SPSBIC 2019

24th – 27th June, Minna Nigeria

2ND SCHOOL OF PHYSICAL SCIENCES BIENNIAL INTERNATIONAL CONFERENCE (SPSBIC 2019)

PROCEEDINGS

THEME:
SUSTAINABLE ENERGY IN CHANGING CLIMATE: THE ROLE OF SCIENCE AND TECHNOLOGY

FEDERAL UNIVERSITY OF TECHNOLOGY
MINNA, NIGER STATE, NIGERIA

PREFACE

This is the second international Conference organized by the school of Physical Sciences of the Federal University of Technology, Minna Nigeria the school is relatively new and comprising of the Departments of Chemistry, Geography, Geology, Geophysics, Mathematics, Physics and Statistics. It was exercised from the former school of Natural and Applied Sciences on the 6th of November 2014.

The school of Physical Sciences 2nd Biennial International Conference is an interdisciplinary forum for the presentation of new ideas, recent developments and research findings in the field of Science and Technology. The Conference provides a platform to scholars, researchers in the academics and other establishments to meet, share and discuss on energy, climate change and sustainable energy use and development. Submissions were received both nationally and internationally and severally reviewed by our international program committee. All contributions are neither published elsewhere nor submitted for publication as asserted by contributor.

We wish to express our gratitude to the school for challenging us to organize the second international conference. Special thanks to the former Dean of the School Prof. A. S. Abubakar who initiated the conference and to the present Dean Prof. Jonathan Yisa for keying into it. The Vice Chancellor Prof. Abdullahi Bala have given immense support to the Conference, thank you sir. Our special appreciation to the keynote speakers for accepting our invitation to give a talk at the conference. Special thanks to all members of the organizing committee and sub-committees for their dedication, determination and sacrifice towards achieving a fruitful and successful conference.

Prof. Kasim Uthman Isah
The Local Organizing Committee Chairman

THEME OF THE CONFERENCE:

Sustainable Energy in Changing Climate: The Role of Science and Technology

SUB-THEMES OF THE CONFERENCE:

- Political, Economic and Technical Challenges in Energy Development;
- Sustainable Energy on Climate and Disaster resilience;
- Energy for Sustainable Development, Benefits and Challenges for Poverty Alleviation;
- Implication of Fossil Divestment and Green Bonds for Financial and Energy Market;
- Energy Use And Environmental Impact for Energy Sustainable Development ;
- Climate Change Through Sustainable and Innovative Energy Technological Development;
- Analysis on Scientific Research in Technology and Energy for Sustainable Development

INTERNATIONAL PLANNING COMMITTEE

Chemistry			
Prof. F. A. Adekola (PhD Analytical Chemistry) Department of Chemistry University of Ilorin, Nigeria Email: fadekola@hotmail.com	Prof. J. N. Egila (Analytical/Environmental Chemistry) Department of Chemistry University of Jos, Nigeria	Prof. Dagne Ermias (Natural Product Chemistry) African Laboratory of Natural Products, Department of Chemistry University (Art Kilo), Ethiopia Email: edagne@gmail.com	Dr. Hasmerya Maroof Computational Chemistry/Chemometrics, Department of Chemistry, University Teknologi Malaysia Email: hasmerya@kimia.fs.utm.my
Prof. Mohamed Noor Hasan Chemoinformatics/Chemometrics, Department of Chemistry, University Teknologi Malaysia Email: mnoor@utm.my, mnoor@yahoo.com	Dr. Nor Kartini Abu Bakar, Department of Chemistry, Faculty of Science, University of Malaya, Malaysia Email: kartini@um.edu.my	Dr. J. O. Jacob, Department of Chemistry, School of Physical Sciences, Federal University of Technology, Minna, Nigeria Email: john.jacob@futminna.edu.ng	Dr. Abdullahi Mann, Department of Chemistry, School of Physical Sciences, Federal University of Technology, Minna, Nigeria Email: abdumann@yahoo.com
Dr Hairul Anuar Tajuddin, Dept. of Chemistry, University of Malaya, Malaysia hairul@um.edu.my **hairultajuddin@gmail.com**			
Geography			
Prof. N.G. Nsofor Department of Geography Federal University of Technology Minna, Nigeria. Email: nsoforng50@yahoo.com	Prof. Haruna Kuje Ayuba Department of Geography Nasarawa State University, Keffi PMB 1022Keffi, Nigeria.	Prof. S. M. Hassan Department of Geography and Environmental Management University of Abuja, Nigeria.	Prof. A. I. Tanko Department of Geography Bayero University Kano, Nigeria Email; aitanko.geog@buk.edu.ng

	Email: hkayuba@yahoo.com	Email; shuaibhassan123@gmail.com	
Dr. Paul Tengbe Department of Geography Furra Bay College, University of Sierra Leone, Freetown Email; dr.paultengbe@yahoo.com	Prof. Alessandra Giannini International institute of Climate and Society (IRI) The Earth Institute University of Colorado, USA Email; Alesall@iri.columbia.edu		
Mathematics			
Dr. Farhad Ali Fluid Dynamics, Heat and Mass Transfer, Department of Mathematics. City University of Science and Information Technology, Pashewar, Pakistan Email: farhadali@cusit.edu.pk	Prof. Frank Sottile, Department of Mathematics, Texas A and M University, College Station, TX 77843, USA Email: sottile@math.tamu.edu	Prof. Oluwole D. Makinde, Applied Mathematics Department, University of the North, South Africa Email: dmakinde@yahoo.com makinded@sun.ac.za	Dr. Patrick Oseleka EZEPUE Director of Research Innovation and Creativity, Hallam University, SheffieldS1 1WB, UK Email: p.ezepue@shu.ac.uk
Dr. O. A. Ajala Department of pure and Applied Mathematics Ladoke Akintola University of Technology, Ogbomoso, Nigeria. E-mail**:** oaajala@lautech.edu.ng	Dr. A. J. Omowaye Department of Mathematics Federal University of Technology, Akure Nigeria E-mail: ajomowaye@futa.edu.ng omowaye_2004@yahoo.co.uk	Dr. Amos Popoola Department of Mathematics Osun State University, Osogbo, Nigeria E-mail: amos.popoola@uniosun.edu.ng	Prof. R. B. Adeniyi Numerical Analysis Department of Physics, University of Ilorin, Nigeria Email: raphade@unilorin.edu.ng
Materials Science/Nanoscience			

Professor Arunachala Kannan, Ira A. Fulton Schools of Engineering, The Polytechnic School PRLTA 335A, 7171 E Sonoran Arroyo Mall Arizona State University Mesa, AZ 85212; Email: amk@asu.edu	Dr. S. Ambali Department of Chemical Engineering, Federal University of Technology, Minna, Nigeria. Email: kasaka2003@futminna.edu.ng	Prof. A. S. Afolabi Department of Chemical and Metallurgical Engineering, Botswana University of Science and Tecgnology, Bostwana. Email: afolabi@biust.ac.bw	Dr, Nafarizal Bin Nayan, (nanoscience/nanotechnology and electronics) Email: nafa@uthm.edu.my Shamsuddin Research Centre, Office for Research, Innovation, Commercialization and Consultation, Universiti Tun Hussein Onn Malaysia
Prof. M. Aibinu, Department of Mechatronics, Federal University of Technology, Minna, Nigeria. Email: maibinu@gmail.com	Dr. Olayemi, Dept of Biology, F. U.T., Minna Email: isreal.olayemi@futminna.edu.ng	Dr. Mohammed Saidu Dept. Civil Engineering Department of Mechatronics, Federal University of Technology, Minna, Nigeria Email: mohammed_saidu@futminna.edu.ng	
Physics			
Prof. Fabian Ezema Department of Physics, Federal University of Technology, Minna, Nigeria	Dr. Mayeen Uddin Kahandaker, Department of Physics, University f Malaya, 50603, Kuala Lumpur, Email: mu_khandaker@um.edu.my	Prof. A. O. Musa, Department of Physics, Bayero University, Kano, Nigeria Email: aomusa2011@gmail.com	Prof. K. J. Oyewumi, Department of Physics, University of Ilorin, Nigeria Email: kjoyewumi@unilorin.edu.ng
Dr. Muhammad Arif in Agam Department of Physics, Universiti Tun Hussian Oon Malaysia Malaysia, Email: arif@uthm.edu.my	Dr. Oluwafemi Stephen Ojambati Department of Science and Technology, University of Twente, 7500 AE Enschede, The Netherlands Email: o.s.ojambati@utwente.ni	Dr. Zaidi Bin Embong, Department of Physics, Universiti Tun Hussian Oon Malaysia Malaysia Email: zembong@gmail.com	Dr. Umaru Ahmadu, Department of Physics, Federal University of Technology, Minna, Nigeria Email: u.ahmadu@yahoo.com

Prof. E. E Udensi, Department of Physics, Federal University of Technology, Minna, Nigeria Email: eeudensi@yahoo.com	Dr. Nasir Naeem Department of Physics, University of Abuja, Abuja, Nigeria. Email: nassnaeem@gmail.com	Prof. O. D Oyedum Department of Physics, Federal University of Technology, Minna, Nigeria Email: oyedidavid@futminna.edu.ng	Dr. Matthew T. Kolo Department of Physics, Federal University of Technology, Minna, Nigeria Email: mat_479@yahoo.com
Dr. Adetona Abbass Geophysics Department of Physics, Federal University of Technology, Minna, Nigeria Email: **tonabass@gmail.com**	Prof. SADIQ Umar, Nuclear Physics Department of Physics, Ahmadu Bello University, Zaria, Nigeria Email: sadiqumarx@yahoo.co.uk	Prof. V. Chukwuma, Atmospheric Physics Department of Physics, University of Ilorin, Nigeria Email: victorchukwuma@yahoo.com	Dr. Ibrahim Aku Department of Physics, Federal University of Technology, Minna, Nigeria ibrahimaku@futminna.edu.ng
Statistics			
Prof. Benjamin Agboola Oyejola Professor of Statistics (Biometry, Applied Statistics, Experimental Design and Econometrics) Department of Statistics University of Ilorin, Ilorin, Nigeria. **Email:** **boyejola@unilorin.edu.ng** **and** **boyejola2003@yahoo.com**	Prof. E.O. Asiribo Professor of Statistics (Biostatistics, Experimental Design and Time Series) Department of Statistics Federal University of Agriculture Abeokuta, Nigeria Email: asiribo@yahoo.com	Prof. Shehu Usman Gulumbe Professor of Statistics (Multivariate Statistics and Repeated Measures) Department of Mathematics Federal University Birin Kebbi Kebbi State, Nigeria. Email: shehu.gulumbe@fubk.edu.ng,	Dr. I. U. Shittu Associate Professor of Statistics (Time Series, Probability and Stochastic processes) Department of Statistics, Federal University of Technology, Minna, Nigeria. Email: shittu.olanrewaju@gmail.com, oi.shittu@ui.edu.ng
Dr. A. Isah Associate Professor of Statistics (Spatial	Dr. Alexander Hapfelmeier *Ph.D.*		

Statistics, Probability theory, and Sample Survey) Department of Statistics, Federal University of Technology, Minna, Nigeria. Email: aish@futminna.edu.ng	Institut Fur Medizinsche Statistik UndEpidemiologe Technical University of Munich Klinikum rechts derIsar Ismaninger Str. 22. Email: alexander.hapfelmeier @tum.de.		
Geology			
Dr. U. S. Onoduku, Department of Geology, Federal University of Technology, Minna, Nigeria, **onoduku.usman@futminna.edu**	Prof. Wan Hasia Abdullahi, Department of Geology, University of Malaysia, Malaysia, wanhasia@um.edu.my	3. Dr. Idris-Nda Abdullahi, Department of Geology, Federal University of Technology, Minna, Nigeria, 08036273815, idrisnda@futminna.edu.ng	Prof. Okosun Edward Agboneni, Department of Geology, Federal University of Technology, Minna, Nigeria, eaokosun@yahoo.com
Dr. Waziri M. N., Department of Geology, Federal University of Technology, Minna, Nigeria **nuhuwaziri@futminna.edu.ng**	Dr. Che Vivian, Department of Geology, University of Buea, Cameroon, +237675030802, chevivian@gmail.com	Dr. Agyingi Christopher, PhD (Associate Professor of Sedimentology and Petroleum Geology) Department of Geology, University of Buea, Cameroon Tel: +237677875030 Email: agyingi@ubuea.cm and cm_agyingi@yahoo.co.uk	Cheo Emmanuel Suh, PhD (Professor of Economic Geology and Microtectonics) Department of Geology, University of Buea, Cameroon Tel: +237677292940 Email: chuhma@yahoo.com
Dr. Isah Goro Aliyu, Department of Geology, Federal University of Technology, Minna, Nigeria, isahgoro@futminna.edu.ng	Dr. Ako Thomas Agbor, Department of Geology, Federal University of Technology, Minna, Nigeria akoagbor@futminna.edu.ng		

LOCAL ORGANISING COMMITTEE

Prof. Kasim Uthman Isah (**Chairman)**

Dr. Abubakar Usman

Dr. Shehu Usman Onodoku

Dr. Mairo Muhammed

Dr. Umaru Mohammed

Mr. Elijah Yanda Shaba (**Secretary)**

TECHNICAL COMMITTEE

Dr. Adamu Alhaji Mohammed (**Chairman)**

Dr. T. A. Ako

Dr. J. O. Tijani

Mr. J. Mayaki

Dr. Eichie Julia Ofure (**Secretary)**

LOGISTICS COMMITTEE

Dr. U. S. Onoduku (**Chairman)**

Dr. A. A. Rafiu

Dr. Samshideen Ajoye

Dr. J. O Jacob

Dr. (Mrs) S. H. Waziri

Dr. U. S. Mohammed

Mr. I. S. Onotu

Mr. S. E Abdulkabir

Mr. E. Y. Shaba (**Secretary)**

KEYNOTE SPEAKERS

Prof. Daniel Ayuk Mbi Egbe

Prof. Daniel Ayuk Mbi Egbe received his BSc in Physics and Chemistry in 1991 from the then University of Yaoundé (now University of Yaoundé 1), Cameroon. In 1992, he moved to Germany where he obtained a MSc and PhD in Chemistry in 1995 and 1999, respectively, from the Friedrich-Schiller University of Jena. He completed his habilitation in Organic Chemistry at the same institution in 2006

Prof. Egbe is a member of Organic Electronics Association (OE-A), and a board member of the World University Service (WUS) in Germany. He is the initiator of the German-Cameroonian Coordination Office, initiator and International Coordinator of the African Network for Solar Energy (ANSOLE), initiator and chairperson of ANSOLE e.V., an institution legally representing ANSOLE, and initiator of the Cameroon Renewable Energy Network (CAMREN). He is also the initiator and coordinates the research platform BALEWARE (Bridging Africa, Latin America and Europe on Water and Renewable Energies Applications). He was part of the team engaged in developing research programs at the Pan African University Institute of Water and Energy Sciences (including Climate Change) (PAUWES) in Tlemcen, Algeria. In 2016 he was appointed the first Distinguished Brian O´Connell Visiting Fellow of the University of the Western Cape, South Africa. He is the director of the VolkswagenStiftung-sponsored Summer Schools on sustainable energetics and on water.

He is presently member of the Institute of Polymeric Materials and Testing (IPMT), Johannes Kepler University Linz, where he researches and lectures. He is a PhD supervisor and visiting lecturer at the African Centre of Excellence in Energy for Sustainable Development (ACE-ESD) of the University of Rwanda in Kigali.

Prof. Egbe's main research interest is the design of semiconducting materials for organic photovoltaics and other optoelectronic applications, has published more than 120 peer-reviewed articles, speaks 5 languages and is father of 4.

Daniel.egbe@ansole.org, daniel_ayuk_mbi.egbe@jku.at Skype: danielegbe1

Kazeem Ojoye

Kazeem OJOYE was born on 9 October 1967 in Ibadan, the capital city of Oyo State. He enrolled into the Technical University in Munich where he graduated with a bachelor's degree in Computer Engineering. He worked at several places in Germany Between 1990 to 1997.

He was Project Manager Migration of the Telekom SIP Platform from the (MSP) to the new Telekom Corporate SIP Platform, Project Manager Emergency/Outage Telephony Concept for UniCredit, with UNIFY, T-Systems, Technical Project coordinator Teleopti Upgrade of Version 8. He joined the services of BMW as a logistic specialist. While in BMW he worked in several departments which include communication specialist and customer consultants.

Currently, Kazeem Ojoye is the application manager in charge of ICT at Unicredit direct Services in Munchen, He is the financial secretary of Nigeria in Diaspora organization (NIDO0 in Germany, the principal consultant for multivate consulting, UK and Germany, consultant for renewable energy, Chairman, Youth Empowerment Enlightenment and Self Sustainability Initiative (YEESSI), Project Manager at Bruder-Hilfe among others.

He speaks English, Deutsch and French. He is happily married with children

TABLE OF CONTENTS

CHEMICAL SCIENCES

Studies of Biogas Production of Some Selected Animal Wastes and Their Co-Digestion

Mohammed S., Buhari I., Muhammad M.U., and Adamu S.M

Abstracts

Production of biogas through anaerobic digestion of organic waste materials provide an alternative renewable energy source and also eco-friendly method. In the present investigation, biogas production from poultry dropping, turkey dung, cow dung and co-digestion (of two each) in the ratio of 1:1 was evaluated. The same volume of digesters were employed for biogas generation. The digestion process was carried out for a retention time of 7-days for eight weeks. The biogas production was subsequently measured by downward displacement. The samples of tested substrates were analyzed for pH, ash, moisture content and percentage organic matter. For sole digestion, the cumulative biogas production revealed values of 2531.43cm^3, 2495.71cm^3 and 2511.43cm^3 for turkey dung, cow dung and poultry dropping respectively. For co-digestion the gas yield of 1311.43cm^3, 2624.29cm^3 and 742.86cm^3 was obtained for turkey dung with poultry dropping, turkey with cow dung and poultry dropping with cow dung respectively. The results obtained showed that the type of waste had significant effect on the quantity of biogas produced. All the substrate used appeared to be good source for biogas production. Assessment of cumulative biogas production revealed that only co-digestion of turkey dung with cow dung enhanced the biogas production.

Key words: Biogas, Co-digestion, Animal waste and Renewable energy

1.0 INTRODUCTION

The renewable energy sources can contribute to solve the present and future energy problems. For their economic progress, African countries need sustainable energy supplies. Unreliable energy supply may end up with low level of private investment in African continent. Therefore, improvement in the quality and magnitude of energy services in developing countries is required to meet developmental objectives including the Millennium Development Goals (MDGs).

Biomass in the form of mainly fuel wood and charcoal is the dominant energy source in Sub-Saharan Africa. Though it appears cheap, overexploitation of this biomass leads to serious negative environmental consequences. Fossil energy sources are the most widely used energy supplies in the world today. However, the increased prices of oil and increased awareness of climate changes is promoting the use of alternative environmentally friendly renewable energy sources such as biogas (Khanal, 2008). Among the alternative energy sources, biogas production from organic wastes has worldwide application as it yields good quality fuel and fermented slurry, which may be used as a manure or soil conditioner. In addition, it helps to a great extent in the abatement of pollution. Biogas has a very positive impact on the environment since less CO_2 is formed during its combustion than it is used for photosynthesis by the plants (Navickas, 2007).

The content of biogas varies with material being decomposed and environmental conditions involved (Anunputtikul and Rodtong, 2004).Potentially, all organic waste materials contain adequate quantities of the nutrients essential for the growth and metabolism of the anaerobic bacteria in biogas production. However, the chemical composition and biological availability of the nutrients contained in these materials vary with species, factors affecting growth and age of the animal or plant (Anunputtikul and Rodtong, 2004). Various wastes have been utilized for biogas production and they include amongst others; animal wastes (Alvarez *et al*., 2006), industrial wastes (Uzodinma *et al.*, 2007), food processing wastes (Arvanitoyannis and Varzakas, 2008), plant residues (Ofoefule and Uzodinma, 2008) etc. One treatment method for improving the biogas production of various feedstocks is co-digesting them with animal and/or plant wastes (). The objective of this study was to assess the biogas potential from turkey dung, poultry droppings and cow dung in sole and co-digestion.

2.0 MATERIALS AND METHODS

The materials used in this investigation as substrates were cow dung, turkey dung and poultry droppings all of which were agricultural waste materials.

2.10 Sampling and Sample Treatment

The waste materials were collected fresh from various locations in Sokoto metropolis. The substrates were sun dried for seven day. The dried samples were grounded using wooden pestle and mortar and then sieved using standard test sieve to have uniform size of substrates. The cow dung was collected from Kofar Kware area in Sokoto, while Turkey dung and Poultry droppings were collected from poultry house at Shehu Shagari College of Education Sokoto.

2.20 Fabrication of Digesters

Six digesters were fabricated using empty cleaned Milo tins and rubber tube 0.8cm diameter. A hole was bored on the cover and the tubes were inserted into the hole. The tube was tightened using a strip of rubber. The gas was collected by downward displacement of water in the measuring cylinders of 1000cm^3 capacity.

2.30 Slurry Preparation

From the powdered dried samples, slurries were prepared by mixing 300g of each substrate with 1200cm^3 of water to obtain 1:4, substrate to water ratio. For co-digestion, 150g of each substrate were weighted and mixed with 1200cm^3 of water.

2.40 Method of Analysis

The physical characteristics pH, moisture content, ash content and organic matter were analyzed.

2.41 Moisture Content

Moisture content was determined using procedure given by AOAC, 2000. About 3 g of sample to the dish and then placed in an oven for 3 h at 105°C. The percent of moisture is computed using the formular

Moisture (%) = $\frac{W1-W2}{W1} \times 100$

Where: W1 = weight (g) of sample before drying, W2 = weight (g) of sample after drying.

2.42 Ash Content

Ash was determined using the procedure given by Baraem, 2017. About 2 g of sample into the crucible. The crucible was placed in muffle oven at 550 °C and heated overnight. The percentage ash is computed using

% Ash = $\frac{weight\ of\ ash}{original\ sample\ weight} \times 100$

2.43 Determination of pH

Determination of pH of the diluted substrate in each digester was done directly using digital pH meter. An electrode was inserted into samples of substrate that was diluted using distilled water.

2.44 Determination of Organic Matter

The amount of organic matter was calculated by differ-ence as follows:

Organic matter, % = 100 – (ash + moisture)

3.0 RESULTS AND DISCUSSION

In this experimental work, the following results were obtained:

Table 1: Charging Temperature and pH of the Digesters

Digesters	Temperature(^{0}C)	pH
A (TD)	29	5.4
B (CD)	29	5.3
C (PD)	30	5.6
D (TD/PD)	29	5.3
E (CD/TD)	31	5.4
F (CD/PD)	29	5.4

TD= Turkey droppings, CD= Cow dung, PD= Poultry dung. Co-digestion was in the ratio (1:1)

The production of biogas is depended on the optimum biodegradation process. Temperature and pH are some of the process parameters that play an important role in the anaerobic process. Bacteria work in temperature of mesophillic condition (25-40^{0}C) with optimum temperature of 35^{0}C and thermophillic condition of (50-65^{0}C). The bacteria also work in a specific pH range and shows maximum activity in the optimum pH. The optimum pH needed by acidogenic

bacteria is in 5-6.5, whereas optimum pH for methanogenic bacteria is higher than 6.5 (Akens, 2005). It is evident from table above that the pH of wastes in each digester ranged from 5.3-5.6 which is in conformity with the optimum pH range for biogas production. The temperature in all the digesters ranged from29-31^{0}C which happens to be in the range of mesophillic 25-40^{0}C which is allowed for biogas production.

Table 2: Physicochemical properties of the wastes

Substrates	Moisture (%)	Ash (%)	Organic matter (%)
TD	23.00	6.50	70.50
CD	13.50	14.00	72.50
PD	4.00	8.50	87.60

TD= Turkey droppings, CD= Cow dung, PD= Poultry dung.

From the table above, it can be seen that turkey dung had maximum moisture content of 23.00% and poultry droppings the least with moisture content of 4.00%. The maximum ash content was recorded in cow dung as 14.00% while turkey dung gave the lowest value of 6.5%. The percentage organic matter in all the substrates varied between 70.50% (turkey dung) to 87.60% for poultry droppings.

Table 3: Quantity of biogas production by each digester (Biogas production in cm^3/day for 1st week).

Digesters/ Week	A	B	C	D	E	F
1	-	-	-	-	-	-
2	-	-	-	-	-	-
3	-	-	-	-	20	-
4	20	-	40	10	30	-
5	40	40	60	30	100	20
6	100	50	70	50	110	50
7	110	70	90	60	120	60
Mean	38.57	22.86	37.14	21.43	54.29	18.57

It is observed from the table above, gas production was not recorded on the first day in all the digesters. On first day there was no production of biogas (Adeyemo, et al., 2008), thus suggesting that fermentation has not started. From day 3-6 the gas production was fairly slow, this is predicted because biogas production rate in batch condition is directly equal to specific

growth of methanogenic bacteria (Napharatana, et al., 2007). For sole digesters (containing only one kind of substrate), digester A which contains turkey dung as feedstock produced highest average biogas (38.57ml) which can be attributed to its more water content, thus increasing the degree of digestion as bacteria can easily access liquid substrate for relevant reaction to take place easily (Buysman, 2010) while digester B (cow dung) gave lowest average biogas of 22.86ml. Cow dung alone resulted less biogas probably due to its partial fermentation that usually takes place in the intestinal tract of the animal (Deublein and Steinhauser, 2008). Though blending or co-digestion of waste is one of the optimization techniques known to improve biogas production, as seen in the table it is only co-digestion of cow dung and turkey dung (digester E) enhanced biogas production. This might be due to less favorable situation of substrate mixtures (in digester D and F) to microorganism.

Table 4: Mean Weekly Biogas Production in cm^3 for eight weeks

DIGESTERS/ WEEKS	A	B	C	D	E	F
Week 1	38.57	22.86	37.14	21.43	54.29	18.57
Week 2	260.00	160.00	235.71	184.29	191.43	128.57
Week 3	442.86	291.43	550.00	368.57	304.29	337.14
Week 4	530.00	530.00	768.57	442.86	451.43	182.86
Week 5	607.14	917.14	637.14	208.57	767.14	68.57
Week 6	385.40	450.00	230.00	69.43	570.00	7.14
Week 7	211.43	110.00	48.57	15.71	242.86	-
Week 8	54.29	14.29	4.29	1.43	42.86	-

The graphs in figure 1 & 2 showed the variations in the biogas production for all the six digesters in different week. The maximum biogas production was observed for digester B in the 5th week with mean value of 917.14ml followed by digester E with mean value of 767.14ml in the same week. Digester C had its highest production in the 4th week with 637.14ml as mean value thereafter yield decreases gradually for the weeks left. The 5th week also recorded the maximum quantity of biogas of 607.14ml for digester A. Digesters D and F have recorded the least yield although a significant amount has been recorded in 4th and 3rd week with mean values of 442.86ml and 337.14ml respectively, which could be due to the nature of the blended subsrates.

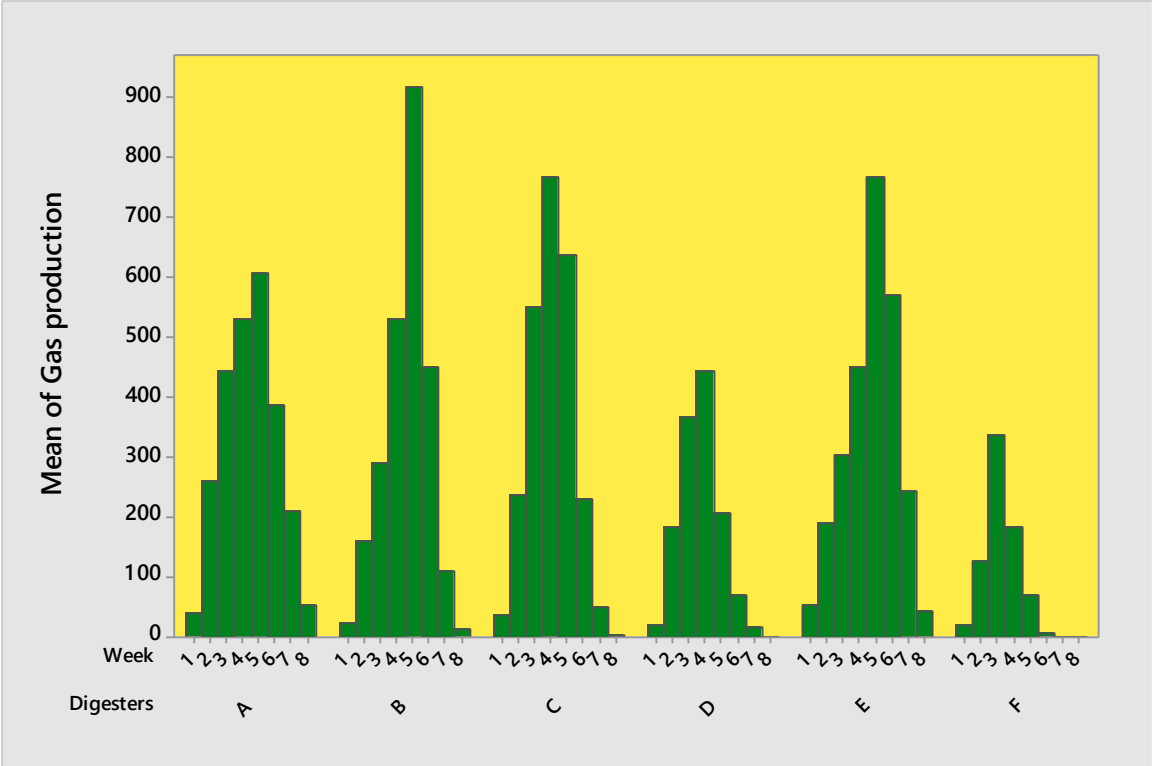

Figure 1: Weekly mean biogas yield of the digesters in cm^3

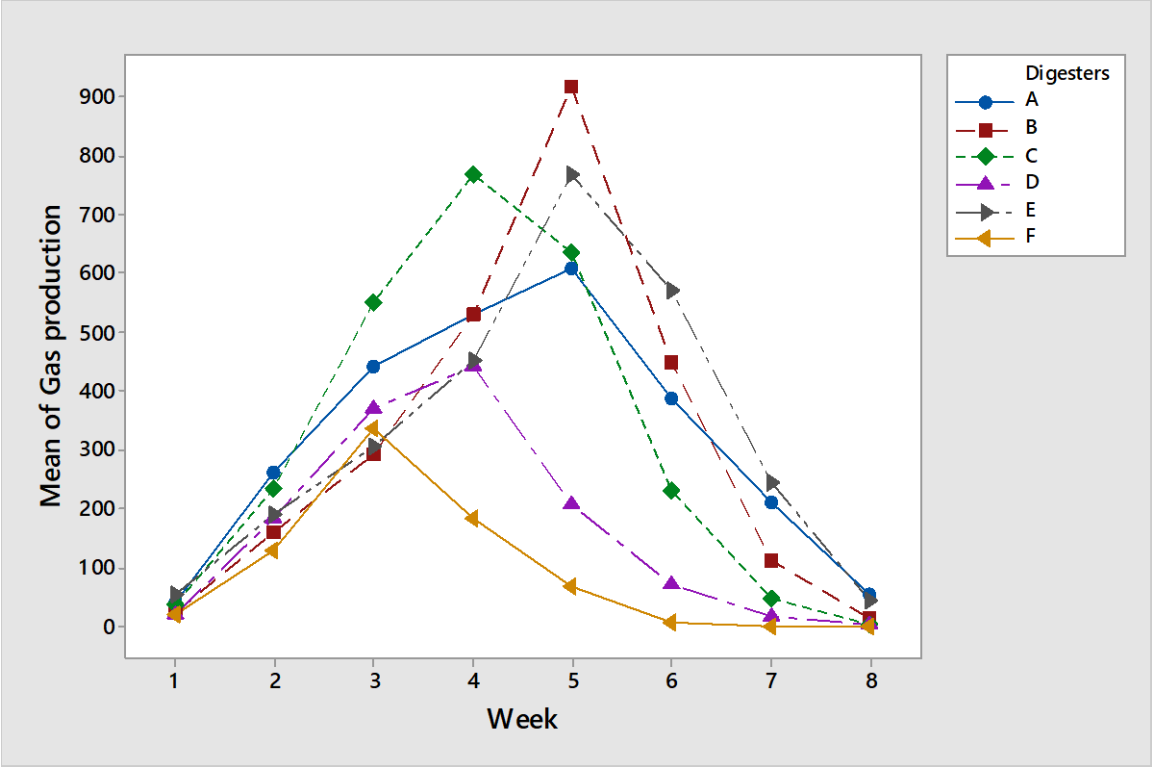

Figure 2: Weekly mean biogas yield of the digesters in cm^3

4.0 CONCLUSION

It was evident from the result that, all the three substrates used in this investigation are good materials for biogas production and maximum biogas production was observed during 3-5 week of digestion. However, the volume of biogas produced is dependent of the waste material. This study also showed that biogas production was less and gradual in the first week of the investigation. This suggests that the biogas producing microorganisms are in the lag phase of growth where acclimatization or adaptations of the cells take place. This report is in consonance to that of Ozor *et al.*,(2014*)*. It is also evident from our findings that only co-digestion of cow dung with turkey dung enhanced biogas generation.

REFERENCES

Anunputtikul W and Rodtong S, (2004) The Joint International Conference on "Sustainable

Nwagbo EE, Dioha IJ, Gulma MA, (1991) Nigerian. J. Solar Energy. 10: 145 – 149.

Zuru A.A., Saidu H., Odum E. A. and Onuorah O.A. (1998) *Nigerian Journal of Renewable Energy*. 6 (1&2): 43 – 47.

Alvarez R, Villica R and Liden G (2006) *Biomass and Bioenergy*. 30: 66-75.

Uzodinma EO, Ofoefule AU, Eze JI. and Onwuka ND, (2007), *Trends Appl. Sci. Res*. 2 (6): 554-558.

Arvanitoyannis I.S. and Varzakas T.H. (2008), *Crit. Rev. Food Sci. Nut*. 48 (3): 205-247.

Ofoefule AU and Uzodinma EO, (2008), *Nigerian. J. Solar Energy*. 19: 57 – 62.

Ofoefule AU, Uzodinma EO and Onukwuli OD, (2009) *International Journal of Physical Sciences.* 4(8): 535-539.

Mshandete A, Kivaisi, AK, Rubindamayagi M and Mattiasson B, (2004) *Bioresource Technology*. 95: 19 – 24.

Nielsen H.B and Angelidaki I, (2008) *Water Science Technology*. 58: 1521 – 1528.

Adeyemo S.B and Adeyeniju A.A (2008) improving Biogas Yield Using Media Materials *Journal of Engineering and Applied Sciences. 3(2):207-210*

Napharatana A, Pullamanappelli P.C and Clark W.P (2007) Kinectic and Dynamic Modelling of
Batch Anaerobic Digestion of Municipal Solid Waste via Stirred Reactor Waste Management 27:595-603

Baraem P (2017) Ash Content Determination S.S Nielson, *Food Analysis Laboratory Manual Food Science Text Series Sringer International Publishers*

O. C. Ozor, M. V. Agah,K. I. Ogbu,A. U. Nnachi, O. E. Udu-ibiam and M. M. Agwu (2014) Biogas Production Using Cow Dung From Abakaliki Abattoir In South-Eastern NigeriaI *International Journal of Scientific & Technology Research* 3: 238

Energy and Environmental (SEE)", Hua Hin, Thailand. 1-3 Dec, 2004, 238- 243.

Phytochemical and Antibacterial Studies of *Ensete gilletii* Leaf Extract and Fraction

[1]Tanko, E., [2]Dauda, B. E. N., [3]Mann, A. A., [4]Oyeleke, S. O., [5]Fadipe, L. A.,
[1,2,3,5]Department of Chemistry, [5]Department of Microbiology, Federal University of Technology, Minna, P. M. B, 65,
Minna, Niger State, Nigeria
Email: ezekieltanko@gmail.com

ABSTRACT

Ensete gilletii (family *musaceae*) is ethnomedicinally used for the treatment of diarrhoea, dysentrieae, stomach ache, digestive disorder, cholera, fever, urinary infection and gonorrhoea. The quantitative determination of the phytochemicals constituents revealed the presence of alkaloids, flavonoids, phenolic compounds, Saponins and tannins with the values (3.970, 3.900, 12.712, 0.419 and 18.857 mg/cm^3, respectively).The preliminary phytochemical screening of the Leaf extracts revealed the presence alkaloids, flavonoids, phlobatannins, reducing sugar, saponins, tannins and terpenoidal compounds; While the preliminary phytochemical screening for the VLC fraction (L1 –L4) revealed the presence of flavonoids, plobatannins, reducing sugar, tannins and terpenoidal compounds. The thin layer chromatography (TLC) sprayed with chromogenic reagents ($FeCl_3$) also revealed the present of phenolic compounds. Antibacterial susceptibility test of crude ethanol extract of the leaf of *Ensete gelletii* against Gram-positve (*B. subtilis, S. aureus, S. Pyogenes*) and Gram-negative (*E. coli, K. pneumonaie, S. Typh* and *S. dysentriea*) at (40, 80, 120 and 160 mg/cm^3) test bacteria isolates revealed a broad spectrum of activity in dose dependent manner. The zone of inhibition ranged from (16 to 29 mm) in the leaf extract (16 to 31 mm) which is significantly different from the standard antibiotics (Ampiclox) at (40 mg/cm^3). *S. pyogenes* and *S. dysentriea* were resistant against the leaf extract. The Minimum Inhibitory Concentration (MIC) and Minimum Bactericidal Concetration (MBC) of the fractions were also observed to be lower when compared with the leaf crude extract. The MIC ranged (25 to 100 mg/cm^3) while the MBC ranged from (50 to 100 mg/cm^3) in all the susceptible organisms. The broad spectrum activity displayed than the standard antibiotic drugs (Ampiclox) suggest that the leaf part of the plant could be used as pharmaceutically important agents in drug formulation in the treatment of numerous diseases.

INTRODUCTION

Nature has endowed man with abundant natural resources, especially plants and their medicinal potentials. Over the years, man has exploited these medicinal plants, some for therapeutic purposes. Because of the unique medicinal potentials discovered from these plants, people have been using these plants for their health care needs (Tee *et al.*, 2015). Traditional medicines have been universally employed for treatment of various ailments and as basic template for many pharmaceutical drugs (Abbott, 2014). It has been reported that 80 % of the world's

population relies on medicinal plants for their primary health care needs (World health Organization (WHO, 2014).

Therefore, continuing exploration for novel chemical classes derived from medicinal plants is one of the practical and promising approaches that attract researchers in the quest for new chemotherapeutics (Daniels and Malomo, 2014). *Ensete gilletii* is a wild banana (Family *Musaceae*) commonly called wild banana (English), Ayaɓar dāji (Hausa), *Uhia unune* (Igbo), *Egbo ogede* (Yoruba), *Ayabaladde* (Fulani) and *Gbmamiyai* (Gbagyi) has a wide distribution range (West Tropical Africa to Malawi, Nigeria, Benin, Cote d'ivore, Sierra Leon, Togo, Central Republic of Africa, Cameroun and Democratic Republic of Congo) (Scott, 2013). *E. gilletii* is a large monocarpic flowering plants and one of the three genera in the banana family, *Musaceae*, with unbranched pseudo-stem of concentric layers of fleshy leaf-petioles arising to 1.5 meters high from a swollen base, not suckering like *Musa* specie, and dying after flowering. It resemble banana plants (Tesfaye *et al*., 2016), but they have a long, paddle-shaped leaves with crimson midribs. The fruits are similar in appearance to those of banana, but they are dry, seedy plant. The seeds coats are black, ovoid, and have about 0.4 – 0.5 mm diameter and 0.5 – 0.7 mm long with a conspicuous white, powdery endosperm. The entire plant dies after fruiting and is widely used for household, domestic and personal uses (Afolayan *et al*., 2014, Tesfaye *et al*., 2016).

Ensete gilletii is used by rural people for the treatment of various ailments. In Nigeria, information from local sources revealed that the roots have reportedly been used to treat various ailments such as dysentery, diarrhoea, stomach ache, digestive disorder, cholera, fever, urinary infection, gonorrhea, malaria, menstrual pains, typhoid fever, insect bites, skin infections, treatment of wounds and general weakness. The flower, stem and leaves and roots of *musacea* family have reportedly been used in the treatment of diabetics, diarrhoea, dysentery and easy delivery among pregnant women (Sethiya, 2016). Although much work have been carried out

on the other species, *Ensete superbum, Ensete ventricosum* among others. Literature on *Ensete gilletii* however, is scanty, although it has been reported that the ethyl acetate and ethanol seed extracts of the plant have a promising antibacterial and fungal activities (Afolayan *et al*., 2014). A review of literature reveals no work has been carried out on the leaf extracts and the fractions of *Ensete* plant. This work therefore presents the results of the phytochemical and antibacterial potentials of the extracts and fractions of both the leaf of *E. gilletii* against selected bacteria in comparison with standard antibiotic drug.

Materials and Methods

Collection of Plant

Fresh leaves of *Ensete gilletii* were collected from a farmland in Sarkin Pawa in Munya Local Government Area, Niger State, Nigeria in the month of December, 2018. The plant was duly authenticated by the herbarium at National Institute of Pharmaceutical Research and Development (NIPRD), Idu-Abuja, Nigeria, and a voucher specimen deposited (Voucher no. NIPRD/H/6991). The fresh leaf collected was cut into pieces, air-dried at room temperature. The dried sample was then pulverized.

Extraction Procedures

Pulverized leaves (1 kg) of *Ensete gilletii* was exhaustively extracted with 70 % ethanol by hot maceration continuously at water bath (temperature, 70°C) for several days until the extractant became colorless. The resulting solution was decanted, filtered and then concentrated in *vacuo* and finally dried over a water bath to afford a deep brown pasty mass coded ethanol leaf extracts (L) (109.6 g, 10.96 % recovery).

Fractionation of Crude Extracts

Vacuum – Liquid Chromatography (VLC) of Crude Extracts L

Ethanol leaf extract (L) (pasty brown mass, 20 g) was fractionated using vacuum – liquid chromatography (400 g silica gel, mesh 60-120, increasing polarity of $CHCl_3$:MeOH (100-0: 0-100). The resultant eluates were collected in factions of 100 cm^3 each and identical fractions pooled based on TLC profile in various solvent systems to give four major fractions coded L1-L4. The pooled fractions were sprayed using chromogenic reagents: $FeCl_3$ (test for phenolic compounds), Dragendorff's (test for Alkaloids) and LiebermannBuchard's reagents reagents (test for steroidal compound). The chromatogram is shown on palate I.

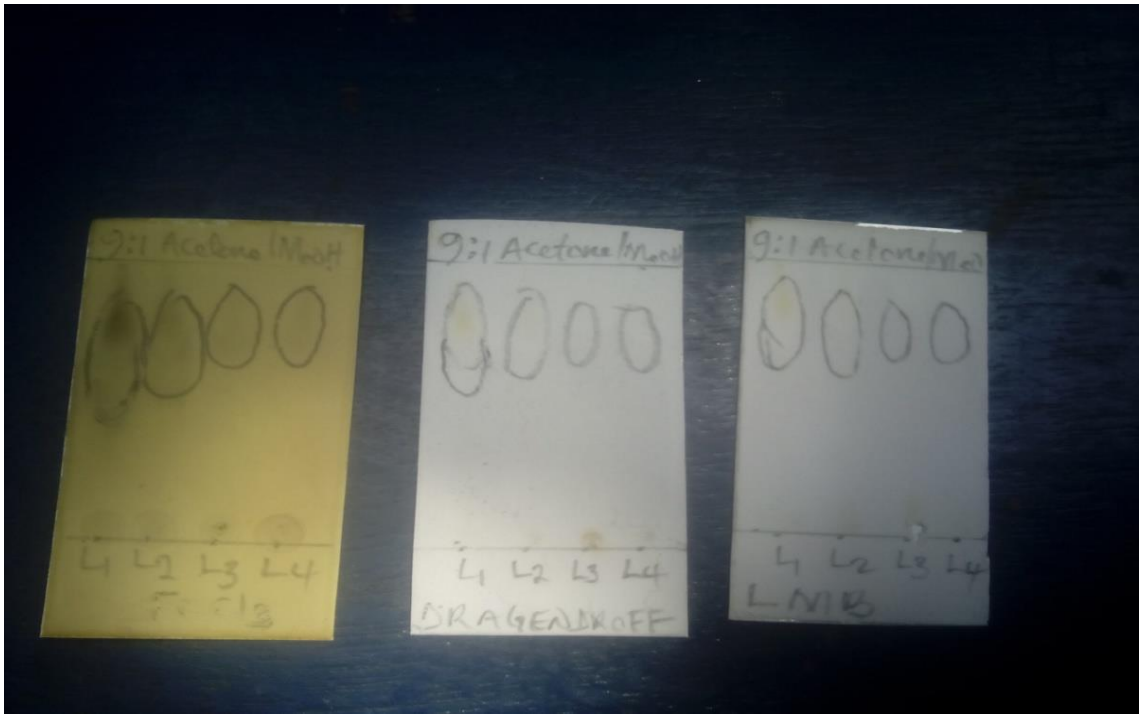

A B C

Plate I: Chromatograms of the TLC (solvent system: Me_2CO:MeOH (9:1) of the leaf fractions (L1-L4) sprayed with Chromogenic reagents $FeCl_3$ (A) (Bluish-black, Dragendorff's (B) (no colour) and LiebermannBuchard's (C) reagents (no colour)

Qualitative and Quantitative Screening

The various classes of the phytochemical present in the ethanol leaf extract of *E. gilletii* detected using various standard methods (Sofowora, 1993; Harbone, 1998; Trease and Evans, 2002; AOAC, 2010).

Antibacterial Assay

Source of organisms and bacterial culture

Crude ethanol leaf extract (L) and Fractions (L1-L4) tested against overnight cultures of three Gram – positive (*Staphylococcus aureus*, *Bacillus subtilis* and *Streptococcus pyogens*) and four Gram – negative (*Escherichia coli*, *Salmonella typhi*, *Klebsiella pneumoniae and Shigella dysentriae*) bacterial strains. All obtained from the Department of Microbiology, Federal University of Technology Minna, Niger State, Nigeria.

The Antimicrobial screening of the crude ethanol leaf (L) extracts and the fractions (L1-L4) were carried out using agar dilution method as described by Sofowora, 1993 and Trease and Evans (2002).

Results and Discussion
Preliminary Phytochemical Screening

Results of preliminary phytochemical screening (qualitative) of crude leaf extracts of *E. gilletii* is presented in Table 1 and 2.

Table 1: Quantitative phytochemical Screening of Ethanol Leaf (L) Extract of *Ensete gilletii*

	Concentation (mg/g) Phytoconstituents				
Extract	Alkaloids	Flavonoids	Phenolic compounds	Saponins	Tannins
L	3.97±0.00	3.548±0.33	12.712±1.32	0.419±0.89	18.857±0.19

Table 2.: Phytochemical Constituents of the Crude Leaf Ethanol Extracts and the various Fractions of *Ensete gilletii*.

Phytochemicals	Test	Observation	L	L1	L2	L3	L4

Alkaloids	Dragendorff's reagent	Orange recipitate	+	-	-	-	-
Anthraquinones	Borntrager's test	Pink redclour	-	-	-	-	-
Cardiac glycosides	Keller Killani's testtest	Reddish-brown precipitate	-	-	-	-	-
Flavonoids	NaOH reagent	Intense yellow colour	++	++	+	+	+
Phlobatannins	Borntrager's test	Red precipitate	++	++	+	+	+
Reducing sugar	Fehling's test	Brick red precipitate	++	+	+	+	+
Saponins	Frothing Test	Persistent froth	+	-	-	-	-
Steroidal compound	Libermann Burchard's test	Greenish colour	-	-	-	-	-
Tannins	$FeCl_3$ test	Bluish-black colour	++	++	++	+	+
Terpenes	Salkwiski's test	Layer of reddish brown colour	+	+	+	-	-

Key: + = present, ++ = moderately present

Table 3: Susceptibility Test for Ethanol Crude Leaf Extracts of *E. gilletti*

Test Organisms	Concentration (mg/cm^3)				Standard drug
	40	80	120	160	40
Bacillus subtilis	NA	NA	17	21	31
Escherichia coli	NA	16	22	28	36
Klebsilla pneumonieae	NA	NA	21	27	31
Salmonella typhi	17	21	23	29	29
Staphyloccus aureus	NA	22	24	29	36
Shigella dysentriae	NA	NA	NA	NA	34
Streptococcus pyogenes	NA	NA	NA	NA	26

NA= No activity

Table 4: Minimum Inhibitory Concentration (MIC) and Minimum Bactericidal Concentration (MBC) of Ethanol Crude Leaf Extracts of *E.gilletii*.

Test Organisms	MIC	MBC	Ampiclox
Bacillus subtilis	120	120	40
Escherichia coli	80	120	40
Klebsiella pneumoniea	120	120	40
Salmonella typhi	40	80	40
Staphyloccus aureus	80	120	40
Shigella dysentriae	NA	NA	40
Streptococcus pyogenes	NA	NA	40

NA= No activity

Table 4: Susceptibility Test for Crude Ethanol Leaf (L) Fractions of *E. gilletii*

Organisms	Fractions (Concentration 200 mg/cm^3)				Standard drug
	L1	L2	L3	L4	Ampiclox
Bacillus subtilis	24	NA	NA	18	31
Escherichia coli	NA	19	18	21	36
Klebsiella pneumonia	20	18	23	17	31
Salmonella typhi	21	17	NA	21	29
Staphyloccus aureus	18	NA	NA	17	36
Shigella dysentriae	19	22	20	20	34
Streptococcus pyogenes	NA	18	NA	NA	26

NA=No activity

Table 5: Minimum Inhibitory Concentration (MIC) and Minimum Bactericidal Concentration (MBC) of Ethanol Leaf (L) Fractions of *E.gilletii*

(Concentration 200 mg/cm^3)	
MIC	MBC

Test Organisms	L1	L2	L3	L4	L1	L2	L3	L4	Ampiclox
Bacillus subtilis	25	NA	NA	100	50	NA	NA	100	40
Escherichia coli	NA	100	100	50	NA	100	100	50	40
Klebsiella pneumoniea	50	100	50	100	100	100	50	100	40
Salmonella typhi	50	100	NA	50	100	100	NA	50	40
Staphyloccus aureus	100	NA	NA	100	100	NA	NA	100	40
Shigella dysentriae	100	50	50	50	100	50	100	50	40
Streptococcus pyogenes	NA	100	50	NA	NA	100	50	NA	40

NA= No activity

The quantitative phytochemical screening revealed the presence of alkaloids, flavonoids, phenolic compound, saponins and tannins (3.97±0.00, 3.548±0.33, 0.419±0.89, 12.712±1.32, and 18.857±0.19 mg/g, respectively) (Table 1).

Qualitative phytochemical screening of the crude leaf extract and fractions also revealed the presence of alkaloids, flavonoids, phlobatannins, reducing sugar, saponins, Tannin and terpenes (Table 2). Fractions L1- L4 also contains flavonoids, phlobatannins, reducing sugar, saponins and Tannin. Afolayan *et al.*, 2014 reported the presence of similar phytochemicals in hexane, ethyl acetate and ethanol extract of *E. gilletii*. The used of chromogenic reagents ($FeCl_3$) revealed the presence of Phenolic compounds (Plate 1).

Antibacterial susceptibility test of crude ethanol leaf (L) extract of *E. gelletii* against *B. subtilis, S. aureus, S. pyogenes, E. coli, K. pneumonaie, S. dysentriea* and *S. typhi* at 40, 80, 120 and 160 mg/cm^3 revealed a broad spectrum of activity in dose dependent manner. The zone of inhibition ranged from 16 to 29 mm in the leaf extract which is significantly different from the

standard antibiotics (Ampiclox) at 40 mg/cm^3. *S. pyogenes* and *S. dysentriea* were resistant against the leaf extract (Table 3.).

The Minimum Inhibitory Concentration (MIC) and Minimum Bactericidal Concentration (MBC) which is the minimum concentration required inhibiting the growth of the microorganism or completely kill the microorganism respectively were also recorded. *S. typhi* have the lowest MIC and MBC (40 and 80 mg/cm^3 respectively), *S. aureus* and *E. coli* have an MIC of 80 mg/cm^3 and an MBC of 120 mg/cm^3 while *B. subtilis* and *K. pneumoniae* have the highest MIC and MBC (120 mg/cm^3 each) in the leaf extract.

Antibacterial susceptibility test of fractions have a wider zone of inhibition in all the test bacteria isolates at 200 mg/cm^3 than the crude extract with zone of inhibition ranging from 18 to 24 mm in fraction 1 to 4 of the leaf. *S. pyogenes* and *E. coli* were resistant against fraction L1; *B. subtilis* and *S. aureus* against fraction L2, L3; *S. typhi* against fraction L3 (Table 4). MIC and MBC of the fractions were also lowered when compared with the crude leaf extract. The MIC ranged from 25 to 100 mg/cm^3 while the MBC ranged from 50 to 100 in all the susceptible organisms (Table 5).

The curative properties of plants are due to the presence of various phytochemical constituents such as alkaloids, flavonoids, phenolic compounds, saponins, steroidal compounds, tannins and terpenoidal compounds (Kumar *et al.*, 2013). These phytochemicals are known to have *in vitro* antimicrobial/antibacterial activity (Mann *et al.*, 2008; Doughari *et al.*, 2010; Ahmad and Wudil, 2013; Adesina *et al.*, 2013).

2013). Therefore, the presence of this phytochemicals in the crude and fractions of the extract may have contributed the observed spectrum of activity.

Conclusion

The studies revealed that the pathogens used in this study were susceptible to both the leaf and the stem of *E. Gilletii*, thus suggesting the usefulness of this plant as pharmaceutically active

agent in drug formulation in the treatment of numerous diseases. The fractions of the extracts obtained from this plant could provide a basis for the isolation of active compounds of broad spectrum antimicrobials.

REFERENCES

Abbott, R. (2014). Documenting Traditional Knowledge. *World Intelectual Property Organization*, pp 1-10.

Adesina, S. K., Idowu, O., Ogundaini, A. O., Oladimeji, H., Olugbade, T. A., Onawunmi, G. O. & Pais, M. (2013). Antimicrobial Constituents of Leaves of *Eacalypha wilkesiana* and *Acalypha hispida*. *Journal of Phytotheraphy Research*, 14, 371-374.

Afolayan, M., Salisu, A., Adebiyi, A., Idowu, D. & Fagbohun, A. (2014). In-vitro Antioxidant, Antimicrobial and Phytochemical Properties of Wild Banana (*Ensete gilletii*) (E. A. J. De Wildman) seed Extracts. *International Journal of Advanced Chemistry*, 2 (2), 59-61.

Ahmad, J. M. & Wudil, A. M. (2013). Phytochemical Screening and Toxicological Studies of Aqueous Stem Extracts of *Anogenesis leiocarpus* in Rats. *Asian Journal of Scientific Research*, 5 (4), 781-788.

Association of Official Analytical Chemistry (AOAC) (2010). Official Methods of Analysis. 19th Edition. *Association of Official Analytical Chemists, Washington DC*.

Daniels, O. & Malomo, O. (2014). Preliminary Studies on the Antimicrobial Effects and Phytochemical Studies of Some Nigerian Medicinal Plants on Some Human Pathogens. *International Journal of Current Microbiology and Applied Sciences*, 3 (3), 910-923.

Doughari, J. H. (2010). Phytochemoicals: Extractions, Basic Structures and Mode of Action as Potential Chemotherapeutic Agent. *Journal of Pharmaceutical Research*, 5 (3), 1-33.

Harbone, J. B. (1998). *Phytochemical Methods*: *A Guide to Modern Techniques of Plant Analysis*, (3rd ed., pp. 1-32). London: Chapman and Hall, Ltd.

Kumar, V. S. & Navaratnam, V. (2013). Neem (Azadirachta indica): Prehistory to Contemporary Medicinal Uses to Human Kind. *Asian Pacific Journal of Tropical Biomedicines*, 3 (7), 505-514.

Mann, A., Yahaya, Y., Banso, A. and John, F. (2008). Phytochemical and Antimicrobial Activity of *Terminalia avicennioides* Extracts Against Some Bacteria Pathogens Associated with Patients Suffering from Complicated Respiratory Tract Diseases. *Journal of Medicinal Plants Research,* 2 (5), 094 – 097.

Scott, J. A. (2013). *Ensete Livingstonianum*, International Union for Conservation and Natural Resources (IUCN). Red List of Threatened Species, *http://dx.doi.org/10.2305/IUCN.uk.*

Sethiya, N., Brahmbhat, K., Chauhan, B. & Mishra, S. H. (2016). Pharmacognostic and Phytochemical Investigation of the Seeds and Pseudostem of *Ensete* superbum (Roxb.) Cheesman. *Journal of Natural Products and Resources*, 7 (1), 51-58.

Sofora, A. (1993). *Medicinal Plants and Traditional Medicine in Africa*. NY: John Wiley and Sons. pp 102.

Tee, L. H., Ramanan, R. N., Tey, B. T., Chan, E. S. & Azrina, A. (2015). Phytochemicals and Antioxidant Capacities from *Dacryode srostrata* Fruits. *Journal of Medicinal Chemistry*, 5, 23-27.

Tesfaye, A., Guaide, A. & Melese, M. (2016). Phytochemistry, Pharmacology and Nutraceutical Potential of *Enset* (*Ensete Ventricosum*). *International Journal of Emerging Technology and Advanced Engineering*, 6 (10), 2250-2459.

Trease, G. E. & Evans, W. C. (2002). *Pharmacognosy*. (15th ed.). *Saunder Publisher, London*, pp. 214-393.

World Health Organization (WHO) (2014). Antimicrobial Resistance: Global Report Surveillance. *World Health Organization*, 20 Appia Avenue, Geneva, Switzerland, pp 1-29.

Sustainable Energy Production, Science and Technology Development in Nigeria: the Role of Chemistry Education.

YAKUBU, Abdullahi Adinoyi
Department of Science Education,
School of Science and Technology Education,
Federal University of Technology, Minna Niger State.
E-mail: abdullahiyakub74@yahoo.com Phone No: 07065699399
ABDULKADIR, Suleiman Alabi
Department of Chemistry,
School of Secondary Education (Sciences), Kwara State College of Education,Oro.
E-mail: suleimanabdul1999@gmail.com Phone No: 08037515086
YERIMA, Habiba
Department of Chemistry,
School of Secondary Education (Sciences), Niger State College of Education, Minna.
E-mail: yerima2012@gmail.com Phone No: 07032130516
&

AHMAD Isma'il
Department of Chemistry,
School of Secondary Education (Sciences), Federal College of Education, Zaria.
E-mail: ahmadismaila835@gmail.com Phone No: 08066029333

Abstract

The significant gap between demand and supply of Energy has led to recurrent power shortcuts in Nigeria, resulting to persistent problem in sustainable energy production which further affects the rate of Science and Technology Development in the country. This Paper sought to assess The Role of Chemistry Education in sustainable Energy Production, Science and Technology Development in Nigeria. The Paper further established the Relationship between Energy Production, Science and Technology Development in Nigeria. Literatures on the state of Energy Production, Science and Technology Development Plans, Challenges, Impacts of Politics and Economy on Science and Technology Development in Nigeria were reviewed, respectively. Heavy reliance on oil, Lack of adequate quality and quantity of chemistry delivery to the needs of Nigerians and Nigeria, ineffective government agencies to supervise the rate of science and Technology Development in Nigeria, were identified as some of the challenges facing sustainable energy production, Science and Technology Development in Nigeria. The Role of Chemistry Education identified includes but not limited to: Review of Chemistry Curriculum, where chemistry is delivered as not only a body of knowledge but also a veritable instrument for self – reliance, growth and development in the country. The Paper recommended among others, the establishment of Programs such as Solar Energy Education Program (SEEP),Biotechnology Energy Production Program (BEPP) and Nuclear Energy Education Program (NEEP), which will be headed by the Ministry of education, Power and steel in collaboration with Research institutes to Develop, Implement and Evaluate Chemistry curriculum and Delivery in all schools Nationwide.

Keywords: Sustainable Energy Production, Science and Technology Development, Chemistry Education,

Introduction

On a Separate Research conducted by the Economic Community of West African Countries (ECOWAS) and World Bank in Aliyu, et al, (2018) revealed that Nigeria has the largest economy in Sub - Saharan Africa, but a limitation in the power sector declines its rate of growth and development. This implies that, sustainable energy production has a great influence in improving growth and development through Science and Technology. Nigeria is endowed with large oil, gas, hydro and solar resources having potentials to generate 12,522 Megawatts (MW) of electric power from existing plants, but unfortunate enough was only able to generate around 4,000MW at the end of 2016, which is insufficient for consumption (Daramola, 2015 & Ojo, 2016). These have However, affected investment, industrialization, science and technology development and other sectors of the Economy. Various stake holders, pressure group, Unions and other agencies protested on the state of energy production in Nigeria as the then Federal Government under the leadership of the then President Good luck Ebele Jonathan had no choice than to privatize its distribution companies which gave rise to a wide range of tariff thereby affecting other sectors of the economy and standard of living among Nigerians (Sadiq, 2017). Stake holders have no choice than to seek for possible solutions to sustainable energy, Science and Technology development in Nigeria.

Various Research findings (John, 2014; Adeoye, 2016 & Azare, 2017) have revealed that the nature of Science is systematic in approach and tentative in content, which implies that science have a defined process and product skills in arriving at a specific conclusion. Tentative nature of sciences makes sciences to have applications in the Physical Sciences such as Physics, Chemistry, Geography, Biology, Geology, Mathematics and other professions of human endeavor such as Medicine, Education, Petrochemicals, Brewery industries, Engineering, and Pharmacy. The knowledge or product of sciences can only be meaningful when it finds application to the benefit of an individual and his entire community, this application is called Technology (Adeoye, 2016), These revealed that Technology is a product of science which is also dynamic in Nature, as all things been equal no society or nation develops technologically above its quality of science delivery, so for any nation that aspires to be great must pay great attention to the quality of its science and Technology development (John, 2014 & Jimoh, 2015). Moreover, a society having scientifically literate or enlightened individuals through Chemistry education, solemnly, do have a higher chance to develop progressively in the area of sustainable Energy production, Science and Technology development, which will yield significant result when Chemistry curriculum reflects the needs of the ever changing society (Anne, 2017).

Chemistry Education is a veritable instrument for the growth, development, survival and emancipation of the human race thus, needs to be given good quality attention (Mogbo, 2014 & Anne, 2017).The importance of chemistry education in the development of any nation cannot be underrated especially in Nigeria where the National income rests on Petroleum and Petrochemical industries. Moreover, the Federal government of Nigeria seems to have realized the importance of chemistry education as an important key for development by stating in its national policy on education that the goals of science education shall be to inculcate inquiry knowledge and rational mind for the conduct of a good life and democracy through science and Technology (FRN, 2007).

The broad aim of Chemistry Education relates both to individuals and to society in general (Anne, 2017). At the level of the individual it aims to prepare students to realize their full potentials, function and participate responsibly in society as good citizens, agile workers, enlightened consumers and family members having interest of the society at heart in the area of science and technology development (Adeoye, 2016 & Azare, 2017). Thus, the ultimate aims of Chemistry Education in every society is to provide people with knowledge of scientific concepts needed for the fulfillment of the socio – economic and cultural needs of the society among others includes, the Mining industries, Medicals, automobiles, Petrol and Petrochemical industries, Textile industries, cement and glass industries and Brewery industries (Bichi, 2015 & Balogun, 2016).

The Proceeds from the work of the Scientists and Technologists are used up by the society. However the Society itself is not stagnant, it is dynamic in Nature as Nigeria being a developing nation cannot be an exception. However, for any nation to be developed it must be able to meet the needs of the changing society in the area of science and Technology through effective science delivery (Mogbo, 2014 & Anne, 2017). Therefore, this study intends to assess Sustainable Energy, science and Technology Development in Nigeria: The role of Chemistry Education.

State of Energy Production in Nigeria

The extent of energy production in the country needs to be evaluated base on the rate of demand and supply. According to the International Energy Agency (IEA) in (Wakili, 2017), the total Nigerian primary energy supply was 118,325 Kilotonnes of oil equivalent (Ktoe) excluding electricity trade, in 2016 Biomass and waste dominated with 82.2%, renewable sources only accounted for a small share of the energy supply that is, hydropower only accounted for 0.4%

wind and solar are also utilized but at an insignificant level. At present, Biomass is the dominant energy source for cooking and heating purposes in our households. According to the Global Initiatives on Accessible, Clean and Efficient Energy (GIACEE), Sustainable for all (SE4ALL) in (Sadiq, 2015 & Aliyu, et al, 2018) revealed that little progress has been made with regards to providing access to non – solid cooking fuels since 1990 as only 26% of the population had access to non – solid cooking fuel in 2010 with a big difference between urban and rural area. Electricity having a share of 2% in the total final energy consumption, electricity remains a marginal source of energy in Nigeria as it only represents 9% of the households total energy consumption (Ojo, 2016). Electricity consumption from residential and commercial sectors represented 80% of the total electricity demand; the rest was covered by the industries, street lightening and special tariff sectors (Wakili, 2017). The share of large consumers such as industry and large commercial areas only represented 15 of the total electricity consumption. As a result of high economic growth and demographic pressure, in 2008, the energy commission of Nigeria (ECN) together with the International Atomic Energy Agency (IAEA) projected a demand of 15,730MW for 2010 and 119,200MW for 2030 under the reference scenario (7%) yearly economic growth (Sadiq, 2015 & Aliyu, et al, 2018). Other actors like the defunct Power Holding Company of Nigeria (PHCN) or world Alliance for Decentralized Energy (WADE) have also developed scenario though, the results of these studies varies widely but they all conclude that the current gap between supply and demand is already very substantial and that it will become more entrenched under a business as usual scenario.

During the administration of president Umaru musa Yar'adua, vision 20 – 20:20 was designed to ensure Nigeria becomes one of the top 20 economies of the world by 2020 (Ayomide, 2015), it emphasizes the importance of the development of energy infrastructure as a means to attain the final objective as the target of 40,000MW by 2020 was mentioned in the document. As part of the sustainable energy for All (SE4ALL) initiatives (Sadiq, 2015 & Aliyu, et al, 2018), the Federal Ministry of Power (FMP) jointly with the Economic Community of West Africa States (ECOWAS) centre for renewable Energy and Energy Efficiency (ECREEE) and the Nigerian Energy Support Program (NESP) are on the process of elaborating National Renewable Energy and Energy Efficiency Action Plans (Ojo, 2016 & Wakili, 2017).

Science and Technology Development Plan in Nigeria

Research findings (John, 2014; Jimoh, 2015 & Adeoye, 2017) have revealed that the level of Science and Technological development of any society or country lies on the strength of its economic base. Immediately after Independence in 1960, the Federal government of Nigeria

seems to have realized the significance of showing more interest in its economic base, thereby mapped out a development plan on Science and Technology development through its National Economic Council (NEC) (Lewis, 2017). The NEC outlined its development plan from 1962 – 1985 which spread across four stages.

The first National Development plan started in 1962 – 1968 though the plan aim at a target saving of about fifteen percent of the gross Domestic Product (GDP) by 1985, which was an annual investment of 15% of the GDP during the period, the highest priority were accorded to Agriculture accounting for about 65% of the GDP. However, Mining was the fastest growing sector of the economy as various projects completed during the first development plan includes the Oil Refinery, Niger dam, Sugar Mill, Paper Mill. Though, the plan had a major setback as a result of the civil war which lasted from 1967 – 1970. However, the plan was judged to be successful in the field of insurance through the establishment of Nigerian insurance Company, Lagos Stock exchange and various chambers of commerce.

The second National Development Plan lasted from 1970 – 1974. The highest National priority was accorded to Agriculture, Industry, Transportation and Man power development while at the second order of priority were accorded to social services and utilities such as electricity, communication and water supplies while in the field of education the goal was restoration of facilities and services damaged or disrupted by the civil war, development, expansion, improve quality and quantity of teachers all over the country.

The third National plan lasted from 1975 – 1980 the major objective of the plan includes but not limited to diversification of the economy through the implementation of a wide range of building materials, agro allied, petrochemicals and other industrial projects due to the importance given to Oil sector government revenue increased. This gave rise to more foreign exchange for the country. Large program of expansion of secondary, technical and university were included and aimed at overcoming the shortage of high level manpower.

The fourth National Development Plan lasted from 1981 1985 the main goal of the plan among others includes strengthening of the economic infrastructure particularly power, water supply, telecommunication, land transportation with emphasis on the railways, housing and health, efforts were also made to diversify the economy away from the overdependence on oil by laying emphasis on export potentials of existing industries such as textile, tyres, coal, pulp and paper industries, traditional crops such as cocoa, groundnut palm produce and rubber were actively exploited, in the area of education more primary, secondary, pre – vocational, and

technical schools were established, training and retraining of teachers in technical colleges and vocational training schools for the training of craftsmen, artisan and technicians.

Impacts of Politics and Economy on Science and Technology Development in Nigeria

Immediately after the era of Nigerian Economic Development plan which was pioneered by the National Economic Council (NEC) in 1984, Nigeria had witnessed a lot of political reformations and economic changes as result of change in political mantra from 1984 to 2019, which further influenced the level of Science and Technology Development to date.
During General Ibrahim Badamosi Babangida's administration, various agencies and programs were initiated among which includes the Federal Environmental Protection Agency in 1985, Jibia water treatment plant and Challawa Cenga Dam Kano in (1992), Oil Mineral producing Area Development Commission were constituted as share of oil royalties raise to state of origin from 1.5% to 3% (Lewis, 2017), creation of economic policies through Structural Adjustment Programs (SAP) in 1986 its policies among others includes but not limited to Privatization of public enterprise, deregulation of the agricultural sector and relaxation of foreign investments (Ajakaiye, 2013). Moreover, in 1986 – 1988 these policies were executed and the Nigerian economy actually grow with some shortcomings which made the government return to an inflationary economic policy and partially reversed the deregulatory initiatives following mounting political pressure and economic growth slowed correspondingly as capital flight resumes apace under the influence negative real interest rate (Ajakaiye, 2013).

During the reign of General Sani Abacha the Petroleum Trust Fund (PTDF) was established and inaugurated on March 25th 1995 under the chairmanship of General Muhammadu Buhari, (Morris, 2012) the Fund was formed to undertake major economic issues which Nigeria was suffering, major development plan were in road construction, provision of Drugs, restructuring of major insurance companies that supports the Small and medium Scale enterprises across the country (Lewis, 2017). The Policy of privatization halt privatization program of the previous administration which reduced inflation rate of 54% inherited from the previous administration to 8.5% between 1993 – 1998, while oil was at an average of $15 per barrel as Abacha's administration became the first to record unprecedented economic achievement which over saw an increase in the country's foreign exchange reserve from $ 494 Million to $ 9.6 Billion by the middle of 1997, he further reduced the external debt from N36 Billion to N27 Billion in 1997 (Willian, 2014).

On 29th May, 1999 when Nigerian political track drifted from Military to Democracy, Chief Olusegun Obasanjo's administration also brought in various programs and policies among which includes the creation of Niger delta Development Commission, Resuscitated the National Fertilizer Company in Kaduna and Onne, Port Harcourt, Independent Corrupt Practices Commission (ICPC), Economic and Financial Crime Commission and his administration also increased the share of oil royalties and rent to the state of origin from 3% to 13% (Encyclopaedia Britannica). The economic growth and debt payment before his administration revealed that the Gross domestic Product (GDP) growth had been painfully slow since 1987 and only managed to increase to 3% between 1999 – 2000. However, the growth rate doubled to 6% before 2007 (Lewis, 2017). The Nigerian foreign reserve rose from $2 billion in 1999 to $43 billion in 2007 and the naira exchange rate to the US dollar and other major currencies during this period was highly regulated and artificially high (Morris, 2012).

In 2007, During Umaru Musa Yar'adua administration pointed out seven point agenda among which includes critical infrastructural development in power and transportation, wealth creation through diversification of the economy and focus on development issues in the Niger Delta as solutions to the current developmental challenges facing country, but by 2010 the country was struggling to realize to realize many of the stated goals as the power sector was not adequately funded, infrastructural deficit was not closed down and the troublesome process of reforming land use regulation hampered a reform of the land use law (Lewis, 2017).

During President Goodluck Jonathan's administration a road map for power sector reform was launched on 2 August, 2010. In a study conducted by the World Bank in (Sadiq, 2015) revealed that lack of access to financing and electricity were cited as Nigerian main obstacles to Development surpassing corruption. The government then oversees privatization of the sector to enhance efficient and reliable power infrastructure to Nigerians (Fashina, 2017). A Canadian consultancy firm which specializes on transportation and energy infrastructure projects was contracted to serve as transaction adviser for the handover of state electricity assets. On 13 December, 2011 the 2012 fiscal year's budget removed any provision for the existing fuel subsidy though about 80% of Nigerians opposed the plan to remove the fuel subsidy (ACE – Nig). Prof. Tam David – West former petroleum minister expressed concern that the planned removal of the fuel subsidy will squeeze the economy, increase inflation and hurt both businesses and public while other view the action as ill – timed (Atanda, 2010).

During President Muhammadu Buhari administration 2015 – 2018, Nigeria suffered a decline in commodity prices which triggered an economic recession (Akinrinade, 2016), naira

depreciated in the black market leading to a gulf between the official exchange rate and the black market rate, a resulting shortage in foreign exchange hit various businesses including petroleum marketers (Fashina,2017). In May, 2016 the government announced a rise in the official pump price of petroleum to curtail shortfall in the commodity as a result of foreign exchange shortages (Odanyeo, 2017). In 2016, the country's economy decline by 1.6 % and in 2017 per capital economic growth is projected to be negligible (Fashina, 2017). Though the administration has not shown dedicated efforts to diversify sources of government spending as the 2018 budget signaled an expansionary fiscal policy with funds dedicated to infrastructural projects such as strategic roads, bridges and power plants (Aliyu, et al 2018). In Niger Delta despite the amnesty program to ameliorate the conditions of the Peoples lives and settle militant activities, there are still intermittent attacks on oil facilities by groups such as the Niger Delta Avengers, this has significantly affected oil production leading to cuts in exports and government revenue as the avengers are waging conflict for greater economy and political autonomy (Adarmola, 2015).

Challenges to Sustainable Energy Production, Science and Technology Development in Nigeria

The significant gap between demand and supply of electricity has led to recurrent power shortcuts, thus the heavy reliance on gas, limited technical / technological know – how, lack of energy efficiency practices and infrastructure maintenance, inadequate regulations and attack on energy infrastructure, contributes to the challenges facing sustainable energy production in Nigeria.

In the area of Science and Technology Development, despite the huge government revenue and reliance on oil sector, diversification of the economy becomes necessary since oil revenue alone cannot meet up with the needs of the ever changing and developing country like Nigeria, especially in the area of Science and Technology Development. These reasons been that government have shown little or no significant impact to provide facilities, materials to influence effective learning of Sciences (Chemistry) using Science Technology and Education (STE) models, lack of adequate training and retraining of workers, lack of adequate technical/ technological know – how and inadequate government agencies to supervise the rate of science and technological development in the country and proffer solutions to relevant authorities immediately. Therefore, this study will tend to evaluate the role of chemistry education in ensuring sustainable energy, Science and technology Development throughout the country.

The teaching of chemistry being the foundation and backbone of sciences at secondary school levels have not being encouraging over the years, these makes most chemistry students not to identify their divine potentials in terms of being creative and productive, which would have helped them to be self reliant and useful to themselves and the society, but rather subject their potentials to the streets by involving in social vices such as Destruction and Theft of oil pipelines, Power plants, Drug addiction, Kidnapping thereby becoming a threat to the government which further impedes development in the country.

The Role of Chemistry Education for Sustainable Energy, Science and Technology Development in Nigeria

The need for chemistry curriculum changes by incorporating Science and Technology is evident in the perception by science educationists, Government and other stake holders that chemistry education have not in the past been relevant to the needs of the broad cross – section of students and the society (Adeoye, 2016). Various research findings have attributed this to the quality and quantity of chemistry delivery in the area of changing the existing chemistry curriculum to meet the demand of the society as the chemistry teaching methods should be student centered and not teacher centered where the students should be allowed to explore their environment and take responsibility for their learning with little guide by a facilitator (John, 2014: Jimoh, 2015 & Adeoye, 2016).

It is now being argued that a chemistry curriculum that is more personally and socially relevant would be more appropriate for secondary students, especially those who will be future consumers of chemistry rather than the future producers in the area of energy production (Akinrinade, 2016; Wakili, 2017 & Azare, 2017). Therefore, if Chemistry is presented as a human endeavor which develops through the efforts of people and which affects the lives of people through improved standard of living, then we can vividly accept the relevance of chemistry education in the society. For instance, in Energy production the major goals should be to teach basic principles and concepts relating to heat, light and other forms of energy, study technological changes, adaptations and examine mankind's need for utilization of energy. Sustainable energy can be produced through chemistry education among which includes Biotechnology Energy, Nuclear Energy, Solar Energy and Hydroelectric Power.

Biotechnology is being used to produce energy based on naturally produced organic materials such as maize, cassava, though there are places in the world where industrial plants convert sugar from cane into ethanol which can be used to fuel cars. In North America cereals such as

Maize, Wheat, Barley are fermented to produce a variety of products including fuel (Ojo, 2016). However, alcohol is potentially a cleaner source of energy than fossils because it is sulphur free. Therefore, During Chemistry learning all the necessary instructional and improvised materials should be made available to the students whom will work as a team find out how energy can be produced from Maize, Cassava or sugar cane. If this method reflects in the chemistry curriculum throughout the nation may mean that every Nigerian chemistry students will know how to produce energy from Maize or Cassava which will further improve science and Technology development in the country.

The Nuclear Energy is the bedrock of nuclear technology, primarily responsible for production of power (electricity) (Aliyu, et al, 2018). Today however, Man has produced and still producing lots of destructive arms and ammunitions example includes Atomic bomb, Hydrogen Bomb, missiles of all forms. Nuclear Chemistry is a concept taught in most secondary schools in Nigeria, these explains how energy can be radiated or produced from the nucleus of an atom, this can be taught effectively using a curriculum that outline modules of activities which students will use to explore and take control of their learning with little guide by a facilitator to identify how nuclear energy is produced from an atom, These will further improve science and Technology Development in the country.

Water as a Chemistry concept can be outlined in the Curriculum on the principles of Damming and Electrolysis on techniques and principles of power generation from water using improvised material as outlined in the curriculum. These will improve Chemistry students' potentials on Hydro Electric Power (HEP) generation nationwide, thereby aids Energy Production potentials among enlightened chemists, science and technology development nationwide.

Recommendations

i. Government and other stake holders should accept the fact that chemistry Education is a vital tool for sustainable energy production, science and technology development in Nigeria, by providing all the necessary materials for effective learning outcome.
ii. Government, international agencies and other stake holders should assist in funding Chemistry Education Projects.
iii. Government should establish programs and institutions which should include but not limited to Solar Energy Education Project (SEEP), Nuclear Energy Education Program (NEEP), Biotechnology Energy Production Program (BEPP), Science Process Skills Program (SPSP) and Chemistry Entrepreneurship Skill Acquisition Program (CESAP)

headed by the Ministry of Education in collaboration with Ministry Science and Technology, Ministry of Power Through Research Institute such as Energy Research Institute of Nigeria (ERIN) or Institute of Science and Technology Development of Nigeria (ISTDN) which should be saddled with the responsibility of developing, implanting, supervising and evaluating a new chemistry curriculum Nationwide.

iv. International organization such as United Nations International Children Emergency Fund (UNICEF), World Health Organization (WHO) and other stake holders should assist the government in funding the program.

v. Effective and Regular Training and Retraining of workers at all levels**.**

vi. Most of the programs should be extended to higher institution of learning nation wide

vii. Improved incentives for Science Teachers on the basis of professional development index, so as to encourage continuous research among chemistry Teachers.

viii. Free Education and scholarship should be given to students in the area of science and Technology to increase students enrollment especially Females in Northern Nigeria.

ix. Government and other agencies should organize frequent and regular Seminars, Conferences and workshops among stake holders Nationwide.

x. Government Policies and Programs should be reviewed from time to time in favor of Energy Production, Science and Technology Development in not only Secondary Schools but also higher institutions of learning.

xi. Curriculum change should not only be limited to Chemistry but also Physics and other science related subjects.

References

Adaramola, M. S (2015). "On wind Speed Pattern and Energy Potential in Nigeria" Energy Policy 39 (5), 2501 – 2506.

Adegbese, M. U (2015). Ibrahim Badamosi Babangida: The Military, Power and Politics. *Adonis & Abbey. Publisher, PP, 19 - 40.*

Adeoye, M . I (2016). Science and Technology for National Development. The effects of students interaction pattern on cognitive achievement in Chemistry. Perspectives on crucial issues on Nigeria and African Education. *Publication of Institute of Education, University of Nigeria, Nsukka 1.1 – 6.*

Ajakaiye, O. N (2013), The Structural Adjustment Program and changes in the structure of Production in Nigeria, NCEMA Monograph series No, 20.

Akinrinade, S. P (2016). "Nigeria's Economy – Weighing the Balance" Africa Today, November/ December.

Aliyu, G. N; Abubakar, H. A; Rufai, A. Y & Tukura, T. S (2018). " A review of Renewable Energy Development in Africa: A Focus in South Africa, Egypt and Nigeria" *Renewable and Sustainable Energy Reviews 81:* 2502 – 2518.

Anne, O. S (2017). Enhancing Science Education through Professional Development of Science Teachers on inquiry – based teaching strategy in a dwindling Economy, *A paper presented at the 5th School of Science and Technology Education Futminna international conference oct, 3 – 6, pp, 120 – 128.*

Ariyo, K. A. (2016) Effect of concepts maps on senior secondary students' retention in electrolysis concepts. *Perspective on crucial issues on Nigerian and African education (1) 112 – 127.*

Atanda, O. G (2010). Nigeria Since Independence: The first twenty five years Vol 29 – Science and Technology, Ibadan Heinemann Educational Books.

Ayomide, E. O (2015). Nigerian Government and Education since 1990s, Longman Publishing company, Lagos.

Azare, G. D (2017). The Problems Hindering the effective Management of Education in Nigeria. *A paper presented at the annual national conference of education planners and Managers at Ahmadu Bello University, Zaria. May 3rd – 10th*

Balogun, T. O (2016). Interest in Science and Technology education in Nigeria. *Journal of the Science Teachers Association of Nigeria (STAN) 43, (1 & 2), 92 – 99.*

Baruwa, Y (2014). Intellectuals, Economics, Reforms and Social changes constraints and Opportunities in the Nigerian Technocracy, Dakar, CODESRIA.

Bichi, T. A (2015). Science, Society and Science Teaching Effectiveness in Nigeria. *Journal of Science Teachers Association of Nigeria (STAN), (45) 14 – 20.*

Fashina, O. J (2017). " Economic Crises, Social Unrest and the Academia" in Ogunye, I. et al (eds), Citadels of Violence, Lagos, Committee on the Defence of Human Rights (CDHR) Lagos, pp 100 – 144.

Federal Republic of Nigeria (2004 – 2014). National Policy on Education, Lagos: *NERDC press National Policy on education (5th Edition) NERDC Publishers.*

First National Development Plan 1962 – 1968, Federal Ministry of Economic, Development and Reconstructions, Lagos.

Fourth National Development Plan 1981 – 1985, Federal Ministry of Economic, Development and Reconstructions, Lagos.

Jimoh, O. J (2015) Integrated science in Nigeria. A view of the problems and prospects *led paper I 45th annual conference proceedings of Science Teachers Association of Nigeria (STAN), 209 – 219.*

John, P. O (2014). Problems and prospects of science and technology education in Nigeria. *Journal of the science Teachers of Nigeria 49 (1 & 2) 92 – 99.*

Lewis, H. M (2017). Growing Apart: Oil, Politics and economic Change in Indonesia and Nigeria. *University of Michigan Press p. 178* ISBN 0-472-06980-2

Lewis, O. N (2017). " From Prebendalism to predation: The Political Economy of decline in Nigeria." *Journal of modern African Studies 34 (1). 79 – 103.*

Mogbo, W. (2014), Science and Technology for Sustainable Growth and Development, *Federal University of Technology, Minna, News letter 3(8).pp 20.* ISBN, 0795.1035.

Morris, J. I (2012). " Ideas & Trends: A Nigerian Miracle", The New York times. Retrieved 9. April 2012.

National Policy on education (NPE), (2014), *Federal Republic of Nigeria, Lagos: NERDC press (5th, Edition).*

Obotetukudo, S. H (2014). The Inaugural addresses and Ascension speeches of Nigerian elected and Non – elected Presidents and Prime Ministers from 1960 – 2010. University Press of America, P. 121.

Odanyeo, O. H (2017) A comprehensive History Textbook on Science and Technology.

Ojo, G. K (2016). "Prospects of Localism of Community Energy Projects in Nigeria" *Local Environment* 19 (8) 933 – 946.

Okeke U. M. O (2015). Science education in Nigerian schools since 1960, *A paper presented at the international conference on comparative education for Nigeria. University of Lagos, Lagos.*

Olusegun Obasanjo Encyclopedia Britannica 21 May, 2014 retrieved 23 February, 2015.

Sadiq, Z. I (2015). "Current Status and Future Prospects of Renewable Energy in Nigeria" *Renewable and Sustainable Energy Reviews* 48: 336 – 346.

Second National Development Plan 1970 – 1974, Federal Ministry of Economic, Development and Reconstructions, Lagos.

Third National Development Plan 1975 – 1980, Federal Ministry of Economic, Development and Reconstructions, Lagos.

Wakili, M. O (2017). " Nigeria: Mambilla Power Projects Gets $5.79bn for takeoff. *Daily Trust (Abuja).* Retrieved 2017 -11- 02.

Optimization of some Selected Parameters in the Deacetylation Process of Chitosan Extraction from African Giant Land Snail Shell (*Archachatinamarginata*) using Response Surface Method

Kunle Isaac[1*] and Abdulfatai Jimoh[2]

[1,2] Department of Chemical Engineering, Federal university of Technology, Minna,Nigeria

[1]Ohimahisaac@gmail.com, fatai2011@futminna.edu.ng,* Corresponding author

Abstract

Chitin is the second most abundant naturally occurring polymer found on the earth after cellulose, it's commonly found in the exoskeleton and shells of insects, mollusks, crustaceans and even in fungal cell walls. The partial N-deacetylation of chitin leads to the production of chitosan, which is an improvement on the poor physiochemical properties of chitin thereby ensuring that chitosan is far more advantageous in terms of application than chitin.

This study was undertaken to investigate the effect of some selected parameters on the deacetylation process of chitosan extraction from African giant land snail shell (*Archachatinamarginata*) using Response Surface Method. A chemical approach was utilized in the chitin and chitosan production. The chitin was extracted from the snail shell after deproteination and demineralization reactions were carried out while the chitosan was obtained after deacetylation of the chitin. The deacetylation stage was optimized using four input variables, viz. NaOH concentration, Chitin to Solvent ratio, Reaction temperature and Reaction time with the aid of Design expert version 7 response surface method, where the central composite design methodology was used to design the experiment. Thereafter the analysis of results and optimization of the extraction process was carried out using the same Design expert software. From the results obtained, it was discovered that the extraction process of chitosan from African giant land snail shell (*Archachatinamarginata*) gave a DA yield of67.9%at NaOH concentration, Chitin to Solvent ratio, Reaction temperature and Reaction time of40%, 1:13.50, 75^{o}C and 120 minutes respectively. A good correlation exists between the experimental chitosan yields and the predicted chitosan yields as was confirmed by validation experiment carried out and also by the square of the correlation coefficient of the developed model which was estimated to be 0.9293.

Keywords: African giant land snail shell, Central composite design, Chemical method, Chitosan yield, extraction, optimization, Response Surface Method.

1. Introduction

Chitinpolymer (poly (β-(1→4)-N-acetyl-D-glucosamine))is a natural polysaccharide, it is the second most abundant natural occurring polymeron the earth after cellulose(Islem, and Marguerite, 2015). This chitin polymer can easily be found in the skeletal or exoskeletal structure of lower animals (particularly crustacea, mollusks and insects), fungi (where it exists as the principle fibrillar polymer of the cell wall), yeast and green algae(Gbenebor,*et al.*, 2017).

However, chitin's poor solubility has placed a limitation in its applicationsince it is insoluble in most solvents(Shanta, *et al.*, 2015). The need to overcome this limitation has resulted in the birth of chitosan which is derived by the chemical modification of chitin (Islem, and Marguerite, 2015). Similarly, Islem, and Marguerite, (2015) reported that modified chitin (chitosan) is far more advantageous to use and opens new frontiers for its application.

The cationic, non-toxic, biodegradable and biocompatible polyelectrolytic nature of chitosan has made it one of the most widely distributed biopolymers (Enyeribe, *et al.*, 2017). These cationic properties of the chitosan imbue it with unique properties that can be exploited by biotechnologists; including applications in the fields of medicine, material science and crop science (Russell, 2013).

2. Literature Review

According to Russell, (2013)the steps leading to the extraction of chitosan include the deproteination and demineralization of the snail shell which would yield chitin after which the deacetylation of this chitin giveschitosan. However, several factors and process parameters play an important role in each the stages involved.

Mahmoud, *et al.*, (2007) and Wassila,*et al.*,(2013) reported that the biological approach or a chemical approach could be utilized in the chitin extraction phase althoughIslem, and Marguerite, (2015)reported that despite drawbacks associated in the use of the chemical approach it is still the most widely utilized method in chitin extraction. A typical chemical extraction of chitin involves the use of an acid reagent for the demineralization phase and an alkaline reagent for the deproteination stage. Howbeit, extensive research has placed emphasis on the use of HCl as the acidic reagent and NaOH as the alkaline reagent (Hongkulsup, *et al.*, 2016;Joshy, *et al.*, 2016). Other organic and inorganic acids such as HNO_3, H_2SO_4, CH_3COOH, HCOOH, and $C_6H_8O_7$have been used while successes in the use of other alkalines such as Na_2CO_3, $NaHCO_3$, K_2CO_3, $Ca(OH)_2$, Na_2S, $NaHSO_3$, and Na_3PO_4 has also been reported (Varun,*et al.*, 2017 2013; Islem, and Marguerite, 2015).

The demineralization (decalcification) stage can be carried out before the deproteination stage however as a rule of thumb it is preferable to carry out the deproteination stage first as this sequence helps to control foaming which is a by-product of the release of CO_2 in the demineralization stage (Joshy, *et al.*, 2016). The application of the biological method in chitin

extraction bypasses the need for individual deproteinization and demineralization steps since the processes occur simultaneously unlike the chemical method in which each step (deproteination and demineralization) occur separately (Shanta, *et al.,* 2015). Despite this advantage implementation of the biological approach to chitin extraction is still plagued by factors such as the longer reaction time and the excessive amount of residual protein that is generated as by-product(Hongkulsup, *et al.,* 2016).

Table 2.1: Comparison of chemical and biological methods in chitin recovery (Wassila, *et al.*, 2013)

		Chemical method	Biological method
			In-situ
Chitin Recovery	Demineralization	Mineral solubilization by acidic treatment using an acidic reagent such as HCl, HNO_3, H_2SO_4 CH_3COOH and HCOOH.	This is carried out by lactic acid produced by bacteria through the conversion of an added carbon source.
	Deproteination	Protein solubilization by alkaline treatment	This is carried out by proteases secreted into the fermentation medium or by adding exo-proteases or proteolytic bacteria

Chitosan (modified chitin) is formed by the deacetylation of chitin. This deacetylation is simply the removal of the acetyl groups from the molecular chain of chitin, leaving behind a compound (chitosan) with a high degree chemical reactive amino group (-NH2). An advantage in the use of chitosan over chitin is its solubility in most solvents thereby opening up new frontiers for its application (Shanta, *et al.*, 2015). However, no matter the method employed in the deacetylation of chitin (enzymaticor alkali deacetylation) the most important factor to consider is the molecular weight and the degree of deacetylation of the chitosan.

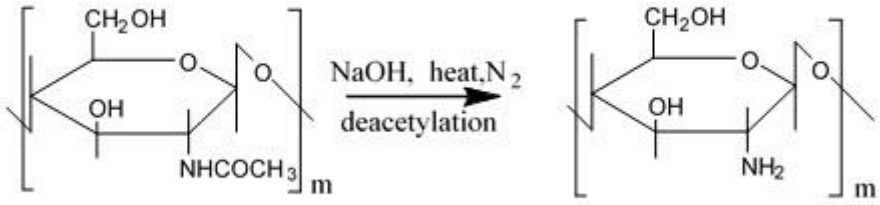

Figure 2.1 Chemical deacetylation of chitin using a Basic (alkaline) reagent (Shanta et al., 2015)

The alkali deacetylationis the most preferred form of chitin deacetylation. During the course of deacetylation, part of polymer N-acetyl links are broken with the formation of D-glucosamine units, which contains a free amine group thereby increasing the polymer's solubility in aqueous medium(Nisha, and Pandharipande, 2016). In other words,chitosan can be defined as a co-polymer of glucosamine and N-acetylglucosaminewhich is obtained by the removal of the acetyl groups in the chitin during whichthe acetamide groups (-NHCOCH3) of chitin are converted into amino groups (-NH2) leading to chitosan formation (Ameh, *et al.*, 2013; Nisha, and Pandharipande, 2016).

The use of an acidic reagent in place of an alkaline reagent in the chemical deacetylation of chitin would lead to the hydrolysis of the polysaccharide. As such only alkaline methods can be employedwith the added benefit that the use of alkaline deacetylationprocess is favourable industrially in that its low cost and ease of use makes it suitablefor the mass production of chitosan commercially (Shanta, *et al.*,2015; Islem, and Marguerite, 2015).

Majekodunmi, (2016)reported that enzymatic deacetylation occurs when chitin deacetylase catalyses the hydrolysis of N-acetamido bonds in chitin to produce chitosan. This enzymatic activity has been reported in several fungi and insect species. Common examples of such enzymes which have been extracted from fungi include Mucor rouxii, Absidiacoerulea, Aspergillus nidulans and two strains of Colletotrichum lindemuthianum.

A major difference between chitin and chitosan lies in the fact that chitin is not readily soluble in diluted acetic acid although it is soluble in highly toxic solvents such as lithium chloride and dimethylacetamide. In terms of deacetylation Nisha, and Pandharipande, (2016) reported thatchitin with a degree of deacetylation of 75% or above is known as chitosan.

2.1Properties of Chitosan

2.1.1Degree of Deacetylation (DD)

The degree of deacetylation determines the content of free amino groups (-NH2) in the polysaccharides and this can be used to differentiate between chitin and chitosan (Wassila, *et al.*, 2013). Ideally chitin with a degree of deacetylation of 75% or above is known as chitosan (Nisha, and Pandharipande, 2016).Gbenebor, *et al.*,(2017) reported that properties such as solubility, viscosity, ion-exchange capacity, flocculation ability, tensile strength, ability to chelate metal ions, immune adjuvant activity and reaction with amino group are all dependent on the degree of deacetylation with a higher the degree of deacetylation representing a higher the number of amino groups present(Majekodunmi, 2016).

2.1.2 pH value

According to Kaewboonruang, (2016) chitosan has a typical PH value that falls in the range of 6.0 to 7.5 as chitosan's with PH value within this range exhibit better physiochemical properties.

2.1.3 Colour

Generally, a white chitosan is desirable due to aesthetics. Howbeit, the chitosan's color does not affect its properties (Islem, and Marguerite, 2015).

2.1.4Solubility

Chitosan should have a solubility of above 50% in 1% acetic acid as its solubility in 1% acetic acid serves as a clear distinction between it and chitin (Shanta, *et al.*, 2015).

2.1.5Molecular Weight

According toMahmoud,*et al.*,(2007) and Thillai, *et al.*, (2017) the molecular weight of chitin is always greater than that of chitosan with the molecular weight of chitin usually been over a million Dalton's (>1 × 10^6DD) and that of chitosan been classified as low MW (< 50 kDa), medium MW (50 – 150 kDa) and high MW (> 150 kDa).

2.1.6 Viscosity

Hossain, and Iqbal, (2014) reported that the factors that affect the viscosity of chitosan include the degree of deacetylation, the molecular weight, pH, and temperature. They also reported that smaller particle sizes resulted in chitosan of higher viscosity and molecular weight with a higher molecular weight resulting in a higher viscosity.

2.2Importance of Chitosan

2.2.1 In Food Industry

The non-toxic nature of chitosan makes it applicable as a colouring agent, flavouring agent and dietary fiber in food (Shanta, *et al.*, 2015). it can also be applied to fresh food produce by coating or spraying in other to increase the shelf life of such food produce and it has been tested extensively on vegetables and fruits (Muxika*et al.*, 2017).

2.2.2 In Medical Industry

Chitosans attractive biological activities (antifungal, antibacterial, antitumor, immunoadjuvant, anticholesteremic agent) and bioadhesivity (especially of chitosan and its derivatives) makes it possible for them to be used as absorption promoters, for drug delivery in both implantable and injectable forms, hydrating agents, as well as for film production and wound healing (Islem, & Marguerite, 2015, Shanta, et al., 2015).

2.2.3 In Industry

Muxika et al., (2017) reported that an application of chitosan in industry is in 3D printing (also known as Additive Manufacturing) where chitosan is mixed with other biocompatible components such as gelatine and silica. Similarly, it can also be used in various industries as fillers in bio-polymer composite materials (Gbenebor, et al., 2017).

2.2.4 In Wastewater Treatment

In wastewater treatment chitosan act as chelating agent and heavy metals trapper where chitosanhas been effectively used in the removal of arsenic, dies such as orange 3 (DO3) and disperse blue 3 (DB3) and even select heavy metals such as $Cu^{2+}$from contaminated wastewater (Muxika*et al.*, 2017)

3. Methodology

3.1 Sample Preparation

The snail shells were scraped free of loose tissue, washed and dried. The product was thenpulverized into fine snail shells powder

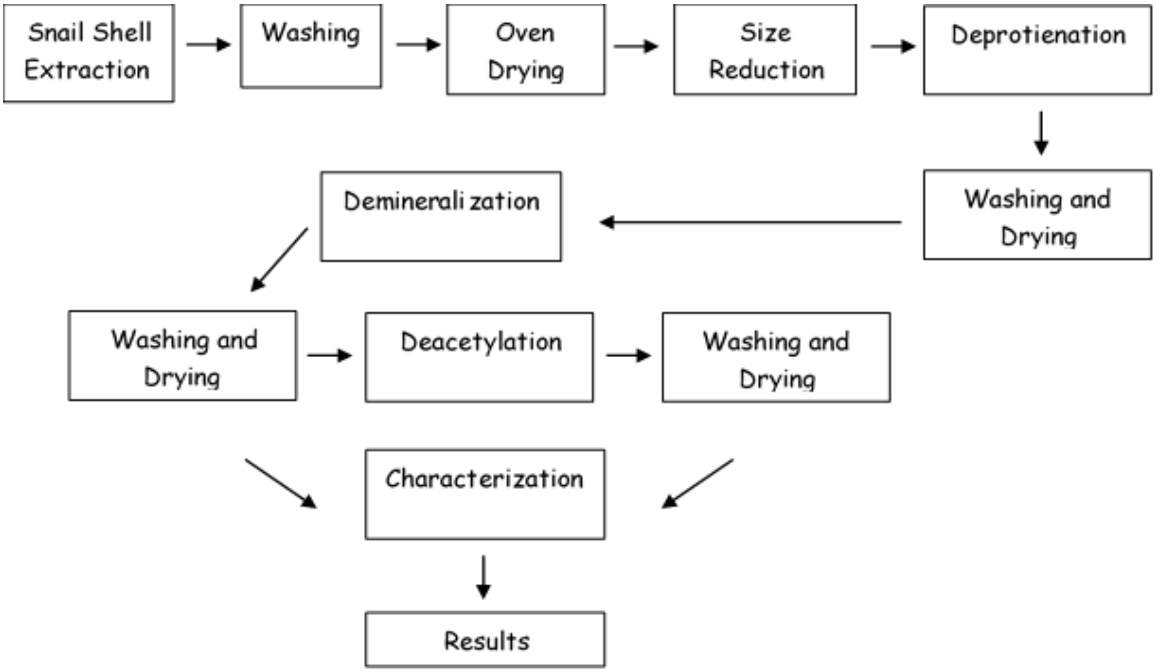

Figure 3.1: Schematic of chitin and chitosan recovery

3.2Obtainment of Chitin

Hongkulsup, *et al.*,(2016) reported that the deproteination stage and the demineralization stage are the two phases required in the extracton of chitin.In this study chitin was obtained through the stages of deproteinization which involves the extraction of protein matter in alkaline medium mainly with NaOH and demineralizationstage involves acid treatment to remove inorganic matters mainly calcium carbonate with HCl(Shanta, *et al.*, 2015).

Similarly, according to Joshy, *et al.*, (2016) the four major parameters affecting the extraction of chitin include the reagent used, the reagents concentration, the reaction temperature and the reaction time. The deproteination reaction was carried out at 4% NaOH concentration, 1:10 sample to alkali ratio, reaction temperature of 50 ^{o} C and reaction time of 1 hour. Similarly, the demineralization stage occurred at 2M HCl concentration, sample to acid ratio of 1:5, a reaction temperature of 60 ^{o} C and reaction time of 3 hours

3.3Obtainment of Chitosan

The optimization of the deacetylation of Chitin(brings about the formation of Chitosan) was carried out using design expert.This deacetylation stage was optimized using DESIGN EXPERT (Version 7.0.0, Stat Ease, Inc., USA) software. The process parameters considered for the deacetylation stage include the NaOH concentration, the Sample to Alkali ratio, the Reaction Temperature and the Reaction time.This factors where chosen because they are the main factors that affect the attainment of adequate molecular weight chitosan

Table 3.1: Process parameters under investigation

Variables	Low	High
NaOH Concentration (%)	30	50
Chitin to Alkali Ratio (w/v)	7	20
Reaction Temperature (^{o} C)	90	120
Reaction Time (minutes)	90	150

3.4Chitosan Characterization

3.4.1Degree of Deacetylation (DD)

The degree of deacetylation determines the content of free amino groups (-NH2) in the polysaccharides (Wassila, et al., 2013).The DD was determined from the Fourier Transform Infrared Spectroscopy (FTIR) as reported by (Gbenebor, et al., 2017).

$$DD = 100 \times \left(1 - \frac{\left(\frac{A_{1655}}{A_{3450}}\right)}{1.33}\right) \qquad (1)$$

Where the A1655and A3450 are the absorbance at 1655 cm^{-1} of the amide I band as a measure of the N-acetyl group content and 3450 cm^{-1} of the hydroxyl band.

3.4.2pHvalue

The pH value was determined by the method reported by Kaewboonruang, (2016)where 5 ml of distilled water is added to 20g of the air-dried chitosan and stirred using a glass rod after which the electrode of the digital standardized pH meter is inserted into it and the pH read off the meters display

3.4.3Solubility

1g of the chitosan was dissolved in 1M acetic acid and vigorously stirred for 30 minutes after which the residue is filtered out and weighed (Majekodunmi, 2016).

$$\%\, Solubility = \frac{Initial\ weight - Weight\ of\ residue}{Initial\ weight}\ x\ 100\% \qquad (2)$$

3.4.4 Molecular Weight

The molecular weight was determined by employing Mark-Houwink equation

$$\eta = KM^a \qquad (3)$$

Where η is the intrinsic viscosity, M is average molecular weight, K and a are constants, whose values depend on the polymer type and the chosen solvent as reported by (Hossain, and Iqbal, 2014).

3.4.5 Viscosity

The viscosity of chitosan samples was determined by a Brookfield viscometer. Where the chitosan sample was dissolved in 1% of acetic acid at 1% concentration of the sample on a dried basic.The chitosan viscosity was measured in centipoises (cps) (Hossain, and Iqbal, 2014).

3.4.6 Moisture Content

This was determined by gravimetric method where the crucible was dried in an oven at 80°C for 20 minutes, and then cooled in a desiccator and weighed (W1)g, 2g of the sample wasthen placed into the crucible and reweighed (W2)g, the crucible with the sample was dried in the oven at 105°C until a constant weight was obtained after successive cooling in the desiccator and weighing.It was then transferred from the oven to the desiccator to cool and then quickly weighed (W3)g. The percentage moisture content is calculated using formula (Enyeribe, *et al.*, 2017).

$$\%\ Moistue\ content = \frac{(W_2(g) - W_3(g))}{(W_2(g) - W_1(g))}\ x\ 100\% \quad (4)$$

4. Results and Discussion

4.1 Optimization of Chitosan Production

The deacetylation of Chitin is what brings about the formation of Chitosan.This deacetylation stage was optimized using DESIGN EXPERT (Version 7.0.0, Stat Ease, Inc., USA) software. The process parameters considered for the deacetylation stage include the NaOH concentration, the Sample to Alkali ratio, the Reaction Temperature and the Reaction time.

Table 4.1: Optimization of chitosan production from Snail shell

Run Number	A: NaOH concentration (%)	B: Chitin to Alkali ratio (w/v)	C: Reaction Temperature (°C)	D: Reaction Time (mins)	Actual DD Yield (%)	Predicted DD Yield (%)
1	50.00	20.00	90.00	150.00	74.3	74.16
2	50.00	20.00	90.00	90.00	77.3	75.60
3	40.00	13.50	105.00	60.00	84.0	85.64
4	40.00	13.50	105.00	120.00	82.7	81.53
5	40.00	13.50	105.00	180.00	83.2	83.49
6	60.00	13.50	105.00	120.00	76.5	78.74
7	30.00	7.00	120.00	150.00	82.0	82.90
8	40.00	26.50	105.00	120.00	70.0	73.20
9	50.00	7.00	120.00	150.00	82.0	82.11
10	50.00	7.00	90.00	150.00	84.0	82.88
11	30.00	7.00	120.00	90.00	84.6	83.61

12	40.00	13.50	105.00	120.00	79.3	81.53
13	30.00	20.00	90.00	150.00	69.4	69.10
14	30.00	7.00	90.00	90.00	70.6	71.18
15	50.00	7.00	120.00	90.00	84.0	83.50
16	40.00	0.50	105.00	120.00	82.0	80.72
17	50.00	20.00	120.00	90.00	83.0	80.78
18	50.00	20.00	120.00	150.00	77.3	75.92
19	40.00	13.50	135.00	120.00	80.5	82.25
20	50.00	7.00	90.00	90.00	80.3	80.85
21	40.00	13.50	105.00	120.00	82.7	81.53
22	40.00	13.50	105.00	120.00	83.8	81.53
23	30.00	20.00	120.00	90.00	84.5	84.82
24	30.00	20.00	120.00	150.00	82.3	80.63
25	30.00	20.00	90.00	90.00	71.1	69.86
26	40.00	13.50	105.00	120.00	81.7	81.53
27	30.00	7.00	90.00	150.00	72.8	73.90
28	40.00	13.50	105.00	120.00	80.0	81.53
29	20.00	13.50	105.00	120.00	74.1	73.79
30	40.00	13.50	75.00	120.00	67.9	68.07

Table 4.2:Analysis of Variance (ANOVA) forchitosan production from snail shell

Source	Sum of Squares	Degree of Freedom	Mean Square	F Value	p-value Prob > F
Model	740.35	14	52.88	14.09	< 0.0001
A- NaOH Concentration	38.00	1	38.00	10.13	0.0062
B- Chitin to Alkali ratio	86.64	1	86.64	23.09	0.0002
C- Reaction Temperature	298.21	1	298.21	79.47	< 0.0001
D- Reaction Time	7.48	1	7.48	1.99	0.1784
AB	14.44	1	14.44	3.85	0.0686
AC	93.12	1	93.12	24.82	0.0002
AD	0.64	1	0.64	0.17	0.6855
BC	5.76	1	5.76	1.53	0.2344
BD	11.22	1	11.22	2.99	0.1043

CD	10.89	1	10.89	2.90	0.1091
A^2	51.86	1	51.86	13.82	0.0021
B^2	39.50	1	39.50	10.53	0.0054
C^2	74.67	1	74.67	19.90	0.0005
D^2	15.95	1	15.95	4.25	0.0570
Residual	56.29	15	3.75		
Lack of Fit	41.23	10	4.12	1.37	0.3834
Pure Error	15.06	5	3.01		
Cor Total	796.64	29			

$R^2 = 0.9293$ C.V. % = 2.45

The analysis of the variance (ANOVA) for the response surface quadratic model is shown in Table 4.2. The model expression developed that relates the Deaetylation (DA) yield and the four reaction parameters considered (A, B, C, D) is considered suitable because its p-value is less than 0.05. The model F-value of 14.09 implies the model is significant. The F-value is the ratio of the Model SS / Residual SS and shows the relative contribution of the model variance to the residual variance where large number indicates more of the variance being explained by the model and a small number says the variance may be more due to noise (Shridhar, *et al.*, 2010). The model fit is also checked with the correlation factor R^2 which equals to 92.93%.

The significant factors from the ANOVA analysis are the quadratic effects of the NaOH concentration (A^2), the chitin to alkali ratio (B^2), and the reaction temperature (C^2) and with p-values of 0.0021, 0.0054, and 0.0005 respectively. Other significant factors are the interaction effect of NaOH concentration and Reaction Temperature (AC) including the linear effects of the NaOH concentration (A), the linear effects of the Chitin to Alkali ratio (B) and Reaction Temperature (C) with p-values of 0.0002, 0.0062, 0.0002, and < 0.0001 respectively. The other factors have no statistically significant effect.

In this study the value of the determination coefficient ($R^2 = 0.9293$) indicates that the sample variation of 92.93% is attributed to independent variables and 7.17% of the total variation is not explained by the model. The value of the coefficient of variation (C.V. % = 2.45) gives the precision and reliability of the experiment carried out where a lower value indicates a better precision and reliability of the experiment. The models p-values of < 0.0001 shows that the quadratic model is a suitable model for this study

The model equation governing the DA yield is represented by the following coded equation

$$\text{DA Yield} = 81.70 + 1.26A - 1.90B + 3.52C - 0.56D - 0.95AB - 2.41AC - 0.20AD + 0.60BC - 0.84BD - 0.82CD - 1.38A^2 - 1.20B^2 - 1.65C^2 + 0.76D^2$$

The linear effect of A, B and C, the Interaction effect of AB, AC, BD and CD and the quadratic effect of A^2, B^2 and C^2 are the generally determining factors of the deacetylation of chitin produced from snail shell. The quadratic effect of D^2 can be considered as the secondary factors of the response. In this statistical analysis the linear effect of reaction temperature (C) has the highest coefficient between the four independent variables. This implies that the response depends largely on this factor.

4.2 Effect of Interaction between process parameters and chitosan yield

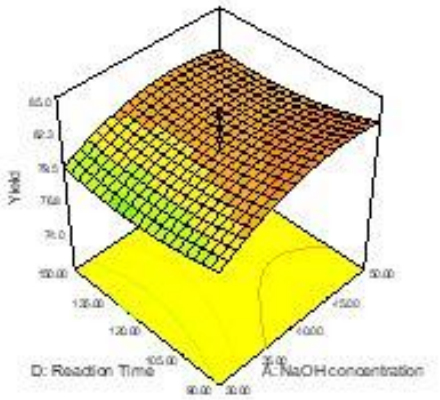

Figure 4.1: Surface plot of DA Yield % against the interaction effect of NaOH concentration and Chitin to Alkali ratio

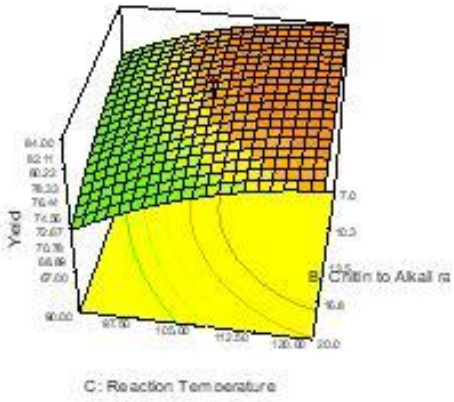

Figure 4.2: Surface plot of DA Yield % against the interaction effect of NaOH concentration and Reaction Temperature

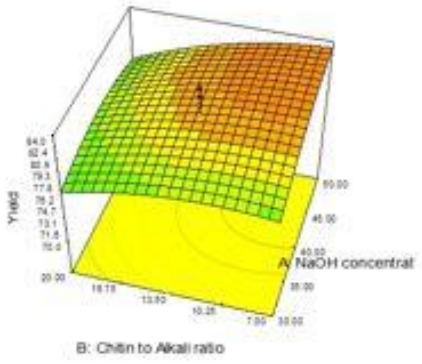

Figure 4.3: Surface plot of DA Yield % against the interaction effect of NaOH concentration and the Reaction Time

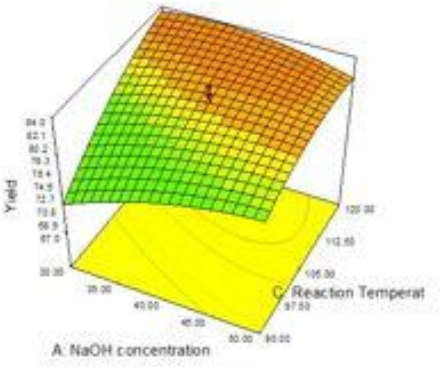

Figure 4.4: Surface plot of DA Yield % against the interaction effect of Chitin to Alkali ratio and the Reaction Temperature

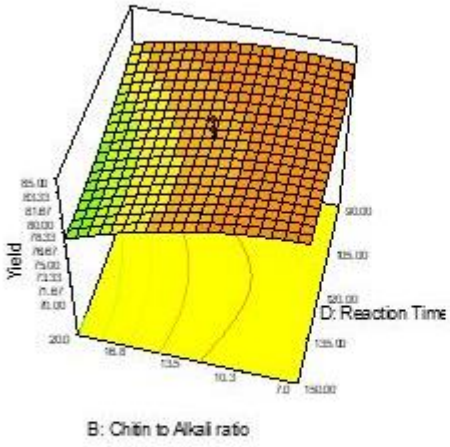

Figure 4.5: Surface plot of DA Yield % against the interaction effect of Chitin to Alkali ratio and the Reaction time.

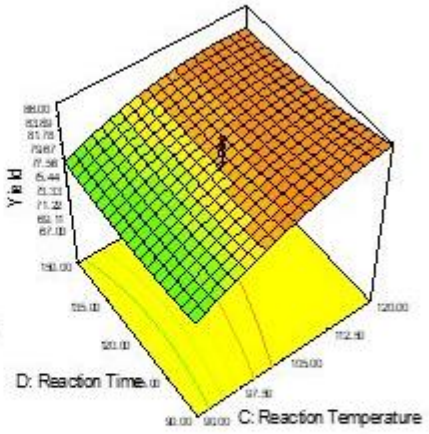

Figure 4.6: Surface plot of DA Yield % against the interaction effect of Reaction temperature and the Reaction time.

The surface plot of the DA yield % againstinteraction effect of NaOH concentration and the Chitin to Alkali ratiorepresented by Figure 4.1 shows that there was an increase in the DAyield as the NaOH concentration increased howbeit when the chitin to alkali ratio is considered there was an increase in the DA yield as the chitin to alkali ratio decreased. In terms of the interaction effect of NaOH concentration and the Chitin to Alkali ratioan optimum DA yield of 77% was obtained at a 30% NaOH concentration and a chitin to alkali ratio of 1:20.

Figure 4.2 represents the surface plot of the DA yield % against the interaction effect of NaOH concentration and Reaction Temperature. From the plot it was observed that an increase in the reaction temperature resulted in a similar increase in the DA yield %. Howbeit a drop in the NaOH concentration resulted in a decline in the DA yield %. The interaction effect of the NaOH concentration and Reaction Temperature resulted in a DA yield of 71.54% which was obtained at a 30% NaOH concentration and a reaction temperature of 90 ^{o}C.

Figure 4.3 represents the surface plot of the DA yield % against the interaction effect of NaOH concentration and the Reaction Time. From the plot it was observed that an increase in the NaOH concentration resulted in an increase in the DA yield % while an increment in the reaction time resulted in a dip in the DA yield %. However, at reaction time above 135 minutes there was a slight increment in the DA yield%. The interaction effect of the NaOH concentration and the Reaction Time resulted in a DD yield% of 78.12% was obtained at a 30% NaOH concentration and a reaction time of 135 minutes.

The surface plot of the DA yield % against the interaction effectof Chitin to Alkali ratio and the Reaction temperaturerepresented by Figure 4.4 shows that anincrease in the reaction temperature favors the increase of DA yield % while a decrease in the chitin to alkali ratio also favors an increase in the DA yield %. Theinteraction effect of Chitin to Alkali ratio and the Reaction temperature resulted in an optimum DA yield % of 72.1% was obtained at a chitin to alkali ratio of 1:20 and a reaction temperature of 90 ^{o}C.

From Figure 4.5 it shows the surface plot of the DA yield % against the interaction effect ofChitin to Alkali ratio and theReaction time. From the plot it was observed that a decrease in both the chitin to alkali ratio and the reaction time resulted in an increase in the DA yield %.The interaction effect of Chitin to Alkali ratio and the Reaction time resulted in an optimum DA yield % of78.12% was obtained at a reaction time of 150 minutes and a chitin to alkali ratio of 1:20.

The surface plot of the DA yield % against the interaction effect of Reaction temperature and the Reaction time represented by Figure 4.6. From the plot it was observed that an increase in the reaction temperature favored an increase in the DA yield %. However, an increase in the reaction time resulted in a slight dip in the DA yield %. This trend continued until a reaction time of 120 minutes were further increment in reaction time resulted in a slight increment in the DA yield %. The interaction effect of reaction temperature and the reaction time resulted in an optimum DA yield % of 76.56% at a reaction temperature of 90 ^{o} C and reaction time of 120 minutes.

4.3 Properties of Synthesied Chitosan

The properties of the synthesized chitosan are presented in table 4.3

Table 4.3 Properties of Synthesied Chitosan

Properties	Result/Value
Colour	White
pH	7.09
Solubility in 1 % acetic	Soluble
%Solubility	87.2
Solubility in water	Insoluble
Viscosity (cps)	220
Molecular weight (DD)	2.91×10^5
Moisture content (%)	3.25
Ash (%)	1.42
% DD	75.85
Yield (per 1g of chitin)	0.531
% Yield (per 1g of chitin)	53.01

Yield (per 100g of Snail shell)	7.04
% Yield (per 100g of Snail shell)	7.04

4.4 Structural analysis of Synthesied Chitosan

4.4.1Scanning Electron Microscopy (SEM) Analysis of Chitosan

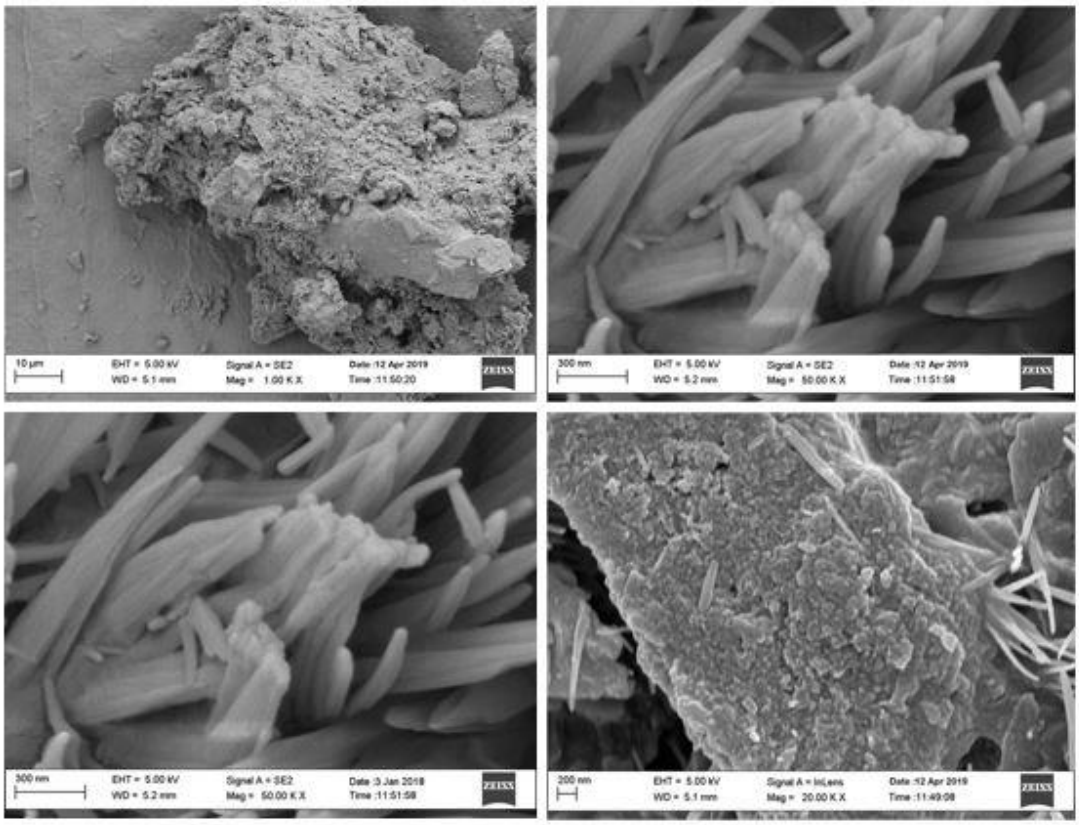

Figure 4.7SEM micrograph of the synthesized chitosan

The SEM micrographs represented by Figure 4.7 shows the surface morphology of the synthesized chitosan. Under the electron microscopic examination, chitosan showed non-homogenous and non-smooth surface with straps and shrinkage which corresponds to the SEM morphology of standard extracted chitosan (Islam*et al.*, 2011).

4.4.2Fourier Transform Infrared Spectroscopy (FT – IR) Analysis of Chitosan

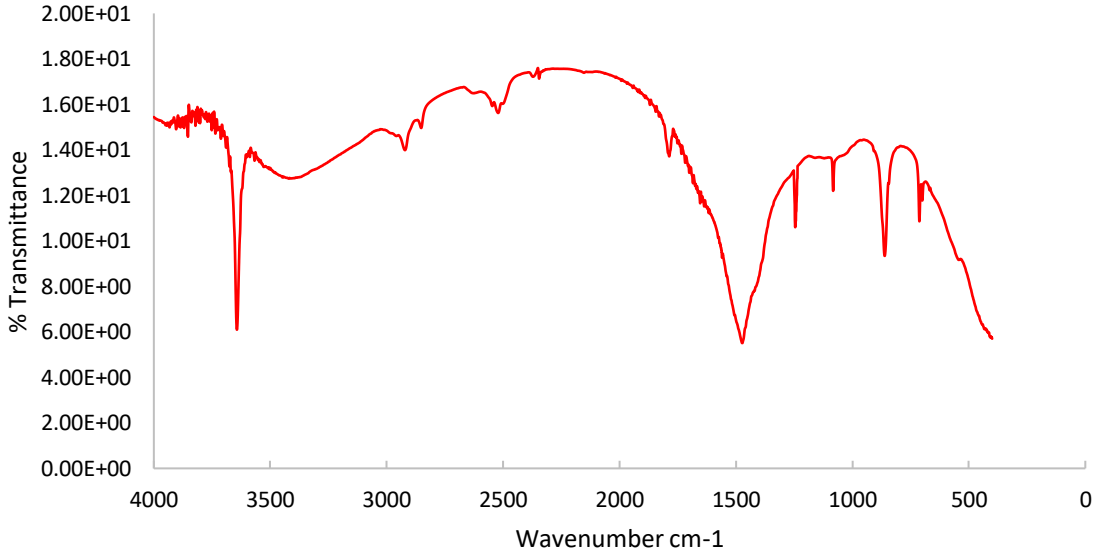

Figure 4.8: FT-IR spectra of synthesized Chitosan

The FTIR spectra for the synthesized chitosan gave a characteristic wide band of NH at 3386.34 cm^{-1} which corresponded to the N-H stretching vibrating band of free amino acids. Likewise, the band observed at 1786.77 cm-1 corresponded to the carbonyl group band. The band at 3642.39 cm-1 is a result of the stretching primary hydroxyl groups of tertiary O-H stretching as reported by (Thillai, *et al.*, 2017; Abdulkarim, *et al.*, 2013)

Table 4.13: Wavenumbers and chemical group of FT-IR absorption bands for chitosan

S/N	Standard Chitosan Wavelength in cm^{-1}	Synthesized Chitosan Wavelength in cm^{-1}	Group
1.	3450	3642.39	OH hydroxyl group
2.	3360	3386.34	N-H group-stretching vibration
3.	2920, 2880, 1430, 1320	2918.74, 2851.24	Symmetric or asymmetric CH_2 stretching vibration
4.	1275,1245	1245.79	Attributed to pyranose ring
5.	1730	1786.77	Carbonyl group vibration
6.	1660	1600.15	C=O in amide group (amide I band)
7.	1560	1473.19	NH-bending vibration in amide group
8.	1590	1473.19	NH_2 in amino group
9.	1415, 1320	1245.79	Vibrations of OH, CH in the ring
10.	1380	1473.19	CH_3 in amide group
11.	1255	1245.79	C–O group
12.	1150, 1040	1082.84	–C–O–C– in glycosidic linkage
13.	850, 838	861.60	CH_3COH group

5. Conclusion

Most of the process parameters have a significant effect on thedeacetylation (DA) yield %. From the ANOVA analysis the significant factors are the quadratic effects of the NaOH concentration (A^2), the chitin to alkali ratio (B^2), and the reaction temperature (C^2) because their p-values are less than 0.05 respectively. Similarly, the interaction effect of NaOH concentration and Reaction Temperature (AC) including the linear effects of the NaOH concentration (A), the linear effects of the Chitin to Alkali ratio (B) and Reaction Temperature (C) can also be considered as having a significant effect in terms of DD yield %with p-values less than 0.05 respectively. The other factors have no statistically significant effect.

The surface plot shows the interaction effect of the various process variables considered against the DA yield %.The optimization data from this studyresulted in an optimum DA yield of at NaOH concentration, Chitin to Solvent ratio, Reaction temperature and Reaction time of 40%, 1:13.50, 75 ^oC and 120 minutes.

The successful extraction of chitosan fromtheAfrican Giant Land Snail Shell (*Archachatinamarginata*) and the optimization of process variables involved in its extraction provides data on how these various process variables viz NaOH concentration, Chitin to Solvent ratio, Reaction temperature and Reaction timeaffect the extraction of chitosan from the African Giant Land snail shell. Similarly, it provides a market for the utilization of these snail shell and also shows the viability of the theAfrican Giant Land snail shell as a suitable raw material for chitosan extraction. The strutural analysis of the synthesised chitosan shows that the synthesied chitosan has similar properties with standardied chitosan as reported in literature.

References

Abdulkarim, A., Isa, M.T., Abdulsalam, S., Muhammad, A.J. andAmeh, A.O. (2013), Extraction and Characterization of Chitin and Chitosan from Mussel Shell. *Civil and Environmental Research*, Vol 3, 108 – 114.

Ameh A.O., Isa M.T., Adeleye T.J. and Adama K.K. (2013). Kinetics of demineralization of shrimp exoskeleton in chitin and chitosan synthesis. *Journal of Chemical Engineering and Materials Science.*,Vol 4, 32 – 37.

Enyeribe, C.C., Kogo A.A., Yakubu M.K., Obadahun, J., Agho, B.O. andKadanga, B. (2017), Effect of Degrees of Deacetylation on The Antimicrobial Activities of Chitosan. *International Journal of Advanced Research and Publications,*Vol 1, 55 – 61.

Gbenebor, O.P., Akpan, E.I. and Adeosun, S.O., (2017), Thermal, structural and acetylation behavior of snail and periwinkle shells chitin. *Progress in Biomaterials,*Vol 1, 13 – 19.

Hongkulsup, C., Khutoryanskiy, V. and Niranjan, K., (2016), Enzyme assisted extraction of chitin from shrimp shells (Litopenaeusvannamei). *Journal of Chemical Technology and Biotechnology,*Vol 91, 1250 – 1256.

Hossain, M.S., and Iqbal, A., (2014), Production and characterization of chitosan from shrimp waste. *Journal of the Bangladesh Agricultural University*, Vol 12, 153 – 160.

Islam, M., Shah, M., Masum, M., Rahman, M., Ashraful, I.M., Shaikh, A.A. and Roy, S.K. (2011). Preparation of Chitosan from Shrimp Shell and Investigation of Its Properties, *International Journal of Basic and Applied Sciences,*Vol 11, 77 – 80.

Islem, Y., and Marguerite, R., (2015), Chitin and Chitosan Preparation from Marine Sources: Structure, Properties and Applications. *Journal of Marine Drugs,*Vol13, 1133 – 1174.

Joshy, C.G., Zynudheen, A.A., George, N., Ronda, V., andSabeena, M. (2016), Optimization of Process Parameters for the Production of Chitin from the Shell of Flowertail Shrimp (Metapenaeusdobsoni). *Society of Fishery Technology India,*Vol53, 140 – 145.

Kaewboonruang, S., Phatrabuddha, N., Sawangwong, P., andPitaksanurat, S., (2016),Comparative Studies on the Extraction of Chitin – Chitosan from Golden Apple Snail Shells at the Control Field. *IOSR Journal of Polymer and Textile Engineering,*Vol 3, 34 – 41.

Mahmoud, N.S., Ghaly, A.E. and Arab, F., (2007), Unconventional Approach for Demineralization of Deproteinized Crustacean Shells for Chitin Production. *American Journal of Biochemistry and Biotechnology,*Vol3, 1 – 9.

Majekodunmi. O.S., (2016), Current Development of Extraction, Characterization and Evaluation of Properties of Chitosan and Its Use in Medicine and Pharmaceutical Industry. *American Journal of Polymer Science,*Vol6, 86 – 91.

Muxika, A., Etxabide, A., Uranga, J.P., Guerrero, K. and de la Caba., (2017), Chitosan as a bioactive polymer: Processing, properties and applications. *International Journal of Biological Macromolecules,*Vol 105, 1358 – 1368.

Nisha, P. andPandharipande, S.L., (2016), Review on synthesis, characterization and bioactivity of chitosan. *International journal of engineering sciences & research technology,*Vol 5, 334 – 344.

Russell, G.S., (2013), A Review of the Applications of Chitin and Its Derivatives in Agriculture to Modify Plant-Microbial Interactions and Improve Crop Yields. *Journal of Agronomy,*Vol3, 757 – 793.

Shanta, P., Paras N.Y. and Rameshwar A., (2015), Applications of Chitin and Chitosan in Industry and Medical Science: A Review. *Nepal Journal of Science and Technology,*Vol 16, 99 – 104.

Shridhar, Bagali S., Beena,K.V., Anita,M.V. and Paramjeet,K.B. (2010), Optimization and characterization of Castor Seed Oil. *Leanardo Journal of Science,*Vol1, 59 – 70.

Thillai N. S., Kalyanasundaram, N., and Ravi, S. (2017). Extraction and Characterization of Chitin and Chitosan from Achatinodes. Natural Products Chemistry & Research, Vol5, 1 – 5.

Wassila A., Leila A., Lydia A. andAbdeltif A. (2013). Chitin Extraction from Crustacean Shells Using Biological Methods – A Review. *Food Technology Biotechnology*,Vol51, 12 – 25.

Characterization of Selected Ore Deposits for The Determination of Elements and Oxides Composition of Gold in Niger State For Industrial Application

Isaac A. Joseph*[1]; Elizabeth J. Eterigho[2] and J.O. Okafor[3]

Chemical Engineering Department, Federal University of Technology, Minna, Niger State, Nigeria.

E-mail: *[1] isaacchemeng@yahoo.com, [2]betyeterigho@gmail.com, [3]Jo.okafor@futminna.edu.ng

Abstract:

This work presents the determination of elemental and oxide composition of gold ores from different mining locations in Niger State, Nigeria. The aim is to provide useful information on the availability of elements and its oxides of high economic values that can serve as raw materials for industrial applications. These ores samples were collected from four different locations. The chemical analyses of the ores were carried out using X-ray fluorescence (XRF) spectrometry. The results show that Paiko Ore consists essentially of Si (58 %), Fe (2.1 %), Au (1.23 %), Mg (0.8 %), SiO_2 (71.9 %), Al_2O_3 (7.1 %), Fe_2O_3 (2.9 %) and MgO (1.26 %) while Garatu Ore consist mainly of Si (63.5 %), Fe (2.7 %), Au (0.7 %), SiO_2 (53.7 %), Al_2O_3 (10.2 %) and Fe (3.9 %). The essential composition of Chanchaga ore are Si (75.4 %), Fe (7.7 %), Ca (1.1 %), Au (1 %), SiO_2 (23.16 %), Fe_2O_3 (11.1 %), CaO (1.5 %) and TiO_2 (1%) while Ore sample from Maitunbi consists of Si (69.5 %), Fe (4 %), Au (0.88 %), SiO_2 (40.7 %), Al2O3 (9.9 %). The high amounts of Au, Si, SiO_2 and TiO_2 in these ores show that they are suitable raw materials for industrial applications.

Keywords: elemental composition, oxide composition, gold ore

1. INTRODUCTION

Currently, there is an increased search for locally available raw materials around the world. This is in a bid to expand scope of industrial development, job creation and increase in gross domestic products (GDP). One of the ways of achieving this is through quantitative and qualitative analysis of these available raw minerals in their ores at various locations in the country.

Niger State has the fourth largest gold deposit in Nigeria while the first, second and third are in Zamfara, Kaduna and Kebbi State respectively (BluePrint, 2016). This deposit is in both Primary (eluvia) and secondary (alluvia) (SRMEAMK, 1987). The primary deposit (i e. eluvia) results from where there is chemical reactions between wall rocks in the Earth's Crust and ore bearing hydrothermal (hot fluid) mineralization solutions; metal bearing to form gold precipitate (Weick, 1994; Zhu *et al.*, 2011). Secondary (alluvia) deposit is formed from mechanical and chemical process of weathering and erosion, and the physical re-concentration of gold bearing sediment into placer deposits (Weick, 1994) and it is usually in free and native form (Ogundare *et al.*, 2014). The ore deposit in this region has similar elements composition but different content with ore sample reported by Ayin and Gul (2014) from Canakkale, Turkey. This is similar to gold ore sample reported by Ogundare *et al.* (2014) from Itagunmodi,

Osun State of Nigeria. There are some similarities between oxide composition of ore from Niger and that of Rio de Janeiro-Brazil by Rojas *et al.* (2015). Gold ore is usually associated with several other mineral elements such as silver, silicon, magnesium, calcium and many others (Ariffin, 2006; Marcello *et al.*, 2006). It also has associate oxides such as silicon oxide (SiO_2), aluminum oxide (Al_2O_3), iron oxide (Fe_2O_3). However, the percentage of these elements and oxides varies from one location to another as a result of variation in geological formation. The amount of Au, Cu and S present in the ore are usually a thing of concern as it determine the viability, rate of recovery of gold, the ease and method of the ore processing. The amount of gold present in any ore is the major factor local miners consider before going into mining and processing of gold ore. The local miners by experience do a quantitative determination of the amount of gold present in any ore by washing some collected samples over slux box. If reasonable amount is recovered from washed samples, then mining and processing continue otherwise, they stop and go to another location. Cupper and Sulphur are less desired in gold ore as they reduces the recovery of gold. Large amount of sulphur in the ore can make extraction by, coal-oil agglomerate, borax and cyanide method unsuccessful (UNEP, 2012; Veiga *et al.*, 2006).

The numbers of gold mining sites in Niger State is currently unknown however, new discovery of gold deposits are made on daily basis by local miners in the region. Some of the locations of ore within Niger State are: Chanchanga, Paiko, Maitunbi, Garatu, Rafi, Shiroro, Borgu, Lapai, and Magama (SRMEAMK, 1987; IOEPN, 2016). Despite the abundance of gold ore in Niger State, it is only the local miners that are currently exploring and mining the ore deposits. The local miners only recover a portion of the gold from the ore and then discard the sand without the knowledge of other associated minerals or amount of gold left in the ore. This present study is aimed at the determination of the elemental and oxide composition of this gold ore, with the interest of identifying possible raw materials from the ores.

2. Materials and Methods

Samples of the ores were collected from the mining sites at Maitunbi and Chanchaga (both in Chanchaga LGA), Paiko, in Paiko LGA and Garatu, in Bosso LGA of Niger State. Samples from Paiko and Garatu were in elluvia deposit while samples from Maitunbi and chanchaga were in allovia deposit. The method used is described in Section 2.1

2.1 Method

Ore samples were pulverized and their particle sizes were reduced in order to enhance easy liberation of gold and other associated minerals. The chemical analyses were conducted in Spectrometry Laboratory Services, Kaduna, Nigeria using XRF (Nitron 3000) using Copper-Zinc method. The XRF machine was powered on and initialized after which it was allowed to stabilize for 5 minutes. The Cu-Zn method was chosen due to its wide coverage of elemental and sesquioxide detection and intensity. The data were subjected to analyses in triplicates and this automatically takes the average. This procedure was followed for all the samples to get the percentage chemical composition in oxide and elemental form. Sieve analysis was carried out in Civil Engineering Laboratory, Federal University of Technology, Minna, Niger State with a set of eleven sieves. A know mass of ground samples were poured into the set of sieves and shaken for ten minutes and each of the retained masses by the sieves were collected, weighed and recorded for further computation and plotting of the particle size distribution curves.

3. Results and Discussion

Table.1 is the results of the elemental composition of the ore samples from Paiko, Gurara, Charchanga and Maitunbi with other reported results. The main elements in Paiko sample is Si (33.6 %) followed by Al (3.8 %), Fe (2.1 %) and Au (1.2 %, element of interest). The result from Garatu showed the main elements Si (25.1 %) followed by Al (5.4 %), Fe (2.7 %), K (1.4 %) and Au (0.7 %). Sample from Chanchaga has its main element as Si (10.8 %), followed by Fe (7.7 %), Al (3.9 %), Ca (1.067 %) and Au (1.01 %, element of interest). The result of the elemental composition of ore sample from Maitunbi shows that Si (19.0 %) is the main element present in the ore followed by Al (5.2 %), Fe (3.99 %) and Au (0.88 %,). The detailed XRF analysis of the samples shows that sample from Paiko has the highest percentage of Au followed by ore from Chanchaga and Maitunbi while the least is from Garatu.

Table1. Elemental Composition of gold ore in some sites in Niger State

Element Present in the Ores (%)	Paiko	Garatu	Chanchaga	Maitunbi	Canakkale, Turkey. Ayin and Gul (2014)	Osun, Nigeria. Ogundare *et al.* (2014)
Mg	0.759	0.598	<LOD	0.454	0.02	0.0000048
Si	58.054	63.59	75.473	69.505	-	-
P	<LOD	<LOD	<LOD	<LOD	41	0.0002158
S	0.232	0.356	0.049	0.017	-	0.0000448
Cl	0.021	<LOD	<LOD	<LOD	0.8	0.0000399
K	0.776	1.144	0.175	0.614	-	-
Ca	0.239	0.203	1.067	0.658	0.03	0.0000
Ti	0.126	0.19	0.576	0.35	0.05	0.0000219
V	0.006	0.009	0.027	0.012	-	0.003
Cr	0.009	0.008	0.02	0.009	-	0.0000233
Mn	0.047	0.085	0.059	0.047	-	0.0000
Fe	2.055	2.745	7.737	3.99	-	0.0000731
Co	<LOD	<LOD	<LOD	0.016	3.51	0.0023
Ni	<LOD	<LOD	<LOD	<LOD	0.00418	0.0000
Cu	0.013	0.035	<LOD	<LOD	-	0.0000061
Zn	0.019	0.052	0.013	0.006	0.0182	0.0000067
As	<LOD	<LOD	0.002	<LOD	0.0079	0.0000102
Se	<LOD	<LOD	<LOD	<LOD	0.01375	0.0000
Rb	<LOD	<LOD	<LOD	<LOD	0.0051	-

Sr	0.002	0.003	0.005	0.005	-	0.00000091
Zr	0.004	0.005	0.008	0.018	-	-
Nb	<LOD	<LOD	<LOD	<LOD	-	-
Mo	<LOD	0.003	<LOD	<LOD	-	-
Pd	<LOD	<LOD	<LOD	<LOD	-	-
Ag	<LOD	<LOD	<LOD	<LOD	-	-
Cd	<LOD	<LOD	<LOD	<LOD	0.012	0.00000362
Sn	<LOD	<LOD	<LOD	<LOD	-	-
Ba	0.036	0.079	0.032	0.043	-	-
W	0.007	<LOD	<LOD	<LOD	-	-
Au	1.231	0.724	1.010	0.875	-	0.0006119
Pb	0.226	0.397	<LOD	<LOD	0.001885	0.0019
Bl	<LOD	<LOD	<LOD	<LOD	-	0.00000156
Bal	3.765	5.421	3.931	5.226		-
Total	99.997	99.997	99.996	99.997		

* LOD: Low Detection *Bal: Balance; amount of elements that could not be detected

The 33.6 % and 25.07 % silicon from Paiko and Garatu samples respectively could be of great interest as silicon is considered to be the second source of industrial economy in the manufacturing of computer. The high silicon was recorded in primary deposit of Paiko and Garatu while lower silicon content was recorded in secondary deposit from Chanchaga (10.8 %) and Maitunbi (19 %), this is shown on Figure 1.

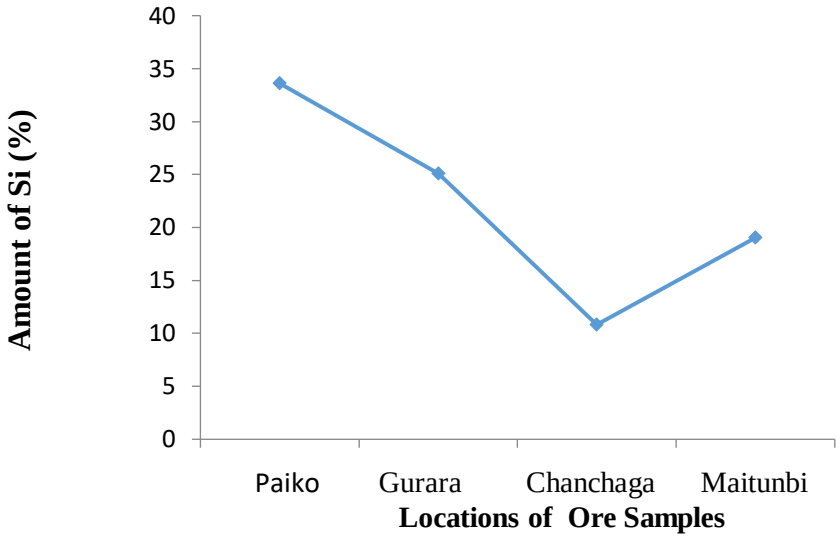

Figure 1: Amount of Si in Gold Ore Samples

Lead, a radioactive element was found in ore samples from Paiko (0.226 %) and Garatu (0.397 %) while the presence of lead in Chanchaga and Maitunbi ore samples is at low detection (Figure 2). Consumption of accumulated lead around gold processing areas of Paiko and Garatu can lead to adverse effects on livestock and humans. A toxicological study may be required within the gold mining and process areas of Paiko and Garatu in order to ascertain the safety of people living around the area.

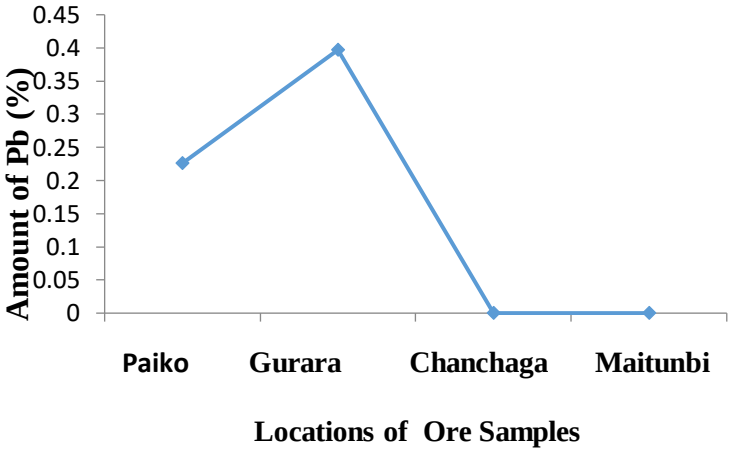

Figure 2: Amount of Pb in Gold Ore Samples

The results indicate that sulphur is present in all the samples with Garatu having the highest percentage of 0.35 %, and Maitunbi having the lowest of 0.017 % (Figure 3). The presence of sulpur in the ore could make the extraction of the gold unsuccessful using borax (UNEP, 2012; Appel and Na-Oy, 2012; Veiga *et al.*, 2014) however, this can be overcome by calcination (Robinson, 1988) of the ore followed by oxidation (Veiga *et al.*, 2014).

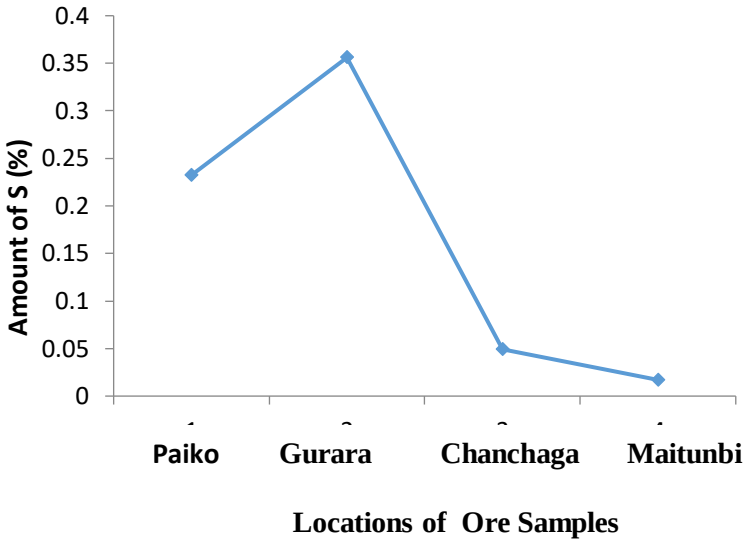

Figure 3: Amount of S in the Ore samples

From Figure 4 the ore sample from Chanchaga has the highest amount of iron (7.737 %) followed by those of samples from Maitunbi (3.99 %) and Garatu (2.745 %) while Paiko (2.055 %) has the least amount of iron. The Brownish colour of the collected ore from the different locations is also an evidence of the presence of iron is ore.

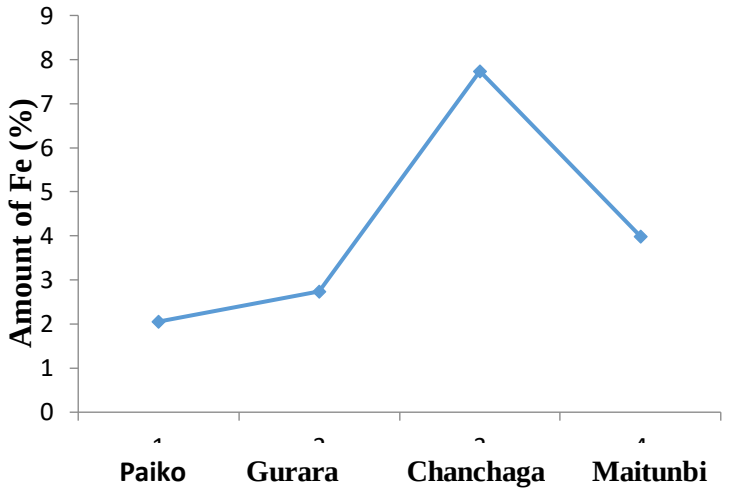

Figure 4: Amount of Fe in the Ore Samples

It was noted that Paiko (1.231 %), Garatu (0.724 %), chanchaga (1.01 %) and Maitunbi (0.875 %) have higher percentages of gold compared to 0.0019 % gold in Osun, Nigeria, O.0019 % in Indonesia and 0.0018 % of gold in Canakare, Turkey. This higher percentage of gold content in the ore samples from Niger state offer a better income for both Government and the local miners if appropriate methods are used for the extraction, separation and purification (Figure 5).

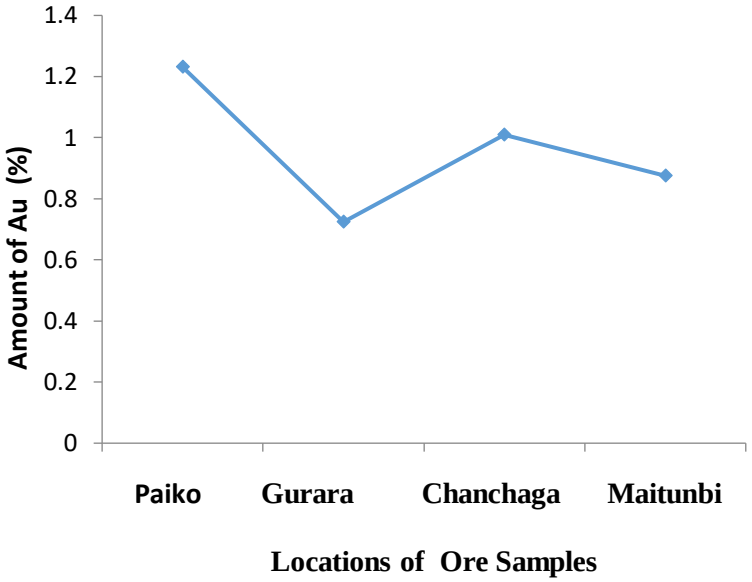

Figure 5: Amount of Au in the Ore samples

In Table 2, SiO_2 is the main component in Paiko sample having the highest percentage of 71.905 % followed by Garatu ore (53.658 %) and Maitunbi ore (40.717 %). while ore sample from Chanchaga has the lowest percentage of 23.16 % silica, this is presented in Figure 6.

Table 2: Oxide Composition of Gold Ore in some Sites in Niger State

Oxide Content (%)	Paiko	Garatu	Chanchaga	Maitunbi	Rio de Janeiro, Brazil
CuO	0.016	0.044	0	0	-
NiO	0	0	0	0	-
Fe_2O_3	2.939	3.925	11.063	5.705	7.66
MnO	0.061	0.11	0.076	0.061	0.08
Cr_2O_3	0.014	0.012	0.029	0.013	0.01
TiO_2	0.21	0.318	0.962	0.584	0.94
CaO	0.334	0.285	1.494	0.922	0.48
Al_2O_3	7.115	10.246	7.43	9.877	15.95
MgO	1.26	0.992	0	0.754	1.35
ZnO	0.024	0.065	0.016	0.008	-
SiO_2	71.905	53.659	23.16	40.717	62.33
Cr_2O	-	-	-	-	0.01
K_2O	-	-	-	-	4.6
P_2O_5	-	-	-	-	0.13

LOI	-	-	-	-	5.7
Total	83.878	69.656	44.23	58.641	99.84

Rajas *et al.* (2015)

The high presence of silica in Paiko and Garatu Ore are about the average content in Maitumbi ore which can serve as a good source of silicon for computer industry (Idrisa *et al.*, 2015). This will also maximize the use of the ore and bring about an increase in the income of the miners and increased GDP. The local miners in the region are ignorant of the presence of silicon in the ore as they discard the sand after extracting the gold by crude method.

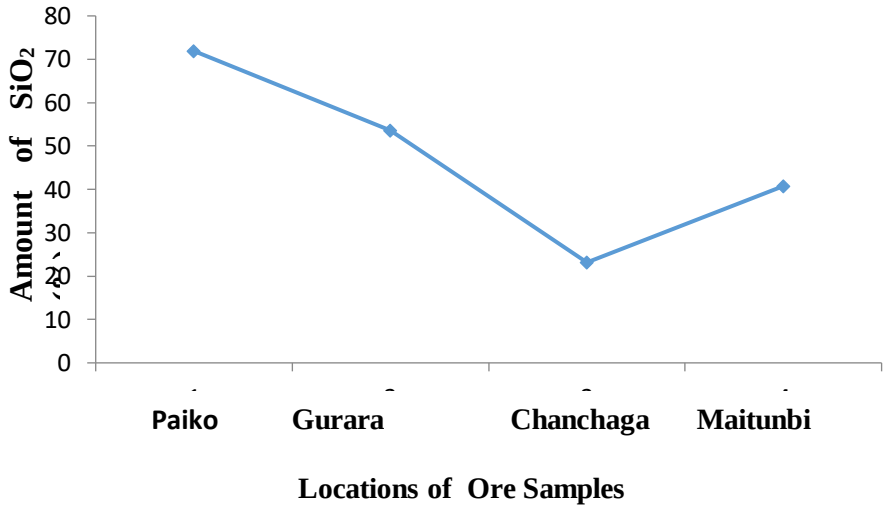

Figure 6: Amount of SiO_2 in the Ore samples

Alumina (Al_2O_3) is an important raw material in engineering processes such as insulation of materials, manufacturing of refractories. This alumina is found in all the samples collected. Highest amount of Al_2O_3 is found in Gurara (10.246 %) followed by Maitunbi (9.877 %) and Chanchaga (7.43 %) while sample from Paiko has the least amount of Al_2O_3. This is clearly shown in Figure 7. According to Report by Rajas *et al.* (2015) 15.95 % Al_2O_3 was present in ore sample collected from Rio de Janeiro, Brazil which is higher than the amount of Al_2O_3 from all the samples in this study.

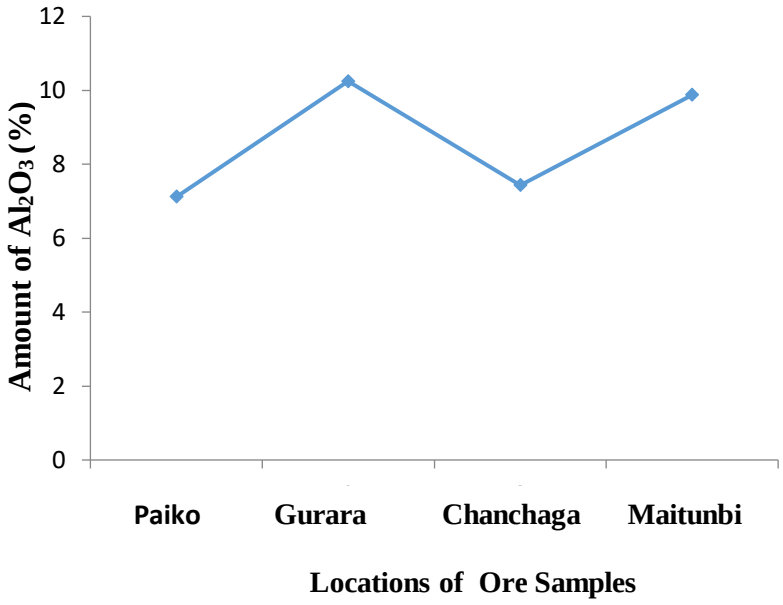

Figure 7: Amount of Al_2O_3 in the Ore Samples

The pH of ore samples helps to provide information on the acidity or basicity of the sample as well as the right process rought to be adopted in the extraction process of the mineral constituents. Table3 contain the pH of the four samples from Niger state which ranges between 6.55 to 6.80. The colour of the both samples from Paiko and Garatu is brow, this could be due to the presence of iron in it while the deck-brow colour of chachaga ore is largely due to the high percentage of iron and iron oxide in the ore. The black colouration of Maitunbi ore may be likely do decayed organic materials.

Table 3: Physical Properties of Gold Ore.

Local	pH	Colour
Paiko	6.55	Brown
Chanchaga	6.93	Dark-Brown
Garatu	6.59	Brow
Maitunbi	6.80	Slightly black

The results of the particle size distribution for gold ore from Chanchaga, Paiko, Garatu and Maitunbi are shown in figure 8. The particle size distribution for both Chanchaga and Maitunbi has some sililarities as a result of the same method of manual granding of the ore while Paiko and Garatu are abit different because the samples were collected from different milling machine. It was noticed that in all the samples gold particles were clearly seen at 0.3 mm and 0.15 mm (more pronuced). Gold particles at other sieve sizes were not seen, this might be due to poor gold libration at those particle sizes.

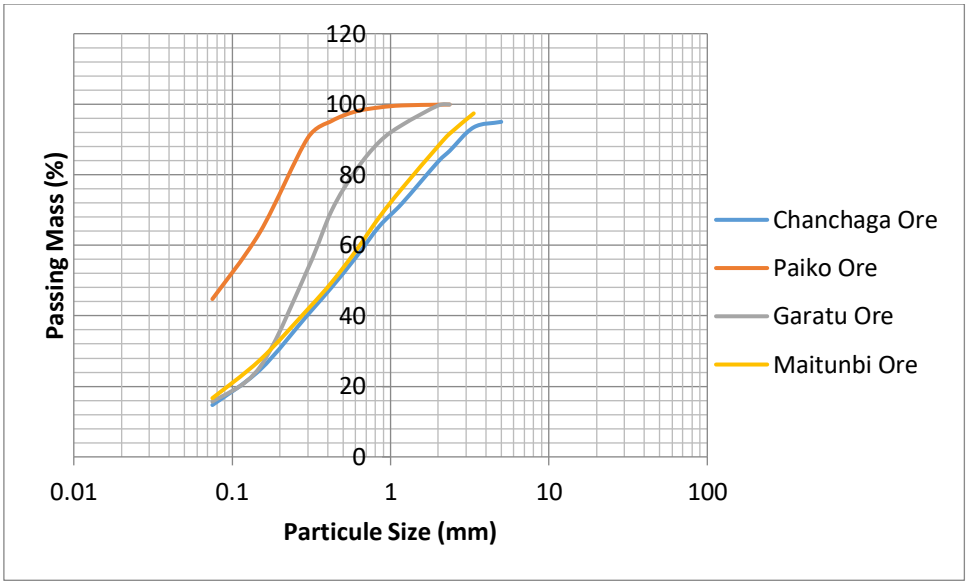

Figure 8: Particle size distribution of gold ore samples from Niger State

4. Conclusion

The high presence of high percentage of gold in ore samples from Paiko (1.231 %), Garatu (0.724 %), Chanchaga (1.01 %) and Maitunbi (0.875 %) are indications of the potentiality of the ores for gold mining. These could be used as raw material for jewelry, medical and electronic industries. The high percentage of the gold and low sulphur content in (Garatu, ,0.35 %, and Maitunbi, 0.017 %) shows that the extraction of gold from these sites can be done by an environmentally friendly method using coal-oil agglomerate and borax method compared to the current non environmentally friendly method of mercury extraction in Niger State. Visible gold liberation was recorded at 0.3 mm and 0.15 mm. The high silicon (33.6 % in Paiko, 25.07 % in Garatu, 10.8 % in Chanchaga and 19 % in Maitunbi) and silica content (71.905 % in Paiko, 53.658 % in Garatu, 40.717 % in Maitunbi and 23.16 % in Chanchaga) in the ore samples is a great potential that the government can harness for economic purpose. As silicon is one of the major components used in the production of computer processor in computer industry and as well as the production of solar energy converter.

References

Ariffin, K. S. (2006). Geology, Genesis of Gold Deposit and Occurrences in Malaysia. School of Materials and Mineral Resources Engineering Universiti Sains Malaysia.

Aydin, B., Basturkcu, H., Gul, A. (2014). Influence of Pre-aeration on Cyanide Leaching of a Non-refractory Sulphide Gold and Silver Ore. *Physicochemical Problems of Mineral Processing.* 51(2) Pp647-660.

Blueprint (2016). An Insight into Nigeria's Gold Deposit. Retrieved from www.blueprint.ng/an-insight-into-nigerias-gold-deposite/, October 23, 2017.

Idrisa, W. E., Nasiru, A. S., Abba, K. A. and Umar, A. A. (2013). Extraction and Quantification of Silicon from Silica Sand obtained from Zauma River, Zamfara State, Niferia. European Scientific Journal. Vol. 9 (15). Pp 160-168

Investment Opportunities and Export Potentials in Niger State, Niger State, Nigeria (IOEPN, 20016). Presentation of Niger State at the 1st Northern Central Nigerial- China, Business and Investment Forum. Venue: Hilton Hotel, Guangzhou, China, 13th -14th April,

Marcello, Veiga M., Stephen, M. Metcalf, Randy, F. Baker, Bern Klein, Gillian Davis, Andrew Bamber, Shefa Siege, Patience Singo (2006). Removal of Barriers to Introduction of Cleaner Artisanal Gold Mining and Extraction Technologies. Global Mercury Project, Coordination Unit, Vienna. Retrieved from www.globalmercury.org/, June 15, 2018.

Ogundare, O. D., Mosobalaje, O. A., Adelana, R. A., Olusegun, O. A. (2014). Beneficiation and Characterization of Gold from Itagunmodi Gold Ore by Cyanidation. *Journal of Minerals and Materials Characterization and Engineering,* 2, 300-307.

Robinson, J.J. (1988). The extraction of gold from sulphidic concentrates by roasting and cyanidation. J. S. At,. Inst. Min. Metal vol. 88(4) pp. 117-130.

Rojas, R. H., Torem, M. L. Merma, A.G., Bertolino, M. L. and Monte, M.B.M., Gomes, F.M (2015).Mineralogical Characterization of a Gold Ore Through a Computational liberation Analysis. Retrieved from www.cetem.gov.br>CAC00610013 on May 2018.

Steel Raw Material Exploration Agency Malali, Kaduna (SRMEAMK, 1989). Preliminary Investigations of the Mineral Resources of Niger State. Niger State Development Company Ltd. Project NSDC/INV/188/Vol.1/167.

United Nations Environment Programme (USEPA) (2012). Reducing Mercury Use in Artisanal And Small-Scale Gold Mining. A UNEP Global Mercury Partnership document produced in conjunction with Artisanal Gold Council. Retrieved from www.artisanalgoldcouncil.org

Veiga, M M, Maxson, P A and Hylander, L D (2006). Origin and consumption of mercury in small-scale gold mining. Journal of Cleaner Production, 14 (3-4): 436-447

Weick R. J (1994). Gold Occurences. New Foundland Labrador, Canada. Retrieved January 14,1018 from http://www.gov.nl.ca/

Zhu Y; Fang, A. and Juanjuan T. (2011). Geochemistry of hydrothermal gold deposits: A Review. Geoscience Frontiers 2(3) Pp 367-374.

Synthesis of Titanium Dioxide Nanoparticles

Mustapha S.[1,3], Ndamitso M.M.[1,3], Abdulkareem S.A.[2,3], Tijani J.O.[1,3]
Etsuyankpa M. B. and Sumaila A.[1,3]

[1]Department of Chemistry, Federal University of Technology, PMB 65, Bosso Campus, Minna, Nigeria
[2]Department of Chemical Engineering, Federal University of Technology, PMB 65, GidanKwano Campus, Minna, Niger State, Nigeria
[3]Nanotechnology Research group, Center for Genetic Engineering and Biotechnology, Federal University of Technology, Minna, PMB 65, Niger State, Nigeria
E-mail: **saheedmustapha09@gmail.com**

Abstract

Different techniques such as hydrothermal, co-precipitation, chemical vapour deposition, microemulsion and sol-gel among others have been used for the synthesis of titanium dioxide nanoparticles (TiO_2-NPs). Among these, the sol-gel synthesis is a promising method because of its mild experimental conditions. This review summarized this commonly used technique (sol-gel) and other steps via this, for the synthesis of TiO_2-NPs and also facile factors which include pH and calcination temperature that affect synthesized TiO_2 nanoparticles. It was found that these factors affect the agglomeration of titanium nanoparticles.

Keywords: Sol-gel, synthesis, calcination temperature, TiO_2 nanoparticle

1. Introduction

Nanotechnology is a field of science and technology for the production of nanoscale materials with unique properties which are widely used in modern material sciences research. The synthesis involved in the production of these nanoscale-based materials using different techniques including chemical, physical, irradiation, and biological methods have resulted in environmental pollution [1]. Therefore, the quest for clean, safe, eco-friendly, and less or non-toxic techniques for the synthesis of nanoparticles is insatiable. However, through academic and technological research approach, the use of non-toxic, inexpensive, highly photoactive, and easily synthesizable nanoparticles could be obtained.

Titanium oxide (TiO_2) has been considered a non-toxic nanomaterial that possesses a high concentration of hydroxyl groups, stability and catalytic efficiency [2]. Titanium dioxide is also known as titania naturally exists in three forms namely anatase, rutile, and brookite. Both the anatase and rutile forms have tetragonal shapes while brookite has orthorhombic shape. Other phases that can be produced synthetically are TiO_2B, TiO_2H (hollandite-like form), TiO_2R (ramsdellite-like form), TiO_2II (α-PbO_2-like form), akaogiite (baddeleyite-like form, 7 coordinated Ti), TiO_2O, cubic form, and TiO_2 OII (cotunnite $PbCl_2$ like) [3].

There are copious methods of preparing titanium oxide nanoparticles, including sol-gel, hydrothermal, precipitation, chemical vapour deposition, microemulsion, laser ablation and thermal decomposition of organometallic precursor etc. The commonly used methods were hydrothermal, co-precipitation, sol-gel and microemulsion. Among these, the sol-gel method has been found to be the most outstanding due to the generation of high-quality surface morphologies [4].

Titanium dioxide nanoparticles (TiO_2-NPs) have been utilized in industrial and commercial applications for solar cells, memory devices, adsorption of pollutants and wastewater purifications [5-7]. Although, numerous investigations have been carried out on the practical applications of these nanoparticles. The major setbacks have been the cost of the preparation processes. The production of TiO_2 nanoparticles equally faced with these problems. Here, we reported a short review on the commonly used technique for the synthesis of TiO_2 nanoparticles.

2. Methods for TiO_2 Nanoparticles Synthesis

Several techniques have been employed for the synthesis of titanium oxide nanoparticles which include laser ablation, solvothermal, precipitation, sol-gel, hydrothermal, hydrolysis, microemulsion and chemical vapour deposition. These methods have been categorized into three major classes: (1) liquid phase (2) gas phase and (3) vapour phase.

The production of TiO_2 is being certified by their properties, economical operations, and environmental friendliness during application. Thus, among these techniques, wet chemical methods have been known to be the best and these include microemulsion, hydrothermal/solvothermal, precipitation and sol-gel which have been well studied. But the sol-gel method is reported to be simple, economical and most often used to synthesize TiO_2 nanoparticles. However, there are still ongoing researches on the synthesis of TiO_2 using sol-gel. Scholars came up with logical steps in the production of these nanoparticles and were found indomitable in various forms of applications.

2.1 Sol-gel method

Among the wet chemical methods, sol-gel is a sophisticated method for the production of titanium dioxide. The method helps to control the stability and phase formation of the precursor. During this process, an integrated network gel is produced while the metal alkoxides serve as the typical precursor on the addition of water to form a colloid. The formation of colloid is as a result of hydrolysis and polycondensation reactions. However, the four stages

that occur during sol-gel formation are hydrolysis, condensation, growth, and agglomeration of particles.

This process proceeds by hydrolytic polycondensation of titanium precursors being alkoxides or chlorides in the presence of solvents, modifiers, and organic templates. The reaction starts with hydrolysis, which is the formation of Ti-OH moieties by the substitution reaction of water with Ti-OR groups. The precursors undergo condensation reactions to produce Ti-O-Ti by oxolation or Ti-OH-Ti bonds by olation[8]. The mechanisms for the formation of TiO_2 nanoparticles are presented as follows:

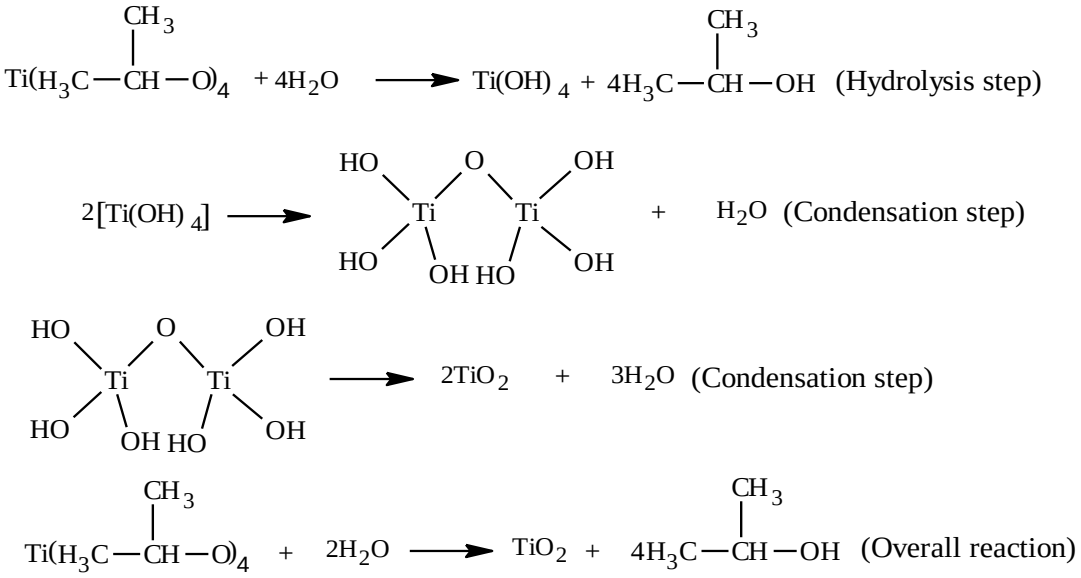

Scheme 1: Hydrolysis and condensation reactions of titanium isopropoxide for TiO_2 production [9].

In general, the sol-gel method consists of the transformation of a system from a liquid phase (sol) toward a solid phase (gel).The various precursors such as organic alkoxides and acetates, in addition to inorganic salts like chlorides, are utilized for the synthesis of nanoparticles. Alcohols are greatly used among various kinds of solvents, although some other solvents could be used for some alkoxides as depicted in scheme 2.

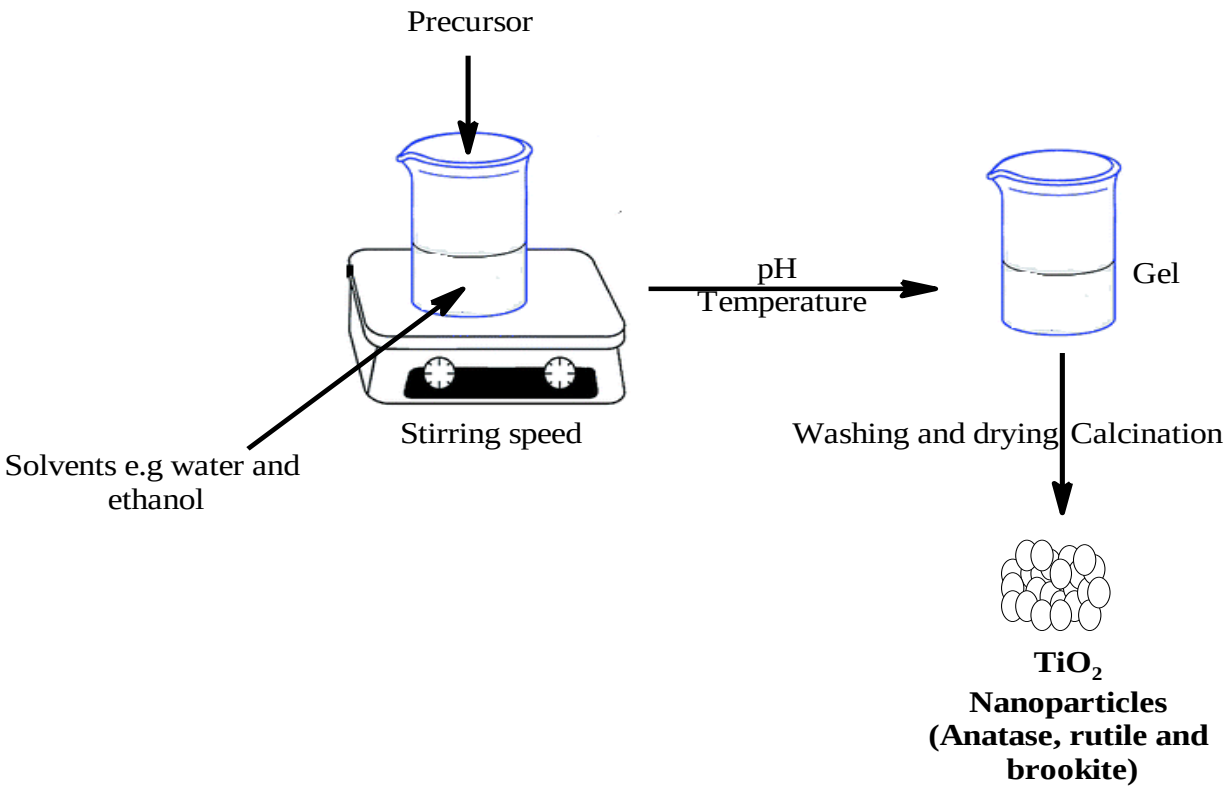

Scheme 2: Preparation of TiO_2 nanoparticles using Sol-gel technique

Some parameters such as the order of addition of reactants, the temperature, stirring time, the ratio of water to titanium, the solubility of reagents in the solvent and the pH affect the homogeneity of the gel. Calcination temperature and pH are paramount factors which help in giving the nanoparticles better surface areas. Among the researchers who worked on the production of TiO_2-NPs using the sol-gel method to examine some of the properties of the produced nanoparticles using various instruments such XRD (X-ray diffraction), SEM (scanning emission microscope), PL (photo-luminescence), HRTEM (high-resolution transmission microscopy), BET (Brunauer Emmett Teller), TGA (thermogravimetry analysis) and SAED (selected area (electron) diffraction) were Sharma et al. [4], Kashyout et al. [9], Phonkhokkong et al. [10], Khan et al. [11], Vijayalakshmi and Rajendra [12], Kavitha *et al.* [13], Salah et al. [14] and Bessekhouad et al.[15].

3. Factors affecting TiO_2 nanoparticles

The forms of TiO_2 depends on the arrangement of titanium and oxygen atoms in the crystal lattice. Therefore, it has been reported that the solvent, precursor type, particle size, calcination temperature, pH, additives, and stirring time affect sol-gel synthesized TiO_2 nanoparticle

phases [16-17]. It has been reported that the particle sizes of the synthesized nanoparticles produced increase just as their surface areas increase [18-19].

3.1 Effect of calcination

Calcination is a thermal treatment process in the absence or a limited supply of air required for thermal decomposition. The effect of calcination temperature on the phase of TiO_2 from 100 to 1000 °C was evaluated by Pavel and Radovan [19]. The authors reported that at 500 °C, the observed peaks conform to anatase phase but as the peak grows to 800 °C, the anatase phase was transformed to rutile. They concluded that 600 °C was convenient to achieve higher efficiency nanoparticles due to the finer grains of the anatase phase of TiO_2 synthesized.
Abdullahi et al. [20] demonstrated the effect of calcination temperature on nanocomposite used in the photocatalytic degradation of phenol under the visible light. The nanocomposite (ZnO/TiO_2) at 600 °C was found to be more effective in the destruction of the pollutant as a result of the formation of hydroxyl radical on the surface of the nanocomposite. They also deduced that the formation of anatase phase enhanced the degradation of the targeted pollutant.

Aphairaj et al. [21] calcined TiO_2 powder at 300-1000 °C. At a temperature of 300-500 °C, the length of the nanotubes-nanofibers structure of the calcined samples was smaller than the sample before calcination and was aggregated. As the temperature increased, the surface morphology of the calcined sample had increased particle sizes attributable to the phase transformation change from anatase to rutile.

Thus, calcination temperature controls the crystalline phase of a nanoparticle of its homogeneity and surface area. Also, the particle size of TiO_2 was found to increase with calcination temperature, suggesting that the effect of different calcination temperatures could help in the degradation of pollutant substances.

3.2 Effect of pH

The pH medium significantly affects crystal structure and surface morphology such as the size and the entanglement of TiO_2 nanostructures [22-24]. Due to the small particle size, the Van der Waals interaction is significant; this interaction increases exponentially as the particle size decreases. These facts favour the growth of clusters. Ibrahim and Sreekantan[25] reported that lower acidity promotes anatase structure while high acidity results in rutile phase formation. This shows that the degree of crystallinity of anatase is pH dependent and lower acidity enhances the crystallinity, which also promotes the formation of big crystallite size. Mutuma et al. [26] reported the formation of pure TiO_2 rutile phase calcined at 800°C and mixed phase (anatase and brookite) at 600 °C in a strongly acidic medium. While in the investigation

reported by Cassaignon et al. [27], a rutile crystalline phase was formed at the pH conditions less than 4.5 and only anatase structure formed at pH greater than 4.5.

However, the possibility of anatase structure in acidic medium is apparent. Therefore, investigation of TiO_2 nanoparticles synthesized by a facile sol-gel method under acidic and basic medium is necessary for the clarification of the crystal forms, microstructure and optical properties of TiO_2 nanoparticles.

4. Conclusion

TiO_2-NPs have been extensively investigated during the last decade due to their wide view of applications. In summary, it is observed that the synthesis of this nanomaterial was mostly done using the sol-gel technique due to the high quality of TiO_2 nanoparticles produced. The sol-gel technique has emerged as a promising processing route for the synthesis of nanosized particles because of the simplicity and high purity nanopowders resulting from the availability of high purity chemicals raw materials. Changes in composition, structure, and morphology of the TiO_2 nanoparticle are strictly dependence with the pH and calcination temperature.

Acknowledgements

The authors appreciate the financial supports received from the Tertiary Education Trust Fund (TETFund) of Nigeria under a grant number TETFUND/FUTMINNA/2017/01 is highly appreciated.

References

[1] M. Troester, H. Brauch, and T. Hofmann (2016). Vulnerability of drinking water supplies to engineered nanoparticles Water Research **96**: 255-279.

[2] H. Qian, Y. Hu, Y.Liu, M. Zhou, and C. Guo(2012). Electrostatic self-assembly of TiO_2 nanoparticles onto carbon spheres with enhanced adsorption capability for Cr(VI). Materials Letters**68**: 174-177.

[3] S.G. Ullatti, and P. Periyat(2017). Sol-Gel Synthesis of Titanium Dioxide. Sol-Gel Materials for Energy. Environment and Electronic Applications **1**: 271-283.

[4] A. Sharma, R.K. Karn, and S.K. Pandiyan (2014). Synthesis of TiO_2 Nanoparticles by Sol-gel Method and Their Characterization. Journal of Basic and Applied Engineering Research **1**(9): 1-5.

[5] K. Zhang, K.C. Kemp, and V. Chandra(2012). Homogeneous anchoring of TiO_2 nanoparticles on graphene sheets for waste water treatment. Materials Letters **81**: 127-130.

[6] Y. Li, W. Zhang, X. Li, and Y. Yu(2014). TiO_2 nanoparticles with high ability for selective adsorption and photodegradation of textile dyes under visible light by feasible preparation. Journal of Physics and Chemistry of Solids **75**: 86-93.

[7] H. Lu, J. Wang, M. Stoller, T. Wang, Y. Bao, and H. Hao (2016). An Overview of Nanomaterials for Water and Wastewater Treatment. Advances in Materials Science and Engineering **1**: 1-10.

[8] S.Z. Islam, S. Nagpure, D.Y. Kim, and S.E. Rankin(2017). Synthesis and Catalytic Applications of Non-Metal Doped Mesoporous Titania. Inorganics **5**(15): 1-43.

[9] A.B. Kashyout, M. Soliman and M. Fathy(2010). Effect of preparation parameters on the properties of TiO_2 nanoparticles for dye sensitized solar cells. Renewable Energy **35**: 2914-2920.

[10] T. Phonkhokkong, S. Thongtem, C.S. Thongtem, A.Phuruangrat,and W. Promnopas(2016). Synthesis and Characterization of TiO_2Nanopowders for Fabrication of Dye Sensitized Solar Cells. Digest Journal of Nanomaterials and Biostructures **11**(1): 81-90.

[11] M.A. Khan, M.S. Akhtar, and O. Yang(2010). Synthesis, characterization and application of sol-gel derived mesoporous TiO_2 nanoparticles for dye-sensitized solar cells. Solar Energy **84**: 2195-2201.

[12] R. Vijayalakshmi, and V. Rajendran(2012). Synthesis and characterization of nano-TiO_2 via different methods. Archives of Applied Science Research **4**(2): 1183-1190.

[13] M. Kavitha, C. Gopinathan, and P. Pandi(2014). Synthesis and Characterization of TiO_2Nanopowders in Hydrothermal and Sol-Gel Method. International Journal of Advancements in Research and Technology **2**(4): 102-108.

[14] A. Saleh, F.A. Rasin, and M.A. Ameen(2009). TiO_2 nanoparticles prepared by sol-gel. Journal of Materials Science and Engineering **3**(12): 81-84.

[15] Y. Bessekhouad, D. Robert,and J.V. Weber (2003). Preparation of TiO_2 nanoparticles by Sol-Gel route. International Journal of Photoenergy**5**: 153-158.

[16] L. Agartan, D. Kapusuz, J. Park, and A. Ozturk(2013). Effect of H_2O/TEOT ratio on photocatalytic activity of sol-gel derived TiO_2 powder, Nanomater. Energy**2**: 280-287.

[17] M. Islam,and S. Basu(2015). Effect of morphology and pH on (photo) electrochemical degradation of methyl orange using TiO_2/Ti mesh photocathode under visible light. Journal of Environmental and Chemical Engineering **3**: 2323-2330.

[18] Y. Chen, X. Xu, J. Fang, G. Zhou, Z. Liu, X. Wu, J. Chu,and X. Zhu (2014). Synthesis of BiOI-TiO_2 Composite Nanoparticles by Microemulsion Method and Study on Their Photocatalytic Activities. The Scientific World Journal **1**: 1-8.

[19] K. Pavel, and K. Radovan(2015). The Effect of Calcination on the Structure of Inorganic TiO_2 Nanofibers. Oct 14th-16th2015, Brno, Czech Republic, EU. NanoCon.

[20] N.S.A. Abdullah, S. So'aib, and J. Krishnan(2017). Effect of Calcination Temperature on ZnO/TiO_2 Composite in Photocatalytic Treatment of Phenol under Visible Light. Malaysian Journal of Analytical Sciences **21**(1): 173-181.

[21] D. Aphairaj, D.Wirunmongko, P.Chaloey-arb, S. Pavasupree, and P. Limsuwan(2011). Effect of calcination temperatures on structures of TiO_2 powders prepared by hydrothermal method using Thai leucoxene mineral. 9thEco-Energy and Materials Science and Engineering Symposium, Chiang Rai, Thailand, 25-28 May 2011

[22] J. Xue, Q.Shen, F.Yang, W. Liang, and X. Liu (2014). Investigation on the influence of pH on structure and photoelectrochemical properties of CdSe electrolytically deposited into TiO_2 nanotube arrays, Journal of Alloys and Compound**607**: 163-168.

[23] A.M. Selman, Z. Hassan, and M. Husham (2014). Structural and photoluminescence studies of rutile TiO_2 nanorods prepared by chemical bath deposition method on Si substrates at different pH values. Measurement **56**: 155-162.

[24] V.S. Mohite, M.A. Mahadik, S.S. Kumbhar, V.P. Kothavale, A.V. Moholkar, K.Y. Rajpure, and C.H. Bhosale (2015). Photoelectrocatalytic degradation of benzoic acid usingsprayed TiO_2 thin films. Ceramic International**41**: 2202-2208.

[25] S.A. Ibrahim, and S. Sreekantan (2010). Effect of pH on TiO_2 nanoparticles via sol gel method. International Conference on X-Rays & Related Techniques in Research & Industry, June 9-10, 2010, Aseania Resort Langkawi, Malaysia,pp. 84-87.

[26] B.K. Mutuma, G.N. Shao, W.D. Kim, and H.T. Kim (2015). Sol-gel synthesis of mesoporous anatase-brookite and anatase-brookite-rutile TiO_2 nanoparticles and their photocatalytic properties, Journal of Colloid Interface and Science**442**: 1-7.

[27] S. Cassaignon, M. Koelsch, and J.P. Jolivet (2007). From $TiCl_3$ to TiO_2 nanoparticles (anatase, brookite and rutile): thermohydrolysis and oxidation in aqueous medium. Journal of Physical Chemistry and Solids **68**: 695-700.

Physicochemical Properties of Forest Surface Soils in Kogi State, Nigeria

Azeez, A.A[1]*. Iyaka, Y.A[2] . & Ndamitso, U.U[3].

[3&2]Department of Chemistry, Federal University of Technology, Minna,
[1]Department of Chemistry, Kogi State College of Education, Ankpa.
[3]Muhd.ndamitso@futminna.edu.ng,
[2]iyaka.yahaya@futminna.edu.ng,
[1]Azeezakeem25974@gmail.com
* Corresponding author

Abstract

Soil is an essential component for growth of plants and survival of organisms. In this work, the soil samples are forty forest surface soils of Kogi state randomly collected at the depths of 0–20cm and subjected to physicochemical examination using standard routine laboratory tests to assess the quality of soil. In addition, mean, range and Pearson's moment correlation were employed to analyze the data. The results showed that sand, silt and clay contents ranged from 51.80 % - 94.00 %, 3.50 % - 31.00 % and 2.00 % - 22.60 % respectively. Texturally, the soils were predominantly sandy loam and loamy sand with sand dominating the particle fractions of the soil. Soils were moderately acidic with mean pH values 5.46 ranging from 4.47-6.84. Electrical conductivity mean value of the saturation extract was 0.237 dSm^{-1} which ranged from 0.036 dSm^{-1} to 0.574 dSm^{-1} indicating non-saline nature of the soils and suitable for plants growth and soil microbial processes. The soils were non- calcareous in nature and having calcium carbonate content ranges from 0.08 % - 2.00 %. The available mean of soil organic matter was 8.85 % (ranged from 3.19 % - 13.35 %) indicating high soil organic matter. These results showed that organic matter is better protected and had potentials for storing organic carbon of appreciable concentration. Similarly, the mean of cation exchange capacity showed 15.01 $cmolckg^{-1}$ (ranged 12.20 $cmolc.kg^{-1}$-18.60 $cmolckg^{-1}$) indicating moderate. Finally, pH showed strong positive correlation with soil organic matter, cation exchange capacity and calcium carbonate content while soil electrical capacity showed negative correlation with pH, soil organic matter and calcium carbonate content. From this study, it was ascertained that these forest soils possess potential to hold nutrients and make it readily available for plant to absorb which in turn possess the capacity to support ecosystems.

Keywords: forest, physio-chemical properties, soil nutrient, surface soil

Introduction

Soil is a vital part of the Earth. It serves as a natural medium for plants growth (Osuocha *et al*., 2016). Soils are the naturally occurring physical materials covering of the earth's surface and a mixture of organic matter, minerals, gases, liquids and organisms that together support life. The earth's body of soil is the pedosphere (skin of the earth), which has four functions namely: a medium for plant growth; a means of water storage, supply and purification; a modifier of earth's atmosphere and a habitat for organisms. All of which, in turns, modify the

soil. Soil, as an integral element of the natural environment, is a non-renewable resource (Massas *et al*., 2013). According to Keesstra *et al*. (2016), soils play an important role in global food security, water security, biofuel security and human health. To Decock *et al*. (2015), soil is a key component of the earth system as it controls the geochemical, biological, erosional and hydrological cycles and offers services, goods and resources for human kind.

Soil is a significant determinant of the economic status of nations. Soil ecosystem services fulfils human needs (Robinson *et al*., 2012), assigning economic value to things that contribute to human well-being. Based on this, soil quality has received great attention in recent years (Sinha *et al*., 2014). Specifically, Khormali *et al* (2009) refers to soil quality as a concept that includes soil physical, chemical and biological factors and it is used as a framework for the evaluation of soil. The quality of soils does not depend on its ability to supply adequate nutrients alone but the nutrients must be in the right proportion as needed by plants (Ayeni and Adeleye, 2011). In addition, high quality soils not only produce better food and fibre, but also help to establish natural ecosystems and enhance air and water quality (Griffiths *et al*., 2010).

The quality of growth and reproduction of forest cannot be understood without the knowledge of its soil nutrient. The soil and vegetation have a complex interrelation, because they develop together over a long period of time, the selective absorption of nutrient elements by different tree species and their capacity to return them to the soil brings about changes in soil properties (Sharma *et al*., 2010). Soil helps secure and renew the forest. Forests also help secure and renew the soil. The forest covers and protects the soil from extreme heat and cold while slowing the natural forces of erosion like water, wind, and gravity. The nutrients strength of a forest soil to maintain and support the plant growth generally depends on its physical, chemical and biological properties. Researchers have reported that the nature of parent material has been found to influence development and characteristics of soils (Umeri *et al*., 2016). Soil sustains the forest and provides raw materials for its life: fallen leaves, woody debris, and dead animals recycle through the soil.

The estimation of soil available nutrient contents in a complex heterogeneous system is of a great pedological as well as ecological importance (Olojugba and Fatubarin, 2015). Trees affect the forest ecosystem by manipulating its constituents prominent to changing future forest vegetation (Frouz *et al*., 2013c). Tree cover in turn, influences the growth and development of physical and chemical properties of soil. These properties sustain and support the plant growth in forest soil. Soil physical and chemical properties play a central role in transport and reaction of water, solutes and gases in soils, their knowledge is very important in

understanding soil behaviour to applied stresses, transport phenomena in soils, hence for soil conservation and planning of appropriate agricultural practices (Olorunfemi *et al*.,2018).

A good knowledge of the variations of soil physical and chemical properties their interactions as it relates to micronutrient status is essential for good land evaluation which is a pre-requisite for sound land use planning (Lawal *et al*., 2013). Assessing soil physicochemical properties are used to understand the potential status of nutrients in forest soils. This knowledge can ascertain whether the forest soils are useful to meet plants requirement for rapid growth. For this reason, the present study attempts to evaluate the physiochemical properties of forest surface soils in Kogi state of Nigeria.

Materials and Methods

Description of the Study Area

This research was conducted in the forest vegetative sites of Kogi state, Nigeria. The capital of Kogi state (Lokoja) is located on the confluence of Rivers Niger and Benue at Lokoja on Latitude 6° 44' North and Longitude 7° 44' East. Going by the present composition of the state, Kogi State is quintessentially Nigeria, with three dominant ethnic groups namely; Igala, Ebira and Okun (Yoruba) and several minorities (Omotola, 2008). Kogi state has a total land area of 28,313.53 square kilometres and on the basis of the 1991 Nigerian national population census, the total population of Kogi state was 2,141,756 (Ali *et al*., 2012).

Kogi state just as many other states in Nigeria is blessed with natural resources. It has expensive fertile land for agriculture all over the state, coal at Okobo, Ankpa, huge deposits of iron ore at Ajaokuta and limestone at Obajana. The climate of the Kogi state is a tropical climate with two distinct seasons [rainy season (March – October) and dry season (November – March)]. The rainfall regime shows double maxima which is separated by a comparatively low rainfall period (dry period) in August called August Break. The mean annual rainfall ranges from 1,560mm at Kabba in West to 1,808mm at Anyigba in the East. Average monthly temperature varies from 17ºC to 36.2ºC. The temperature shows some variation throughout the years. The state is known for cultivation of arable crops such as yam, cassava, maize, groundnut, cowpea etc (Omotola, 2008).

Sample Collection and Preparation

A total of 40 composite soil samples were collected at forty forest locations within villages of East, Central and West of Kogi State and used for this study. These forests are uncultivated and comprise of shrubs, woodlands and deciduous trees without the protection of the state forest reserve agency. From each forest location, five soil samples were randomly collected in different points and pooled together to form a composite sample for that location. They were collected from surface at the depths of 0–20 cm by scooping surface soils of the sampling areas using a stainless steel hand trowel. After collection, each composite was then labelled, transferred to a separate clean plastic container and transported to the laboratory.

Prior to analysis, the composite soil samples were air- dried at room temperature for two weeks in the laboratory, ground (using a ceramic mortar and pestle), sieved (using a 2-mm sieve) and stored in well labelled sample plastics for laboratory analysis. The prepared soil samples were analyzed by means of internationally-accepted classical methods.

Determination of Physico-chemical Properties

Soil particle sizes were determined using the hydrometer method described by Gee and Or (2002) and classification was carried out using the USDA classification system (Soil Survey Staff, 2009). The pH and Electrical conductivity of the soil samples were measured in distilled water at ratio 1:1 as demonstrated by Osayande *et al*. (2015). Calcium carbonate content was estimated following the procedure described by Rowell (1994). The organic carbon was determined using the Walkley - Black wet oxidation procedure and the soil organic matter content was determined by multiplied organic carbon with 1.724 (Nelson and Sommers, 1982). The cation exchange capacity (CEC) at pH 7.0 was determined following the procedure described by Chapman (1965).

***Quality** Control*

All reagents and chemicals were of high analytical grade and high purity distilled water was used for all dilutions. All glassware and plastic containers used were soaked in 10% v/v HNO_3 solution overnight (Onianwa, 2001) and rinsed thoroughly with distilled water before used to avoid contaminants.

Statistical Analysis

Data obtained was statistically analyzed using mean and range. Pearson's correlation analysis was also used to establish significant relationship between the selected physiochemical properties of soils.

Results and Discussion

Table 1: Particle Size Distribution of the Experimental Forest Surface Soils

Sampling Site	Sand (%)	Silt (%)	Clay (%)	Texture	Silt/Clay	Silt and Clay (%)

1	60.50	25.00	14.50	Sandy loam	1.72	39.50
2	62.50	20.50	17.00	Sandy loam	1.21	37.00
3	86.00	8.50	5.50	Sandy	1.55	14.00
4	55.50	25.90	18.60	Sandy loam	1.39	44.50
5	62.10	21.00	16.90	Sandy loam	1.24	37.90
6	90.00	6.00	4.00	Sandy	1.50	10.00
7	82.00	10.00	8.00	Loamy sand	1.25	18.00
8	54.90	28.50	16.60	Sandy loam	1.72	45.10
9	63.20	18.90	17.90	Sandy loam	1.06	36.80
10	67.50	17.30	15.20	Sandy loam	1.14	32.50
11	56.90	26.40	16.70	Sandy loam	1.58	43.10
12	77.00	12.90	10.10	Loamy sand	1.28	23.00
13	80.10	10.90	9.00	Loamy sand	1.21	19.90
14	85.40	8.90	5.70	Sandy	1.56	14.60
15	71.50	15.80	12.70	Loamy sand	1.24	28.50
16	92.00	4.70	3.30	Sandy	1.42	8.00
17	58.90	30.00	11.10	Sandy loam	2.73	41.10
18	52.10	31.00	16.90	Sandy loam	1.83	7.90
19	75.00	14.50	10.50	Loamy sand	1.38	25.00
20	59.30	26.40	14.30	Sandy loam	1.85	40.70
21	56.90	26.00	17.10	Sandy loam	1.52	43.10
22	94.00	3.50	2.50	Sandy	1.40	6.00
23	59.60	22.00	18.40	Sandy loam	1.20	40.40
24	73.90	18.00	8.10	Loamy sand	2.20	26.10
25	66.80	18.30	14.90	Sandy loam	1.23	33.20
26	76.00	13.00	11.00	Loamy sand	1.18	24.00
27	93.00	5.00	2.00	Sandy	2.50	7.00

28	66.50	21.30	12.20	Sandy loam	1.75	33.50
29	69.50	18.80	11.60	Sandy loam	1.62	30.40
30	71.20	14.90	13.90	Loamy sand	1.07	28.80
31	90.10	6.00	3.90	Sandy	1.54	9.90
32	76.20	13,80	10.00	Loamy sand	1.38	23.80
33	51.80	25.60	22.60	Sandy loam	1.13	48.20
34	81.00	11.00	8.00	Loamy sand	1.38	19.00
35	72.10	18.50	9.40	Loamy sand	1.97	27.90
36	89.40	6.40	4.20	Sandy	1.52	10.60
37	79.10	12.50	8.40	Loamy sand	1.49	20.90
38	68.10	18.90	13.00	Sandy loam	1.45	31.90
39	82.90	10.00	7.10	Loamy sand	1.41	17.10
40	57.40	24.00	18.60	Sandy loam	1.29	42.60
Overall mean	71.70	16.77	11.53	Loamy sand	1.50	28.35
Overall range	51.80-94.00	3.50-31.00	2.00-22.60		1.06-2.73	6.00-48.20

Soil particle distribution of Kogi State forest surface soils in Table 1 showed that, the overall mean of sand fraction was 71.70% (ranged 51.80%-94.00%), silt had 16.77% (ranged 3.50%-31.00%) and clay had 11.53 % (ranged 2.00%-22.60%). Thus sand fraction was the highest, followed by silt and then clay. This was in agreement with the findings of Adugna and Abegaz (2016) that found sand content of soils of forestland to be the highest. The results revealed that the textures of Kogi state forest soils are mainly sandy loam and loamy sand textured at the surface. This was in conformity with what Uquetan *et al*. (2017) reported.

The silt/clay ratio ranged from 1.06 - 2.73 with mean 1.50 was above 0.15 indicating that the soils are relatively young with high degree of weathering potential. This is in harmony with report from Sharu *et al*. (2013) and Jimoh *et al*. (2016) on the soils. More so, the finding showed that mean of 28.35 % silt plus clay content ranged 6.00% - 48.20%. This is because about 48% of the soil samples contained more than 30% (clay + silt) contents. This has shown that silt plus clay content is a relatively important determinant of soil organic matter level in soils. The capacity of soils to maintain organic carbon is influenced by its clay plus silt content (Bationo *et al*., 2007).

Table 2: pH, Electrical Conductivity (EC), Calcium Carbonate Content ($CaCO_3$), Soil Organic Matter (SOM) and Cation Exchange Capacity (CEC) of the Experimental Forest Surface Soils

Sampling Site	pH	EC (dSm^{-1})	$CaCO_3$(%)	SOM (%)	CEC (cmolckg-1)
1	4.64	0.456	0.20	5.01	12.50
2	5.65	0.141	1.30	9.93	15.80
3	4.81	0.343	0.43	6.62	13.30
4	5.78	0.124	1.43	9.98	16.20
5	5.85	0.114	1.50	10.09	16.60
6	5.33	0.255	0.83	8.38	14.30
7	6.39	0.070	1.80	11.67	17.40
8	4.49	0.574	0.18	3.19	12.00
9	4.46	0.538	0.08	3.31	12.20
10	5.91	0.105	1.63	11.49	17.00
11	6.33	0.076	1.75	11.63	17.30
12	4.79	0.372	0.40	6.59	13.10
13	6.46	0.062	1.85	11.68	17.50
14	5.51	0.177	1.13	9.86	15.20
15	4.73	0.414	0.33	6.51	12.80
16	6.07	0.080	1.68	11.62	17.20
17	5.43	0.202	0.95	9.83	14.80
18	4.49	0.478	0.10	3.35	12.30
19	5.29	0.301	0.73	8.32	14.00
20	4.70	0.450	0.28	6.49	12.60
21	5.48	0.187	0.98	9.83	14.90
22	5.21	0.309	0.63	8.19	13.70
23	6.84	0.036	2.00	13.35	18.60

24	5.57	0.150	1.23	9.91	15.60
25	6.02	0.087	1.65	11.60	17.10
26	5.78	0.132	1.35	9.97	16.00
27	5.83	0.128	1.43	10.00	16.40
28	4.74	0.401	0.38	6.57	12.90
29	4.59	0.476	1.25	4.97	12.40
30	5.51	0.167	1.08	9.85	15.00
31	5.26	0.308	0.63	8.24	13.80
32	6.63	0.046	1.80	11.73	17.80
33	5.40	0.237	0.88	8.41	14.50
34	5.41	0.212	0.90	8.61	14.70
35	4.81	0.361	0.48	6.71	13.40
36	5.52	0.158	1.18	9.90	15.40
37	6.70	0.043	1.90	13.26	18.30
38	4.93	0.328	0.55	8.17	13.50
39	5.88	0.108	1.57	10.91	16.80
40	5.31	0.282	0.78	8.38	14.10
Overall Mean	5.50	0.237	1.03	8.85	15.01
Overall Range	4.47-6.84	0.036-0.574	0.08-2.00	3.19-13.35	12.20-18.60

Soil pH

The results in Table 1 also, show that the overall mean pH of studied Kogi state forest surface soils ranged from 4.47 to 6.84 with a mean value of 5.50 indicating that the soils were moderately acidic to almost neutral. The mean value reported in this study is within the range for optimum plant growth and in almost the same range with pH of some selected soils of rain forest zones of Delta state, Nigeria which ranged from 4.72 to 6.52 at the surface soils reported by Umeri *et al*. (2017). Also, these pH values are within those obtained by Osakwe and Akpoveta (2012) and consistent with findings of Uquetan *et al*. (2017) who observed pH of 4.2- 6.0 in natural forest of Akamkpa, Cross River State, Nigeria. In addition, the mean pH of

5.50 obtained is within the ideal pH range of 5.5-7.0 for optimum growth and nutrient availability to plants (Brady and Weil, 2010).

Electrical Conductivity (EC) of the soil

The overall mean EC of studied Kogi state forest surface sampled soils was 0.237 dSm^{-1} (ranged 0.036 dSm^{-1} to 0.574 dSm^{-1}). Here, all the soil sampled (100%) were salt free (i.e. no saline). However, the EC values recorded from these forest surface soils were within the normal range of less than 1 dS/m which are considered non-saline and suitable for plants growth and soil microbial processes according to Deshmukh (2012) and Nachtergaele et al. (2009). Similar result was also reported by Jimoh et al. (2016) in Northern Guinea Savanna zone of Nigeria.

Calcium Carbonate Content of the soil

The overall mean $CaCO_3$ content of the studied Kogi state forest surface soils showed 1.03% (ranged 0.08% to 2.00%). On the basis of $CaCO_3$ rating suggested by Nachtergaele et al. (2009), the soils of the studied soils were non- calcareous in nature.

Soil Organic Matter (SOM) content

Additionally, the overall mean percentage of soil organic matter of studied Kogi state forest surface soils was 8.85% (ranged 3.19% to 13.35%). These values of organic matter contents are considered high for forest soils. The higher SOM content exhibited by the topsoil in this study is also consistent with that demonstrated by Ahukaemere et al (2012); Straaten et al, (2015) and Adugna and Abegaz (2016) in forestlands. The higher organic matter under these forest lands might be attributed to continuous accumulation of un-decayed and partially decomposed plant and animal residues mainly in the surface soils of forestland.

Cation Exchange Capacity (CEC) of the Soil

The overall mean of CEC of the studied Kogi state forest surface soils was 15.01$cmolc.kg^{-1}$ (ranged 12.20 $cmolc.kg^{-1}$-18.60 $cmolc.kg^{-1}$). Soil CEC has been classified as very low (<10cmolc.kg-1), low (10-15$cmolc.kg^{-1}$), moderate (15-20$cmolc.kg^{-1}$) and high (>20$cmolc.kg^{-1}$) (Abe et al., 2010). On the basis of this classification, 50% of the surveyed forest sites have CEC values >15 cmol $kg^{-1}$and 50% have moderate CEC. CEC is an important property of soil because it is a useful indicator of soil fertility and nutrient availability for flora growth (Hazelton and Murphy 2007). Thus high SOM increases cation exchange capacity (CEC).

Table 3: Correlation between Studied Physico-chemical Properties of Soils

physico-chemical properties	Correlation coefficient (r)
Soil pH and SOM	0.92
Soil EC and pH	-0.59

Soil CEC and SOM	0.95
Soil pH and CEC	0.95
Soil pH and $CaCO_3$	0.98
Soil EC and SOM	-0.98

Table 3 showed relationship existed among soil physicochemical properties which positively or negatively, interfered with nutrient availability (Onwudike, 2015).

Based on the Pearson correlation coefficient data analysis, the observed soil pH showed significant positive correlation with SOM and the correlation coefficient is 0.92 which indicated the higher the pH (i.e. the lower the acidity level of the soil), the higher the SOM. Also, soil EC showed negative correlation with pH (r= – 0.59). This means that at low soil pH value, there is high soluble salt content and therefore high electrical conductivity. The research findings consistent with the study of Nur Aini et al. (2014) who reported that soil EC had significant negative relationship with the soil pH.

In addition, soil CEC was correlated with SOM for all the soils which showed correlation coefficient of 0.95. This means that, there is a strong correlation between the CEC values, and the amount of organic matter present in the soil as Organic matter is a major source of negative electrostatic sites. The research findings conform to the works of Olorunfemi et al. (2018) and Fasinmirin and Olorunfemi (2012) who all reported that soil samples with higher values of CEC were found to have high levels of organic matter and pH levels. More so, there is a significant positive correlation between soil CEC and pH with correlation coefficient of 0.95. This finding conform to the works of Olorunfemi et al. (2018) who all reported that soil samples with higher values of CEC were found to have high pH levels.

Further more, a positive correlation existed between soil pH and $CaCO_3$ with correlation coefficient of 0.98. This relationship was strong and significant which indicated that pH increased with increased in the amount of $CaCO_3$ present. Finally, organic matter was shown to correlate negatively with electrical conductivity (r = -0.98) suggesting that soils high in organic matter tend to favour the immobilization of soluble ions in soils. This indicated that soil EC decreased with an increased in SOM. This finding is supported by the works of Nelson et al. (2017) who all reported that SOM had significant strong negative relationship with the soil EC.

Conclusion and Recommendation

In conclusion, the forest soils in this studies area contain significant quantities of all the nutrients analysed. These forest soils proven to contain high soil organic matter, non-saline (i.e. free from salt) and non- calcareous in nature. Also, the soils were predominantly sandy loam and loamy sand and possess suitable pH for normal forest ecosystems. These soils have moderate CEC values and this might be due to their high organic matter, presence of low amount of $CaCO_3$ and very low soluble salt in the soil.

In addition, pH showed strong positive correlation with SOM, CEC and $CaCO_3$. Also, soil EC showed negative correlation with pH and SOM. Correlation results showed that relationships existing among soil physicochemical properties interfered with nutrient availability. This conforms to the findings of Tsozue et al. (2016) who showed that plant nutrient availability depends on relationships among soil physicochemical properties.

It is therefore recommended that, the conservation of these forests in Kogi state is an urgent need for the proper management practices of the forests which will in turn increase the quality of soils and the forest. This will reduce indiscriminate destruction of forest cover and protection of the top soils.

References

Abe, S. S., Buri, M. M., Issaka, R. N., Kiepe, P. & Wakatsuki, T. (2010). Soil fertility potential for rice production. *Journal of Agricultural Research quarterly*, Vol. 44(4), 343–355.

Adugna, A. & Abegaz, A. (2016). Effects of land use changes on the dynamics of selected soil properties in northeast Wellega, Ethiopia. *SOIL*, Vol. 2, 63–70.

Ahukaemere, C.M., Ndukwu, B.N. & Agim, L.C. (2012). Soil quality and soil degradation as influenced by agricultural land use types in the humid environment. *International Journal of Forest, Soil and Erosion*, Vol. 2 (4), 175–179.

Ali, S., Yusufu, B., Moses, S.E. & Abu, M. (2012). The Scramble for lugard house: Ethnic identity politics and recurring tensions in Kogi State, Nigeria. *Canadian Social Science*, Vol. 8(1), 130–135.

Ayeni, L.S. & Adeleye, E.O. (2011). Soil nutrient status and nutrient interactions as influenced by agro wastes and mineral fertilizer in an incubation study in the Southwest Nigeria. *International Journal of Soil Science*, Vol. 6 (1), 60–68.

Bationo, A., Kihara, J., Vanlauwe, B.,Waswa, B. & Kimetu, J. (2007). Soil organic carbon dynamics, functions and management in West African agroecosystems. *Agricultural systems*, Vol. 94, 13–25.

Brady, N.C. & Weil, R.R. (2010). *Elements of the nature and properties of soils*. 3rd edition. Pearson Education, Inc., Upper Saddle River, New Jersey. Pp. 74–89.

Chapman, H.D. (1965). *Cation exchange capacity*. In Methods of Soil Analysis (Number 9 in the Series Agronomy), Part 2, A. Black, ed., American Institute of Agronomy, Madi-son, Wisconsin, 891–901.

Decock, C., Lee, J., Necpalova, M., Pereira, E. I. P., Tendall, D. M. & Six, J. (2015). Mitigating N_2O emissions from soil: From patching leaks to transformative action. *Soil*, Vol. 1, 687–694.

Deshmukh, K.K. (2012). Studies on chemical characteristics and classification of soils from sangamner area, Ahmadnagar District, Maharastra. *Rasayan Journal of .Chemistry*, Vol. 5(1), 74–85.

Fasinmirin, J. T. & Olorunfemi, I. E. (2012). Comparison of hydraulic conductivity of soils of the forest vegetative zone of Nigeria. *Applied Tropical Agriculture*, Vol. 17(1), 64–77.

Frouz, J., Liveckova, M., Albrechtova, J., Chronakova, A., Cajthaml, T, Pizl, V., Hanil, L., Stary, J., Baldrian, P., Lhotakova, Z., Simackova, H. & Cepakova, J. (2013c). Is the effect of trees on soil properties mediated by soil fauna? A case study from post-mining sites. *Forest Ecology and Management*, Vol. 309, 87–95.

Gee, G. W. & Or, D. (2002). Particle size distribution. In: Dane, J. H and Topp, G. C. (eds). Methods of soil Analysis. Part 4, Physical methods. *Soil Science American Book Series* No.5, ASA and SSSA, Madison, W.I. Pp. 255–293.

Griffiths, B.S., Ball, B.C. & Bohanec, M. (2010). Integrating soil quality changes to arable agricultural systems following organic matter addition, or adoption of a ley-arable rotation. *Applied Soil Ecology*, Vol. 46 (1), 43–53.

Hazelton, P. & Murphy, B. (2007). *Interpreting Soil Test Result*: What Do All the Numbers Mean? Australia: CSIRO Publishing. Pp. 64– 71.

Jimoh, A.I., Malgwi, W.B., Aliyu, J. & Shobayo, A.B. (2016). Characterization, classification and agricultural potentials of soils of gabari district, Zaria, Northern guinea savanna zone Nigeria. Biological and Environmental *Sciences Journal for the Tropics*, Vol. 13(2), 102–113.

Keesstra, S.D., Bouma, J., Wallinga, J., Tittonell, P., Smith, P., Cerda, A., Montanarella, L., Quinton, J.N., Pachepsky, Y., Putten, W.H.V., Bardgett, R.D., Moolenaar, S., Mol, G., Jansen, B.& Fresco, L.O. (2016).The significance of soils and soil science towards realization of the United Nations Sustainable Development Goals. *Soil*, Vol. 2, 111–128.

Khormali, F., Ajami, M., Ayoubi, S., Sirinivasarao, C.H. & Wani, S.P. (2009). Role of deforestation and hillslope position on soil quality attributes of loss-derived soils in Golestan province, Iran. *Journal of Agriculture, Ecosystem and Environmental*, Vol. 134, 178–189.

Lawal, B.A., Ojanuga, A.G., Isada, P.A. & Mohammed, T.A. (2013). Characterization, classification and agric potentials of soils on a Toposequence in Southern Guinea Savanna of Nigeria. World Academy of Science Engineering and Technology. *International Journal of Biology, Veterinary, Agricultural and Food Engineering*, Vol. 7 (5), 146–150.

Massas, I., Kalivas, D., Ehaliotis, C. & Gasparatos, D. (2013). Total and available heavy metal concentrations in soils of the Thriassio plain (Greece) and assessment

of soil pollution indexes. *Environmental Monitoring and Assessment*, Vol. 185 (8), 6751–6766.

Nachtergaele, F., Velthuizen, H. V. & Verelst, L. (2009). *Harmonized World Soil Database*. (Version 1.1). FAO, Rome, Italy and IIASA, Laxenburg, Austria. Pp. 1–38.

Nelson, A.M., Tamungang, E.B.N., Antoine, D.M., Georges, K.K. & Kenneth, M. (2017). Assessment of physico-chemical and heavy metals properties of some agricultural soils of Awing-North West Cameroon. *Archives of Agriculture and Environmental Science, Vol.* 2(4). 277–286.

Nelson, D.W. & Sommers, I.E. (1982). Total carbon, organic carbon and organic matter. In: Page et al., (eds). *Methods of Soil Analysis part 2. Agronomy 9 second edition* .ASA and SSA Madison Wisconsin. Pp. 595–624.

Nur Aini, I., Ezrina, M.H. & Aimruna, W. (2014). Relationship between soil apparent electrical conductivity and pH value of Jawa series in oil palm plantation. *Agriculture and Agricultural Science Procedia,* 2, 199 – 206.

Olojugba, M.R. & Fatubarin, A.R. (2015). Effect of seasonal dynamics on the chemical properties of the soil of a Northern Guinea savanna ecosystem in Nigeria. *Journal of Soil Science and Environmental Management*, Vol. 6(5), 100–107.

Olorunfemi, I.E., Fasinmirin, J.T. & Akinola, F.F. (2018). Soil physico-chemical properties and fertility status of long term land use and cover changes: A case study in Forest vegetative zone of Nigeria. *Eurasian Journal of Soil Science*, Vol. 7 (2) 133 – 150.

Omotola, S.J. (2008). Democratisation, identity transformation, and the rising ethnic conflict in Nigeria. *Philippine Journal of Third World Studies*, Vol. 23(1), 71–90.

Onianwa, P.C. (2001). Roadside topsoil concentrations of lead and other heavy metals in Ibadan, Nigeria. *Soil Sediment Contamination*, Vol.10 (6), 577–591.

Onwudike, S.U. (2015). Effect of land use types on vulnerability potential and degradation rate of soils of similar lithology in a tropical soil of Owerri, Southeastern Nigeria. *International Journal of Soil Science*, Vol. 10, 177-185.

Osakwe, S. A., Akpoveta, V. O. (2012). Effect of cassava processing mill effluent on physical and chemical properties of soils in Abraka and Environs, Delta State, Nigeria. *The Pacific Journal of Science and Technology*, Vol. 13 (2), 544–552.

Osayande, P. E., Oviasogie, P. O. Orhue, E. R., Irhemu, P., Maidoh, F. U. & Oseghe, D. O. (2015). Soil nutrient status of the otegbo fresh water swamp in Delta State of Nigetria. *Nigerian Journal of Agriculture, Food and Environment*. Vol. 11(2), 1–8.

Osuocha, K. U., Akubugwo, E. I., Chinyere, G.C. & Ugbogu, A.E. (2016). Seasonal impact on phytoaccumulation potentials of selected edible vegetables grown in Ishiagu quarry mining effluent discharge soils. *African Journal of Environmental Science and Technology*, Vol. 10, 34–43.

Robinson, D.A., Hackley, N., Dominati, E.J., Lebron, I., Scow, K.M., Reynolds, B., Emmett, B.A., Keith, A.M., De Jonge, L.W., Schjonning, P., Moldrup, P., Jones, S.B. & Tuller, M. (2012). Naural capital ecosystem services and soil change. *Vadose Zone Journal*, Vol. 11, 5–10.

Rowell, D.L. (1994). *Soil Science: Methods and Applications*. Longman Group. Prentice Hall, Harlow. Pp. 345. ISBN: 0582087848.

Sharma, C.M., Sumeet, G., Ghildiyal, S.K. & Sarvesh, S. (2010). Physical properties of soils in relation forest composition in moist temperate valley slopes of the central western Himalaya. *Journal of Forest Science*, Vol. 26(2), 117–129.

Sharu, M., Yakubu, M. & A.I. Tsafe, S. N. A. (2013). Characterization and Classification of Soils on an Agricultural landscape in Dingyadi District, Sokoto State, Nigeria. *Nigerian Journal of Basic and Applied Sciences*, Vol. 21(2), 137–147.

Sinha, N. K., Chopra, U. K., Singh, A. K., Mohanty, M., Somasundaram, J. & Chaudhary, R. (2014). Soil physical quality as affected by management practices under maize–wheat system. *National Academy Science Letter*, Vol. 37, 13–18.

Soil Survey Staff (2009). *Soil survey field and laboratory methods manual*. Soil survey investigations report no. 51. USDA, Natural Resources Conservation Service, National Soil Survey Centre, Kellogg Soil Survey Laboratory, USA. Pp.457– 459.

Straaten, O.V., Corre, M.D., Wolf, K., Tchienkoua, M., Cuellar, E., Matthews, R.B. &

Veldkamp, E. (2015). Conversion of lowland tropical forests to tree cash crop plantations loses up to one-half of stored soil organic carbon. Conversion of lowland tropical forests to tree cash crop plantations loses up to one-half of stored soil organic carbon. *National Academic Science*, Vol. 112 (32), 99–56.

Tsozue, D., Tematio, P. & Tamfuh, P.A. (2016). Relationship between soil characteristics and fertility implications in two typical dystrandept soils of the Cameroon Western Highland. *International Journal of Soil Science*, Vol. 11, 36–48.

Umeri, C., Onyemekonwu, R.C. & Moseri, H. (2017). Analysis of Physical and Chemical Properties of Some Selected Soils of Rain Forest Zones of Delta State, Nigeria. Agricultural Research & Technology: *Open Access Journal*, Vol. 5(4), 555– 668.

Umeri, C., Moseri, H. & Onyemekonwu, R.C. (2016). Effects of nitrogen and phosphorus on the growth performance of maize (Zea mays) in selected soils of Delta State, Nigeria. *Advances in Crop Science and Technology*, Vol. 4 (1), 1–4.

Uquetan, U. I., Eze, E. B., Uttah, C.1., Obi, E.O., Egor, A. O.& Osang, J. E.(2017). Evaluation of Soil Quality in Relation to Land use Effect in Akamkpa, Cross River State, Nigeria. *Applied Ecology and Environmental Sciences*, Vol. 5(2), 35–42.

Thermal Degradation Kinetics of Chemically Modified Wood Sawdust Using Thermogravimetric Analysis (TGA)

Blessing A. C. Enwere[1] Ruth A. Lafia-Araga[2*], M.A.T Suleiman[2] and St. S. Ochigbo[2,]

Department of Chemistry, FCT College of Education, Zuba, Abuja
[2,] Department of Chemistry, School of Physical Sciences, Federal University of Technology, Minna
[1]chibless2013@gmail.com
[2]rutharaga@yahoo.ca
[2]smatsule@yahoo.com
[2]stephenochigbo@futminna.edu.ng
*Corresponding author

Abstract

The kinetic study of the thermal degradation of NaOH modified *Gmelina arborea* sawdust was investigated by thermogravimetric analysis (TGA). Samples were treated with 4% NaOH solution for a period of 30 and 90 minutes. Thermogravimetric analysis was carried out at five different heating rates of 10, 20, 30 and 50°C min^{-1} from a temperature range of 50 to 650C° at a constant nitrogen flow rate of 20 ml min^{-1}. The activation energy and other kinetic parameters of the decomposition process were calculated by model free Kissinger and Ozawa methods. TG and DTG analysis revealed that sample treated for 90 minutes presented the highest onset and peak degradation temperature of 274.04°C and 372.11°C respectively. The activation energy (E_a) obtained by Kissinger and Ozawa methods were 183.32 and 184.69 KJ/mol, while the pre-exponential factor (lnA) was 6.97 x 10^4 and 7.00 x 10^4 min^{-1} respectively. Therefore, alkali treatment with 4% NaOH solution for 90 minutes imparted a significant improvement on the thermal stability of *Gmelina arborea* sawdust. This implies that this sample will withstand higher temperature without appreciable degradation when compounded with a thermoplastic polymer in polymer matrix composites.

Keywords: Chemical Modification, Activation energy, Thermal Degradation, Kinetic parameters and Thermogravimetric analysis.

1. Introduction

Wood sawdust is a natural polymeric material that is obtained as by-product of the timber milling processes. It is naturally abundant, light weight, renewable and of low cost. Despite these advantages, wood also suffers a number of disadvantages. First, it is hygroscopic, absorbing moisture from the surrounding environment. This leads to poor resistance against fungal and insect attack, swelling and shrinkage resulting from water absorption and desorption (Kokaefe *et. al*., 2018). In addition, wood is very polar due to the presence of hydroxyl groups in the cellulose. This leads to poor adhesion or compatibility when compounded with a non-polar thermoplastic resin in composites applications (Yang *et. al*., 2007). Furthermore, wood is thermally unstable, degrading at temperatures above 200°C. Therefore, lower processing temperatures are generally needed because of the possibility of lignocellulosic degradation

and/or the possibility of volatile emissions that could affect composite properties (Sanadi *et. al*., 1997). Therefore, there is need to alter the cell wall chemistry in order to achieve the properties of interest. One modification method used in wood is the alkaline treatment (mercerization). Alkaline treatment results in the disruption of the hydrogen bonding in the network structure of the wood polymers, thereby increasing the surface roughness. It reduces fibre diameter, increases aspect ratio, increases the amount of crystalline cellulose and removes natural and artificial impurities (Kalia *et. al*., 2009). In addition, it increases the thermal stability of the wood samples by degrading the heat sensitive components (Olakanmi *et. al.*, 2015).

The effect of alkaline treatment on the thermal stability and the degradation kinetic analysis of the devolatilization of wood can be monitored by thermogravimetric analysis (TGA). In the literature, the TGA analysis and behavior of different materials such as agricultural residue, plastic, rubber-derivative, natural fibers, and various types of biomass during thermal degradation has been described. The measurements are used mostly to determine the composition of wood sawdust and to predict their thermal stability at temperatures up to 650°C (El-Sayed, and Mostafa 2014). Usually biomass decomposition is discussed in terms of its three main components namely lignin, cellulose and hemicelluloses (Gasparovic *et al*., 2009).

Slopiecka, *et al.* (2012), examined the pyrolysis of wood and main wood compounds through thermogravimetry and revealed that the thermal decomposition of wood by TGA proceeds via three stages namely, water evaporation, active and passive pyrolysis. Kumar *et al*., (2010) investigated the thermal decomposition of corn stoves by TGA in nitrogen and air atmospheres and concluded that there are three distinct stages of weight loss in both conditions and that the kinetic parameters were similar only at slow heating rates. At higher heating rates, the second stage occurred very rapidly and activation energy was higher than activation energy in nitrogen atmosphere.

As a result of the simplicity of the Ozawa and the Kissinger models and the fact that they require fewer data and have fast procedures for their calculation, these models have been used extensively to study the thermal degradation kinetics of biomass (Gasparovic et al., 2009; Lv *et al.*, 2010; Okoroigwe, 2015). It is therefore in order to adapt these models for this research work to study the kinetics of thermal degradation profile of alkali modified wood sawdust. Therefore, this study aims to determine the kinetics parameters that define the thermal degradation process of alkali treated wood sawdust. The study compares Kissinger and Ozawa methods of kinetic models for wood sawdust and provides evidence for further applications of

the thermochemical conversion of alkaline modified wood sawdust as potential filler in polymer matrix composites production.

2 Literature review

2.1 Kinetics Study

The rate of wood sawdust modification can be associated with its chemical composition through evaluation of the kinetic parameters. The aim was to ascertain the extent to which the modification of OH groups on the wood components with NaOH contributes to the thermal stability as well as improvement on the performance and applications of such a renewable lignocellulosics materials. Radhakumari *et al.*, (2015) investigated the kinetic study of the pyrolysis process of Algal biomass using a thermogravimetric analyzer. The samples were heated over a range of temperature from 200 to 1000 °C at three different heating rates of 5, 10, and 30 °C/min at a constant N_2 flow rate of 30 $mLmin^{-1}$. The result obtained from thermal decomposition process indicates that there are three main stages of events such as dehydration, active and passive pyrolysis. The maximum decomposition of the biomass samples occurred between 220–650 °C. In the DTG thermograms, the temperature at maximum weight loss rate changed with increase in heating rate. The activation energy of the pyrolysis reaction was determined by model free Kissinger-Akahira-Sunose and Ozawa-Flynn-Wall methods. The Coats-Redfern method was used to obtain kinetic parameters such as activation energy, pre-exponential factor, and reaction order. Pyrolysis process was simulated with the obtained kinetic parameters and results obtained were in good agreement with experimental data.

2.1.2 Kinetics models

There are many models employed in the analysis of non-isothermal solid-state kinetic data obtained from thermogravimetry analysis (TGA). The models are separated into two major groups namely, Model- fitting method: which involves appropriating a given kinetic data to the thermogravimetric curves obtained so that the model used will be one that gives the most suitable statistical fit, through which the kinetics parameters could be evaluated. The broad use of this method is attributed to the fact that it had direct capacity to calculate the activation energy and pre-exponential factor from a particular thermogravimetric analysis. The limitation lies in its inability to determine reaction mechanism (Slopiecka *et al.*, 2012).

This method includes the Friedman model which obtains ($-E_a/R$) value for a given value of conversion (α) through a graph of $\ln(d\alpha/dt)$ against $1/T$ from equation 1

$$\ln (d\alpha/dt) = \ln [Af(\alpha)] - E_a/RT \quad (1)$$

Where f(α) is the reaction model which depends on the reaction mechanism and α is the conversion rate which depends on the initial and final mass of the sample.

Another is modified Coats-Redfern model which is multi-heating rate application of the equation below

$$\ln[\beta/T^2(1-2RT/E_a)]=\ln[-AR/(E_a\ln(1-\alpha)]-E_a/RT \quad (2)$$

In applying the modified Coats-Redfern method in equation 2, it encompasses a plot of [ln (β/T^2)] against 1/T since ($1-2RT/E_a$) on the left- hand side of the equation is a constant. The slope of the plot is equal to

$-E_a/R$.

Model-free method: This method requires many kinetics curves to perform the investigation. The model has numerous advantages over the model fitting method which includes its simplicity and error free quality. It allows measurement of activation energy from a given degree of conversion. Also, the method gives polymer scientists opportunity to find the reliance of activation energy with conversion factor using thermogravimetric and differential thermogravimetric thermograms obtained at various heating rates with no prediction of the reaction mechanism and order of the reaction. The model-free approach does not require assumption of specific reaction models, and yields unique kinetic parameters as a function of either α conversion (isoconversional analysis) or temperature (non-parametric kinetics). Of the two methods, the isoconversional approach is more frequently implemented, and is increasingly being used in biomass thermochemical conversion study (Poletto *et al.*, 2012; Jayabal et al., 2012).

2.2.3 Theoretical approach of the kinetics study

Thermodegradation performance of natural biomass could be explained through a simple rate equation of,

$$d\alpha/dt = k(T)f(\alpha) \quad (3)$$

In the equation above α is the degree of conversion, t is the time, k stands for rate constant while f(α) stands for the reaction model which depend upon the mechanism of the degradation reaction. The value of α typically reflects the progress of the overall conversion of a reactant to products which is defined as:

$$\alpha = (m_i-m_t)/ (m_i-m_f) \quad (4)$$

where m_i stands for the initial mass of sample, m_t is the mass at temperature T and m_f is the mass for final sample. The rate constant k is usually defined by Arrhenius equation as,

$$k = A \exp(-E_a/RT) \quad (5)$$

The E_a in the equation is the apparent activation energy in $KJmole^{-1}$, A is pre-exponential factor in min^{-1}, R is gas constant which is equal to 8.314 $JK^{-1}mole^{-1}$, while T is absolute temperature in Kelvin. Combination of equation 3 and 5 gives rise to the fundamental equation 6 below which is used to calculate the kinetic parameter.

$$d\alpha/dt = A \exp(-E_a/RT)f(\alpha) \quad (6)$$

For an active thermogravimetric analysis, incorporating the non-isothermal heating rate ($\beta = dT/dt$) into equation 6 generates another equation,

$$d\alpha/dT=(A/\beta)\exp(-E_a/RT)f(\alpha) \quad (7)$$

Finally, equations 6 and 7 are the basic equations used in analytical process to calculate activation energy and pre-exponential factor from TGA results (Poletto *et al.*, 2012; Slopiecka *et al.*, 2012).

3. Methodology

3.1 Materials

The *Gmelina arborea* sawdust was collected from wood sawmills in the Federal Capital Territory (FCT), Abuja, Nigeria during milling operation. The sawdust was cleaned manually and dried at 105°C for 24 hours. It was then ground using a local milling machine into powder. Finally, the sample was sieved to obtain particles between 40 and 100 meshes (150-400µm) and kept in air tight desiccators.

3.2 Modification with NaOH

About 2.00 g of the sawdust sample each was separately soaked in 100 cm^3 of 4 % NaOH solution for different times of 30 and 90 minutes using a magnetic stirrer (Jayabal *et al.*, 2012). The samples were neutralized with 2% H_2SO_4 to remove excess NaOH. Then washed several times with deionized water until a pH of 7 was obtained and dried in an oven at 105°C until a constant weight was achieved.

3.3 Thermogravimetric analysis

Thermogravimetric analysis of treated and untreated sawdust was performed using a Perkin–Elmer Pyris TG 6 (USA) thermogravimetric analyzer. The thermogravimetric (TG) analysis was carried out with 5 to 7 mg of the sample. The sample was heated from 50°C to 650°C under a nitrogen atmosphere at a flow rate of 20 cm^3min^{-1}. TGA and DTG curves were obtained

and sample weight loss as a function of temperature was recorded at five different heating rates of 10, 20, 30, 40 and 50°C min^{-1}. The results obtained were used in the kinetic analysis.

3.4 Kinetic methods

3.4.1 Kissinger model

This model enables polymer scientists to estimate the kinetic parameters of a solid-state reaction where the reaction mechanism is not known. According to Slopiecka *et al*. (2012), Kissinger formed a model free non-isothermal technique for the determination of the kinetics of biomass degradation, which does not require the calculation of activation energy (Ea) for every conversion value. The equation is;

$$\ln (\beta/T_p^2) = - E_a/ RT_p + \ln (AR/E_a) \quad (8)$$

The Kissinger model gives researchers opportunity to get the value of activation energy from a linear plot of $\ln (\beta/T_p^2)$ against $1/T_p$ for a chain of analysis at different heating rates β (°C/min). T_p is the maximum degradation temperature of sample on the DTG curve. The activation energy (E_a) was calculated from the slope of the plot, which is equal to $-E_a/R$ while the intercept is equal to $\ln (AR/E_a)$ and was used to calculate the pre-exponential factor.

3.4.2 Flynn Wall Ozawa model

This is an integral model that involves a plot of lnβ against $1/T_p$ at a fixed value of conversion (α) rate to obtain a slope which is equal to –1.052Ea/R where g(α) is fixed for a given value of conversion. From the slope the activation energy can be calculated. The equation is given as follows; $\ln(\beta) = \ln [AE/Rg(\alpha)] - 5.33l - l.052\ E_a/RT$

(9)

4 Results and Discussion

4.1 Effect of modification on thermal characteristics

The thermal stability of unmodified and modified sawdust samples was obtained by TGA measurements. The thermograms of mass loss at five heating rates (10, 20, 30, 40, 50 °C) and derivative curves in relation to temperature are shown in Figures 1- 3. Data extracted from these curves are presented in Table 1. There are two main stages of mass loss as shown in the DTG curves. The first stage occurred between 50°C and 150°C which can be related to evaporation of water and possibly, the volatilization of extractives from the wood sawdust. The results show that the unmodified sample had the highest percentage weight loss of 1.88% around this temperature region when compared with the modified samples that recorded weight loss as low as 0.13%. The high extractives content in unmodified sample promotes its thermal

degradation at lower temperature due to their high volatility and could be responsible for this observation. Also, the presence of higher number of OH groups on the surface of untreated sawdust could be responsible for the high % moisture content at this degradation temperature. In addition, research has shown that the free OH groups in wood are reduced with alkali treatment (Olakanmi *et al.*, 2015). Therefore, a reduction in the moisture content of the NaOH treated sample is expected. The second stage with a major weight loss occurred within the range of 220°C and 400°C could be attributed to the degradation of hemicellulose, cellulose, and lignin. It has been observed that lignocellulosic materials, being chemically active, decompose thermo-chemically in the range of 150°C to 500°C. Hemicellulose degrades between 150°C to 350°C, cellulose between 240°C to 350°C and lignin between 250°C and 500°C (Lafia-Araga *et al*., 2017; Mohammed *et al.*, 2017; Lafia-Araga *et al.*, 2018).

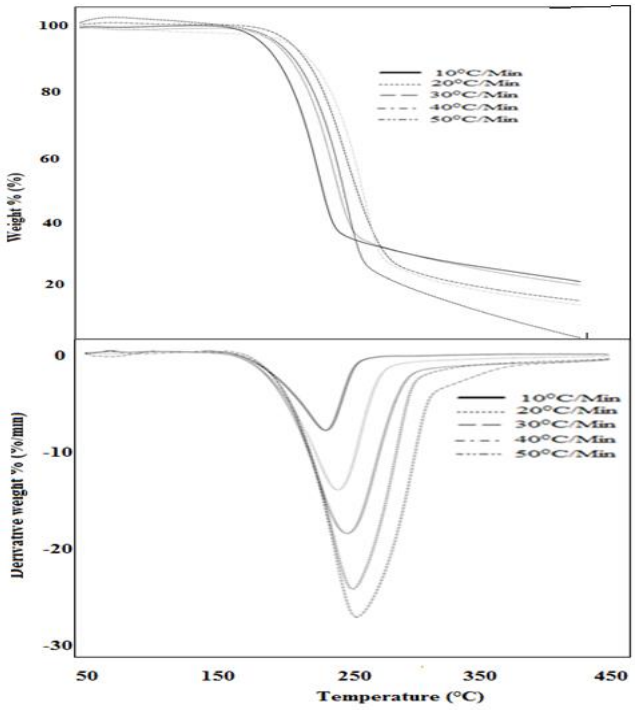

Figure 1: TGA and DTG curves of unmodified sawdust sample

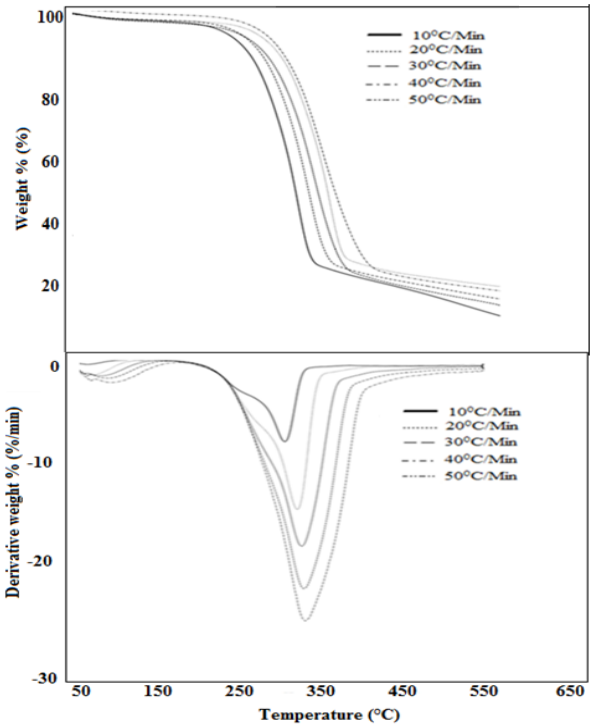

Figure 2: TGA and DTG curves of sawdust sample soaked for 30 minutes

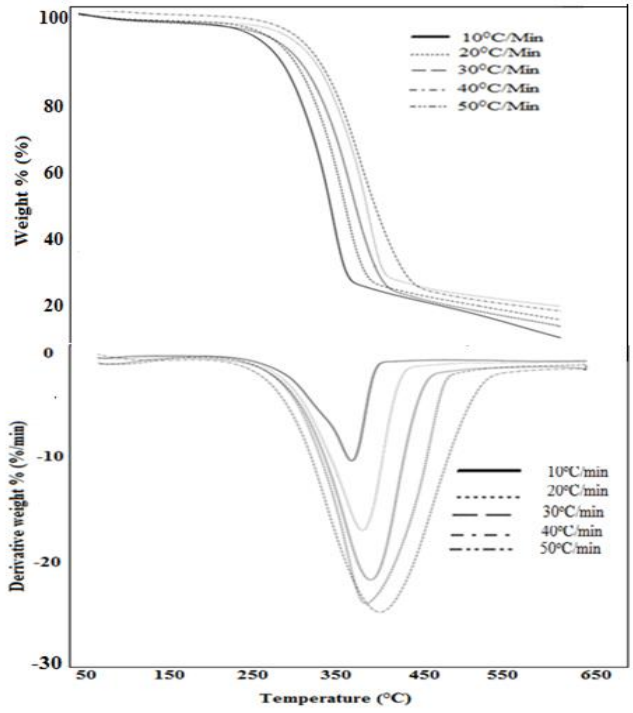

Figure 3: TGA and DTG curves of sawdust sample soaked for 90 minutes

Table 1: Thermal Degradation data for unmodified and sawdust modified for 30 and 90 minutes

Samples	T_{onset} (°C)	T_p (°C)	$T_{50\%}$ (°C)	Degradation temperature range (°C)	Moisture (%)
Unmodified	230.33	260.20	265.00	220.20---358.12	1.80
30 min	256.37	337.04	345.33	220.10---401.22	1.57
90 min	274.04	372.11	361.15	226.22---413.34	0.13

Although, the samples displayed a general increase in onset temperature, T_{onset} and degradation peak temperatures, T_p, the T_p of the samples increased from 260.20°C in unmodified sample to a highest value of 372.11°C in sample treated for 90 minutes sample, while samples soaked for 30 minutes had T_{onset} and T_p of 256.37 and 337.04°C respectively. This shows improvement in thermal stability which could be due to hemicellulose removal from the wood sawdust by alkaline treatment. This is expected to have possibly improved the thermal properties by reduction in heat transfer coefficient (Mishra, and Bhaskar, 2014). The high T_p value for wood flour treated for 90 minutes is in agreement with the findings of Abdullah *et. al.* (2019). Olakanmi, *et al*., (2015), also investigated the use of alkaline treated *Daniela oliveri* wood flour as reinforcement in virgin HDPE and reported that wood flour treated with 4% NaOH solution for 150 minutes produced composites that exhibited the highest T_{onset} and T_p of 375°C and 495°C respectively. Also, Zierdt *et al.,* (2015), reported the results of the TGA investigations that showed that the application of 10 % NaOH alkaline treatment for 60 min effectively enhanced the thermal stability of beech fibers. In general, it has been observed that alkalination of wood flour with NaOH at specified concentration and time has the ability to improve the thermal properties of wood flour (Choudhury, 2007; Okoroigwe, 2015; Mohammed, *et al*., 2017; Lafia-Araga, *et al*., 2017). It is therefore necessary to note that samples modified for 90 minutes can be conveniently compounded with a polymer matrix at temperatures as high as 250°C to 300°C. Furthermore, the rate of wood degradation showed an increase with increase in heating rates. This is due to the higher thermal energy given to the samples which led to improved heat transfer between the surrounding and inside the samples. At low heating rate, the decomposition is influenced by volatilization of water, extractives degradation, breakdown of hemicellulose and degradation of lignin and cellulose (Poletto *et al.,* 2012).

4.2 Kinetic analysis using Kissinger model

The results extracted from thermogravimetric analysis were elaborated according to model free methods to calculate the kinetic parameters. When the decomposition temperature of wood

sawdust reached its degradation peak, the influence of the heating rates upon the maximum degradation temperatures obeys the Kissinger method according to equation (8). The Kissinger plots of $\ln\beta/T_p^2$ against $1/T_p$ for the decomposition process of unmodified and modified sawdust are shown in Figures. 4-6. The regression equations and the square of the correlation coefficient (R^2) are also presented. The activation (E_a) and pre-exponential factor (A) were derived from the slope and intercept of plotting regression line, respectively. The results obtained from Kissinger methods for activation energy and pre-exponential factor are presented in Table 2. The unmodified sample has activation energy of 69.96 KJ/mole, pre-exponential factor of 1.50 x 10^4 min^{-1}. Sample treated for 30 minutes has activation energy of 102.93 KJ/mole and pre-exponential factor of 2.84 x 10^4 min^{-1} while that treated for 90 minutes displayed an activation energy of 183.32 KJ/mole and pre-exponential factor of 6.97 x 10^4 min^{-1}. This implies that samples soaked for 90 minutes will withstand a higher energy barrier than that soaked for 30 minutes when subjected to thermal degradation reaction. Lv *et al.*, (2010), investigated the thermal degradation kinetics of hemicellulose from corn stalk and reported higher activation energy of 213.3 $KJmol^{-1}$ and pre-exponential factor of 46.2 min^{-1} using the Kissinger model. The calculated squares of the correlation coefficient R^2, corresponding to linear fitting in Figures 4-6 are higher for all sample and are in the range of 0.960 to 0.990 except the unmodified sample that had the least value of 0.789. This could be due to alkaline modification of sawdust which led to improved thermal stability. The observed increase is in agreement with the finding of Slopiecka *et al., (*2012) , who reported higher correlation coefficient in the range of 0.975 to 0.996.

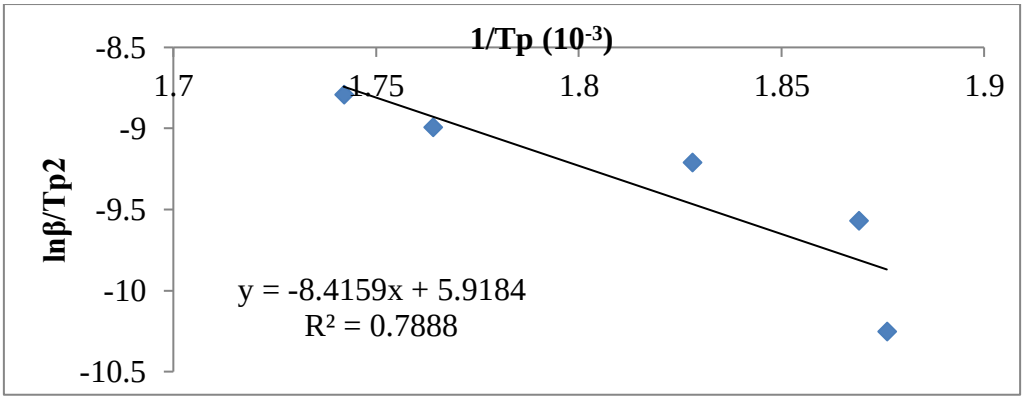

Figure 4: Linearization curve of Kissinger model for unmodified sample

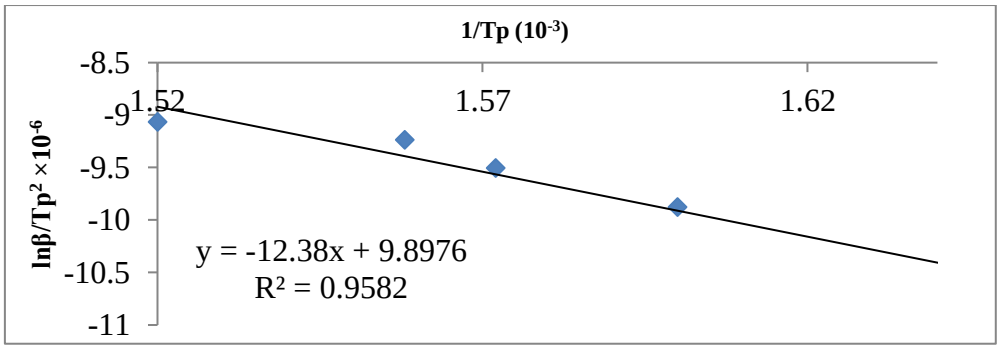

Figure 5: Linearization curve of Kissinger model for sample treated for 30 minutes

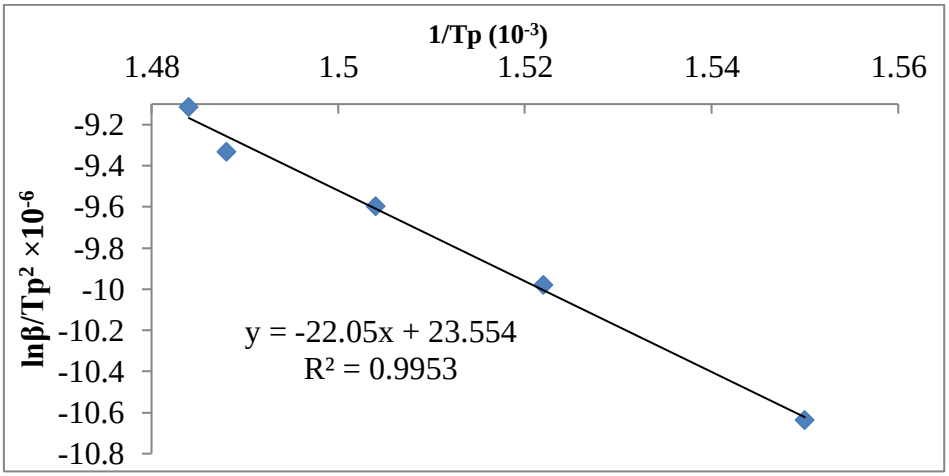

Figure 6: Linearization curve of Kissinger model for sample treated for 90 minutes.

4.3 Kinetic analysis using Ozawa model

The impact of heating rate, (β), on the maximum temperatures of the DTG curves was given by the Ozawa formula in equation (9). Ozawa plot of lnβ and $1/T_p$ for all the samples are presented in figures. 7-9. Kinetic parameters obtained from Ozawa equation for all samples are given in Table 2. The unmodified sample showed activation energy of 75.26 KJ/mole, pre-exponential factor of 2.74 x 10^4 min^{-1}. The sample treated for 30 minutes presented an activation energy of 74.61 KJ/mole and pre-exponential factor of 2.88 x 10^4 min^{-1} while sample treated for 90 minutes sample showed a higher activation energy of 184.69 KJ/mole and pre-exponential factor of 7.00 x 10^4 min^{-1}. Again, correlation coefficient, R^2, corresponding to linear fitting in Figures. 7-9 are higher for all sample and are in the range of 0.970 to 990 except the unmodified sample that had the least value of 0.827.

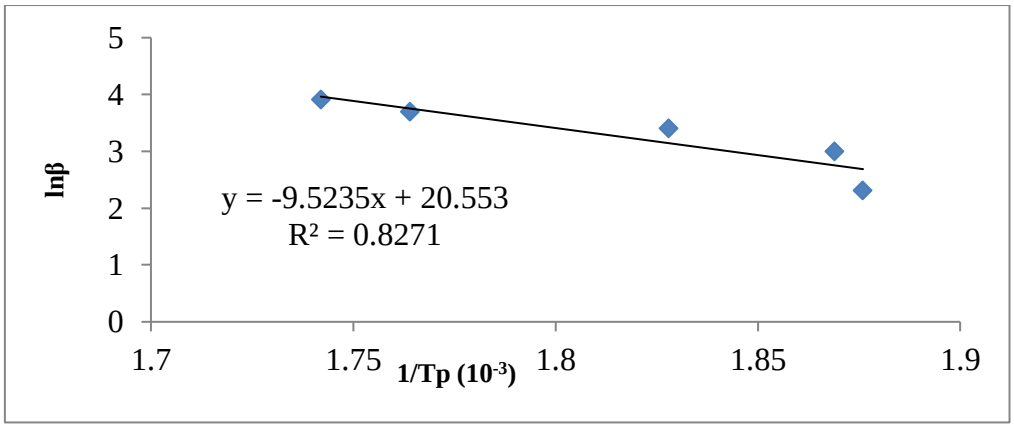

Figure 7: Linearization curve of Ozawa model for unmodified sample.

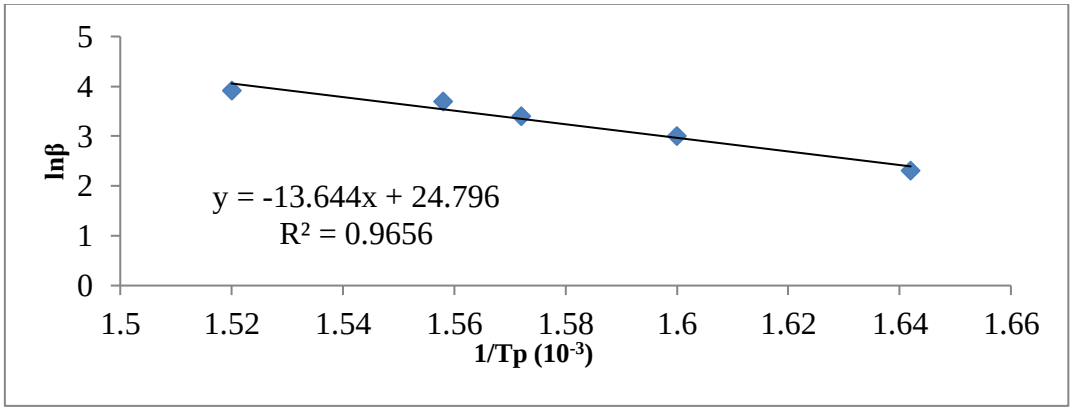

Figure 8: Linearization curve of Ozawa model for sample treated for 30 minutes.

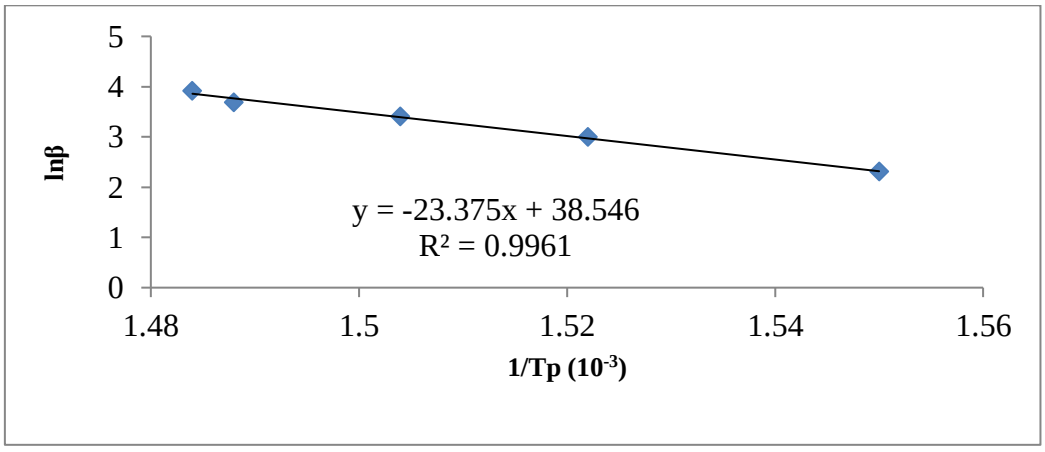

Figure 9: Linearization curve of Ozawa model for sample treated for 90 minutes

Table 2: Summary of kinetic parameters obtained by Kissinger and Ozawa Models for unmodified and samples modified for 30 and 90 minutes

Samples	Kissinger			Ozawa		
	E_a (kJmole^{-1})	A (min^{-1}) x 10^4	R^2	E_a (kJmole^{-1})	A(min^{-1}) x 10^4	R^2
Unmodified	69.96	1.50	0.789	75.26	2.74	0.827
30 minutes	102.93	2.84	0.958	74.61	2.88	0.966
90 minutes	183.32	6.97	0.995	184.69	7.00	0.996

The Kissinger and Ozawa models are differential and integral thermal analysis model which have been widely applied in the calculation of kinetic parameters of lignocellulosic materials at different heating rates. Though there are varieties of kinetic models used in calculation of kinetic parameters of biomass, only Kissinger and Ozawa models do not require prior knowledge of reaction mechanism before calculation of activation and pre-exponential factors. From the results in Tables 2, it was observed that the unmodified sample recorded the least activation energy in both Kissinger (69.96 KJ/mole) and Ozawa (75.26 KJ/mole) model. This is in line with the findings of Mohammed *et al*. (2017), who reported activation energy of wood fiber as low as 24.59 KJ/mol. This implies that unmodified sawdust is thermally reactive as confirmed by the thermogravimetric analysis in Figure 1 and will readily undergo thermal degradation reaction. From the results, all the kinetic parameters progressively increased with an increase in duration of treatment. However, sample treated for 90 minutes had the highest activation energy (183.32 and 184.69 KJ/mole), pre-exponential factor (6.97×10^4 and 7.00×10^4 min^{-1}) with a better linear fit factor of (0.995 and 0.996) using the Kissinger and Ozawa models respectively. The value of correlation coefficient (R^2) was found to be equal to 1 which shows that both Kissinger and Ozawa kinetic models can adequately be used to determine the kinetic process the thermal degradation of wood sawdust. In addition, this could imply that treatment of wood sawdust with NaOH solution for 90 minutes duration enhances their resistance to thermal degradation to an extent, since higher activation energy implies slower reaction. This is in line with the results of previous researchers (Gasparovic *et al.*, 2009; Lv *et al.*, 2010, Jayabal *et al.*, 2012). It was also observed that values obtained by Kissinger model for treated samples was lower than those from Ozawa model except in samples treated for 30 minutes that had an activation energy value as low as 74.61 KJ/mole. This could mean higher thermal reactivity of the sample. The observed differences could be due to differences in

modification duration and calculation methods employed (Yao *et al.,* 2007, Okoroigwe, 2015;). Furthermore, higher activation energy value for samples treated for 90 minutes could mean that this sample will withstand higher temperature without appreciable degradation when compounded with a thermoplastic polymer. It is worth to note that this samples also possessed the highest onset and peak degradation temperatures.

The reason for the calculation of the activation energy and pre-exponential factor of samples was to help wood polymer composites industries to develop a simple approach that will be of benefit in having an improved perceptive on thermal degradation profile of wood sawdust especially the Nigerian wood which is deficient in most literature. The values obtained in this study agree with those in previous research works (Radhakumari *et al.,* 2015; Okoroigwe, 2015; Yao *et al.,* 2008), hence future potential use of NaOH modified *Gmelina arborea* sawdust in wood reinforced polymer composite as filler could be considered.

5 Conclusion

Highest thermal stability was found in wood sawdust treated with at 90 minutes. Also, the activation energy obtained in this study ranged from 69.96 - 183.32 KJ/mole in Kissinger model and 74.61 - 184.69 KJ/mole in Ozawa model for untreated and samples treated for 30 and 90 minutes respectively. This information will help wood processing factories and chemist to understand the thermal decomposition of wood sawdust which can then be employed in wood thermoplastic composites industry. From these results, it can be concluded that treating wood flour with 4% NaOH at 90 minutes had significant improvement on the thermal properties and thermal decomposition kinetic of *Gmelina arborea* sawdust. This could mean that this sample will withstand higher temperature without appreciable degradation when compounded with a thermoplastic polymer and so encourages its use as filler in polymer matrix composites. Finally, the results of this study on kinetic parameter is vital since activation energy is the energy barrier reactants must overcome to form the product. Knowledge of the activation energy will provide useful information on the optimum energy required to start a reaction; in this case, thermal degradation.

References

Abdullah, C. I., Azzahari, A. D., Abd. Rahman, N. M., Hassan, A., Yahya, R (2019). Optimizing Treatment of Oil Palm-Empty Fruit Bunch (OP-EFB) Fiber: Chemical, Thermal and Physical Properties of Alkalized Fibers. *Fibers and Polymers*, Vol. 20(3), 527-537.

Choudhury, D. (2007). Non-Isothermal Thermogravimetric Pyrolysis Kinetics of Waste Petroleum Refinery Sludge by Iso-Conversional Approach. *Journal of Thermal Analysis and Calorimetry*, Vol. 89(3), 965-970.

El-Sayed, S.A., Mostafa, M.E. (2014). Pyrolysis Characteristics and Kinetic Parameters Determination of Biomass Fuel Powders by Differential Thermal Gravimetric Analysis (TGA/DTG). *Energy Conversion Management*, Vol. 85, 165–172.

Gašparovič, L., Koreňová, Z., Jelemenský, L. (2010). Kinetic Study of Wood Chips Decomposition by TGA. *Chemical Papers*, Vol. 64(2) 174–181.

Jayabal, S., Sathiyamurthy, S., Loganathan, K. T., Kalyanasundaram, S. (2012). Effect of Soaking Time and Concentration of Naoh Solution on Mechanical Properties of Coir Polyester Composites. *Bulletin of Material Science, Indian Academy of Sciences*, 35(4), 567–574.

Kalia S., Kaith B. S., Kaur I. (2009). Pretreatments of Natural Fibres and Their Application as Reinforcing Material in Polymer Composites - A Review. *Polymer Engineering & Science*, 49(7), 1253-1272.

Kokaefe D., Poncsak S., Boluk Y. (2008). Effect of Thermal Treatment on the Chemical Composition and Mechanical Properties of Birch and Aspen. *BioResources*, 3(2), 517-537.

Kumar A., Wang L., Dzenis Y., Jones D., Hanna, M. (2008). Thermogravimetric Characterization of Corn Stoves as Gasification and Pyrolysis Feedstock. *Biomass and Bioenergy*,32(5), 460-467.

Lafia-Araga, R.A., Enwere, B.A.C., Suleiman, M. A. T., Ochigbo, S. S. (2017). Study of the Thermal Degradation Profile of Chemically Modified Wood Sawdust. *Proceeding of FUT Minna 1st SPS Biennial International Conference,* 778- 786.

Lafia-Araga, R. A., Hassan, A., Yahya, R., Rahman, N.A., Salleh, F.M. (2018). Water Absorption Behavior of Heat-Treated and Untreated Red Balau Sawdust/LDPE Composites: Its Kinetics and Effects on Mechanical Properties. *Journal of Thermoplastic Composite Materials*, 1–19. DOI: 10.1177/0892705718799823.

Lv G-J., Wu S., Lou, R., (2010). Kinetic Study of Thermal Decomposition of Hemicelluloses isolated from Corn Stalk, *BioResources*, 5 (2), 1281-1291.

Mishra, G., & Bhaskar, T. (2014). Non-Isothermal Model Free Kinetics for Pyrolysis of Rice Straw. *Bioresource Technology*, doi: http://dx.doi.org/10.1016/j.biortech.2014.07.045

Mohammed, U.G., Adoga, I., Umaru, M., Alechenu, A. A., Abdulsalami, S. K. & David, O. A. (2017). Thermogravimetric Characteristic and Kinetic of Catalytic Co-Pyrolysis of Biomass with Low- and High-Density Polyethylene. *Biomass Conversion Bio references*, DOI 10.1007/s13399-017-0261-y.

Okoroigwe, E. (2015). Combustion Analysis and Devolatilisation Kinetics of Gmelina, Mango, Neem and Tropical Almond Woods Under Oxidative Condition. *International Journal of Renewable Energy Research*, 5(4), 1024-1033.

Olakanmi E.O, Ogunesan, E.A., Vunai, E, Lafia-Araga R.A, Doyoyo M and Meijboom R. (2015). Mechanism of Fiber/Matrix Bond and Properties of Wood Polymer Composites Produced from Alkaline Treated Daniella Oliveri Wood Flour. *Polymer Composites*, DOI 10.1002/pc.23460.

Poletto, M., Zattera, A. J., Santana, R. M. C (2012). Thermal Decomposition of Wood: Kinetics and Degradation Mechanisms. *Bioresource Technology*, Vol. 126, 7-12.

Radhakumari, M., Prakash, D.J., Satyavathi, B. (2015). Pyrolysis Characteristics and Kinetics of Algal Biomass Using TGA Analysis Based on ICTAC Recommendations. *Biomass Conversion Bio references*, DOI 10.1007/s13399-015-0173-7.

Sanadi A. R., Caulfield D. F and Jacobson R. E. *Agro-Fibre Thermoplastic Composites*. In: R. M. Rowell., R. A. Young and J. K. Rowell, editor. Paper And Composites from Agro-Based Resources. Boca Raton: CRC Press, 1997. 377- 401.

Slopiecka, K., Bartocci, P., & Fantozzi, F. (2012). Thermogravimetric Analysis and Kinetic Study of Poplar Wood Pyrolysis. *Applied Energy*, 97(5), 491-497.

Yang H. S., Wolcott M. P., Kim H. S., Kim S., Kim H. J.(2007). Effect of different compatibilizing agents on the mechanical properties of lignocellulosic material filled polyethylene bio-composites. *Composite Structures*, Vol. 79(3): 369-375.

Yao, F., Wu, Q., Lei, Y., Guo, W., Xu, Y. (2008). Thermal Decomposition Kinetics of Natural Fibers Activation Energy with Dynamic Thermogravimetric Analysis. *Polymer Degradation Stability*, Vol. 93(1), 90-98.

Zierdt, P., Theumer, T., Kulkarni, G., Däumlicha, V., Klehm, J., Hirscha, U. Weber, A. (2015). Sustainable Wood-Plastic Composites from Bio-Based Polyamide 11 and Chemically Modified Beech Fibers. *Sustainable Materials and Technologies*, Vol. 6, 6-14.

Isolation of Gymnemic Acid from Gymnema Sylvestre Aerial Part Extract and Evaluation of Its Antidibetic Effect on Alloxan Induced Diabetic Rats

Mann,A., Andrew, K., Ibikunle, G. F. and Muhammad, H. L.

Department of Chemistry, Federal University of Technology, PMB 65, Minna, Niger State, Nigeria
Corresponding author:keziaandrew@yahoo.com; 08036799660

Abstract

Diabetes mellitus, a human metabolic disorder affects about 10% of the world population and is a major global concern. Conventional treatment for the disease using synthetic drugs (chemotherapy)poses serious challenge. The study of plants with potential antidiabetic activity may give a new lead in the treatment approach of diabetes. The study is aimed at evaluating the antidiabetic effect of gymnemic acid isolated from Gymnemasylvestreaerial parts sourced from the Nigerian ecosystem,Tafa Forest, Baddegi, Katcha Local Government area of Niger Stateon alloxaninduced diabeticrats.Defatted methanol aerial parts of G. sylvestre was precipitated which is the gymnemic acid and this was evaluatedfor its antidiabetic activity. Rats weighingbetween 120-200 g weregrouped into six and fasted overnight with blood withdrawn from their tail at regular intervals and the GA effect on blood glucose measured using glucometer.Administration of alloxan results in hyperglycaemic state as evident in the significant raise in blood glucose level in untreated diabetic rats (496.78 - 588.04 mg/dL) when compared to theuninduced group (109.56-110.64 mg/dL). However, dose dependent reduction in BGL was observed in diabetic rats treated with GA (411.34 - 209.40 mg/dL at 150 mg/kg, 459.32 - 159.27 mg/dL at 300 mg/kg and 506.68 - 86.53 mg/dL at 600 mg/kg). The blood glucose reducing activity was also accompanied by improvement in body weight of rats.TheGA showed a significant suppressive rate (82.92% at 600 mg/kg) when compared with lower dosage (49.33%at 150 mg/kg and 65.33% at 300 mg/kg). The suppression rate of GA at higher dosage was high in comparison to that of the standard drug (81.53% at 5mg/kg). It is concluded that GA shows a significant hypoglycemic activity at 600 mg/kg bodyweight dose in alloxan induced diabetic rats.

Keywords: Gymnemic acid, *Gymnemasylvestre*, Antidiabetic, Diabetes mellitus, Blood glucose level

INTRODUCTION

Diabetes mellitus (DM), a human metabolic disorder results when the insulin producing β cells in the pancreas is damaged- type I diabetes and or a decline in the sensitivity of the body muscles and liver cells to insulin action- type II diabetes (Oyedemi*et al*., 2009); due to the body inabilityto produce enough insulin to compensate for the impaired ability to use insulin (Deshpande *et al.*, 2008). The disease affectsabout 10% of the world population. Symptoms of diabetic patient include; frequent urination, are susceptible tothirst and hunger (Tedong, 2006). Other symptoms are;numbness, loss of sensation and coordination, imbalance and feet

pains,imbalance in carbohydrate, protein and lipid metabolism resulting to chronic blood glucose (sugar) leading to severe complications which could result to death (Ghorbani*et al.*, 2010). With treatment, complications such as blindness, atherosclerosis, and impotence may occur. For the treatment of this disease, market is filled with different synthetic anti-diabetic drugssuch as insulin sensitizers (biguanides, thiazolidinediones), insulin secretagogues (sulfonylureas, meglitinides), α-glucosidase inhibitors, incretin agonists and dipeptidyl peptidase-4 inhibitors (Lorenzati*et al.*, 2010), but the associated side effect of these drugs with long term use has paved way for plant-based products.It is estimated that 3.4 million patients died from diabetes-related complications in 2004. According to a report by World Health Organization (August, 2011), about 346 million people have diabetes worldwide.According to a recentresearch conducted by the International Diabetes Federation (IDF), about 425 million persons are said to be living with DM worldwide, with nearly 50% of these population undiagnosed (IDF, 2017). With Africa and Asia contributing a significant fraction to this population with over 151 million of people who lived with diabetes in year 2000, 194 million people in 2003, 246 million in 2006, 285 million in 2010 and 415 million in 2015 (Adeloye*et al.*, 2017) and 425 million in 2017 with an estimated increase to 629 million in 2045 (IDF 2017). In Africa, there are over 16 million people with the burden of diabetes and this number is likely to increase to 41 million by 2045. The estimated prevalence of diabetes in Africa is 1% in rural areas, and ranges from 5% to 7% in urban sub-Saharan Africa (Ogbera*et al.*, 2014). Without serious action, this number is likely to double by 2030, there is a need to look inward and proffer drastic measures to control the prevalence of the disease.

The first anti-diabetic drug, metformin, isolated from *Galega officinalis*, is an herbal formulation (Tiwari *etal.*, 2014). Various plant extracts like aloe (*Aloe vera L*), bitter Melon (*Momordica charantia*), fenugreek (*Trigonellafoenumgraecum*), Asian ginseng (*Panax ginseng*) and American ginseng (*Panax quinquefolius L*), gymnema (*Gymnemasylvestre*), milk thistle (*Silybummarianum*), nopal (*Opuntia streptacantha*), salacia (*Salacia oblonga; SalaciaReticulate*), and formulations like those of chromium have been used and clinically tested for their anti-diabetic activity as well as their potential side effect (Shane, 2009).

Gymnema sylvestre(Retz.) R. Br. (Asclepiadaceae) also popularly known with these local names:kashe*zaki* (Hausa) and*enugi-bata* (Nupe)in Nigeria, is well distributed across a large area, occurring from East Africa to Saudi Arabia, India, Sri Lanka, Vietnam and southern China, as well as Japan (Ryukyu Islands), Philippines, Malaysia, Indonesia and Australia. In

addition, it occurs throughout most of West Africa and extends to Ethiopia and South Africa. In Niger State, the plant is often found around river coasts of adjoining forests especially River Gbako in Katcha Local Government, Niger State, Nigeria.*G.Sylvestre*has long been used as a treatment for diabetes (Vishwa, 2015). Popularly known as sugar destroyer(*Kashezaki* in Hausa) due to its ability to suppress sweetness of sugar in traditional medicine practice and most notably in the control of blood glucose. A number of studies have evaluated the effects of *G.Sylvestre*on blood sugar in animals (Thakur *et al*., 2012). Scientific investigations conducted onthe herb proved it as a lipid-lowering agent, for weight loss and for the inhibition of caries primarily in rodent studies. This planthas good prospects in the treatment of diabetes as it shows positive effects on blood sugar homeostasis, controls sugar cravings, and promotes regeneration of pancreas.Indigenous medicinal plants are interestingly and largely underexplored source for the discovery of potential "lead" for chemotherapy drug development. Within the last 10 years, a number of Gymnema products, including Gymnema capsules, Gymnema tea, Bioshape®, and Diaxinol® have appeared in the world market.

Chemotherapy, the conventional treatment for diabetes is of health concern owing to some factors including; drug resistance, cost, adverse side effects and inaccessible nature of the available anti-diabetic drugs especially for a developing country like Nigeria. Despite the fact that Nupe ethno-medicine is very rich in recipes such as chewing the leaves of *G.Sylvestre*to suppress sweet-taste, these claims have not been supported with pharmacological investigations. To the best of our knowledge from available literature, gymnemic acid is yet to be reported to be isolated, evaluatedand purified from indigenous*G. Sylvestre*aerial parts sourced locally from Nigerian ecosystem particularly fromTafa Forest, Baddegi,Katcha Local Government, Niger State, Nigeria.

Sample collection and Identification

Freshand healthy-looking aerial parts of*G. Sylvestre*were collected from their natural habitat atTafa Forest near Baddegi, Katcha Local Government, Niger State, Nigeria in the month of January, 2018.The material was identified by chewing few leaves of the plant for a minute or two and the mouth rinsed with clean water, few grains of sugar was placed in the mouth. Disappearance of the sugar sweetness confirms it to be *G. Sylvestre*.For further identification, the plant was identified by a plant taxonomist at the National Institute for Pharmaceutical Research and Development, Idu-Abuja, Nigeria and a voucher specimen kept for future reference.

Extraction, Isolation and Purificationof Gymnemic acidbyHoopers' Method as reportedby Krishna *et al*.(2012) with slight modifications

Processing of *G.*sylvestreAerial Parts

Aerial parts of *G. Sylvestre*were collected from its natural habitat in the morning by hand picking and kept in plastic sealable bags. The parts werewashed thoroughly under running tap water and air-dried under shade for about two (2) weeks. About 500 g of the washed air-dried aerial partswas and finally crushed and pulverized into powdery form, sieved with a 40 sieve mesh and kept in plastic sealable bags for further use. The woody fibres of the stem was discarded and the powdered material stored in air-tight container for further use.

Extraction and Isolation of *G.sylvestre*Aerial Parts

The dried powdered aerial parts were subjected to Soxhlet sequential extraction with petroleum ether and methanol in acontinuous hot extraction as shown in step 1 to 3 below. The solvent soluble extracts collected, filtered and evaporated to fine dry precipitates using Rotary evaporator.

Step 1: Extraction with Petroleum Ether

About 350 g of dry aerial parts powder was packed into a cleansoxhlet extraction unit. 3.5 liters of petroleumether (60-80^{o}C) added and extracted for 24-36 h till all the components soluble inpetroleum ether are removed. Petroleum ether extract was then collected andevaporated using Rotary evaporator.Petroleum ether extraction is only used for defattingdried aerial parts powder.

Step 2: Extraction with 90% Methanol

The resultant defatted powdered dry aerial parts extract from step 1 above was then packed in a soxhlet thimble and extracted continuously with 90% methanol until the material was completely exhausted. The solvent, methanol was afterwards removed from the methanol soluble extract under reduced pressure using rotary evaporator to give thick paste (brown gum).

Step 3:Isolation of Pure Gymnemic Acid from Methanol Extract

A known amount of the thick paste(brown gum) of the methanol extract from step 2 above was dissolved in 1% aqueous KOH solution and continuously stirred for 45 min to 1 h. The solution was then filtered using filter paper to separate the undissolved particles and dilute HCl added slowly under constant stirring, during whichthe gymnemicacidwas precipitated.

Precipitatedsolution was filtered under suction and the precipitate(greenish amorphous powder) was dried. The greenish amorphous powderprecipitateobtainedis thepure gymnemic acid.

Tests for Identification of Gymnemic Acid:

The identification of theisolated gymnemic acid was carried out and noted for its abilitytoabolish the sense of sweetness, froth test, test for acidity, Liebermann-Burchard color test, phenolic test, melting point and solubility test.

Evaluation of the Antidiabetic Activity of Gymnemicacid Isolated from the Locally Sourced *G.sylvestre*Aerial Parts.

Toxicity Study:

Toxicity study was carried out according to the OECD guidelines. Precipitate dissolved in DMSO was administered to 6 rats at different dosage (1600 mg/kg body weight, 1900 mg/kg body weight and 5000mg/kg body weight) and observed for 24 h for any change in autonomic or behavioral response to determine the safe dose (Khatune*et al*., 2016).

Induction of Diabetes

Freshly prepared solution of alloxan monohydrate (110mg/kg) was injected intra-peritoneally in overnight fasted rats. After 3 days, blood sample was collected from the tail-vein of overnight fasted rats and measured using a glucometer.Animals with marked hyperglycemia were selected for the study (Lenzen, 2008).

Experimental Design:

The experimental rats were divided into six groups with three animals in each group: Group I-Diabetic, treated with gymnemic acid (150mg/kg body weight/15 days) orally. Group II-Diabetic, treated with gymnemic acid (300mg/kg body weight/15 day) orally, Group-III-Diabetic, treated with gymnemic acid (600 mg/kg body weight/15 days) orally,Group IV–Diabetic, treated with standard drug (Glibenclamide (10mg/kg bodyweight/15 days),Group V–Control (diabetic), Group VI – Control (Uninduced).Rats were fasted overnight and blood was withdrawn from the tail on the 3rd, 6^{th,} 9th, 12th and 15thdays. The changesin body weight was observed throughout the treatment period at five day interval in experimental animals.After the 15th dose of treatment with the precipitate, the rats were sacrificed and blood samples collected in centrifuge tubes for lipid profiling.

Determination of Blood Glucose Level

The blood glucose level in mg/dl was determined during the periods of treatment within three days intervals using finetestautocoding glucometer which was done by collecting the blood through orbital puncture of the tail-vein of rats (Khatune*et al*., 2016).

Collection of Blood Sample

Collection of sample for biochemical analyses was as described by (Yakubu *et al*., 2003).The animals were anasthesized with chloroform and blood was collected through cardiac puncture into a clean, dry centrifuge tubes. The blood sample was allowed to stand for 10minutes at room temperature and then centrifuged at 1000rpm for 15min to get the serum for the determination of; serum lipid profile (plasma cholesterol concentration, triglyceride concentration, serum HDL-C and LDL-C)

Statistical Analysis

Values were analyzed using statistical package for social science (SPSS) version 16 and presented as means ± SE of the mean. Comparisons between different groups were carried out by one-way analysis of variance (ANOVA) followed by Duncan's Multiple Range Test (DMRT). The level of significancewas set at $P < 0.05$ (Adamu and Johnson, 1997) as reported by Shittu and Tanimu 2012.

RESULTS AND DISCUSSION

Phytochemical composition

Table 1 present the qualitative phytochemical compositions of methanolaerial parts extract of *G.sylvestre*. The results revealed the presence of terpenoids, alkaloids, phenols,tannins, flavonoids, saponins and reducing sugar but steroids &phlobatannins were absent.

Table 1. Quatitative phytochemical composition of methanol aerial parts extract of *G.sylvestre*

Phytochemicals	Inference
Terpenoids	+
Alkaloids	+
Phenols	+
Tannins	+
Flavonoids	+
Reducing sugar	+
Saponins	+

Steroids	-
Phlobatannins	-

Key: + = present, - = absent

Fasting Blood Glucose (FBG)

The effect of the precipitate from methanol extract of *G.sylvestre*aerial parts (gymnemic acid)on fasting blood glucose level of alloxan induced diabetic rat is presented in Table2. A significant (P<0.05) and progressive increase in blood glucose level was observed in diabetic untreated rats throughout the experimental period. The group of rats treated with gymnemic acid at dosage 150, 300 and 600 mg/kg produced 49.33%, 65.33% and 82.92 % hypoglycemic effect compared with 81.53% recorded for glibenclimide treated rats (Table 2).

Serum lipid profile

Table 3 shows the effect of gymnemic acidon serum lipid profile of alloxan induced diabetic rat. A significant (P<0.05) increase in triglycerides (292.85, 210.71,192.87 and 309.83in mg/dL) and total cholesterol(77.77, 77.77, 83.33 and 98.90 in mg/dL) and reduction in high density-lipoprotein (96.42, 117.85, 128.57 and 98.78 in mg/dL) and lowdensity-lipoprotein{65.78, 51.92,45.97 and 72.34 (mg/dL)}levels were observed in diabetic untreated rat when compared with the normal glycemic rats and other experimental group. Administration of gymnemic acid at dosage of 150, 300 and 600 mg/kg triggered a significant (P<0.05) and dose dependent decrease in the elevated triglycerides, total cholesteroland increase in high and low density-lipoprotein comparedtodiabetic untreated rats.

Table 2:Effect of gymnemic acidon fasting blood glucose level of alloxan induced diabetic rat in mg/dL

	Post Induction Days					
	3	6	9	12	15	% Glucose reduction
150 mg/kg	411.34±3.44^{ab}	356.35±5.43^{b}	380.45±8.94^{c}	299.26±4.32^{ab}	208.40±3.89^{ab}	49.33±5.20^{a}
300 mg/kg	459.32±7.56^{b}	357.68±4.32^{b}	213.90±9.34^{b}	177.38±1.89^{b}	159.27±2.89^{ab}	65.33±5.2^{b}
600 mg/kg	506.68±9.45^{c}	482.16±6.23^{c}	317.26±8.34^{ab}	150.90±1.89^{b}	86.53±1.45^{a}	82.92±5.47^{c}
Standard	591.18±11.97^{d}	382.90±3.24^{ab}	320.68±8.09^{ab}	278.31±2.89^{ab}	109.19±0.67^{b}	81.53±5.37^{c}

Control	496.78±8.09[c]	497.37±2.89[c]	513.89±8.35[d]	578.69±13.45[c]	588.04±11.89
Uninduced	109.56±1.86[a]	110.35±0.89[a]	109.24±0.97[a]	108.36±1.78[a]	110.64±0.67[b]

Data are MEAN±SEM of triplicate determination. Values along the same row with different superscript alphabet are significantly different ($p<0.05$)

Table 3: Lipid Profile

	Cholesterol (mg/dL)	Triglyceride (mg/dL)	HDL-Cholesterol (mg/dL)	LDL-Cholesterol (mg/dL)
150 mg/kg	77.77±2.93 [ab]	292.85±3.21 [b]	96.42±0.89 [a]	65.78±1.87 [b]
300 mg/kg	77.77±1.98 [ab]	210.71±2.34 [a]	117.85±1.90 [b]	51.92±2.13 [a]
600 mg/kg	83.33±0.97 [b]	192.87±4.32 [a]	128.57±0.34 [b]	45.97±1.90 [a]
Standard	66.89±0.89[a]	197.08±1.90 [a]	138.90±3.43[bc]	48.09±1.03 [a]
Control	98.90±1.92 [c]	309.83±3.43 [c]	98.78±1.89 [a]	72.34±2.34 [c]
Uninduced	58.88±1.90[a]	201.98±2.87 [a]	150.54±4.34 [c]	45.34±2.21 [a]

Data are MEAN±SEM of triplicate determination. Values along the same row with different superscript alphabet are significantly different ($p<0.05$)

Table 4: Body weight in g

	0	5	10	15
150 mg/kg	161.78±3.45	158.93±3.24	154.34±3.45	156.83±3.45
300 mg/kg	157.90±2.98	155.08±2.84	151.98±2.98	155.90±2.94
600 mg/kg	161.89±3.95	158.76±3.90	158.62±3.90	164.90±5.43
Standard	159.78±4.45	156.97±2.34	159.76±3.56	165.78±4.32
Control	161.75±3.89	158.68±3.54	149.89±2.89	124.53±3.97

Uninduced	158.97±2.89	161.97±2.34	167.98±5.67	171.90±4.97

Discussion

Blood glucose is a key marker for the diagnosis and prognosis of diabetes mellitus. Alloxan selectively destroys the pancreatic insulin secreting β-cell leaving the less active cell behind thus, making diabetes to set in. The evaluation of hypoglycemic activity of antidiabetic agent using alloxan-induced hyperglycemia model has been widely accepted (Etukand Muhammed, 2010). Results from the present study revealed that administration of alloxan results in hyperglycaemic state as evident by a remarkedelevation in blood glucose level from normal to the range of 411-591 mg/dL. However, dose dependent reduction in blood glucose level was observed in alloxan-induced diabetic rats treated with gymnemic acid as obtained from the study (from 411.34-208.40 mg/dL at 150 mg/kg15 days body weight and 506.68-86.53 mg/dL at 600 mg/kg/15 days body weight of rats). The blood glucose reducing activity was accompanied by improvement in the body weights of the rats during recovery (154.34-156.84, 151.98-155.90, 158. 62-164.90 weight in g). Possible mechanism for the reduction in blood glucose level-body weight improvement could be as a result of increased insulin secretion by the pancreatic stimulation and the prevention of absorption of glucose in the gut (Borhanduddlin*et al*., 1994). The insulin deficiency cause drastic elevation in glucose level due to excessive production of endogenous glucose and cause changes in body weight (Ramachandran*et al*., 2011) which may be due to excessive breakdown of tissue protein and lipid caused by insulin defficiency as observed in diabetic untreated rats.

Since, lipid abnormalities accompanied with atherosclerosis is the major cause of cardiovascular disease in diabetes, for ideal treatment of diabetes, in addition to glycemic control, there need be apositive effect on lipid profiling. High level of TC and LDL are major coronary risk factors (Temme*et al*., 2002). Furthermore, several studies suggested that TG itself is independently related to coronary heart disease (Khatune*et al*., 2016). The abnormalities in lipid metabolism lead to elevation in the levels of serum lipid and lipoprotein that in turn play an important role in occurrence of premature and severe atherosclerosis, which affects patients with diabetes (Khatune*et al*., 2016). Hence, measurements of biochemical parameters are necessary to prevent cardiac complications in diabetes condition (Ravi *et al*., 2005).

In the present study, administration of alloxan revealed a significant increase in cholesterol, LDL and triglyceride. However, administration of the gymnemic acid from *G.sylvestre* tend to

restore the elevated parameters towards normal level thereby reflecting the hypolipidemic property of this compound.The reduction in total cholesterol concentration (when compared with 98.90 mg/dL for control diabetic rat to 83.33mg/dL for diabetic rat treated with 600 mg/kg body weightin serum of rats following the administration of the gymnemic acid) might have resulted from inhibition of cholesterol biosynthesis in the liver (Sinclair *et al*., 2001), and the inhibition of the absorption of cholesterol via the small intestine (Evers, 2008). The dose dependent reduction in triacylglycerol recorded in this study (309.83mg/dL for control diabetic rat to 192.87mg/dL for diabetic rat treated with 600 mg/kg body weight gymnemic acid) could also be attributed to the presence of alkaloids and saponins, which could result in the reduction of the absorption of dietary glucose in the gastrointestinal tract due to 'autointoxication' or "leaky gut' (Evers, 2008).

The dose dependent increase in serum HDL levels of rats (98.78 mg/dL for control diabetic rat to 128.57 mg/dL for diabetic rat treated with 600 mg/kg bodyfollowing the administration of gymnemic acid)suggested a possible boost of HDL-C biosynthesis in the liver promoted by the presence of flavonoids (Renaud *et al*., 1999). Therefore, more cholesterol would be transported from peripheral tissues to the liver for excretion and could be the reason for the reported trend in the serum cholesterol concentration.

The observed increase and decrease in the serum HDL-C and LDL-C levels respectively as compared to diabetic untreated rat (98.78 mg/dL), suggests a reduced risk of developing atherosclerosis following repeated administrations of gymnemic acid to diabetic rats.

CONCLUSION

Although there are many phytoconstituents that could combat diabetes, a single phytoconstituent that could be used in the treatment of the disease would be a plus andgymnemic acid fulfills this criteria. The masses needto be made aware of the factthat diabetes mellitus could result from over-accumulation of sugar molecules especially sucrose along with fat molecules(especially in the northern part of Nigeria with high level of sugar consumption) since they are posing a big threat after cardiac problems and cancer. From thisresearchwork, it can be concluded that gymnemic acid (a precipitate from the methanolic extract of *G.sylvestre* aerial parts sourced locally from Nigeria ecosystem) might be that single phytoconstituent needed to combat diabetes and is a safe and effective ethno-medicinal compound for the treatment of diabetes.

REFERENCES

Adeloye, D., Ige, J. O., Aderemi, A. V., Ngozi, A., Emmanuel, O. A., Asa, A.&Gbolahan, O. (2017). Estimating the Prevelance, Hospitalization and Mortality from Type II Diabetes Mellitus in Nigeria: A Systematic Review and Meta-analysis.*Biomedical Journal*, 7.

Deshpande, A. D., Harris-Hayes, M. &Schootman, M. (2008). Epidemiology of Diabetes and Diabetes-Related Complications. *Phys. Ther*, 88:1254-1264.

Etuk, E. U. & Muhammed, B. J. (2010). Evidence Based Analysis of Chemical Method of Induction of Diabetes Mellitus in Experimental Rats. *International Journal of Research and Pharmacological Science*, 1(2):139-142.

Evers, B. M. (2008). Small Intestine. In: Townsend CM, Beauchamp RD, Evers, B. M., Mattox, K. L., eds. Sabiston Textbook of Surgery. 18th ed. St. Louis, Mo: WB Saunders; chap 48.

Ghorbani, A.,Varedi, M., Hadjzadeh, M. R. &Omrani, G.H. (2010) Type-1 Diabetes Induces Depot- Specific Alterations in Adipocyte Diameter and Mass of Adipose Tissues in Rat. *Experimental Clinical Endocrinology for Diabetes*,118:442-448.

International Diabetes Federation (2017). Diabetes atlas. 8th ed. Brussels: International Diabetes Federation.

Khatune, N. A., Bytul, M. R., Ranjan, K. B. & Mir, I. I. W. (2016). Antidiabetic, Antihyperlipidemic and Antioxidant Properties of Ethanol Extract of *Grewiaasiatica* Linn. Bark in Alloxan Induced Diabetic Rats.*BMC, Complementary and Alternative Medicine*, 16:295.

Krishna, R.B., Reddy, S.R.R., Javangula, H., Swapna, D. & Reddy, K.J. (2012). Isolation and Characterization of Gymnemic Acid from *Gymnemasylvestre* R.Br. in Control of Diabetes.*International Journal of Life Science & Pharmacology Research*, 2(1):1-8.

Lenzen, S. (2008). The Mechanisms of Action of Alloxan and Streptozotocin Induced Diabetes. *Diabetology*, 51:216-26.

Lorenzati, B.,Zucco, C.,Miglietta, S., Lamberti, F. & Bruno, G. (2010). Oral Hypoglycemic Drugs: Pathophysiological Basis of their Mechanism of Action. *Pharmaceuticals*,3:3005- 3020.

Organization for Economic Co-operation and Development (OECD) (2002). Guidelines for testing of Chemicals / Section 4:Health Effects Test, 423: Acute Oral Toxicity – Acute Toxic Class Method. Paris: OECD.

Ogbera, A. O. &Ekpebegh, C. (2014). Diabetes Mellitus in Nigeria: The past, Present and the Future. *World Journal of Diabetes*,5:905-11.

Oyedemi, S. O., Bradely, G., &Afolayan, A. J. (2009). Ethnobotanical Survey of Medicinal Plants Used for the Management of Diabetes Mellitus in the Nkonkobe Municipality of South Africa. *Journal of Medicinal plants Research*, 3:1040-1044.

Ramachandran, R.,Zhao,X.F.&Goldmam,D.(2011).*Proceeding of nationalacademic science USA*.108(38);15858-63.

Ravi, K., Rajasekaran, S. & Subramanian, S. (2005). Anti-hyperlipidemia effect of *Eugeniajambolana* seed kernel on streptozotocin-induced diabetes in rats. *Food Chemical Toxicology*, 43: 1433-1439.

Shane, McWhorter, L. (2009). Dietary Supplements for Diabetes: An Evaluation of Commonly Used Products.*Diabetes Spectrum*, 22; 4:206–213.

Shittu, O. K. and Tanimu, M. (2012). Proximate Analysis of Wheat Supplemented Diet and its Anti-trypanosomal Effect on Infected Rat. *International Journal of Applied Biological Research*, 4(1 & 2):109-103.

Tedong, L., Dzeufiet, P. D. D., Asongalem, A. E., Sokeng, D. S. P., Callard, P., Flejou, J. F. & Kamtchouing, P. (2006). Antihyperglycemic and Renal Protective Activities of *Anacardiumoccidentale*(Anacardiaceae) Leaves on Streptozotocin Induced Diabetic Rats.*African Journal of Traditional Medicine*, 3(1):23-25.

Thakur, Gulab S., Rohit, Sharma, Bhagwan, S.,Sanodiya,Mukeshwar P., Prasad G. B. K. S.& Prakash, S. Bisen (2012). *Gymnemasylvestre*: An Alternative Therapeutic Agent for Management of Diabetes. *Journal of Applied Pharmaceutical Science*, 2(12):001-006.

Tiwari, P., Mishra, B.N. &Sangwan, N.S. (2014). Phytochemical and Pharmacological Properties of *Gymnemasylvestre*: An Important Medicinal Plant. *Bio-Medical Research International*, Article ID 830285, 18 pages.

Vishwa, R. L. (2015).Isolation of Gymnemicacid from *Gymnemasylvestre*.*International Journalfor Exchange of Knowledge*, 2 (1):117-123.

World Health Organization, (2011), Global atlas on cardiovascular disease prevention andcontrol. Geneva, World Health Organization.

In-vitro Antibacterial Activity of an Extract, Fractions and Terpenols from Lantana camara Linn Leaves against Selected Oral Pathogens

[1*]Fadipe, L, A., [2]Babayi, H., Abiola, B. F. & [1]Nnabuchi, F

[1]Department of Chemistry, Federal University of Technology, Minna, Niger State, Nigeria
[2]Department of Microbiology, Federal University of Technology, Minna, Niger State
*Corresponding Author: labake.fadipe@futminna.edu.ng

Abstract

Ethnomedicinally, the leaves of *Lantana camara* (family: Verbenaceae) has a lot of applications, some of which includes in the treatment of bacterial infections. Successive and exhaustive partitioning of the crude methanol extract of the leaves (L) gave rise to the chloroform (Lc) and ethyl acetate (Le) fractions which both revealed the presence of terpenes and steroidal nucleus. Fractionation and purification of the ethyl acetate fraction (Le) led to the isolation of two long chain terpenols which were structurally elucidatedas 3, 7, 11, 15-tetramethyl-2-hexadecen-1-ol (2-Phyten-1-ol) and 3, 7, 11, 15- Tetramethylhexadeca- 2, 6, 10, 14- tetraen-1-ol (geranylgeraniol)using physical, chemical and spectral properties in comparison with literature data. Antibacterial assay of the crude extract, L (2500-10,000 µg/cm^3), its two fractions, Lc and Le (2500-10,000µg/cm^3 each) and the two isolated compounds (100 µg/cm^3) in comparison with amoxillin and ampiclox (100µg/cm^3) against selected Gram positive and Gram negative oral pathogens revealed that L and Lc exhibited no inhibitoryactivity; Le displayed a broad spectrum activity, while, the isolated compounds inhibited growth of only Gram positive pathogens.The results obtained from this study have provided some evidence for the ethnomedicinal use of the *Lantana camara* leaves as an antibacterial agent.

Keywords: Isolation, *Lantana camara*, Leaves, Oral pathogens, 2-Phyten-1-ol, Geranylgeraniol

Introduction

Natural products, such as medicinal plants have over the centuries been a source of very active therapeutic agents due to the presence of various secondary metabolites. These metabolites are known to display extensive range of bioactivities, thereby enhancing immune systems and giving resistance against several diseases in order to protect the body from harmful pathogens (Khalid *et al*., 2018). The emergence of bacterial resistance strains to most antibacterial agents has made it pertinent to keep investigating natural products, especially plants, as possible alternatives because of their availability, cheapness and low toxicity (Patil*et al*., 2015). *Lantana camara* Linn (Verbenaceae) is an ornamental evergreen, perennial, aromatic shrub. Though considered a noxious weed, it is a medicinal plant that possesses much potential (Mamta*et al*., 2012). It is commonly known as Red sage/Lantana weed/Wild sage/Curse of Barbados (English), Kashinkuda (Hausa), Anya nnunu (Igbo) and Ewonadele (Yoruba). It is native to the

tropics and sub-tropics, highly invasive in many countries, growing up to a height of 1-3 m and a width of 2.5 m. Leaves are oppositely arranged, ovate in shape, rough, scabrid, bright green, hairy and aromatic when pulverized; stems possess prickles; flowers are small, clusters, most often orange/bright yellow in color with other varieties, such as white, blue, pink red and dark red, changing color with age and occurs year round. Fruits are also small, drupaceous, shinning and are either dark purple, greenish-blue, dark blue or black having two nutlets that are often dispersed by birds (Burkill, 1985; Ghisalberti, 2000; Lonare*et al*., 2012; Vedavathi*et al*., 2013). Traditionally, various organs of the plant are useful in different parts of the world in the treatment of different diseases, such as asthma, ulcers, rheumatism, malaria, dysentery, toothache, epilepsy, leprosy, itches, chicken pox, eczema, cataract, flu, yellow fever, skin problems, blood pressure and as an abortifacient (Burkhill, 1985; Abdullah *et al*., 2009; Hiteshi*et al*., 2012; Ingawale and Goswami-Giri, 2014). There has been a great variation in the phytochemical constituents of *L. camara* which differ for different climates and geographical region (Musyimi*et al.,* 2017), but generally, a significant presence of phenolic compounds, especially flavonoids and tannins, alkaloids, sterols, terpenoids, fatty acids, aromatics and glycosides (Burkhill, 1985; Mamta*et al*., 2012; Kalita*et al*, 2012; Vedavathi*et al*., 2013; Ingawale and Goswami-Giri, 2014; Charan and Kamlesh, 2015; Jafaar*et al*., 2018) has been reported and several classes of these compounds have been isolated from different organs of the plant. One of the commonly isolated compounds from the plants is the triterpenoids (Lai *et al*., 1998; Misra and Laatsch, 2000; Sharma *et al*., 2000; Wahab*et al*., 2003; Yadav and Tripathi, 2003; Hitesh*et al.,* 2012; Ingawale and Goswami-Giri, 2014; Patil*et al*., 2015).The plant has antimycobacterial (Begum *et al*., 2008), antibacterial (Patil*et al*., 2015), analgesic (Kalyani*et al*., 2011), antifungal (Das and Godbole, 2015; Fayaz*et al*., 2017), antioxidant (Anwar *et al*., 2013), wound healing (Swamy*et al*., 2015), mosquito repellant (Akumu*et al*., 2014) and antimicrobial (Lyumugahe*et al*., 2017) properties to mention a few.

Terpenes /Terpenoids are small molecules synthesized by plants and are the largest and most diverse group of bioactive compounds, mostly made up of essential oils. They are made up of units of five carbon atoms in the order C_5, C_{10}, C_{15}, C_{20}, C_{25}, C_{30} and C_{40} structures, where they exist as either acyclic or cyclic (Seigler, 2012). They are known to exhibit significant antimicrobial, antibacterial, antiviral, anti-inflammatory and anticancer potentials (Mahato and Sen, 1997).This study presents the isolation and characterization of two of the terpenols of the plant, as well as investigation of the antibacterial potentials of the crude methanol extract, its

chloroform and ethyl acetate fractions and the isolated terpenolsagainst some oral pathogens in comparison with amoxillin and ampiclox.

Materials and Methods

Extraction of plant material

The leaves of *L. camara* were collected from Kakuri, Chikun Local Government Area of Kaduna State in the month of February, 2018. The leaves were air-dried, pulverized and 700 gwas cold macerated with methanol for a week until a colorless extractant was obtained. The resulting solution was filtered, concentrated *in-vacuo* and brought to dryness over a water bath. Crude MeOHextract was labeled 'L' (17 % recovery).

Preliminary qualitative screening

i) Liebermann-Burchard's test: Addition of few drops of acetic anhydride to a chloroform solution of the extract, L followed by addition of 1 cm^3 of conc. H_2SO_4 down the side of the test tube. Formation of a pink, purple or blue-violet color/green, greenish-blue color after a few minutesis indicative of terpenoids and steroidal nucleus respectively.

ii) Salkowskii's test: Addition of few drops of conc. H_2SO_4 to a chloroform solution of extract, L. Formation of a yellowor red coloration in the lower layer indicates the presence ofterpenoids and steroidal sapogenins respectively.

Thin Layer Chromatography (TLC)

Stationary phase: Silica gel 60 F_{254}pre-coated TLC sheets (0.25 mm thickness)

Mobile phases: (a) Hexane: $CHCl_3$ (4: 1), (b) hexane:EtOAc (9:1) and (c)$CHCl_3$: EtOAc (9:1)

Chromogenic reagents: All chromatograms were (i) viewed under UV light (254 and 366 nm) and developed with: (ii) I_2 vapor and (iii) Liebermann-Burchard's reagent and heated to 120^oC

Solvent partitioning

A portion of extract L (90 g) was solubilized in 500 cm^3 of distilled water, homogenized and allowed to stand for an hour. The resulting mixture was filtered and the filtrate partitioned exhaustivelyand successively in a separatory funnelwith chloroform (100 cm^3 x 7)and ethyl acetate (100 cm^3 x 10) until the extractant was colorless. Both mixtures were concentrated *in-*

*vacuo*and dried at room temperature to afforda fraction labeled as the $CHCl_3$ fraction (Lc, dark green gummy mass, 0.98%) and EtOAc fraction (Le, blackish-green gummy mass, 1.7%). Both fractions were screened for the presence/absence ofterpenes and steroidal nucleus.

Isolation and characterization of compounds

The ethyl acetate fraction, Le(1.5 g) was applied to the surface of a prepared flash column packed with silica gel (60-120 mesh, 30 g, wet method) and eluted sequentially with varying proportions of increasing polarity of petroleum ether: EtOAc (100:0 to 0:100). Similar fractions were pooled based on their TLC profile and concentrated *in-vacuo* to yield 5 major sub-fractions, Le1 – Le5. Sub-fraction Le1 (obtained from pet. Ether: EtOAc, 19: 1) yielded a significant yellow spot along with some steroidal and terpenoidal spots on TLC. Further subjection of fraction Le1 to a shorter column (silica gel, mesh 230-400 nm, increasing polarity of petroleum ether: $CHCl_3$ afforded yellow oil (compound I) from pet ether: $CHCl_3$ (9:1). From a mixture of pet ether: $CHCl_3$ (4: 1), a sub-fraction which revealed a major and minor spot on TLC was purified by washing severally with methanol to which the minor spot was soluble. The insoluble major spot revealed a single spot on TLC (compound II). Both compoundswere subjected to physical, chemical and spectral characterization.IR and UV were both recorded in $CHCl_3$ using FTIR 8400 spectrometer and UV-3101PC spectrophoton respectively. ^{1}H-NMR, ^{13}C-NMR and DEPT-135 spectra were recorded in $CDCl_3$ on Jeol 400 Brukerspectrometer operating at 400 MHz, while, GC-MS was recorded using Agilent Model 7890 GC with split/splitless injector interfaced to an Agilent 5975 mass selective detector. The MS operating condition was ionization voltage 70eV and ion source 240^{o}C. GC was fitted with a DB-5 fused silica capillary column (30 x 0.32 mm, film thickness 0.25 μm)

Antibacterial Assay

Sources of organisms

Samples from dental abscesses and tooth decay were collected from patients who presented pathological symptoms at dental unit of General Hospital Minna, Niger State, Nigeria, by rubbing the lesions with sterile swab sticks. The swab sticks were then transferred to sterile normal saline containers and transported in ice pack to the Microbiological laboratory, Federal University of Technology, Minna, Niger State, Nigeria.

Identification of clinical isolates

The identity of each strain was confirmed by standard bacteriological methods (Cheesebrough, 2010) and 16s rRNA gene sequencing. The organisms, include, Gram positive strains: *Micrococcus luteus*, *Streptococcusmutans*, *Streptococcus pneumoniae*and *Streptococcus pyogenes*; Gram negative strains: *Klebsiellapneumoniae* and *Pseudomonas aeruginosa*

Standardization of test organisms

The method of Collins *et al*., (1995) was employed. Sterile nutrient broth (5 cm^3) was inoculated with a loopful of each organism and incubated for 24 h. 0.2 cm^3 of the 24 h culture was then sub-cultured into a 20 cm^3 sterile nutrient broth and incubated at 37ºC for 5 h to standardize the culture to10^6cfu/cm^3/organism. A loopful of each standardized culture was then used for the assay.

Antibacterial testing

The antibacterial activity of crude methanol extract of *L. camara* leaves, L, its chloroform (Lc) and ethyl acetate (Le) fractions all at concentrations ranging from 2500 -10,000 µg/cm^3were tested against the oral pathogens using the agar dilution test (Collins *et al*. 1995). The activity of each test compound was compared withplates for standard control (amoxicillin and ampiclox; 100 µg/cm^3 each). Extract sterility control (ESC), organism viability control (OVC) and medium sterility control (MSC) were also prepared. All plates were incubated aerobically at 37ºC for 24 h and checked for growth/no growth of organism.

Determination of minimum inhibitory concentration (MIC)

The MIC of theethyl acetate fraction (Le) was determined by microbroth dilution technique as described by (Collins *et al*., 1995). Under septic condition, a loopful of each standardized oral pathogen was inoculated into nutrient broth containing 2500, 3000, 4000, 4500, 5000 and 10,000 µg/cm^3 of fraction Le. All were incubated for 24 h at 37ºC. The MIC was determined by observing tubes with lowest concentration of fraction Le that inhibited the growth of each organism.

Determination of minimum bactericidal concentration (MBC)

The MBC ofethyl acetate fraction (Le) was determined using the Collins *et al* (1995). A loopful of each MIC tube was inoculated into solidified sterile nutrient agar and incubated at 37°C for 24 h. Plates that failed to show any visible growth after 24 h were recorded as MBC.

Results and Discussion

Subjection of ethyl acetate fraction (Le) to gas chromatography-mass spectrometry revealed the presence of fifteen major compounds: germacrene D (a sesquiterpene), diazoprogesterone (steroidal), santolinatriene (a monoterpene), lilac alcohol A and C (monoterpenes), phytol (diterpene alcohol), (Z, Z) - α- farnesene (a sesquiterpene) and geranylgeraniol (a monoterpene), while others were long chain fatty acids,fatty acid methyl esters, some steroidal, phenolic and alkaloidalcompounds.

Characterization of compound I

Physical properties: Light yellow viscous oil, 23 mg, 296 $gmol^{-1}$ and $C_{20}H_{40}O$ (both as revealed by GC-MS). **Chemical properties**: Single spotted on TLC (Hex: $CHCl_3$, 4: 1, R_f 0.55) (Hex: EtOAc, 9: 1, R_f 0.59), blue fluorescence spot under UV, bright yellow (I_2) and purple (Liebermann-Burchard's reagent). Compound was soluble in petroleum ether, $CHCl_3$, Me_2CO, EtOH; insoluble in water. **Spectral properties:FTIR (cm^{-1}):** 2924.5 (C-H stretching), 3310.8 (broad, O-H intermolecular stretch), 1558.1 (C=C stretching) and 1325.0 (C-H bending). **UV (λmax, nm):** 177 (non-conjugated C=C) and 179 (-OH). **GC-MS (m/z, intensity, %):**296 ($C_{20}H_{40}O^+$, 15%, M^+), 278 (M-H_2O, 10%), 263 (M-H_2O + CH_3, 10%),123 ($C_9H_{15}^+$, 30%), 71 ($C_4H_7O^+$,100%, base peak), 57 ($CH_3CH_2CH_2CH_2^+$, 35%) and 43 ($CH_3CH_2CH_2^+$, 40%). **^{1}H-NMR (δ ppm):** Most of the peaks appeared as clusters and were upfield indicating the presence of quite a number of methylene and methyl groups. The most de-shielded peaks were weak and ranged between δ3.78 - 4.91indicating the presence of nucleophilicgroups, -OH and alkene (Table 1). **^{13}C-NMR (δ ppm):**revealed eleven proton de-coupled peaks of which peak at C-6, C-8, C-10 and 12 was of highest intensity/bolder singlet; followed by peaks atC-16 and C-20, C-18 and C-19, indicating that there were more than one carbon atoms resonating at those frequencies. Downfield peaks at δ121.5 and 128.9 are indicative of a methine anda quaternary carbon at C-2 and C-3 respectively, while a peak at δ50.4 indicates a primary alcohol (Table 1). **DEPT (δ ppm):** revealed that of the 11 peaks displayed by ^{13}C-NMR (though a total of 20 carbons), one was quaternary (nulled), four were methine (positive), ten were methylene (negative), while, five were methyl (positive).

Table 1: ^{1}H-, ^{13}C- NMR and DEPT-135^{o} of compound I in comparison with literature values*

Position	^{1}H (ppm)	^{1}H (ppm)*	^{13}C (ppm)	^{13}C (ppm)*	DEPT (ppm)
1	3.97 (d)	4.18	50.4 (H_2C-OH)	58.9	50.4 (neg.)
	4.22 (s)	5.05			
2	4.91 (t)	5.39	121.5 (HC=)	123.8	121.5 (pos.)
3	-	-	128.9(= C-)	139.2	Null.
4	1.90 (t)	1.94	37.4 (-CH_2)	39.6	37.4 (neg.)
5	1.22 (m)	1.31	23.5 (-CH_2)	24.9	23.5 (neg.)
	1.28				
6	1.08 (m)	1.19	34.8 (-CH_2)	37.8	34.8 (neg.)
	1.01				
7	1.25 (m)	1.40	30.8 (-CH-)	33.3	30.8 (pos.)
8	1.08 (m)	1.19	34.6 (-CH_2)	37.7	34.1 (neg.)
	1.01				
9	1. 17 (m)	1.25	23.2 (-CH_2)	24.6	23.2 (neg.)
10	1.08 (m)	1.19	34.1 (-CH_2)	37.7	34.1 (neg.)
11	1.25 (m)	1.40	30.5 (-CH-)	33.2	30.5 (pos.)
12	1.08 (m)	1.19	34.6 (-CH_2)	37.7	34.1 (neg.)
13	1.17 (m)	1.25	23.0 (-CH_2)	24.3	23.0 (neg.)
14	1.08 (t)	1.19	37.8 (-CH_2)	39.9	37.8 (neg.)
15	1.35 (t)	1.62	26.9 (-CH-)	28.1	25.9 (pos.)
16	0.90 (d)	0.91	21.9 (-CH_3)	23.2	21.9 (pos.)

17	1.40 (s)	1.79	15.5 (-CH_3)	16.3	15.5 (pos.)
18	0.81 (s)	0.87	20.7 (-CH_3)	21.0	20.7 (pos.)
19	0.83 (s)	0.89	20.7 (-CH_3)	21.0	20.7 (pos.)
20	0.88 (s)	0.91	21.9 (-CH_3)	23.2	21.9 (pos.)

Keys:s, singlet;d, doublet; t, triplet; m, multiplet;pos., positive peak; neg., negative peak; null, nullified peak; *ACD/ChemDraw (Product Version 15)

A comparative study of the obtained physical, chemical and spectroscopic data of compound I with those published in literature, revealed to be 3, 7, 11, 15-tetramethyl-2-hexadecen-1-ol/ 3, 7, 11, 15-tetramethylhex-2-en-1-ol/2-Phyten-1-olas shown in Figure 1

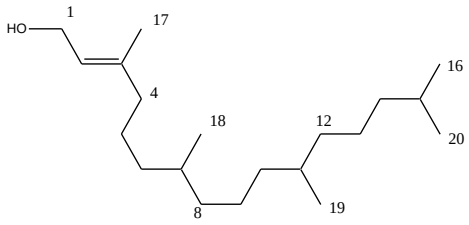

Figure 1: Structure of Compound I (3, 7, 11, 15 -Tetramethyl-2-hexadecen-1-ol)

The compound,2-Phyten-1-ol is an acyclic diterpene unsaturated alcohol (aliphatic diterpenoid alkene alcohol) commonly found in plants, a building block of the chlorophyll molecule and a precursor for the manufacture of vitamins E and K1 (Byju*et al*., 2013). It is useful as a food additive and exhibits significant biological activities, such as anti-spasmodic (Pongprayoon*et al*., 1992), anti-cancer (Lee *et al*., 1999), anti-tubecular (Saikai*et al*., 2010), anti-convulsant (Costa *et al*., 2012), anti-mycobacterial (Bhattacharya and Rana, 2013) and anti-schistosomal properties (de Moraes*et al*., 2014). The compound has been isolated from several plants (Mcneil*et al*., 2012; Passos*et al*., 2012; Thakor*et al*., 2016; Phantangare*et al*., 2017).

Compound II

Physical properties: A colorless viscous volatile oil, 18 mg, 290.5 $gmol^{-1}$ and $C_{20}H_{34}O$ (both as revealed by GC-MS). **Chemical properties**: Single spotted on TLC (Hex: $CHCl_3$, 4: 1, R_f 0.58) (Hex: EtOAc, 9: 1, R_f 0.61), blue fluorescence spot under UV, bright yellow (I_2) and purple (Liebermann-Burchard's reagent). Compound was soluble in petroleum ether, $CHCl_3$,

CH_2Cl_2, Me_2CO, slightly soluble in EtOH and insoluble in water. **Spectral properties:FTIR (cm^{-1}):** 3321 (broad, O-H intermolecular stretch), 3079 (=C-H stretch), 1640 (C=C stretching) and 1452 (C-H bending).**UV (λmax, nm):**184 (-OH) and 201(C=C). **GC-MS (m/z, intensity, %):** 290.5 ($C_{20}H_{34}O^+$, 10%, M^+), 273 (M-H_2O, 10%), 258 (M-H_2O + CH_3, 15%), 69 ($C_4H_5O^+$, 100%, base peak), 81 ($C_5H_7O^+$, 52%), 55 ($C_4H_7^+$, 25%), 41 ($C_3H_5^+$, 58%) and 31 (CH_2OH^+). **^{1}H-NMR (δ ppm):**The most de-shielded peak at 5.11 ppm (a weak triplet) was assigned to the sp^2 hybridized methine carbon atom at C-2 neighboring the C-OH group at C-1, followed by a very weak triplet at4.99 ppm which was also assigned to sp^2 hybridized methine carbon atoms at C-6, C-10 and C-14;while a weak singlet at 4.88 ppm and a doublet at 4.04 ppm were assigned to the –OH group and hydroxylic proton at C-1 respectively. Shielded peaks of which most were sharp singlets were attributed to methylene peaks at 1.90 ppm (C-4, C-5, C-8, C-9, C-12 and C-13), while, peaks at 1.53 ppm was assigned to methyl peaks at C-17, C-18 and C-19) as shown in Table 2. **^{13}C-NMR (δ ppm):** This revealed thirteen proton de-coupled peaks of which peaks at C-4, C-8 and C-12, C-5 and C-9, C-6 and C-10, C-7 and C-11, C-17, C-18 and C-19 were of higher intensities, indicating that more than one carbon atoms were resonating at those frequencies. The most de-shielded peak at 139.5 ppm was assigned to the tertiary carbon atom bearing a sp^2 and sp^3 hybridized carbon atoms at C-3.Other de-shielded peaks ranged from 133.8 to 120.2 ppm, all peaks of high intensities,indicating the presence of several sp^2 hybridized carbon atoms in the molecule (C-2 and C-3, C-6 and C-7, C-10 and C-11, C-14 and C-15). Another de-shielded peak at 51.4 ppm was assigned to a carbon atom bearing a nucleophilic –OH group (C-1). Other peaks which were more shielded were assigned to methine, methylene and methyl carbons respectively (Table 2). **DEPT (δ ppm)** revealed that of the 13 peaks displayed by ^{13}C-NMR (though a total of 20 carbons), four were quaternary (nulled), four were methine (positive), seven were methylene (negative), while, five were methyl (positive).

A comparative study of the obtained physical, chemical and spectroscopic data of compound II with those published in literature, the compound was identified as 3, 7, 11, 15-Tetramethylhexadeca- 2, 6, 10, 14- tetraen-1-ol/tetraprenol/Geranylgeraniol/Geranylgeraniol as shown in Figure 2

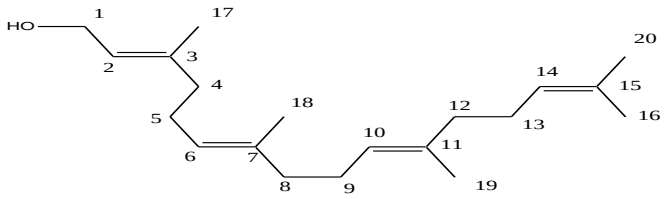

Figure 2: Structure of compound II (Geranylgeraniol, GGOH)

The compound, geranylgeraniol is a long chain diterpene alcohol/isoprenoid/ polyprenol that has been isolated from some plants and is involved in various physiological processes (Ho *et al*., 2018). The compound reportedly exhibited bactericidal activity against *S. aureus* (Inoue *et al*., 2005), anti-mycobacterium and anti-leshmanial activities (Vik*et al*., 2007). The volatile nature of the compound makes GGOH a valuable starting material for perfumes and pharmaceutical products (Tokuhiro *et al*., 2009).

Table 2: ^{1}H-, ^{13}C- NMR and DEPT-135^{o} of compound II in comparison with literature values*

Position	^{1}H (ppm)	^{1}H (ppm)*	^{13}C (ppm)	^{13}C (ppm)*	DEPT (ppm)
1	4.04 (d)	4.18	51.4 (-CH_2OH)	58.9	51.4(neg.)
	4.88 (s)	5.05			
2	5.11 (t)	5.39	120.7 (-CH)	124.6	120.7 (pos.)
3	-	-	133.8 (-C-CH_3)	139.5	Null.
4	1.90 (s)	2.00	36.9 (-CH_2)	39.7	36.9(neg.)
5	1.90 (s)	2.00	25.8 (-CH_2)	26.7	25.8(neg.)
	1.81				
6	4.99 (t)	5.20	121.1 (-CH)	124.3	121.1 (pos.)
7	-	-	132.4 (-C-CH_3)	135.7	Null.
8	1.90 (s)	2.00	36.9 (-CH_2)	39.7	36.9(neg.)
9	1.90 (s)	2.00	25.8 (-CH_2)	26.7	25.8(neg.)
	1.81				

10	4.99 (t)	5.20	120.7 (-CH)	124.3	120.7(pos.)
11	-	-	132.4 (-C-CH_3)	135.7	Null.
12	1.90 (s) 1.83	2.00	36.9 (-CH_2)	39.7	36.9(neg.)
13	1.90 (s) 1.81	2.00	25.1 (-CH_2)	26.4	25.1(neg.)
14	4.99 (s)	5.20	120.2 (-CH)	123.5	120.2(pos.)
15	-	-	129.9(-CH-CH_3)	132.0	Null.
16	1.65 (s)	1.82	22.5 (CH_3)	24.6	22.5 (pos.)
17	1.53(s)	1.79	15.8 (CH_3)	16.4	15.8 (pos.)
18	1.53 (s)	1.79	15.8 (CH_3)	16.4	15.8(pos.)
19	1.53 (s)	1.79	15.8 (CH_3)	16.4	15.8(pos.)
20	1.44 (s)	1.70	17.2 (CH_3)	18.6	17.2(pos.)

Keys: s, singlet; d, doublet; t, triplet; pos., positive peak; neg., negative peak; null, nullified peaks; *ACD/ChemDraw (Product Version 15)

Table 3: Antibacterial activity of ethyl acetate fraction of *Lantana camara*leaves (Le)

Test Organisms	Concentration (µg/cm^3) of test compounds against test organisms							
	**Ethyl acetate fraction (Le)						Ampiclox	Amoxicillin
	2500	3000	4000	4500	5000	10,000	100	100
Gram positive								
M. luteus	-	-	-	-	+*	+	+	+
S. mutans	-	-	-	+*	+	+	+	+

S. pneumoniae	-	-	-	-	+*	+	+	+
S. pyogenes	-	-	+*	+	+	+	+	+
Gram negative								
K. pneumoniae	-	-	-	-	+*	+	+	+
P. aeruginosa	-	-	-	-	+	+	+	+

Keys: +, activity; -, no activity, *, MBC, **the fraction was only static on *P. aeruginosa*, but cidal on all other test organisms

Table 4: Antibacterial activity of the terpenols from the ethyl acetate fraction of *Lantana camara* leaves (Le)

Test Organisms	Activity of test compounds against test organisms at 100 µg/cm^3			
	Compound I	Compound II	Ampiclox	Amoxicillin
Gram positive				
M. luteus	+	+	+	+
S. mutans	+	+	+	+
S. pneumoniae	+	+	+	+
S. pyogenes	+	+	+	+
Gram negative				
K. pneumoniae	-	-	+	+
P. aeruginosa	-	-	+	+

Keys: +, activity; -, no activity

The crude methanol extract (L) and the chloroform fraction (Lc) of the leaves of *Lantana camara* from concentrations ranging from 2500 to 10,000 µg/cm^3 displayed no activity against any of the tested oral pathogens, an indication that the extract and $CHCl_3$ fraction might not be useful in the treatment of oral infections and other infections caused by such organisms. The EtOAc fraction inhibited the growth of all oral pathogens tested. The fraction was cidal on all

the test organisms, except on *P. aeruginosa*, supporting the ethnomedicinal uses of the plant. The observed inhibitory effects may be due to the presence of mid-polar bioactive compounds which all probably acted synergistically (Doughari and Obidah, 2008). Although, the activity displayed by the fraction was at higher concentrations in comparison to that exhibited by the standard drugs at 100 µg/cm^3 (Table 3); sometimes the antibacterial activity of a fraction could be enhanced at lower concentrations with further fractionation and purification (Ndip*et al*., 2009).

The two oils isolated from the ethyl acetate fraction of the plant (compounds I and II) both inhibited the growth of the Gram positive oral pathogens only in comparison to the standard drugs all at 100 µg/cm^3 (Table 4); an indication that both compounds do not possess broad spectrum activity or might become enhanced at higher temperature. Long chain diterpenes possessing the –OH group(s) have been reported to exhibit good bactericidal activity against some Gram positive strains at very low concentrations (Inoue *et al*., 2005, Vik*et al*., 2007).

Conclusion

The ethyl acetate fraction (Le) at concentrations ranging from 4000 – 10,000 µg/cm^3 exhibited a broad spectrum activity against the oral pathogens, while, and the two long chain terpenols isolated from it; 2-Phyten-1-ol (compound I) and Geranylgeraniol(compound II) both inhibited the growth of Gram positive oral pathogens. The results obtained from this study have provided some evidence for the ethnomedicinal use of the leaves of *L. camara* as an antibacterial agent.

References

Abdullah, M. A., Hassandarvish, P., Ali, H. M., Noor, S. M. & Mahmoud, F. H. et al. (2009).Acceleration of wound healing potential by *Lantana camara* leaf extract in experimental rats.*J. Med. Sci.* 3, 75-79

Akumu, E. O., Anthoney, S. T., Mutuku, C. N., Jackie, K. O. & Edwin, M. (2014).Phytopharmacological evaluation of *L. camara* leaves' smoke.*Int. J. of Pharmacy and Biological Sciences*, 4 (2), 28-34

Anwar, F., Shaheen, N., Shabir, G., Ashraf, M., Alkharfy, K. M. &Gilani, A. H. (2013).Variation in antioxidant activity and phenolic and flavonoid contents in the flowers and leaves of Ghaneri (*Lantana camara* L.) as affected by different extraction solvents.*Int. J. of Pharmacology*, 9 (7), 442-453

Begum, S., Wahab, A. &Siddiqui, B. S. (2008).Antimycobacterial activity of flavonoids from *Lantana camara* Linn.*Nat. Prod. Res*., 22 (6), 467-470

Bhattacharya, A. K. &Rana, K. C. (2013).Antimycobacterial agent, (E)-phytol and lauric amide from the plant *Lagasceamollis.Indian J. Chem*. 52B, 901-903

Burkill, H. M. (1985). The *useful plants of West Tropical Africa* vol. 5. Royal Botanical Gardens, Kew

Byju, K., Vasundhara, G., Anuradha, V., Nair, S. M. & Kumar, N. C. (2013). Presence of phytol, a precursor of vitamin E in *Chaetomorphaantinnina*.*Mapana J. Sci*., 12 (2), 57-65

Charan, S. &Kamlesh, C. (2015).Micropropagation and analysis of phytochemical profile of *Lantana camara* whole plant extraction.*World J. of Pharm. and Pharm. Sci*. 4 (8): 1907-1919

Cheesebrough, M. (2010).*Distinct Laboratory Practice in Tropical Countries*.Part 2. UK: Cambrigde University Press, pp. 35-38

Collins, C. H., Lynes, P. M. & Grange, J. M. (1995).*Microbiological Methods*. 7th ed. UK: Butterworth Heinemann, Ltd., pp. 175-190

Costa, J. P., Ferreira, P. B., Sousa, D. P., Jordan, J.&Freitas, M. (2012).Anticonvulsant effect of phytol in a pilocarpine model in mice.*Neurosci.Lett*., 523, 115-118

Das, L. &Godbole, S. (2015). Antifungal and phytochemical analysis of *Lantana camara*, *Citrus limonum* (Lemon), *Azadirachtaindica* (Neem) and *Hibiscus rosasinensis* (China Rose). *J. of Pharmacy Research*, 9 (7), 476-479

de Moraes, J., de Oliveira, R. N., Costa, J. P., Junior, A. L. G., de Sousa, D. P., Freitas, R. M., Allegretti, S. M. & Pinto, P. L. S. (2014). Phytol, a diterpene alcohol from chlorophyll, as a drug against neglected tropical disease - *Schistosomiasismansoni*.*PLOS Neglected Tropical Diseases* 8 (1), e2617

Doughari,J. H. &Obidah, J. S. (2008). Antibacterial potentials of stem bark extracts of *Leptadenialancifolia* against some pathogenic bacteria. *Pharmacology on line*, 3, 172-180

Fayaz, M., Bhat, M. H, Fayaz, M., Kumar, A. & Jain, A. K. (2017). Antifungal activity of *Lantana camara* L. leaf extracts in different solvents against some pathogenic fungal strains. *Pharmacologia*, 8, 105-112

Ghisalberti, E. L. (2000). *Lantana camara* L. (Verbenaceae).*Fitoterapia*, 71, 467-486

Hitesh, H.S., Mayukh, B. & Mahesh, A. R. (2012).Isolation and characterization of chemical constituents of aerial parts of*Lantana camara*.*Int. J. of Pharm. Res. and Bio-Sci*., 1 (6), 198-207

Ho, H. J., Shirakawa, H., Giriwono, P. E., Ito& Komai, M. (2018). A novel function of geranylgeraniol in regulating testosterone production. *Biosci.Biotechnol.Biochem*., 82 (6), 956-962

Ingawale, G. S.&Goswami-Giri, A. S. (2014).Isolation and characterization of bioactive molecule from *Lantana camara*.*Asian J. Res. Chem*., 7 (3), 339-344

Inoue, Y., Hada, T., Shiraishi, A., Hirose, K., Hamashima, H. & Kobayashi, S. (2005). Biphasic effects of geranylgeraniol, terprenone and phytol on the growth of *Staphylococcus aureus.Antimicrobial Agents and Chemotheraphy*, 49, 10.1128/AAC. 49.5. 1770-1774. 2005

Jafaar, N. S., Hamad, M. N., Alshammaa, D. A &Abd, M. R. (2018). Preliminary phytochemical screening and high performance thin layer chromatography [HPTLC] detection of phenolic acids in *Lantana camara* leaves cultivated in Iraq.*Int. Res. J. of Pharm*., 9 (7), 59-64

Kalita, S., Kumar, G., Karthik, L. &Rao, K. V. B. (2012).A review on medicinal properties of *Lantana camara* Linn.*Res. J. Pharm. and Tech*., 5 (6): 711-715

Kalyani, L., Lakshmana, R. & Mishra, U. S. (2011).Antibacterial and analgesic activity of leaves of *Lantana camara*.*International Journal of Phytomedicine*, 3, 381-385

Khalid, S., Shahzad, A., Basharat, N., Abubakar, M.& Anwar, P. (2018).Phytochemical screening and analysis of selected medicinal plants in Gujrat.*J.PhytochemistryBiochem*, 2,108

Lai, J. S., Chan, Y. F., Huang, K. F. & Chin, I. (1998).Triterpenoids, flavonoids and a mixture of campesterol, stigmasterol and β-sitosterol from the stem of pink flowering taxa of *Lantanacamara*.*Pharm. J. (Taipei)*, 50, 385-392S

Lee, K. L., Lee, S. H. & Park, K. Y (1999). Anticancer activity of phytol and eicosatienoic acid identified from *Perilla* leaves. *J. Korean Soc. Food Sci. Nutr*., 28, 1107-1112

Lonare, M. K., Sharma, M., Hajare, S. W. &Borekar, V. I. (2012).*Lantana camara*: Overview on toxic to potent medicinal properties. *Int. J. Pharm. Sci. Res*., 3 (9), 3031-3035

Lyumugahe, F., Uyisenga, J. P., Bayingana, C. &Songa, E. B. (2017). Antimicrobial activity and phytochemical analysis of *Vernoniaaemulans*, *Vernoniaamygdalina*, *Lantana camara*and *Markhamialutea* leaves as natural beer preservatives. American *J. of Food Tech*., 12 (1), 35-42

Mahato, S. B. &Sen, S. (1997). Advances in terpenoid research 1990-1994. *Phytochemistry*, 44, 1185-1236

Mamta, S., Jyoti, S. &Sarita, K. (2012). A brief review on: Therapeutic values of *Lantana camara* plant. *Int. J. of Pharm. & Life Sci*. (IJPLS), 3 (3), 1551-1554

Mcneil, M. J., Porter, R. B. & Williams, L. A. (2012).Chemical composition and biological activity of the essential oil from Jamaican *Cleome serrata*.*Nat Prod. Comm*., 7, 1231-1232

Misra, L. &Laatsch, H. (2000).Triterpenoids, essential oil and photooxidative 28-13-lactonization of oleanolic acid from *Lantana camara*.*Phytochemistry*, 54, 969-974

Musyimi, D. M., Opande, G. T., Chesire, J., Sikuku, P. A. &Buyela, D. K (2017).Antimicrobial potential and screening of phytochemical compounds of *Lantana camara* Linn. IJRDO- *J. of Biological Sciences*, 3(6), 18- 35

Ndip, R. N., Ajonglefac, A, N., Wima, T., Luma, H. N., Wirmun, C. &Efange, S. M. (2009). In-vitro antimicrobial activity of *Ageratum conyzoides* (Linn.) on clinical isolates of *Helicobacter pylori*.*African Journal of Pharmacy and Pharmacology*, 3 (11), 585-592

Passos. J. L., Barbosa, L. C., Demuner, A. J., Alvarenga, E. S., Silva, C. M. &Barreto. R. W. (2012). Chemical characterization of volatile compounds of *Lantana camara* L. and *Lantana radula* Sw. and their antifungal activity.*Molecules*, 17, 11447-11445

Patil, G., Khare, A. B., Huang, K. F. & Lin, F. M. (2015). Bioactive chemical constituents from the leaves of *Lantana camara* L. *Indian J. of Chemistry*, 54B, 691- 697

Phatangare, N. D., Deshmukh, K. K., Murade, V. D., Hase, G. J. &Gaje, T. R. (2017). Isolation and characterization of phytol from *Justiciagendarussa*Burm.f. –An anti-inflammatory compound.*Int. J. of Pharmacognosy and Phytochemical Research*, 9 (6), 864-872

Pongprayoon, U., Baeckstreom, P., Jacobson, U., Lindstreom, M. &Bohlin, L. (1992). Antispasmodic activity of β-datascenone and e-phytol isolated from *Ipomoea pescaprae*. *PlantaMedica*, 58, 19-21

Saikai, D., Parihar, S., Chanda, D.*et al.*, (2010).Anti-tubecular potential of some semisynthetic analogues of phytol.*Bioorg. Med. Chem. Lett.*, 20, 508-512

Seigler, D. S. (2012).*Plant secondary metabolism*. Springer Science and Business Media pp. 668

Sharma, O. P., Singh, A. & Sharma, S. (2000). Levels of lantadenes, bioactive pentacyclictriterpenoids in young and mature leaves of *Lantana camara* var. aculeate.*Fitoterapia*,71, 487-491

Swamy, M. K., Sinniah, U. R. &Akthar, M. S. (2015). *In vitro* pharmacological activities and GC-MS analysis of different solvent extracts of *Lantana camara* leaves collected from tropical region of Malaysia. *Evidence-based Complementary and Alternative Medicine*, 2015, 1-9

Thakor, P., Mehta, J. B., Patel, R. R. &Thakkar, V. R. (2016). Extraction and purification of phytol from *Abutilon indicum*: cytotoxic and apoptotic activity. *RSC Advances*, 6 (54), 48336-48345

Tokuhiro, K., Muramatsu, M., Ohto, C., Kawaguchi, T., Obata, S., Muramoto, N., Hirai, M., Takahashi, H., Kondo, A., Sakuradani, E. & Shimizu, S. (2009). Overproduction of geranylgeraniol by metabolically engineered *Saccharomyces cerevisiae*. Appl. Environ.Microbiol.,75 (17), 5536-5543

Vedavathi, T., Bhargavi, K., Swetha, G. &Mythri, K. (2013).Estimation of flavonoid, phenolic content and free radical scavenging activity of fresh unripe fruits of *Lantana camara* Linn.(Verbenaceae).*Int. J. of Res. in Pharmacology and Pharmacotherapeutics*, 2 (issue 1), 286-294

Vik, A., James, A. &Gundersen, L. L. (2007). Screening of terpenes and derivatives for antimycobacterialactivity ; identification of geranylgeraniol and geranylgeranyl acetate as potent inhibitors of *Mycobacterium tuberculosisin-vitro*. *PlantaMedica*, 73 (13), 1410-1412

Wahab, A., Siddiqui, B. S. & Begum, S. (2003). Pentacyclictriterpenoids from the aerial parts of *Lantana camara*.*Chem Pharm Bull (Tokyo)*, 51, 134-137

Yadav, S. B. &Tripathi, V. (2003).A new triterpenoid from *Lantana camara*.*Fitoterapia* 74, 320-321

Preparation, Characterization and Application of Activated Carbon From *Terminalia Avicennioides Pods* For the Removal Of Heavy Metals From Electroplating Effluent

Akoyi, A. K., Yisa, J. & Jacob, J. O.

Department of Chemistry, Federal University of Technology, P. M. B. 65, Minna, Niger State, Nigeria.

Corresponding Authors email:
*kabirabdulkadir30@gmail.com

Abstract

In this study, activated carbons were produced from Terminalia avicennioides pods by chemical activation using 50% ortho-phosphoric acid and 1M NaOH labeled as Acid treated Terminalia avicennioides activated carbon (ATAC/H_3PO_4) and Base treated Terminalia avicennioides activated carbon (BTAC/NaOH) respectively. The activated adsorbents were used for the removal of Ni, Cd, Fe and Zn ions from an electroplating effluent using batch adsorption process. Physico-chemical properties such as pH, bulk density, moisture content, ash content, volatile matter and fixed carbon analysis were carried out. The effects of the process parameters such as the solution pH, contact time, adsorbent dosage, and temperature were studied. Increase in pH of solution between 3 to 7 led to increase in the percentage removal and subsequently decreased above 7. Zn had the highest percentage removal of 95% at 35°C using ATAC/H_3PO_4 and 93% using BTAC/NaOH. The contact time shows highest percentage removal of 78.30% and 85.72% for Zn and Fe using ATAC/H_3PO_4 and BTAC/NaOH respectively at solution pH of 7. The results showed that the removal efficiency of the metal ions by ATAC/H_3PO_4 and BTAC/NaOH still increases at 0.9g of the sample dosage but declines with continuous increase in temperature. However, higher percentage removal of the metal ions was observed at 0.9g sample dosage and 35^oC temperature.

Keywords: *Adsorption, Heavy metals, electroplating effluent*

1.0 Introduction

Heavy metals are class of pollutants which are very poisonous to the environment even at very low concentrations (Srivastava and Goyal, 2010). They are very toxic to both animals and human beings (Jaishankar *et al.*, 2014), and are non-biodegradable and persistent in the environment (Haware and Pramod 2011).

Pollution by heavy metal has become one of the most serious environmental concerned due to their persistence and toxicity **(**Jaishankar *et al*., 2014**).** These metals sometimes act as a pseudo element of the body while at certain times they may even interfere with metabolic processes.

Heavy metal pollution is caused through various sources, including, industrialization population growth, climate changes and domestic activities. Some of the industries which generate effluent containing varieties of waste products especially heavy metals generally get discharged into the water bodies (Nargawe and Sharma, 2016).

Many industries discharged effluent containing heavy metals into the environment due to the high cost of treatment and lack of effective materials and treatment methods (Gangadhar *et al.*, 2012*)*. The heavy metals in the effluent, if not properly treated are transported from the industrial sites by run-off water to contaminate water sources, downstream and become major contaminants of marine, ground, and even surface water (Neeta and Gupta, 2016).

Conventional methods employed to remove heavy metals such as reverse osmosis, ion exchange, chemical precipitation, electrodialysis, solvent extraction, electrochemical reduction and membrane separation are expensive and inefficient when treating effluents with low concentration of heavy metals (Norhafizah *et al.*, 2011).

In addition, some of these methods generate secondary wastes and in some cases are not effective in the removal of contaminants especially heavy metals. Thus, the demand to develop technologies that will lead to an effective removal of these ions from industrial effluent has become a great challenge.

2.0 Methodology

2.1 Sample Collection and Preparation

Terminalia avicennioides seeds were collected from Tswachiko village, in Agaie Local Government Area of Niger state. Seeds were washed severally with tap water in order to remove dirt's and dusts. The sample was further sun-dried for 2 weeks, squashed with hand slightly to remove the excesses of leaves attached to the seeds and later ground using wooden mortar and pestle to reduce the particle size and to obtain a fine powdery form of the sample.
Metal plating effluent was collected from the effluent storage point of the electroplating section at the Scientific Equipment Development Institute (SEDI), in Niger State. It was carefully bottled in a plastic container and stored in the laboratory for analysis.

2.2 Digestion of electroplating Effluent

$10cm^3$ of the electroplating effluent was measured into a $250cm^3$ beaker. $2cm^3$ of conc. HCl and 5 cm^3 of conc. HNO_3 were then added, heated in a fume cupboard on a hot plate for about 15 minutes to a final volume of $5cm^3$. $15cm^3$ of deionized water was added to the resultant solution and filtered with whatman filter paper No. 45. The filtrate was made up to $50cm^3$ with deionized water. This process was repeated until the desired volume was obtained, and was analysed for the heavy metals content using Atomic Absorption Spectrophotometer (Varian AA 240 FS, USA) in a Multi-User science laboratory of the chemistry department, Ahmadu Bello University Zaria.

2.4 Carbonization

2.4.1 Chemical Activation and Carbonization with Acid

100g of the powdered material to be carbonized were weighed and partially treated with $400cm^3$ of 50% ortho-phosphoric acid for 24hours. The steeped sample was sun-dried and then carbonized in a muffle furnace at the carbonization temperature of 490^oC for 40 minutes to produce an activated carbon. The activated carbon produced were first washed in 0.5M KOH and rinsed thoroughly with excess distilled water until a pH of between 7.0-7.5 was attained, oven dried for 30mins, powdered well and labeled as Acid treated *Terminalia avicennioides* activated carbon *(ATAC/H_3PO_4)* before storing in an airtight container ready for analysis (Hesham *et al*, 2012; Zalilah *et al.*, 2015).

2.4.2 Chemical Activation and Carbonization with Base

100g of the powdered *Terminalia avicennioides* seeds were weighed and partially soaked in $400cm^3$ of 1M NaOH for 24hrs in order to activate the sample prior to carbonization. The steeped sample was sun-dried and then carbonized in a muffle furnace at the carbonization temperature of 490^oC for 40 minutes to produce an activated carbon. The activated carbon produced were washed with 0.5M acetic acid and further rinsed thoroughly with distilled water until a pH of 7.5-8.0 was attained, oven-dried for 30mins and powdered well, labeled as Base treated *Terminalia avicennioides* activated carbon *(BTAC/NaOH)* and stored in an airtight container ready for use (Madu and Lajide, 2013 ; Zalilah *et al.*, 2015).

2.5 Determination of Percentage % Yield of Activated carbon

The percentage (%) yield of the activated carbon produced is the ratio of the weight of the resultant activated carbon to the original precursor weight on a dry basis which was determined using the relation (Ambursa *et al*., 2011).

$$\% \text{ Yield} = \frac{X_1}{X_o} X\ 100$$

Where; Xo = Original mass of precursor on dry basis, and X_1 = Weight of sample after activation, washing and drying.

2.6. Activation Burn Off

Burn off refers to the weight difference between the original samples and activated carbon divided by the weight of the original samples. It was calculated using the equation; (Ambursa *et al*., 2011).

$$\% \text{ Burn off} = \frac{Xo - X_1}{X_O} X\ 100$$

Where; Xo = Weight of sample before activation and carbonation and X_1 = Activated carbon weight.

3.7 Physico-chemical Tests

The activated carbon produced were subjected to preliminary physico-chemical tests such as the pH, bulk density and proximate analysis (moisture content, ash content, volatile matter and fixed carbon) using standard procedures as described in the literature for each of the parameters with little modifications in some cases.

3.7.1 Determination of Activated Carbon pH

The standard pH test method for the determination of activated carbon (ASTMD3838-80) was employed. 1.0g each of the ATAC/H_3PO_4 and BTAC/NaOH was weighed using a Metler analytical weighing balance and transferred into a separate 25cm^3 beakers. 100cm^3 of distilled water was added and stirred for one hour. The samples was allowed to stabilize, then the pH was measured using a pH meter (Ekpete and Horsfall, 2011)

3.7.2 Determination of Bulk Density

5g of the activated carbon; ATAC/H_3PO_4 and BTAC/NaOH were weighed separately and transferred into a 10cm^3 graduated cylinders. The cylinder was tamped gently on a cotton wool while activated carbon was being added until the entire original sample was transferred completely into the cylinder. Tamping was continued for 5 minutes until there was no further settling produced. The volume was recorded and the apparent density was calculated on the dry using the formula below:

$$\text{Bulk Density} = \frac{\text{Sample weight(g)}}{\text{Sample volume } (cm^3)} X\ 100$$

3.7.3 Determination of Moisture Content

Determination of the moisture content was carried out using the thermal drying method. 1.0g of the dried activated carbons were weighed and placed in a washed, dried and weighed crucible. The crucibles were left open and placed in an oven and dried at 105ºC for 4 hours until a constant weight was obtained (Ekpete and Horsfall, 2011). The percentage moisture content was thus calculated as follows:

$$\% \text{ Moisture content (M)} = \frac{(X-Y)}{(X-Z)} X\ 100$$

Where X = Weight of crucible +original sample, Y = Weight of crucible + dried sample and Z = Weight of empty crucible.

3.7.4 Determination of Ash Content

1.0g activated carbon was placed in a crucible of a known weight, heated at 750˚C for 2 hours while the crucible was left open. The sample was then cooled in a desiccator and weighed afterwards. The weight of sample before and after heating was used to determine the ash content using the equation below (Smrutirekha, 2014).

$$\% \text{ Ash content} = \frac{\text{Ash weight (g)}}{\text{Sample weight (g)}} \text{ X } 100$$

$$(\%)\ A_C = (X-Z)/(Y-Z)100$$

Where A_C = Ash content, Z = Mass of empty crucible, Y = Mass of crucible + sample and X = Mass of crucible + ash sample.

3.7.5 Determination of Volatile matter

A known quantity of sample was taken in cylindrical crucible closed with a lid. It was then heated to 925ºC for exactly 7 and half minutes in a muffle furnace. Then the crucible was cooled in a desiccator and weighted.

Volatile matter (VM) on dry basis

$$VM = \frac{100[100(Y-X)-M(Y-Z)]}{[(Y-Z)(100-M)]} \text{ X } 100$$

Where Y = Mass of crucible, lid and sample before heating, X = Mass of crucible, lid and contents after heating and Z = Mass of empty crucible and lid

M = % of moisture determined above.

3.7.6 Determination of Fixed Carbon

Fixed carbon content (FC) was determined using the formula:

FC= 100 - (Ash content + Moisture content + Volatile matter)

3.8 The effect of Process Parameters

The activated carbon was employed for the batch adsorption study to evaluate for its efficiency on the removal of heavy metals with emphasis on the effects of the pH, contact time, adsorbent dosage and temperature. The process were carried out at a constant pH of 7.0, adsorbent dosage of 0.5g, contact time of 120mins, agitation speed of 200rpm and at room temperature except otherwise mentioned.

3.8.1 pH

Adsorption experiments were carried out at solution pH of 3, 5, 7 and 9. The acidic and alkaline pH of the effluent was maintained by adding the necessary amounts of 0.1M hydrochloric acid and 0.5M potassium hydroxide solutions (Nazar *et al.*, 2013). 100ml of the effluent were transferred into 250cm^3 conical flasks, and agitated at 200rpm for 120 minutes with 0.5g of the adsorbent (Chigondo, 2013). The mixtures were filtered and analyzed for residual metal ions using AAS.

3.8.2 Contact Time

In order to determine the optimum time for the adsorption of Fe, Cd, Zn and Ni, using *Terminalia avicennioides* seeds, 50ml of the effluent was contacted with 0.5g of the adsorbent, pH of the effluent adjusted to 7.0 respectively, the solutions were agitated at 200rpm for different contact time (30mins, 60mins, 90mins and 120mins). The mixtures were filtered and analyzed for residual metal ions using AAS.

3.8.3 Dosage

Different doses of the adsorbent (0.1, 0.5, 0.9) was mixed with the effluent and the agitated in a mechanical shaker at 200rpm for 120mins at the pH of 7.0. The percentage of different

adsorption doses were determined by keeping all other factors constant (Nazar *et al.*, 2013). The mixtures were filtered and analyzed for residual metal ions using AAS.

3.8.4 Temperature

The adsorption experiments for temperature variation was carried out at pH of 7.0 using 0.5g sample, 120mins contact time, but different temperatures between (25°C-55°C). The mixtures were filtered and analyzed for residual metal ions using AAS.

3.8.5 Removal Efficiency

Optimal process conditions will be used for the adsorption equilibrium and kinetics justification. The effect of the adsorption properties such as the adsorbent dosage, contact time and the pH on the removal efficiency was determined using the formula below as presented by Said *et al*. (2014).

$$\text{Removal efficiency (\%)} = \frac{C_o - C_e}{C_e} \times 100$$

Where C_o = heavy metal concentration (mg/L) at initial time, C_e = heavy metal concentration (mg/L) at the equilibrium condition.

3.0 Results and Discussion

Table 3.1 Effluent Initial Metal Ion Concentration before Treatment

Metal	Concentration (mg/L)	WHO/UNICEF (2010) Permissible Limit (mg/L)
Cadmium	0.260	0.003
Iron	4421.111	0.30
Nickel	288.176	0.02
Zinc	27.289	3.00

(WHO/UNICEF, 2010).

Table 3.1 Shows the initial metal ions present in the digested effluent sample collected as revealed by the Atomic Absorption Spectroscopy (AAS). This result revealed higher concentrations of heavy metals (Cadmium 0.260mg/L, Iron 4421.111mg/L, Nickel 288.176mg/L and Zinc 27.289mg/L) as compared to the WHO/UNICEF permissible limit.

3.0 Physico-chemical Analysis

Parameters	*ATAC/H_3PO_4*	*BTAC/NaOH*
Percentage Yield (%)	62.50	43.20
Percentage Burn off (%)	56.90	37.66
pH	7.18	7.64
Bulk density (cm^3/g)	0.83	0.59
Ash Content (%)	9.20	13.47

Moisture Content (%)	4.20		4.60
Volatile Matter (%)		17.28	12.42
Fixed Carbon (%)		69.32	69.51

3.1 Percentage Yield and Percentage Burn Off

Activated carbon yield in any particular chemical process is an important variable when scaling up the process (Abechi *et al*., 2013). The *ATAC/H_3PO_4* sample yielded better (62.50%) than that of *BTAC/NaOH* with a percentage yield of (43.20%). However, the percentage burn off of *ATAC/H_3PO_4* and *BTAC/NaOH* were found to be 37.66% and 56.90% respectively.

3.2. Characteristics of *ATAC/H_3PO_4* and *BTAC/NaOH* Activated Carbons

The physico-chemical characteristics such as pH, bulk density, the moisture content, ash content, volatile matter and fixed carbon describe the *ATAC/H_3PO_4* and *BTAC/NaOH* suitability as an adsorbent for the adsorption process and also an indication of whether the activated carbon can be used commercially.

3.2.1 pH of *ATAC/H_3PO_4* and *BTAC/NaOH*

The pH value of activated charcoal is its acidity or basicity with the value of 6-8 usually acceptable for most applications (Egwu *et al.,* 2015). Studies revealed that the values of pH affect the surface and binding capacity of adsorbent due to exchange of H^+ ions with metal ions. However, different pH values favors different adsorbent or metal of interest as lower pH can favor the removal of some metal ions (Sheel *et al.*, 2016). The surface of *ATAC/H_3PO_4* and *BTAC/NaOH revealed an alkaline pH of* 7.18 and 7.64 respectively. Too high or too low pH indicates that acid/base wash was incomplete.

3.2.2 Bulk Density

The bulk density test shows the flow consistency and packaging quantity of an activated carbon sample (Smrutirekha, 2014). Bulk density measures the weight of material that can be contained in a given volume under specified conditions. The macro-porous carbon has a bulk density above 1cm^3/g (pore space volume for gram of carbon). The meso-porous carbon has a bulk density ranging between 0.85-1.0cm^3/g. The micro-porous carbon has a value less than 0.85cm^3/g (Sabino *et al*., 2016). Since *ATAC/H_3PO_4* and *BTAC/NaOH* sample bulk densities are 0.83cm^3/g and 0.59cm^3/g respectively, it revealed that *ATAC/H_3PO_4 and BTAC/NaOH* are both expected to have a good efficiency in the removal of heavy metals.

3.2.3 Ash Content

Ash is the non-carbon or mineral additives that do not combine chemically with the carbon surface. For activated carbons, an ash content of between 1-20% is better and primarily depends on the type of raw material. High ash content above 20% is undesirable for activated carbon since it reduces the mechanical strength of carbon and affects adsorptive capacity (Smrutirekha, 2014). Another study revealed less than 15% ash content to be more efficient (Sabino *et al*., 2016). High ash content in precursor materials contain high levels of impurities that lead to the blockage of pores, thus reducing the surface area of the activated carbon produced. Lower ash content of *ATAC/H_3PO_4* should impact positively on its quality. Therefore, the lower the ash value, the better the activated carbon for use as adsorbent **(**Atef, 2016). *ATAC/H_3PO_4* and

BTAC/NaOH activated carbons are expected to be a good adsorbent because of their low percentage ash content of 9.20 and 13.47 respectively.

3.2.4 Moisture Content

The moisture contents for *ATAC/H_3PO_4* and *BTAC/NaOH* were 4.20 and 4.60% respectively as shown in Table 3.1. However, the general expected moisture content for an ideal activated carbon is that it should be less than 3% **(**Atef, 2016). If the percentage moisture content of activated carbon becomes too high, micro-organisms especially fungi will degrade the carbon during their metabolic processes. In addition, micro-organisms can multiply within the macro and micro-pores of an activated carbon, blocking the pore structure, thus, the absorptive capacity of the carbon is reduced. When activated carbon is exposed to air, it adsorbing moisture from atmosphere thereby increasing its moisture content **(**Atef, 2016). Low amount of moisture is an indication that the activated samples would be good adsorbents for use for adsorption (Egwu *et al.*, 2015).

3.2.5 Volatile matter and Fixed Carbon

Volatile matters are those products with the exception of moisture, given off by a material as gas or vapor during the carbonization process. Physico-chemical analysis data on Table 3.1 showed that the samples treated with *ATAC/H_3PO_4* and *BTAC/NaOH* contained 17.28% and 12.42% volatile matter and yielded 69.32% and 69.51% fixed carbon respectively.

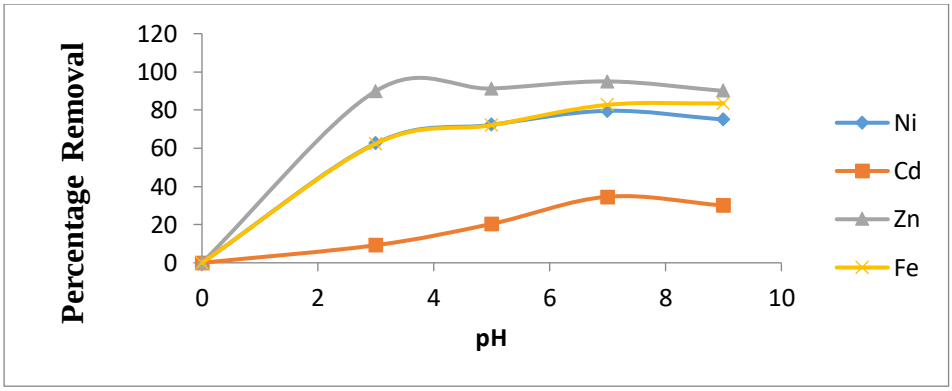

Fig:3.1: Effect of pH on heavy metal removal by *ATAC/H_3PO_4*

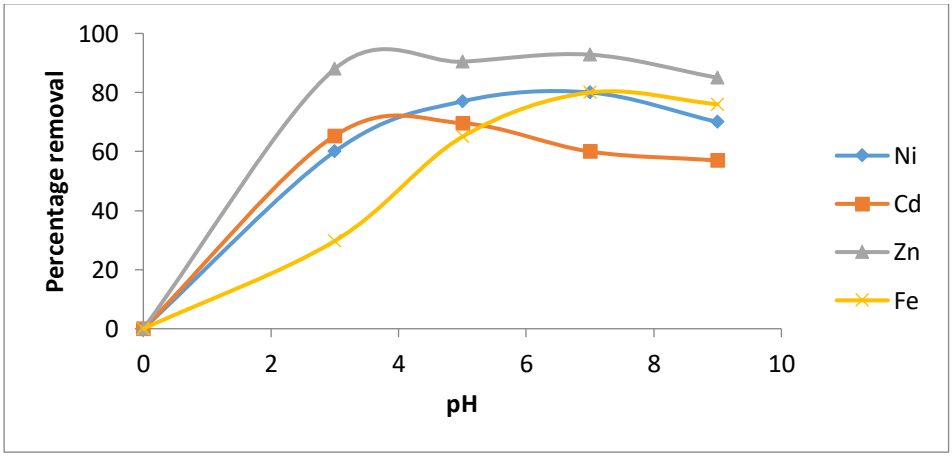

Fig:3.2: Effect of pH on heavy metal removal by *BTAC/NaOH*

It is clear from figures (3.1 and 3.2) that the percentage removal is higher at acidic pH (5.0 – 7.0), reaching maximum of about 95% and 93% for Zn for both acid and base treated adsorbents respectively. The higher percentage removal of the Zn could be attributed to its smaller atomic

size in comparison with Ni, Fe and Cd respectively. However, the percentage removal decreased gradually with the decrease in pH. The maximum adsorption capacities observed at pH 7.0. Adsorption values at pH greater than 7.0 gives rise to lead precipitation, so that active sites would have achieved saturation above a certain range of pH values. The results obtained are in close agreement with reported studies (Mutasim *et al.*, 2017). These obtained results could be explained as, in acidic media i.e. when the pH of solution were less than 4, the elevated hydrogen ions (H+) rival the metal ions from reaching the free available sites on the adsorbent surface and prevent the ions from bounding with activated carbon surface due to the repulsive forces. Besides that, it is also noted when the pH values reaches 5 and above, the adsorption process were enhanced and removal percentage get maximum quantities due to the lower hydrogen ions (H+) that exist, Hence, these ions got better chance to occupy the free sites of the active surface. Later on, when the pH precede toward basic region, the recorded values of removal ions increased significantly specifically at pH of 7. However, pH 9 mostly recorded lower values and shows a decline in the percentage removal. This can be attributed to ions precipitated by the formation of hydroxide anions due to their dissolution reaction (Mutasim *et al.*, 2017 and Barkat *et al.*, 2009).

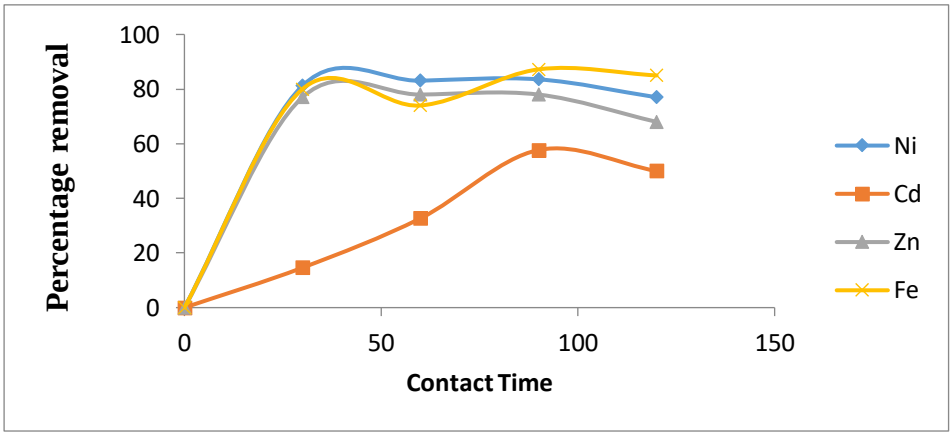

Fig:3.3: Effect of Contact time on heavy metal removal by *ATAC/H_3PO_4*

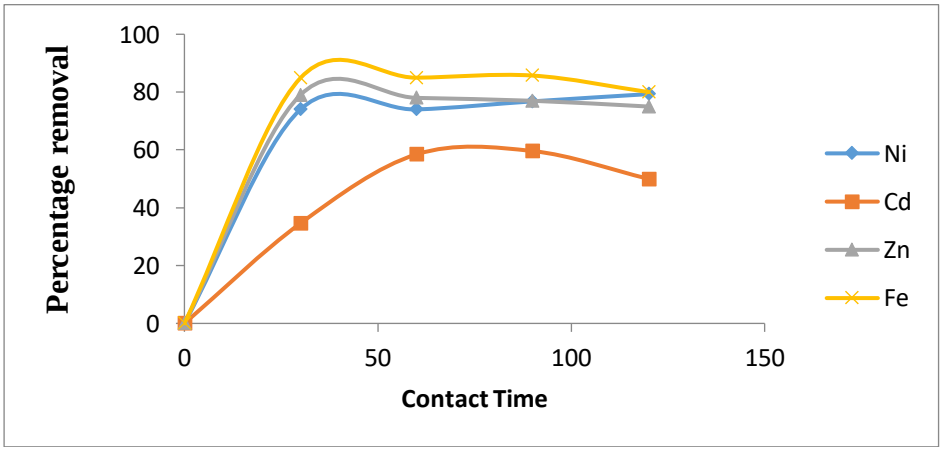

Fig:3.4: Effect of Contact time on heavy metal removal by *BTAC/NaOH*

The effect of contact time on the removal Ni, Cd, Zn and Fe on acid and base treated AC are shown in Figures 3.3 and 3.4 respectively. The amount of the adsorbed metal ions increases with increasing time having a higher percentage removal at 90mins until it began to decrease after 120mins. A decrease in the adsorption capacity is indicative of equilibrium due to saturation of adsorption sites. Rapid adsorption of metal ions during the initial stages was due

to the large initial concentration gradient between the adsorbate in solution and the number of available vacant sites on the adsorbent surface (Mutasim and Yusuf, 2015).

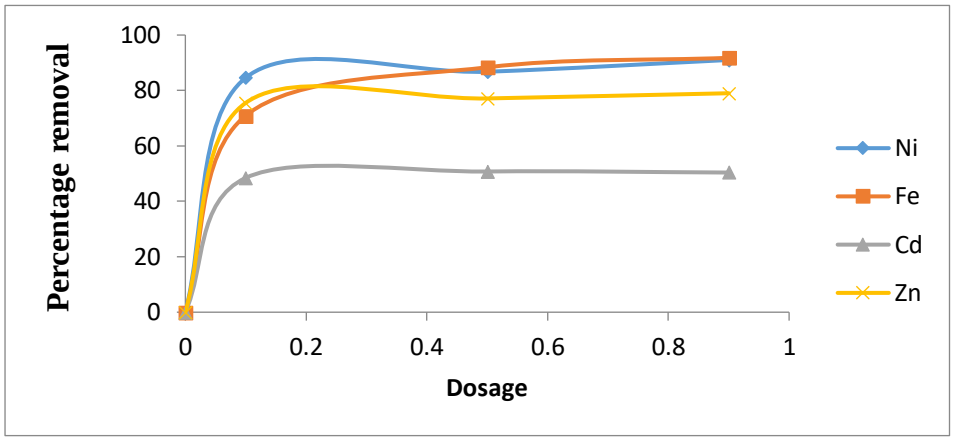

Fig:3.5: Effect of dosage on heavy metal removal by *ATAC/H_3PO_4*

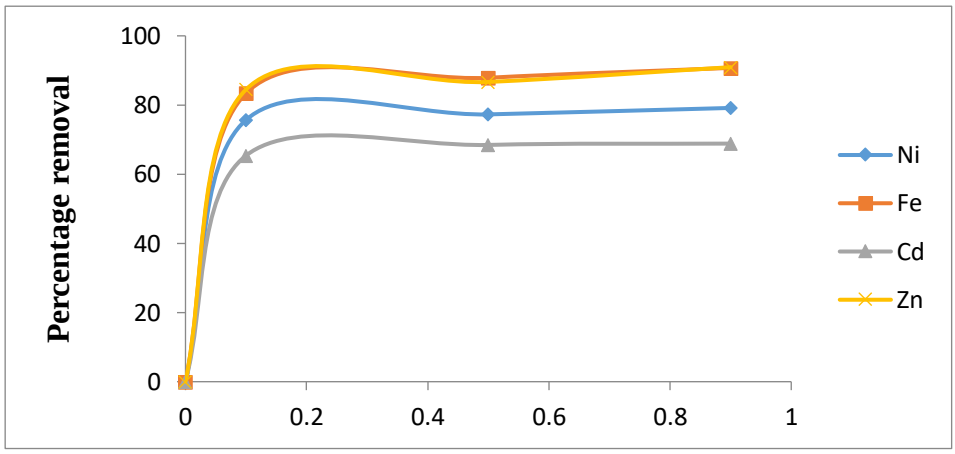

Fig:3.6: Effect of dosage on heavy metal removal by BTAC/NaOH

The effect of adsorbent dose on the removal percentage of Ni, Cd, Fe and Zn ions using *ATAC/H_3PO_4* and *BTAC/NaOH* was illustrated in Figure 3.5 and 3.6 respectively. Different doses of adsorbents ranging from 0.01 – 0.9g were considered and other process parameters were maintained constant (pH – 7.0, Agitation speed of 100rpm, contact time – 120mins and at room temperature. An increase in adsorption capacity with increasing adsorbent dose up to a maximum of 0.9g giving the corresponding optimum percentage removal of Ni (91%), Cd (50%), Zn (79%) and Fe (92%) on ATAC/H_3PO_4 and Ni (79%), Cd (69%), Zn (91%) and Fe (91%) on BTAC/NaOH. On the other hand, it was found that further addition over 0.9g made little or no enhancement in the adsorption process, because there was almost negligible increase in the removal efficiency over the specific adsorbent dose. The initial increase in adsorption capacity as adsorbent mass increases may be due to the increase in the number of exchangeable sites for metal ion adsorption, after which equilibrium was reached (Mutasim *et al.*, 2017).

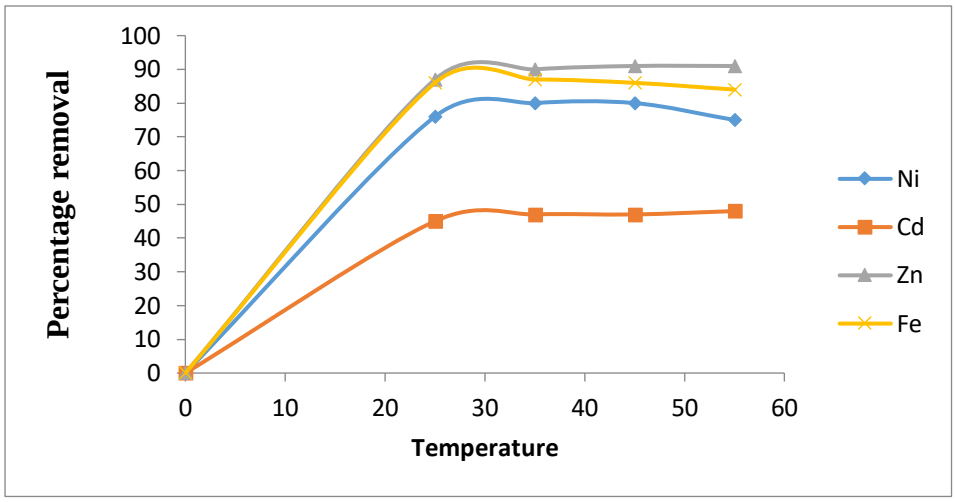

Fig:3.8: Effect of Temperature on heavy metal removal by *ATAC/H_3PO_4*

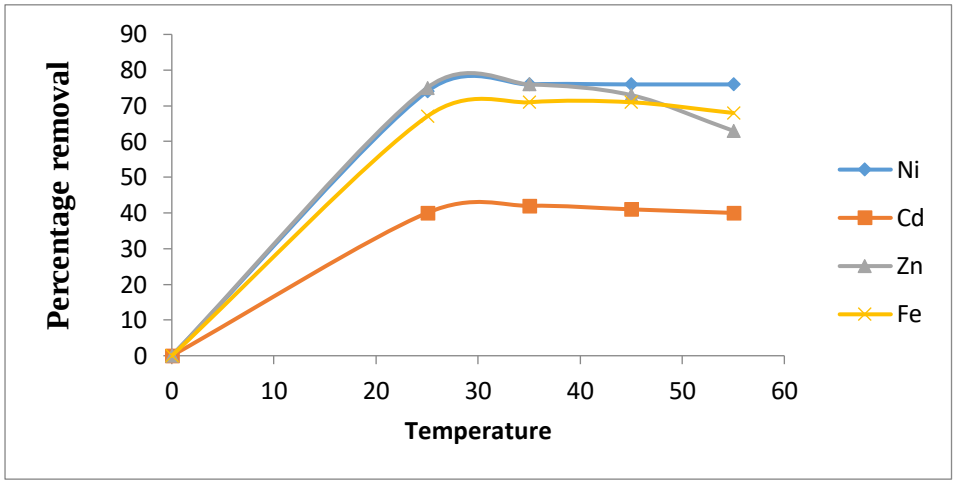

Fig:3.9: Effect of Temperature on heavy metal removal by *BTAC/NaOH*

Effect of temperature on the removal percentage of Ni, Cd, Fe and Zn ions on *ATAC/H_3PO_4 and BTAC/NaOH* are shown in Figures 3.8 and 3.9 respectively. Temperature range of 25-55°C were used for the experiments, adsorbent dose 0.9g, contact time of 120mins and pH 7.0. Adsorption of these metals by the adsorbent witnessed increase in removal percentage and adsorption capacity at 35°C, while as from 45 to 55°C, no significant change with further increase of temperature. Higher rate of adsorption were observed mostly at 35°C with Ni (80%), Cd (47%), Fe (87%) and Zn (90%) for *ATAC/H_3PO_4* whereas Ni (76%), Cd (42%), Fe (71%) and Zn (76%) were observed for BTAC/NaOH. However, low rate of adsorption was generally observed at 55°C within the studied range of temperatures. This indicates that the removals of these metal ions are exothermic (Mutasim and Yusuf, 2015). The high removal percentage may be due to the high diffusion rate of metal ions into the pores as the surface area and pore volume of the adsorbent were large, However, at high temperature the kinetic energy of the species is low and hence contact between the metal ions and the active sites of activated carbon is not sufficient, resulting in reduced removal efficiency (Mutasim *et al.*, 2015).

4.0 Conclusion

Extensive research and knowledge about these low cost adsorbent such as activated carbons from plants materials for the removal of heavy metals will make them more productive and allow their full scale application in the industrial effluent treatment. The prepared activated carbon, *ATAC/H_3PO_4* and *BTAC/NaOH* used in this study is found to have a high capability

for removing Ni, Cd, Fe and Zn ions from aqueous solution with *ATAC/H_3PO_4* being more effective in the process. Adsorption method was successfully applied for the removal Ni, Cd, Fe and Zn ions from aqueous solution. However, the removal efficiency of the ions were found to dependent largely on various parameters such as pH of the solution, contact time, adsorbent dosage and temperature. The pH of the solution played a key role in enhancing the ability of adsorbents towards the metal ion. Increase in the pH of solution from 3 to 7 led to increase in the removal efficiency and subsequently decreased above 7. The results obtained showed that the removal efficiency of these ions by *ATAC/H_3PO_4* and *BTAC/NaOH* increased with time, which is significant in the first stage but decreased subsequently. The experimental results showed that the removal efficiency of the metal ions by *ATAC/H_3PO_4* and *BTAC/NaOH* will decreases with increase in adsorbent dosage, and temperature respectively.

5.0 References

Abechi, S. E., Gimba, C. E., Uzairu, A. & Dallatu, Y. A. (2013). Preparation and Characterization of Activated Carbon from Palm Kernel Shell by Chemical Activation.*Res. J. Chem. Sci.*3(7): 54-61.

Ahmaruzzaman, M. & Vinod K. G. (2011). Rice Husk and Its Ash as Low-Cost Adsorbents in Water and Wastewater Treatment. *Industrial & Engineering Chemistry Research*. 50: 13589–13613.

Ambursa, M.M., Faruk,U.Z., Uba, A., Sahabi, D. M., Atiku, F.A. & Koko, R. A. (2011). Comparative Efficiency of Base Activated Carbon and Acid Activated Carbon for Sorption of Heavy Metals from Waste Water. *Journal of Chemical and Pharmaceutical Research.* 3(6):732-741.

Amin, M. T., Alazba, A. A. & Manzoor, U. (2014). A review of removal of pollutants from water/wastewater using different types of nanomaterial.http://dx.doi.org/10.1155/2014/825910.

Atef, S. A. (2016). Physical, Chemical and Adsorptive Characteristics of Local Oak Sawdust Based Activated Carbons. *Asian Journal of Scientific Research, 9: 45-56.*

Barkat, M., Nibou, D., Chegrouche, S., & Mellah, A. (2009). Kinetics and thermodynamics studies of chromium (VI) ions adsorption onto activated carbon from aqueous solutions. Chemical Engineering and Processing: Process Intensification, 48 (1), 38-47.

Cao, J., Wu, Y., Jin, Y., Yilihan, P. & Huang, W. (2014). Response surface methodology approach for optimization of the removal of Chromium (VI) by NH2-MCM-41, *J. Taiwan Inst. Chem. Eng.* 45: 860-868.

Chigondo, F., Nyamunda1, B.C. Sithole1, S.C. &Gwatidzo, L. (2013). Removal of lead (II) and copper (II) ions from aqueous solution by baobab (Adononsiadigitata) fruit shells biomass. *Journal of Applied Chemistry (IOSR-JAC). 5(1): 43-50.*

Egwu, C. N., Evbuomwan, B. O. & Ibrahim, A. O. (2015). Determination Of Physico-Chemical Properties Of Low Cost Adsorbent Produced From Activated Coconut Wastes. *The International Journal ofScience &Technoledge.*3:265.

Ekpete, A. O. & Horsfall, M. N.R. J., (2011). *Research Journal of Chemical Sciences* 1(3):10-15.

Gangadhar G., Maheshwari U. and Guptac S. (2012).Application of Nanomaterials for the Removal of Pollutants from Effluent Streams.*Nanoscience& Nanotechnology*-Asia, 2:140-150.

Gin, W.A., Jimoh, A.*, Abdulkareem, A.S. &Giwa, A. (2014). Adsorption of Heavy Metal ions from Electroplating Wastewater Using Watermelon Peel Activated Carbon: Kinetics and Isotherm Studies. *International Journal of Scientific & Engineering Research*, 5:304-314.

Hesham, R. L., Jane, M. & Mary, M. M. (2012). The Preparation of Activated carbon from Agroforestry Waste for wastewater Treatment. *African Journal of Pure and Applied Chemistry*. 6(11), 149-156.

Jaishankar, M. Tseten, T., Anbalagan, N., Mathew , B. B. Beeregowda, K. N. (2014).

Toxicity, Mechanism and Health Effects of Some Heavy Metals. *Interdiscip Toxicol*.; 7(2): 60–72.

Madu, P. C. & Lajide L. (2013). Physicochemical characteristics of activated charcoal derived from melon seed husk.Journal of Chemical and Pharmaceutical Research, 5(5): 94-98.

Mutasim, H. E. & Yusuf M I. (2015), Evaluation of the Adsorption Capacities of Activated Charcoal from Sudanese Wooden Parts of Prosopis juliflora, Acacia Nilotica, and Rhamnus Frangula, *International Journal of Emerging Technology and Advanced Engineering*. 5(4): 582-587.

Mutasim H. E., Rashida, M. H., Sumia, A. N., Mawia, H. E. (2017). Preparation and Characterization of Activated Carbon from Palm Tree Leaves Impregnated with Zinc Chloride for the Removal of Lead (II) from Aqueous Solutions. *American Journal of Physical Chemistry. 6(4): 59-69.*

Nakkeeran, E., Rangabhashiyam, S., Giri, N.M.S. &Selvaraju, N. (2016). Removal of Cr(VI) from Aqueous Solution Using StrychnosNux-vomica Shell as an Adsorbent. Desalination and Water Treatment.1-14.

Nazar, A. E., Mutaz A. E. & Mohammed A. E. (2013).Physico-Chemical Characterization and Freundlich Isotherm studies of Adsorption of Fe(II), from aqueous solution by using Activated carbon prepared from Doum fruit waste. Archives of Applied Science Research. 5 (5): 149-158.

Nargawe, T. &Sharma, D. (2016). Baobab fruit shell (*Adansoniadigitata*) as a Natural Adsorbent for Copper and Lead Removal from Industrial Effluent.Research Journal of Chemical and Environmental Sciences.*Res J. Chem. Environ. Sci.* 4 (2): 32-38.

Neeta, S. & Gupta, S. K. (2016).Adsorption of Heavy Metals: A Review. *International Journal of Innovative Research in Science, Engineering and Technology*.5: 2267- 2281.

Norhafizah, B. A. H., Nurul, A. B. R. & Wong C. S. (2011). Removal of Cu(II) from Water by Adsorption on Papaya Seed. Asian Transactions on Engineering (ATE ISSN: 2221–4267). 01: 49-55.

Obaroh, I. O., Abubakar, U., Haruna, M. A., & Elinge, M. C. (2015). Evaluation of some heavy metals Concentartion in River Argungu. *Journal of Fisheries and Aquatic Science.* 10:581-586.

Sabino, D. G., Giusy L., Mariangela, G. & Michele, N. (2016). An Overview of Low Cost Adsorbents for Wastewater Treatment.1-95.

Said, N., Amalina, R., Mazza, S. A. A., Syafiqah, A. K. & Hajar, A. M. S. (2014). Rock Melon Activated Carbon (RMAC) for Removal of Cd(II), Ni(II) and Cu(II) from Wastewater: Kinetics and Adsorption Equilibrium.

Sheel, R., Indu, S., Joy, S. &Naik, R. M. (2016). The Removal of Nickel from Waste Water by Modified Coconut Coir Pith.*Chemical Sciences Journal*.7: 1-6.

Smrutirekha, D. (2014). Characterization of Activated Carbon of Coconut Shell, Rice Husk and Karanja Oil Cake. National institute of Technology Rourkela-769008.

Srivastava, S., & Goyal, P. (2010). Novel biomaterials: decontamination of toxic metals from wastewater. Springer, NY.

Vadivel S., Manickam A., & Ponnusamy S. (2012). Physico-chemical and adsorption studies of activated carbon from Agricultural wastes.

WHO/UNICEF, (2010). Report of WHO/UNICEF joint monitoring programme on water supply and sanitation. New York and Geneva. United Nations Children's Fund and the World Health Organization.

World Health Organization & UNICEF (2013). Progress on Sanitation and Drinking-Water, World Health Organization, Geneva, Switzerland.

Zaharaddeen, N. G. (2015).Preparation, Characterization And Evaluation Of Optimal Activated Carbons Derived From *Prosopis Africana* Seed Hulls For The Removal Of Chlorophenols From Aqueous Solution. 1-24.

Zalilah, M. Y., Norzila O., Hamdan, R. & Ruslan, N. N. (2015). Characterization of Phosphoric Acid Impregnated Activated Carbon Produced From Honeydew Peel. *Jurnal Teknologi.* 76(5). 15-19.

Evaluating Chemical Composition and Biogas Generation from *Rothmannia Longiflora* (Gaude) Fruit Peel

Kwazo H.A., Muhammad M.U., Mohammed S., and Hadi B.A.

Abstract

Many researches on biogas have lately gain large interest particularly on the less known and underutilize waste plants parts in order to exploit their energy potential. This waste discarded plant fruits being an energy carrier as the society is replacing fossils fuels with renewable alternatives due to its market stability, low cost, sustainability, substitute fuel energy composition, greener output and colossal fossil fuel depletion and decrease the massive usage of fossil fuels. This study is aimed at evaluating the biogas potential of fruit peels for their possible utilization as means of energy. The results obtained from proximate analysis were; moisture content (27.33±0.47%), ash content (13.17±0.47%), crude protein (2.51±0, 04), crude lipid (2.33±0.24%), crude fibre (3.67±0.47%), carbohydrate (78.32±0.41) and energy value (344.29). The peel was also found to contained 0.29 ± 0.02 mg/100g phosphorous, 376.67 ± 62.35mg/100g potassium, 59.5 ± 0.82% organic matter, 29.75 ± 0.71 % carbon, 0.8 ± 0.05 % Nitrogen and 43.14 ± 0.07 C:N. The average volume of biogas obtained from the peel of *Rothmannia longiflora* fruits from digesters A to E were 912.8, 950.0, 550.0, 925.0 and 1475 cm^3 respectively at an average temperature of 30^0c and pH of 5.3. The preliminary test shows that only digester A and E gave blue flame while B, C and D does not show any flame when the flame test was carried out on the produced biogas. Blue flame obtained were persistence for more than 10 minutes on the biogas produced. The results indicated that the fruit peel could be a potential viable energy source.

Key words: Proximate, Biogas, *Rothmannia longiflora* fruit peel, flammability.

Introduction

Rothmannia longifloa is a member of the family Rubacea which is a shrub or small tree up to 9m tall. The fruit is a globose to ellipsoid berry, 3.5-7cm x 5-6cm, green-blackish; with 10

indistinct ribs, glabrous, many-seeded, the calyx persistent. Seed lens-shaped, 6-8mm x 1-1.5mm, brown-red (Jansen, 2005). The plant is known locally as "Gaude" or "Katambiri" in Hausa, "Obesaledo" in Edo, "Nwaebotri" among the efik "Aberekamwo" in igbo land and "Iroro" at Yoruba land (Awosan *et al*, 2014). The fruit is commonly used in africa to make blue-black mark-ings on the hands, face and body, sometimes to imitate tattooing. In Nigeria a dye and an ink-like extract (Katambiri) is made from finely crushed seed (Bringmann *et al* ,1999). This study is therefore aimed at evaluating the energy potential of this fruit peels in order to establish purposeful utilization of this less known or underutilize plant fruit of *Rothmannia longiflora.*

Materials and Methods

Rothmania longiflora fruits were randomly plucked from different trees at Wanke bush along Lungu road in shagari local government of sokoto state, Nigeria.

The fruits were collected from different branches of the selected trees using method adopted by Ayaz *et al, (2*002), Asaolu and Asaolu, (2002). The fresh fruits samples were authenticated at the Herbarium unit of the biological science department Usmanu Danfodiyo University, Sokoto. The seed were separated manually from the peel, the peel were air dried and mechanically grounded into fine powder using blender. The powder was stored in a covered plastic container for analysis.

Proximate Analysis

The moisture content was determined at 105^0c in an oven, Ash content was determined at 550^0c. Crude protein, lipid and fiber were determined according to the AOAC (1990) procedures. Crude nitrogen was determined using the Kjeldahl procedure and crude protein value was obtained by multiplying nitrogen value by a factor of 6.25, while available carbohydrate was estimated by difference according to the equation below:

$$CHO = 100 - (\%Ash + \%\ crude\ protein + \%\ crude\ lipid + \%\ crude\ fiber)$$

$$Energy\ value\ (Kcal) = [(\%\ CHO \times 4) + (\%\ crude\ protein \times 4) + (\%crude\ lipid \times 9)]$$

(Hassan *et al.*, 2008)

Mineral Analysis

The sample 0.5g was put into Kjeldahl digestion flask to which 24cm^3 of a mixture of concentrated nitric acid (HNO_3), Conc H_2SO_4 and 60% $HClO_4$ (9:2:1 V/V) was added. The flask was allowed to stand overnight to prevent excess foaming (Sahrawat *et al*, 2002). The flask was put on a heating block and digested to a clear solution, cooled and the content filtered into 50cm^3 volumetric flask. The solution was then diluted. Blank solution was prepared in similar manner without sample being added. The solution was used for mineral analysis. The mineral content (calcium, magnesium, iron, zinc, copper, manganese, lead, chromium, cobalt and cadmium) were analyzed using AAS. Sodium and potassium were analysed using atomic emission spectrometry while phosphorous was determine by colorimetry using Vanadomolybdate (blue) method (AOAC, 1990).

Determination of nitrogen content

Two gram (2g) of the dried sample was weighed into Kjeldahl digestion flask and 0.5g of Kjeldahl tablet was added followed by addition of 10 cm^3 of concentrated tetraoxosulphate (VI) acid. The content was then heated in Kjeldahl digestion unit until the digest became clear (approximately 2hours). After the digest had been completed, the flask was cooled diluted with 10cm^3 distilled water and filtered with a Whatman No1 filter paper in a 100cm^3 volumetric flask and made up to the mark with distilled water. 10cm^3 of homogenous aliquot solution was pipette into distillation flask and 20cm^3 of 45% NaOH solution was added. The content was diluted to about 200cm^3 with distilled water and distilled using micro-kjeldahl distillation apparatus. The distillate was collected in receiving flask containing 10cm^3 boric acid indicator solution. After the distillation, the distillate was titrated with standardized 0.01M HCl to the

end point. Blank was determined using all the reagents in the same quantities as described above. The process was carried out in triplicate and the crude protein (CP) calculated using equation. (AOAC, 1995)

$$\%\mathrm{N} = \frac{(\mathrm{S} - \mathrm{B}) \times 0.1\mathrm{M\ HCl} \times 0.014 \times \mathrm{D} \times 100}{\text{weight of sample } \times \mathrm{V}}$$

Determination of Organic Matter

The organic matter (Volatile solid) was determined by subtracting the percentage of moisture and ash content from 100% (Garba, 1999).

$$Organic\ matter = 100\% - (\%Ash + \%Moisture\ content)$$

Determination of percentage carbon

The percentage carbon was estimated using equation as adopted by Abba *et al* (2014)

$$\%C = 0.5 \times organic\ matter$$

Determination of Carbon-Nitrogen Ration

The **carb**on to nitrogen ratio was evaluated by calculating the ratio of organic carbon content to that of nitrogen content (Bagudo, 2008)

$$C{:}N = \frac{\%\ Organic\ carbon\ in\ the\ sample}{\%\ Nitrogen\ in\ the\ sample}$$

Biogas Generation

The four (4) cylindrical tins, 500cm^3 capacity were used as digesters for this batch anaerobic digestion. A hole was based on the top of the cap of the digester, tube of urine bag was inserted through the hole and glued using araldite to make it air tight. The first set of digesters A was loaded with 100g of substrate and 200cm3 of distilled water (100% sample). The second set of digesters (B) were loaded with the mixture of 70g substrate and 30g cow dung the homogenized with 200cm^3 water while third set of digesters were loaded with 50g substrate and 50g cow dung and finally the set of digesters (E) were loaded with 100g of cow dung and homogenized

with the same quantity of distilled water (200 cm^3). The volumes of the biogas generated were collected continuously in the urine bag for 30 days. Whenever the urine bag is filled it contents will be transferred into a fresh bag and kept as adopted by Abba *et al*, (2014).

Results and Discussion

Table 1-4 present the results of proximate, element composition, volume of biogas generated and percentage yield on average volume of *Rothmannia longiflora* fruit peel.

Table 1: Proximate Composition of *Rothmannia longiflora* Fruit Peel

Components	Peel (%) dry weight
Moisture	27.33 ± 0.47
Ash	13.17 ± 0.47
Crude protein	2.51 ± 0.04
Crude lipid	2.33 ± 0.24
Crude fibre	3.67 ± 0.47
Available CHO	50.99 ± 0.41
Organic Matter	59.50 ± 0.82
Energy	234.97

Table 2: Elements composition of *Rothmannia longiflora* fruit peel (mg/100g dry weight)

Minerals elements	Concentration
Nitrogen (%)	0.80 ± 0.05
Carbon (%)	29.75 ± 0.71
Phosphorous (mg/100g)	0.29 ± 0.02
Potassium (mg/100g)	376.67 ± 62.35
C/N	37.19

Table 3: Volume of Biogas Produced

Week	Biogas volume (cm^3)					Temp.^{0}c
Sample	A	B	C	D	E	31
1st week	150	400	0	500	700	30
2nd week	600	700	200	800	1200	29
3rd week	1400	1300	1000	1100	2000	30
4th week	1500	1400	1000	1300	2000	30
Average	912.5	950	550	925	1475	30

Table 4: Results of percentage yield on average volume

Digester	Average Volume (cm^3)	Percentage Yield (%)

A	912.5	18.96
B	950	19.74
C	550	11.43
D	925	19.22
E	1475	30.65
TOTAL	4812.5	100

Discussion

During anaerobic digestion, microorganisms action indicated that the relative moisture, ash and volatile solid in a given plant material influences the amount of biogas produced (Abdulrahim *et al.*, 2015). Table 1 and figure 1 shows the results of proximate composition obtained from the peel of *Rothmannia longiflora* fruit. The percentage moisture, ash, crude lipid, crude fiber, crude protein, organic matter, available CHO and energy present in biomass are some of the key parameters that influence heating values of solid fuels. The moisture content present in the biomass determine combustion tendency of solid fuels. However, biomass sources that contain higher moisture content proved less efficiency during combustion and hence, to have low heat value which may be attributed to higher use of heat to remove water from the biomass during combustion process. Higher moisture content results to significant amount of heat loss, which eventually does not encourage the solid biomass fuels. Considering the amount of moisture content from fruit under study 27.33±0.47% proves efficient during combustion and hence has more heat value. This value was higher than 2.52±0.14% *L. siceraria*, 2.61±0.03% *J. curcas*, 2.04±0.01% *A.* indica, 1.52±0.02 *R. communes* all of defatted cakes (Baki, 2015) and lower than tomato having 83.15% and breads 55.82%. (Leta *et al.*, 2015). The ash content was found to be (13.17±0.47 %) in the peel *of Rothmannia longiflora*, this indicates that the sample has less impurity that may cause problem to the furnace when stirring heating is applied. High ash content grant valuable substrate for biofertilizer (Ezeonu *et al.*, 2002).This value was lower compared to *Grewia Mollis* (43.14%), *Lannea sp* (44.23%), *Sterculia setigera* (41.18%), *Ficus capensis* (48.08%), *Ficus trichopofda* (49.02%) and *Piliostigma thonnigii* (47.06%) as stated by Ubwa *et al*, (2013). Generally the ash content obtained from fruit peel of *Rothmannia*

longiflora proved to be efficient for biofuel production although less efficient while compared to others.

The percentage crude proteins obtained in *Rothamannia longiflora* fruit peel was 2.51 ±0.04% It is generally accepted as a fact in the biogas technology that protein-rich biomass substrates should be avoided due to inevitable process inhibition and *Rothmannia longiflora* contain low protein content and become suitable for biogas generation. *Rothmannia longiflora* has C/N of 37.19% and substrate compositions with a low C/N ratio are considered difficult to handle and may lead to process failure (Kovács *et al.,* 2013). The optimum yield of biogas is in the range of C/N ratio of 20 – 30 (Dioha *et al.,* 2014) which will make it suitable in biogas production.

The crude lipid content of the fruit peel was 2.33±0.24%, the lower the crude lipid present in the biomass the more the biodegradability of cellulose for biogas production. This revealed that *Rothmannia longiflora* fruit peel has more efficiency; this disagreed with the findings by Dhana *et al.,* (2010) on *Com stover* (64.31%) as less effective in biofuel production as opined by Damirbas (2007).

As shown in table 2 the carbon content of the analyzed was found to be 29.75 ± 0.71% higher than Neem leaves (14.00%) and lower than Bagasse with 53.27% (Dioha *et al.,* 2014). Carbon, nitrogen, potassium and phosphorus from *Rothmannia longiflora* fruit peel, were found to have important role in viability of biomass for fuel production. Carbon influences the combustion process and calorific value of the solid fuels, also known to have undergone oxidation with hydrogen and exothermically releases thermal energy which is more intense with high carbon contents in a sample (Abdullah, 2013).

The microbial population involved in the bioconversion of organic materials into biogas requires sufficient nutrients to grow and multiply. Each specie required both a source of carbon and nitrogen. The nitrogen contents in the sample indicates that *Rothmannia longiflora* fruit peel (0.80 ± 0.05%) may have lower emission of NOx upon combustion while compared with the nitrogen content from groundnut and Rape seed cake with higher content, which could be

attributed to the protein nature of the cakes that could also prolong combustion that affect the environment as reported by Maishanu and Hussein, 1991.

The role played by potassium in the synthesis of carbohydrates cannot be over emphasized, it assist in the synthesis of proto plasmic protein and is believed to increase vigour in plants (Abdulrahim *et al.,* 2015). This research showed that the potassium level for *Rothmannia longiflora* fruit peel is high for use on farm land in order to become more fertile and increase crop production as well as healthier growth as stated by Baki *et al.,* (2004). Even though, the nitrogen and phosphorus content in this study shows the reduction in nutrient of the plant part. Taking in to consideration of their analyzed compositions they still satisfy the requirement for use as biofertilizer.

In an attempt to biogas generation from fruit peel, the average volume of biogas obtained from digesters A to E were 912.8,950, 550,925 and 1475 cm^3 respectively at an average temperature of 30^0C and pH of 5.3. The results obtained indicate that the peel of *Rothmannia longiflora* produced appreciable amount of biogas (912.5cm^3) which has 18.96% yield compared to the biogas produced by cow dung (1467cm^3) with percentage yield of 30.65 % been used as control in this study. Preliminary assessment of biogas produced was carry out where by a flame test were employed to evaluate the biogas produced, digesters A and E shows a persistent blue flame for more than ten (10) minutes while in the remaining digesters no flame was observed. Therefore, observation of the blue flame on digester A which is 100% *Rothmannia longiflora* fruit peel indicate that the peel could be a good potential sources of biogas energy generation. realize

Conclusion

The results obtained from the study shows that the peel of *Rothmannia longiflora* contained considerable amount of carbohydrate, moisture, ash content organic matter and total solids. However crude protein, crude lipids and fiber were found in lower percentage which shows that the percentage compositions of the parameters are accepted for biogas generation. Similarly, the significant concentration of Carbon, Nitrogen, Potassium and Phosphorous were

found to have an impact role in viability of biomass for fuel production. Inaddition the peel has display to be a good potential for energy generation. Further works are on for the analysis of biofuel generated from the peel.

References

Abba A, Faruq U.Z, Birnin-Yauri U.A, Yarima M.B and Umar K.J (2014). Study on Production of Bigas and Bio-ehanol from Millet Husk. *Annual Research and Review in Biology* 4**(5)**:817-827 SCIENCEDOMAIN International.

Abdullahi, A. S. (2013). Biodiesel production and characterization from Calabash and Pumpkin. Thesis submitted to the Department of pure and Applied Chemistry, Usmanu Danfodiyo University, Sokoto for the award of PhD in Renewable Energy. Pp 35. Unpublished

Abdulrahim U. Rabah A. B. Baki A. S. Orjiude J. E. and Idris A. D. (2015). Biogas production using guinea corn and rice husk. *J. Microbiol. Biotech. Res.*, 5 (5):53-62 (http://scholarsresearchlibrary.com/archive.html) ISSN : 2231 –3168 CODEN (USA) : JMBRB4

Adamu A.S, Ojo J.O and Oyetunde J.G (2017) Evaluation of Nutritional Values in Ripe, Unripe, Boiled and Roasted Plantain (*Musa paradisiacal L*) Pulp and Peel. *European Journal of Basic and Applied Science* 4**(1)** ISSN2059-3058

AOAC (1990) Official Methods of Analysis. 14th Edition Association of Official Analytical chemist. Washington DC.

AOAC (1995) Official Methods of Analysis 15th Edition. Association of Official Analytical Chemist, Washington DC.

Asaolu-Barko E and Asaolu S.S (2002). Proximate and Mineral Composition of Cooked and Uncooked *Solomum Melangena*. *International Journal of Food Science and Nutrition* 53:615-624.

Awosan E.A, Lawal I.O, Ajikigbe J.M and Borokimi T.L (2014). Antimicrobial Potential of *Rothmannia longiflora Salis* and *Canna* inica lim extract against selected strains of fungi and bacteria. *African Journal of Microbiology Research*. 8**(24)**:2376-2390.

Ayaz, F.A, hung, H.S, Chuang L.T, Vander-Jagt D.J and Glew R.H (2002). Fatty Acid Composition of Medlar (*Mespilus germanica* L). *Italian* J*ournal of Food Science* 14**(4)**:439-446.

Bagudo B.U, Garba B, Dangoggo SM and Hassan L.G (2008) comparative study of biogas production from locally sourced substrate materials. *Nigerian Journal of Basic and Applied Science.* 16**(2)**:209-216.

Baki, A. S (2015). Potentials of Biofuels Production from Residual cakes of *Lagenaria sicenaria, Jatropha curcas, Azadirachta indica* and *Racnnus communis*. A PhD thesis submitted to postgraduate school, Usmanu Danfodiyo University, Sokoto Nigeria. Pp 74-124. Unpublished.

Bringamann G, Schlauer J, Wolf K, Rischer H, Buchbom U, Kreiner A, Thiele F, Duschek M and Ake-Assi L (1999). Cultivation of *Triphyophyllum Pettatum*.(Dioncophyllaceae), the part-time carnivorous plant carni plant Newsl. 28:7-13

Chinnici F, Bendini A, Gaiani A and Riponi C (2004). Radical Scavenging Activities of Peels and Pulp from Golden Delicious Apple as Related to their Phenolic Composition. *Journal of Agricultural and Food Chemistry* 52:4684-4689.

Damirbas, A. (2007). Combustion System for Biogas Fuel, Energy Source Part A, **29**: Pp 303-312.

Dhana, M. S, Prasad, S, Johnshi, H. C, Renu, S., and Chaudhary, A. (2010). Effect of Pre-treatments for Delignification and Sugar Recovery for Ethanol Production from Corn Stover.

Dioha I. J, Ikeme C.H, Nafi'u T, Soba N. I. and Yusuf M.B.S (2014). Effect of Carbon to Nitrogen Ratio on Biogas Production. *International Research Journal of Natural Sciences*. 2 **(1)** Pp. 27-36, Published by European Centre for Research Training and Development UK (www.ea-journals.org) 27

Ezeonu, F. C, Udedi, S. C. Okaka, A. N. C and Okonkwo, C. J. (2002). Studies on Brewers Spent Grains (BSG) Biomethanation: l-Optimal Conditions for Digestion. *Nigerian Journal of Renewable Energy*, 10 (1, 2): Pp 53-57

Garba B (1999). Challenges in Energy Biotechnology with Special Reference to Biogas technology. A Paper Presented at the 12th Annual Conference of the Biotechnology Society of Nigeria at the National Institute of Fresh Water Fisheries Research Institute (NIFFRI). New Bussa

Hassan L.G, Muhammad M.U, Umar K.J and Sokoto A.M (2008). Comparative Study on the Proximate and Mineral Content of Seed and Pulp of Sugar Apple (*Annona squamosa*). *Nigerian Journal of Basic and Applied Sciences* 16**(2)**:174-177.

Hassan L.G, Umar K.J, Abdullahi S and Muhammad A.S (2005) Proximate Composition and physicochemical Properties of Seed and oil of *Cassia siamen*. *Bulletin of science Association of Nigeria (SAN in Proceeding of Annual Conferenc*e 26:373-380.

Hassan L.G, Usman B.B, Kamba A.S and Hassan SW (2009). Nutritional Composition of Vegetable Spaghetti (Hasta La Pasta) Fruit. N*igerian Food Journal* 27**(2)**:41-49

Jacob A.G, Eong D.I and Tijjani A (2015). Proximate Mineral and Ant-nutritional Composition of Melon (*Citrullus lanatus*)seed. *British Journal of Research*. www.british.org. 22**(5)**:142-151. ISSN 2394-3718.

Jansen P.C.M (2005)..*Rothmannia longiflora* salesh (Internet) Record from Protaou.Janson PCM and Cordan D. (Editors) PROTO:Wageningen, Netherlands (http://www.proto44.org/search.asp). Accessed 3 may 2017

John O.J Mann A, Olanrewaju I.A and Ndamisto M.M (2016). Nutritional Composition of Selected Wild Fruits from Minna Area of Niger State, Nigeria. World Academy of Science, Engineering and Technology. *International Journal of Nutrition and Feed Engineering*. 10**(1**)

Johnson J.T, Iwang E.U, Hemen J.T, Odey M.O Efiong E.E and Eteng O.E (2012) Evaluation of Antinutrient Content of Water Melon (*Citrullus lanatus*). Scholars Research Library. Annals of biological Research 3(**11)**:5145-5150. ISSN 0976-1233. Available online at www.scholarsresearchlibrary.com

Kaur C. and Kapoor H.C (2001). Antioxidants in Fruits and Vegetables the Millenniums Health. *International Journal of Food Science and technology 36:203-723*

Kim-shapiro D.B, Godwin M.T, Patel R.P and Hogg N (2005). Role of Nitrite in Haemoglobin Mediated Hypotic Vasodilation. *Journal of inorganic Biochemistry* 99**(1)**:237-246.

Kovács E, Wirth R, Maróti G, Bagi Z, Rákhely G, et al. (2013) Biogas Production from Protein-Rich Biomass: Fed-Batch Anaerobic Fermentation of Casein and of Pig Blood and Associated Changes in Microbial Community Composition. PLoS ONE 8(10): e77265. doi:10.1371/journal.pone.0077265

Leta D. Solomon L. Chavan R. B. Daniel M. and Anbessa D (2015). Production of Biogas from Fruit and Vegetable Wastes Mixed with Different Wastes. Environment and Ecology Research 3**(3)**: 65-71, 2015 DOI: 10.13189/eer.2015.030303

Krishna G and Ronjhan S.K (1983). Laboratory Manual for Nutrition Research. Vikas Publishing Hause.PUK ltd Ghaziabad up (India) Pp. 121-123

Maishanu, S. M., and Hussaini, H. B. N. (1991). Studies on Factors Affecting Biogas Generation from *Pistia stratiotes. In 32nd annual conference of Nigeria society of microbiology, University of Ilorin,* Pp. 7-11

Marroquin-Andrade L, Cuevas-Sanchez J.A, Ramirez D.G, Reyes L, Reyes-Chumacero A and Reyes-Trejo B (2011). Proximate Composition, Mineral Nutrient and Fatty Acid of the Seed of Ilama, *Annona diversifolia* saff. *Scientific Research and Essays* 6*(14)*:3089-3093. Doi:10.5897/SRE10.1159.ISSN 1992-2248.

Mohammed S.S, Paiko Y.B, Mann A, Ndamitso M.M, Mathew J.T and Maji, S (2014). Proximate, mineral and anti-nutrientional composition of *Curcurbita maxima* Fruits Part. *Nigerian Journal of Chemical Re*search 19**(1)**:37-49.

Muhammad M.U, Kamba A.S, Abubakar L, and Bagna E.A (2010) Nutritional Composition of Pear Fruit*s (Pyrus communis*). *African Journal of Food Science and Technology* 1(**3)**:76-81ISSN 2141-5455.. Available online http://www.interesjournals.org/AJFST.

Muhammad S, Hassan L.G, Dangoggo S.M, Hassan S.W, Umar R.A and UMar K.J (2015) Nutritional and Anti-nutritional Composition of *Sclerocarya birrea* Peels. *International Journal of Science, Basic and Applied Research* (IJSBAR) 21**(2)**39-48 ISSN 2307-4531

Musa N.M, Ikeh P.O, Hassan L.G and Mande G. (2014) Proximate and Mineral Composition of the Pulp of *Chrysophyllum albidum* fruit. *Chemsearch Journal* 5**(2)**:20-24 ISSN 2276-207X

Ola F.L and Obah G (2000). Food Value of two Nigerian Edible Mushrooms(*Termitomyceles stratus* and *Termitomyceles robustas*). *The Journal of Technoscience,* 4:1-3

Sahrawat K.L, Kumar G.R and Rao J.L (2002). Evaluation of Triacid Dry Ashing Procedures for Determine Potassium, Calcium, Magnesium, Iron, Zinc, manganese and copper in plant materials. *Communication of Soil Science and Plant Analysis*. 33(**1&2)**:95-102

Silva R.M, Andrade P.B, Valento P, Ferreres F, Seabra R.M and Ferreira M.A (2004). Quince (*Cydonia olonga* miller) fruit (Pulp, Peel and Seed). And Jam: Antioxidant Activity. *Journal of Agricultural and food Chemistry* 52:4702-4712

Umaru H.A, Adamu R., Dahiru and Nadro M.S (2007) Level of Anti-nutrient Factors in Some Wild Edible Fruits of Northern Nigeria. *African Journal of Biotechnology* 6**(6)**:1935-1938. Available online at http://www.academicjournal.org/AJB.

Van-burden T.P and Robinson W.C (1981). ::Formation of Complexes Between Protein and Tannic Acid" *Journal of Agricultural Food Chemistry* Vol 1.Pp 77

World Health Organization (WHO) "Evaluation of Certain Food Additive" Technical Report Series 913 (Geneva,WHO) Pp. 20-32.2002.

Soetan K.O, Olaiya C.O and Oyewolw O.E (2010). The importance of mineral elements for humans, domestic animals and plants: a review, African journal of Basic and Applied science research, 2(5):4839-4843.

Appel, I.J (1999). Clin.cadiol:1111-1115.

Fallon, S. and Enig M.G (2001). Nourishing traditions: the cookbook that challenges politically correct nutrition and the diet dictorats. PP: 40-45.

Oluyemi E.A, Akilua A.A, Adenuya A.A and Adebayi M.B (2006). Mineral content of some commonly consumed Nigerian food. Science focus 11(1):153-157.

Melaku U, Clive E.W and Habtanon F (2005).content of zinc, iron, calcium and their absorption inhibitors in ethiopia. Ournal of food composition analysis. 18:803-817.

Mielcarz, G.W., Howard A.N, William N.R, Kinsman G.D., Moriguchi Y, Mizushina and Yamoriy (1997). Copper and zinc status as a risk factor for ischemic heart diseases. A comparison between Japanese in brzil and Okinawa. Journal of trace element exp.med.10:29-35.

Anhawange B.A, Ajibola, V.O, and Oniya S.J (2004). Chemical studies of the seeds of moringa oleifera and deuterium microcarpum. Journal of biological science 4(6): 711-715.

Eastmond D.A, Macgreger J.T and Sleninki R.S (2008). Trivalent chromium: assessing the Genotoxic Risk of the essential Trace element and widely used in Human and animal nutrition supplement. Critical review toxicology 38,173-190

WHO (1996). Guideline for Drinking Water Quality 2nd Edition Vol 2. World Health Organization. Geneva.

Ubwa, S. T. Asemave, K. Oshido , B. Idoko A. (2013). Preparation of Biogas from Plants and Animal Waste. *International Journal of Science and Technology* 2**(6)** Publications UK. All rights reserved. Pp 480

Appendix

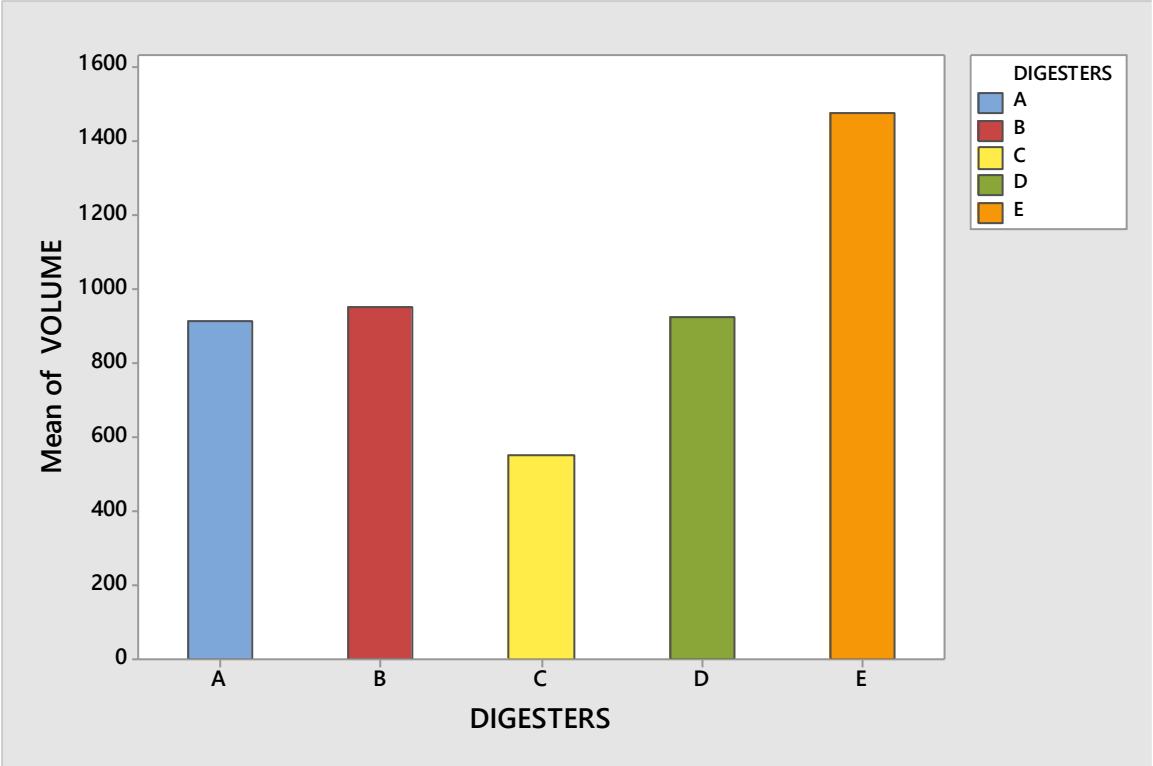

Figure 1: Mean Volume of Biogas Produced in cm^3

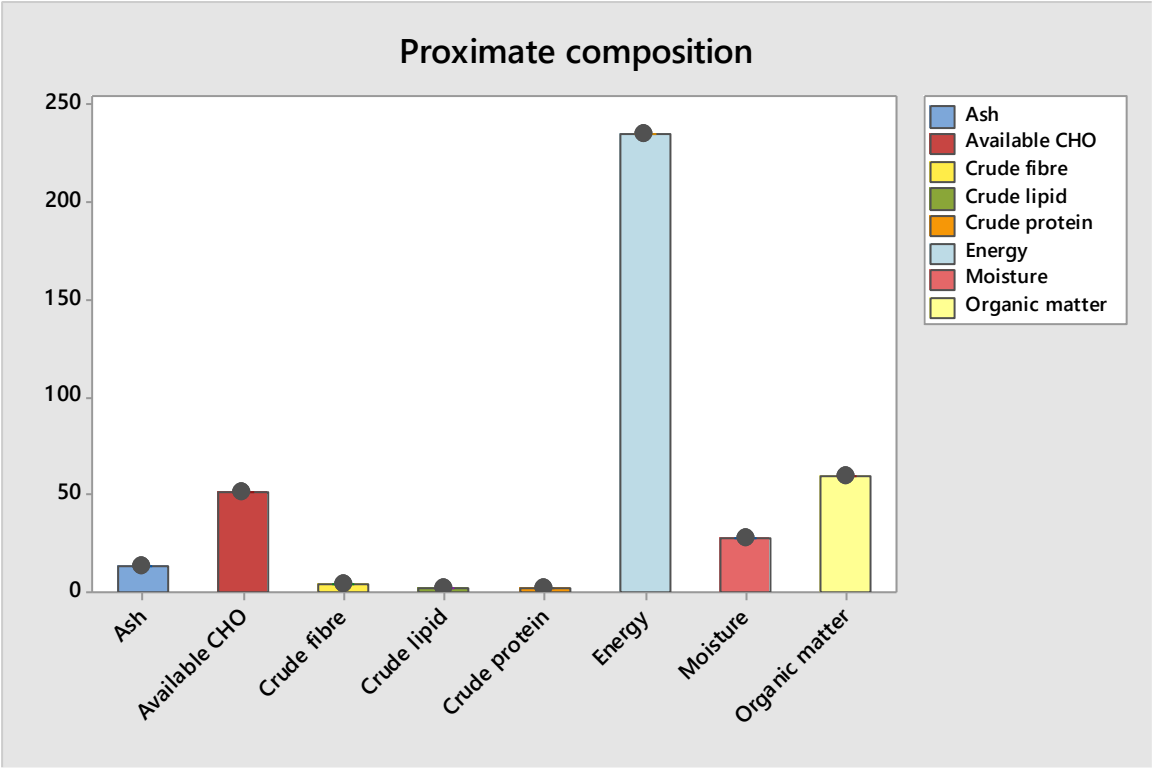

Figure 2: Proximate Composition in %

Determination of Selected Heavy Metals in Soil and Water from Jatau–GarinGabas Gold Mining Site in Niger State

Alexander Ikechukwu Ajai,[1*]Abdulrahman Ali Yusuf,[2]JimohOladejoTijani[2]

Department of Chemistry, Federal University of Technology, Minna, Nigeria

ajiyusuf20@gmail.com

[*]Corresponding author

Abstract

Concentrations of Cd, Fe, Ni, Pb and Zn in soil and water collected within and around local artisanal gold mining sites in Jatau – GarinGabas village of Rafi Local Government Area of Niger State were determined using Atomic Absorption Spectrophotometry (AAS) technique. The mean concentration for Ni was 103.38 and 186.11 mg/kg for the soil samples and between 0.01 and 0.23 mg/l for the water samples; Fe, between 273.35 and 476.71 mg/kg for the soil samples, and 0.28 and 2.87 mg/l for the water samples; Zn between 49.90 and 117.47 mg/kg for the soil samples, and 1.05 and 2.08 mg/l for the water samples; Pb varied widely from 19.0 and 28.39 mg/kg for the soil samples, while for the water samples it ranged between 0.17 and 0.58 mg/l; Concentration of Cd in soil samples ranged between 0.22and 0.85mg/kg and 0.001 and 0.003 mg/l for the water samples. The order of occurrence in the soil samples were Fe > Ni > Zn >Pb> Cd for the soil samples, and Fe > Zn >Pb> Ni > Cd for the water samples. All heavy metals tested in the soil samples except Pb were found to have exceeded the permissible limits set by the World Health Organisation. Similarly, Pb and Fe in the water samples tested exceeded the permissible limits. The study revealed that the water bodies and the soil around the mining site were polluted with tailings from the mines during the process of washing the minerals,and therefore not fit for drinking and agricultural activities respectively. Regular monitoring of mining activities should be carried out from time to time to ensure a safe environment for man and other living organisms in the area.

Introduction

Mineralexploration and exploitation have been identified as one of the anthropogenic activities contributing significantly to environmental degradation and deterioration due to the release of potentially toxic elements into soil, water and air (Udosen*et al*, 2018).

Literature Review

According to report by expert committee on metals, all essential elements become toxic at high intake and the margin between levels that are beneficial and those that are harmful may be small (Abdallah, 2014). Copper, zinc, cobalt, nickel, chromium, manganese, iron, selenium, silicon, tin, fluorine, iodine, molybdenum and vanadium are essential trace elements, while lead, cadmium, mercury are non-essential. Heavy metals are natural component of the earth crust; they enter our bodies via food, drinking water and air (Uzairu*et al.*, 2015). Some heavy metals (such as copper, selenium and zinc) are essential to maintain the metabolism of the human body. However, at higher concentration, they can lead to poisoning (Tijjani*et al.*, 2014).

Soil is a very important natural resource to man as it is a source of his life on this planet. Without soil the earth would be lifeless (Ujoh*et al.*, 2014). Water plays an important role in the world economy, as it functions as a solvent for many chemical substances and facilitates industrial cooling and transportation. Approximately 70% of the freshwater used by man goes to agriculture. However, pollution of water by natural and anthropogenic means is a source of worry globally, and as such, requires adequate attention (Tijjani*et al.*, 2014).

The aim of this research is to determine the effects of mining activities on the levels of heavy metals in soil and water around Jatau-GarinGabas local mining site.

Methodology

Sample Location

Jatau – GarinGabas, is located between latitudes $10^0 11^1 04''$N and longitudes $6^0 15^1 12''$E. It is an agrarian community in Rafi Local Government Area of Niger State, Nigeria (NIGIS, 2013). It is 104 km from Minna the state capital. The area enjoys both wet and dry seasons with a total annual rainfall of between 804.5-1767.1 mm (NIGIS, 2013). Mean annual temperature is about 27.7^0C with a relative humidity of 30% in dry season and 70% in wet season. Average daily wind speed is 89.9km/hr. Average daily vapour pressure is 26Hpa (Niger State Ministry of Information, 2009). The land rises from about 300 m along the Niger valley to between 300-900 m above sea level in the uplands (Niger State Ministry of Information, 2009).

Sample Collection

Soil and water samples were collected at various points from the mining site. Water samples were collected from 3 different points along the river around the mining sites. The first water sample labelled A was collected approximately 100 m before the mining site, and B from the

actual mining site, and C, 100 m after the mining site. Each water sample was acidified with dilute HNO_3 to avoid oxidation and stored for laboratory analysis (Amadi*et al*., 2015).

Soil samples were collected at a depth of 0-15 cm and 15-30 cm according to the method reported by Agbalaje (2015), making 2 different samples from each point. The soil samples were collected from three different points; the actual mining site, approximately 100 m before it and 100 m after it. The 2 samples from the same point were pulled together to form a composite for each of the sampling points. They were stored in a black polythene bag, labelled and transferred to the laboratory for further analysis (Musa *et al*., 2016).

Sample Digestion

The procedure reported by Chiroma*et al*. (2014) with some modifications was used for the digestion of the water samples. 50 cm^3 of the water sample was accurately measured into a 100 cm^3beaker.10 cm^3 of concentrated HNO_3 was added to it. The solution was heated on a hot plate at 95ºC. The solution was then reduced to 30 cm^3. It was allowed to cool before being filtered using Whatman No. 1 filter paper and then transferred into a 100 cm^3 standard flask. The solution was then diluted to the mark with distilled water and stored for analysis. The digested samples were analysed for 5 heavy metals, namely: Ni, Pb, Fe, Zn and Cd using Atomic Absorption Spectrophotometry (Buck Scientific 210VGB). Same procedure was applied to all the water samples collected.

The procedureby Rao*et al*. (2017) with some modifications was used for digestion of the soil samples. 2.0 g of the soil sample was weighed into a 100 cm^3 beaker and 8.0 cm^3 of aqua-regia (1:3 HNO_3 and HCl) was added. The mixture was heated on a hot plate for 30 minutes at 90ºC. The sample was dissolved after evaporation to near dryness with 10 cm^3 of 2% nitric acid and then filtered through Whatman No. 1 filter paper into a sample bottle before itwas then diluted to the mark with distilled water. It was stored and later analysed for selected heavy metals (Ni, Pb, Fe, Zn and Cd) using Atomic Absorption Spectrophotometry (Buck Scientific 210VGB).

Results and Discussion

From the results on the physicochemical properties of the water sample (Table 1), it can be observed that the pH of the water samples ranged from 5.33 to 6.34, which indicates that the samples were fairly acidic; this could be attributable to the mining activities going on at the locations. The value of COD ranged between 115.15 and 135.80. According to Odukoya (2015),the concentrations of COD observed in surface waters range from 20 mg/L or less in unpolluted water to greater than 200 mg/L in waters receiving effluents. According toTsafe*et al*. (2016), industrial wastewaters may have COD values ranging from 100 mg/Lto 60,000

mg/L. The concentrations of COD observed in this study showed that the water may be polluted with discharge from the mining site. The BOD levels obtained ranged from 51.29 to 60.89 mg/L. The BOD levels of the samples are also high. However, COD levels are generally higher than the BOD (Musa and Jiya, 2014).

Table 1: Physicochemical Properties of Water Samples

Location	pH	COD (mg/L)	BOD (mg/L)	TOC (mg/L)	Turbidity (NTU)
A	6.01 ± 0.01	135.80 ± 2.2	57.43 ± 1.2	2.61 ± 0.3	0.56 ± 0.8
B	5.33 ± 0.04	126.21 ± 2.4	60.89 ± 1.7	2.99 ± 0.6	0.85 ± 0.7
C	6.34 ± 0.03	115.53 ± 1.5	51.29 ± 1.4	2.21 ± 0.2	0.46 ± 0.5

Where A, B and C are 100 m before, at and 100 m after the local mining site located at Jatau village respectively.

Organic carbon in freshwaters arises from living material (directly from plant photosynthesis or indirectly from terrestrial organic matter) and also as a constituent of many waste materials and effluents (Alhassan*et al*, 2016). Consequently, the total organic matter in the water can be a useful indication of the degree of pollution, particularly when concentrations can be compared upstream and downstream of potential sources of pollution, such as sewage or industrial discharges or urban areas. The TOC in the analysed water samples from the mining site ranged from 2.21 to 2.99 mg/L. This high concentration of TOC may be due to the presence of tailings in the water. TOC concentrations in municipal wastewaters range from 10 to > 100 mg/L (Adelekan and Abegunde, 2015). The type and concentration of suspended matter controls the turbidity and transparencyof the water. Turbidity values from the study were between 0.46 and 0.85 NTU. Turbidity results from the scattering and absorption of incident light by the particles, and the transparency is the limit of visibility in the water.

Concentration of nickel in the water samples ranged between 0.01 and 0.23 mg/L, which wereabove the permissible limit of 0.02 mg/L set by WHO (1993). The values of Ni in this present study were similar to those obtained by Wong *et al.*(2016) which ranged from 0.15 – 0.21 mg/L for water samples. The values of Fe in the water samples ranged from 0.28 to 2.87 mg/L (Table 2). They were slightly higher than the limit of 0.2 mg/L set by WHO in 1993.

Concentration of Zn in water samples ranged between 1.05 to 2.08 mg/L as shown in Table 2. The permissible limit of Zn in water according to WHO (1993) standards is 2.6 mg/L (Adelifa*et al.*, 2016). In all the collected water samples, concentration of Zn was obtained below the permissible limit. In all the collected water samples, concentration of Pb ranged between 0.17 and 0.58 mg/L as presented in Table 2. According to WHO (1993) standards, permissible limit forPb in water is 0.01mg/L (Mutune*et al*. 2014). Concentration of Pbin the water was above the permissible limit. Pb as a water contaminant accumulates with age in bones, kidney and liver. It can enter the human body through uptake of food (65%), water (20%) and air (15%) (Nkwocha*et al.*, 2014).

Table 2: Heavy Metal Concentrations in the Water Samples (mg/L)

Sample location	Ni	Fe	Zn	Pb	Cd
A	0.10 ± 0.01^{b}	0.55 ± 0.20^{b}	1.47 ± 0.32^{b}	0.28 ± 0.44^{b}	0.001 ± 0.00^{a}
B	0.23 ± 0.00^{c}	2.87 ± 0.75^{c}	2.08 ± 0.59^{c}	0.58 ± 0.15^{c}	0.003 ± 0.01^{c}
C	0.01 ± 0.00^{a}	0.28 ± 0.23^{a}	1.05 ± 0.25^{a}	0.17 ± 0.12^{a}	0.002 ± 0.02^{b}
WHO Standard (1993)	0.02	0.2	2.6	0.01	0.005

Values with different superscripts on each column are statistically significant at ($p < 0.05$).
A is a well before the mining site, B is a water body at the actual mining site in Jatau village and C is a well located after the mining site.

Concentration of Cd in all the collected water samples ranged between 0.001 and 0.003 mg/L as shown on table 2. In all the collected water samples, concentration of Cd was recorded below the maximum permissible limit of 0.005 mg/L set by WHO (1993).

For the physicochemical properties of the soil samples presented on Table 3, the pH of all the samples were found to be acidic (between 6.00 and 6.40); this may be as a result of the sorption of metals in the soil (Mordi*et al.*, 2013). The electrical conductivity values were found to vary significantly across the sites; 2.94 μScm^{-1} (for point A), 3.46 μScm^{-1} (for point B) and 2.48

μScm^{-1} (for point C). The variation observed in electrical conductivity between sites could be attributed to soluble salts in the soil samples. The organic matter content ranged from 1.74 to 2.89. This relatively high value could be due to the lower soil moisture contents during the dry season which retards the activities of the micro-organisms involved in the organic matter decomposition, thereby accumulating more organic matter (Gyang and Ashano, 2014).

Table 3: Physicochemical Properties of Analysed Soil Samples

Location	pH	Organic matter (g/kg)	CEC (cmol/kg)	Electrical conductivity (dsm^{-1})
A	6.20 ± 0.04	2.87 ± 1.24	4.12 ± 1.25	2.94 ± 1.71
B	6.00 ± 0.02	1.74 ± 0.90	2.18 ± 1.11	3.46 ± 1.82
C	6.40 ± 0.03	2.89 ± 1.08	5.28 ± 1.36	2.48 ± 1.63

Where A, B and C are 100 m before, at and 100 m after the local mining site located at Jatau village respectively.

The levels of Cation Exchange Capacity (CEC) ranged from 2.18 to 5.28 cmol/kg. This high CEC value could influence the ability of the soil to hold onto essential nutrients (Amadi and Nwankwoala, 2015).

The concentration of Ni in soil samples collected within the mining site varied between 103.38and186.11 mg/kg. The permissible limit set by WHO (1993) is 35 mg/kg, the concentration values were all above the permissible limit especially at point B with a value of 186.11 mg/kg which was highest. The values of Ni in this present study were similar to those obtained by Wong *et al.*(2016) in a study carried out around Pearl River Delta in China, which ranged from 98.50 – 165.00 mg/kg for the soil samples studied. Although Ni has been considered to be an essential trace element for human and animal health,it is absorbed easily and rapidly to harmful levels by plants (Wong *et al.*, 2016).

Concentration of Fe in all the collected soil samples ranged between 273.35 and 476.71 mg/kg (Table 4). In all the soil samples, concentration of Fe was above the permissible limit of 200 mg/kg set by WHO (1993).This could pose perilous threats to residents in the locality.

Excess amount of Fe causes rapid increase in pulse rate and coagulation of blood in the blood vessels, hypertension and drowsiness(Gyang*et al.*, 2014).

In this study, the concentration of Zn in the soil (Tables 4) at the actual mining site and at locations approximately 100 m before and after it varied between 49.90and117.47 mg/kg. It showed the highest concentration of 117.47 at point B which is the actual mining site. This is higher than the results obtained by Sourav*et al*. (2014) which stood at between 25.95 and 72.22 mg/kg. The WHO (1993) standard for Zn is 50 mg/kg. This high concentration could be attributed to the anthropogenic activities like breaking up ores around the gold mine that also contain Zn, which are subsequently translocated to areas close to the mine by erosion or human activities. The values in this study were however lower than the results obtained by Tsafe*et al*. (2016) who got values ranging from 185- 373 mg/kg for evaluation of heavy metals uptake and risk assessment of vegetables grown in Yargalma in Northern Nigeria.

Zn is one of the important trace elements that play a vital role in the physiological and metabolic process of many organisms. Nevertheless, higher concentrations of Zn can be toxic to living organisms (Nkwocha*et al.*, 2014).

The concentration of Pbin the soil samples from the study area also varied widely from 19.00–28.39 mg/kg (Table 4). The WHO (1993) recommended limit forPb is 85 mg/kg.The values were fairly low and below the recommended limits. The low concentration indicates that the environment is relatively safefrom the adverse effects of Pb which may result from the mining activitiestaking place around the area, which is usually accompanied by other harmful by-products (Odukoya 2015).

Table 4: Heavy Metal Concentration in the Soil Samples (mg/kg)

Sample location	Ni	Fe	Zn	Pb	Cd
A	120.15 ± 1.05^{b}	378.25 ± 1.3^{b}	49.90 ± 0.2^{a}	24.55 ± 0.9^{b}	0.22 ± 0.17^{a}
B	186.11 ± 2.5^{c}	476.71 ± 2.1^{c}	117.47 ± 1.6^{c}	28.39 ± 0.5^{c}	0.85 ± 0.51^{c}
C	103.38 ± 2.0^{a}	273.35 ± 2.2^{a}	61.20 ± 0.1^{b}	19.00 ± 0.1^{a}	0.31 ± 0.28^{b}
WHO Standard (1993)	35.00	200.00	50.00	85.00	0.80

Values with different superscripts on each column are statistically significant at ($p < 0.05$). Where A, B and C are 100 m before, at and 100 m after the local mining site located at Jatau village respectively.

Concentration of Cd in soil samples ranged between 0.22and 0.85 mg/kg (Table 4).The maximum permissible limit for Cd in soil is 0.8 mg/kg according to WHO (1993). From the results of the soil samples collected, concentration of Cdobtainedfrom all locations were below the WHO permissible limit, except for point B, which is the actual mining site. Consequently, the mining activity at point B had given rise to pollution of the soil within the environment, which could expose the inhabitants to various environmental hazards caused by Cd.

Conclusion

The study shows that heavy metal pollution of water and soil is of environmental concern within the perimeter of the gold mining site in Jatau village. The heavy metal concentrations in the soils varied significantly by sampling sites and metal type. The soil samples from the mining site are more contaminated with heavy metals with maximum concentrations of 186.11 mg/kg Ni; 476.71 mg/kg Fe; 117.47 mg/kg Zn; 28.39 mg/kg Pb and 0.85 mg/kg Cd. The surface water around the mining site had concentrations of 0.23 mg/L Ni; 2.87 mg/L Fe; 2.08 mg/L Zn; 0.58 mg/L Pb and 0.003 mg/L Cd. This research also revealed that heavy metals at location B (Table 4) had the highest concentration of iron (476.71 mg/kg).

From this study, it was observed that the most polluted soil is that of the actual mining site, as it had the highest concentration of all the heavy metals analysed. The results imply that

pollution of such environment by heavy metals could have adverse effect on human health and the environment, and cultivation of crops around the area may result to significant bioaccumulation of the heavy metals into the food chain.

References

Abdallah, M. I. M. (2014). Evaluation of some heavy metals residue in whole milk powder used at confectionary plant regarding the public health significance. *Animal research institute, agricultural research center, Giza Egypt,* 88, 375-384.

Abera, M. (2014).Determination of levels of some heavy metals (Pb, Cr and Cd) in three commercially available brands of milk powder found in Harar town, Eastern Hararge, Ethiopia.*Spanish Journal of Food Science and Technology*, 34, 441-449

Adelekan, B. A, and Abegunde, K. D (2015).Heavy Metals Contamination of Soil Groundwater at Automobile Mechanic Villages in Ibadan, Nigeria. Int. J. Phy. Sci. 6(5):1045-1058.

Adelifa, E.O., Onwordi, C.T., and Ogunwande, I.A. (2016). Level of heavy metals uptake on vegetables planted on poultry dropping dumpsite. *Archives of Applied Science Research*, 2(1), 347-353.

Agbalaje, O.L. (2015). Assessment of heavy metals in soils around Etelebou flow station in Bayelsa State, Nigeria. *Unpublished M.Sc. thesis, Dept of Environmental Technology, Federal University of Technology, Owerri, Nigeria*, pp.129.

Alhassan, S., Abdul, N., Nazeef, U., Ali, R., Muhammad, A., Muhammad, Z., & Muhammad (2016).Comparative study of heavy metals in soil and selected medicinal plants.*Journal of Chemistry*, 2013, 5.

Chiroma T. M., Ebewele R. O., and Hymore F. K. (2014).Comparative assessment of heavy metal levels in soil, vegetables and urban grey waste water used for irrigation in Yola and Kano. *International Refereed Journal of Engineering and Science (IRJES)*, pp. 01-09

Gyang, J.D., and Ashano, E.C. (2014). Effects of mining on water quality and the environment: A case study of parts of the Jos Plateau, North-central Nigeria. *The Pacific Journal of Science and Technology*, 11(1), 631-639.

Mordi, R. I., Udom, G. N., and Zuofa, K. (2013).Properties, classification and management implication of soils in the backswamps of the upper deltaic plain.Science forum.*Journal of pure and applied sciences*, 5(2), 171-182.

Moses, Y. (2016). Evaluation of levels of heavy metals in soil and well water within selected automobile mechanic workshops in Lokoja, Nigeria.*Soil Science*, 163, 463-471

Musa, H. D., andJiya, S. N. (2014).An assessment of mining activities impact on vegetation in Bukuru, Jos-Plateau State Nigeria using Normalized Differential Vegetation Index (NDVI).*Journal of Sustainable Development*, 4(6), 150-159.

Mutune, A. N., Makobe, M. A., andAbukutsa-Onyango, M. O. O. (2014). Heavy metal content of selected African leafy vegetables planted in urban and peri-urban Nairobi, Kenya. *African Journal of Environmental Science and Technology*, 8(1), 66-74.

Nazir, R., Khan, M., Muhammad, M., Hameed, R., Naveed R., Surrya, S., Nosheen, A., Muhammad, S., Mohib, U., and Muhammad, R., Zeenat, S. (2015). Accumulation of heavy metals (Ni, Cu, Cd, Cr, Pb, Zn, Fe) in the soil, water and plants and analysis of physico-chemical parameters of soil and water Collected from Tanda Dam kohat. *J. Pharm. Sci. & Res. Vol*. 7(3), 2015, 89-97.

Ndana M (2010). ED-XRF analysis of tantalite deposit of Mai-Kabanji, North -Western Nigeria, *J. Environ. Chem. Ecotoxicolo*. 2(6):185-188.

NIGIS (2013): Niger State Geographic Information System; an overview of Niger State and its 25 local government areas, Vol. 1, 22-25.

Nkwocha, E. A., Dakiky, M. K., Khamis, M. H., Manassra, A. N., and Mereb, M. R. (2014). Selective Adsorption of Chromium (VI) in Industrial Waste Water using Low-Cost Abundantly available Adsorbents. *Journal of Advance in Environmental Research*, 6, 533-540.

Odukoya, A. M. (2015).Contamination assessment of toxic elements in the soil within and around two dumpsites in Lagos, Nigeria.*Ife Journal of Science*, 1**7**(2), 351-361

Rao P. S., Tarence T., Amreen H., andAshish D. (2017).Determination of heavy metals contamination in soil and vegetable samples from Jagdalpur, Chhattisgarh State, India.*International Journal of Current Microbiology and Applied Sciences*, 6(8), 2909-2914.

Sourav, C.,Obasi, N. A., Akubugwo, E. I., Ugbogu, O. C., &Chinyere, G.C. (2014). Heavy metals bioavailability and phyto-accumulation potentials of selected plants on burrow-pit dumpsites in Aba and Ntigha dumpsite in IsialaNgwa of Abia State, Nigeria, *Nigerian Journal of Biochemistry and Molecular Biology*, 27(1), 27-45.

Tijjani, M. N., Kenneth, J., and Yoshinar, H. (2014).Environmental impact of heavy metals distributions in water and sediments of Ogunpa River, Ibadan Area, South Western Nigeria.*Journal of Mining and Geology*, 40(1), 73-83.

Tsafe, A. I., Hassan, L. G., Sahabi, D. M., Alhassan, Y., and Bala, B. M. (2016).Evaluation of Heavy Metals Uptake and Risk Assessment of Vegetables Grown in Yargalma of Northern Nigeria.*J. Basic and Appl. Sci. Res*. 2(12): 6708-6714.

Uba, S., Uzairu, A., Harrison, G. F. S., Balarabe, M. L., and Okunola, O. J. (2014).Assessment of heavy metal bioavailability in dumpsites of Zaria metropolis, Nigeria.*African Journal of Biotechnology*, **7**(2), 122-130.

Ujoh, F. I., and Alhassan, M. M. (2014), Assessment of Pollutants in Streams around a Cement Plant in Central Nigeria, *International Journal of Science and Technology*, Volume 4, 3.

Udosen, E, D., Benson, N. U. Essien, J. P. and Ebong, G. A. (2018).Evaluation of selected heavy metalswithin artisanal mining site in SuleTankarkar.*International Journal Soil of Science*. 1, 27-32.

Uwumarongie, E. G., and Okieimen, F. E. (2016). Spatial distribution and speciation of arsenic, chromium and copper in CCA contaminated soil in Bende, Southeast Nigeria. *Journal of Chemical Society of Nigeria*, 33(1), 112-121.

Uzairu, A., Uba, S., Sallau, M. S., Abba, H., and Okunola, J. O., (2015). Seasonal fractionation of metals in some dumpsite soils in Zaria metropolis, Nigeria. *Journal of Environment and earth Science*, 2(3), 2224-3216.

Wieczorek, J., Wieczorek, T., and Bieniaszewski, T. (2014). Cd and lead content in cereal grains and soil from cropland adjacent to roadways. *Polish Journal of Environmental Studies*, 14, 535-540.

WHO (1993). World Health Organisation, Guidelines for drinking-water quality, World Health Organization, Geneva.

Wong, C. S. C., Li, X. D., Zhang, G., Qi, S. H., and Peng, X. Z (2016).Atmospheric depositions of heavy metals in the Pearl River Delta, China.*Atmosphere and Environment*, 37, 767-776.

Yusuf, A. A., Arowolo, T. A., and Bamgbose, O. (2014). Cadmium, Copper and Nickel levels in vegetables from industrial and residential areas of Lagos City, Nigerian. *Food Chemical Toxicology*, 41, 285-291.

Persulfate and Ferrioxalate as Solutions of Electron-Hole Recombination in Tio_2 and Zno Photocatalytic Degradation of Malachite Green: Process Intensification

Dalhatou Sadou[1*], Tarkwa Jean Baptiste[2], Mohamed Raoul Ibrahim[1] and Yaya Sali[1]

[1]Department of Chemistry, Faculty of Sciences, University of Maroua, Cameroon.

[2]Department of Inorganic Chemistry, Faculty of Sciences, University of Yaoundé I, Cameroon.

*Corresponding author: dalsaous@yahoo.fr

Abstract

In this work, the effect of persulfate and/or ferrioxalate on the photocatalytic degradation of malachite green was studied. The results obtained showed, firstly, that the degradation efficiency of MG by the different systems were such that UV/TiO_2< $UV/TiO_2/S_2O_8^{2-}$ < $UV/TiO_2/Fe^{3+}/S_2O_8^{2-}$. In fact, the addition of persulfate and/or ferrioxalate oxidants hinderedelectron-hole recombination and intensified the TiO_2 and ZnO photocatalytic process.

Keywords: Electron-hole pair, Malachite Green, Photocatalytic degradation, radical sulfate, Semi-conductor.

1. Introduction

In the recent literature, the performances of the semiconductors TiO_2 and ZnO for the photocatalytic degradation of organic substances are known. However, their yield is limited by the recombination phenomenon of the electron-hole pairs. On the other hand several works have shown that the doping of these semiconductors by certain metals decreases this phenomenon, but this solution was laborious and the percentage of recombination remained always high.

2. Literature Review

Semiconductors based photocatalysis has known as an environmental friendly, cost effective and green process for effective degradation of harmful organic contaminants in aqueous solution in recent decades. In heterogeneous photocatalysis for water treatment, TiO_2 and ZnO semiconductors were widely used photocatalysts because of their excellent UV absorbency and high photocatalytic activity, as well as their low cost and non-toxicity (Sajan et al., 2016; Czech and Hojamberdiev, 2016). In the photocatalytic process, the organic

contaminants were degraded under a light irradiation sufficient for the activation of the photocatalyst material. However, under light irradiation, electron-hole pairs were formed and then in a reaction with adsorbed molecules (O_2, H_2O etc…) produced highly reactive species such as superoxide ions O_2^- and hydroxyls radical $HO^\bullet$ (Nosaka and Nosaka, 2017). These reactive species can oxidize most of the organic pollutants in the solution until the high mineralization yield (Gaya and Abdullah, 2008).). Unfortunately, the fast electron-hole (e-/h+) recombination is a major problem for practical applications as it hindered significantly the overall photocatalytic efficiency (Li et al., 2015).

Therefore, to overcome this drawback several strategies based on thermodynamic requirements and kinetics processes taking place in photocatalysis were explored such as coupling two or more semiconductor, supporting of a semiconductor onto a suitable support with strong electric field strength, the doping of these semiconductors by certain metals etc… [Li et al., 2018, Ramírez and Ramírez, 2016).But these solutions were laborious and the percentage of recombination remained always high.Hence, the main objective of this study is to investigate on the effect of persulfate and ferrioxalate ions in the degradation of MG via TiO_2 and ZnO photocatalysis processes. Moreover, plausible mechanism of photogenerated charges separation and MG oxidation will be proposed to deepen the understanding of the system.

3. Methodology

A follow-up by UV-visible spectrophotometry of the decolourisation of Malachite Green (MG) was performed. For these experiments, a batch photoreactor with a capacity of 250 mL has been used. This cylindrical reactor is double-jacketed in order to maintain the system at a constant temperature (25 ± 1°C) to avoid thermal fluctuation. A stirring system of the solution with a magnetic bar ensures the homogenisation of the reaction medium. In addition, the photoreactor is provided with a low-pressure mercury vapour pencil UV lamp emitting a monochromatic radiation of wavelength $\lambda = 365$ nm (Pen-ray Lamps Group). This lamp is protected by a quartz tube to avoid any contact with the solution.

4. Results and Discussion

Three systems: UV/TiO_2 alone, in the presence of persulfate (UV/TiO_2/PS), then in the simultaneous presence of persulfate and ferrioxalate (UV/TiO_2/PS/FO), were studied for the degradation of 250 mL of MG (10 mg/L). The evolution of the concentration of MG versus time is presented in Figure 4.1.

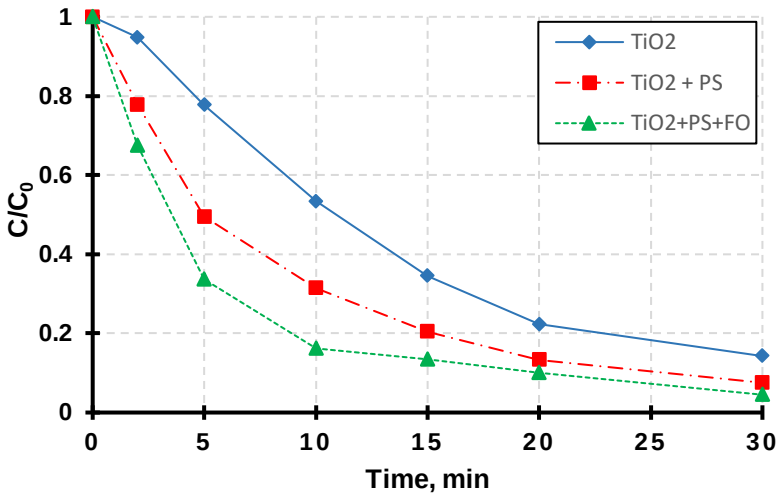

Figure 4.1: Effect of PS and FO on the concentration of MG versus time; [MG] = 10 mg/L; [PS] = 2 mmol.L^{-1}, [FO] = 0,1 mmol.L^{-1}, pH = 6,8 ; V = 250 mL.

According to this figure, the presence of PS and OF enhancedthe degradation yield of MG by 21% and 15.34% respectively within 10 min of irradiation.

Indeed, the acceleration of MG decolourisation can be attributed to the additional production of hydroxyl radical $OH^{\bullet}$ and sulphate radicals $SO_4^{\bullet-}$. The production of $OH^{\bullet}$resultedfrom the decomposition of H_2O_2 during the photoreduction of ferric ions Fe^{3+}(1) whereas $SO_4^{\bullet-}$ resulted from the activation of persulfate $S_2O_8^{2-}$ by Fe^{2+} ions (2). In addition, the semiconductors photogenerated electrons can reduceFe^{3+}ions into Fe^{2+} ions (3), which can decompose hydrogen peroxide via classic Fenton reaction (4)to produce supplementary $HO^{\bullet}$ radicals. Moreover, these photogenerated electrons reduced persulafte ions to generate $SO_4^{\bullet-}$ radical (5). Thus, the increase of these species results in the improvement of MGdegradation (6) & (7).

$$Fe^{3+} + H_2O_2 + hv \longrightarrow Fe^{2+} + HO^{\bullet} + HO^{-} \quad (1)$$

$$Fe^{2+} + S_2O_8^{2-} \longrightarrow Fe^{3+} + SO_4^{\bullet-} + SO_4^{2-} \quad (2)$$

$$\mathbf{Fe^{3+} + e^{-} \longrightarrow Fe^{2+}} \quad \mathbf{(3)}$$

$$Fe^{2+} + H_2O_2 \longrightarrow Fe^{3+} + HO^{\bullet} + HO^{-} \quad (4)$$

$$\mathbf{S_2O_8^{2-} + e^{-} \longrightarrow SO_4^{\bullet-} + SO_4^{2-}} \quad \mathbf{(5)}$$

$$MG + \mathbf{HO^{\bullet}} \longrightarrow \text{Products} \longrightarrow \longrightarrow CO_2 + H_2O + \text{mineral ions} \quad (6)$$

$$MG + \mathbf{SO_4^{\bullet-}} \longrightarrow \text{Products} \longrightarrow \longrightarrow CO_2 + H_2O + \text{mineral ions} \quad (7)$$

It follows that the $S_2O_8^{2-}$ and Fe^{3+} ions react with the electrons expelled towards the conduction band (3) & (5), limiting the hole-electron recombination phenomenon ($h^+ + e^-$). In addition, Fe^{2+} ions generated fromPhoto-Fenton reaction (1) and Fe^{3+}reduction with photogenerated electrons (3) also activate the $S_2O_8^{2-}$ ions (2). Figure 4.2 summarizes the different reactions that took place in the solution.

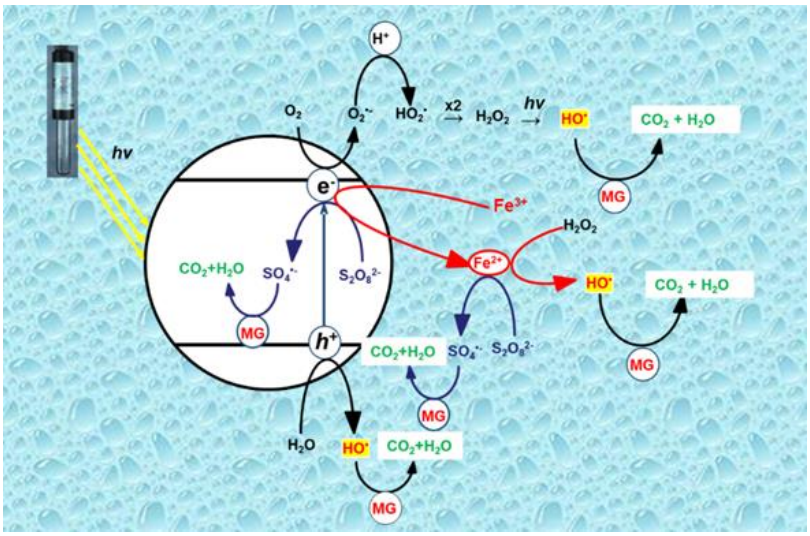

Figure 4.2: Different reactions that took place in the reaction medium

5. Conclusion

The $SO_4^{-\bullet}$ radicals are powerful oxidants in the same way as the $HO^\bullet$ radicals, and have the advantage of being non-selective, highly mobile and more stable. Therefore, these oxidants species demonstrated an effective degradation of MG from aqueous solution.From this work, two main advantages emerged from the addition of PS and FO in the photocatalysis process: (i) Optimal production of oxidizing species ($SO_4^{-\bullet}$ and $HO^\bullet$), which increased the removalrate of the organic pollutant; (ii) High reduction of electron-hole recombination rate, improving the efficiency of the process. To know the role played by each species in the rest of this work, we intend to carry out complementary experiments of the scavenger effect.

References

Sajan, C. P., Wageh, S., Al-Ghamdi, A. A., Yu, J., & Cao, S. (2016). TiO_2 nanosheets with exposed {001} facets for photocatalytic applications. *Nano Research*, 9(1), 3-27.

Czech, B., & Hojamberdiev, M. (2016). UVA-and visible-light-driven photocatalytic activity of three-layer perovskite Dion-Jacobson phase $CsBa_2M_3O_{10}$ (M= Ta, Nb) and oxynitride crystals in the removal of caffeine from model wastewater. *Journal of Photochemistry and Photobiology A: Chemistry*, 324, 70-80.

Nosaka, Y., & Nosaka, A. Y. (2017). Generation and detection of reactive oxygen species in photocatalysis. *Chemical reviews*, 117(17), 11302-11336.

Gaya, U. I., & Abdullah, A. H. (2008). Heterogeneous photocatalytic degradation of organic contaminants over titanium dioxide: a review of fundamentals, progress and problems. *Journal of Photochemistry and Photobiology C: Photochemistry Reviews*, *9*(1), 1-12.

Li, X., Shen, R., Ma, S., Chen, X., & Xie, J. (2018). Graphene-based heterojunction photocatalysts. *Applied Surface Science*, *430*, 53-107.

Li, X., Yu, J., Low, J., Fang, Y., Xiao, J., & Chen, X. (2015). Engineering heterogeneous semiconductors for solar water splitting. *Journal of Materials Chemistry A*, *3*(6), 2485-2534.

Hernández-Ramírez, A., & Medina-Ramírez, I. (2016). *Photocatalytic semiconductors*. Springer International Pu.

Biosynthesis and Antibacterialstudies of Chitosan Stabilized Silver Nanocomposite

[*1]Sumaila, A., [1]Ndamitso,M. M., [1]Iyaka, Y. A., [2]Abdulkareem, A. S
[1]*Department of Chemistry, Federal University of Technology Minna, Niger State Nigeria*
[2]*Department of Chemical Engineering, Federal University of Technology Minna Nigeria*
*Author for correspondence: muminislam2012@gmail.com

Abstract

The preparation and antibacterial potential of chitosan stabilized silver nanocomposite is reported. Chitosan-Silver nanocomposite was prepared by incorporation of silver nanoparticles onto chitosan polymer matrix by reduction method. The nanocomposite wascharacterized by UV-visible spectroscopy, Fourier Transform Infrared (FTIR) spectroscopy, X-ray Diffraction (XRD) analysis and High-ResolutionScanning Electron Microscopy (HRSEM). Antibacterial activity of the chitosan stabilized silver nanocomposite against *K. pneumoniae*, *P. aeruginosa*, *S. aureus* and *S. Pyogimase*was carried out by Agar – well diffusion method. The UV–visible spectrum at maximum absorption band of 426.5 nm andXRD analysis demonstrated the formation of semi – crystalline chitosan stabilized silver nanocomposite.The nanocomposite exhibited strong antibacterial activity against all the tested bacteria than chitosan and silver nanoparticles alone but most active against *K.pneumonia*e and *P. Aeruginosa.*

Keywords: Chitosan, Nanosilver**,** Incorporation**,** Characterization, Antimicrobial activity

Introduction

Chitosan is a second most abundant low – cost natural biopolymer after cellulose (Hajji *et al*., 2014). Chitosan is prepared by deacetylation of chitin, which is the structural component in the exoskeletons of crustaceans, radulas of molluscs and beaks of cephalopods (Yang, 2011). Recently, chitosan has attracted significant interest due to its antimicrobial activityin the field of biomedicine which is influenced by a number of factors such as the species of bacteria, concentration, pH, solvent and molecular mass (Mahmoud and Seid, 2016).

The antimicrobial properties of chitosan can be improved by doping with nanoparticles of metals and metal oxides such as copper, gold, titanium, zinc and silver (Sharma, 2015).Of all these metals, antimicrobial of silver is the one whose nanoparticles is well known due to its strong toxicity against a wide range of microorganisms other advantages include stability at high temperature and low volatility (Sharma, 2015). Thus, this study report the preparation and antibacterial activity of chitosan stabilized silver nanocomposite. The preparation nanocomposite was characterized by FTIR, XRD, Uv-visible spectroscopy and HRSEM. In order to evaluate the antibacterial activities, *K. pneumoniae*, *P. aeruginosa*, *S. aureus* and *S. pyogimase* were selected as the tested bacteria.

MATERIALS AND METHODS

Materials

Leaves of *Nicotiana tabacum* wereobtained from a vegetable farm in TungaAwaje area of Paiko, Niger State Nigeria. Chitosan was extracted fromcrab shells via the methods reported by Hajji *et al.*, (2014). Silver nitrate ($AgNO_3$) and glacial acetic acid with percentage purity of 99% were obtained from Sigma Aldrich Chemicals Limited. All chemicals and reagents used in this work were of analytical grade and used as received without further purification.

Method

Preparation of Aqueous Leaf Extract

The fresh leaves of *Nicotiana tabacum* were washed with distilled water, sun dried and later ground to fine powder. To 10 g of the leaves, 100 cm^3 distilled water, was added and boiled at 80° C in water bath for 15 minutes. This was allowed cools and subsequently filtered through Whatmann No.1 filter paper and stored at room temperature for further use.

Phytochemical qualitative analysis

The phytochemical screening of aqueous leaf extract of *Nicotiana tabacum* was doneusing standard procedures earlier employed by Okere*et al.*, (2016).

Preparation of Chitosan - Silver Stabilized Nanocomposite

For the preparation of chitosan – silver stabilized nanocomposite, 40 cm^3 of 1.0 wt% chitosan solution and the 40 cm^3 of 1M $AgNO_3$ solution were mixed in the 100 cm^3 conical flasks. To this mixture, 5 cm^3 aqueous leaf extract of *Nicotiana tabacum* was then added. The mixture was stirred on a magnetic stirrer at 250 rpm for 2 hours and subsequently allowed to age for 24 hours. The changes in colour from colourless to pale brown then to dark brown, signifies the formation of nanosilver. The obtained chitosan – silver nanocomposite was freeze dried at -42^{0}C and then characterized.

Antibacterial activity of chitosan – silver stabilized nanocomposite

The antibacterial activities of chitosan – silver nanocomposite were analyzed by agar well diffusion method on Muller- Hinton plates against *K. pneumoniae, P. aeruginosa, S. aureus* and *S. pyogimase*. Individually, single colony of bacterial strain was grown in nutrient broth and maintained on a shaker at 37 °C for 24 hours. After 24 hours incubation,each bacterial

strain was spread into the Muller-Hinton agar plates using sterile cotton swabs. The control and synthesized nanocomposite of the same concentrations (250mg/l) were poured into the wells and the plates were incubated at 37 °C for 24 hours. After incubation, the zone of inhibition was measured.

Results and Discussion

Results of Phytochemical Screening of Aqueous Leaf Aqueous Extract

In this study, the qualitative and quantitative phytochemicals analysis of the aqueous leaf extract of *Nicotiana tabacum* was done and the result is presented in Table 1. Table 1shows presence of alkaloids, flavonoids, phenols and tannins and their respective amount and absence of reducing sugars, steroids and saponins in the extract.

Table 1: Qualitative and quantitative phytochemical analysis of aqueous leaf extracts of *Nicotiana tabacum* (mg/g)

Class of compounds	Aqueous extracts	Amount (mg/g)
Total Alkaloids	+	72.722
Steroids	+	65.223
Total Phenols	+	135.405
Total Flavonoids	+	23.667
Tannins	+	45.704
Reducing sugars	-	-
Saponins	-	-

Key: Positive (+), Negative (-)

Previously, aqueous leaf extracts of *Nicotiana tabacum* have been positively tested for steroids, flavonoids, tannins, phenols and alkaloid by Sunil *et al.* (2010), Shekins*et al*. (2016) and Patil *et al.* (2015) and their results were in agreement with the outcome of this study. From the Table 1, it can be seen that total phenols compared to other phytochemicals has the highest amount of 135.405 mg/g, followed by alkaloids with a concentration of 72.722 mg/g and an considerable amount of tannins (45.704 mg/g) while total flavonoids was in a appreciable amount of 23.667 mg/g. Therefore, the presence of this phytochemicals in good amount is an indication of their impact on the biosynthesis of silver nanoparticles as reducing agents.

UV–visible spectroscopy analysis of chitosan – silver stabilized nanocomposite

The formation of the nanosilver by reduction of $AgNO_3$ in the acetic acid solution of chitosan in the presence of aqueous leaf extract of *Nicotiana tabacum* ion was monitored by UV–visible spectroscopy. During the reduction process, colourless solution of chitosan containing $AgNO_3$ gradually changed to brown, which signifies the conversion of Ag^+ into Ag^0 (Ge*et al.*, 2014). The presence of nanosilver in the composite was confirmed by UV–visible spectrum (Figure 1) with a maximum absorption band at426.5 nm, which corresponds to the typical plasmon resonance band of nanosilver (Sotiriou, *et al.*, 2010).

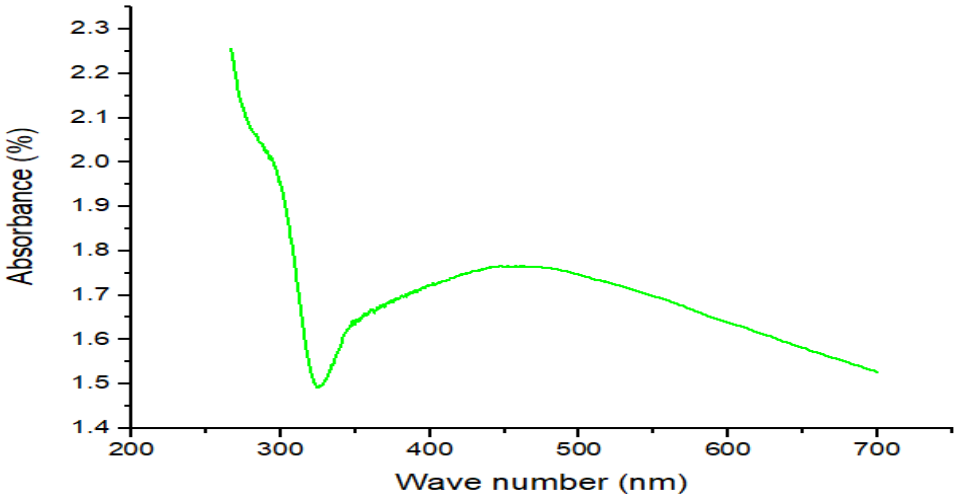

Figure 1: UV–visible spectra of chitosan – silver nanocomposite

FTIR of chitosan stabilized silver nanocomposite

FTIR analysis was carried out to identify the functional groups developedfor the interaction between the chitosan polymer matrix and the nanosilver. The FTIR spectra for the chitosan stabilized silver nanocomposite are shown in Figure 2. As shown in figure 2, a characteristics absorption band was observed at 1646.82 cm^{-1} which was assigned as C - Nstretch while N - H was at observed at 3290.80 cm^{-1}. The C–H bond interaction due to Amide II band was at 1396.04 cm^{-1} and the C–O skeletal stretch characteristic of polysaccharides was observed at 1019.88 cm^{-1}. The band at 2858.91 cm^{-1} wasassigned to the alkane C-H-stretching respectively (Wang, *et al*., 2016). The single peak at 3290.80 cm^{-1} corresponds to N – H is in agreement with the previous studies resultreported (Ahmad, *et al*., 2011).

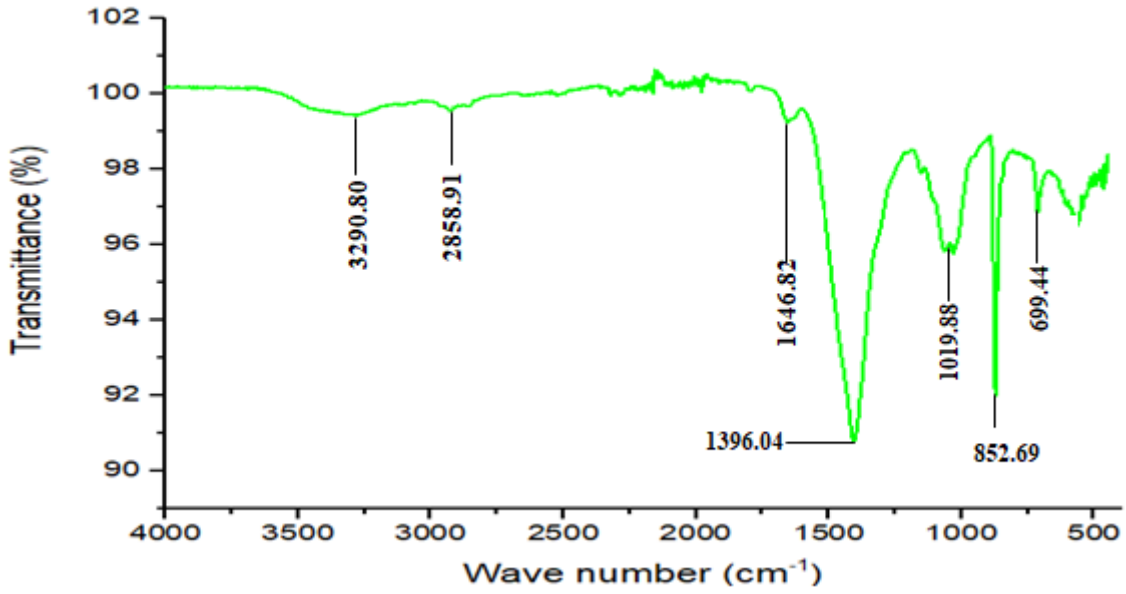

Figure 2: FTIR of the Synthesized Chitosan – Silver Nanocomposite

XRD study of the prepared chitosan – silver nanocomposite

The phase structure of the prepared chitosan – silver nanocomposite was investigated using XRD technique. Figure 2 shows the diffractogram of the prepared nanocomposite. The presence of chitosan and nanosilver were apparent from the diffractogram, while other peaks may be attributed to the impurity phases due to biomolecules of the leaf extract (Astalakshmi, *et al.*, 2013)

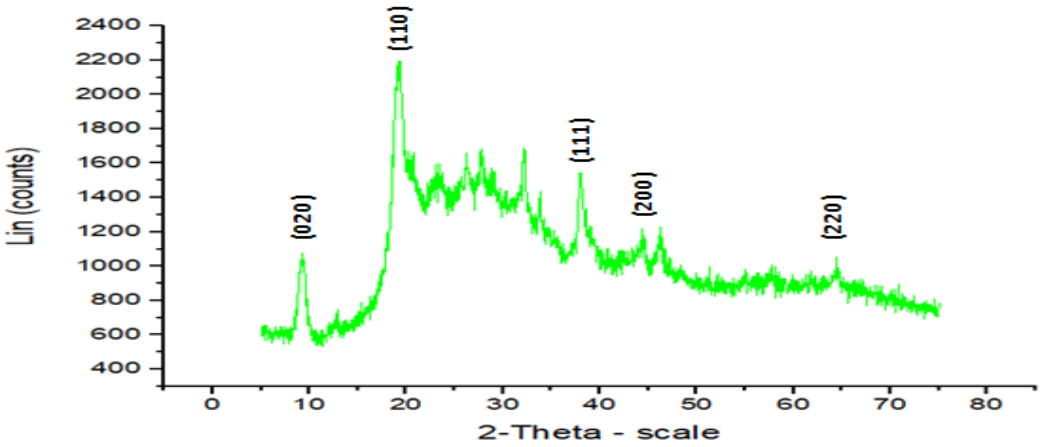

Figure 3: XRD pattern of chitosan–silver nanocomposite

The diffraction peaks observed at 2θ values of 9.29° and 19.30^{0}with crystal plane (020) and (110) correspond to a diffractogram of a typical chitosan, while the diffractogram at 2θ of

38.04°, 44.65^0 and 64.45° indexed (111), (200) and (220)miller indices are assigned to silver nanoparticles (Shameli, *et al*., 2011).

High Resolution Scanning Electron Microscope (HRSEM) of chitosan stabilized silver nanocomposite

Surface morphology of prepared chitosan stabilized silver nanocomposite was analyzed using the HRSEM technique. The HRSEM image of the nanocomposite in Figure 4 showed distribution of silver nanoparticles on the chitosan surface and embedment of some of the nanoparticles into chitosan to create pores.

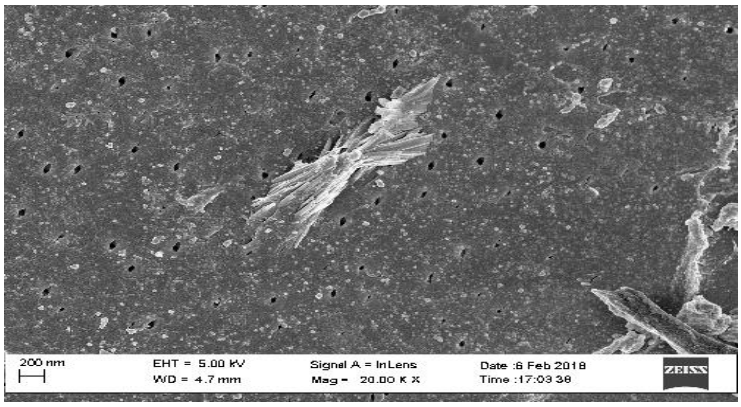

Figure 4: HRSEM image of chitosan stabilized silver nanocomposite

Electron Dispersive Spectroscopy (EDS)

Electron Dispersive Spectroscopy (EDS) is ananalysiscarried out to scanfor elementsthat made up a sample through amplitude of wavelength for the x-ray emitted after the electron was hit by the electron beam. X- rays can only be emitted by atoms that contain minimum of K - shell and L - shell where the electron is allow to displace from one energy level to another. EDS could not determine hydrogen because atom of hydrogen contains only K - shell is not detectable (Swapp, 2012). Figure 5 is an elemental dispersive spectrum showing the main elements that made up chitosan – silver nanocompositewhile Table 2shows the weight percent of the element.

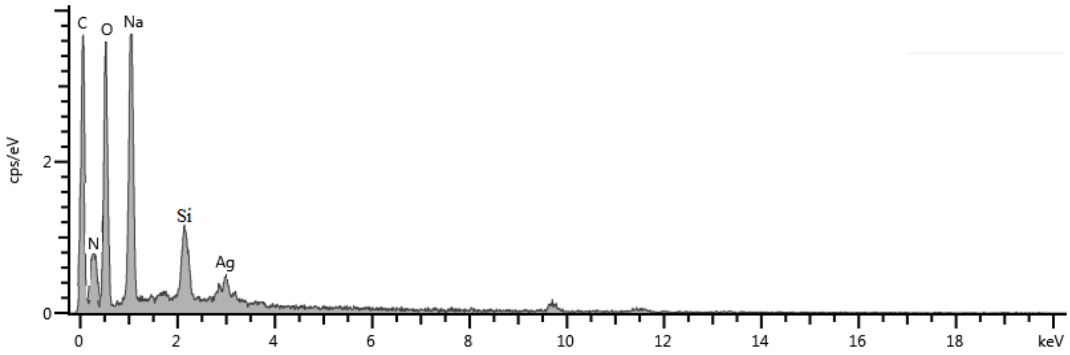

Figure 5: EDS Spectrum for Chitosan – silver nanocomposite

Table 2: Elemental weight (%) composition of chitosan – silver nanocomposite

Atomic number	Element symbol	Name of element	Weight %
4	C	Carbon	15.50
7	N	Nitrogen	12.98
8	O	Oxygen	40.67
11	Na	Sodium	26.87
14	Si	Silicon	0.43
108	Ag	Silver	3.55

Antimicrobial activity

The ability of chitosan – silver nanocomposite to inhibit growth of the tested strains is shown in Table 3. The inhibitory activity was measured based on the diameter of the clear inhibition zone. The results from this study revealed that chitosan - silver nanocomposite clearly showedbetterinhibitory effect against all the tested bacteria strains compared to chitosan and silver nanoparticles alone.

Table 3: Antimicrobial activity of chitosan – silver nanocomposite film forming solutions

Inhibition zone diameter (mm)

Indicator organisms	Chitosan – silver nanocomposite	Chitosan	Silver nanoparticles
Klebsiella pneumoniae,	27.00	-	26.00
Staphylococcus aureus	29.00	10.00	25.00
Streptococcus pyogimase	28.00	-	23.00
Pseudomonas aeruginosa,	24.00	11.60	20.00

ND: not detected

Conclusion

The present study reported the greensynthesis of chitosan stabilized silver nanocomposite and its application in antimicrobial activity. The aqueous leaf extracts *Nicotiana tabacum* was used as reducing agent and the presence of silver nanoparticles on the surface of chitosan was

confirmed by XRD result. The nanocomposite exhibited efficient activity against all the tested bacterial strains.

Acknowledgement

The authors would like to acknowledge the financial support from Tertiary Education Tax Fund (TETFund) Nigeria with grant number TETFUND/FUTMINNA/2016-2017/6thBRP/05 through Institution Based Research (IBR) of Federal University of Technology, Minna, Nigeria.

REFERENCE

Ahmad, M. B., Lim, J. J., Shameli, K., Ibrahim, N. A., and Tay, M.Y. (2011). Synthesis of Silver Nanoparticles in Chitosan, Gelatin and Chitosan/GelatinBionanocomposites by a Chemical Reducing Agent and Their Characterization, *Molecules*, 16, 7237 - 7248.

Astalakshmi, A., Nima, P., and Ganesan, V. (2013) A green approach in the synthesis of silver nanoparticles using bark of *Eucalyptus globulus,* Labill, *International Journal Pharmaceutical Scientic Research*, 23, 1, 47 - 52.

Ge, L., Li, Q., Wang, M., Ouyang, J., Li, X., and Xing, M. M(2014). Nanosilver particles in Medical Applications: Synthesis, Performance, and Toxicity, *International Journal of Nanomedicine*, 9: 2399–2407.

Gu, H.W., Ho, P. L., Tong, E., Wang, L., and Xu, B. (2003). Presenting vancomycin on nanoparticles to enhance antimicrobial activities", *Nano Letter*., 3, 1261 - 1263.

Hajji, S., Younes, I., Ghorbel-Bellaaj, O., Hajji, R., Rinaudo, M., and Nasri, M., (2014). Structural differences between chitin and chitosan extracted from three different marine sources, *International Journal Biology Macromolecules*, 65, 298 – 306.

Kuppusamy, P., Mashitah, M., Yusoff, M., Maniam, G. P., and Govinda, N. (2016). Biosynthesis of metallic nanoparticles using plant derivatives and their new avenues in pharmacological applications, *Saudi Pharmaceutical Journal*, 24, 4, 473 – 484.

Mahmoud, H., and Seid, M. J. (2016). Evaluation of different factors affecting antimicrobial properties of chitosan, *International Journal of Biological Macromolecules*, 85, 467- 477.

Okere O. S., Ejike U. D., Mubarak, L. L., and Paul, J. (2016). Phytochemical Screening of Tobacco (*Nicotiana tabacum*) and Its Effects on Some Haematological Parameters and Histopathology of Liver and Brain in Male Rats*International Journal of Biochemistry Research &*Review, 14, 4, 1 – 9.

Patil RS, Desai AB, Wagh SA (2015) Comparative study of antimicrobial compounds extracted from leaves of Nicotiana tabacum and cigarette. World J. Pharm. Pharm. Sci. 4(3):1511-1518

Pawan, K., Ashok, C., and Rajesh, T. **(**2013**).** Synthesis of Chitosan-Silver Nanocomposite and their Antibacterial Activity, *International Journal of Scientific and Engineering Research*, 4, 4, 868 – 872.

Shameli, K., Ahmad, M.B. Zargar, M., Yunus, W.M., Ibrahim, N.A., Shabanzadeh, P., and Moghaddam, M.G. (2011). Synthesis and Characterization Silver/ Montmorillonite/ Chitosan Bionanocomposites by Chemical Reduction Method and their Antibacterial activity, *International JournalNanomedicine*,6, 271 - 284.

Sharma, D. (2015). Biogenic synthesis of nanoparticles: A Review. *Arabian Journal of Chemistry*, http://dx.doi.org/10.1016/j.

Sotiriou, G. A. Sannomiya, T. Teleki, A. Krumeich, F. Vörös, J., and Pratsinis, S.E. (2010). Non-toxic dry-coated nanosilver for Plasmonic Biosensors, *Advanced Functional Material*, 21, 20, 24, 4250 – 4257.

Shekins OO, Dorathy EU, Labaran ML, Joel P (2016) Phytochemical screening of tobacco (Nicotiana tabacum) and its effects on some haematological parameters and histopathology of liver and brain in male rats. Int. J. Biochem. Res. 14(4):1-9.

Sunil K, Paras S, Amit J, Mukesh SS (2010) Preliminary phytochemical screening and HPTLC fingerprinting of Nicotiana tabacum leaf. J. Pharm. Res. 3(5):1144-1145.

Swapp, S. (2012) Scanning Electron Microscopy (SEM). http://serc.carleton.edu/research_education/geochemsheets/techniques/SEM.html

Wang, Y., Pitto-Barry, A., Habtemariam, A., Romero-Canelon, I., Sadler, P. J.,and Barry, N. P. E. (2016). Nanoparticles of Chitosan Conjugated to Organo-Ruthenium Complexes, *Inorganic Chemistry Frontier*,**3**, 1058 - 1064.

Sustainability of Biodiesel and Bioethanol Production as a Substitute for Fossil Fuels in Developing African Countries

Adewusi S. G, Okunola O. J and Obadimu C.O.
Department of Chemistry, Federal College of Education, Zaria
Department of Applied Chemistry, Federal University Dutsin-Ma, Katsina State
Department of Pure and Applied Chemistry, Akwa Ibom State University Ikot Akpaden Mkpatenin LGA, Akwa Ibom State.

Abstract

The changing in our climate as a consequence of anthropogenic activities which fossil fuel exploration and usage has contributed significantly is becoming a global phenomenon. This has underpins our current way of life and hopes of people in the developing countries for improved lives. Biofuels – bioethanol and biodiesel derived from plants seem to be an elegant solution to this dilemma because they decrease dependency on fossil fuels and only return recently sequestered carbon dioxide to the atmosphere. The governments of many industrialized and developing countries are therefore creating and expanding policies and research programmes to increase the production and use of biofuels. Nevertheless, the growing demand for biofuel to be produced from crops previously used for food has raised concern about the long-term economic, environment and social sustainability of the alternative fuels. With particular focus on developing Africa countries, this paper discusses the viability of biodiesel and bioethanol as a substitute for fossil fuels especially providing energy from local crops, creating jobs and alleviating poverty, and most important reduction in green house gas (GHS) emissions. However, sustainability of these potentials will not be realized without careful and thorough assessment and regulations.

Keyword: *Biodiesel, Bioethanol, Substitute, Fossil fuels*

Introduction

High economic growth, underway for several decades in most developing countries across the globe, has resulted in robust demand for various energy sources. A greater need for mobility and peoples' aspirations for improved living conditions have together become the main driver for increasing primary oil demand, which is projected, according to most recent energy "outlooks" by the IEA and OPEC, to rise by about 1.0% per year, reaching approximately 105 million barrels per day (mb/d) level by 2030 (OFID/IIASA, 2009).

The transport sector, in particular, relies almost entirely on oil supplies for fuel. Several factors, including energy price increases, increased market volatility, in particular during 2008 and

2009; heavy dependence of many countries on imported oil; lingering debate about the ultimate size of remaining, recoverable fossil fuel reserves; and, not least, growing concerns about the environmental impact of fossil fuel usage have provided the impetus for the current strong interest in, and support for, biofuels in many parts of the world. In developing African countries, the contribution of biofuels as an alternative energy source is currently very small, but this may change, should the high growth rates of the last few years be sustained in the coming years and decades (Mandil and Adnan, 2010).

What are Biofuels?

Biofuels are combustible materials directly or indirectly derived from biomass, commonly produced from plants, animals and micro-organisms but also from organic wastes. Biofuels may be solid, liquid or gaseous and include all kinds of biomass and derived products used for energetic purposes (2). This "bioenergy" is one of the so-called renewable energies. Besides the traditional use of bioenergy (3), 'modern bioenergy' comprises biofuels for transport, and processed biomass for heat and electricity production. Biofuels provide an opportunity for agriculture to work with the energy sector in a mutually beneficial way. In tropical sub-Saharan Africa, the biofuels market is still at its infancy and requires much needed attention from policy makers and financial institutions to develop and grow this industry to fruition so that we do not eventually end up as importers, like we do for other sectors.

Energy consumption is today regarded globally as an index of development. On the overall, energy consumption in Africa is less than 5% of the global consumption, though 13% of the world's populations and 10% of the world crude oil reserves are in Africa (Bugaje and Mohammed, 2008). Also, 85% of the people in Africa still live in rural areas without electricity access. Yet Africa is fortunately blessed with not only abundant sunshine (solar energy), but plentiful wind energy, wood and biomass resources, etc more than most other continents of the world. These could be mobilized to address the eminent energy crisis facing the continent in a sustainable manner.

Biofuels, such as biodiesel, and bioethanol (all sourced from renewable agricultural resources), have great potentials of not only providing an alternative automobile transport fuel but also creating other downstream industries utilizing ethanol as raw material. Falling back to agriculture to provide fuel using non-edible raw materials such as seed oils of *Jatropha caucus* (bini-da-zugu), *Ricinus communis* (castor), *Lannea microcarpa* (African grapes), *Vitex doniana* (African olive), etc and the less edible ones such as sugarcane molasses, would not only be sustainable sources but will help check desertification and reverse the green house

effect. Plantations of Jatropha in the Southern fringes of the Sahara, for example, will surely reduce the desertification process and ensure environmental sustainability (Bugaje, 2010).

Global trends in biofuels demands and supply

Global production of biofuels has been growing rapidly in recent years, more than tripling from about 18 billion litres (10 million tonnes of oil equivalent {Mtoe}) in 2000 to about 60 billion litres (42 Mtoe) in 2008. Supply is dominated by bioethanol, which accounted for approximately 84% of total biofuel production in 2008. Despite this exponential increase, biofuels still represent a very small share of the global energy picture. Total biomass accounted for 3.5% of total primary energy supply in 2007, according to the OPEC World Oil Outlook (OPEC/ WOO, 2009), with liquid biofuels accounting for about 0.28% of total energy demand and about 1.5% of transport sector fuel use (IEA /WEO, 2009).

Currently, production is concentrated in a small number of countries (Table 1). Together the US and Brazil account for about 81% of total biofuel production and about 91% of global bioethanol production Since 2005, the US has surpassed Brazil as the largest bioethanol producer and consumer, accounting for 50% of global production in 2008 (SCOPE, 2009). The EU follows as the third major producer with 4.2%. In contrast, about 67% of biodiesel is produced in the EU, which is also the largest consumer, with Germany and France combined accounting for 75% of total EU production and 45% of global production.

Table 1 Biofuel production in 2008

billion litres	Bioethanol		Biodiesel		Total biofuels		Share in total
World	*67.0*	*(32.8)*	*12.0*	*(9.4)*	*79.0*	*(42.2)*	*100.0%*
US	34.0	(16.7)	2.0	(1.6)	36.0	(18.2)	45.6%
Brazil	27.0	(13.2)	1.2	(0.9)	28.2	(14.2)	35.7%
EU	2.8	(1.4)	8.0	(6.3)	10.8	(7.6)	13.7%
China	1.9	(0.9)	0.1	(0.1)	2.0	(1.0)	2.5%
Canada	0.9	(0.4)	0.1	(0.1)	1.0	(0.5)	1.3%
India	0.3	(0.1)	0.02	(0.0)	0.32	(0.2)	0.4%

Source: REN 21 (2009). Note: units are billion litres; Mtoe (in brackets) was calculated. Share in total is in volume.
[Other countries not named in Table 1.1 have a combined 0.8% share of the world total.]

According to a recent study by Hart's Global Biofuels Center (Hart/GBC 2009), global demand for ethanol and biodiesel combined is expected to nearly double between 2009 and 2015 from 95.3 to 183.8 billion litres (50.5 to 100.8 Mtoe) (Tables 1.2a and 1.2b). Ethanol, while accounting for 80% of this latter figure, will only represent 12% to 14% of total global gasoline demand. Although global ethanol supply generally matches demand in 2009 and 2010, it is expected to exceed it in 2015, reaching 168.6 billion litres (82.6 Mtoe) compared to expected

demand of 147.3 billion litres (72.2 Mtoe). Similarly, biodiesel supply is projected to almost double by 2015, reaching 94 billion litres (73.6 Mtoe), and will also exceed the estimated demand of 36 billion litres (28.2 Mtoe) that year. Hart/GBC estimates supply based on current capacity and projected capacity to be in place by the 2015 time frame. Hart/GBC based their demand figures on the assumption that policy requirements and targets will be implemented and fulfilled and by using gasoline and on-road diesel demand figures estimated in another Hart/GBC study. The apparent supply/demand imbalance, according to Hart/GBC, will be taken care of by 2015 through some or all of several expected routes; 1) governments increasing blending limits; 2) many proposed projects cancelled; 3) continued low utilization rates; and 4) many existing plants scrapped. Interestingly, projected supply is well above targeted demand, which increases uncertainty in the motor fuels market, and creates a disincentive to invest in both the upstream and downstream of this domain. The supply/demand medium-term outlooks (2009, 2010 and 2015) for major ethanol and biodiesel producers and consumers are summarized in Tables 2 and 3.

Table 2 Global ethanol medium-term supply and demand

billion liters	2009		2010		2015	
Country	Supply	Demand	Supply	Demand	Supply	Demand
*World **	*83.4 (40.9)*	*82.2 (40.3)*	*101.4 (49.7)*	*99.4 (48.7)*	*168.6 (82.6)*	*147.3 (72.2)*
USA	42.4 (20.8)	42.4 (20.8)	49.2 (24.1)	49.2 (24.1)	61.7 (30.2)	60.5 (29.6)
Brazil	27.5 (13.5)	22.0 (10.8)	29.7 (14.6)	25.9 (12.7)	54.0 (26.5)	47.2 (23.1)
EU	3.4 (1.7)	4.8 (2.4)	4.4 (2.2)	6.0 (2.9)	6.0 (2.9)	9.2 (4.5)
China	3.1 (1.5)	8.5 (4.2)	3.4 (1.7)	8.8 (4.3)	12.8 (6.3)	11.5 (5.6)
India	1.7 (0.8)	0.8 (0.4)	1.8 (0.9)	1.6 (0.8)	9.3 (4.6)	2.1 (1.0)
Indonesia	0.7 (0.3)	0.18 (0.1)	2.2 (1.1)	0.6 (0.3)	6.5 (3.2)	1.1 (0.5)
Malaysia	0	0	0	0	0	0

Table 3 Global Biodiesel medium-term supply and demand

billion liters	2009		2010		2015	
Country	Supply	Demand	Supply	Demand	Supply	Demand
World*	***48.2 (37.7)***	***13.1 (10.3)***	***59.6 (46.7)***	***18.3 (14.3)***	***94.4 (73.9)***	***36.5 (28.6)***
USA	2.8 (2.2)	2.8 (2.2)	3.1 (2.4)	3.1 (2.4)	8.4 (6.6)	8.4 (6.6)
Brazil**	2.9 (2.3)	1.0 (0.8)	4.5 (3.5)	1.8 (1.4)	6.0 (4.7)	2.1 (1.6)
EU	18.6 (14.6)	9.6 (7.5)	21.5 (16.8)	12.8 (10.0)	28.1 (22.0)	16.1 (12.6)
China	5.3 (4.1)	0	6.3 (4.9)	0	11.5 (9.0)	3.5 (2.7)
India	1.8 (1.4)	0	2.0 (1.6)	0	4.2 (3.3)	4.1 (3.2)
Indonesia	2.9 (2.3)	0.08 (0.1)	7.4 (5.8)	0.2 (0.2)	10.4 (8.1)	0.5 (0.4)
Malaysia	4.3 (3.4)	0.25 (0.2)	5.5 (4.3)	0.25 (0.2)	10.5 (8.2)	0.3 (0.2)

*Source: Hart/GBC 2009. Note: Units are billion litres, Mtoe (in brackets) was calculated. *World was calculated as the sum of regional supply/demand data provided in the above source **Petrobras has set a target of 0.8 billion litres (0.6 Mtoe) per year by 2011 (Biodiesel magazine, August 2006)*

Over the medium term, the US and Brazil are likely to continue to dominate ethanol supply and demand. However, their combined share of production may decrease to 73% of the global total, as the role of countries in the Asia-Pacific region, mainly China, India, Indonesia and Malaysia, rapidly increases. By 2015, the latter region's total production could represent about 22% of global supply.

With respect to biodiesel, the EU is assumed to continue dominating consumption in 2009 and 2010, but its share is also projected to decrease, from 60% to 40%, by 2015 as consumption in Asia-Pacific grows steadily. This region also captures a significant share of biodiesel production, about 50%, by 2015. Table 4 provides a comparison between the outlooks for biofuel supply provided by Hart/GBC, EIA, and OPEC.

Table 4 Comparison of medium-term outlooks for biofuel supply

	2007	2008	2009	2010	2015
Hart/GBC, billion liter/yr			131.6 (78.6)	161 (96.4)	263 (156.5)
EIA, mb/d	1.1 (37.0)			1.9 (63.9)	2.8 (94.1)
OPEC, mb/d		1.3 (43.7)	1.5 (50.4)	1.7 (57.1)	2.2 (74.0)

In a detailed analysis of biofuels for transport, the OECD and FAO (2008) expect the global use of bioethanol and biodiesel to nearly double from 20052007 to 2017 (Table 5). Most of this increase will be due to biofuel use in the US, the EU, Brazil and China. But other countries not yet considered could also develop towards significant biofuel consumption. Indonesia, India, Australia, Canada, Thailand, the Philippines and Japan are all likely important producers and consumers in the foreseeable future. The OECD and FAO (2008) also evaluated the role of feedstocks for the global production of biofuels until 2017 (Table 6) by taking policies in place in early 2008 into account and assuming them to be constant over the period to 2017. In total, biofuel feedstocks would increase from 50 Mt in 2005 to 193 Mt in 2017. As a result 9% of the global production of wheat and coarse grains plus oilseeds and vegetable oil would supply 5% of global gasoline and diesel demand with biofuels.

Biofuels in Africa

Biofuel expansion drivers in Africa

The European Union has proposed mandatory biofuel blends with petroleum of five per cent by 2015, and 10 per cent by 2020 (to be reviewed in 2014), as a mechanism to reduce carbon emissions. Since the EU is unable to meet its biofuel target due to insufficient agricultural land available in Europe, this has created an international market for biofuels. European and other investors are placing strong pressure on African countries to make more land available for biofuel feedstock to meet European biofuel and global carbon reduction targets.

Table 5 Increase of biofuels use from 2005 – 07 to 2008 and projection to 2017

	Fuel ethanol plus biodiesel			
	2005-07 to 2008		2005-07 to 2017	
	PJ	%	PJ	%
Australia	26	323%	46	582%
Brazil	104	36%	435	150%
Canada	20	117%	63	371%
China	12	37%	98	297%
Columbia	9	156%	12	206%
Ethiopia	0.02	32%	0.83	1240%
EU Total	135	60%	520	231%
India	5	30%	20	137%
Indonesia	3	180%	71	4522%
Malaysia	2		5	
Mozambique	0.05	163%	0.54	1617%
Peru	0.04		0.04	
Philippines	1	259%	4	1010%
South Africa	0		8	
Tanzania	0.24	179%	1.44	1085%
Thailand	2	71%	26	925%
Turkey	0.32	35%	0.42	47%
USA	361	76%	759	160%
World Total	679	63%	2071	193%

Source: UNEP, 2009

Table 6 Global demand and area for biofuel feedstocks until 2017

	2005	2007	2017	2005 to 2007			2007 to 2017		
				absolute	%	% p.a.	absolute	%	
Wheat and coarse grains									
Total demand, Mt	1622	1702	1930	80	4.90%	2.50%	228	13.40%	1.30%
of which, biofuel Mt	46	93	172	47	102.20%	51.10%	79	84.90%	8.50%
of which: biofuels, %	2.80%	5.50%	8.90%						
Total production, Mt	1615	1661	1906	46	2.80%	1.40%	245	14.80%	1.50%
Area harvested, Mha	525	531	539	6	1.10%	0.60%	8	1.50%	0.20%
Yield, t/ha	3.08	3.13	3.536	0.05	1.70%	0.80%	0.41	13.00%	1.30%
Oilseeds and vegetable oil									
Total demand, Mt	96	105	143	9	9.40%	4.70%	38	36.20%	3.60%
of which, biofuel, Mt	4	9	21	5	125.00%	62.50%	12	133.30%	13.30%
of which: biofuels,%	4.20%	8.60%	14.70%						
Total production, Mt	99	106	143	7	7.10%	3.50%	37	34.90%	3.50%
Area harvested, Mha	145	142	164	- 3	- 2.10%	-1.00%	22	15.50%	1.50%
Yield, t/ha	0.68	0.75	0.872	0.06	9.30%	4.70%	0.13	16.80%	1.70%
Biofuel feedstocks total									
Total demand, Mt	1718	1807	2073	89	5.20%	2.60%	266	14.70%	1.50%
of which, biofuel, Mt	50	102	193	52	104.00%	52.00%	91	89.20%	8.90%
of which: biofuels,%	2.90%	5.60%	9.30%						

OECD/FAO (2008)

Africa's interest in this market is driven predominantly by the need for economic growth, especially among rural communities. Biofuel production represents an opportunity to boost rural economies by supplying international markets for fuel crop products and, in turn, opening markets for agricultural surpluses. The concern is that the economic benefits of biofuels to African countries may be minimal, especially if raw feedstock is exported for processing elsewhere (von Maltitz and Brent, 2008; Haywood *et al.*, 2008). Of the 40 countries within sub-Saharan Africa, 14 are landlocked. Further, nearly 40 per cent of Africa's population lives in landlocked countries where transport costs on average are 50 per cent higher than in coastal countries. Biofuel production offers African countries importing petroleum a means to achieve energy security and the possibility of reducing the foreign currency demands for importing oil. However, as a continent, Africa has the lowest per capita energy consumption. Low consumption levels reflect low economic development, and also hinder economic development. Biomass in the form of charcoal and fuelwood continues to be the main fuel source for most sub-Saharan countries (see Table 7). Biofuels are a relatively new concept and although bioethanol was used as a petroleum supplement in the past in countries including Malawi, South Africa and Zimbabwe, it is only in the last few years that large-scale biofuel production has been seriously considered.

Table 7. Annual energy consumption characteristics of some Africa and to global trends

	Energy use per capita (kgoe)	Total energy from biomass and waste in %	Electricity consumption per capita (kWh)	Liquid fuel consumption per capita*
World	1796	9.7	2678	751
Sub-Saharan Africa	681	56.3	542	117
Ghana	397	66.0	266	122
Tanzania	530	92.1	61	45
Kenya	484	74.6	138	101
Mozambique	497	85.4	450	39

Source: Compiled from World Bank 2008
****Calculated from 2004 oil consumption and population data at www.eia.doe.gov/emeu/international June 2009***

Biofuel projects in Sub-saharan Africa

It is impossible to obtain an accurate figure for the status of biofuel projects across Africa. The situation is very dynamic with new investments being announced monthly, often to simply disappear. A large number of projects are in the planning phase, but few are fully operational. Hagan (2007), for instance, suggests that current projects in 10 West African countries represent an investment of US$126 million, with plans to install processing capacity for 70 million litres of biodiesel and 165 million litres of bioethanol per year. But, as far as can be ascertained, none of these projects are operational. On an Africa-wide scale, the proposed biofuel expansion equates to tens of millions of hectares.

African biofuel projects can be divided into four basic types based on the scale of production and intended use of the biofuels (see Figure 2).

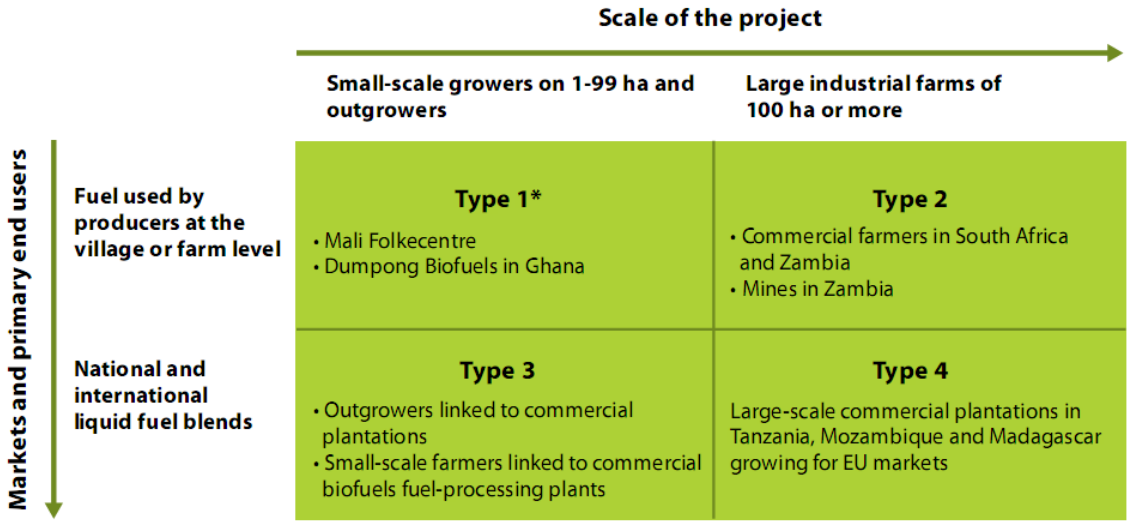

Figure 1 Typical biofuel projects grouped by scale of farming activity and intended use of the biofuel product

In Type 1 and 2 projects, biofuels are produced to meet local needs. These projects are typically small and have been initiated in several African countries including Mali, Ghana, Mozambique, Tanzania and Zambia. These projects are often initiated by nongovernmental organisations (NGOs) and supported by national governments or international donors. Although mostly based on small growers who provide the feedstock (Type 1), some largescale farmers and mining companies are also planting biofuel crops to meet their own fuel requirements (Type 2). Biofuels are commonly part of a mixed cropping system for both small and large-scale farmers.

In contrast, Type 3 and 4 projects are dedicated biofuel production enterprises established specifically to meet the demands for national and international fuel blends. As such, armers benefit from cash income rather than fuel security. Large corporations are the main investors in these types of projects. In Mozambique, Nigeria, Zambia, Tanzania, Ghana and other countries, large jatropha (for biodiesel) and sugarcane (for bioethanol) plantations ranging from thousands to tens of thousands of hectares are currently being planned and planted (Type 4). Similar trends are evident in West Africa with palm oil. Malawi has been producing bioethanol for the past 20 years and currently uses a 10 per cent blend with petrol (see Box D). Industrial sugar production is already practised in most countries with suitable climates, and bioethanol production can build on this as a basis, possibly by just using the molasses, which is regarded as a waste product. In other places, such as in Zambia, companies are attempting to initiate industries based entirely on small-scale farmers (Type 3). However, smallscale farmers are most commonly involved as outgrowers linked to larger industrial plantations (Type 3). In these instances, a proportion of the farmer's landholding is converted to feedstock production. The biofuel industry provides support and inputs, financing, technological assistance and a market. Arguably, biofuels are an attractive farming option on account of the assistance received by the farmers, rather than the intrinsic value of the biofuel crop itself (Haywood *et al*., 2008).

Since Type 1 and 2 projects are aimed at only meeting local fuel needs, they are not considered to have major negative social or environmental impacts; indeed, their proponents see potential positive impacts. If these projects prove to be non-viable, the repercussions will be minimal. By contrast, the magnitude of Type 3 and 4 projects could result in extensive land transformation and consequential biodiversity loss. In addition, unless well managed, there is a high risk of unintended negative social consequences, such as food insecurity and

communities displaced from their land. In Type 3 and 4 projects, there are also concerns that industrial plantations provide either a large number of poorly paid job opportunities if not mechanised, or better-paid but fewer opportunities if mechanised.

Competing biofuel feedstocks

Sugarcane, Jatropha curcas and palm oil are the three main feedstocks being promoted and grown in Africa, but other feedstocks are also being considered such as sweet sorghum, cassava and cashew apples (Table 8). Sugarcane is grown in many African countries, and is a well understood and established crop. Sugarcane produces more biofuel per hectare than any other currently used biofuel crop. Areas in Africa have high sugarcane potential: Zambia has reported production of up to 200 tonnes per hectare (t/ha), which is three times the international norm of 65 t/ha. Malawi and Ethiopia already produce bioethanol from sugarcane and many other countries are considering the option. In addition there is the potential for cogenerating electricity from sugarcane bagasse (and presumably sweet sorghum) as an added benefit (Naylor *et al*. 2007).

Table 8 Indicative yields and fuel equivalents from common biofuel crops

	Sugar	Sugar molasses	Sweet sorghum	Maize	Cassava	Jatropha[2]	Palm oil	Soybean	Canola	Sunflower
Litres fuel/t	60-80	240	40	366-470	160	350	230	227	400	400
Tonnes/ha[1]	13-105	4.5	60[3]	1-5 (USA) 9	3-8 (Thai) 80	2-8	20	2.67	1.4	1-2.5
Biofuel yield l/ha	780-8400	1080	2400	366-3760	480-1280	700-2800	4736	446	552	400-1000
Petrol equivalent/ha	3833	756	1680	2625	1304					
Diesel equivalent/ha						690	4451	420	550	660
High protein animal feed as a byproduct	no	no	no	yes	no	no	no	yes	yes	yes

[1] *Yields vary with location and management. All yields are based on commercial agricultural values. Where possible, the petrol or diesel equivalent is based on data from best practice situations as given by Naylor et al. 2007.*

[2] *These relatively conservative estimates for jatropha are yet to be verified in production systems.*

[3] *With new varieties and where two crops can be grown per year, yields of sweet sorghum may be much higher.*

Jatropha has sparked major interest throughout Africa, with projects currently being implemented in many African countries with suitable climates. South Africa does not support growing jatropha as the country fears that the plant may become a noxious weed. Enthusiastic claims for jatropha's drought hardiness and yields are being tempered by the realisation that jatropha is only likely to yield more than one t/ha of oil in areas with more than 800 mm of rain and where plantations are well managed. Despite the large-scale plantings, and high expectations, many uncertainties still surround the long-term viability of jatropha (Jongschaap *et al*. 2007; Achten *et al*. 2008).

African palm oil can produce up to 20 t/ha of fruit which gives about 4.5 t/ha of oil. It has been extensively grown for cooking oil, especially in West Africa. Palm oil plants require high rainfall and humidity; this limits plantations to tropical rainforest areas and raises concerns about deforestation (Naylor *et al*., 2007).

Sweet sorghum, though not currently produced for biofuels, is generating widespread interest as it approaches sugarcane production levels, but in areas of lower rainfall and possibly with less fertilisation. Extensive agronomic trials are being undertaken by the International Crops Research Institute for the Semi-Arid Tropics (ICRISAT), for instance in Zambia and Botswana. A further advantage is that it may be possible to produce both sorghum grain for food and sugar for ethanol concurrently from the same field (Woods, 2001).

Maize is the key bioethanol crop in America but although farmers are promoting it as a biofuel crop for South Africa, the Government has discouraged its use because of concerns about food security (Department of Minerals and Energy, 2007). Most African maize is a staple food crop and too important as a food to be seriously considered for first-generation biofuel.

Biofuels for Sustainable Development

Land needed to meet fuel security

On a global scale, biofuel production using first generation technologies can only realistically replace a small percentage of fossil fuel. For many African countries, the situation is very different and even first-generation biofuels can provide full fuel self-sufficiency from very limited land areas (see Table 9). Land availability varies widely: countries such as Malawi, Rwanda, Burundi and South Africa have limited land, while countries such as Mozambique, Angola and Zambia have extensive land available. One must use caution in interpreting 'availability,' however, because much of this land is forested and is subject to customary claims. Reliable statistics on land availability are scant and most land is currently being used in some way. Agricultural productivity per hectare in Africa currently falls way below international norms (see Figure 2). It is therefore possible that agricultural intensification could generate an extensive agricultural surplus that could be diverted into biofuels without affecting local food security. However, caution must be used in ensuring families negatively affected by biofuel expansion are able to benefit in meaningful ways.

Table 9 Rough estimates on land needed to meet five per cent (two per cent for South Africa) biofuel targets and total fuel needs (based on von Maltitz and Brent 2008)

	Botswana	Namibia	Tanzania	S. Africa	Mozambique	Zambia
Diesel use in l/yr x 10^6	281	445	667	7987	381	327
Petrol use in l/yr x 10^6	301	325	202	10 289	107	210
Percent of total land needed to meet transport fuel needs	0.9	0.9	1.2	14.6	0.8	0.8
Land needed to meet biofuel targets in ha	26 078	38 917	53 855	307 375	30 631	56 286
Estimates of jobs created to meet biofuel targets[2]	12 251	18 608	26 399	142 919	15 036	27 046
Estimates of jobs created to meet national fuel usage[2]	245 028	372 160	527 980	n/a	300 712	270 458

[1]All calculations based on sugarcane and jatropha as feedstock, as per Table 2. Values are not linked to specific country or growth conditions and assume suitable land is available.
[2]These figures are based on 0.5 jobs per hectare for biodiesel and 0.33 jobs per hectare for sugarcane, as used in Econergy 2008. Most would be low-paying labourer jobs.

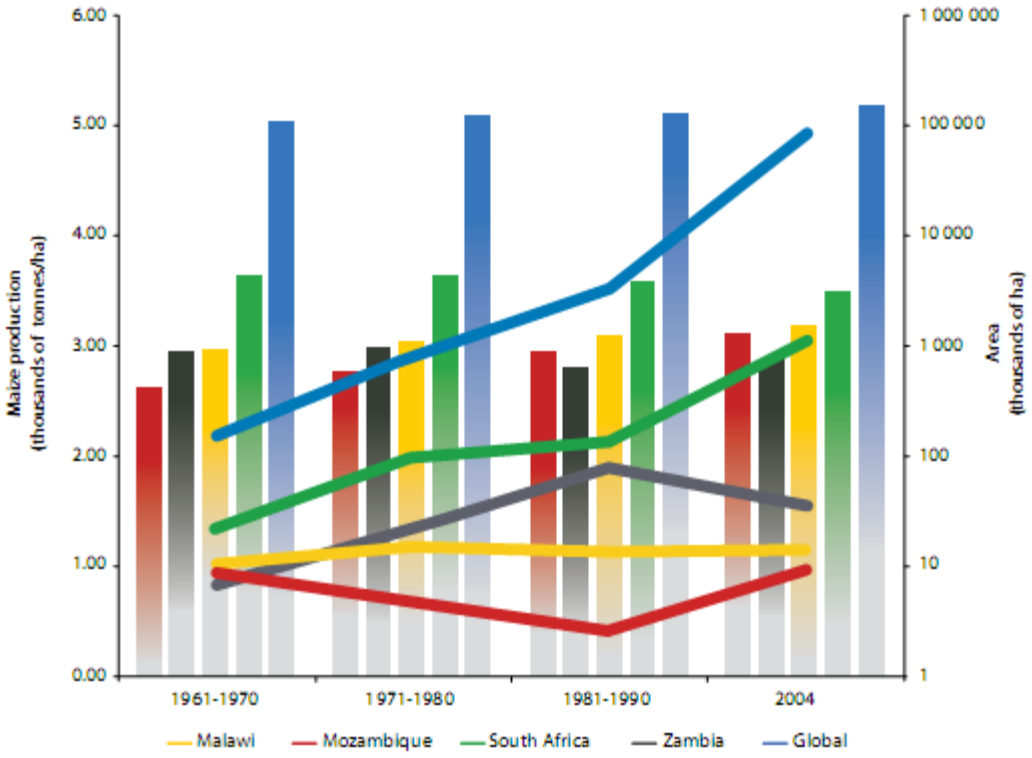

Figure 2 Maize productivity in some Africa countries
Source: von Maltitz et al. (2009)

Second-generation biofuels would have even greater benefits as they achieve significant 'wellto-wheel' reductions in greenhouse gas (GHG) emissions and require dramatically less land when compared with first-generation biofuels. This is because most biomass, including many organic wastes, can be used as feedstock. Additionally, second-generation biofuels perform better as internal combustion (IC) engine fuels, as they do not have any of the

technical problems of degradation and material incompatibility associated with first-generation biofuels (DTI 2006).

Social Consideration

Globally, the most serious concerns about biofuel expansion focus on the potential impact on global food prices and thereby poverty (Eide 2008; Royal Society, 2007). At the global level, the immediate net effect of higher food prices on food security is likely to be negative (FAO, 2008). Although sub-Saharan African countries are feeling the pinch from rising food prices, biofuel production at regional and national levels need not diminish regional food security. It has been suggested that biofuel production may help stabilise agricultural food production by giving farmers assured markets for their surpluses, stimulating changes in food aid policies and stabilising agricultural production (von Maltitz and Brent 2008; Haywood *et al.*, 2008). A Food and Agricultural Organisation report (2008) states that while higher agricultural prices could revitalise the role of agriculture as an engine of economic growth over the medium- to long-term, urban residents and the large number of net food buyers in rural areas are likely to be negatively affected, with the poorest households the most affected. Other sources provide evidence for localised food insecurity where land has been converted from smallholder agriculture to commercially produced biofuels (ABN, 2007). Depending on the global market prices of biofuels, and the feedstock and production model (and therefore the net area of agricultural land diverted from food to fuel), such impacts could play out at the national level through reduced food self-sufficiency at household or national levels.

Land Dispossession

Dispossession of land or resources is another key potential concern in sub-Saharan Africa. Most available land is communal and governed by customary law. Communal land users do not have secured individual tenure to the land's resources. Large-scale biofuel plantations may displace current land users. Where land is governed by a chief or traditional authority, economic benefits to the traditional authority or community as a whole may well overrule existing resource use rights enjoyed by individual members. Caution must be used, however, given increasing evidence that local or customary leaders do not always act in the community's best interest when there are personal benefits to be gained (Brockington 2007; Oyono *et al.*, 2006). Conversion of land for new uses must be based on adequate prior information as well as representative consultation.

Gender Inequalities

Women make up most of Africa's agricultural workforce as they are responsible primarily for growing food crops in rural areas whereas men are responsible for cash-generating crops such

as cotton and tobacco. Even though women play the prominent role in agriculture, there is much inequality. From an African perspective this inequality stems from traditional socio-cultural roles, and results in women being denied equal access to means of production such as land, credit, appropriate technology and extension services. It is anticipated that in small-scale production, the emerging biofuel industry will have the greatest labour impacts on rural women. Converting land used by women predominantly for food crops to growing energy cash crops instead might cause the partial or total displacement of women's food-growing activities towards increasingly marginal land or divert their labour towards activities whose proceeds they have less access to or control over. This would undermine the ability of women to ensure a secure food supply to feed their families (Kajoba, 2002; Rossi and Lambrou, 2008). In addition, if land traditionally used by women is switched to energy crops, women may then be marginalized in household decision-making about agricultural activities because they control less land.

Disease

HIV/AIDS is another serious challenge to agricultural development and, in turn, sustainable biofuel production. HIV/AIDS tends to affect the most productive age group and is characterized by repeated periods of illness. This affects the available agricultural workforce and increases medical expenditure. The extent and severity of HIV/AIDS impacts are most pronounced where periods of sickness or death coincide with peak agricultural seasons. If Africa is to be a global biofuel player, it needs to develop and implement robust policy response options to promote equal opportunities for women and men within the context of HIV/AIDS. This applies particularly to access to food and resources such as assets, capital, technology, agriculture and rural development services, as well as employment opportunities and decision making processes.

Financial Viability

The factors and criteria affecting biofuels' economic/financial viability are national and local in their scope and specifics. Factors include: (a) the cost of biomass materials, which varies depending on land availability, agricultural productivity, labour costs, etc; (b) biofuel production costs, which depend on the plant location, size and technology; (c) fossil fuel costs in individual countries, which depend on fluctuating global petroleum prices and domestic refining characteristics; and, (d) the strategic benefit of substituting imported petroleum with domestic resources. The economics of biofuel production and use will therefore depend upon the specific country and project situation (Thomas and Kwong 2001).

Biofuel production is often a high up-front cost venture, and many programs require government support in the initial start-up phases. Access to affordable financing is a major constraint. Traditional banks are unwilling to provide financing due to market uncertainties and perceived high risks. Investors and financiers have limited data and information on which to base sound judgments and decisions. Biofuels require a ready market both locally and internationally to guarantee economic viability. Reliable and competitive markets are not yet fully developed in Africa, and the continent has limited access to international biofuel markets. Market prices for feedstock and fossil fuels largely determine biofuel competitiveness. Given that these prices are highly volatile, investing in biofuel requires closer examination of the longterm market potential and other determinants to minimise the risks. This is particularly important for smallholders, who have limited capacity to weather failed investments. Investors need the security of markets and if the market is to be national, then they may need the assurance of mandatory blending with petroleum products. Economies of scale are also crucial, as is having the knowledge and capacity to select the appropriate feedstock and technology. Lessons can be learned from economic analyses undertaken for selected feedstocks in various countries. This means that the users of renewable energy technologies, and the suppliers of these systems, must all see a financial benefit. This will enable the optimum growth of renewable energy markets; otherwise, renewable energy will always depend on external finance, grants and short-term policy obligations. For smallholders, evidence suggests that an outgrower approach will generate greater returns to poor people than a more capital-intensive plantation approach due to the greater use of unskilled labour and accrual of land rents to smallholders (Arndt et al. 2008).

In all, links between biofuels and sustainable development are varied and complex. On the one hand, biofuels may imply improved energy security, economic gains, rural development, greater energy efficiency and reduced GHG emissions compared to standard fuels. On the other hand, production of energy crops could result in the expansion of the agricultural frontier, deforestation, monocropping, water pollution, food security problems, poor labour conditions and unfair distribution of the benefits along the value chain. The positive impacts and trade-offs involved vary depending on the type of energy crop, cultivation method, conversion technology and country or region under consideration.

Conclusion

Our conclusion that biofuels are potential substitute for fossil fuels is a future prediction. There exist a number of sustainability issues that need to be resolved. Questions often raised include:

'How much land is required to meet current policy targets?'; 'What volume of biofuels can be produced globally, regionally and nationally?'; and 'What implications will biofuels have on land use and local livelihoods?' Establishing accurate answers to these questions is difficult because they are dependent on a number of interacting scientific, social, environmental and economic factors such as the yield of the feedstock, the conversion efficiency, the location of the end user and the type of end use. Hence, where land is available, it is important to ascertain that biofuels are the most appropriate land use and will provide greater benefits to the current land users and owners.

References

Achten, W. M. J., Verchot, L., Franken, Y. J., Mathijs, E., Singh, V. P., Aerts, R. and Muys, B. (2008). Jatropha biodiesel production and use. Biomass and Bioenergy 32 (12): 1063-1084.

Bugaje, I. M. (2010). Global Energy Crisis – **The Untapped Opportunities for** Commercial Agriculture **and Biofuel Development in** Sub-Saharan Africa. Paper for presentation at the African Rural and Agricultural Credit Association (AFRACA) Fourth Agribanks Forum, co-hosted by the Central Bank of Nigeria, and holding at Sheraton Hotel and Towers, Abuja, May 5-7, 2010.

Bugaje, I. M. and Mohammed, I. A. (2008) Biofuels Production Technology. Publisher - Science and Technology Forum, Nigeria. ISBN: 978-057-061-8.

Coelho, S. T. (2005). 'Biofuels – advantages and trade barriers' prepared for the united nations conference on trade and development, February.

Department of Minerals and Energy 2007. Biofuel industrial strategy of the Republic of South Africa. The Republic of South Africa. http:// www.dme.gov.za.

DTI (2006). Second generation transport biofuels: A mission to the Netherlands, Germany and Finland. Global Watch Mission Report, UK.

Determination of Phase Equilibria and Construction of Closed Phase Equilibria Diagrams for Quaternary Na, K//SO4, B4O7−H2O and KCl−K2SO4−K2B4O7−H2O Systems at 25°C by Means of Translation Method

Sherali Tursunbadalov

Department of Chemistry, Faculty of Natural and Applied Sciences, Nile University of Nigeria, Plot 681, Cadastral Zone C-OO, Research & Institution Area, FCT Abuja, Nigeria,

+234 805 069 21 18, s.tursunbadalov@nileuniversity.edu.ng

Abstract

The phase equilibria in the two quaternary Na,K//SO_4,B_4O_7−H_2O and KCl−K_2SO_4−$K_2B_4O_7$−H_2O systems at 25°C were investigated by means of translation method. There are 3 points saturated with 3 solid phases, 7 curves saturated with 2 solid phases and 5 fields saturated with 1 solid phase in the Na, K//SO_4, B_4O_7−H_2O system. The quaternary KCl−K_2SO_4−$K_2B_4O_7$−H_2O system contains only one invariant point saturated with 3 different solid phases and 3 monovariant curves saturated with 2 different solid phases. Closed phase equilibria diagrams for both of the systems were constructed by means of translation method on the basis of obtained data.

Introduction

The two quaternary Na,K//SO_4,B_4O_7−H_2O and KCl−K_2SO_4−$K_2B_4O_7$−H_2O systems are the subsystem of the more complex quinary Na,K//Cl, SO_4, B_4O_7-H_2O system whose phase equilibria data facilitates extraction of solid phases from the natural brines and industrial wastes containing sulfates, chlorides and borates of sodium and potassium at the isotherm of 25°C.
Experimental determination of phase equilibria in quaternary systems is a tedious work which requires considerable amount of time, large amounts of analytical chemicals and relevant workforce, while preliminary prediction of phase equilibria in systems by means of translation method provides roadmaps which facilitates further comprehension of the phase equilibria and exploitation of the resources. The translation method which is explained in more details in literature[1] obeys the three main principles of the physicochemical analysis consistency, continuity and compatibility principles and derived from the third compatibility principle[2].
This work presents the results of determination of phase equilibria and construction of closed phase equilibria diagrams for the two quaternary Na,K//SO_4,B_4O_7−H_2O and KCl−K_2SO_4−$K_2B_4O_7$−H_2O systems at 25°C by means of translation method. The method which has already proven its advantages was used in determination of phase equilibria in several multicomponent water-salt systems[3-5].

Methodology

The main operation of the method is the determination of the invariant points on the overall (n+1)-component system by the techniques of the method that ensure the formation of the rest

of the geometrical figures namely the curves, fields and volumes etc. of the overall composition. There are three main techniques of the method used for the determination of the invariant points of the overall composition:

i. Determination of the invariant points of (n+1)-component system which are generated by the simultaneous translation that is extension of invariant points of the relevant n-component subsystems. This technique allows extension of two and three different curves from different subsystems depending on the solid phase composition of the overall system.

ii. Determination of composition of invariant points of (n+1)-component system generated from unilateral extension of points of n-component subsystems into the overall composition. This technique allows the extension of the invariant points of the subsystems that are not extended along with other points simultaneously.

iii. Determination of the intermediate points that enclose the curves and the fields of the overall (n+1)-component composition which are formed from the two initial techniques. The intermediate points form at the intersection point of the curves of overall composition that are not linked with each other.

Points, curves and fields of the n-component subsystems transform into the curves, fields and volumes of the overall (n+1)-component system respectively when the subsystems enter into the composition of the overall system. Because the method fully obeys the Gibbs' phase rule, the intersection and linkage of the generated curves by extension of the invariant points along with the ones extending between them, take place in consistence with the reduced Gibbs' phase rule for the isothermal-isobaric processes.

Consequently by the determination of phase equilibria by means of translation method; closed phase equilibria diagrams for quaternary systems and total phase equilibria diagrams for quinary and higher component systems are obtained that can be used in utilization of the complex natural resources.

The phase equilibria in quaternary systems are determined on the basis of data on relevant ternary subsystem. For the determination of phase equilibria in the quaternary $Na,K//SO_4,B_4O_7–H_2O$ and $KCl–K_2SO_4–K_2B_4O_7–H_2O$ systems at 25°C the available data in relevant ternary subsystems were used[6].

Prediction of phase equilibria and construction of quaternary phase equilibria diagrams

The quaternary Na, K// SO_4, B_4O_7 −H_2O system at 25°C

The quaternary $Na,K//SO_4,B_4O_7–H_2O$ system is composed of four $Na_2SO_4–K_2SO_4–H_2O$, $Na_2B_4O_7–K_2B_4O_7–H_2O$, $Na_2SO_4–Na_2B_4O_7–H_2O$ and $K_2SO_4–K_2B_4O_7–H_2O$ ternary subsystems

There are 5 solid K_2SO_4 – arcanite (KS), $K_2B_4O_7·4H_2O$–(KB4), $Na_2B_4O_7·10H_2O$–(NB10), $Na_2SO_4·10H_2O$–(S10) and $Na_2SO_4·3K_2SO_4$–(GS) phases in equilibrium in the

Na,K//SO_4,B_4O_7–H_2O system at 25°C. All of the four listed ternary subsystems of the quaternary Na,K//SO_4,B_4O_7–H_2O system are well investigated by means of solubility method[6]. The Table 1 shows the list of invariant points at the ternary subsystems of the quaternary Na,K//SO_4,B_4O_7–H_2O system along with their relevant equilibrium solid phases.

Table 1. Ternary invariant points and relevant equilibrium solid phases in the quaternary Na, K//SO_4, B_4O_7–H_2O system at 25°C[6]

Ternary Subsystem	Invariant Point	Equilibrium Solid Phases
Na_2SO_4–K_2SO_4–H_2O	E_1^3	S10 + GS
	E_2^3	GS + KS
$Na_2B_4O_7$–$K_2B_4O_7$–H_2O	E_5^3	KB4 + NB10
Na_2SO_4–$Na_2B_4O_7$–H_2O	E_3^3	S10 + NB10
K_2SO_4–$K_2B_4O_7$–H_2O	E_4^3	KS + KB4

The capital letter E, whose; subscript shows the serial number and superscript shows the complexity of the relevant systems denote the invariant points throughout this work. The extension of points as quaternary curves is indicated by arrows whose directions show the direction of the extension of the generated curves. Because the curves formed from the latter extension and the curves that extend between the determined quaternary points vary from each other they are represented by arrows and solid curves respectively.

The Figure 1 shows set of ternary phase equilibria diagrams arranged on an unfolded prism that reflects the ternary composition of the quaternary Na,K//SO_4,B_4O_7–H_2O system. The diagram in Figure 1 is constructed on the basis of the data in Table 1. Three of the ternary subsystems contain one invariant point saturated with two different solid phases each, while the fourth ternary Na_2SO_4–K_2SO_4–H_2O system includes two invariant points.

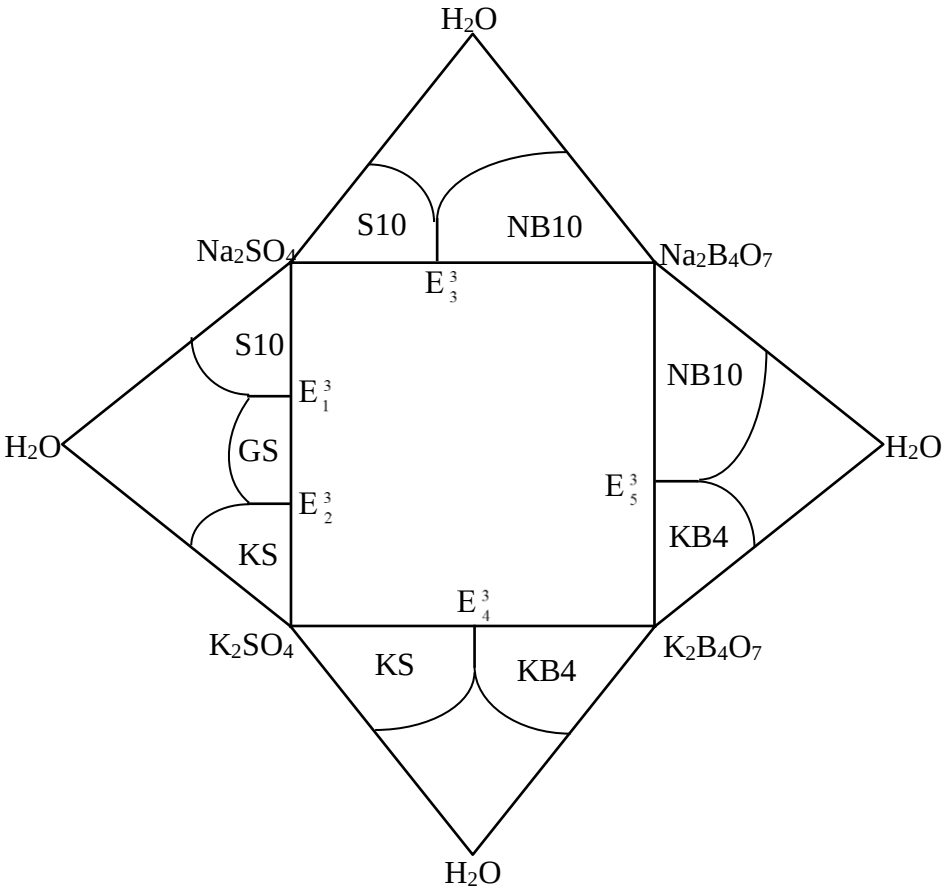

Figure 1. Unfolded prism reflecting the ternary composition of the quaternary Na, K//SO_4, B_4O_7–H_2O system at 25°C

The Figure 2 shows the schematic phase equilibria diagram of the system obtained by folding the prism in Figure 1. The extensions of the ternary invariant points as the quaternary monovariant curves into the quaternary composition are shown with arrows whose directions are shown by the direction of the arrow. Two quaternary points in equations (1) and (2) are generated as a result of extension of 2 ternary invariant points, while the third point in the system is generated as independent translation of the ternary E_2^3 point. The $Na_2B_4O_7{\cdot}10H_2O$ phase completes the composition of the quaternary point generated from extension of the latter E_2^3 point as given in equation (3).

$$E_1^3 + E_3^3 \rightarrow E_1^4 = S10 + NB10 + GS \quad (1)$$

$$E_5^3 + E_4^3 \rightarrow E_3^4 = NB10 + KS + KB4 \quad (2)$$

$$E_2^3 + NB10 \rightarrow E_2^5 = GS + KS + NB10 \quad (3)$$

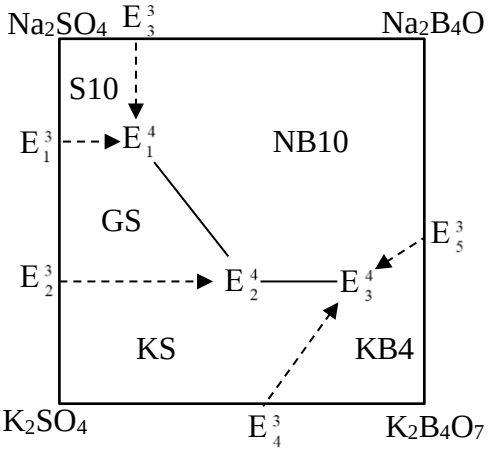

Figure 2. Schematic phase equilibria diagram of the quaternary Na, K//SO_4, B_4O_7–H_2O system at 25ºC constructed by translation method[7].

The quaternary KCl–K_2SO_4–$K_2B_4O_7$–H_2O system at 25°C

The quaternary KCl–K_2SO_4–$K_2B_4O_7$–H_2O system is composed of three ternary KCl–K_2SO_4–H_2O, K_2SO_4–$K_2B_4O_7$–H_2O and KCl– $K_2B_4O_7$–H_2O subsystems which are well investigated by the solubility method at 25ºC[6]. There are three solid K_2SO_4 – arcanite (KS), $K_2B_4O_7 \cdot 4H_2O$–(KB4), and KCl–(KC) phases in equilibrium in the KCl–K_2SO_4–$K_2B_4O_7$–H_2O system at 25ºC and each ternary subsystem includes one invariant point saturated with the relevant solid phases given in Table 2. Every ternary invariant point in Table 2 is saturated with two different solid phases along with a liquid phase in equilibrium.

Table 2. Ternary invariant points and relevant equilibrium solid phases in quaternary $KCl–K_2SO_4–K_2B_4O_7–H_2O$ system at 25°C[6]

Ternary Subsystem	Invariant Point	Equilibrium Solid Phases
$KCl–K_2SO_4– H_2O$	E_1^3	KC + KS
$K_2SO_4–K_2B_4O_7–H_2O$	E_2^3	KS + KB4
$KCl– K_2B_4O_7–H_2O$	E_3^3	KC + KB4

The unfolded prism in Figure 3 which is constructed on the basis of data in Table 2 shows the ternary composition of the quaternary $KCl–K_2SO_4–K_2B_4O_7–H_2O$ system at 25°C.

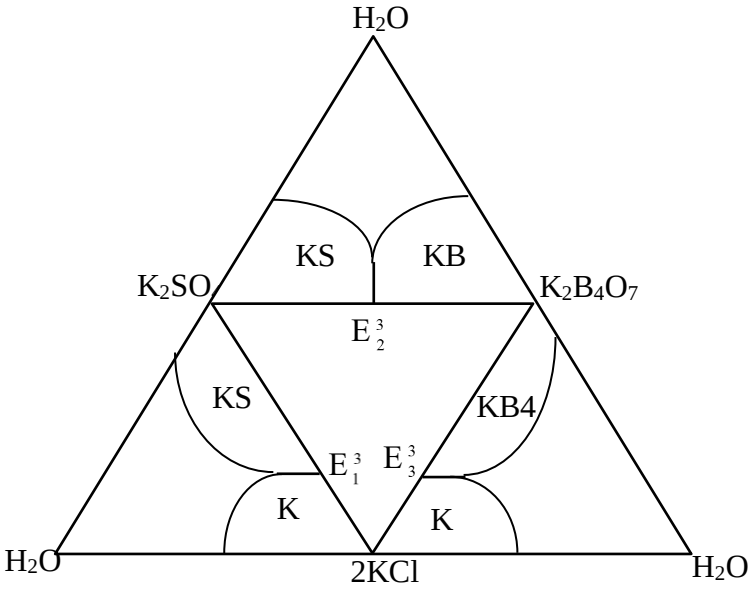

Figure 3. Unfolded prism reflecting the ternary composition of the quaternary $KCl–K_2SO_4–K_2B_4O_7–H_2O$ system at 25°C

The schematic phase equilibria diagram in Figure 4 is constructed by folding the prism in Figure 3. The arrows represent the monovariant curves formed as a result of transformation of the relevant ternary invariant points. The only one quaternary E_1^4 invariant point is generated from extension and intersection of the quaternary curves formed from the ternary invariant points. The equation (4) shows the generation of the latter quaternary invariant point along with its equilibrium solid phases from the combination of ternary invariant points.

$$E_1^3 + E_2^3 + E_3^3 \rightarrow E_1^4 = KS + KC + KB4 \quad (4)$$

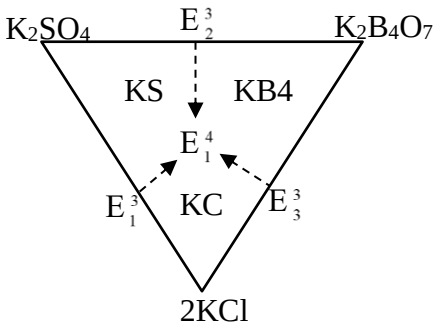

Figure 4. Schematic phase equilibria diagram of the quaternary KCl–K_2SO_4–$K_2B_4O_7$–H_2O system at 25°C constructed by translation method[7].

Results and discussion

In this section the constructed diagrams in the previous section will be simplified for better visualization and readability. The invariant points represented by E and the arrows that show the directions of the translation of the points as curves into the overall composition will be shown as the only intersection points of the relevant curves and the plain solid curves respectively. The Figure 5 and Figure 6 give the final version of the phase equilibria diagrams of the quaternary Na, K//SO_4, B_4O_7–H_2O and KCl–K_2SO_4–$K_2B_4O_7$–H_2O systems at 25°C. There are 3 points, 7 curves and 5 fields in the quaternary Na, K//SO_4, B_4O_7–H_2O system, while the quaternary KCl–K_2SO_4–$K_2B_4O_7$–H_2O system contains only 1 invariant point and 3 monovariant curves on the overall composition at 25°C.

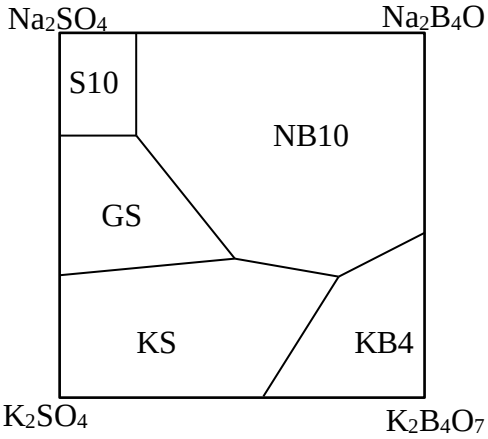

Figure 5. Final version of phase equilibria diagram of the quaternary Na, K//SO_4, B_4O_7–H_2O system at 25°C

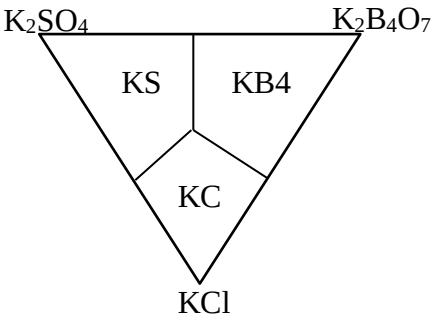

Figure 6. Final version of phase equilibria diagram of the quaternary KCl−K_2SO_4−$K_2B_4O_7$−H_2O system at 25°C.

Two of the curves in KCl−K_2SO_4−$K_2B_4O_7$−H_2O system have different history of formation than the other 5 curves in the system. They extend between the quaternary invariant points and 5 curves are generated from the extension of the ternary invariant points into the quaternary composition. All of the 3 curves in the KCl−K_2SO_4−$K_2B_4O_7$−H_2O system form as a result of extension of the relevant ternary points into the overall composition of the system.

The obtained results in this work guide tracking of crystallization and dissolution pathways in the investigated quaternary systems and can be used in utilization and comprehensive exploitation of the natural sources that contain chloride, sulfate and borates of the sodium and potassium[7]

Conclusions

There are three quaternary invariant points saturated with three different solid phases, seven monovariant curves saturated with two different solid phases and five divariant fields saturated with one solid phase in the Na, K//SO_4, B_4O_7−H_2O system at 25°C. Two of the curves have different nature of formation as they extend between the quaternary invariant points while the other five curves generate from the extension of the relevant ternary points into the overall quaternary composition of the system. The quaternary KCl−K_2SO_4−$K_2B_4O_7$−H_2O system 25°C is characterized to possess three monovariant curves saturated with two different solid phases and one invariant point saturated with three solid phases. All the three curves are generated from extension of the relevant ternary points into the overall quaternary composition of the system. The result obtained in this work will pave the way for further experimental investigation of the systems and guide crystallization and dissolution processes in the investigated systems.

References

1. Tursunbadalov, S., Soliev, L. (2016). Phase equilibria in multicomponent water−salt systems. *Journal of Chemical and Engineering Data*, 61, 2209−2220.
2. Goroshchenko,Y.G.: (1982) *The Centroid Method for Imaging Multicomponent Systems;* Naukova Dumka: Kiev [in Russian].

3. Tursunbadalov, S., Soliev, L. (2017). Crystallization and dissolution in multicomponent water−salt systems. *Journal of Chemical and Engineering Data*, 62, 3053−3063.
4. Soliev, L.; Tursunbadalov, Sh. (2008). Phase equilibria in the Na,K//SO_4,CO_3,HCO_3−H_2O system at 25 °C. *Russian Journal of Inorganic Chemistry*, 53, 805−811.
5. Soliev, L.; Tursunbadalov, Sh. (2010). Phase equilibria in the Na,K//SO_4,CO_3,HCO_3−H_2O system at 0°C. *Russian Journal of Inorganic Chemistry*, 55, 1295−1300.
6. Zdanovskiy, A.B.; Soloveva, E.F.; Lyakhovskaya, E.I.; Shestakov, N.E.; Shleymovich, R.E.; Abutkova, A.B.; Cheromnikh, L.M.; Kulikova, T.A. *Handbook of experimental data on solubility of multicomponent water-salt systems*, Vol. I. Khimizdat: Saint Petersburg, **2003** [in Russian].
7. Tursunbadalov, S., Soliev, L. (2017). Determination of Phase equilibria and Construction of Phase Diagram For the Quinary Na,K//Cl, SO_4, B_4O_7-H_2O system at 25°C. *Journal of Chemical and Engineering Data*, 62, 698−703.

Synthesis of Zirconium Oxide (Zro2) Supported Clay Catalyst and its Application in Biodiesel Production using Castor Oil (Ricinus communis)

Izuegbunam Chidiebere[1*] and Eterigho Elizabeth[2]

[1,2]Department of Chemical Engineering, Federal University of Technology, Minna, Nigeria

[1]chidosky4learning@gmail.com

*Corresponding Author

Abstract

Zirconia supported clay catalyst, a heterogeneous solid catalyst was produced by wet impregnation at different proportions of 1:2 and 1:1 tagged A and B respectively. The properties of the catalysts were characterized using Brunauer-Emmett-Teller (BET), Scanning Electron Microscopy (SEM), X-Ray Diffraction (XRD), Energy Dispersive X-ray (EDX), and Fourier Transform-Infrared Spectroscopy (FT-IR). The characterized catalysts showed improved and enhanced catalytic properties for reaction. The synthesized catalysts A and B were used for biodiesel production through Transesterification reaction using castor oil, at a reaction time of 3hr, temperature of 60^{o}C, catalyst loading of 2.5wt/wt% and methanol to oil ratio of 6:1. Both catalysts showed catalytic activity, however catalyst B had a better percentage yield of 91.4 % biodiesel as compared to that of catalyst A of 88.8% biodiesel.

Keywords: Catalyst, Castor Oil, Biodiesel, Transesterification, Zirconia

Introduction

For several decades, energy crisis have being confronting the world due to the excessive utilization of the world's depleting oil reserves by the ever-increasing human population. The world's economy is largely dependent on the transportation of goods and services, while transportation itselfisdependent on energy from petroleum. In fact, the transportation sector is 96% dependent on fossil fuels with an annual worldwide fuel consumption of 62% (Yahaya *et al.*, 2014). This is despite other sources of energy such as coal, natural gas, hydroelectricity and nuclear power. Apart from the ever-increasing prices of petroleum fuels, more worrying issues associated with utilizing these fuels include health standards and environmental degradations. These concerns have led to the search for sustainable alternatives; biofuel (Yahaya *et al.*, 2014).

Generally, biodiesel is mainly produced by Transesterification process. Transesterification is the reaction of lipid with an alcohol in the presence of a catalyst to form esters and a by-product; glycerol. It is, in principle, the action of one alcohol displacing another from an ester, referred to as alcoholysis (cleavage by an alcohol) (Eterigho *et al.*, 2017). In transesterification

mechanism, the carbonyl carbon of the starting ester ($RCOOR^1$) undergoes nucleophilic attack by the incoming alkoxide (R^2O^-) to give a tetrahedral intermediate, which either reverts to the starting material, or proceeds to the transesterified product ($RCOOR^2$). Transesterification consists of a sequence of three consecutive reversible reactions. The first step is the conversion of triglycerides to diglycerides, followed by the conversion of diglycerides to monoglycerides, and finally monoglycerides into glycerol, yielding one ester molecule from each glyceride at each step (Deepak *et al.*, 2016). Feedstocks for biodiesel production can be classified into edible and non-edible oils. Examples of the edible oils are soybean, corn and canola. Non-edible oils such as animal fats, castor oil, jatropha curcas, and waste oils such as yellow grease and soybean soap stock have been used in the production of biodiesel. Results have shown that these sources serve as good replacement for diesel.

There are basically two types of catalysts that are used in the production of biodiesel namely homogenous and heterogeneous catalysts (Hilary, 2013).Homogenous and heterogeneous catalysts have their unique differences in terms of advantages and disadvantages. The advantages of heterogeneous catalysts include but not limited to non-corrosiveness, environmental benign, ability to catalyze esterification and transesterification reaction simultaneously (Hilary, 2013),and can be recycled. However, the disadvantages are: high reaction temperature, pressure and more process time as they have low micro porosity and therefore, low diffusion limitation.

Clays have attracted increasing interest due to their application as heterogeneous catalysts in both gas and liquid systems; their innate surface acidity play an important role in many reactions (Fatimah, 2014). Clay's structure collapses at high temperatures and must be stabilized (Egi *et al.,* 2012). Kaolinite is a clay mineral material of an industrial kaolin group; it is the principal clay mineral substance existing in kaolin mineral group (Olu *et al*., 2017). Kaolinite clay is the most essential and useful kaolin used industrially in term of clay that consist of primarily minerals with properties variation that is amenable; hence making it very useful for various industrial applications. The chemical compositions of kaolinite clay varies from colocations in term of the ratio of alumina : silica and the degree of purity (Olu *et al*., 2017). Zirconium dioxide presents considerable interest in the field of heterogeneous catalysis, due to its original acid–base and redox properties. Zirconia (ZrO_2) finds extensive use as a ceramic material, it also has important applications in catalysis. Due to its unique chemical properties (i.e., surface acidity and basicity), it is a valuable catalyst for reactions involving elimination, dehydration, hydrogenation, and oxidation (Mohammed *et al.*, 2014). Zirconia has

great contribution towards catalysts' activity improvement in the production of biodiesel (Eterigho *et al.*, 2017).

Methodology

The raw clay was obtained from Enhandiagu, Enugu State while the castor oil was obtained from NARICT (National Research Institute for Chemical Technology). Zirconium Oxochloride was obtained from Panlac Chemicals.

Sample Preparation and Pre-treatment

The clay was sieved using 250 µm mesh sieve. 300 g of the clay was suspended in a 1000 cm^3beaker containing distilled water for 6 hours. Moore and Reynolds technique of soil minerals purification was utilised to treat the clay in order to remove any organic particles left in the clay(Moore and Reynolds, 1998; Olu *et al*., 2017). This method involves the treatment of the sample with 30 % hydrogen peroxide solution until all effervescence stopped. The pre-treated clay was allowed to stay overnight after which the supernatant was decanted. The slurry was oven dried at 100^oC for 24 hr.

Chemical Modification of Clay

200 g of the clay sample was added to 1.0 L of 0.50 mol/L of hydrochloric (HCl) acid and thoroughly mixed using magnetic stirrer for 4 hours at 300 rpm. The mixture was centrifuged for 20 minute at 1000 rpm. This was washed with distilled water to remove any trace of Cl^- ions, and was dried at of 100^oC for 24 hr.

Zirconium Synthesis.

According to Eterigho *et al*. (2011) and Hasanudin (2016), $Zr(OH)_4$ catalyst was prepared by dissolving $ZrOCl_2 \cdot 8H_2O$ into demineralized water followed by hydrolysis with addition of NaOH to form $Zr(OH)_4$ gels at a pH of 10. The resulting zirconium hydroxide was washed thoroughly to remove Cl^- ions from the gels. This was confirmed by argentometric titration of the solution using potassium chromate (K_2CrO_4) as an indicator, filtered and dried in an oven at 100^oC for 24 hours.

Preparation of Zirconium Supported Clay Catalyst

The zirconia was impregnated by introducing it into the modified clay and allowed to age at room temperature for 18hr. This was dried in an oven at 120°C for 24 hours. Finally, the solid was calcined in a muffle furnace at 600°C for 5hr to obtain zirconia-clay catalyst. (Eterihgo *et al*., 2017).

Characterization of Catalyst

The prepared catalysts were characterized using Fourier Transform Infrared Spectroscopy (FTIR), X-ray Diffraction (XRD), Brunauer-Emmet-Teller (BET), Scanning Electron Microscopy (SEM) and Energy Dispersive X-ray (EDX).

Characterization of Castor Oil

The castor oil was characterized for its specific gravity, density, flash point, kinematic viscosity, acid value, iodine value, moisture or water content and free fatty acid (FFA). Determinations of these properties were carried out using the experimental description reported by the American Standards and Testing Materials (ASTM).

Transesterification of Castor Oil

The Transesterification reaction of the castor oil was carried out using the synthesised A and B catalysts. The catalyst was placed in a 250 cm^3 round bottom flask withmethanol to oil molar ratio of 6:1, catalyst loading 2.5 wt/wt %, at a reaction time of 3hr and temperature of 60°C, under constant stirring. After completion of the reaction, the products were allowed to settle overnight in a separating funnel and the biodiesel was sequestrated and washed (Nurdin *et al.*, 2015; Yacob *et al.*, 2017).

Results and Discussion

Catalyst Characterization

The results of the characterization of the synthesized catalysts (zirconia supported clay catalyst) areas presented in Table 1 indicating their surface area, functional group, its surface morphology and its crystallinity.

Brunauer-Emmet-Teller (BET) Analysis

Table 4.1: BET Analysis for Catalyst A and Catalyst B

Sample	**Surface area (m^2/g)**	**Pore volume (cc/g)**	**Pore size (nm)**
Catalyst A	360.526	0.2300	2.433
Catalyst B	360.526	0.2300	2.433

The BET analysis of both catalyst A and B produced no appreciable difference in their surface area, pore volume and pore size. It also showed that the surface area, pore volume and pore size of the synthesised catalysts was greatly improved, seeing that there was great improvement

from the known surface area of zirconia (120m^2/g) as reported by Dominik and Reinhard (2002).

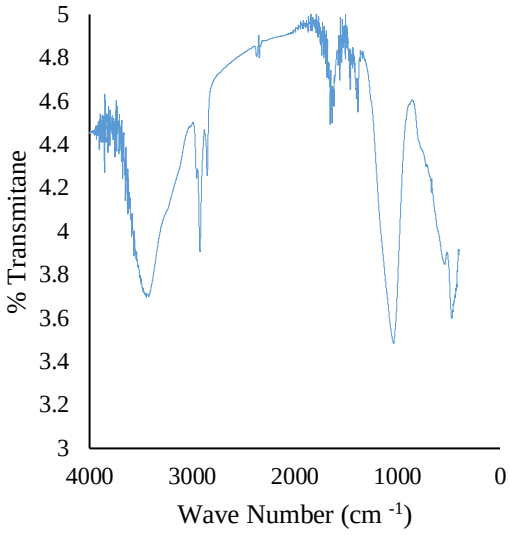

Figure 4.1: FTIR Spectra of Catalyst A

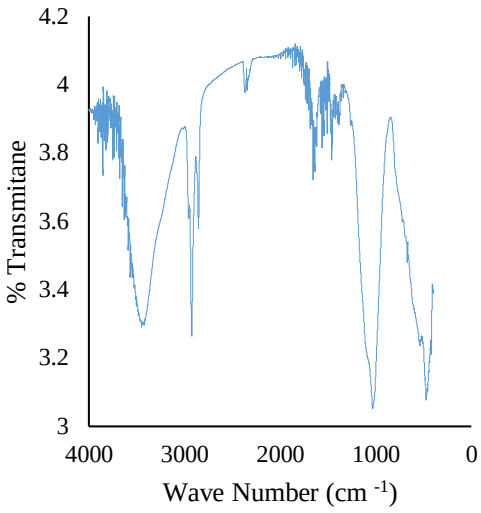

Figure 4.2: FTIR Spectra of Catalyst B

The observed FTIR absorption peak at about 457 cm^{-1} regions is due to the presence of Zr–O vibration, which confirms the formation of ZrO_2 structure, the prominent peaks observed at 1019 cm^{-1} is attributed to the presence of O–H bonding. The peaks observed at 1558 cm^{-1} are due to presence of adsorbed moisture in the sample and the presence of peaks at 3425–3495 cm^{-1} could be due to the stretching of O–H groups which is a characteristic of a highly hydrated compound (Singh and Umesh, 2014). The similarity in the FTIR spectra of both catalyst A and B reveals that both catalysts have the same functional groups. However, the peak intensity of catalyst B are higher as such indicating the presence of more zirconia in catalyst B as confirmed by its impregnation ratio of 1:1 when compared with catalyst A with an impregnation ratio of 1:2.

4.2.3 Scanning Electron Microscopy (SEM)

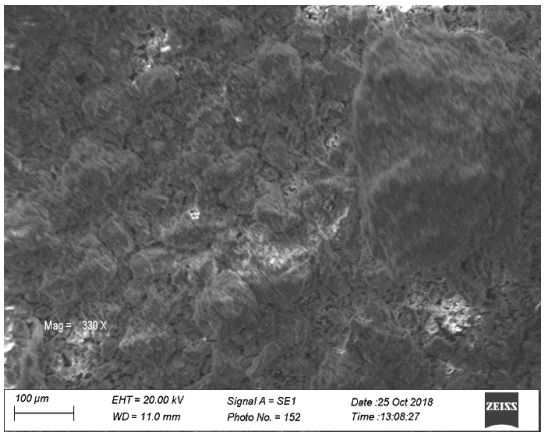

a

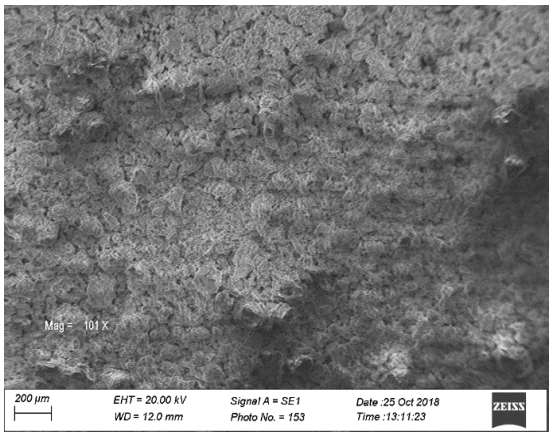

(d)

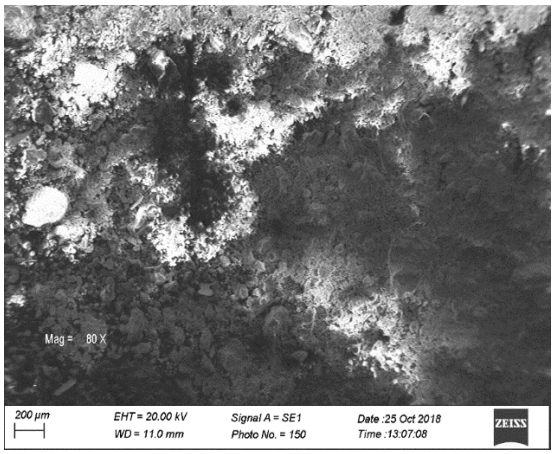

b

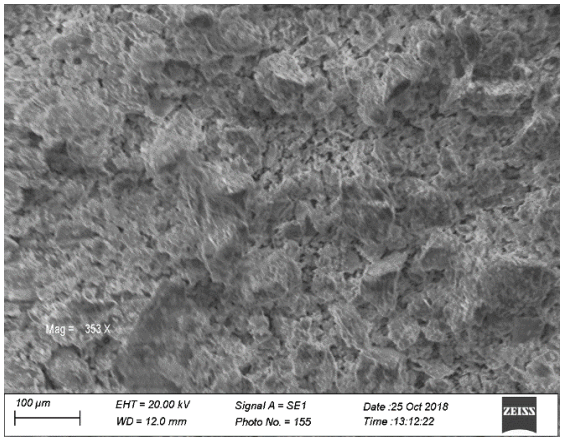

(e)

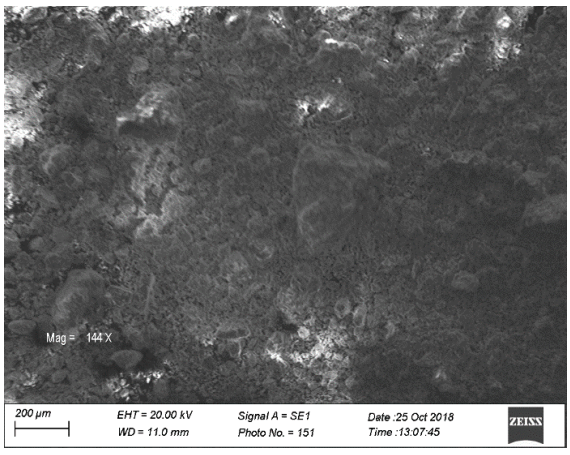

c

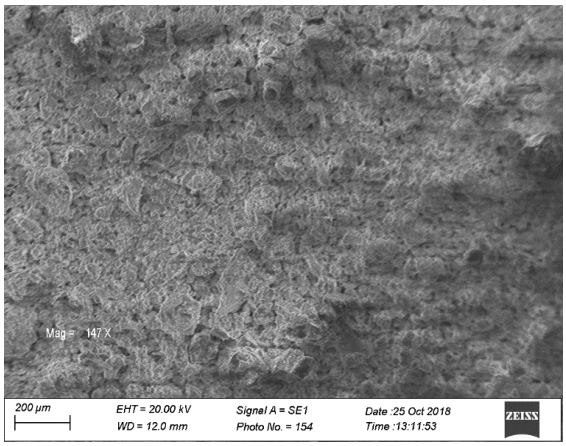

(f)

Figure 4.3: SEM micrograph of Catalyst A (a, b and c) and Catalyst B (d, e and f)

Both SEM micrographs of catalyst A and B exhibited well-shaped particles that are crystalline in shape which is as that reported by Eshed*et al.,(* 2011) and Omar*et al.*,(2011). However, a

closer look at the SEM micrographs of catalyst A and B reveals the presence of more well-shaped spherical particles in catalyst B and this can be attributed to the fact that there is a higher ratio of ZrO_2 in catalyst B.

Table 4.2: Elemental Weight Composition of Catalyst A (EDX)

Element	Atomic %	Weight %
Al	26.53	19.27
Si	51.05	38.59
Zr	13.39	32.88
S	1.23	1.06
K	7.80	8.21

Table 4.3: Elemental Weight Composition of Catalyst B (EDX)

Element	Atomic %	Weight %
Al	22.40	13.98
Si	47.62	30.94
Zr	23.18	48.92
S	-	-
K	6.80	6.15

The Energy Dispersive X-ray (EDX) of both catalysts (A and B) reveals the presence of several elements. The Energy Dispersive X-ray (EDX) confirmed the presence of zirconium in the both catalysts. However, the Energy Dispersive X-ray (EDX) shows that twice as much zirconium in catalyst B as there is in catalyst A which is as a result of the ratio of impregnation. It also reveals the presence of other compounds like Al, Si, K, and S for both catalysts with the exception of sulphur that was not present in catalyst B. Catalyst A show more presence of silica and alumina than that of catalyst B which might be as a result of the clay content/dosage ratio. Whereas the presence of potassium and sulphur are more in catalyst A which is impurities associated with clay.

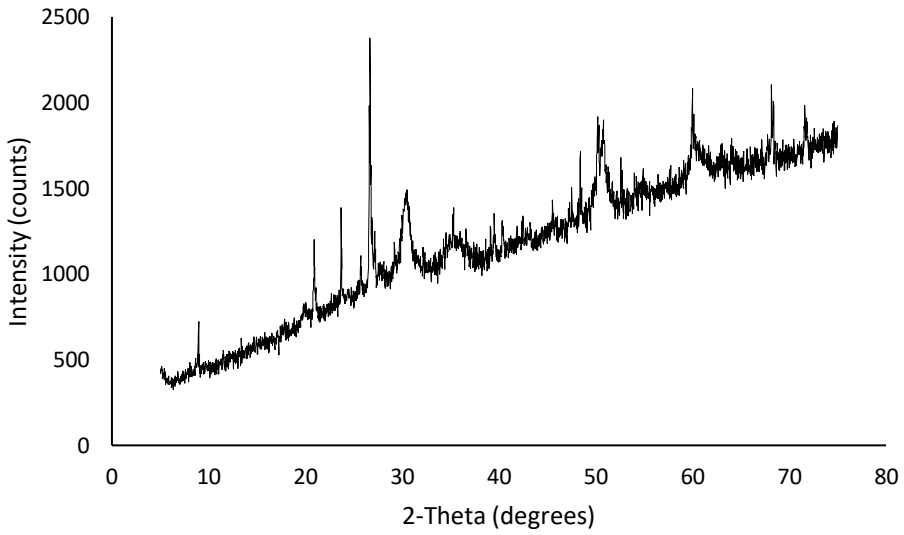

Figure 4.6: X-ray Diffraction (XRD) analysis of Catalyst A

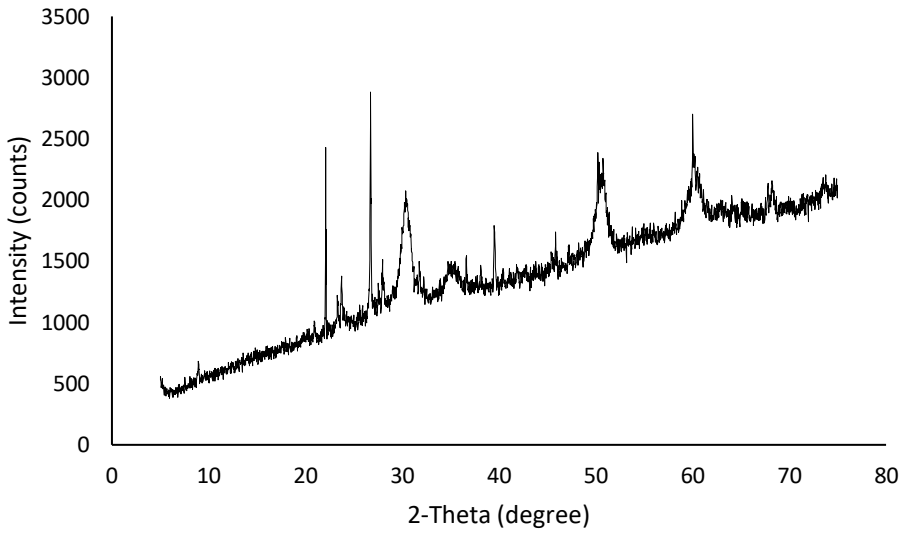

Figure 4.7: X-ray Diffraction (XRD) analysis of Catalyst B

The characteristic peaks at 2θ value obtained from the XRD diffractograms of both catalyst samples (A and B) at 22°, 28°, 30°, 50° and 60° are similar as the typical zirconia peaks reported by Sani*et al.,*\ (2011). The XRD patterns of the synthesized zirconium oxide catalyst (A and B) are also similar to that reported by Omar, *et al.* (2011) and Sani *et al.* (2011). Omar, *et al.* (2011) reported that the crystal structure of ZrO_2 remained the same because the crystalline structures of modified zirconia are the same with parent ZrO_2 in pattern. Both catalyst A and catalyst B exhibited predominantly peaks of similar monoclinic ZrO_2. The XRD diffractograms of both catalyst samples revealed a tetragonal-monoclinic phase transition. This is because the tetragonal peak at 2θ = 30°, 34° and 50° was prominent alongside those of the monoclinic phases. Where typical tetragonal phase of zirconia occurs at 2θ = 24°, 28°, 34°, and 50° (Omar, *et al.,* 2011; Sani, *et al.*, 2011).

Comparing the produced biodiesel with standard revealed that it conforms with standard as shown in Table 4.5.

Table 4.5: Comparism between Synthesized Biodiesel and Standard Biodiesel properties

Properties	**Units**	**Castor Oil Biodiesel using catalyst A**	**Castor Oil Biodiesel using catalyst B**	**ASTM D6751**
Density 40°C	g/cm^3	0.944	0.945	-

Kinematic Viscosity at 40°C	mm^2/s	5.3	4.7	1.9 – 6.0
Flash Point	-	138	162	130 min
Pour point	° C	-5	-8	-
Cetane Index	-	51	63	47 min
Cloud point	-	7 ° C	3 ° C	-
Iodine value	mg I/100g	87	83	-
Ester value	wt. %	99.4	169.12	-
pH Value	-	7.41	7.15	-
Biodiesel Yield	%	88.8	91.4	-

Conclusion

The characterization of both catalysts A and B showed the presence of more of zirconia in catalyst B than in catalyst A. This fact was corroborated by the FTIR analysis where higher peak intensities of catalyst B indicated the presence of a higher concentration of Zr–O vibration, which confirm the formation of ZrO_2 structure.

The use of chemically modified clay as support was very good as evident in the surface area of the synthesized catalysts where it showed the presence of silica which has good surface area helping to increase the surface area of the synthesized catalysts

In terms of biodiesel synthesis, catalyst B could be said to be better in the production of biodiesel as a yield of 91.4% was obtained as against a yield of 88.8% obtained when catalyst A was used. It was observed that the biodiesel produced using catalyst B showed a higher cetane number of 63 as against that of 51 when catalyst A was used. Other biodiesel properties such as flash point, kinematic viscosity at 40°C and the ester value are all favourably in terms of the use of catalyst B for biodiesel production.

References

Yacob, A.R Mahgoub, A. Saied, M. Muhammad, A. B.& Zaki, M. (2017).Acid Modified Jourdiqua Clay for Methanolysis of Castor Oil*; Journal of Pharmacovigilance*,DOI: 10.4172/2329-6887.1000240.

Dominik, E & Reinhard, K (2002). The Stoichiometry of Hydrogen Reduced Zirconia and Its Influence on Catalytic Activity.Part 1: Volumetric and Conductivity Studies. *Article in Physical Chemistry Chemical Physics*4, 795-801.www.researchgate.net/publication/ 236269387

Deepak, V., Janmit, R., Amit, P. & Manish, J. (2016).A Critical Review on Production of Biodiesel from Various Feedstocks. *Journal of Scientific and Innovative Research.* 5(2), 51-58.

Egi, A. Ghozali, M., Savitri & Wuryaningsih, S. R. (2012). Biodiesel Production of Jatropha Curcas Oil By Bentonite as Catalyst; *Proceeding of International Conference on Sustainable Energy Engineering and Application.* Inna Garuda Hotel, Yogyakarta, Indonesia. ISBN 978-602-18167-0-7.

Eshed, M. Pol, S. Gedanken, A. & Balasubramanian, M. (2011). Zirconium Nanoparticles Prepared by the Reduction of Zirconium Oxide Using The RAPET Method. Beilstein *Journal of Nanotechnology*, 2(1), 198 – 203

Eterigho, E. J. Farrow, T. S.& Ejejigbe, S. E. (2017). Sulphated Zirconia Catalyst Prepared From Solid Sulphates by Non-Aqueous Method: *Iranian Journal of energy & environment* 8(2): 142-146 doi: 10.5829/ijee.2017.08.02.07.

Eterigho**,** E.J. Lee, J. G. M. & Harvey, A. P. (2011). "Triglyceride Cracking for Biofuel Production Using a Directly Synthesised Sulphated Zirconia Catalyst", *Journal of Bioresource Technology*, 102(10), pp. 6313-6316. www.elsevier.com/locate/biortech

Fatimah, I. (2014). Preparation of ZrO_2/Al_2O_3-Montmorillonite Composite as Catalyst for Phenol Hydroxylation; *Journal of Advanced Research* 5, 663–670.

Hasanudin & Addy Rachmat 2017, Production of Biodiesel from Esterification of Oil Recovered from Palm Oil Mill Effluent (POME) Sludge using Tungstated-Zirconia Composite Catalyst; Indonesia *Journal of Fundamental and Applied Chemistry* idDOI: 10.24845/ijfac.v1.i2.42

Hasanudin, R. A. (2016). Production of Biodiesel from Esterification of Oil Recovered from Palm Oil Mill Effluent (POME) Sludge Using Tungsten – Zirconia Composite Catalyst

Hilary, R. (2013). "The Use of Thermally Modified Koalin as a Heterogeneous Catalyst for Producing Biodiesel" *Materials and Processes for Energy Communicating Current Research and Technological Developments* (A.Méndez Vilas, Ed.).

Mohammed, H. A. YongMan, C.& Allen, W. A. (2014). Preparation of Zirconium Oxide Powder Using Zirconium Carboxylate Precursors: *Advances in Physical Chemistry*. 8 http://dx.doi.org/10.1155/2014/429751.

Nurdin, S. Rosnan, N.A. Ghazali, N.S. Gimbun, J. Nour, A.H.& Haron, S.F. (2015). Economical Biodiesel Fuel Synthesis from Castor Oil using \Mussel Shell Base (MC – BS). *International Conference on Alternative Energy in Developing Countries and Emerging Economies.*79(2015),576 – 587.

Olu, S. C. Dim, P. E. Kovo, A. S. Okafor, J. O.& Izuegunam, C. I. (2017). Adsorption of Cr (VI) and Cu(II) ions Onto Kaolinite Clay.*International Journal of Recent Engineering Science.* 4(6) ISSN: 2349-7157

Omar, W.N. & Amin, N.A. (2011). Biodiesel Production from Waste Cooking Oil Over Alkaline Modified Zirconia Catalyst. *Fuel Processing Technology*, 92(2011), 2397 – 2405.

Sani, Y.M. Alaba, P.A. Raji-Yahya, A.O Aziz, A.R.&Daud, W.A. (2015). Acidity and Catalytic Performance of Yb-Doped SO2-4 /Zr Catalysts Synthesized Via Different Preparatory Conditions for Biodiesel Production.*Journal of Taiwan Institute of Chemical Engineers*, 1(2015), 1 – 10.

Singh, A.K. & Umesh, T.N. (2014). Microwave Synthesis, Characterization, and Photoluminescence Properties of Nanocrystalline Zirconia. *The Scientific World Journal*, 1(2014), 1 – 8.

Yahaya, M. S. Wan, M. A. Wan, D. A. R.& Abdul, A. (2014). Activity of Solid Acid Catalysts for Biodiesel Production: A Critical Review. *Applied Catalysis A: General*. 470, 140– 161.

The Kinetic and Thermodynamic Study of the Removal of Selected heavy Metals from a Nigerian Brewery Wastewater Using Activated Carbon From Cheese Wood (alstonia boonei)

[1*]Shaba, E.Y., [1]Mathew, J. T, [2]Musah, M., & [1]Agboba, E. I.

Department of Chemistry, Federal University of Technology, P. M. B. 65, Minna, Niger State, Nigeria.

Department of Chemistry, Niger State College of Education, Minna, Nigeria
Corresponding Authors email:
* elijah.shaba@futminna.edu.ng

Abstract

An adsorbent was developed from the bark of *Alstonia boonei* for removing Pb, Ni and Fe ion from brewery wastewater using a batch adsorption process. Various process parameters that include adsorbent dosage, contact time, solution pH and temperature where studied. For the effect of temperature, Pb had its highest percentage removal of 80.48% at 40°C, for Ni 90.26% at 60°C and Fe 98.76% at 50°C. The effect of solution pH shows highest percentage removal of 98.39% and 99.85% for Fe and Ni respectively at solution pH of l0 while Pb had its highest percentage removal of 79.9% at the solution pH of 2 The result also shows highest percentage removal of 76.01% and 99.19% at adsorbent dosage of 1.5g for Pb and Fe respectively, and 96.8 % at 0.5g for Ni. Also, the highest percentage removal of Pb and Ni was at 60 minutes indicating 82.48% and 96.l9% respectively while Fe showed highest percentage removal of 99.12% at contact time of 30 minutes. Negative values of entropy change ΔS° and Gibbs free energy change ΔG° indicate that this adsorption process is spontaneous. The adsorption process follows pseudo second-order kinetics. The surface functional groups and surface area of the adsorbent was examined by Fourier Transformed Infrared Technique (FT-IR) and Brunauer Emmett Teller (BET).

Keywords: *Adsorption, Heavy metals, wastewater*

1. Introduction

Water bodies have been contaminated due to increase in population and rapid industrialization which is a major concern to the environment (Gunatilake, *et al*., 2015). These industrial effluents are likewise the principal source of heavy metals in wastewater (Malu *et al*., 20l4), these heavy metals are hazardous and courses different disorders which include cerebrum, brain and liver damage (Srivastava *et al*., 2015 and Wang *et. al.,* 2015). Heavy metals get into the brewery wastewater through the grains which are utilized as basic materials, since they are typically developed with herbicides, fungicides and bactericides that contain heavy metals (Cejka *et al*., 2011).

Several techniques such as precipitation, filtration, ion exchange, advanced oxidation, reverse osmosis and so forth have been used for the removal of heavy metals from aqueous solution. However, these techniques have their very own current restrictions such as high operational cost, delicate working conditions, low efficiency (Sud, *et. al*., 2011). Adsorption using activated carbon is recognize to play a great industrial significant in removal of heavy metals from wastewater, due to its accessibility, sustainable, low cost, and high efficiency (Abdel-Fattah, *et al*., 2015).

Due to these facts researchers all over the globe have fused on the development of alternative method, as well as more environmentally friendly process. Activated carbon has been recognized as an important material in purification of water, due to its unique properties such as high porosity and high surface area, has been known as an (Silgado *et al*., 2014). However commercial activated are costly which has necessitated the development of activated carbon from a cheaper materials (Samson, 2015), such as *Alstonia boonei* which is an agricultural by-

products that are available at little or no cost that can be used for preparation of the activated carbon.

Activated carbon have various application which include recovery of solvents, removal of odor medical application, color removal, water purification, desalination, purifying agent in food processing and catalyst support (Yahya *et al*., 2016). The production of activated carbon from agricultural byproducts has potential economic and environmental impacts by converting unwanted low-value agricultural waste to high-value adsorbents (Ekpete *et al*., 2017).

2. Methodology

2.1 Sample Collection and Preparation

The Cheese wood (*Alstonia boonei*) was gathered from Kure Market in Minna Niger State,Nigeria. The Cheese wood was then thoroughly washed twice with distilled water and dried for 3 weeks in the laboratory at room temperature. The sample was crushed with mortar and pestle and sieved with 63µm mesh to obtain a fine sample. The industrial effluent was collected from the Nigerian Breweries, Kakuri, Kaduna State, Nigeria.

2.2 Carbonization (Pyrolysis) and Activation of the Adsorbent

A known amount of Cheese wood (5.00 g) was weighed inside a crucible and then placed in a muffle furnace and heated at a temperature of 600ºC for 15 minutes. The sample was then removed and placed in a desiccator to cool. This process was repeated severally until a desired quantity of the sample was obtained. 30.00g of the carbonized sample was added to 500cm^3 of 0.5mol/dm^3 HNO_3 in l000 cm^3 beaker and was allowed to stay for 24hours to ensure activation of the sample. It was washed severally with deionized water until a pH value of 7 was obtained (Narin *et. al.*, 2005). It was then filtered and the residue was oven dried for 24 hours at 110 ºC and then cooled and stored in a polyethene bag for further use.

2.3 Digestion of Industrial Effluent for the Heavy Metals Analysis

10cm^3 of the industrial effluent was measured into a 250cm^3 beaker. 2cm^3 of conc. HCl and 5cm^3 of conc. HNO_3 were added into the beaker and the solution was heated on a hot plate for 15 minutes to a final volume of 5cm^3 in a fume cupboard. 15cm^3 of deionized water was added to the solution in the beaker and filtered with whatman filter paper No. 45. The filtrate was made up to 50cm^3 with deionized water. This process was repeated until the desired volume was obtained, and was taken to the Atomic Absorption Spectrophotometer for analysis.

2.4 Batch Adsorption Experiment

2.4.1 Adsorbent Dosage Effect

50cm^3 of effluent was measured into a 250cm^3 conical flask and 0.5g of activated carbon was added to it and shaken on a mechanical shaker for 60 minutes. This process was repeated for the dosage of l.0g, l.5g, and 2.0g activated carbon. The content of each conical flask was filtered and the filtrate taken for AAS analysis.

2.4.2 Contact Time Effect

The effect of contact time 30, 60, 90, and l20 minutes were experimented respectively. 0.5g activated carbon was weighed into four different conical flasks containing 50 cm^3 each of the effluent and were placed on a mechanical shaker. After each time, the samples were filtered with Whatman filter paper and the filtrates were taken for AAS analysis.

2.4.3 Solution pH Effect

50cm^3 of the effluent was measured inside four different conical flasks. The pH of the effluent in the l^{st} conical flask was made to 2, the pH of the 2^{nd} conical flask made to 4, the pH of the 3^{rd} made to 6, and the pH of the 4^{th} made to 8 using either 0.lM HCl or 0.lM NaOH (Nasrabadi *et. al.*, 20l0). 0.5g of activated carbon was introduced into each conical flask and macerated with a glass rod and placed on a mechanical shaker for 60 minutes. The samples were then filtered, and the filtrate taken for AAS analysis.

2.4.4 Effect of Temperature

50Cm^3 of the wastewater was placed into four different 250cm^3 conical flask. 0.5g of the activated carbon was added to the effluent in each flask. A series of the flask was placed in a water bath shaker at temperatures of 30°C, 40°C, 50°C, and 60°C respectively for 30 minutes each. The content was then filtered with filter paper and the filtrate was analysed using Atomic Absorption Spectrophotometer (AAS).

2.5 Data Analysis

The adsorption capacity q_e (mg/g) of the raw sample and activated carbon were calculated using the expression;

$$q_e = \frac{(Co-Ce)V}{M} \quad (1)$$

where Co is the initial concentration in mg/dm^3, Ce is the final concentration in mg/dm^3, V is the volume of effluent in dm^3, and M is the mass of the adsorbent in grams. The percentage removal of heavy metals was calculated using the expression:

$$\%\text{removal of heavy metals} = \frac{Co-Ce}{Co} X\ l00 \quad (2)$$

2.5.1 Adsorption Kinetics

Two kinetic models were used to examine the adsorption mechanism of the heavy metals.

2.5.2 Pseudo First Order

This is given as: $\frac{dqt}{dt} = K_1\ (q_e - q_t)$ (3)

The integral form of this equation is (Santhy and Selvapathy 2006)

$In(q_e - q_t) = Inq_e - k_1 t$ (4)

where q_e (mg/g) and q_t (mg/g) are the amounts of adsorbed adsorbate at equilibrium and at time t, respectively, and k_1 (min^{-1}) is the rate constant of pseudo first-order adsorption.

2.5.3 Pseudo second-order equation

The sorption kinetics can also be described by pseudo second-order model. The linear form of pseudo second- order equation is expressed as (Bulut and Ozacar 2008).

$t/q_t = 1/k_2 q^2_e + t/q_e$ (5)

where k_2 (g/mg min) is the equilibrium rate constant of pseudo second-order adsorption.

The applicability of the two models above can be examined from the linear plot of $In(q_e - q_t)$ against t, and t/q_e against t, respectively.

2.5.4 Thermodynamic parameters

The value of ΔH and ΔS were calculated from the slope and intercept of the linear van Hoff's plot respectively, using the relation:

$$InK = \frac{\Delta S}{R} - \frac{\Delta H}{RT} \quad (6)$$

Where:

ΔS = entropy change for the process

ΔH = enthalpy change for the process

R = gas constant

T = absolute temperature

The distribution coefficient (Kd) of the activated charcoal surface was calculated using the equation,

$$Kd = \frac{(Ci-Ce)}{Ce}\frac{V}{M} \quad (7)$$

Where C_i= the initial concentration of the metal ion, C_e= the equilibrium concentration of the metal ion, V = the volume of the solution equilibrated in cm^3 and m = mass of the adsorbent in g

The change in free energy (ΔG) for the specific adsorption has also been calculated using the equation

$\Delta G = -RT\ InK$ (8)

3. RESULTS AND DISCUSSION

Results

Table l: Results of the physicochemical properties of the adsorbent

Parameters	Values
Bulk density (g/cm3)	0.26
Ash content (%)	6.00
Moisture content of Activated Adsorbent (%)	0.1
Electrical conductivity (µS/cm)	2.8 x l0^2
Iodine number (mg/g)	110.48
Volatile matter (%)	2.17
Fixed carbon (%)	91.63
Micro pore width (nm)	6.538
Pore diameter (nm)	2.427
Pore volume (cc/g)	0.2158
Surface area (m^2/g)	418.3-1344

Table 2: Adsorption kinetic constants for activated carbon

Metal ions	Pseudo-first order			Pseudo second order		
	ln ($q_e - q_t$) = Inq_e – K_lt			$t/q_t = 1/K_2q_e^2 + t/q_e$		
	R^2	q_e (mg/g)	K_1	R^2	q_e (mg/g)	K_2
Pb	0.0228	1.1630	-0.0210	0.954	454.55	0.00017
Ni	0.1401	0.0501	-0.0454	0.8668	l25	-0.00035
Fe	0.5889	0.0021	-0.0760	1	500	-0.01000

The experimental adsorption capacity q_e (mg/g) for Pb, Ni and Fe are 445.598mg/g, 239.l38mg/g and 499.878mg/g respectively.

Table 3: Thermodynamic parameters Enthalpy Change, ΔH°, and Entropy Change, ΔS°. **for Pb, Ni and Fe**

Item	Pb	Ni	Fe
R^2	0.1495	0.5666	0.3008
ΔH° KJ/mol	-12.8	-19.37	-31.68
ΔS° (J/mol.K)	0.0054	0.1164	0.0316

Table 4: Gibbs free energy Change (ΔG°) for Pb, Ni and Fe

ΔG° (kJ/mol) Temp. (k)	Pb	Ni	Fe
303	-14.44	-54.64	-41.25
313	-14.49	-55.8	-41.57
323	-14.54	-56.97	-41.89
333	-14.59	-58.13	-42.2

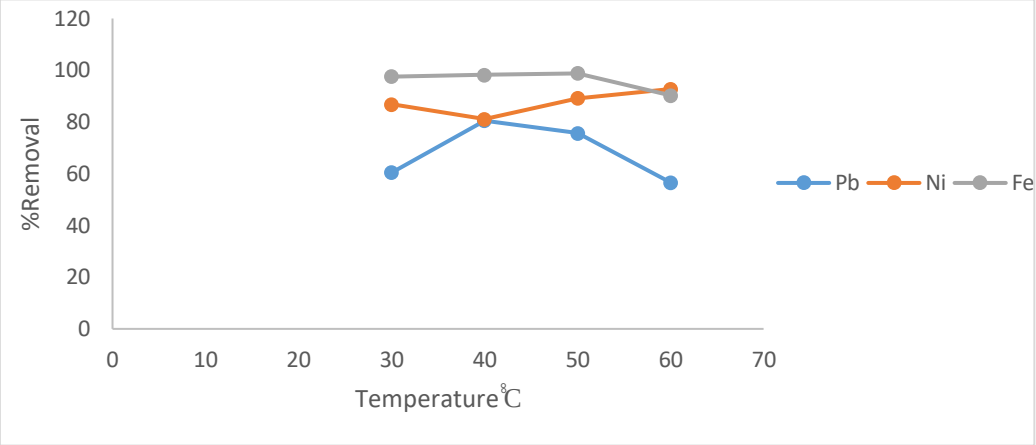

Figure l: Effect of Temperature on Pb, Ni, and Fe

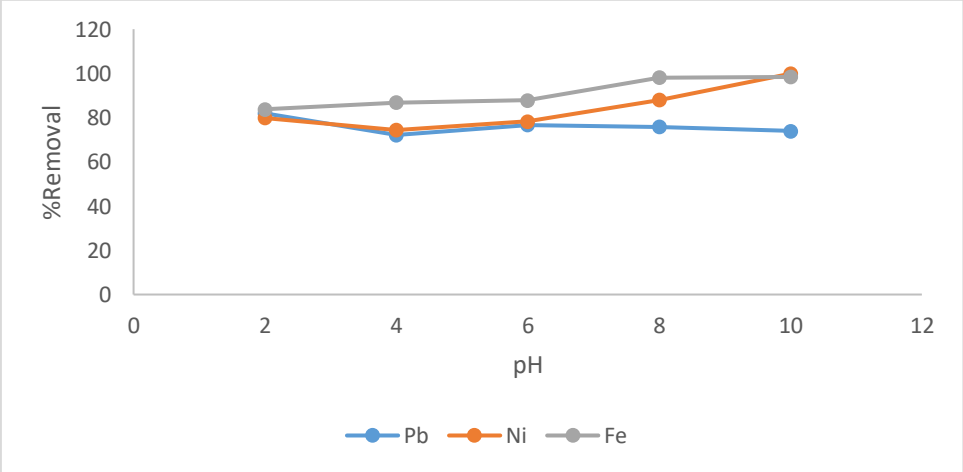

Figure 2: Effect of solution pH on Pb, Ni, and Fe adsorption

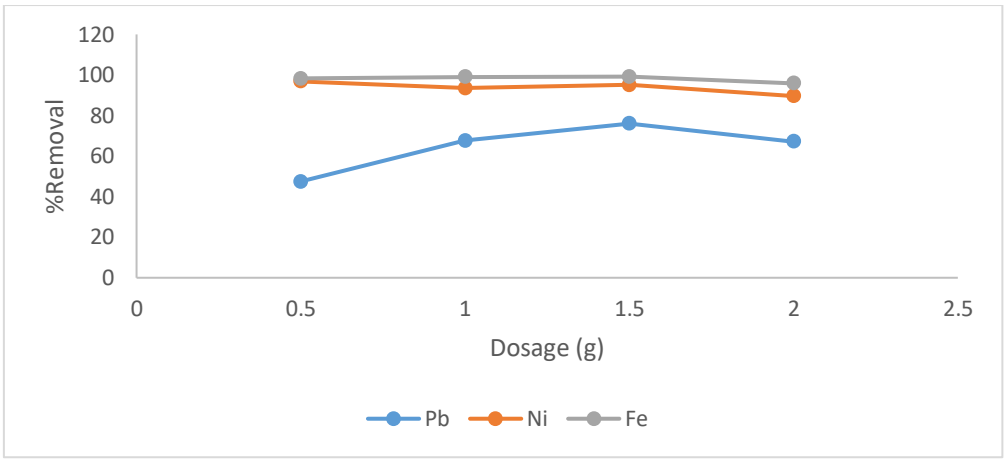

Figure 3: Effect of Adsorbent Dosage on Pb, Ni, and Fe Adsorption

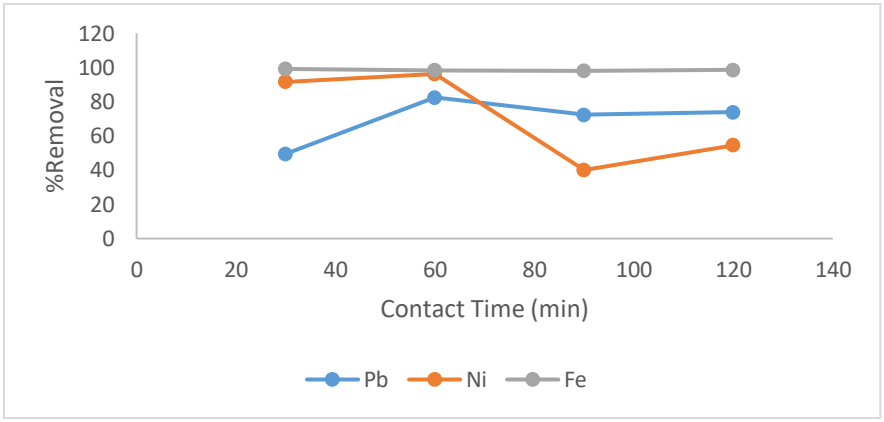

Figure 4: Effect of Contact Time on Pb, Ni, and Fe Adsorption

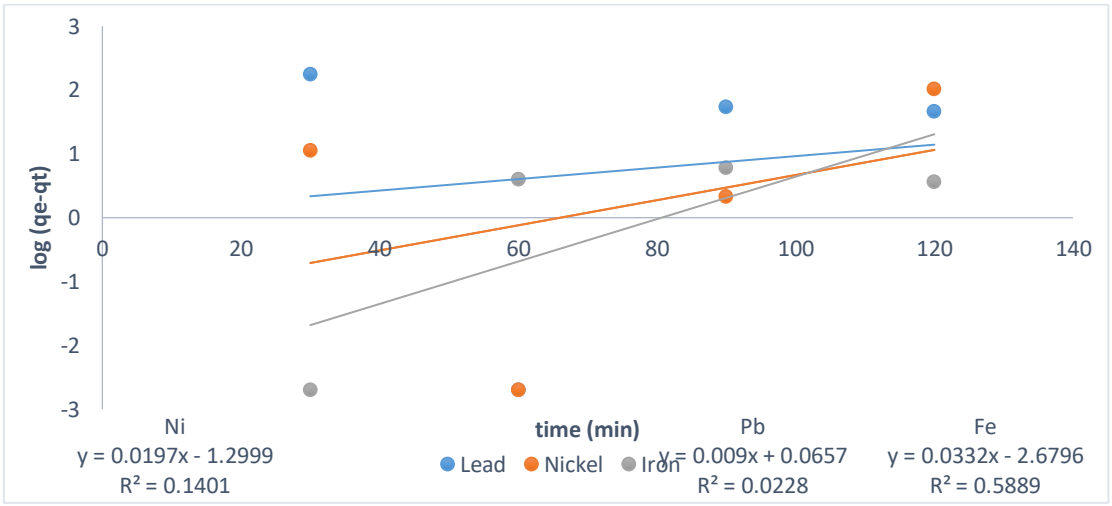

Figure 5: Pseudo first order kinetic plot for Pb, Ni, and Fe adsorption

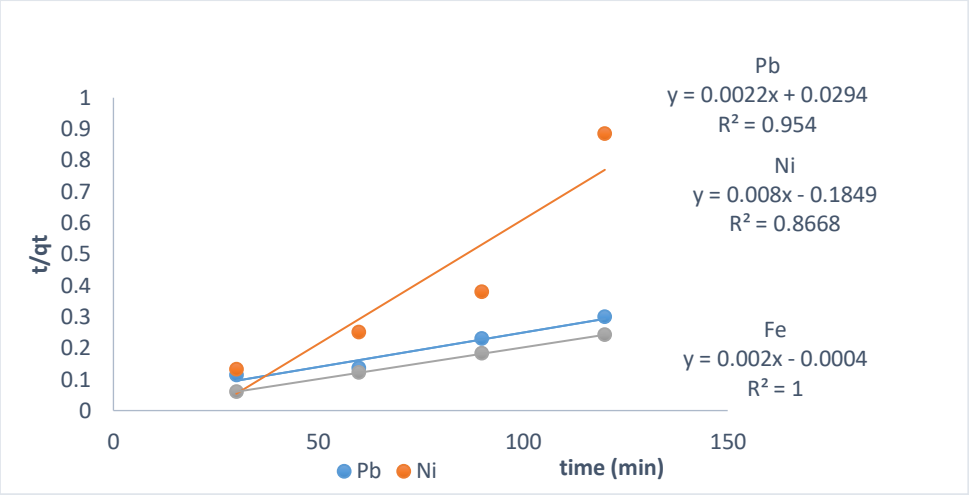

Figure 6: Pseudo second order kinetic plot for Pb, Ni, and Fe adsorption

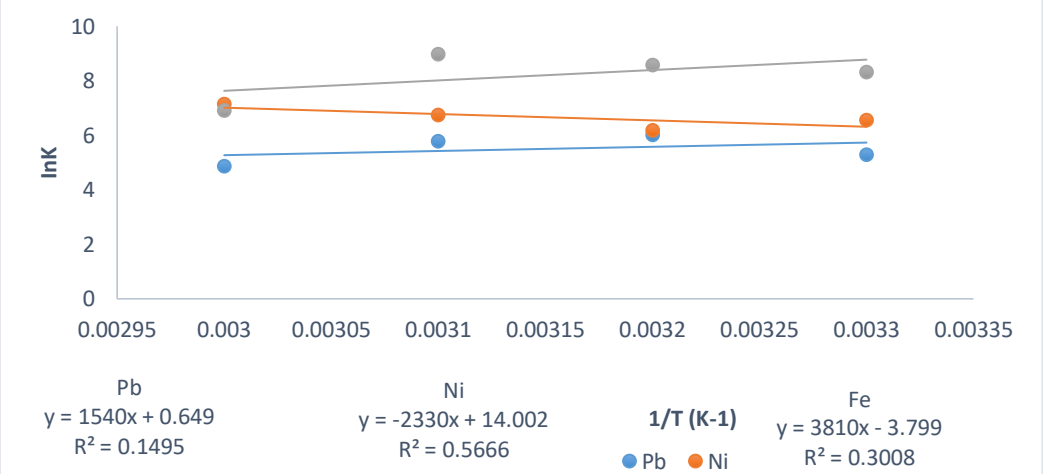

Figure 7: Van Hoff's thermodynamic plot for the adsorption of Pb, Ni and Fe

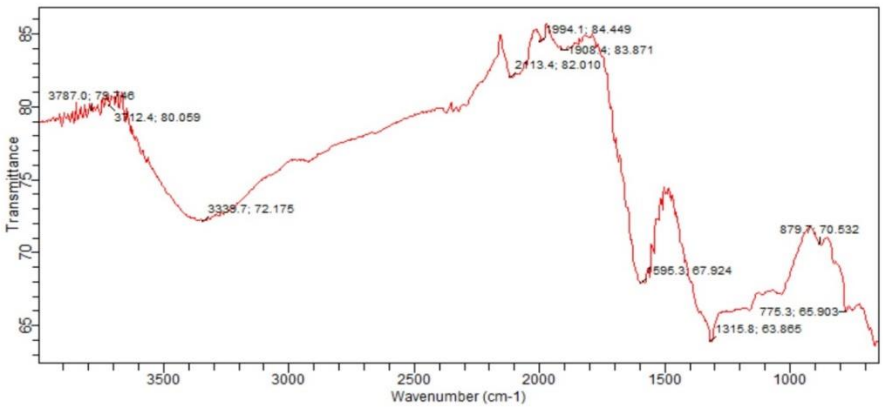

Figure 8: FTIR spectrum of Activated Carbon Prepared from *Alstonia boonei*

3.2 Discussion

From the result of the physicochemical analysis in table 1 6% ash content was obtained for this study; good activated carbon is expected to have low ash content (Abubakar *et al*., 2012). The ash content is linked to the pore structure of the activated carbon and also reflects the purity of

the activated carbon (Nworu *et al*., 2018), which greatly influences the adsorptive capacity of the prepared activated carbon (Ahmed *et. al.*, (2008).
The result of the moisture content of the activated *Alstonia boonei* was 0.1% as presented in table 1.It has been reported by Shaarani *et al*. (2010) that a good activated carbon must have a low moisture content to avoid water vapours competing in adsorption process and fill the adsorption sites within the pores, thus reducing the efficiency of the activated carbon. The moisture content obtained in this study is lower than the 4.20 % reported Maina and Anuka (2014).
The range of particle size and degree of activation affects bulk density, which have an effect on adsorption per unit volume. Bulk density of 0.26g/cm^3 was obtained for this study which is lower than the 0.509g/cm^3 reported by Olafadehan *et al*. (2012). TIGG Corporation, (2012) reported that higher density provides greater volume activity and indicates better-quality activated carbon.

The iodine number of 110.48 mg g^{-1} was obtained from the analysis.Iodine number is directly linked to the adsorption capacity of an activated carbon since It is a measure of the microspore content of the activated carbon and is obtained by the adsorption of iodine from solution by the activated carbon sample (Lillo-Rodenas *et al*., 2003). It is used to measure the porosity and adsorbent capacity of activated carbon (Ekpete and Horsfall, 2011).

Volatile matter of 2.17 was obtained. The study revealed fixed carbon of 91.63 %. Surface properties of the of the activated carbon (BET surface area, pore volume, and pore size distributions) were evaluated by nitrogen adsorption-desorption isotherm the result revealed micro pore width of 6.538 nm, pore diameter 2.427nm, pore volume of 0.2158 cc/g and surface area 418.3- 1344 m^2/g for BET and Langmuir model respectively. The result is in similar to the 311 to 1044 m^2/g surface area and 0.18 to 0.59 cm^3/g pore volume obtained for *Spent Tea Leaves* activated carbon by Singh *et al*. (2015). The result is higher than 179.7 m2 /g and micropore volume 0.081 cc/g (Yakout *et al*., 2015).
The result of shows that the as the temperature increases from 30°C to 40°C the percentage removal of Pb increases from 60.40% to 80.48% and Fe ion also increases from 97.59% to98.78% as the temperature increases from 30-50°C as shown in figure 1 This phenomenon is attributed to the increased kinetic energy of the metallic ions due to the increase in temperature of the system which leads to the increased mobility of the Pd and Fe ions to the adsorption sites.
Meanwhile, there was decrease in percentage removal of Ni from 86.83% to 81.13 %. As the temperature increases before an increase in percentage removal from 81.13% to 89.l3% and respectively. From the result It is observed that the percentage removal of Pb < Ni < Fe which may be attributed to their atomic size.
The effect of solution pH on adsorption of Pb, Ni and Fe is shown in figure 2. The highest percentage removal of Pb was at solution pH of 2, while Ni and Fe highest percentage removal was at pH l0. The low bio-sorption of Fe and Ni at lower pH may be attributed to the higher concentration and greater mobility of H^+.
The highest percentage removal of Pb, Ni and Fe are 8l.94%, 99.85%, and 98.39% respectively.
The result in this study shows an increase in percentage removal of Pb ions from 47.49% to 67.64% to 76.015% as adsorbent dosage increases from 0.5g to 1.0g to 1.5g respectively. This continuous increase percentage removal with increasing adsorbent dosage is due to the increased surface area of adsorbent dosage with increasing amount of adsorbent. Ranjan and Krishna (20l4) gave a similar report using activated carbon from *polyathia longifolia* for the kinetic studies on bio-sorption of fluoride.

The lowest percentage removal of Pb, Ni and Fe was observed at the highest adsorbent dosage of 2g. This phenomenon can be attributed to the agglomeration of the adsorbent due to the large quantity of activated carbon, forming clusters which tends to reduce the surface area of the adsorbent and block the its pore space.

The result obtained for the effect of contact time on Pb, Ni and Fe as presented in figure 4.7 shows the rapid adsorption of Pb and Ni in the first 60 minutes and Fe in the first 90 minutes of the adsorption process. This is due to the availability of free pore space in the adsorbent in the early minutes of contact time and so these metals will readily fill up those spaces. The maximum percentage removal for Pb and Ni was 82.48% and 96.l9% respectively at contact time of 60 minutes, while the maximum percentage removal for Fe was 99.96% at contact time of 90 minutes.

The thermodynamic parameters, namely free energy (ΔG^o), enthalpy (ΔH^o) and entropy (ΔS^o) have an important role in determining spontaneity and heat change for the adsorption process. The values of entropy change ($\Delta S°$) and enthalpy change ($\Delta H°$) were obtained from intercept and slope of the plot of InK versus 1/T (K^{-l}).

The estimated values of the thermodynamic parameters for the four operation temperatures were calculated and presented in table 4 and 5. The negative values of the change in free in energy ($\Delta G°$) confirms the adsorption process is spontaneous and does not require energy input outside the system while the positive value of the entropy change ($\Delta S°$) confirms the spontaneity of the adsorption process (Zhou *et al*., 2014). The negative value of $\Delta H°$ -12.6, -19.37 and -31.69 kJ/mol for Pd, Ni and Fe respectively indicates that the adsorption is exothermic in nature, and in such instance, increase in temperature leads to increase in adsorption rate since the adsorbed molecules gain more kinetic energy and are readily desorbed. In other words, in exothermic adsorption process, the rate of adsorption-desorption increases.

In adsorbed state, the adsorbate is held on the surface of the adsorbent by attractive forces (bond). Depending on the nature of attractive forces, adsorption can be classified as physical adsorption (physisorption) or chemical adsorption (chemisorption) as reported by Alzaydien in 2016. The $\Delta H°$ values for physical adsorption is in the range of -10kJ/mol to 40kJ/mol (Alkan *et al*, 2004), this shows that the adsorption in this study is physical adsorption since the $\Delta H°$ values obtained is less than 40kJ/mol, while it has been reported that chemical adsorption are rarely less than 80kj/mol and sometimes exceed 400kj/mol (). Chemisorption has higher enthalpy of adsorption values because in chemisorption, the chemical bonds are stronger, while the physical adsorption has lower enthalpy of adsorption because weak forces such as vanderwaal's forces exist.

Fourier transform Infrared spectroscopy was used to study the functional group and obtained information on the chemical structure of the prepared activated carbon. The surface chemistry of the activated carbon was determined by the type, quality and bonding of the functional groups. Figure 8 from the result shows the spectra of activated carbon from *Alstonia boonei.*

The broad band around 3100-3600 cm^{-l} is attributed to the presence of hydroxyl group, either aliphatic alcohol/phenol or adsorbed water molecule. The 2200-2000cm^{-l} is possibly caused by C≡C stretch. The band around 1650-1500 cm^{-l} is possibly caused by the stretching vibration of C=O in carboxyl, ketones, aldehydes or lactone group. The band around 1400 cm^{-l} is attributed to the presence of NO_2. 1400-1000 cm^{-l} indicates C-F bond and 800-600 cm^{-l} indicates C-Cl bond.

The mechanism of the adsorption of Pb, Ni and Fe ions by activated carbon from *Alstonia boonei* were examined by using the pseudo-first and pseudo second models. The pseudo-second order kinetics has higher correlation coefficient (R^2) values in comparison to the correlation coefficient values of the pseudo-first order. Also, the calculated adsorption capacity (qe) values for the pseudo-second order kinetics for Pb, Ni and Fe were found to be 454.55mg/g, l25mg/g, and 500mg/g respectively, which are very much closer to the

experimental adsorption capacity (qe) values of Pb, Ni and Fe, which are 445.598mg/g, 239.138mg/g and 499.878mg/g respectively, while the calculated qe values for the pseudo-first kinetics for Pb, Ni and Fe which are l.l630mg/g, 0.050lmg/g, and 0.002l mg/g respectively, are nowhere close to the experimental qe values. Therefore, the pseudo second order model best fits the experimental data than the first order and is more relevant to this study.

4.0 Conclusion

Activated carbon prepared from *Alstonia boonei* bark which is abundant in Nigeria can be used as effective sorbents for purification of drinking and waste waters. From the results obtained, it is evident that activated carbon produced from *Alstonia boonei bark* can remove 80.48%, Pb, 99.19% of Fe and 99.85% of Ni ions which also dependent on parameters such as time, adsorbent dosage, pH and temperature.

The thermodynamic parameters indicated that the adsorption process is spontaneous. .

5.0 REFERENCE

Abdel-Fattah, M. E. Mahmoud, Ahmed S.B., M. D. Huff, J. W. Lee, & Kumar S. (2015). Biochar from woody biomass for removing metal contaminants and carbon sequestration. Science Direct. *Journal of Industrial and Engineering Chemistry*, 1(2), 1-15.

Abubakar, M., Alechenu, A. A., Manase, A. & Mohammed, J. (2012): A Comparative Analysis and Characterization of Animal bones as Adsorbent. *Advances in Applied Science Research*, 3(5): 3089-3096.

Alkan, M., Demirbas, O., Elikcapa, S., & Dogan, M., (2004) Sorption of acid red 57 from aqueous solution onto sepiolite. *J. Hazard. Mater*. ,116, 135–145.

Alzaydien**, S. A. (**2016). Physical, Chemical and Adsorptive Characteristics of Local Oak Sawdust Based Activated Carbons. *Asian Journal of Scientific Research.* 9 (2), 45-56.

Ashutosh, T. & Manju, R. R. (2015). Heavy Metal Removal from Wastewater Using Low Cost Adsorbents. *Journal of Bioremediation and Biodegradation* .6, 2155-6199.

Cejka, P., Horak, T., Dvorak, J., Culik, J., Jurkova, M., Kellner, V. & Haskova, D. (2011). Monitoring of the distribution of some heavy metals during brewing process. *Ecological chemistry and Engineering.* 18 (1), 67-*74.*

Chandra, S., Singh, A., & Tomar, P. K. (2012) Assessment of water quality values in Porur Lake Chennai, Hussain Sagar Hyderabad and Vihar Lake Mumbai, India. *Chem. Sci. Trans. 1: 508-515.*

Cheesbrough, M. (2006). District laboratory Practice in Tropical Countries. Part 2. *Cambridge University Press. pp.* 143-157.

Dawodu, F.A. & Ajanaku, K.O. (2008). Evaluation of the effects of brewery effluents disposal on public water bodies in Nigeria. *Terrestrial and Aquatic Environmental Toxicology*, 2(1),1-17

Ekpete, O. A. & Horsfall, M. (2011). Preparation and characterization of activated carbon derived from fluted pumpkin stem waste (*Telfairia occidentalis hook* f). *Research Journal of Chemical Sciences*, 1 (3),10–17.

Ekpete, O. A. Marcus, A. C. & Osi, V. (2017). Preparation and Characterization of Activated Carbon Obtained from Plantain (*Musa paradisiaca*) Fruit Stem**.** *Journal of Chemistry*, 1-6.

Galadima, A., Garba, Z. N., Leke, L., Almustapha, M. N. & Adam, I. K. (2011). Domestic Water Pollution among Local Communities in Nigeria. Causes and Consequences. *European Journal of Scientific Research.* 52 (4), 592-603.

Gunatilake, S. K. (2015). Methods of Removing Heavy Metals from Industrial Wastewater. *Journal of Multidisciplinary Engineering Science Studies*, 1 (1), 12-18.

Halder, J. N. & Islam, M. N. (2015). Water pollution and its impact on the human health. *Journal of environment and human.* 2(1):36-46.

Inyang, U.E., Bassey, E. N. & Inyang, J. D. (2012). Characterization of Brewery Effluent Fluid. *Journal of Engineering and Applied Sciences.* 4, 68–76.

Lillo-Rodenas, M.A., D. Cazorla-Amoros and A. Linares-Solano, (2003). Understanding chemical reactions between carbons and NaOH and KOH: an insight into the chemical activation mechanism. *Carbon*, 41: 267-275.

Maina, N. S. & Anuka, A. A. (2014). Production of activated carbon from Atili seed shells. *Leonardo Electronic Journal of Practices and Technologies*. 25, 95-209.

Malu, S.P., Andrew, C., Abah, J. & Oko, O.J. (2014). Determination of Heavy Metals in Brewer's Spent Grains Obtained From Benue Brewery Limited (BBL), Makurdi, North Central Nigeria. *Journal of Natural Sciences Research.* 4(1), 119-122.

Milojkovic, J., Mihajlovic, M., Stojanovic, M., Lopicic, Z., Petrovic, M., Sostaric, T. & Ristic, M., (2014). Pb (II) removal from aqueous solution by *Myriophyllumspicatum* and its compost: equilibrium, kinetic and thermodynamic study. *J. Chem. Tech. Biotech.* 89:662-670.

Ninnekar, H. Z. (1992). Biodegradation of environmental pollutants. *Journal of Environmental Biodegradation*. 5,149-154.

Nworu, J. S., Ngele, S. O., Nwabueze, E., Okhifo, A. & Peretomode, T. M. (2018). Quantitative Characterization of Activated Carbon from Cow, Donkey, Chicken and Horse Bones from Ezzangbo in Ebonyi State, Nigeria. *American Journal of Applied Chemistry***,** 6(5): 169-174.

Obasi, A. & Ogochukwu, A. (2017). Bioremoval of Heavy Metals from a Nigerian Brewery Wastewater by Bacterial Application. *Food and Applied Bioscience Journal*, 5(3):165–175.

Olafadehan, O.A., Jinadu , O.W., Salami, L. & Popoola, O. T. (2012). Treatment of Brewery Wastewater Effluent Using Activated Carbon Prepared From Coconut Shell. *International Journal of Applied Science and Technology*, 2(1) 165-178

Salem, H. M., Eweida, E. A. & Farag, A.. (2000). Heavy Metals in Drinking Water and Their Environmental Impact on Human Health. ICEHM2000 , 542- 556.

Samson, M. L. N. (2015). Activated carbon from corn cob for treating dye waste water. Environmental Science, 10(3), 88-95.

Shaarani, F. W. & Hameed, B. H. (2010). Ammonia-Modified Activated Carbon for the Adsorption of 2,4-dichlorophenol. *The Chemical Engineering Journal*, 169(1), 180-185.

Silgado, K. J., Marrugo, G. D. & Puello, J. (2014). Adsorption of chromium (vi) by activated carbon produced from oil palm endocarp. *Chemical Engineering Transactions*, 37, 721-726.

Silgado, K. J., Marrugo, G.D. & Puello J. (2014). Adsorption of chromium (vi) by activated carbon produced from oil palm endocarp. *Chemical Engineering Transactions*, 37, 721-726.

Singh, J., Doshi, V. & Lim, X. Y. (2015). Investigation on *Spent Tea Leaves* Derived Activated Carbon For CO_2 Adsorption R. Menon,. *Journal of Engineering Science And Technology Eureca* . 50 – 61.

Srivastava, S., Agrawal, S. B. & Mondal, M.K., 2015. A review on progress of heavy metal removal using adsorbents of microbial and plant origin. *Environmental Science and Pollution Research.* 22, 15386-15415.

Sud, G. Mahajan, & M. P. Kaur. (2008). Agricultural Waste Material as Potential Adsorbent For Sequestering Heavy Metal Ions from Aqueous Solutions. *Science Direct. Bioresource Technology*. 99 (14), 6017–6027.

Uchimiya, I. M., Lima, K. T., Klasson, S. C. Chang, L. H. Wartelle, J. E. & Rodgers. (2010). Immobilization of heavy metal ions (Cu-II, Cd-II, Ni-II, and Pb-II) by broiler litter-derived biochars in water and soil. ACS. *Journal of Agricultural and Food Chemistry*.58(9), 5538–5544.

Wang, Z., Liu, G., Zheng, H., Li, F., Ngo, H.H., Guo, W., Liu, C., Chen, L. & Xing, B., (2015). Investigating the Mechanism of Bio char's removal of lead from solution. *Journal of Bioresource Technology*. 177, 308-317.

Yahya, M.A., Zanariah, C.W., Ngah, C. W., Hashim, M. A. & Al-Qodah, Z. (2016). Preparation of Activated Carbon from Desiccated Coconut Residue by Chemical Activation with NaOH *Journal of Materials Science Research*. 5(1), 24-31.

Yakout , S. M., Daifullah , A. M., & El-Reefy, S. A. (2015). Pore Structure Characterization of Chemically Modified Biochar Derived From Rice Straw. *Environmental Engineering and Management Journal*, 14 (2), 473-480.

Zhou, Z., Lin, S., Yue, T., & Lee, T. C. (2014). Adsorption of food dyes from aqueous solution by glutaraldehyde cross-linked magnetic chitosan nanoparticles. *Journal of Food Engineering*. 126, 133–141.

EARTH SCIENCES

Effect of Weather Variables on Reservoir Inflow for Hydroelectric Power Generation in Jebba Dam, Nigeria

Ndace Danladi1[1]* M. B. Yunusa[2]
[1, 2]Department of Geography Federal University of Technology Minna Nigeria
[2]mb.yunusa@futminna.edu.ng
1*ndaceisah@gmail.com
*Corresponding author

Abstract

This study examined the effect of weather variable on reservoir inflow for hydro-electric power generation in Jebba Dam, Nigeria. The study utilized monthly rainfall, temperature, evaporation, reservoir inflow and outflow from 1993 to 2017. The study objectives were achieved by analysing mean annual trend of rainfall, temperature, evaporation, reservoir flows, for 25 years. Hypothesis was tested for relationship between the weather variables (rainfall, temperature, evaporation) on the amount of reservoir inflow, while the effect of reservoir inflow, and reservoir outflow on the amount of energy generated was tested using correlation coefficient at 5% significant level. The amount of energy generated for the period of study was analysed on monthly basis to know the season more electricity was generated. From the study it reveals that the month of March generate more electricity of (273724 mwh) and the lowest in the month of July (155098mwh). All the weather variables show an increasing trend, while the reservoir inflow pattern exhibit fluctuations at various levels. The results also revealed that rainfall, temperature, evaporation, has a direct effect on the reservoir inflows and subsequently on dam levels and also that reservoir inflow, and outflow have strong relationship with the amount of energy generated which signify that climate variability has a big impact on reservoir inflow and energy production. It was recommended that future hydropower plant investments in the country should take careful consideration into the climatic variables impact on the potential for energy generation.

Keywords: Reservoir inflow, reservoir outflow, temperature, evaporation, rainfall, hydroelectric power generation

1. Introduction

Water is a vital resource to support life on earth. Unfortunately, it is not evenly distributed over the world by season or location; it is also a critical limiting factor for economic and social development in many parts of the world. The recent rapid growth in human population and water use for social and economic development is increasing the pressure on water resources and the environment, as well as leading to growing conflicts among competing water use sectors (agriculture, urban, tourism, industry) and regions (Gleick *et al.*, 2009; World Bank, 2006). One of the most efficient ways to manage water resources for human needs is by the construction of dams that create reservoirs for storage and future distribution (ICOLD, 1999; Asmal, 2009). Large dams constitute a significant tool for the economic development of nations for years. Globally, there are 5000 large dams as at 1950 (ICOLD, 1998); three quarters of these were in North America, Europe, and other industrial regions. By the year 2000, the

number of large dams had risen to more than 45,000, and these were spread among more than 140 countries (ICOLD, 1998). On average, two large dams were built per day for half a century (WCD, 2000). Today, the number of large dams exceeds 50,000 (Berga, *et al.*, 2006).

Nigeria as a nation has more than four decades of history on hydro-electric power development in Africa South of Sahara starting with the Kainji Dam on the lower part of River Niger. The primary purpose of these dams (Jebba, Kainji on River Niger and Shiroro on River Kaduna) was to serve as engine of growth and development. This role has been performed creditably well by supplying not only Nigeria but also those neighboring countries for which River Niger is a common wealth, with the needed energy to power the growing economy. In this study we are concern with the hydro electric power generation dam, the reservoir and climatic elements that are of interest are rainfall, Evaporation, temperature and reservoir inflow and outflow pattern.

2. Literature Reviews

Kabo-Bah, *et al.* (2016) studied Multiyear Rainfall and Temperature Trends in the Volta River Basin and their Potential Impact on Hydropower Generation in Ghana. The effects of temperature and rainfall changes on hydropower generation in Ghana from 1960–2011 were examined to understand country-wide trends of climate variability. Moreover, the discharge and the water level trends for the Akosombo reservoir from 1965–2014 were examined using the Mann-Kendall test statistic to assess localized changes. The annual temperature trend was positive while rainfall showed both negative and positive trends in different parts of the country. However, these trends were not statistically significant in the study regions in 1960 to 2011. Rainfall was not evenly distributed throughout the years, with the highest rainfall recorded between 1960 and 1970 and the lowest rainfalls between 2000 and 2011. The Mann-Kendall test shows an upward trend for the discharge of the Akosombo reservoir and a downward trend for the water level. However, the discharge irregularities of the reservoir do not necessarily affect the energy generated from the Akosombo plant, but rather the regular low flow of water into the reservoir affected power generation.

Kachaje, Kasulo, and Chavula (2016) assessed the potential impacts of climate change on hydropower: on micro hydropower scheme, Malawi. The study reveals that Climate change has the potential to affect hydropower generation by either increasing or reducing flows (discharge) and the head. The study analyzed trends in weather time series (air temperature and rainfall) data from 1980 to 2011 in connection to changes in river discharge and their associated impacts on hydropower generation profile. The Mann-Kendall (MK) test was used to detect trends in air temperature, precipitation and discharge. Correlation analysis was also used to uncover the relationship between discharge and precipitation as well as between discharge and temperature. The MK results highlighted significant rising rates of air temperature, precipitation and discharge in some months and decreasing trend in some other months, suggesting significant changes have occurred in the area.

Bekoe & Logah (2013) assessed the impact of droughts and climate change on electricity generation in Ghana, Ghana has occasionally being experiencing harsh weather conditions such as flooding and hydrological droughts. Electricity power for the country depends mainly on

hydropower generated from a hydropower dam at Akosombo built in 1965. The 2006/2007 electricity power rationing, equating to about 24hrs light in 48 hrs was the severest power rationing ever witnessed in Ghana and the consequences were catastrophic. Out of about 1180MW generated by the two hydropower dams, only about 400MW was produced. This affected all sectors of the economy including industry, mining and domestic. Manufactures were reducing output, this paper analysis 37 years of rainfall in the Volta basin and intake water levels in the Dam site on the Volta lake for hydropower generation to establish whether in reality, the main causes of the power rationing due to low water levels in the Akosombo dam was due to drought. The paper establishes that the 1983, 1997 and 2006/7 power rationing was truly as a result of hydrologic drought whereas the 2003's was not. The paper also suggests that if climate change effects on the water resources of the country are not managed sustainably, drought and floods could affect hydropower generation in future.

3. Methodology

Mean monthly rainfall, evaporation, temperature, reservoir Inflow, outflow, and amount of energy generated for a period of twenty five (25) years from 1993-2017 over the study area were obtained from the hydroelectric-dam Jebba Station in their hydrological unit and generation room. The statistical techniques that were use are all toward establishing relationship between hydropower generations, and weather variables on reservoir for electricity generation in Jebba dam and these includes, time series analysis, Pearson Product moment correlation analysis, using Statistical Package for Social Scientists (SPSS) tool. These methods are briefly discussed in following sections:

3.1 Trends of weather variables

This was achieved using time series analysis to detect the trend in weather variables. Trend analysis presents the long term movement of the time series to detect the patterns of weather variables (temperature, evaporation, and rainfall), and reservoir inflow over the hydro station presented using graphs.

3.2 Effects of weather variables on reservoir

This was assessed using correlation analysis as shown in equation 1. This was meant to determine the degree of relationship between climate variables and reservoir inflow.

$$R_{xy} = \frac{\frac{1}{n}\sum_{i=1}^{n}(x_i-\bar{x})(y_i-\bar{y})}{\sqrt{\frac{1}{n}\sum_{i=1}^{n}(x_i-\bar{x})^2.\frac{1}{n}\sum_{i=1}^{n}(y_i-\bar{y})^2}} \quad \text{eqn (1)}$$

Where, R_{xy} is the correlation coefficient, n is the sample size, $x_i$and y_i are the variables being correlated and x and y are the mean values of variables being correlated. The computed correlation values were tested for statistical significance at 5% significance level.

3.3 *Analysis of the mean monthly reservoir inflow and outflow, and mean monthly energy generated*

This was analyse using trend analysis and the variation on amount of energy generated in the study area by getting the overall mean of energy generated for the time frame of study (1993-2017) for each month .

3.4 *Examine the relationship between the reservoirs inflow, outflow patterns on the amount of energy production*

This was achieved using Pearson Product moment correlation co-efficient using Statistical Package for Social Scientist (SPSS) version 20.0 software package. The test was tested at 0.05 level of significance.

4. Results and Discussion

4.1 Analysis of rainfall trend over the study area

The rainfall data collected from the study area was subjected to linear trend analysis in order to show the trend of rainfall for the time frame of study (1993-2017). The trend in figure1 graphically shows that rainfall in the study area has been fluctuating and the pattern shows gradual increase over the years reaching its zenith in the year 2013 with 122.20mm, although there is also a wide range of fluctuation in the amount of rainfall ranging from the lowest which is the year 2009, 2005, and 2006 with 77.81mm, 78.10mm, 81.07 respectively. With an increase in 2016, 2003, and 2000 with about 115.35mm, 111.54mm, 103.38 accordingly. The study area does not seem to have a major shortage in amount of rainfall as shown in figure 1.

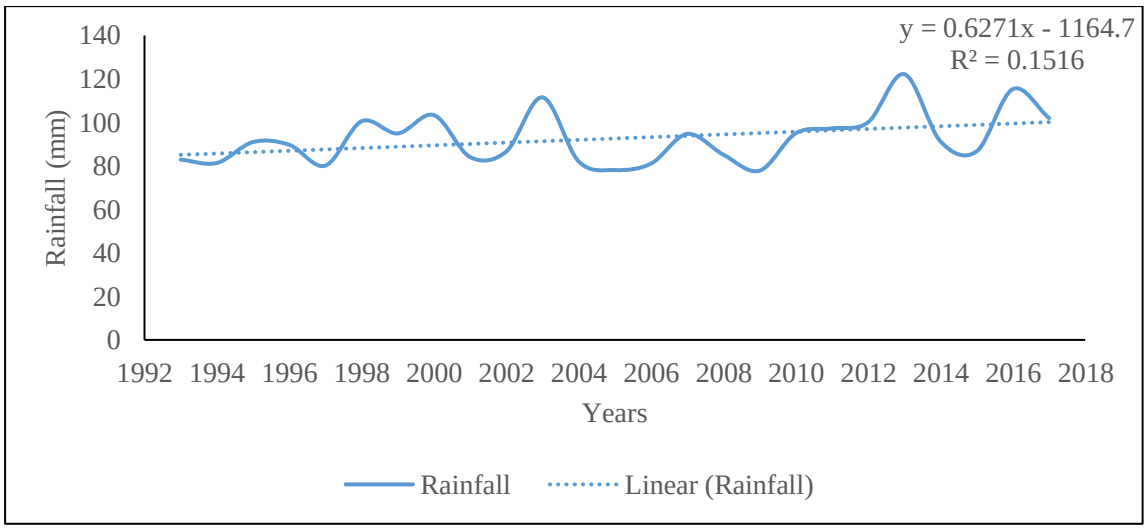

Figure 1: Mean Annual Trend of Rainfall in Jebba Dam (1993 to 2017).
Source: Authors' Data Analysis, 2019.

4.2 Analysis of temperature trend over the study area

shows the Trend of Temperature in the study area for the period of twenty five years (1993-2017) it shows that the temperature of the study area has been on the increase and has been fluctuating, with the lowest annual recorded in the year 1993, 1994, 1995, and 1997 with 28.58ºC, 28.63ºC, 28.75ºC, 28.71ºC, respectively showing a sharp drop to 31^0C below average. With the increase starting from 29.04ºC year 1999, reaching it highest in 2010 with 30.75^0C. This increase could be as a result of climate change. An increase in temperature is capable of

increasing evaporation rate and it is also capable of increasing precipitation which might lead to flooding thereby causing destruction and break down of equipment required for electricity generation. This further proves the claim made by Cole, Elliot and Strobl (2014).

Similarly, Salami, Sule and Okeola (2011) who worked on same Kainji dam noted that the value of (Mann-Kendall) was positive which demonstrates an existence of a positive trend that is statistically significant and indicates that an increase in temperature would be noticeable. In view of the above it is important to note that regulating global temperature will amount to checking and maintaining the factors responsible for climate change more seriously as suggested by Salami, *et al.* (2015).

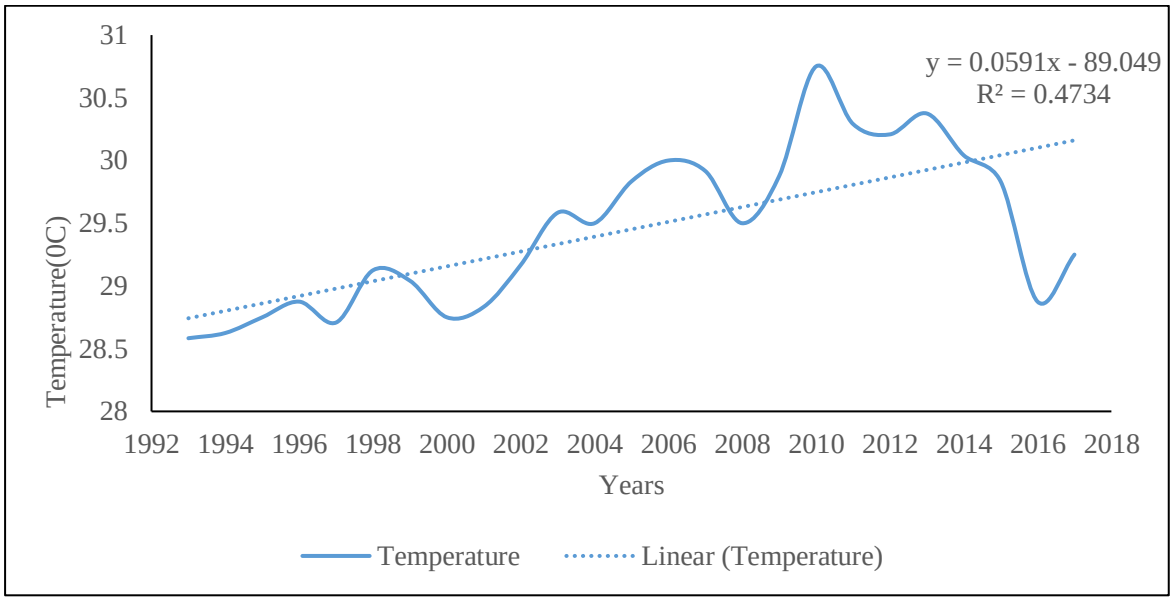

Figure 2: Mean Annual Trend of Temperature in Jebba Dam (1993 to 2017)
Source: Authors' Data Analysis, 2019.

4.3 Analysis of evaporation trend over the study area

The evaporation data collected from the study area was analyzed in order to show the pattern of change for the time frame of study for twenty five years (1993-2017). Figure 3 shows that the evaporation in the study area for the time frame of study has been fluctuating though not too significant because at the year 2002, despite increased evaporation rate of about 19.45mm, which mark the highest amount of evaporation within the study period the station was still able to generate an annual mean power generation of 173869.3mwh which is high when compared with the average amount the station has been generating using the time frame of study. Similarly, the rate of evaporation in the year 2011 dropped sharply to an average of 16.16mm and the power generated was still about 213942.5mwh which is above average. Also, the average evaporation for 2012 is 16.19mm while the amount of power generated in 2012 is among the highest with the figures of about 224478.4mwh in the period of time under study. High rate of evaporation is capable of reducing the amount of water in the reservoir, thereby resulting to shortage in power generation. Though, it can cause increment in precipitation. Cole, Elliott and Strobl (2014) also observed that the greatest loss of potential water resources from hydroelectric facilities comes from the evaporation of water from the surface of reservoirs.

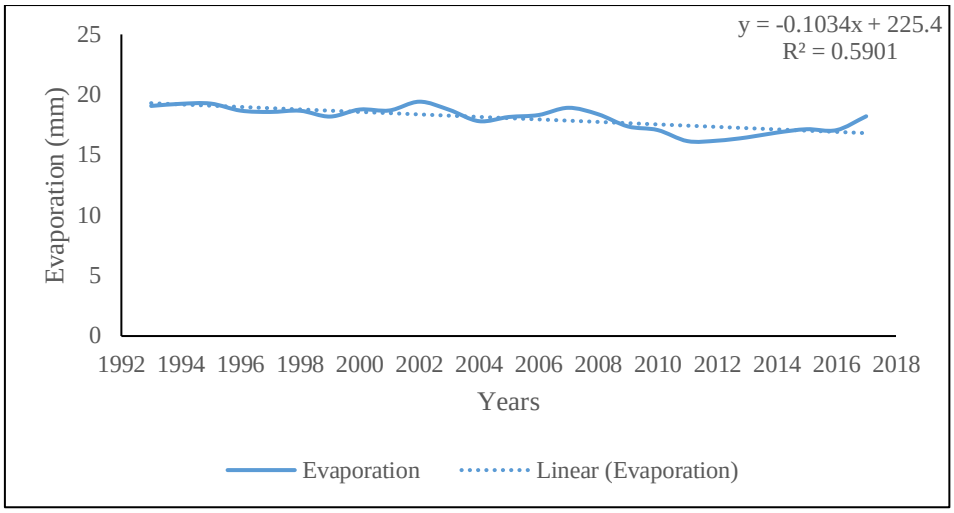

Figure 3: Mean Annual Trend of Evaporation in Jebba Dam (1993 to 2017)
Source: Authors' Data Analysis, 2019.

4.4 Analysis of Trends in reservoir inflow over the study area

The reservoir inflow data collected from the study area was also subjected to time series analysis to show the pattern of reservoir inflow for the time frame of study as shown in Figure 4 shows the Trend of reservoir inflow in the study area for the period of twenty five years (1993-2017).

The graphs provides visual presentation of reservoir inflow pattern which has been within and out of the country. It is important to note that reservoir inflow in Jebba dam is a major factor that determine the amount of power generated. In river Niger in Jebba we have two patterns which brings about reservoir inflow. In the months of May to October precipitation in the northern parts of Nigeria south of Niamey produces flood that quickly reaches Jebba area with a peak of 4,000- 6,000 m^3/sec in the second flood originates from the rivers headwater region from rivers of high annual rainfall in the Fouta Djallon highlands in Guinea and passes through sub-arid region and deltaic swamps in Timbuktu. These floods lead to high water levels which always give rise to water release at the dam sites which eventually have negative consequences on the study area. The flow regime of the River Niger below the Jebba dam is governed by the operations of the Kanji and Jebba. The study reveals that the reservoir inflow exhibit a negative trend though with various degrees of fluctuation from the year 1993, which record the lowest inflow with about inflow of 714.166. And with much increament in the second year of the study period 1994, with an inflow of 1287.333 and a sudden decrease in 1996, and 1997 with inflow of this 934.6667, and this 915.75 respectively while year 1998 to 2017 exhibit tremendous fluctuation at various levels.

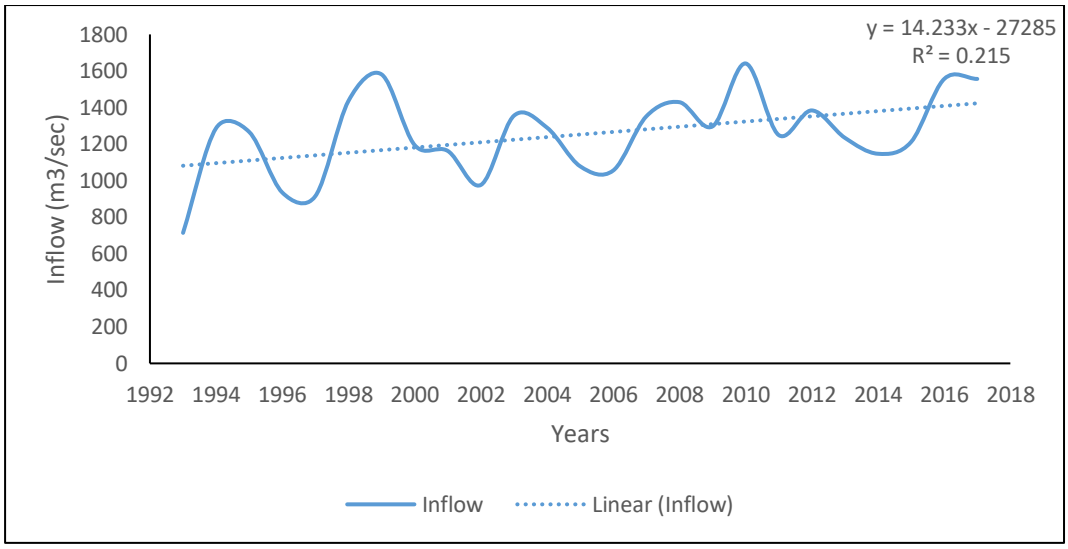

Figure 4.Mean Annual Trend of Reservoir Inflow in Jebba Dam (1993 to 2017)
Source: Authors' Data Analysis, 2019.

4.5 Analysis on the Effect of Weather Variables (Evaporation, Rainfall, and Temperature) on the Reservoir Inflow Pattern

Table 1: Correlation between Rainfall, Temperature and Evaporation on Reservoir Inflow

Variables		Rainfall	Temperature	Evaporation
Reservoir Inflow	Pearson Correlation	.467*	.301	-.326
	Sig. (2-tailed)	.019	.144	.112
	N	25	25	25

* .Correlation is significant at the 0.05 level (2-tailed).

Table 1 show that the correlation between rainfall and reservoir inflow is 0.467* this shows that there is a positive significant relationship between rainfall and reservoir inflow which signify that an increase in rainfall will lead to increase in the amount of water which will be available for energy generated and vice versa.

Temperature also shows it in positive direction with the r value between temperature and reservoir inflow in the study area been 0.301. This implies that it is positive but not very strong at 0.05 level of significant and changes in temperature since climate change will certainly increase global air temperature, considerable regional impacts on the availability of water resources will occur concerning quantity and seasonality (IPCC, 2007b). At first glance, increased global precipitation would appear to suggest more water available for hydroelectric power production. However, higher temperatures will lead to increased evapotranspiration levels thus reducing the runoff (Harrison *et al.*, 1998).

Lastly table 1 evaporation shows it have strong negative correlation relationship with reservoir inflow at 0.05 level significant as the r value between them is -0.326 which indicate a strong

negative relationship between evaporation and reservoir inflow. This means an increased in the amount of evaporation will lead to decrease in the reservoir inflow but not statistically significant.

4.6 Analysis of mean monthly inflow and mean monthly outflow

The summary of mean monthly reservoir inflow, and outflow on the study area is presented in figure 5 and figure 6 respectively during the 25years of the study. The peak reservoir inflow occur during the month of September which is 2058.2 m3/s and October with 1989.84m3/s, and the low flow occur during the months of July and June with values of 843.16m3/s and 897.28 m3/s respectively, also from January to may, august and November, December exhibit fluctuations across the months

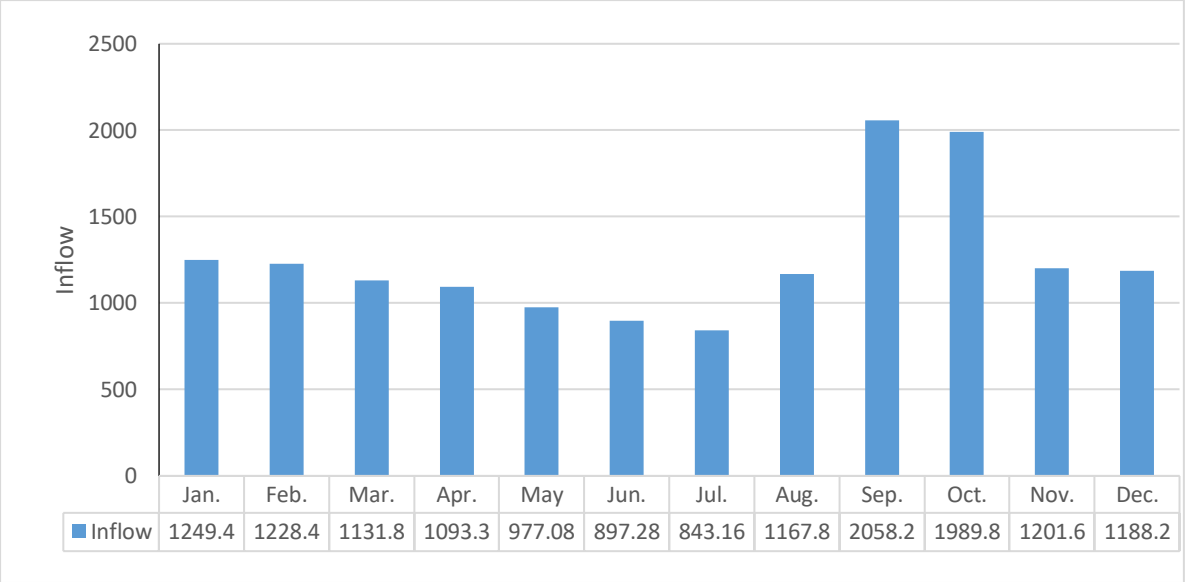

	Jan.	Feb.	Mar.	Apr.	May	Jun.	Jul.	Aug.	Sep.	Oct.	Nov.	Dec.
Inflow	1249.4	1228.4	1131.8	1093.3	977.08	897.28	843.16	1167.8	2058.2	1989.8	1201.6	1188.2

Figure 5: Mean Monthly Trend of Reservoir Inflow in Jebba Dam (1993 to 2017)
Source: Authors' Data Analysis, 2019.

While reservoir out flow record it peak in the month of October with 2037.04 m3/s and September 1949.24 m3/s respectively and the lowest reservoir out flow was on the month of July 842.88m3/s and various fluctuation across the remaining months from January, to December as shown in figure 6

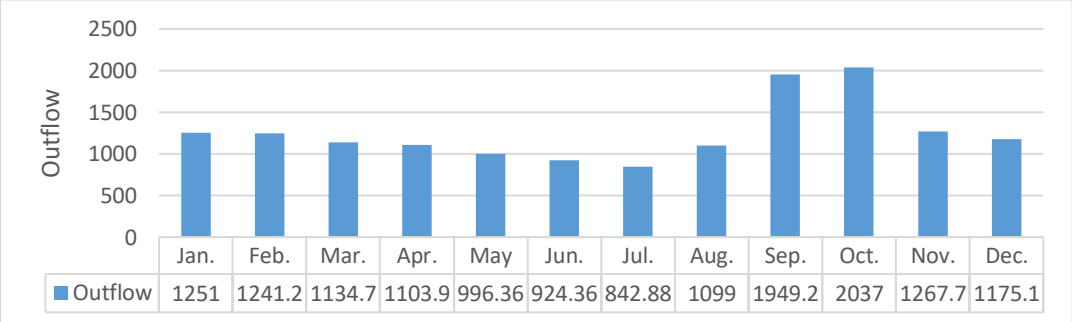

	Jan.	Feb.	Mar.	Apr.	May	Jun.	Jul.	Aug.	Sep.	Oct.	Nov.	Dec.
Outflow	1251	1241.2	1134.7	1103.9	996.36	924.36	842.88	1099	1949.2	2037	1267.7	1175.1

Figure 6: Mean Monthly Trend of Reservoir Outflow in Jebba Dam (1993 to 2017)
Source: Authors' Data Analysis, 2019

4.7 Analysis of mean monthly energy generated

The mean monthly energy generated was obtained after analysing data on the amount of energy generated and used to plot the graph in figure 7, various degree of fluctuation are observed. From January to February, March and April with an average mean of 226278mwh, 207603mwh, 273724mwh, and 197979mwh, respectively. The month of May with 183595mwh, marks the period of decline in the amount of energy generated to the month of July with an average of 155098mwh which is the lowest as the study reveals. While the month of June generates 162045mwh Although the month of August with a mean of 195274mwh marks the period of increase in energy generation and this increase continues to September, with October, and a down word decrease from November to December having an average of 249887wmwh, 266122mwh, 223790mwh, and 218711 respectively. And the months with highest amount of energy generation accordingly are march, October, September, November, January, This is so because of the inflow pattern of the Jebba reservoir which is as a result of the river flow regime characterized by two distinct flood periods occurring annually, namely the white and black floods. The black flood derives its flow from the tributaries of the Niger outside Nigeria (flows from October-May, though the flow will have been drastically reduced in May). It arrives Jebba reservoir in November while the White flood is a consequent of flows from local tributaries especially the Sokoto-Rima and Malendo River systems. The White flood is heavily laden with silts and other suspended particles (flows from June to September) and arrives Jebba in August. So the low flow period in Jebba reservoir is between April and July of each year and April is the beginning of the wet season period in the study area. This must have contributed to the low amount of power generated during the April to July period.

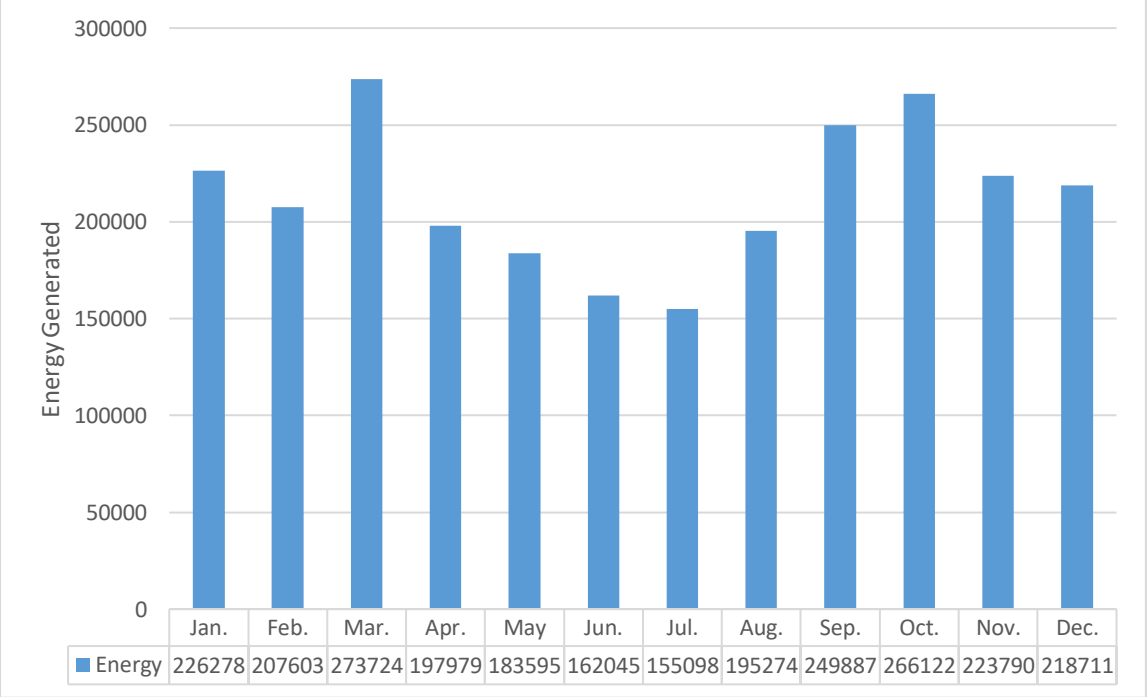

Figure 7: Mean Monthly Trend of Energy Generated in Jebba Dam (1993 to 2017)

Source: Authors' Data Analysis, 2019

4.7 Correlation Between Reservoir Inflow and Outflow on the amount of energy generated

The effect of reservoir inflow and out flow patterns on amount of energy generated was assessed using the Pearson's Product Moment correlation co-efficient using SPSS version 20, software package at 0.05 level of significance and result presented in table 2**.**

Table 2: Correlation Between Reservoir Inflow and Outflow on the amount of power generated

Variables		Reservoir Inflow	Reservoir Outflow
Energy	Pearson Correlation	.637*	.634*
	Sig. (2-tailed)	.001	.001
	N	25	25

* .Correlation is significant at the 0.05 level (2-tailed).

Table 2 shows that reservoir inflow and the amount of energy generated have correlation of 0.637* The result shows a significant positive relationship at 0.05 level of significance. This implies that a change in reservoir inflow will definitely affect the amount of energy generated. This findings is in agreement with Jimoh (2008), who revealed that reservoir inflow in Kainji dam is a major factor that determines the amount of energy generated because rainfall and inflow covering 4,000 km and over nine countries across West Africa is being received at the dam.

Lastly From table 2 also shows the r value between the reservoir outflow and amount of energy generated is 0.634* the result shows a significant positive relationship at 0.05 level of significance which means that it is a strong positive relationship, that implies the more the reservoir outflow the more amount of energy generated since the reservoir outflows is crucial to reservoir balance, the reservoir useful life, as well as reservoir discharge. And the amount of electricity to be produced by a hydropower facility will mainly depend on the volume of water passing through the turbine in a given amount of time, the water head and efficiency of the turbine. While the fluctuations in the quantity and timing of river discharge rate affects much the production of hydroelectric power (Koch, *et al.,* 2011).

5. Conclusion

Hydropower generation is highly dependent on available water resources. The impact of rainfall, temperature, evaporation, variability has a direct impact on reservoir inflow which in turn have much effect on amount of electricity generation. This study examined the historical rainfall, temperature, evaporation, reservoir inflow, and outflow data across twenty five years in jebba reservoir to understand specific trends over time. The study also examined the discharge irregularities of the Jebba Reservoir from 1993-2017 as way to contextualize the implications of climate variability on the performance of hydropower plants.

Weather variables (rainfall, temperature, evaporation,) and the hydro meteorological parameters (reservoir inflow, reservoir outflow) within Jebba Dam were subjected to multiple

analyses. The trends of the weather variables and hydro parameters for the time frame of study were shown using trend line. Rainfall, temperature, shows an increasing trend, except for evaporation which shows a downward decrease while the reservoir inflow and outflow pattern show a steady fluctuation in the movement of the flow sometimes increase and decrease trend. Mean while all the variables and the parameters exhibit fluctuations at various levels while statistical analysis revealed that there is increased electricity generation during the dry season than the rainy season. However, the amount of energy generated in March, August, September, and October is high and can be comparable to the amount generated in the dry season months. Pearson correlation co-efficient shows that reservoir inflow and outflow have significant relationship with the amount of energy generated, while rainfall also have a significant relationship with the amount of reservoir inflow temperature have little significant relationship with the amount of reservoir inflow and evaporation have negative relationship to reservoir

References

Amos T. K., Chukus, J., Diji, K. N., Yacob, M., Daniel, O., and Komlani, A. (2016). Multiyear rainfall and temperature trends in the volta basin and their potential impact on hydropower generation in Ghana. Available at www.mdpi.com journal/climate.

Bekoe, E.O. and Logah, F.V. (2013). The impact of droughts and climate change on electricity generation in Ghana. *Journal of environmental Sciences,* vol (1): 13,13-24. Available online at www.mhikari.com

Berga, L., Buil J.M., Bofill, E.De cea,) C Garcia Perez,). A, Manueco, G., Polimon J., Soriano, A and Yague, J (2006). Dams and reservoirs societies and environmental in the 21st century. In proceeding of the international symposium on dams in societies of the 21st century, Barcelona Spain, 18 June 2016 London. Tayior and Francis group.

Cole, M.A., Elliott, J.R. and Strobl, E.C. (2014). Climate Change Hydro-dependency and the African Dam Boom, *Proceedings on Climate Change Workshop*. Department of Economics, University of Birmingham, United Kijngdom

Gleick, H.P. Cooley, H., Cohen, M, Morikawa, M., Morrison, J, and Palaniappan, M. (2009). The world's water 2008-2009: the biennial report on fresh water resources. Island pr, washington, D.C

Harrison, G, P., Whittington, H.W., Gundy, S.W. (1998). Climate change impacts on Hydroelectric power inproc univ power ENGCONF. 19998sep 1:391-394

ICOLD (International Commission on Large Dams) (1998). World register of dams Paris ICOLD. International environmental and social panel of experts for Laos Nam thennis multipurpose project. Report No 11-23 February 2007

IPCC (2007b). Climate change: the physical science basis contribution of working Group 1 to the fouth Assessment Report of the intergovernmental panel on climate change; IPCC cambridge UK.

Jimoh, O.D. (2008). *Operation of Hydropower Systems in Nigeria.* Department of Civil Engineering Federal University of Technology, Minna Nigeria

Kachaje, O. Kasulo V, and Channla G. (2016). The potential impacts of climate change on hydropower: An assessment of Lujeri micro hydropower scheme, malaui Africa *Journal of environmental science and technology vol.*10 (12) pp 476-484

Koch F, Prasch M., Bach, H., Manser, W., Appel, F., and Weber, M. (2011). How will hydroelectric power Generation Develop under climate change scenario? A case study in thse upper Danube Basin.Energies

Salami, A.W. and Olukami, D.O. (2002). Assessment of impact of hydropower dams reservoir outflow on flood regime Nigeria experience *Journal of environmental hydrology*, vol.16 no 2: 62-92

Salami, A.W., Mohammed, A.A., Adeyemo, J.A. and Olalokun, O.K. (2015). Assessment of Impact of Climate Change on Runoff in lake basin using statistical methods *International Journal of Water Resource and Environmental Engineering.* Vol (7) 2.716 available at www.academicjournal.org/ijwree

World Commission on Dams (2000). Dams and development. A new framework for decision making earthscan publication ltd London and sterling, VA.

World Bank, 2006. Reengaging in agricultural water management challenges and options, washington, D.C

Influx of Foreign Water Borehole Drilling Rigs into Nigeria: a Blessing or Curse?

[1]Ameh, I. M., [1]Amadi, A. N. [1]Unuevho, C. I., [2]Okunlola, I. A and [3]Shaibu, I.

Corresponding Author's Email Address:geoamehmark@gmail.com
Phone: +2348032400236
[1]Department of Geology, Federal University of Technology, Minna.
[2]Al-Hikma University, Ilorin, Nigeria.
[3]Department of Geology, Federal University, Gusua, Zamfar

Abstract

Nigeria in recent times has continued to witness the influx of foreign multinational drilling companies into the country. The multinational water borehole drilling companies are currently in our country in their numbers. They have continued to carry out their drilling activities without supervision from any quota. Our young geologist, hydrogeologist, geophysicist and water engineers have remained unemployed. Little is done on groundwater development by government and non-governmental organisations saddled with the responsibility. There is an increase in the numerical strength of hydrogeologist, geophysicist and water scientist and engineers within the country as more than 20 institutions of higher learning turn out graduates in their hundreds every year. It is sad to say, while we have qualified professionals and well trained graduates in search of job opportunities, these foreign hydrogeology related companies have deliberately refuse to employ Nigerian geologist and hydrogeologists except as casual staffs. This makes one conclude that there exist a high level of contemptuous disregard for Nigerian laws by these foreign hydrogeological companies and also the relevant law enforcement authorities within the country are not leaving up to their responsibilities in penalizing such illegal act. As at this moment the unprofessional, deliberate, manipulative and explosive activities of the multinational water borehole drilling companies as it affect the hydrogeology profession in Nigeria have remained unchecked.

Key words: Multinational drilling companies, hydrogeologist and unprofessional practices.

Introduction

Nigerian is the most populous black nation in the world and one of the fastest growing nations in the African continent in particular and the world in general. The demand for potable water is quite high in response to increase in human population (Amadi *et al.*, 2017). To bridge the gap in water supply and demand, it is crucial that wells/boreholes are delivered in a cost effective manner. Cost effectiveness does not necessarily mean cheaper boreholes but rather optimum value derived over long term compared to money invested. This should result in boreholes continuing to function through their designed lifespan of 20 to 50 years (Olabode and Bamgboye, 2013).

There is an increase in the numerical strength of hydrogeologist, geophysicist and water scientist and engineers within the country as more than 20 institutions of higher learning turn out graduates in their hundreds every year. The hydrogeological sector of Nigerian has witnessed the influx of foreign water borehole drilling companies, a development which ordinarily should be a plus to the hydrogeologists, but instead, what is obtained leaves one in doubt. On the contrary, majority of these foreign companies do not contribute significantly to the hydrogeology profession in Nigeria. The aggregate drilling companies coming into the country ideally should be a major source of revenue for the country through the Ministry of Water Resources via the National Water Resources Institute (NWRI), Standard Organisation of Nigeria (SON), Council of Nigerian Mining Engineers and Geoscientists (COMEG) and other relevant government agencies.

One of the fundamental benefits of foreign investment should be technology transfer (Lukeman, 2015). It is sad to say, while we have qualified professionals and well trained graduates in search of job opportunities, these foreign hydrogeology related companies have deliberately refuse to employ Nigerian geologist and hydrogeologists except as casual staffs (Plate I). An average of 20 personnel is what an average water drilling company is supposed to engage. These employees consist of professionals, administrative staff, drivers, security and cooks among others. Against this, the existing foreign drilling companies which are now numbering up to 150 have deliberately refused to engage indigenous professionals, you can now imagine the number of graduate that should have been employed. Instead, these foreign companies under the pretence of visitation, tourism visas or work permits bring in their nationals to take up relevant positions at the expense of Nigerian professional hydrogeologists (Lukeman, 2015). Most times on the expiration of their visa duration they are returned back to their country only to be replaced by a new set of their nationals. Permit me to say is that the salaries of these nationals working in Nigeria are been paid to their families back in their home countries, living them with little or no money to put back into the Nigerian economy from where the money is been generated.

Plate I. Drilling Operations by Artisans

One wonders why this kind of dubious, callous and malicious practice by these foreign companies has remained unchecked by the agencies of government responsible for the correction of such anomalies. Despite the huge income these foreign companies make from water borehole drilling in Nigeria, little or nothing is put back into the economy by them. As a matter of fact, most of the materials the used are imported from their country of origin even when we have them available in our country.

This makes one conclude that there exist a high level of contemptuous disregard for Nigerian laws by these foreign hydrogeological companies and also the relevant law enforcement authorities within the country are not leaving up to their responsibilities in penalizing such illegal act.

Recently investigation reveals that averages of 5 boreholes are drilled daily in many states of the country underlain by Basement Complex. For the past four years borehole drilling rigs with the capacity of drilling up to 300m depth in Basement Terrains have found their way and some are still finding their way into the country in their numbers. This is coupled with the fact that few indigenous water borehole drilling rigs available cannot attain reasonable drill depth recommended by professionals most times in the basement areas. This has given room to the influx of foreign drilling rigs invading the country.

The expatriate quota administration which should have taking care of the expatriate quota position and monitoring of expatriate quota to be jointly carried out by the Interior Ministry and the Nigerian Immigration Service has not been effective in the hydrogeologic sector. The local content initiative make room for indigenous professionals; that for every expatriate

position, there must be at least two Nigerian with relevant basic academic qualification understudying the position held by the expatriate (Lukeman, 2015).

Aim

The aim of this study is to unravel the unchecked, unprofessional, deliberate manipulative and explosive activities of the multinational water borehole drilling companies as it affect the hydrogeology profession in Nigeria.

Code of Conduct and Ethics

Professionally the activities of these drilling companies is worrisome, considering the fact that professional ethics to be considered before, during and after borehole development are often deliberately been ignored. The Nigeria Code of Practice for Water Well Construction (Nigerian Industrial Standard NCP 027:2010) approved by the governing council of SON clearly spells out best practices for drilling sustainable boreholes. According to unofficial report none of these current multinationals companies in the country are in compliance with this code and little or nothing is been done to correct the wrong.

Pre-drilling Geophysical Investigation

Pre-drilling geophysical investigation is a prerequisite to drilling activities. It enables one to locate a feasible point(s) for groundwater exploitation. The formation type, aquifer type and drill depth are some of the inferred products of geophysical investigation. In Nigerian most often the electrical resistivity method is mostly used for groundwater investigation, employing simple arrays of Wenner or Schlumberger.

The case is not the same with most of the multinationals carrying out drilling activity in Nigeria. In difficult terrains they just prefer drilling alone without involving themselves in pre-drilling geophysical investigation, so as not to take any responsibilities for abortive boreholes. In areas were groundwater are easily accessible at proximate depth they unprofessionally used the 'water witching' method, using brass or copper lines (Plate II). This unconventional and deceptive kind of survey has no scientific base as the principle behind the survey cannot be defined. No data is generated during the survey; therefore reference cannot be made to any of such manipulative practice, courtesy of the multinational water drilling companies.

Plate II. 'Water witching'

Borehole Drilling

The major functional area of these multinational companies is the drilling aspect which most of them refer to as '*punching*', this is due to their possession of modern rigs with mounted compressor which have the capacity of drilling up to 300m in the basement terrain (Plate III).

Most of the foreign drillers are not licensed by the NWRI as specified by the code of conduct, and to the best of our knowledge no penalties has been visibly melted on any of the companies in accordance with provision related to breach of grant of license under rules made pursuant to the code of practice. The requirements for water well drilling as specified by the code of practice is not even known by these multinationals, such as the siting distance requirement as specified in the code and shown in Table 1. The most frequently problem associated with the current multinationals are drilling without well design, record keeping, sample logging and proper development.

Plate III. Borehole Drilling Rig

Table 1. Minimum Sitting Distance Requirements for Standard Well Construction (Nigerian Industrial Standard, 2010)

Separation of Well from	**Minimum Separation Distance (m)**
Water Supply boreholes	50
Hand dug water wells	20
Septic drain field	35
Septic tank	20
Drain field of system with more than 10,000L/day of sewage inflow	100
Permanent building or structure	3
Livestock pen	75
Streams, canals, irrigation ditches or laterals, and other permanent, temporary, or intermittent body of water	20
Approved solid waste dump including burial ground	1000
Coastlines	1000

Well Design and Well Development

Well development as defined in the code of practice for water well construction is "the act of bailing, jetting, pumping or surging water in well to remove drilling fluids, fines, and

suspended materials from within the well screen, gravel pack, and aquifer to establish the optimal hydraulic connection between the well and the aquifer" (Figure 1).

The current practice of the multinational drillers does not put into practice this well development code as stated above. The only practice visible in site from these drillers is blowing or air lifting with air compressor which in most cases hardly exceeds 20 minutes, not minding weather the hole is clean or not they pull out their equipment unchallenged and proceed to continue in another site. Grouting of well is not been practiced by these drillers not to talk of approved grouting materials. Pumping test of no kind is performed after drilling because hydrogeologists and water engineers are not often involved in the development processes.

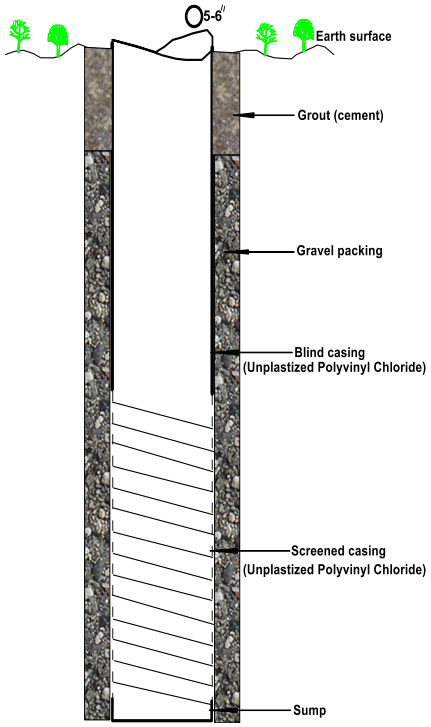

Figure 1. Well Design for Basement Complex Terrain

.

Gravel Pack Design

The major reason behind water well gravel packing is to ensure that optimal efficiency of water well completed in any aquifer is reached. Under section 5.8.1 of the code of practice for water well construction, it is stated that "the gravel used in gravel-packed wells shall come from clean sources and shall be thoroughly sieved, washed and disinfected before being placed in the well. Under no circumstances shall crushed rock and/or laterite be used as gravel pack material".

The above is not in view with the current type of foreign drillers that we have in the country. Crushed rocks are not only been used by these set of driller but weathered crushed rocks and sometimes the cuttings from the drilled holes are being pushed back into the annulus as grave pack materials.

With the inappropriate use of crushed rock without known average specific gravity and uniformity coefficient, disinfection of the gravel with a free chlorine residual of at least 50ppm as specified in the code of practice is not being carried out by these companies (plates IV and V).

It is noteworthy that many younger hydrogeologists are asking many pertinent questions that have remained unanswered. Where do we go from here?

Plate IV. Granite Chippings for gravel packing. Plate V. Inappropriate Gravel packing of a borehole

Professional Bodies

The drilling business is not unconnected with the activities of government and non-governmental professional bodies and institution such as Council of Nigerian Mining Engineers and Geoscientist (COMEG), National Water Resources Institute (NWRI), Nigerian Association of Hydrogeologist (NAH) and Nigerian Association of Hydrological Sciences (NAHS) among others. All these associations and agencies of government are responsible to

the public in discharge of their professional duties, for instance rule 6 of COMEG clearly state the responsibility of the function of its members to the public;

The inadequacy and short coming of our professional bodies to defend and protect our professional practice has given rise to unprofessionals (quacks) to dominate and to an extent

Council of Nigerian Mining Engineers and Geoscientists (COMEG)

Rule 6: Responsibility to the public

6.1 In discharging his/her responsibility to his/her employer and to the profession, a member shall have full regard to and protect the public interest as much as possible.

6.2 A member shall maintain dignity and interest in the welfare of the community and shall endeavour to assist the public to arrive at a correct general understanding of the technical phases of issues of public interest related to his/her discipline. He/she shall discourage and challenge every untrue, unfair and exaggerated statement on technical subjects especially when such statement leads to uneconomic public enterprise.

6.3 A member shall promote public appreciation of the profession through advancing the state of knowledge in his/her own efforts and by his/her encouragement of sound technical training

control the drilling business in Nigeria (Olasehinde and Amadi, 2009). Unions and associations such as; The Borehole Drillers Association of Nigeria (BODAN) and Association of Water Well Drilling, Rig Owners and Practitioners (AWDROP) have unapologetically taken up the responsibility of the professional bodies. Sad to say is that some so called professionals have comfortably aligned them self's with this unions.

Conclusion and Recommendations

The multinational water borehole drilling companies are currently in our country in their numbers. They have continued to carry out their drilling activities without supervision from any quota. Our young geologist, hydrogeologist, geophysicist and water engineers have remained unemployed. Little is done on groundwater development by government and non-governmental organisations saddled with the responsibility.

It is high time the Nigerian Association of Hydrogeologists and other agencies of government saddled with the responsibility of water resources in Nigerian wake up and hear the cry of younger hydrogeologists and water engineers watching the deterioration of the highly exalted profession before their own eyes is unacceptable by the young geoscientist.

Reference

Amadi, A.N., Olasehinde, P. I., Obaje, N.O., Unuevho, C.I., Yunusa, M.B., Keke, U. and Ameh, I.M., (2017). Investigating the Quality of Groundwater from Hand-dug Wells in Lapai, Niger State, North-central Nigeria using Physico-chemical and Bacteriological Parameters. Minna Journal of Geoscience, 1(1), 77 – 92.

Council of Nigerian Mining Engineers and Geoscientists (COMEG), (1990). Code of conduct and ethics for professionals registrable with the Council of Nigerian Mining Engineers and Geoscientists.

Lukeman, A. O., (2015). The Influx of Foreign Quarries, *A blessing or curse*? The Rock Post. Issue 2, 70-72.

Nigerian Industrial Standard, NCP 027:2010, (2010). Code of Practice for Water Well Construction, ICS 23.040.10. Standard Organisation of Nigeria.

Olabode, O. T., and Bamgboye, O. A., (2013). Why Borehole Drilling and Construction Projects Fail. A paper presented at a seminar organized by the Association of Water Well Drilling Rig Owners and Practitioners (AWDROP) at Kakanfo Inn, Ibadan.

Olasehinde, P. I. and Amadi, A. N., (2009). A review of Borehole Construction, Development and Maintenance Techniques around Owerri and its Environd, Southeastern Nigeria. *Journal of Science, Education and Technology*, 2(1), 310 – 321.

Trend Dynamics of Rainfall on Vegetation Pattern over Mokwa Local Government Area of Niger State, Nigeria

***[1]Umar A., [1]Muhammed M. and [1]Suleiman M. Y.**

[1]Department of Geography, Federal University of Technology Minna, Niger State
*ahmedumaru4@gmail.com
ummubahiyya@futminna.edu.ng
Suleym080563@gmail.com
* Corresponding author

Abstract

Over the years, the rainfall trend couples with urbanization as a result of increase in population have been going on in the study area. The increasing population and demand for land is threatening the existence of vegetal cover which demands effective measurement and understanding of the health dynamics of vegetal cover in the study area. The study analyses trend dynamics of rainfall on Vegetation pattern over Mokwa Local Government Area. Gridded satellite daily rainfall data for the periods of 1987-2017 and data from remote sensing images for 1987, 2002 and 2017 were extracted and used. The satellite image was used for Land Use Land Cover (LULC) change and Normalized Difference Vegetation Index (NDVI) analysis, while gridded satellite data was used for Standardized Precipitation Index (SPI) and simple linear regression was used to depict correlation in rainfall and vegetation. Findings revealed that the year 1994 had the highest positive value of SPI (1.62) and lowest value in 2000 (-2.75), four years were observed to be above normal wetness with five years below normal dryness. The NDVI value was observed to be between 0.81 and -1 in 1987 but decreased to between 0.405 and -0.12 in 2017. The results of LULC change show a decrease of 15.5% in vegetation cover from 1987 to 2017 with an increase of 15.42% in non vegetation areas and 0.13% increase was observed in the water body during the study period. The linear regression of R^2=0.743 indicated a positive relationship between rainfall and vegetation cover. It was concluded that the spatial trend in rainfall are not spatially distributed along longitudinal or latitudinal directions. However vegetation cover was found to be decreasing throughout the study period. The study recommends further investigation on urbanization and agricultural activities responsible for vegetation dynamics in the study area.

Keywords: Dynamics, Land Use, Rainfall, Trend, Vegetation

1. Introduction

Over the years, the rainfall trend coupled with urbanization as a result of increase in population has been going on in the study area. The increasing population and demand for land is threatening the existence of vegetal cover which demands effective measurement and understanding of the health dynamics of vegetal cover across the country. In recent times, the dynamics of Land use Land cover and particularly settlement expansion in the study area requires a powerful and sophisticated system such as remote sensing and geographic information system (GIS), which provides a general coverage of large areas analysis. The study aimed at analysis of trend in rainfall and Vegetation dynamics over Mokwa Local Government Area (LGA). Land cover pattern of a place is an outcome of natural and socioeconomic factors and their utilization by man in time and space. Studies have shown that there remain only few landscapes on the earth that is still in their natural state. Man's activities on earth have had a

deep effect on the natural environment thus resulting into a non observable pattern in the land use land cover over time. Investigating the state or the amount of vegetation is one of the paramount objectives in the field of land surface related remote sensing applications.

The availability of frequent data that are internally consistent over a sufficient period and provide information on the spatial complexity as well as on the temporal dynamics of vegetation is prerequisite for successful monitoring of vegetation cover (Seiler, 2010). Remote sensing of the vegetation condition is based on the fact that healthy plants have more chlorophyll and therefore absorbs more Visible (VIS) radiation and reflects more Near-InfraRed (NIR) radiation (Rimkus, *et al.*, 2017). High spatial and temporal rainfall trends have been a big problem in monitoring agricultural phenomenon over Africa, because any excessive or deficit of rainfall amount may result to change in vegetation and or failure. It is necessary to emphasize that the vegetation (and hence Normalized Difference Vegetation Index (NDVI) values) response to the meteorological conditions in a given year depends on the geographical region and environmental factors such as vegetation type, soil type and land use (Usman *et al.*, 2013). Poor land utilization practices, especially in subsistence farming and nomadic pastoral economies in the majority of the African countries have accelerated the loss of natural vegetation and exacerbated the problem of climate change (Bamba, 2015).

Historical baselines of forest cover are needed to understand the causes and consequences of recent changes and to assess the effectiveness of land-use policies (Kim *et al.*, 2014). There are now more concerns about vegetation changes and its attendant consequences on the environment. It is evident that the Nigerian natural vegetation if not conserved and sustainably managed will lose its natural state (Fashae, *et al.*, 2017). There is therefore an urgent need to create awareness about the consequences of these changes and bring a halt to the trend. Also increase in population has resulted in increase in consumption of wood for domestic purposes aggravate the environmental degradation and land use change. Bush burning and uncontrolled grazing are carried out elsewhere in the study area thereby contributing immensely to the vegetation dynamics.

Many methods and in particular various vegetation indexes have been introduced to quantify certain vegetation parameters. However, all of them take into account that vivid green vegetation shows a specific reflection signal in the red and near infrared part of the electromagnetic spectrum (Seiler, 2010). Therefore, in most cases NDVI values are complexly analyzed with meteorological and agro-meteorological drought indicators such as the Standardized Precipitation Index (Gebrehiwot *et al.*, 2011; Gaikwad and Bhosale, 2014; Stagge *et al.*, 2015). For the analysis of LULC change supervised classification developed spectral

signatures of known categories and each pixel allocated to the cover type to which it is most popular. Image classification methods are many, but there is no single "best" method to image classification. However the choice depends on available algorithms within the image-processing software (Horning *et al.*, 2010).Supervised classifications using Maximum Likelihood Classifier (MLC) was used because of its popularity, simplicity and above all its proven high degree of accuracy. The classified land use and land cover maps may contain some sort of errors because of several factors, from classification technique to the method of satellite data capture. This study analyses trend dynamics of rainfall on vegetation pattern over Mokwa LGA of Niger State, Nigeria.

2.0 Study Area

Mokwa Local Government Area (LGA) in Niger state, is located between Longitude 4º45'00" to 5º 45'05'' East and Latitude 8º45' 00'' to 9º 40' 00"North and covers a total land area of 4,338km^2. The population by 2006 national population census is 242,858 with a projected population of 341,200 by 2016 (National Population Commission of Nigeria) (Figure 1).Meteorological research confirms that Rainfall is highly seasonal and controlled by the irregular movement of the Inter-Tropical Discontinuity (ITD). Onset is usually by April/May and cessation in October with an average record of 200 days of rainy days for year with an average mean annual rainfall of 1,300mm (Adefolalu, 1986). However the temperature rarely falls below 20ºC. The wet season average temperature is about 20ºC. The peak is 38ºC in February to March and 35ºC in November to December while the mean relative humidity is 33-83%.The vegetation of the study area falls within the vegetation zone of Guinea Savanna which is a major vegetation zone across Niger state. It consists of wood land and light forest. The common tree found in this zone are; Sheabutter, Neou oil, African locus bean or Niffa, Axle-wood and thinning's piliostigma tree. Agriculture is the main economic activity of the people in the study area.

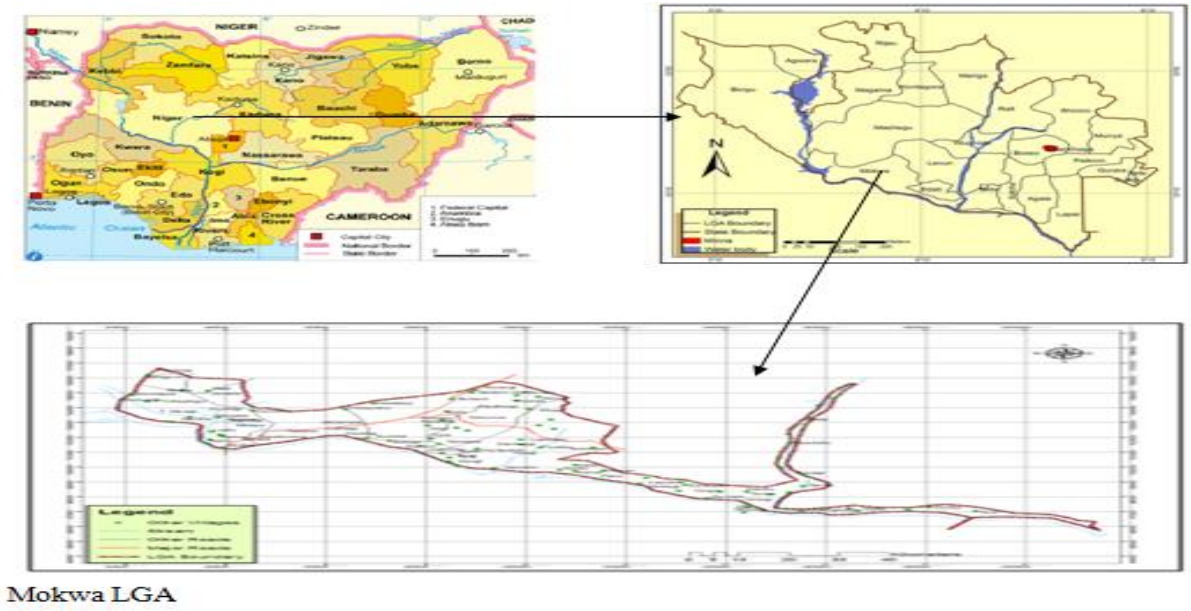

Figure 1 The Study Area (Mokwa Local Government Area, Niger State).
Source: Niger State Geographic Information System (NIGIS)

3. Materials and Methods

3.1 Data Acquisition

The research used daily satellite grid rainfall estimates data and satellite imagery. The data were source from www.globalweather.tamu.edu. The datasets has a spatial resolution of 0.25^0 consisting of three (3) hourly/daily rainfall estimates from 1979 to 2017. LandSat-5 image Thematic Mapper (TM) for 1987, LandSat 7 Enhance Thematic Mapper Plus (ETM^+) for 2002, and LandSat 8 Operational Land Imager (OLI) 2017 all with 30m Resolution, sourced from United State Government via www.usgs.gov were used.

3.2 Methodology

The annual mean rainfall amount for the entire study area data record (1987–2017) were computed and analyzed. The annual rainfall values were computed for each data point from the daily rainfall amount using equations 1.

$$AR = \sum_{n-I}^{d} R \qquad (1)$$

Where, AR is the annual rainfall amount at each data point.

R is the daily rainfall amount at each data point,

d is the number of days, and

I is the months of the year.

n is the total number of years.

SPI is a normalized index representing the probability of occurrence of an observed rainfall amount when compared with the rainfall climatology at a certain geographical location over a long – term reference period.

The Standardized Precipitation Index (SPI) is expressed in the form $\frac{X-\bar{X}}{\sigma}$ (2)

Where σ is the standard deviation

X is annual rainfall for a given period.

$\bar{X}$ is annual mean rainfall for a given period

Negative SPI value represent rainfall deficit (dryness), while positive SPI values indicates rainfall surplus (wetness). The SPI values ranges from -2.00 to 2.00 representing extremely dry and extremely wet respectively. From the mean annual rainfall values from 1987 – 2017, the average rainfall for the study area were computed. For the mapping of spatial pattern of trends from point data, Inverse Distance Weight (IDW) was the interpolation method adopted to monitor the distribution of rainfall which was acquired from nine rainfall data points within the study area. The analysis was done using ArcGIS 10.3 analysis tool. NDVI was calculated as the difference between reflectance in Near Infrared and Visible radiation.

$$\text{NDVI} = \frac{(NIR-VIS)}{(NIR+VIS)} \quad (3)$$

Where NIR is Near Infrared (fourth band of landSat images) and

VIS is Visible band (third band).

The final NDVI products were depicted in the geographic grid with equal latitude and longitude intervals. The NDVI values ranges from -1 to +1. The negative index value can be recorded over the clear water bodies while values are close to 0 over the land without vegetation. The index value equal to 1 indicates perfect growing vegetation conditions. Rainfall and vegetation value were analyzed by the use of simple linear regression. To Examine the LULC Changes over the Study Area from 1987 – 2017 the images were subjected to the following procedures

Image analysis involves Information extraction from satellite imagery which is preceded by Image Pre-Processing steps such as image registration, radiometric correction, image enhancement and display (Rodriguez-Galiano, *et al*., 2012). Image registration is meant to correct image displacement, while radiometric correction is meant to adjust the radiation values to the standard values. Failure to observe them or observance with imprecision may render change detection meaningless.

Image Classification Three land cover types were analysed for this research as adopted by Agbor*et al*., 2012 (Table 1). Supervised classifications using Maximum Likelihood Classifier

(MLC) were used because of its popularity, simplicity and above all its proven high degree of accuracy.

Table 1 Land Use and Land Cover Classification

S/NO	Land Cover Type	Description of the Land Cover Types
1	Vegetation	All Agricultural lands, forest, grasslands, trees, shrub land, natural and semi- natural vegetations
2	Non Vegetation	All residential, commercial and industrial areas, roads, Settlement and infrastructures
3	water Body	Rivers, streams, dams, lakes and ponds

Source: Ahmad (2018)

Accuracy assessments produce information that describes reality on the study area. References (sample) were identified from Google Earth and using a different training site. This were done using Kappa coefficient (k). The kappa coefficient is a measure that considers significantly unequal sample sizes and likely probability of expected values for each class. Mathematically the equation is express in equation 4

$$K = \frac{d-q}{N-q} \qquad 4$$

Where d = total number of cases in diagonal cells of the error matrix,

N = total number of samples.

In order to assess the impact of rainfall trend on vegetation dynamics, the NDVI and SPI values were statistically analysed through the use of simple linear regression to know the level of impacts if there is any in the study areas. The linear regression equation is express in equation 5 as:

$$Y = a + bx \qquad 5$$

Where Y is the dependent variable; x is the independent variable

b is the slope of the line; a is the y intercept

4.0 Results and Discussion

4.1 Results of SPI values for the study area.

The computation of Standardized Precipitation Index for the study area (Figure 2) revealed an increase in rainfall from 1987 to 1996. The year 1994 had the highest positive value of SPI (1.62), while lowest value was in year 2000 (- 2.75), four years (1988, 1989, 1994 and 1995) were observed to be above normal wetness with five years (1999, 2000, 2001, 2011 and 2012) below normal dryness. The temporal trend in rainfall for the study area indicates that the first decade of the study period witness normal wetness of positive SPI value. While the second and

third decade witness an alternate positive and negative SPI value meaning that some years were wet while others were dry.

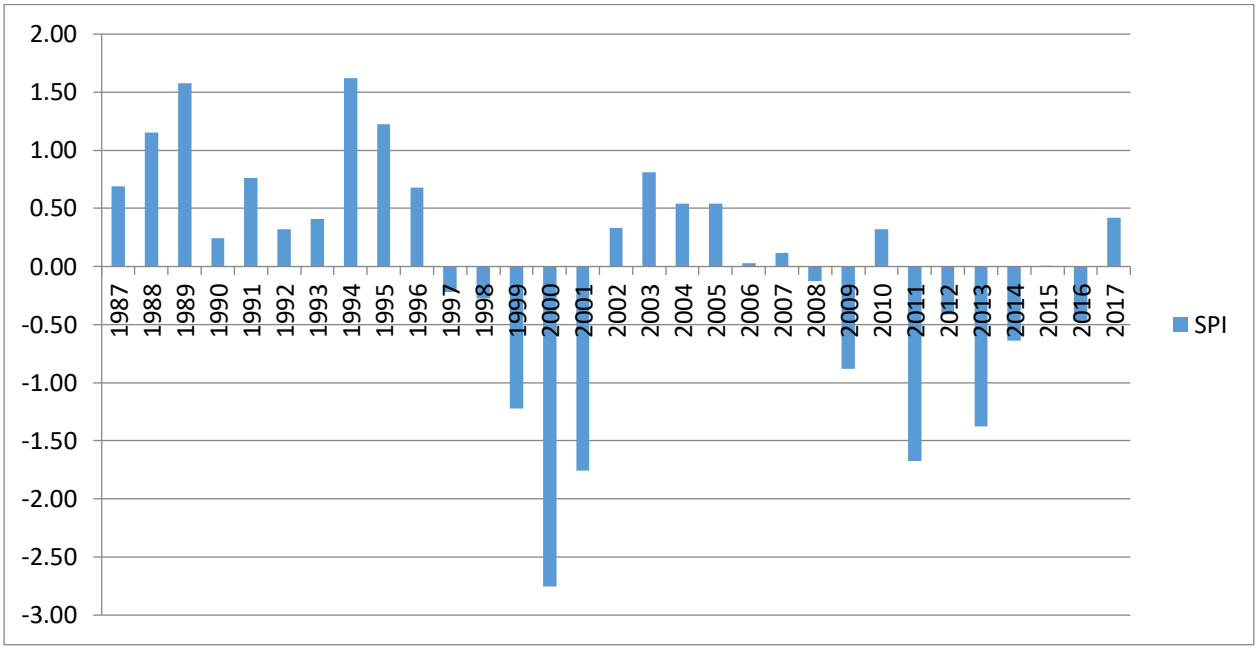

Figure 2 SPI values over the study area

Source: Ahmad (2018)

4.2 The results of spatial trends in mean rainfall from 1987 – 2017 in the study area.

The maps of spatial trend (Figure 3) indicates that the mean annual rainfall from 1987 – 2002 (a) indicates a value of 1500.16mm as the highest occurring in the north – eastern part with the lowest value of 1108.02mm in the north – western parts of the LGA; 2002 – 2017 (b) shows a value of 1275.15mm as the highest occurring in the south – eastern part with the lowest value of 769.08mm in the north – western part of the LGA and 1987 – 2017 (c) revealed a value of 1390.49mm as the highest occurring in the south – eastern part with the lowest value of 946.007mm in the north – western part of the LGA. The spatial trends in annual mean rainfall from 1987-2017 shows a wider range of trend of about 444.483mm. This wider range of trend contributes to the fact that some parts of the LGA may witness wetness while other parts may be witnessing dryness. This trend may be attributed to the large area coverage of the LGA. The spatial trend in rainfall may not be attributed to the longitudinal or latitudinal variation as some area of the same longitude and latitude has different amount of mean rainfall. This signals that there may be other factors like temperature variation contributing to increase in rainfall in such areas. Urbanization and deforestation are visibly taking place in the study area as a result of increase in population as confirm by LULC change analysis.

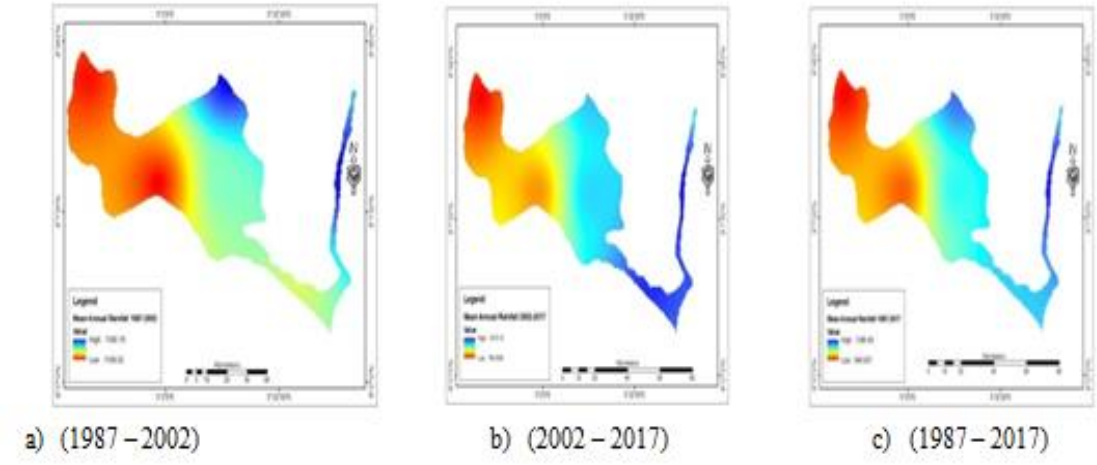

Figure 3 The spatial trends in mean rainfall from 1987 – 2017 in the study area.

Source: Ahmad (2018)

4.3 Results of NDVI analysis in the study area

The NDVI analysis (Figure 4) indicates a value between 0.81 and -1 in 1987 (a). In 2002 (b) the NDVI value was observed to be between 0.52 and -1. It further decreases to between 0.405 and -0.12 in 2017 (c).

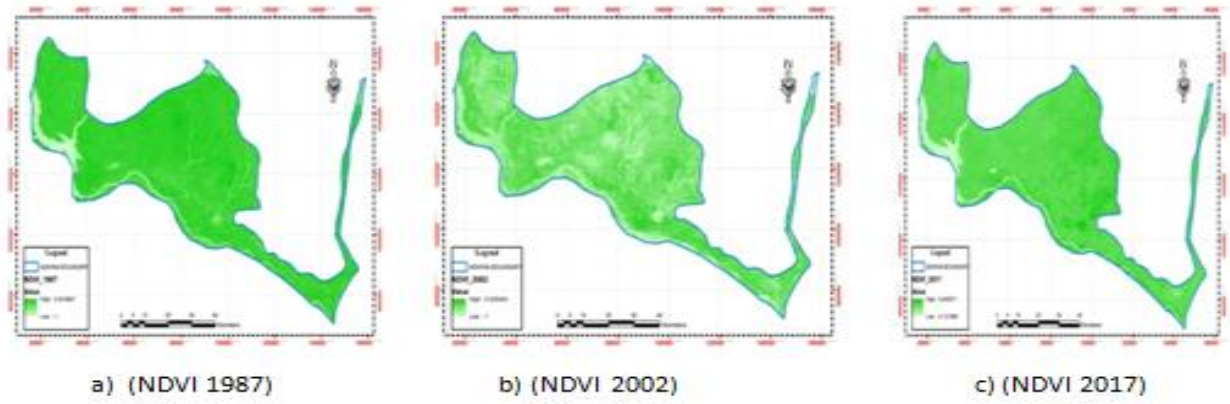

Figure 4 NDVI analyses in the study area

Source: Ahmad (2018)

NDVI values in the analyzed area were determined by the amount of rainfall and other factors such as urbanization, population increase and agricultural activities. On average, the active rainy season in the study area lasts from the end of April or beginning of May until the middle or end of October. The spatial pattern of the NDVI trend is closely related to the spatial trend of rainfall. The NDVI analysis indicates that a high value of NDVI 0.8 in 1987 was drastically decreased to 0.4 in 2017. This high rate of decrease in vegetation cover may not be unconnected to the fact that since late 1990's rapid urbanization as a result of population increase have been going on in the area. The population increase also resulted to mass deforestation in the area as

people compete for fire wood for both domestic and commercial purposes. The rate of deforestation in the LGA took a different dimension in late 2000 as some group of individuals settled around Mokwa – Bokani axis of the local government. These groups of people source their income from fire wood sales in commercial quantity most at time load of trailer for onward movement to other parts of the country. The wide use of charcoal from early 2000 to date has also contributed a lot in time of decrease in vegetation cover. Although government has put in place some agencies to control the trend, however their active control of tree falling has not yielded any positive result.

4.4 The LULC Changes in the study area for 1987, 2002 and 2017

From the various spatial temporal analysis of categorical LULC of the LGA it is obvious that the land use has been changing in size noticeably over the years.

The result of LULC in Table 2 shows a decrease in vegetation cover from 2999.43KM^2 (69.12%) in 1987 to 2615.81KM^2 (60.30%) in 2002 (Figure 5). As the vegetation cover decreases, the non vegetation areas continue to increase from 1008.42KM^2 (23.20%) in 1987 to 1344.78KM^2 (31.00%) in 2002, while Water body was observed to have increase from 330.55KM^2 (7.62%) in 1987 to 376.10KM^2 (8.67%) in 2002. The vegetation cover further decreases to 2326.03KM^2 (53.62%) in 2017, while the non vegetation areas further increased to 1675.33KM^2 (38.62%), however, the water body was observed to have decreases to 336.19KM^2 (7.75%) in 2017. This high percentage of vegetation cover is in agreement with the work of Suleiman, *et al. (*2014), Agbor *et al.* (2012) and Mansur *et al.* (2017) who reported high rate of vegetation cover in most parts of guinea savanna of Nigeria in 1980ce.

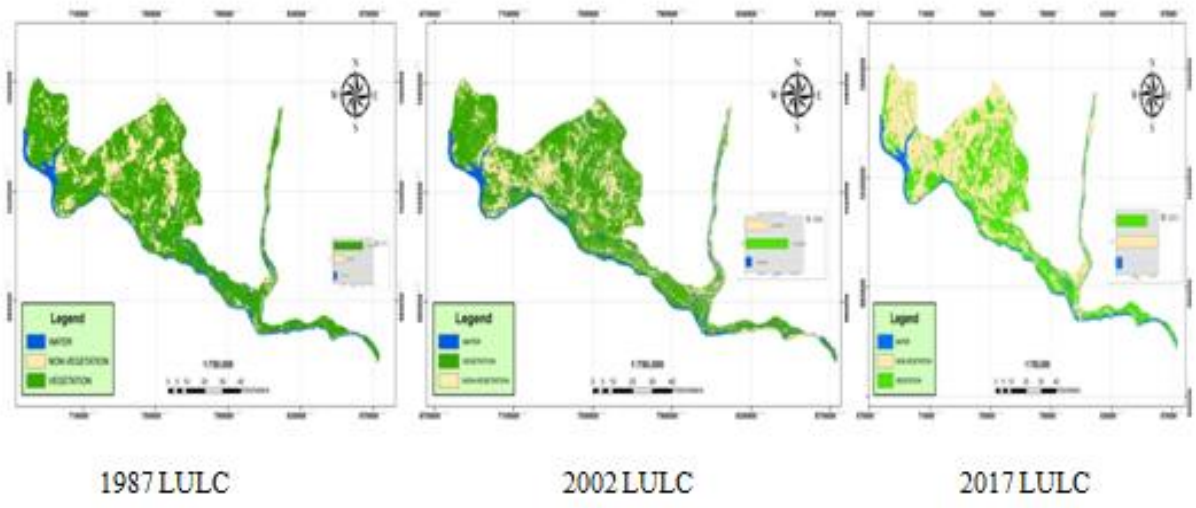

Figure 5 LULC Change analysis in the study area

Source: Ahmad (2018)

Table 2 Summary Statistics of LULC Distribution of Mokwa (1987, 2002 and 2017)

Classification Type	1987		2002		2017		Change	
Area Cover in	(KM^2)	(%)	(KM^2)	(%)	(KM^2)	(%)	(KM^2)	(%)
Vegetation	2999.43	69.12	2617.81	60.3	2326.03	53.62	672.39	15.5
Non Vegetation	1008.42	23.26	1344.78	31	1676.33	38.62	668.92	-15.42
Water Body	330.55	7.6	376.1	8.67	336.19	7.75	5.64	-0.13
Total	4338	100	4338	100	4338	100	1347	

Source: Ahmad (2018)

A decrease of 15.5% was recorded in vegetation class from 1987 to 2017. However increase of 15.42% in non vegetation areas was observed from 1987 to 2017. While 0.13% increase was observed in the water body.

Accuracy assessment of the classified Images of 1987, 2002 and 2017 in the Study Area

The overall accuracies of the classified images (1987, 2002 and 2017) were 77%, 78% and 80% with Kappa coefficient of 0.712, 0.738, and 0.760 respectively.

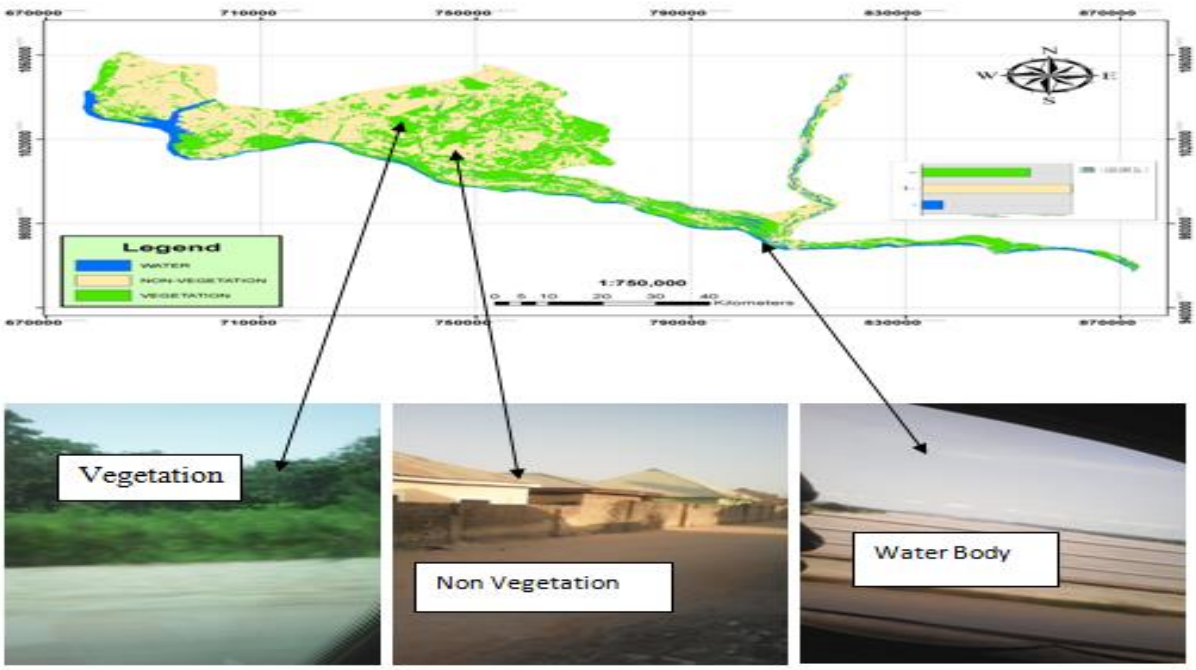

Figure 6 Accuracy assessments of the classified images

Source: Ahmad (2018)

4.5 Results of Linear Regression for the study area.

The linear regression analysis (Figure 7) revealed a value of R^2 = 0.743 which indicates a positive relationship between rainfall and vegetation dynamics which is in agreement with the work of Bamba, (2015) who found linear correlation between rainfall and NDVI to be high in large areas of the savannah region mainly it achieve 0.8 over Ghana and Nigeria. The high values are mainly observed in region where the annual rainfall is around 1000 mm. So the vegetation growing depends directly on rainfall.

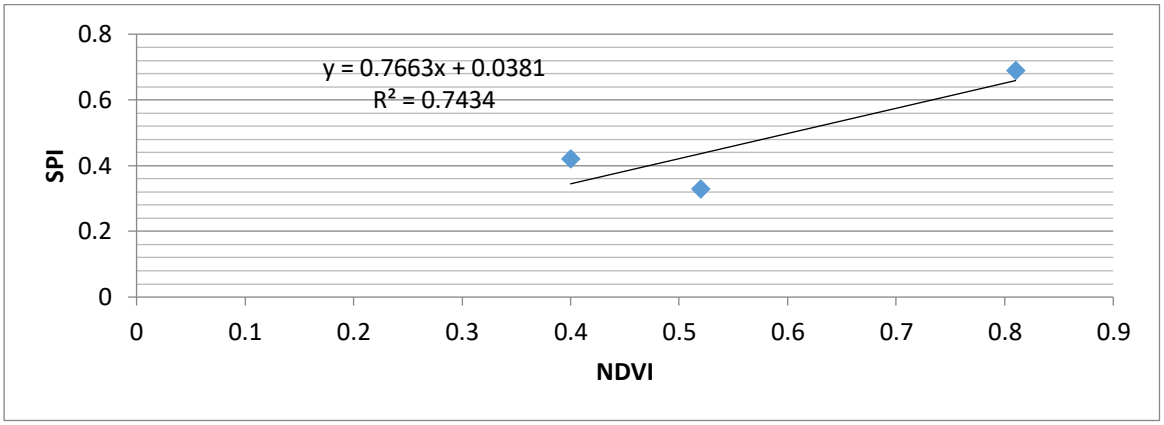

Figure 7 Linear Regressions for the study area.

Source: Ahmad (2018)

5. Conclusion and Recommendations

The study was able to analyze rainfall trend and vegetation dynamics in Mokwa LGA and observe that there has been different pattern for the entire study period. There was a decrease in rainfall in the second half of the study period and a decrease in (NDVI) for that region concurrent with rainfall decrease. The map of spatial trend in rainfall revealed that rainfall over the study area is not spatially distributed. The temporal trend in rainfall shows a positive trend in the first decade of the study period and was characterized by alternation of positive and negative trends in the last two decades of the study period. The NDVI analysis indicates that the vegetation cover over the study area has continued to decrease throughout the study period. Positive linear relationships were observed between rainfall and vegetation dynamics in the study area.

The study recommends further investigation on other factors such as urbanization, population increase and agricultural activities as rainfall alone cannot be responsible for vegetation dynamics in the study area.

The State Ministries of Environment and Agriculture with other relevant agencies should advocate for afforestation practice in the study area so as to reclaim the lost forest.

Urban expansion due to population increase should be checked through re-planning of town so as to fill the undeveloped areas within the town.

References

Adefolalu, D. O. (1986). Rainfall trends in Nigeria.*Theoretical and Applied Climatology* 37, 205-219.

Ahmad, U. (2018) Comparative Rainfall and Vegetation Trend Dynamics in Mokwa and Rijau Local Government Areas of Niger State, Nigeria Unpublished M. Tech Thesis, Department of Geography Federal University of Technology, Minna

Bamba, A., (2015). Land Use Change, Vegetation Dynamics and Rainfall Spatio-Temporal Variability over West Africa. Unpublished Doctor of philosophy Degree Thesis Submitted to the School of Postgraduate Studies, the Federal University of Technology Akure, Nigeria

Fashae, O., Olusola, A and Adedeji, O. (2017). Geospatial Analysis of Changes in Vegetation Cover over Nigeria. Bulletin of Geography. *Physical Geography Series*, No. 13 17-28 http://dx.doi.org/10.1515/bgeo-2017-0010

Gaikwad, Y. and Bhosale, R. (2014). Survey on predictive analysis of drought in India using AVHRR–NOAA remote sensing data, *International Journal of Advance Foundation and Resource Computation.*, 1, 2348–4853,

Gebrehiwot, T., van der Veen, A., and Maathuis, B.(2011). Spatial and temporal assessment of drought in the Northern high - lands of Ethiopia. *International Journal of Applied Earth Observation*, 13, 309–321, https://doi.org/10.1016/j.jag.2010.12.002, 2011

Horning, N., Robbinson, J.A., Sterling, E.J., Turner, W. and Spector, S. (2010). Remote Sensing for Ecology and Conservation: A Handbook of Techniques. Oxford University Press, Oxford, New York

Kim, D.H., Sexton, J.O., Noojipady, P., Huang, C., Anand, A., Channan, S., Feng, M. and Townshend, J.R. (2014). Global, Landsat-based forest-cover change from 1990 to 2000. *Remote sensing of Environment,* 155: 178-193.

Rimkus, E., Stonevicius, E., Kilpys, J., Maciulyte, V. and Valiukas, D., (2017)Drought identification in the eastern Baltic region using NDVI. Earth System Dynamics, 8, 627–637, https://doi.org/10.5194/esd-8-627-2017.

Seiler, R., (2010). Characterisation of Long-Term Vegetation Dynamics for a Semi-Arid Wetland Using NDVI Time Series from NOAA-AVHRR. In: Wagner W., Székely, B. (eds.): ISPRS TC VII Symposium – 100 Years ISPRS, Vienna, Austria, IAPRS, XXXVIII, Part 7B.

Stagge, J. H., Kohn, I., Tallaksen, L. M., and Stahl, K. (2015). Modeling drought impact occurrence based on meteorological drought indices in Europe, *Journal of Hydrology*, 530, 37–50, https://doi.org/10.1016/j.jhydrol.2015.09.039.

Usman, U., Yelwa, S. A., Gulumbe, S. U., and Danbaba A.(2013). Modelling Relationship between NDVI and Climatic Variables Using Geographically Weighted Regression, *Journal of Mathematical Sciences and Applications*, 1, 24–28.

Agro-Climatic Site Suitability Selection for Sugarcane Production in Southern Parts of Adamawa State, Nigeria

Ishaku V. M.[1]* Yahaya T. I.[2]
[2, 1]Department of Geography, Federal University of Technology, Minna, Nigeria
[2]iyandatayo@futminna.edu.ng
[1]mabusa045@yahoo.com
*Correspondent author

Abstract

In this work, agro-climatic factors were used in the selection of suitable sites for sugarcane production in the southern parts of Adamawa state of Nigeria. Eleven local government areas were covered with total area of about 20,739.30 Km.^{2} Data on rainfall, temperature, relative humidity, sunlight, soil, relief and drainage were transformed into spatial datasets and integrated in the process of Weighted Sum overlay in ArcGIS 10.2 and in line with the FAO guidelines on suitability analysis for the sites selection. Following the analysis and integration of the agro-climatic factors used, four degrees of suitability were arrived at, which are, Most suitable, Moderated suitable, Marginally suitable and Not suitable sites for sugarcane production. The final results revealed that, Most suitable sites for sugarcane production in the study area cover total area of about 880.93 Km^2 (that is 4.25% of the study area), Moderately suitable sites cover about 11,808.08 Km^2 (56.94%), Marginally suitable sites cover about 5,927.10 Km^2 (28.58%) and sites that are Not suitable cover about 2,123.19 Km^2 (10.23%). Therefore, sites that are considered good for sugarcane production in the study area (that is Most suitable and Moderately suitable degree of suitability combined) cover about 12,689.01 Km^2. This is about 61% of the total area of study. These sites are vast enough to support production of sugarcane in a quantity that can boost the economy of Adamawa state and the country at large. It is therefore, advised that, the state government as well as all the stakeholders in the business of sugarcane production, should key into this finding with the aim at promoting sugarcane production in the state. The business should be encouraged, by making the environment conducive for both foreign and local investor in sugar production. Experts in the business of sugarcane should be partnered to devise ways of booting the production of sugarcane in the state and that will strengthen the already weak economy base of the state.

Keywords: agro-climatic, site suitability, sugarcane, suitability analysis, spatial data

Introduction

For maximum crop production, especially commercially inclined ones, the knowledge of areas that will be good for the cultivation of the crop in questions is paramount. Sugarcane and any other crop, yield best on a certain climatic environment. Srivastava & Rai (2012) agrees with that, as noted in their words: climate plays an important role in all the phases of sugarcane crop (and of course any other crop). They stressed further that, sugarcane stands in the field for 12-24 months, therefore it passes through all possible limits of weather parameters such as rainfall, temperature, sunshine, and humidity. Consequently, all climatic parameters have significant role in the crop's growth, yield, quality and of course juice content.

The major source of income in Adamawa state is the monthly federal allocation and that is not the best for the state's economy. The state is blessed with vast arable lands that could be used

for agriculture (Federal Republic of Nigeria, 2017). The federal allocation must not blind us from seeing some other potential source of revenue, such as agriculture. Therefore, Adamawa state needs to look into this sector with the aim at augmenting her economic base for the good of the citizens of the state and the country at large. Consequently, in this work, is an effort made in the area of agriculture, to encourage the government and the farmers in the state to invest in the cultivation of sugarcane so as to diversify the state's source of income. The researchers are positive that, by studying the agro-climatic factors and to use them in selecting sites suitability for sugarcane growth in the study area, one of the most important steps would have been taken.

In this study, two objectives were pursued to come up with sites selection for sugarcane production in the southern parts of the Adamawa state. These are: to analysed the major agro-climatic parameters that influence the optimum growth of the sugarcane crop and to come up with a comprehensive sites selection for sugarcane cultivation in the study area.

1. Literature Review

Srivastava & Rai (2012) stated that, sugarcane is a taxa represented by stout, jointed, fibrous stalk of 2-6 m with sugar is a tall perennial grass of the genus *Saccharum* of family Poaceae. Sugarcane is a perennial crop with determinate growth habit; its yield is located in the stem as sucrose and the yield formation period is about two-thirds to three quarters of its cultivated life span (Vooren, 2008). There are six species that are included in the classification of sugarcane. Among the species known are *officinarum, spontaneum, barberi, sinense, edule* and *robustum.* These species survive in both tropical and sub-tropical regions (Tarimo & Takamura, 1998). According to Letstalkagric (2017), sugarcane is used as a sweetener in beverages and various foods. It is also used in making confectionaries, example bread, cakes and biscuits. In the production of alcohol example ethanol, sugarcane is useful too. The by-productions of the processing are used in the following ways: cane residue (bagasse) can be used as fuel, manure or fodder.

The concept, "land (site) suitability" is a measure of how well the qualities of a land unit match the requirements of a particular form of land use (FAO, 1976). Land use evaluation is a procedure that involves a lot of information which is distinguished by its geographical and multivariate character (Daniel *et al.*, n.d.).). Land use suitability assessment provides important reference for planning, planning management, planning implementation and planning evaluation (Lingjun & Yan, 2008). **Methodology**

3.1 Preamble

Both climatic and physical parameters were integrated to achieve the aim of this study. The climatic parameters used were rainfall, temperature, sunlight and relative humidity. However, physical parameters include the soil types, relieve and drainage. These were used based on the fact that, they are the major parameters that have great influence in the growth of the crop. These parameters were converted to spatial datasets in Geographic Information System (GIS) environment and were integrated to select sites that are good for the growth of sugarcane. In the end, quantitative agro-climatic map of the study area showing spatial distribution of the degrees of site suitability for sugarcane production were produced.

Study Area

Adamawa state is one of the states in north eastern Nigeria with its capital Yola. It is one of the largest states in the country and occupies about 36,917 square Kilometres. It is located between latitudes 7°N and 11°N and longitudes 11°E and 14°E. The state has common boundaries with Taraba state in the south-west, Gombe state in the north-west and in the north with Borno state. In the eastern part, the state shares an international boundary with the Republic of Cameroon (Adebayo & Tukur, 1999). However, the study area, that is the southern parts of the Adamawa state consists of only eleven (11) Local Government Areas and lies between latitude 7°N and 10°N (Field work, 2019).

According to Adebayo & Tukur (1999), Adamawa state is characterised with varied rainfall ranging from 700mm in the north-western part to 1600mm in the southern part. By and large, the mean annual rainfall is less than 1000mm in the central part of the state. This region includes, Song, Gombi, Shelleng, Guyuk, Numan, Demsa, Yola and part of Fufore Local Government Areas (LGAs). Northern strip and southern part have over 1000mm in the other hand. This variation of the annual rainfall amount is as the result of the altitudes of the stations.

The major vegetation formation of the state is divided into three zones: The Southern Guinea Savannah, the Northern Guinea Savannah and the Sudan Savannah. However, each formation is characterised by interspersion of thickets trees Savannah, open grass Savannah and fringing forest in the river valleys (Adebayo & Tukur, 1999).

Data Source and Analysis

The dataset used for the study are grouped in two; as pointed earlier: the climatic data and physical data. Climatic data used include: Rainfall, Temperature, Sunlight, and Relative Humidity (RH); while physical data are soil, Relief and Drainage. Therefore, their source varied. Data on rainfall, temperature, sunlight and RH were obtained from Global Weather Data for SWAT (GWDS) and NASA Prediction of Worldwide Energy Resources (POWER). The data from GWDS were from 1979 to 2014 (35 years). NASA POWER data also covered a period of 35 years, which is from 1982 to 2017. All the climatic data were in numeric forms which were later processed into spatial datasets for this work. Dataset on soil type were obtained from Global Soil Survey and NRCS (Natural Resources Conservation Service) map of 2005 from United State Department of Agriculture (USDA). For the Relief of the study area, http://data.biogeo.ucdavis.edu/data/diva/ alt/NGA_Alt.zip was the source used to obtain the related data. Drainage dataset was extracted from Google.com.ng/maps. These data were in JPEG formats and imagery and *added* (imported) in the Arc Map environment where they were *geo-referenced* and captured for used in the study.

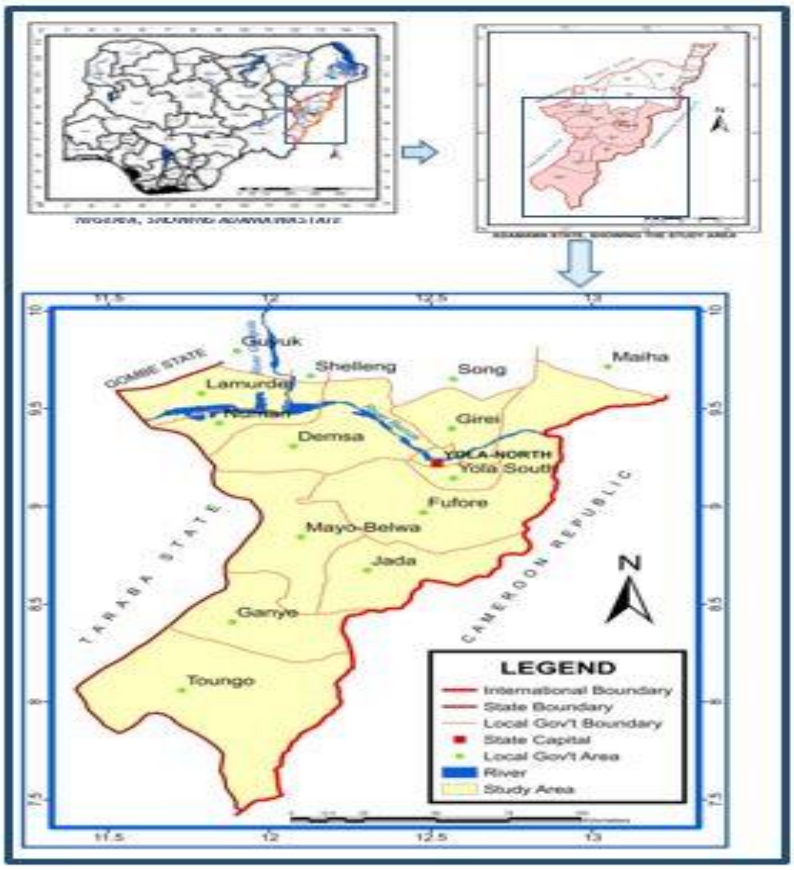

Figure 1. Location of the Study Area
Source: Map and Research, 2017

Preparation and Creation of Criteria Maps

The four climatic data used in this work, were analysed in the Microsoft Excel to produce tabular datasets for use in the Arc Map (ArcGIS 10.2) environment. Averages for each point (coordinate) in the study area captured for the period of 35 years were computed. Subsequently, the tables were added in the Arc Map environment, where the *Display XY Data* command, was used to display the values computed for all the points. These points and their values for each dataset were displayed across the study area automatically. In order to produce a spatial

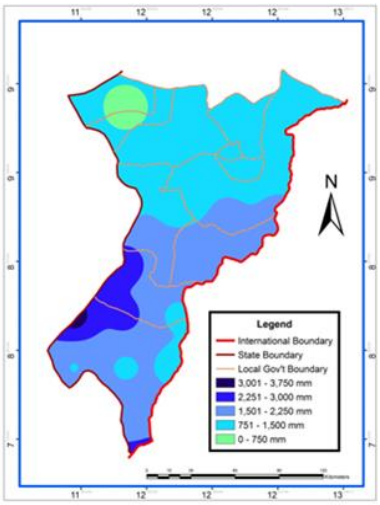

Figure 2. Mean Annual Rainfall

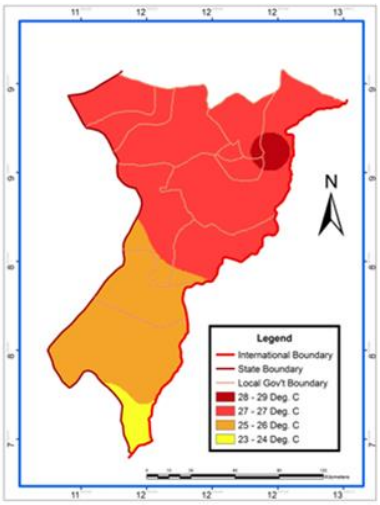

Figure 3. Mean Annual Temperature

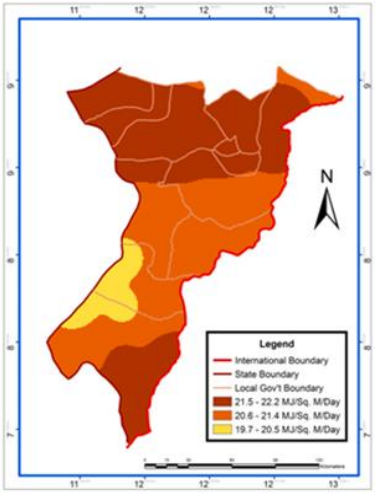

Figure 4. Mean Annual Sunlight

representation of the datasets over the study area, *interpolated* command were used on each of the climatological dataset. Therefore, on each dataset, a map was produced showing various units depending on the range of values computed and they served as criteria used for further analysis. The other three physical data (soil, relief and drainage) which were in form of thematic maps for soil and drainage, and imagery for relief were geo-referenced following their retrieval from the sources stated early to come up with compatible datasets for used in ArcGIS environment. In the end, seven (7) datasets were produced for this study (figures 2-8).

3.5 Reclassification of Datasets

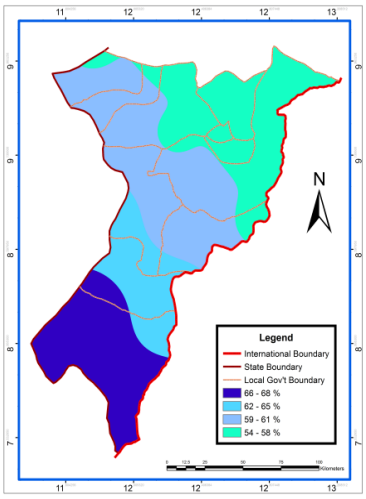

Figure 5. Mean Annual Relative

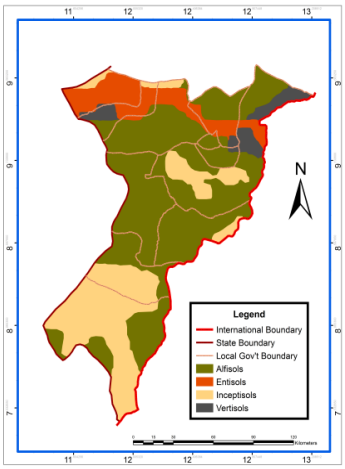

Figure 6. Soils Types

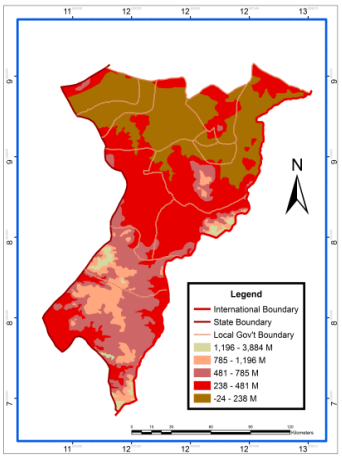

Figure 7. Relief

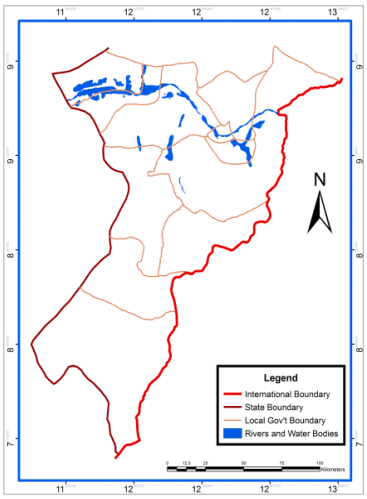

Figure 8. Major Drainage

The climatic datasets having been produced through the process of *interpolation* in Arc Map environment are automatically in form of raster map and can be used directly for further analysis. However, the physical data needed to be converted into raster maps by digitising them. Therefore, various units on the physical datasets (maps) were digitised as polygons. In the Arc Map10.2 environment, each unit digitised, a value is assigned on the *attribute table* for each dataset. For instance, the various temperature regions have their attribute tables produced and each region's value recorded against it on the table.

All the datasets were further *reclassified* for integration in the weighted sum overlay process. On each dataset's attribute table, areas that meet the required condition for sugarcane cultivation were reassigned value **1**, while areas that do not were given **0**. The reclassification process was guided by the requirements in table 1. The datasets which were initially having various units shown by different colours (figures 2-8) now were changed to two (2) units, that is areas that are suitable and areas that are not suitable for sugarcane cultivation in the study area. These two units were depicted with green colour for areas that are suitable and red colour for areas that are not suitable (figures 9-15). It was this analysed agro-climatic parameters (reclassified datasets), that were integrated to come up with the final result (figures 16 and 17).

Figure 9. Reclassified Rainfall

Figure 10. Reclassified Temperature

Figure 11. Reclassified Sunlight

Figure 12. Reclassified Relative Humidity

Figure 13. Reclassified Soil

Figure 14. Reclassified Relief

Figure 15. Reclassified Drainage

Table 1: Conditions for Agro-Climatic Site Selection for Sugarcane Production in the Study Area

Serial Number	Criterion	Ideal Condition for Sugarcane Cultivation	Source
1	Mean Annual Rainfall	Between 750 to 1500 mm	Mondale (2017)

2	Mean Annual Temperature	Between 25 to 40°C	Directorate of Sugarcane Development (2013); Asiafarming.com (2018)
3	Relative Humidity	At least 70%	Srivastava and Rai (2012), Binbol *et al*.
4	Sunlight	18-36 MJ/m^2 Daily	NETAFIM (n.d)
5	Soil Types	Deep loamy soil, heavy clay soil, sandy loam soil	SC (2012), Letstalkagric (2017), Republic of South Africa (2014)
6	Relief	Highland and Medium highland	Sugarcane Production (2012)
7	Drainage	Well drained Land, Not waterlogged	Rhum Agricole (n.d), (Tarimo & Takamura (1998)

Source: Field work, 2019

Weighted Sum Overlay

Weighted Sum is a data analysis process which works by multiplying the designated field values for each input raster by the specified weight. It then sums (adds) all input raster datasets together to create an output raster (Esri, 2016). Weight here, means importance attached to a criterion, which could be in percentage or ratio. For this study, the value of 1 was assigned to each of the reclassified dataset used, signifying that equal importance were given to each.

The seven reclassified criteria (figures 9-15) were integrated through the process of W*eighted Sum* overlay explained in previous paragraph of this section. This process could be expressed mathematically as follows:

Weighted Sum output *= wightedSum (weighted Sum Table[Criteria 1, Value *weight Value], [Criteria 2, Value*weight value], [Criteria 3, Value*weight value].....[Criteria N, Value*weight value])* (Esri, 2016)

Overlay in more clear terms means that units on the reclassified maps which have only values **0**s and **1**s were all combined so that, where for instance 1 and 1 meet the resultant value will be 2, and where 1, 1, and 1 meet the result is 3.Therefore, On the overlaid map, the maximum value on the weighted sum table (also on the map) is 6, meaning that; the area(s) in question meet(s) all the six conditions with the exception of drainage, which is the seventh criterion used. This was later superimposed on the overlaid map to remove places with major water bodies which are considered not suitable. Therefore, some places meet five, others four, three and zero respectively as shown in figure 16.

In line with the FAO guidelines on land suitability analysis, areas that have value **6**, were assigned S1, areas with value **5** were assigned S2; while areas with **4** were assigned S3; and areas with values **3** and **0** were assigned N. Consequently, the final result generated from weighted sum overlay (integration of all the datasets used in this study) shows only four (4) degrees of site suitability for sugarcane production in the study area. These are:
Most suitable (areas with S1),

Moderately suitable (areas with S2),

Marginally suitable (areas with S3), and

Not suitable (areas with N) (figure 17)

Results and Discussions

Results of the Analysed Datasets

The analysed datasets are shown in figures 9 to 15. These are the reclassified datasets as discussed in section 3.5 of this work. They display the areas that are good and areas that are not good for sugarcane growth in the southern parts of Adamawa state. The area coverage for each unit of suitability on the maps is computed and the result displayed in table 2 as explained earlier. This is the transformation of the initial criteria dataset used for this study, from multi-units maps to di-unit maps showing only areas that are good with value **1** (green in colour) and areas that are not good with value **0** (red in colour) for sugarcane growth. These nevertheless, are the maps that were combined through the process of weighted sum overlay to come up with agro-climatic site selections for sugarcane production in the study area.

Table 2: Area Coverage for Reclassified Datasets

S/N	DATA	SUITABILITY			
		Suitable		Not Suitable	
		Km^2	%	Km^2	%
1	Rainfall	20,008.99	96	730.31	4
2	Temperature	20,048.59	97	690.71	3
3	Sunlight	20,739.30	100	0	0
4	RH	6,621.21	32	14,118.09	68
5	Soil	12,888.40	62	7,850.90	38
6	Relief	14,667.20	71	6,072.10	29
7	Drainage	19,867.40	96	871.90	4

Source: Field work, 2019

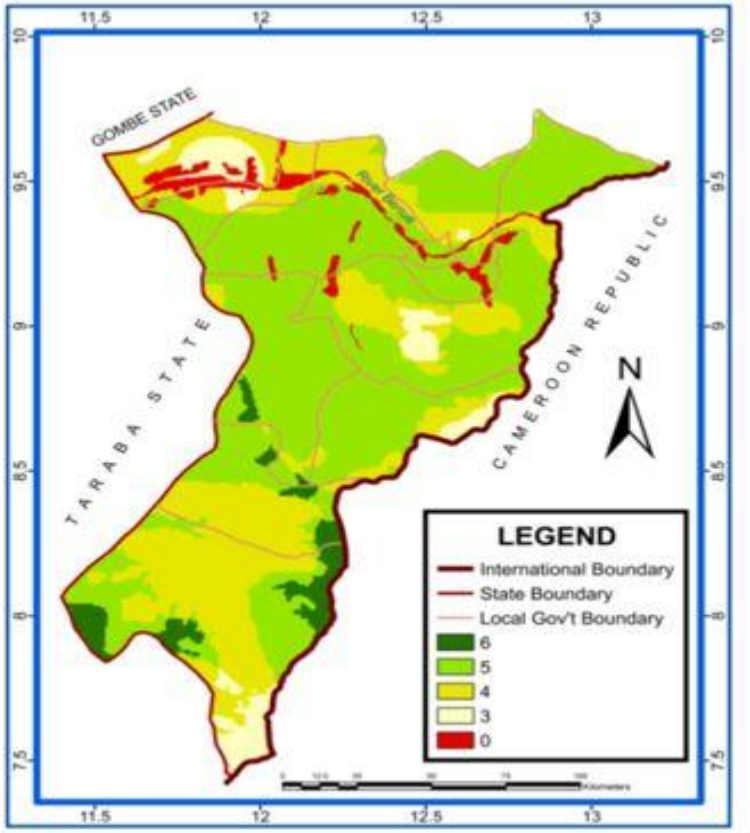

Figure 16 Integrated Datasets for Sites Suitability Selection

Datasets Integration and Degree of Suitability

Following the integration of all the analysed dataset as explained in section 3.6 the result of the finding is shown in figure 16. On the map, values for degree of suitability for each site are shown. That is, 6, 5, 4, 3, and 0 depending on the number of conditions a given area meets for sugarcane growth. This map is further analysed to come up with four degree of suitability as discussed in 3.6 of this work, that is Most suitable, Moderately suitable, Marginally suitable and Not suitable for sugarcane production.

As can be seen in figure 17, the areas that are Most Suitable for sugarcane growth are spread over places like Toungo and partly in Ganye, Jada and Mayo-Belwa Local Government Areas (LGAs). Moderately suitable areas cover the largest area, and these areas are spread across all the LGAs in the southern parts of Adamawa state, however, are more pronounced in the central part and towards the northern part of the study area. The Marginally suitable areas for sugarcane growth in the study area are mostly located in Toungo, Ganye, Fufore, Numan, Demsa, Lamurde and Girei LGAs axis. Finally, areas that are Not suitable for sugarcane growth are dotted in Southern part of Toungo, Jada, Fufore, Yola-North, Yola-South, Girei, Numan,

Demsa and Lamurde LGAs. The area coverage of each degree of suitability is shown in table 3.

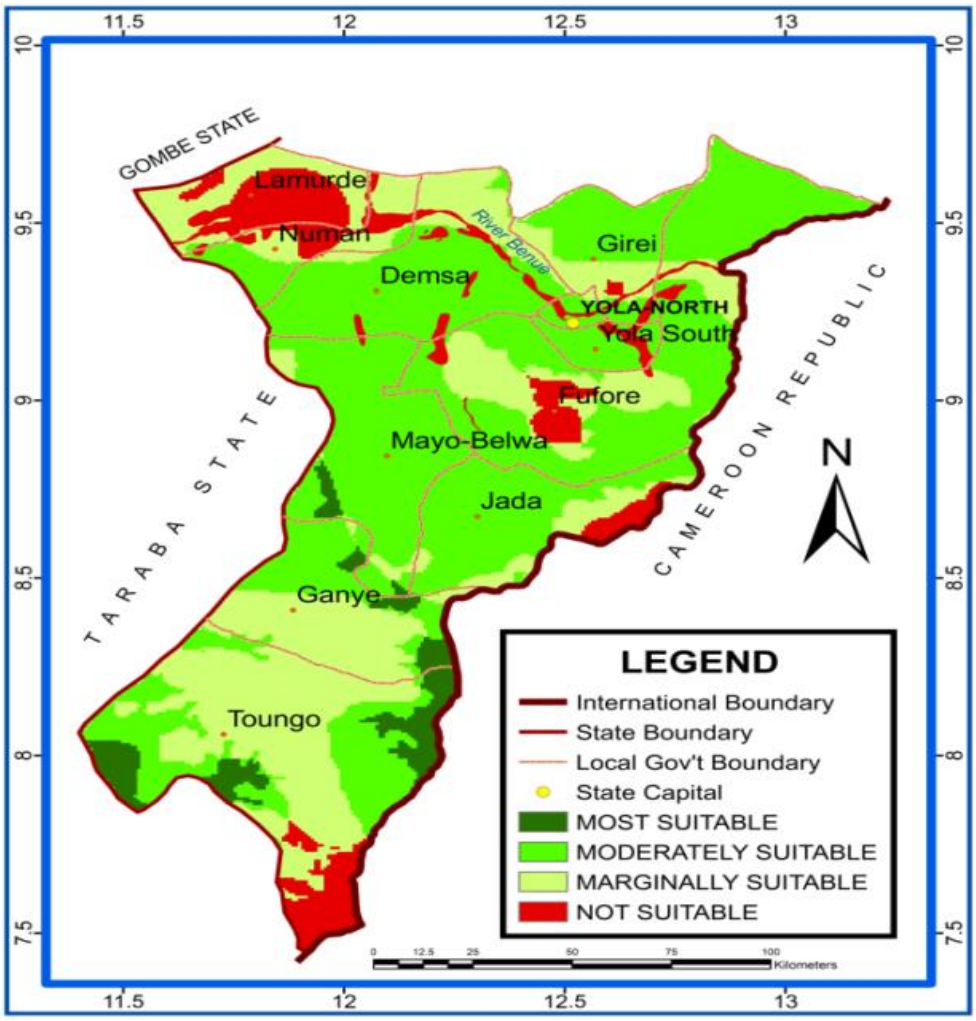

Figure 17. Degree of Suitability for Sugarcane Production in Southern Parts of Adamawa state

Table 3: Degree of Suitability for Sugarcane Production in the Study Area

Degree of Suitability	Weighted Sum Value	FAO Classification	Area Coverage (Km^2)	Percentage Coverage (%)
Most Suitable	6	S1	880.93	4.25
Moderately Suitable	5	S2	11,808.08	56.94
Marginally Suitable	4	S3	5,927.10	28.58

Not Suitable	3, 0	N	2,123.19	10.23
Total			**20,739.30**	**100**

Source: Field Work, 2019

Conclusions and Recommendations

This study leaned on the agro-climatic factors in selecting the site suitability for sugarcane production in the southern parts of Adamawa state of Nigeria, and result shows the spatial distribution of the degree of site suitability. These are Most suitable, Moderately suitable, Marginally suitable and Not suitable sites for sugarcane growth in the study area.

From the finding, the sites that are suitable for sugarcane production cover the greater part of the study area, that is about 12,689.01 Km2 (61%) see table 3. These areas encompass the Most suitable and Moderately suitable degree of suitability in the study area. This size of land as suitable for sugarcane growth in more than 450 Km^2 (45, 000 hectares) used by Zimbabwe to produce 600,000 tons of sugar annually before land seizure in 2002 (Tyler, 2008). These lands are underutilised for sugarcane cultivation in the state. The authors believe that, if this land could be put to use for sugarcane production, the state as well the country's economic base could be strengthened. Because it could result into chain-benefits, ranging from job creation, infrastructural development, and most importantly source of revenue for the state and all the stakeholders.

Therefore, this large area of land as suitable for sugarcane production shows that, the southern parts of Adamawa state, is one of the right places to invest in sugarcane business. Presently, the only company that produces sugar and its by-products is the Dangote Group of Company which bought the forma Savannah Sugar Company Limited, and it has not being able to utilise the whole area. This shows that, there is room for more investors.

The authors therefore, recommend that, the state government should spare headedly key in to this finding in this work. They should take it serious, if they really strive to diversify the economy of the state, because depending on federal allocation is a risky idea. Even the federal government depends majorly on the oil, which price in the international market affects it. When the price of oil falls in the market, it usually affect our economy, thus there are urgent need to find other source of revenue.

References

Adebayo A. A. & Tukur A. L. (1999). *Adamawa state in maps*. First edition. Yola. Paraclete Publishers.

Akobundu, I.O. (1987). *Sugarcane*. In Weed Science in the Tropics I.O. Akobundu, (ed). John Wiley and Sons New York. 414 – 446.

Daniel, J. D., Adebayo, E. F., Shehu, J. F., & Tashikalma, A. K. (2013). Technical efficiency of resource-use among sugarcane farmers in the Northeast of Adamawa state, Nigeria. *International Journal of Management and Social Sciences Research (IJMSSR)*, 2 (6), 13—18, ISSN: 2319-4421

Daniel, P. D. L., Carlos, B. & Tatiana, D. (n.d.). Land suitability evaluation using combination of exploratory data analysis with a geographical information system on sugarcane areas. Scientific registration no: 2148.

Esri (2016). How weighted sum overlay works. Retrieved from http://desktop.arcgis.com/en/arcmap/10.3/tools/spatial-analyst-toolbox/how-fuzzy-overlay-works.htm.

FAO. (1976). A framework for land evaluation: *Soils Bulletin*: 32, Food and Agriculture Organization of the United Nations, Rome.

Federal Republic of Nigeria. (2017). Adamawa state. Retrieved from Nigeria.gov.ng/index.php/2016-04-06-08-39-54/north-east/adamawa-state.

Letstalkagric (2017). Sugarcane farming guide. Retrieved from http://www.letstalkagric.com/crops/sugarcane-farming-information-guide.

Lingjun, L. & Yan, H. (2008). Study on land use suitability assessment of urban-rural planning based on remote sensing—a case study of Liangping in Chongqing. *The International Archives of the Photogrammetry, Remote Sensing and Spatial Information Sciences.* 37 (8), 123-130.

Srivatava A. K. & Rai M. K., (2012). Sugarcane production: impact of climate change and its mitigation. *Bio Diversit AS*. 12 (4) 214-227 doi: 10.13057/biodiv/d130408.

Tarimo, A. J. P. & Takamura, Y. T. (1998). Sugarcane production, processing and marketing in Tanzania. *African Study Monographs,* 19(1): 1-11.

Tyler, G. (2008). Background Paper for the Competitive Commercial Agriculture in Sub-Sahara Africa (CCAA) Study. The African Sugar Industry – A Frustrated Success Story. Retrieved from http://www.siteresouce.worldbank.org/in.Tafrica/resource/257994T 12154571 7825 67/ch6sugar PDF. Retrieved 15/11/08.

Vooren, P. Z. J. (2008). *Sugarcane ethanol contributions to climate change mitigation and the environment*. (ed). The Netherlands. Wageningen Academic Publishers. ISBN: 978-90-8686-090-6, e-ISBN: 978-90-8686-652-6. doi: 10.3920/978-90-8686-652-6

Pollution Potential of Leachate from Dumpsites in the Federal Capital Territory, Nigeria.

By

Oluyori, A. O.[1*], Abubakar, A. S.[2], Usman, M. T[2] and Suleiman, Y. M.[2]
1. Laurmann and Company Ltd., Plot 596 Ahmadu Bello Way, Garki II, Abuja
2. Department of Geography, Federal University of Technology, Minna
*oluyoriaustine@gmail.com; 08035906370

Abstract

Leachate is extremely polluted wastewater which is regardedto have potent pollution treat on water resources in the environment.Heavy metal, microbiological, physico-chemical and nutrient parameters in leachate samples collected from municipal solid waste dumpsites in the FCT were analyzed and reported to assess the pollution potential of leachate on the biophysical environment of the study area. The results obtained were compared to NSDWQ standard to check the risk of leachate on the environment. The range concentration of heavy metals in leachate are Fe-0.2265mg/L (KUJ) to 10.3971mg/L (GSA), Cd-0.0069mg/L (ABJ) to 0.3857mg/L (MPP), Cr-0.1050mg/L (MPP) to 0.7776mg/L (KWL). Cu-0.0057mg/L (BWR) to 0.5261mg/L (KWL), Pb-0.0672mg/L (AJT) to 1.5071mg/L (KWL), Mn-0.0408mg/L (TGM) to 1.0026mg/L (GSA), Ni-0.0051mg/L (GLD) to 0.3646mg/L (KWL) and Zn-0.0024mg/L (KWL) to 0.4897mg/L (KSH).Concentration of Cd, Cr and Pb in leachate from the dumpsites were above the permissible level by NSDWQ for surface and groundwater while Cu and Zn were within the tolerable limit. Reported range concentration of Microbiological and Nutrient parameters in leachate samples were: Total coliform-126.33CFU/100mL (KUJ) to 205.33CFU/100mL (KWL), E.coli-122.00CFU/100mL (DTS) to 161.00CFU/100mL (AJT), Cl^--2.83mg/L (KWL) to 560.11mg/L (MPP), NO_3^--0.31mg/L (KSH) to 2.08mg/L (MPP) and SO_4^{2-}-0.26mg/L (DTS) to 728.67mg/L (MPP).Concentration of Total Coliform and E coli were above the NSDWQ guidelines in leachate from all the dumpsites in the study area. The concentration of $NO_3^-$was within the NSDWQ guidelinesin leachate from all the dumpsites.

Physico-chemical parameters in leachate characterized shows pH values of 6.78 (GSA) to 8.60 (AJT), DO-4.27mg/L (TGM) to 5.94mg/L (KWL), BOD-3.02mg/L (KWL) to 8.27mg/L (AJT), TS-1.26mg/L (KUJ) to 9.81mg/L (KWL), TSS-1.89mg/L (MPP) to 8.32mg/L (GLD), Alkalinity-1.04mg/L (MPP) to 3.07mg/L (DTS) and EC-512.33µs/cm (BWR) to 1051.33µs/cm (AJT). The results show that the leachate from the dumpsites has potential to impact water resources in the study area. As such, there is need for government to overhaul her approach towards management of waste dumpsites whether they are open or closed and also to develop better waste management practices to mitigate anticipated impact and its attendant implications.

Keywords: Leachate, Waste dumpsite, Municipal Solid Waste Management, Pollution, Impa*ct.*

Introduction

The symbiotic relationship between man and the environment and the equilibrium between the two is the prime need of the present day's sustainable life. However, rapid urbanization and fast lifestyle have led to the formation of various types of toxic compounds within the ecosystem which are less degradable and harmful to living things. Uncontrolled and unscientific garbage or solid waste disposal systems with the associated problem of infiltration of solutes (pollutants) into the soil and accumulation at any particular depth of soil leading to the contamination of the groundwater reserves is a major problem nowadays and it is expected to increase with time if no proper precautions are taken.

The FCT is located between latitude 8^0 25'and 9^0 25'North of the equator and longitude 6^0 45'and 7^0 45'East of Greenwich Meridian (Figure 1). The territory covers approximately an area of 8,000 square kilometres and occupies about 0.87% of Nigeria. The territory is bordered by four states namely; Niger to the West, and North West, Nassarawa to the East, Kogi to the South and Kaduna to the North of the territory (Magaji, 2009).

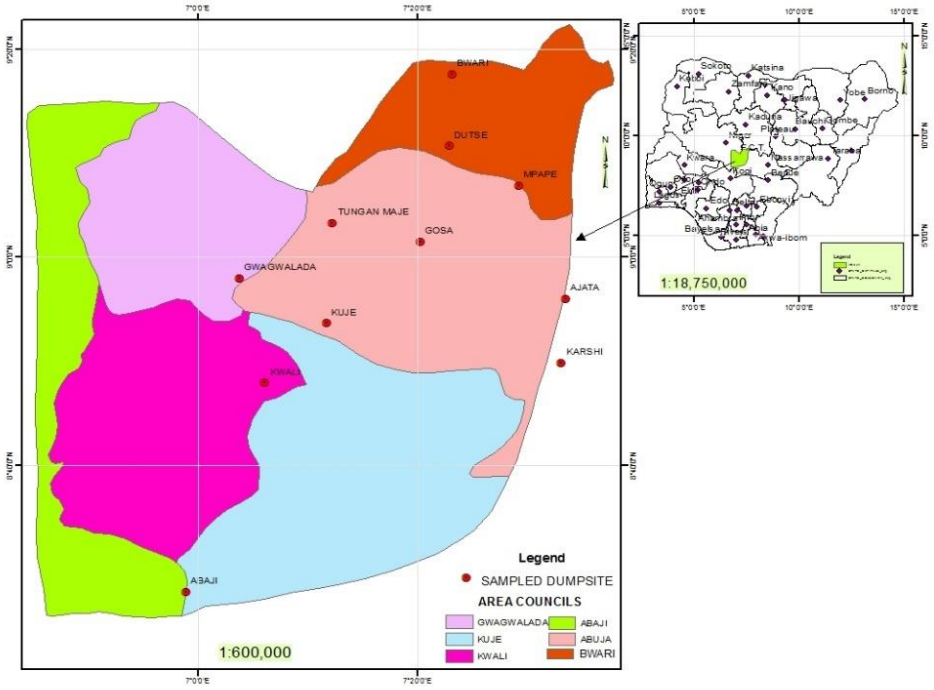

Figure 1: The Study Area (Federal Capital Territory, Abuja, Nigeria indicating the designated Dumpsites)

Table 1 gives a summary of the locational attributes of the dumpsites and the selected research control sites, there are also information about the waste dumping methods implored in the dumpsites as well as the status of the dumpsites.

Table 1 Dumpsites with their Locational Attributes

Dumpsite	Classification Remarks	Code	Latitude	Longitude	Elevation (m)
KUJE	+, α	KUJ	8.89392	7.19637	314
TUNGAN MAJE	+, α	TGM	9.05452	7.20566	332
DUTSE	+, α	DTS	9.17816	7.38310	475
AJATA	*, α	AJT	8.93323	7.56084	416
KARSHI	+, α	KSH	8.83053	7.55398	400
BWARI	+, α	BWR	9.29340	7.38813	565
GOSA	+, μ	GSA	9.02511	7.33994	387
MPAPE	*, μ	MPP	9.11455	7.48980	568
KWALI	+, α	KWL	8.79805	7.10252	190
GWAGWALADA	+, α	GLD	8.96625	7.06330	218
ABAJI	+, α	ABJ	8.46129	6.98303	172

Source: Oluyori, 2018

Key:

- Status of Dumpsite
  - * = Dumpsites that have been closed, investigation was on post closure impact.
  - + = Dumpsites that are open and active, measured for current impact level.

- Methods of Waste Dumping
  α= Open Dumping
  μ= Controlled Dumping

Literature Review

Pollution occurs when a product added to our natural environment adversely affects nature's ability to dispose it off. A pollutant is something which adversely interferes with health, comfort, property or environment of the people. Generally, most pollutants are introduced in the environment as sewage, waste, accidental discharge and as compounds used to protect plants and animals (Misra& Mani,1991).

Open dumps are the oldest and the most common way of disposing of solid waste, although in recent years thousands have been closed, many still are being used. In many cases, they are located wherever land is available, without regard to safety, health hazard and aesthetic degradation. The waste is often piled as high as equipment allows. In some instances, the refuse is ignited and allowed to burn while in others, the refuse is periodically levelled and compacted. As a general rule, open dumps tend to create a nuisance by being unsightly, breeding pests, creating a health hazard, polluting the air and sometimes polluting groundwater and surface water (Keller, 1982).

Leachate corresponds to atmospheric water that has percolated through waste, interacting with bacteriological activity and especially organic substances. Its composition is a function of the nature and the age of the landfill, the type of wastes, the method of burying, the geological nature of the site, the climate (Amina *et al.*, 2004).Leachate varies widely in composition depending on many interacting factors such as the composition and depth of waste, availability of moisture and oxygen, landfill design, operation and age (Reinhart and Grosh, 1998).

This study is aimed at assessing the pollution potential of leachate from government approved and operated dumpsites in the FCT as it relates to water resources component of the environment.

Methodology

Eleven (11) government approved and operated dumpsites covering the entire FCT was considered see Table 1. The choice of the leachate was based on the view that leachates in dumpsites ultimately leak, percolate, and contaminate the groundwater; hence its analysis can give an indication of a potential for environmental pollution.

Leachate samples were collected from the 11 dumpsites in the May, 2017 from randomly selected leachate drains at the dumpsites as adapted from Uba*et al.* (2008), Adeolu*et al*, (2011).The samples were collected in well-labelled clean polythene bottles rinsed with the leachates prior to the sample collection. Randomly sampled leachate from different locations within each dumpsite and were thoroughly mixed and composite samples taken for analysis. The samples for microbiological analysis were aseptically taken in 50ml sterile universal containers.Samples were analyzed using standard procedures defined by APHA, (2005).

Physico-chemical parameters like Electrical Conductivity (EC), temperature, total suspended solids (TSS) and pH were measured in-situ with the aid of JENWAY 4590 meter. The composition of parameters such as Dissolved oxygen (DO), Biochemical Oxygen Demand (BOD), Total solids, Alkalinity, Total coliform, E coli, Nitrate, Chloride, Sulphate and Heavy metals (Fe, Cu, Cr, Cd, Pb, Zn, Mn and Cu) were determined in the laboratory using AAS Thermo Scientific iCE 3000 at the National Advanced Laboratories, National Science and Technology Complex, Sheda, Abuja.

The evaluation of potential risk of leaching to groundwater and surface water was performed by the pollutant concentrations in the leachate being compared directly to the applicable water quality standards, such as the Nigerian Drinking Water Standards (SON, 2007), with the appropriate consideration of dilution that may occur, and also to establish the pollution potential and strength of the leachates from the selected dumpsite.

Results and Discussions

The physico-chemical characteristics of leachate depend primarily upon the waste composition and water content in the total waste (Mohan and Gandhimathi, 2009). The characterization of leachates (Heavy metals, Microbiological, Nutrient and Physico-chemical parameters) across the dumpsites are presented in Tables1 to 3.

Table 1 Mean values of Heavy metals in dumpsite leachate and NSDWQ Acceptable Standard

Dumpsites	Fe (mg/L)	Cd (mg/L)	Cr (mg/L)	Cu (mg/L)	Pb (mg/L)	Mn (mg/L)	Ni (mg/L)	Zn (mg/L)
KUJ	0.2265	0.1386	0.1428	0.0059	0.2390	0.0614	0.0163	0.3158
TGM	8.2612	0.0530	0.1763	0.0824	0.5524	0.0408	0.0078	0.2755
DTS	0.9410	0.0526	0.1451	0.0610	0.4683	0.2879	0.0749	0.2829
AJT	1.4273	0.0348	0.2517	0.3440	0.0672	0.0955	0.0986	0.285
KSH	8.2721	0.0418	0.2011	0.2274	0.3128	0.9627	0.1438	0.4897
BWR	7.3291	0.0784	0.1330	0.0057	0.2519	0.2313	0.1067	0.4053
GSA	10.3971	0.0518	0.1784	0.0243	0.7849	1.0026	0.1353	0.3039
MPP	4.5780	0.3857	0.1050	0.1483	0.2276	0.3036	0.2241	0.1248
KWL	7.2233	0.0000	0.7776	0.5261	1.5071	0.2340	0.3646	0.0024
GLD	0.3515	0.1136	0.2059	0.0158	0.2189	0.1089	0.0051	0.1935
ABJ	6.4288	0.0069	0.6921	0.4683	0.2005	0.1932	0.3245	0.0021

NSDWQ STANDARD	0.3	0.003	0.05	1	0.01	0.2	0.02	3

Source: **Oluyori, 2018**

Table 1 shows the mean concentration of Fe in leachate ranged from 0.2265mg/L (KUJ) to 10.3971mg/L (GSA). The ranking order of mean Fe concentration in dumpsite leachate show that GSA>KSH>TGM>BWR>KWL>ABJ>MPP>AJT>DTS>GLD>KUJ. The relatively high value in GSA is attributable to the dumping of iron and steel scraps in large quantities alongside waste stream in this dumpsite, a reasonably evident presence of 'sharps' and 'medication materials were sighted in the raw wastes characterized from this site. The concentration of Cd was undetected in the leachate samples from KWL, while the mean value ranged from 0.0069mg/L (ABJ) to 0.3857mg/L (MPP) in the remaining dumpsites. Mean values for Cr in the leachate samples was between 0.1050mg/L (MPP) and 0.7776mg/L (KWL). The recorded values for Cu were in the range of 0.0057mg/L (BWR) and 0.5261mg/L (KWL). Level of Pb in the leachate samples collected across the dumpsites ranged between 0.0672mg/L (AJT) and 1.5071mg/L (KWL). The recorded values for Cu was in the range of 0.0057mg/L (BWR) and 0.5261mg/L (KWL). The range of mean concentration values for Mn are from 0.0408mg/L (TGM) to 1.0026mg/L (GSA). The Concentration range for Ni in the leachate samples are 0.0051mg/L (GLD) and 0.3646mg/L (KWL). The mean values of Zn are between 0.0024mg/L (KWL) and 0.4897mg/L (KSH).

The mean concentration of Cd, Cr and Pb in leachate from all the dumpsites were all above the permissible level by NSDWQ for either surface or groundwater while Cu and Zn were within the tolerable limit, this is indicative of potential for heavy metal pollution to surface or groundwater through surface runoff or leaching as the case may be. However, Fe, Mn and Ni in leachate showed divergent concentration pattern in which values exceeded NSDWQ guidelines in some dumpsites and were within the guidelines in other dumpsites (Table 1).

Table 2 Mean values of Microbiological and Nutrient parameters in dumpsite leachate and NSDWQ Acceptable Standard.

Dumpsites	Total coliform (cfu/100ml)	E.coli (cfu/100ml)	Cl^- (mg/L)	NO_3^- (mg/L)	SO_4^{2-} (mg/L)
KUJ	126.33	139.00	23.93	0.5587	1.2533
TGM	154.33	125.00	15.43	0.432	2.5667
DTS	131.67	122.00	17.57	0.6147	0.2620
AJT	151.00	161.00	25.83	0.4680	3.1967
KSH	143.67	144.33	19.07	0.3113	1.1433
BWR	128.67	149.67	14.50	0.4187	1.5600
GSA	134.33	145.33	15.30	0.3187	1.3600
MPP	156.33	145.33	560.11	2.0800	728.67
KWL	205.33	158.33	2.83	ND	639.67
GLD	135.67	145.67	15.90	0.8147	1.8833
ABJ	182.77	153.09	2.67	0.1306	569.40
NSDWQ STANDARD	10	0	250	50	100

Source: **Oluyori, 2018** **ND = Not Detected**

Table 2 shows concentration level of Microbiological and Nutrient parameters in leachate samples from the dumpsites. Total coliform was observed to have a minimum concentration value of 126.33CFU/100mL (KUJ) and a maximum concentration value 205.33CFU/100mL (KWL). The concentration of E.coli ranged between 122.00CFU/100mL (DTS) and 161.00CFU/100mL (AJT).Total coliform and E.coli are used as indicators to measure the degree of pollution and sanitary quality of well water, because testing for all known pathogens is a complicated and expensive process. The concentration of Total Coliform and E coli were above the NSDWQ guidelines in leachate from all the dumpsites in the study area. Total coliform bacteria are not likely to cause illness, but their presence indicates that your water supply may be vulnerable to contamination by more harmful microorganisms. E.coli in drinking water indicates the water has been contaminated with fecal material that may contain disease causing microorganisms, such as certain bacteria, viruses, or parasites.

Analysis of Nutrients parameters in leachate showed the following range of values from the waste dumpsites, Cl^- showed a concentration range between 2.83mg/L (KWL) to 560.11mg/L (MPP). The mean levels of $NO_3^-$was in the range of 0.31mg/L (KSH) and 2.08mg/L (MPP). The concentrations range for $SO_4^{2-}$was from 0.26mg/L (DTS) to 728.67mg/L (MPP). The concentration of $NO_3^-$was within the NSDWQ guidelinesin leachate from all the dumpsites, while if similar for Cl^-except in MPP where the value was above the guideline. In the case of SO_4^{2-}, the concentration at KUJ, TGM, DTS, AJT, KSH, BWR, GSA and GLD were within stipulated NSDWQ guideline while the concentration at MPP, KWL and ABJ were outside the NSDWQ acceptable guideline.

Physico-chemical parameters that were analyzed are summarized in Table 3, which shows that pH values of the leachates from the various sites range from 6.78 (GSA) to 8.60 (AJT) which

generally indicates slight acidic and alkaline conditions of the leachate, with the GSA dumpsite characterized with the most acidic pH value while AJT dumpsite had the most alkaline pH character, the observation at AJT can be attributed to the methane fermentation phase of the dumpsite which has already been closed as observed by Adeolu*et al.*, (2011).

Table 3 Mean values of Physico-chemical parameters in dumpsite leachate and NSDWQ Acceptable Standard.

Dumpsites	pH	DO_2 (mg/L)	BOD (mg/L)	TS (mg/L)	TSS (mg/L)	Alkalinity (mg/L)	Conductivity (µs/cm)	Temperature ºC
KUJ	7.49	5.02	5.66	1.26	5.58	2.05	844.67	28.67
TGM	8.14	4.27	6.31	2.06	6.47	2.16	907.33	28.03
DTS	6.84	5.52	8.09	2.45	4.72	3.07	961.33	28.13
AJT	8.6	5.92	8.27	2.11	5.12	2.52	1051.33	27.80
KSH	7.33	5.36	7.23	2.55	4.24	2.47	706.67	27.43
BWR	7.23	5.12	6.89	2.49	4.76	2.20	512.33	27.67
GSA	6.78	5.81	7.15	3.10	5.23	2.33	905.67	28.83
MPP	7.11	5.02	3.15	6.24	1.89	1.04	1038.33	27.03
KWL	7.49	5.94	3.02	9.81	6.81	2.94	1023.33	27.23
GLD	6.84	5.52	5.09	1.89	8.32	2.72	965.67	28.60
ABJ	7.01	5.36	2.85	8.73	6.06	2.73	910.77	24.24
NSDWQ STANDARD	6.5 – 8.5	NA	NA	N/A	500	N/A	1000	AMBIENT

Source: **Oluyori, 2018** **N/A = Not Available**

As landfill age increases, the biodegradable faction from organic pollutants in leachate decreases due to anaerobic decomposition occurring in the landfill site. The minimum concentration of DO was 4.27mg/L at TGM while the maximum concentration was 5.94mg/L at KWL. The concentration level of BOD ranged from 3.02mg/L (KWL) to 8.27mg/L (AJT). The mean value of TS was reported to range from 1.26mg/L (KUJ) to 9.81mg/L (KWL). TSS reported a value in the range of 1.89mg/L (MPP) to 8.32mg/L (GLD). Alkalinity ranged from 1.04mg/L (MPP) to 3.07mg/L (DTS). EC showed variation in sites though the range 512.33µs/cm (BWR) to 1051.33µs/cm (AJT). A pattern of decrease in the level of conductivity as observed was AJT>MPP>KWL>GLD>DTS>TGM>GSA>KUJ>KSH>BWR. Temperature range was from 27.03ºC (MPP) to 28.83ºC (GSA).

The value of pH in leachate from all the dumpsites was within the NSDWQ guideline except in the case of AJT which was above the permissible range for pH. The concentration of TS in leachate from all dumpsites was within prescribed limits, while the concentration of EC in leachate from KUJ, TGM, DTS, BWR, KSH, GSA, GLD and ABJ were with the permissible

limit the concentration of EC in leachate from MPP, KWL and AJT was above the threshold level.

The relatively high concentration of Pb, Cu, Cr in KWL shows that the dumpsite receives waste streams from batteries, florescent tubes as well as the location of the site in the proximity of right of way of a recently constructed power transmission line with part of the metallic construction waste still in place. AJT recorded maximum mean values for E. coli, pH, BOD and Electrical Conductivity, this could be adduced to the operational state as a recently closed dump site with significant reduction in the concentration of hydrogen ions. MPP recorded the highest mean value for all the nutrients analyzed in this study (Cl^-, NO_3^-andSO_4^{2-}), this dumpsite was closed in 2005 is still actively releasing the water-soluble salts to the environment as a result of surface water ingression and age. GSA reported maximum mean values for Fe, Mn and Temperature, while also recording the lowest pH value of all the dumpsites which is tending toward acidity.

Figures2 to 5 indicates the overall pattern of leachate characterization within the study area. Average characterization of leachate quality of Heavy metals showsthe following values: - Fe (5.0396 mg/L), Cd (0.0870 mg/L), Cr (0.2735 mg/L), Cu (0.1736 mg/L), Pb (0.4391 mg/L), Mn (0.3202 mg/L), Ni (0.1365 mg/L) and Zn (0.2437 mg/L) as seen in Figure 2. When compared with the NSDWQ guidelines for drinking water, the overall concentration of Fe, Cd, Cr, Pb and Mn in leachate of the study area were above the threshold limit while the concentration values of Cu, Ni and Zn were within tolerable limits. On the whole Fe, Cd, Cr, Pb and Mn are characterized as toxic for the water resources in the study area.

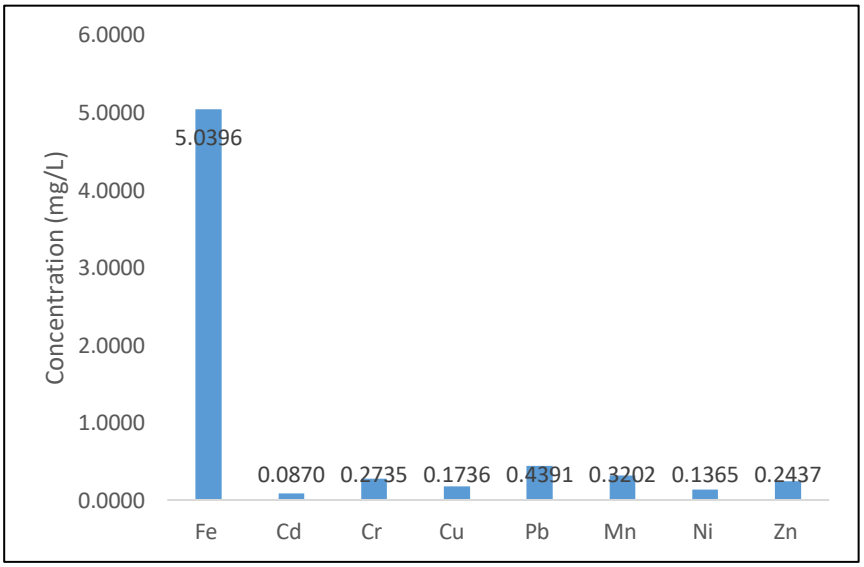

Figure 2 Overall picture of Heavy Metal in Leachate in the study area

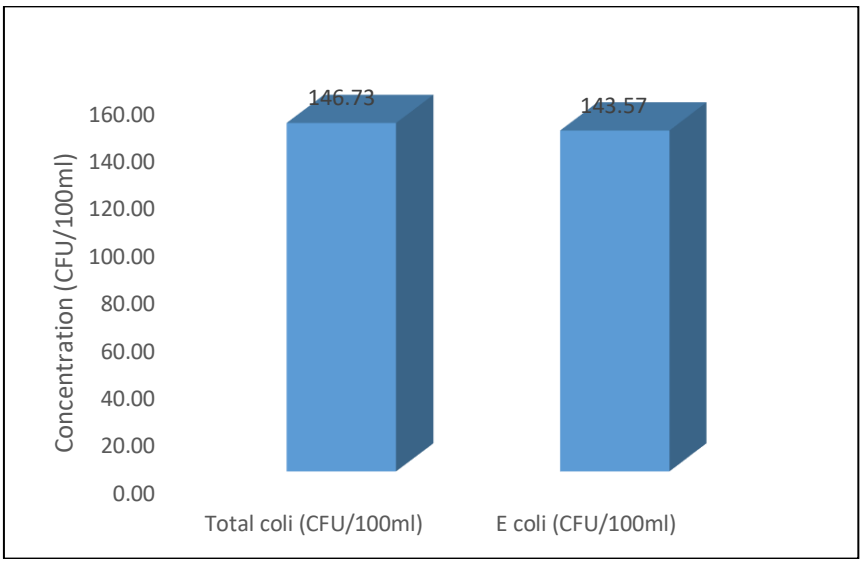

Figure3 Overall picture of Microbial Parameter in Leachate in the study area

Microbial Parameters showed that average concentration of Total Coliform was 146.73 cfu/100ml and E.coli was 143.57 cfu/100ml (Figure 3). Average concentration of both microbiological parameters in the study area falls outside the allowable limit prescribed by NSDWQ guidelines, hence the pollution potential of microbiological parameters is highly probable. The mean values for physico-chemical parameters are as follows: - pH (7.35), DO (5.35 mg/L), BOD (6.09 mg/L), TS (3.39 mg/L), TSS (5.31 mg/L), Alkalinity (2.35mg/L), Electrical Conductivity (891.67 us/cm) and Temperature (27.94^{o}C) as seen in Figure 4.Nutrients recorded overall mean values of Chloride, 71.05 mg/L, Nitrate, 0.6017 and Sulphate, 138.16 mg/L (Figure 5). Average mean values when compared with available standard benchmark for physico-chemical and nutrient parameters were observed to be within allowable limits.

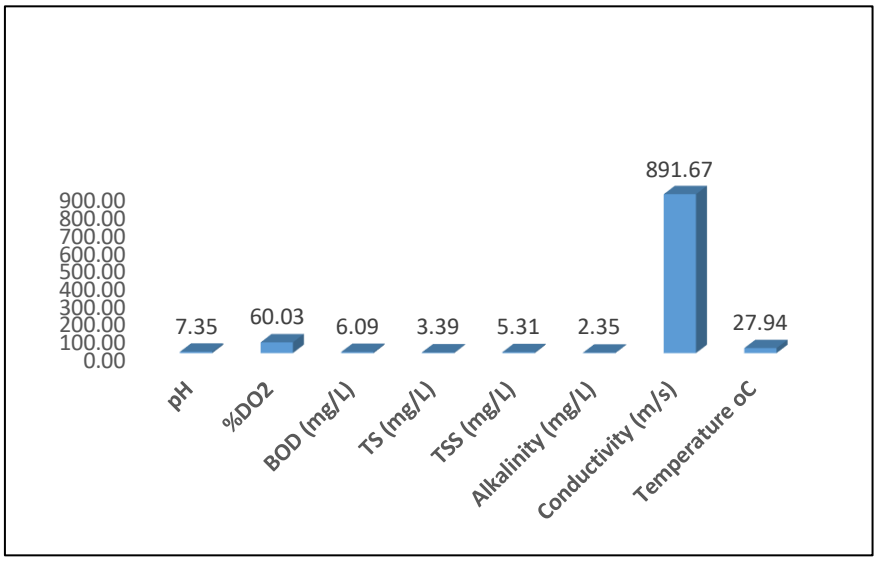

Figure 4 Overall picture of Physico-chemical Parameters in Leachate in the study area

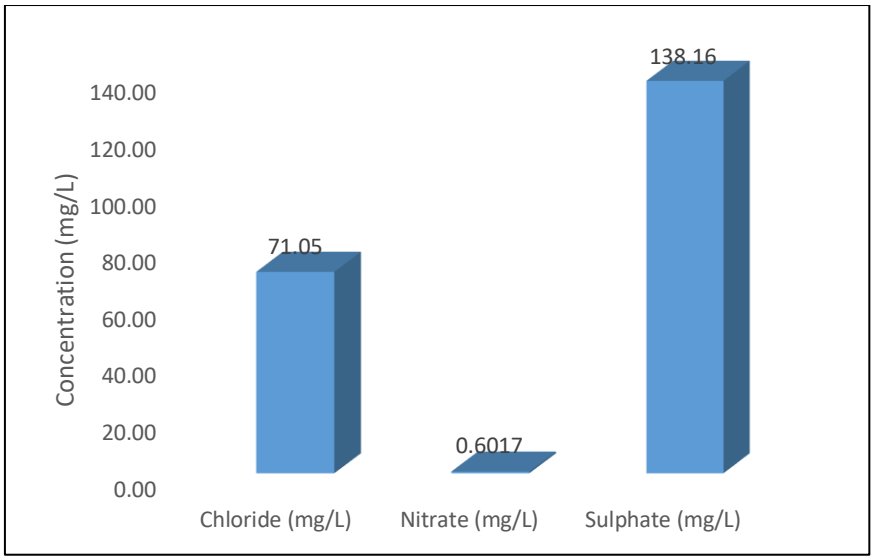

Figure 4.5Overall Picture of Nutrient in Leachate in the study area

Conclusionand Recommendations

The concentration level of leachate quality parameters in the dumpsites within the study area was found to vary over locations (spatially) and seasons (temporal). Parameters like Heavy metals (Cd, Cr and Pb), Microbiological content in leachate from all the dumpsites in the study area exceeded the permissible limit allowed by NSDWQ standard. The high concentrations of the pollutants in the leachate have potential to reach and contaminate water resources within the study area and thus threatening sustainable development. Therefore, there is an urgent need for strategy to be put in place for leachate collection and treatment as part of dumpsite management strategy to deal with active and post closure impact of dumpsite leachate to mitigate potential impact water resources.

References

Abubakar, B. S. and Adejoh, B. (2011). Pollution Potential of leachate from selected soil waste dumpsites in Kakuri, Kaduna, Nigeria. *Journal of engineering and applied sciences*, 3, 45-51

American Public Health Association, APHA (2005). American Water works Association and Water Pollution Control Federation, Standard Method for Examination of Water and Wastewater, APHA, AWWA and WPCF, 46, New York.

Amina, C., Abdekader, Y., Elkbri, L., Jacky, M. and Alain, V. (2004). Environmental impact of an urban landfill on a costal aquifer (El Jadida, Morocco). *Journal of African Earth Science*, 39: 509-516.

American Public Health Association, APHA (2005). *American Water works Association and Water Pollution Control Federation*, Standard Method for Examination of Water and Wastewater, APHA, AWWA and WPCF, 46, New York.

Keller, E.A., (1982). Environmental Geology. 3rd Edn., Bell and Howell Company, pp: 301.

Misra, S.G. and Mani, D. (1991). Soil Pollution. 1st Edn., Efficient Offset Printer, ABC., New Delhi, India, pp: 6-42.

Nigerian Standard for Drinking Water Quality (NSDQW) 2007. Nigerian Industrial Standard NIS 554, Standard Organization of Nigeria, pp15-30.

Oluyori, A. O. (2018). *Effect of Waste Dumpsite on the Biophysical Environment in the Federal Capital Territory, Nigeria*. Part of Unpublished PhD Post Field Report presented to Department of Geography, Federal University of Technology, Minna, Nigeria.

Reinhart, R.D. and Grosh, C. J. (1998). Analysis of Florida Municipal Solid Waste Landfill Leachate Quality, Report #97-3, *Florida Center for Solid and Hazardous Waste Management*

Predictive mapping of the mineral potential using geophysical and remote sensing datasets in parts of Federal Capital Territory, Abuja, North-Central Nigeria

Ejepu, J.S.*[1], Abdullahi S. [1], Abdulfatai, I.A. [1] and Umar, M.U. [3] and Sabo M.L. [2]

1 Department of Geology, School of Physical Sciences, Federal University of Technology, Minna, Niger State, Nigeria.
2 Department of Physics, School of Physical Sciences, Federal University of Technology, Minna, Niger State, Nigeria.
3 Department of Geology and Mining, Faculty of Applied Sciences and Technology, Ibrahim Badamasi Babangida University, Lapai, Niger State, Nigeria.
* Correspondence: ejepu.jude@futminna.edu.ng; Tel: +2348034065079

Abstract

GIS modelling is gaining wide application in providing solutions to wide–ranging geoscientific problems. A knowledge based Mineral Prospectivity Mapping (MPM) using Fuzzy Logic has been adopted in this study for a regional scale mapping of mineral potential in Sheet 185 Paiko SE, North–Central Nigeria. Mineral Prospectivity Mapping (MPM) is a multi-step process that ranks a promising target area for more exploration. This is achieved by integrating multiple geoscience datasets and using mathematical tools to determine spatial relationships with known mineral occurrences in a GIS environment to produce mineral prospectivity map. The study area is bounded within Latitudes 9° 00′ N to 9° 15′ N and 6° 45′ to 7° 00′ E. The study area is underlain by rocks belonging to the Basement Complex of Nigeria which include migmatitc gneiss and schist, granites of different compositions and textures and alluvium. The datasets used in this study include aeromagnetic, aeroradiometric, structural, satellite remote sensing and geological datasets. Published geologic map of the Sheet 185 Paiko SE was used to extract lithologic and structural information. Landsat images were used to delineate hydroxyl and iron-oxide alterations and to identify linear and fault structures and prospective zones at regional scales. ASTER images were used to extract mineral indices of the OH-bearing minerals including alunite, kaolinite, muscovite and montmorillonite to separate mineralized parts of the alteration zones. Aeromagnetic data were interpreted and derivative maps of First Vertical Derivative, Tilt derivative and Analytic signal were used to map magnetic lineaments and other structural attributes while the aeroradiometric dataset was used to map hydrothermally altered zones. These processed datasets were then integrated using Fuzzy Logic modelling to produce a final mineral prospectivity map of the area. The result of the model used predicted well the known deposits and also highlighted areas where further detailed exploration may be conducted.

Keywords: *Geophysical methods, Mineral exploration, Fuzzy logic models, Geographic Information Systems, Remote sensing*

1.0 Introduction

Modern mineral exploration efforts in recent times have adopted the integration of different datasets from various sources and surveys. Therefore, an important phase in mineral exploration should involve the collection, analysis, interpretation and integration of remotely sensed, geological, geophysical and geochemical datasets. This is done in order to map prospective areas for further more detailed investigations. Mineral Prospectivity Mapping (MPM) is basically classified into empirical (data driven) and conceptual (knowledge driven)

methods (Bonham-Carter, 2009, Yousefi and Carranza 2016). In the data driven method, known mineral deposits are used as 'training points' for examining spatial relationships between the known deposits and geological, geochemical and geophysical features of interest. The identified relationships between the input data and the training points are quantified and used to establish the importance of each evidence map and finally integrated into a single mineral prospectivity map. Examples of the empirical methods used are weights of evidence, logistic regression and neural networks.

However, in the conceptual (knowledge driven) method, conceptualisation of knowledge about the mineral deposit is devised in order to create a mappable criterion. These include making inferences about threshold values in criteria that control the mineralisation style. The areas that satisfy most of these criteria are delineated as being the most prospective. These methods are subjective based on the geologist's input and the proposed exploration model. By selecting a conceptual method one can benefit from the expertise of the geologists during the modelling process exceeding the capabilities of pure statistics. The methods belonging to this branch include Boolean logic, index overlay (binary or multi-class maps), the Dempster-Shafer belief theory, and fuzzy logic overlay.

Hence, the choice of methods to be applied are often made based on the availability of disparate datasets and modelling goals (Nykänen and Salmirinne, 2007). The fuzzy logic method has been recently widely implemented for the data integration and MPM purposes (Bonham-Carter 2009; Carranza and Hale, 2001; Masoud *et al.*, 2014; Zhang *et al.*, 2007). The fuzzy method enables evidence maps to be combined into a series of steps regarded as an inference net (flowchart), instead of combining them in a single operation. The inference net is a simulation of the logical process defined by a specialist (Quadros *et al.* 2006).

In this study the fuzzy logic technique was selected due to its flexible capability to demonstrate its potential for exploration of the hydrothermal and structural controlled mineralization in the study area located within the Federal Capital Territory (FCT) Abuja, North-Central Nigeria. Several studies have shown the feasibility of multispectral remote sensing for mapping the hydrothermally altered rock (Adegoke and Bulus. 2015; Aliyu et al. 2018; Ejepu *et al.*, 2018). Spectral discrimination of potential areas of gold mineralization (hydrothermal alteration zones) is a common application of remote sensing data analysis (Gabr *et al.*, 2010). Here, Advanced Spaceborne Thermal Emission and Reflection Radiometer (ASTER) data was processed and analysed for gold mineralization mapping in the study area.

Structural controls and the distribution pattern of hydrothermal alteration zones have been used as indicators of mineralized zones within the study area. Hence, a GIS-based spatial analysis was applied to evaluate mineral potential in the study area by using mineral favourability maps in order to define areas for detailed investigations.

2.1 Study area

2.2 Geology of the area

The study area forms part of reworked part of the West African Craton and underlies about 60% of Nigeria's land mass (Odeyemi, 1993). The Basement Complex has been described by Rahaman (1988), as a heterogeneous assemblage, which includes migmatites, gneisses, schists and a series of basic to ultrabasic metamorphosed rocks. Pan African Granites and other minor intrusions such as pegmatite and Aplites dykes and quartz veins have intruded these rocks (Figure 1).

All these rocks were affected and deformed by the Pan-African thermotectonic event. Detailed reports of the lithological description, age, history, structure and geochemistry of the basement complex of Nigeria are given in Oyawoye (1964), Black (1980), Ajibade, Woakes and Rahaman (1987), Rahaman (1988), Caby *et al.*, (1981) and Dada (2006).

2.2.1 The Metasediments

The Metasedimentary/Metavolcanic series consist of phyllites, schists, amphibolites, quartzites and serpentinites. The series comprises low grade, metasediment-dominated belts trending north- south and considered to be Upper Proterozoic super crustal rocks that have been infolded into the migmatite-gneiss complex. The lithological differences include fine to coarse grained clastics, politic schists, phyllites, carbonate rocks (marble and dolomitic marbles) and mafic metavolcanics (amphibolites). Rahaman and Ocan (1978) and Grant (1978) suggested the existence of many basins of deposition while Oyawoye (1972) and Mc Curry (1976) considered the schist belt as relict of a single supracrustal cover. Olade and Elueze (1979) considered the schist belt to be fault-controlled rift-like structures.

2.2.2 The Migmatite – Gneiss Complex

The Migmatite-Gneiss complex comprises the most widespread group of rocks and is considered as the Basement Complex *sensu stricto* (Rahaman, 1988; Dada, 2006). It comprises migmatites, orthogneisses, paragneisses, quartzites, calc-silicate rocks, biotite-hornblende schist and amphibolites. On account of petrography, the Pan African orogeny culminated in the recrystallisation of many of the constituent minerals of the Migmatite-Gneiss Complex by partial melting with most of the rocks showing medium to high grade amphibolites facies metamorphism. The Migmatite-Gneiss Complex displays ages varying from Pan African to Eburnean with three main geological phenomena recorded (Dada *et al.*, 1987); the first at 2,500 Ma, involved in initiation of crust forming process and of crustal growth by sedimentation and orogeny; the second event was the Eburnean; 2,000 $\pm$ 200 Ma, marked by the granite gneisses, which structurally obliterated the older rocks and reset the geochronological clock to give rise to granite gneisses, migmatites and other similar lithological units.

2.3 Structural Geology of the Region

The structural elements in Nigerian Basement include joints, fractures, lineations and folds (minor and major). The E-W trending structures are deep seated in origin and ancient in age and resulted from various thermotectonic deformational episodes mostly of the Eburnean and Pan-African Orogeny (Oluyide, 1988), (Olasehinde, 1999 and Olasehinde *et al.*, 2013). The dominant surface structural trend in the basement is essentially NE-SW trends in common with the tectonic grains of the schist belt. The NW- SE and E-W trends are locally dominant. Several sets of fractures having NW-SE, NNW-SSE, NNE-SSW and NE-SW directions were produced by transcurrent movement and shearing (Olasehinde, 2010) were also observed in the study area.

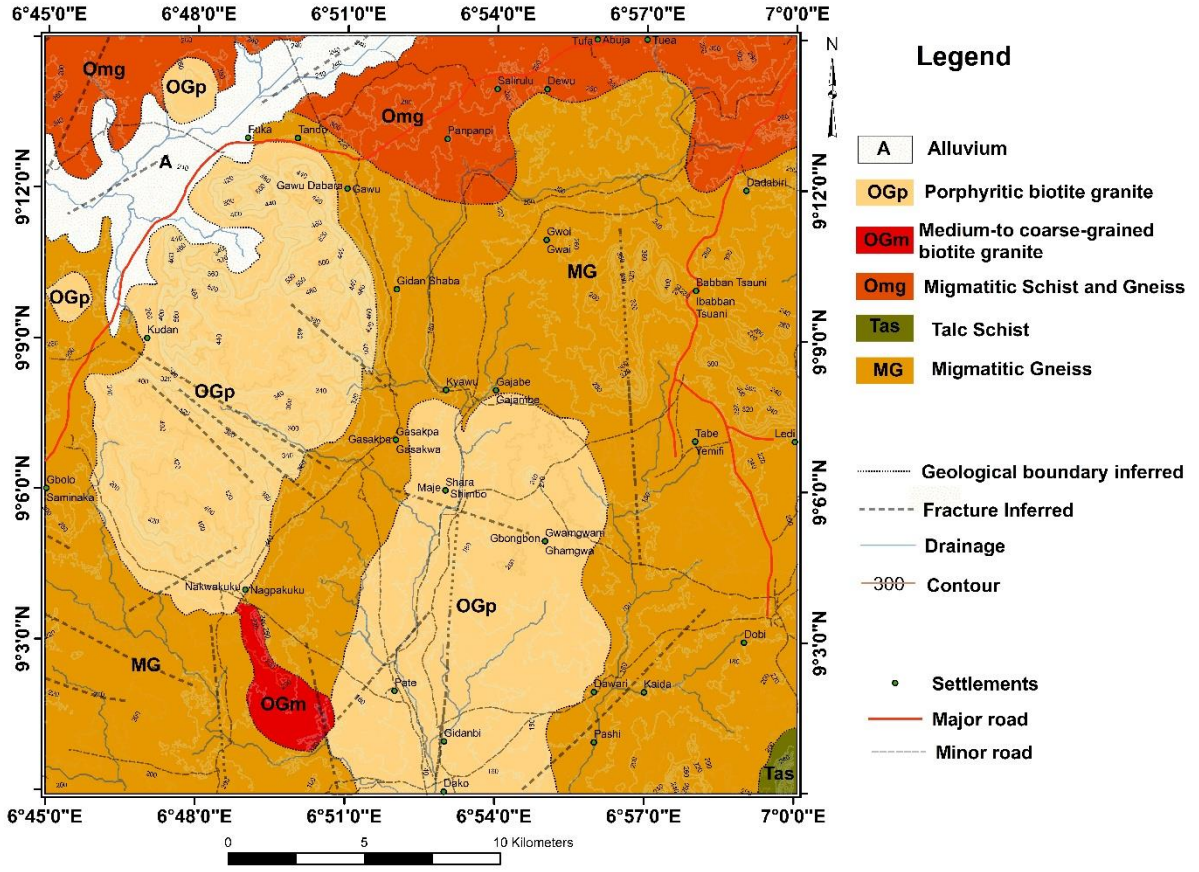

Figure 1: Geologic map of the area. Some fault lines are digitized from published geologic map. (Source: Nigerian Geological Survey Agency (NGSA), 2009).

3. Materials and Methods

In mineral exploration studies, method selection and tools to be applied are often dependent upon the mode of occurrence and formation of targeted mineral deposits (Gupta, 2003). This research has its target on Gold occurrences, which occur in fractures and are related to shear zones. Therefore, the best surface indications for these features are structural controls and hydrothermal alterations. These features are usually expressed as lineaments and lithological contrasts, respectively.

3.1 Satellite Imagery

3.1.1 Landsat 8 OLI

The satellite imagery used was clipped from the Landsat 8 scene LC81890542018016LGN00, from 20 January, 2018 from the earthexplorer.usgs.gov website, collected by sensors OLI (Operational Land Imager) and TIRS (Thermal Infrared Sensor). Landsat 8 band specifications are presented in Table 1. This scene was chosen due to its near perfect quality (9/9), the virtually non-existent cloud coverage (0.98/100) and due to the relatively low solar elevation (49.55°).

Table 1: Landsat band specifications. Source: USGS/NASA, 2015.

Sensor	Band	Spectral Resolution (µm)	Spatial resolution (m)
OLI	Band 1 - Coastal	0.435-0.451	30
	Band 2 - Blue	0.452-0.512	30
	Band 3 - Green	0.533-0.590	30
	Band 4 - Red	0.636-0.673	30
	Band 5 - NIR	0.851-0.879	30
	Band 6 - SWIR-1	1.566-1.651	30
	Band 7 - SWIR-2	2.107-2.294	30
	Band 8 - Pan	0.503-0.676	15
	Band 9 - Cirrus	1.363-1.384	30
TIRS	Band 10 - TIR-1	10.6-11.19	100
	Band 11 - TIR-2	11.50-12.51	100

3.1.2 ASTER

The extent of the study area was clipped from the ASTER Scene AST_L1T_00301282002100954_20150424050755_62951 of 28th of January, 2002 from https://earthdata.nasa.gov/. The scene has solar elevation of 59° and perfect cloud cover cloud cover of 0%. ASTER band specifications are presented in Table 2. It provides higher spatial, spectral, and radiometric resolutions than traditional Landsat data (Abrams and Hook, 2001). The ASTER channels are more contiguous in the shortwave infrared region than those of Landsat, yielding increased accuracy in the spectral identification of rocks and minerals (Crósta and Filho, 2003). More spectral bands provide a better understanding of the geology and soils of the earth surface. This is what makes ASTER data superior over other sensors for lithological mapping (e.g., Ninomiya *et al.*, 2005, 2006, Gad and Kusky, 2006, 2007).

The digital pre-processing, processing and preliminary lineament mapping of the SRTM, Landsat 8 and ASTER data were executed using ENVI software. Atmospheric correction of Landsat 8 OLI and ASTER images were performed using the FLAASH module of ENVI software. Spectral resampling has been used to downscale the spatial resolution of the SWIR bands of the ASTER data to 15 m.

Table 2. ASTER band specifications

System	Band	Spectral range (μm)	Spatial resolution	Radiometric resolution
VNIR	1	0.52 - 0.60	15 m	8 bit
	2	0.63 - 0.69		
	3	0.78 - 0.86		
SWIR	4	1.60 - 1.70	30 m	8 bit
	5	2.145 - 2.185		
	6	2.185 - 2.225		
	7	2.235 - 2.285		
	8	2.295 - 2.365		
	9	2.360 - 2.430		
TIR	10	8.125 - 8.825	90 m	12 bit
	11	8.475 - 8.825		
	12	8.925 - 9.275		
	13	10.25 - 10.95		
	14	10.95 - 11.65		

3.1.3 SRTM DEM

The National Imagery and Mapping Agency (NIMA), National Aeronautics and Space Administration (NASA) and German Aerospace Centre (DLR) collaborated to launch the SRTM Mission on February 11, 2000 with the primary objective of acquiring elevation data on a near-global scale and generate the most complete high-resolution digital topographic database of the Earth. Using the Space borne Imaging Radar-C and X-Band Synthetic Aperture Radar (SIR-C and X-SAR) hardware, SRTM collected data that were used to generate a digital elevation model with data points spaced every 1 arc second of latitude and longitude (approximately 30 metres at the equator). The absolute horizontal and vertical accuracy is better than 20 metres and 16 metres, respectively. SRTM uses radar interferometry. The 30 m SRTM data was downloaded from http://dwtkns.com/srtm30m/. This site is an interface that attempts to ease the pain of downloading 30-meter resolution elevation data from the Shuttle Radar Topography Mission website.

High-pass convolution filters (directional edge) from a Kernel 3 x 3 matrix were applied to the SRTM DEM image to emphasize the structures parallel to the direction of each filter (Drury, 2001). The directional filters were applied for the azimuths 0º, 45º, 90º, 135º, 180º, 225º, 270º and 315º for a comprehensive cover of the area using the ENVI software (Exelis Visual Information Solutions, Boulder, CO, USA)

3.1.4 Aero geophysical Data

The aeromagnetic inversion method is based on processing of the total field magnetic anomaly. Total magnetization is the rock property associated to its magnetic anomaly and geologic origin ([35]) in the direction of the earth's field. The total field aeromagnetic anomalies include both induced and remnant magnetic fields. This is a reflection of variations in the amount and type of subsurface magnetic minerals, hence, important for geophysical prospecting of mineral resources. The aeromagnetic data was obtained from Nigeria Geological Survey Agency (NGSA). The data were captured for NGSA from 2005 to 2010 by Fugro Airborne Surveys as part of nationwide airborne geophysical surveys. The data were acquired along a series of NE–SW profiles with a flight line spacing of 500 m and terrain clearance of 80 m. For this study one half degree sheet covering the study area was utilised. The total magnetic intensity field was International Geomagnetic Reference Field (IGRF, 2009) corrected and a super-regional field of 32,000 nT was deducted from the raw data. Oasis montaj software was used to grid the data at 125 m spatial resolution using the minimum curvature gridding method (Briggs, 1974)

and subsequently subjected to Reduction to the Magnetic Equator (RTE) and further processing were carried out in order to investigate the presence of buried structures that might be relevant in mineral exploration.

The aeroradiometric data was acquired using a high-sensitivity 256-channel airborne gamma ray spectrometer. The data of the survey was available in the form of total count, Potassium, equivalent Uranium, and equivalent Thorium data in a digital form. Enhancement and interpretation processes was done by using Oasis montaj software.

3.2 Data processing

3.2.1 Alteration mapping

The most important mineralogical difference between altered and unaltered rocks is the abundance of alteration minerals such as alunite, montmorillonite and kaolinite in the altered rocks. Furthermore, the difference between mineralized and non-mineralized altered rocks is the presence of abundant secondary iron minerals such as goethite, hematite, limonite and jarosite in association with other alteration minerals. In altered rocks, the change in abundance of any of the above-mentioned alteration minerals would lead to a slight change in the reflectance value that depends on that mineral's spectral characteristics.

3.2.2 Landsat 8 OLI

The following common digital processing techniques were used: Red, Green, Blue (RGB) colour composites, Principal Component Analysis (PCA), directional spatial filters and band ratios. Rationing is a common procedure used for feature enhancements based on the division of every pixel value of one band by the homologous pixels of the other band (Prost, 1983). A ratio is created by dividing brightness values, pixel by pixel, of one band by another so as to enhance spectral differences and suppress illumination differences. Band ratios of Landsat 8 OLI data are used to enhance rock alteration. Ratios exaggerate some subtle differences in spectral response. A false colour composite can then be made in such a way that to each ratio band is then assigned one of the three primary colours with the lighter parts (high DN values) of the band contributing more colour to the composite.

In this study, band ratios 4/2, 5/6, and 6/7 (RGB) has been used. This combination is selected for their sensitivity to lithologic variables, and for their lack of statistical redundancy (Crippen *et al.*,1990). The ratio of bands 4/2 enhances rocks with an abundance of ferric iron oxide (limonite) responsible for the hydrothermal alteration or the oxidation of Fe-Mg silicates. The ratio of bands 5/6 enhances rocks which are rich in ferrous iron and band ratio 6/7 enhances rocks having Al-OH, such as those clay and sulphate minerals produced from hydrothermal fluids.

3.2.3 ASTER data

A hybrid method based on the combination of band ratio images and the PCA method of Zhang *et al.*, (2007) who used the four mineralogical indices proposed by Ninomiya (2003) for hydrothermal alteration mapping. The formulae of Ninomiya (2003) indices are listed below:

OHI = (band 7/band 6) (band 4/band 6)

KLI = (band 4/band 5) (band 8/band 6)

ALI = (band 7/band 5) (band 7/band 8)

CLI= (band 6/band 8) (band 9/band 8)

where OHI is the index for OH-bearing minerals, KLI is the kaolinite index, ALI is the alunite index, and CLI is the calcite index. Each index was thresholded and then merged spatially to map the alteration zones using the mineralogical indices for each alteration mineral. Results obtained from these indices include feasibility-abundance maps of the OH-bearing minerals including alunite, kaolinite, muscovite and montmorillonite from the SWIR surface reflectance

data.

An ASTER band ratio image (bands 4/8, 4/2, and 8/9 in RGB respectively) has been created for better separation of the mineralized parts of the alteration zones (Figure 4). The ratio 4/8 was chosen to increase the response of the iron oxides in the altered mineralized rocks. The ratio 4/2 separates altered mineralized rocks from all the other background materials (both altered non-mineralized and the unaltered rocks). Finally, and for better contrast for the resulting image, 8/9 ratio was chosen to make an image for averaged values from all the rock units in the image area.

3.3 Aeromagnetic data

3.3.1 Vertical, total gradient and Tilt derivatives

First vertical derivative can be applied either in space or frequency domain. It is proposed by Nabighian (1984), using 3D Hilbert transforms in the x and y directions. It is used in this study to supress deeper anomalies while enhancing shallow features with their boundaries so as to make lineaments extraction easier. This is achieved by the vertical derivative amplifying short-wavelengths at the expense of longer ones, therefore making it easier for shallower causative sources to be mapped. Also, the analytic signal (total gradient) can be calculated either in space or frequency domain, producing a maximum directly over discrete bodies as well as their edges. Analytic signal is formed through the combination of the horizontal and vertical gradients of the magnetic anomaly (Ansari and Alamdar, 2009) and its amplitude is independent on the magnetisation direction. This filter applied to reveal the anomaly texture and highlight discontinuities also enhance short- wavelength anomalies (Roest *et al.,* 1992).

The amplitude of the signal peak of analytic signal is directly proportional to the edge of magnetization. Hence source edges are easily determined. The magnetic tilt derivative (TDR) combines all three gradients (X, Y and Z) to produce what is a called a tilt angle. This product highlights very subtle, near surface structures in the dataset where the zero-contour line of the grid is said to represent geology contacts or edges of bodies.

3.3.2 Aeroradiometric data

Gamma-ray spectrometry (GRS) can be very helpful in mapping surface geology. The method provides estimates of apparent surface concentrations of the most common naturally occurring

radioactive elements comprising potassium (K), equivalent uranium (eU), and equivalent thorium (eTh). The use of the method for geological mapping is based on the assumption that absolute and relative concentrations of these radio elements vary measurably and significantly with lithology. The aeroradiometric technique assists considerably in mapping surface structure, lithological units and identification of hydrothermal alteration zones. The radiometric data are gridded to obtain total count, potassium, equivalent thorium and equivalent uranium maps to show the surface distribution of these elements. Also, producing K/eTh ratio map help to map hydrothermally altered zones, since a reduction in eTh and a rise in K is an indicator of

alteration environments in an ore deposit (Ostrovskiy, 1975). Finally, A ternary map is created by combining the three radioelements concentration in the RGB colours.

3.4 Lineament extraction

3.4.1 Surface lineament extraction

In order to extract lineaments from the remotely sensed datasets, directional spatial filters are applied so as to modify pixel values of the remotely sensed images based on the values of neighbouring pixels using 3X3 kernels allowing for edge enhancement in a particular direction (Gupta, 2003; Lillesand and Kiefer, 2004; Schowengerdt, 2007). The main applications of this type of filters include: obtaining sharper and more detailed images, edge enhancement and reducing local illumination effects (Gupta, 2008). Four directional filters depicted in (Figure 2) were applied to the Landsat 8 OLI, ASTER and SRTM DEM datasets. All lineaments from various remotely sensed datasets were merged to form a composite surface lineament map of the study area and subsequently plotted as a Rosette diagram. To group these features, the classification used by Batista *et al,*. (2014) was adopted, where the N-S and E-W limits comprise a margin of 10º in clockwise and anti-clockwise directions.

N - S		
-1	-1	-1
0	0	0
1	1	1

W - E		
-1	0	1
-1	0	1
-1	0	1

NW -SE		
-1	-1	0
-1	0	1
0	1	1

NE - SW		
0	-1	-1
1	0	-1
1	1	0

Figure 2. Directional spatial filters applied to Landsat 8 imagery Richards and Jia, 2006.

3.4.2 Magnetic Lineament extraction

Magnetic lineaments were delineated using the CET Grid Analysis plugins included in Oasis montaj software. The CET grid analysis is a new technique developed by Centre for Exploration Targeting (CET), University of Western Australia consists of a number of tools that provide automated lineament detection of gridded data, which can be used for first-pass data processing. As explorers often have large volumes of gridded data to interpret, these tools provide a rapid unbiased workflow that reduces the time with which one can interpret gridded data.

The extension is specifically designed for mineral exploration geophysicists and geologists looking for discontinuities within magnetic and gravity data. The CET Grid Analysis provides a step-by-step trend detection menu which offers two different approaches to trend estimation. The first method, *Texture analysis-based image enhancement*, is suitable for analysing regions of subdued magnetic or gravity responses where texture analysis can first enhance the local data contrast. The second method, *Discontinuity structure detection*, is useful in identifying linear discontinuities and edge detection. These methods use a phase-based approach will ensure that even features lying in low contrast regions will be detected. Edge detection proceeds with Lineation Detection, to find edges in magnetic or data irrespective of their orientation or contrast with the background and Lineation Vectorisation, to generate trend line estimates from the edge information detected by the phase congruency transform. The phase congruency transform is a contrast-invariant edge detection method based on observing the local spatial frequencies (Kovesi 1997, 1999).

3.5 Final fuzzy integration procedure

The fuzzy logic method allows weights to be assigned to each evidential layer based upon informed decisions and opinions. The fuzzy-set theory defines a degree of membership in a set represented by a value between 0 and 1. The value of the membership function can be determined by two methods. One method is to calculate according to the membership function curve; the other is to assign values artificially according to geological knowledge. The fuzzy model in mineral prediction consists of two steps: (1) fuzzification of data (2) fuzzy synthesis of fuzzified data. Fuzzy synthesis is executed using the operator. The most basic fuzzy operators are: fuzzy AND; fuzzy OR; fuzzy algebraic product; fuzzy algebraic sum; and fuzzy gamma.

The fuzzy Sum operator highlights the maximum values available for all input criteria. The sum fuzzy operator assumes that the more favourable input is better. The resulting sum is an increasing linear combination function that is based upon the number of criteria entering the analysis. The fuzzy gamma operator was used to calculate the final prospectivity map in the present study. The fuzzy Gamma type is an algebraic product of fuzzy Product and fuzzy Sum, which are both raised to the power of gamma. The generalize function is as follows: $\mu(x) = (\text{FuzzySum})^{\gamma} * (\text{FuzzyProduct})$. The final prospective map was prepared with fuzzy $\gamma = 0.9$ operator.

4.0 Results and discussion

4.1 Alteration mapping: Hydrothermal deposits develop along faults and fractures. Increased permeability along faults probably controlled the pathways followed by fluids that deposited metals and gangue minerals (Boleneus *et al.*, 2001). Therefore, faults and major fractures are considered as potential localizers for ore deposition. The major faults were delineated from enhanced aeromagnetic data, Landsat 8 OLI, SRTM satellite image and geological map of the study area.

The detection of alteration zones using Landsat 8 OLI images marked by the presence of iron oxides, hydroxyl- bearing minerals and hydrothermal clays was made possible from false colour composite image band ratios of 6/4, 4/2 and 6/7 in red, green and blue (Sabins, 1997; Knepper, 1989; Khalid and AbdelHalim, 2014; Pour *et al*., 2014; Ducart *et al*., 2016). Primary colours of red, green and blue are indicative of high ratio value band ratios of 6/4, 4/2 and 6/7 respectively. High band ratio values of two colours are depicted in the pixel as a combination of two colours proportional to their values. High 6/4 values (red) give a high composition of iron oxides (both ferric and ferrous); large 4/2 values (green) represent a large component of ferric oxides associated soils. For example, iron oxide-rich parts of the alteration are considered to be the main target for gold exploration.

Furthermore, high 6/7 values (blue) represent the presence of hydrothermal clays since the band 6 covers the reflectance peak of hydrothermal clays whereas band 7 contains a reflectance trough of the clays. A large 6/4 and 4/2 band ratio values in the same pixel will display as yellow, while high band ratios of 6/4 and 6/7 value in one pixel will be displayed as pink. The largely blue areas in the study area of the band ratio composite map correlates well with areas having high lineament densities. These are areas are rich in iron oxide minerals and hydrothermally altered clays (Figure 13). Ferric minerals are found doting around other parts of the study area.

The method for Landsat OLI was adapted also to create the ASTER alteration images. In this case, iron oxides, hydroxyl- bearing minerals and hydrothermal clays as possible false colour composite image band ratios of 4/8, 4/2 and 8/9 in red, green and blue were created. A large

4/8 and 4/2 band ratio values in the same pixel will display as yellow, while high band ratios of 4/2 and 8/9 value in one pixel will be displayed as blue. Mapped mineralogical units related to gold deposits maybe used as an exploration tool in areas around the study area where promising locations are expected. It is to be noted that several field visits were carried out for updated lithological mapping resulting in the production of the geological map that provided useful information for this study.

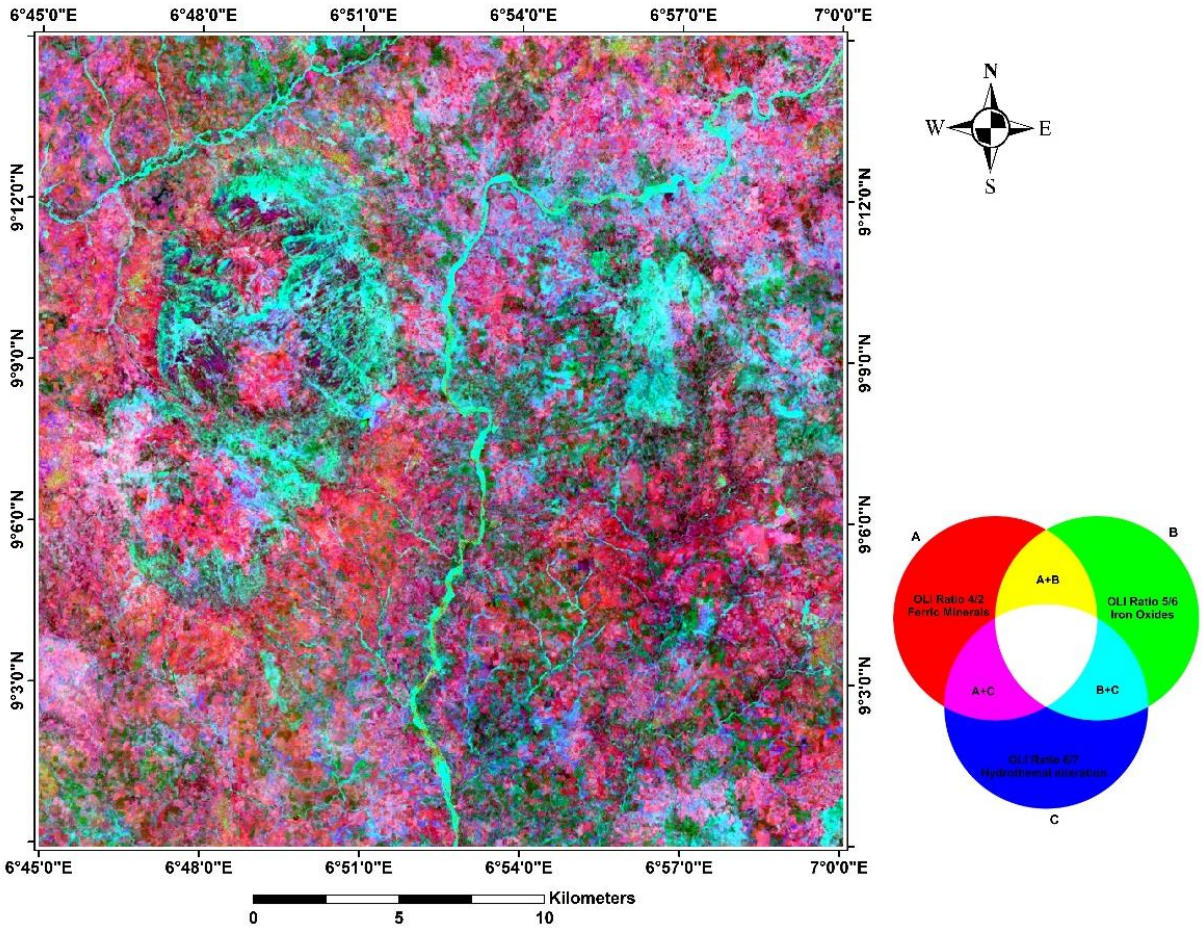

Figure 3: Landsat False Colour Composite

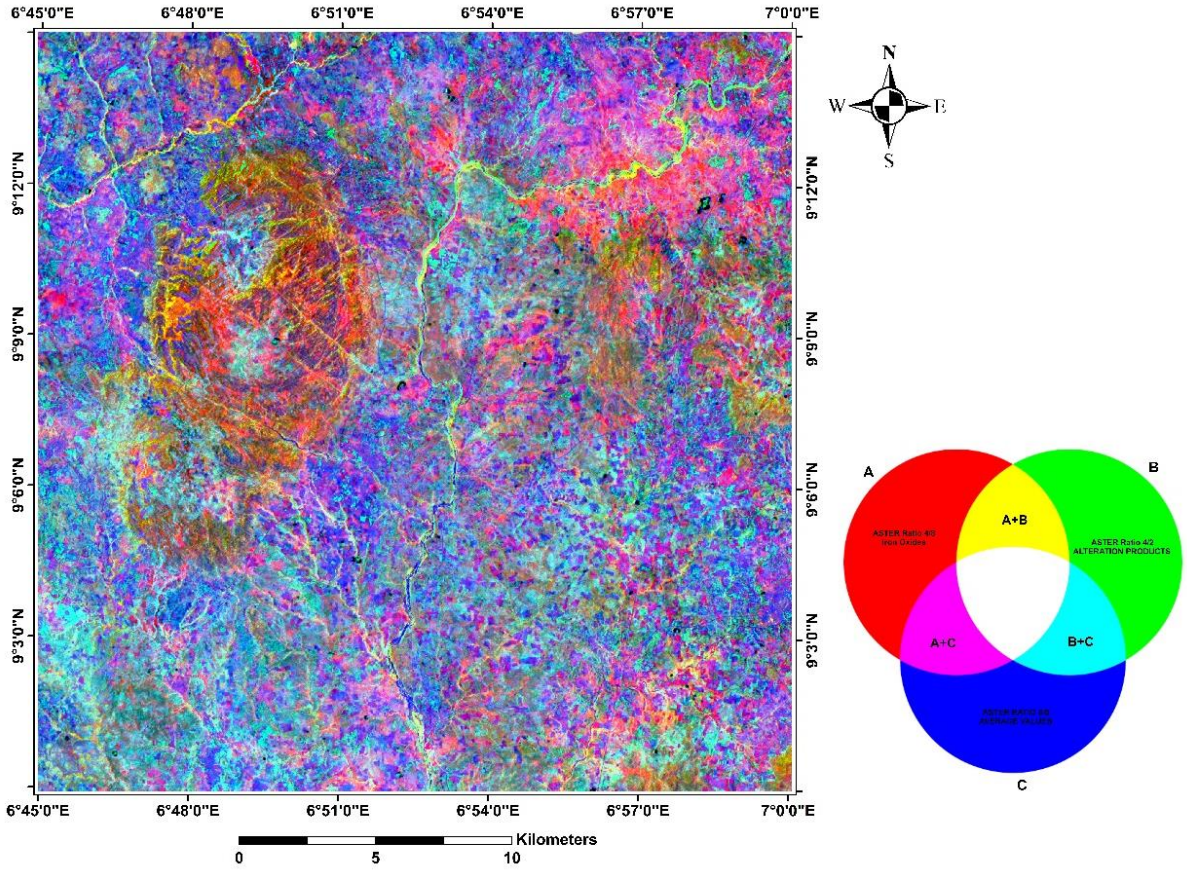

Figure 4: ASTER False Colour Composite

4.2 **Aeromagnetic data analyses**

Residual magnetic anomaly image (Reduced to Equator (RTE) (Figure 4) shows an amplitude variation in the range of -481 to 336 nT in the study area due to wide variation of susceptibility values of various lithologic units (magnetic/moderate-magnetic basement). High amplitude, short wavelength anomaly pattern in the north-eastern and north-western part of the area shallow nature of the basement. Since the contact is unconformable, the boundary in magnetic anomaly image is gradational. The magnetic bodies are oriented in the NE-SW direction marked in the magnetic anomaly image. This is also evident in the hill shade image of the residual magnetic anomaly map.

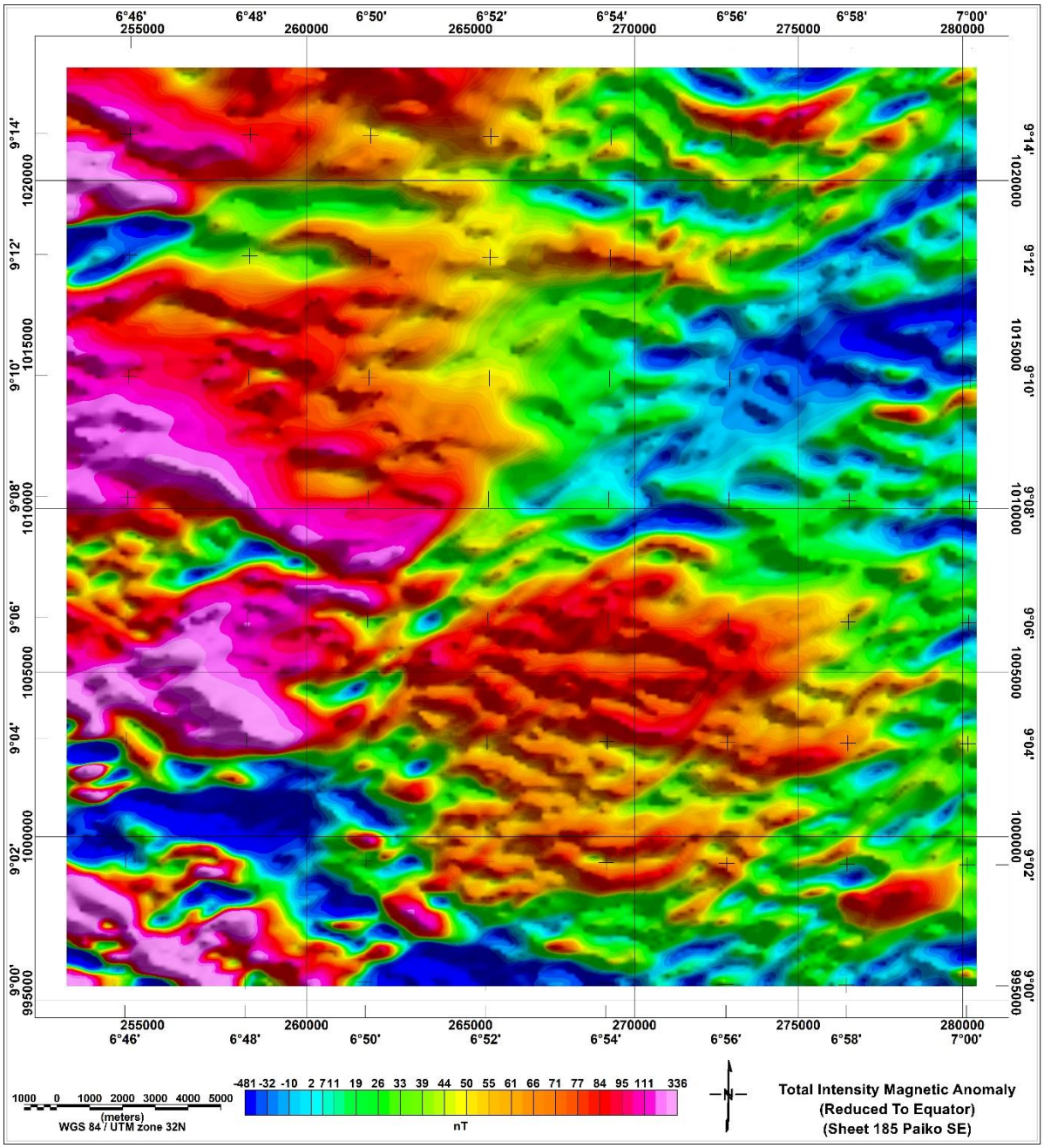

Figure 5: Total Intensity Magnetic Anomaly map of Sheet 185 (Paiko SE). Areas in magenta are of high magnetic intensity, while blue coloured areas have low magnetic intensities. Data was processed using Oasis montaj software.

Detailed structural fabric has been deciphered based on study of First vertical derivative image (Figure 6) and tilt derivative image (Figure 7). All zones of magnetic minima as well as displacements/discontinuities of magnetic anomalies were interpreted as linear structures. Some of these negative anomalies have remarkable positive anomalies at the edges, though not all of the structures are lined with these positive anomalies. The presence of linear, negative and positive anomalies next to each other is due to the general geometry of magnetic anomalies (Telford *et al.*, 1990).

First vertical derivative image indicates that magnetic linears generally trend NE-SW sectors with minor NE-SW and E-W components. Linears along NE-SW directions are dominant with

minor E-W and NW-SE components. Here, the basement faults (NE-SW) are better resolved. The amplitude of the signal peak of analytic signal is directly proportional to the edge of magnetization. Hence source edges are easily determined. The analytic signal has a form over causative body that depends on the locations of the body (horizontal coordinate and depth) but not on its magnetization direction. of magnetization. Analytic signal is often effective at highlighting geologically meaningful subtle anomalies (Lyatsky *et al.*,2004). Tilt Derivative revealed short wavelengths and enhanced the presence of magnetic lineaments as well as boundaries of magnetic bodies within the study area using its zero-crossing.

The radiometric response in the ternary map (Figure 10) to some extent corresponds with the surface rock units of the study area and shows a close spatial correlation with the rock units. The visual inspection of this map shows that high concentration of K, eTh and eU radioactive elements are displayed in lighter colour and related to Older Granites.

The composite image does not provide colour discrimination between older granites (OGp) and the (OGm). This can be discussed to the resemblance of radioelement content and the redistribution of radioelements concentration in the overburden because of high weathering process. There was however, a discrimination between the Migmatitic rocks (MG).

4.3 Fuzzy integration

The fuzzy logic technique was used to construct a prospectivity mapping model for hydrothermal gold deposits and highlighted potential exploration targets in the study area. Some evidence maps were used for evaluating the importance of each data set in data analysis algorithm. The prospectivity map highlighted three potential exploration targets for gold mineralization within the study area. The predicted favourable zones coincide spatially with anomalous zones for stream sediment Au, Ag, Zn and Pb contents (Figure 10) and suggested for future detailed exploration.

5.0 Conclusion

Satellite imagery and aerogeophysical datasets were used to map hydrothermal alteration zones and extract the structural lineaments. Based on the exploration model considered for the study area, appropriate evidence maps include hydrothermal alteration, host rock and structural maps were developed, weighted and reclassified. Finally, fuzzy operators are applied to produce mineral prospectivity map. Mineral prospectivity map comparison with field studies and this revealed that the fuzzy logic model describes fairly well the favourability of the hydrothermal gold deposits in the study area. All produced maps in this study should be perceived as the preliminary evaluation of the study area in a reliable manner. The maps are a valuable data source for the detailed studies to be conducted in the future.

The results of remotely sensed images, aeromagnetic, aeroradiometric datasets and geology were integrated to produce a composite favourability map of the study area (Figure 10). The predominant tectonic trends are NE – SW, NW – SE and the E – W. The NE-SW (the predominant in the Basement Complex areas) was the most developed one among these trends and represents the preferred orientation of ore deposits. Also, a number of hydrothermally altered zones are mapped from the Landsat OLI and ASTER images. Since these zones have one or more structures associations, they serve as channel pathways for migrating hydrothermal fluids that contemporaneously reacts with rock formation which got altered subsequently. The alteration zones marked by low magnetic intensity and significant radiometric response lie within or close to a structure that has a NE – SW trend identified previously. The coincidence areas of these alteration zones and high complexity lineaments indicated a high possibility for the occurrence of gold mineralization in other similar locations. Thus, as mentioned previously,

the close concordance between these known mineralization locations and the interpreted structural complexities sheds a light towards the similar mapped features that may be new promising sites. However, precise detection and evaluation of these ores need more geological and geophysical follow up survey with finer spacing.

As a consequence, the use of satellite images for hydrothermal alteration mapping and spatial data modelling during the early stages of mineral exploration has been found to be very successful in delineating the hydrothermally altered rocks. Conceptual fuzzy-logic method also gives a flexible tool to test exploration models in an easily understood manner for geologists. The uncertainties of the fuzzy-logic modelling could not be estimated easily, but an expert validation process would in many cases be appropriate and lead to reliable results.

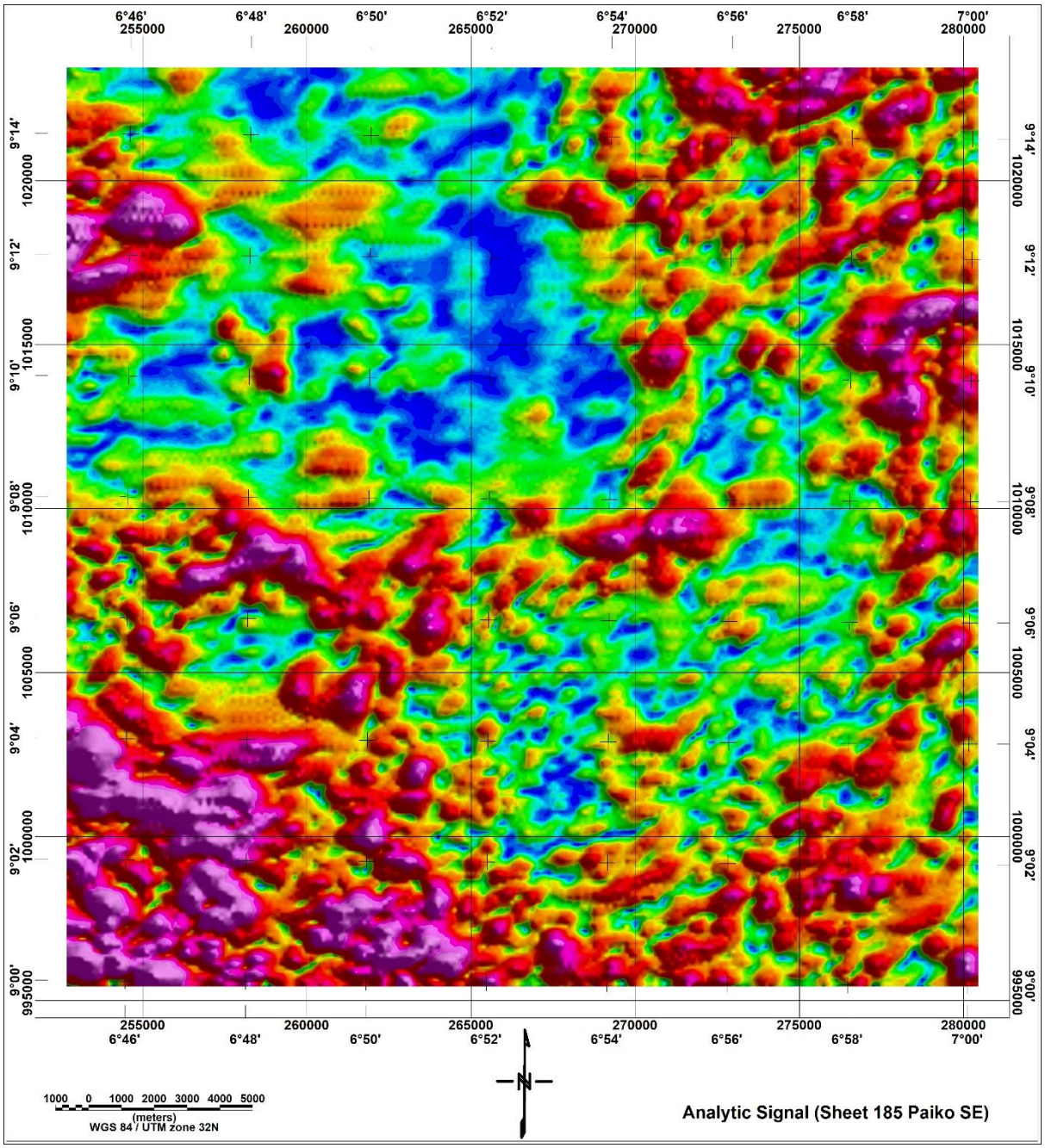

Figure 6: Analytic Signal map of Sheet 185 (Paiko SE). Data was processed using Oasis montaj software. Maxima, represented by areas in magenta, show edge/contact of discreet bodies.

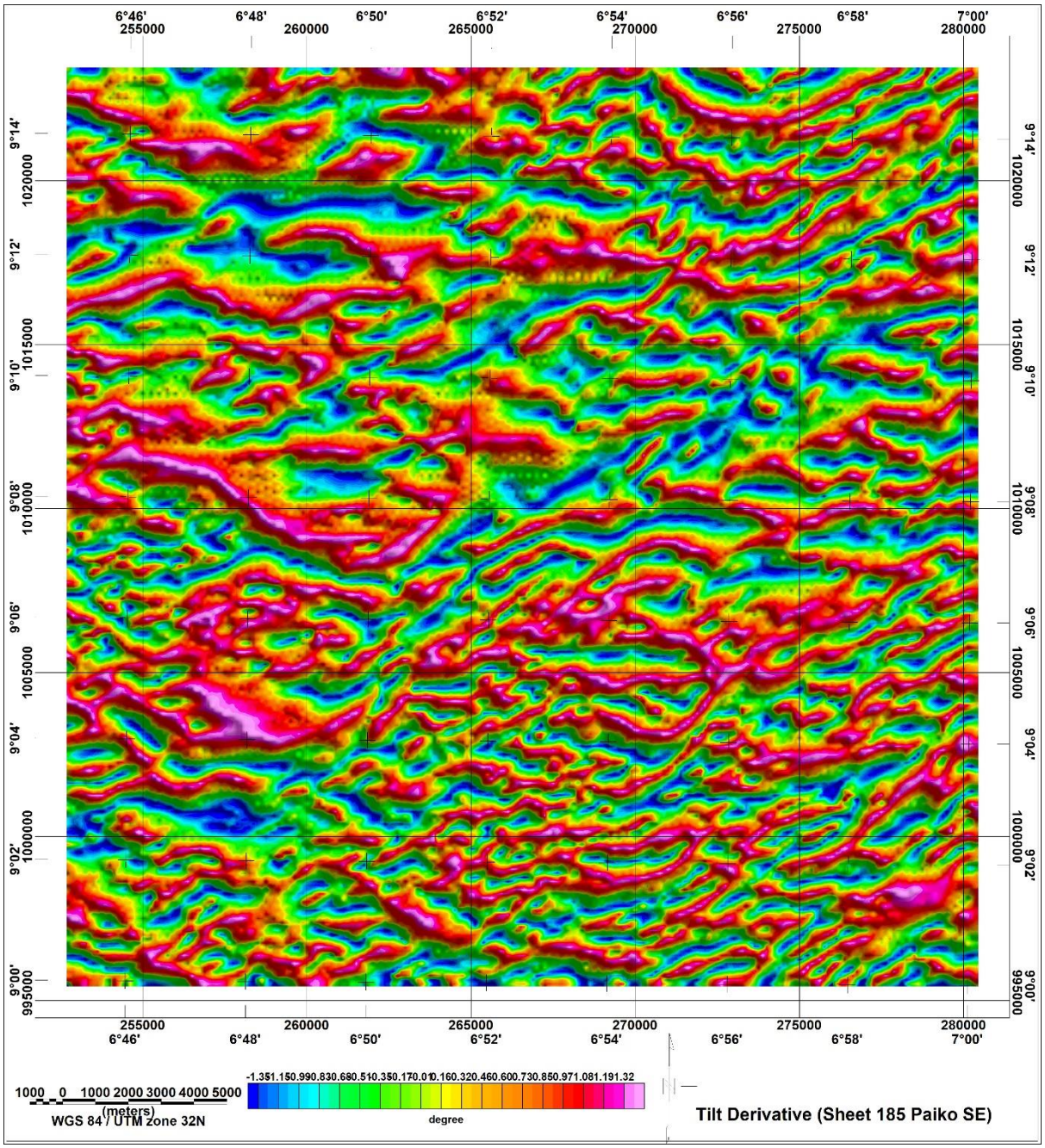

Figure 7: Tilt Derivative map of Sheet 185 (Paiko SE). Data was processed using Oasis montaj software. Minima, represented by areas in blue, allowed for the delineation of magnetic lineaments.

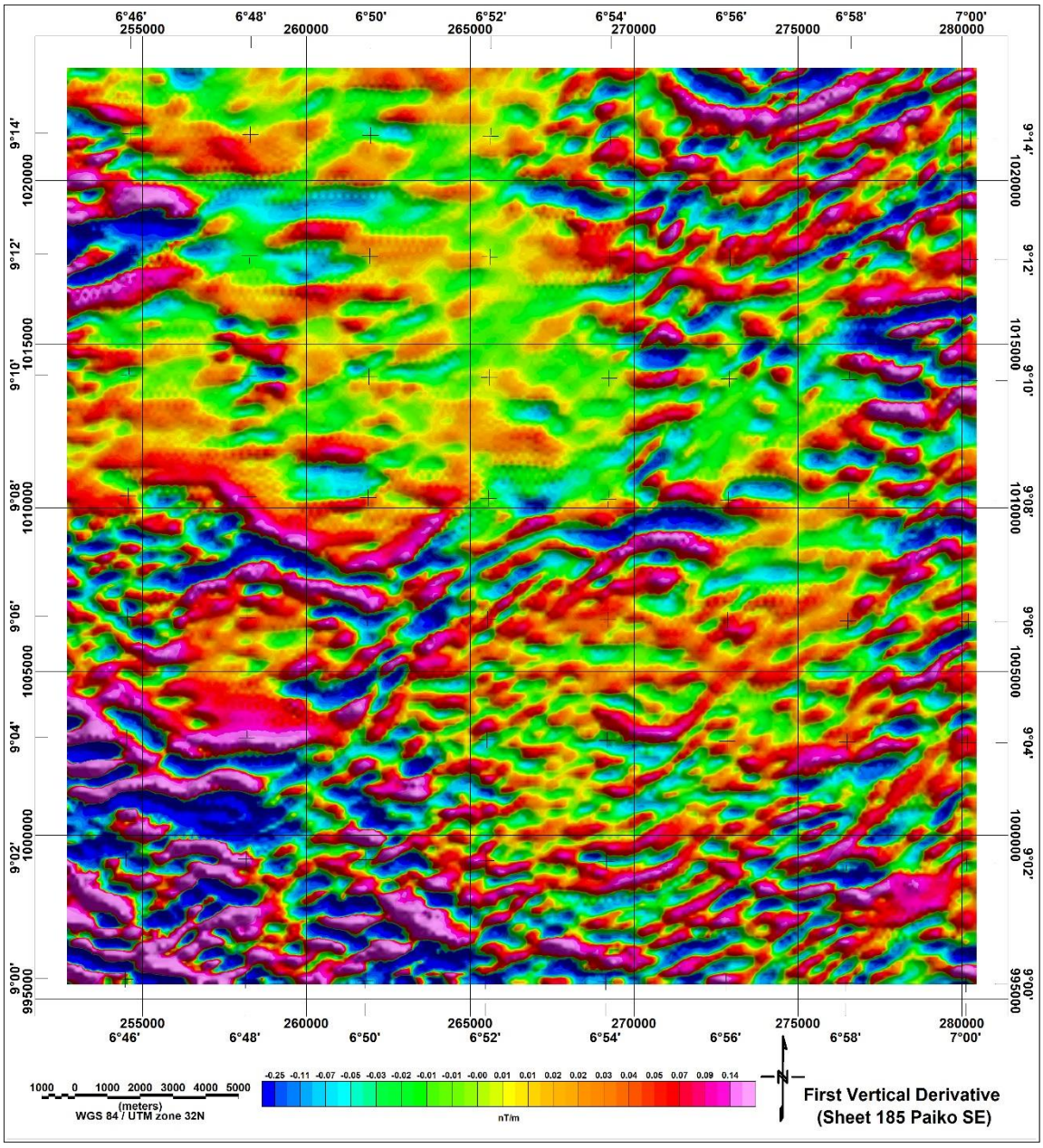

Figure 8: First Vertical Derivative map of Sheet 185 (Paiko SE). Data was processed using Oasis montaj software.

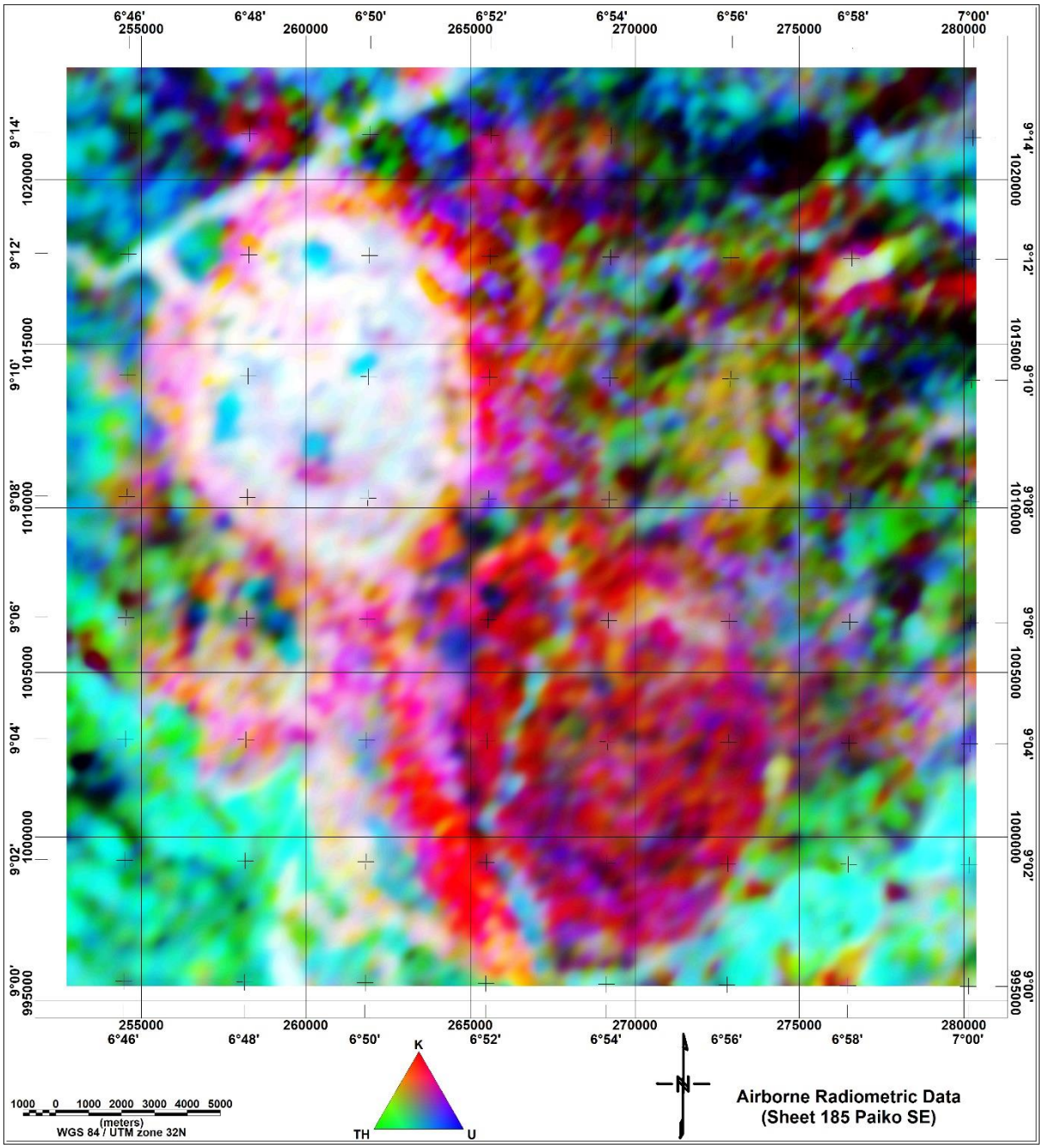

Figure 9: Ternary Map of Sheet 185 (Paiko SE). Data was processed using Oasis montaj software. Areas in magenta represent zones of high K content. Areas in green represent zones of high Th content while areas in blue highlight areas enriched in U.

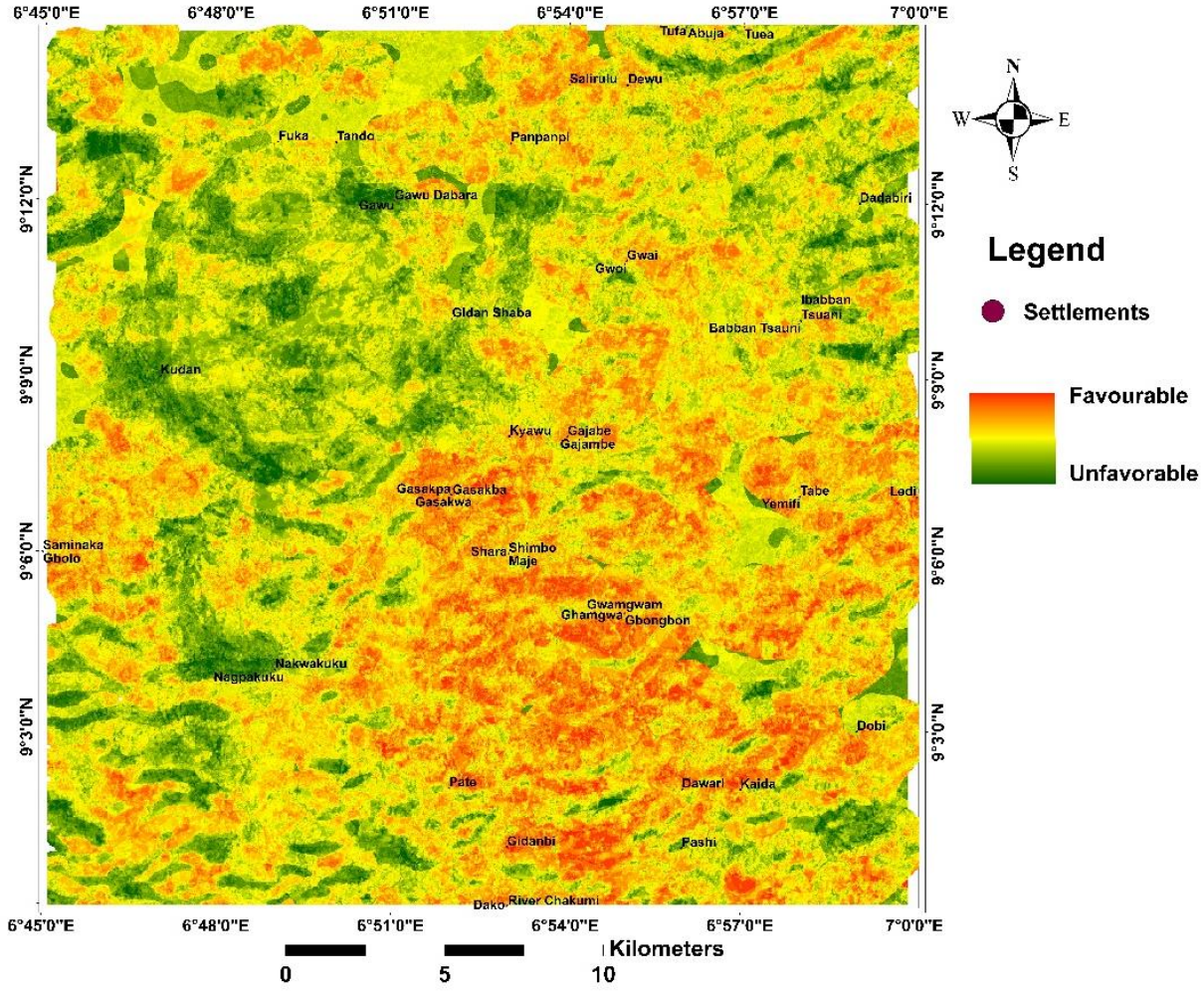

Figure 10: Favourability map of Sheet 185 (Paiko SE). Areas in orange are delineated as areas more favourable to mineralisation. Green areas have been adjudged unfavourable.

References

Abrams, M., Hook, S., 2001. ASTER User Handbook (version 2). Jet Propulsion Laboratory, Pasadena, CA-91109, USA. 135 pp.

Adegoke, K.M. and Bulus, L.G. (2015). Satellite Remote Sensing for Mineral Deposit Assessment of Clay in Mubi Local Government Area of Adamawa State, Nigeria, *Geosciences*, Vol. 5 No. 1, 2015, pp. 26-30. doi: 10.5923/j.geo.20150501.03.

Adegoke, K.M., Bulus L.G. (2015). Hydrological and Morphometric Analysis of Upper Yedzaram Catchment of Mubi in Adamawa State, Nigeria. Using Geographic Information System (GIS), *World Environment*, Vol. 5 No. 2, 2015, pp. 63-69. doi: 10.5923/j.env.20150502.03.

Ajibade, A. C., Woakes, M. & Rahaman, M.A., 1981. Proterozoic crustal development in the Pan-African regime of Nigeria. In Kroner, A. (Ed.), *Precambrian Plate Tectonics, Elsevier*, Amsterdam.

Aliyu, J. A., Mazlan H. and Amin Pour, A.B (2018). Identification of hydrothermal alteration minerals associated with geothermal system using ASTER and Hyperion satellite data: a

case study from Yankari Park, NE Nigeria, Geocarto International, DOI: 10.1080/10106049.2017.1421716.

Ansari, A.H., Alamdar, K., 2009. Reduction to the pole of magnetic anomalies using analytic signal. World Appl. Sci. J. 7, 405–409.

Batista, C. T., Veríssimo, C. U. V., Amaral, W. S. (2014). Levantamento de feições estruturais lineares a partir de sensoriamento remoto – uma contribuição para o mapeamento geotécnico na Serra de Baturité, Ceará. Geologia USP. Série Científica, 14(2), 67-82. http://dx.doi.org/10.5327/Z1519-874X201400020004.

Black, R. (1980). Precambrian of West Africa. *Episodes*, 4, 3–8.

Boleneus DE, Raines G, Causey J *et al.*, (2001) Assessment method for epithermal gold deposits in northeast Washington State using weights-of-evidence GIS modeling. US Department of the Interior, US Geological Survey, Menlo Park.

Bonham-Carter, G.F., Agterberg, F.P., Cheng, Q., Behnia, P., Raines, G., and Kerswill, J., 2009, Correcting for bias in weights-ofevidence applications to assessing mineral processing: IAMG-2009 Conference Proceedings, Stanford University.

Briggs IC (1974). Machine contouring using minimum curvature. Geophysics 39(1):39-48.

Caby, R. Bertrand, J.M.I. and Black, R. (1981). Pan African ocean closure and continental collision in the Hoggar-Iforas segment, central Sahara. In: A Kroner (Editor) Precambrian plate tectonic. *Elsevier, Amsterdam*, 407-434.

Carranza EJM, Hale M (2001) Geologically-constrained fuzzy mapping of gold mineralization potential, Baguio district, Philippines. Nat Resour Res 10:125–136.

Crippen, R. E., E. J. Hajic, J. E. Estes, and R. G. Blom (1990). Statistical band and band-ratio selection to maximize spectral information in color composite displays, in preparation for submission to international Journal of Remote Sensing.

Crósta, A.P., Filho, C.R.d.S., 2003. Searching for gold with ASTER. Earth Observation Magazine 12 (5), 38–41.

Dada, S. S., Lancelot, J. R. and Briqueu, I. (1987). Age and origin of a Pan-African charnockitic complex: U-Pb and Rb-Sr evidence from the charnockitic complex at Toro, Northern Nigeria. Abtr. Vol. 14 Coll. Afri. Geol. Berlin, 72-73.

Dada, S.S. (2006). Proterozoic evolution of Nigeria. In Oshi O. (Eds.), *The Basement Complex of Nigeria and its Mineral Resources* (A tribute to Prof. M. A. Rahaman). (pp. 29-44). Akin Jinad and Co. Ibadan.

Ducart, D. F., Silva, A. M., Toledo, C. L. B., & deAssis, L.M. (2016). Mapeamento de óxidos de ferro usando imagens Landsat-8/OLI e EO-1/Hyperion nos depósitos ferríferos da Serra Norte, Província Mineral de Carajás, Brasil. Brazilian Journal of Geology. 46, 331-349.

Ejepu J.S., Arikawe, E.A. and Abdullahi, S. (2018). Geological, Multispectral and Aeromagnetic Expressions of Pegmatite Hosted Mineralization of Keffi Sheet 208 NE,

North-Central Nigeria. American Journal of Modern Physics and Application. Vol. 5, No. 4, pp. 53-69.

Emanuel J. Caranza (2002). Geologically-Constrained Mineral Potential Mapping (Examples from the Philippines). ITC Publication Number 86 International Institute for Aerospace Survey and Earth Sciences (ITC) Hengelosestraat 99, 7514 AE Enschede, The Netherlands.

Gabr, S.S., Hassan, S.M. and Sadek, M.F. (2015). Prospecting for new gold-bearing alteration zones at El-Hoteib area, South Eastern Desert, Egypt, using remote sensing data analysis. Ore Geology Reviews, Elsevier.

Gad, S., Kusky, T., 2006. Lithological mapping in the Eastern Desert of Egypt, the Barramiya area, using Landsat thematic mapper (TM). Journal of African Earth Sciences 44, 196–202.

Gad, S., Kusky, T., 2007. ASTER spectral ratioing for lithological mapping in the Arabian Nubian shield, the Neoproterozoic Wadi Kid area, Sinai, Egypt. Gondwana Research 11, 326–335.

Grant, N.K. (1978). Structural distinction between a sedimentary cover and an underlying basement in 600 m.y. old Pan-African domain of northwestern Nigeria, West Africa. *Geological Society American Bulletin* 89: 50-58.

Gupta, R.P., 2003. Remote Sensing Geology, second ed. Springer- Verlag, Berlin.

International Geomagnetic Reference Field - 11th Generation (2009). https://www.ngdc.noaa.gov/metaview/page?xml=NOAA/NESDIS/NGDC/MGG/GeophysicalModels/iso/xml/IGRF11.xml&view=getDataView&header=none.

Khalid A., Elsayed Z. and AbdelHalim H. (2014). The Use of Landsat 8 OLI Image for the Delineation of Gossanic Ridges in the Red Sea Hills of NE Sudan. *American Journal of Earth Sciences*. Vol. 1, No. 3. pp. 62-67.

Knepper, D. H., Jr., (1989). Mapping hydrothermal alteration with Landsat Thematic Mapper data, Lee, Keenan, ed., Remote sensing in exploration geology — A combined short course and field trip: 28th International Geological Congress Guidebook T182, p. 13–21.

Kovesi, P., 1997. Symmetry and Asymmetry from Local Phase, in: Tenth Australian Joint 593 Converence on Artificial Intelligence. pp. 2–4. 594.

Kovesi, P., 1999. Image Features from Phase Congruency. The MIT Press, Videre: Journal of 595 Computer Vision Research Volume 1, 1–26.

Lillesand, T.M., Kiefer, R.W., 2004. Remote Sensing and Image Interpretation, fifth ed. John Wiley and Sons, Inc., New York.

Masoud Moradi & Sedigheh Basiri & Ali Kananian & Keivan Kabiri (2014). Fuzzy logic modeling for hydrothermal gold mineralization mapping using geochemical, geological, ASTER imageries and other geo-data, a case study in Central Alborz, Iran. Earth Sci Inform DOI 10.1007/s12145-014-0151-9.

Masoud, M., Sedigheh, B., Ali K. and Keivan, K. (2014). Fuzzy logic modeling for hydrothermal gold mineralization mapping using geochemical, geological, ASTER imageries and other geo-data, a case study in Central Alborz, Iran. Earth Sci Inform. DOI 10.1007/s12145-014-0151-9.

McCurry, P. (1976). The geology of the Precambrian to Lower Palaeozoic rocks of northern Nig. A review In: C.A. Kogbe (Editor) geology of Nigeria. *Elizabethan press Lagos*, 15-39.

Morteza Tabaei, Mahin Mansouri Esfahani, Pezhman Rasekh, Ali Esna-ashari (2017). Mineral prospectivity mapping in GIS using fuzzy logic integration in Khondab area, western Markazi province, Iran. Journal of Tethys: Vol. 5, No. 4, 367–379.

Ninomiya, Y., 2003. A stabilized vegetation index and several mineralogic indices defined for ASTER VNIR and SWIR data. Proceedings of IEEE 2003 International Geoscience and Remote Sensing Symposium: IGARSS'03, 3, pp. 1552–1554.

Ninomiya, Y., Fu, B., Cudhy, T.J., 2005. Detecting lithology with Advanced Spaceborne Thermal Emission and Refection Radiometer (ASTER) multispectral thermal infrared "radiance-at-senseor" data. Remote Sensing of Environment 99, 127–135.

Ninomiya, Y., Fu, B., Cudhy, T.J., 2006. Corrigendum to "Detecting lithology with Advanced Spaceborne Thermal Emission and Refection Radiometer (ASTER) multispectral thermal infrared 'radiance-at-sensor' data". Remote Sensing of Environment 101, 567.

Nykänen V, Salmirinne H (2007) Prospectivity analysis of gold using regional geophysical and geochemical data from the Central Lapland Greenstone Belt, Finland. Gold in the Central Lapland Greenstone Belt: Geological Survey of Finland, Special Paper 44: 251–269.

Odeyemi, I. B. (1988). Lithostratigraghic and structural relationships of the upper Precambrian metasediments in Igarra area. In: Precambrian Geology of Nigeria. *Geological survey of Nigeria,* pp. 111-125.

Olade, M.A. and Elueze, A.A. (1979). Petrochemistry of Illesha Amphibolites and Precambrian Crustal Evolution in the Pan-African Domain of Southwestern Nigeria. Precambrian Research, 8, Pp.308-318, 1979.

Olasehinde P. I. (1999): An integrated geologic and geophysical exploration technique for groundwater in the Basement Complex of West Central Nigeria. *Water Resources Journal*, 10, 46-49.

Olasehinde P. I., Ejepu S. J. & Alabi A. A. (2013). Fracture Detection in a Hard Rock Terrain Using Radial Geoelectric Sounding Techniques. *Water Resources Journal* 23(1&2), 1-19.

Olasehinde, P. I. (2010). The Groundwaters of Nigeria: A Solution to Sustainable National Water Needs. *Federal University of Technology, Minna Inaugural Lecture Series 17.*

Oluyide, P .O. (1988). Structural trends in the Nigerian Basement Complex. In: Precambrian Geology of Nigeria. *Geological Survey of Nigeria*, pp. 93 - 98.

Ostrovskiy, E.A., 1975. Antagonism of radioactive elements in wallrock alteration fields and its use in aerogamma spectrometric prospecting. Int. Geol. Rev. 17 (4), 461–468.

Oyawoye, M.O. The Geology of the Nigerian Basement Complex, Nigeria, J. Min. Geol. and metal. Soc. (1), Pp. 7-102, 1964.

Pour, A. B., Hashim, M. & Marghany, M. (2014). Exploration of gold mineralization in a tropical region using Earth Observing-1 (EO1) and JERS-1 SAR data: a case study from Bau gold field, Sarawak, Malaysia. Arab J Geosci 7: 2393. https://doi.org/10.1007/s12517-013-0969-3.

Prost, G. (1983). Mineral exploration with Skylab photography in Central Colorado. *Economic Geology*, vol. 78, pp. 633-640.

Quadros TF, Koppe JC, Strieder AJ et al (2006) Mineral-potential mapping: a comparison of weights of evidence and fuzzy methods. Nat Resour Res 15:49–65.

Rahaman, M.A. & Ocan, D. (1978). On Relationship in the Precambrian Migmatite-gneiss on Nigeria. *Journal of Mining and Geology, 15*, 23-32.

Rahaman, M.A. (1988). Recent advances in the study of the Basement Complex of Nigeria. Precambrian Geology of Nigeria, *Geological Survey of Nigeria Publications,* 11-43.

Rasekh Pezhman, Kiani Farshid, Asadi Hooshang & Tabatabaei Seyed Hassan (2016). Mineral Prospectivity Mapping by Fuzzy Logic Data Integration, Kajan Area in Central Iran. 34th National and the 2nd International Geosciences Congress.

Roest, W.R., Verhoef, J., Pilkington, M., 1992. Magnetic interpretation using 3-D analytic signal. Geophysics 57, 116–125.

Sabins, F. (1997). Remote Sensing: Principles and interpretation (2nd ed.). NY: Freeman.

Sabins, F. (1997). Remote Sensing: Principles and interpretation (2nd ed.). NY: Freeman.

Schowengerdt, R. A. (2007). Remote Sensing: Models and Methods for Image Processing, 3rd ed., Academic Press, London.

Telford W. M., Geldart, L. P. & Sheriff, R. E. (1990). Applied geophysics, Cambridge University Press.

USGS/NASA (2015). Landsat 8 (L8) Data User's Handbook; USGS/NASA: Sioux Falls, SD, USA, p. 106.

Yousefi, M. and Carranza, E.J. (2014). Fuzzification of continuous-value spatial evidence for mineral prospectivity mapping. Computers & Geosciences. 74. 10.1016/j.cageo.2014.10.014.

Zhang, N. and K. Zhou (2015). Mineral prospectivity mapping with weights of evidence and fuzzy logic methods: Journal of Intelligent and Fuzzy Systems, 29, 2639–2651, http://doi.org/10.3233/IFS-151967.

Zhang, X., Pazner, M., and Duke N. (2007). Lithologic and mineral information extraction for gold exploration using ASTER data in the south Chocolate Mountains (California) ISPRS Journal of Photogrammetry & Remote Sensing 62 (2007) 271–282.

Zhang, X., Pazner, M., Duke, N., 2007. Lithologic and mineral information extraction for gold exploration using ASTER data in the south Chocolate Mountains (California). Photogrammetry & Remote Sensing 62, 271–282.

Identification and Mapping of Suitable Ecotourism Site in Old Oyo National Park Using Geospatial Techniques

J. O. Bakare[1], G. N Nsofor[2] and M. Muhammed[3]

[3]Department of Geography, Federal University of Technology Minna, Nigeria
[2]Department of Geography, Federal University of Technology Minna, Nieria,
[1]Department of Geography, Federal University of Technology Minna, Nigeria
[3]ummubahiyya@futminna.edu.ng
[1]bakarejoe@gmail.com
Corresponding author (bakarejoe@gmail.com)

Abstract

Ecotourism is considered as the most attractive subset of tourism industry which can contribute to natural resource conservation and local development under proper management.
This paper is centers on Identification and Mapping of Suitable Ecotourism site in Old Oyo National Park(OONP) Using Geospatial Techniques. The research used satellite data and weighted overlays ofthe suitable ecotourism sites gotten using geospatial techniques of land use land cover analysis and weight analysis in ArcGIS after the criteria had been determined through consultation with the experts. The auxiliary data from analytical hierarchy process were then integrated with other GIS datasets to mapsuitable ecotourism sites in Old Oyo National Park Oyo state Nigeria. Theanalysis indicates that the highly suitable areas are mainly located at Mguba and Tede range which is located at the south western andsouth-east of the study area characterized by some historic features such as ibuya pool, vast terrain and abundant of wildlifeThe moderately suitable areas are mostly located in Tede and Maguba range of the reserve which is abundantly blessed with great terrain and vegetation, since most of these are largely free from urban settlements with a unique and outstanding natural beauty, diverse attractions and great tourism potential. The marginally suitable areas arelocated in Sepeteri and Oyo ile range which houses the relic historical site of old Oyo settlement such as defense wall,Agbaku cave, Majiro cave,Majiro grinding industrial siteand different rock view and shape.These area are majorly rocklike in terrain. The non-suitable areas of the forest are at the extremely southern part of Tede range which is made up of water body and extreme north of Oyo ile range which is majorly rock.The study recommends that in order to optimally use the area and preserve the natural environment, proper holistic management and policies that will involve the surrounding communities should be put in place while the highly suitable ecotourism sites should be made biodiversity hot zone within the reserve
Keywords:GIS, LULC, Ecotourism, Potential sites and OONP

1. Introduction

In recent years, ecotourism sector, as a subset of tourismindustry, plays a great role in improving the economy of developed countries and their local people. Moreover, ecotourismpreserves the natural, bioenvironmental and cultural values of those areas (Sharpley, 2000).

Ecotourism is a form of tourism in which the main motivation of the tourists is the observation and appreciation of nature as well as the traditional cultures prevailing in natural areas. It also contains educational and interpretation features thereby generating economic benefits for the host communities, organizations and authorities managing natural areas with conservation purposes,providing alternative employment and income opportunities for local communities; and Increasing awareness towards the conservation of natural and cultural assets, both among locals and tourists according to United Nations World Tourism Organization(UNWTO, 2002). Ecotourism can be defined as an opportunity to promote the values in the protected areas and to finance related stakeholders. Ecotourism means "responsible travel to natural areas that conserves the environment, sustains the well-being of the local people, and involves interpretation and education" according to The International Ecotourism Society (TIES, 2015). Ecotourism is as old as man itself because the first ecotourism site in the world was planted by God and it served as a source of employment to the first man in the world history apart from its leisure nature.

Ecotourism, or ecological tourism, has been a growing phenomenon since the 1950s and 1960s as the First World grew in its appreciation of nature and its vulnerability to human development and population growth (Roche and Wallington, 2014).Ecotourism emerged as an alternative form of tourism in the 1990s to mitigate the faults ofconventional (mass) tourism in meeting the needs of sustainable development. It has since become widespread in Thailand and is adopted not only in natural areas (Leksakundilok, 2006)

Ormsby *et al.* (2006) found out that ecotourism ventures have sustained the economy of most nations, for example, East African countries like Kenya, Tanzania and part of West Africa like Senegal. Ecotourism accounts for a large share of some countries' Gross Domestic Product (GDP) and so contributes to livelihoods of many people, as in Kenya, Madagascar, Nepal, Thailand and Malaysia (Isaacs, 2000). When ecotourism is supported in protected areas, it is

often argued that economic benefits will accrue to local communities (Marsh, 2000). Some of the economic benefits which local communities can derive from ecotourism are employment opportunities, development associated with infrastructure (e.g. better road network and water) and ecotourism businesses (Hall, 2006a; Marsh, 2000; Weiler and Scidl, 2004).

Old Oyo National Park (OONP) is a 2512km^{2}expanse of conserved natural landscape which ishaving its fair share of deforestation and forest degradation (Chibuzor, 2017 in press). Despite it being a conserved area, forest degradation is still taking its toll on it, which call for a need of prompt action to save the naturalness and biodiversity of the forest of which ecotourism will play a big role. This can also serveas source of income generation to the state and nation if it is fully harnessed. Old Oyo National Park has different ranges that comprise criteria tenable for ecotourism, hence necessitated the need for this research work. The study sought to identify and map suitable ecotourism sitesin Old Oyo National Park..

2. Literature Review

Xiang (2017) examined ecotourism development evaluation and measures for forest parks in Chinabased on the principles of ecotourism, by developing an evaluation index systemto assess the current situation and problems of ecotourismdevelopment in forest parks from a national perspective. Adopting the Delphi Method; a forest park ecotourism development evaluation index system was established. Theindex contains 57 indicators including ones for the number of ecotourism and ecotourism revenue, ecotourism productsdevelopment, ecotourism interpretation and education,green infrastructure development, environmental quality andprotection, community participation, ecotourism management using a field survey and a mail survey to obtain data.

The forest park survey consisted of an on-the-spot survey and a survey conducted by post.There were 382 questionnairesaltogether (of which, about 89% were field survey). Atotal of 354

copies were responded to by the manager of forestpark, achieving a validity of 92.67% using SPSS18.0 software. The questionnaire was analyzed by means of <0.05 forsignificant difference and F test. When choosing surveysamples, the number and proportion of forest parks in eachprovince was taken into consideration. The questionnaire was tested by Cronbach's α reliability analysis and obtained the α coefficient of 0.870, indicatingthat the questionnaire data have a high degree of credibility.

He concluded that China's ecotourism in forest parks is undergoing a stage of steady development and ecotourism products available are rich and distinctive. More attention is paid to the construction of environmental interpretation systems thereby green infrastructure is making progress and the natural ecological tourism environment is good while communities that participatein ecotourism receive economic benefits and ecotourismmanagement continues to improve.

Bhaya and Chakrabarty (2016) considered a GIS based ecotourism infrastructure planning for Promotion of tourism in Jungle Mahal of West Bengal, India in order to identify potential ecotourism sites through the use of remote sensing and GIS techniques in forest dominated area of West Bengal. They used LANDSET- 8 satellite imagery to generate the land use and land cover through classified supervisedtechnique using maximum likelihood classifier specification and relative relief of the area gotten from the ASTER(Advanced Space borne Thermal Emissionand Reflection Radiometer) while the Digital Elevation Model (DEM) was generated. Various criteria such as spot height of 702 – 0 m elevation, dense to moderate forest cover, water bodies' availability, road network, soil type were used to identify ecotourism potential site selection which led to generation of various maps that were overlain in ArcGIS to identify the ecotourism potential sites. The study concluded thatjungle Mahal appeared as an ideal ecotourism destination where thousands of local people could be employed.They also pointed out areas that should be afforested immediately,where expansion of settlement and cultivation should be restricted, instead of large - scale cultivation, thrust area should be

forestry and forestbased economic activity like agro forestry, horticulture, sericulture,aquaculture, animal husbandry to meet the demand of tourists as well as the local tribal people of the jungle so that Mahal will see the new path for socio- economic development..

Onojeghuo and Onojeghuo (2015b), applied remote sensing techniques in mapping and showingthe distribution and structure of forest landscapes across protected areas in two states (Cross Riverand Delta) within the Niger Delta. It was observed that the total area of forest landscape for 1986,2000 and 2014 across the identified protected areas were 535,671 ha, 494,009 ha and 469,684 ha(Cross River) and 74,631 ha, 68,470 ha and 58,824 ha (Delta) respectively. The study showed that annual deforestation rates for protected areas across both states from 1986 to 2000 were 0.8%.However, the overall annual deforestation rate between 2000 and 2014 was higher in Delta (1.9%)compared to Cross River (0.7%). The study showed accelerated levels of forest fragmentationacross protected areas in both states as a side effect of the prevalence of agricultural practices andunsupervised urbanization.

The study area for our study is located in Oyo State, South West part of Nigeria at latitude 8º 10' N and 9º 05' N and longitude 3º 35' E and 4º 42' E with 'Saxophone' shaped like and a total land mass of 2759.052km^2 making it the fourth largest national park in Nigeria. Old Oyo National Park is surrounded by Eleven (11) Local Government areas out of which Ten (10) fall within Oyo State and one (1) in Kwara State. There are Atisbo(Tede/Ago-Are), Atiba (Oyo), Irepo (Kisi), Oorelope (Igboho), Saki East (Ago-Amodu), Iseyin (Iseyin), Orire (Ikoyi), Itesiwaju (Otu), Olorunsogo (Igbeti), Saki West(Saki), and bounded by Kaima (Kwara state).(Oladeji *et al*., 2012)

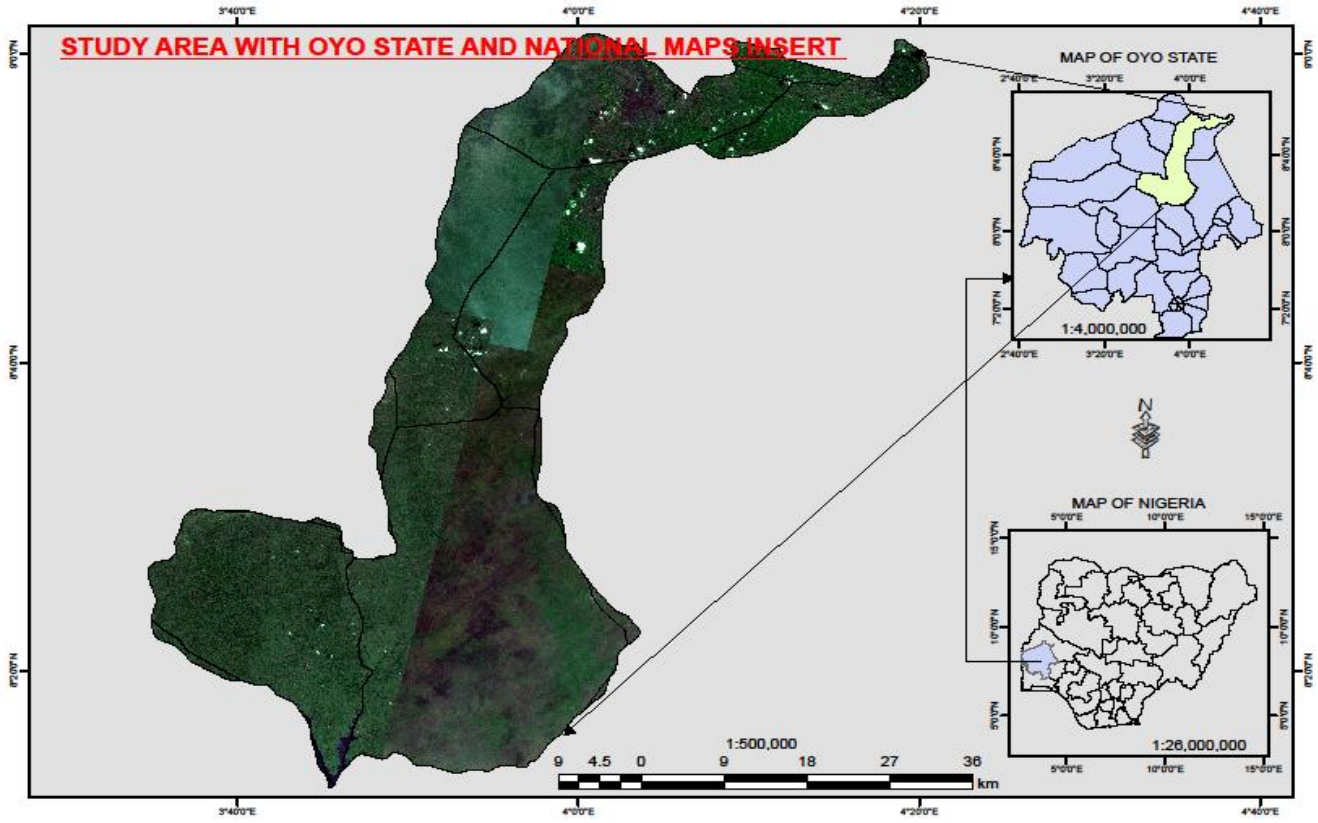

Fig 1:0: Map of Nigeria showing Oyo State and map of Oyo state showing the study Areas.

Source: Authors'' fieldwork, 2018

3. Methodology

A combination of different approaches was used during the analysis of the data using the spatial analysis of the ArcGIS tool box. This was made easier with data gathered during the field work. A classification scheme of Anderson et al. (1976) level 1 classification was adopted and modified into five classes representing forest land, rock out crop, shrub land, water body and open space. The supervised maximum Likelihood image classification was used to generate the land use and land cover map, some factors (Landscape/Naturalness, Topography and road) and criteria (land use and land cover, Elevation/slop, road proximity to cultural site). These wereconsidered for determining ecotourism sites. The Model(DEM) was used to generate the elevation and slope map.The proximity to cultural site was done through buffering which were

then integrated into to map in ArcGIS togenerate the ecotourism site map through weight analysis.

3.1 Data collection

Satellite image of Old Oyo National Park (OONP)was downloaded from the United States Geological Survey (USGS) website (http://glovis.usgs.gov/). OLI satellite image of 2018was used of 30m resolution and spectral range of 10.4 -12.5, band 5, 4, 3 for land use land cover image classification.

Table 1:0: Factors and Criteria for Land Suitability Analysis of Ecotourism

Factors	Criteria	Unit	High	Moderate	Marginal	Not suit
Landscape/ Naturalness	Land use/land cover	Value range	Near range High	Middle range Moderate	Far range Marginal	Not visible Not
Topography	Elevation	Meter	0-100m	100-300m	> 400 m	0-100 m
	Slope	degree	0-5°	5-25°	25-35°	> 35°
Road	Proximity to cultural sites	Kilometer	0-15km	15-30km	30-45km	> 45 km

Source: Authors' fieldwork, 2018

4. Results and Discussion

The land use change map of OONP in figure 2.0, shows that forest land was the dominant land cover features of about 1321.9254 km^2 (47.35 %) of the total area,and covers majorly the central and northern part of the study area. This is followed by shrub and fallow land which covers an area of 857.9682km^2 (30.73 %) predominantly at the south west and south east of the study area. The bare soil and open space areaaccounts for about 225.7713km^2 (8.09 %)

majorly visible at the south-western area of the reserve. Rock out crop is 196.9083 km^2 (7.05%) well pronounced at the northern part of the study area and are made up of caves such as Agbaku cave and some historical sites of Old Oyo Ile relics, Koso relics. Water covers about 189.2934 km^2 (6.78%) abundantly found at the southern part of the study area. A quick glance at the forest reserve, forest vegetation still carries the largest part of the reserve.

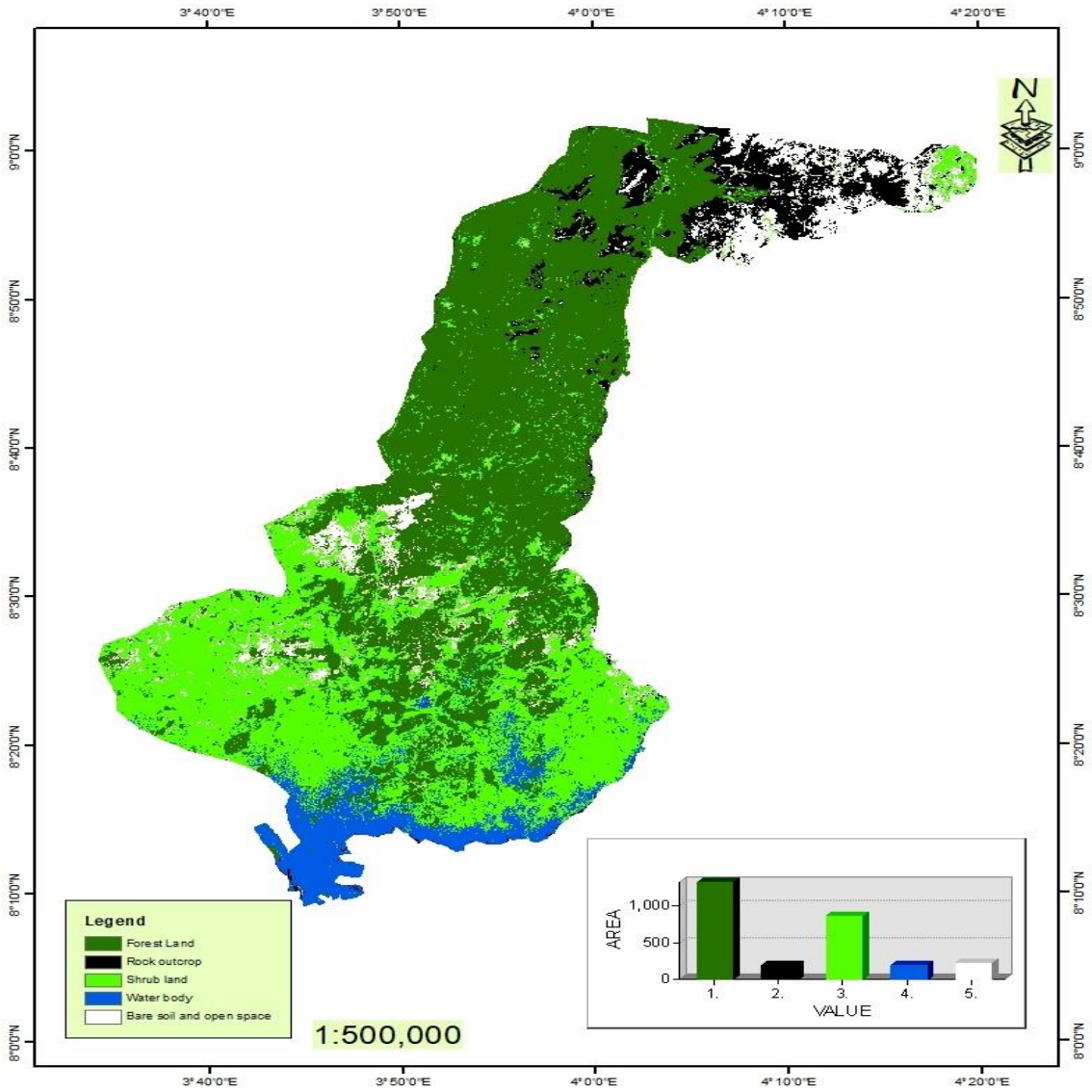

Fig 2.02018 Land Use and Land Cover of the Old Oyo National Park

Source: Authors' work, 2018

4.1: Mapping potential areas of ecotourism in the study area.

For mapping potential areas for ecotourism in the study area, some factors and criteria were used such as land use and land cover type, elevation/slope, road proximity to cultural site. Thesewere prepared as map layers as shown in figure 3.0. Based on the ecotourism area mappedusing weighing analysis from the criteria, the highly suitable areas for ecotourism site is found at the south westernpart of the study area which contains historic ibuya pool, which is traditionally significant for Sepeteri people as part of traditional worship center of one of their gods in the olden days, and some part of south-east of the map.(seefigure 3.0)

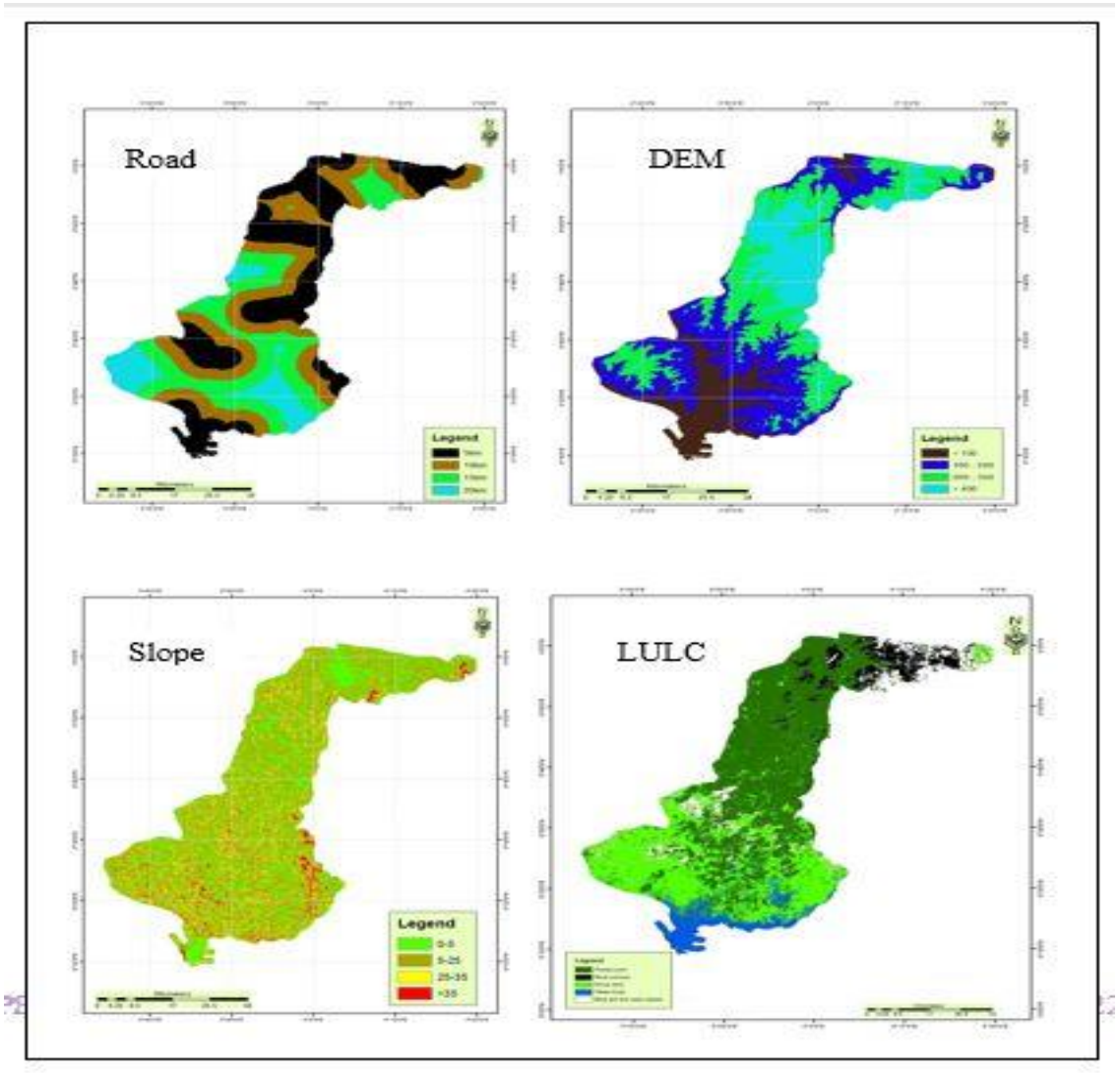

Fig 3.0Criteria for ecotourism mapping in map layers
Source: Authors' work, 2018.

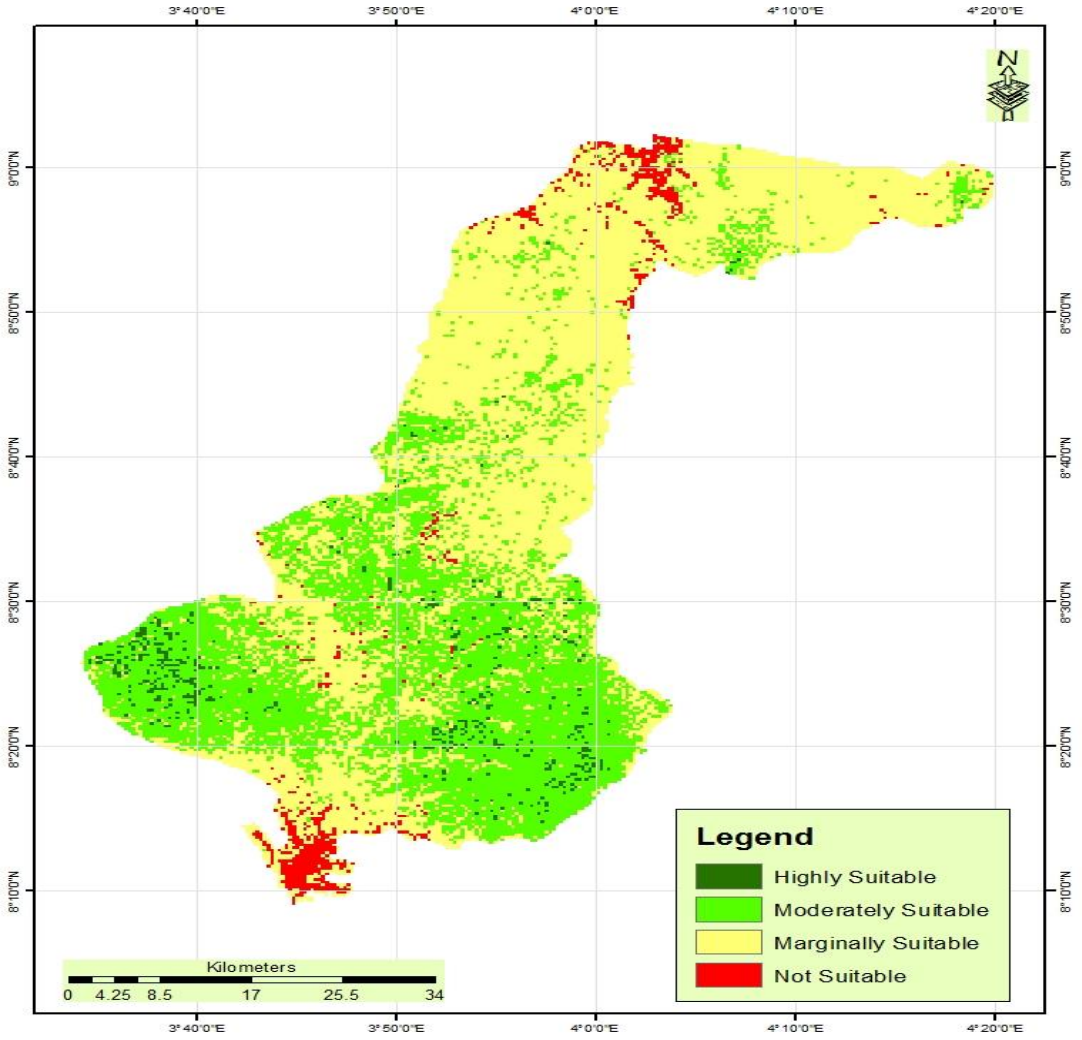

Fig 4.0 Ecotourism map of thestudy area

Source: Authors' work, 2018.

Table 4.1 shows the area of land covered by each ecotourism area in the order of their suitability.The most highly suitable area covers a total land mass of 57.35km^2, that is, about 2.1 % of the total land mass of 2759.052km^{2,}, moderatelysuitable area carries 1053.905km^2(38.2%) the second highest in land mass of the study area, while marginally suitable area carries the highestland massof 1552.184km^2(56.3%), and not suitable area accounts for 95.6157km^2(3.4%).(see table 2.0).

Table 2.0 Ecotourism suitability area

Weight Analysis scale	Area (km^2)	Percentage (%)
Highly suitable	57.34698	2.078503
Moderately suitable	1053.905	38.19809
Marginally suitable	1552.184	56.25788
Not suitable	95.6157	3.465528

Source: Author's fieldwork, 2018

5. Conclusion

Ecotourism development is visualized as a development tool – not just in promoting tourism growth but also to conserve biodiversity of species in area where it is established and also aid in climate change regulation.It also has capacitytoreduce poverty particularly in the rural areas. Poverty is widespread as pervasiveeconomic pursuits in those areas are limited to agriculture, livestock, and trans-boundary trade. All these activities suffer from low productivity, and are subsistence oriented. Ecotourism is expected to preserve forest reserve against forest degradation and also engage neighboring communities in higher productivity by linking them to more commercial activities.In order to optimally use the area and preserve the natural environment, a proper holisticmanagement and policies that will involve the surrounding communities should be put in place while the highly suitable ecotourism sites should be make biodiversity a hot zone within the reserve. The study has also shown that GIS and remote sensing are an indispensable tool for mapping suitable ecotourism sites.

References

Ayeni, D. A. (2010). Tourism as a Means of Income Generation for Developing Countries: Focus on Nigeria. *Journal of Environmental Technology*, *2*(1), 42-52.

Bhaya S, Chakrabarty A (2016) A GIS Based Ecotourism Infrastructure Planning for Promotion of Tourism in Jungle Mahal of West Bengal. J Remote Sensing & GIS 5: 181. doi:10.4172/2469-4134.1000181

Brockington, D., Duffy, R., & Igoe, J. (2012). *Nature unbound: conservation, capitalism and the future of protected areas*. Routledge.

Banerjee, U. K., Kumari, S., Paul, S. K., & Sudhakar, S. (2002). Remote Sensing and GIS based ecotourism planning: A case study for western Midnapore, West Bengal, India. *Map Asia*.

Chibuzor J.I (2017)Time Series Analysis of Forest Loss and Degradation in the OldOyoNational Park: A project submitted to the department of geography inpartial fulfillment of the requirements for the award of masterof geographic information system in the faculty of the socialsciences, university of Ibadan, Ibadan Nigeria, *in press*

Hall, M. (2006a). Stewart Island. In G. Baldacchino, ed. Extreme tourism: Lessons from the World's Cold Water Island. pp 219-232. Amsterdam: Elsevier

Isaacs, J. C. (2000). The limited potential of ecotourism to contribute to wildlife Conservation. The Ecologist, 28(1): pp. 61-69.

Marsh, J. (2000). Tourism and national parks in Polar Regions. In: R. Butler and S. Boyd,Eds. tourism and national parks-issues and implications. pp. 127-136. Chichester: Wiley Making Tourism More Sustainable – A Guide for Policy Makers, UNEP and UNWTO, 2005, P. 11-12 Retrieve on February 24, 2018, from www. Word Tourism Organization.com

Sharpley, R. (2000). Tourism and sustainable development: Exploring the theoretical divide. Journal of Sustainable tourism, 8(1), 1-19.

Miller, G. 2001. Corporate responsibility in the UK tourism industry.Tourism Management, 22:589-598.

Mohammed, S. O., Gajere, E. N., Eguaroje, E.O., Shaba, H., Ogbole, J. O., Margut, Y. S., Onyeuwaoma, N. D., Kolawole, I. S. (2013). Spatio-temporal Analysis of the National Parks in Nigeria Using Geographic Information System. Ife Journal of Science vol. 15, no. 1(2013)

Leksakundilok, A. (2006). Community participation in ecotourism development in Thailand (University of Sydney, Geosciences) Malaysia. (2001). Rural tourism master plan. Kuala
Lumpur: Ministry of Culture, Arts and Tourism. Malaysia. (2006). Ninth Malaysia plan. Government of Malaysia Printers: Kuala Lumpur.

Ogunsesan, D., Oyedepo, J., Oates, J., Adeofun, C. O., Ikemeh, R. and Bergl, R., (2011). GIS –Supported Survey of Lowland Rain Forests in South-Western Nigeria. Proceedings of the Environment Management Conference, Federal University of Agriculture, Abeokuta, Nigeria, 2011.

Onojeghuo, A. O. and Onojeghuo, R. O. (2015b). Protected Area Monitoring in the Niger Delta using Multi-Temporal Remote Sensing. Environments 2015, 2:500 – 520; doi:10.3390/environments2040500

Roche C., Wallington B. 2014. What is ecotourism? (http//.www.ewt.org.za). Downloaded 10th of December, 2017.

The International Ecotourism Society (TIES, 2015): Definition of ecotourism retrieve from https://ecotourism.org

United Nation World Tourism Organization (2015). UNWTO Annual Report 2014, UNWTO, Madrid

United Nations World Tourism Organization (UNWTO, 2002) Annual Report

Weiler, S., and Seidl, A. (2004). What's in a name? Extracting econometric drivers to assess the impact of national park designation. Journal of Regional Science, 44:245-262.

Xiang Baohui (2017) Ecotourism Development Evaluation and Measures for Forest Parks
in China. Journal of Resources and Ecology, 8(5):470–477. DOI: 10.5814/j.issn.1674764x.2017.05.004 www.jorae.cn

An Assessment of the Spatial Distribution and Facilities of Public Primary Schools in Shomolu Lga, Lagos State

Taiwo, Praise O.1* Uluocha N. O.2 Odekunle M. O.3, Adenle A. A.4, Sule I.5

[1] Department of Geography, University of Lagos, Nigeria
[2] Department of Geography, University of Lagos, Nigeria
[3]Department of Physics, Federal university of Technology, Minna, Nigeria

[1]praisetaiwo@gmail.com
[2]nuluocha@unilag.edu.ng
[3]Odemary@futminna.edu.ng
[4]Ade.ademola@futminna.edu.ng

Abstract

The research analyzed the spatial distribution of public primary schools and a total of 53 primary schools were identified with the population of pupils at 13,753 across the study area. All the schools in the study area were purposively sampled and used in the study. Most of the attribute data were obtained at the State Universal Basic Education Board (SUBEB) Maryland, Ikeja and also Local Government Education Authority, Gbagada phase II, Somolu. The study also revealed inequality firstly in the distribution of schools in the study area with wards like (Bariga ward D, Somolu ward H etc.) having none, secondly , the Nearest Neighbour Index and Point Density Analysis revealed the cluster pattern of the distribution of schools resulting to inequality in the distribution of schools in the study area. An administrative map of the study area obtained from the Local Government Area was geo-referenced and digitized in ArcGIS 10.3.1 for the base map through digitizing process. An overlay analysis was performed and all the coordinates of the UBE primary schools were displayed on the composite map. A GIS database was created where the spatial and attribute data were encoded and query analysis was carried out.

The study recommends among others, provision of functional facilities (especially the recreational facilities) by the Lagos State Ministry of Education and the Local Government Area of study.

Keywords: Spatial Distribution, Public Primary School, Map, GIS, Analysis, Education, Teachers.

1. Introduction

In regards to public services, Educational services can be said to be one of the most important on the provision list to members of any locality. The efficiency of the educational sector is strongly advocated by both the promoters of social equality, social justice and modern day democracy, who view education as a precondition for advanced development and competitive edge (Taiwo C.O. 1980). So governments are striving to provide educational institutions of all levels (nursery and primary, secondary, universities) in order to accelerate progress and prosperity (Fuende HD et al 2013).

The Universal Basic Education, UBE, came as a replacement of the Universal Primary Education as an innovation to enhance the success of the first nine years (6 years of Primary School, 3 years of Junior Secondary School education) of schooling. This scheme is monitored by the Universal Basic Education Commission, UBEC, and has made it "free", "compulsory" and a right of every child. (Aderinoye, 2007).

World Bank recommended that the following data were needed for rationalizing and drawing up of both the urban and rural school map. Schools which includes physical aspects, site, type of building, usage, capacity, teachers (numbers, qualification, and age), students enrolment in school, individual data on age, sex, previous schools, home, location, mode of transport, time taken in home/school journey, parental background, rural and urban area data which include land use administration map on a large scale, planning reports, settlement patterns etc. The facility also includes classrooms, toilets, furnishings, materials and supplies, fire suppression systems, security, information technology etc. (World Bank, 2014).

1.1 Scope and Limitation

The scope of this research is formal education and it is limited to the distribution of public primary schools in Shomolu Local Government Area, Lagos State. The content scope of the research covered the location, mapping, and generating of geo-database of the primary schools infrastructure in the study area.

1.2 Aim and Objectives

Aim:

The aim of the study is to examine the spatial distribution of public primary educational institutions in Shomolu Local government area in Lagos state, Nigeria and identify the factors associated with the observed pattern.

Objectives:

The specific objectives in achieving the aim of the study include:

- To identify and map the locations of Public Primary Schools in the study area.
- To determine the spatial pattern of public primary educational facilities in Shomolu local government.

- To compare the Teacher to Pupils population ratio with the set standards of UNESCO and UBE.
- To examine the characteristics of the educational facilities (which includes: Type of building, numbers of classrooms, classroom situation, type of toilet, roof condition, play room, playground facilities etc.)
- To create a Web-Based Geo-database for the public primary schools in Shomolu LGA.

1.3 Justification for the study

The primary education level, which acts as a very vital aspect of the nation's educational system that deserves to be handled with great care and caution. Errors committed in the organization and management of this level of education might affect other levels and thus seriously mar the lives of the people and indeed the overall development of the nation. This is one good reason why all the stakeholders must show enough concern for those issues that concern the organizing and managing of our primary system (Durosaro, 2004).

Unavailability of data that shows the distribution pattern of the schools in the study area has made it very difficult for people to see at a glance how these schools are spread. Also, in taking sound decisions on the management of primary education in Nigeria, there is the need to ensure availability of accurate data on the system (FGN/UNESCO/UNDP, 2003). A GIS database provides a comprehensive framework and organization of spatial as well as non-spatial data. Such as a map that will show the distribution pattern of the public primary schools in Shomolu L.G.A of Lagos State

As a step towards improving the standard of public primary schools' education in the study area, it will be necessary to provide the public and decision makers of the state with information such as location, staff strength, available facilities, status of public primary school, to enhance proper planning and decision making. The information provided will enable the government and educationists in policy and decision making such as planning for the future expansion, distribution of materials or facilities among these schools in the study area.

1.4 Study Area

The area known today as Shomolu Local Government area was formerly known as Mushin East Local Government area when it was carved out of the defunct Mushin Town Council in 1976. On December, 1996, Kosofe Area was again carved out and became Kosofe Local

Government while the remaining area retained Shomolu Local Government Which lies between latitude 6º31'12''N and 6º33'36''N and Longitude 3º22'22''E and 3º24'36''E. Bordered by Kosofe Local Government in the north, Lagos Island in the West, Lagos Mainland in the South and Mushin Local Government in the East. The population of Shomolu Local Government according to the 2006 census stands at 402,673 person, with an area of 106.5km^2. The Local Government Headquarters is located at Number 2, Durosinmi Street, Shomolu, off Oguntolu Street. The present Shomolu Local Government comprises areas like the community road, Akoka, areas East of Ikorodu up to Anthony, Oke side interchange, including Somolu Bashua, Bariga, part of Akoka, Igari, Obanikoro, pedro village, Abule Okuta, Seriki village, Apelehin and Ilaje.

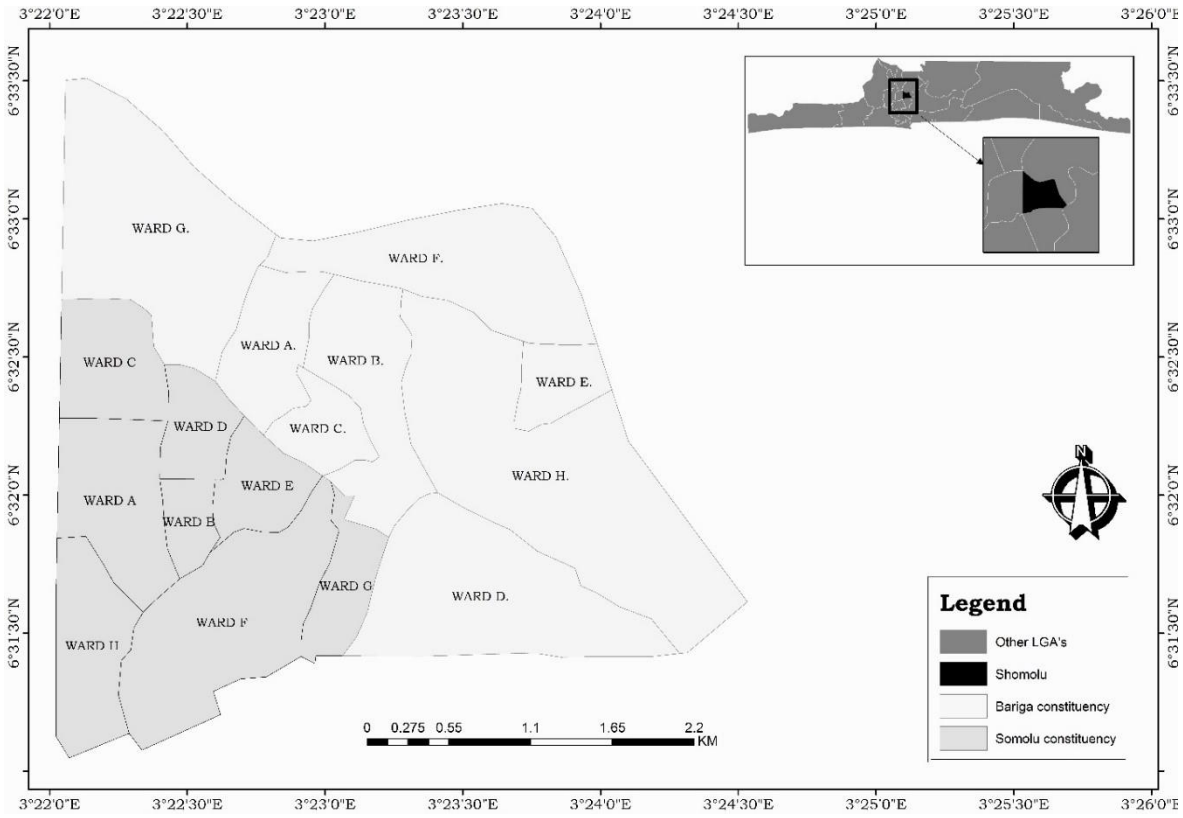

Figure 1. Study area map of Somolu LGA showing the distribution of the wards

2. Literature Review

2.1 Millennium Development Goal

In this priority area the millennium development goal is to ensure that by the year 2015, children everywhere, boys and girls alike, will be able to complete a full course of primary schooling and those girls and boys will have equal access to all levels of education (Susan, 2004).

2.2 Definition of Basic Education

United Nations Economic, Scientific, and Cultural Organization (UNESCO) define basic education as the first nine years of schooling; the first five or six years are often identified as primary education and the rest as lower secondary education. It also includes basic education for youth and adults who did not have the opportunity to complete a full cycle of primary education (Ikpasaja, 2014).

The agency which coordinates the affairs of this sub sector is the Universal Basic Education Commission (UBEC). Other coordinating agencies in this sector include National Commission for Nomadic Education and National Mass Education Commission.

2.3 National Policy on Education

Universal Primary Education (UPE)

Universal Primary Education (UPE) is a goal stated in many national development plans and pursued with vigour by governments of most developing countries. Primary education is seen as the first step in laying the foundation for future educational opportunities and lifelong skills. Through the skills and knowledge imbued, primary education enables people to participate in the social, economic and political activities of their communities to their fullest potential (Globalisation of Education Policies, 2000).

In 1976, the Universal Primary Education (UPE) programme was introduced in the country and was launched on Monday 6th September by the Olusegun Obasanjo Military Administration at Oke Sunna Municipal Primary School, Lagos to provide free and compulsory education to children at the primary school level. Unfortunately, the Scheme was faced with several challenges because structures were hurriedly put in place, teachers were trained haphazardly and there was an inadequate funding of the primary education sector. This however, brought about declining enrolment in public primary school. Teachers to pupil's ratio were high and at the long run, education was meant only for the wealthy children (not for all the children as proposed earlier). Children who are supposed to be in the school learning are outside the street hawking goods for their parents. The vision of Education for All (EFA) regardless of their socio-economic background was ignored (Omotere and Adunola, 2010).

Universal Basic Education (UBE)

Universal Basic Education (UBE) is a reformed programme in Nigeria's basic education delivery (from primary one, all through to junior secondary school class 3) and is to reinforce the implementation of the National Policy on Education (NPE) in order to provide greater

access and ensure quality throughout the Federation as it is free and compulsory (Adomeh et al, 2007).

Nigeria is adopting Universal Basic Education (UBE) and as a process of fulfilling the aim of Education For All (EFA) as endorsed at the World conference on education held in Jomtien, 1990 (Arhedo, 2009). The UBE Programme is a nine (9) year basic educational programme, which was launched and executed by the government and people of the Federal Republic of Nigeria to eradicate illiteracy, ignorance and poverty as well as stimulate and accelerate national development, political consciousness and national integration. Former President Olusegun Obasanjo flagged off UBE on 30th September 1999 in Sokoto State.

According to Omotere and Adunola (2010), Universal Basic Education is broader than Universal Primary Education of the 1970s, which focused on providing educational opportunities for primary school age children. Universal Basic Education stresses the inclusion of girls and women and a number of non-privilege groups: the poor, street and working children, rural and remote populations, nomads, migrant workers, indigenous people, minorities, refugees and the disabled. It also extends to the first level of secondary education (JSS 3).

2.5 Laws and other Basic Regulations Concerning Education in Nigeria

The National Policy on Education was enacted in 1977 and undergone three revisions, the most recent one in 2003. Since 1981, a number of decrees have been passed providing the legal framework of education in the country (International Bureau of Education (IBE) - UNESCO, 2006).

i. The **Decree No. 16** of 1985 places special emphasis on the education of the gifted and talented children within the National Policy on Education.

ii. The National Commission for Mass Literacy, Adult and Non-formal Education, which was established by **Decree No. 17** of 26 June 1990 and formally inaugurated on 5 July 1991, is charged with the responsibility of developing strategies, coordinating programmes, monitoring and promoting literacy and post-literacy programmes nationwide.

iii. In 1993, the National Minimum Standards and Establishments of Institution Amendments **Decree No. 9** was promulgated. It provides for religious bodies, non-governmental organizations and private individuals to participate in the provision of tertiary education.

iv. By a recent decree, all companies operating in Nigeria which have up to 100 employees on their payroll shall contribute 2% of their pre-tax earnings to the Education Tax Fund for the funding of education.

v. The most crucial strategy for sustainable education development in Nigeria is the Universal Basic Education (UBE) Scheme, which was launched in 1999. In May 2004, the Nigerian Legislature passed the UBE bill into law. The **Universal Basic Education Act** represents the most significant reform and addresses comprehensively the lapses of the Universal Primary Education (UPE) and the issues of access, equality, equity, inclusiveness, affordability and quality.

2.6 The State of Education in Nigeria of the Nation

The federal government reported that the falling standard of education in Nigeria is caused by "acute shortage of qualified teachers in the primary school level." It is reported that about 23% of the over 400,000 teachers employed in the nation's primary schools do not possess the Teachers' Grade Two Certificate, even when the National Certificate of Education (NCE) is the minimum educational requirement one should possess to teach in the nation's primary schools (Africa Economic Analysis (2008). Due to lack of teachers, however, holders of the Teacher's Grade II Certificates (TC II) are still allowed to teach in some remote primary schools (Better Future Foundation Amodu (BFFA) – Nigeria, (2014).

2.7 Standards

Standards are set of yardsticks in the units of measurement of variables which appear in the statement of principles. Standards are not absolute but relative and are more or less a form of guides.

Standards for Setting of Public Primary School:

i. United Nations Education Scientific and Cultural Organization (UNESCO) standard (1996): (UNESCO) prescribed the ratio of 1:25 in public primary schools. (Chukwu, 2011).

ii. Universal Basic Education Plan, (2010-2019): reveals that, for effective teaching and learning, the teacher/pupils ratio shall be 1.35 in primary schools (Kakuri, nd), and with the walking distance (3-4km) for all learners of primary school-going age Federal Ministry of Education - FMoE (2009).

2.8 School Mapping (SM)

It bothers on availability as relates to even spread (as stated by the Federal Ministry of Education (1999) is developing in the entire citizenry a strong consciousness for education and a strong commitment to its various promotion. It is quite obvious from the above phenomenon that the objective of developing the entire citizenry cannot be achieve unless the public education facilities are evenly distributed over the country's landscape. (Hite J. 2008).

School Mapping (SM) also helps to investigate and ensure the efficient and equitable distribution of resources within and between school systems when large-scale reform or significant expansion of an educational system takes place (Caillods, 1983).

Hite (2004) explained that, school mapping as a technical exercise has become a relatively normalized and institutionalized practice in education's planning. More than simply being a tabular, graphical or cartographical representation of a particular space or place, school mapping involves the consideration and inclusion of various forms of technical data that impact and populate the physical and social context of analysis. School mapping comprises physical location analysis of schools. In order for this to be accomplished knowledge of the settlements and population of the area is required.

2.9 Geographic Information System (GIS)

Geographic Information System is a better, more precise, and flexible spatial analysis tool for representing schools and their physical, social and geopolitical contexts. It also provides a different way to understand and plan those contexts geospatially (Hite J. 2008).

Geographic Information System is a discipline for capturing, storing, analysing, managing and presenting data and associated attributes which are spatially referenced to Earth. The use of GIS in Education involves combining statistical inferences to geographic information. Statistics in education might be used with GIS to present a clear picture of educational facilities and activities such as ratio of students to teacher, number of students in a class and student density in school and schools distribution in district (Eray, 2012).

2.10 Related Studies

In the study of Sule, Abdullahi and Bungwon (2012), private primary school locations in Kaduna metropolis were determine by the use of handheld GPS receiver. Thematic map, nearest neighbour and Buffer zone analysis reveals that, the schools are not evenly distributed as some areas have the schools concentrated at particular places while some areas have none, and some settlements are deficient in private schools while others have excess.

Akpan and Njoku (2013) identified the educational facilities in Ikot Ekpene LGA including their geometric properties and created a GIS database for both the public and 21 private schools in the study area. The authors observed that spatial location of schools in the LGA is uneven and almost randomly distributed such that some wards were essentially educationally deprived making children to trek long distances to schools.

Another study by Olamiju and Olujimi, (2011) analyzed the locations of public educational facilities in Akure, Nigeria. They found out that population figures were not considered in allocation of educational facilities in the region. This trend shows that there is no equitable distribution of educational facilities in Akure area. Ibrahim (2009) studied the spatial analysis of the distribution of social facilities in Sabon Gari LGA, Kaduna State, and found out that there is an uneven distribution of social facilities in Sabon Gari LGA of Kaduna State.

In another study in Yola North LGA, Adamawa state by Aliyu (2013) clearly depicts the process of using thematic map and nearest neighbour analysis in determining the distribution pattern of the post-primary schools. The study reveals how the schools were located on digital map and shows that random pattern of distribution exists within the study area. The potentials of GIS technology in database design and creation has been demonstrated and found to be more efficient than the manual approach.

The use of GIS for analyzing the distribution of facilities is not new in Kano State, like the study of Ahmed M. et al (2013) where thematic map and nearest neighbourhood analyses were used and found out that the pattern of distribution of Police Stations in Kano Metropolis is generally random and uneven, with a little clustering at the center. One and two kilometre buffer zones were generated and the result shows that the old city of Kano and the eastern part of the metropolis were fully served while the west and southern part were underserved.

Also, in another research conducted by, Kibon and Ahmed (2013), where they made use of thematic map and nearest neighbour analysis shows that, the distributions of Health facilities in Kano Metropolis are in clustered.

The study of Olubadewo, Abdulkarim and Ahmed (2013), indicates the use of technology (GIS) for education planning have proved to be very important in the decision making in Fagge L.G.A by providing the planners integrated geographic scenario of location of school. The Thematic map and nearest neighbour analysis shows that the distribution of primary schools in the area is more concentrated than other areas, while the buffer zones show that schools are closer to roads and Markets. The database shows there are 222 classrooms, 12,693 pupils and 558 teachers in the areas at which the result shows a perfect significant relationship between

the number of teacher and pupils. The tool of the analysis (Nearest Neighbour) was used to analyze the pattern of the distribution and the result shows the schools are dispersed.

2.11 Distribution of Schools

Findings derived from Al-zeer (2005), Akpan and Njoku (2013), Olamiju and Olujimi, (2011), Aderamo and Aina, (2011) among others, have shown that educational infrastructures are unevenly distributed within a region and majority of the people struggle to gain access to infrastructures in order to improve their quality of live.

According to Abbas (2009), he stated that issues of centrality, location and accessibility have a vital role to play in the utilization of education infrastructure by the people. However, Green *et al*. (2008) stressed that achieving equitability is possible only if the areas that are under or overprovided are identified and corrective action is applied through appropriate planning and implementation. Determining the spatial mismatch between supply and demand is established by: deciding on suitable standards pertinent to a specific facility, which will be related to the demand (the population who will use the facility); acceptable travel costs (time or distance) to the facility and the capacity of existing facilities (based on size and functionality), (Green *et al*., 2008).

Distribution of educational facilities or schools have an effect on the participation rate in school education geographic location of primary schools as indeed public facilities in Nigeria has not taken into account inequalities among region, different social groups and geographical area (Ikpasaja, 2014).

3. Methodology

3.1 Data

Data needed for this study were collected from both primary and secondary sources.

Primary Sources of Data:

GPS Survey: It was used to acquire the coordinates of each public primary school.

Interview: An inventory of some of the public primary school infrastructures and their characteristics alongside the pupils and teachers characteristics were obtained through oral interview. An inventory check list was designed and used to identify and take records of the attributes of these infrastructures. The essence of the interview was to seek for primary information on the condition of the infrastructures available.

Secondary Sources of Data:

A list showing the names of all the public primary schools and their addresses in the study area was acquired from the Local Government Education Secretariat alongside the administrative boundary map of Somolu LGA. The attributes of the public primary schools which include the data on teachers, students and the facilities were obtained from State Universal Basic Education Board (SUBEB) Maryland, Ikeja and also Local Government Education Authority, Gbagada phase II, Somolu. Existing literatures including journals, textbooks, conference proceedings, seminar papers, theses, reports and web references were equally made use of.

3.2 Data Analysis

The analysis of the data employed both the descriptive and overlay analysis. Appropriate maps/diagrams and tables were used to illustrate the distribution of the available infrastructures in the study area. Identification and mapping of the public primary schools and their available facilities in the study area was achieved by using the name and address of each school to identify each primary school in the study area. The Handheld GPS Receiver captured the actual coordinate of the schools. The coordinates and other attributes of the schools were copied to Microsoft excel and saved as CSV (comma delimited) format, then imported into ArcGIS 10.3.1 using the add XY option at the sub-section of the file option in the tools menu. This procedure overlaid the points (coordinates) on the geo-referenced administrative map of the study area. The spatial distribution of primary schools in the study area was analyzed by using the location of each school which was used to determine the general spatial distribution of schools within the administrative wards in the study area. This was done by overlaying the coordinates of the schools on the base map of the study area. The digitized features was overlaid with the schools coordinates to form composite maps showing the primary schools. Point density analysis was performed and the density of the public primary schools by measuring the quantity of each location and derives a spatial relation of the locations with the measured quantities. To develop a geo-database for the primary schools in the study area, the following data were collected and used in the development of the database.

i. The study area map

ii. List showing Primary schools names and addresses.

iii. Geographical coordinate of Primary Schools.

iv. All the necessary attributes for each Primary school were entered into its layer's/theme's attribute table.

This was done by adding required number of fields (columns) to the table and entering the data for all the Primary school in their corresponding records (rows). Attributes collected included; school name, address of school, year of establishment, number of teachers, Type of building, numbers of classrooms, classroom situation, type of toilet, roof condition, play room, recreational facilities, Furniture facilities, water and power supply. The coordinates and attributes of the UBE Primary school were copied to Microsoft Excel and saved as CSV (comma delimited) format which is recognizable and accepted by the ArcCatalog extension of ArcGIS. This file was later imported into Arc Map environment using the add XY, Command at the tools menu. The system can be updated to reflect changes in any school attributes as well as appending more attributes in ArcGIS interface by an authorized ArcGIS application user. To assess the characteristics of the primary education infrastructure, queries were carried out on the database using both the query builder to assess the characteristics of some of these available infrastructures in the schools and Microsoft Excel (Pivot Table command) to analyze attribute characteristics based on the wards distribution.

Also, an account was created online with the ArcGIS online platform (maps.arcgis.com). The shapefiles used containing the boundary details and coordinate of the wards with their attributes were compressed to a ZIP format (.zip extension) then exported to the web map platform. The web map was created and also shared followed by the creation of the web application. The web application was designed with the web application builder using a new template, widgets were added (some includes summary, print, share, about, my location, chart, bookmark, stream etc.) then the application was saved and also shared.

4. Results and Discussions

4.1 Spatial Distribution of Public Primary Schools

Primary school provides the foundation for educational journey of any child. A total of 53 primary schools were identified to cater for 13,753 students across the study area. The geographic coordinates of each of these primary schools were collected and the concept of point on polygon overlay analysis was used to map the primary schools in the study area. See Appendix II. Identifying geographic patterns is important for understanding how geographic phenomena behave. One can get a sense of the overall pattern of features and their associated

values by mapping them. Table 1 gives the pattern of distribution of primary schools among the various wards in the study area.

A total of 53 primary schools were identified to cater for 13,753 students across the study area. Table 1 and figure 2 shows that, there are fifty three (53) public primary schools in Somolu Local Government Area, Lagos State. The local government is divided into two LCDA's, Somolu and Bariga LCDAs. They both have 8 wards each labelled alphabetically illustrated in Table 1 and Figure 2. Figure 3 shows a presentation of the variations of the numbers of schools in each ward.

Table 1. Distribution of Public Primary Schools (2017)

	Wards	No of Schools	AK	Wards	No of Schools
Bariga	Bariga Ward A	1	**Somolu**	Somolu Ward A	4
	Bariga Ward B	1		Somolu Ward B	0
	Bariga Ward C	1		Somolu Ward C	2
	Bariga Ward D	0		Somolu Ward D	3
	Bariga Ward E	1		Somolu Ward E	0
	Bariga Ward F	8		Somolu Ward F	9
	Bariga Ward G	9		Somolu Ward G	0
	Bariga Ward H	14		Somolu Ward H	0
				Grand Total	53

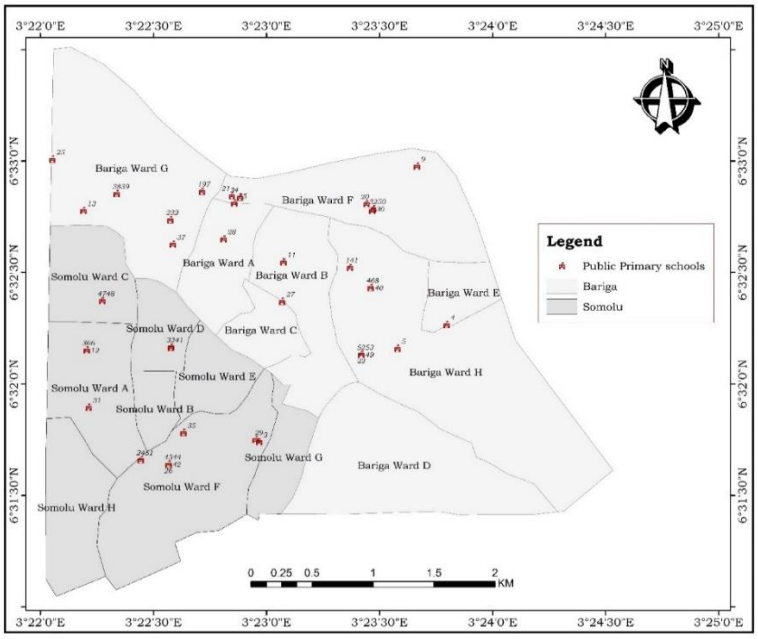

Figure 2. Distribution of Public Primary Schools (2017)

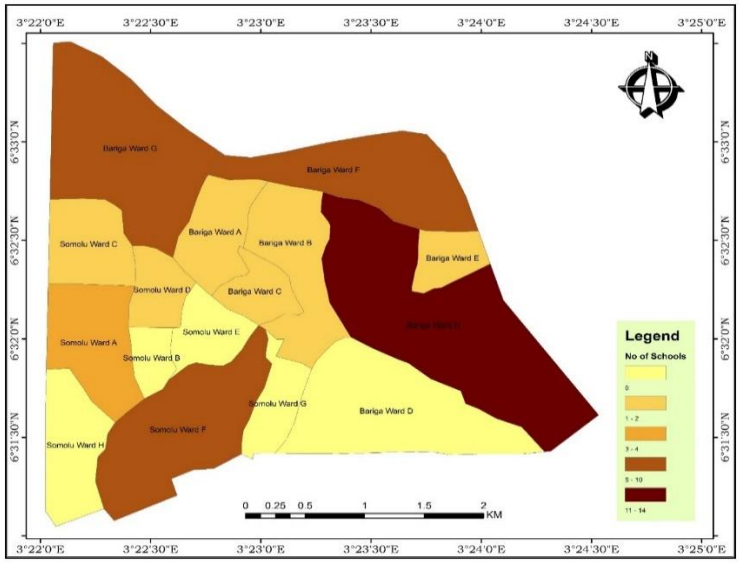

Figure 3. Number of Public Primary Schools in each Ward(2017)

4.2 Nearest Neighbour Index Summary

The result of the Nearest Neighbour Summary (figure 4.) showed that the Observed Mean Distance was 81.7603 Meters, the Expected Mean Distance: 192.4746 Meters, the Nearest Neighbour Ratio: 0.424785, the z-score: -8.011231, the p-value: 0.000000.

Given the z-score of -8.01123058131, there is a less than 1% likelihood that this clustered pattern could be the result of random chance.

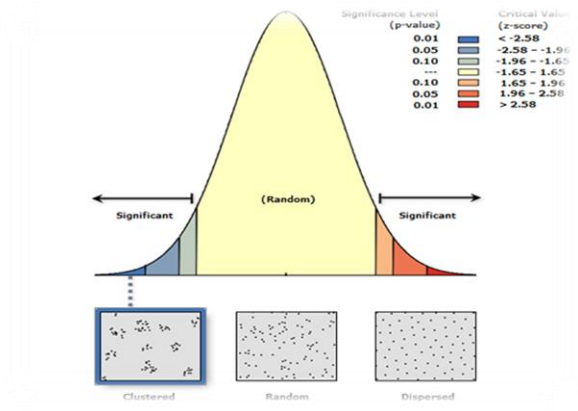

Figure 4. Nearest Neighbour Summary Result

4.3 Point Density Analysis Summary

The point density analysis shows vividly the clustered and uneven distribution of schools in the study area. It also further established and exposed the facts that wards with larger numbers of schools (Bariga Ward H, Somolu Ward F amongst others) when compared with the others are unevenly distributed within the wards. Generally, the public primary schools are concentrated and clustered within the central part of the study area as identified in figure 5..

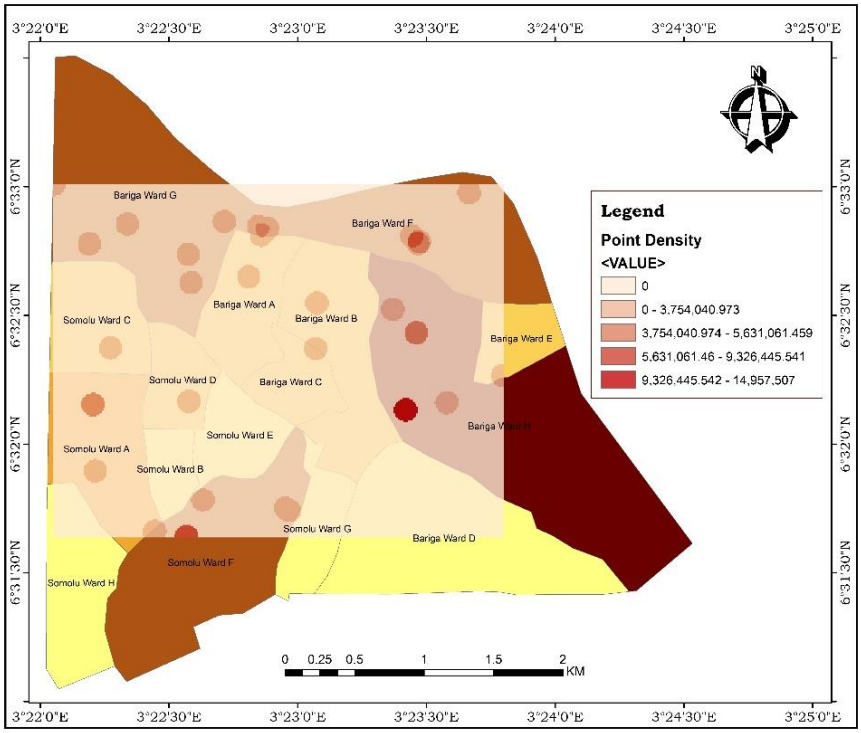

Figure 5. Point Density Analysis

The pattern of distributions of the Primary Schools in the study area also reveals the inequality firstly in terms of the distribution of the public schools in each ward compared to other wards. For example, (Bariga ward H, Somolu ward F) with 10 or more schools while some others (Bariga ward D, Somolu ward H, Somolu ward B etc.) have none.

4.4 Teachers and Facilities Distribution Analysis

Table 2 and Table 3 Number of Teachers for each qualification in the public primary schools in the study area and Distribution of building conditions of the public primary schools in each ward.

Table 2. Total Number of Teachers and their Qualifications.

Qualifications	No(s) of Teachers
HIGHER DEGREE WITH TEACHING QUALITY	14
HIGHER DEGREE WITHOUT TEACHING QUALITY	1
FIRST DEGREE WITH TEACHING QUALITY	184
FIRST DEGREE WITHOUT TEACHING QUALITY	27
HND WITH TEACHING QUALITY	3
HND WITHOUT TEACHING QUALITY	7
N.C.E	241
DIPLOMA IN EDUCATION	19
O.N.D	23
ACE,ACIE OR EQUIVALENT	4
TC 11 OR EQUIVALENT	7
TC II REFERRED	2
BELOW TC 11	82

Table 3. Building Conditions of the Public Primary Schools in each Ward.

WARDS	NO AVAILABLE	NO IN USE	NO REQUIRE	GOOD	MINOR REPAIR	DILAPIDATED
Bariga Ward A	0	15	15	0	0	0
Bariga Ward B	18	8	0	6	12	0
Bariga Ward C	0	0	0	0	0	0
Bariga Ward D	0	0	0	0	0	0

Bariga Ward E	14	13	6	14	0	0
Bariga Ward F	88	73	7	30	48	0
Bariga Ward G	96	67	15	70	39	10
Bariga Ward H	157	123	22	106	15	14
Somolu Ward A	50	40	13	30	0	0
Somolu Ward B	0	0	0	0	0	0
Somolu Ward C	22	21	34	0	0	15
Somolu Ward D	18	18	18	11	12	0
Somolu Ward E	0	0	0	0	0	0
Somolu Ward F	71	42	19	23	13	15
Somolu Ward G	0	0	0	0	0	0
Somolu Ward H	0	0	0	0	0	0
Grand Total	**534**	**420**	**149**	**290**	**139**	**54**

Most of the public primary schools met with the UNESCO standard (1996) which put the classroom capacity to one teacher to twenty five pupils in a classroom (1:25), though the total pupils/teachers ratio meets the standard (teacher - pupils ratio of 1:20). The classroom/Teacher ratio of the public primary schools is up to the UNESCO standard of (1:25). More than half of the total classrooms (54.3%) are in good condition and 26% in need of minor repairs, which makes a considerable amount of usable classrooms available, though there are still some cases of dilapidated classrooms which accounts for 10.3% of the available classrooms.

Secondly in terms of facilities, inequality in distribution also exist between the various wards that make up the study area. From the result generated in the study, Conditions among distribution of facilities whereby some Schools have excess in a particular facility alongside scarcity in others of the same facility. Although when seen generally as a whole, the standard of the facilities are sufficient or considerably enough except for the recreational facilities. The percentage of available recreational facility is 17.4% of the total required for the study area which shows a reduction in keeping the health and the enhancement of the teaching-learning process that is generated with the presence of sufficient recreational facilities.

4.5 Web Based Geo-database of Public Primary Schools

A Web Application was created using the ArcGIS online platform after exporting the shapefiles using the web map interface.

The images below (figure 6. shows some of the stages in the web map and afterwards the web map application created.

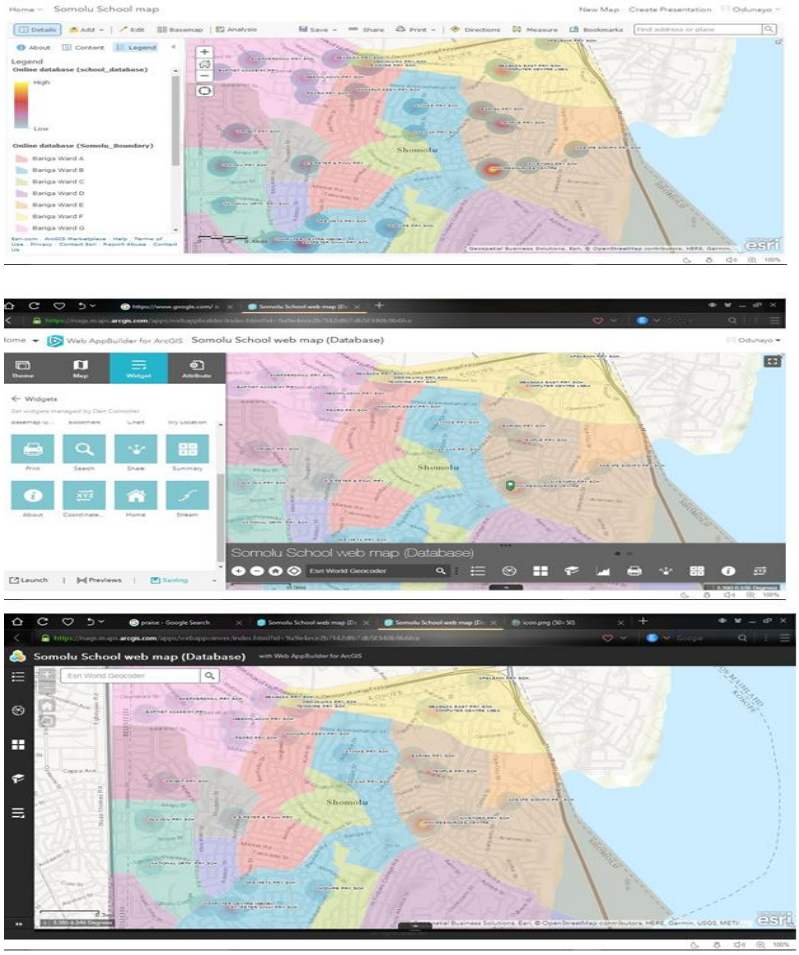

Figure 6. Web Application Previews.

The link of the Web Map application is:
https://nags.maps.arcgis.com/apps/webappviewer/index.html?id=9a9e4ece2b7f42dfb7db5f340b9b6fce

4.6 Discussion of Result Summary

This study of the Public Primary Schools in Somolu Local Government Area, Lagos State, Nigeria using Geographic Information System Technique identified and located a total of 53

Primary schools in the study area and these schools are supervised and monitored by two major organization bodies which are the State Universal Basic Education Board (SUBEB) Maryland, Ikeja and also Local Government Education Authority, Gbagada phase II, Somolu.

The results from the study shows a clustered pattern of distribution of public primary schools exists in the study area and the study also successfully mapped out all the Public Primary schools and displayed their spatial location over the entire study area.

The study shows that the standards set by UNESCO for the public primary schools in the study area were met as a whole when all public primary schools are considered. More and less in different standard categories such as: Numbers of Teachers, Teachers Qualification, Numbers of Classrooms, Classroom qualities etc. results to deficiencies amongst some schools in the study area. There is inequality in the distribution of educational facilities in all the ten wards comprising the study area and most of the educational infrastructure such as classrooms, Building conditions, Toilets, Recreational facility, furniture, Water and Power sources are inadequate

5. Conclusion

Generally, the quality of education that children receive bears direct relevance to the availability or lack, of physical facilities and overall atmosphere in which learning takes place. Therefore, this study analyzed the spatial distribution and generated a database for public primary schools in Somolu LGA, Lagos State. The study has conclusively shown that there is inequality in the distribution of educational facilities in all the ten wards in the study area. This study has effectively showcased the capability of GIS as a veritable tool for decision support system for planning and management of the Universal Basic Education facilities. It is a cost effective and fair method of tracking the status of the necessary infrastructure to ensure an effective teaching–learning to take place and it should be encouraged and adopted for policy making and implementation. The aim of this project was achieved as all the public primary schools were identified and mapped and a GIS database for public primary schools facilities in Somolu Local Government area alongside a web application has been developed. The spatial distribution of the schools was analyzed. The database provides users with a working environment for data management. It also allows for efficient query of information needed for school administration and management.

The following recommendations are hereby made based on the data analysis, research findings and conclusion of the research:

Firstly, the deficiency in the availability of recreational facilities across the public primary schools needs to be adequately addressed to make up the shortfalls in the existing facilities.

Secondly, public primary schools with inadequacies in the necessary facilities should be provided for, to improve the teaching-learning process.

Thirdly, periodic upgrade of existing facilities should be carried out to meet up with the growing population.

6. References

Aderinoye, R. A. (2007*). Mass Literacy in Nigeria: Efforts and Challenges*. in Journal of the Community and Adult Education Society of Nigeria. Vol. 5, No 1

Adomeh, I.O.C, Arhedo, A. and Omoike, D. (2007). *Comtemporary issues in history of education in O.O. Aluede and D.Omoike (eds): trends in history of eduction in Nigeria* (pp 221-139) Agbor: Krisbec Publications 121-139

Ahmed, M. N., M. U. Mohammed and Y. IDRIS (2013). A GIS-Based Analysis of Police Stations Distributions in Kano Metropolis. *IOSR Journal of Computer Engineering (IOSR-JCE),* Vol. 8**,** pp72-78.

Akpan P. E. and Njoku E. A. (2013). *Towards a Sustainable Distribution and Effective Management of School Facilities in Ikot Ekpene LGA of Akwa Ibom State*: A Geographic Information Systems Option MCSER-Mediterranean Center of Social and Educational Research Vol 4.15

Aliyu A., M. A. Shu'aibu and R. M. Aliyu (2013). Mapping and Spatial Distribution of Post Primary Schools in Yola North Local Government Area of Adamawa State, Nigeria. *International Journal of Science and Technology,* 2.

De La Fuente H, Rojas C, Salado M, Carrasco J, Neutens T (2013*). Socio-spatial inequality in education facilities in the Concepcion metropolitan area (Chile)*. Current Urban Studies 1(4):117-129.

Caillods, F. (1983). *School Mapping and micro-planning in education,* Module I: *Training materials in educational planning, administration and facilities.* IIEP/UNESCO 7 - 9, rue Eugene - Delacroix, 75116 Paris, France.

Durosaro, D. O. (2004), *Resource Allocation and Utilization for University Education in Nigeria, Trends and Issues,* in: E. G. Fagbamiye and D. O. Durosaro, eds., *Education and Productivity in Nigeria* (NAEAP) 51-67.

Eray, Okan (2012). Application of Geographic Information System (GIS) in Education, *Journal of Technical Science and Technologies*.

Federal Ministry of Education - FMoE, Nigeria (2003): Education Sector Status report, Nigeria.

Federal Ministry of Education - FMoE, Nigeria (2006): Strategic Plan for Educational Enhancement and Development. Nigeria.

FGN/UNESCO/UNDP, 2003. A Decade of Basic Education data in Nigeria (1988 – 1998).

Federal Ministry of Education, - FMoE, Nigeria (2009). Roadmap for the Nigerian Education Sector.

Globalisation of Education Policies (2000): *Extent of External Influences on Contemporary Universal Primary Education Policies in Papua New Guinea* - excerpts are from the complete text of Thomas Webster - book from the University of Papua New Guinea Press.

Hite, J. S. (2008). *School Mapping and GIS in Educational Micro-Planning*. International Institute for Education Planning. United Nations Educational, Scientific and Cultural Organization (UNESCO), Paris, France.

Ikpasaja, Ernest (2014): *Spatial Distribution and Accessibility to Public Primary School in Akwa-Ibom State: A case study of Uyo Local Government Area*. Unpublished MSc project report, Regional Centre for Training in Aerospace Survey (RECTAS) Library, Ile-Ife,Osun State, Nigeria.

International Bureau of Education (IBE) – UNESCO, (2006): Laws and other basic regulations concerning education.

Olamiju Isaac Oluwadare and Olujimi Julius (2011). *Regional Analysis of locations of Public Educational Facilities in Nigeria: The Akure region experience.* Journal of Geography and Regional Planning. Vol. 4(7), pp. 431.

Omotere, Adunola (2010): *The Challenges Affecting the Implementation of Universal Basic Education in Nigeria* Chapter One. Published Online By: Ego Booster Books, Osun State, Nigeria.

Susan J. Peters (2004). *Inclusive Education: An EFA Strategy for All Children*. World Bank. Online document.

Sule J. O, H. S. Abdullahi and J. Bungwon (2012), Acquisition of Geospatial Database for Primary Schools in Kaduna Metropolis, *Research Journal of Environmental and Earth Science*.

Taiwo CO. *The Nigerian education system: Past present and future Lagos*. Thomas Nelson (Nigeria) Ltd. 1980; 66-90.

WORLD BANK (2014). Education is fundamental to development and growth. "The First 7": *Conference on Early Childhood Development Policies.* World Bank

Geospatial Distribution and Locational Impacts of Filling Stations in Minna Metropolis

Odekunle, M. O[1*]; Adesina, E.A.[2]; Lateef Q.A.[1] Acha, S[1], Ahmed, Y[1]

[1] Department of Geography, Federal University of Technology, Minna, Nigeria.

[2]Department of Surveying and Geo-informatics, Federal University of Technology, Minna, Nigeria.

[1] odemary@futminna.edu.ng,
[2]joefodsolutions@gmail.com
* Corresponding author

Abstract

This research analyzed the geo-spatial distribution of filling stations outlets in Minna Metropolis using Global Positioning System (GPS) receiver; Garmin 76X to determine their spatial locations. The updated georeferenced street shape file of the study area was sourced from the Niger State Geographical Information System (NGIS) and imported to ArcGIS environment with data integration and transformation of the geographical coordinate of the filling stations. Standard of planning by Department of Petroleum Resource (DPR) was adapted

by Environmental Guidelines Standard was also used as a standard for the study. The study discovered 83 filling stations located along the 10 roads in the study area, of which 73.973% belong to indigenous marketers, 20.55% belong to multinational marketers and 4.82% belong to NNPC. Correlation exist between hierarchy of road and filling stations, Bosso, Western by-pass, Eastern by-pass, Bida, Kpakungun and Paiko road (all major roads) have the highest number of filling stations whereas minor roads like Shehu Musa and Shehu Kangiwa roads have low density of filling stations. The locational pattern of the filling stations is clustered with significant difference between the pattern and random pattern at both 95 and 99% level of significance. The major factors governing the location of filling stations are the traffic flow, exit site from the city and closeness to Motor Park. 83.13% of the filling stations met 15 meter distance to the road as standard. However, 60% of the stations met distance of 100 metre to the utilities but with side by side closeness to built-up. Thus, many stations does not meet the standard of 400 metre distance to nearby stations but were located without separation. The research recommended that agencies in charge of regulation should ensure that filling stations operators comply with standards through enforcements.

Keywords: ArcGIS, ArcMap, Coordinate System, Department of Petroleum Resources, Filling station, Geo-referencing, Global positioning system.

1. Introduction

Petroleum products are highly inflammable and hazardous, their explorations, transportation and citing of filling stations must not be taken with levity like other products but handle with cares as they are capable of life and properties destructions. According to World Health Organization (2016), millions of lives with more than billions of properties were lost to fire outbreaks due to mishandling of petroleum product.

Minna as the capital city of Niger state is one of highly populated settlements in Niger state and by implication with high transportation system (National Population Commission 2006, Niger State Bureau of Statistics 2012). The demand for petroleum becomes more very high as a result of shortfall in supply of electricity from the national Grid. The petroleum filling stations become lucrative as a result leading to concentration of filling stations in the strategic places of Minna especially along major and main road, cited with unconformity with Department of Petroleum Resources Guidelines.

In Nigeria, Department of Petroleum Resources Environmental Act amended Decree no 37 of I997 serve as safety rules and guide in protection of environment from potential hazard of close proximity of filling stations to build up area. However, Nigeria Department of Petroleum Resources (DPR) under ministry of petroleum and Environmental Guidelines and Standards (EGAS) of 1991 serve as comprehensive working documents with serious consideration for preservation and protection of Niger Delta region and by extension the Nigeria environment (Department of Petroleum Resources, 2016).

Recently, number of filling stations in metropolis of Minna has increased tremulously; best reason for such unprecedented increased includes the growing number of people that brought about increase in the number of vehicles. The profit attractive of petroleum both at black and

control market makes more people to ventures; marketers take advantage of this and build petroleum filling stations randomly without considering the certain environmental effects of such location. Because petroleum are highly in flammable and a times centre of district business in most built up areas. Therefore environmental impacts assessment of Petroleum filling station distribution should not be neglected but ascertained.

2. Literature Review

The largest industry in Nigeria nation economy is the petroleum industry or sector as opined by Baghebo and Atima (2013) which provides approximately 90% of foreign exchange earnings of the country with about 80 percent of Federal revenue and a major determinant to the rate of growth of Gross domestic product of the nation.

Petroleum industry in Nigeria is distinguished by type of actors that is otherwise known as sector (Ehinomen and Adeleke, 2012). They further itemized that the actors in the Nigeria industry or petroleum economy consisting both private and public organizations. The public actors are the government functionaries and agents such as the Nigerian National Petroleum Corporation (NNPC) and its subsidiaries, the Petroleum Products Pricing Regulatory Authority (PPPRA), the Department of Petroleum Resources (DPR), among many others. The private segments on the other hand consist of both indigenous and foreign actors that own oil block. The indigenous actors are the private marketers which numbered about 2000 in 1983, after the act which established them was formulated , private investors increased to 7988 in 2012 with much more competition with the major marketers who are foreign and multinational marketers that includes Conoil Public Limited Company, Oando Nigeria Public Limited Company., African Petroleum Public Limited Company, Mobil Oil Nigeria Public Limited Company, MRS Nigeria Public Limited Company, and Total Nigeria Public Limited Company among many other company.

Mshelia, Abdullahi and Dawha (2015) study revealed that the standards for citing petroleum stations have not been adhered by most of the petroleum outlets and this is thereby posing serious dangers on residents living in close proximity to petroleum filling stations in Maiduguri and Jero. The hazards causing to their study includes injury to aquatic life, harmful effects to human's health and environmental pollution from generating plant exhaust.

Hazards are harmful physical environmental elements to man that can be caused by forces that are extraneous to him. These hazards are also seen as threat to future source of danger having the potential to cause harm to people such as death, injury, disease and stress among others; harm to human activities including economic development, educational activities and sustainable development; harm to property damage and economic loss and environmental harm loss of plant and animal, aquatic organism and its biodiversity, pollution and loss of amenities. Mshelia, Abdullahi and Dawha (2015) further suggested that government in partnership with all the petrol stations should constantly be mounting public enlightenment campaign using bill boards, posters and media houses to enlighten the public at large on the hazards associated with petroleum products mishandlings with respect to human health and the environment so as to discourage residing close to petrol stations as mitigation control measures.

3. Methodology

This section discusses the study area, data and methodology used for the study. It discusses data sources and types, data collection procedures, sampling techniques and methods of data analysis. Thus, the primary data used for this study includes collection of geographical

coordinates, field survey, interview and the secondary data includes land use and road map of the study area.

The criteria used in siting of filling stations was obtained from DPR office in Minna, Niger State, before proceeding to field to obtain geographical coordinate (x and y) of the existing filling stations in the study area. The shape files of the updated road and land use maps were also obtained from Niger State GIS office in Minna, Niger State. Checklist was drafted after detailed information on the filling stations has been sourced.

Field operation was made to acquire the geographical location (x and y) of the existing filling stations using Global Position System (Garmin 76X Model). The filling stations were categorized into three (3) for comparison and they includes multinational (major) marketers, indigenous (independent) marketers and NNPC stations.

To achieve the goal of the study, different sets of data were used. These include the filling stations data sourced from DPR and field survey, land use map and road map. These data were imported, georeferenced to the same coordinate and datum, and integrated in the ArcGIS 10.3 environment for the analysis.

3.1 The Study Area

Minna is located geographically on latitude 9^0 36' 50'' and longitude 6^0 33' 25'', with a population estimation of 304,113 (National Population Commission, 2006). It is the capital of Niger state and is connected to neighbouring cities by road with Abuja for instance being about 150km away. The city is linked to both Lagos and Ibadan in the south and to other places in the north. Minna is situated at 243 meters above the sea level, have a geological base of basement complex that consist of gneiss and magmatite that are undifferentiated. Urban development of the city is limited in the north east direction of the city due to continuous steep of granite. Figure 1 shows the map of the study area.

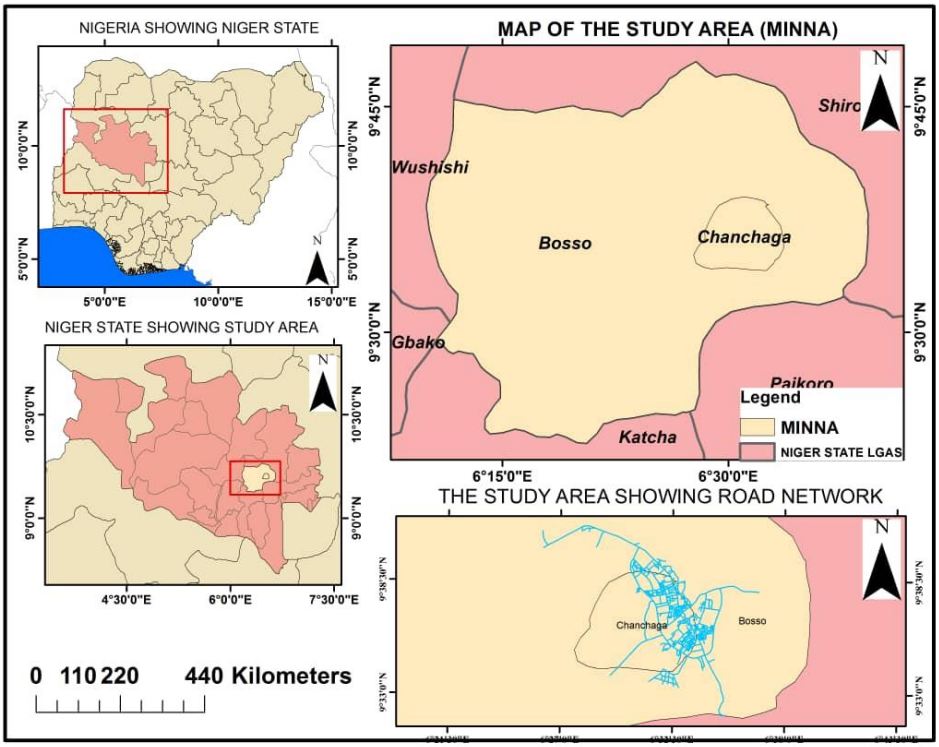

Figure 1: Map of the study area showing the road network

3.2 Geo-referencing and digitizing the map

The digitized shape files of the updated road and map obtained from Niger state GIS office was imported into Arc Map environment of ArcGIS 10.3 software. Major landmarks in the area like Mobil Round About, Federal University of Technology Bosso campus, Kpakungun Junction and Air force base in Maikunkele were used as georeferencing point of the road shape file. The shape file and the geographical coordinate were auto rectified and transformed to same coordinate system using UTM (Universal Transverse Mercator) of Global Coordinate System (GCS) projection with Minna Zone 32N being used as datum. The UTM was used in light of the fact that it is metric and has the ability to calculate distance, length and other measurement that may not be possible with geographic coordinate.

3.3 Data processing

The geographical coordinates of the existing filling stations were entered into Excel Microsoft application software to create database. Information on the existing filling stations which includes company name, address and road location, latitude and longitude coordinates was stored with column and row. The data were saved in the folder created in C drive and exported it to ArcGIS environment to show spatial pattern and arrangements using map with further analysis. In order to achieve the objective of mapping out filling stations in the study area. Pattern analysis was carried out using spatial statistics tools in ArcMap environment to identify

the location pattern by using nearest neighbour index (NNI) and the Z-score value to determine the pattern of distributions.

The nearest neighbour index (Rn) according to Muritala (2015) is the ratio between the observed and expected values that varies from zero (when all points are in one location and distance between each point and its neighbour is equal to zero) and (for a perfect uniform or symmetrical point pattern spread out on an indefinite large area). A values of $Rn = 1$ indicate a random pattern since the observed distance between neighbours is equal to the one expected for random distribution. The nearest neighbour formula is given as:

$$\boldsymbol{Rn = 2 đ \sqrt{n / A}} \quad (1.1)$$

where,

Rn = description of the distribution

d = the mean distance between the nearest neighbours (km)

n = the number of the points in the study area

A = the area under study (km^2)

The Z-score is the number of standard deviation from mean of data point which is technical way of measuring deviation below or above mean population and apply to compare result from test analysis to normal population distribution, the Z-score formula for a sample is given as:

$$\boldsymbol{z = (x - \mu) / \sigma} \quad (1.3)$$

where,
X = value of the element
μ = population mean
σ = standard deviation

3.4 Filling station and physical planning standards

Filling station business is regulated by DPR, a department under the Ministry of Petroleum Resources saddled with responsibility to register and regulate the downstream petroleum sector. In addition, there exists Niger State Urban Planning Department Agency (NSUPDA) whose duty is to regulate all development within the metropolitan of Minna. In order to achieve the second objective which is comparing location of the filling stations with standards of DPR and EGAS, proximity analysis (buffering) was used. This was achieved using buffering analysis tools available in ArcGIS 10.3 software.

3.4.1 Distance to road

The physical planning Standards by DPR (2016) grant of approvals to construct and operation of petrol station, the distance from the road to station must not less to fifteen (15) meter. Because filling station is a point location and road being a line feature, a buffering of 15 metres

was created on the road and data query was made in ArcMap environment (Figure 4). To avoid the clustering of the road buffering result of 15 meters distance standard of filling to road, filling stations that does not conform to the standard was extracted and presented in map and table for easy visual interpretations.

3.4.2 Proximity of filling stations to utilities

The various utilities considered for this study include churches, mosques hospital, schools and other places of gathering merged together as layer to obtain their proximity to filling stations for vulnerability assessment. 100 metres buffering was created on the filing stations and query of data was created by location in ArcMap environment to determine possible associated hazard of proximity. The selections of locations that are within 100 meters distance to the utilities were identified by the query.

3.5 Factors that determine filling stations distribution in Minna Metropolis

Filling station business exists in a geographic space and has spatial dimensions of which such place for this business has to possess. The DPR is responsible for issuance of license to operators and ensure standards are complied with, marketers consider some factors in business location choice. The result of the interview conducted by IPMAN official in Minna revealed that the following are the factors the operators take into consideration in selecting site for building filling station.

1. Traffic flow: This is one of the most paramount factors operators considered in citing filling station. Marketers build station along main roads that have continues and heavy traffic flow because they attract more customers. In other words the more the heavy traffic flow the more the demand of fuel.

2. Exit roads**:** Filling stations were usually built along the exit roads that link the city (Minna) to other neighbouring cities. Example of such roads like Paiko, Bida/Kpakungu, Eastern bye-pass, Bosso and Western bye pass road have the greater number of station compare to other roads partly because they are the exit road from Minna to all parts of the country. Petroleum had been compare to food as such anyone driving out of the town has to full his tank (with fuel). In fact finding showed that most filling stations are built on the exit road where customers will find it easier to enter filling station and fuel their motor vehicle. In addition, the marketers assumed that vehicle driving-in the town (Minna Town) had already fuel their vehicle at their source/origin.

3. Closeness to Motor Park: Filling station business targets drivers, especially public transport drivers, so filling stations were built very close to motor park especially those for intercity or intra transport.

4. Convenience: This was another factor consider by marketers for choosing their business location. Though marketers are attracted by heavy traffic flow, they prefer re built-in their station in places away from traffic jam heart were the passengers may find it convenience to

park and fuel their vehicle. Hence, stations are built where there is enough space for customers to maneuver the vehicle when entering or exiting after fueling.

5. Near Nodal Towns/Junctions**:** Filling stations are also built close to nodal towns or junction because nodal towns are potential markets for filling station, filling station were built along them. However, this is more applicable to peri-urban stations. Vehicles are coming from different side of the junction and therefore likely to stop and get fueled.

4. Results and Discussion

4.1 Results

This involves the presentation of results from the processed data, analysis, and discussion of results. Figure 2 shows the map of the spatial distribution of the existing filling stations in the study area while Figure 3 depicts the nearest neighbor analysis to determine the pattern distributions of the filling in the study area.

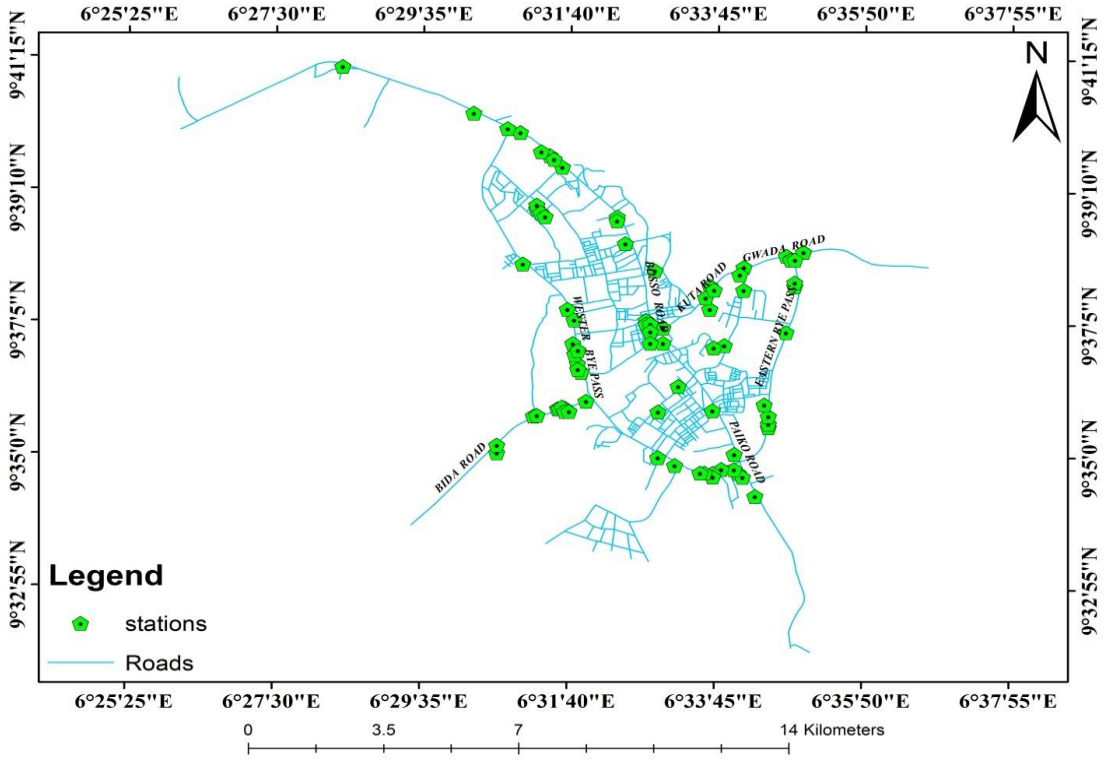

Figure 2: Existing filling stations spatial distribution in Minna Metropolis

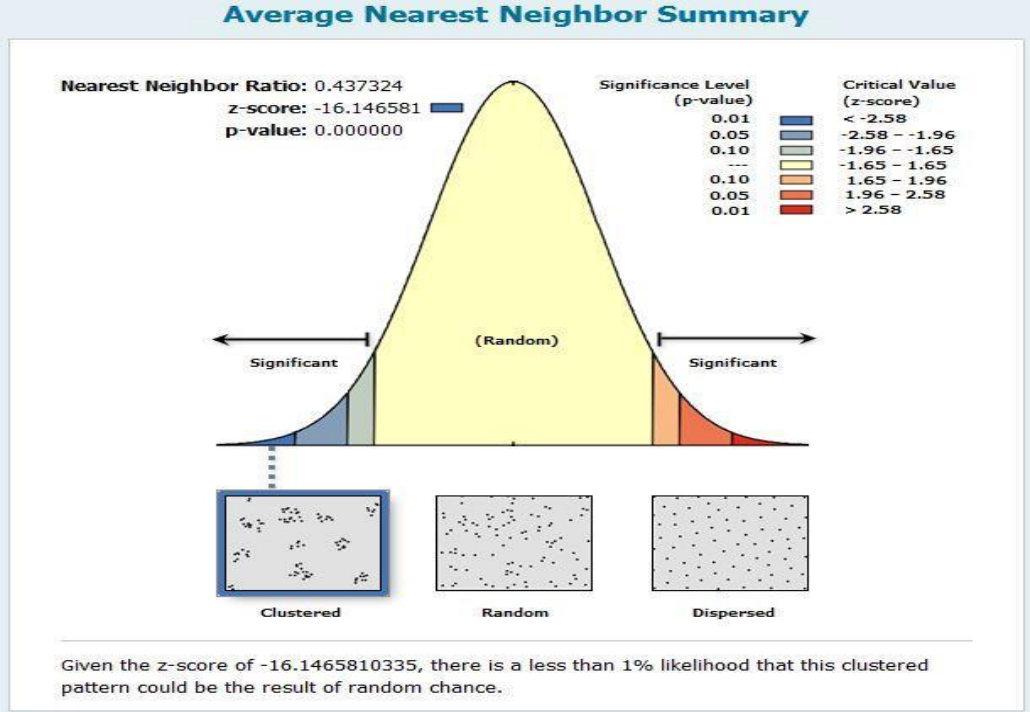

Figure 3: Nearest neighbor analysis of filling station

Table 1 shows the percentage location of filling stations in Minna metropolis. Figure 4 shows the 15meters distance road buffer used on the existing filling stations while Figure 5 is the map of the filling stations that does not meet the 15 metres distance to road in the study area.

Table 1: Location of filling stations by road in Minna Metropolis

S.N	Road	Type	F	Percentage
1.	Bida Kpakungun	Major	10	12
2.	Bosso	Major	9	11
3.	David Mark	Major	3	4
4.	Eastern byepass	Major	10	12
5.	Western byepass	Major	20	24
6.	Ibo	Major	4	4.8
7.	Kuta Gwada	Minor	8	9.64
8.	Paiko	Major	7	8.43
9.	Shehu Musa	Minor	3	3.61
10.	Bala Shamaki	minor	4	4.8
11.	Shehu Kangiwa	Minor	5	6.24
	Total		**83**	**100**

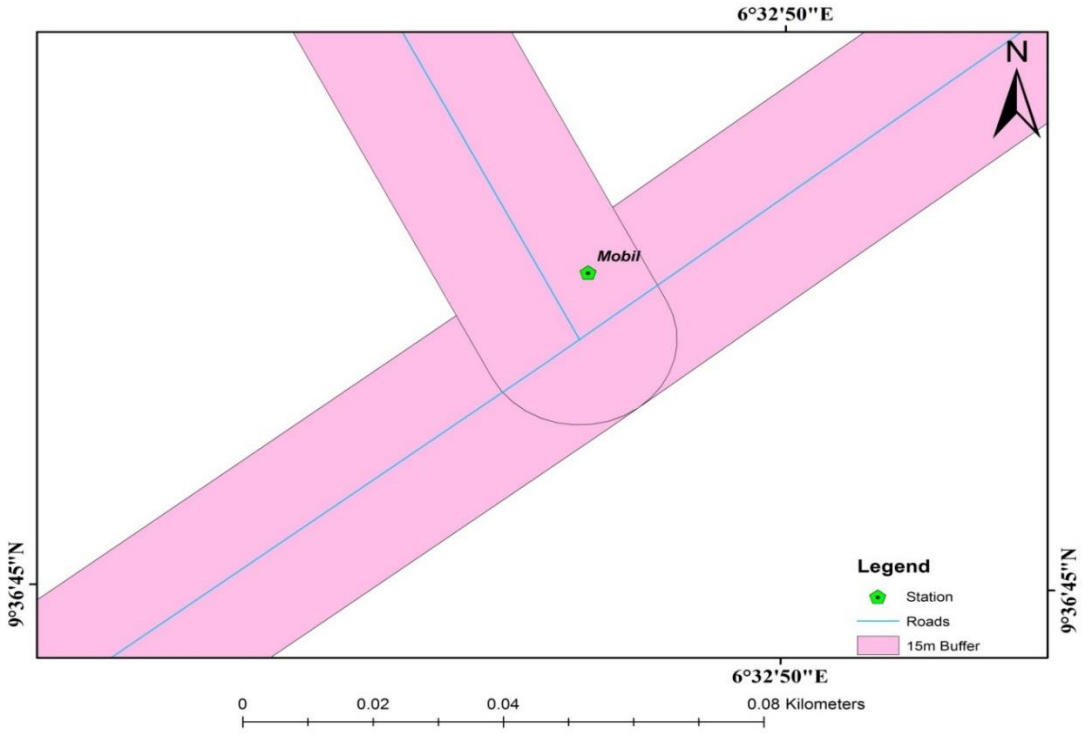

Figure 4: Filling stations and 15 metres distance road buffering

Figure 5: Filling Stations not meeting 15 metres distance to road in Minna Metropolis

Thus, Table 2 shows the filling stations that are not conforming to the 15 meters standard because the distance from the road to station must not less to fifteen (15) meter. Figure 6

depicts the map of the existing filling Stations in the study area in relation to 400 meter distance buffered to each other. Figure 7 is the map the shows the spatial distribution of filling stations in relation to utilities. Figure 8 is the map of the filling stations and 100 metre distance buffered from utilities while Figure 9 depicts the filling stations and 100 metres buffered distance to the utilities in the study area.

Table 2: Filling stations not conforming to 15 meter standard

SN	Distance (m)	Filling Stations
1	5.00	Oando filling station, Kpakungu
2	9.00	Total filling station Tunga
3	18.00	Garima filing station, Bosso
4	37.00	Muhabat filling station, Tudun Fulani
5	79.00	Forte oil, Kuta round about
6	81.00	Mobil filling station, Mobil round about
7	83.00	Under construction

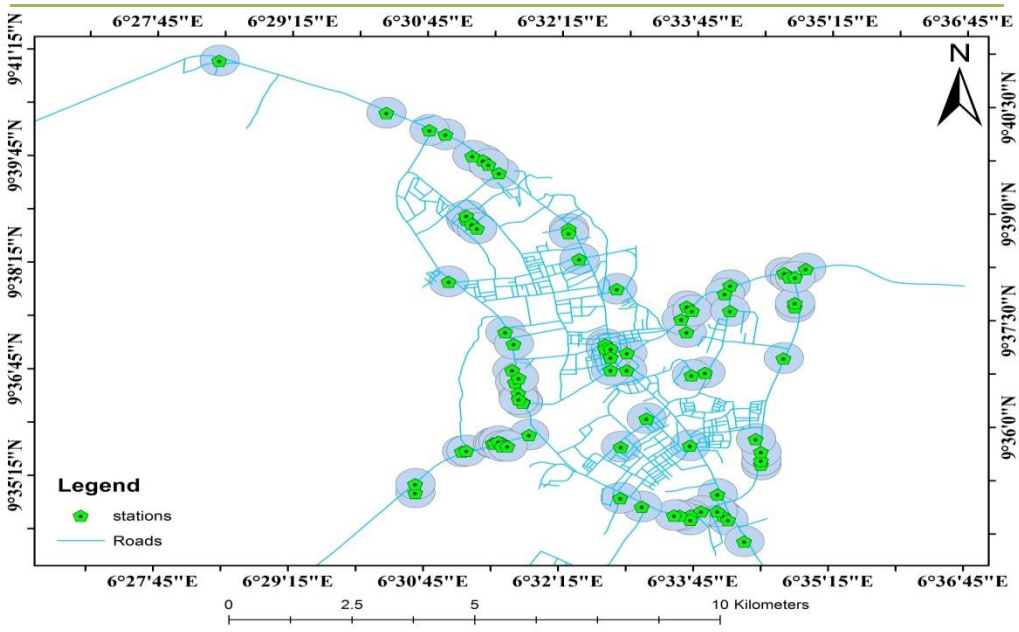

Figure 6: Filling Stations in Relation to 400 meter Distance to each other

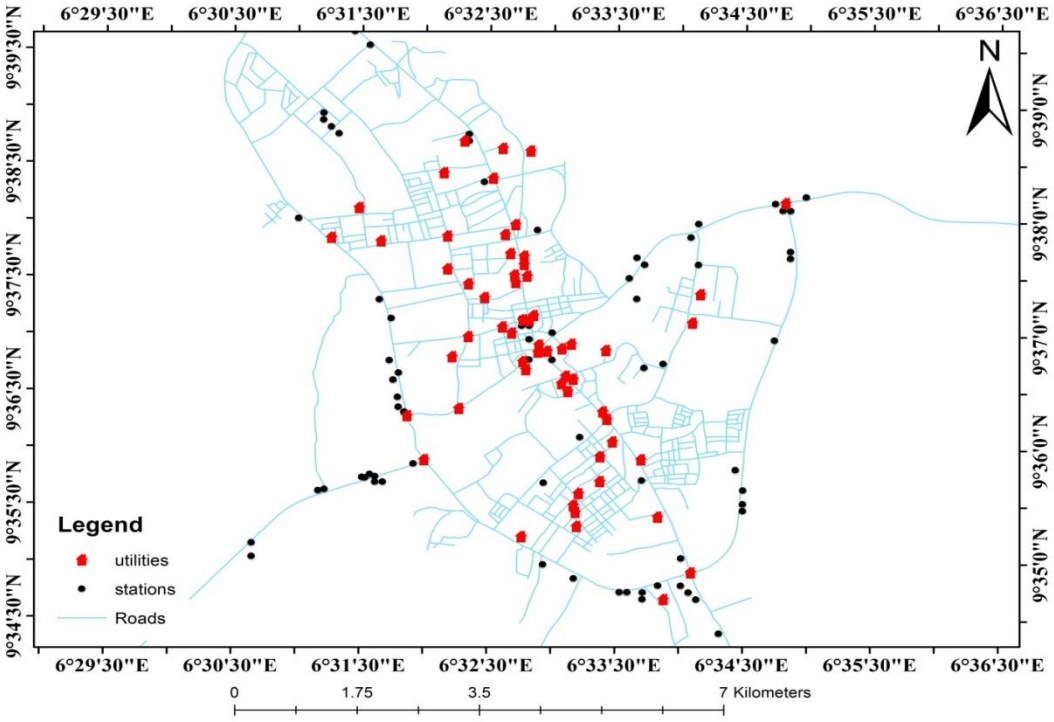

Figure 7: Spatial distribution of filling stations in relation to utilities

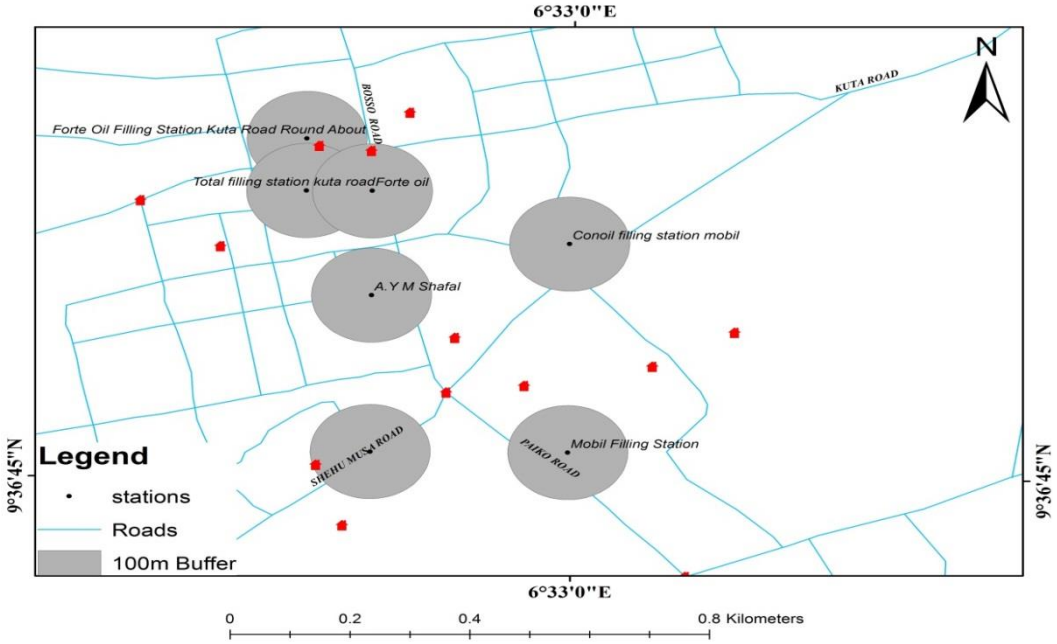

Figure 8: Filling stations and 100 metres distance from utilities

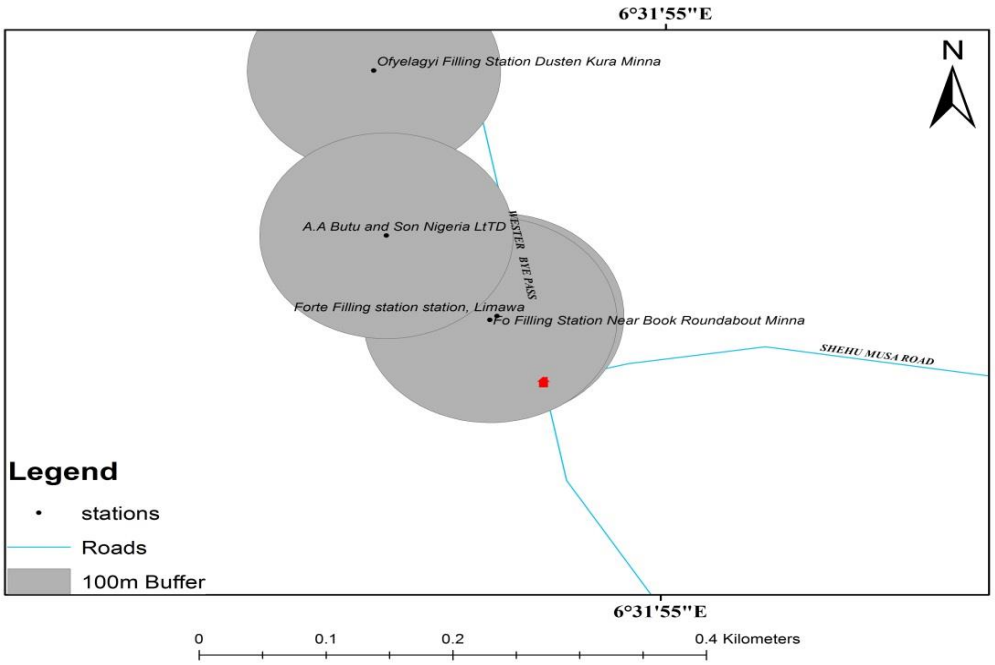

Figure 9: Filling Stations and 100 metre Distance to Utilities

4.2 Discussion of results

The finding revealed that there exist eighty three (83) filling stations at the time of this study which are distributed along eleven (11) roads in the area (Table 1). The filling stations distribution is not uniform between the roads, Western bye-pass road has the highest number of stations (20), Eastern bye pass and Bosso road have (14) and (12) each respectively. These three (3) roads account for about average of the filling stations in the area (representing about 53%). Because the roads are major roads in the metropolis, the result is not surprising; they are the longest and linked connect Minna with other neighbouring city and town. Short or access roads have least number of filling stations. This result supports that of Muritala (2012) that filling stations are mostly built in town centres rather than on the extreme exit of roads and use to be dominated on the exit side of the town.

For instance out of eighteen filling stations along Bosso Mobil to Tunga road, eight (44%) are built on the exit side along Minna to Suleja-Way, fourteen (52%) in Eastern and Western bye pass and Maikunkele road and three (30%) in Kpakungu road are found on exit side from Minna to Bida (Figure 2).

The study discovered that 86.31% of the filling stations are located on the major road and 13% on minor roads (Table.1). Attempt was made to see if there exist any relationship between the road rank and the number of filling station using Pearson product moment correlation and it was discovered that there is significant relationship even at alpha value of 0.00 because the p-value for the relationship is 0.0000. In other words, the higher rank of the road the more the number of filling stations located along it.

The result shows that seven stations (8.43%) did not conform to the criteria of 15 meters distance to road (Figure 4 and 5). The stations are within major roads (e.g. Bosso and Tunga road) and none is within minor roads. This confirms that most of the filling stations meet the standard criteria of locating 15 metres distance from road because of Minna road network. Because most road networks in Minna are beautify with pedestal pathway, this constitute to factors why filling stations met the standard.

The finding discovered that 454 meters is the longest distance between neighboring filling stations; this was between solid mark filling station along Maikunkele road and Salihi filling station. Shortest distance less to metre was observed where stations lie to each other. Figure 6 show that more than one quarter of the stations does not maintain 400 meters to their neighbors. 9.64% of the stations met the minimum distance requirements of 400 meters to neighbors' as standard.

The filling stations that had not conformed to the standard were found mostly in main roads. The possible reason for the play out may be due to Bosso -Tunga road, East and Western bye-pass and Bida road that are major road that link Minna to other neighbouriing settlement, presence of market, shopping mall on these areas and the fact that regulators to does not strict to law enforcing but ignored by give waver especially in heavy traffic roads.

The study findings revealed that most filling stations meet this standard (60%) and only few of the stations could not meet the standard. Those stations that do not meet the standard are major and indigenous marketers with non-belonging to NNPC. Although, filling stations in Minna metropolis are located within built up but in particular proximity distance of filling station to utilities is one of the main standards the regulator are strictly with because of their usefulness.

4.3 Summary of findings

This research analyzed the location of filling stations in Minna Metropolis and subjected the location to the physical planning standards put in place by the regulatory agency, DPR and EGAS. The research findings discovered eighty three (83) filling stations currently operating in the study area. Among filling stations existing in the area, about 72.29% are owned by Independent marketing companies, 22.89% by six major marketers and 4.82% by NNPC. Total Nigeria plc top the major marketers with six filling stations with Mobile Nigeria have the least number among the major marketers.

The number of stations correlated significantly with road hierarchy. Major roads like Bosso Mobil Tunga, Eastern and Western byepass with Kpakungu/Bida road have higher number of filling stations. About 78% of the stations were located on the major main roads and 14% on the minor roads.

Though the filling station exhibit linear pattern because they are cited mainly on road side where drivers can easily get the product, the overall pattern off distribution is clustered with nearest neighbour value (Rn) of 0.43 (less than 1) and z-value of -16.14. There was significant different between the observed pattern and the random pattern at both 95% and 99% level of significance and its 99% likely that the pattern is cause by chance. The major factors influencing the location of the filling stations are traffic flow, exit side of the town, nearness to

inter urban Motor Park, convenience and existence of nodal towns or junction. Most filling stations met the requirement of minimum 15 meter distance from the road (96%). In the same vein however, 60% of the filling stations met the minimum distance of 100 meter to utility. Many stations had not met the criteria of 400 meter minimum distance to other neighboring stations but they were located side by side without road separation.

5. Conclusion

5.1 Conclusion

The research made the following conclusions:

1. The filling stations in Minna metropolis are not equally distributed but concentrated along major roads especially Bosso road, Bida road, Eastern bye-pass and Western bye-pass road.

2. There is significant correlation between the hierarchy of the road and number of filling station. Filling station retailers prefer highways linking Minna town with other towns and cities like Suleja, Abuja, Kaduna, Bida, Kotangora among others where the people mingle all the time.

3. The independent marketers dominated the petroleum retail business (filling Station) and this is good for the economy. Indeed the independent marketers were established with intention to diversify the economy, create opportunity for Nigerian to participate in downstream petroleum sector and reduce the monopoly of multinational companies that initially dominated the sector.

5. Most Filling station complies with the standards pertaining to distance from the road due to pedestal pathways of Minna road network and from public buildings and utilities especially hospital. Many stations do not meet the 400 meter distance to other nearby stations. In fact it is common in the metropolis to see two stations lying back to back especially in the major roads.

6. This study was able to create the database for filling stations in Minna Metropolis, the DPR ,EGAS and Niger State City Development Office and Niger State GIS which are currently trying to create spatial database for the city can utilize this data. A similar study can be carried out in all states of the federation.

5.2 Recommendation

The research also made the following recommendations:

1. The regulators (DPR, EGAS, fire service and town planner) must make it mandatory for every filling station operators to include the geographic location of the site when processing license. This will aids in spatial database management updating.

2. Regulatory agencies need to look into the issue of discrepancies regarding the compliance to standards, take appropriate measures that ensured that only site that meet the minimum standards are allowed to do the business.

3. Filling stations are mostly located on some roads as found by the study, hence the need to give priority for the roads with less number of filling stations when given license to operators.

4. The vulnerability assessment shows that built up located at distance of 20 meter to filling station are in danger in case of fire outbreaks, authorities should enforce law and other to secure lives and properties from fire outbreaks.

References

Baghebo, M. and Atima, T. O. (2013). The impact of petroleum on economic growth in Nigeria. Global Business and Economics Research Journal, 2(5): 102-115.

Department of Petroleum Resource, DPR (2016) Procedure Guide for Grant of and Approval to Construct and Operate Petroleum Products Retail Outlets. Issued by DPR, Ministry of Petroleum Resources

Ehinomen C. and Adeleke A. (2012) An Assessment of the Distribution of Petroleum Products in NigeriaE3 Journal of Business Management and Economics Vol. 3(6). pp. 232-241, June, 2012 Available online http://www.ejournals.org.

Helsinki, (2000). Environmental Protection Act 86/2000. 4th Feb. 2000. In: P. M. Nieminen, 2005: Environmental Protection Standards at Petrol Stations: A comparative study between Finland and selected European countries. Tempere University of Technology, Publication. 534. P. 27.

Mshelia M., Abdullahi J. and Dawha E. (2015) Environmental Effects of Petrol Stations at Close Proximities to Residential Buildings in Maiduguri and Jere, Borno State, Nigeria, Vol. 20, No. 4.

Niger State Bureau of statistics (2012). Facts and Figure about Niger State handbook printed under the auspice of Nigeria statistical development (NSDP)

World Health organization (2016). Safe Piped Water: Managing Microbial Water Quality in Piped Distribution Systems by Richard Ainsworth.

Hydrogeochemical Evaluation of Groundwater Quality in Auchi and Its Environs

***[1]Umoru T.A., [2]Amadi A.N., [2]Unuevho C.I., [1]Sule, T.U.N., [2]Waziri, N. M. and [2]Ameh I.M.**

[1]Department of Mineral and Petroleum Resources Engineering, Auchi Polytechnic, Auchi

[2]Department of Geology, Federal University of Technology, Minna

*Corresponding Author's Email: geoama76@gmail.com or umorutiti5@gmail.com

Phone Number: +234-8037729977 or +234-7062238600

Abstract

The quality of groundwater is determined by its physical, chemical, bacteriological and radiological characteristics. The hydrogeochemical evaluation of groundwater quality in Auchi and its environs is conducted to ascertain its potability and facies types. Geologic mapping of the area revealed that the area is dominated by ferruginized sandstone. Thirty (30) groundwater samples were collected from the study area and sent to the laboratory analysis for chemical and microbial analyses. Prior to the laboratory analyses, physical parameters were determined insitu using a multi-meter. The It was observed that the hydrochemical parameters of the groundwater falls within the permissible limits of the NSDWQ of 2007 and WHO standard of

2004, with the exception of pH and iron concentration. The pH of the groundwater is 5.75±0.0707 indicating acidic water, and the iron concentration has a value of 0.375±0.1061 mg/l, which is beyond the permissible limits.

The concentration sequence of the major cations of the groundwater in the study area is Ca^{2+}> Na^{+}>Mg^{2+}>K^{+}, with Na^{+} value of 1.07±0.2121 mg/l, K^{+} 0.1950±0.0778 mg/l, Ca^{2+} 2.5750 ±1.2516 mg/l and Mg^{2+} 0.7750± 0.2756 mg/l. The concentration sequence of the major anions of the groundwater in the study area is Cl^{-}> HCO_3^{-}>NO_3^{-}>SO_4^{2-}, with Cl^{-} value of 28.6500±4.4548 mg/l, HCO_3^{-} 21.4000±8.6267 mg/l, SO_4^{2-} 0.3550±0.1485 mg/l and NO_3^{-} 1.2500±0.9051 mg/l. The electrical conductivity (EC) of groundwater in the study area ranges from 49.10 to 580.40 µS/cm. It falls within the permissible limits for NSDWQ and WHO. The total dissolved solids (TDS) in the groundwater of the study area have an average value of 42.95 mg/l, indicating fresh water. Stiff plots of the groundwater in the study area reveals that they are from the same aquiferous formation, and has a Calcium Bicarbonate (Ca-HCO_3) hydrochemical facies.

Keywords: Hydrochemical facies, Groundwater quality, Auchi, Cations, Anions.

1. Introduction

Water is essential for human existence, many people in developing countries do not have access to potable water. In achieving sustainable development goal, adequate supply of safe and clean water is one of the most important factors (Ibrahim *et al.*, 2012), and groundwater which is the water present in the subsurface of the earth at the zone of saturation more safe for consumption than surface water and it serves as a major source of potable water supply (Amadi *et al.*, 2012). The quality of groundwater is pertinent to its suitability for domestics and purposes. Thus, there is need to evaluates the hydrogeochemical evaluation of the groundwater in Auchi and its environs in ascertaining its potability, hydrochemicalfacies and and the groundwater trend in the area.

2. Materials and Methods

Study Area Description

The study area lies in the south-south geo-political zone of Nigeria, and situated between latitude latitude N 7º00′00″ to N 7º10′00″ and longitude E 6º10′00″ to E 6º20′00″.and it can be accessed through the Auchi-Benin express road.

Geomorphology

The study area is characterized by two distinct seasons; the dry and rainy seasons. The dry seasons which occurs between November-April and it is associated with hamattan that comes up between late November and February which is characterized by dust knew winds as a result of the North East or trade wind. The rainy season spans from April-November, with an average of about 100cm-15cm, the south west trade wind brings the rain for wet season. The vegetation of the area falls within the guinea savannah which is characterized with few grasses, shrubs and few scattered moderate height trees of about 6m tall. The vegetation is dense during the rainy season and less dense during the dry season, and it is always altered during dry season due to degradation by fire, animal grazing and farming activities, thus enhancing erosion in the

area (Matthew, 2002). The topography of the area is undulating with a ruggy relief. Figure 1 shows the topographic map of the study area.

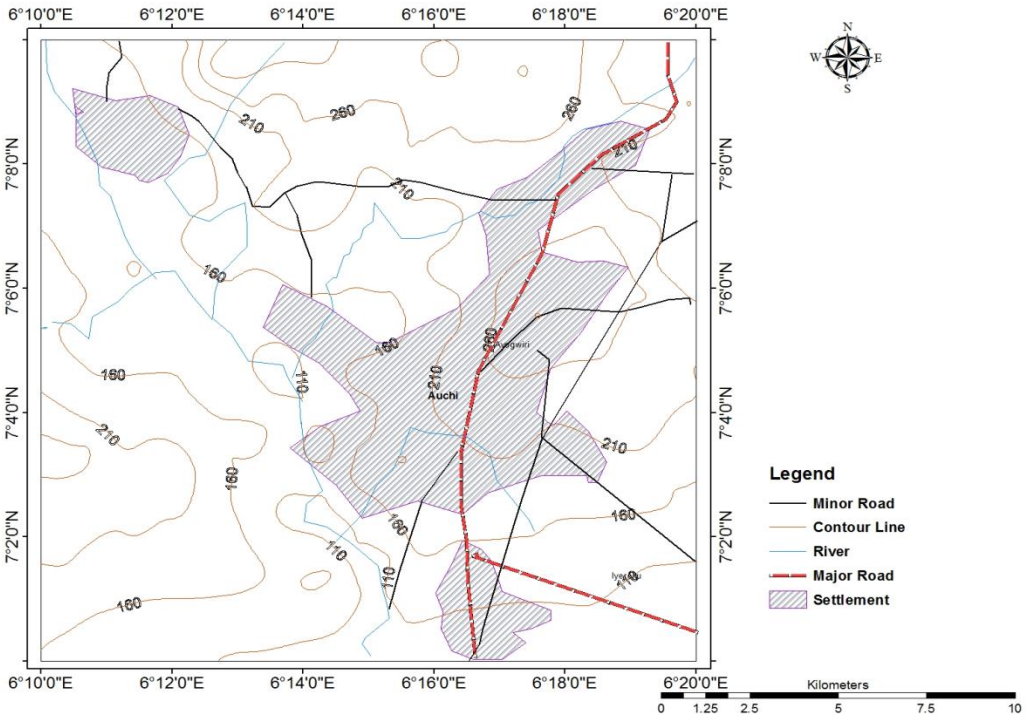

Figure 1: Topographic map of the study area (Office of Surveyor General of the Federation, 2009)

Geology and Hydrogeolgy of the Study Area

The study area lies within the Anambra basin, which is one of the sedimentary basins in Nigeria, and it's distinctively belonging exclusively to Nigeria (Okogbue, 2005). It is a structural depression located at the south-western of the Benue Trough. The basin is the Upper Senonian – Maastrichtian and Paleocene basin at the end of the Benue Trough in which Nkporo Shales and younger sediments accumulated, and which extended towards the southwest as the

Niger Delta basin (Reyment, 1965), with a lithological units of Nsukka, Ajali, Mamu and Nkporo Formation.

The area is widely covered by ferruginized sandstone, sandstone and clayey sand and it is drained by River Orle and River Niger (Sule *et al.*, 2014) and poses a detrital drainage system. The aquifer of the basin is the Ajali sandstone within the false-bedded Sandstone formation which is about 457m thick (Macaulay, 2008). Figure 2 shows the geology map of Nigeria.

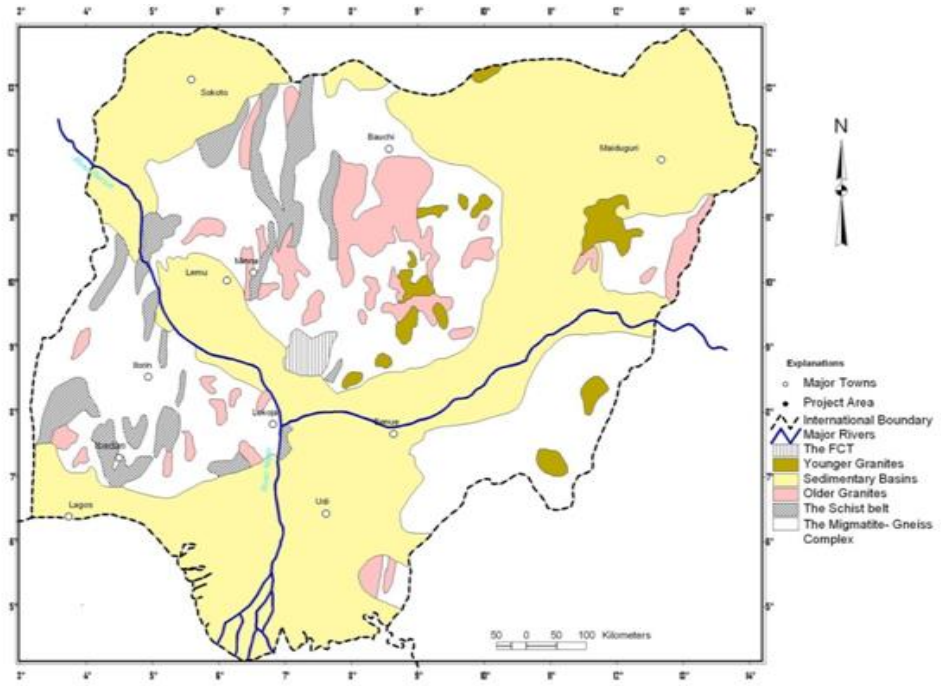

Figure 2: Geology map of Nigeria (Ajibade, 1983)

3.0 Methodology

Sample Collection and Laboratory Analysis

Groundwater samples were collected in two sets of one litre containers for both cation (which was stabilized with dilute hydrochloric acid) and anion analysis. An insitu testing was done to determine the physical parameter of the groundwater by the use of a Model PHS-3B pH Meter

Uniscope to measure the temperature, pH and electrical conductivity of the groundwater samples. The laboratory analysis of the groundwater samples was done with the aid of an Atomic Absorption Spectrophotometer (AAS), Spectronic 20D+ spectrophotometer, oven, incubator and titration apparatus. The groundwater physico-chemical parameters is compared with World Health Organization (WHO) standard of 2004 and Nigerian Standard for Drinking Water Quality (NSDWQ) of 2007. Figure 3 shows the groundwater samples location in the study area.

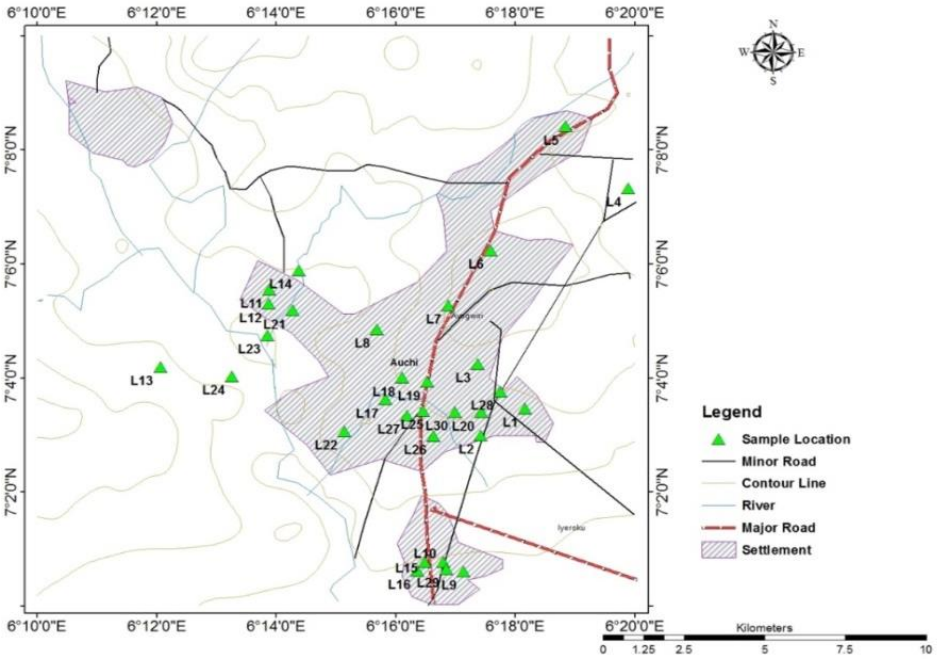

Figure 3: Groundwater sample location in the study area

4.0 Results and Discussion

The geostatistical result of the groundwater physico-chemical analysis is shown in table 1.

Table 1: Geostatistical results of the groundwater physico-chemical parameters in the study area

Descriptive Statistics						
	N	**Minimum**	**Maximum**	**Mean**	**Median**	**Std. Deviation**
Na	30	0.760	7.530	1.7450	1.0700	1.6318
K	30	0.120	1.100	0.2767	0.1950	0.2368
Ca	30	1.450	13.800	3.6190	2.5750	2.9789
Mg	30	0.500	4.730	1.1450	0.7750	1.0195
Cl	30	15.200	145.100	38.1667	28.6500	30.4629
HCO_3	30	10.200	96.700	27.1067	21.4000	20.2481
SO_4	30	0.140	1.410	0.6093	0.3550	0.3277
pH	30	4.3	7.0	5.8367	5.7500	0.6955
EC	30	49.100	580.400	1.3395	85.6500	125.7812
TDS	30	24.800	290.300	67.1500	42.9500	62.8647
Fe	30	3.820	0.170	3.9900	0.8130	0.3750
Mn	30	0.183	0.000	0.1830	0.0395	0.0265
Zn	30	0.700	0.052	0.7500	0.2226	0.1285
Cu	30	0.082	0.000	0.0820	0.0153	0.0000
Cr	30	0.034	0.000	0.0340	0.0038	0.0000
Cd	30	0.031	0.000	0.0310	0.0037	0.0000
Ni	30	0.000	0.000	0.0000	0.0000	0.0000
Pb	30	0.024	0.000	0.0240	0.0025	0.0000
V	30	0.000	0.000	0.000	0.0000	0.0000
THC	30	0.120	0.000	0.120	0.0150	0.0000
P	30	3.520	0.110	3.630	0.7710	0.4550

NH4N	30	0.155	0.004	0.159	0.04500	0.0265
NO_2	30	0.229	0.000	0.229	0.03640	0.0140
NO_3	30	7.480	0.200	7.680	2.0140	1.2500
COD	30	30.100	2.400	32.500	11.8700	9.6500
BOD5	30	4.000	0.000	4.000	1.5000	0.0000
Sal	30	0.240	0.022	0.262	0.06047	0.0390
Col	30	11.200	0.000	11.200	0.9867	0.0000
Turb	30	9.600	0.000	9.600	0.7933	0.0000
TSS	30	15.900	0.000	15.900	1.3067	0.0000
DO	30	2.300	4.900	7.200	6.1867	5.9500

Figure 4 shows the major cations and anions concentration (mg/l) in the groundwater samples of the study.

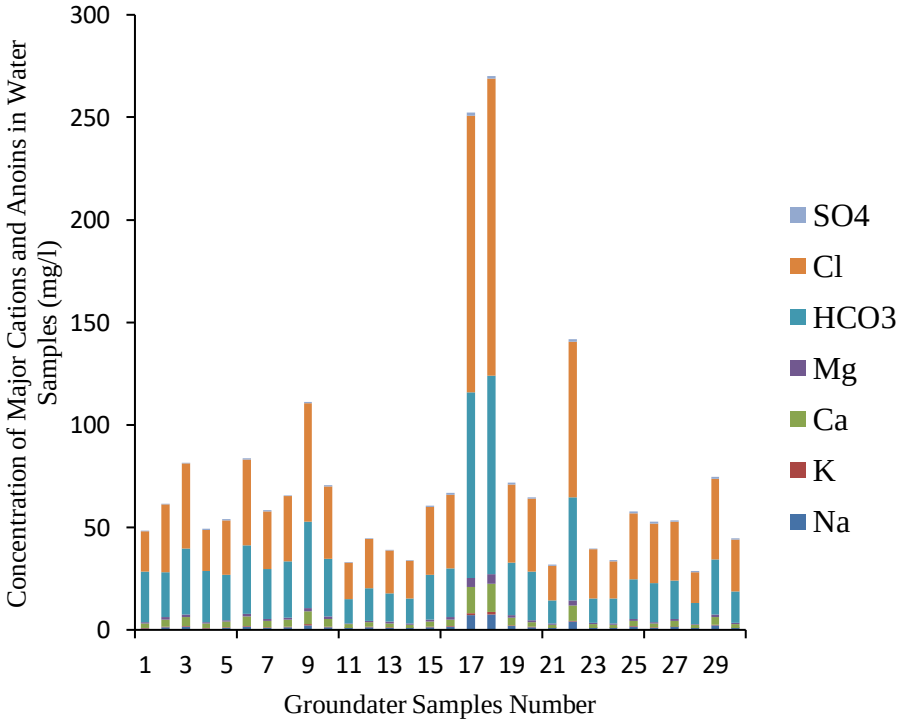

Figure 4: Major cations and anions concentration (mg/l) in the groundwater of the study area

The cation Na^+ has a value of 1.07±0.2121 mg/l, K^+ 0.1950±0.0778 mg/l, Ca^{2+} 2.5750 ±1.2516 mg/l and Mg^{2+} 0.7750± 0.2756 mg/l. The concentration sequence of the major cations of the groundwater in the study area is Ca^{2+}> Na^+>Mg^{2+}>K^+. The anoin Cl^- has a value of 28.6500±4.4548 mg/l, HCO_3^- 21.4000±8.6267 mg/l, SO_4^{2-} 0.3550±0.1485 mg/l and NO_3^- 1.2500±0.9051 mg/l. The concentration sequence of the major anions of the groundwater in the study area is Cl^-> HCO_3^->NO_3^->SO_4^{2-}.

The electrical conductivity (EC) of groundwater in the study area ranges from 49.10 to 580.40 µS/cm. It falls within the permissible limits for NSDWQ and WHO.

The total dissolved solids (TDS) in the groundwater of the study area have an average value of 42.95 mg/l. Table 2 shows the classification of groundwater based on total dissolved solids content (after Freeze and Cherry, 1979).

Table 2: Classification of Groundwater Based on TDS Content (Freeze and Cherry, 1979)

Groundwater	TDS (mg/l)
Freshwater	0 – 1, 000
Brackish water	1, 000–10, 000

Saline water (seawater)	10, 000–100, 000 (35, 000)
Brine water	> 100, 000

*TDS > 2, 000 – 3, 000 mg/l is too salty to drink

The TDS of the groundwater in the study area falls within the range of 0 to 1000 mg/l, thus it is classified as fresh water.

The hydrochemical parameters of the groundwater lie within the permissible limits of the NSDWQ of 2007 and WHO standard of 2004. However, the pH of the water samples has a range of 4.30 to 7.00 and an average value of 5.75 (5.75±0.0707). The iron concentration has a range of 0.17 to 3.99 mg/l and an average value of 0.375 (0.375±0.1061 mg/l). Figure 5 shows the iron concentration map of the study area.

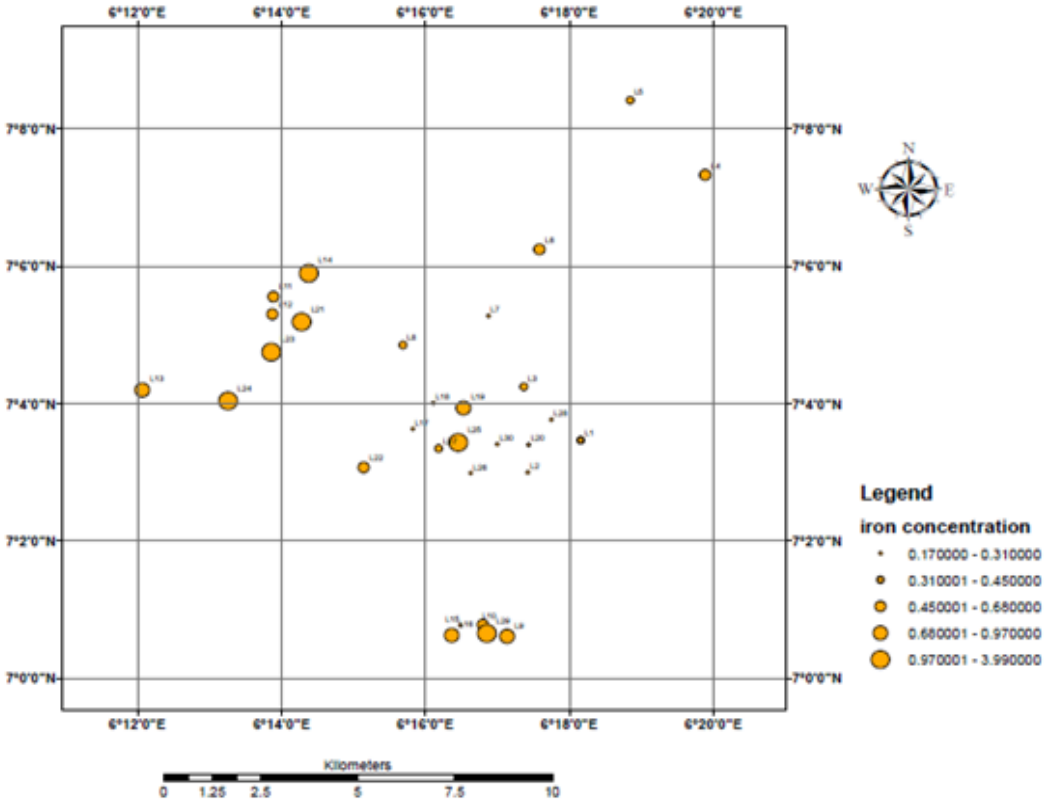

Figure 5: Iron concentration distribution map of the groundwater in the study area

Groundwater hydrogeochemical characterization

The groundwater hydrogeochemical characterization of the study area was done using Stiff (1951) diagram, Schoeller (1962) plot, Gibbs (1970) plot, Piper (1944) diagram and correlation analysis of the physico-chemical parameters of the groundwater.

Stiff diagram shows the composition of water with respect to its major cations and anions in a polygonal shape made from four horizontal axes with zero at the center mark. The cations are

plotted on the left-half from the zero mark and anions on the right-half side from the zero mark of the plot. This represents the hydrochemical pattern and signatures of each groundwater samples. The hydrochemical pattern and signatures are alike with same water chemistry and it shows that the groundwater is from the same aquifer formation. Figure 6 shows the Stiff diagrams of the groundwater samples in the study area.

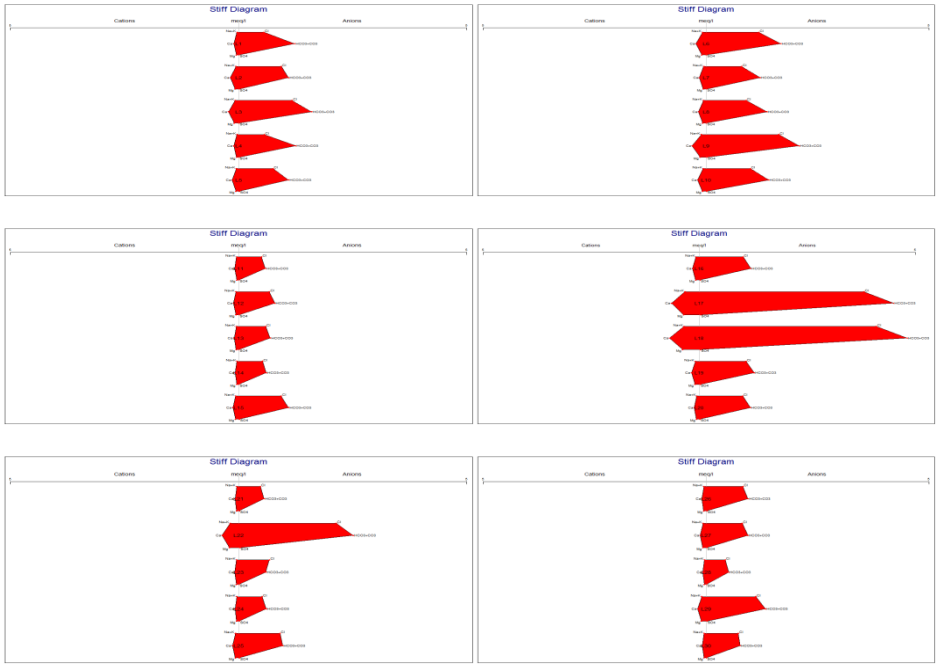

Figure 6: Stiff diagrams of the groundwater samples in the study area

Correlation analysis of the some physico-chemical parameters in the groundwater samples shows that the concentration of cations and anions has a positive relationship with the temperature, pH and electrical conductivity of the water samples. It has a negative relationship with the dissolved oxygen in the water samples. The dissolved oxygen has a positive relationship with the HCO_3^- concentration. It also reveals that the concentration of heavy metals in the groundwater in the study area has a negative relationship with the electrical conductivity, dissolve oxygen, total dissolve solids, temperature, cations and anions concentration. The heavy metals have a positive relationship with the colour, pH, NO_2 and NO_3 concentration of

the groundwater. Table 3 shows correlation of the physico-chemical parameter of the water samples in the study area.

Table 3: Correlation of some physico-chemical parameter of the groundwater in the study area

	TDS	DO	Col.	Temp	pH	EC	Na^+	K^+	Ca^{2+}	Mg^{2+}	HCO_3^-	Cl^-	SO_4^{2-}	NO_2	NO_3	Fe	Mn	Zn	Cu
TDS	1																		
DO	-0.053	1																	
Col.	-0.131	-0.456	1																
Temp	0.439	0.023	-0.076	1															
pH	0.236	-0.233	0.174	0.048	1														
EC	1.000	-0.055	-0.129	0.439	0.238	1													
Na^+	0.992	-0.063	-0.136	0.471	0.190	0.992	1												
K^+	0.970	-0.038	-0.172	0.472	0.106	0.969	0.990	1											
Ca^{2+}	0.949	-0.019	-0.191	0.471	0.056	0.948	0.976	0.997	1										
Mg^{2+}	0.981	-0.043	-0.160	0.472	0.133	0.981	0.996	0.998	0.991	1									
HCO_3^-	0.944	0.043	-0.224	0.500	0.034	0.943	0.965	0.986	0.990	0.981	1								
Cl^-	0.980	-0.018	-0.168	0.447	0.117	0.979	0.990	0.995	0.990	0.996	0.984	1							
SO_4^{2-}	0.806	-0.182	0.091	0.305	0.211	0.807	0.781	0.743	0.714	0.758	0.715	0.762	1						
NO_2	-0.241	-0.312	0.809	-0.335	0.240	-0.239	-0.247	-0.281	-0.298	-0.267	-0.333	-0.281	-0.132	1					
NO_3	-0.040	-0.566	0.675	-0.195	0.038	-0.038	-0.045	-0.079	-0.097	-0.068	-0.150	-0.070	0.129	0.606	1				
Fe	-0.222	-0.455	0.720	-0.413	0.206	-0.220	-0.220	-0.256	-0.275	-0.242	-0.318	-0.273	-0.072	0.884	0.559	1			
Mn	-0.141	-0.377	0.661	-0.366	0.197	-0.139	-0.143	-0.183	-0.205	-0.167	-0.247	-0.185	-0.032	0.752	0.711	0.809	1		
Zn	-0.161	-0.383	0.745	-0.349	0.308	-0.159	-0.176	-0.231	-0.259	-0.209	-0.304	-0.233	-0.029	0.884	0.706	0.877	0.888	1	
Cu	-0.196	-0.455	0.678	-0.367	0.251	-0.195	-0.204	-0.237	-0.255	-0.225	-0.287	-0.237	-0.043	0.822	0.760	0.842	0.877	0.872	1

Schoeller plot is a semi-logarithm diagram representing the water chemistry and concentration in meq/l of major ion in the water. A Schoeller plot of the groundwater shown in Figure 7 reveals that the predominate cations in the groundwater in the study area is Ca^+ and Na^+ while the predominate anion are Cl^- and HCO_3^-.

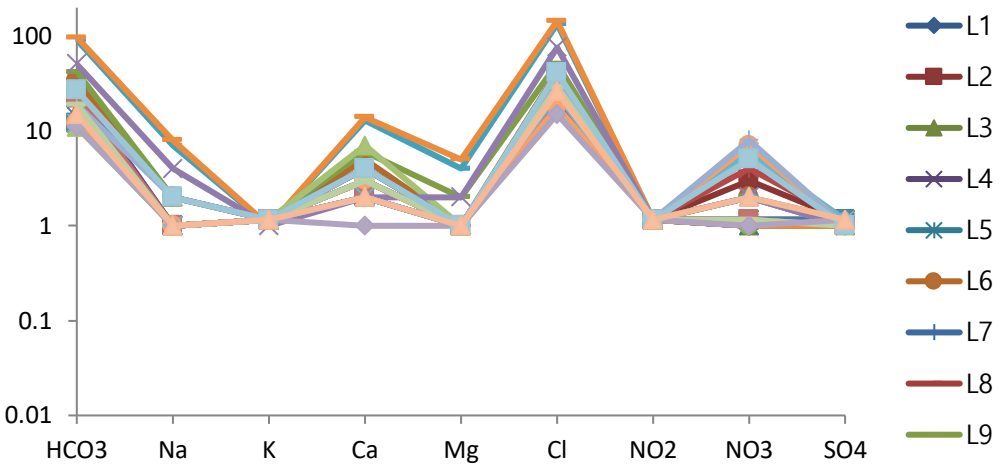

Figure 7: Schoeller plot of groundwater sample in the study area

Gibbs plot reveals the major natural mechanism controlling the water chemistry. It is a plot of TDS versus the weight ratio of $(Na^+ + K^+)/(Na^+ + K^+ + Ca^+)$. The Gibbs plot of the groundwater is shown in Figure 8. It reveals that the major natural mechanism controlling the groundwater chemistry in the study area is rock-water interaction, with little influence of precipitation on the groundwater chemistry.

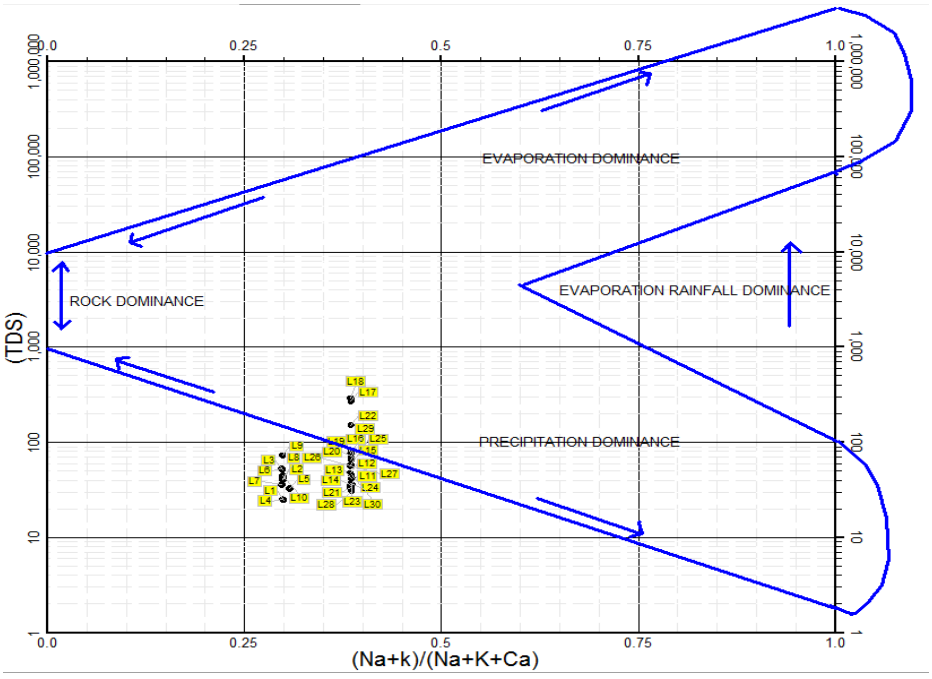

Figure 8: Gibbs plot of groundwater sample in the study area

Piper diagram is a graphical representation of two trilinear diagrams representing the major ion cations (Na^+, K^+, Ca^{2+} and Mg^{2+}) and anions (Cl^-, CO_3^{2-}, HCO_3^- and SO_4^{2-}) in water and a centered diamond shaped diagram. The plots represent percentages of the total cation and/or anion concentrations, such that the water with very different total ionic concentrations can occupy the same position in the diagrams. The trilinear plots requires three paramters each, therefore the cations are reduced from four to three by grouping Na^+ and K^+, while the anions are reduced by grouping CO_3^{2-} and HCO_3^-. The plot on the diagram is projected on a straight line within the central diamond field, to represent mixing of groundwaters between two end-member solutions. This identify the hydrochemical facies of the groundwater. Figure 9 shows a Piper diagram of the groundwater in the study area. This indicates that the groundwater in the study area is of calcium bicarbonate (Ca-HCO_3) hydrochemical facies.

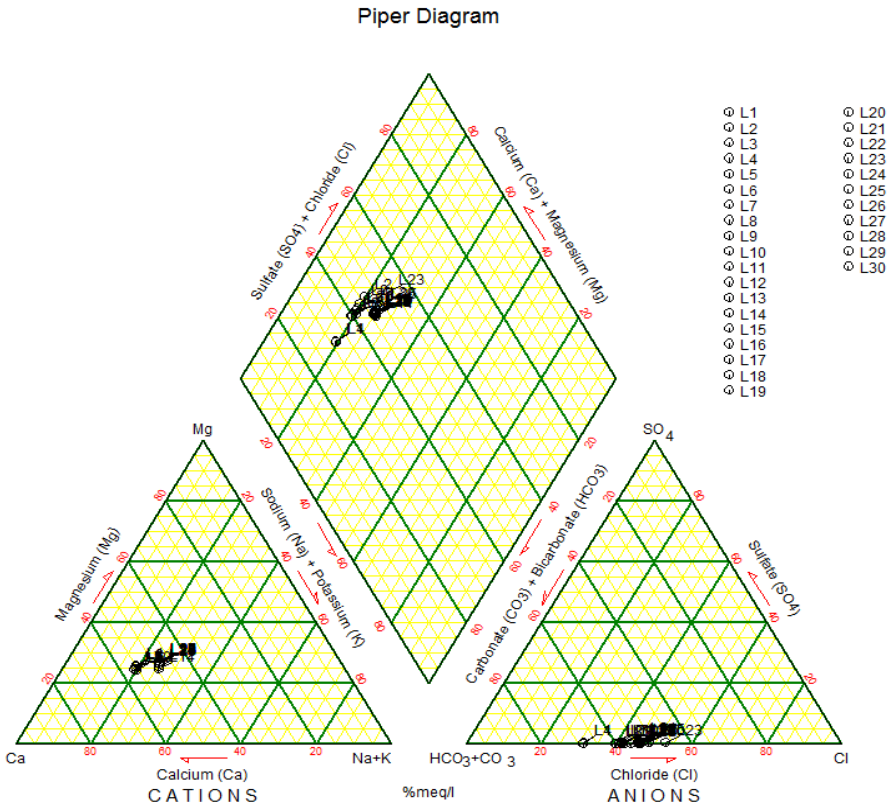

Figure 9: Piper diagram classifying the water samples in the study area

5. Conclusion and Recommendations

Conclusion

The area is widely covered by ferruginized sandstone, sandstone and clayey sand, with the Ajali Sandstone as the aquifer formation. The hydrochemical parameters of the groundwater in the study area falls within the permissible limits of the NSDWQ of 2007 and WHO standard of 2004, with the exception of pH and iron concentration. The groundwater in the study area has a pH value of 5.75±0.0707 indicating acidic water. The iron concentration has a value of 0.375±0.1061 mg/l, which is above the permissible limit. The high concentration of iron in the groundwater has a secondary health hazard to human. It is probably responsible for the high cases of health challenges that comprises of skin wrinkles, damage of health skin cells, water borne diseases, fatigue, joints pain and weight loss. The ferruginized sandstone in the study area is suggested to be responsible for observed colour of groundwater in some location. Also, the groundwater in the study area is from the same aquiferous formation as shown by the Stiff plot, and has a Calcium Bicarbonate (Ca-HCO_3) hydrochemical facies of the groundwater.

Recommendations

A periodic evaluation and assessment of the groundwater in the study area should be carried out, for effective monitoring and management of its quality. Also the host communities should be sensitized on the health challenges of low pH value and high iron concentration of the groundwater in the study area and the need for water treatment before consumption.

References

Ajibade, A. C. (1983). Proterozoic Crustal Development in the Pan - African Regime of Nigeria. In Kogbe, C. A. (Ed.). Geology of Nigeria. Jos, Nigeria, Rock View Limited; 57 - 63.

Amadi, A. N., Olasehinde, P. I., Yisa, J., Okosun, E. A., Nwankwoala, H. O., & Alkali, Y. B. (2012). Geostatistical assessment of groundwater quality from coastal aquifer of Eastern Niger Delta, Nigeria. *International Journal of Geosciences*, 2(3), 51 - 59.

Freeze, R. R. & Cherry, J. A. (1979). *Groundwater*. Englewood Cliffs, New Jersey, Prentice-Hall.

Gibbs, R. J. (1970). Mechanisms controlling world water chemistry. *Science* 170, 1088 - 1090.

Ibrahim, S. I., & Ajibade, L.T. (2012). Assessment of Water Quality and Domestic Uses in Medium-Sized Towns of Niger State, Nigeria. *Transnational Journal of Science and Technology,* 2, 5 - 15.

Macaulay, O. O. (2008). *Hydrogeological Pratices; with application to Nigerian Groundwater Terrains*, Ilorin: Pios Publications.

Matthew, E. O. (2002). *Groundwater Supply and Development in Nigeria.* 2nd edition. Jos: Mecon Geology and Engineering Service Limited.

Nigerian Standard for Drinking Water Quality (2007). Nigerian Industrial Standard, NIS: 554, 1 - 14.

Office of Survey General of Federation (1993). Topographic Map of Auchi. Abuja - Nigeria.

Okogbue, C. O. (2005). Hydrocarbon Potential of the Anambra Basin: Geology, Geochemistry and Geochemistry Perspectives, Proceeding of the First Seminar Organized by the Petroleum Technology Development Fund (PTDF), University of Nigeria, Nsukka.

Piper, A. M. (1944). The Interpretation of chemical water analysis by means of patterns. Journal of Petroleum Technology, 3(10), 15 - 17.

Reyment, R. A.(1965). Aspects of the Geology of Nigeria: The Stratigraphy of the Cretaceous and Cenozoic deposits. In: Nwajide, C. S., (Ed.). *Geology of Nigeria's Sedimentary Basins*, (pp. 46). Lagos, CSS Press.

Schoeller, H.(1962). *Les EauxSouterraines*. Mason et Cie, Paris, France.

Stiff, H. A. (1951). A Graphic Procedure in the Geochemical Interpretation of water analyses. Transactions of American Geophysical Union, 2, 914 - 923.

Sule T. U. N., Umoru, A.T. & Oyathelemeh, E. (2014). Lithological Examination and Resistivity Trend Pattern Investigation of Groundwater Research in PhilipaIdogho Campus, Auchi Polytechnic, Auchi. *Journal of Environment and Earth Science*s, 2(4), 57 - 65.

World Health Organization (WHO, 2004). Guideline for drinking water quality. 4th edition. World Health Organization. Geneva, Switzerland.

Comparative Study of Sustainability of Resettlement Scheme In Part of Niger State Nigeria

Yisa Moses Kodan

Center for Human Settlements and Urban Development
Federal University of Technology, Minna

Abstract

The Sustainability of resettlement has one underlying goal of reinstating affected inhabitants quickly into their old lives and if possible more improved and lasting situations. Muregi and Akare has suffered floods for decades; the three (3) most recent ones are in 2008, 2009 and 2012. This caused displacement of people from their usual dwelling places resulting into varying impacts on infrastructure, crops, health, education, environment as well as damage to property. It seems that the resettlement programme is affecting the environment negatively because it iseasily observed that deforestation, overgrazing of lands are problems in Nigeria particularly in the resettlement areas which recur from time to time. This paper examine the people's perception on the sustainability of this resettlement schemesin Niger State. The study is empirical in nature and intends to analysis the sustainability of resettlement. Structural questionnaires were used, data collected were subjected to statistical analysis. Findings shows that the scheme has benefited both the resettlers and host communities in Muregi as compared to Akare by providing access to basic infrastructure and social services such as roads, schools, health services, safe drinking water and market access to their products.

Key words: Sustainability, Resettlements and Scheme

Introduction

Sustainability is not only one of the principles of engagement in development planning process but also a challenge in most developing countries. In planning circles the notion of development is often equated to sustainable development, which is simply seen as development for the present without comprising that of the future generation (Bruntland, 2007). This notion has guided the development of projects worldwide including large dams and the resettlement of its affected people. In Nigeria for instance, issues of sustainability has become an important language among development practitioners and a critical ingredient in planning and designing of development projects.

The Sustainability of resettlement has one underlying goal of reinstating affected inhabitants quickly into their old lives (cultural, economic and physical aspects), and if possible more improved and lasting situations. Achieving this goal comes with implicit and explicit challenges that arise because of land acquisition, compensation and integrating resettles into their new home through community participation. In the process, housing, community

structures and systems, social networks, and social services can be disrupted (Raschid-Sally.et al, 2008).

Resettlement scheme may be defined as a planned project or programme involving the transfer of people most probably through selection and control from one region to another. When resettlement schemes are considered, governments in developing countries, in general, and in Africa, in particular, make decisions as to when, where and how reestablishment should take place.

Resettlement of people can either be forced or voluntary. Disasters, such as wars, floods and earthquakes, among others, are some of the reasons that could force Man to move out of an area that he is familiar with, to resettle in an entirely new area. Government acquisition of land for development projects is another cause. All over the world resettlement programs abound. Nigeria is no exception to these phenomena. Most programs involve Government decisions, which leave the affected people with very little room to manoeuvre (Ajibola, 2009).

Although resettlement is increasingly seen in development theory as an important livelihood strategy for poor people (Tan 2008), implementing state-sponsored resettlement schemes and bringing about livelihood change is a complex process. Experience in Nigeria, elsewhere in Africa, and the world over, show the fact that things can often go very wrong in resettlement operations unless managed with meticulous care (Abbute 2003; De Wet 2004). Any resettlement programme involving the movement of hundreds of thousands of people over large distances has many risks and dangers attached to it. Even if in principle it is a good idea to move people from a less fertile area to new productive areas, the question of how far in practice is a planned resettlement programme actually a good policy needs to be answered.

The study areashas suffered floods for decades; the three (3) most recent ones are in 2008, 2009 and 2012. This caused displacement of people from their usual dwelling places resulting into varying impacts on infrastructure, crops, health, education, environment as well as damage to property (NSEMA, Assessment of Floods Report, 2013). The general problem of the communities is the frequent flood disaster that occurs yearly and it has being a serious problem which claims a lot of lives and properties. A lot of money has being sunk in developing a resettlement schemes called New Bussa, New Gbajigbo, New Muregi and New Akare by providing infrastructure facilities, yet the community are not ready to move away from the disaster prone area. Some noticeable challenges of resettlement scheme are the cost required for implementation of full resettlement programme could exceed the financial capacity of the State or may be the planning process involved in the resettlement was not properly managed

and implemented. Some other outstanding problems that affect the resettlement are the absence of social infrastructure in the settlement sites. For example in the absence of schools, health facilities, motorable roads, communication networks, etc., could make the life of resettles burdensome. Problems associated with these and similar other factors could create a challenge not only on the target group but also on the country's economy, host communities and the natural environment.

Many scholars (such as Abiy 2004; Belay 2004:24; Hammond 2008) argue that though the resettlement programme is expected to be implemented voluntarily in consultation with the host community and careful preparation (FDRE 2003), in practice these principles are not appropriately implemented. For them, many resettlers were physically forced to move, and the planning and execution of the programme was hastily and poorly done without the consultation of the host community.

Though there are studies on resettlement planning and implementation, to what extent the resettlers developed assets (physical, social, financial, human and natural) and secured their livelihoods is not known. It seems that the resettlement programme is affecting the environment negatively because it is easily observed that deforestation, overgrazing of lands, etc. are problems in Nigeria particularly in the resettlement areas which recur from time to time. Therefore, this paper will examine the people's perception on the sustainability of this resettlement schemein Niger State.

Study area

The study area is located between longitude 4^0 20' E to 4^0 50' E and latitude $9^0$51' N to 10^0 57' N in northern Nigeria. The study area cut across Mokwa and Wushishi local government area in Niger State. It is located along River Niger and River Kaduna Confluence. Akare is located at about 7km from Wushishi town in Wushishi local government area of Niger state, on the south eastern direction. The area lies between latitude $9^0$54'N to $9^0$72'N and longitude 6^0 38'E to 6^0 51'E of the equator.

Resettlement: Concepts and Theories

Resettlement is a programme that many governments in developing countries have been implementing; however, with mixed results. Resettlement as a policy action or intervention strategy differs from one case to another depending on the objectives of the programme. Most resettlement programmes have the objectives, firstly of poverty reduction, mainly targeting the poor communities especially the landless and, secondly, regional

development targeting those with own resources to invest in agricultural activities. It is quite difficult to define resettlement without referring to other related terms that describe population movement such as migration, colonisation and transmigration. "Resettlement, colonisation, or transmigration all refer to the phenomenon of population redistribution, either planned or spontaneous" (Rahmato 2003:1). According to Rahmato, different countries give emphasis to different terms, for instance, 'transmigration' implying government sponsored programmes in Indonesia, 'colonisation' referring to occupation of uncultivated land in Latin America, and 'resettlement' seems to be the more appropriate expression in the Ethiopian context that implies moving people to new locations. For Rahmato, resettlement is the phenomenon of population redistribution either in a planned or spontaneous manner: relocating people in areas other than their own for the purpose of converting "transient populations- nomadic pastoralists, transhumant or shifting cultivators- to a new way of life, based on sedentary forms of agricultural production" (Rahmato 2003: 2). According to Abbute (2002:25), "resettlement involves the movement of communities from one environment to the other, and changes or modifies the physical and social environment in which settlers find themselves in and adapt to". Piguet and Dechassa (2004:134) also define resettlement as a "planned or spontaneous redistribution of phenomena of population". According to Woube (2005:19):

Resettlement is defined as the process by which individuals or a group of people leave spontaneously or un-spontaneously their original settlement sites to resettle in new areas where they can begin new trends of life by adapting themselves to the biophysical, social and administrative systems of the new environment.

All of the above definitions emphasise that in the process of resettlement settlers could move voluntarily or involuntarily from their areas of origin to the new resettlement sites and this phenomenon is not without consequences. To Woube (2005:19), in this spontaneous or planned movement from their original settlement to new sites, people have to adapt to the biophysical, social and administrative system of the new environment. According to Woube (2005:25-27), during the relocation or adaptation process, resettlers may face physical and mental stress and different kinds of impoverishment risks. In order to minimise these risks, resettlement programmes, planned or spontaneous, should be planned, implemented and evaluated appropriately. Although this study mainly targets the planned resettlement programme, it is very difficult to demarcate the difference between planned and spontaneous resettlement schemes.

The Rationale behind Resettlement Schemes

Worldwide experience suggests that resettlement, caused by development projects, conflicts or other socio-economic, political and environmental factors, is a risky process that often leads to impoverishment and rarely results in sustainable development (Brown, Magee and Xu 2008; Cernea and McDowell 2000; Hwang 2010; Ohta and Gebre 2005). Other studies have shown that living conditions and livelihoods of resettled people improved after resettlement (Agnes, Solle, Said and Fujikura 2009; Manatunge, Takesada, Miyata, and Herath 2009, Nakayama, Gunawan, Yoshida, and Asaeda 1999). Different countries undertake resettlement programmes for different purposes and objectives depending on their social and political situations. These include poverty reduction, the improvement of social services and restoring the income and livelihood of affected people (Cernea 2008:89; Cernea 2009a:52; Pankhurst 2009:13-15).

From the Brazilian experience, one can learn that resettlement is helpful in creating new growth centres and reducing regional imbalances. These include creating conditions to integrate regions into the market economy, establishing conditions for effective agricultural transformation of the semi-arid and arid regions, redirecting labour migration to agricultural areas in order to minimise migration to the urban areas, and stimulating a process of industrialisation (Helena and Heneriques 1988:322).

According to Oberai (1992:16), the principal objective of the resettlement programme in Malaysia was “to develop land for the landless and the unemployed” in order to assist the rural poor such as those with small and fragmented holdings. In Malaysia, “land development and settlement constitutes one of the most important instruments of the regional development programme”. Land development and settlement were reported to have increased rural production, raised rural income and reduce rural-urban migration in Malaysia (Obeari 1992:79).

The Somalian experience also indicates that the objectives of the resettlement programme were to 1) attain redistribution of Somalia’s population so as to increase productive rural enterprise, and 2) provide social services to Somalia’s largely nomadic population (Ragsdale and Ali 1988:205). Kassahun (2003:3), basing his argument on the Ethiopian experience, also postulates that resettlement is “a way out of pressing pressures caused by food shortages, land fragmentation and congestion faced by producers, rampant unemployment, marginality of land and decline in productivity in areas under cultivation.” Pankhurst and Piguet (2009:9)

Voluntary vs Involuntary Resettlement

Under the planned resettlement schemes there are both voluntary and involuntary resettlement (Woube 2005:31). According to Woube, a voluntary resettlement scheme is a process whereby people move to resettlement sites willingly. Such schemes manifest a more or less sound resettlement planning methodology through which the resettlers are well informed about the new resettlement sites as well as when and how they will be resettled. Involuntary resettlement, however, takes place when an external agent imposes it on people in a planned and controlled manner due to external circumstances that force them to do so (World Bank 2004:4).

Yntiso (2004:106) recognises that the distinction of resettlement schemes as voluntary and involuntary is more theoretical than empirical. Yntiso (2009:127) argues that these two distinct forms of displacement fail to highlight the specific conditions of resettlement. In an attempt to tackle this limitation, Yntiso (2004:106 – 107; 2009:127) has proposed a modified and more practical conceptual scheme, which identifies four major types of resettlement: voluntary, inducedvoluntary, involuntary or forced, and compulsory-voluntary movements. This classification is based on the nature of willingness to move and the causes of displacement.

Much has been written about the consequences of involuntary resettlement which involves forceful displacement or dispossession of people for the purpose of developmental projects (Cernea and McDowell 2000; De Wet 2006; Muggah 2008; Oliver-Smith 2005; Scudder 2005). These studies have explored reasons, types and processes of people relocating and the mechanisms of how to improve the livelihoods of resettlers. In turn, they have come up with useful concepts, analytical approaches and models that have broadened our knowledge and understanding of relocation as a social phenomenon as a whole. The focus of this research, however, is on planned voluntary resettlement, where an agency or institution (mostly governments) secures land and recruits people to settle on this land and engage in farming activities. Most planned voluntary resettlement programmes aim to achieve either both or one of the two fundamental objectives: poverty reduction and promotion of regional economic growth through agricultural activities (Zhibin 2003:2). However, it should be borne in mind that most resettlement programmes are designed to meet certain political benchmarks and not poverty reduction.

According to Morris and Roth (2010:5), “resettlement of the old kind that is forced, harmful, and unjust is rejected, but resettlement of a new kind that is based on prior informed consent is

still possible". While the shift to a voluntary basis is a welcome evolution in resettlement practices, onthe-ground realities may substantially differ from expectations.

According to FDRE (2003b:1 – 3), any development initiative planned for implementation in a settlement area should adhere to the main principles of voluntary and informed consultation, the objective of improving life sustainably, environmental sustainability, cooperation, self-reliance, cost sharing, community- led, transparency, responsibility, etc., starting at its inception and going through to its planning and implementation stages.

a) Voluntary and Informed Consultation

The implementation of a settlement programme should be planned through a consultation process involving both settlers and receiving communities. There should be transparent, detailed and all-inclusive discussions among the settlers, receiving communities and others concerned. The participation of all concerned in the planning, implementation and monitoring and control of the economic and social development activities helps maximise possible options as well as choose the most effective among those options. For this participation to be effective, all sides have to obtain in advance accurate information and analysis concerning the settlers, the recipient communities and the status of the natural resources of the settlement areas.

b) **The Objective of Improving Life Sustainably**

The action taken in a settlement area should free citizens from dependency on aid caused by human induced environmental deterioration or by drought so that they may maintain themselves sustainably through their own efforts. This makes it essential to implement plans that spring from the communities themselves and are in harmony with the ecosystem dynamics as well as being consistent with the national vision of development. Therefore, all plans should incorporate the requisite environmental considerations. The action for environmental protection should be planned and implemented in such a way as to create economic capacity.

c) Environmental Sustainability

The economic and social development activities carried out in a settlement area should be based on a coherent environmental management plan that enhances the quality of the environment and maximises its productivity sustainably. Special care and protection must

be given to fragile natural and human made environments that can be easily damaged or destroyed and cannot be easily replaced. Therefore, consultations should be carried out on the environmental, economic, social and cultural impacts of any activity aimed at implementing the settlement programme.

d) Cooperation, Self-Reliance and Cost-Sharing

The implementation of a settlement programme should involve the settlers, the receiving local community, as well as governmental and other actors, in cooperative and mutually supportive interaction. The settlement programme should foster self-reliance and eliminate the spirit of dependency**.**

e) Community-led Administration, Transparency and Responsibility

The implementation of settlement activities and the sustainability of development plans should be clearly visible to both the settlers and the receiving local community. This can be effective if there is a community-led administration which is transparent and responsive.

f) Improvement and Enrichment through Action and Experience

The settlement programme should be enriched and improved, using knowledge gained through implementation, monitoring and control. The implementation should vary according to what the diversity in time and space calls for. For this reason, resettlement should not take place in one go but should rather be initiated by family or local community representatives and, upon evaluation and realisation of its effectiveness, the accumulated positive experience can be used to develop a strategy for a more extensive implementation.

Finally an impact assessment needs to be carried out on the planned activities aimed at implementing the settlement programme in order to predict their positive and negative effects on the ecological, socio-economic conditions so as to strengthen the positive and, when possible, avoid (or at least minimise) the negative consequences. An impact statement is then prepared, based on the assessment as to whether that particular resettlement programme is bringing about sustainable development or not.

Resettlement and Livelihoods: Linkages

Pankhurst (2009:13) notes that ‘despite all the recent expansion in research, there is much that we still do not know about resettlement, especially about the behavioural response of

various populations and subgroups, and about their own initiatives for coping and reconstruction'. At this juncture a theoretical synergy is required to explain resettlers' initiatives, i.e. the role of the people in coping with displacement as a response to foreseen risks. The sustainable livelihood approach developed beyond the concern for development induced displacement may fill the gap (Scoones 1998:4). The presentation of livelihood strategies and the attention the framework renders to societal institutions make it ideal for the topic under study. McDowell (2002:11) calls for such a theoretical blend and the need to ascertain how people respond to the risk of processes of impoverishment, and the role of institutions, associations and other forms of relationships in mediating their access to and control over the resources necessary to rebuild livelihoods.

The livelihood framework has five key features, according to Chimhowu and Hulme (2006:729) that make it especially relevant for studying resettlement. Firstly, it views resettled households as making a living in a variety of ways of which farming may be just one. Secondly, livelihood approaches emphasise the need to see land as just one among several assets/capitals required to make a living. Thirdly, livelihood approaches place the interaction of the various capitals within a broader policy environment. Fourthly, the framework allows us to investigate livelihood dynamics in a given geographical and historical context. Livelihoods are not static but change in response to various internal and external stimuli. Fifthly, the focus on risk and vulnerability is appropriate for resettled households in frontier regions.

Materials and Methods

This research is empirical in nature and intends to analysis the sustainability of resettlement in Muregi and Akare in Niger State. It was designed to collect information from all parameters that is needed to solve the research problems. The research makes use of both theoretical and investigative method for collection of data,also data was collect from residents of Bussa, Gbajigbo, Muregi and Akare on reasons for locating in such area, the infrastructure available, and its adequacy and otherwise. This provide opportunity to assess the coping strategies adopted and planning implication to sustainable resettlement in Niger State and Nigeria in general.

Data Sources

In this study, both secondary and primary sources of data will be use to carry out a comparative analysis of sustainability of resettlement scheme in Muregi and Akare, to assess and compare

the various infrastructure available in area and examine the resettled households assests vital to realise resettles sustainable livelihood outcome. Primary sources include a household survey, key informants' interview and observations. The major primary data will be collected through *survey of* settler households in Muregi and Akare to solicit a wide variety of information about their assets (physical, social, financial, human and natural), their livelihood strategies and the risks settlers faced, livelihood outcomes, etc. A key informants' interview will be conducted by the researcher Moreover, *observations* will be employed by the researcher to gain a deeper understanding of the areas. Observations will be employed to obtain a better grasp on processes of livelihood generation, the type, nature, state and use of household assets, livelihood strategies and outcomes.

Data Analysis

The analysis will follow the framework reviewed. The framework focused on the context of resettlement, risks of relocation, livelihood assets of settlers, institutional influences in access to livelihood assets, livelihood strategies and livelihood outcomes. The analysis will be done, based on the before and after situation as well as on spatial comparison. The quantitative data collected through questionnaire will be prepared by cleaning, coding and entering them into a computer. These data will be then analysed with the help of the Statistical Package for Social Science. Descriptive and inferential statistical analysis will be use. Firstly, descriptive statistical procedures including cross tabulations, frequency distributions, percentages, arithmetic means, line and bar graphs, indexes, etc. will be used to provide comparisons between the two areas' resettled households livelihoods and their perceptions related to the resettlement programme.

Results

Resettlers Knowledge about Resettlement

Information exchange is an important tool in creating awareness that enables the participants to make a decision to resettle. The current voluntary government sponsored resettlement programme document highlights the importance of information exchange with people in sending districts and consultation with the host community to enable participants to make their own choices regarding the program. Table 1 shows the extent to which information was shared with participants in the resettlement programme in the study areas.

Table 1: Information exchange about the programme

Were you well informed about resettlement?	Muregi (n=130)		Akare (n=120)	
	f	%	f	%
No	2	2	0	0
Yes	128	98	120	100
If Yes, source of information?				
Media	1	1	7	6
Government Officials	124	97	117	98
Previous Settlers	4	3	8	7
Others	2	2	-	-
What was your reaction to the programme?				
Accepted it	127	97.7	108	90
Rejected it	2	1.53	7	6
Indifferent	1	0.77	5	4

As depicted in Table 1, almost all of the respondents were well informed about the programme and most of the resettlers obtained information from government officials at different levels. Most of them also accepted the invitation to resettle.

Resettlers Perception towards Resettlement Process

Resettlers were asked whether the resettlement process was voluntary or not. As depicted in Table 2, more than 98 percent of the resettled households confirmed that the resettlement process was voluntary.

Table 2 Perception of resettlers about the relocation process

Variables	Muregi (n=130)		Akare (n=120)	
	f	%	f	%
How did you come to this settlement sites?				

Voluntary	128	98.5	117	97.5
Involuntary	0	0	1	0.8
Self-organised	2	1.5	2	1.7
Did your family members come with you?				
No	34	26	55	46
Yes	96	74	65	54
How did you assess the site selection of the resettlement areas?				
Highly inconvenient	2	1.5	2	1.7
Inconvenient	26	20	16	13.3
Don't Know	7	5.4	3	2.5
Moderately convenient	94	72.3	91	75.8
Highly convenient	1	0.8	8	6.7
Were you happy about leaving your former home village?				
No	18	14	16	13
Yes	112	86	104	87

The resettled households' perspective on what it meant when it was stated that the moving process was voluntary was not just the absence of physical force; issues like how much information one had before making a decision, and having an option to return if one did not like the new place were also considered as aspects that made this new resettlement programme voluntary in nature. These aspects were issues that gave the resettlers more choice and more options, and in relation to this the programme leant more to the voluntary side than to the other way.

Perceptions about the Push-Pull Factors

Respondents were asked to mention the push factors that forced them to resettle in order of importance. According to the survey data, the main push factors for the resettled

households in the two districts were related to shortage of farm land, landlessness, food insecurity, shortage of rainfall, land degradation, among others.

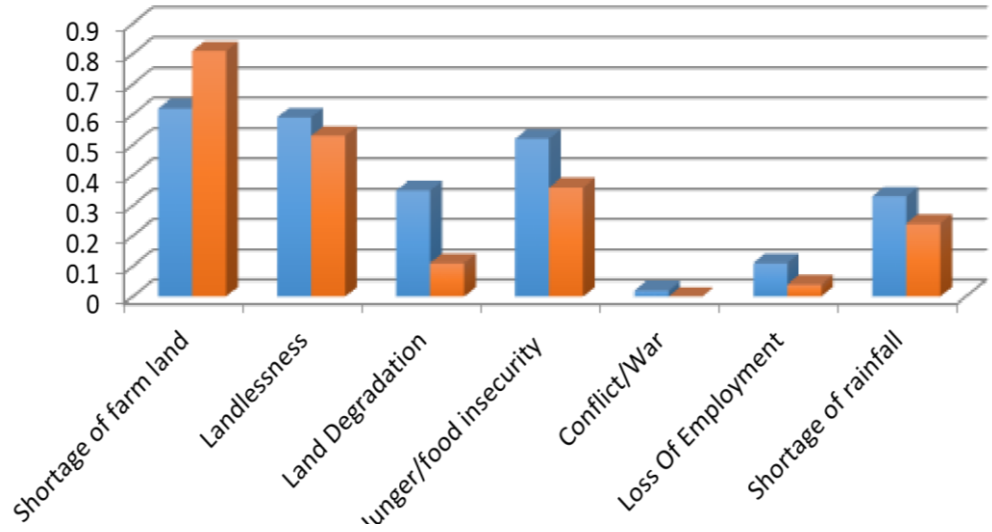

Figure 2: Push factors affecting households to resettle

More than 80 percent of the resettlers in Akare and 62 percent of them in Muregi were forced to relocate due to shortage of farm land at their places of origin. Since there was not enough arable land to match the population growth, this led to land fragmentation and low productivity. Most of these households had farmland, but they perceived it as inadequate to improve or even sustain the households' livelihood.

The respondents were also asked to what extent the reality met their expectations. Accordingly, more than 75 percent in Muregi and 68 percent in Akare found the reality on the ground below their expectations. The reason was that most of the promises were not implemented in practice.

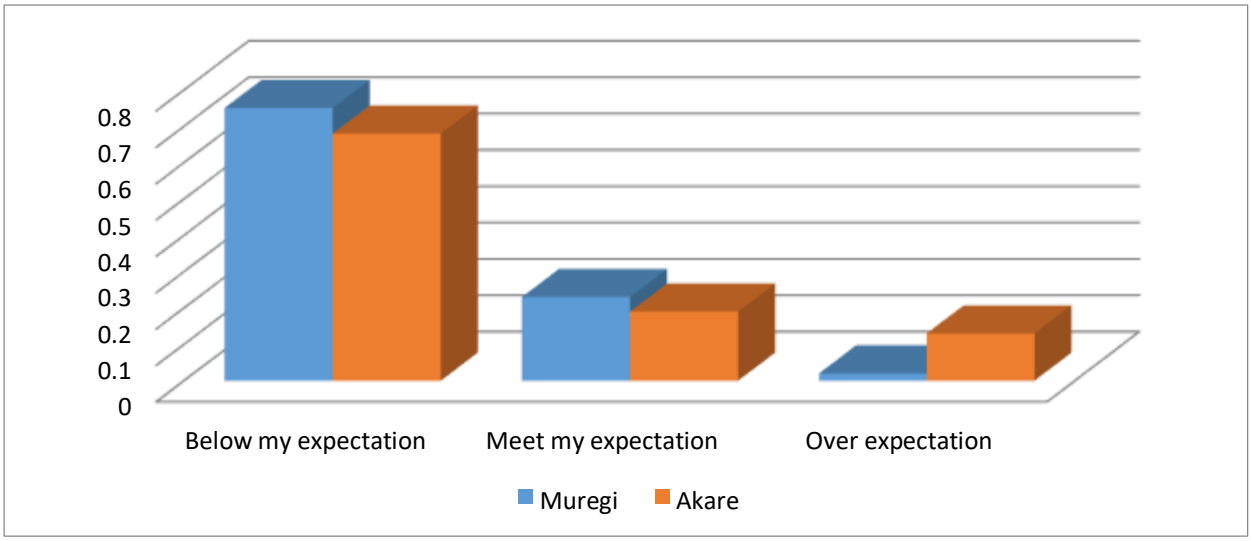

Figure 2: Reality as compared to expectation/promises

Table 3: Perceptions regarding occurrence of conflicts

Items	Muregi (n=130)		Akare (n=120)	
	f	%	f	%
Conflict with the host community or other settlers?				
No	88	68	75	63
Yes	42	32	45	38
If Yes, reasons for conflict?				
Religion	-	-	2	4
Competition for land	20	48	25	56
Forest destruction	6	14	-	-
Animal feed	8	19	10	22
Language	-	-	2	4
Others	1	2	6	13
If yes, how was it solved?				
by community elders	32	76	21	47

by village social courts	4	10	10	22
by district court	4	10	8	18
by religion head	-	-	2	4
Others	3	7	3	7

As depicted in Table 3, a significant number of respondents (32 percent in Muregi and 38 percent in Akare) reported that there had been conflict during the last one year. The main reasons for conflict occurrence in both districts were competition for land, followed by animal feed. The data also showed that conflict occurrence due to religion and language/ethnicity was very minimal among respondents in the study areas.

Respondents were also asked how the conflicts had been solved when they occurred. In both areas, the majority of conflicts were solved by community elders. Some of the conflicts related to land title and ownership issues were also solved by courts at district and village levels.

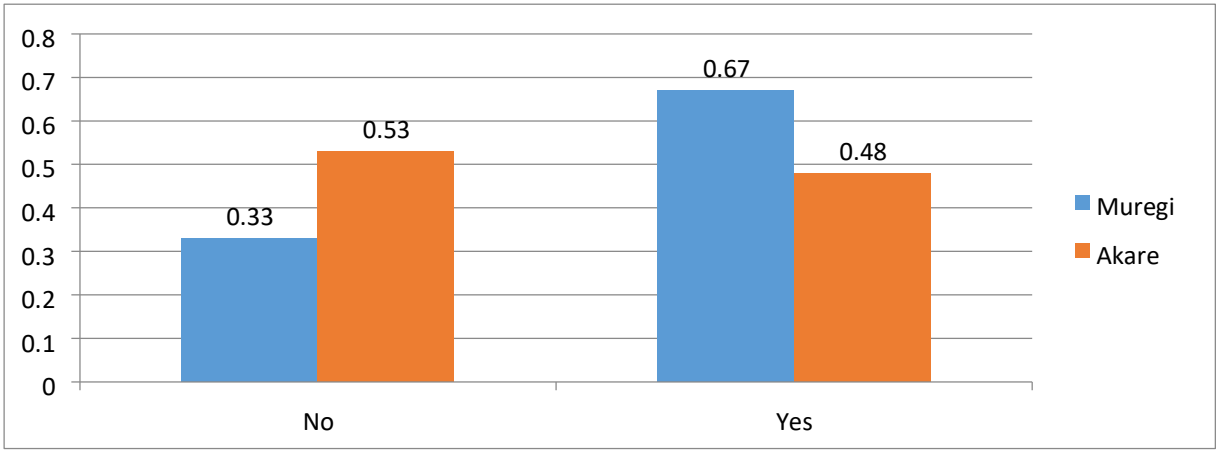

Figure 3: Have your problems been solved after resettlement?

Resettlers were also asked whether their problems were solved after resettlement or not. More than 33 percent of respondents in Muregi and more than 53 percent in Akare confirmed that their problems were not solved. In both districts there was a general perception that the information they had received in their home areas about the resettlement programme was different from the reality.

Conclusion

This study analysed the resettlement in Muregi and Akare resettlementscheme in Niger State to the implementation processes and outcomes of the new resettlement programme. This study concludes that the results are mixed and challenges the generic representation of the resettlement scheme as a failure or a success. Despite the many challenges the government experienced in this resettlement programme, there are evidences that clearly shows the successes of the programme. The planned state-led resettlement programme had brought relief to households facing food insecurity, raise the assets and incomes of the poor resettled households at least in the short run. The programme has benefited both the resettlers and host communities in Muregi as compared to Akare by providing access to basic infrastructure and social services such as roads, schools, health services, safe drinking water and market access to their products. Some of the impoverishment risks and vulnerabilities have been reduced after resettlement. The average land holding size of resettlers at the area of resettlement was much higher than before resettlement in both research sites. With this successes, however, there were many challenges that the scheme faced in planning and implementing the resettlement programme.

References

Abbute, W. (2013). Resettlement as a response to food insecurity: The Case of the Southern Nations, Nationalities, and Peoples' Region (SNNPR) in *People, space and the state: migration, resettlement and displacement in Ethiopia* edited by A Pankhurst and F Piguet. Addis Ababa: ESSSWA and the United Nations Emergencies Unit for Ethiopia/UNEUE/.

Bohle, M G. (2007). *A delicate balance: land use, minority rights and social stability in the horn of Africa*. Addis Ababa: Institute for Peace and Security Studies.

Bruntland, H G. (2007). Living with vulnerability: livelihoods and human security in risk environments. Bonn: United Nations University, Institute for Environment and Human Security.

Brown, H, Magee, D. and Xu, Y. (2008). Socioeconomic vulnerability in China's hydropower development. *China Economic Review* 19(4):614–627.

Cernea, M. (2008). Compensation and benefit sharing: Why resettlement policies and practices must be reformed. *Water Science and Engineering* 1(1): 89-120.

Cernea, M and McDowell, C. (2000). Reconstructing resettlers' and refugees' livelihoods in *Risks and Reconstruction: Experiences of Resettlers and Refugees edited by* M Cernea and C McDowell. Washington, DC. : The World Bank.

Chambers, R and Conway, G. (1992). Sustainable rural livelihoods: practical concepts for the 21st century. *IDS Discussion Paper* 296.

Chimhowu, A and Hulme, D. (2006). Livelihood dynamics in planned and spontaneous resettlement in Zimbabwe: converging and vulnerable. *World Development* 34 (4):728–750.

De Wet, C. (2005). The Experience with dams and resettlement in Africa. Cape Town: World Commission on Dams.

Getachew, D. (2009). Resettling the discourse on resettlement schemes towards a new approach In: Proceedings of the 16th International Conference of Ethiopian Studies. Addis Ababa, Ethiopia.

Ohta, I and Gebre, Y. (2005). *Displacement risks in Africa: refugees, resettlers and their host population*. Kyoto: Kyoto University Press.

Oliver-Smith, A. 2005. Communities after catastrophe-reconstructing the material, reconstituting the social in *Community building in the Twenty-First Century* edited by E Hyland. New Mexico: School of American research press.

Pankhurst, A. 2009. Revisiting resettlement under two regimes in Ethiopia: the 2000s programme reviewed in the light of the 1980s experience in *Moving people in Ethiopia: development, displacement and the state* edited by A Pankhurst and F Piguet. London: James Currey, Eastern African Series.

Terminski, B. 2013. *Development-Induced Displacement and Resettlement: Theoretical Frameworks and Current Challenges*. Geneva, Switzerland.

World Bank. 2010. Reducing poverty, protecting livelihoods, and building assets in a changing climate social implications of climate. Washington DC: The World Bank.

Woube, M. 2005. Effects of Resettlement Schemes on the Biophysical and Human Environments: The Case of the Gambela Region, Ethiopia. Boca Raton, Florida: Universal Publisher.

Yntiso, G. 2009. Why did resettlement fail? Lesson from Metekel. In *Moving people in Ethiopia:*

development, displacement and the state edited by A Pankhurst and F Piguet. London: James Currey, Eastern African Series.

Geographic Information Systems (GIS) and its Role to Physical Development Control: a Case Study of Part of Oyo East Local Government Area, Oyo State.

By
Mr. Ajani, Ayodeji Olatubosun
(ayodejiajani013@gmail.com)
07063391862
Mr. Ilesanmi, Oluwatosin Ibukunoluwa
(hillesanmet@gmail.com)
08136789067
Surv. Oyeyode, Ajiboye Oyesiji
(boyee4real@yahoo.com)
08154046095
Department of Geographic Information Systems (GIS),
Federal School of Surveying, Oyo

Abstract
The primary concern of this study is to employ Geographic Information Systems (GIS) in developmental control in some part of Oyo East Local Government area using its spatial analytical capabilities. GIS provides useful techniques for capturing, maintaining, and analyzing spatial data. Satellite imagery was acquired and updated through the technology of Global Positioning System (GPS) and it was converted to digital format using ArcGIS software. The identification of the spatial problem initiated the following order of operations: database design phase, which involves the conceptual, logical and physical design of the study area. The database creation and the analyses were also performed using ArcGIS based on the set criteria by the Town Planning rules and regulations. Buffering analysis were carried out to draw buffer round the major and minor roads which were later overlaid on the buildings in order to determine conformity to set back rule and also the classification of land use in the study area.

Keywords: Geographic Information Systems (GIS), Database, Land Use, Development Control.

Introduction

For any system to work as expected, there is always the need for control and balance which is a form of regulation for necessary operation that is why development control is seen as a mechanism that is put in place to maintain standard over all developments that is, all developments shall be subjected to the need for planning permission being granted by local planning authority before development commence. It reduces the negative effect that accompanies physical development.

Development control is one of the measures applied by physical planning agencies particularly, Local Planning Authorities. Development control is a tool use to ensure that developers do not deviate from building plans approved for them in the course of implementation (construction) on the plot earmarked for such. This is aimed at enhancing environmental quality, improved housing condition, privacy in residents and free flow of air among other factors.

The state of the physical environment particularly the urban centers today is a major source of global concern. The concern is greater in respect of developing nations like Nigeria. This is evident from the fact that the urban environment is greatly of man's making called urbanization, by which increase proportion of people are drawn into the cities.

Urbanization can also be regarded as a consequence of urban population increase, most especially rapid exodus of people from the rural communities (concerned chiefly with agriculture) to urban community (generally larger) where the activities are primarily governmental oriented, trading, manufacturing, and of allied interest.

The first ever known form of development control measure in the country was in year 1863 town improvement ordinance of Lagos. The 1928 Town Planning Ordinance only ameliorated the situation of haphazard development with the establishment of Lagos Executive Development Board (LEDB). The LEDB, through the ordinance built houses in Lagos Island and housing scheme in Surulere, Ikoyi, Apapa and Industrial layouts at Ijora and Iganmu. Other town and country planning legislation after 1928 and before 1946 had similar orientation in control of development in the sense that they restricted enforcement of modern planning Regulation as it were to just Lagos city area and more importantly to the Government Reserved Areas (GRAs).

This study has used the technology of Geographic Information Systems in identifying the challenges of the development control in relation to the planning regulations applicable to the study area and the degree of contravention in Oyo West Local Government, Oyo State.

Statement of Problem

Urban ever-increasing development, irregular population growing up and immigrations to the cities have led to unplanned and uncontrollable urban development and changes in urban space structure and also ushered in a new pattern of development in form of squatter settlement and slum areas. This development pattern is associated with gross disregard for regulation guiding physical development and creating enormous problems for city managers. It's beginning to have an arm twisted effects on the Town Planners who are responsible for orderly arrangement of land uses, aesthetic and economic improvement of the region which they serve. Also there were no past efforts at controlling physical development and if there were, solving the problem

of development control was not based on proper studies and understanding of the situation at hands, hence solution were inadequate.

Aim of the Study

The aim of this study is to apply GIS tools in development control to check building line regulations, and checking the acceptable standard established on the area of land for specific use, and monitoring purposes with the view to identifying the structures/ development along the roads challenges of development control in the study area, using the 'Oyo State Urban and Regional Planning Board' space standard for physical development in as a guide.

Objectives

- Design a spatial database for the study area
- Conversion of existing analogue map to digital format by digitizing
- Examine all available standard and regulations governing the provision control and maintenance of setback to roads
- Determine the buildings that compliances to the laid down rules and regulation of town planning
- Database creation for the study area
- Performing spatial analyses operation required e.g. buffering, overlay, querying and classification
- To supply information on development and administrative policies formulated to serve as a spatial decision support system (SDSS).

Study Area: Oyo-East Local Government Area is one of the four Local Government in Oyo town, Oyo State. The LGA headquarter is in Kosobo and is located between Latitude $8^0.5^I$N and $9^0.5^I$N of the equator and also between Longitude 2^0E and 4^0E of the Greenwich Meridian. Oyo East Local Government is bounded in the north by Ejigbo and Ogo-Oluwa Local Governments, in the south by Afijio Local Government; in the west by Oyo West Local Government and; in the east by Iwo Local Government respectively and has 10 political wards with a population of 153453 according to 1991 population census data (NPC1991)

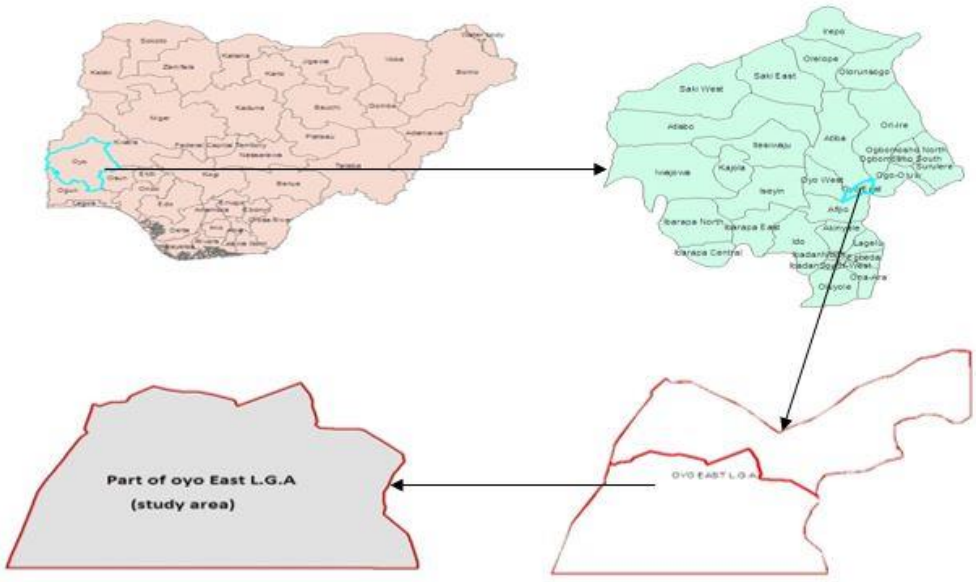

Fig1: Diagram of the study area

Literature Review

The focus of most developing and developed nations in recent time is to develop a way of improving situation in the urban centers. There is no gain saying that the urban centre is a place of beehive of activities necessary for the development of any nation. This cannot be without the attendant problem of congestion, slum, waste disposal, drainage and overcrowdings. Most developed cities have developed strategies to cope and deal with this situation at least to wear a pretence look of orderliness.

Ogundele (2011), Opined that the state of the physical environment particularly the urban centers, today is a major source of global concern. The concern is greater in respect to developing nations like Nigeria. This is evident from the fact that the urban environment is greatly of man's making. He further explained that the issue of agglomeration of population into urban areas leads to the quest for more basic utilities and facilities to commensurate with the demographic structure. Okekeogbu (2011), stated that Urbanization is a development process that is occurring all over the world, particularly in developing countries. Consequent on urbanization, there is pressure on the land, resulting in slums, change of use, and illegal developments. Development control, which includes monitoring is an activity undertaken by Town Planning Agencies, to ensure that plans are implemented as designed. Planning agencies

are empowered by legislation. Unfortunately, rapid urbanization has out-paced the existing urban management of Nigerian cities and this continues to be a challenge.

Ogundele (2011), stated that development control is one of the measures applied by physical planning agencies particularly, local planning authority to ensure that developers do not deviate from building plans approved for them in the course of implementation (construction) on the plot earmarked for such. This is aimed at enhancing environmental quality, improved housing condition, privacy in residents and free flow of air among others.

Obabori, Obiuwevbi, and Olomu (2007), defined development control as mechanism put in place to maintain standard. It reduces the negative effects that accompany physical development. There are restrictions introduced to prevent certain acts that are detrimental to stake holders in the built environment. The concept of zoning, covenants and other forms of regulating agreement are being used to guide developers and beneficiaries.

Fagbohun (2007), defined development control as the process by which an authority responsible for town planning exercises its statutory power to control all development. The essence of development control is therefore to maintain acceptable standards of physical development in urban and rural environment, and to monitor and order the use of land, especially in urban space.

In order to create an environment which has a quality of acceptable standards of health and efficiency and which enables the individual, the family and the community to live, work, recreate and worship in a satisfactory manner. This led to the establishment of Oyo State Urban and Regional Planning Board in 2008 in accordance with Oyo State Urban and Regional Planning Board Law, 2001 which necessitated a pragmatic, proactive and sustainable change in the administration of physical planning and development in the state.

Database Design

Database being the heart of GIS, is defined as an organized method of data collection, and storage capable of use by the relevant applications with the data being accessed by different logical path (Ajibade, 2000). It is nothing more than a computer based record keeping system whose overall objective is to record and maintains information or data. The storage capacity and other parameters which together determine the user friendliness of a database are of immense importance (Obi, 2003).

In database design, there is need for reality, which is referred to as the phenomenon that actually exist, including all aspects, which may or may not be perceived by individuals (view of reality) and can be use for a particular application or groups of applications (Kufoniyi, 1998).

The design is carried out in three phases namely:

- The conceptual design
- The logical design
- The physical design

Conceptual Design

This deals with the representation of human conceptualization of reality i.e. how the view of reality will be represented, and the entities of interest include:

Roads viewed as line, Communities viewed as polygon, Buildings viewed as polygon, Land use as polygon

Logical Design

The conceptual data model is transformed into data structure capable of being represented in the computer. In a relational data model, data are separated into tables. Each table contains item of data called fields, fields are object (Attribute of entities). The logical design is meant to provide redundancy-free data set. Each fact is stored only once in the database, the output of this stage is a data structure. The logical schema are RD_ID Road Identification, RD_NM Road Name, RD_TYPE Road Type and RD_WIDTH Road Width.

Physical Design

This stage is referred to as the implementation stage. It involves the representation of the data structure in a format of the implementation software. This include definition of field i.e. field name, field type, whether (String, Boolean, Number date etc.) and field width.

Data Sources

Using GIS in controlling physical development control involves the collection of spatial and attributes data of the entities. This project relied on the secondary data source.

- The acquired data sets include:
- Street guide map of Oyo at scale of 1:25,000
- Satellite imagery of Oyo at resolution of 1m

The primary source involves the use of GPS technology to pick the coordinates of known points in the study area. Ground truthing was also done to validate secondary data acquisition. Non spatial data were obtained through direct observation.

Geometric Data Acquisition

An A 3 Musket scanner was used to scan the street guide map of the study area. The analogue map was scanned, geo-referenced, and on-screen digitization of the roads was carried out with ArcGis 10.3 software.

Entities were identified and created according to specification for the project. Each entities were digitized in separate layers. The entities are: Boundary, Buildings, Roads, Land use class

Spatial Analyses and Information Presentation

Parameter used for GIS Analysis

As stated in the early part of the paper, one of the objectives of carrying out the study is to assess the degree to which town planning rules and regulations have been adhered to in the study area this is reflected in the analysis carried out base on the study for this study.

The following are some parameters used:

1. Setback: if a minimum setback of 6m from the collector roads, 12m from the minor roads and 18m from Oyo-Ibadan and Oyo-Ogbomosho roads respectively
2. If recommended land allocation for different uses was observed

Buffering Operation

Roads Set Back

Buffering was done to check the buildings that contravene the building line regulations. Buffer operation was carried out to the specified criteria according to Oyo State Urban and Regional Planning Board as shown in the table below

INPUT THEME	BUFFERED DISTANCE	OUTPUT THEME
MINOR ROADS	6M	BUFFER OF MINOR ROAD BY 6M
MAJOR ROADS	18M	BUFFER OF MAJOR OF 18M

Table 1 buffered distances at specified criteria

Overlay and Intersect Operation

After buffering of both minor and major roads, overlay operation of buildings layer on roads buffer layer was performed to know those buildings that intersect the roads buffer zone to know the buildings that contravened the roads set back. The result of the overlay operation of both major and minor roads buffer and buildings is shown in fig 2 and fig 3

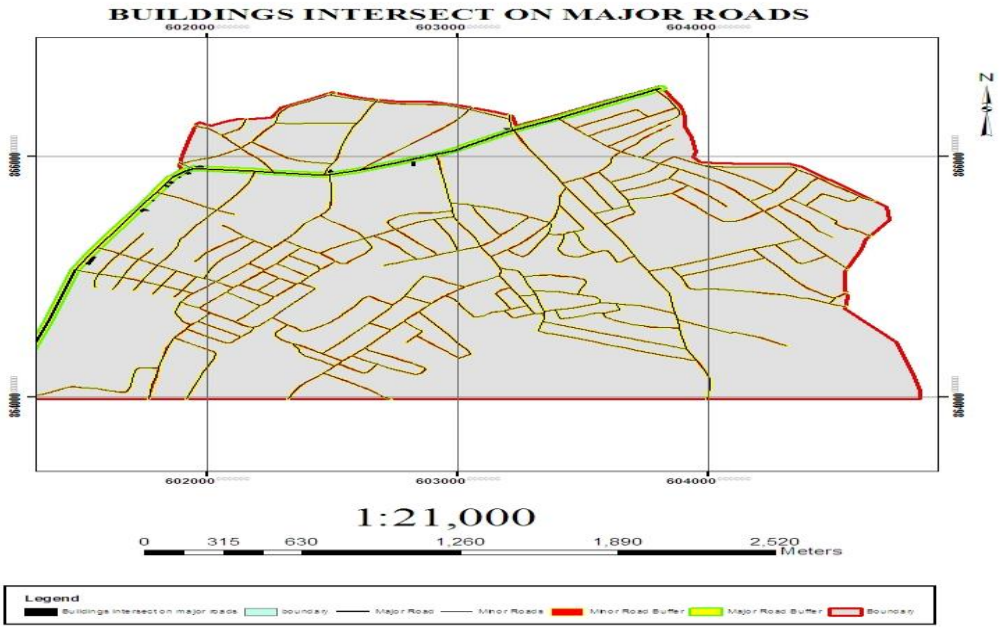

Fig 2: Map showing building that intersects the major roads set back

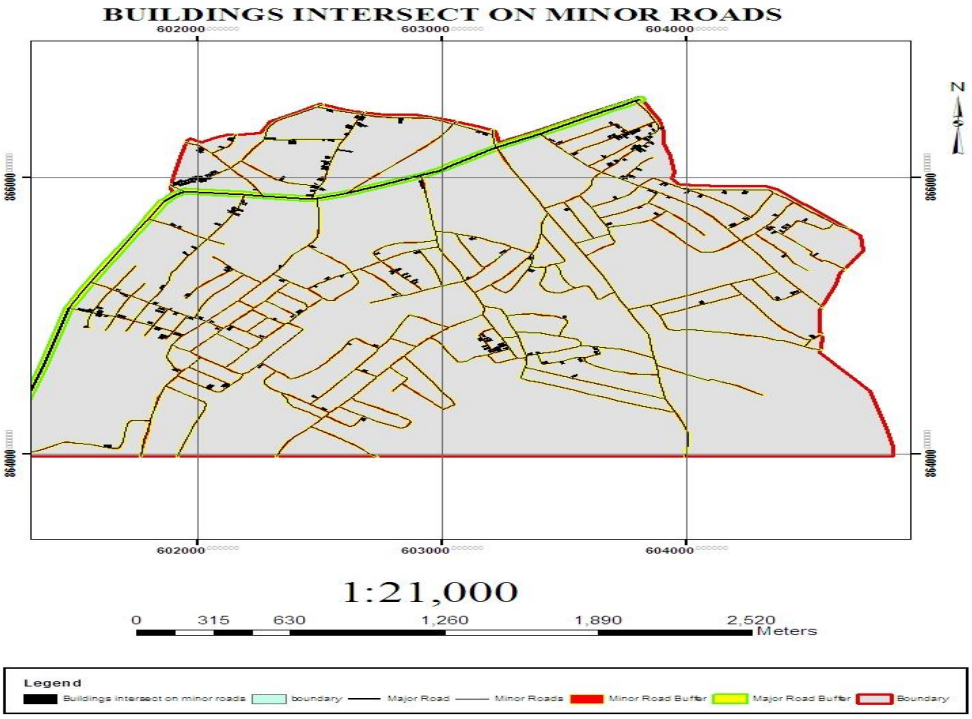

Fig 3: Map showing building that intersects the minor roads set back

Land Use Classification

Acceptable standard have been established over time on areas of land for specific uses, amenities and services. Such standard include that of major and auxiliary land use: residential, commercial, industrial, public and semi-public, recreation and circulation.

Land Use	Percentage
Residential (Dwelling plot)	50-60
Local/Neighborhood commercial market area	3-4
Park/Playground and other open spaces	10-12
Roads and Right of way	15-20
Public and semi-public use	4-6
Industrial	As required

Table 2: Neighbourhood Land use estimate (source: J.B Falade and Leke Oduwaye 1998)

The table below showed the land use estimation and the land used observed in the study area

LAND USE TYPE	% EXPECTED	% OBSERVED
Residential (Dwelling plots)	50-60	49.265
Neighborhood Commercial (market) area	3-4	1.98

Parks/ Playground and other open spaces	10-12	19.26
Roads and street (Right of ways)	15-20	16.31
Public and semi-public use (Schools, Hospitals and worshipping place)	4.0-6.0	13.18

Table 3: land use expected and land use observed

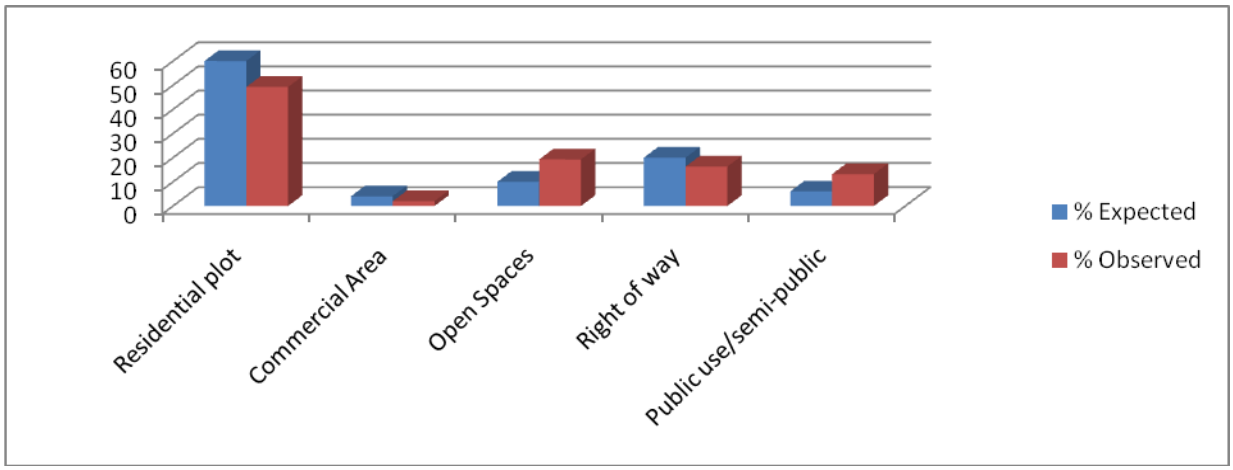

Fig 4: Bar chart showing the land use estimation and land use observed

General Observation

The general observation on land use classes and noncompliance with the buildings set- back, in the study area showed that the land use classification is still within the range of the land use estimation, though some buildings that falls in the residential zone are used for commercial purposes and some building are mixed used for both residential and commercial purpose. Many buildings are located close to road most especially on minor roads. The buildings in Jabata and Owode are clustered together which does not allow for ventilation, while the buildings in Araromi, Folatyre are well spaced and arranged compare to Jabata.

Summary

The study attempted to assess conformity to planning regulations with a view to control the physical development using GIS analytical tools. It has been able to identify some cases of incompatible land use and conversion, contraventions in building guidelines as it relates to the set-back rules. The study discovered that a lot of researches have been carried out on

development control but the use of GIS as a developmental control tool has not been fully utilized thus, the need to embark on this research

The study discovered that Oyo East has a mixed land use: Kosobo, Fola Tyre, and Araromi are residential areas and well organised except for some buildings in these areas which are used for both commercial and as a resident. Owode is a commercial area with some residential buildings, Jabata is the only community that is not well planned due to the fact that is a traditional and core area in the study area.

Conclusion

The contribution and importance of GIS at this era cannot be overemphasized given it problem solving spatial analytical functions. The demonstration of this is shown in this project work, where a spatial database was created and spatial analysis like overlay, buffering, and queries were performed. This was aimed at checking contravention to development control regulations, which is to serve as an instrument i.e. spatial decision support system (SDSS) to the relevant bodies in any urban areas in the country that have similar developmental problems.

Recommendations

Based on the summary of findings, it is hereby suggested that if the followings should be addressed and implemented by various organs of governments and the people concerned, this will help minimize the problems arising from contraventions in the study area.

- Enlighten the people of the importance of an organized and well planned environment and issues relating to development control.
- Planning intervention is urgently needed in the study area, because of the rapid development. This intervention should be in area of preparation of schemes and layout to conform to the developmental changes coupled with strict enforcement on the part of the Planning Authority to maintain a healthy environment.
- Preparation of Oyo East: it has been gathered that there is no master plan for Oyo East. It thus necessary to prepare a master plan of Oyo East to avoid future haphazard development. This will guide the development of the town and also make provision for the facilities which will cope with the increasing population as the town grow. The master plan will also make provision for land use zoning and serve as a check to haphazard development. The master plan will also serve as an instrument in the hand of the development control department to guide the development of the town.

- There is urgent need of GIS analyst to be introduced in control departments, of planning offices at all tiers of Government, for effective development control and other policy issues as it relate to spatial entities.

References:

Fagbohun P. O (2007): *Population and Urbanization in Nigeria,* Bluesign Publication Shomolu Lagos.

Obabiri A. O and Obiuwevbi (2007): *Development Control an important Regulator of settlement Growth:* A Case study of Ekpoma, Nigeria. A journal of Human Ecology Vol 2 (4), PP 285-291.

J.B Falade and Leke Oduwaye (1998): Essentials of Landscape and Site Planning

Ogundele F.O (2011): *Challenges and Prospect of Physical Development Control, A Case study of Festac Town, Lagos Nigeria.* African journal of Political Science and International Relation Vol 5 (4), PP174, 175.

Okekeogbu C.J (2011): *Development Control and Local Planning Authourity in Enugu, Nigeria*. A Journal of Environmental Management and Safety, Vol 2, No1, PP 56-66.

Geological and Geoelectrical Prospecting for Manganese Ore within Tashan-Kade In Tegina Sheet 142, North-Central Nigeria

[1*]Unuevho, C.I., [1]Amadi, A.N., [1]Okesipe, D.O., [1]Adeniji, O. J. [2]Udensi, E.E, [3]Goki, N.G.

[*] Correspondence e- mail address : unuevho@gmail.com
[1] Department of Geology, Federal University of Technology, Minna
[2] Department of Physics, Federal University of Technology, Minna
[3] Department of Geology and Mining, Nassarawa State University, Keffi

ABSTRACT

Although manganese has attained the status of elements in critical global demand, the deposit in Tashan-Kade has remained hitherto unreported and yet to be appraised. This study is a preliminary attempt to appraise the deposit by delineating its surface spatial extent and ascertaining its subsurface thickness, through surface lithologic mapping and 2D geoelectrical prospecting. The 2D geoelectrical data was acquired with ABEM Terrameter (SAS 4000) and twenty one metal electrodes arranged in Werner Alpha field array, along a 100 m long traverse oriented along outcrop foliation dip direction. The geoelectrical data comprised electrical resistivity (ER) and induced polarization (IP) measurements. The data was processed and interpreted using RES2DINV software. The lithologic outcrops are migmatitic schist, amphibolites, granite and manganese ore. The migmatitic schist and amphibolites strike NW – SE and dip 30°W. Broken particles of the migmatitic schist are attracted by a horse shoe magnet, indicating magnetite content. Samples of the manganese ore were inert to dilute mineral acids, thereby precluding rhodochrosite. The ore shows a schistose texture and a sooty residue, which are indications of pyrolusite. The 2D inverse ER and IP models respectively reveal ER values lower than 200 Ωm and IP values higher than 2 ms in the western part of the traverse. The geoelectrical values agree with observations of rubbles of manganese ore outcrops on the western part of the traverse. The ER and IP values are respectively lower than 80 Ωm and 2 ms where the outcrops of the ore bodies are continuous sheet-like bodies. A surface spatial extent of 540,000 m^2 of manganese ore deposit was delineated between longitudes E 6°11′ 45″ to E 6°12′ 00″ and latitudes N 10°8′ 10″ to N 10° 9′ 00″, from inferred subsurface extension captured from 2D geoelectrical models and outcrop locations of the ore. The spatial area and 8 m mean subsurface ore thickness obtained from the 2D geoelectrical models constitute 4, 320,000 m^3 gross volume for the ore deposit.

Keywords: Manganese ore, critical global demand, 2D geoelectrical models

INTRODUCTION

The recent (October, 2018) commissioning of Pb-Zn ore processing plant in Cross River State of Nigeria is a demonstration of the country's commitment to develop the solid mineral sector to augment revenue from the petroleum industry. However more attractive opportunities lie in the minerals that have been declared to be in critical global demand. One of such minerals is

manganese. Up till date, the manganese deposit in Tashan-Kade area of northern Nigerian basement has neither been reported in contemporary geosciences literature nor attention given to its spatial delineation. Surface lithological mapping and 2D geoelectrical tomography were conducted in this work for preliminary prospection and delineation of the deposit in Tashan-Kade.

Tashan-Kade lies within longitude E6°11'50" to E6°12'50" and latitude N10°5'0" to N10°5'40" of Tegina Topographic Sheet 142, within the part of Northern Nigeria Massif called Birnin Gwari Schist Belt (figure 1)

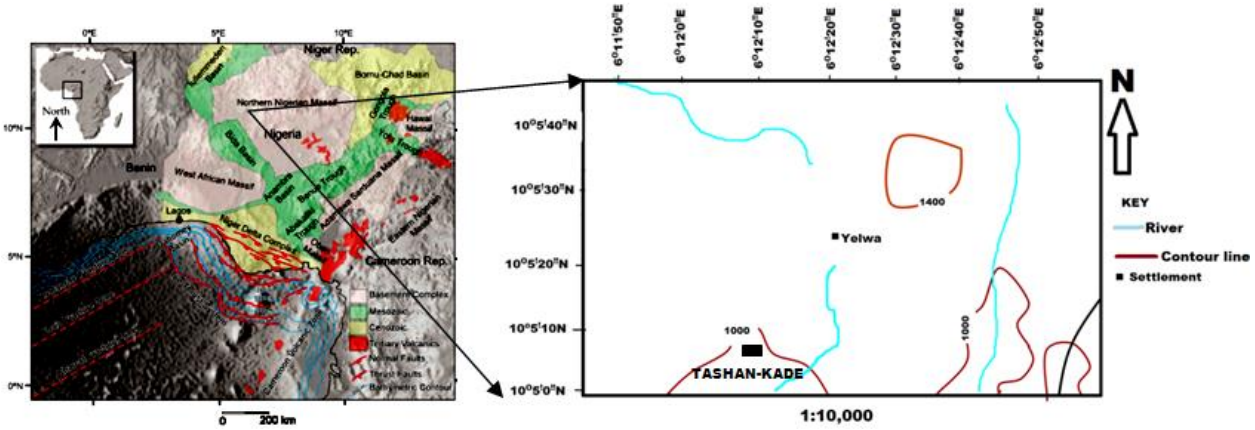

Figure1. Location of Tashan-Kade

Wright and McCurry (1970) first reported lenses of manganese ore in the western part of Northern Nigerian Massif. They remarked that the ore occurs as manganiferous layers interbedded with quartzite. Obaje (2009) documented manganese ore deposits within present states of Katsina, Kebbi and Zamfara- all in the western part of Northern Nigerian Massif. Moon *et al.* (2006) emphasized that mineral prospecting studies are crucial for discovering, qualifying and quantifying new deposits, even during exploitation, in order to expand reserves and to increase project span. They added that rock and soil sampling, chemical analysis and geophysical techniques constitute the traditional procedure for discovering and characterizing new mineral deposits. Cortes *et al.* (2016) employed the combination of resistivity method and geological mapping to delineate copper sulphide mineralization within metamorphosed, silicified and fractured sandstone in the northern edge of Camaqua sedimentary basin in southern Brazil. They associated low resistivity (less than 20 Ωm) with the ore deposit. Moreira *et al*. (2016) employed low resistivity (between 73 and 300 Ωm) to delineate supergenic manganese ore within regolith interval in Heliodore region of southern Minas Gerais in southern Brazil. Viera *et al.* (2016) characterised manganese ore deposit in Itapira, south-eastern Brazil, with high chargeability of about 20 mv/v, from 2D IP surveying. Srigutomo *et al.* (2016) also associated low resistivity and high chargeability (greater than 10 ms) with manganese ore deposit.

Libbey *et al.* (1948) remarked that most of mined manganese consists of one or both of two oxides, namely psilomelane and pyrolusite. The description and identification of igneous rocks in hand specimen, using texture and mafic mineral index was given by Chernicoff and Whitney (2007). They were able to identify granite, granodirite, diorite, gabbro, peridotite, rhyolite,

dacite and basalt. They further combined mineral content with grain size and foliation to identify slate, phyllite, schist, gneiss and amphibolites. Gandhi *et al.* (2016) classified configuration of ore mineral deposits into sheet bodies, vein bodies and lensoid or lenticular bodies.

METHODOLOGY

Lithologic mapping of the rocks was conducted. The igneous rocks were identified on the basis of texture and mafic colour index (MCI). Felsic rocks contain 0 – 15% feldspar and quartz. Granite is a felsic in which potassium feldspar (pale orange to pink coloured minerals) is greater than plagioclase feldspar (light gray coloured minerals). Metamorphic rocks were identified in hand specimen, using the combination of mineral content with presence or absence gnessic and schistose mineral foliation. Amphibolites were identified as rocks with glossy greenish or black minerals, with cleavages meeting at 60˚/ 120˚. Schists were recognized as rocks with light gray to gray minerals that split along unidirectional schistose planes.

Manganese ore was identified using effervescence with hydrogen peroxide(H_2O_2) solution, dark gray colour, brownish black streak colour, dull metallic luster and hardness of 6 – 6.5 on Mohr Hardness Scale. The outcrops of the rocks and manganese ore were plotted on a base map produced on 1: 10,000 scale from Nigeria's Tegina Topographic Sheet 142. The manganese outcrops were delimited eastwards by amphibolites outcrops. To ascertain subsurface continuity of the ore westward, a 2D geoelectrical survey was conducted along a 100 m long westward traverse, close to the westward limit of the amphibolites. The traverse starting position is N10˚8 '8.29" and E6˚11 '55.28". The 2D geoelectrical data was acquired with ABEM Terrameter (SAS 4000), using the Werner Alpha geometry with twenty electrodes arrayed along outcrop dip direction. The starting electrode spacing (minimum electrode spacing) was 5 m. This was expanded consecutively in multiples of 2, 3, 4 and 5 to give six levels of measurements and 63 data points. RES2DINV computer program was used to process and interpret the 2D geoelectrical data. The resistivity of manganese ores (< 300 Ωm) given by Keller and Frischknecht (1970), Cortes *et al.* (2016) and Moreira *et al.* (2016) guided the identification of manganese ores in the inverse resistivity subsurface model. The identification was supported by manganese ore IP values (> 10 ms) given by Srigutomo *et al.* (2016). Subsurface intervals with resistivity < 300 Ωm and IP > 10 ms were recognized as bearing manganese ore. The identified subsurface extension of the manganese ore bodies was combined with its outcrop locations to delineate the spatial extent of the deposit. The area of spatial extent of the deposit was manually determined. The gross volume of the ore was estimated as the product of its average thickness and the spatial area.

DATA PRESENTATION AND ANALYSIS

LITHOLOGIC OUTCROPS

Outcrops found during the surface lithologic mapping are schist, amphibolites, and granite and manganese ore. The schist and amphibolites strike NW – SE (140˚) and dip 30˚W. The schists are light gray in hand specimen. This suggests presence of biotite or hornblende, and quartz. One of such outcrops is figure 2.

Figure 2. Biotite or hornblende and quartz bearing schist
(E6°12'32.33" ; N10°8'27.61")

Some of the schists display migmatitic texture. An example of this is outcrop shown in figure 3.

Figure 3. Schist displaying migmatitic texture
(E6°12'1.07" ; N10°8'5.86")

Figure 4 is one of the amphibolite outcrops. The rock is dark green in colour, banded and fine grained. The green colour and 60°/ 120° cleavage pattern seen in magnifying hand lens suggest that amphiboles predominantly compose the rock.

Figure 4. Amphibolite outcrop
(N10° 8' 11.09"N: E6° 12' 2.62")

The granite outcrops bear many schist zenoliths. These granites belong to the Older Granite series that intruded into the older basement. Figure 5 is representative of the Older Granite outcrops.

Figure 5. Schist zenolith bearing Older Granite outcrop
(N 10° 8' 41.30"; E6° 12' 50.51")

Pieces of fragments of the migmatitic schist are attracted by a horse- shoe magnet. This indicates the presence of magnetite in them. Figures 6 and 7 are some outcrops of the manganese ore.

Figure 6. Manganese ore outcrop
(N10° 8' 6.74" ; E 6° 12' 2.18"E)

Figure 7. An outcrop of manganese ore
(N 10° 8' 17.38"; E 6° 12' 4.15")

Samples from the outcrops stain hands black and are dark gray in colour. They display dull metallic luster, give a black streak, and exhibit schistose texture. They are identified to be pyrolusite. They are unaffected by dilute mineral acid, and give a hardness of 6 – 6.5 on Mohr scale. This indicates that manganese carbonate ore (rhodocrosite) is absent in the samples.

Figure 8 shows the locations of the various lithologic outcrops and the 2D geoelectrical traverse starting location.

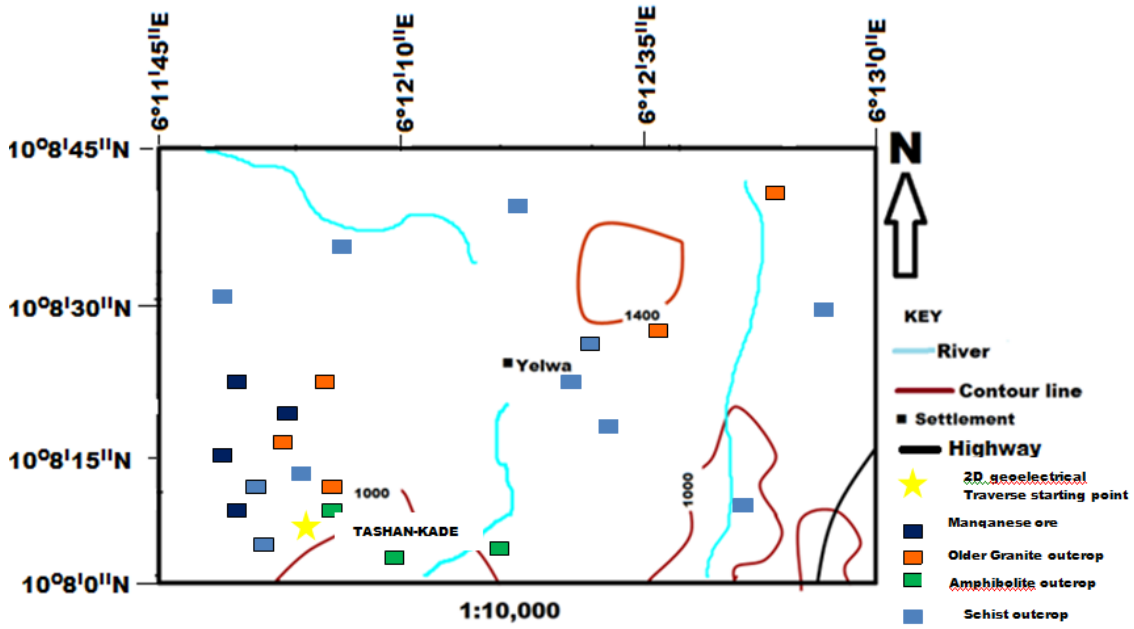

Figure 8. lithologic outcrops and 2D Geoelelectrical traverse starting point locations

Geoelectrical Prospecting For Sites with New Opportunities in Shallow Fractures for Waterborehole Drilling Within Kadna, North-Central Nigeria

Christopher Imoukhai UNUEVHO[1*], O. Johnson AJIROBA[2], A. Nnosike AMADI[1], K. Mosto ONUOHA[3], E. Emeka UDENSI[4]

[1] Department of Geology, Federal University of Technology, Minna, Nigeria
[2]Kwara State's Ministry of Industry and Solid Minerals Development, Ilorin, Nigeria
[3]Department of Geology, University of Nigeria, Nsukka
[4]Department of Physics, Federal University of Technology, Minna, Nigeria
*Corresponding Author: unuevho@gmail.com

Abstract

Kadna is an urban sprawl of Minna within Northern Nigeria Massif in north-central Nigeria. Her residents obtain potable water from six boreholes that tap water from basement fractures at depths shallower than 50m. These have become inadequate to satisfy the potable water needs of the growing population of the town. An appraisal of the shallow fracture system is vital to recognizing fresh opportunities within the system for locating productive water boreholes. The appraisal was accomplished by combining surface geological mapping with geoelectrical sounding conducted using SAS 4000 ABEM Terameter. Rock lithologies were identified from

texture and mafic colour index of fresh rock samples. Electrical resistivity (ER), spontaneous potential (SP) and induced polarization (IP) sounding data were acquired along ten traverses aligned with foliation strike. The Etrex Garmin GPS (global positioning system) was employed to determine geographic coordinates and surface elevation (with respect to sea level) of the sounding stations. WinResist inversion software was used to process and analyse the ER data. The IP and SP data were analysed using Microsoft Excel. The outcropping lithologic units are migmatite, schist, and amphibolites with NNE strike and 25 - 35° E dip. Older granites intruded these outcrops and outcrops of quartzite. Fractures between 20 and 50 m depths were grouped together as shallow fractures. Their ER value varies between 60 and 600 Ωm, with the highest value (400 – 600 Ωm) characterizing the NW part. The western and eastern parts are characterised by 50 – 150 Ωm ER value and 9 – 18 m thick fracture intervals. Their basal elevation decreases outward in radial pattern from 280 m in mid-western part to 190 m in the east, 100 m in the north and western parts. Its SP value decreases from -70 mv in the mid-western part to + 20 mv in the eastern part, following basal elevation decrease trend. The eastern part is a broad groundwater convergence area by virtues of low ER and basal elevation values, and positive SP values. The IP values increase (up to 70 ms) eastward, thereby supporting presence of water filled fractures. These attributes characterise the groundwater convergence areas where the existing water boreholes are located. This study reveals that undrilled part of Kadna with these groundwater indicative attributes in the shallow fracture system lies within latitude N9.50° to N9.560° and longitude E6.597° to E8.810°.
Keywords: Shallow fractures, groundwater indicative attributes, groundwater convergence area

Introduction

Kadna is inhabited by mostly middle level civil servants. Six boreholes presently provide potable water for the inhabitants, from shallow fractures. Since the boreholes are hand-pumped, they tap water from fractures shallower than 60m depth. However, this water source has become inadequate due to rising population. This study was conducted to delineate areas in Kadna where potential shallow fracture aquifers are yet to be tested by drilling.

The town is an urban sprawl of Minna within latitudes N9°33'30" to N9°34'30" and longitudes E6°32'30" to E6°36'30" in north- central Nigerian Basement Complex (Figure 1).

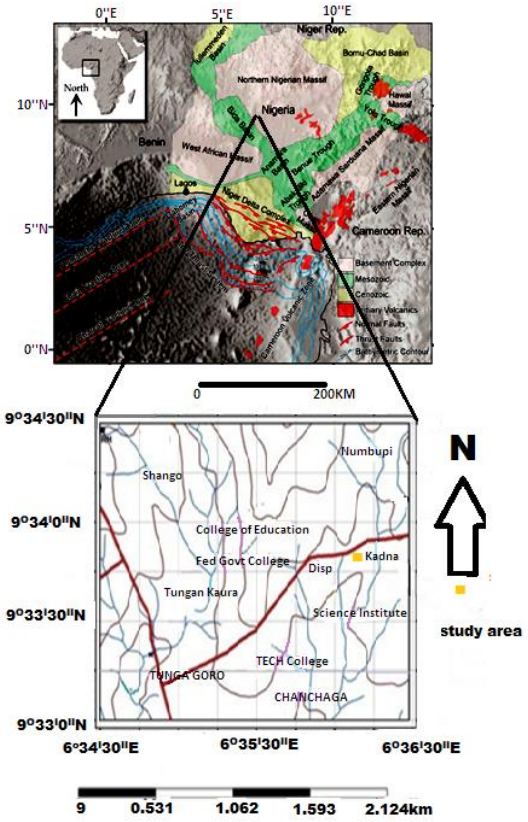

Figure 1. Location of Kadna

This was approached by integrated interpretation of geological and surface 1D geoelectrical data comprising electrical resistivity(ER), spontaneous potential (SP) and induced polarization (IP) data. Such integrated analysis of multiple geosciences data is yet to be deployed for aquifer exploration in Kadna.

Schist Belts, Older Granites, and undeformed acid and basic dykes are the principal petro-lithological units that constitute Nigerian Basement Complex. The rocks of the Schist Belts are pelites, semi-pelites, quarzites, marble, banded iron formation, amphibolites, and minor felsic to intermediate metavolcanic rocks. Oluyide (1988) found that fractures within the complex trend majorly N-S, NNE-SSW, NE-SW, NNW-SSE and NW-SE. He noted subsidiary E-W fractures as well. Ajibade et al. (2008) acknowledged aquifer attribute of fracture zones within fresh rocks, and described them as basement aquifers. They noted that the fractures are frequently shallow, and are commonly penetrated by boreholes that are 30-40 m deep or sometimes up to 50 m deep. Unconfined fractures and confined fractures are described within the Nigerian basement by Olorunfemi (2009) and Ojo and Olorunfemi (2013). They described a confined fracture as a fractured basement interval that is sandwiched between fresh basement above and below.

Prospects for drilling productive boreholes are commonly generated by Direct current(DC) resistivity method in the basement complex (Ayuk et al., 2014; Ojoina, 2014; Wright, 2015). This is because the DC resistivity method is the most suitable among all geophysical methods for delineating aquifers in hard rock terrains (Ratnakumari et al., 2012). Tswako et al. (2017) found that success rate in drilling is improved by delineating groundwater convergence areas

from integrated interpretation of ER, SP and IP data to. Dan-Hassan (1999) and Unuevho et al. (2016) revealed that boreholes are commonly productive within groundwater convergence areas in the Nigerian Basement Complex.

This work seeks to delineate groundwater convergence areas within shallow fractures that are yet to be drilled for water in Kadna.

Material and Method

Rock outcrops were mapped to determine their lithology and structural attitude. Lithology was ascertain from texture and mafic colour index (MCI) of fresh outcrop samples. The percentage of green, gray and black minerals in the samples constitute the MCI. Felsic rocks were identified as non-foliated rocks with 0 – 15 % MCI. Granite was recognized as felsic rocks with higher proportion of potassium feldspar (pale orange to pink colour) than plagioclase feldspar (light gray in colour). Schists were recognized from schistose texture and light to gray colour. Amphibolites were identified by the presence of amphiboles (glossy minerals with $60^{\circ}/120^{\circ}$ intersecting cleavage planes. Outcrops that display both granitic and gnessic textures were called migmatites. Outcrops constituted solely of fused yellowish browm to white quartz were identified to be quartzite. Geological map of the area was produced from the plot of the oucrop locations on a base map of scale 1 : 10,000. Joint directions were determined and plot as Rosette diagram, using Rock Work software.

ABEM SAS 4000 Terrameter was employed to conduct one dimensional (1D) geoelectrical sounding at a total of fifty stations along ten traverses, giving an average of five stations per traverse. The traverses were aligned with foliation strike, and separated by 50 – 100 m along foliation dip direction. The geoelectrical sounding comprise electrical resistivity (ER), spontaneous potential (SP) and induced polarization (IP) measurements. Schlumberger field array was employed with a maximum current electrode spacing of 200m. Global positioning system (GPS of etrex Garmin – legend type) was used to determine the geographical coordinates and surface elevation of the sounding stations. The ER data was analysed using WinResist inversion software. Microsoft Excel was employed to analyse the IP and SP data.s

One- dimensional (1D) geoelectrical sounding – comprising resistivity, spontaneous potential (SP) and induced polarization (IP) – was conducted at 50 stations, using Schlumberger array along a traverse of 200 m maximum electrode spacing. The sounding was performed using SAS 4000 ABEM Terrameter, along 10 traverses oriented along foliation strike, with an average of 5 stations per traverse. The traverses were separated by 50 – 100 m along foliation dip direction. Geographic coordinates of the sounding stations were determined using global positioning system (GPS, the etrex Garmin-legend type). The electrical resistivity data were analysed using *WinResist* inversion software. The IP and SP curves were plotted using *Microsoft Excel* and then analysed.

Fracture intervals were identified from the 1D resistivity inverse models. Fractures deeper than 60 m were grouped together as deep fractures. The depth to the base of each deep fracture interval was subtracted from the corresponding sounding station's surface elevation. This gives the basal elevation of the fracture's interval with respect to sea level. The deep fracture interval

thickness was obtained as the difference in depth to top and base of the interval. Iso resistivity, IP and SP maps were generated by contouring the respective parameters against the stations' geographic coordinates. Fracture thickness and basal elevation maps were also generated. Topographic depressions were identified on the basal elevation map. Topographic depressions characterized by low resistivity and increasing SP positivity were inferred to be groundwater convergence zones.

VES 1 (N9°33'42" ; E6°35'52")

Distance	Resistivity
1.00	43.7140
1.50	52.0470
2.00	52.2490
3.00	54.0000
5.00	51.5760
7.00	41.1540
10.00	44.0740
15.00	46.7050
20.00	56.9410
25.00	63.4570
30.00	322.1200
40.00	151.9700
50.00	244.9300
60.00	198.4300
70.00	225.8900
80.00	293.0300
100.00	137.8800

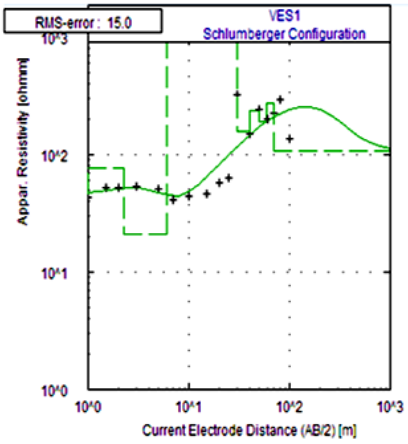

No	Res	Thick	Depth
1	46.5	1.0	1.0
2	76.2	1.3	2.3
3	21.0	3.8	6.1
4	967.5	24.2	30.3
5	157.1	9.7	40.0
6	236.6	9.7	49.7
7	189.1	9.8	59.5
8	276.0	9.6	69.1
9	107.5	-.-	-.-

Shallow fracture

VES 2 (N9°33'42.9" ; E6°35'50.83")

Distance	Resistivity
1.00	15.8780
1.50	21.3150
2.00	26.2410
3.00	26.5420
5.00	26.7910
7.00	27.2330
10.00	36.2450
15.00	42.2570
20.00	81.2310
25.00	138.7600
30.00	208.2130
40.00	151.9700
50.00	125.1400
60.00	198.4300
70.00	166.3100
80.00	192.3800
100.00	233.5100

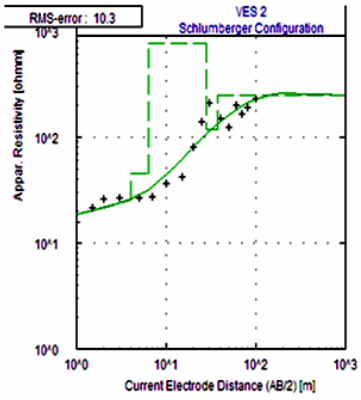

No	Res	Thick	Depth
1	17.6	0.7	0.7
2	25.5	3.3	4.0
3	45.7	2.4	6.4
4	767.8	21.4	27.8
5	117.8	9.6	37.5
6	249.3	-.-	-.-

Shallow Fracture

VES 11 (N9°33'41.7" ; E6°36'1.9")

Distance	Resistivity
1.00	80.1660
1.50	78.5490
2.00	73.2330
3.00	53.6770
5.00	32.4810
7.00	26.6780
10.00	27.6620
15.00	40.6620
20.00	56.1900
25.00	62.6990
30.00	53.5560
40.00	41.9370
50.00	60.2510
60.00	66.9590
70.00	74.3030
80.00	92.5680
100.00	114.0300

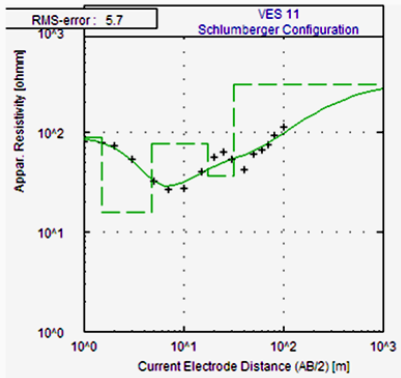

VES 19 (N9˚33'50.73"; E6˚35'44.604")

Distance	Resistivity
1.00	355.2000
1.50	295.8400
2.00	239.2800
3.00	156.1500
5.00	91.1090
7.00	72.1750
10.00	34.5450
15.00	36.1630
20.00	80.3100
25.00	84.9200
30.00	64.3010
40.00	80.5700
50.00	100.6700
60.00	126.1300
70.00	145.7500
80.00	161.9300
100.00	190.9200

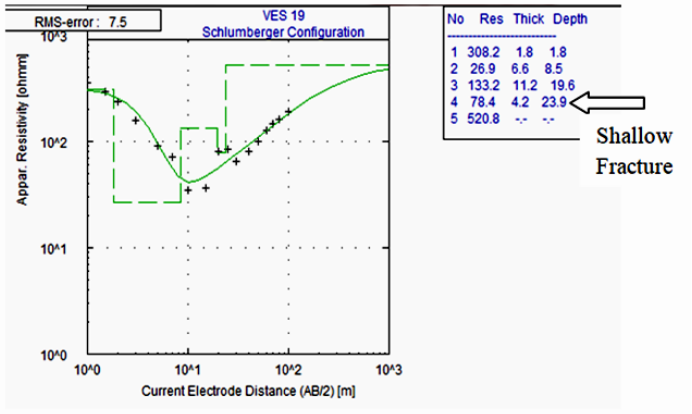

VES 49 (N9˚33'21.4"; E6˚35'45.5")

Distance	Resistivity
1.00	138.1100
1.50	162.2900
2.00	143.1800
3.00	85.0130
5.00	47.4650
7.00	47.8990
10.00	50.8370
15.00	66.3480
20.00	82.8040
25.00	98.8900
30.00	92.4340
40.00	76.6000
50.00	98.1720
60.00	120.5900
70.00	126.9100
80.00	130.6500
100.00	144.7300

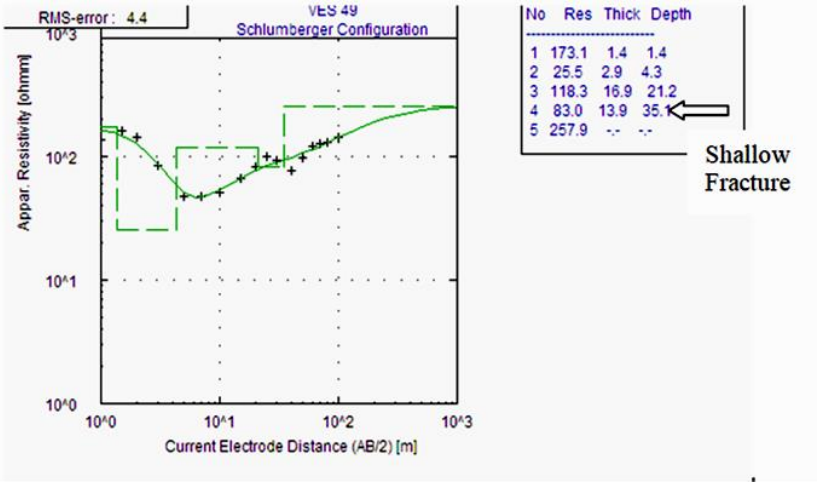

The Impact of Urbanization on Microclimate of Lokoja, Kogi State, Nigeria

ShehuYahuza Atta[1*]Aishetu Abdulkadir[2*]Mairo Muhammed[3]

[1]Department of Geography, Federal university of Technology, Minna, Nigeria
[3]ummubahiyya@futminna.edu.ng
[2]abuzaishatu@futminna.edu.ng
[1]yahuzashehu@yahoo.com
* yahuzashehu@yahoo.com

ABSTRACT

Nigerian urban centres are perhaps the fastest growing cities in Africa and as with other urbanizing countries of Africa in general, are experiencing the most damaging effects of climate change. The urbanizing town of Lokoja as it stands today consists urban footprints capable of absorbing and releasing heat. This research aims at examining the impact of urbanization on the microclimate of Lokoja, Nigeria. Dataset used for the study includes Landsat 5 (TM) of 1990, Landsat 7 (ETM+) of 2010 and Landsat 8 (OLI) of 2018. The land use was classified into four classes from 1990 - 2018 to monitor the changes that have taken place over time. The spatio-temporal pattern of UHI was determined through extraction of LST. Result shows that: a) with a negative annual rate of change in both bare soil and vegetation each year, built-up areas have been on increase with an annual rate of change of 7.52km^2. This therefore suggest a rapid rate of urbanization; b) as the built-up area increased in size (210.65 km^2) so was the surface temperature (8.90^{o}C), water body (10.76 km^2: 7.59^{o}C) and bare soil (-74.14 km^2: 5.48^{o}C) while vegetation cover increased by 6.76^{o}C, its area extent decreased (-147.26 km^2). These changes were responsible for the rise in the mean surface temperature from 21.30^{o}C in 1990 to 34.43^{o}C in 2010 and 28.48^{o}C in 2018, creating a condition for urban heat island; c) the study revealed a direct relationship between the changing pattern among the various landuse/cover types and the variations in the surface temperatures of these landuse/cover types within the study period.It is suggested that specific growth management policies that will help to provide more vegetation cover should be adopted to minimize the urban heat island effect on the environment.

Keywords:environmental criticality index, land surface temperature, land use land cover, Lokoja, urban heat islands

1. Introduction

The ubiquitous and spontaneous nature of the global urbanization process has been an issue of concern over the years. Urbanization is seen as a key process, a complex set of socio-economic, political, demographic, cultural and environmental development that have resulted into an increase in the proportion and density of population and resource consumption in towns and cities within urban settlements (Reinhard and Yasin, 2011). In 2014, urban population accounted for 54% of the total population of the globe; an increase by approximately 1.64% per year is expected between 2015 and 2030 (WHO, 2013). From forecasted growth, 70% of

the world population will live in cities by 2050 (WHO, 2013). Nearly 90 per cent of the increase will be in Africa and Asia, the fastest urbanizing global regions (UNDESA, 2014).

Unprecedented Urbanization has been a common feature of countries across developing world since the last century (Aderamo, 2010). Nigerian urban centres are perhaps the fastest growing cities in Africa (Onibokun 1997, UNDESA, 2014). The country has many large urban centres with too few well-planned cities and towns. Nigeria has a dense network of urban centres owing to a peculiar urbanization history - most of these cities having transformed in recent times, as a result of their political administrative reclassification. Many were recently designated as capital cities within the administrative structure of the country (Ibrahim *et al.*, 2014).

The impact of urbanization on urban areas around the world is usually felt as it affects urban structures; areas, density, mobility and transport, infrastructure, the city-related production, human behaviour as well as private households at different dimension and extent (Reinhard and Yasin, 2011). Although these effects are not as critical as, for example, climate change (Woods *et al*., 2015). For instance, since 1978, intense urbanization in southeast China has led to an increase in mean temperature of 0.05°C per decade. Likewise, Tanko*et al.*, (2017) found out that urbanization accounted for 80.5% increment in the land surface temperature (LST) of Kano Metropolis in Nigeria. The climatic impact of urbanization may lead to a scaled-down climatic condition referred to as microclimate. In other words, microclimate is defined as a combination of meteorological parameters that create a localized climatic condition, which is different from its surrounding areas (Hogan, 2012). Microclimate is related to global climate change in two ways. First, the measurement of global climatic parameters and their related trends are dependent on acquiring data in microclimate settings. Secondly, global climate change impacts differently in areas with different microclimates (Woods *et al.*, 2015). As a result, an understanding of how local micro-climate is changing and its associated factors will lead to a better understanding of the impacts of future global climate changes.

The characteristics of an urban climate can be summarized as the “five island effects”, namely, urban heat island (UHI), urban humid island, urban arid island, urban turbid island, and urban rainy island (Zhang *et al*., 2016). Among these characteristics, the urban heat island (UHI) is considered the most influential in terms of its effect on human and natural environment. UHIs have a particular influence on general discomfort, heat stroke, sunburn, dehydration and respiratory problems (EPA, 2016). UHIs significantly affect human health and well-being. For example, Tan *et al*. (2010) found evidence that the UHI effect resulted in heat-related mortality in Shanghai.

In general, the impacts of UHIs stated above are concentrated at a regional scale and, while the contribution of UHI intensities to the global climate change is debatable, it is true that UHIs may exacerbate heat load in cities if they are coupled with global warming (EPA, 2016). Therefore, how to minimize UHI intensities within a city is a key policy question (United Nations, 2016).

Bearing this in mind, a clear understanding of the relationship between urban growth and microclimate otherwise known, as UHI is therefore critical in terms of formulating effective planning policies to mitigate the UHI effect in cities

2. Literature Review

The trend towards urbanization is only accelerating and 96% of all urbanization by 2030 will occur in the developing world (UN, 2015). The built up urban land areas in these developing countries is expected to increase from the present 200,000km2 to 600,000 km2 in 2030 and the 400,000km2 increase will be equal to the world`s total combined urban area in 2004 (Payne *et al*., 2018). Progression in urbanization is considered as the most prominent driver of land cover changes in the history of human civilization (Adedokun, 2011).

Ecosystems concentrated most human impacts on environment and lead to many meteorological problems. One of them is urban heat island, which refers to the difference in temperature between the urban area and its surrounding non-urban areas due to urbanization (Ward *et al*., 2016).

Researches have long been done using different types of remote sensing data to derive land cover and UHI patterns, such as Landsat, ASTER, SPOT, and IKONOS (Hussain and Shan, 2015 and Li *et al*., 2016). Of these, Landsat (TM, ETM, OLI) provides the most commonly used remote sensing data, for three reasons:

a) They are freely available to researchers;

b) Their world-wide coverage with medium spatial resolution (30×30m); and

c) Their long-term temporal coverage (data are available since 1972) which enables researcher to monitor changes over a much needed longer time span (Zhang *et al*., 2013).

Study that have been conducted both globally and locally utilizing Landsat data to quantify the extent of LUCC and UHI include;Muthoka and Ndegwa (2014) studied the dynamism of land use changes on surface temperature over Kenya, focusing on Nairobi city. The study showed a

reduction in vegetation cover to bare land or built-up; an evidence of a growing city. Njoroge, Nda'Nganga, Wariara&Maina (2011) assessed the landscape change and occurrence at watershed level in city of Nairobi. The study observed significant changes in the spatial configuration of the landscape of Nairobi city between 1976 and the year 2000. According to the study, land use related to human activities such as built areas increased to the detriment of wetland and vegetated areas, signifying the city's growth. According to studies (e.g. Zhang *et al*., 1995, Schats and Kucharik, 2014), land surface reflectivity is one of the most important parameters that characterize the earth's radioactive regime and its impact on biospheric and climatic processes.

3. METHODOLOGY

STUDY AREA

Figure 1 shows Lokoja, Kogi State. Lokoja is located within longitudes 6°41'E and 6°45'E and latitudes 7° 45' N and 7° 51' N. It is the administrative headquarters (Capital) of Kogi State situated at the confluence of the Niger and Benue rivers within the lower Niger trough with an estimated area of 63.82 sq km. According to Ukoje*et al*. (2014), the actual urban area of Lokoja is defined by "The land use (designation of Lokoja Metropolitan Area) order of 2nd October, 1991". This makes all parcels of land within an 16 km radius of a circle around the Lokoja General Post Office located within the geographical coordinates of approximately 07°48' 05" N, 06°44′ 39"E to be part of the planning area of Lokoja Metropolitan Area. The planning area therefore encompasses portions of five Local Government Areas, which include Lokoja LGA (Lokoja Township), Kogi LGA (North East), Adavi LGA (South West), Ajaokuta LGA (South) and Bassa LGA (East). These areas include Lokoja as well as several small size localities within the 16 km radius.

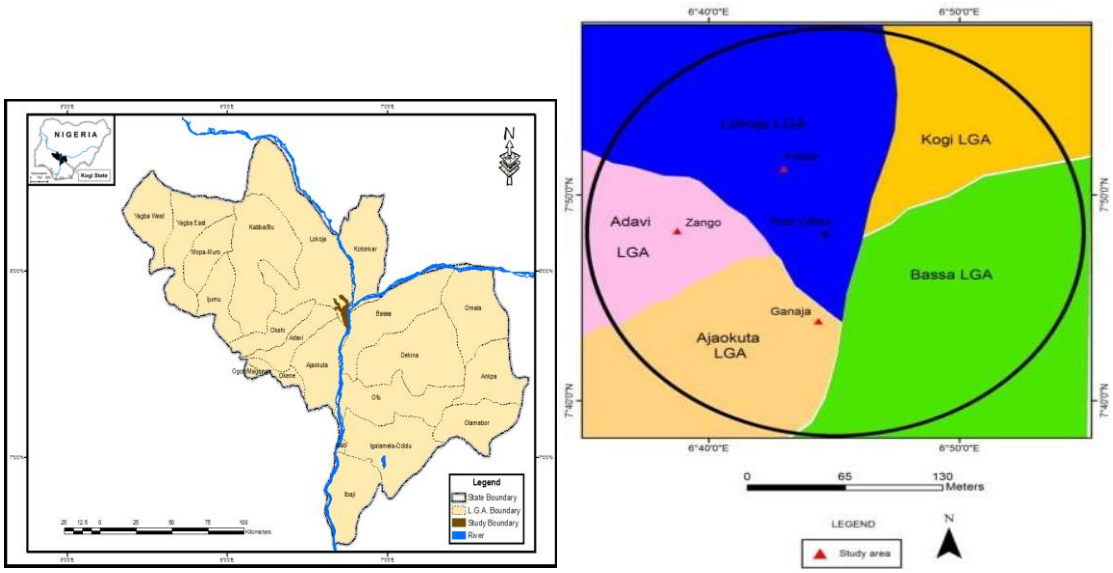

Figure 1. Map Of Nigeria Showing Kogi State And Map Of Lokoja Metropolitan Area

Source: Department of Lands and Survey, Kogi State Ministry of Works, 2018

METHODOLOGY

The Materials used for this study comprises both primary and secondary data. Furtherance to the objectives of this study, Ground control points (GCP) from ground truthing was collected as primary data using GPS handheld technology for creating signature or training site. Existing situation of the study area was reported partly from personal observation.

Landsat data; TM, ETM and OLI obtained from USGS were used in this study as describe earlier. Their properties are presented in Table1. Other geo-spatial data like Shapefiles, and base map of Lokoja were obtained from National Space Research and Development Agency (NSRDA) and land and survey department of the Kogi State ministry of works, lands, housing and urban development for extraction and delineation of area of interest.

Table 1: Satellite Data Used With Their Acquisition Dates

S/N	Sensor	Path / Row	Source	Date of acquisition	Scale/resolution
1	LANDSAT TM	189/054-055	GLCF	29 October 1990	30
2	ETM+	189/054-055	GLCF	31 October 2009	30
3	OLI	189/054-055	GLOVIS	31 December 2018	30

Source: Author's Analysis, 2018

*TM = Thermal Band, ETM+ = Enhance Thematic Mapper Plus and OLI = Operational Land Imager

DATAPREPARATION

LAND USE/COVER CHANGE DETECTION

The band 4,3,2 used for Landsat TM and ETM and band 5,3,2 used for Landsat 8 (OLI) were enhanced using histogram equalization, rectified to a common UTM coordinate system (WGS84). A supervised classification with support vector machine algorithm was conducted to classify the imageries. Training sample sets were collected based on ground truth data gathered during field checks. On completion it was run on mosaic.

LAND SURFACE TEMPERATURE ESTIMATION

After applying geometric and radiometric correction, the LST from Landsat images were estimated using thermal band 6 of Landsat TM/ETM and thermal band 11 of Landsat OLI based on the method adopted in (Lu *et al.*, 2014). This procedure is demonstratedin the equation 1, 2, 3, 4 and 5below.

Radiometric Calibrations

$$L_\lambda = \text{gain} \times DN + \text{bias} \quad (1)$$

Where;

L_λ is the normalized atmospheric reflectance at a particularwavelength.

I. Conversion to At Sensor Spectral Radiance (Qcal -to- Lλ)

$$L_\lambda = \left(\frac{LMAX_\lambda - LMIN_\lambda}{Q_{calmax} - Q_{calmin}} \right) \left(Q_{cal} - Q_{calmin} \right) + LMIN_\lambda \quad (2)$$

$L_\lambda = G_{rescale} \times Q_{cal} + B_{rescale}$

Where
L_λ= Spectral radiance at the sensor's aperture [W/(m2srμm)]

Q_{cal} = Quantized calibrated pixel value [DN]
Q_{calmin} = Minimum quantized calibrated pixel value corresponding to LMIN^ [DN_λ]
Q_{calmax} = Maximum quantized calibrated pixel value corresponding to LMAX) [DN_λ]
$LMIN_\lambda$ = Spectral at-sensor radiance that is scaled to Q_{calmin} [W/ (m^2sr μm)]
$LMAX_\lambda$= Spectral at-sensor radiance that is scaled to Q_{calmax} [W/ (m^2sr μm)]
$G_{rescale}$ = Band-specific rescaling gain factor [(W/ (m^2sr μm))/ DN]
$B_{rescale}$ = Band-specific rescaling bias factor [W/ (m^2sr μm)]

II. Conversion to TOA Reflectance (Lλ-to-ρλ)

$$\rho_\lambda = \frac{\pi \bullet L_\lambda \bullet d^2}{ESUN_\lambda \bullet \cos\Theta_s} \quad (3)$$

Where;

ρ_λ = Planetary TOA reflectance [no unit]
π = Mathematical constant approximately equal to 3.14159 [no unit]
L_λ = Spectral radiance at the sensor's aperture [W/ (m^2sr μm)]
d = Earth-Sun distance [astronomical units]
$ESUN_\lambda$ = Mean of exo-atmospheric solar irradiance [W/ (m^2 lam)]
Θ_s = Solar zenith angle [degrees]

III. Conversion to At-sensor Brightness Temperature (L λ -to- T)

$$T_B = \frac{K_2}{\ln\left(\frac{K1}{L\lambda} + 1\right)} \quad (4)$$

Where T_B is the at-sensor brightness temperature in Kelvin; L_λ equals TOA radiance and K_1= 607.76 W/ (m^2sr μm) and K_2=1260.56 W/ (m^2srμm) are pre-launch calibration constants. The generated brightness temperature values as derived from the above equation will then be converted to emissivity-corrected LST in Kelvin using the following equation:

$$T_S = \frac{T_B}{1 + [(\lambda \times T_B / \propto]\text{In}\in} \quad (5)$$

Where λ is the wavelength of emitted radiance equals 11.5 μm; α = hc/b (1.438×10^-2 mk); b refers to Boltzman constant as 1.38 × 10^-23 J/K; h is the Planck's constant 6.626× 10^-34 JS; C refers to the velocity of light 2.998× 10^8 m/s; and ε is the surface emissivity.

The calculated temperature in Kelvin was then converted into centigrade for ease of interpretation by subtracting 272.15 from the result, which is the conversion rate of kelvin to Celsius.

ENVIRONMENTAL CRITICALITY

In order to identify the level of combined environmental criticality in Lokoja metropolis based on LST and the density of Built-up area, Environmental criticality index was employed. This index not only measures the extent of impact that may affect the environment but as well quantify the degree and magnitude of impact that a particular area may receive based on the degree of the combined values or magnitude of the input layers.
The Environmental Criticality index based on land use/land cover was carried out using equation 6.

$$ECI = \frac{LST}{LULC} \quad (6)$$

Where;

ECI = environmental criticality index

LST = land surface temperature
LULC = land use land cover

4. RESULTS AND DISCUSSION

EXTENT OF LANDUSE AND LAND COVER DYNAMICS

Table 2 shows the Land use and land cover dynamics of Lokoja metropolis from 1990 to 2018and the changes they had undergone within the span of 28 years.

From the classified Landsat imageries of 1990, 2010 and 2018, four-land uses/cover were identified. The different land use types as observed in the study area showed significant increase during the study period with the exception of bare soil and vegetation cover. There was a negative annual rate of change i.e. a reduction in both bare soil and vegetation each year by -2.65km^2 and -5.26 km^2 respectively. This can be attributed to the rural–urban migration and transformation of the new capital city, hence, built-up area increased by 7.52km^2. It is evident that the effect of Lokoja's expansion was on vegetation cover and bare soil. The increase witnessed in built-up area is an indication of the continuous influx of people into Lokoja metropolis due to its status as an administrative headquarters.

Table 2: Land Use/Land Cover Classification (1990-2018)

LULC Class	**Area (km^2) 1990**	**Area (km^2) 2010**	**Area (km^2) 2018**	**Change in extent (km^2)**	**Annual rate (km^2)**
Built-up area	30.78	70.32	241.43	210.65	7.52
Vegetation	274.79	226.75	127.53	-147.26	-5.26
Water body	36.50	56.73	47.26	10.76	0.38
Bare soil	463.83	452.11	389.69	-74.14	-2.65
Total	**805.91**	**805.91**	**805.91**		

Figures 2, 3 and 4 shows the LULC distribution over LokojaMetropolis for the years of 1990, 2010 and 2018 respectively. As observed from the map, the proportion of built-up areas has steadily increased while bare soil and vegetation has decreased in terms of area coverage.

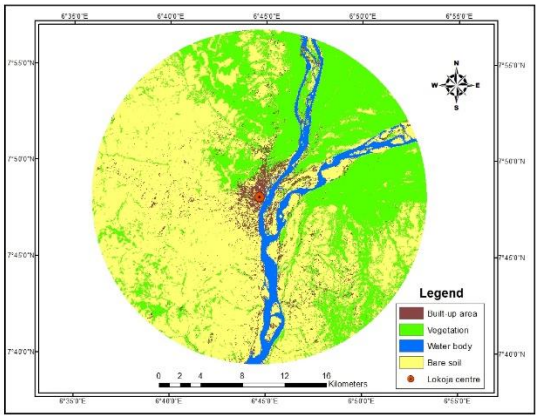

Figure 2. LULC of Lokoja Metropolis In 1990

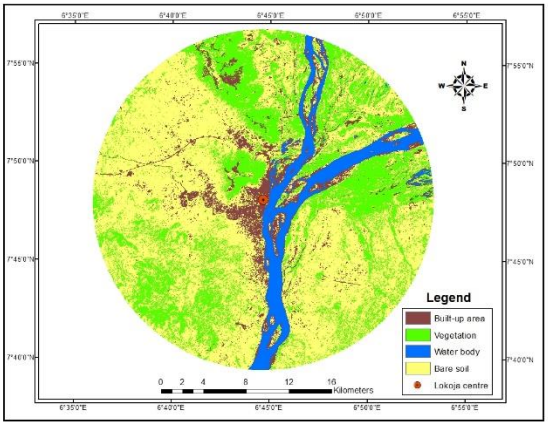

Figure 3.LULC Of Lokoja Metropolis In 2010

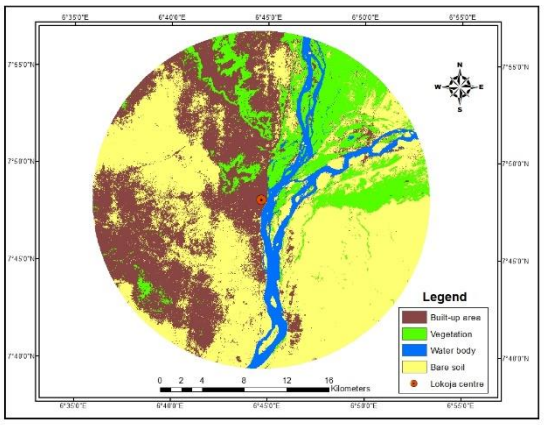

Figure 4.LULC Of Lokoja Metropolis In 2018

LAND SURFACE TEMPERATURE OF LAND USE AND LAND COVER TYPES

Table 3 shows the average values of surface radiant temperature for each of the land use/cover type in 1990, 2010 and 2018. It is clear that for the three epochs, built up area exhibits the highest surface radiant temperature (22.50˚C in 1990, 39.03℃ in 2010 and 31.40℃ in 2018), and followed by bare soil (24.43 ˚C in 1990, 38.20℃ in 2010 and 29.90 ˚C in 2018). The implication of this is that the increase in non-evaporating and non-transpiring surfaces such as stone, metal and concrete brings up the surface radiant temperature. The lowest radiant temperature in 1990 is exhibited by water body (18.21℃), and followed by vegetation (20.07℃). This pattern differs in 2010 where vegetation cover exhibited 32.56℃ and water bodies exhibited 27.92℃. The trend continued into 2018. From this study, the resulting mean surface of temperatures for the 1990, 2010 and 2018 are 21.30℃, 34.43℃ and 28.48℃ respectively.

Table 3: Land Use and Land Cover Class Temperature (1990-2018)

LULC Class	Mean Surface Temperature of LULC Class (˚C)				Average of Change over 28 years (˚C)
	1990	**2010**	**2018**	**Change**	
Built-up	22.50	39.03	31.40	8.90	
Vegetation	20.07	32.56	26.83	6.76	**7.18**
Water body	18.21	27.92	25.80	7.59	
Bare soil	24.43	38.20	29.90	5.48	
Mean Land Surface Temperature	**21.30**	**34.43**	**28.48**		

It is evident from Table 3 that vegetation covers had shown a considerably low radiant temperature in the three epochs, because dense vegetation can bring about a decrease in the amount of heat stored in the soil and surface structures through transpiration. The exposed bared soil showed a significant increase in temperature over vegetation. In effect surface soil water and vegetation contributed to the broad variation in the surface radiant temperatures of both vegetation cover and bare soil. Land use and land cover changes do have intense effect on the surface radiant temperature of a location.

Figures 5, 6 and 7 shows the map of LST distribution over LokojaMetropolis for the years of 1990, 2010 and 2018 respectively.The resulting GIS analysis showed that land use and land cover changes witnessed in Lokoja town are due to conversion of vegetation cover to other land use and land cover types within the study period and this had given rise to an average increase of 7.18℃ in surface radiant temperature. The implication here is that with the annual rate of increase of the built-up area (190.5%) and annual rate of decline of vegetation cover (22.6%), surface radiant temperature will be on the increase and this may create an environment for urban heat island. This agreed with Adebayo (2010) in his research that urban heat island were always created in the urban centers partly due to the nearly absence of vegetation covers.

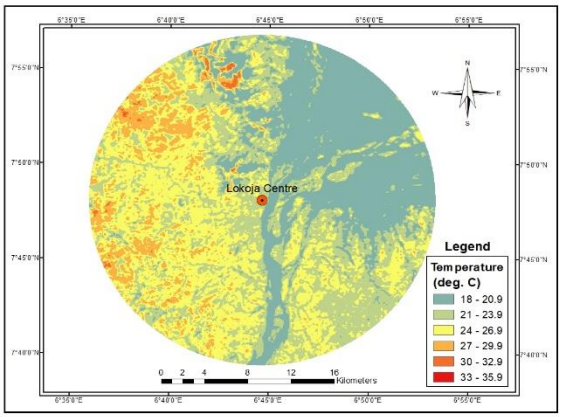

Figure 5.LST of Lokoja Metropolis In 1990

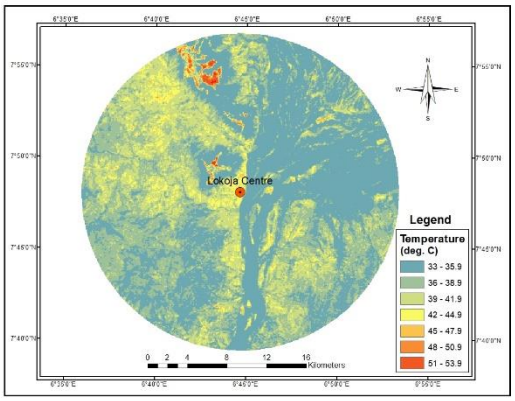

Figure 6.LST of Lokoja Metropolis In 2010

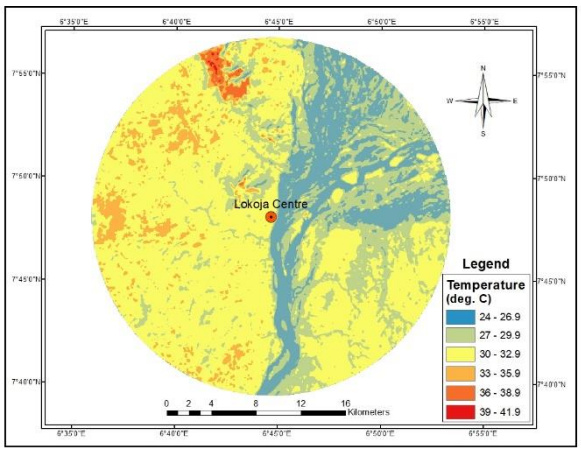

Figure 7.LST of Lokoja Metropolis In 2018

RELATIONSHIP BETWEEN LST ANDLANDUSE LAND COVER

Figure 8 shows the environmental criticality index based on LST and LULC. The spatial patterns of slopes extracted from the ECI model reveal rather interesting spatial variations. It can be observed from the figure 8 that the denser the buildings in an area, the higher the LST and the severe the UHI and vise-versa. Note, however, that the intensity of such influence is different for different areas. For example, the impact of LCC on UHI is stronger in southeast and nearby areas in Lokoja. However, the resultant ECI layer highlight the existence of UHI in the study area; where urban areas fall within severe to high criticality level while suburbs fall within moderate level and surrounding rural and bare land areas fall within low to non-level criticality. The changes in LST coincide with the corresponding changes of built-up area is an indication of the presence of urban heat island in the area. The two parameters show significant relationship in same direction throughout the years as observed in the study. The results in this research showed the association between UHI and land cover. It therefore implies that increase of UHI through LC changes is resulted from replacing vegetation areas with impervious surface areas (i.e. urban expansion) (Morini*et al.*, 2016). This is because impervious surfaces are low albedo features and thereby reflect a small amount of solar radiation while absorbing the rest (see the literature review for more details). This characteristic of impervious surface areas lead to increase of LST and thereby UHI. This confirmed the causal mechanism criterion.

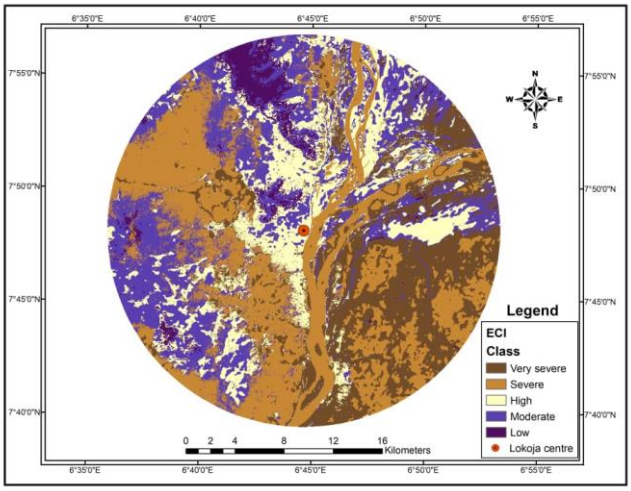

Figure 8. Environmental Criticality Index based on LST and LULC

5. CONCLUSION

The result of the work shows that urbanization processes majorly contributed to land use/cover change in Lokoja. This rapid urbanization is highly related to the administrative functions, socio-economic and industrial potentials of the city.

The spatio-temporal pattern of UHI in Lokoja metropolis was found to be in line with the amount of land cover changes in Lokoja for the three epochs i.e. the rate of conversion and transformation of land use types such as the increasing built up at the expense of vegetation is one of the contributing factor to the increase in the urban heat island temperature.

The environmental criticality index (ECI) investigation indicated that the UHI effect is influenced by land cover patterns, but the density of built-up area has a significant role in increasing UHI. Thus, it can be concluded that changes in UHI intensity is a function of LCCs particularly changes in built-up density. Recommendations include

1. For cities to promote sustainable development and redress the problems associated with rapid urbanization, it is recommended that monitoring systems through reliable data like Remote Sensing and GIS should be adopted as tools, which will enable planners and decision makers, arrest problems before they occur, as well as manage changes in dynamic environments.

2. Urban expansion can be directed in a desirable and sustainable way through protecting the vegetation cover, which always serves as the ecosystem service provider to the urban centers and also, policy makers should incorporate afforestation and establishments of green belts and parks into the urban planning schemes.
3. In this research, the relationship between UHI and LCC were established using ECI unlike previous studies that utilized ordinary least square method (OLS). Overall, the above findings bear research implication. It is then suggested that future studies should employ ECI that is geographic in nature rather than global models such as OLS to understand the relationship between UHI and its explanatory factors.

REFERENCES

Adebayo W.O (2010) The Human Environment: Something to Everyone, University of Ado-Ekiti; *The TwentyNineth Inaugural Lecture* 75pg.

Adedokun, M. (2011) "An analysis of spatial pattern of urban activities in a traditional African city: a case study of Ilorin, Nigeria." *European Journal of Humanities and Social Sciences* 10, no. 1: 408-421.

Aderamo A.J. (2010). Changing Structure of intra-urban road network in Ilorin Nigeria (1960-2000). Ilorin Journal of Business and social sciences vol. 8 Nos, 182 pp 65-76 MJT press.

EPA. 2016. *Heat Island Impacts*. United States Environmental Protection Agency: Available: http://www.epa.gov/hiri/impacts/index.htm [Accessed 11/04/2018].

Hogan, M. 2012.*Microclimate*. The Encyclopedia of Earth Available: http://editors.eol.org/eoearth/wiki/Microclimate [Accessed 4/04/2018].

Hussain, E. & Shan, J. 2015. Object-based urban land cover classification using rule inheritance over very high-resolution multisensor and multitemporal data. *GIScience& Remote Sensing***,** 1-19.

Ibrahim R. Babatunde, Adetona N. Adewale&Olawoyin O. Rachael (2014). "Correlates of Urbanization and House Rent in Ilorin, Nigeria".*Global Journal of Science Frontier Research: (H) Environment &Earth Science*. Volume 14, Issue 2, Version 1.0. Global Journals Inc. (USA). Pg. 33-38.

Li, X., Li, W., Middel, A., Harlan, S., Brazel, A. & Turner, B. 2016. Remote sensing of the surface urban heat island and land architecture in Phoenix, Arizona: Combined effects of land composition and configuration and cadastral–demographic–economic factors. *Remote Sensing of Environment*, 174**,** 233-243.

Lu, D., Song, K., Zang, S., Jia, M., Du, J. &Ren, C. 2014. The Effect of Urban Expansion on Urban Surface Temperature in Shenyang, China: An Analysis with Landsat Imagery. *Environmental Modeling & Assessment*, 20**,** 197-210.

Morini, Elena &Touchaei, Ali &Castellani, Beatrice & Rossi, Federico &Cotana, F. (2016). The Impact of Albedo Increase to Mitigate the Urban Heat Island in Terni (Italy) Using the WRF Model. Sustainability. 8. 999. 10.3390/su8100999.

Muthoka M.J., Ndegwa M.C., 2014. Dynamism of Land Use Changes on Surface Temperature in Kenya: A Case Study of Nairobi City. *International Journalof Science and Research*, 3, 38-41. ID: 020131389

Njoroge J.B.M., Nda'Nganga K., Wariara K., Maina M.G., 2011. Characterising changes in urban landscape of Nairobi city, Kenya.*ActaHorticulturae*, 911, 537–543.http://dx.doi.org/10.17660/ActaHortic. 2011.911.63,

Onibokun, A. G. (1997). Nigerian cities in the Twenty first century.*Being a lecture delivered at the 1997 world habitat day celebration.* CASSAD: Nigeria.

Reinhard, M. Y., S. (2011). Impacts of urbanization on urban structures and energy demand: What can we learn for urban energy planning and urbanization management?*Urban & Regional Planning.Sustainable cities and society (1) 45-53.*

Schats J., Kucharik J.C., 2014. Seasonality of the Urban Heat Island Effect in Madison, Wisconsin.*Journal of Applied Meteorology and Climatology,* 53, 2371-2386. DOI: 10.1175/JAMC-D-14-0107.1

Tan, J., Y. Zheng, X. Tang, C. Guo, L. Li, G. Song, X. Zhen et al. 2010. "The Urban Heat Island and Its Impact on Heat Waves and Human Health in Shanghai." International Journal of Biometeorology 54: 75–84.doi:10.1007/s00484-009-0256-x.

Tanko I. A, Suleiman Y. M, Yahaya T. I. and Kasim A. A. 2017. Urbanization Effect on the Occurrence of Urban Heat Island over Kano Metropolis, Nigeria.*International Journal of Scientific & Engineering Research* Volume 8, Issue 9, September-2017 293 ISSN 2229-5518

Ukoje JE, Makanjuola MI, Oluleye EK (2014). Analysis of Urban Expansion and Land Use Land Cover Change in Lokoja, Nigeria. Paper Presented at the Second Regional Conference on Remote Sensing and Geographical Information Systems Applications: Space Based Technology for Disaster Management and Mitigation, held at the Federal University Lokoja, Kogi State, Nigeria. November 10th- 13th, 2014

UNDESA (United Nations Department of Economic and Social Affairs). 2014. *World UrbanizationProspects: 2014 Revision.* New York: United Nations Department of Social and Economic Affairs.

United Nations. 2015. *Transforming our World: The 2030 Agenda for Sustainable Development*. United Nations: New York, NY.

United Nations. 2016. *Sustainable Solutions for an urban future*. Available: http://www.un.org/sustainabledevelopment/blog/2015/04/over-100-mayors-adopt-declaration-to-combat-climate-change-support-sustainable-cities/ [Accessed 20/04/2018].

Woods, H. A., Dillon, M. E. &Pincebourde, S. 2015. The roles of microclimatic diversity and of behavior in mediating the responses of ectotherms to climate change. *Journal of Thermal Biology,* 54**,** 86-97.

WHO (2013). Annual report 2013. WHO Centre for Health Development, Kobe, Japan.

Zhang, H., Qi, Z.-F., Ye, X.-Y., Cai, Y.-B., Ma, W.-C. & Chen, M.-N. 2013. Analysis of land use/land cover change, population shift, and their effects on spatiotemporal patterns of urban heat islands in metropolitan Shanghai, China.*Applied Geography*, 44**,** 121-133.

Zhang Y.C., Rossow W.B., Lacis A.A., 1995. Calculation of surface and top of atmosphere radiative fluxes from physical quantities based on ISCCP data sets, 1., Method and sensitivity to input data uncertainties.*Journal of Geophysical Research*, 100, 1149-1165. DOI: 10.1029/94JD02747

Sensitivity of the Guinea and Sudano-Sahelian Ecological Zones of Nigeria to Climate Change

Salihu, A. C.[1*], Abdulkadir, A.[1], Nsofor, G. N.[1]

Suleiman, Y. M.[1], Ojoye, S. and Otache, M. Y.[2]

[1]Department of Geography, Federal University of Technology, Minna, Nigeria

[2]Department of Agricultural and Bioresources Engineering, Federal University of Technology, Minna, Nigeria

[1*]asalihuc@gmail.com

* Corresponding author

Abstract

The aim of this study is to assess the sensitivity of Guinea and Sudano-Sahelian Ecological Zones of Nigeria to climate change. Data used comprises of observed and simulated temperature and precipitation data. The observed data are that of Climate Research Unit (CRU TS 4.2) and the simulated data are that of CMIP5 both found in the Royal Netherland Meteorological Institute archive Known as KNMI database. Climate change analysis was performed based on three IPCC's scenarios. Three climatic periods of (2019-2048), (2049-2078) and (2071-2100) with reference to two baseline periods of (1959-1988) and (1989-2018) were considered. Findings reveal that Guinea and Sudano-Sahelian Ecological Zones of Nigeria is highly sensitive to climate change. This is noticed from the rise in temperature from 1^{o}C in the first climatic period (2019-2048) to as high as 6^{o}C in the third climatic period (2071-2100). Similar trend was observed for rainfall where there is increase in rainfall amount from 0.5mm/day to 2.5mm/day. This anticipated condition has serious implications on water resources, from increase in stream flow, rise in reservoirs, soil moisture changes and flooding.

Keywords: Sensitivity, Climate change, Ecological zones,

1. Introduction

It is known and established in literature that there is intrinsic relationship between climate change and water resources. This is even more so as empirical studies in recent past have shown the impact of the former on the later (Hagemann *et al.*, 2013 and Adam *et al.*, 2016). Water resources of the world in general and in Nigeria are under heavy stress due to increased impact of climate change but the severity of the impact varies from one region to another. According to the Intergovernmental Panel on Climate Change (IPCC) (2014), climate change is defined as "change in the state of the climate that can be identified (e.g. using statistical tests) by

changes in the mean and/or the variability of its properties, and that persists for an extended period, typically decades or longer". It refers to any change in climate over time, whether due to natural variability or as a result of human activity. This usage differs from that in the United Nations Framework Convention on Climate Change (UNFCCC), where climate change refers to a "change of climate that is attributed directly or indirectly to human activity that alters the composition of the global atmosphere and that is in addition to natural climate variability observed over comparable time periods". However, this study adopts IPCC (2014) definition.

Climate change is increasing the frequency and severity of extreme hydrological events such as floods and droughts around the world (Guoyong *et al.,* 2016).Water is an indispensable element of life; the water resources of river basins are highly dependable and sensitive to climate variability and change; due to inter-connection between the climate system, hydrological cycle and water resources system. Thus, if the trends in climate contexts that took place over the last three decades continue to prevail unabatedly, West Africa will no doubt experience decreased freshwater availability (Ayansina *et al.,* 2018). Also, compared to previous decades, it is observed that since the early 1970s, the mean annual rainfall has decreased by 10% in the wet tropical zone to more than 30% in the Sahelian zone while the average discharge of the region's major river systems dropped by 40 to 60% (Yunana *et al.,* 2017). This sharp decrease in water availability will be complicated by greater uncertainty in the spatial and temporal distribution of rainfall and surface water resources (Guoyong *et al.,* 2016).

2. Literature Review

Climate change is a burning issue of the 21st century and its attendant consequences on different environmental components cannot be under estimated. A range of related literature has been reviewed. Gebre and Ludwig (2015) assessed the hydrological response of climate change of four catchments of the upper Blue Nile River basin in Ethiopia using new emission scenarios based on IPCC fifth assessment report (AR5). The future projection period were divided into two future horizons of 2030`s (2035-2064) and 2070`s (2071-2100). All the five GCMs projection showed maximum and minimum temperature increases in all months and seasons in the upper Blue Nile basin. The change in magnitude in RCP8.5 emission is more than RCP4.5 scenario as expected. There is considerable average monthly and seasonal precipitation change variability in magnitude and direction. Ahmed *et al.* (2017) assessed climate change impact on surface water resources in the Rheraya catchment, Morocco. An ensemble of five regional climate models from the Med-CORDEX initiative was considered to

evaluate future changes in precipitation and temperature, according to the two emissions scenarios RCP4.5 and RCP8.5. The future projections for the period 2049–2065 under the two scenarios indicate higher temperatures (+1.4°C to +2.6°C) and a decrease in total precipitation (−22% to −31%). Gneneyougo *et al.* (2017) examined climate change and its impact on water resources in the Bandama Basin, Côte D'ivoire. Simulation results for future climate from HadGEM2-ES model under representative concentration pathway RCP4.5 and RCP8.5 scenarios indicate that the annual temperature may increase from 1.2°C to 3°C. These increases will be greater in the north than in the south of the basin. The monthly rainfall may decrease from December to April in the future. During this period, it is projected to decrease by 3% to 42% at all horizons under RCP4.5 and by 5% to 47% under RCP8.5.

Furthermore, Adefisan (2018) analysed climate change impact on rainfall and temperature distributions over West Africa from three IPCC Scenarios. The analysis considered two climatic periods which are 2000 to 2029 as present and 2070 to 2099 as future. The result showed that temperature increases over West Africa countries in all the months under each of the scenarios. Scenario A2 with the highest emission of 800 ppm shows the highest increase of temperature and rainfall over West Africa followed by scenario A1B with emission of 720 ppm and the least is that of B1 with the lowest emission of 550 ppm. The result also showed that rainfall increases over most part of West Africa in all the scenarios with the exception of coastline that a little decrease in amount of rainfall was estimated. Xiaoli *et al,* (2018) investigated potential impact of climate change to the future stream flow of Yellow River Basin based on CMIP5 data in China. During future period of 2021–2050, the seasonal precipitation presents a slightly increasing trend in spring and autumn, while a very slightly decreasing trend with the rate of 2.99 mm/day a in summer. During the period of 2021–2050, the basin average temperature shows an obviously increasing for two RCPs. The changing rate of seasonal temperature for RCP8.5 more than 0.4°C, which is higher than that of RCP4.5. Minsung *et al,* (2019) examined change in extreme precipitation over North Korea using multiple climate change scenarios. A comparison of regional averages in each future relative to the reference period showed that precipitation with a 20-year frequency precipitation was projected to increase as much as 43.4mm/year under RCP4.5 and 80.7mm/year under RCP8.5 in comparison with the reference period. Ruotong *et al,* (2019) evaluated the multi-model projections of climate change in different RCP scenarios in an Arid Inland Region, Northwest China. The maximum air temperature simulated by different GCMs exhibited an increasing trend in all the three RCP scenarios at different time scales, and the increase in autumn was the most obvious with a maximum amplification of 2.8°C. In contrast, the projected largest

increase in the seasonal minimum air temperature occurred in summer, with the highest amplification of 2.5ºC.

The conclusion drawn from this review is that most of these studies undertaken at local scale in different countries are in tandem with global trend of continuous increase in temperature and evapotranspiration with a decrease in rainfall and surface runoff. However, the rate of change varies from one location to another. More so, the change in climatic elements has led to manifestation of extreme events such as drought and flood. Consequently, there is need to continuously undertake research in this area in order to unearth the likely impact of climate change. This will help in advancing timely adaptation strategies, mitigation measures and formulation of policies to tackle the effect of climate change. Hence, the aim of this study is to assess the sensitivity of Guinea and Sudano-Sahelian Ecological Zones of Nigeria to climate change.

3. Methodology

The study area lies between Longitudes 3°E to 15°E of the Greenwich meridian and Latitudes 8°N to 14°N of the equator. The area covers the Guinea and Sudano-Sahelian Ecological Zones of Nigeria. It is bordered to the north by Niger Republic, to the east by Republic of Cameroun, to the south by the tropical rainforest and to the west by Benin Republic (Figure 3.1). The two predominant air masses that influence the weather and climate of these zones are Tropical Continental (cT) air mass and Tropical Maritime air mass (mT) (AbdulKadir *et al.*, 2015). The former is dry and dusty which originates from Sahara desert, while the later is dense and moist which originates from Atlantic Ocean. The rainfall distribution shows a mean of 1100mm/year

around the Guinea to about 700mm/year in the Sahel zone. The temperature show a range of 24°C to 30°C in Guinea to as high 44°C in the Sahel zones (Abdussalam, 2017).

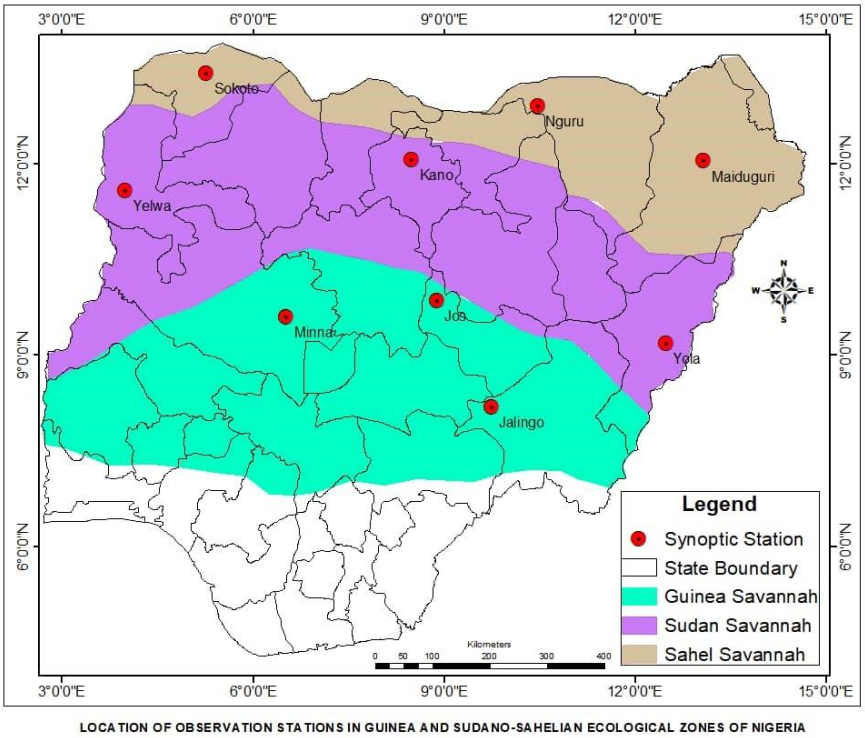

Figure 3.1: Study area

The present study concentrated on three basins namely: Kainji Lake Basin (KLB), Sokoto – Rima Basin (SRB) and Komadugu – Yobe Basin (KYB) spread across the Guinea and Sudano-Sahelian Ecological Zones of Nigeria. The daily temperature and precipitation data used were from archive of Royal Netherland Meteorological Institute Known as KNMI Climate Explorer. It comprises of observed and simulated temperature and precipitation data. The observed data are that of Climate Research Unit (CRU TS 4.2) and the simulated data are that of CMIP5 both found in the KNMI database. The respective coordinates of each basin was used to derive the observed and simulated rainfall and temperature records.

Climate change analysis was performed based on three IPCC's scenarios. These scenarios are RCP8.5, RCP4.5 and RCP2.6 as defined by Intergovernmental Panel on Climate Change (IPCC) Fifth Assessment Report. Three climatic periods of (2019-2048), (2049-2078) and (2071-2100) with reference to two baseline periods of (1959-1988) and (1989-2018) were considered. The sensitivity of each basin based on changes in rainfall mm/day and temperature in degree Celsius were then studied and compared. Seasonal changes of the dry season (November, December, January, February, March and April) denotes as NDJFMA, and wet season (May, June, July, August, September and October) denotes as MJJASO and were computed and compared for each of the three IPCC scenarios. The computation is as follows:

$$PI_1 = \left(\frac{t_n}{t_0}\right) 100 \quad (1)$$

Where PI_1 = percentage impact for temperature t_n = temperature under a given scenario

t_0 = temperature of the reference period 100 = percentage

PI_2 is computed from the equation:

$$PI_2 = \left(\frac{p_n}{p_o}\right) 100 \quad (2)$$

Where PI_2 = percentage impact for rainfall p_n = precipitation under a given scenario

p_o = precipitation from the reference period 100 = percentage

4. Results and Discussion

4.1: Evaluation of models performance for temperature and rainfall

The veracity of the CMIP5 multi-model ensemble mean simulation compare with observed rainfall and temperature in the Guinea and Sudano-Sahelian Ecological Zones of Nigeria was evaluated using statistical metrics. The metrics are root mean square error (RMSE), mean absolute error (MAE) and Nash-Sutcliffe efficiency (NSE) see table 4.1. The results indicate that for seasonal dry temperature, Sokoto – Rima Basin (SRB) has the highest error between the simulated and observed seasonal dry temperature given as RMSE (1.55)and MAE (1.45) while Kainji Lake Basin (KLB) has the least error given as RMSE (1.14) and MAE (1.05). As for NSE, KLB has the highest value (0.94) follow by Komadugu – Yobe Basin (KYB) (0.89) and then SRB (0.86). This implies that the CMIP5 multi-model ensemble mean is better able to reproduce the seasonal dry temperature in KLB than in the KYB and SRB respectively. Seasonal wet temperature in KYB has the highest error between the simulated and observed seasonal wet temperature given as RMSE (0.65)and MAE (0.55) while SRB has the least error given as RMSE (0.57) and MAE (0.55). As for NSE, all the three basins have the same value each given as (0.98). This implies that the CMIP5 multi-model ensemble mean reproduce the same seasonal wet temperature across the three basins.

Table 4.1 Evaluation metrics between historical observed and simulated seasonal temperature and rainfall (1959 – 1988)

TEMPERATURE	KLB			SRB			KYB		
	RMSE	MAE	NSE	RMSE	MAE	NSE	RMSE	MAE	NSE

Seasonal Dry	1.14	1.05	0.94	1.55	1.45	0.86	1.14	1.10	0.89
Seasonal Wet	0.60	0.55	0.98	0.57	0.55	0.98	0.65	0.55	0.98
RAINFALL									
Seasonal Dry	0.32	0.30	0.99	0.17	0.16	0.99	0.13	0.12	1
Seasonal Wet	1.29	1.05	0.94	0.78	0.60	0.98	0.96	0.95	0.96

Source: Author's Computation, 2019

Seasonal dry rainfall in KLB has the highest error between the simulated and observed seasonal dry rainfall given as RMSE (0.32)and MAE (0.30) while KYB has the least error given as RMSE (0.13) and MAE (0.12). As for NSE, KYB has the highest value (1.0) denoting perfect reproduction of seasonal dry rainfall in the basin. KLB and SRB have the least NSE value each (0.99). This implies that the CMIP5 multi-model ensemble mean is better able to reproduce the seasonal dry rainfall in KYB than in KLB and SRB. Seasonal wet rainfall across these basins reveals that KLB has the highest error between the simulated and observed seasonal wet rainfall given as RMSE (1.29)and MAE (1.05) while SRB has the least error given as RMSE (0.78) and MAE (0.60). As for NSE, SRB has the highest value (0.98) follow by KYB (0.96). This implies that the CMIP5 multi-model ensemble mean is better able to reproduce the seasonal wet rainfall in SRB than in the KYB and KLB respectively. On a general note, despite the variations in the ability of the CMIP5 multi-model ensemble mean to reproduce seasonal dry and wet temperature and rainfall across the three basins, the errors between the observed and simulated are within the acceptable threshold. The error mergins for temperature (0.57 - 1.55) and rainfall (0.13 - 1.29) are in tandem with (1.78 - 2.10) reported by Vera and Díaz (2013) for South America and also consistent with those found in most regions of the world (Kumar *et al.*, 2014). NSE of (0.8) threshold is in the range of 'very good values' as recommended by Moriasi *et al*. (2007) cited in (Miguel *et al.*, 2018) for general performance ratings. Thus, we can conclude that these CMIP5 multi-model ensemble mean is good at simulating the precipitation and temperature in Guinea and Sudano-Sahelian Ecological Zones of Nigeria.

4.2: Projected changes in seasonal temperature: dry season (NDJFMA)

The spatial distribution of seasonal dry **(**NDJFMA**)** temperature over KLB, SRB and KYB are shown on (figure 4.1 and 4.2) respectively. The first column is the projection for the first baseline period (1959-1988) while the second column is the projection for the second baseline

period (1989-2018). The first, second and third row is respectively for (2019-2048), (2049-2078), and (2071-2100) future climatic periods. It is observed that temperature will increase from the first climatic period to the third climatic period with reference to the first and second baselines of (1959-1988) and (1989-2018) respectively in the KLB, SRB and KYB. Looking at the differences between first climatic period (2019-2048) and third climatic period (2071-2100) it shows that base on (1959-1988) baseline, seasonal dry temperature in KLB will increase for RCP8.5 from (1^{o}C to 5.8^{o}C), RCP4.5 from (1^{o}C to 2.5^{o}C) and RCP2.6 from (1^{o}C to 1.5^{o}C).

1959 – 1988 Baseline **1989 – 2018 Baseline**

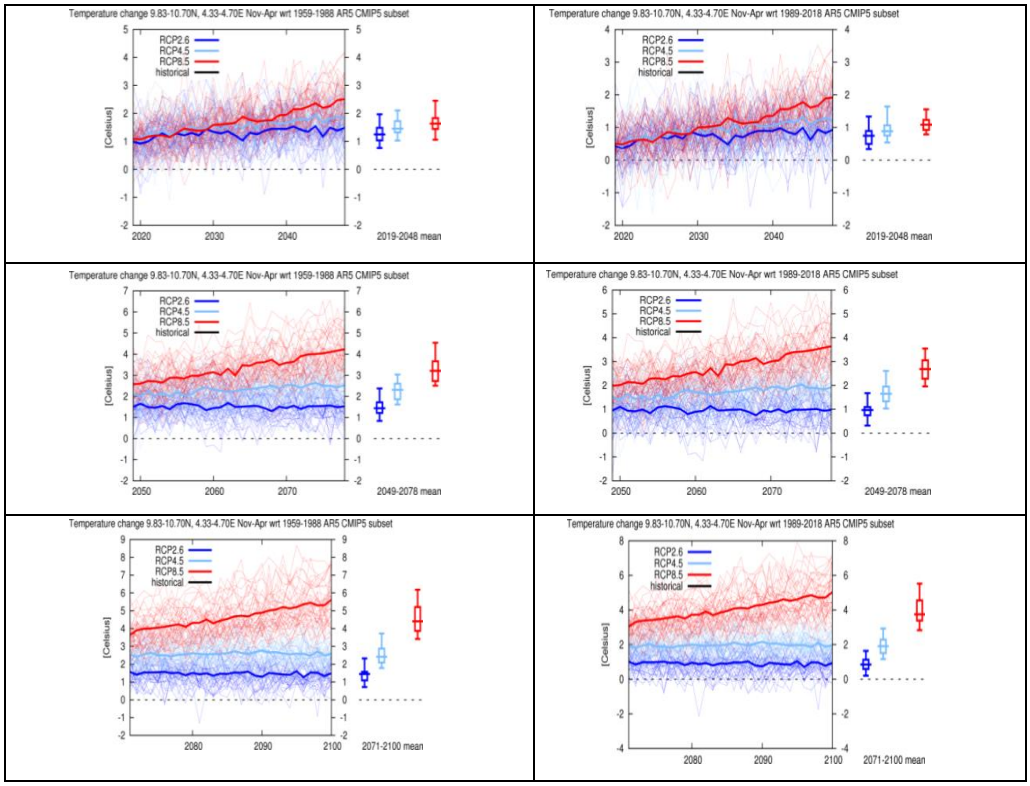

Figure: 4.1 Projected changes in seasonal temperature: dry season (NDJFMA) relative to (1959 – 1988) and (1989 – 2018) baselines for KLB

SRB **KYB**

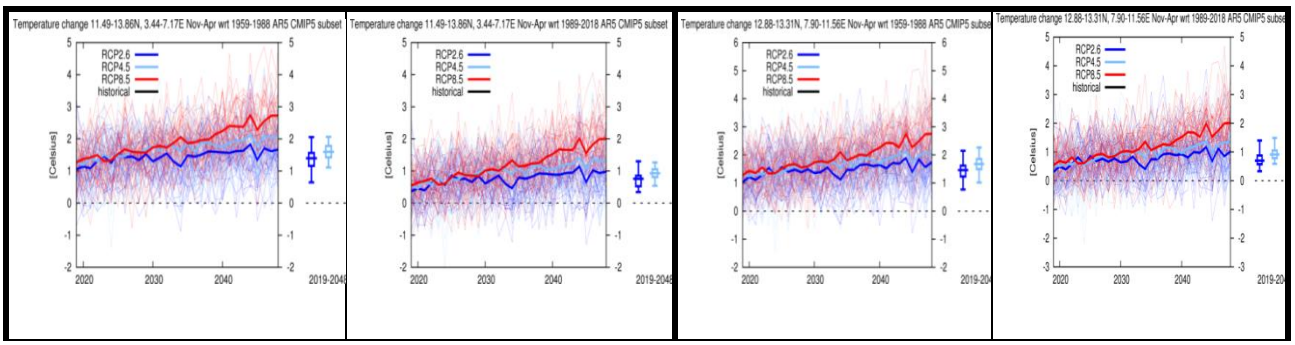

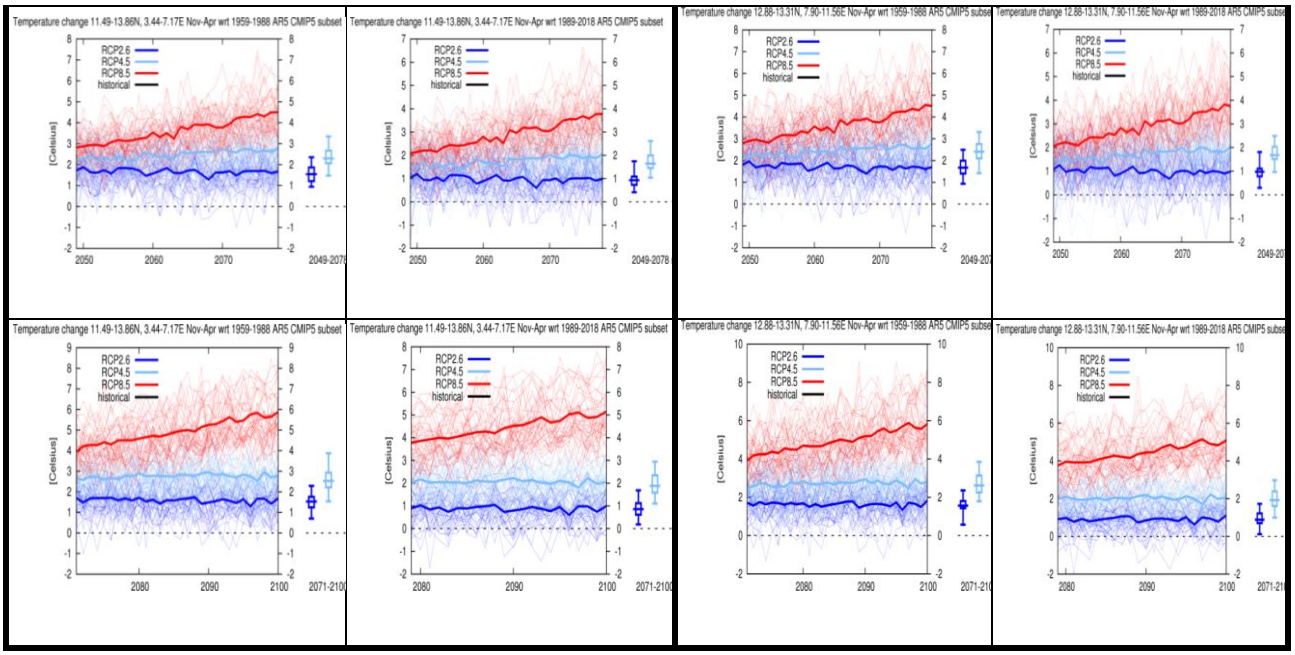

Figure: 4.2 Projected changes in seasonal temperature: dry season (NDJFMA) relative to (1959 – 1988) and (1989 – 2018) baselines for SRB and KYB

The respective values of these for (1989-2018) baseline are RCP8.5 from (0.4ºC to 5ºC), RCP4.5 from (0.5ºC to 2ºC) and RCP2.6 remain as (0.5ºC). As for the SRB it reveal that base on (1959-1988) baseline, seasonal dry temperature will increase for RCP8.5 from (1.2ºC to 5.9ºC), RCP4.5 from (1ºC to 2.9ºC) and RCP2.6 from (1ºC to 1.8ºC). The respective values of these for (1989-2018) baseline are RCP8.5 from (0.4ºC to 5.1ºC), RCP4.5 from (0.4ºC to 2ºC) and RCP2.6 from (0.4ºC to 1ºC). Similarly, those for KYB show that base on (1959-1988) baseline, seasonal dry temperature will increase for RCP8.5 from (1.2ºC to 5.9ºC), RCP4.5 from (1.2ºC to 2.8ºC) and RCP2.6 from (1.2ºC to 1.9ºC) in the KLB. The respective values of these for (1989-2018) baseline are RCP8.5 from (0.5ºC to 5ºC), RCP4.5 from (0.5ºC to 2ºC) and RCP2.6 from (0.5ºCto 1ºC). These findings are in agreement with the work of Adefisan (2018) that observed throughout the entire West Arica, there is a general temperature increase. Looking at the scenario A1B, the minimum temperature over Southern part of West Africa located at around 10°N (18°C) in the present (2000-2029) but has increased to (22°C) in the future (2070-2099). That the respective values of these for A2 are (18°C and 30°C) while those of B1 are (24°C and 26°C). Thus, it can be deduced that the warming trends observed in KLB, SRB and KYB between climatic periods (2019-2048), (2049-2078), and (2071-2100) are indications that obviously Guinea and Sudano-Sahelian Ecological Zones of Nigeria are sensitive to climate change.

4.1.3: Projected changes in seasonal temperature: wet season (MJJASO)

Distribution of seasonal wet (MJJASO) temperature over KLB, SRB and KYB are shown on (figure 4.3, and 4.4) respectively. The first column is the projection for the first baseline period (1959-1988) while the second column is the projection for the second baseline period (1989-2018). The first, second and third row is respectively for (2019-2048), (2049-2078), and (2071-2100) future climatic periods. Looking at the differences between first climatic period (2019-2048) and third climatic period (2071-2100) it show that base on (1959-1988) baseline, seasonal wet temperature in KLB will increase for RCP8.5 from (0.8ºC to 5.1ºC), RCP4.5 from (0.8ºC to 2.5ºC) and RCP2.6 from (0.8ºC to 1.2ºC). The respective values of these for (1989-2018)

1959 – 1988 Baseline **1989 – 2018 Baseline**

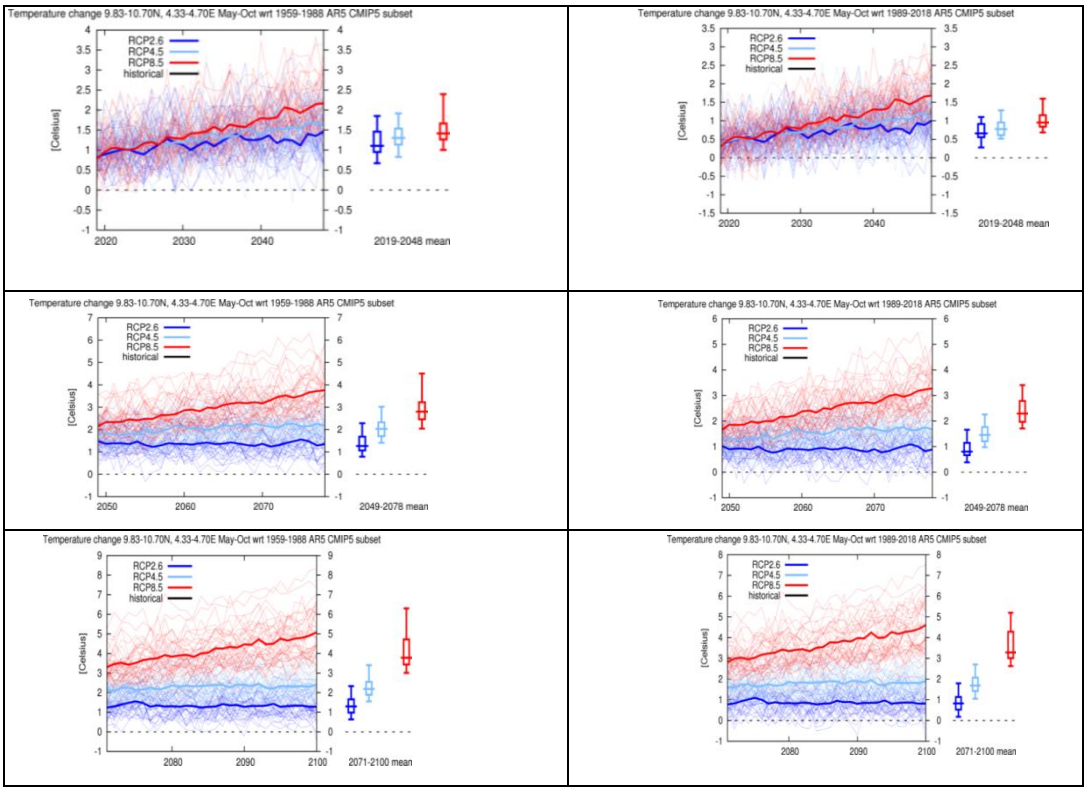

Figure: 4.3 Projected changes in seasonal temperature: wet season (MJJASO) relative to (1959 – 1988) and (1989 – 2018) baselines for KLB

SRB **KYB**

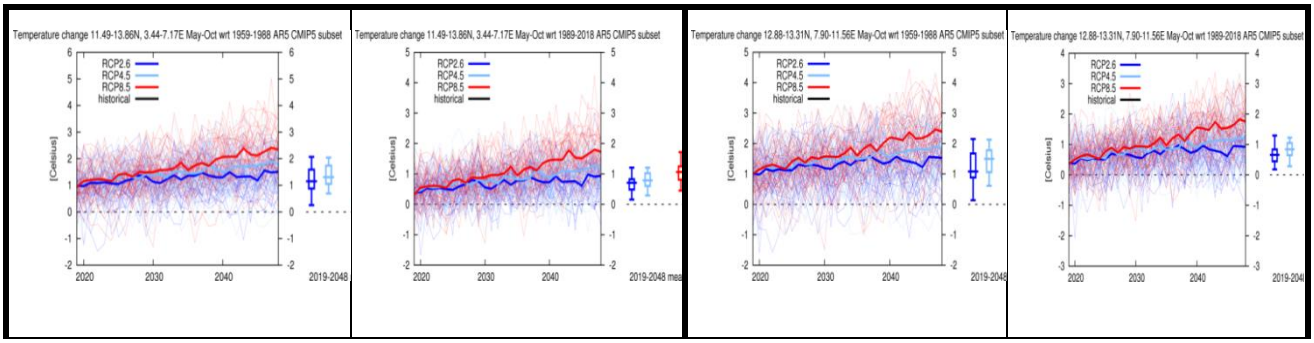

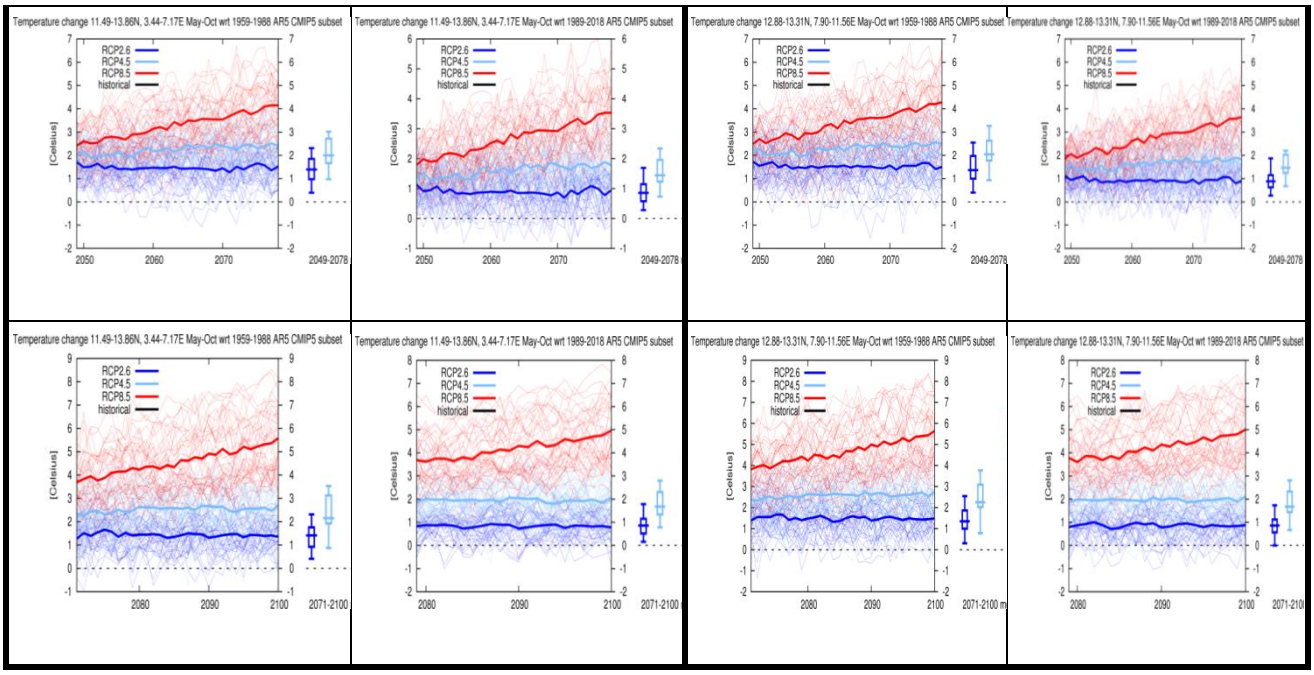

Figure: 4.4 Projected changes in seasonal temperature: wet season (MJJASO) relative to (1959 – 1988) and (1989 – 2018) baselines for SRB and KYB

baseline is RCP8.5from (0.4ºC to 4.6ºC), RCP4.5 from (0.5ºC to 1.9ºC) and RCP2.6 from (0.5ºC to 0.9ºC). As for the SRB it reveal that base on (1959-1988) baseline, seasonal wet temperature will increase for RCP8.5 from (1ºC to 5.7ºC), RCP4.5 from (1ºC to 2.8ºC) and RCP2.6 from (1ºC to 1.2ºC). The respective values of these for (1989-2018) baseline are RCP8.5 from (0.2ºC to 5ºC), RCP4.5 from (0.2ºC to 2ºC) and RCP2.6 from (0.2ºC to 1.9ºC).

Similarly, those for KYB show that base on (1959-1988) baseline, seasonal wet temperature will increase for RCP8.5 from (1ºC to 5.8ºC), RCP4.5 from (1ºC to 2.9ºC) and RCP2.6 from (1ºC to 1.5ºC). The respective values of these for (1989-2018) baseline are RCP8.5 from (0.4ºC to 5ºC), RCP4.5 from (0.4ºC to 2ºC) and RCP2.6 from (0.4ºC to 1ºC). This finding is in tandem with the work of Demircan *et al.* (2017) that between (2016 and 2099) it was expected that there will be an increase between 1°C and 6°C in seasonal wet temperature of Turkey. This is also consistent with that observed by Navneet (2017) in India where seasonal wet temperature compared to baseline for 2020s will be between 1.4 and 2.0°C, for 2050s it will range between 2.8 and 3.6°Cand for 2080s it will be 4.0 and 6.7°C. Thus, it can be deduced that the warming trends observed in KLB, SRB and KYB between climatic periods (2019-2048), (2049-2078), and (2071-2100) are indications that obviously Guinea and Sudano-Sahelian Ecological Zones of Nigeria are sensitive to climate change. More so, it is imperative to mention that despite the increasing trends of seasonal dry and wet temperature in the future years, the increase is slightly more in dry than wet season.

4.1.5: Projected changes in seasonal rainfall: dry season (NDJFMA)

Future seasonal dry rainfall projections comprising of November, December, January, February, March and April (NDJFMA) over KLB, SRB and KYB are considered (Table 4.2). Differences between and among the future first (2019-2048), second (2049-2078) and third (2071-2100) climatic periods relative to (1959-1988) and (1989-2018) baselines are found in the rainfall amounts (mm/day).

Table 4.2 Projected changes in seasonal (dry) rainfall (mm/day) relative to (1959 – 1988) and (1989 –2018) baselines

Scenario	**RCP2.6**			**RCP4.5**			**RCP8.5**		
Basin	KLB	SRB	KYB	KLB	SRB	KYB	KLB	SRB	KYB
1959 – 1988 baseline average (mm/day)									
2019-2048	+0.6	+0.5	-0.2	+0.4	+0.4	+0.4	+0.7	+0.5	+0.2
2049-2078	+0.5	+0.6	-0.2	+0.6	+0.5	+0.2	+0.7	+0.6	+0.4
2071-2100	+0.6	+0.1	+0.2	+1.4	+0.5	-0.2	+0.9	+0.7	+0.4
1989 – 2018 baseline average (mm/day)									
2019-2048	+0.7	+0.4	+0.4	+0.3	+0.3	+0.1	+0.6	+0.5	-0.2
2049-2078	+1.2	+0.6	+0.4	+0.8	+0.7	+0.2	+0.8	+0.5	+0.6
2071-2100	+0.4	+0.5	+0.3	+1.5	+0.7	+0.2	+0.6	+0.6	+0.4

Source: KNMI Climate Explorer

The positive changes that signifies increase in rainfall amount is mostly observed over the three basins. This means that seasonal dry rainfall amount will increase in the future. As observed in the three climatic periods, the increase will be highest for the first climatic period such that RCP8.5 (+0.7mm/day), RCP4.5 (+0.4mm/day) and RCP2.6 (+0.6mm/day) while the second climatic period will be the least found as RCP8.5 (+0.5mm/day), RCP4.5 (+0.2mm/day) and RCP2.6 (+0.3mm/day). Furthermore, the differences with respect to the two baselines of (1959-1988) and (1989-2018) periods show that the seasonal dry rainfall will be higher with reference to (1989-2018) baseline when compared with (1959-1988) baseline. The (1989-2018) baseline found RCP8.5 (0.7mm/day), RCP4.5 (0.7mm/day) and RCP2.6 (0.6mm/day) compared with RCP8.5 (0.6mm/day), RCP4.5 (0.5mm/day) and RCP2.6 (0.1mm/day) for the (1959-1988) baseline. Across the three basins, seasonal dry rainfall will be highest in the KLB given as RCP8.5 (0.8mm/day), RCP4.5 (1.5mm/day) and RCP2.6 (1.2mm/day) follow by SRB given as RCP8.5 (0.7mm/day), RCP4.5 (0.7mm/day) and RCP2.6 (0.6mm/day). The least increase is in KYB given as RCP8.5 (0.6mm/day), RCP4.5 (0.4mm/day) and RCP2.6 (0.3mm/day).

4.1.6: Projected changes in seasonal rainfall: wet season (MJJASO)

Seasonal wet rainfall projections comprising months of May, June, July, August, September and October (MJJASO) over KLB, SRB and KYB are considered (Table 4.3).

Table 4.3 Projected changes in seasonal (wet) rainfall (mm/day) relative to (1959 – 1988) and (1989 –2018) baselines

Scenario	**RCP2.6**			**RCP4.5**			**RCP8.5**		
Basin	KLB	SRB	KYB	KLB	SRB	KYB	KLB	SRB	KYB
1959 – 1988 baseline average (mm/day)									
2019-2048	+3	-1.2	-0.8	+2	+0.2	+1.4	+1.5	+0.8	+1.5
2049-2078	+2.81	-0.8	-	+3	+0.6	+1.2	+2	+1.2	+1.8
2071-2100	+1.2	+0.2	+1.2	+0.5	+0.4	+1	+4	+0.8	+2

1989 – 2018 baseline average (mm/day)									
2019-2048	+3.8 +2.2	-1		+2.1	+0.5	+2	+1.5	+0.8	+1.5
2049-2078	+1.4	-0.8	+0.8	+2.5	+2	+2	+2.1	+1.2	+1.8
2071-2100	+0.4	-1	+2	+1.2	+0.7	+2.5	+2.7	+1	+1.5

Source: KNMI Climate Explorer

Just like seasonal dry rainfall over these basins, the seasonal wet rainfall exhibit similar pattern of increasing rainfall up till the end of 21stcentury. The values for the KLB is found as 0.8mm/day, 0.8mm/day and 1.2mm/day for RCP8.5, RCP4.5 and RCP2.6 respectively during the seasonal dry rainfall while 2.1mm/day, 2.5mm/day and 1.4mm/day for RCP8.5, RCP4.5 and RCP2.6 respectively during the seasonal wet rainfall. The respective values for KY B is found as 0.6mm/day, 0.2mm/day and 0.4mm/day for RCP8.5, RCP4.5 and RCP2.6 respectively during the seasonal dry rainfall while 1.8mm/day, 2mm/day and 0.8mm/day for RCP8.5, RCP4.5 and RCP2.6 respectively during the seasonal wet rainfall. This shows that Guinea and Sudano-Sahelian Ecological Zones of Nigeria is sensitive to climate change resulting to increase in the seasonal wet rainfall amount (0.8mm/day to 4mm/day) between the first and third climatic periods.

5. Conclusion

Based on the findings of this study, it could be deduced that Guinea and Sudano-Sahelian Ecological Zones of Nigeria to climate change. This is noticed from the rise in temperature from 1^{o}C in the first climatic period (2019-2048) to as high as 6^{o}C in the third climatic period (2071-2100) being the end of 21st century. Similar trend is observed for rainfall where there is increase in rainfall amount from 0.5mm/day in first climatic period to 2.5mm/day in the third climatic period. This anticipated condition has serious implications on water resources, from increase in streamflow, rise in reservouir, soil moisture changes and flooding.

References

AbdulKadir, A., Usman, M. T., and Shaba, A. H. (2015). An Integrated Approach to Delineation of the Eco-climatic Zones in Northern Nigeria. *Journal of Ecology and the Natural Environment*, Vol. 7(9), pp. 247-255, doi:10.5897/jene2015.0532.

Adam, B., Martin, H., Magdalena, N., and Adam, V. (2016). Increasing Water Resources Availability under Climate Change. *International Conference on Efficient & Sustainable Water Systems Management toward Worth Living Development*, 2nd EWaS 2016

Adefisan E. A. (2018). Climate Change Impact on Rainfall and Temperature Distributions over West Africa from Three IPCC Scenarios. *J Earth Sci Clim Change* 9: 476. doi: 10.4172/2157-7617.1000476

Ahmed,M.,Yves,T.,Lahoucine,H.,Denis,R.,andLionel,J.(2017).ClimateChangeImpactsonSurfaceWaterResourcesintheRherayaCatchment(HighAtlas,Morocco).*HydrologicalSciencesJournal*, Volume62,issue6.doi:10.1080/02626667.2017.1283042

Ayansina, A., Maren, R., John, F. M., Tabitha, M. (2018). Rainfall variability and drought characteristics in two agro-climatic zones: An assessment of climate change challenges in Africa. *Science of the Total Environment*, 630, 728–737. doi: 10.1016/j.scitotenv.2018.02.196

Demircan, M., Gurkan, H., Eskioglu, O., Arabaci, H., and Coskun, M. (2017). Climate Change Projections for Turkey: Three Models and Two Scenarios. *Turkish Journal of Water science and Management.*Vol 1: Issue 1.

Gebre, S. L., Tadele, K., and Mariam, B. G. (2015). Potential Impacts of Climate Change on the Hydrology and Water resources Availability of Didessa Catchment, Blue Nile River Basin, *Ethiopia. Journal of Geology and Geosciences*, 4: 193, doi:10.4172/2329-6755.1000193

Gneneyougo, E. S., Affoue, B. Y., Yao, M. K., and Tie, A. G. (2017). Climate Change and Its Impacts on Water Resources in the Bandama Basin, Côte D'ivoire. *MDPI Journal/ Hydrology*, 4, 18, doi: 10.3390/hydrology4010018.

Guoyong, L., Maoyi, H., Nathalie, V., Xuesong, Z., Ghassem, R. A., and Ruby, L. L. (2016). Emergence of new hydrologic regimes of surface water resources inthe conterminous United States under future warming. *Environmental Research Letters*, 11. doi:10.1088/1748-9326/11/11/114003

Hagemann, S., Chen, C., Clark, D. B., Folwell, S., Gosling, S. N., Haddeland, I., Hanasaki, N., Heinke, J., Ludwig, F., Voss, F., and Wiltshire, A. J. (2013). Climate Change Impact on Available Water Resources obtained using multiple global climate and hydrology models, *Earth System Dynamics*, 4, 129-144. doi.org/10.5194/esd-4-129-2013, 2013.

Intergovernmental Panel on Climate Change (IPCC) (2014). *Synthesis Report.* Contribution of Working Groups I, II and III to the Fifth Assessment Report of the Intergovernmental Panel on Climate Change [Core Writing Team, R.K. Pachauri and L.A. Meyer (eds.)]. IPCC, Geneva, Switzerland, 151 pp.

Kumar D, Kodra E, Ganguly A. 2014. Regional and seasonal intercomparison of CMIP3 and CMIP5 climate model ensembles for temperature and precipitation. *Clim. Dyn*. 43(9–10): 2491–2518. https://doi.org/10.1007/s00382-014-2070-3.

Miguel A. L., Omar V. M., Ernesto H. B., and Gabriela V. M. (2018). Evaluation of CMIP5 retrospective simulations of temperature and precipitation in northeastern Argentina. *International Journal of Climatology* published by the Royal Meteorological Society.doi: 10.1002/joc.5441

Minsung K., Jang H., and Jaehyun A. (2019). Change in Extreme Precipitation over North Korea Using Multiple Climate Change Scenarios. *MDPI Journal/water*. doi:10.3390/w11020270

Ruotong W., Qiuya C., Liu L., Churui Y., and Guanhua H. (2019). Multi-Model Projections of Climate Change in Different RCP Scenarios in an Arid Inland Region, Northwest China. *MDPI Journal/water*. doi:10.3390/w11020347

Vera C. S., Díaz L. (2013). Anthropogenic influence on summer precipitation trends over South America in CMIP5 models. *Int. J. Climatol.* 35:3172–3177. https://doi.org/10.1002/joc.4153.

Xiaoli Y., Weifei Z., Liliang R., Mengru Z., Yuqian W., Yi L., Fei Y., and Shanhu J. (2018). Potential impact of climate change to the future streamflow of Yellow River Basin based on CMIP5 data. Published by Copernicus Publications on behalf of the *International Association of Hydrological Sciences*. https://doi.org/10.5194/piahs-376-97-2018

Yunana, D. A., Shittu, A. A., Ayuba, S., Bassah, E. J., and Joshua, W. K. (2017). Climate Change and Lake Water Resources in Sub-Saharan Africa: Case Study of Lake Chad and Lake Victoria. *Nigerian Journal of Technology,* 36 (2), pp.648-654. doi:org/10.4314/njt.v36i2.42

Impact of Weather on Guinea Corn Production In Kaduna State, Nigeria

MOHAMMED, Usman Kawu and OJOYE, S.
Department of Geography
Federal University of Technology, Minna

ABSTRACT

Weather variations has become a topical issue in recent time because of its largely detrimental impacts on natural and human systems. The study examines the impact of weather on guinea core production in Kaduna State, it analyse the trend of rainfall and temperature over the past 20 years (1999-2018) and examine the impact of these weather variables on guinea corn production. Rainfall, temperature and guinea corn yield was acquired, data collected were

subjected to regression analysis. The findings show that the coefficient of variation as seen above of maximum temperature 4.4 and minimum temperature 2.72 shows that there is a consistency in the variation although not too strong. The findings also show that there is uneven pattern of rainfall implying that crop yield differs from year to year. This is as a result of the relationship between rainfall and Guinea corn in this investigation. The study thereby recommend that Guinea corn production should be regressed on other environmental factors such as soil fertility.

Key words: Weather, Rainfall, Temperature and Guinea corn

Introduction

Year-to-year variations in crop yields pose a significant risk to subsistence farmers or people depending on local supply (Headey, 2011; Schewe *et al*., 2017). Annual crop yields depend on several factors. In addition to weather conditions, the occurrence of weeds, diseases, and pests can result in yield fluctuations (Gregory *et al.,* 2009). Weather has emerged as a global concern in the past 20 years and weather impacts are already being experienced through increasing temperatures, variable rainfall and climate related extreme events. Guinea corn is one of the major cereal crops widely grown in Nigeria, and a very important staple food for the populace particularly in the northern part of the country (Tashikalma *et al*., 2012). The Nigerian guinea corn production was 11.5 tons in 2010 and forecast was 11.7 tons in 2011 (United States Department of Agriculture, 2010). The crop yield has increased because of the acceptance by farmers of improved varieties developed by local research institutes.

The impact of weather on crop production in Kaduna State has received limited attention despite the fact that over 60% of the active populations are farmers. Studies on weather variations have revealed that the potential impacts of weather will include every aspect of the four dimensions of food security; food availability (production and trade), food accessibility, food stable supplies, and food utilization (Nwafor, 2007). Olarenwaju (2012) reported that many of the problems facing agricultural production are weather related. It is against this background that this study analyse the trend of rainfall and temperature over the past 20 years (1999-2018) and examine the impact of these weather variables on guinea corn production in in Igabi Local Government Area of Kaduna State.

Igabi Local Governmnet Area lies on latitudes 10^0 25′ 28″ N and 11^0 35′ 53″ N and Longitudes 7^0 21′ 49″ E and 7^0 50′ 00″ E (Figure 1.1). The area covers an area approximately 3,727 square kilometers and shares boundaries with Kaduna North, Kaduna South, Zaria, Kajuru, Kauru, Igabi and Birnin-Gwari Local Government Councils. Turunku is the headquarters of Igabi LGA which was the seat of power of the famous Queen Amina of Zazzau. The study area has an average annual rainfall of 1250mm. The rains occurs between months of April – October when the South Westerly humid winds brings in rain. The dry seasons last between November and March when the prevailing North Easterly winds (Harmattan) brings with it dusty, dry and cool air of the Sahara desert ushering in the dry season. The mean annual rainfall in the study area ranged from 1000mm to 1500mm. The month of August-September recording highest rains of 300mm (Yamusa, Abubakar and Falaki, 2015). The rainy season starts between 10th of April to 20th of May and extends to October. The temperature of the study area resembles that of the North Central Zone of the country. Temperature ranges between 25^0 C – 35^0C during the dry season. The temperature may rise to about 42^0C in March/April which is the hottest period. The coldest month is December/January. During the harmattan popularly referred to as the West Africa Doctor, temperature sometimes reaches freezing point (Record from the nearest meteorological station over a period of 15years) (Yamusa, Abubakar and Falaki, 2015).

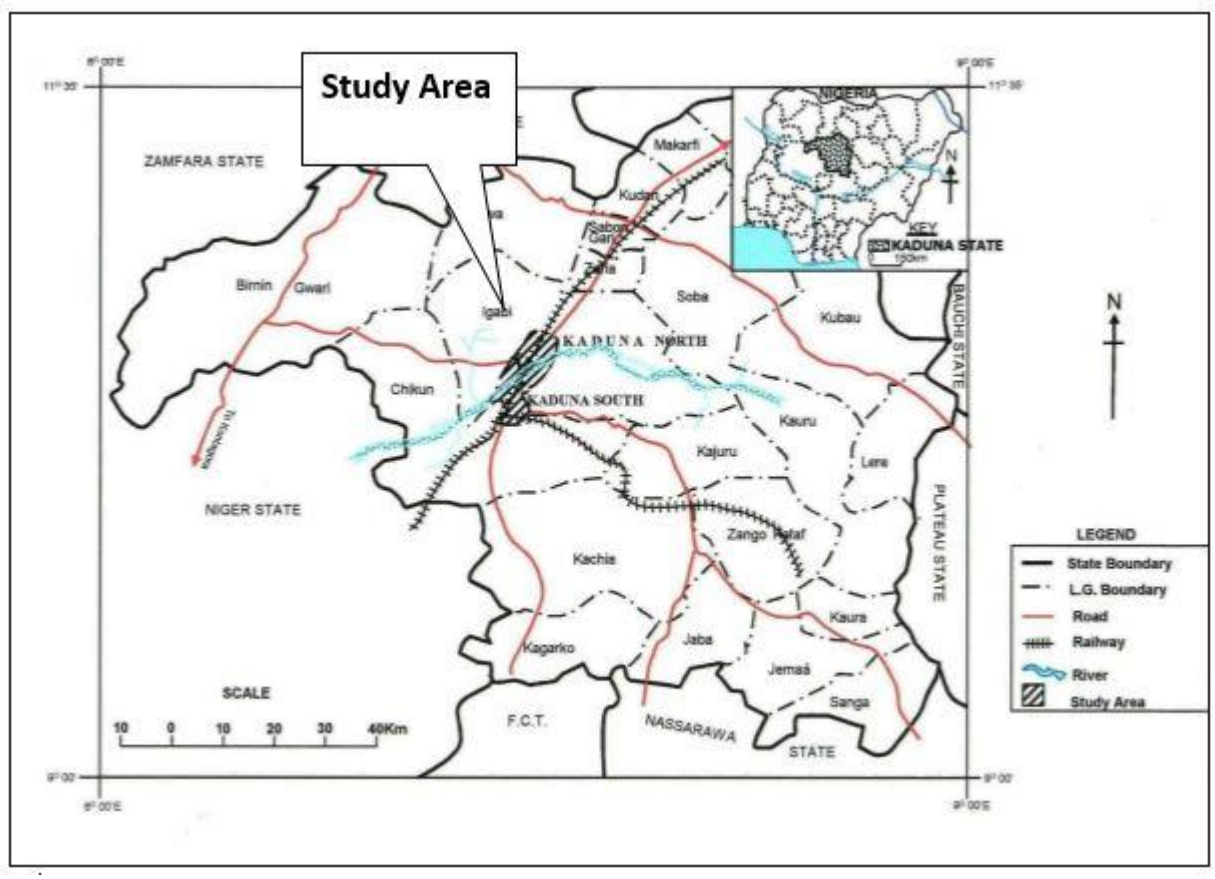

Figure 1.1: Kaduna Map showing Igabi

Source: Kaduna State Ministry of Land and Geoinformatics, 2018

Literature Review

Weather plays an important role in agricultural production (Stern, 2011). It has a profound influence on crop growth, development and yields; on the incidence of pests and diseases; on water needs; and on fertilizer requirements (Tenge, 2011). This is due to differences in nutrient mobilization as a result of water stresses, as well as the timeliness and effectiveness of preventive measures and cultural operations with crops (Timofeev, 2012). Weather aberrations may cause physical damage to crops and soil erosion (Stern, 2011). Weather factors contribute to optimal crop growth, development and yield (Bradshaw, 2013). They also play a role in the incidence and spread of pests and diseases. Susceptibility to weather-induced stresses and affliction by pests and diseases varies among crops, among different varieties within the same crop, and among different growth stages within the same crop variety (Selvaraju *et al*, 2015).

Even on a climatological basis, weather factors show spatial variations in an area at a given time, temporal variations at a given place, and year-to-year variations for a given place and time. For cropping purposes, weather over short periods and year-to-year fluctuations at a particular place over the selected time interval have to be considered. For any given time unit, the percentage departures of extreme values from a mean or median value, called the coefficient of variability, are a measure of variability of the parameter.

Greenhouse gases emissions from human activities are responsible for weather variation (Li *et al.* 2011). Weather variations leads to increased temperatures, changing rainfall patterns and amounts, and a higher frequency and intensity of extreme climate events such as floods, cyclone, droughts, and heatwave (Roudier *et al*. 2011). Temperature increases and erratic rainfall patterns affect crop agriculture most directly and adversely (Lansigan *et al*. 2013;4 Almaraz *et al.* 2016). Variation in weather over time affects guinea corn production adversely (Behnassi 2011). The channels of the impacts are depicted in Figure 2. Variations in weather generally involve changes in two major climate variables: temperature and rainfall. The increase in temperature shortens the phenological phases of crops (such as planting, flowering and harvesting) (Liu *et al*. 2010; Teixeira *et al*. 2011) and affects plant growth and development. The fluctuations and occurrence of extreme weather events reduce guinea corn yields significantly, particularly at critical crop growth stages (Lansigan *et al*. 2000; Teixeira *et al.* 2011).

Rainfall extremes, through droughts and floods are very detrimental to guinea corn productivity. Higher and/or heavy rainfall results in higher yield losses through flooding (Roudier *et al.* 2011). In contrast, insufficient rainfall leads to greater drought frequency and intensity, while increased evaporation leads to complete crop failure (Liu *et al.* 2010). Overall, temperature and rainfall changes reduce the cropped area, production level and yield. This reduction or fluctuation in guinea corn yield warrant farmers' adaptability to minimise these adverse effects. However, adaptation strategies at the farm level vary from area to area and

from farm to farm. Farmers' adaptive capacity is determined by their socio-demographic characteristics, farm characteristics and accessibility to institutional factors

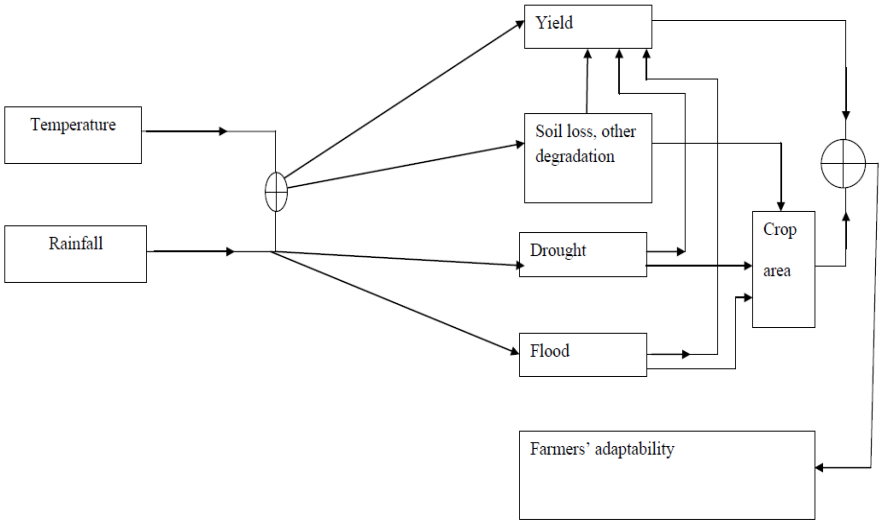

Figure 1.1: Conceptual framework of weather impacts on guinea corn production

Materials and Methods

Quantitative data technique was used, rainfall and temperature data from Nigeria Meteorological Agency (NIMET) of the Nigerian College of Aviation Technology (NCAT) School Zaria and Guinea corn yield was also obtain from Kaduna State Agricultural Development Agency for a period of 20 years (1999 – 2018).

Methods of Data Analysis

The trends of rainfall and temperature variations was analyses using Standardized Precipitation Index (SPI), mean and Diurnal Temperature Range (DTR). Rainfall and maximum temperature were obtained on daily and monthly basis for a period of 20 years (1999 to 2018) and converted into mean annual value using the statistical technique. Multiple linear regression was used to examine the impact of rainfall and temperature and guinea corn production.

Results

The relationship of crop and rainfall gave a negative relationship and others positive relationship. The relationship of both rainfall and temperature on Guinea showed a strong negative relationship. From the 2 it can be deduced that there is a constant increase in temperature. This shows that there is yearly change in temperature that can alter the yield of Guinea corn in the study area. The coefficient of variation as seen above of maximum temperature 34.2 and minimum temperature 32.3 shows that there is a consistency in the variation although not too strong.

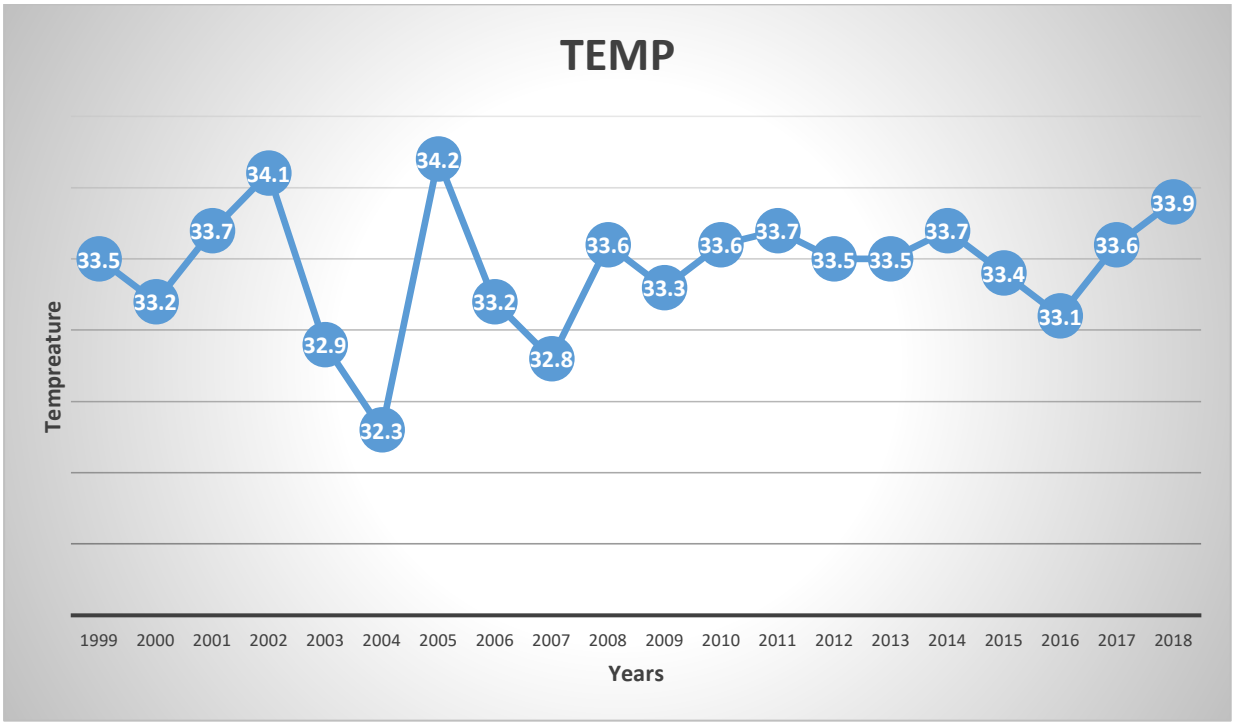

Figure 2: Pattern of Maximum Temperature in the study area

The figure showed the trend of temperature over the years in the study area, a close look at the graph reveals that the temperature from 2010 was constantly increasing except for the fall in 2016, but they never went below 32°C in 2004. The year 2005 experienced the highest temperature of 35°C. Figure 3 shows the annual total rainfall in the study area from 1999-2018. The average rainfalls were gotten from the estimate of rainfall in a year.

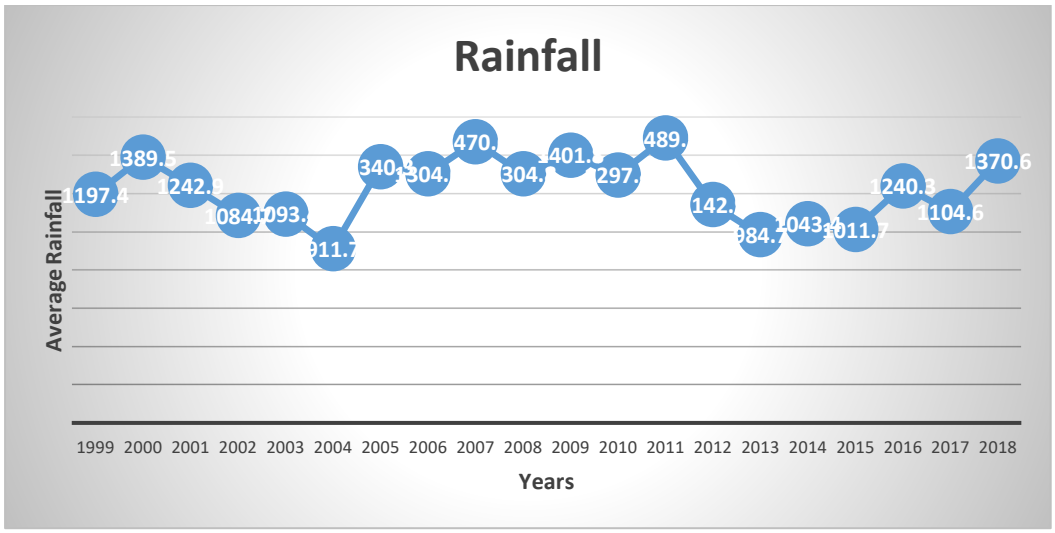

Figure 3: Rainfall pattern in the study area

The graph in figure 3 displays the pattern of rainfall in the study area. A look at the graph shows that there has not been constant rainfall pattern in the study area. But the graph has it that 2012 recorded the highest rain fall followed by 2007. From the graph it is observed that the rainfall pattern fluctuates. this is to show that the rainfall pattern was not stable throughout the decade. The data on Guinea corn yield per tones covers a period of (20) twenty years, that is 1999-2019 and the area cultivated in hectare is presented in figure 4.

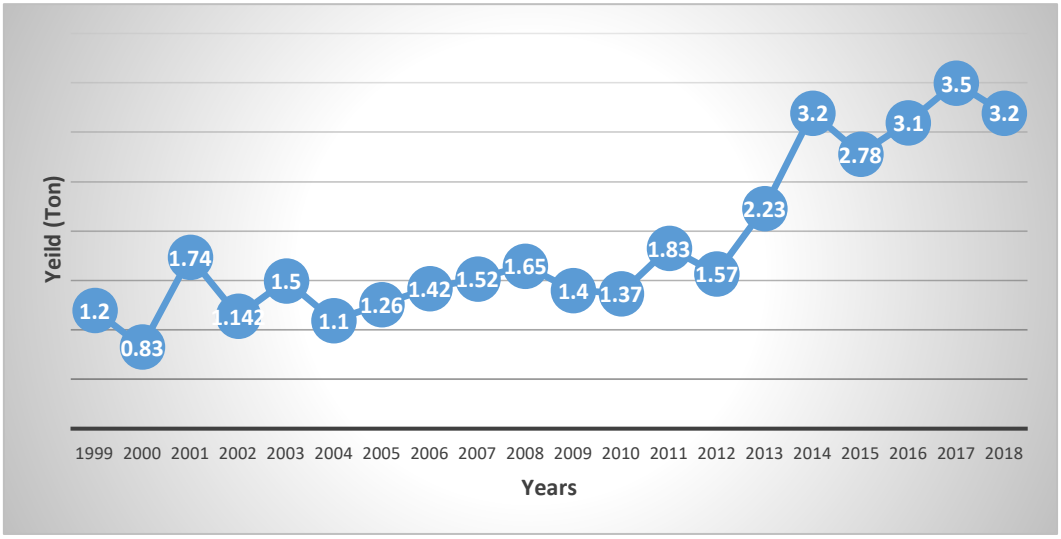

Figure 4: Guinea Corn yield in the study area

Impact of Rainfall and Guinea corn Yield

Figure 5 showed the rainfall pattern over the years. This shows that there is uneven pattern of rainfall implying that crop yield differs from year to year. This is as a result of the relationship between rainfall and Guinea corn in this investigation.

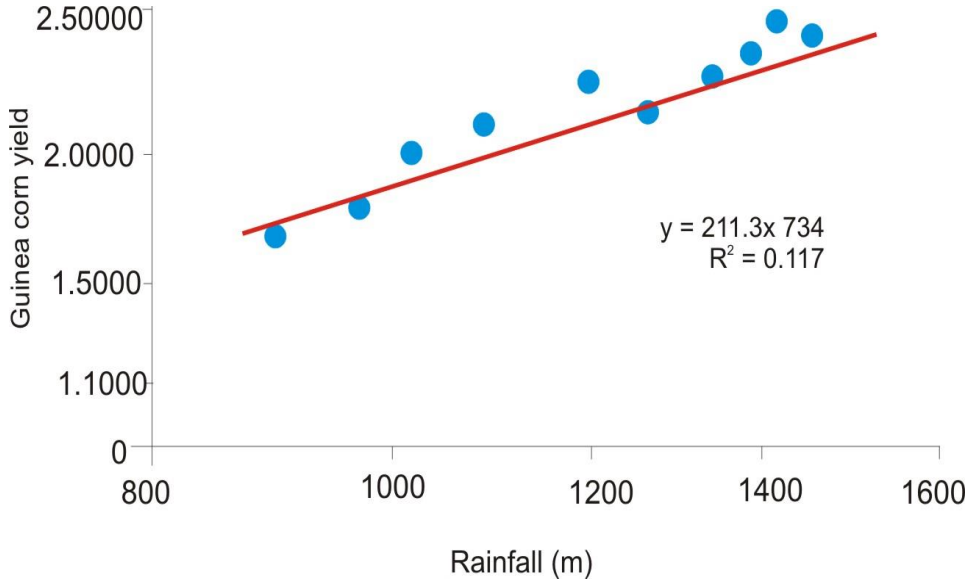

Figure 5: Line graph showing the relationship between annual rainfall and Guinea corn yield

It is also noted that Guinea corn yield in the study area is uneven; this is as a result of the area coverage which differ from year to year. This goes a long way to affect the amount of Guinea corn and the coefficient of variation in the study area. The relationship between temperature and guinea corn yields in the area using the Pearson correlation technique where Guinea corn is dependent variables and temperature, the independent variable. The mean value of crops against the numbers of hectare of land cultivated and the mean value of temperature were used to determine their relationship.

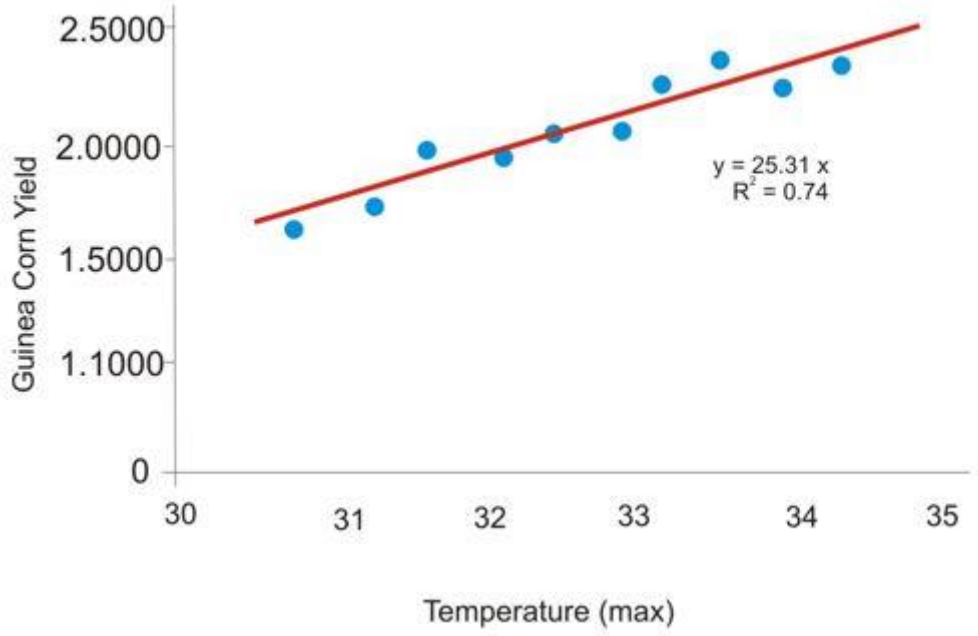

Figure 6: Line graph showing the relationship between temperature and Guinea corn yield

In line with the aim of this study which is to examine the relationship between rainfall and temperature variability on Guinea corn production, multiple regression was applied. The annual yield was regressed against rainfall and temperature to established the relationship that exist between them. Thus, these results were obtained from the regression, as shown in the table below:

Table 1. Summary of the analysis

Variables	Regression value	Remarks
Temperature	0.74	There exists a strong positive relationship between temperature and Guinea corn yield
Rainfall	0.117	There exists a strong positive relationship between temperature and Guinea corn yield

Conclusion

In the relationship between rainfall and Guinea corn yield which has a positive relationship means that there exists relationship between the two parameters. This could be as a result of the data being a secondary data and the author could not monitor the collection which could have some errors. It observed that any amount of rainfall above 1800mm will have a negative effect on Guinea corn yield. Too much rain could lead to water logging. The correlation between rainfall, temperature and Guinea corn yield all show a positive relationship. This means that combination of rainfall and temperature has a great influence on Guinea corn yield and other environment factors such as, soil fertility, seed variety or type etc. The study concluded that the relationship between climatic elements and Guinea corn yield in Igabi local government area is positively significant. This means that rainfall and temperature influence Guinea corn yield but other environmental factor such as soil fertility, type, and temperature technology etc. should also be put into consideration.

References

Ajetomobi, J.O. (2016). Effects of weather extremes on crop yields in Nigeria. *African journal of food, agriculture, nutrition and development*, 16(4): 11168-11184.

Ako, B. D. and Olorunfemi, M.O. (1999). Geoelectrical survey for groundwater in the newer basalts of Jos, Plateau State. *Journal of Mining and Geology*, 25; 247- 250.

Akullo, T. (2014). The effect of weather on crop yields: A case study of the maize crop in Masindi District Western Uganda. A thesis submitted in partial fulfillment of the requirements for the award of the Masters of Arts Degree in Geography of Makerere University.

Alistair, B. F. (2003). Bad Meteorology: Raindrops are shaped like teardrops. Pennsylvania State University. Archived *from the original on 2012-08-04. Retrieved 2008-04-07.*

Ammani, A.A., Ja'afaru, A. K., Aliyu, J. A. and Arab, A. I. (2012). Climate change and maize production: empirical evidence from Kaduna State, Nigeria. Journal of Agricultural Extension, 16(1): 1-7

Aondoakaa, S.C. (2012). Effects of climate change on agricultural productivity in the Federal Capital Territory (FCT), Abuja, Nigeria. Ethiopian Journal of Environmental Studies and Management, 5(4): 559-566.

Awotoye, O. O. and Matthew, O. J. (2010). Effects of temporal changes in climate variables on crop production in tropical sub-humid southwestern, Nigeria. *African Journal of Environmental Science and Technology*, 4(8): 500-505.

Baiyegunhi, L.J.S. and Fraser, G.C.G. (2009). Profitability of sorghum production in three Villages of Kaduna State, Nigeria. *Journal of Applied Sciences Research*, 5(10): 1685-1691.

Bast, J.L. (2010). Seven Theories of Climate Change. The Heartland Institute, Arlington Heights, Illinois. http://www.physicsclassroom.com/class/circles/Lesson-4/Kepler-s-Three-Laws

Bello, O. B., Ganiyu, O. T., Wahab, M. K. A., Mahmud, J., Azeez, M. A. and Abdulmaliq S. Y. (2015). Evidence of climate change impacts on agriculture and food security in Nigeria. *International Journal of Agriculture and Forestry*, 2(2): 49-55.

Crate, S. A. and Nuttall, M. (2009). Anthropology and Climate Change: From Encounters to Actions. *Walnut Creek, CA: Left Coast Press. pp. 70–86, i.e. the chapter 'Climate and weather discourse in anthropology: from determinism to uncertain futures' by Nicholas Peterson & Kenneth Broad.*

De Wit, M. and Stankiewicz, J. (2012). Changes in surface water supply across Africa with predicted climate change. *Science*, 311, 1917-1921

Emmanuel, M. A. and Fanan, U. (2013). Effect of variability in rainfall characteristics on maize yield in Gboko, Nigeria. *Journal of Environmental Protection*, 4, 881-887.

Enete, A. A. & Onyekuru, A. N. (2014). Challenges of agricultural adaptation to climate change: empirical evidence from southeast Nigeria. *Tropicultura*, 29(4), 243-249.

Fan, Z., Bräuning, A. and Thomas, A. (2011). Spatial and temporal temperature trends on the Yannan Plateau (Southwest China) during 1961–2004. *International Journal of Climatology*, 31(20): 78–90.

Gray, W.M. (2009). Climate Change: Driven by the Ocean, Not Human Activity. 2nd Annual Heartland Institute Conference on Climate Change, New York, 8-10 March 2009. http://tropical.atmos.colostate.edu/Includes/Documents/Publications/gray2009.pdf.

Green, U. (2007). The British and the Making of a Capital City, 1913-1960. In Ashafa, A.M (ed) *Urbanization and Infrastructure in Nigeria Since the 20th Century*. Kaduna State University, Kaduna-Nigeria.

Gujarati, R. (2003). *Fundamentals of Social Research Methods. An African perspective*. Cape Town: Juta Co Ltd.

Igwe, K.C., Uguru, J. O., Shomkegh, S. A. and Igwe, C. O. K. (2014). Climate change and growth rate of food grain output in Nigeria (1970-2010). *Journal of Scientific Research & Reports*, 3(3): 397-406.

Intergovernmental Panel on Climate Change [IPCC] (2012). Third assessment report mitigation IPCC, Switzerland.

IPCC (2013) Climate Change; The Physical Science Basis, Summary for policy makers, Observed Changes in the Climate System P 15, IN IPCC AR5, WG1. IPCC. https://www.ipcc.ch/pdf/assessment-report/ar5/wg1/WGIAR5_SPM_brochure_en.pdf.

International Institute for Sustainable Development [IISD], (2013). Community-based adaptation to climate change Bulletin. A summary of the second International Workshop on Community-based adaptation to climate change. IISD reporting services.

Jatau, B. S., Fadele, S.I. and Agelaga, A. G. (2013). Groundwater investigation in parts of Kaduna South and environs using Wenner Offset Method of Electrical Resistivity Sounding. *Journal of Earth Sciences and Geotechnical Engineering*, 3(1): 41-54

Kaduna State Ministry of Land and Geoinformatics, 2018.

Kandlinkar, M & Risbey, J. (2010). Agricultural impacts of climate change: If adaptation is the answer, what is the question? *Climatic change*, 45, 529-539.

Khanal, R.C. (2012). Climate change and organic agriculture. *The Journal of Agriculture and Environment* 10, 100-109, Review paper.

Kondwani, M. (2013). Climate change impact on rainfed corn production in Malawi. A thesis submitted in partial fulfillment of the requirements for the degree of Master of Science in the Department of Civil, Environmental and Construction Engineering in the College of Engineering and Computer Science at the University of Central Florida, Orlando Florida.

Labaris, A., Yusuf, K.S., Medugu, N.I. and Barde, M.M. (2014). Problems of guinea corn marketing in Nasarawa State, Nigeria. *International Journal of Science, Environment and Technology*, 3(5): 1790-1796.

Moran, M. J. and Shapiro, H. N. (2006). "1.6.1". Fundamentals of Engineering Thermodynamics (5 ed.). John Wiley & Sons, Ltd. p. 14. ISBN 978-0-470-03037-0.

Moses, O. (2016). Assessment of drought in Kaduna State, Nigeria between 2000 and 2014. *Journal of Mining and Geology*, 28: 403-412.

NAERLS (2012). *Field Situation Assessment of 2012 Wet Season Agricultural Production in Nigeria*. Zaria: NAERLS.

Nigerian Environmental Study/Action Team [NEST] (2013). *Climate change in Nigeria. A communication guide for reporters and educators.* Ibadan: NEST pp. 5-16.

Ofor, R., Ibeawuchi, Y. and Oparaeke, U. (2009). Crop protection problems in production of maize and guinea corn in Northern Guinea Savanna of Nigeria and control measures. *Environ. J. Environ. Stud., 2*(2): 41-49.

Odjugo, P.A.O. (2010). An analysis of rainfall pattern in Nigeria. *Global Journal of Environmental Science*, 4(2): 139-145.

Odjugo, P. A. O. (2011). Regional evidence of climate change in Nigeria. *Journal of Geography and Regional Planning*, 3(6), 142-150, June 2010 Available online at http://www.academicjournals.org/JGRP

Odjugo, P. A. O. (2012). Climate change and global warming: the Nigerian perspective. *Journal of "Sustainable Development and Environmental Protection",* 1(1), 5-17. http://www.ierdafrica.org/resources

Olayinka, A.I. and Olorufemi, M.O. (1992). Determination of geoelectrical characteristics in Okene area and implication for borehole siting. *Journal of Mining and Geology*, 28: 403-412.

Omojolaibi, J.A. (2014). Climate Change and Sustainability Development in Sub-Saharan Africa, an Application of Panel Coointigration to Some Selected Countries. In: Iregha P.B. Babatolu J.S. and Akinnubi, R.T., Eds., Climate Change and Crop Production in Nigeria: An Error Correction Modelling Approach. *International Journal of Energy Economics and Policy*, 4, 297-311.

Oyedele, E. (2011). Migration Phenomenon and Violent Conflict Generation in Kaduna Metropolis. *Lapai Journal of Humanities*, 2: 192-206. IBB University. Niger State.

Pielke, S.R. (2009). Climate Change: The Need to Consider Human Forcings besides Greenhouse Gases. Earth Observation Satellite (EOS), 90, 413. https://doi.org/10.1029/2009eo450008.

Roberts, J.M., Schlenker, W. and Eyer, J. (2012). Agronomic Weather Measures in Econometric Models of Crop Yield with Implications for Climate Change. *Ame. J. of Agric. Econs.* 2012; 1093: 1-17.

Rosegrant, M.W. Ewing, M, Yohe, G. Burton, I., Huq, S. and Valmonte-Santos, R. (2013). Climate change and agriculture: threats and opportunities. Deutsche Gesellschaft fur Technische Zusammenarbeit (GTZ). Climate protection programme for Developing Countries. Federal Ministry for Economic Cooperation and Development, Germany.

Rosemary, K. (2012). Impacts of climate change on crop production practices among small holder farmers in Guruve District, Zimbabwe. A dissertation submitted in partial fulfillment of the requirements of a Master of Science degree in Sociology and Social Anthropology, Department of Sociology, University of Zimbabwe.

Shehu, S. (2011). The Growth and Development of Kaduna Metropolis, 1913-2000. In Ashafa, A.M (ed) Urbanization and Infrastructure in Nigeria Since the 20th Century. Kaduna State University, Kaduna-Nigeria. *Environmental Monitoring Assessment*, 1, 277-298.

Tashikalma, A. K., Stephen, J. and Umaru, A. (2012). Economic analysis of sorghum production in Michika Local Government Area of Adamawa State, Nigeria. *Journal of Sustainable Development in Agriculture and Environment*, 5(1): 10 – 20

United States Department of Agriculture (2010). Nigeria grain and feed annual. Grain Report, Number NI0007. *United States Department of Agriculture,* 11pp

World Bank (2015). Shock Waves: Managing the Impacts of Climate Change on Poverty.

Wooldridge, T. (2001). *Interviewing the Art of Science In Handbook of Quantitative Research*. London: Denzin and Lincoln eds Sage Publications Thousand oaks.

Mineralogical and Caloric Evaluation of Selected Nigerian Coals and their Potentials as Alternative Sources of Energy

ONODUKU Usman Shehu, AKO Thomas Agbor and MOHAMMED Laminga Mohammed

DEPARTMENT OF GEOLOGY, FEDERAL UNIVERSITY OF TECHNOLOGY, PMB, 65, MINNA, NIGERIA

Corresponding Author-onoduku.usman@futminna.edu.ng

ABSTRACT

Forty coal samples (4 samples per deposit) from ten coal deposits that span over Anambra Basin and Benue Trough were sampled and analyzed for their mineralogical and calorific characteristics. These coal deposits include Onyema, Okpara, Ogboyoga, Okaba, Owukpa, Ibobo, Udane Biomi and Iva Valley in the Anambra Basin and Lafia Obi and Maiganga in the Benue Trough. XRD technique was used for the mineralogical analysis while bomb calorimeter was used to determine the calorific values of the coals.The X Ray Diffractograms of the coals show that quartz is the dominant mineral in most of the coals. Other minerals detected include halite, anhydrite, magnetite, magnesite, hematite, dolomite and kaolinite. The calorific values of the coals are Iva Valley (5990kj/kg), Okaba (4723kj/kg), Ibobo (4640kj/kg), Obi – Lafia (4345kj/kg), Owukpa (3780kj/kg), Onyema (3742kj/kg), Okpara (3569kj/kg), Maiganga (2861kj/kg), Udane – Biomi (2625kj/kg) and Ogboyoga (2220kj/kg). Based on the analysed calorific values, the coals are classified as Iva Valley (B), Okaba (C), Ibobo and Obi-Lafia (D), Owukpa, Onyema and Okpara (E), Maiganga and Udane Biomi (F) and Ogboyoga (G).In terms of the technological applications of the studied coals, the calorific values of the coal deposits are sufficiently high and indicate their suitability for the generation of power.

1. INTRODUCTION

Nigerian coals were major source of power generation and income to the country before the advent of the oil boom in the early seventies when emphasis was shifted to oil (Obaje, 2009). This brought a nearly complete halt to research and continuous exploration and appreciation of the country's coal resources. However, with current dwindling power supply and decreasing reliance on oil all over the world, coal is positioned to regain its past glory in the energy mix of Nigeria. The coal reserves are in the excesses of three billion (3,000,000,000) tons of indicated reserves spread over seventeen coal fields and over six hundred million (600,000,000) tons of proven reserves (RMRDC, 2015). This shows that more new coal deposits are being discovered in the country and this trend must be matched with continuous and up to date analyses to determine the qualities of these coal deposits. These coal deposits and resources are spread over 13 states of the Federation but geologically restricted to the Benue Trough (Northern, Central-, and Southern-Benue Troughs) and the adjacent Anambra Basin. Some of the notable coal deposits in Nigeria include the Okaba, Owukpa, Inyi, Ogboyoga, Udane Biomi, Ibobo, Onyeama, Okpara, Iva Valley, Kwangshir-Jangwa along River Dep, Maiganga and GidanSidi Coal deposits.

2.0 GEOLOGICAL SETTING OF BENUE TROUGH AND ANAMBRA BASIN

2.1. The Benue Trough

The Benue Trough is one of the Nigeria's inland basins that are bounded in the north by the Chad basin and in the south by the Bida Basin (Figure 1). The Benue Trough is a fundamental tectonosedimentological feature in the evolution of the Cretaceous and Tertiary geology of Nigeria (Nwajide, 2013). The trough is a part of the extensive West and Central Africa plate consequent upon the initiation of proto-equatorial Atlantic (Nwajide, 2013). According to Nwajide, 2013, the precise bounds and dimensions of the Benue Trough are yet to be accurately determined and defined. This he attributed to the burial of its limits under the younger basins, the Anambra and the Niger Delta basins in the South-West and the Chad basin in the North East. Also theco-existence and continuity of the Trough's structures with those of the Niger Republic's basin (Termit basin) to the North added to the complicity of determining the Northern boundary and dimension of the Benue Trough (Figure 1).

The Trough can be arbitrarily taken to extend to and terminate at the right angular bend into the Termit Basin in Niger Republic and this will make an estimated total length of the Trough in Nigeria to be roughly 1,300km and an estimated narrowest and broadest width of 125km at

the immediate SouthEast of the Jos Plateau and 250km across Auchi to Gboko axis respectively (Nwajide, 2013). In the Northeastern part where the Trough bifurcates into two arms (the Northern Gongola arm and the Southern Yola arm), the width of the trough is estimated at over 200km. the sediment thickness across the trough range from 5km in the Northeast to over 12km in the Southwest.

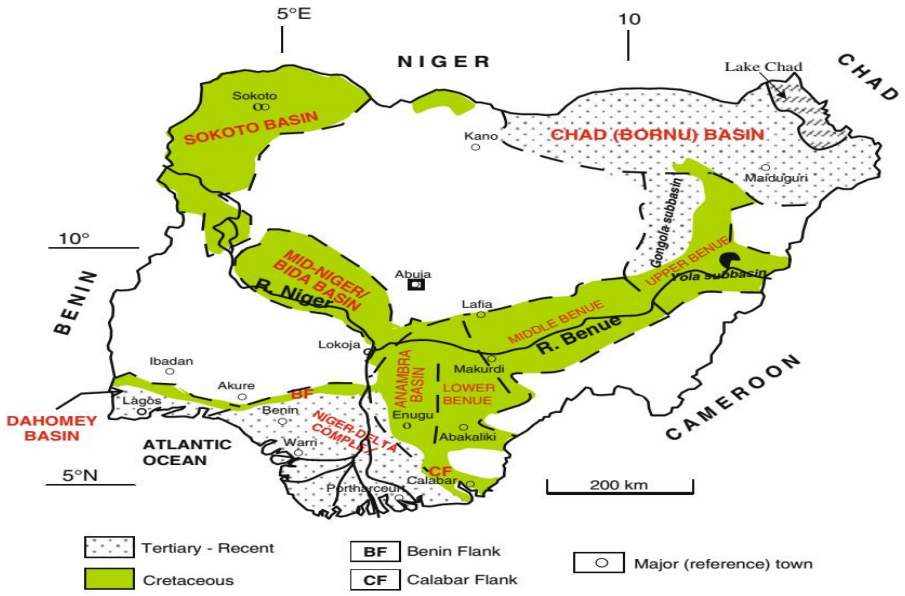

Figure 1: Sedimentary basins of Nigeria (Adopted from Obaje, 2009).

Nwajide (2013) has adopted the Northern, Central and Southern segments as the subdivisions for the Benue Trough as against the hither to Upper, Middle and Lower Benue Trough used by previous authors. The gross characteristics of the Trough are defined by its structural orientation, configuration and the inherent lineaments.

Various theories that culminated into the origin of the Trough have been summarized and discussed by several authors (Nwachukwu, 1972; Wright *et al*, 1985; Wright, 1989;Genik,1992; Obaje,2009;Nwajide,2013). According to these authors, two geologic events viz, the rift fault system and plate tectonics were postulated for the origin of the Benue Trough. Coal resources within the Benue Trough are stratigraphically restricted to the Mamu, Ajali and Nsuka formations, Lafia Formations and the Gombe Formation of the Southern, Central and Northern Benue Trough segments respectively.

2.2. The Anambra Basin

Nwajide (2013) and Wright *et al*. (1985) defined the Anambra Basin as "the upper Senonian-Maastrichtian to Paleocene depositional area located at the Southern end of the Benue Trough, within which the Nkporo Group and younger sediments accumulated, and which extended towards the Southwest as the Niger Delta Basin". This definition is both geologic and geographic and it refers to the sediments-filled area between the southernmost end of the Benue Trough and the Northern end of the Niger Delta. There seems to be a sort of sedimentological continuity among the three interrelated basins, their respective different lithological characteristics notwithstanding (Figure 2).

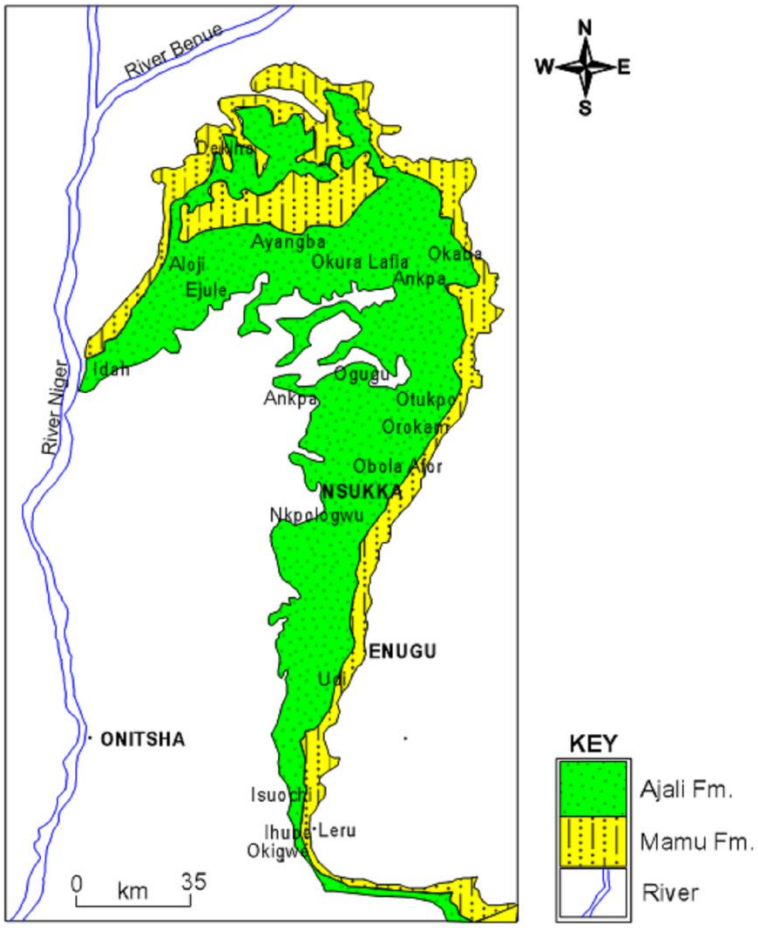

Figure 2: Geological map of Anambra Basin (Adopted from Chiaghanam*et al.*, 2013)

Stratigraphically, the Anambra Basin consists of the uppermost coal measures which are made of the Nsukka, Ajali and Mamu Formations, underlain by the Awgu Formation (Chiaghanam*et al.*, 2013).

2.3. The Coal Measures

The Nigerian coals are sub-bituminous (black coals) of Cretaceous age and lignites (brown coals) of Tertiary age (Nigerian Geological Survey Agency, NGSA bulletin, 2nd edition, 1987). However, the coal deposit at Obi, near Lafia in Nasarawa state has been described as coking coal. Generally, the quality of a coal depends largely on its geological age, hence the Nigerian coals and lignites which are dated Cretaceous to Tertiary age are believed to be of poorer quality than the older Carboniferous coals of Europe and America. The black coals occur in strata of two different ages in the Lower and Upper Coal Measures and are almost entirely restricted to the Benue Trough and the Anambra basin of Nigeria. The Upper Coal Measures are hosted by the Nsukka Formation while the Lower Coal Measures are hosted by the MamuFormation.TheMamu Formation consists of alternations of sandstones, siltstones, mudstones, coal seams and rare shales. This is overlain by the Ajali Formation which is mainly sandstone. The Ajali Formation is in turn overlain by the Nsukka Formation typically comprising of sandstones, blackshales, coal, mudstones and marine limestones. The coals of the lower measures are of medium quality, non-coking and sub-bituminous. They are excellent for gas making and produces high tar-oils, self-binding under pressure, suitable for production of liquid fuels. Conversely, the coals of the upper measures are thinner and of poorer quality.

3.0 MATERIALS AND METHODS

3.1 Field Work and Samples Collection

During field work, ten coal locations were selected within the country for this study. The ten locations were chosen to cover the whole length of Benue Trough and parts of the Anambra basin. Coal samples from Ibobo, Udane-Biomi and Ogboyoga(Kogi State), Iva Valley and Okpara (Enugu State) were obtained from coal seams exposed on the field either along river banks and/or beds, or in areas where the coal seams or beds have been exposed by erosion. Samples from Onyema (Enugu State), Owukpa (Benue State) and Kwaghshir (Lafia-Obi) (Nassarawa State) were obtained from old and abandon coal mines while in Okaba (Kogi State) and Maiganga (Gombe State) the samples were obtained from the recent mine sites.

Four representative coal samples were obtained at each of the ten study sites with the aid of a geological hammer. The sampling was done randomly but in areas where the coal seams were well exposed as in Maiganga, the samples were collected at the various coal seams seen in the mine site. During the sampling, a bulk sample of about 300g each of coal was collected from four points within each of the study areas. The samples collected were sealed in polythene bags and were subsequently transferred into polyvinyl chloride (PVC) canisters and labeled

appropriately for later transport to the laboratory for the various analyses. The coordinates and elevations of the sampling locations were taken with an Etrex Garmin model of GPS (Global Positioning Satellite). Coal samples were collected from freshly exposed mine faces (at Maiganga, Okaba, Ibobo), exposed seams as a result of weathering (at Ogboyoga, Onyema, Iva Valley, Udane Biomi and Okpara) and core samples at Lafia Obi coal deposits. Location maps of the coal deposits were prepared from the GPS coordinates using ArcGis version 10.2.2.

3.2 Laboratory Analyses

Pulverized coal samples were analyzed for mineralogical and calorific characteristics of forty samples (4 samples per coal deposit) from the ten studied coal deposits.

3.2.1 Mineralogical analysis of the coals

The quality and content of minerals in the studied coals were determined by chemical procedures of X-ray diffraction (XRD) method. The coal samples were analyzed for mineralogical constituents using X-ray diffraction (XRD). A pw 3830 X-ray generator Philips PANalytical instrument activated at 25 mA and 40 kV was used for this analysis. The pulverized samples were dried in an oven at 100 °C for 12 h to eliminate the water adsorbed. The samples were compressed into rectangular aluminum holders utilizing an alcohol dabbed spatula and after that clipped into the sample holder of the instrument. The samples were scanned step by step from 5 to 85 degrees 2 theta scale at space of 0.02 and counted for 0.5 sec for each step. The XRD analysis was carried out at the Engineering Materials Development Institute (EMDI) of National Agency for Science and Engineering Infrastructure (NASENI), Akure, Nigeria.

3.2.2 Calorific analysis of the coals

The calorific value was determined based on ASTM D5865 standards. The Ballistic Bomb Calorimeter was first standardized with benzoic acid having 6.32 kCal/g as its calorific value. Different samples of the coals of 0.5 g were placed in the crucibles. The bomb body was fastened in place and plugging the thermocouple into the bomb body. The pressure discharge regulator was closed, and oxygen was admitted into the bomb till the pressure increases to 25 bars. The knob for firing was depressed and released for the bomb to be fired. Heat was given off and the maximum deflection scale of the galvanometer was documented. The maximum deflection obtained in the galvanometer was transformed to energy charge of the sample matter by contrasting the rise in galvanometer deflection with that achieved when a sample of

identified calorific amount of benzoic acid is combusted. The heat, Qin kCal/g given off from the sample is calculated from;

$$Q = \frac{G(\text{meter deflection X calibration constant}}{\text{original mass of sample}} = \frac{(\partial 3 - \partial 1)\,\gamma}{Z} \quad \ldots\ldots\ldots\ldots\ldots\ldots\ldots\ldots\ldots\ldots\ldots\ldots\ldots\ldots 3.6$$

Where:

∂_1=deflection of galvanometer without sample

∂_3=deflection of galvanometer with sample

Z =mass of sample in gram

γ =calibration constant

The calorific value analysis was carried out at the Engineering Materials Development Institute (EMDI) of National Agency for Science and Engineering Infrastructure (NASENI), Akure, Nigeria.

4.0 RESULTS AND DISCUSSION

4.1Field Results

Forty coals samples (four per sample site) obtained from ten coal deposits were used for the various analyses carried out in this study (Figure 5). The coal samples were obtained from the various coal fields (active and non-active mining) spread across the Nigerian coal-bearing sedimentary facies.

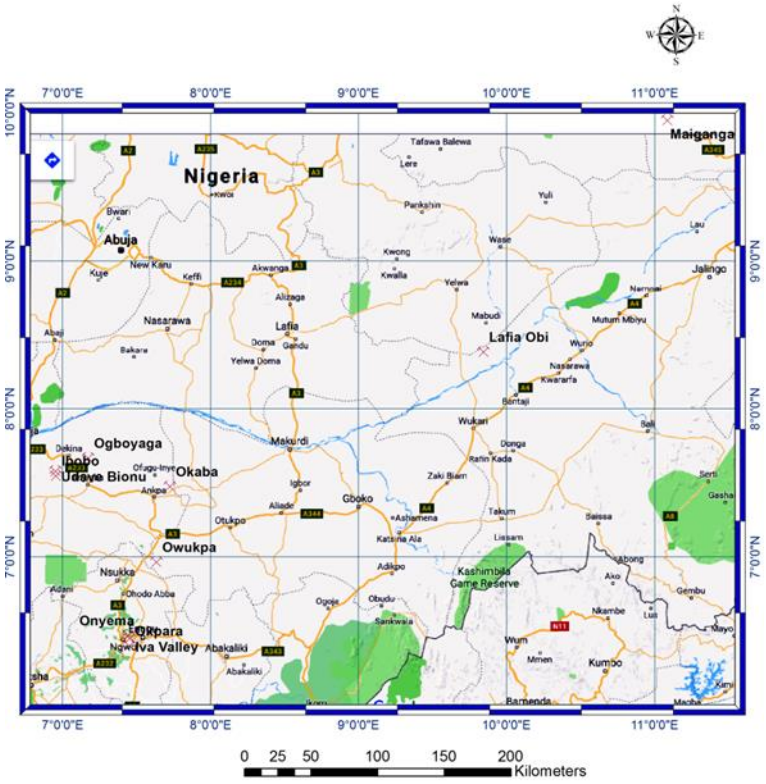

Figure 3: Location map of the coal fields where samples were taken for the study

The coal deposits where the samples were obtained are Lafia Obi, Okpara, Onyema, Okaba, Maiganga, Udane Biomi, Ibobo, Owukpa, Iva Valley and Ogboyoga. The samples are grab samples (Ibobo and Owukpa coals), channel samples (other coals deposits) except for Lafia Obi coal where core samples were obtained from the Nigerian Coal Corporation site office at Obi, Nasarawa State (Table1).

Table 1: Information on the coal sampling points (sample origin, latitude and longitude)

Coal Deposit	Sample origin	Latitude	Longitude
Ibobo	Run-off-mine	N 07 33 01.1	E 006 57 15.5
Udane Biomi	River channel	N 07 34 51.2	E 006 57 07.5
Ogboyoga	River bank	N 07 40 15.2	E 007 10 26.1
Okaba	Mine face	N 07 28 43.2	E 007 43 33.9

Owukpa	Abandoned mine	N 06 58 04.9	E 007 38 04.9
Onyema	Coal outcrop	N 06 28 19.9	E 007 26 43.2
Okpara	Coal outcrop	N 06 24 00.2	E 007 27 05.5
Iva Valley	Coal outcrop	N 06 27 02.0	E 007 27 09.2
Maiganga	Mine face	N 09 57 08.1	E 011 05 15.2
Lafia Obi	Core sample	N 08 23 13.2	E 009 50 39.9

4.2 Mineralogy of the coals

The X-ray Diffraction patterns of the studied coals are presented in appendix A and their corresponding minerals in Table 2. The X Ray Diffractograms of the coals show that quartz is the dominant mineral in most of the coals. Other minerals detected include halite, anhydrite, magnetite, magnesite, hematite, dolomite and kaolinite. These minerals are commonly reported in coal samples from most parts of the world (Ryemshak*et al*., 2015).

Table 2: Minerals identified from the XRD analyses of the studied coals

Coal deposit analyzed	Minerals identified
Onyema	Quartz, Anhydrite, Hematite,
Obi - Lafia	Quartz, Magnetite, Anhydrite, Magnesite
Maiganga	Quartz, Magnetite, Anhydrite, Magnesite
Ogboyoga	Quartz, Kaolinite, Rutile
Iva Valley	Quartz, Dolomite
Ibobo	Quartz, Hematite
Udane Biomi	Quartz, Dolomite
Okaba	Quartz, Dolomite
Okpara	Quartz, Halite, Anhydrite

Owukpa	Quartz, Dolomite

These minerals affect the processing and utilization of coals. There are two ways in which mineral matters can be associated with coals; these are exempted minerals association (minerals that are distinct from the coal) and included minerals association (minerals strongly linked with the coal). The most frequent minerals recognized in coals are quartz, kaolinite, calcite, gypsum and feldspar, and intermittently ankerite, dolomite, siderite, iron-oxyhydroxides and sulphates (Ryemshak*et al*., 2015).

4.3 Calorific values of the coals

The calorific values of the coals as determined are indicated in Table 3.

Table 3: Calorific values of the coals

Coal Deposit	Average Calorific Value (Kcal/kg)
Iva Valley	5990
Okaba	4723
Ibobo	4640
Obi – Lafia	4345
Owukpa	3780
Onyema	3742
Okpara	3569
Maiganga	2861
Udane – Biomi	2625
Ogboyoga	2220

Table 4: Classification of coals based on calorific values (After Kumar and Saxena, 2014)

Grade	**Calorific Value Range (in Kcal/kg)**

A	Exceeding 6200
B	5600 – 6200
C	4940 – 5600
D	4200 – 4940
E	3360 – 4200
F	2400 – 3360
G	1300 – 2400

On the basis of coal classification based on their respective calorific values according to (Kumar and Saxena, 2014), the analysed coals are classified as indicated in Table 5.

Table 5: Classification of the analyzed coals based on calorific values

Grade	Analysed Coal Deposits
B	Iva Valley
C	Okaba
D	Ibobo
D	Obi - Lafia
E	Owukpa
E	Onyema
E	Okpara
F	Maiganga
F	Udane - Biomi
G	Ogboyoga

4.4 Uses of the studied coals

The trends in the mineralogical and calorific values of the studied coals have earlier been discussed under the various subheadings.The calorific values of the entire coal deposits are sufficiently high and can be utilized for the generation of power. The Iva Valley coal deposit with the greatest heating value of 6,712Kcal/kg could be the most excellent for heating and generation of power.

5. CONCLUSION

The selected ten studied Nigerian coals are situated within the Benue Trough and Anambra Basin.The Nigerian coal deposits and resources are spread over 13 states of the Federation but geologically restricted to the Benue Trough (Northern, Central-, and Southern divisions) and the adjacent Anambra Basin. There are also reported cases of coal shows in the Bida and Sokoto Basins, the Ogwasi - Asaba lignite deposit in Niger Delta, Southern part of Nigeria. Some of the notable coal deposits in Nigeria include the Okaba, Owukpa, Inyi, Ogboyoga, Udane Biomi, Ibobo, Onyema, Okpara, Iva Valley, Obi - Lafia, Kwangshir-Jangwa, River Dep, Maiganga, Okobo and GidanSidi Coal deposits.

The X Ray Diffractogram of the coal samples showed that quartz is dominant in most of the coals. Other minerals include halide, anhydride, magnetite, magnesite, hematite, dolomite, kaolinite and rutile.

On the basis of the Kumar and Saxena (2014) classification based on calorific value, the analyzed coals are grouped as Iva Valley – grade B, Okaba – grade C, Obi- Lafia - grade D, Ibobo – grade D, Onyema-grade E, Owukpa – grade E, Okpara – grade E, Udane Biomi-grade F, Maiganga-grade F and Ogboyoga G.

In terms of the technological applications of the studied coals,the calorific values of the coal deposits are sufficiently high and indicate their suitability for the generation of power.

6. REFERENCES

ASTM D5865-13, Standard Test Method for Gross Calorific Value of Coal and Coke, a Standard – ASTM D5865, 2007 ASTM International, West Conshohocken, PA, 2013, www.astm.org.

Chiaghanam, O.I., Chiadikobi, K.C., Ikegwuonu, O.N., Omoboriowo, A.O., Onyemesili,O.C. &Acra, E.J. (2013).Palynofacies and Kerogen Analysis of Upper Cretaceous (Early Campanian to Maatrichtian) Enugu Shale and Mamu Formation in Anambra Basin, South-eastern, Nigeria.*Coal Geology*, 26, 233 – 260.

Genik, G.J. (1992).Regional Framework, Structural and Petroleum aspects of Rifts Basin in Niger, Chad and the Central African Republic (CAR).*Tectonophysics*, Elsevier. ISO 1172.*Journal of Mining and Geology*, 44, 11–18.

Kumar, V. &Saxena, V.K. (2014).Studies of the Variation in Coal Properties of Low Volatile Coking Coal after Benefication.*International Journal of Computational Engineering Research*, 4(1), 39 – 57.

Nwachukwu, S.O. (1972). The Tectonic Evaluation of the Southern Portion of the Benue Trough.*Geological Magazine*, 109(5), 411-419.

Nwajide, C.S. (2013).*Geology of Nigeria's Sedimentary Basins*. Lagos, CSS Bookshop Ltd., 565p.

Nigeria Geological Survey Agency Bulleting, 2nd Edition, (1987) Petroleum Geology using Aromatic Biological Markers as a Tool for Assessing Thermal Maturity of Source Rocks in the Campano-MaastrichtianMamu Formation, Southeastern Nigeria.

Obaje, N.G. (2009). *Geology and Mineral Resources of Nigeria*. Springer Dordrecht Heidelberg London, New York, 221p.

Ryemshak, S.A. &Jauro, A. (2013).Proximate Analysis, Rheological Properties and Technological Applications of Some Nigerian Coals*International Journal of Industrial Chemistry*, 4(7), 1-7.

Raw Material Research and Development Council (2015). Brief on Nigerian Coals

Wright, J.B., Hastings, D.A. & Williams, H.R. (1985).*Geology and Mineral Resources of West Africa*.London, George Allen and Unwin, 187p.

Appendix A: X-Ray Diffractograms of the Studied Coals

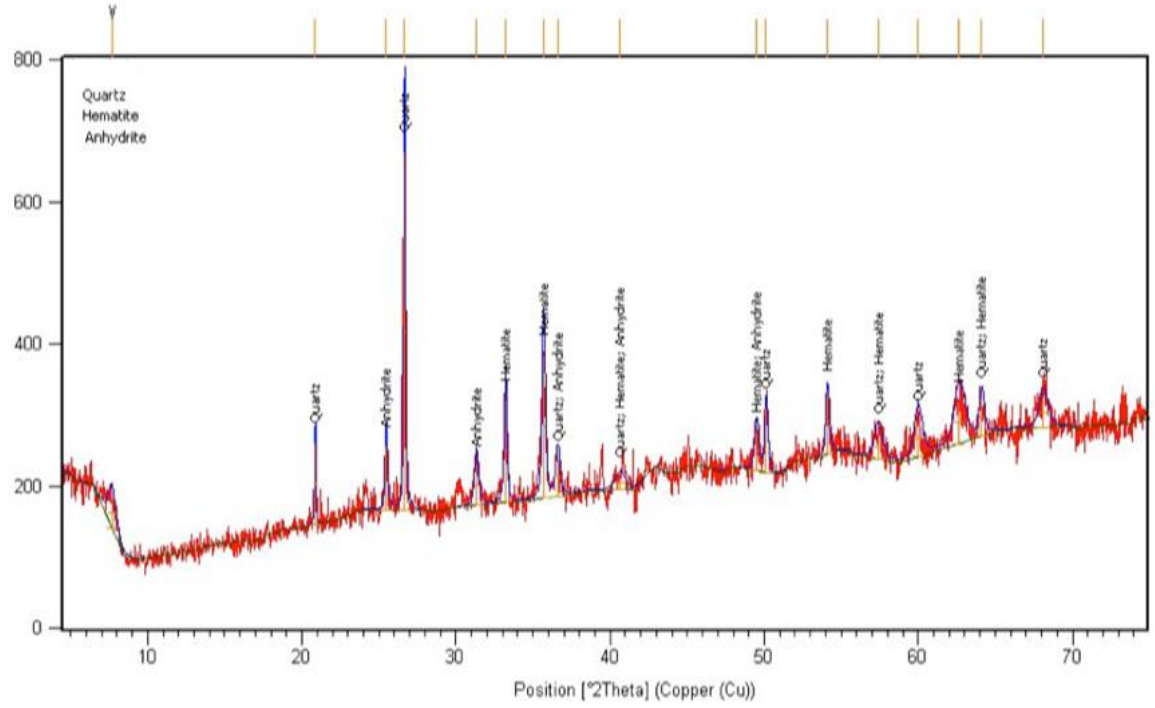

X-ray Diffractogram of Onyema coal

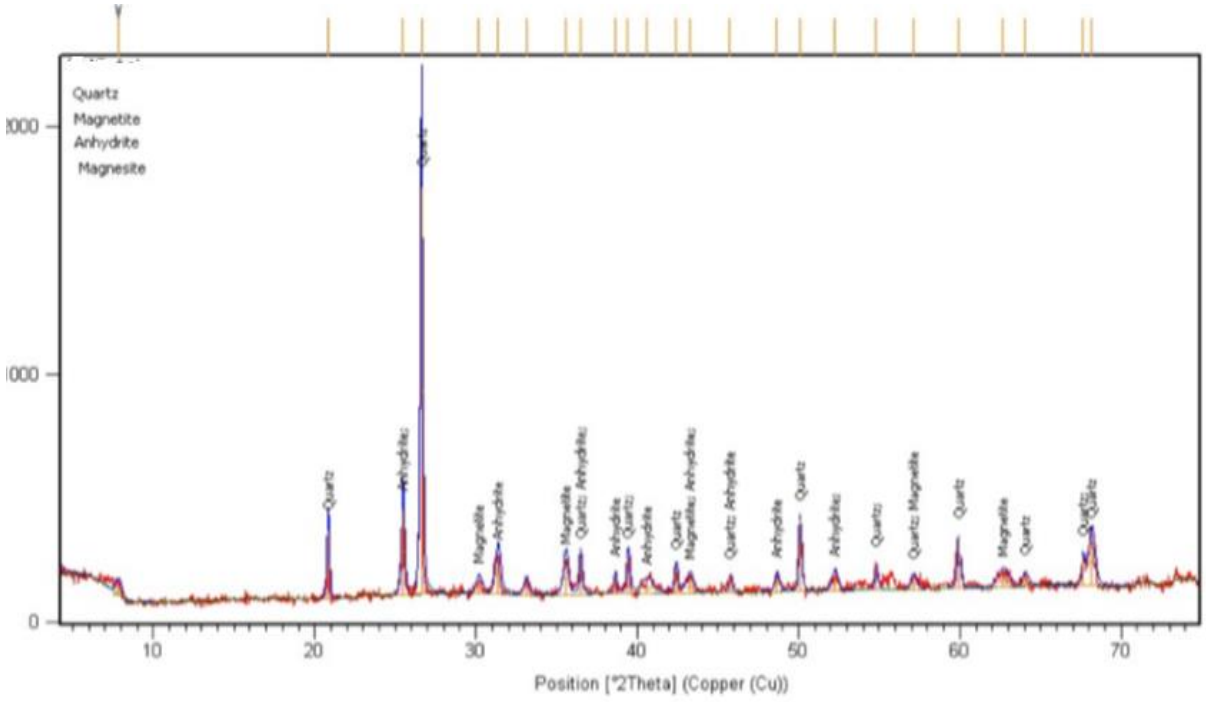

X-ray Diffractogram of Lafia Obi coal

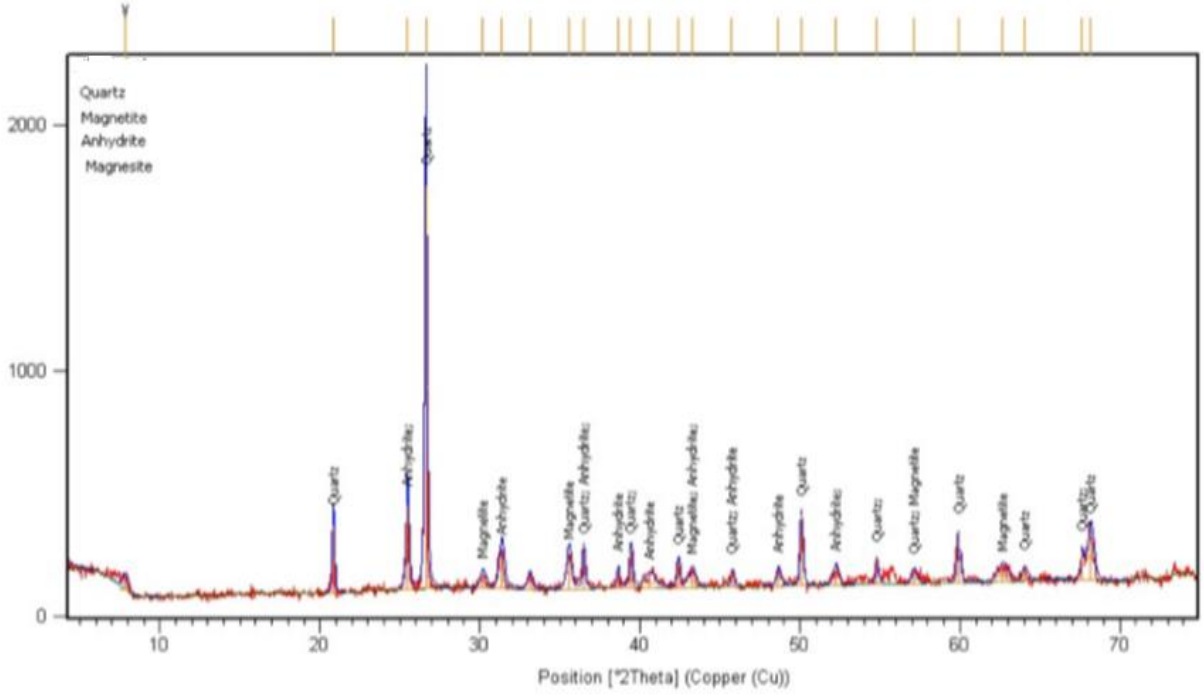

X-ray DiffractogramofMaigangacoal

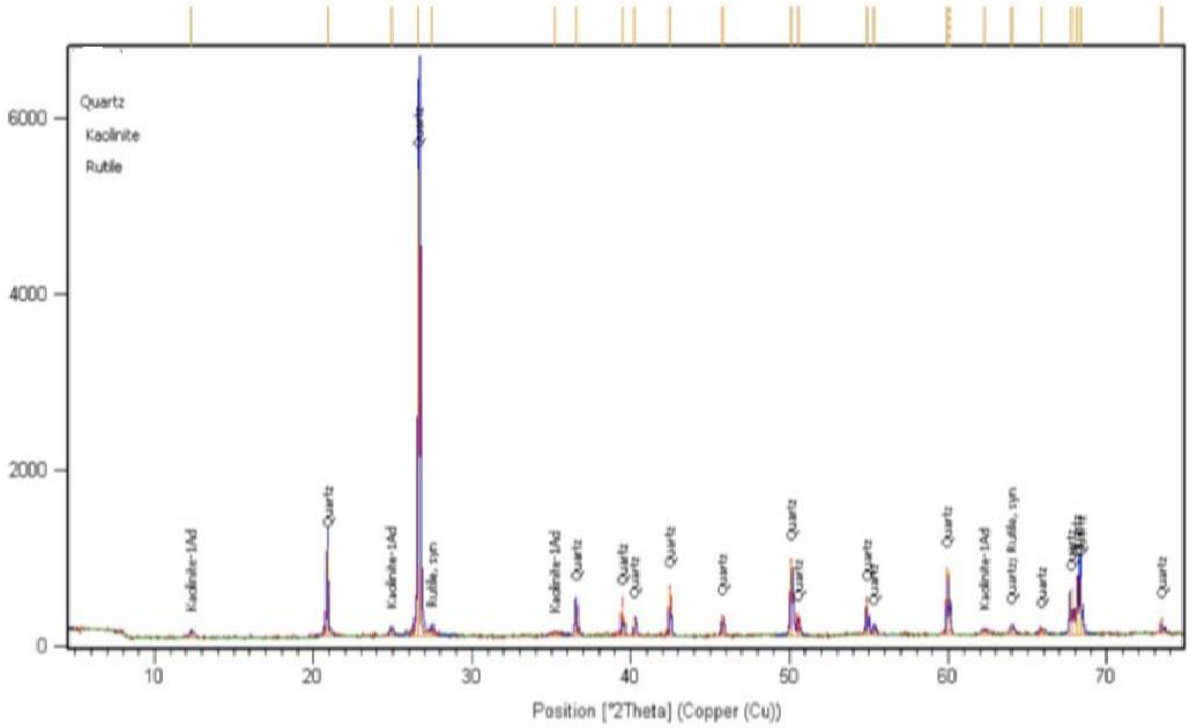

X-ray DiffractogramofOgboyogacoal

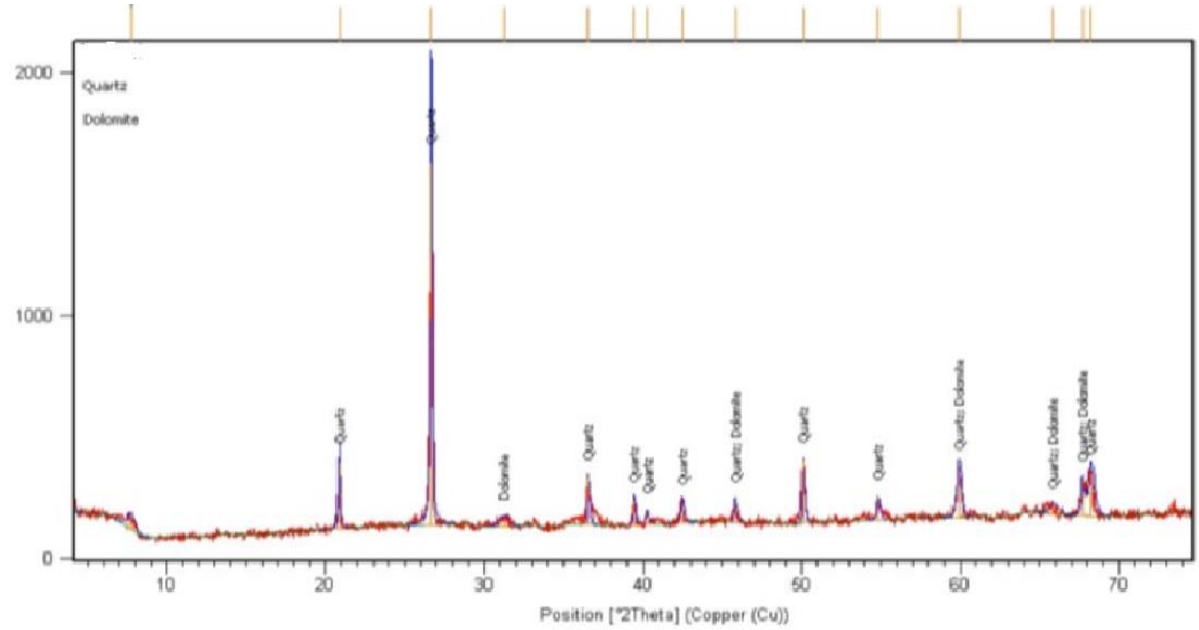

X-ray Diffractogramof Iva Valley coal

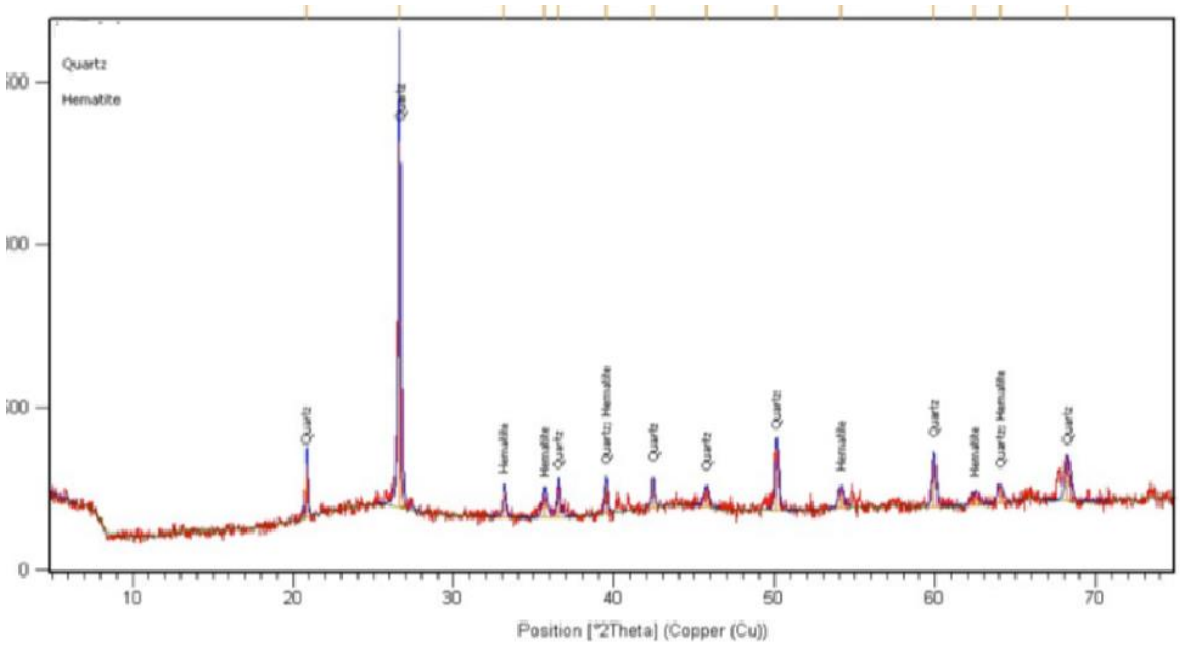

X-ray DiffractogramofIbobocoal

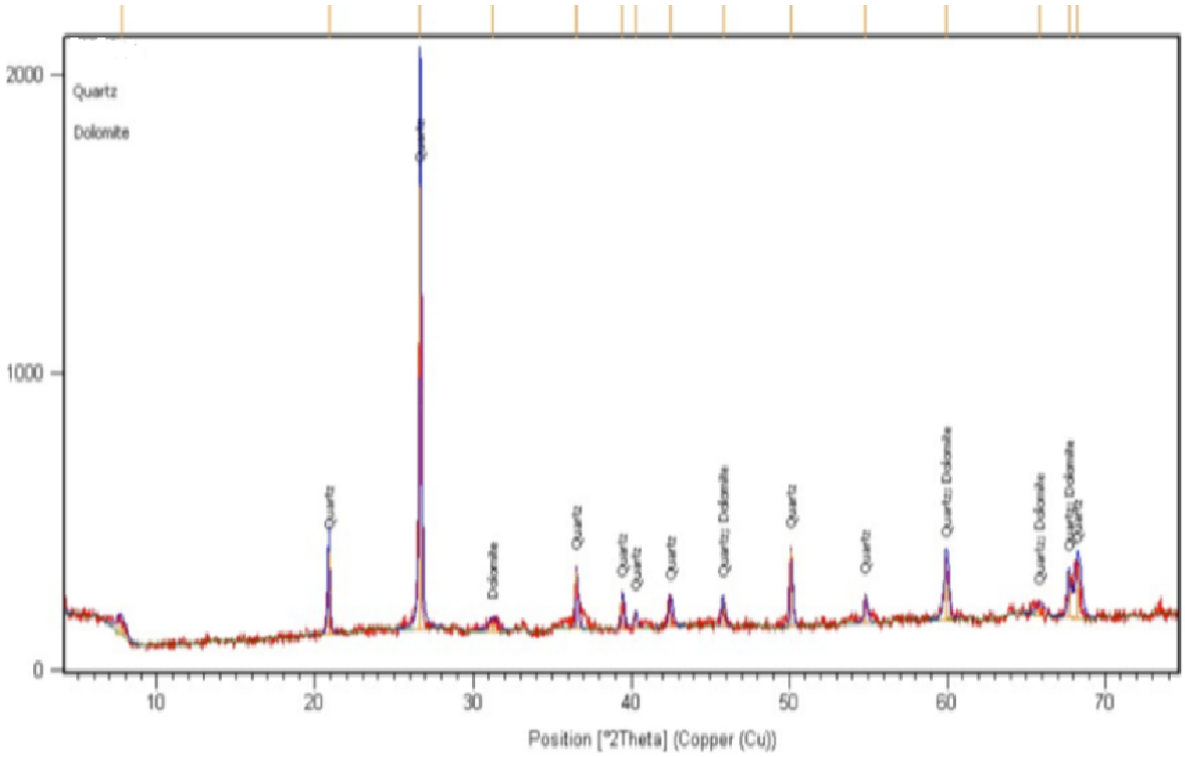

X-ray Diffractogram of Udane Biomi coal

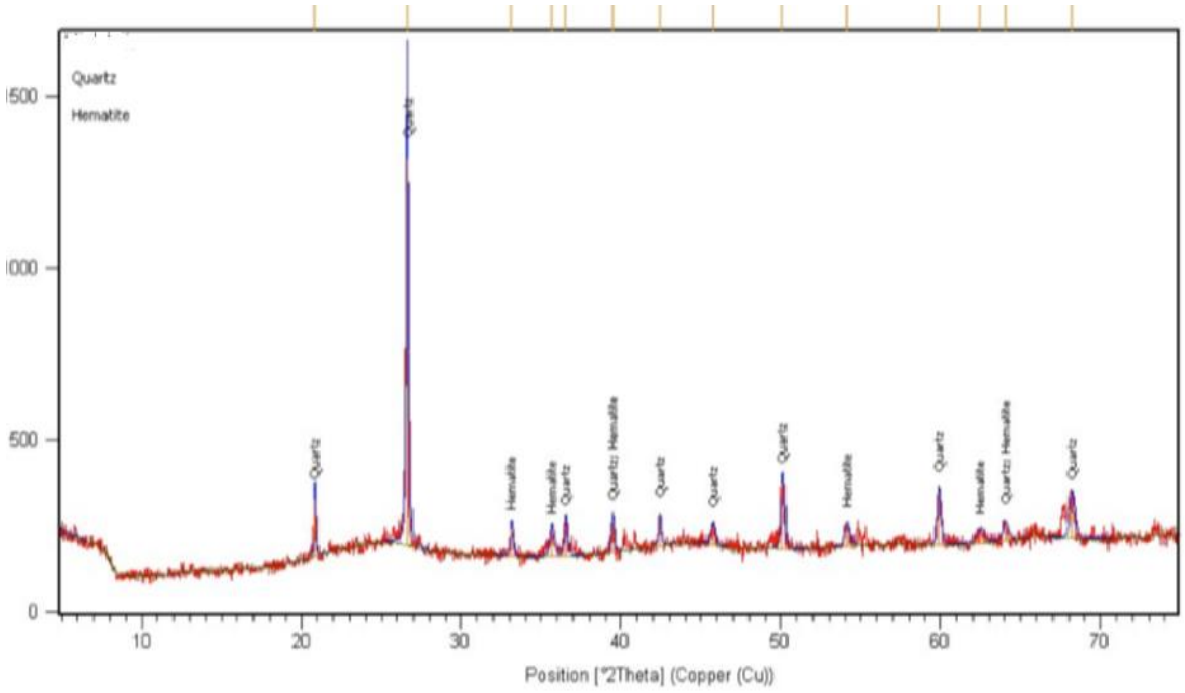

X-ray Diffractogram of Okaba coal

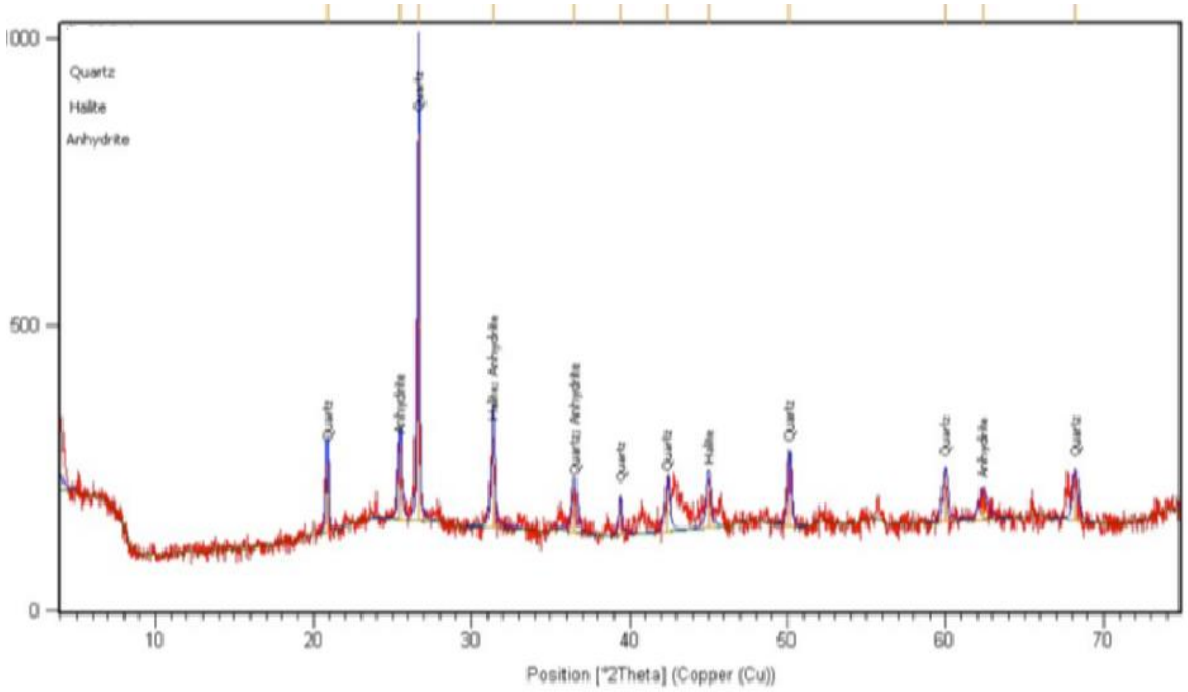

X-ray Diffractogram of Okpara coal

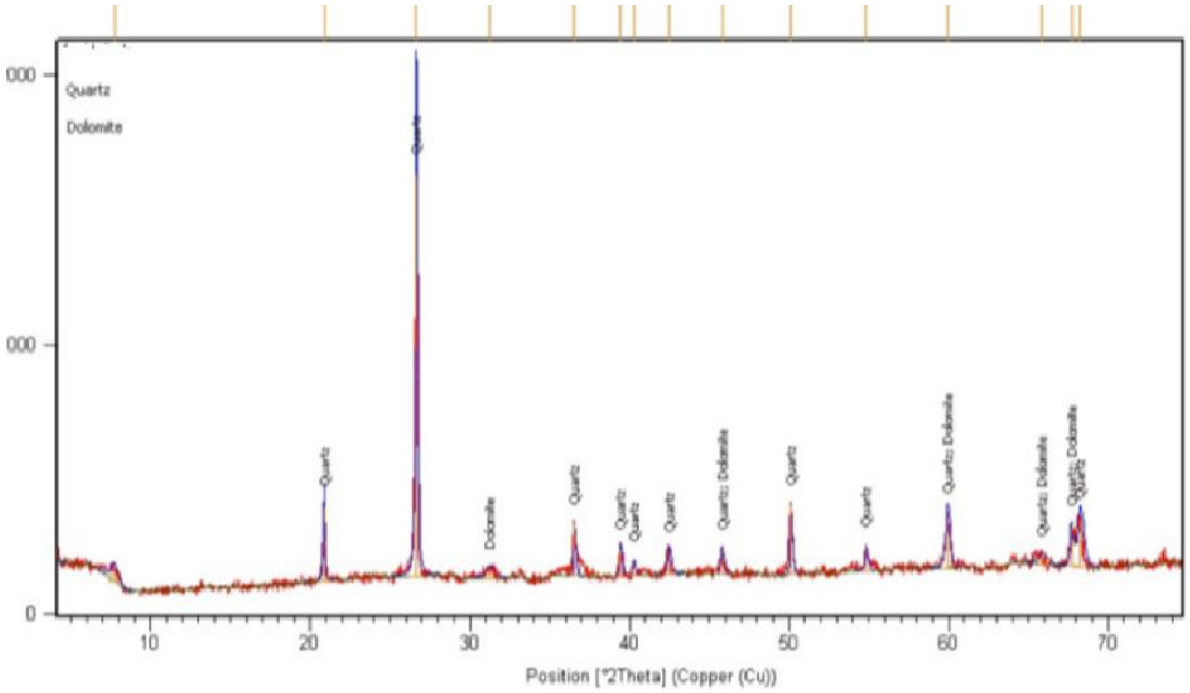

X-ray Diffractogram of Owukpa coal

Investigation of Groundwater Quality in parts of Onitsha, Southeastern Nigeria

B.A. Igbomor and A.N. Amadi*
Department of Geology, Federal University of Technology, Minna
*Corresponding Author's email: geoama76@gamil.com
Phone Number: 08037729977 or 07030579700

Abstract

The physico-chemical and microbial characteristics of water defines its quality. The groundwater quality in Onitsha was investigation in the present study from the point-view anthropogenic interference. The concentrations of the major ions were found to be below the recommendations by Nigeria Standard for Drinking Water Quality (NSDWQ) and World Health Organization (WHO) except chloride. High chloride content in groundwater may be an indication of urban groundwater contamination as well as proximity to marine source. The water type in the area as revealed from Piper Diagram is calcium-chloride type. The pH of the groundwater is slightly acidic and it explains the paucity of carbonates in the groundwater system in the area. Carbonates are easily converted to bicarbonates under acidic condition. The concentrations of iron, lead, manganese, chromium and cadmium in the groundwater were found to be 73.3%, 23.3%, 20.0%, 13.3% and 10.0% respectively higher than their maximum permissible limit by NSDWQ and WHO. The slightly acidic medium enhances the dissolution, release and migration of these metals into the aquiferous system. Based on the Water Quality Index (WQI), the groundwater in the area was categorized into 5 ranging from excellent water

(24%), good water (27%), poor water (17%), very poor water (24%) and water unsuitable for drinking (10%). High concentration of chloride, iron, lead, manganese, chromium and cadmium in the groundwater in some locations are responsible for the poor water quality in the area. It can be attributed for the huge human activities going on in the area. The spatial distribution of WQI shows that wells close to dumpsites or untreated industrial effluent are deteriorated with respect to quality. Metal pollution index (MPI) indicates that iron lead and manganese show moderate pollution status while chromium and cadmium reflects light pollution. The results MPI agreed with the findings of WQI, which confirms the efficacy of these models in groundwater pollution studies.

Keywords**:** *Groundwater, Assessment, Onitsha, Southeastern Nigeria*

1. Introduction

Groundwater is the water found in the intercalated pore spaces saturated in the subsurface below the water table. It accounts for about 98% of the world's available fresh water and is the most valuable resources for various activities of man. The chemistry of groundwater is influenced majorly by the mineralogy of the host rock, the residence time and the anthropogenic activities dominant in the area (Abimbola *et al.,* 2002; Amadi *et al.,* 2014). In most developing countries of the world like Nigeria, due to high population in most urban centres there is increase in industrial and human activities coupled with environmental degradation and indiscriminate refuse disposal tend to make groundwater vulnerable to contamination, (Adelana *et al.,* 2003; Adelana *et al.,* 2005; Ocheri, 2006; Longe and Enekwechi, 2007; Efe, 2008, Amadi et al; 2010; Idris-Nda et al; 2015 and Ezeabasili, 2014). Groundwater is the most sort after in most cities in Nigeria as a result of paucity of surface water and the broken down of public water supply has led to the increase in demand of groundwater due to its protective nature and indirect contact with the surface (Amadi *et al.,* 2014).

World health organization (WHO, 2004) report estimate that more than a billion people globally lack access to potable water and sanitation, with most of them in Sub-Sahara Africa. Drinking polluted water increases the risk of cholera, typhoid fever, hepatitis, increased blood pressure and metabolic poison (WHO, 2017; Zietz et al, 2007; Adepoju-Bello and Alabi 2005). Although they are treatable and preventable, they are the number one killer disease in Africa (WHO, 2004). Many chemical constituents of groundwater can potentially cause adverse human health effects, the detection of these constituents in water is often slow, difficult and expensive which limits early warning capability and affordability. Reliance on water quality determination alone is not enough to protect public health because it is not economically

feasible to test all drinking water quality parameters, thus the use of monitoring effort should be employed. The study area is a densely populated commercial nerve centre in southeastern Nigeria host to many industries and markets, with serious sanitation pose by these industries and markets. The urban population depend on groundwater for drinking and domestic purposes. The objective of this paper is to discuss the physicochemical parameters based on compliance the of the groundwater in Onitsha to Nigeria and WHO standard for drinking water quality and the use of Water Quality Index (WQI) and Metal Pollution Index (MPI) to access the overall quality rating the groundwater in the study area.

2. Materials and Methods

2.1 Location, Geology and Hydrogeology of the Area

The study was carried out in Onitsha area, located in the southeastern part of Nigeria. The area extent of the study area is approximately 46.65 km^2 and bounded within Latitudes $6^{\circ}6'00^{II}$ N to $6^{\circ}9'30^{"}$ N and Longitudes $6^{\circ}46'00^{II}$ E to $6^{\circ}50^{I}00^{II}$ E in the topographical map of Nigeria, sheet 300. (Figure 1). Located within the tropics with two prominent seasons. The dry and wet season, April to October is the period of rainfall with average monthly rainfall of 2000 mm. The dry season is between November to March. The mean annual rainfall is between 1,500 mm to 2,500 mm. Temperature ranges between 22^0C to 27^0C. The study area is majorly drained by Nkisi, Anambra and the Idemili rivers which are tributaries to River Niger.

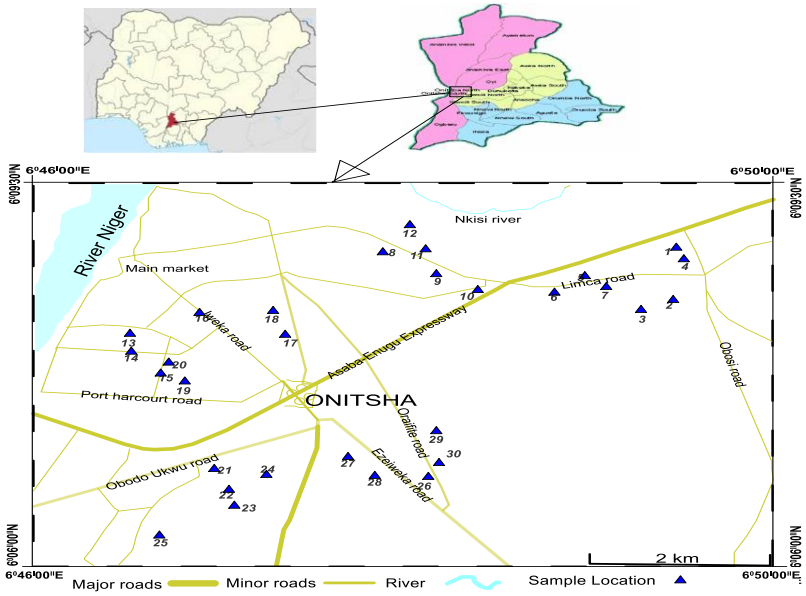

Figure 1. Map of Nigeria showing the study area.

Geologically Onitsha is located within the Anambra basin, it is underlain by cretaceous to recent sedimentary formations that are of varying aquifer potentials which belong to Ameki

group consisting of the Nanka sand, Nsugbe sandstone and Ameki formation, (Nwajide, 2013). The area is underlain by the Alluvial plain sands, Ameki/Nanka sands and the Imo shale with different ability to hold and transmit water(Nfor *et al* 2007). The area is mostly cover by lateric soil with variable thickness, underlain by a thick coarse sandy horizon with lenses of medium shale to medium sand occurring with the coarse sand. The thickness of the coarse sand range between 8 – 27m. The coarse sand horizon is underlain with clay with a range of thickness from 6 m at southern part to 23 m in the east (Isikhueme and Omorogieva; 2015). Below the shale and sand horizon at about 102 m is the top of a medium grained sand zone which is the main aquifer which varies in thickness from 23 m to more than 92 m. The aquifer is prolific and extends within the study area (Isikhueme and Omorogieva; 2015). Figure 2 shows the subsurface stratigraphy and the various aquiferous horizons from unconfined, semiconfined to confined in the region. At the base of the unconfined aquifer lie the semi-confined and the confined upper, middle and deep aquiferous horizons made up of sandstone within the Ameki Formation (Isikhueme and Omorogieva; 2015).

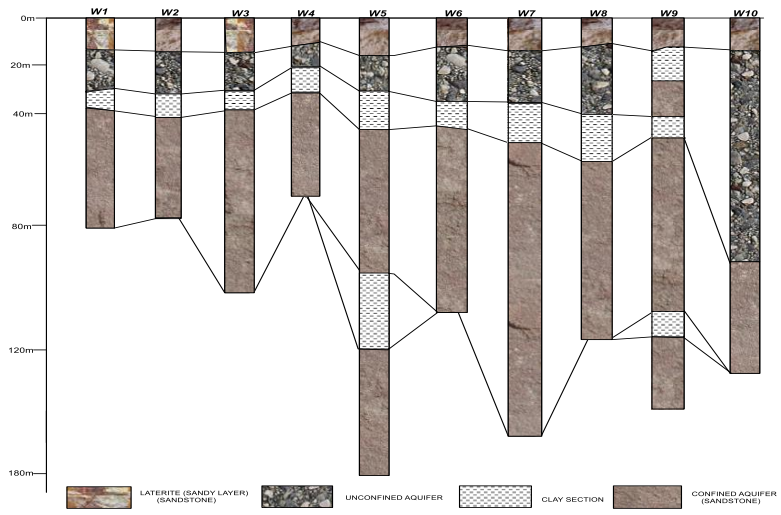

Figure 2: Lithologic log from wells within Onitsha (After Isikhueme and Omorogieva; 2015).

2.2 Sampling and Laboratory Analysis

A preliminary investigation was conducted to locate areas that of interest within the study area and establish sampling points. Samples were collected from boreholes (Figure 1) in tight capped high quality polyethylene bottles, they are rinsed with the same water which has to be taken as samples. Electrical conductivity (EC), total dissolved solids and pH were measured using a model PHS-3D pH meter uniscope immediately after sampling and the coordinate of the borehole taking with a hand held Global Positioning System (GPS, Model GARMIN GPSMAP 78S). The samples were immediately transferred to the laboratory. Each of the

groundwater samples was analyzed for various physicochemical parameters such as pH; electrical conductivity (EC); total dissolved solids (TDS); turbidity; colour; major cation-sodium (Na^+), potassium (K^+), calcium (Ca^{2+}) and magnesium (Mg^{2+}); major anions-bicarbonate (HCO_3^-), chloride (Cl^-), and sulphate (SO_2^-). Minor constituents such as nitrate (NO_3), nitrite (NO_2), phosphate (PO_4), and ammonium nitrogen. Heavy metals such as iron (Fe), manganese (Mn), copper (Cu), arsenic (As), zinc (Zn), lead (Pb) cadmium (Cd) and nickel (Ni). Test methods followed are the standard procedures recommended by American Public Health Association (APHA, 2008). Statistical analysis was done using Statistical Program for Social Sciences (SPSS 16.0) obtain from the physicochemical parameters and the suitability of the water was examined based on percent compliance of the measured data with respect to Nigeria Standard for Drinking Water Quality (NSDWQ, 2007) and World Health Organization standard (WHO, 2007). The groundwater hydrochemical facie will be classified by graphic procedure (Piper, 1944).

2.3 Metal Pollution Index (MPI)

Metal Pollution Index (MPI) is a method of rating water quality that shows the composite influence of individual parameters on the overall quality of water (Tamasi and Cini, 2004). The rating is a value between zero and one, reflecting the relative importance individual quality considerations. The higher the concentration of a metal compared to its allowable standard, the worse the quality of the water (Amadi, 2011). It has a wide application and it is used as indicator of the quality of river water (Lyulko et al., 2001; Amadi, 2012), as well as drinking water (Nikoladis et al 2008). The MPI represents the sum of the ratio between the analyzed parameters and their corresponding national standard values (Tamasi and Cini 2004; Amadi, 2012) as shown:

$$MPI=\Sigma[Ci/(MAC)i]$$

Ci is the metal concentration in water sample, MAC_i is the maximum allowable concentration.

2.4 Water Quality Index(WQI)

To understand the overall quality of groundwater, the WQI was used.WQI is defined as a rating reflecting the composite influence of different water quality parameters on the overall quality of water(Batabyal and Chakraborty; 2015). The objective of WQI is to turn complex water quality data into information that is understandable and useable by the public (Amadi; 2011). The Nigeria Standard for Drinking Water Quality (NSDWQ, 2007) was used for the calculation of WQI. The water quality index was calculated using the Weighted Arithmetic Index method. The quality rating scale for each parameter (qi) was calculated by using the expression: qi=(ci/si)x100. Relative weight (wi) was calculated by a value inversely proportional to the

recommended standard (si) of the corresponding parameter: wi= 1/si. Overall WQI = Σ qiwi /Σwi. The computed WQI values are classified into five categories: excellent water (WQI= 50); good water (WQI=50–100); poor water (WQI=100–200); very poor water (WQI=200–300); and water unsuitable for drinking (WQI> 300).

The Geographic Information System (GIS) was integrated to generate a map that includes information relating to water quality and its distribution over the study area. The spatial analysis was carried out using sufer 11 software. The physicochemical parameters from groundwater samples from each location were computed using WQI (Table 2). All the WQI values with their location details were included separately into the attribute table of the software to generate a spatial distribution of water quality map.

3. Results and Discussion

Table 1: Statistical summary of the Physico-chemical Parameters

Parameters(mg/L)	Minimum	Maximum	Mean (Ci)	NSDWQ,2007	WHO,2007
PH	4.92	7.11	5.728	6.5-7.5	6.5-7.5
Conductivity (µs/cm)	44	575	253.87	1000	1000
Colour (Pt.Co)	0.00	1.8	0.2	15	15
Turbidity (NTU)	0.00	1.24	0.172	5	5
TDS	29.48	385.25	158.204	500	500
COD	3.2	23.1	9.703	10	-
Bicarbonate	23.4	90.1	53.327	100	-
Sodium	0.18	1.29	0.6407	200	200
Potassium	0.09	1.21	0.3683	150	-
Calcium	0.85	5.11	1.9913	200	-
Magnesium	0.13	2.41	1.165	200	-
Chloride	33.49	320	133.97	250	250
Nitrite	0.005	0.18	0.0426	0.2	0.2
Nitrate	0.305	8.2	2.0508	50	10
Sulphate	0.024	3.00	0.5302	100	250
Iron	0.172	1.165	0.5333	0.3	0.3
Manganese	0.019	0.281	0.1200	0.200	0.1
Zinc	0.142	0.721	0.3327	3.00	5.0
Copper	0.012	0.18	0.0512	1.00	0.5
Chromium	<0.001	0.081	0.0082	0.05	0.05
Cadmium	<0.001	0.0012	0.0098	0.001	0.03
Lead	<0.001	0.08200	0.0156	0.01	0.01

The statistical summary of groundwater analysis (Table 1) with respect to the Nigeria Standard for Drinking Water Quality (NSDWQ, 2007) and World Health Organization (WHO, 2007)

standard. The pH shows acidic property (4.92 to 7.11) with mean value of 5.73, pH shows the water is acidic and this can be attributed to precipitation as the major source of recharge. Water with low pH gives sour taste to water, corrode pipes and increase element mobility (EPA, 2009). Electrical conductivity ranged between 44 µs/cm to 575 µs/cm with a mean value of 353.87 µs/cm, indicating low mineralization in the study area. The maximum value for total dissolved solid is 385.25 mg/l, shows the groundwater is freshwater and suitable for drinking. The turbidity and colour values were <1 NTU to 2.6 NTU and <1 Pt.co to 5.4 Pt.co respectively. The physical parameters lie within the permissible limit for Nigeria and WHO standard for drinking water quality. The major ion analysis shows that calcium ion (Ca^{2+}) is the leading cation and chlorine ion (Cl^{-}) is the dominant anion in the groundwater samples from the study area. The range of the cation abundance was recorded as Ca>Mg>Na>K and the order for anion Cl>HCO>SO_4. The overall concentration pattern of major ions in milligram/liter are Cl>HCO>Ca>Mg>Na>SO_4>K. All major ions values lie within the permissible limit for Nigeria and WHO standard except for chlorine which was found to above the standard in some locations. The concentration of chlorine range between 33.49 to 320 in some locations it is way above the 250 mg/l acceptable limit for Nigeria and WHO standard. This gives a clue the elevated concentration of chloride in some groundwater of the study area might be from waste water. The influence of waste water on groundwater quality is a well documented worldwide (Forster *et al.*, 2011). The study area is the commercial centre of southeastern Nigeria, it is densely populated and home to many industries and markets. The waste water generated from these industries and household coupled with leakages from septic tanks can be linked to the elevated concentration of chloride in the study area. Concentration of Nitrate and Nitrite ranged between 0.3 mg/l to 8.2 mg/l and <0.05 mg/l to 0.18 mg/l respectively. Other minor constituents in groundwater include phosphate, ranged between <0.05 mg/l to 0.34 mg/l and 0.11 mg/l to 0.21 mg/l for Ammonium Nitrogen, both lie within the Nigeria and WHO standard for drinking water quality. Heavy metals iron, manganese, copper, zinc, chromium, cadmium, and lead were all detected in the water sample while nickel and mercury were found below the detection limits. Concentration of iron varied from 0.17 to 1.17 mg/L with a mean value of 0.53 mg/l, 70% of the groundwater samples show concentration of iron above the 0.3 mg/l limit for Nigeria and WHO standard for drinking water quality. The lateritic nature of the overlying soil and host rocks is likely to cause the elevated iron concentration in the groundwater. The interaction of rainwater during infiltration with the iron-rich sediments was primarily responsible for the high iron content in groundwater. Groundwater occurs at shallow depths in the study area under unconfined conditions in the upper part of the unconsolidated sediments,

a sequences of lateritic gravel, ferruginous sand, with minor clay, has been intersected (Fig. 2). Anthropogenic activities are being carried out in the study area, but the elevated values of iron concentration can be linked to water-rock interaction which is geogenic. Manganese concentrations ranged between 0.02 mg/l to 0.28 mg/l and average of 0.12 mg/l. 20% show values greater than the desirable limit, and this may be because of manganese occur naturally along iron and this can be attributed to some localized effects. Copper and zinc ranged between 0012 mg/l to 0.18 and 0.14 to 0.72 respectively and lie within the acceptable limit for Nigeria and WHO standard. Chromium, cadmium and lead were below detection limit in most groundwater samples, However chromium, cadmium and lead was detected in 26.67%, 13.33% and 30% respectively of the groundwater sample in the study area and with some higher than the desirable limit. Chromium ranged between (<0.001 mg/l to 0.081 mg/l), cadmium (<0.001mg/l to 0.013 mg/l) and lead (<0.001 mg/l to 0.082 mg/l). The elevated concentration of these heavy metals in some locations within the study area can be attributed to the anthropogenic activities domicile in the area through effluent discharge from industries to the surrounding soils and stream channels. They can also be linked to infiltration of urban runoff into groundwater from waste disposed indiscriminately in some open dumpsite located within the study area.

The WQI of all the samples taken were calculated using the procedure explained above and presented in Table 2. The results obtained from this study indicate that the mean concentration of the following parameters: pH, COD, iron, manganese, chromium, cadmium and lead compare to their weight index and the permissible limit of (NSDWQ, 2007) thereby signifying contamination. The computed overall WQI was 101.28, which implies that the water is of poor quality. The high value of WQI obtained is as a result of the high concentration iron, manganese, COD, and traces of lead, chromium and cadmium in the groundwater and can be attributed to natural and human activities taking place in the study area. Table 3 and Figure 4 shows the classification of water quality based on WQI value and distribution of the water samples according to their respective quality rating. Based on the WQI value, water is categorized into 5 groups ranging from excellent water (24%), good water (27%), poor water (17%), very poor water (24%) and water unsuitable for drinking (10%). The WQI ranges from 31.5 to 725.2. The elevated WQI values in location 12, 13 and 14 is as a result of concentration of cadmium and lead above acceptable limit of (NSDWQ, 2007).

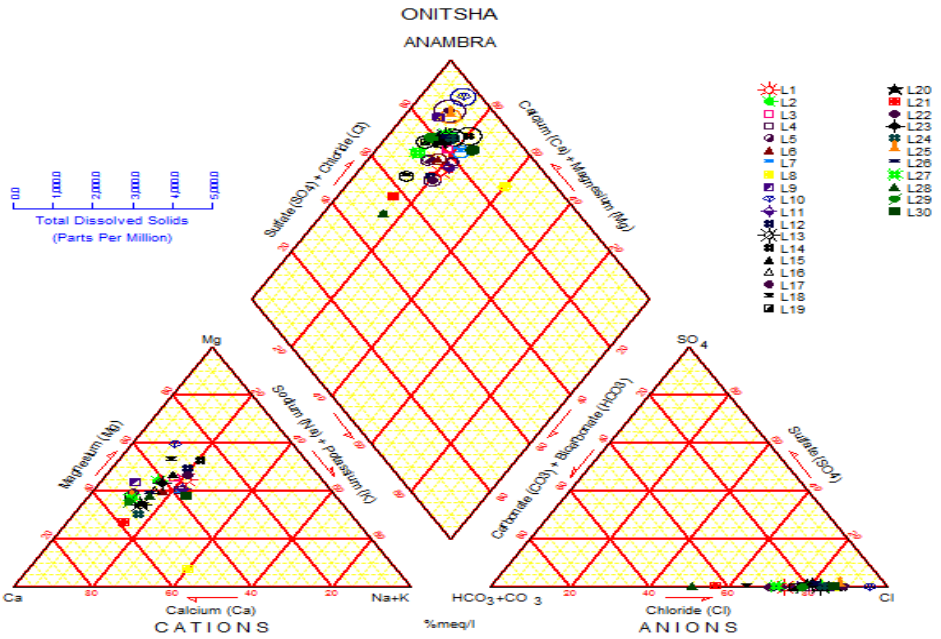

Fig. 3: Piper Diagram

Table 2: Computed WQI Values for the study Area

Parameters (mg/L)	Ci	Si	qi	wi	qiwi
PH	5.728	6.5-7.5	76.27	0.1330	10.140
Conductivity (µs/cm)	253.87	1000.00	25.88	0.0010	0.0260
Colour (Pt.Co)	0.2	15.00	1.33	0.067	0.0891
Turbidity (NTU)	0.172	5.00	3.40	0.200	0.6800
TDS	158.204	500.00	15.82	0.001	0.0158
COD	9.703	10.00	97.03	0.100	9.7030
Bicarbonate	53.327	100.00	53.327	0.010	0.5332
Sodium	0.6407	200.00	0.55	0.005	0.0030
Potassium	0.3683	150.00	0.5847	0.010	0.0058
Calcium	1.9913	200.00	1.050	0.005	0.0053
Magnesium	1.165	200.00	4.450	0.050	0.2225
Chloride	133.97	250.00	67.49	0.004	0.2700
Nitrite	0.0426	0.2000	21.30	5.000	106.50
Nitrate	2.0508	50.00	4.100	0.020	0.0820
Sulphate	0.5302	100.00	0.530	0.010	0.0053
Iron	0.5333	0.300	181.12	3.335	603.67
Manganese	0.1200	0.200	60.00	5.000	300.00
Zinc	0.3327	3.00	11.10	0.333	3.6963
Copper	0.0512	1.00	5.130	1.000	5.1300
Chromium	0.0082	0.0500	16.54	20.00	350.80
Cadmium	0.00098	0.001	98.00	1000	98000
Lead	0.0156	0.0100	156.00	100.00	15600

Table 3: Groundwater Quality Classification based on WQI value

WQI value	Water quality rating	Water samples (%)

<50	Excellent water	24
50-100	Good water	27
100-200	Poor water	17
200-300	Very poor water	24
>300	Unsuitable for drinking	10

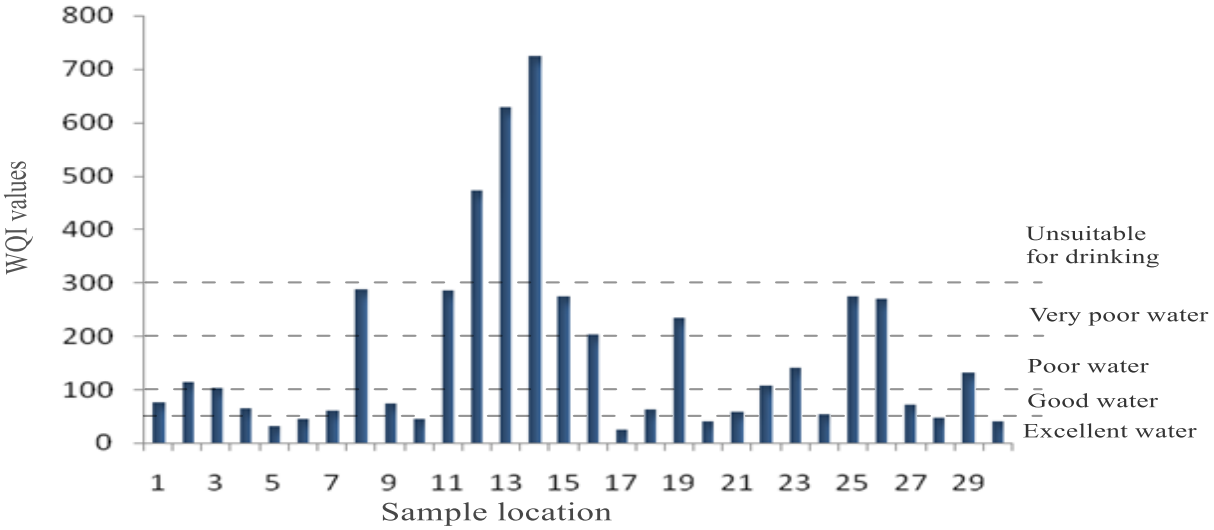

Figure 4. Water quality index (WQI) of groundwater at different locations of the study area

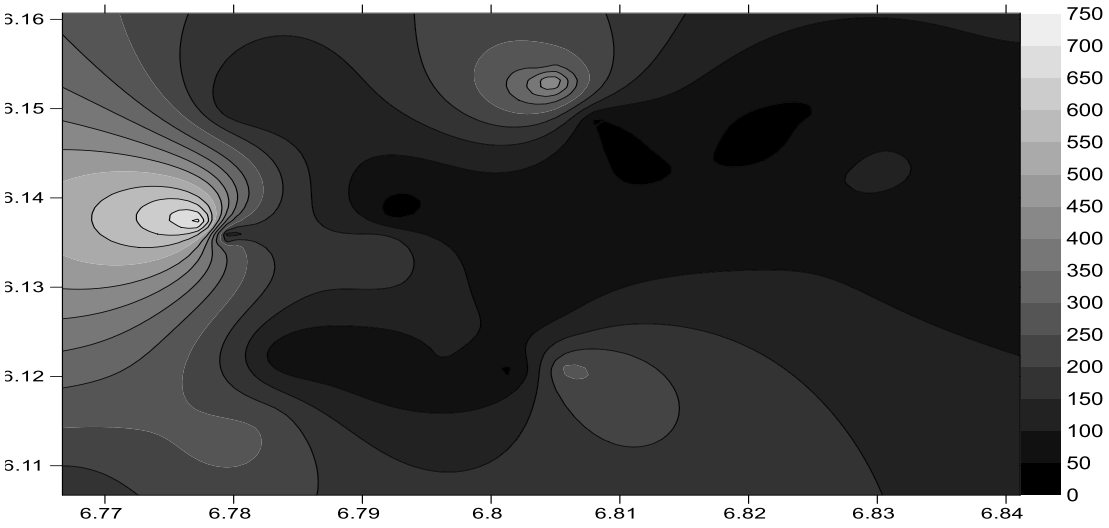

Figure 5: Spatial distribution of water quality based on WQI

The spatial distribution of WQI values (Figure 5) shows that the area is covered by good water and poor water(Table 3) and this can be attributed to iron and manganese concentration in all water sample which a naturally influenced. The elevated values of WQI covering the area with very poor water and water unsuitable for drinking (Table 3) is attributed to the concentration

of heavy metals in some boreholes in proximity to dumpsites and waste water discharge points signifying water pollution and aquifer vulnerability around this locations due to anthropogenic activities taking place in the study area.

Table 4: Calculated Metal pollution Index for the Water in the Area

Parameter (mg/l)	C_i	MAC_I	MPI value	Rating
Iron	0.543	0.300	1.81	Moderately polluted
Manganese	0.120	0.200	0.60	Lightly polluted
Zinc	0.333	3.00	0.11	Lightly polluted
Copper	0.512	1.00	0.51	Lightly polluted
Chromium	0.008	0.05	0.16	Lightly polluted
Cadmium	0.00098	0.001	0.98	Lightly polluted
Lead	0.0160	0.01	1.60	Moderately polluted

Conclusion

The quality of groundwater status has been investigated in this study using physicochemical parameters, water quality index and metal pollution index. the result of the physicochemical parameters shows that the major ions concentration is in this pattern Cl^- > HCO^-> Ca^{2+}> Mg^{2+} >Na^+>SO_4^{2-}>K^+ and in conformity with (NSDWQ, 2007) and WHO standard except for Cl^- in some location above the recommended standard signifying improper sanitation system. The high concentration of iron may be from leaching lateritic soil and host rock, which can also link manganese concentration to localize effects. Concentration of chromium, cadmium and lead can be linked to effluent from industries, waste from paints, electronic waste and improper disposal of battery waste, contributed to the elevated concentration of heavy metals especially around open dumps. The pH value shows acidic property and this contributed to the leaching and subsequent infiltration of these pollutants to the shallow aquifer. Water quality index rate the overall water as of poor quality and heavy metals are the contributing factor. The result from the computed metal pollution index suggests that the groundwater is slightly to moderately affected with respect to heavy metal pollution and it is attributed to the sanitation problem in the area. Spatial distribution also linked area with high water quality index values around dumpsites. Most people in the study area depend on groundwater for drinking and domestic use and the toxic nature of these pollutants even at low concentration; it has become imperative to raise awareness for the overall interest of public health.

References

Abimbola, A.F., A.M. Odukoya, and A.S Olatunji. 2002. Influence of the bedrock on the hydrogeochemistry characteristics of groundwater in northern parts of Ibadan metropolis, Southwestern Nigeria. Journal of Water Resources, Vol.13.pp.1-6.

Adelana, S.M.A., R.B. Bale., and M.W. 2003. Quality of assessment of pollution vulnerability of groundwater in Lagos metropolis, SW Nigeria in: proceedings of the aquifer vulnerability Risk Conference AURO3 Salamenia Mexico, 2, pp.1-17.

Adelana, S.M.A., Bale, R.B., Olasehinde, P. I. and M.Wu.2005.The impact of anthropogenic activities over groundwater quality of coastal aquifer in Southwestern Nigeria. Proceedings on Aquifer vulnerability and Risks.2nd International Workshop and 4th Congress on the Protection and Management of Groundwater. Raggia di Colornoparma.

Adepoju-Bello, A.A. and Alabi, O.M (2005). Heavy metals: A review. The Nigerian Journal of Pharmacy., 37: 41-45

Amadi, A.N., Ameh, M.I and P.I.Olasehinde.2010. Effect of urbanization on groundwater quality within Makurdi Metropolis, Benue State. Proceedings, Annual Conference of the Nigerian Association of Hydrogeologists on Water Resources Development and Climate Change.p49.

Amadi, A.N. (2011). Assessing the Effects of Aladimma dumpsite on soil and groundwater using water quality index and factor analysis. Australian Journal of Basic and Applied Sciences, 5(11), 763-770.

Amadi, A. N., (2011). Quality Assessment of Aba River using Heavy Metal Pollution lndex. American Journal of Environmental Engineering, 2(1), 45-49

Amadi, A.N., Yisa, J., Ogbonnaya, J.C., Dan-Hassan, M.A., Jacob, J.O and Alkali, Y.B. (2012). Quality Evaluation of River Chanchaga Using Metal Pollution Index and Principal Component Analysis. Journal of Geography and Geology; Vol. 4, No; 2. p13-21

Amadi, A.N., Ameh, l.M., Ezeagu, G.G., Angwa, E.M., and Omanayin, Y.A. (2014). Bacteriological and physico chemical analysis of well Water from villages in Edati, Niger State, North-central Nigeria. International Journal of Engineering Research and Development 10(3), 10-16

American Public Health Association (2005) Standard Methods for Examination of Water and Wastewater, 21st edition. American Public Health Association: Washington, D.C.

Batabyal, Asit and Chakraborty, Surajit. (2015). Hydrogeochemistry and Water Quality Index in the Assessment of Groundwater Quality for Drinking Uses. Water Environment Research. 87.10.2075

Efe, S.I. 2008. Quality of water from hand dug wells in Onitsha metropolitan Area. Journal of Environment, Vol.125, pp.5-12.

Ezeabasili A. C., Anike O. C., Okoro B. U. and Dominic C. M. U. (2014): Arsenic Pollution of

Surface and Sub- surface Water in Onitsha, Nigeria. Africa Journal of Environmental sciences and technology. Vol 8(9) pp 491- 497.

Foster, S.; Hirata, R.; Howard, K. (2011) Groundwater Use in Developing Cities: Policy Issues Arising from Current Trends. Hydrogeol. J., 19, 271–274.

Idris-Nda, A., Aliyu, H.K and Dalil, M. (2013), "The challenges of domestic wastewater management in Nigeria: A case study of Minna, central Nigeria", international Journal of Development and Sustainability, Vol. 2 No. 2, pp.1169-1182.

Isikhueme, M.I and Omorogieva; M.O (2015). Hydrogeology and Water Quality Assessment of the Middle Aquiferous Horizon of Onitsha and Environs in Anambra Basin, Eastern Nigeria. British Journal of Applied Science & Technology 9(5): 475-48,

Longe, E.O., and L.O.Enekwechi.2007. Investigation on potential groundwater impacts and influence of local hydrogeology on natural attenuation of leachates at municipal landfill. International Journal of Environmental Science and Technology, Vol.4, No.1, pp.133-140.

Lyulko, I., Ambalova, T. and Vasiljeva, T., (2001). To Integrate Water Quality Assessment in Latvia. MTM (Monitoring Tailor-Made) lll, Proceedings of International Workshop on Information for Sustainable Water Management. Netherdlands, 449-452.

Nfor, B.N, Olobaniyi, S.B and Ogala, J.E (2007). Extent and Distribution of Groundwater Resources in Parts of Anambra State, Southeastern Nigeria. Journal of Applied Science and Environ. Management. Vol 11 (2) 215-221.

NSDWQ, (2007). Nigerian Standard for Drinking Water Quality. Nigerian lndustrial Standard, NIS:554, 1-14.

Nwajide, C.S., 2013. Geology of Nigeria's sedimentary basins. CSS bookshop.p245.

Ocheri, M.I. 2006. Analysis of water consumption pattern in Makurdi metropolis. Journal of Geography and Development, Vol.1, No.1, 71-83.

Piper, A.M., (1944). A graphic procedure in the geochemical interpretation of water analyses. Trans America Geophysical Union, V,25, pp 914-928

Tamasi, G., and Cini R. (2004). Heavy metals in drinking waters from Mount Amiata. Possible risks from Arsenic for public health in the province of Siena. Science of the Total Environment. (327), 41-51.

USEPA, (2009). National Drinking water standards. United States Environmental Protection Agency, Washington, DC. http://www.epa.gov/safewater.

World Health Organization (WHO, 2017). Guidelines for drinking-water quality: fourth edition incorporating the first addendum. Geneva: World Health Organization.

World Health Organization (WHO, 2004). The World Health Report. Geneva. World Health Organization.2004

World Health Organization (WHO, 2007). Guidelines for drinking-water quality. 4th. ed. World Health Organization. Geneva, Switzerland.

Zietz, B.P., J. Lap and R. Suchenwirth, 2007. Assessment and management of tap w ater Lead contamination in Lower Saxon, Germany. Int. J. Environ. Health Res., 17(6): 407-418.
Adepoju-Bello, A.A. and O.M. Alabi, 2005. Heavy metals: A review. The Nig. J. Pharm., 37: 41-45.

Mineralization Zones Delineation in Part of Central Nigeria Using Analytical Signal, Derivatives, Downward Continuation and Centre for Exploration Targeting Plug-IN (CET).

Tawey M. D[1]* Udensi E. E[2] Adetona A. A[3] Alhassan U. D[4]

Geophysics Department, Federal University of Technology Minna
[4]a.usman@futminna.edu.ng
[3]tonabass@gmail.com
[2] eeudensi@yahoo.com
[1*]Corresponding author:**taweymam@gmail.com**

Abstract

A digitised aeromagnetic data covering part of central Nigeria was acquired and analysed with the aim of delineating mineralisation zones within the area using analytical signal, downward continuation, second vertical derivative and structural complexity analyses of the CET. From the analysis of analytical signal, the map reveals areas of low amplitude of 0.0024m in deep blue colour around south central portion of the area while the pinkish colour that dots all over the area has an amplitude of 0.2157m. This pinkish colouration concentrated around central portion to the western end of the study area. Application of downward continuation and second vertical derivative filters produces similar maps in which prospective zones of mineralisations were mapped out. These mineralisation zones were seen to be concentrated in areas with high magnetic signal of amplitude 0.2157m. Application of structural complexity analysis due to CET located deposits occurrence favourable zones that coincided with zones mapped out from SVD and downward continuation maps. Structural trends as revealed by CET Plug-IN are NE-SW, NW-SE, minor E-W and N-S trends.

Keywords: Mineralisation, Structural Complexity, Analytical Signal and CET

Introduction

Aeromagnetic maps usually reflect variations in the earth's magnetic field resulting from the underlying rocks' magnetic properties (e.g. magnetic susceptibilities). Sedimentary rocks have the lowest magnetic susceptibility, whereas metamorphic and acidic igneous rocks intermediate and basic igneous rocks have the highest magnetic susceptibility (Kearey *et al*., 2002). As such,

large-scale aeromagnetic surveys have been used to locate faults, shear zones and fractures, such zones may serve as potential hosts for a variety of minerals and may be used as guidance for exploration of the epigenetic, stress-related mineralisation in the surrounding rocks (Paterson and Reeves, 1985) Magnetic anomalies are caused by magnetic minerals contained in rocks; such anomalies are usually caused by underlying basement (igneous and/or

metamorphic) rocks or by igneous features such as intrusive plugs, dykes, sills, lava flows and volcanic centre (Gunn, 1997). Magnetic method is one of the best geophysical techniques used for determining depth to magnetic source bodies (and possibly sediment thickness) and delineating subsurface structures. Several articles have been published on the Nigerian basement complex's structural and tectonic framework and mineral constituent using magnetic data (Amigun, 2015a) also make use of magnetic method in the resource assessment of Ajabanoko iron ore deposit and his study demonstrated the potential value of this method to the problems of defining the structural setting, physical characteristic, ore geometry and economic potential of iron deposit as such, the present work focused on interpreting aeromagnetic data over part of central Nigeria with the aim of delineating mineralization zones and structural complexity which are usually host for minerals.

Location and extent of the study area

The study area is a rectangular block shape situated in the part of central Nigeria particularly in the northern Nigerian Basement Complex (Figure 1). It is bounded by latitudes $08^{0}30^{'}$ N and $10^{0}30^{'}$ N and longitudes $07^{0}00^{'}$ E and $09^{0}00^{'}$ E. The study area falls in three states namely Kaduna, Niger, Nasarawa and the Federal Capital Territory (FCT) (Figure 1).

Geology of the study area

The area is exclusively Basement and predominant rock type in the area of study is the Migmatite which almost covered the entire area with an isolated occurrence of younger basalt, granite and granite porphyry, coarse Porphyritic hornblende granite, medium to coarse grained biotite granite, undifferentiated granite Migmatite and granite gneiss, Amphibolites schist and amphibolites, undifferentiated schist including philites granite gneiss and the Migmatite (Figure: 2)

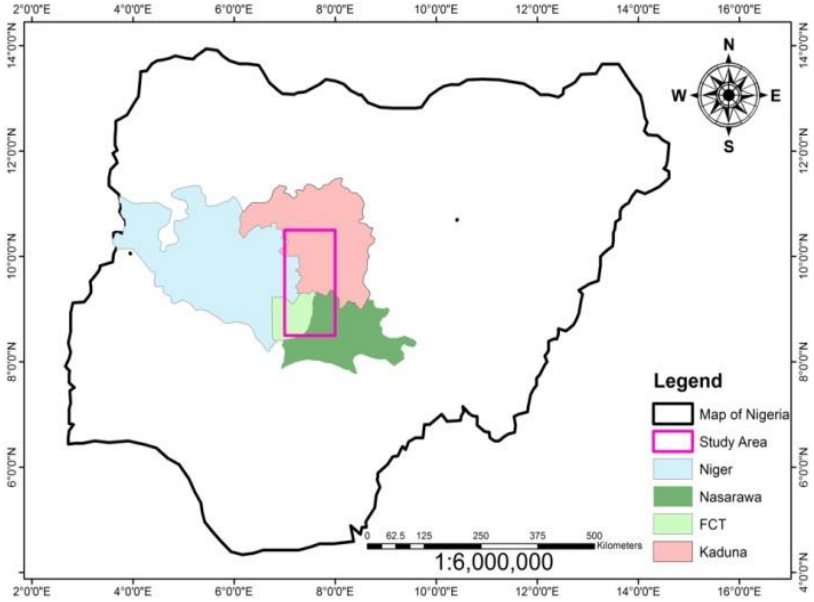

Figure: 1 Location of study area (Google, 2019)

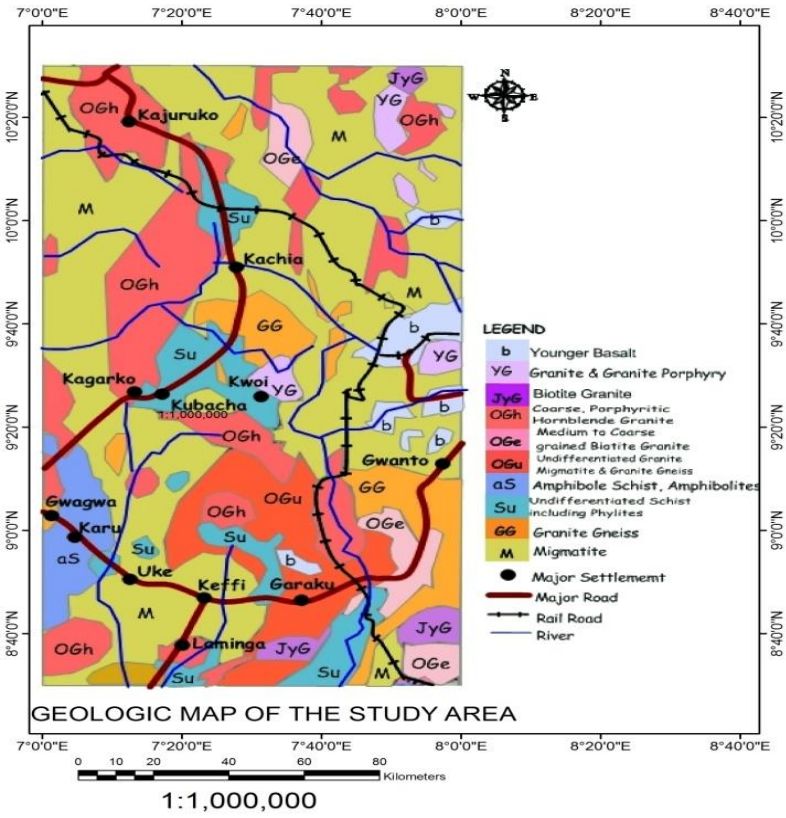

Figure: 2 Geologic map of the area (NGSA, 2006)

MATERIALS AND METHODS

Source of Aeromagnetic Data

The Aeromagnetic Data used for this study which was acquired from the Nigerian Geological Survey Agency (NGSA) Abuja is a new dataset that has been generated from the largest airborne geophysical survey ever undertaking in Nigeria, which is helping to position the country as an exciting destination for explorers. This survey took place between 2005 and 2009 and was financed by Nigerian Federal Government and the World Bank. The survey was conducted in two phases. Phase 1 was financed entirely by the Government of Nigeria. All of the airborne geophysical work data acquisition, processing and interpretation, was carried out by Fugro Airborne Surveys. Phase 1 was completed in September 2007 and included 826,000 line-km of magnetic and radiometric surveys flown at 500 m line spacing and 80 m terrain clearance; and 24,000 line-km of time-domain electromagnetic surveys flown at 500 m line spacing, flight line spacing of 100 meters and 80 m terrain clearance using Fugro's GENESIS EM system. Fugro was also tasked with interpretation of these data. The Phase 2, completed in August 2009, surveyed blocks not covered in Phase 1. It included 1,104,000 line-km of magnetic and radiometric surveys flown at 500 m line spacing and 80 m terrain clearance. These levels of survey are intensive: often a total of seven aircraft of three different types were active at one time. Phase 2 was supported by the World Bank as part of a major project known as the Sustainable Management for Mineral Resources Project.

Methods / Procedures

The procedures involved in this study include:

1. Production of Total Magnetic Intensity (TMI) map of the study area reduced to magnetic pole in color aggregate using Oasis Montaj software
2. Produce Analytical Signal map to locate outcropping areas and showcase places of probable mineralisation zones
3. Production of Downward Continuation map, since, the downward continuation filter when applied to potential field data brings the observation surface closer to the source therefore enhancing the responses from sources at depth from which mineralization zones can be mapped out
4. Computing the Second Vertical Derivative of the data and mapped out the mineralisation zones.
5. Complex structural analysis from Centre for Exploration Targeting (CET) to mapped out complex structural areas which could be probable areas of mineralization

Theories of the Methods

Reduction to Magnetic Pole

Reduction to the pole (RTP) is a standard part of magnetic data processing method, especially for large-scale mapping. RTP operation can transform a magnetic anomaly caused by an arbitrary source into the anomaly that the same source would produce if it is located at the pole and magnetised by induction only. Interpretation of magnetic data can further be helped by RTP in order to remove the influence of magnetic latitude on the anomalies which is significant for anomalies caused by crust. Reduction to the pole is the process of converting the magnetic field from magnetic latitude where the Earth's field is inclined, to the field at a magnetic pole, where the inducing field is vertical (LUO et al., 2010). When the Earth's field is inclined, magnetic anomalies due to induction have forms that are asymmetrically related to their sources, but when the inducing field is vertical, the induced anomalies are directly over their sources (Milligan & Gunn, 1997). Fourier transform is applied to transform RTP from the space domain into the wavenumber domain. The RTP operation in wavenumber domain can be expressed as

$$A_P(u,v) = \frac{A_c A_p(u,v)}{(sinI + icosIcos(D-\theta))^2} \quad 1$$

Where $A_P(u,v)$ be the Fourier Transform of these observed magnetic data, $A_c(u,v)$be the Fourier Transform of the vertical magnetic field, I and D is the inclination and declination of core field, (u,v) is the wavenumber corresponding to the (x, y) directions respectively and $\theta = \arctan\left(\frac{u}{v}\right)$ (LUO *et al.*, 2010). Reduction-to-the-pole (RTP) is a useful and effective operation designed to transform a total magnetic intensity (TMI) anomaly caused by an arbitrary source into the anomaly that this same source would produce if it were located at the pole and magnetized by induction only (Li, 2008).

Analytical method

Analytical signal of TMI has much lower sensitivity to the inclination of the geomagnetic field than the original TMI data, and provides a means to analyses low latitude magnetic fields without the concerns of the RTP operator. Analytical signal is a popular gradient enhancement, which is related to magnetic fields by the derivatives. Roest *et al.*, (1992), showed that the amplitude of the analytic signal can be derived from the three orthogonal gradient of the total magnetic field using the expression:

$$|A(X,Y)| = \sqrt{\left(\frac{\delta m}{\delta x}\right)^2 + \left(\frac{\partial m}{\partial y}\right)^2 + \left(\frac{\delta m}{\delta y}\right)^2} \quad 2$$

Where A(x, y) is the amplitude of the analytical signal at (x, y) and m is the observed magnetic anomaly at (x, y).

While this function is not a measurable parameter, it is extremely interesting in the context of interpretation, as it is completely independent of the direction of magnetisation and the direction of the Earth's field (Milligan & Gunn, 1997). This means that all bodies with the same geometry have the same analytic signal. Analytic signal maps and images are useful as a type of reduction to the pole, as they are not subject to the instability that occurs in transformations of magnetic fields from low magnetic latitudes. They also define source positions regardless of any remnant magnetization in the sources (Milligan & Gunn, 1997).

Upward/Downward Continuation of the field

The amplitude of a magnetic field above a source varies with elevation as an exponential function of wavelength. This relationship can be readily exploited with FFT filters to re-compute the field at a higher elevation (upward continuation) or lower elevation (downward continuation) (Foss, 2011). A potential field measured on a given observation plane at a constant height can be recalculated as though the observations were made on a different plane, either at higher or lower elevation. As described by Gunn (1997), the process has a frequency response of $e^{-h}(u^2 + v^2)^{\frac{1}{2}}$ (where h is elevation). This means that upward continuation smooth out high-frequency anomalies relative to low-frequency anomalies. The process can be useful for suppressing the effects of shallow anomalies when detail on deeper anomalies is required. Downward continuation on the other hand sharpens the effects of shallow anomalies (enhances high frequencies) by bringing them closer to the plane of observation. For upward continuation (where z is positive downward) (Telford et al., 1990)

$$f(x, y, -h) = \frac{h}{2x} \iint \frac{F(x,y,0)dxdy}{\{(x-x')+(y-y')+h^2\}^{\frac{1}{2}}} \quad 3$$

Where $F(x, y, -h)$= Total field at the point $p(x', y' - h)$ above the surface of which

$F(x, y, 0)$ is known h = elevation above the surface

Vertical Derivatives

Vertical derivative (or alternatively named vertical gradient) filters preferentially amplify short-wavelength components of the field at the expense of longer wavelengths (Foss, 2011). Vertical derivative filters are generally applied to gridded data using FFT (Fast Fourier

Transform) filters. Various vertical derivatives of the magnetic field can be computed by multiplying the amplitude spectra of the field by a factor of the form:

$$\frac{1}{n}\left[(U^2+V^2)^{\frac{1}{2}}\right]^n \quad 4$$

Where n is the order of the vertical derivative, (U, V) is the wavenumber corresponding to the (x, y) directions respectively. The first vertical derivative is physically equivalent to measuring the magnetic field simultaneously at two points vertically above each other, subtracting the data and dividing the result by the vertical spatial separation of the measurement points. The second vertical derivative is the vertical gradient of the first vertical derivative and so on. The formula for the frequency response of these operations shows that the process enhances high frequencies relative to low frequencies, and this property is the basis for the application of the derivative process which eliminates long-wavelength regional effects and resolves the effects of adjacent anomalies. The second vertical derivative has even more resolving power than the first vertical derivative, but its application requires high quality data as its greater enhancement of high frequencies results in greater enhancement of noise. Higher orders of derivatives are virtually never used to produce interpretation products (Gunn et al., 1997a).

Complex structural analysis

Centre for Exploration Targeting (CET) is a suite of algorithms which provides functionalities for enhancement, lineament detection and structural complexity analysis of potential field data (Holden et al. 2008; Core et al. 2009). This technique automatically delineate lineaments and identify promising areas of ore deposits via outlining regions of convergence and also divergence of structural elements using several statistical steps that include texture analysis, lineation delineation and Vectorisation and complexity analysis to generate contact occurrence density map. This method identifies magnetic discontinuities using combination of texture analysis and bilateral symmetric feature detection Geosoft, (2012). It then identifies regions of discontinuity and analyses structural associations to locate crossing, junctions, and change of direction of strike. Finally, by measuring the density of the structural contacts and the diversity in the strike structures as a heat map, it facilitates picking the areas that are perceived to be prospective. Nonetheless, since the workflow is directly applied to gridded datasets, any geophysical data sensitive to the geologic structure could be subjected to this to delineate ridges or edges of the geologic structure and when using magnetic data in this process, it is highly recommended to pole reduce the data first so that the anomalies are shifted over their causative structures (Geosoft, 2012).

RESULTS AND DISCUSSIONS

Total Magnetic Intensity TMI/TMI Reduced to Magnetic pole

From total magnetic intensity map (Figure: 3A), the magnetic intensity of the study area ranges from 32950.05nT minimum to 33087.93nT maximum. The area is marked by both high and low magnetic closures, which could be attributed to Factors such as degree of rock strikes, difference in rock lithology of the area, difference in rock magnetic susceptibility of the area, and differences in the depth at which these rocks occur. Areas around the southern part and from the center to the western end of the area are mark with high magnetic closure attributed to the exposed basement nature of the environment while the long wavelength anomaly at the south central portion of the area is attributed to areas that are covered with thick layer of sediment (Figure 3A). To place the anomalies from the residual magnetic field directly over the magnetic field resulting from causative rocks that bring about these anomalies, the TMI grid was transformed into reduction to the pole (RTP) grid using the 2D-FFT filter in Geosoft software to make easy the interpretation of the magnetic data set. The reduction to pole magnetic anomaly image (Figure 3B) depicts both low and high frequencies coming from the magnetised rocks in the region. These strong anomalies with high frequencies are observed directly at the east of the area through the central portion to the western end of the area. The map of RTP also helps to sharpen the contacts between the magnetic high and low patterns and also emphasized on anomalously magnetic susceptible zones possibly coming from deeper sources.

Analytic Signal

The most significant feature of the analytical signal is that it does not dependent on the magnetization field of the source rock. The mineral deposits with high concentrations always show high analytical signal amplitudes. This shows that analytical signal amplitude depends on the magnetizing amplitude of the causative body (Nabighian, 1972; Roest and Pilkington, 1993). High analytical signal amplitudes are recorded which could be areas of large mineral deposits and a closer look at Analytic signal map (Figure: 4), the amplitudes ranges from 0.024m around south central portion of the study area and extreme north central portion of the area to 0.2157m.Thus, areas around central portion of the study area to the western end of the map also have the highest amplitude. They are areas of freshly intruding rocks as such are areas

expected to be zones of mineralisation. Areas around north western end part of the study area, southern part and eastern part of the study area also have some dots of high amplitude anomalies as such are also expected areas of mineralisation. With the application of this filter, structures with trend NE-SW and NW-SE were mapped were also out in black strikes (Figure: 4).

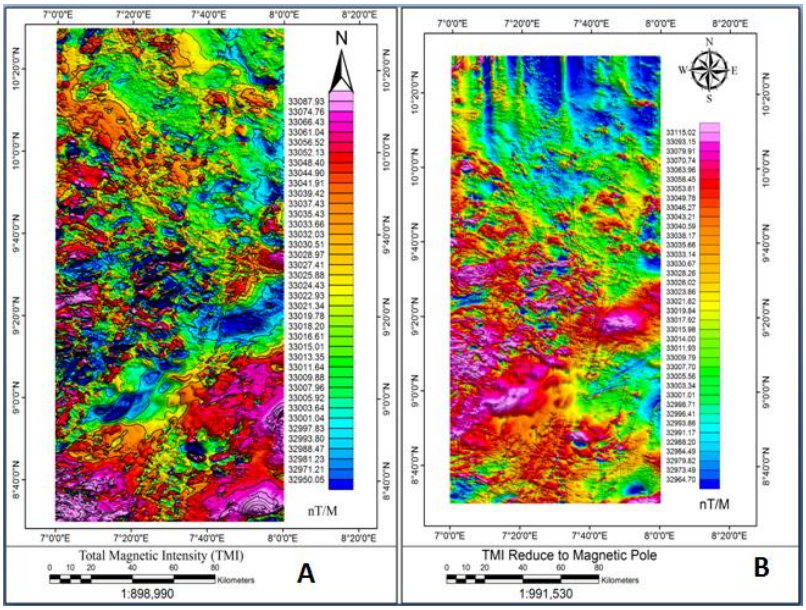

Figure: 3 TMI and TMI Reduce to Pole

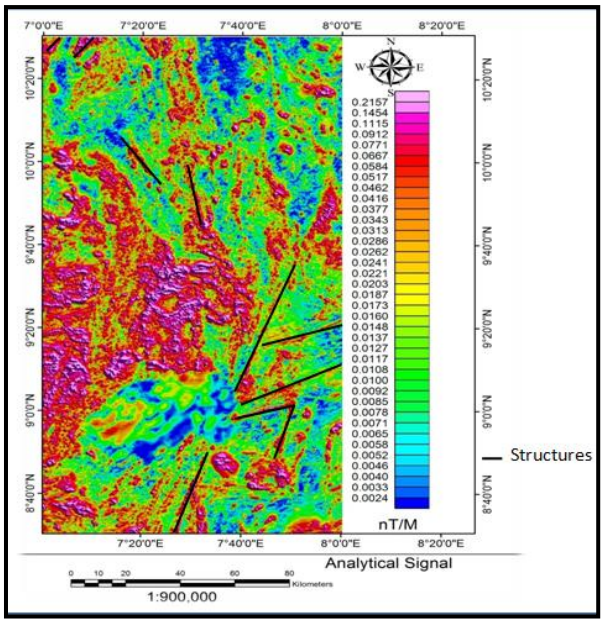

Figure: 4 Analytical Signal Map

Downward Continuation

The application of downward continuation filter enhanced responses from shallow depth sources by effectively bringing the plane of measurement closer to the source. When this filter was applied to the data, produces (Figure 5.A). From the map produced (Figure 5.A), mineralization zones were inferred and mapped out by labeling. These are areas around A, B, C, D, E, F, G and H in (Figure 5A).

Second Vertical Derivative

Second vertical derivative filter was applied to enhance subtle anomalies while reducing regional trends. This filter is considered most useful for defining the boundaries of anomalies and for amplifying fault trends. The SVD map (Figure: 5B) reveals the boundaries of those shallow anomalies clearly. This made it possible to delineate the various mineralization zones with some

Structures mapped out in black strikes. Just as the case of downward continuation map (Figure 5A), Figure 5 B is very similar to the downward continuation map and the boundaries of anomalies (mineralization zones) are represented by areas around A, B, C, D, E, F, G and H in (Figure 5B).

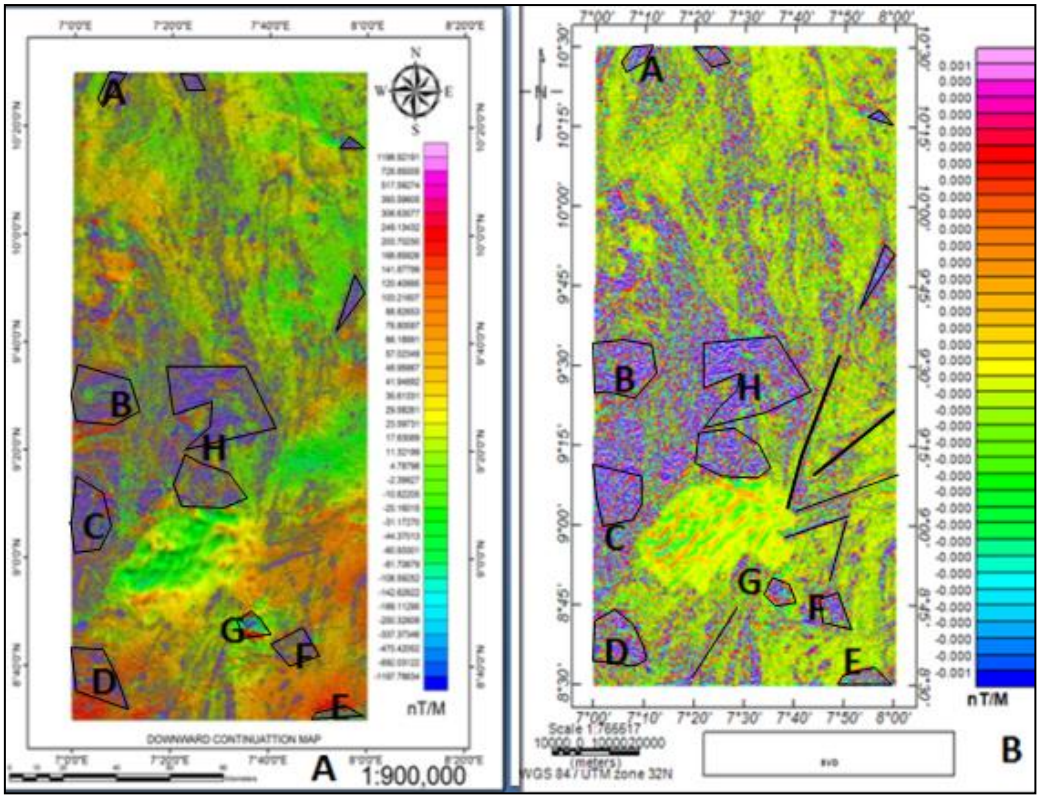

Figure: 5 Downward Continuations and Second Vertical Derivative Map

Structural Complexity Map and Interpretation

The structural complexity analysis is used here to locate deposit occurrence favourability. Texture Analysis was selected from CET window followed by a displayed Standard Deviation dialog. A running window generated a measure of randomness of the texture and two statistical methods were supplied, these are the entropy method and the standard deviation but the standard deviation provides a smoother representation of the degree of randomness that overcomes the inherent noise in the data. For the input filename (grid), pole reduced magnetic grid was selected, for the output filename (grid), standard deviation was entered and the map produced (Figure: 6A). This map is very similar to the Analytical signal map produced (Figure: 4). Here, the structures are seen beginning to align themselves and the application of phase symmetry produces the map in (Figure: 6B) where structures were singled out.

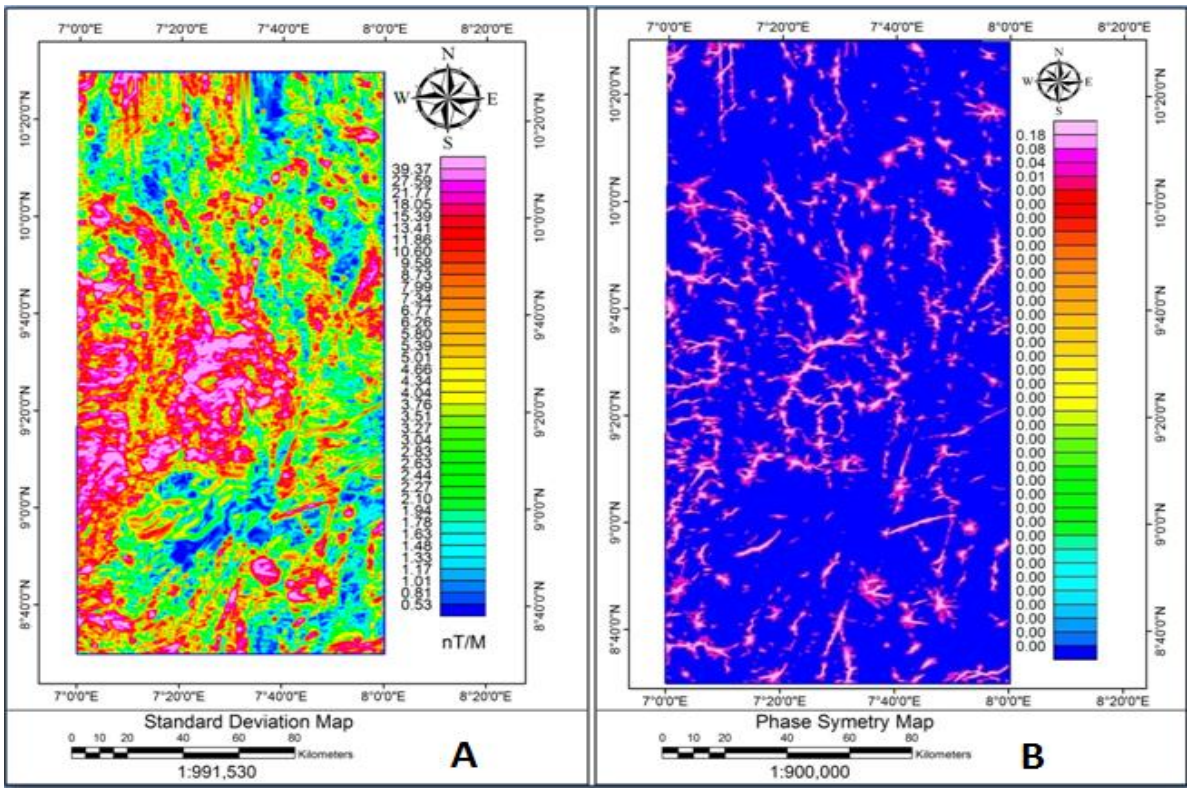

Figure: 6 Standard Deviation and Phase Symmetry Maps

While application of skeletal to vectors PLUG-IN produce the map (Figure: 7A). These structures are overlay on the orientation entropy map (Figure: 7B). The orientation entropy map picks only the localized junctions where the structures bend or changes direction as indicated in the map. The generated map (Figure: 7B) indicated areas of junctions of high densities lineament overlaid by the structures in (Figure: 7A). These are areas favourable for hosting minerals as these areas on this map when compared with downward continuation and second vertical derivative map (Figure: 5A and 5B) both have these mineralization zones in similar portions on the maps. These are areas favourable for hosting deposits of interest and could be further explore in more detail.

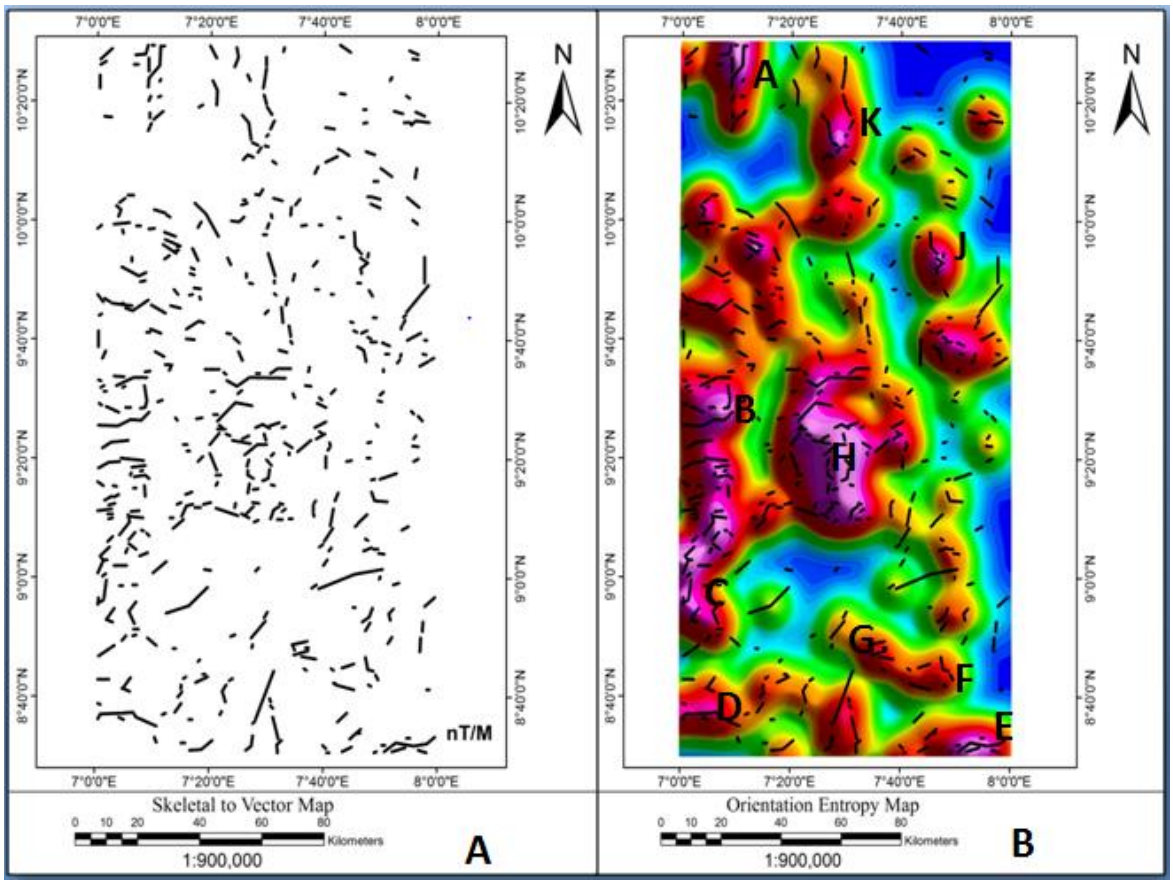

Figure 7Skeletal to Vectors and Orientation Entropy Maps

Conclusions

From the analysis of analytic signal (Figure: 4), areas of high amplitude were observed which are envisage to be areas of probable large mineral deposit having amplitude of 0.2157m from the central portion of the map toward the western end of the study area. Anomalies of the same amplitude dot other parts of the area. The map also revealed structures that were mapped out having NW-SE and NE-SW trends. The second vertical derivative and downward continuation maps (Figure: 5A and 5B) reveals boundaries of mineralisation zones that were mapped out and labeled A, B, C, D, E, F, G and H within the study area while the structural complexity analysis generated a map (Figure: 7A and 7B) that picks or indicated areas of junctions of high density overlayed by the structures produced. These are areas favourable for hosting minerals as areas of high structural densities when compared with SVD and downward continuation maps (Figure: 5 A and B) confirmed both three maps to have the mineralization zones on a similar portions of the individual three maps. Structural maps produce from CET analysis (Figure: 7 A) reveals the area having structures of dominant NE-SW and NW-SE trends.

References

Amigun, J. O. (2015). Application of Magnetic Data in Resource Assessment and Quantification of Magnetite Ore Reserve of Ajabanoko Iron Deposit, Okene area, Nigeria International Journal of Emerging Technology and Advanced Engineering,5(3), 77 – 82

Core, D., Buckingham, A., Belfield, S., 2009. Detailed structural analysis of magnetic data — done quickly and objectively, SGEG Newsletter.

Foss, C. 2011). Magnetic data Enhancement and Depth Estimation. (H. Gupta, Ed.) Encyclopedia of Earth Sciences Series, 736-746.

Geosoft (2012) Manual ; how to create structural complexity map

Gunn, P. J. 1997. Application of aeromagnetic surveys to sedimentary basin studies. Australian Geological Society Organisation (AGSO) Journal of Australian Geology and Geophysics, Vol. 17, No. 2, Pp. 133-144.

Gunn, P., Maidment, D., & Milligan, P. (1997a). Interpreting aeromagnetic data in areas of limited outcrop. *AGSO Journal of Australian Geology & Geophysics, 17*(2), 175–185.

Holden, E.J., Dentith, M., Kovesi, P., 2008. Towards the automatic analysis of regional aeromagnetic data to identify regions prospective for gold deposits. Comput. Geosci. 34, 1505–1513.

Kearey, P., & Brooks, M. (2002). An Introduction to Geophysical Exploration: London, *Blackwell Scientific Publications*.

Li, X. (2008). *Magnetic reduction-to-the-pole at low latitudes.* Fugro Gravity and Magnetic Services. Houston, USA.: Fugro .

LUO, Y., XUE, D.-J., & WANG, M. (2010). Reduction to the Pole at the Geomagnetic Equator. *Chinese Journal of Geophysics, 53*(6), 1082-1089.

Milligan, P., & Gunn, P. (1997). Enhancement and presentation of airborne geophysical data. *AGSO Journal of Australian Geology & Geophysics, 17*(2), 63-75.

Nabighian, M. N. (1972). The analytic signal of two dimensional magnetic bodies with polygonal cross-section: its properties and use for automated anomaly interpretation. *Geophysics,* 37, 507-517.

NGSA, (2006). Geology and Structural Lineament Map of Nigeria.

Paterson, N.R. and Reeves, C.V. 1985. Applications of gravity and magnetic surveys: the state-of-the-art in 1985. Geophysics 50, Pp. 2558-94.

Roest, W., Verhoef, J., & Pilkington, M. (1992). Magnetic interpretaion using 3-D analytical signal. *Geophysics, 57*, 116-125.

Roest, W. R. and Pilkington, M. (1993). Identifying remanent magnetization effects in magnetic data.Geophysics, 58: pp. 653–659

Telford, W. M., Geldart, L. P., and Sheriff, R. E. (1990). Applied Geophysics. Cambridge University Press, second edition.

Access to Modern Energy and Rural Governance In Niger State

ABDULLAHI, Habib

Department of Urban and Regional Planning
Niger State Polytechnic Zungeru
Tel: 07037751773
Email: Abdulllahihabibib31@gmail.com

ADEWUYI A. TUNDE

Center for Disaster Risk Management
Federal University of Technology, Minna
Tel: 08068166939
Adex22ng@yahoo.com

ABSTRACT

Rural energy consumption involves principally household energy uses, which is the biggest energy user in the sector, with cooking being the major end use of about 85% of total rural energy use.The problem of access to modern energy services is a major developmental issue confronting rural communities globally. Rural energy also produce inefficiently, as a result, they require substantial time and effort to collect, and as local resources stocks decrease, they increasingly have to be sourced from further afield. This significantly reduces the time available for productive activities. If managed ineffectively, such resources use can also degrade the environment and create negative spillover effects in other sectors. This study investigate the access to modern energy and rural governance in Bosso Local Government Area of Niger State, It also access the impacts of existing energy resources on rural people and their livelihood. Survey research approach was adopted; questionnaires were distributed to some sample communities in the local government. Responses were subjected to statistical analysis. Frequencies, standard deviations, percentages and means were used to give explanations on the demographic and socioeconomic characteristics of different households as they impinge on household energy use patterns. The findings shows that Electricity, Kerosin, Firewood, Charcoal and sawdust are the available source of energy within the study area, and finding reveal that firewood; 21.7% on daily basis is high in rural areas, while the urban use more of kerosene on daily basis 18.5%. It also discovered that lack of awareness on the risk of rural energy and the relative advantage of modern energy source were not carried out by the relevant stakeholders. The study recommends that awareness on the risk of rural energy should be encouraged.

Key words: Modern Energy, Rural Governance and Environment

Introduction

Rural areas are geographically secluded community with low population density and frequently characterized by a low level of income and education (Niez, 2010). The nature of rural areas varies from place to place and different types of rural areas are defined by how accessible they

are from the urban areas. This range from the rural urban fringe; the very edge of the city, beyond the suburb, where country side and city merge to the extreme (remote) rural areas. The major distinction between rural communities and urban centres is that while urban centres are large, impersonal and complex in social structure; rural areas are small, intimate and simple in organization.

Energy access is given as a target indicator for achieving the seventh objective of the MDGs, which is to ensure environmental sustainability. Northern areas of Nigeria in particular highly rely on inefficient traditional biomass, use mainly for cooking and heating purposes. More than 80 % of the households fulfill their primary energy demands with traditional biomass like firewood. These resources of energy burn inefficiently, thereby giving rise to energy loss. The surrounding environment is also degraded through the depletion of forest resources and that in many areas there is an increasing shortage in firewood supply, which ultimately increases work burden for women whose responsibility, is to collect it. Health damaging pollutants like carbon monoxide, benzene, nitrogen oxides, etc are emitted when these forms of energy resources are used indoors. Moreover, deaths from indoor air pollution, arising from the burning of biomass fuels (Proceedings of a Workshop held by OFID in Abuja, Nigeria June 8-10, 2008).

Energy is one of the most important inputs for sustaining people´s livelihood (Clancy, J.S., and Skutsch, M., 2002). Due to lack of modern energy services in rural areas, rural people have less opportunities for income and employment generation. Therefore, particularly low income levels in rural areas makes the provision of modern energy services unaffordable to most communities. The resulting heavily dependance on traditional energy sources means less energy efficiency; over exploitation of forest resources and a loss of biodiversity; greater health hazards due to indoor air pollution; and reduce capacity to mitigate climate change (Proceedings of a Workshop held by OFID in Abuja, Nigeria June 8-10,2008).

Nigeria is an energy poor country, where a large portion of the population at rest does not have access to contemporary day energy services like electricity. Major portion of the total population lives in remote areas. According to an estimate rural population contributes up to 70 per cent of the total in Nigeria and has only biomass and kerosene oil as major energy resources. Out of that 70%, only 16% of rural population has grid-connected electricity for domestic and commercial use. Rural communities living in Niger State especially in Bosso local government area face deficiency of firewood to meet their household energy demands. Most of the rural villages have relatively small population and distant from the main diffusion lines of the national grid, so it is usually considered as not economically feasible to connect these villages to the main transmission lines of the grid. (Abro, R., 2003). Renewable energies has vast potential to supply energy for various applications and has capacity to raise the socio-economic, health and indoor-environmental standards for rural people of Nigeria.

The predominance of firewood as the prime source of energy for cooking, despite of its ineptitude and detrimental impact on human health and environmental degradation, could be attributed to its availability as a free source of energy. Traditional biomass energy sources such as animal dung, firewood and crop residues, play important roles in local household energy consumption. This conventional energy structure is not only a threat to eco-environment but also to rural women and children as well.

The problem of access to modern energy services is a major developmental issue confronting rural communities globally, particularly in Asia and sub – Saharan Africa. According to IEA 2009) worldwide 1,456 billion people do not have access to electricity, of which 83% live in rural areas. In sub – Saharan Africa less than 10% of the rural population have access to modern energy. Currently in Nigeria, it is estimated that over 70% of the population live in rural areas with less than 15% of them having access to modern energy. Most rural societies experience limited access to modern energy services, due to problems of availability and/or affordability, and instead rely on traditional fuels, predominately animal dung, crop residues, and wood for majority of their energy needs. When burned, traditional fuels often produce hazardous

chemicals with negative health impacts, especially when used indoors. The fact that traditional fuels cannot produce a range of modern energy services such as mechanical power and electricity limits their ability to improve other aspects of life, including education and employment.

Also, traditional fuels also produce energy inefficiently, as a result, they require substantial time and effort to collect, and as local resources stocks decrease, they increasingly have to be sourced from further afield. This significantly reduces the time available for productive activities. If managed ineffectively, such resources use can also degrade the environment and create negative spillover effects in other sectors. Given the cultural practices in many rural areas, these impacts are often most felt by women and children.

One of the reasons that traditional energy source is the preferred domestic fuel is that it does not require a complex and expensive infrastructure to be produced and used as a fuel. Furthermore, so far it is the cheapest (usually free) available energy resource for the rural population and urban poor (Onyekuru, 2008). The energy use patterns of urban households may differ to that of the rural households since they have different geographical characteristics. There has been no research known to me carried out to access to modern energy in the study area. It is against these problems that this study sought to investigate the access to modern energy and rural governance in Bosso Local Government Area of Niger State.

Literature Review

Concept and Evolution of Energy.

Over time, humans have developed an understanding of energy that has allowed them to harness it for uses well beyond basic survival (World Wind Energy, 2009). The first major advance in human understanding of energy was the mastery of fire by James Prescott Joule. The use of fire to cook food and heat dwellings, using wood as the fuel, dates back at least 400,000 years. The burning of wood and other forms of biomass eventually led to ovens for making pottery, and the refining of metals from ore. The first evidence of coal being burned as a fuel dates as far back as approximately 2,400 years (WWE, 2009).

After the advent of fire, human use of energy per capita remained nearly constant until the Industrial Revolution of the 19th century This is despite the fact that, shortly after mastering fire, humans learned to use energy from the Sun, wind, water, and animals for endeavors such as transportation, heating, cooling, cooking and agriculture. The invention of the steam engine was at the center of the Industrial Revolution. The steam engine converted the chemical energy stored in wood or coal into motion energy. The steam engine was widely used to solve the urgent problem of pumping water out of coal mines (WWE, 2009). As improved by James Watt, Scottish inventor and mechanical engineer, it was soon used to move coal, drive the manufacturing of machinery, and power locomotives, ships and even the first automobiles. It was during this time that coal replaced wood as the major fuel supply for industrialized society. Coal remained the major fuel supply until the middle of the 20th century when it was overtaken by oil (Bowman and Balch, 2009).

The next major energy revolution was the ability to generate electricity and transmit it over large distances. During the first half of the 19th century, British physicist Michael Faraday demonstrated that electricity would flow in a wire exposed to a changing magnetic field, now known as Faraday's Law. Humans then understood how to generate electricity (WWE, 2009). In the 1880s, Nikola Tesla, a Serbian-born electrical engineer, designed alternating current (AC) motors and transformers that made long-distance transmission of electricity possible. Humans could now generate electricity on a large scale, at a single location, and then transmit that electricity efficiently to many different locations (Oleson, 2009).

Concept of household

A household-dwelling unit consists of the permanent occupants of a dwelling place. Persons who according to the Population Information System of the Population Register Centre are institutionalized, or are homeless, or are abroad, or are registered as unknown, do not form

part of a household-dwelling unit (United Nations, 1998). Additionally, persons living in buildings classified as residential homes do not form household-dwelling units if their living quarters do not meet the definition of a dwelling, also 'the household is central to the development process. Not only is the household a production unit but it is also a consumption, social and demographic unit' (Canberra Group, 2001).

The concept of household-dwelling unit was adopted in the 1980 census. According to UN (1993), a household is based on the arrangements made by persons, individually or in groups, for providing themselves with food or other essentials for living. A household consisted of family members and other persons living together who made common provision for food. Since 1980 subtenants have been classified in the same household-dwelling units with other occupants (Eurostat, 1985). A household comprises one person living alone or a group of people living at the same address, sharing their meals and the household, and having sole use of at least one room. All persons in a household must receive from the same person at least one meal a day and spend at least four nights a week (one, if they are married) in the household. The household includes staff, paying guests and tenants, and also anyone living in the household during the period in which expenditure is recorded. Persons who normally live in the household, but who are absent for a period of more than one month, are excluded (Eurostat, 1985).

Household Energy use

Household energy is energies use in homes mostly for cooking, heating and cooling processes. They are the major uses of energy. Hot water heating is also a sizable use of energy, as is the cooking process with electricity, sawdust, charcoal fuelwood, stove and oven.

According to Khare (2009), almost all the cities of the developing countries are characterized by slums, squatter settlements and other low-income areas which house the majority of urban

dwellers. The people living in those areas have energy consumption patterns entirely different from those of the high-income groups. Instead, the energy consumption patterns of such urban areas are very similar to those in rural areas. The heavy dependence of rural populations and urban poor on non-commercial energy sources has several implications. For instance, the exploitation of vegetation cover is leading to serious problems of ecological balance (Sambo, 2008).

Domestic Energy Use in Rural and Urban settings of Bosso Local Government Area State.

According to Onyekuru (2008), the energy requirements in the both urban and rural areas of Bosso Local Government Area state consist of two different and distinct components. Each possesses a unique characteristic which reflects the economic and social conditions of its inhabitants. One component follows patterns that are similar to cities (urban areas) in industrialized societies. The energy demands of those areas are similar to those of urban settlements in developed countries and reflect energy consumption patterns of the urban well-to-do, who use energy for commercial buildings, amenities, recreation and transport. Thus, the energy problems in that component of human settlements in developing countries are similar to those found in many developed countries (EIA, 2006). The other component (rural areas) involves the slums and squatter settlements whose energy-related problems bear a close resemblance to those of the rural population. The energy requirements of the low-income population, whether living in urban squatter's settlements or rural areas, can be narrowed down initially to domestic needs.

The rapid growth of concentrated populations in urban centers has led to an extreme scarcity of housing, deterioration of living conditions and the breakdown of infrastructure and services, especially transportation, Household and industrial energy supply, water reticulations and health care (Onyekuru, 2008).

The annual per capita energy consumption of the urban poor in the city does not differ significantly from that of the rural poor, since the main share of energy consumption in both cases goes to cooking (Govinda, Gautam and Michael, 2001). However, with rising incomes, the energy consumption patterns of urban households in urban areas of many developing countries tend to increase. Cooking and lighting account practically for all the energy consumed by people in the lowest income group (Sambo, 2008). Appliances and space and water heating account for up to 60 percent of the energy consumed by the rich in the cities. With rising incomes, fuelwood tends to be replaced by kerosene and kerosene replaced by gas/electricity for cooking and lighting (Onyekuru, 2008).

Methodology

This research adopted a survey research design. The design was chosen due to the large number of households in Bosso Local Government Area which could be too cumbersome to investigate. The population of the study consists of the total number of households from the selected rural and urban areas of the state. According to National Bureau of Statistics (2006), an average person per household in Bosso Local Government Area is 7.0. It is estimated that in every average 7.0 number of persons there is a household i.e. dividing the total population of the state/local government area by 7.0 persons to arrive at the expected number of households in any given local government of Bosso Local Government Area (NBS, 2006).

Stratified random sampling technique was employed to choose the dwellingunits where the questionnaires were administered. The study area was stratified according to its residential area density. This process was carried out as such in other wards until the questionnaires were exhausted. In each of the area, households that were not accessed either as a result of the inhabitant's absence or refusal to fill the question were replaced by the nearest available household.

The major instrument to be used for this research was structured questionnaire. The questionnaire was carefully structured by the researcher into four sections. The first section dealt with questions on the social and demographic background of respondents while the second part dealt with the types of energy sources attributable to different energy uses across the urban and rural areas, the third part dealt with the factors that influences the choice of energy used by households and the fourth one dealt with the preferences of household on different energy sources. The questionnaire were written in close ended questions of four likert-scale of Strongly Agree (SA), Agree (A), Disagree (D), Strongly Disagree (SD) which are denoted as 4,3,2 and 1. Where 4, 3 means Yes and 2, 1 means No in the computations.

The research involved quantitative method of analysis. Quantitative method in this study was simple statistics expressed in frequencies, standard deviations, percentages and means; and they were used to give explanations on the demographic and socioeconomic characteristics of different households as they impinge on household energy use patterns.

Results

Energy used for cooking

Information was obtained from the respondents on the types of energy used for cooking (Table 1). Result shows that the most used energy type for cooking in the rural areas is firewood while in the urban areas the most used is charcoal.

Table 1: Energy types used in cooking

Energy type	RURAL HHs			URBAN HHs			TOTAL	
	% of Yes	% of No	Mean	% of Yes	% of No	Mean	R	U
Electricity	1.08	98.9	1.271	4.6	95.3	2.064	92	108
Gas	0	100	1.25	4.5	95.3	1.444	92	108
Kerosene	3.25	96.7	1.5	61	38	2.513	92	108

Firewood	88	11.9	*3.673	10.1	89.7	1.657	92	108
Charcoal	16.2	83.6	1.978	62.9	36	*2.568	92	108
Sawdust	5.43	94.4	1.75	6.4	93.4	1.564	92	108

The table shows that in the rural areas of the state firewood is the most used energy type for cooking (88%) with a mean of 3.6 showing they strongly agree to its use. In the urban area, charcoal is the energy type that is most used for cooking ranking (62.9%) of positive responses with a mean of 2.5 showing they agree to its use followed by kerosene (61%).

Energy used for ironing

In terms of meeting the ironing needs of respondents, most rural respondents relied on charcoal as against electricity in the urban areas (Table 2).

Table 2: Energy types used in Ironing

SOURCES	**RURAL HHs**			**URBAN HHs**			**Total**	
	% of yes	**% of No**	**Mean**	**% of yes**	**% No**	**Mean**	**R**	**U**
Electricity	8.6	91.2	1.5652	58.8	41.1	*2.675	92	102
Petrol	12.9	86.9	1.75	33.5	66.2	2.203	92	104
Charcoal	77	22.8	*3.3695	14.7	85.1	1.953	92	108

The Table shows that in the rural areas of the state charcoal is the most used energy type for ironing ranking (77%) of positive responses with a mean of 3.3 showing they strongly agree to its use. In the urban area, electricity is the energy type that is most used for ironing ranking (59%) of positive responses with a mean of 2.6 showing they agree to its use.

Energy used for home entertainment

Information was obtained from respondents on the source of energy that is used to power radios, televisions and other electronic gadgets for entertainment at home (Table 3). Result show the

most used energy source for home entertainment in the rural areas is Battery while in the urban areas the most used is petrol.

Table 3: Energy types used in Home entertainment

SOURCES	RURAL HHs			URBAN HHs			TOTAL	
	% of yes	% of No	Mean	% of yes	% of No	Mean	R	U
Electricity	17.3	82.6	1.75	27.4	72.2	2.1203	92	108
Petrol	23.8	76	1,739	56.2	43.4	*2.6574	92	108
Battery	59.3	40.1	*2.815	18.5	81.4	1.9907	92	108

The Table shows that in the rural areas of the state battery is the most used energy type for home entertainment ranking (59%) of positive responses with a mean of 2.8 showing they agree to its use. In the urban area, petrol is the energy type that is most used for home entertainment ranking (56%) of positive responses with a mean of 2.6 showing they agree to its use.

Energy used for lighting

In terms of lighting in homes, the rural and urban households mostly rely on same energy types which are kerosene and petrol (table 4).

Table 4: Energy types for lighting

SOURCES	RURAL HHs			URBAN HHs			TOTAL	
	% of Yes	% of No	Mean	% of Yes	% of No	Mean	R	U
Electricity	24.9	74.9	1.8478	35.1	64.7	2.2222	92	108
Gas	0	99.9	1.3913	0.9	98.8	1.3796	92	108
Kerosene /petrol	65.1	34.7	*2.8478	60.1	39.8	*2.9444	92	108

Candle	6.4	93.4	1.9347	1.8	98	1.4259	92	108
Firewood	3.2	96.7	1.5652	0.9	99	1.4259	92	108

The Table shows that in the rural areas of the state kerosene and petrol is the most used energy type for lighting ranking (65%) of positive responses with a mean of 2.8 showing they agree to its use. In the urban area, same kerosene and petrol is the energy type that is most used for lighting ranking (60%) of positive responses with a mean of 2.9 showing they strongly agree to its use.

Energy used for food preservation

Information was obtained from the respondents on the type of energy used in food preservation (Table 5). Result shows the most used energy type for food preservation in the rural areas is firewood while in the urban areas the most used is kerosene.

Table 5: Energy types used in Food preservation

SOURCES	**RURAL HHs**			**URBAN HHs**			**TOTAL**	
	% of Yes	**% of No**	**Mean**	**% of Yes**	**% of No**	**Mean**	**R**	**U**
Electricity	5.4	84.6	1.5760	20.3	79.6	1.8611	92	108
Gas	0	89	1.2717	3.7	96.2	1.5648	92	108
Kerosene	11.8	87.9	1.4456	67.5	32.4	*2.5092	92	108
Firewood	60.9	38.8	*2.7826	24.9	74.9	2.2037	92	108
Charcoal	13.5	85.8	1.6630	12	87.9	1.6111	92	108
Sawdust	5.3	94.5	1.3695	7.3	92.5	1.9722	92	108

The Table shows that in the rural areas of the state firewood is the most used energy type for food preservation ranking (60%) of positive responses with a mean of 2.7 showing they agree

to its use. In the urban area, kerosene is the energy type that is most used for food preservation ranking (68%) of positive responses with a mean of 2.5 showing they agree to its use.

Energy used for cooling

Information was obtained from the respondents on the type of energy used in cooling (Table 6). Result shows the most used energy type for cooling in the both areas is petrol.

Table 6: Energy types used in cooling

SOURCES	RURAL HHs			URBAN HHs			TOTAL	
	% of Yes	% of No	Mean	% of Yes	% of No	Mean	R	U
Electricity	15.87	84.1	1.445	29.1	70.8	2.12	103	63
Petrol	40.3	35.9	*1.5	67.3	32.6	*2.6	98	62

The Table shows that in the rural areas of the state petrol is the most used energy type for cooling ranking (40.3%) of positive responses with a mean of 1.5. In the urban area, petrol is the energy type that is most used for cooling ranking (67.3%) of positive responses with a mean of 2.6 showing they agree to its use.

Daily Frequency of energy types used by households

The study sought to find out the amount of energy used daily by the respondents for various purposes (table 7).The energy use per day by households are distributed as follows; No response (0), less than 4hours per day (1), 4-6hours per day (2), 8hours per day (3) and more than 8hours per day (4).

Table 7: Frequency of energy types used by households

Types	Number of hours of use of energy by Rural HHs					Number of hours of use of energy by Urban HHs					Total	
	4	3	2	1	0	4	3	2	1	0	R	U
Electricit	2.17	5.43	7.6	28.2	56.5	1.85	17.5	14.8	74	0	92	108
Gas	0	0	0	0	100	-	0.92	2.77	1.85	94.4	92	108

Kerosene	0	8.69	23.9	45.6	21.7	*18.5	41.6	25.9	7.40	6.48	92	108
Firewood	*21.7	45.6	10.8	7.6	10.8	9.25	10.1	16.6	2.77	61.1	92	108
Charcoal	18.4	1.08	13.0	44.5	22.8	11.1	12	25	16.6	35.1	92	108
Sawdust	2.17	4.34	1.08	1.08	91.3	1.85	2.77	2.77	0.92	91.6	92	108

From Table 7 it is evident that the most frequently used energy source per day by the rural households is firewood (21.7%), use for more than eight hours while in the urban is kerosene rated 18.5% use for more than eight hours.

Summary of Findings

The most used energy types for cooking in rural and urban areas is firewood and charcoal respectively. Urban households use kerosene for cooking than rural households. The energy type used for ironing in the rural area of Bosso state is charcoal and the least is electricity, while in the urban areas the most used for ironing is electricity while the least is charcoal. In rural areas of the state, battery is the most used for home entertainment while the least is electricity. In the urban area, petrol ranked the most used for home entertainment while the least is battery. In the rural areas of the Bosso, kerosene/petrol is the most used for lighting while the least is gas. The same goes for the urban area, kerosene/petrol also ranked the most used for lighting while the least is also gas. In the rural area, petrol ranked the most used for cooling while the least is electricity. In the urban and urban areas, petrol ranked the most used for cooling and electricity ranked the least used. In the rural areas of the Bosso, firewood is the most used for food preservation while the least is gas. In the urban area, kerosene ranked the most used for food preservation while the less used is gas. In summary, the most used energy type per day in the urban area is kerosene, while in the rural area it is firewood.

This agrees with the position of (World Bank, 2005, NBS, 2006), which notes that in Nigeria traditional energy sources accounts for over 70% Household energy supply. while rural

households rely more on biomass fuels than those in urban areas, a substantial number of urban poor households' in Nigeria rely on fuel wood, charcoal, or wood waste to meet their cooking needs.

Findings also show that households rely on multiple sources of energy especially in the urban areas. The findings agree with those of Akpan, (2007) and Desalu, (2012) that found that household relies on several energy types and sources. Our findings on the reliance of rural households on fuel wood also agrees with Afeikhena (2006) and Yaqub, et al , (2011), findings show that more rural households use fuel wood and other more polluting and less efficient energy sources for cooking.

Conclusion

Based on the research findings, households in rural and urban areas of Niger state responded differently in their energy usage pattern. The use of solid fuel (firewood; 21.7%) on daily basis is high in rural areas, while the urban use more of kerosene on daily basis (18.5%). Their choice of energy use can be related to level of education, age, gender, occupation, weather, accessibility, location, type of food prepared, income, available home appliance and energy price. The use of electricity is mostly associated with its availability, gas is associated with high level of high level of education, cultural belief, high price and high income, petrol is associated with high income, home appliances and high price. Kerosene is associated with its availability and high price, firewood is associated with its cheapness, cultural preference and belief, low level of education and location (rural), charcoal is associated with low energy price and low income, while the use of sawdust is associated with low energy price and low level of education. Households in both rural and urban area of Bosso state responded positive to the use of modern energy for non-cooking activities if such energy was made affordable, available and they earned higher income, while their response to its use for cooking was different as the rural preferred solid fuel for cooking as against the urban. Making modern energy available and

affordable as well as sensitizing households on the impact of traditional energy use to Niger state environment will help ensure a secured and safe environment.

The study recommends that domestic modern energy types be made available, affordable and accessible to households in Bosso. This is because most urban and many rural households showed interest in the use. There is also need for sensitization in both areas; the rural people need to be educated on the negative impact on the environment of the traditional energy types they use, as well as the urban areas that use charcoal for cooking, aside the energy price, most of them prefer firewood for cooking even when electricity or gas is made available and affordable to them.

REFERENCES

Adetunji, M. and Isa, M. (2006). "The demand for residential electricity in Nigeria: a bound testing approach" Department of Economics University of Ibadan, Nigeria.

Ajoa, K. R. and Ajimotokan H. A. (2009), 'Electric Energy Supply in Nigeria, Decentralized Energy Approach'. *Cogeneration and Distributed Generation Journals*, 24 (4); 34-50.

Akpan, M., Wakili, A., and Akosim, C. (2007). "Fuel Wood Consumption Pattern in Bauchi State: A Guide for Energy Planners in Nigeria". An International Journal of Agricultural Science, Environment and Technology, 7 (1); 126-150. Retrieved from ASSET, on 20th July, 2012.

Al- Salman, M. H. (2007), 'Household demand for energy in Kuwait'. *J. King Saud Univ*ersity Vol. 19, pp 51-60.

Anthony, C., Ogbonna, O. and Dantong, J. (2011). "Domestic Energy Consumption Patterns in a Sub Saharan African City: The Study of Jos-Nigeria". Journal of Environmental Sciences and Resource Management, 3.

Archer, K. J., and S. A. Lemeshow. 2006. Goodness-of-fit test for a logistic regression model fitted using survey sample data. Stata Journal 6: 97–105.

Bowman, D.M., Balch, J.K and Artaxo, P. (2009), "Fire in the Earth System". Science journal, 324 (5926); 481–4.

Canberra Group (2001). "Expert group on household income statistics. final report and recommendations". Ottawa. ISBN 0-9688524-0-8.

Davis, M. (1995). "Fuel choice in rural communities". *Energy for Sustainable Development*, 2(3); 45-48.

Department for International Development (DFID) (2000), 'Energy for the Poor: Underpinning the Millennium Development Goals*'. (Research Project)*. Nigeria: DFID.

Department for International Development (DFID) (2005), 'Energy for the Poor: Underpinning the Millennium Development Goals*'. (Research Project).* Nigeria: DFID.

Desalu, O. (2012), "community survey of the pattern and determinants of household sources of energy for cooking in rural and urban south western, Nigeria". *Pan-African Medical Journal, 12.*

Eboh, C. Eric (2009), Social and Economic Research: principles and methods. African Institute for Applied Economics, Enugu, Nigeria.

Energy Commission of Nigeria (ECN) (2003), 'Strategic Planning and Co-ordination of National Policies in the Field of Energy'.*Journal of ECN on energy*. 20(9) pp 56-122, retrieved from www.energy.gov.ng/index.php%3. July 20th, 2012.

Energy Commission of Nigeria (ECN) (2003), "Strategic Planning and Co-ordination of National Policies in the Field of Energy". *Journal of ECN on energy,* 20 (9); 56-122. retrieved from www.energy.gov.ng/index.php%3. July 20th, 2012. Eurostat, (1985). "Family Budgets: Comparative Tables – Federal Republic of Germany, France, Italy, United Kingdom". Eurostat, Luxembourg.

Fagerland, M. W., and D. W. Hosmer, Jr. 2012. A generalized HosmerLemeshow goodness-of-fit test for multinomial logistic regression models. Stata Journal 12: 447–453.

Govinda, R., Gautam, D., and Michael, P. (2001), *The Least Cost Energy Path for India:* Energy Efficient Investments for the Multilateral Development Banks, International Institute for Energy Conservation. New Jersey.

Hertberg, R. and Bacon, R. (2003), *Household Energy and the Poor*: lessons from a Multi Country study accessed 10th March 2012. Retrieved from http://www.worldbank.org/energy/.

Hosier, R. H. and J. Dowd (1987). "Household fuel choice in Zimbabwe". *Resources and Energy,* 9; 347-361.

Hosier, R. H. and Kipondya, W., (1993), "Urban household energy use in Tanzania: prices, substitutes, and poverty". *Energy Policy,* 21(5). http://www.worldbank.org/energy/. Accessed on July 10th, 2012.

Ibidun, O. A. and Afeikhena, T. J. (2006), "dynamics of household energy consumption in a traditional African city-Ibadan". Volume 26 (2); 99-110.

Intergovernmental Panel on Climate Change (IPCC) (2007), '*Technical summary'.*Working Group 1: Assessment Report 4. Geneva, Switzerland: IPCC.

International Energy Agency (IEA) (2010). 'Energy poverty - how to make modern energy access universal'*World Energy Outlook, September, 2010*. Paris, France.

International Energy Agency (IEA), (2002), *World Energy Outlook 2002*. IEA: Paris, France.

International Energy Agency (IEA). (2002). '*World Energy Outlook 2002'* (2nded.). Paris, France: IEA publications.

International Energy Agency (IEA). (2002). *World Energy Outlook 2002* (2nd ed.). Paris, France: IEA publications.

International Energy Agency (IEA). (2006). '*World Energy Outlook 2006'*(3rd ed.): Energy for cooking in developing countries. Paris, France: IEA.

International Energy Agency (IEA). (2006). *World Energy Outlook 2006* (3rd ed.): Energy for cooking in developing countries. Paris, France: IEA.

Kevelaitis, K. (2008). *Solar Energy Implementation in Nigeria*, Bachelor unpublished Degree in Business Studies. Roskilde University, Olabisi, I. A. (1999). Domestic Energy Situation in Nigeria: Technological Implication and Policy Alternative. *Unpublished Seminar Paper*, Department of Sociology. Obafemi Awolowo University Ile Ife.

Khare, D. K. (2009), *Guidelines for the Implementation of Biomass Gasifier*: Ministry of New and Renewable Energy: Government of India. Retrieved from http://www.thebioenergy.com. (accessed August 12th, 2012).

Madubansi, M. and Shackleton, C. M. (2007) "Changes in fuelwood use and selection following electrification in the Bushbuckridge lowveld, South Africa."*Journal of Environmental Management*, 83; 416–426.

Masekoameng, K. E., Simalenga, T. E. and Saidi, T. (2005). ‘‘household energy needs and utilization patterns’’ in the giyani rural communities of limpopo province, south Africa. University of Venda for Science and Technology, South Africa.

Masekoameng, K., Simalenga, T. and Saidi, T. (2005). “Household energy needs and utilization patterns in the Giyani rural communities of Limpopo Province”. Journal of Energy in Southern Africa, 16 (3).

Masera, O. R., Saatkamp, B. and Kammen, D. M. (2000), “From linear fuel switching to multiple cooking strategies: a critique and alternative to the energy ladder model”. *World Development*, 28(12).

Determination of Sedimentary thickness over parts of Middle Benue Trough, North-East, Nigeria using Aeromagnetic Data

By

Salako K. A., Adetona A. A., Rafiu A. A., Alhassan U. D., Aliyu A., and Alkali, A.
Department of Physics, Federal University of Technology Minna, Niger State.

Abstract

High resolution aeromagnetic data acquired by the Nigerian Geological Survey Agency which covers about 18,150 km^2 of some parts of middle Benue trough (that lies between Longitude 9^oE – 10^oE and Latitude 8^oN – 9.50^oN), was processed and interpreted with the goal of estimating the study area sedimentary thickness. Polynomial fitting of order one was used in regional-residual separation of the Total Magnetic Intensity map of the study area. Thereafter, analytical signal, source parameter imaging (SPI) and spectral depth analyses were applied on the residual data. Results from the analytical signal showed that the area is made up of highs and lows magnetic anomalies with varying amplitudes. The SPI result revealed a sedimentary thickness ranging between 101.8 m and 2550.0 m and the depth estimates from the spectral depth analysis showed that the sedimentary thickness of the study area ranges between 1.20 km and 3.20 km. The estimated depths from spectral analytical method were contoured to portray the basement isobaths for the study area. The highest sedimentary thickness from both depth analytic methods agreed in terms of location, this value can supports the hydrocarbon (gas) accumulation in the central and southern part of the study area.

Keywords: Aeromagnetic data, polynomial fitting, analytic signal, source parameter imaging, spectral depth analysis and sedimentary thickness.

1. INTRODUCTION

Exploration of earth's contents have been of major concern to human because it requires an innovative technique to unravel its complexity as a result, geophysical survey method has been adopted to map the structures and lithology of the subsurface. Magnetic method is one of the best geophysical techniques used in delineating or estimating sedimentary thickness and other subsurface structures. Recent interest in the inland basins in Nigeria for petroleum and mineral deposits necessitated the need to study one of the prominent basins in which Middle Benue Trough is one of them, high resolution aeromagnetic data over part of Middle Benue Trough was used to determine the sedimentary thickness in the study area for possible hydrocarbon accumulation. The Middel Benue Trough, Nigeria, is part of the Benue Trough of Nigeria which is the study area of this research, the study area is located between latitude 8^oN and 9.50^oN and longitude 9^oE and 10^oE in north central Nigeria It covers an area of 18,150 km^2, and covers farmlands, villages, towns, game reserves, and natural reserves. The area lies east of the Federal Capital, Abuja.

This present study is based on reconnaissance survey and two depth estimating methods were adopted to determine the sedimentary thickness over part of middle Benue Trough for possible

hydrocarbon potential in the area. The methods are source parameter imaging and spectral depth analysis. The results from these two methods, that is, source parameter imaging and spectral depth analysis would be used to suggest areas with the presence of hydrocarbon potential.

2. LOCATION AND GEOLOGY

The study area is located in the Middle- Benue Trough Nigeria and it lies in the north eastern part of Nigeria and it lies within latitude $8^0.00'$ N and $9^0.50'$ N and longitudes $9^0.00'$ E and $10^0.00'$ E. Figure 1a shows the generalized geology map of Nigeria showing the study Area (Obaje, 2009). The Benue Trough in Nigeria comprises of a progression of rift basins that model a portion of the Central West African Rift System of the Niger, Cameroon, Chad and Benin Basement fracture, subsidence, block faulting and cracking.

Benkhelil (1982 and 1989),pointed out that the Benue Trough generally has been geographically and structurally subdivided into three parts erroneously termed as "lower Benue Trough", "middle Benue Trough" and an "Upper Benue Trough".

The study conducted by Offodile (1976) distinguishes six sedimentary Formations in the middle Benue trough which are Asu River Group, Keana Formation, Awe Formation, Ezeaku Formation, Awgu Formation, Lafia Formation. The work of Cratchley and Jones (1965), Burke *et al.* (1970), Offodile (1976 and 1984), Osazuwa *et al.* (1981) and Offoegbu (1985) and Patrick*et al*., 2013) have more on the geology of the Benue Trough. Figure 1b shows the geological map of the study area (extracted from geology map of Nigeria, produced by the Nigeria Geological Survey Agency 1984).

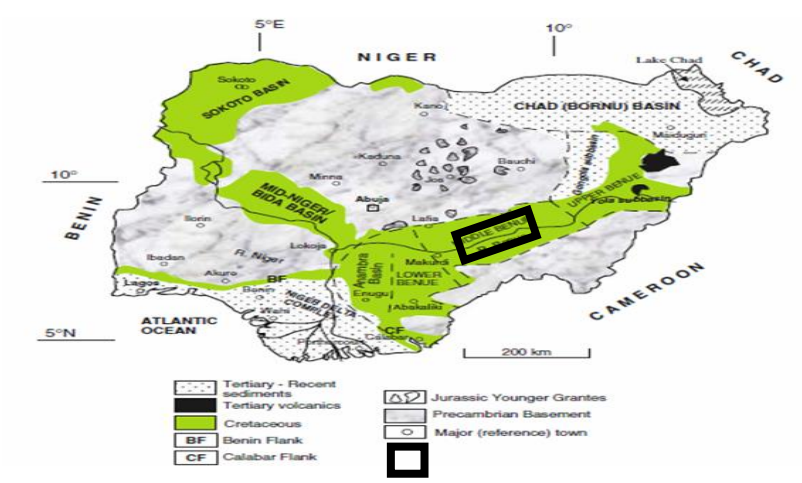

Figure 1a: Geological Map of Nigeria showing the study area in black outline (Source: Obaje, 2009)

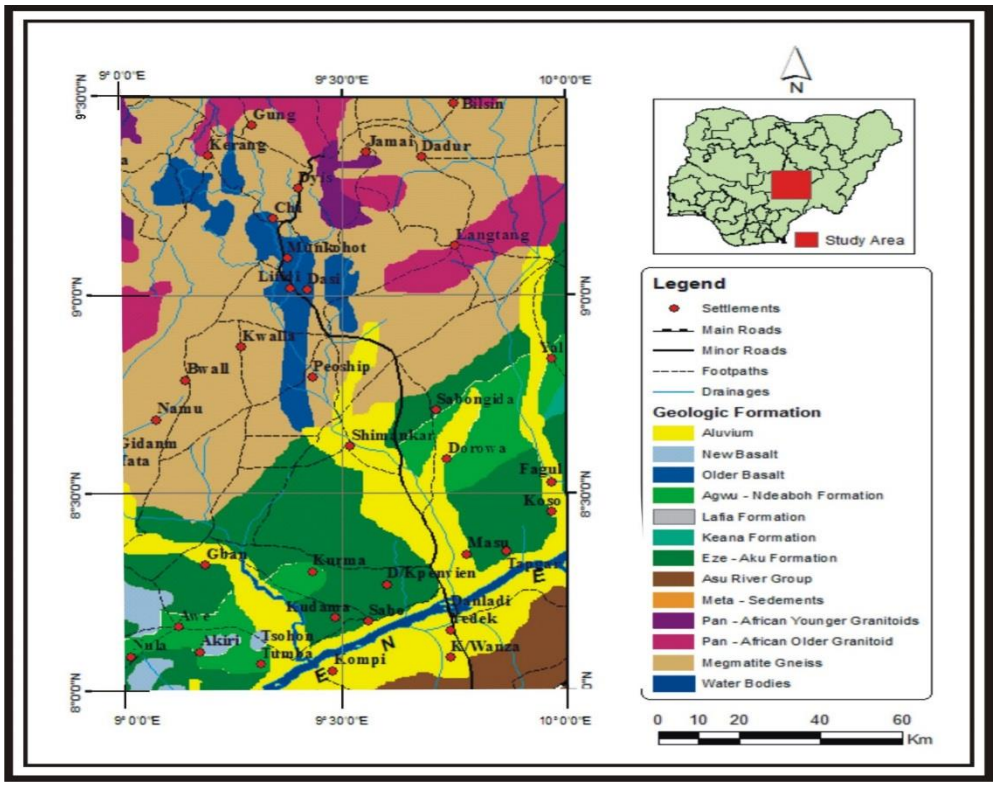

Figure 1b: Geological map of the middle Benue trough (Source: Geological Survey of Nigeria, 1984)

3.0 MATERIALS AND METHODS

For this work, six aeromagnetic maps with sheet numbers 190, 191, 211, 212, 231 and 232 covering the study area was acquired from the Nigerian Geological Survey Agency (NGSA) Abuja as a part of the across the nation aeromagnetic study carried out in 2009 by Fugro Airborne survey. The data was acquired using magnetometers. The survey was conducted along NW-SE flight lines and tie line along NE-SW direction with 500 m flight line spacing, Terrain clearance of 80 m and line spacing of 2 km were used. The magnetic data recording interval during the survey was 0.1 seconds. All grid data were saved and delivered in Oasis Montaj Geosoft raster file format. Each 1:100,000 topographical sheet covers an area of about 3,025 km^2 (i.e. 55 km x 55 km) totalling a superficial area of 18,150 km^2.

The TMI and even the aeromagnetic field sheets used in producing it are the entirety of the effect of all sources generating the magnetic anomaly. In applied geophysics, the issue is to dispose with or lessen to a minimum, the impacts of deep seated, non-profitable sources with minimum disturbance of the resultant anomaly as could reasonably be expected. Thus, this work begins with the separation of the long-wavelength anomalies of the regional field component which is attributed to deep and large scale sources from the shorter wavelength features constituting the residual field assumed to arise from shallow, small scale sources. In view of the simplicity in the trend of the magnetic field in the survey area, the regional field component was removed from the observed data using polynomial fitting method of order two.

The residual anomaly map was later subjected to three automated processing techniques to determine the depth to magnetic basement. The three automated processing techniques are (i) analytic signal, (ii) Source parameter imaging and (iii) spectral analysis

3.1 Analytic Signal method:

The analytic signal method is a notable method for establishing the edges of magnetic anomalies. The analytic signal is not dependent of magnetization direction and Earth's magnetic field direction. This implies that all bodies with similar geometry have the same analytical signal (Milligan and Gunn, 1997).
The function used in the analytic signal method is the analytic signal amplitude (absolute value) of the observed magnetic field at the location (x, y), defined by three orthogonal gradients of the total magnetic field using the expression:

$$|A(x,y)| = \sqrt{(\frac{\partial \mathrm{M}}{\partial \mathrm{x}})^2 + (\frac{\partial \mathrm{M}}{\partial \mathrm{y}})^2 + (\frac{\partial \mathrm{M}}{\partial \mathrm{z}})^2} \qquad (3.1)$$

Where

$A\,(x, y) =$ amplitude of the analytic signal at (x, y),

$M =$ observed magnetic field at (x, y).

3.2 Source Parameter Imaging:

The Source Parameter Imaging (SPI^{TM}) is a technique using an extension of the complex analytical signal to assess magnetic depths. The Source Parameter Imaging TM (SPI^{TM}) function is a fast, simple, and powerful method for calculating the depth of magnetic sources. One merit of the SPI technique is that the depth can be visualized in a raster format and the true thickness determined for each anomaly (Salako 2014).
This approach developed by Thurston and Smith (1997) and Thurston et al. (1998, 1999) uses the connection between source depth and the local wave number (k) of the observed field, which can be calculated for any point within a grid of data through vertical and horizontal gradients Thurston and Smith, (1997). The depth is shown as an image. The basics are that for vertical contact, the peaks of the local wave number define the inverse of depth.

The SPI method (Thurston and Smith, 1997) estimates the depth parameter using the local wave number of the analytical signal (Salako 2014). The analytical signal A1(x, z) is defined by Nabighian (1972) as

$$A_1(x,z) = \frac{\partial \mathrm{M(x,z)}}{\partial \mathrm{x}} - \mathrm{j}\frac{\partial \mathrm{M(x,z)}}{\partial \mathrm{z}} \qquad (1)$$

Where

$A_1(x,z) =$ analytic signal

M(x,z) = magnitude of the anomalous total magnetic field,

Nabighian (1972) have demonstrated that the gradient change constitutes the real and imaginary parts of the 2D analytical signal are connected as follows:

$$\frac{\partial \mathrm{M(x,z)}}{\partial \mathrm{x}} \Leftrightarrow -\mathrm{j}\frac{\partial \mathrm{M(x,z)}}{\partial \mathrm{z}} \qquad (2)$$

Where
$\Leftrightarrow$ implies a Hilbert transform.
Thurston and Smith (1972) defined the local wave number k_1 to be:

$$k_1 = \frac{\partial}{\partial \mathrm{x}}\tan^{-1}\left[\frac{\partial \mathrm{M}}{\partial \mathrm{z}} \Big/ \frac{\partial \mathrm{M}}{\partial \mathrm{x}}\right] \qquad (3)$$

Salako (2014) and Nwosu (2014) expressed that the marks illustrated by Thurston and Smith (1972) used Hilbert transformation pair expressed in (2). The Hilbert transform and the vertical

derivative operators are linear, so the vertical derivative of (3) will give the Hilbert transform pair,

$$\frac{\partial^2 \mathrm{M(x,z)}}{\partial \mathrm{z}\,\partial \mathrm{x}} \Leftrightarrow -\frac{\partial^2 \mathrm{M(x,z)}}{\partial^2 \mathrm{z}} \tag{4}$$

In this manner the analytic signal could be defined based on second-order derivatives, $A_2(x,z)$, where

$$A_2(x,z) = \frac{\partial^2 \mathrm{M(x,z)}}{\partial \mathrm{z}\,\partial \mathrm{x}} - \mathrm{j}\frac{\partial^2 \mathrm{M(x,z)}}{\partial^2 \mathrm{z}} \tag{5}$$

This gives rise to a second order local wave number κ_2 , where

$$k_2 = \frac{\partial}{\partial \mathrm{x}} \tan^{-1}\left[\frac{\partial^2 \mathrm{M}}{\partial^2 \mathrm{z}} \Big/ \frac{\partial^2 \mathrm{M}}{\partial \mathrm{z}\,\partial \mathrm{x}}\right] \tag{6}$$

This k_1 and k_2 are used to determine the most appropriate model and depth estimate of any assumption about a model.

3.3 Spectral analysis:

The method was pioneered by Bhattacharryya (1966) and developed by (Spector and Grant, 1970), it has been utilized widely in the interpretation of magnetic anomalies Onuoha *et al.* (1994), Nwogbo (1997)Eleta and Udensi (2012)Salako and Udensi (2013) Udensi E.E. (2000) Mishra and Naidu (1974). It depends on the expression of Power spectrum for the total magnetic field anomaly.

The approaches used involve Fourier transformation of the aeromagnetic data to compute the energy (or amplitude) spectrum. (Spector and Grant, 1970) demonstrated that the depth could be made using the equation

$$E(r) = \mathrm{e}^{-2\mathrm{hr}} \tag{7}$$

where E(r) = spectral energy

r = frequency

h= depth

The energy or amplitude spectrum is plotted on the Logarithmic scale against frequency. The plot shows the straight line segments which decrease in slope with increasing frequency. The slopes of the segments yield estimates of depths to magnetic sources.

If h is the mean depth of a layer and the depth factor for the ensemble of anomalies is e^{-2rh} hence, a plot of the energy spectrum of a single ensemble of prism against angular frequency r would yield a straight line graph whose slope is directly proportional to the average source depth, h of that ensemble. That is, the logarithm plot of the radial would yield a straight line whose slope,

$$m = -2h$$

$$h = -\frac{m}{2} \tag{8}$$

Equation (3.10) can be specifically applied if the frequency unit is in radian per unit distance (kilometer as it is in this research), if it is unit is in cycle per unit distance as it is in this work, the expression becomes

$$h = -\frac{m}{4\pi} \quad (9)$$

4 Discussion of Result

4.1 Total Magnetic Intensity (TMI)

The total magnetic intensity map (TMI) of the study area (Figure 2) shows variation of highs and lows in magnetic signature, ranging from -54.4nT to 153.5nT. The pink colouration depicts high magnetic signature while blue depicts low magnetic signature, greenish depicts alluvium deposition and yellow indicates intermediary. The high magnetic signature region denoted with **H** is well pronounced at the central part of the of the study area, trending East-West. Although the high magnetic signatures are scattered all round the study area while the low magnetic signature denoted with **L** is well pronounced in the northern part of the study area, though few lows could also be found at Southern part of the study area trending NE-SW.

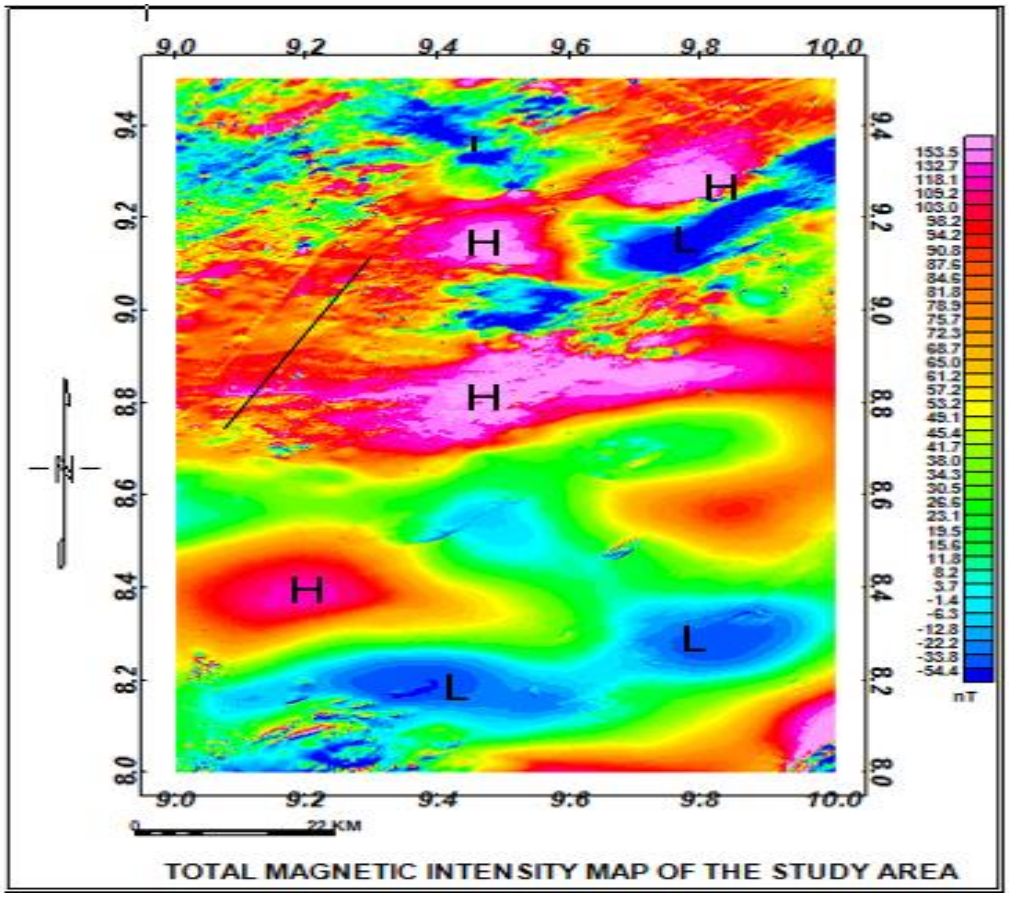

Figure 2: TMI anomaly contour map of the study area (add a background value of 33000nT to each value to get the actual value)

4.2 Regional map of the study area

The TMI is always a combination of the superposition of the impacts of all underground magnetic sources. Normally the targets in this aeromagnetic investigation are the anomalies of the basement rock, and their magnetic field is superimposed in the regional field that originates from larger or more profound sources, and must be separated to get the residual.

A look at the regional map (Figure 3) shows that the northern part is dominated with highs and low magnetic signatures are predominant at the southern part of the study area. The trends appeared in uniform variation (represented by parallel evenly spaced contours) can be observed to run in the NW-SE direction.

The regional field dips gently and uniformly towards the South-western part of the study area from the North-Eastern part

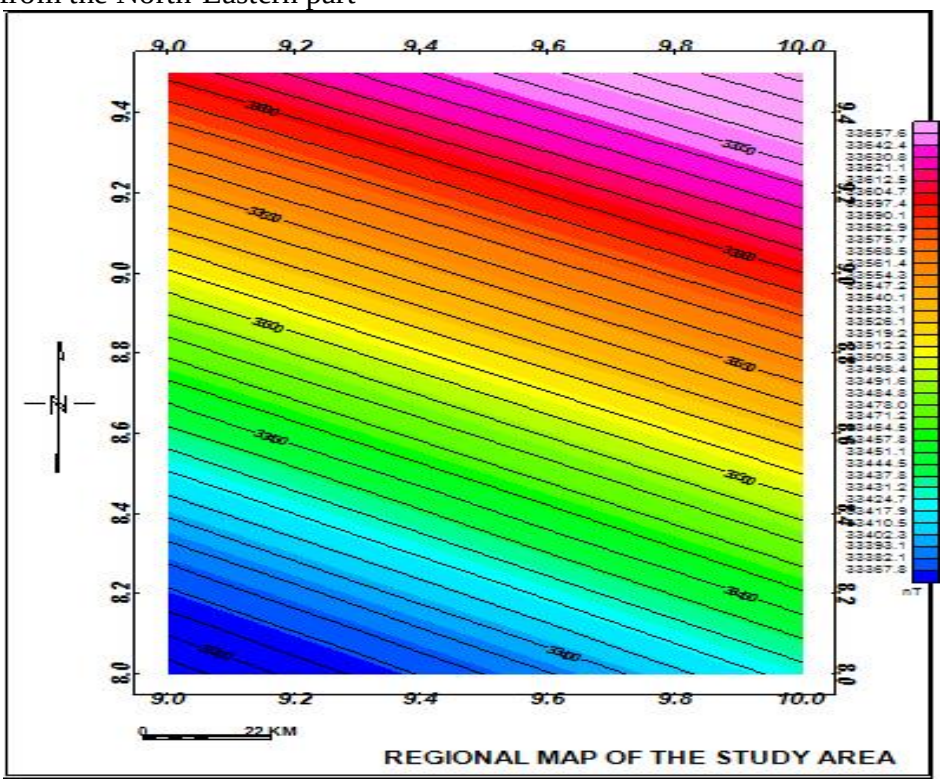

Figure 3: Regional map of the study area

4.3 Residual Map

The residual magnetic intensity map (Figure 4) of the study area shows that the area is made up of magnetic intensity values ranges from -109 nT to 99.9 nT. The negative values imply areas that are magnetically subdued or quiet while the positive values are magnetically responsive. The magnetically subdued areas are the magnetic lows of the study area and this is typical of a sedimentary terrain while the magnetic responsive areas are the magnetic highs regions which are assumed to be due to the likely presence of outcrops of crystalline igneous or metamorphic rocks, deep seated volcanic rocks or even crustal boundaries. The high magnetic anomaly which can probably be attributed to igneous intrusion and shallower sediment is well pronounced in the central part trending approximately East-West similar to the one in TMI map (figure 2). The high magnetic signature can also be found in the North-Eastern part trending North-West while the low magnetic anomalies associated with the sedimentary region was well pronounced in North-Western, North-Eastern, while other scattered at the edges of North-Eastern part of the study area.

About one third of the map can be seen to be greenish (featureless) which may correspond to alluvium deposition in the southern part of the study area.

The varying amplitude of these magnetic anomalies is an indication of different sedimentary thickness in the study area. These variations in the anomaly amplitude may also indicate possibly the occurrences of basement complex rocks containing varying amounts of magnetic minerals.

The traced line on the map is probably a fracture (fault line) At some places on the southern part of the residual map (Figure 4.3) there are anomalies that are not present on the total magnetic map (Fig. 4.1). These anomalies are due to magnetic source of shallow origin.

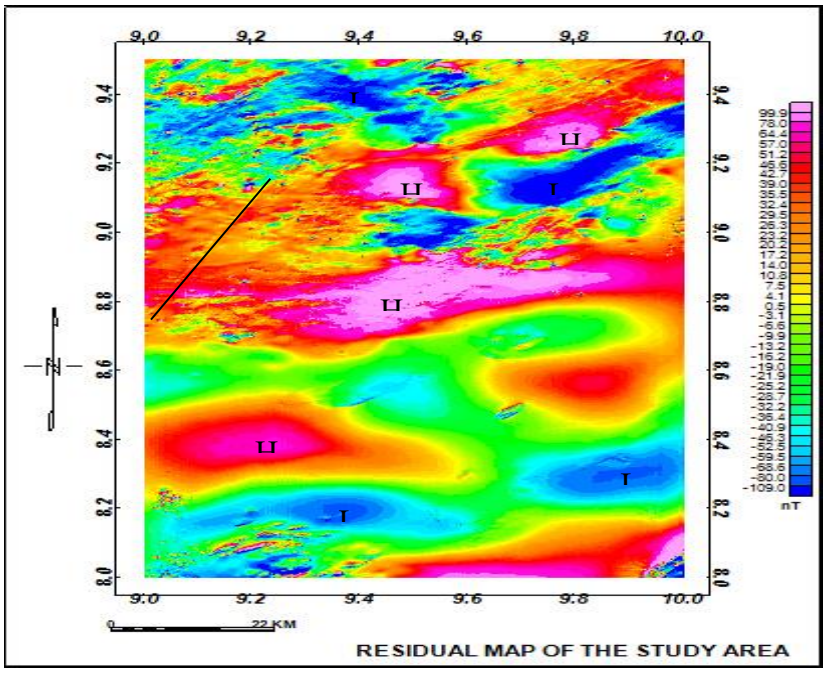

Figure 4: Residual map of the study area

4.4 Analytical signal

The analytic signal map (Figure 5) of the study area indicates contrast in magnetic anomalies amplitude, the lower magnetic anomalies amplitudes ranges from light green to deep blue colour as indicated in the legend. Red, yellow and orange colour depicts areas of higher magnetic anomalies amplitude.

The high amplitude magnetic anomalies were very much pronounced in the northern part and at the edges of the study area. The low amplitude magnetic anomalies were located at the central part and trends towards the south east. The high amplitude magnetic anomaly is probably due to basement intrusion close to the surface.

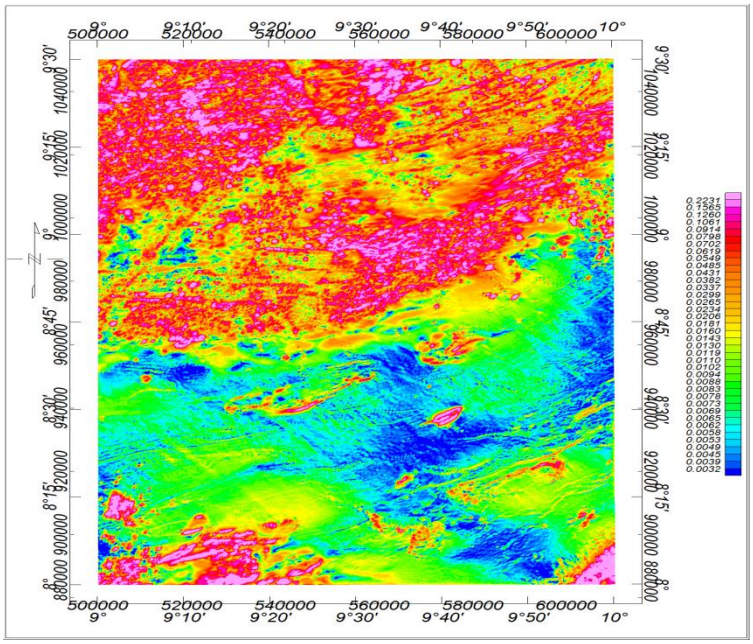

Figure 5: Analytic Signal Map of the Study Area

SPI image and interpretations

The source parameter image (SPI) figure (Figure 6) shows varied colours supposedly demonstrating distinctive magnetic susceptibilities variation in the studied area, and could likewise depicting the undulations in the basement surface. The negatives in the numbers on the legend imply depth. The light blue to deep blue colours indicates areas of thicker sediments or deep lying magnetic bodies, the purple and orange colour depicts areas of shallower sediment or close surface lying magnetic bodies. The white areas/ portion of the SPI are the areas where the derivative used to estimate the local wave number are so small that the SPI structural index cannot be estimated reliably. The model-independent local wave number had been set to zero in that portion.

The source parameter imaging (Figure 6) of the study area shows that most of the features are aligned in the same manner trends as it is in the analytic signal map (Figure 5). The area of highest sedimentary thickness in SPI (Figure 6) conforms to area of lower amplitude magnetic anomalies in analytical signal map (Figure 5).

From Figure (6), the depth to sedimentary/basement interface varies between 101.8 m and 2550.0 m. The thick sediment dominate the southern portion of the area while the least depth dominate major part of the southern portion. However, relatively lower depths are seen scattered around southern part.

According to Ofoha *et al* (2016), the thick sediments which range from 0.98 km to 2.6 km (represented with the blue colour) is synonymous to depth of over burden sediment which has a very important significance as to the hydrocarbon generation potential. And the least depth 0.1 to 0.8 (represented by the magenta, yellow, orange and green colours) indicates shallow seated magnetic bodies that have intruded unto the sedimentary cover and this falls short of the average thickness needed for the accumulation of oil and gas.

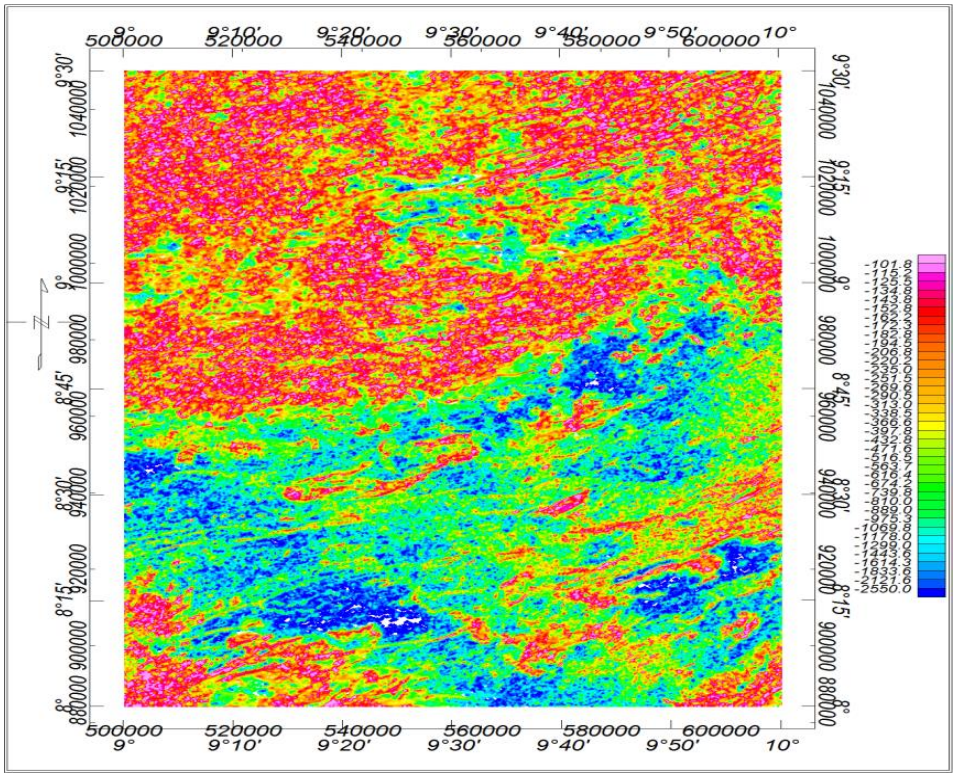

Figure 6: Source Parameter Imaging (SPI) map of the study Area

4.4 Spectral Analysis

The residual map (Figure 4) of the study area was divided into fourteen (Blocks A - N) overlapping magnetic sections in which six (Blocks A - F) covered 55km by 55km data points, three other division (Block G,H and I) covered 110km by 55 km data points, J, K and L covered 110km by 110km and Block M and N covered the remaining 165 km by 55 km part of the study area. In doing this division we ensured that essential parts of anomaly were not cut by the blocks.

The divisions of residual map into spectral sections or blocks were done with Oasis Montaj. The analysis was carried out using a spectral program plot (SPP) developed with MATLAB. Graph of the logarithm of spectral energies against frequencies obtained for blocks A, B, C, and D are shown in (Figure 7) while others are shown in Appendix. The second slope in the plot were used to compute the sedimentary thickness in line with equation 8.

From the result sedimentary thickness ranges from 1.20 km to 3.20 km which largely agrees with the result obtained earlier with SPI that range from 0.101 km to 2.55 km.

Results from the three estimate approaches agreed largely with other published works in the studied area. Nwogbo (1997) got 2km to 2.62km for deeper source and 70m to 0.63km for shallow source from spectral analysis of upper Benue trough; Alkali and Kasidi (2013) obtained two layer depths with the deeper magnetic sources vary between 1.2 km to 4.8 km and the shallower magnetic sources; vary between 0.5km to 1km.

Nwosu (2014) got an average depth of 1079.5 m for shallower source while the deeper magnetic source bodies) have an average depth of 3245m. Alagbe and Sunmonu (2014) using spectral analysis obtained values ranging between 1.22km and 3.45km for depth to magnetic basement

The contour map for the sedimentary thickness is shown in figure 8

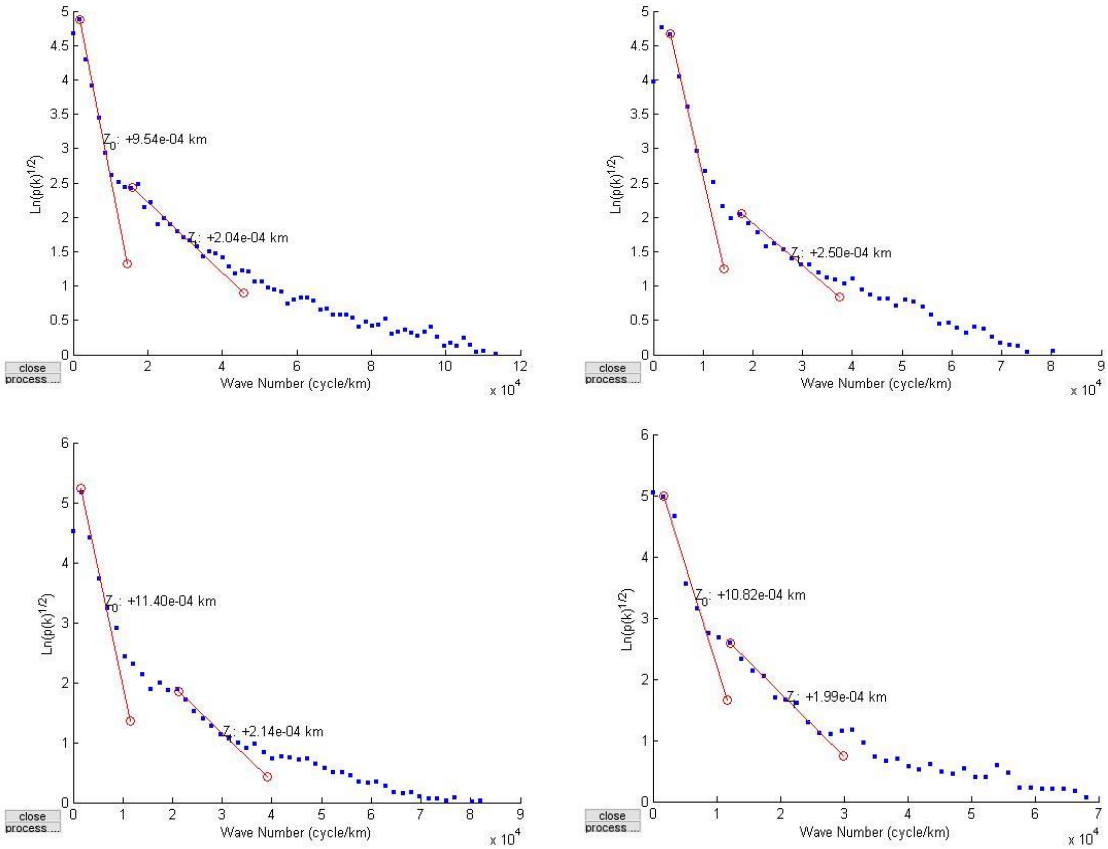

Fig. 7. Typical plots of the logarithm of spectral energies against frequencies obtained for block A, B, C, and D

Table 4.1. Location and depth estimation of sedimentary thickness (Z_t)

Blocks	Longitude (degree)	Latitude (degree)	Sedimentary thickness Z_t(km)
A	9.25	9.25	2.04
B	9.75	9.25	2.50
C	9.25	8.75	2.14
D	9.75	8.75	1.98
E	9.25	8.25	1.20
F	9.75	8.25	1.40
G	9.5	9.25	2.00
H	9.5	8.75	3.20
I	9.5	8.25	1.70
J	9.5	9.0	1.50
K	9.5	8.0	1.84
L	9.25	8.25	2.08
M	9.75	8.25	1.86
N	9.5	8.25	1.65
Average			1.94

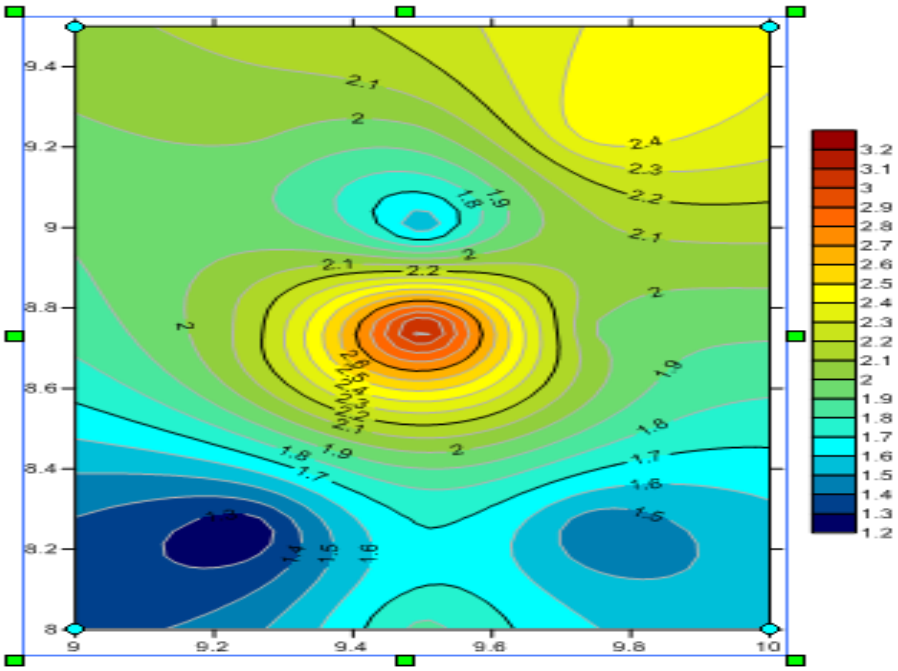

Figure. 4.7 contour map for the sedimentary thickness

CONCLUSION

The results of this study have suggest that the sedimentary thickness of the study area vary between 1.20 to 3.20 km. the high sedimentary thickness can be observed from the central part to the Northern part. These areas correspond to areas with highest magnetic values in total magnetic intensity (TMI) map of Figures 2 and residual map of Figure 4.

hence, the thick sedimentary cover in this region could be associated with hydrocarbon maturation or to series of volcanic activities that led to the formation of intrusive within the Middle Benue Trough.

REFRENCES

Abdullahi, U.A., Ugwu, G.Z., Ezema, P. O. (2014). Magnetic Exploration of the Upper and Lower Benue Trough for Metallic Deposits and Hydrocarbons using 2D/3D. *Journal of Natural Sciences Research,* 4(20), 41-46

Abdulsalam N. N., Mallam A. and Likkason O. K. (2013). Evidence of some tectonic events in the Koton Karifi area, Nigeria, from aeromagnetic studies. *Journal of Petroleum and Gas Exploration Research* Vol. 3(1) pp. 7-15,

Alkali1, S. C. and Kasidi, S. (2013). Determination of Depth to Magnetic Sources Using Spectral Analysis of High Resolution Aeromagnetic Data over IBBI and Environs, Middle Benue Trough, North Central Nigeria. International Journal of Science and Research (IJSR). Pp 1572-1578 retrieved from http://dx.doi.org/10.21275/v5i6.NOV152819 1578

Alagbe O.A, Sunmonu L.A (2014). Interpretation of aeromagnetic data from Upper Benue Basin, Nigeria using automated techniques. *IOSR Journal of Applied Geology and Geophysics* 2: 22–40.

Benkhelil, J. 1988. "Structure etE'volutionGe'odynamique du Basin Intracontinental de la Be'nue (Nigeria)". *Bulletin CentresRecherches Exploration Production Elf-Aquintaine*. 12:29-128.

Benkhelil, J. 1989. "The Origin and Evolution of the Cretaceous Benue Trough (Nigeria)". *Journal of African Earth Sciences*. 8:251-282.

Bhattacharyya, B.K. (1966): Continuous spectrum of the total magnetic field anomaly due to a rectangular prismatic body. *Geophysics,* vol. 31, 97 - 121.

Burke,K.C., Dessauvagie, T. F. J. and Whiteman, A. J., (1970). Geologic history of the Benue Valley and adjacent areas. In: Dessauvagie T.F.J. and Whiteman, A. J. (eds): *African Geology.University of Ibaban Press,* Nigeria, pp. 187-206.

Cratchley, C.R. and G.P. Jones. 1965. "An Interpretation of the Geology and Gravity Anomalies of the Benue Valley, Nigeria". Journal *Geology and Geophysics*. 1:1-26.

Eletta B.E and Udensi E.E (2012). Investigation of Curie point isotherm from the magnetic field of Easter sector of central Nigeria. *Global journal of geoscinces.* 101–106.

Hahn, A., Kind. E.G., and Mishra, D.C. (1976): Depth estimation of magnetic sources by meaI1Sof Fourier amplitude spectra. *Geophysical Prospecting*, vol. 24, 287- 308.

Ikujebi, E. A., Udensi, E. E. and Salako, K. A. (2012). Spectral Depth Analysis of parts of Bornu Basin, Nigeria, Using Aeromagnetic Data. Journal of Science, Technology and Mathematics Education Vol 9(1), pp. 14 – 24.

Milligan, P. R. and Gunn, P. J. (1997) Enhancement and Presentation of Airborne Geophysical Data. J. Aust. Geology and Geophysics, v. 17, pp. 63-75.

Mishra, D.C and Naidu, P.S (1974): Two Dimensional Power Spectrum and Analysis of Aeromagnetic Fields: *Geophysical Prospecting* 22(2),pp 345-353.

Mohammed A.G and Mustapha, A. (2014). Evaluation Of The Magnetic Basement Depth Over Parts Of Bajoga And Environs, Northeastern Nigeria by Stanley's Method. *IOSR Journal of Applied Geology and Geophysics (IOSR-JAGG) Volume 2, Issue 4, PP 47-53*

Nabighian, M. N. (1972). The analytic signal of two dimensional magnetic bodies with polygonal cross-section.its properties and use for automated anomaly interpretation. *Geophysics, 37*, 507-517.

Nwosu O.B(2014) Determination Of Magnetic Basement Depth Over Parts Of Middle Benue Trough By Source Parameter Imaging (SPI) Technique Using HRAM. *International Journal Of Scientific & Technology Research,* 3(1). ISSN 2277-8616

Nwogbo, P.O. (1997). Mapping the shallow magnetic sources in the Upper Benue Basin in Nigeria from aerornagnetic. *Spectra*, 4(3/4), 325-333.

Offodile, M.E.(1976). The Geology of the Middle Benue Nigeria. Cretaceous Research, Paleontological Institute: University of Uppsala. Special Publication. 4:1-166.

Offodile, M.E. 1984. "The Geology and Tectonics of Awe Brine Field". *Journal of Earth Sciences*. 2:191-202.

Ofoegbu, C. O., 1982. An aeromagnetic study of the Lower and Middle Benue Trough of Nigeria,*paper presented at the 6th United Kingdom Geophysical Assembly*, Cardiff, April 5-7.

Ofoegbu C. O. (1984a). Interpretation of Magnetic Anomaly over the Lower and Middle Benue Trough of Nigeria. Geophysical Journal Royal Astronomical Society 79:813-823.

Ofoegbu, C. O. (1984b). Aeromagnetic Anomalies over the Lower and Middle Benue Trough, Nigeria. *Journal African Earth Science,* 3 p.293 – 296.

Ofoegbu C. O. (1985). A review of the geology of the Benue trough, Nigeria. *Journal African Earth Sciences*pp 283 291

Ofoegbu C. O. (1988). An Aeromagnetic Study of part of the Upper Benue Trough, Nigeria. *Journal African Earth Sciences* vol. 7. No.1 pp. 77-90.

Ofoegbu, C.O and Onuoha, K.M (1991):Analysis of the Magnetic Data over the Abakiliki Anticlinorium of the lower Benue Trough, Nigeria. *Marine and Petroleum Geology*. Vol 8,:174-183.

Ofoha, C. C., Emujakporue, G., Ngwueke, M. I., and Kiani I. (2016). Determination of Magnetic Basement Depth over Parts of Sokoto Basin, within Northern Nigeria, Using Improved Source Parameter Imaging (ISPI) Technique *World Scient i f ic News 50, 266-277*

Ofor, N. P., Abubakar, A. T. and Udensi, E. E. (2010). Determination of Depths to Buried Magnetic Rocks under Bida and Baro Area of the Middle Niger Basin, Nigeria, using Aeromagnetic Data. Nigerian Journal of Space Research, Vol 9, pp. 113 – 123.

Onuoha, K. M., Ofoegbu, C. O., Ahmed M.N., (1994) Spectral Analysis of Aeromagnetic Data Over the Middle Benue Trough, Nigeria. *Journal of Mining and Geology* Vol. 30 1994 No.2, pp. 211-217

Osazua, I. B., Ajakaiye, D. E. and Verheiien, P. J. T. 1981. Analysis of the structure of part of the upper Benue rift valley on the basis of new geophysical data. *Earth Evolution Sciences* 2, 126-135.

Patrick,N.O., Fadele, S.I., and Adegoke, I.(2013).Stratigraphic Report of the Middle Benue Trough, Nigeria: Insights from Petrographic and Structural Evaluation of Abuni and Environs Part of Late Albian–Cenomanian Awe and Keana Formations.. *The Pacific Journal of Science and Technology*,14, 557-570 . Retrieved from http://www.akamaiuniversity.us/PJST.htm

Salako, K. A., Udensi, E. E (2013). Spectral Depth Analysis of Parts of Upper BenueTrough and Borno Basin, North-East Nigeria, UsingAeromagnetic Data. *International Journal of Science and Research (IJSR).*Vol 2,8: 2319-7064

Salako (2014). Depth to Basement Determination Using Source Parameter Imaging (SPI) of Aeromagnetic Data: An Application to Upper Benue Trough and Borno Basin, Northeast, Nigeria. Pp 74 -86. *Academic Research International retrieved from* www.journals.savap.org.pk

Spector, A., and Grant, F.S. (1970): Statistical models for interpreting aeromagnetic data. *Geophysics*, vol. 35, 293 - 302.

Thurston, J. B.,and Smith, R. S. (1997). Automatic conversion of magnetic data to depth, dip, and susceptibility contrast using the SPITM method. *Geophysics, 62*, 807-813.

Thurston, J.B., Guillon, C. and Smith, R. (1999) Model-independent depth estimation with the SPITM method: 69thAnnual International Meeting, SEG, Expanded Abstracts, 403–406.

Thurston, J.B., Smith, R. S., and Guillon, C. (2000) A multi-model method for depth estimation from magnetic data: *Geophysics*, 67, 555–561.

Thurston, J.B., Smith, R. S., Dai,T.F., and MacLeod, I. N.(1998) ISPI^{TM} — the improved source parameter imaging method: *Geophysical Prospecting*, 46, 141–151.

Udensi, E. E. (2000). *Interpretation of total magnetic field over the Nupe Basin in westcentral Nigeria using aeromagnetic data*. Ph.D thesis A.B.U. Zaria Nigeria.

Udensi, E.E (2012). Subduing the earth with exploration Geophysics: My contribu Udensi, E.E (2012). Subduing the earth with exploration Geophysics: My contribution. 24th inaugural lecture of Federal University of Technology, Minna

Udensi, E.E (2012). Subduing the earth with exploration Geophysics: My contribution. 24th inaugural lecture of Federal University of Technology, Minna

Wright, J. B., Hastings, D. A., Jones, W. B. and Williams, H. R., (1985). Geology And Mineral Resources of West Africa. George Allen and Unwin (Publishers) Ltd, 40 Museum Street, London WCIA ILU, UK. 187p

Assesment of Water, Sanitation and Hygiene Facilities in some Selected Schools in Potiskum, North Eastern Nigeria and its Implication on Health.

Adamu, H.L and Idris-Nda, A.

Department of Geology, Federal University of Technology, Minna

Corresponding Author: hannatulawan@gmail.com +2348137394545.

Abstract

An assessment of the water, sanitization and hygiene facilities in some selected schools in Potiskum was carried out. The study was aimed at determining both natural and anthropogenic effects on the physical, chemical and bacteriological composition that may affect the potability of groundwater in the schools. Geology and hydrogeology of the area was studied based on existing literature.Water level in wells and boreholes were determined using a dip meter, thirty schools were assessed comprising of twenty primary schools, generally with populations of over 2000 pupils and ten secondary schools, two of which are boarding schools. Thirty water samples were taken from wells and boreholes in the schools, physical parameters were taken at the point of collection while chemical and bacteriological analysis were done in the laboratory using standard analytical procedures. Focussed Group Discussions were held with various stakeholders to establish the present state of WASH education.Potiskum falls within the Nigerian sector of the Chad Basin consisting basically shales, siltstone, sandstone and ironstone. Chad and Keri Keri formations are the most important formations that constitute the aquifers for groundwater storage and transmission. Water level ranges from 12 – 18m, hand dug wells have an average depth range of 15 – 20m while boreholes have a depth range of 45 – 100m. The water has a mean temperature of 32^0C, pH of 6.75 and Electrical Conductivity of 89.53µS/cm. Calcium, chloride and sulphates are the dominant ions in the water, while copper, chromium and iron are the dominant heavy metals. All the analyzed chemical parameters were found to fall within the NSDWQ 2007 and WHO 2006 standards for all the sample locations (schools) except for some few isolated cases. The bacteriological analysis reveal that total coliform is higher is shallow wells than in boreholes. Coliform Bacteria are considered “indicator organisms”; their presence warns of the potential presence of disease-causing organisms and should alert the relevant authorities responsible for the water to take precautionary action. Sanitary facilities found in the various schools are mainly Ventilated Improved Pit (VIP) latrines, ordinary pit latrines and pour-flush systems. Average distance of these sanitary facilities to water points is less than 20m.

INTRODUCTION

An estimated 1.9 billion school days could be gained if the Sustainable Development Goals (SDGs) related to safe water supply and sanitation are achieved and the incidence of diarrhoeal and other related illnesses is reduced (UNICEF, 2017). One way of achieving this is by providing schools with safe drinking water, improved sanitation facilities and hygiene education that encourages the development of healthy behaviours for life. This strategic

approach is known as Water, Sanitation and Hygiene Education (WASH) in Schools. The strategy helps fulfil children's rights to health, education and participation, and has been widely recognized for its significant contributions to achieving the SDGs – particularly those related to providing good health, quality education, promoting gender equality and clean water and sanitation (goals 3,4,5 and 6).

According to Annemarieke, Murat, and Therese, (2012) WASH in Schools not only promotes hygiene and increases access to quality education but also supports national and local interventions to establish equitable, sustainable access to safe water and basic sanitation services in schools. Poor sanitation, water scarcity, inferior water quality and inappropriate hygiene behaviour are disastrous for infants and young children and are a major cause of mortality for children under five. Those conditions arealso detrimental to the health of school-aged children, who spend long hours in schools. The physical environment and cleanliness of a school facility can significantly affect the health and well-being of children. Disease spreads quickly in cramped spaces with limited ventilation, where hand-washing facilities or soap are not available, and where toilets are in disrepair. Too often, schools are places where children become ill.

WASH in Schools aims to improve the health and learning performance of school-aged children – and, by extension, that of their families – by reducing the incidence of water- and sanitation-related diseases by focussing generally on diarrhoeal and worm infections. These are the two main diseases that affect schoolaged children and can be drastically reduced through improved water, sanitation and hygiene in schools (Miguel et al., 2012).The causes of diarrhoea include a wide array of viruses, bacteria and parasites. Diarrhoeal disease affects far more individuals than any other illness. Eighty-eight per cent of diarrhoeal disease is caused by unsafe water supply, inadequate sanitation and hygiene (Prüss-Üstün*et al.*, 2008). Intestinal worm infections including hookworm, whipworm, roundworm and schistosomiasis affect roughly one in four people around the world. Worm infections are spread through unhygienic environments in soil or water and unhygienic behaviour via food or hands. School-aged children have the highest infection prevalence of any group; an estimated 47 per cent of children ages 5–9 in the developing world suffer from a worm infection (Baird, 2012) Such diseases are thought to be entirely attributable to inadequate sanitation and hygiene (Pruss-Ustun*et al.*, 2008)

WASH in Schools also focuses on the development of life skills and the mobilization andinvolvement ofparents, communities, governments andinstitutions to work together toimprovehygiene, water and sanitation conditions.While there are many approachesbased on differing cultural insights andenvironmental and social realities, anyWASH in Schools intervention shouldinclude:

- Sustainable, safe water supply points,hand-washing stands and sanitation facilities;
- Fully integrated life skills education, focusing on key hygiene behaviorsforschool children and usingparticipatory teaching techniques;
- Outreach to families and the widercommunity.

An efficiently and effectively implementedWASH in Schools programme will lead tostudents who:

- Are healthier;
- Perform better in school;

- Positively influence hygiene practicesin their homes, among family members and in the wider community;
- Learn to observe, communicate, cooperate, listen and carry out decisionsabouthygienic conditions and practicesfor themselves, their friends andyounger siblings whosehygiene theymay care for (skills they may apply inother aspects of life);
- Change their current hygiene behaviourand continue better hygiene practices in the future;
- Learn about menstrual hygiene and physical and emotional changes duringpuberty (learning to avoid menstrualodour, discomfort and urinary or vaginalinfections will encourage girls to come toschool during menstruation);
- Practice gender-neutral division ofhygiene-related tasks such as cleaning toilets,fetching and boiling water andtaking care of the sick.

Water supply is important in schools for the following reasons;

- Running a school canteen requires water for preparing food, cooking and washing dishes.
- Promoting hand washing requires a supply of soap and water
- The dignity of prayer and respect for others requires water for washing.
- Shady trees and bright flowers make a school an attractive place, but they require water nearby.
- Clean, odour-free latrines need plenty of water for cleaning.
- Managing the construction and maintenance of a water supply develops skills that can be carried over to other school and community plans.
- Thirsty children don't make good pupils.
- Spraying water helps control dust in classrooms and play areas.
- When traditional community wells dry up, the school well can provide water to those who need it.

Many schools in Potiskum Local Government Area of Yobe State, Northeastern Nigeria lack safe water supply, well designed latrines and hand washing facilities. Which affects enrolment and performance especially in the case of girls.

THE STUDY AREA

Potiskum is situated in Yobe State north eastern Nigeria and falls within latitudes 11˚42'43" N - 11˚48'42" N and longitudes 10˚52'48" E - 11˚4'11" E. It covers an area of 559 $km^2$with an elevation of 100-300m above sea level. Two types of seasons are experienced in Potiskum state, wet season of four months that is between June and October with a low rainfall distribution and a long dry season which normally lasts for eight months which is normally very hot and dry. The hottest months are March, April and May with temperatures ranging from 30°C – 42°C. with average temperature of 32^0C, mean annual evaporation is 1600mm. Vegetation in this area is typically Sudan type with sparsely distributed trees and shrubs.

Potiskum falls within the Nigerian embayment of the Chad Basin; the most important formation as far as ground water availability is concernedare the Keri-Keri and Chad Formations which comprises basically of sandstone intercalated with lenses of clay. The stratigraphy of the Chad

Basin was described to be divided into groups and formations ranging in age from Albian to Recent (Adegoke et al., (1978); Avbovbo et al., (1980); Petters, (1981), Whiteman, (1982); Okosun, (1992, 1995); Ola-Buraimo and Oluwajana, (2012). These formations are; BimaFormation, Gongila Formation, Fika, Gombe, Keri-Keri and Chad Formations. Groundwater in the area is severely limited by climatic factors with a mean annual precipitation of 246mm most of which occurs between June and October peaking in August, the climatic zone is dry-sub humid to semi-arid. Potiskum has a population of 205,876 (NPC, 2006) and represents the third most populated city in the state (Gashua, 127,000 and Nguru, 111,000). A large percentage of this population comprises of school aged children attending about 31 public and private secondary schools in the city.

AIM AND OBJECTIVES

The work is aimed at assessing the efficiency of water, sanitation and hygiene conditions in schools in Potiskum.

The objectives include the determination of the following;

(a) the physical and chemical state of WASH facilities in schools

(b) the principal challenges in providing adequate facilities in a sustainable manner

(c) the existing WASH practices within the community

(d) the available capacities for delivering WASH education, as well as capacity needs

(e) main players involved in the sector and their current and potential roles.

METHODOLOGY

The methodology employed for the studies involves Preliminary studies, Fieldwork and Laboratory analysis.

Previous works and related literature was studied to enhance proper background understanding of the task at hand before embarking on the fieldwork proper. Reconnaissance survey was also done to get familiar with the study area and also to assist in effectively planning of the fieldwork proper and also permit was sorted from relevant authorities to allow for free access to schools for data collection.

The fieldwork was done with the following objectives in mind; observation of the lithology of the various locations (schools) where samples were collected, identifying the means of water supply in each school and its adherence to standard based on source, maintenance as well as protection from pollution, collection of water samples from each school visited taking adequate measures to ensure that water sampling is done in accordance to American Public Health Association (APHA, 1998) standard. A total of 30 water samples from different schools were taken for laboratory analysis after their physical characteristics were determined in-situ in the field.

The laboratory analyses which include both chemical and bacteriological analysis were done in accordance with APHA (1998) procedure. The samples were analyzedat the Department of Water Quality Control and Sanitation, National Water Quality Reference Laboratory Gombe,

Nigeria. The results were compared with the World Health Organization (WHO), 2011 and Nigeria Standard for Drinking Water Quality (NSDWQ), 2007 to determine their suitability for use.

Focussed Group Discussions (FGD) involving all the key players in schools, local government and community to ascertain the state of WASH was also carried. On-the-spot assessment of WASH facilities was conducted to ascertain their current use, functionality and future potential.

RESULTS

i. State of WASH facilities in schools

Table 1 shows the state of WASH facilities in Potiskum including the location coordinates and general comments on the facilities present. Facilities observed in all schools visited include provision of motorised boreholes and hand dug wells for water supply, water cistern latrines for staff quarters while dormitory and class room areas have Ventilated Improved Pit (VIP) latrines or ordinary pit latrines. Water storage facilities are un-Plasticised Polyvinyl Chloride (uPVC) tanks usually mounted on concrete stands with fetching points spread close to the source. Most of these water sources are in poor condition with the surrounding mostly unkempt and wastewater flowing in dirty unplanned drains around the facility.

Mean values and statistical summary for the results of physical parameters of groundwater in all the schools surveyed is shown in Table 2. Electrical Conductivity ranges between 80 to 97 µS/cm which is indicative of potable water with low dissolved solids. The temperature of the water ranges from 27.8 to 36.5°Cwhile the pH ranges between 4.3 to 7.5 which is indicative of slightly acidic to neutral water.

Results of the chemical composition groundwater in the schools sampled is shown in Table 3. Figures 1 and 2 show the mean concentration of major constituents of the water (anions and cations) and the heavy metals. Calcium represents the cation with the highest concentration with a range of 1.6 – 24.10 mg/l (mean of 9.11mg/l). Anions with the highest concentration are sulphate with a range of 8.10 – 22.10mg/l (mean of 16.98mg/l), chloride ranges from 10.6 – 24.2mg/l with a mean of 15.71mg/l while bicarbonate has a concentration range of 0 – 45.8mg/l with a mean of 15.01mg/l. Heavy metal with the highest concentration is copper with a range of 0 – 0.3mg/l and a mean of 0.095mg/l, iron and chromium occur in almost the same concentration in the water.

Total coliform ranges from 0 – 15cfu/100ml with a mean of 10.7cfu, *Escherichia Coli*(E.Coli) and *Feacal Streptococci* are absent in the water. The higher concentration of total coliforms occurs in shallow groundwater sources that are close to poorly designed pit latrines.

Presence of coliforms and chlorides in groundwater are indications of pollution from waste sources close to water sources resulting from poor sanitation facilities.

Table 1: State of WASH facilities in schools in Potiskum

S/N	LOCATION	N	E	REMARK
1	Race Course Primary School	11º42′04″	11º04′49″	Good water storage, not close to the toilet but the pit latrines are unkempt
2	Al-Azahar Secondary School	11º42′59″	11º03′50″	Poor water storage facilities which is very close to the toilets and the pit latrine are unkempt
3	Angulu Primary School	11º43′05″	11º05′30″	Poor hygiene condition, poor storage system with open soak-away and open defecation
4	Government Day Sec School	11º42′44″	11º04′56″	Poor water storage system with VIP latrine that is unkept
5	Trendsetters Islamic Institute	11º42′10″	11º04′40″	Poor water storage facilities with pit latrine that are unkempt.
6	Fika 1	11º42′24″	11º03′10″	Poor water storage condition
7	Fika 2	11º42′24″	11º03′10″	Good storage condition with VIP and water closet system that is unkempt
8	St. Peters Primary School	11º42′29″	11º05′17″	No good water system, poor hygiene condition of toilets though not close to the water source
9	ECWA Children Academy	11º42′13″	11º04′48″	Good water storage system with good VIP latrine
10	Logo Primary School	11º43′20″	11º02′04″	Uncovered well water and VIP latrine that are unkempt but very far from the water source.
11	Kura Primary School	11º42′24″	11º04′20″	Good water storage system. Very poor hygiene condition of the toilets with water source being far from it
12	Chadi Primary School	11º42′34″	11º03′19″	Good water storage facilities. VIP latrine that are very dirty but not close to the water source.
13	Imam Malik Primary School	11º42′49″	11º03′51″	Good water storage condition, good VIP latrine which is not close to the water source.
14	Central Primary School	11º42′25″	11º04′25″	Water storage facilities are good but is very close to the toilets which are unkempt.
15	FCET	11º42′40″	11º05′26″	Good water storage system with fairly good VIP latrine which is not close to the water source
16	St. Paul Primary School	11º42′15″	11º04′42″	Good water storage system, all the toilets are unkempt but are not close to the water source.
17	Sabon Gari Primary School	11º42′29″	11º03′05″	Good water storage system; very poor pit latrine with open defecations but not close to the water source

18	Dambuwa Primary School	11º42′25″	11º04′25″	Good water storage system that is not close to the toilets; good VIP latrine.
19	Kwata Primary School	11º42′10″	11º04′34″	Good water storage system but very poor hygiene condition of toilets with open defecation but is not close to the water source
20	Sabon Layi Primary School	11º41′57″	11º05′09″	Good water storage system poor hygiene condition of the toilets
21	Imam Arabic School	11º42′10″	11º05′11″	Good water storage system, good hygiene condition of toilets which are situated far from the water source
22	Darowa Primary School	11º43′14″	11º03′52″	Good water storage system, poor hygiene condition of the pit latrines.
23	Iqra Secondary School	11º42′26″	11º04′16″	Good water storage system which are not close to septic tanks. The toilets have good hygiene condition
24	GSTC Potiskum	11º43′17″	11º04′16″	Some of the water source are very close to the pit latrine and the toilets have poor hygiene condition.
25	First University Foundation Pri Sch	11º42′17″	11º03′07″	Poor water storage system and poor hygiene condition of toilets.
26	FGGC Potiskum	11º41′53″	11º02′57″	Good water storage condition and good hygiene condition of the toilets
27	Babuti Primary School	11º42′17″	11º05′29″	Poor water storage system and poor hygiene condition of toilets.
28	Tricent Academy	11º42′26″	11º04′16″	Poor water storage system and poor hygiene condition of toilets.
29	FatsumaMai Umar Model School	11º42′15″	11º07′54″	Good water storage system with good hygiene condition of toilets.
30	Ladabi Academy	11º42′04″	11º03′23″	Poor water storage system and poor hygiene condition of toilets.
31	IPS Primary School	11º42′29″	11º05′00″	Poor water storage system and poor hygiene condition of toilets and septic tank is very close to the water source.

Table2: Mean values for the physical parameters of groundwater in the schools

S/No	Locations	Temperature (ºC)	pH	Conductivity (µS/cm)
1	Race Course Primary School	32.2	5.42	90.7
2	Al-Azahar Secondary School	28.8	5.90	84.0
3	Angulu Primary School	28.8	6.70	80.6
4	Government Day Sec School	32.3	6.60	89.6
5	Trendsetters Islamic Institute	35.6	6.50	96.6
6	Fika 1	30.3	7.50	80.2
7	Fika 2	30.3	7.50	80.2
8	St. Peters Primary School	31.4	6.70	89.8
9	ECWA Children Academy	32.0	6.30	90.5
10	Logo Primary School	33.0	7.4	84.8
11	Kura Primary School	35.2	6.7	97.1
12	Chadi Primary School	28.6	6.5	85.0
13	Imam Malik Primary School	30.5	5.4	86.6
14	Central Primary School	30.9	4.3	96.3
15	FCET	31.9	5.4	88.6
16	St. Paul Primary School	36.4	5.5	97.1
17	Sabon Gari Primary School	31.5	5.8	90.5
18	Dambuwa Primary School	31.5	4.8	90.5
19	Kwata Primary School	31.9	6.5	88.6
20	Sabon Layi Primary School	33.8	5.8	92.4
21	Imam Arabic School	32.4	5.6	92.0
22	Darowa Primary School	32.8	4.5	90.7
23	Iqra Secondary School	36.5	5.4	95.4
24	GSTC Potiskum	32.7	4.8	90.9
25	First University Foundation Primary Sch	31.5	6.8	88.7
26	FGGC Potiskum	33.9	6.0	93.7
27	Babuti Primary School	30.4	5.7	87.4
28	Tricent Academy	35.6	7.0	93.7
29	Fatsumamai Umar Model School	30.9	5.4	87.9
30	Ladabi Academy	27.8	6.0	85.8
	Range	**27.8-35.6**	**4.3-7.5**	**80.2-97.1**
	NSDWQ, 2007	**-**	**6.5-8.5**	**1000**
	WHO, 2011	**-**	**6.5-8.5**	**1200**

Table 3: Chemical and bacteriological composition of groundwater in schools in Potiskum

S/No	Location / Parameter	Calcium (Ca^{2+})	Magnesium (Mg^{2+})	Sodium (Na)	Potassium (K)	Manganese (Mn)	Arsenic (As)	Copper (Cu)	Iron (Fe^{2+})	Chromium (Cr^{6+})	Chloride (Cl^-)	Sulphate (SO_4^{2-})	Phosphorus	Bicarbonate (CO_3^{2-})	Nitrate as (NO_3^- - N)	Total Coliform	E. Coli	Faecal Streptococci
1	Race Course Primary School	1.6	0	2.04	3.87	0	0	0.14	0.01	0	14.2	17	0.05	15.3	0.08	6	0	0
2	Al-Azahar Secondary School	4.8	0.49	1.91	4.01	0	0	0.09	0.01	0	14.2	20	0.25	12.3	0.08	13	0	0
3	Angulu Primary School	2.4	0	2.43	4	0	0	0.13	0.01	0	14.2	17	0.27	15.3	0.2	15	0	0
4	Government Day Sec School	2.4	0	2.04	5	0.01	0	0.24	0.02	0	10.6	17	0.26	12.3	0.08	8	0	0
5	Trendsetters Islamic Institute	1.6	0	3.07	1.08	0.01	0	0.06	0.01	0	17.6	13	0.27	9.15	0.12	14	0	0
6	Fika 1	2.4	0	3	0.93	0	0	0	0	0	17.6	8.1	0	18.3	0.14	4	0	0
7	Fika 2	12	2.43	1.93	5.32	0	0	0	0.02	0	14.2	11	0	45.8	0.22	10	0	0
8	St. Peters Primary School	24	0.49	2.06	2.91	0	0.02	0	0.02	0.1	14.2	19.2	0	12.2	0.14	10	0	0
9	ECWA Children Academy	2.4	0	4.7	1.36	0.02	0	0.3	0.06	0	24.2	12.1	0	9.15	0.08	6	0	0
10	Logo Primary School	10.4	0.96	3.92	7.02	0	0	0.13	0.06	0	21.3	12.6	0	21.4	0.05	0	0	0
11	Kura Primary School	2.4	0	2.43	4.2	0	0	0.03	0.02	0	14.2	17.2	0.27	15.3	0.2	15	0	0
12	Chadi Primary School	4.3	0.49	1.91	4.01	0	0	0.09	0.01	0	14.2	20	0.25	12.3	0.15	13	0	0
13	Imam Malik Primary School	4.8	0.49	1.94	4.01	0	0	0.09	0.02	0	14.2	20	0.25	45.8	0.08	10	0	0
14	Central Primary School	24	0.49	2.06	2.91	0	0.01	0	0.02	0	14.2	17.2	0.27	15.3	0.2	10	0	0
15	FCET	2.4	0	4.7	1.36	0.02	0	0.3	0.06	0	24.2	22.1	0	9.15	0.08	10	0	0
16	St. Paul Primary School	13.2	2.49	2.06	2.91	0	0.01	0	0.02	0.1	14.2	19.2	0	12.2	0.14	10	0	0
17	Sabon Gari Primary School	24	0.49	2.06	2.91	0	0.01	0	0.02	0.1	14.2	19.2	0	12.3	0.14	10	0	0
18	Dambuwa Primary School	12	1.49	2.06	2.91	0	0.01	0	0.02	0	14.2	17.2	0.27	15.3	0.2	10	0	0
19	Kwata Primary School	2.4	0	4.7	1.36	0.02	0	0.3	0.06	0	24.2	12.1	0	9.15	0.08	10	0	0
20	Sabon Layi Primary School	13.2	2.49	2.06	2.91	0	0.01	0	0.02	0.1	14.2	19.2	0	12.2	0.14	13	0	0
21	Imam Arabic School	24.1	0.5	2.16	2.92	0	0	0	0.02	0.1	14.2	19.2	0	12.3	0.14	10	0	0
22	Darowa Primary School	16	0	2.4	3.3	0	0	0.14	0.06	0	21.6	13.3	0	21.4	0.2	10	0	0
23	Iqra Secondary School	4.8	0.49	1.91	5.01	0	0	0.1	0.2	0	15.2	20.5	0.26	13.4	0.1	13	0	0
24	GSTC Potiskum	13.2	2.49	2.06	2.91	0	0.01	0	0.02	0.1	14.2	19.3	0	12.2	0.14	13	0	0

25	First University Foundation Primary Sch	2.4	0	2.04	5	0.1	0	0.25	0.03	0	10.6	17	0.27	13.3	0.9	8	0	0
26	FGGC Potiskum	1.1	0	3.1	1.1	0.02	0	0.1	0.01	0	17.7	14	0.37	0	0.13	15	0	0
27	Babuti Primary School	4.8	0.5	2.01	4.11	0	0	0.1	0.01	0	14.2	20	0.25	12.4	0.09	13	0	0
28	Tricent Academy	13.2	2.49	2.06	2.91	0	0.01	0	0.02	0.1	14.3	19.2	0	12.2	0.14	14	0	0
29	Fatsumamai Umar Model School	24	0.49	2.1	2.91	0	0.2	0	0.02	0.1	14.2	19.3	0	12.3	0.15	10	0	0
30	Ladabi Academy	2.4	0	2.04	5.1	0.01	0	0.25	0.02	0	10.6	17.1	0.27	12.4	0.08	8	0	0
	Mean	**9.09**	**0.66**	**2.5**	**3.34**	**0.01**	**0.01**	**0.09**	**0.03**	**0.03**	**15.7**	**17**	**0.13**	**15.1**	**0.16**	**10.4**	**0**	**0**
	NSDWQ, 2007	-	-	250	-	100	-	1.5	200	-	-	20	50	0.2	0.2	10	0	0
	WHO, 2011	100	-	250	150	450	150	2 (1.5)	200	200	250	50	50	0.2	0.2	10	0	0

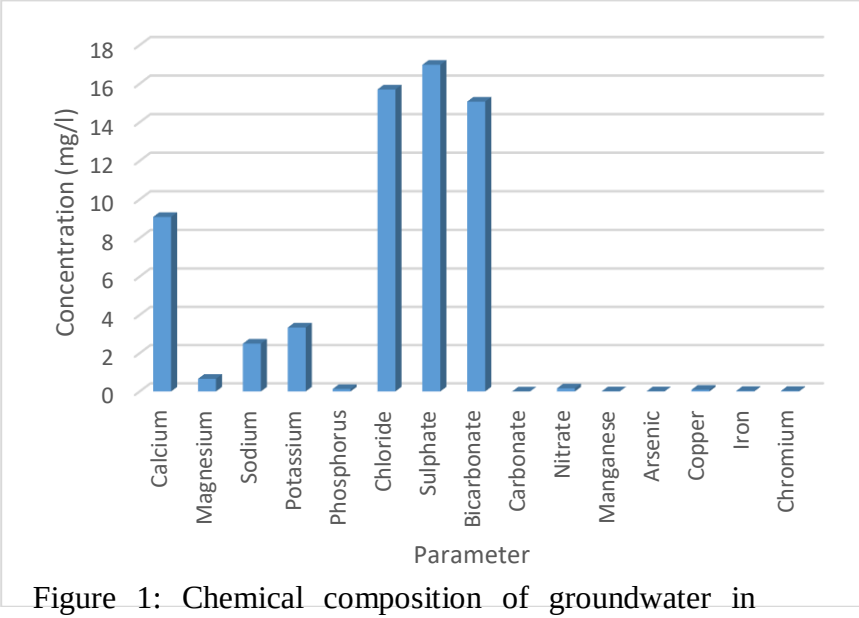

Figure 1: Chemical composition of groundwater in schools in Potiskum

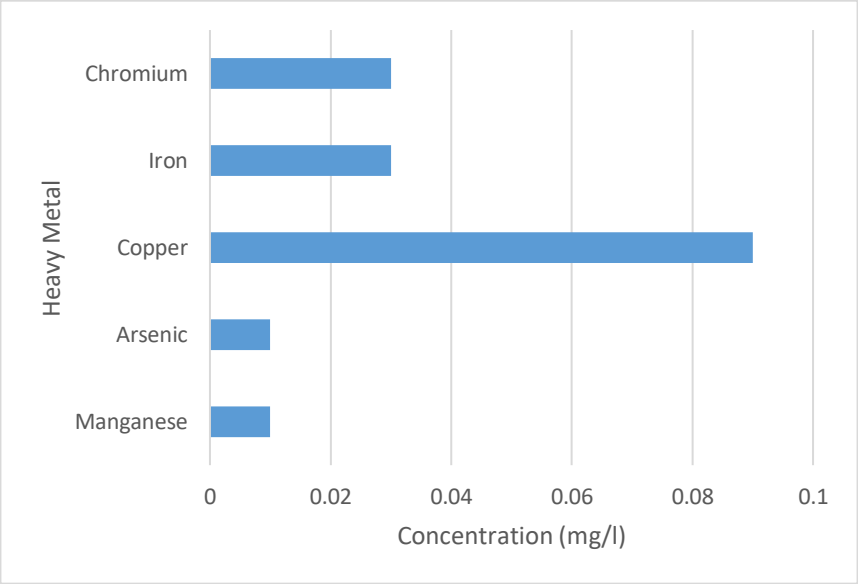

Figure 2: Heavy metal concentration of groundwater in schools in Potiskum

ii. Principal challenges in providing adequate facilities in a sustainable manner.

Results from Focussed Group Discussions involving staff, students and management of the schools indicated that the challenges in providing adequate facilities for WASH is hampered mainly by low finance, improper planning and education. As a result of the local geology and inadequacy of the public water supply all the water needs of the schools is dependent on groundwater through the provision of boreholes and hand dug wells. Hand dug wells are shallow and cannot be used for drinking easily without treatment, boreholes are therefore the best alternative. The cost of drilling motorised boreholes is high and the cheaper hand pump boreholes cannot be installed due to the depth required to reach the aquifer (> 60m, which is the optimal for hand pump). Since sanitation facilities are linked to water supply, design and construction of these facilities is such that minimal water will be required for use. This resulted into construction of ordinary pit latrines and Ventilated Improved Pit (VIP) latrines. These still remain at the bottom of the sanitation ladder; the hope is that with improvement in water supply it should be scaled up to pour flush latrines for the school area.

iii. Existing WASH practices within the community

Information on existing WASH practices in the schools was derived from Focussed Group Discussion and direct observations. Water supply is mostly from motorised boreholes and hand dug wells. Sustainability of the boreholes is mostly hampered by inadequate power supply which make pumping of the wells to be dependent on whenever there is electricity from the public power supply. Some schools had hand dug wells which are used for washing and other utility but not for drinking. While pit latrines are available, they are mostly clean and unkempt which makes using the facilities to be uncomfortable. As a result of the state of the latrines Open Defecation (OD) is still practiced in most of the schools. Hand wash facilities are completely absent in all the schools visited except in staff quarters where hand wash basins are part of the components in the toilet system. Most students are totally unaware of basic sanitation and hygiene education including Menstrual Hygiene Management (MHM) for the females.

iv. Available capacities for delivering WASH education, as well as capacity needs

The management and staff of the schools constitute the first line of communication between the general community and the schools. Presently the staff are not well informed and educated on WASH. Despite the existence of health science and civic education as part of the educational curriculum in Nigeria, effective teaching and learning does not explicitly take the effects of improper sanitation on the overall well-being of the individual.

v. Main players involved in the sector and their current and potential roles.

The main players involved in the sector is government at all levels, Federal, State and Local, Donor Agencies and Non-Governmental Organisations (NGOs).

CONCLUSION

All the analyzed chemical parameters were found to fall within the NSDWQ 2007 and WHO 2011 standards for all the sample locations (schools). In summary, 22 schools out of a total of 30 had either the pH or Total coliform or both not falling within the permissible limits (11 of which had issues with the pH only, 5 had issues with Total coliform while 6 had issues with both). The pH ranged from 4.3 to 6.0 while the Total coliform ranged from 0 to 15cfu/100ml. The low pH may be attributed to an increase in carbon dioxide concentration associated with biological activity resulting from the presence of microorganisms, which lowers pH since pH is controlled by the carbon dioxide – bicarbonate – carbonate equilibrium. The pH of most drinking-water lies within the range 6.5–8.5. most chemical reactions start to take place under particular pH and temperature conditions, low pH will lead to mobilisation of other elements out the environment and into the water leading to increased contamination and eventual pollution of the water.Although pH usually has no direct impact on water consumers, it is one of the most important operational water quality parameters. Careful attention to pH control is necessary at all stages of water treatment to ensure satisfactory water clarification and disinfection. For effective disinfection with chlorine, the pH should preferably be less than 8.0. The pH of the water entering the distribution system must be controlled to minimize the corrosion of water mains and pipes in water systems. Failure to do so can result in the contamination of drinking-water and in adverse effects on its taste, odour and appearance.

Total coliform counts give a general indication of the sanitary condition of a water supply. **Total coliform bacteria** are commonly found in the environment (e.g., soil or vegetation) and are generally harmless. If only total coliform bacteria are detected in drinking water, the source is probably environmental. Total coliforms may include bacteria that are found in the soil, in water that has been influenced by surface water, and in human or animal waste. Coliform bacteria will not likely cause illness. However, their presence in drinking water indicates that disease-causing organisms (pathogens) could be in the water system. Most pathogens that can contaminate water supplies come from the faeces of humans or animals.Whencoliforms have been detected, repairs or modifications of the water system may be required. Boiling the water is advised until disinfection and retesting can confirm that contamination has been eliminated. A defective well is often the cause when coliform bacteria are found in well water.When total coliform bacteria are confirmed (at least 2 samples with coliform bacteria present) in drinking water, it means the water system should be inspected to find and eliminate any possible sources of contamination. Once the source is identified, it can usually be resolved by making system repairs, flushing, and adding chlorine for a short period of time.

It is a known fact that access to water resources and sanitation through improved management of water resources and the development of adequate and sustainable water supply, improved sanitation facilities and hygienic practices is a right for all. Therefore, it must be taken into cognizance that all conditions that affect the cleanliness of water, especially with regard to dirt and infection and specifically to drainage and disposal of sewage and refuse from houses is a concern for all. More practically,

sanitation involves all means of collecting and disposing of excreta and community liquid waste in a hygienic way so as not to endanger the health of individuals or the community as a whole.
From the research carried out, only eight (8) out of a total of thirty schools that were investigated in Potiskum had good water supply and storage system with a healthy hygiene conditions of toilets, septic tanks and environment; eleven (11) had good water supply and storage system but poor hygiene conditions and sanitaryfacilities as well as the general environment while the remaining eleven (11) have very poor water supply and storage systems, hygiene and sanitation conditions and the general environment. This is a clear indication that facilities for WASH are inadequate in most of the primary and secondary schools that were assessed in Potiskum.

In essence, WASH in Schools is a pathway to healthier schools and healthier, better performing children. Sustainable WASH in Schools programmes require the involvement and political leadership of ministries of education as well as related ministries such as health, public works, finance, local governance and water authorities. Without the political commitment evidenced in policies, standards and budgets, WASH in Schools remains externally subsidized. Such small-scale interventions cannot move beyond the pilot stage. If faith-based and private schools do not fall under national policies, mechanisms must be found to promote WASH in those schools as well. In the past, these were considered schools for the privileged and did not generally require development interventions.

RECOMMENDATIONS AND STRATEGIES

The following recommendations and operational strategies is in line with the United Nations Children Fund (UNICEF) standards and guidelines for water, sanitation and hygiene services in schools and other educational facilities.

1. **Water quality:**It should be ensured that water for drinking, cooking, personal hygiene, cleaning and laundry is safe for the purpose intended. Indicators of water quality are; Microbiological quality of drinking water:**(i)**. *Escherichia coli* or thermotolerant coliform bacteria are not detectable in any 100-ml sample. **(ii)**. treatment of drinking water: Drinking water from unprotected sources should be treated to ensure microbiological safety.**(iii)**. Chemical and radiological quality of drinking water. The water should meet World Health Organisation(WHO) Guidelines for Drinking-water Quality or the Nigerian national standards (NSDWQ, 2007) and acceptance levels concerning chemical and radiological parameters. **(iv)**. Acceptability of drinking water: The water should have no taste, odour or colour that would discourage consumption of the water. **(v)**. Water for other purposes: Water that is not of drinking water quality should be used only for cleaning, laundry and sanitation.
2. **Water Quantity:**Sufficient water should be available at all times for drinking and personal hygiene, and for food preparation, cleaning and laundry when applicable. Indicators of water availability include;**(i)**. Basic quantities required; Day schools should have 5 litres per person per day for all schoolchildrenand Boarding schools should have15 20 litres per person per day for all residentialschoolchildren and staff.**(ii)**. Additional quantities required; Flushing toilets 10–20 litres per person per day for conventional flushingtoilets/1.5–3litres per person per dayforpour-

flush toilets Anal washing/cleansing1–2 litres per person per day. These figures should be doubled for boarding schools.

3. **Water facilities and access to water**: Sufficient water-collection points and wateruse facilities should be available in the school, allowing convenient access to, and use of, water for drinking and personal hygiene, and for food preparation, cleaning and laundry. Indicators of access to water include;**(i)**. A reliable water point, with soap or a suitable alternative, should be available at all the critical points within the school, particularly toilets and kitchens. **(ii)**. A reliable drinking water point should always be accessible for staff and schoolchildren.
4. **Hygiene promotion:** Correct use and maintenance of water and sanitation facilities should be ensured through sustained hygiene promotion. Water and sanitation facilities should be used as resources for hygiene education. Indicators of hygiene promotion include;**(i)**. Hygiene education should be included in the school curriculum. **(ii)**. Positive hygiene behaviours, including correct use and maintenance of facilities, should be systematically promoted among staff and schoolchildren. **(iii)**. Availability of facilities and resources enable staff and schoolchildren to practice behaviours that control disease transmission in an easy and timely way.
5. **Toilets:**Sufficient, accessible, private, secure, clean and culturally-appropriate toilets should be provided for schoolchildren and staff. Indicators of toilets availability and sufficiency include;**(i)**. Available toilets should be– 1 per 25 girls or female staff, and 1 toilet plus 1 urinal (or 50 centimetres of urinal wall) per 50 boys or male staff. **(ii)**. Toilets should be easily accessible and no more than 30 metres from all users. **(iii)**. The toilets should be able to provide privacy and security. **(iv)**. The toilets should be child-friendly and appropriate to local cultural, social and environmental conditions. **(v)**. The toilets should be hygienic to use and easy to clean. **(vi)**. The toilets should have convenient hand-washing facilities close by. **(vii)**. The school should put in place a sustainable cleaning and maintenance routine that ensures clean and functioning toilets are available at all times.
6. **Control of vector-borne disease:** Schoolchildren, staff and visitors should be protected from disease vectors. Indicators of effective control measures for vector-borne disease include; **(i)**. The density of vectors in the school is minimized. **(ii)**. Schoolchildren and staff should be protected from potentially diseasetransmitting vectors. c. Vectors should be prevented from contact with schoolchildren and staff or substances infected with related vector-borne diseases.
7. **Cleaning and waste disposal**: The school environment should be kept clean and safe. Indicators of clean environment include;**(i)**. Classrooms and other teaching areas should be regularly cleaned to minimize dust and moulds. **(ii)**. Outside and inside areas should be free of sharp objects and other physical hazards. **(iii)**. Solid waste should be collected from classrooms and offices daily and disposed of safely. **(iv)**. Wastewater should be disposed of quickly and safely.
8. **Food storage and preparation (if applicable)**: Food for schoolchildren and staff should be stored and prepared so as to minimize the risk of disease transmission. Indicators of effective food storage and preparation include;**(i)**. Food handling and preparation should be done with utmost cleanliness (hands should be washed before preparing food). **(ii)**. Contact between raw foodstuffs and cooked

food should be avoided. **(iii)**. Food should becooked thoroughly. **(iv)**. Food should be kept at safe temperatures. **(v)**. Safe should be used at all times.

9. **Child participation:** Good education about hygiene is as important as good sanitary facilities. Life skills-based hygiene education allows children to learn about water and sanitation related behaviours and the reasons why these lead to good health or bad health. The idea is that when children understand and think together about their situations and practices, they can plan and act to prevent diseases, now and in the future.This can be achieved through Participatory education through teachers in schooland by Children's involvement in youth hygiene clubs within and outside the school.
10. **Training of teachers, management and involving parents and community:** An important focus of teacher training should be attitude change towards WASH in Schools.This can be achieved by; **(i)**. Explaining that this programme is not another subject in school, but a life skill used by children at school, at home and in the community to improve their overall health and hygienic living conditions.**(ii)**. Understanding that children do not only receive information but also actively promote good health and hygiene.

    Parents and community members can have important roles in keeping the school clean, safe and healthy, and encouraging children to adopt improved hygienic behaviour.
11. **Scaling up:** The ultimate goal of any WASH in Schools intervention is its long-term sustainability and mainstreaming into the system. Financial sustainability, the development of political interest, cooperation among ministries, a national policy on WASH in Schools in the overall strategy for quality education, and national policies and standards in related sectors are necessary to scale up WASH in Schools.

    To achieve scale-up, an accountable institution, preferably the ministry of education, must take the lead on WASH in Schools and ensure the involvement of all related ministries, such as health, works, finance, local government and water authorities. Political commitment to children's education and health creates an environment that is conducive to the implementation, operation and maintenance of WASH in Schools programmes and enables small-scale pilot projects to scale up effectively.

    Without political commitment and the resulting favourable policies and budgets, WASH in Schools programmes remain externally-subsidized, small-scale interventions, which never grow beyond the pilot phase. In Nigeria, UNICEF, donor agencies, NGOs or others sometimes provide investment costs, but the government and community should always be prepared to cover operation, maintenance and replacement costs of educational materials and facilities, this often comes in the form of counterpart funds which may just be 30 – 50% of the total cost.**(i)**. Financial sustainability;from their inception, WASH in Schools programmes need a financial policy that ensures long-term sustainability. **(ii)**. With input from the ministry of health and other WASH-related ministries, the ministry of education will need to set specific financial policies for WASH in Schools. The ministry of education will also need to define the cost-sharing arrangements, if any, among national authorities, local authorities, communities, schools, children, teachers and parents. **(iii).** In addition, local authorities must help develop mechanisms for financing

replacement costs and variable costs. such as soap, other supplies, operation and maintenance. In many cases, schools, parents, the community or local enterprises will cover those costs, but local authorities must make sure they are accounted for.

REFERENCES

Abebe, L. (1986) Hygienic water quality; its relation to health and the testing aspects in tropical conditions. Department of Civil Engineering, University of Tempere, Finland

Adelana, S.M.A., Bale, R. B., Olasehinde, P. I. And Wu, M. (2005).The impact ofanthropogenic activities over groundwater quality of coastal aquifer in Southwestern Nigeria. Proceedings on Aquifer vulnerability and Risks. 2nd International Workshop and 4th Congress on the Protection and Management of Groundwater. Raggia di Colornoparma.

APHA (1989) *Standard methods for the examination of water and wastewater*, 17th ed. Washington,DC, American Public Health Association.

Annemarieke, M. Murat, S and Therese, D.(2012). Water, Sanitation and Hygiene (WASH) in Schools, a companion to the Child Friendly Schools Manual. United Nations Children Fund (UNICEF). 3 United Nations Plaza New York, NY 10017, USA

Aremu, M. O., Olaofe, O., Ikokoh, P. P. & Yakubu, M. M. (2011) *Physicochemical characteristics of stream, well and borehole water sources in Eggon, Nasarawa State, Nigeria. J ChemSoc Nigeria 36(1):131–136*

ASTM (1976) Standard test for pH of water and waste water. In: *Annual book of ASTM standards. Part31*. Philadelphia, PA, American Society for Testing and Materials, p. 178.deteriorated A-C pipe. *Journal of the American Water Works Association*, 81(2):80–85.

Baird, S. & Hamory, H. (2011) 'Worms at Work: Long-run impacts of child health gains', October 2011, <www.povertyactionlab.org/publication/wormswork-long-run-impacts-child-health-gains>, accessed 31 May 2012.

Edimeh, P. O., Eneji, I. S., Oketunde, O. F. & Sha'ato, R. *(2011) Physico-chemical parameters and some Heavy metals content of rivers Inachalo and Niger in Idah, Kogi State. J ChemSoc Nigeria 36(1):95–101Google Scholar*

HMSO (1978) The measurement of electrical conductivity and laboratory determination of the pH

Kehinde, M.O. (1998).The impact of industrial growth on groundwater quality and availability in: Osuntokun, A(eds) Current Issues in Nigerian Environment, Ibadan Danidan Press.

Langelier, W.F. (1946) Chemical equilibria in water treatment. *Journal of the American Water WorksAssociation*, 38(2):169–178.

McClanahan M.A. & Mancy KH (1974). Effect of pH on the quality of calcium carbonate film depositedfrom moderately hard and hard water. *Journal of the American Water Works Association*, 66(1):49–53.

Stone, A. & Rose, P. (1987). The effects of short-term changes in water quality on copper and zinc corrosionrates. *Journal of the American Water Works Association*, 79(2):75–82.

Miguel, E. and Michael, K. (2004). 'Worms: Identifying impacts on education and health in the presence of treatment externalities', Econometrica, vol. 72, no. 1, pp. 159–217. Abstract available at <http://onlinelibrary.wiley.com/ doi/10.1111/j.1468-0262.2004.00481.x/abstract>, accessed 28 January 2012.

Muhammed, S. (2011). Effect of refuse dumps on ground water quality. Advances in Applied Science Research, 2011, 2 (6):595-599.

Murrel, N.E. (1987) Impact of metal solders on water quality. In: *Proceedings of the annual conferenceof the American Water Works Association, Part 1.* Denver, CO, American Water Works Association,pp. 39–43.

Musa, J.J. and. Ahanonu,J. J.(2013). Quality Assessment of Shallow Groundwater in Some Selected Agrarian Communities in Patigi Local Government Area, Nigeria. International Journal of Basic and Applied Science, Vol 01, No. 03, pp. 548-563.

Nordberg, G.F.Goyer, R.A.and Clarkson, T.W. (1985) Impact of effects of acid precipitation on toxicity of*value of natural, treated and wastewaters*. London, Her Majesty's Stationery Office.

Prüss-Üstün, A. (2008). Safer Water, Better Health: Costs, benefits and sustainability of interventions to protect and promote health, World Health Organization, Geneva, 2008.

WHO (2011). Guidelines for drinking water quality; First addendum to third edition. World Health Organization, Geneva, 515.

MATHEMATICS/STATISTICS

Isotropic and Anisotropic Variogram Models for Interpolating Monthly Mean Wind speed Data of Six Selected Wind Stations in Nigeria

[1]Usman A., [2]Abubakar U. and [3]James M.

[1, 2 & 3]Department of Statistics, Federal University of Technology, Minna

Abstract

Mean Wind speeds often exhibit directionality in which they are increasing or decreasing across a surface; however, microclimatological effects sometimes produce high or low wind speed over a surface that can create confusion during kriging surface construction. The aim of this study was to investigate the appropriateness of anisotropic variogram models within ordinary kriging for interpolation of monthly mean wind speed data of six selected wind stations which include: Sokoto, Maiduguri, Ilorin, Ikeja, Port Harcourt and Enugu in Nigeria. Four types of isotropic and anisotropic variogram models were fitted: Linear, Spherical, Exponential, and Gaussian. Each model was described using the following parameters: the nugget variance, the sill, and the range. Three statistics to aid the interpretation of model output: the residual sum of square (RSS), R^2 and proportion $C/(C_0+C)$ were provided to give the best fitted model for each wind station. The study found that the six wind stations could be best fitted by linear, Gaussian and exponential anisotropic models. Sokoto wind speed showed the strongest spatial distribution (>7.8 m/s), Maiduguri and Enugu, Ikeja and Port Harcourt showed similar wind speed patterns (3.1-4.0) m/s and (2.1-3.0) m/s respectively whereas Ilorin showed a pattern of low wind speeds (<2.0m/s) . These results may assist in identifying wind stations that are suitable for exploitation of wind energy for electricity generation as well as in mitigating losses to structures due to excessive wind events.

Keywords: Anisotropic, geostatistics; semi variance, wind speeds, Nigeria,

1. Introduction

Wind is the horizontal motion of air that pass through a given point in a location and includes the direction from which the wind is coming from. Wind speed is the description of how fast the air is moving at certain point in a location. This is sometimes measured in meters per second. Wind speed, wind direction, air temperature, atmospheric pressure, humidity and solar radiation are important for monitoring and predicting weather patterns. Each of these parameters have numerous impact on the weather and quality of life. Almost every impact of climate variation involves wind speed either

directly or indirectly (Abhishek *et al*, 2010; Tuller, 2004). For instance, one of the ways that air temperature variations affect objects and living organisms is through sensible heat flux density, which is a function of wind speed. According to Troccoli *et al*, (2012), accurate estimates of long-term linear trends of wind speed provide a useful indicator for circulation changes in the atmosphere and are invaluable for the planning and financing of wind energy.

Researches have showed that there have been comparisons of interpolation methods for temperature and precipitation, (Phillips *et al*., 1992; Collins and Bolstad, 1996; Goovaerts, 2000; Price *et al*., 2000; Jarvis and Stuart, 2001; Vicente-Serrano *et al*., 2003) few research efforts have been directed towards comparing the effectiveness of different spatial interpolators in predicting wind speed. Wind speed surface interpolation results suggest that deterministic methods should be avoided because they fail to account for spatial autocorrelation (Bentamy *et al*. 1996; Phillips *et al*. 1997; Sterk and Stein 1997; Venäläinen & Heikinheimo 2002; Oztopal 2006, Cellura *et al*. 2008; Luo *et al.* 2008; Zlatev *et al.* 2009; Akkala *et al*. 2010; Zlatev *et al.* 2010) and various forms of kriging have been shown to outperform other methods for interpolation of surface-level wind speeds (Lanza *et al.* 2001; Luo *et al.* 2008; Akkala *et al.* 2010; Zlatev *et al.* 2010). Although kriging has been shown to improve interpolation results, most previous studies that examined kriging focused on local- to regional-scale wind surfaces within a single country.

Kriging uses probability and spatial correlation to create a surface that is weighted by observed values through a distance and direction based semivariance function that can account for anisotropic spatial patterns and trends in wind behaviour (Luo *et al*. 2008). Isotropy (uniform values in all directions) is assumed during the kriging process unless anisotropy is specified. Consequently, comparisons between isotropic and anisotropic semivariogram-derived surfaces are not often made. Thus far, the use of anisotropy within kriging has been shown to be superfluous for local- and regional-scale modelling,

although Luo *et al.* (2008) hypothesized that it may be more useful for meso- and macro-scale modelling.

In addition to issues of scale and anisotropy, the impact of heterogeneous terrain (or geographic diversity) on wind speed interpolations is also poorly understood. Etienne and Beniston (2012) examined extreme station data (i.e. top 10% of wind speeds) for wind storms in Europe using 'basic' kriging. The results found that topography greatly influences wind speeds and likely contributed to error effects not normally seen in interpolations of larger areas. Additionally, Zlatev *et al.* (2010) divided the United Kingdom into five areas of homogenous terrain to analyse wind speed interpolations and reduce the potential impact of over-smoothing and over fitting. Joyner *et al.* (2015) used cokriging to interpolate wind speeds for multiple European windstorms to account for errors associated with aspect, elevation, and land cover, further alluding to an impact of geographic diversity on wind speed interpolations.

The aim of this study was to investigate the appropriateness of anisotropic variogram models within ordinary kriging for interpolation of monthly mean wind speed data of six selected wind stations which include: Sokoto, Maiduguri, Ilorin, Ikeja, Port Harcourt and Enugu in Nigeria. Different theoretical models such as linear, spherical, exponential, and Gaussian were fitted to determine the best fitted model and finally, draw wind speed spatial distribution maps for each wind station.

2. Materials and Methods

2.1 Study Area and Data Used

Nigeria co-ordinates on latitude 10.00^{o}N and longitude 8.00^{o}E. The climate is tropical; humid in the south and semi-arid in the north. It comprises various ecotypes and climatic zones. There are two main seasons, namely, rainy and dry seasons. The rainy season lasts from March to November in the south and May to October in the north. During December to March, the Nigerian climate is entirely

dominated by the north east trade winds, locally called "harmattan", which originate from Sub-Tropical Anticyclones (STA).This "harmattan" is associated with the occurrence of thick dust haze and early morning fog and mist as a result of radiation cooling at night under clear skies. The climate is dominated by the influence of Tropical Maritime (TM) air mass, the Tropical Continental (TC) air mass and the Equatorial Easterlies (EE) (Ojo, 1977) in (Abiodun *et al*, 2011).

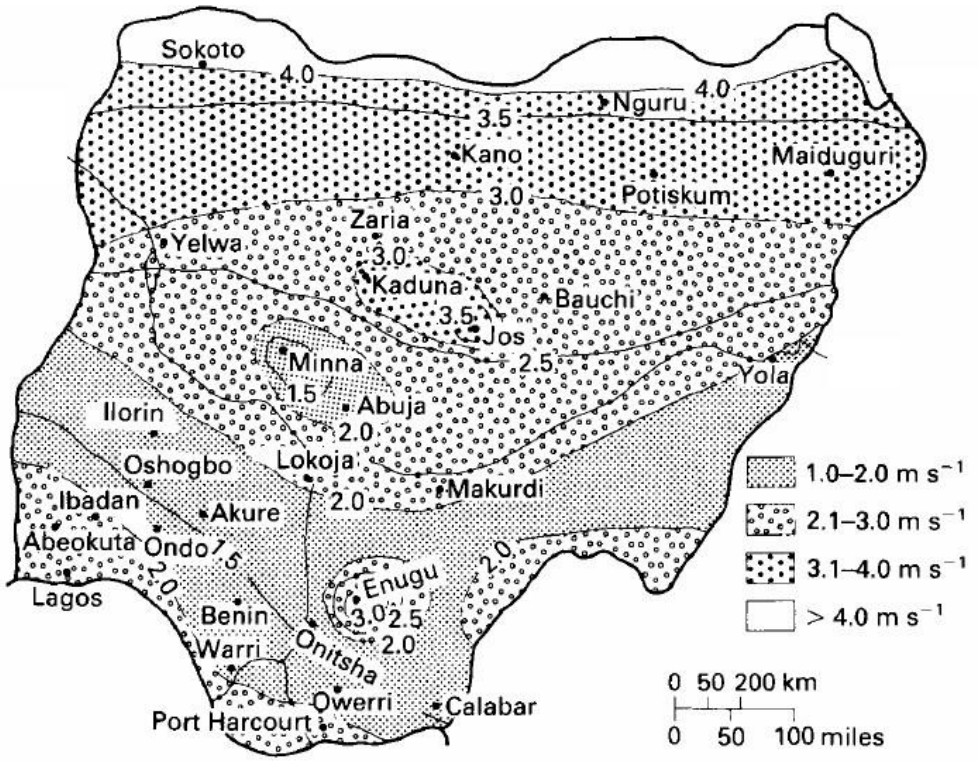

Figure 1**:** Nigeria annual average wind speeds distribution (isovents at 10 m height) showing four different wind speed regimes (Source: Ojosu and Salawu, 1990b)

The monthly mean wind speed data were obtained from archives of the Nigerian Meteorological Agency (NIMET) Oshodi, Lagos, Nigeria. The data obtained covered a period of twenty-six years (1990-2015) for six stations which include: Sokoto, Maiduguri, Ilorin, Ikeja, Port Harcourt and Enugu wind stations. Figure 1 is the map of Nigeria showing the anemometer stations used in the study Some missing entries were observed in the monthly wind speed data and were not replaced. Only one station got some missing observations. In geostatistics, data in the worksheet that are marked as missing are

ignored during data builds and subsequent analyses. These values can be overridden by values specified. Permanent missing values appear as blank cells. The default missing value indicator (MVI) is the numeric value -99.0 but this can be changed in the user preferences window. Missing values appear in output files when a value cannot be interpolated because the location appears in an exclusive polygon or because numerical limitations disallow its computation (such as when a variogram model is inappropriately used during kriging). The examination of the monthly wind speed data indicated that they were not significantly different from a normal distribution (Figure 2).

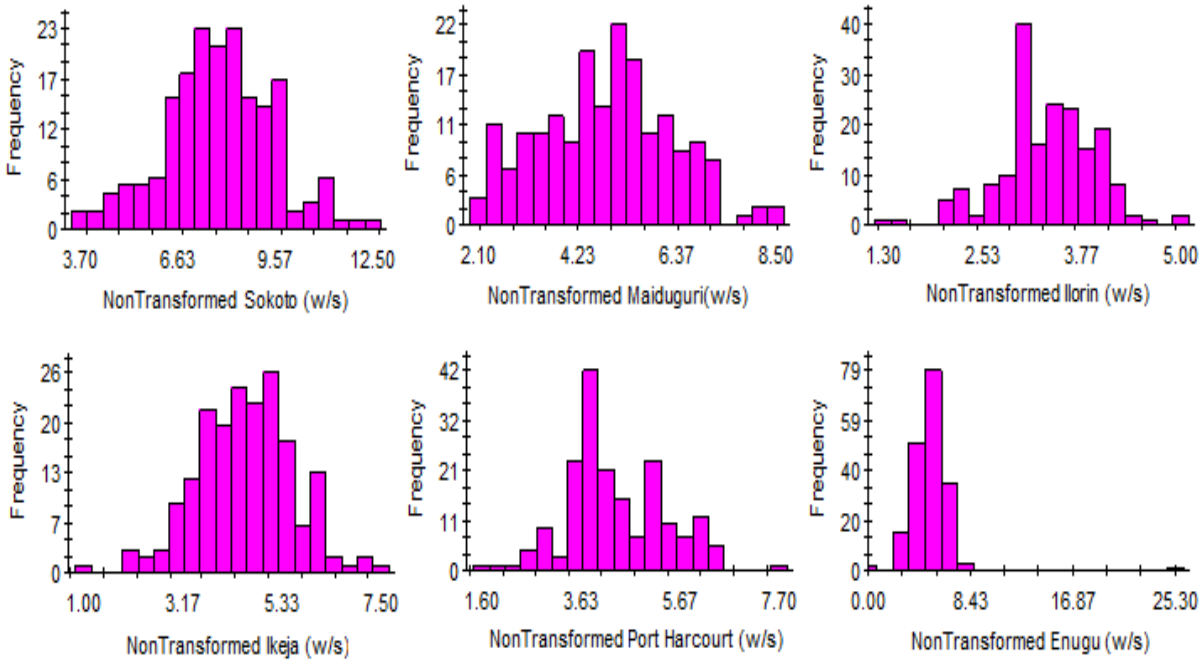

Figure 2: Non transformed frequency distribution for the six selected wind stations

2.2. Geostatistical methods

2.2.1. Kriging

Kriging (Krige, 1966) is a stochastic technique similar to IDW, in that it uses a linear combination of weights at known points to estimate the value at an unknown point. Kriging weights are derived from a statistical model of spatial correlation expressed as semivariograms that characterize the spatial dependency and structure in the data. During surface construction, ordinary kriging was chosen to

interpolate wind station data based on its superiority over other techniques (Luo *et al.* 2008; Akkala *et al.* 2010; Zlatev *et al.* 2010; Luo *et al.* 2011). Ordinary kriging is represented as

$$Z_{OK}^{*}(s_0) = \begin{cases} \sum_{i=1}^{n} \lambda_i Z(s_i) \\ \sum_{i=1}^{n} \lambda_i = 1 \end{cases} \quad (1)$$

where, $Z_{OK}^{*}(s_0)$ is the spatial location s_0; s_i is the location of measurement i; n is the number of observations to consider and λ_i is a real weight.

2.2.2. Semivariance Analysis of Wind Speed Interpolation

In contrast with deterministic methods, kriging provides a solution to the problem of estimation of the surface by taking account of the spatial correlation. The spatial correlation between the measurements points can be quantified by means of the semi-variance function: The experimental variogram measures the average degree of dissimilarity between un-sampled values and a nearby data value and consequently can depict autocorrelation at various distances. The value of the experimental variogram for a separation distance of h (referred to as the lag) is half of the average squared difference between the value at $z(x_i)$ and the value at $z(x_i + h)$ (Robinson and Metternicht, 2006):

$$\hat{\gamma}(h) = \frac{1}{2N(h)} \sum_{i=1}^{N(h)} [z(x_i) - z(x_i + h)]^2 \quad (2)$$

where $N(h)$ is the number of data pairs of measurement points with distance *h* apart. Using an analysis of experimental variogram model of ordinary kriging, a suitable four isotropic and anisotropic variogram models were fitted by different theoretical models such as spherical, exponential, linear, or Gaussian to determine three semivariogram parameters: the nugget (C_0), the sill ($C_0 + C$), and the range (A).

2.2.3 Accounting for Directional Influences— Anisotropic Variogram Models

There are two types of directional components that can affect the predictions in output surface: global trends and directional influences on the semivariogram or covariance (known as anisotropy). A global trend is an overriding process that affects all measurements in a deterministic manner. The global trend can be represented by a mathematical formula (e.g., a polynomial) and removed from the analysis of the measured points but added back in before predictions are made. This process is referred to as detrending

The shape of the semivariogram or covariance curve may also vary with direction (anisotropy) after the global trend is removed or if no trend exists. Anisotropy differs from the global trend because the global trend can be described by a physical process and modelled by a mathematical formula. The cause of the anisotropy (directional influence) in the semivariogram is not usually known, so it is modelled as random error. Even without knowing the cause, anisotropic influences can be quantified and accounted for.

Anisotropy is usually not a deterministic process that can be described by a single mathematical formula. It does not have a single source or influence that predictably affects all measured points. Anisotropy is a characteristic of a random process that shows higher autocorrelation in one direction than in another. For anisotropy, the shape of the semivariogram may vary with direction. Isotropy exists when the semivariogram does not vary according to direction. Isotropic variogram is a graph of semivariance against. separation distance. Where autocorrelation is present, semivariance is lower at smaller separation distances (autocorrelation is greater). This typically yields a curve such as that described in this analysis,

Anisotropic variogram models are similar to those for isotropic variograms but include directional information in the range parameter. Anisotropy refers to a direction-dependent trend in the data. The study used geometric anisotropy, i.e. anisotropy which is expressed as variograms with different ranges

in different directions. The principal anisotropic axis (the major axis of the anisotropic model) is the direction with the longest range, i.e. the direction of major spatial continuity. The best way to evaluate anisotropy is to view the anisotropic semivariance surface (variogram map), and use the azimuth function to define and then set the principal anisotropic axis to the direction aligned with the lowest semivariance values (the direction of maximum spatial continuity, or major axis of the anisotropic variogram model). Anisotropic semivariograms were created during the interpolation procedure to account for directional dependence of wind speeds at varying distances, creating a spatial relationship for each direction that cannot be described by a single formula.

The principal axis is the direction of maximum spatial continuity, or base axis from which the offset angles for anisotropic analyses are calculated. Offset angles in this study are 0º, 45º, 90º, and 135º clockwise from the base axis; points aligned sufficiently close to one or another of these angles are included in the anisotropic analysis for that angle. The axis orientation should correspond to the axis of maximum spatial continuity, i.e. the major anisotropic axis. The default axis is 0º from the north-south (y) axis.

In anisotropic analyses, the offset tolerance determined how closely the alignment between any two points needs to be for those points to be included in the analysis for a given offset angle. Two points will be included in the analysis for a given offset angle if the angle between them is within the offset tolerance from the offset angle. For example, if the angle between two points is 59.3º and the offset tolerance is 15.0º, the points will be included only in the 45º angle class, which would include all angles between 30º and 60º. The default tolerance is 22.5º.

3.0 Results and Discussions

3.1 Descriptive Spatial Statistics

The descriptive spatial statistics of monthly wind speeds for six selected stations are given in Table 1. The calculated spatial statistic included mean centre, standard distance (S_D), minimum and maximum, relative distance (R_D), skewness and kurtosis. The relative distances (R_D) of 66.00%, 50.73% and 50.30% were stronger, which indicated high spatial variability of wind speed for Sokoto, Maiduguri and Enugu stations respectively. While Port Harcourt, Ikeja and Ilorin stations indicated low spatial variability with R_D of 44.95%, 40.52% and 37.70% respectively. Sokoto in the northwest indicated the windiest station with spectacular mean centre wind speeds of 7.02 m/s. Maiduguri and Enugu are in the same mean centre region between 3.44 to 3.56 m/s and Ikeja and Port Harcourt are in the same region between 3.32 to 3.37 m/s. The monthly mean of the wind speed are relatively low in the south west cities of Ilorn (2.34m/s). Studies on the wind speed pattern across Nigeria by Adekoya and Adewale (1992) based on wind data from 30 meteorological stations and Fagbenle and Karayiannis (1994) based on wind data for 18 stations and from 1979-1988 were consistent with current study. Fagbenle and Karayiannis (1994) specifically mentioned that average wind speeds in Nigeria range from about 2 m/s to about 4 m/s with highest average speeds of about 3.5 m/s and 7.5 m/s in the south and north areas, respectively.

Table 1: Descriptive Spatial Statistics for the Six Selected Wind Stations

Station	Mean Center	S_D	Min	Max	R_D (%)	Skew	Kur
Sokoto	7.021	4.634	3.70	12.50	66.002	0.000	0.180
Maiduguri	3.566	1.809	2.10	8.50	50.729	0.120	-0.490
Ilorin	2.341	0.906	1.30	5.00	37.701	-0.350	0.670
Ikeja	3.329	1.349	1.00	7.50	40.522	-0.130	0.430
Port Harcourt	3.373	1.516	1.60	7.70	44.945	0.290	0.190

Enugu	3.447	1.734	0.00	5.30	50.304.	-0.05	0.791

The variations of wind speed across the six stations are due to some roughness of the environment surrounding the stations, variations in the height and position of anemometers, and atmospheric forcing (atmospheric circulation) changes also produce substantial effects. Bichet *et al*. reported that increasing the vegetation roughness length caused by increasing vegetation decreases the land wind speed. Wind speed tend to be higher at well exposed sites than at stations in the vicinity of forests, hills, mountains and other intervening structures such as high rise buildings. The results observed here is expected since the north belongs to the arid and semi-arid ecotypes while the south is dominated by mangrove, swamp forests, tropical rainforests and guinea savanna tall grasslands Bichet *et al*, 2012.

Table 2: Best-fit Isotropic Variogram Models for the Six Selected Wind Stations

Station	**Best-fit Model**	**Nugget (C_0)**	**Sill (C_0+C)**	**Range A**	**RSS**	**R^2**	**C/(C_0+C)**
Sokoto	Spherical	0.1850	2.6860	0.1560	0.618	0.173	0.931
Maiduguri	Exponential	1.475	4.2880	18.0270	0.547	0.718	0.656
Ilorin	Exponential	0.0630	0.3910	0.1060	0.029	0.000	0.839
Ikeja	Spherical	0.0640	1.0940	0.1420	0.085	0.101	0.941
Port Harcourt	Linear	1.0175	1.0175	2.7480	0.059	0.000	0.000
Enugu	Spherical	0.0010	2.4550	0.2400	0.840	0.098	1.000

In order to fit the best isotropic and anisotropic variogram models, three statistics to aid the interpretation of model output was provided in Table 2 & 3: residual sums of squares (RSS)–provides an exact measure of how well the model fits the variogram data; the lower the reduced sums of squares, the better the model fits. When isotropic and anisotropic variogram models were fitted, RSS chooses

parameters for each of the variogram models by determining a combination of parameter values that minimizes RSS for any given model. R^2–provides an indication of how well the model fits the variogram data; this value is not as sensitive or robust as the RSS value for best-fit calculations. And proportion $C/(C_0+C)$ -- this statistic provides a measure of the proportion of sample variance (C_0+C) that is explained by spatially structured variance C. This value will be 1.0 for a variogram with no nugget variance (e.g. Enugu was one indicating the nugget variance is zero where the curve passes through the origin); conversely, it will be 0 where there is no spatially dependent variation at the range specified, (e.g. Port Harcourt was zero indicating no spatially dependent variation where there is a pure nugget effect (Table 2).

Table3: Best-fit Anisotropic Variogram Models for the Six Selected Wind Stations

Station	**Best-fit Model**	**Nugget (C_0)**	**Sill (C_0+C)**	**Range A**		**RSS**	**R^2**	**$C/(C_0+C)$**
				Minor	**Major**			
Sokoto	Linear	2.6430	5.9878	11710.00	11711.00	10.50	0.171	0.559
Maiduguri	Gaussian	1.6520	8.3502	10.636	11.135	11.50	0.406	0.802
Ilorin	Exponential	0.3600	0.9560	29.910	92.640	0.217	0.134	0.623
Ikeja	Gaussian	1.0580	3.5710	16.731	24.872	2.710	0.150	0.704
Port Harcourt	Gaussian	0.9950	2.9240	10.895	21.806	1.980	0.243	0.660
Enugu	Gaussian	2.4230	11.209	911.578	911.578	1.450	0.059	0.784

The study used RSS to judge the effect of changes in model parameters. For isotropic models, spherical model was found to be the best fitted for Sokoto, Ikeja and Enugu with RSS values 0.618, 0.085 and 0.840 respectively; whereas spatial structures of Maiduguri and Ilorin were best fitted by the exponential model with RSS values 0.0.547 and 0.0.029 respectively and linear model was best fitted

for Port Harcourt with RSS value 0.059 (Table 2). The corresponding isotropic variograms were given in figure 3 below.

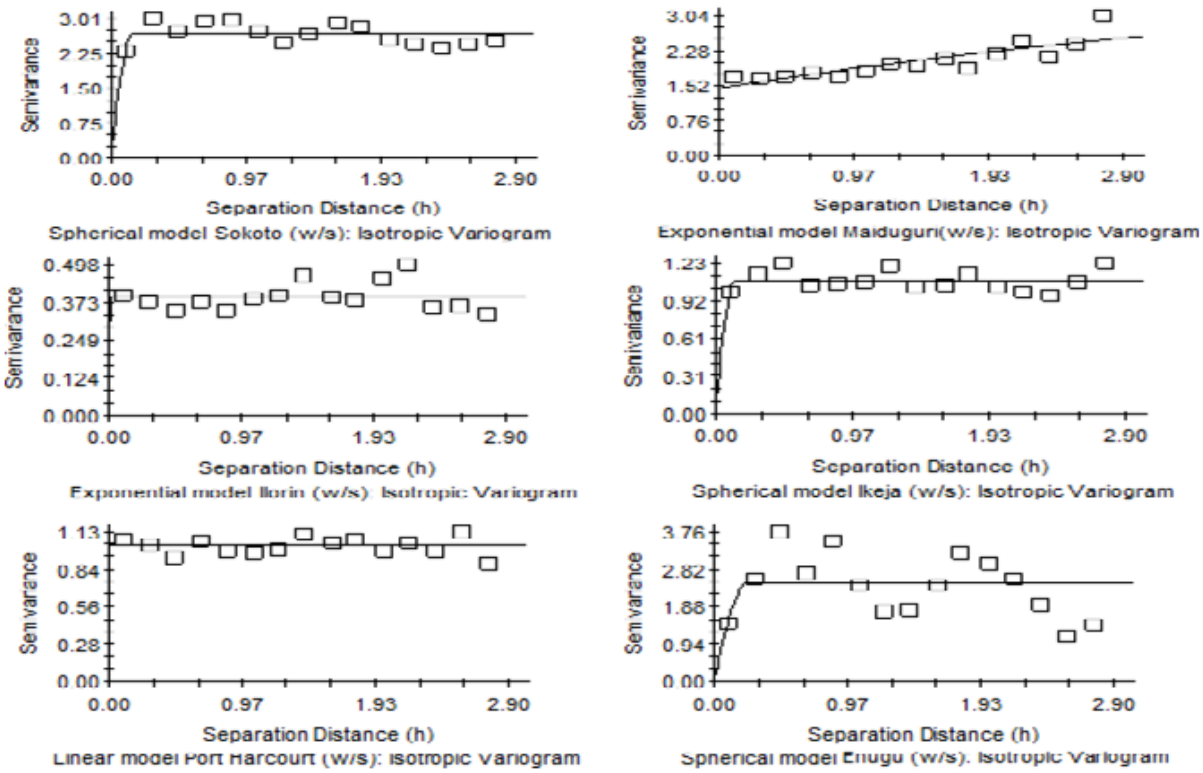

Figure 3: Best fitted Isotropic Variograms for the Six Selected Wind Stations

In other hand, for anisotropic models, linear model was found to be the best fitted for Sokoto, with RSS value 10.50; whereas spatial structures of Maiduguri, Ikeja, Port Harcourt and Enugu were best fitted by the Gaussian model with RSS values 11.50, 2.710, 1.980 and 1.450 respectively and exponential model was best fitted for Ilorin with RSS value 0.217 (Table 3).

The anisotropic variograms were fitted in four different directions. For consistency, the angles in the semivariances are between 0º and 180º, so that a value greater than 180º will appear as that value less 180º (e.g. 225º will be opposite of 90º in the semivariance). The nugget variance is the semivariance intercept of the model and can never be greater than the sill. The best-fitted isotropic and anisotropic models have low nugget variances (Figure 3 & 4). The range is the separation distance over which spatial dependence is apparent and cannot be less than 0. All values of range were greater than or equal

to 0.1060m for isotropic variogram models (Table 2) and greater than or equal to range value from 10.636m to 11.135m for anisotropic variogram models (Table 3). Therefore, all the six selected wind stations had a range value greater than zero indicating existence of a spatial structure for them (Figure 3 & 4). In addition, the ordinary kriging with anisotropic produced an outline map of each wind speed within the larger interpolation grid area. Based on the Nigeria wind speeds classification, winds are classified into four different regimes: very low wind speeds (1.0-2.0 m/s), low wind speeds (2.1- 3.0 m/s), high wind speeds (3.1-4.0 m/s) and very high wind speeds (> 4.1 m/s). High wind speeds appeared in yellow and low wind speeds appeared in blue (Figure 4). The spatial distributions of Sokoto wind speed is stronger (>7.8m/s), Maiduguri and Enugu showed similar wind speed patterns (3.1-4.0m/s) and the spatial distribution of Ikeja and Port Harcourt is between (2.1-3.0m/s) whereas Ilorin showed a pattern of low wind speeds (<2.0m/s).

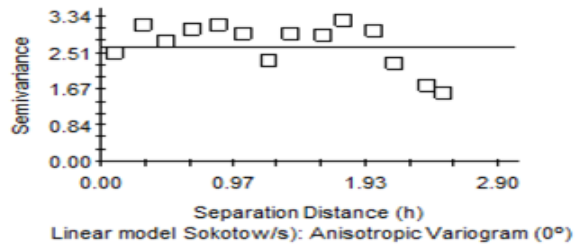

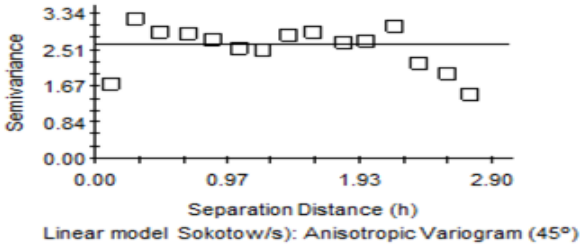

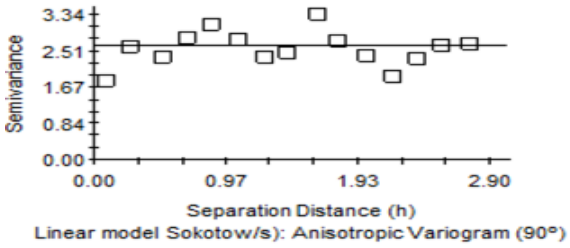

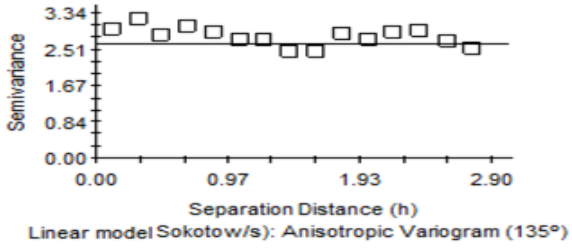

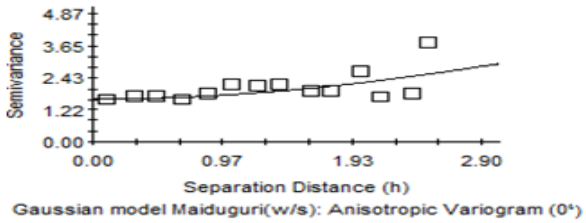

Gaussian model Maiduguri(w/s): Anisotropic Variogram (0°)

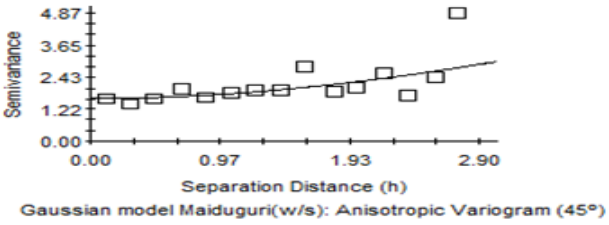

Gaussian model Maiduguri(w/s): Anisotropic Variogram (45°)

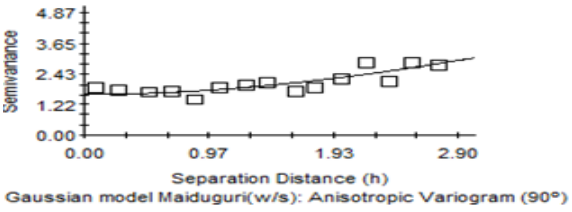

Gaussian model Maiduguri(w/s): Anisotropic Variogram (90°)

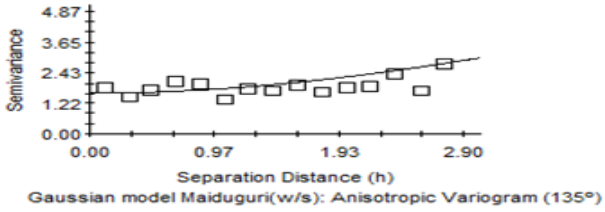

Gaussian model Maiduguri(w/s): Anisotropic Variogram (135°)

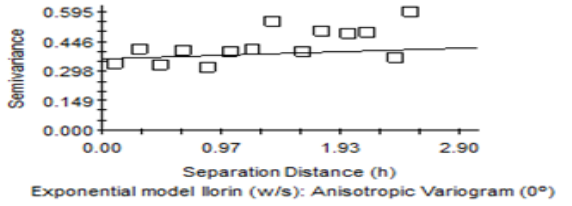

Exponential model Ilorin (w/s): Anisotropic Variogram (0°)

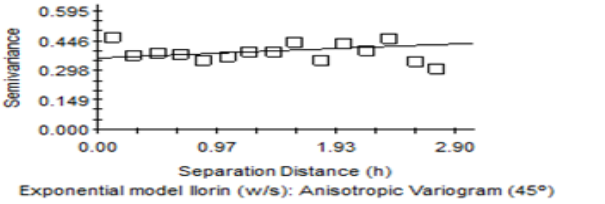

Exponential model Ilorin (w/s): Anisotropic Variogram (45°)

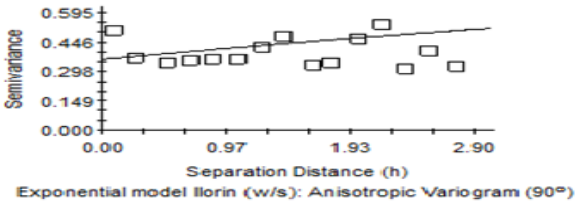

Exponential model Ilorin (w/s): Anisotropic Variogram (90°)

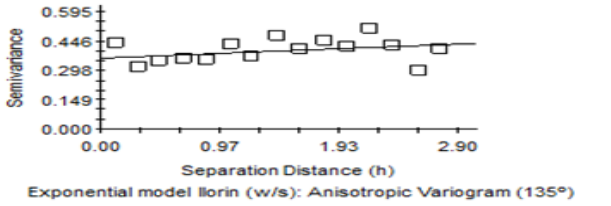

Exponential model Ilorin (w/s): Anisotropic Variogram (135°)

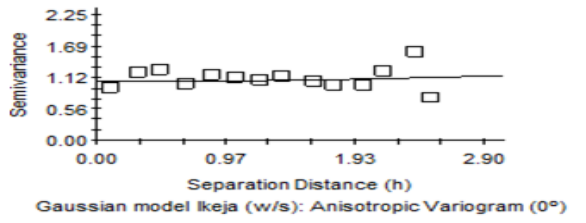

Gaussian model Ikeja (w/s): Anisotropic Variogram (0°)

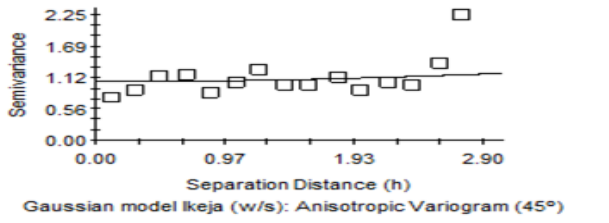

Gaussian model Ikeja (w/s): Anisotropic Variogram (45°)

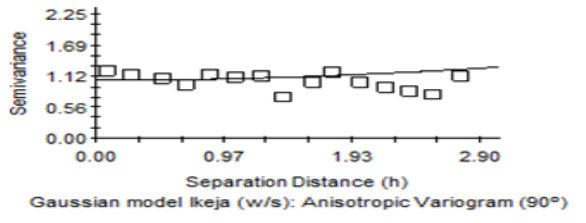

Gaussian model Ikeja (w/s): Anisotropic Variogram (90°)

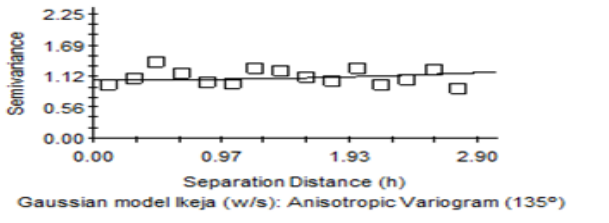

Gaussian model Ikeja (w/s): Anisotropic Variogram (135°)

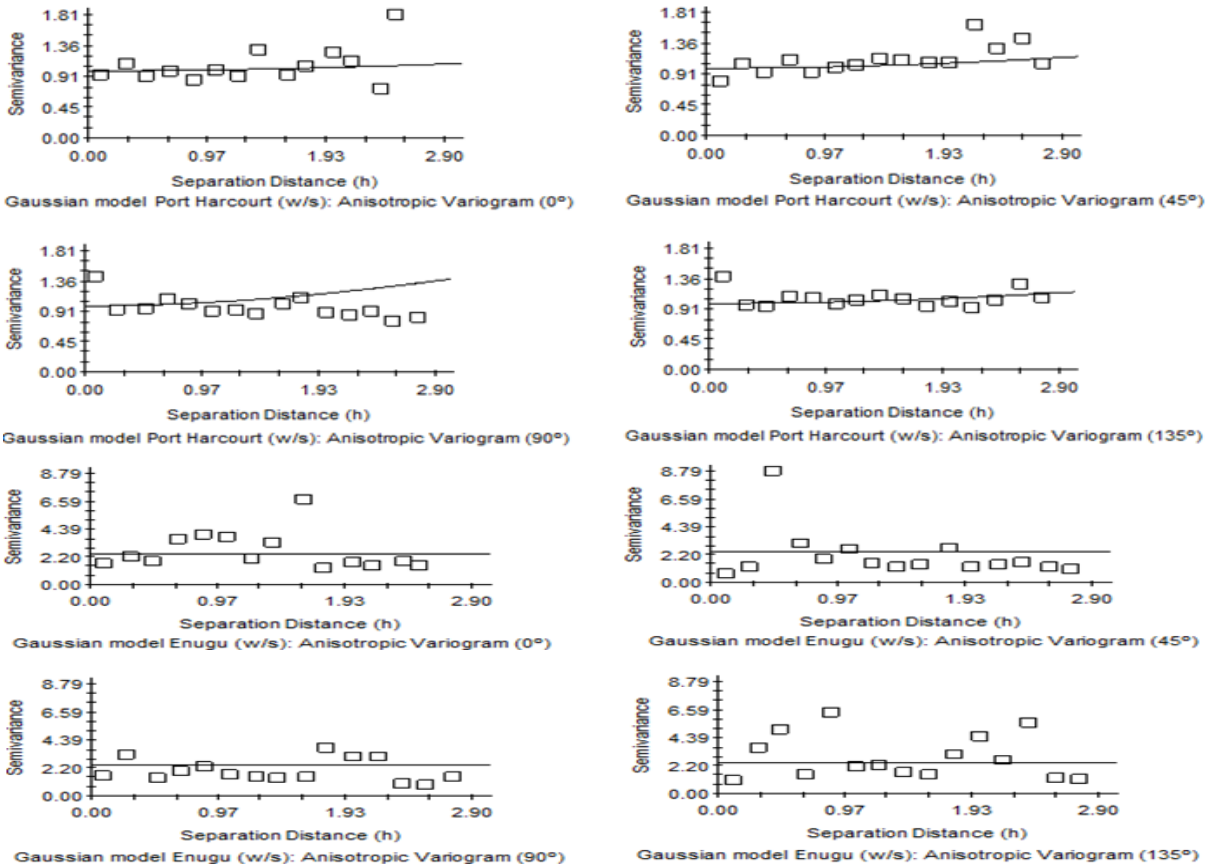

Figure 4: Best fitted anisotropic variograms in the directions N 0° E, N 45° E, N 90° E, and N 135° E with angular tolerance of 22.5 for the Six Selected Wind Stations

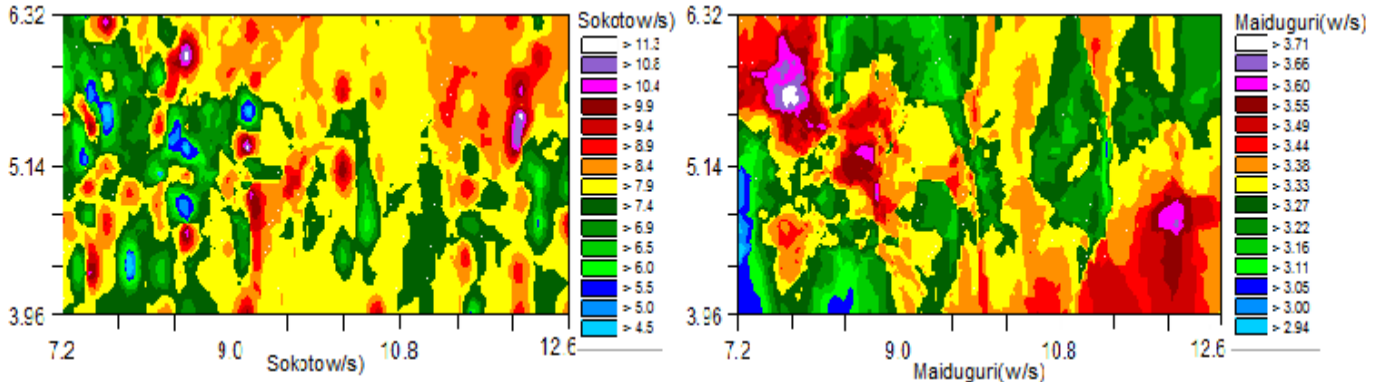

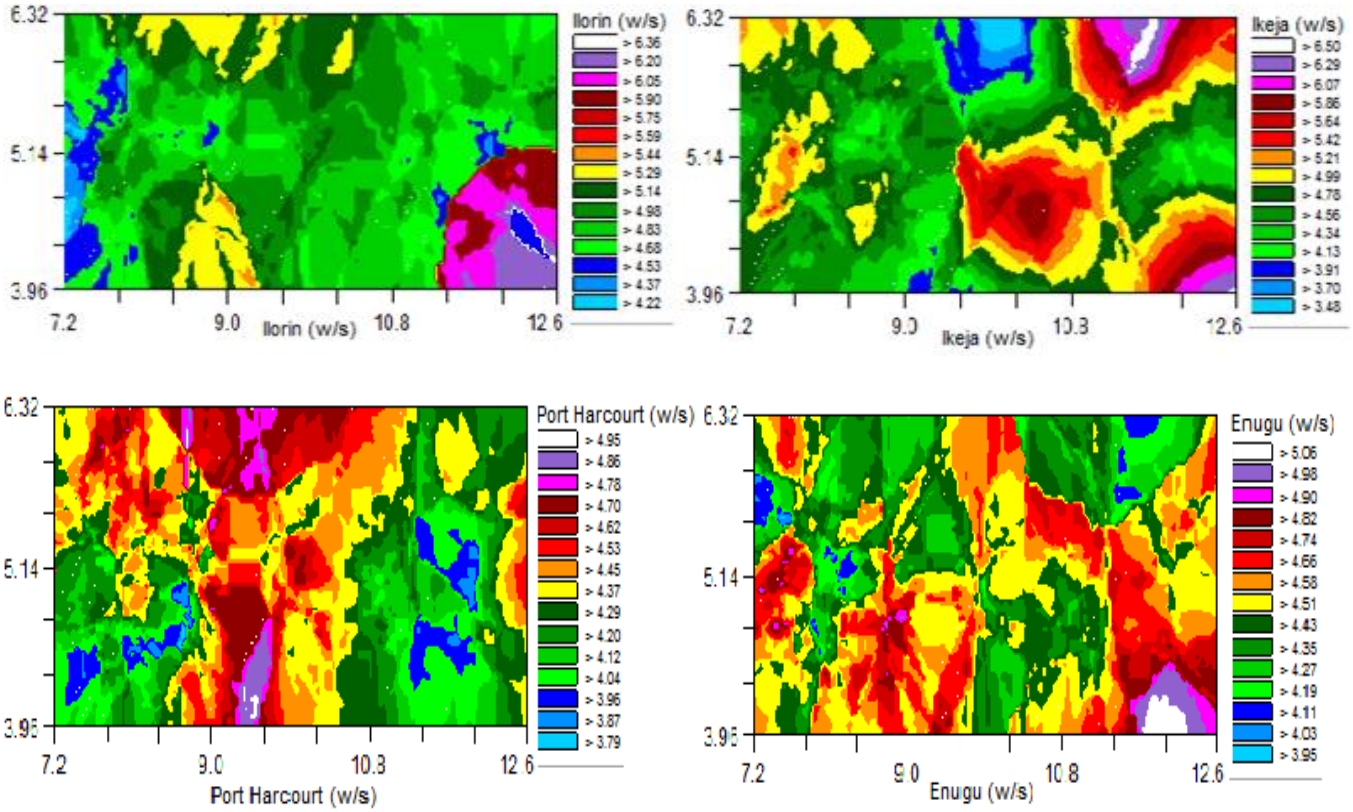

.Figure 5: Anisotropic kriging wind speed interpolation for six selected wind stations

The comparison between estimated and actual values of monthly wind speed for each sample station is given in figure 6. The regression coefficient described at the right corner of the graph represents a measure of the goodness of fit for the least-squares model describing the linear regression equation. A perfect 1:1 fit would have a regression coefficient (slope) of 1.00 and the best-fit line (the solid line in the graph above) would coincide with the dotted 45-degree line on the graph. The standard error refers to the standard error of the regression coefficient; the r^2 value is the proportion of variation explained by the best-fit line; and the y-intercept of the best-fit line is also provided. The SE Prediction term is defined as $SDx(1 - r^2)^{0.5}$, where SD is standard deviation of the actual data (the data graphed on the y-axis).

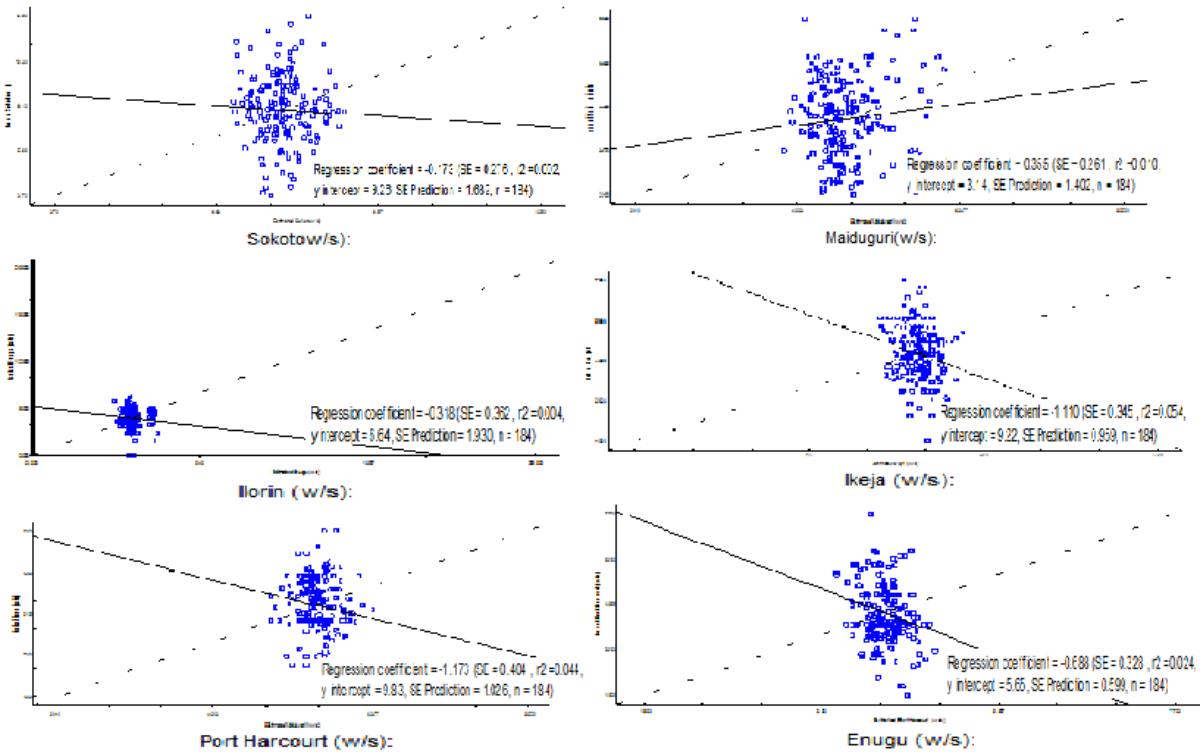

Figure 6: Comparison between actual and estimated wind speed via kriging

4. Conclusions

This study extended previous findings (e.g. Luo *et al.* 2008; Zlatev *et al.* 2009, Carol *et al.* 2016) about the appropriateness of kriging for the interpolation of wind data by analysing isotropic and anisotropic semivariogram-derived kriging surfaces and evaluating a large surface across geographically diverse terrain. A geostatistical approach was applied to investigate the appropriateness of anisotropic variogram models within ordinary kriging on monthly mean wind speed data of six selected wind stations which include: Sokoto, Maiduguri, Ilorin, Ikeja, Port Harcourt and Enugu in Nigeria. The calculated relative distances (R_D) of 66.00%, 50.73% and 50.30% were stronger, which indicated high spatial variability of wind speed for Sokoto, Maiduguri and Enugu stations respectively, whereas Port Harcourt, Ikeja and Ilorin stations indicated low spatial variability with R_D of 44.95%, 40.52% and 37.70% respectively. Sokoto in the northwest indicated the windiest station with spectacular mean centre wind speeds of 7.02 m/s. Maiduguri and Enugu are in the same mean centre region between

3.44 m/s to 3.56 m/s and Ikeja and Port Harcourt are in the same region between 3.32 m/s to 3.37 m/s. The monthly mean of the wind speed are relatively low in the south west cities of Ilorn (2.34m/s). The empirical semivariograms of the six wind stations could be best fitted by linear, Gaussian and exponential anisotropic models.

References

Abiodun, B.J., Salami, A.T. and Tadross, M. (2011).Climate Change Scenarios for Nigeria: Understanding the Bio-Physical Impacts. Climate Systems Analysis Group, Cape Town, for Building Nigeria's Response to Climate Change (BNRCC) Project, Ibadan, Nigeria.

Abhishek, A., Lee, J.Y., Keener, T.C. and Yang, Y.J. (2010). Long-term wind speed variations for Three Midwestern U.S cities. J. Air & Waste Manage. Assoc. 60, 1057 – 1064, doi:10.3155/1047 – 3289.60.1057.

Adekoya L.O., Adewale A.A. 1992. Wind energy potential of Nigeria. Renewable Energy. 2: 35-39.

Akkala A, Devabhaktuni V, Kumar A. 2010. Interpolation techniques and associated software for environmental data. Environ Prog Sustain Energy. 29:134_141.

Bentamy A, Quilfen Y, Gohin F, Grima N, Lenaour M, Servain J. 1996. Determination and validation of average wind fields from ERS-1 scatterometer measurements. Newark, NJ: International Publishers Distributor.

Bichet, A., Wild, M., Folini, D. and Schar, C. (2012). Causes for decadal variations of wind speed over land: sensitivity studies with a global climate model. Geophysical Research Letters, 39, L11701, doi:10.1029/ 2012GL051685.

Carol J. Friedland, T. Andrew Joyner, Carol Massarra, Robert V. Rohli, Anna M. Treviño, Shubharoop Ghosh, Charles Huyck & Mark Weatherhead (2016): Isotropic and anisotropic kriging approaches for interpolating surface-level wind speeds across large, geographically diverse regions, Geomatics, Natural Hazards and Risk, DOI: 10.1080/19475705.2016.1185749

Cellura M, Cirrincione G, Marvuglia A, Miraoui A. 2008. Wind speed spatial estimation for energy planning in Sicily: a neural kriging application. Renew Energy. 33:1251_1266.

Collins FC, Bolstad PV. 1996. A comparison of spatial interpolation techniques in temperature estimation. In *Proceedings of the Third International Conference/Workshop on Integrating GIS and Environmental Modeling*. National Center for Geographic Information Analysis (NCGIA): Santa Fe, NM, Santa Barbara, CA: January 21–25.

Etienne C, Beniston M. 2012. Wind storm loss estimations in the Canton of Vaud (Western Switzerland). Nat Hazards Earth Syst Sci. 12:3789_3798.

Fagbenle R.'L., Karayiannis T.G. 1994. On the wind energy resource of Nigeria. International Journal of Energy Research. 18: 493-508.

Goovaerts P. 2000. Geostatistical approaches for incorporating elevation into the spatial interpolation of rainfall. *Journal of Hydrology* **228**: 113–129.

Lanza L, Ramirez J, Todini E. 2001. Stochastic rainfall interpolation and downscaling. Hydrol Earth Syst Sci. 5:139_143.

Jarvis CH, Stuart N. 2001. A comparison among strategies for interpolating maximum and minimum daily air temperatures. Part II: the interaction between number of guiding variables and the type of interpolation method. *Journal of Applied Meteorology* **40**: 1075–1084.

Joyner TA, Friedland CJ, Rohli RV, Trevi~no AM, Massarra C, Paulus G. 2015. Cross-correlation modeling of European windstorms: a cokriging approach for optimizing surface wind estimates. Spat Stat. 13:62_75.

Krige DG. 1966. Two-dimensional weighted average trend surfaces for ore-evaluation. *Journal of the South African Institute of Mining and Metallurgy* **66**: 13–38.

Luo W, Taylor MC, Parker SR. 2008. A comparison of spatial interpolation methods to estimate continuous wind speed surfaces using irregularly distributed data from England and Wales. Int J Climatol. 28:947_959.

Luo X, Xu Y, Shi Y. 2011. Comparison of interpolation methods for spatial precipitation under diverse orographic effects. Proceedings of the 19th International Conference on Geoinformatics; Jun 24_26. Shanghai, China.

Ojo, O. (1977). The Climates of West Africa, Ibadan, Heinemann.

Ojosu J.O., Salawu R.I. 1990b. An evaluation of wind energy potential as a power generation source in Nigeria. Solar and Wind Technology. 7: 663-673.

Oztopal A. 2006. Artificial neural network approach to spatial estimation of wind velocity data. Energy Convers Manag. 47:395_406.

Phillips DL, Lee EH, Herstrom AA, Hogsett WE, Tingey DT. 1997. Use of auxillary data for spatial interpolation of ozone exposure in southeastern forests. Environmetrics. 8:43_61.

Phillips DL, Dolph J, Marks D. 1992. A comparison of geostatistical procedures for spatial analysis of precipitation in mountainous terrain. *Agricultural and Forest Meteorology* **58**: 119–141.

Price DT, McKenney DW, Nalder IA, Hutchinson MF, Kesteven JT. 2000. A comparison of two statistical methods for spatial interpolation of Canadian monthly mean climate data. *Agricultural and Forest Meteorology* **101**: 81–94.

Robinson, T.P. and G. Metternicht, 2006. Testing the performance of spatial interpolation techniques for mapping soil properties. J. Comput. Elect. Agric., 50: 97-106

Sterk G, Stein A. 1997. Mapping wind-blown mass transport by modelling variability in space and time. Soil Sci Soc Am J. 61:232_239.

Troccoli, A., Muller, K., Coppin, P., Davy, R., Russell, C. and Hirsch, A.L. (2012). Long-term wind speed trends over Australia. Journal of Climate, 25, 170 – 183.

Tuller, S.E. (2004). Measured wind speed trends on the west coast of Canada. Int. J. Climatol. 24:1359 – 1374.

Venäläinen A, Heikinheimo M. 2002. Meteorological data for agricultural applications. Phys Chem Earth Parts A/B/C. 27:1045_1050.

Vicente-Serrano SM, Saz-Sanchez MA, Cuadrat JM. 2003. Comparative analysis of interpolation methods in the middle Ebro Valley (Spain): application to annual precipitation and temperature. *Climate Research* **24**: 161–180.

Zlatev Z, Middleton SE, Veres G. 2009. Ordinary kriging for on-demand average wind interpolation of in-situ wind sensor data. Proceedings of the EWEC 2009. Shanghai, China.

Zlatev Z, Middleton SE, Veres G. 2010. Benchmarking knowledge-assisted kriging for automated spatial interpolation of wind measurements. Proceedings of the 2010 13th Conference on Information Fusion (FUSION). Edinburgh, UK.

Analytical Method of Land Surface Temperature Prediction

[1]M. D. Shehu [2]R. A. Olowu

[1,2]Department of Mathematics, Federal University of Technology, Niger State
[1] m.shehu@futminna.edeu.ng
[2]olowurafiu1985@gmail.com

Abstract

In this paper, we formulated a model for the prediction of Land Surface Temperature (LST) using the Analytical Method, with the incorporation of atmospheric scale height. The following parameters were considered, meridional wind speed "*v"*, scale height of pressure difference "*H"*, coriolis force "*f"*, time "*t"*, gravitational force "*g"* and temperature "*T*". The novelty of this study centers on the attempt to predict and analyze the behaviour of LST for a particular area using shallow water equation. The result revealed that the Land Surface Temperature increases with decrease in altitude, and this re-affirms the efficiency of Shallow Water Equation in making accurate predictions of the Land Surface Temperature.

Keywords: land surface temperature, zonal wind speed, meridional wind speed, scale height, atmospheric altitude.

1.0 Introduction

Weather prediction is an essential method for meteorologists to forecast the weather and lead to more precision in forecasting. Since the weather is a complex and chaotic system, numerical weather prediction also displays a high complexity. Although most people do not know how weather prediction works, they are highly interested in the results, presented by TV weathermen or accessible through the Internet (Albrecht, *et al.*, 2016; Nycander and Doos, 2003)

Land Surface Temperature (LST) is an important variable in climate, Hydrologic, Ecological, Biophysical and Biochemical studies (Ådlandsvik, 2008). LST plays a key role in modeling the surface energy balance and has a substantial impact on analyzing the heat-related issues such as soil moisture, evapotranspiration and urban heat islands (Alexander and Arblaster, 2009; Hallberg and Rhines, 2016), Batteen and Han (1981) considered a Smoothed Particle Hydrodynamics (SPH) approaches were used to solve Shallow Water Equations (SWEs), and this is used to study practical dam-break flows at

South-Gate Gorges Reservoir. The model is first tested on two benchmark collapses of water columns with the existence of downstream obstacle. Subsequently the model is applied to forecast a prototype dam-break flood, which might occur in South-Gate Gorges Reservoir area of Qinghai Province, China. It shows that the SWE-SPH modeling approach could provide a promising simulation tool for practical dam-break flows in engineering scale.

In remote sensing land surface temperature data are usually obtained through the weather satellite, the satellite does not measure the temperature directly; it only scans through the atmosphere and measure the radiant of the sun. A retrieval algorithm is used to obtain the temperature data from the satellite. However, direct estimation of LST from the radiation emitted in the TIR spectral region is difficult to perform with correct accuracy by the satellite, since the radiances measured by the radiometers onboard satellites depend not only on surface parameters (temperature and emissivity) but also on atmospheric effects (Buhler, 1998; Nelson and Markley, 2014)

This necessitated an analytical approach for the prediction of Land Surface Temperature using shallow water equation.

2.0 Model Development

2.1 Shallow Water Equation

The two-dimension form of shallow water equation as given by (Mesinger and Arakawa, 2017) is considered

$$\frac{\partial u}{\partial t} + u\frac{\partial u}{\partial x} + g\frac{\partial h}{\partial x} - fv = 0 \quad (1)$$

$$\frac{\partial v}{\partial t} + u\frac{\partial v}{\partial x} + g\frac{\partial H}{\partial y} + fu = 0 \quad (2)$$

$$\frac{\partial h}{\partial t} + u\frac{\partial h}{\partial x} + v\frac{\partial H}{\partial y} + h\frac{\partial u}{\partial x} = 0 \quad (3)$$

$$\frac{\partial H}{\partial y} = -f\frac{\overline{U}}{g} \tag{4}$$

where,

U represents velocity component in the x- direction

v represents velocity component in the y- direction

h represents depth of the fluid

f represents Coriolis force

t represents time

T represents temperature

g represents acceleration due to gravity

$\overline{U}$ represents average mean wind speed of the atmosphere.

Equation (1) is the momentum equation for u along the x-axis

Equation (2) is the momentum equation for v along the y-axis

Equation (3) is the continuity equation

3.0 Model Formulation

To obtain a mathematical model for the Land surface temperature using the set of equaion (1) to (4) is to define the fluid depth to be consistent with the boundary layer of the troposphere, so the temperature at this lower atmosphere can varies with altitude. A very common way to describe the behavior of temperature and altitude at this atmosphere layer is by its 'scale height'. Scale height is related to the temperature (T) and mean molecular mass (m) of the atmosphere given by the formula:

$$H = \frac{RT}{g} \tag{5}$$

where

H = Scale Height
T = Temperature
R = Universal gas constant
g = Gravitational force

Equation (5) is incorporated into the model formulation due to the existence of various gaseous element within the atmosphere.

By differentiating equation (5) with respect to *y*, yield

$$\frac{\partial H}{\partial y} = \frac{R}{g}\frac{\partial \mathrm{T}}{\partial \mathrm{y}} \tag{6}$$

substituting $\frac{R}{g}\frac{\partial \mathrm{T}}{\partial \mathrm{y}}$ for $\frac{\partial H}{\partial y}$ in equation (4)

$$\frac{\partial \mathrm{T}}{\partial \mathrm{y}} = -f\frac{\overline{U}}{R} \tag{7}$$

To represent the behavior of the atmosphere in other to derive a model for the land surface temperature there is a need to consider the temperature lapse rate "γ"at which temperature decreases with increase in altitude. Combine equation (2) and (3) taking the shallow height of the atmosphere "*h*" to be constant; this leads to a new continuity equations.

$$\frac{\partial u}{\partial t} + u\frac{\partial u}{\partial x} - fv = 0 \tag{8}$$

$$\frac{\partial v}{\partial t} + u\frac{\partial v}{\partial x} + fu = 0 \tag{9}$$

$$\frac{\partial \mathrm{T}}{\partial \mathrm{y}} = -f\frac{\overline{U}}{R} - \gamma \tag{10}$$

where;

Equation (8) represent momentum equation for *u*

Equation (9) represent momentum equation for *v*-

Equation (10) represent lapse rate equation

To obtain solution for our model equation, we consider the analytical method of solution.

3.0 Analytical Method

In this section we employ an analytical method for the solution of our model equation.

Equation (8) , (9) and (10), can be written as

$$\frac{du}{dt} = fv \tag{11}$$

$$\frac{dv}{dt} = -fu \tag{12}$$

Let 0<f<<1, and suppose the solution (u, v) can be expressed in series form as:

$$\mathrm{u}(x,\mathrm{t}) = u_{\circ}(x,\mathrm{t}) + fu_{1}(x,\mathrm{t}) + ... \tag{13}$$

$$v(x,t) = v_o(x,t) + fv_1(x,t) + \ldots \quad (14)$$

Substituting (13) and (14) into equation (11) and (12), respectively

$$\frac{d}{dt}\left(u_o + fu_{1+\ldots}\right) = f\left(v_o + fv_1 + \ldots\right) \quad (15)$$

$$\frac{d}{dt}\left(v_o + fv_1 + \ldots\right) = -f\left(u_o + fu_1 + \ldots\right) \quad (16)$$

Collecting the like power of *f*, we have for

f^o

$$\frac{du_o}{dt} = 0, u_o(x,0) = u_o \quad (17)$$

$$\frac{dv_o}{dt} = 0, v_o(x,0) = v_o \quad (18)$$

f^1

$$\frac{du_1}{dt} = v_o, u(x,0) = 0 \quad (19)$$

$$\frac{dv_1}{dt} = -u_0, v_1(x,0) = 0 \quad (20)$$

Integrating (17) with respect to *t*, we have

$$u_o(x,t) = c_1 = \text{constant}$$

$$u_o(x,0) = c_1 = u_o$$

$$c_1 = u_o$$

Thus

$$u_o(x,t) = u_o \quad (21)$$

Integrating (18) with respect to *t*, we have

$$v_o(x,t) = c_2 = \text{constant}$$

$$v_o(x,0) = c_2 = v_o$$

$$c_2 = v_o$$

Thus

$$v_o(x,t) = v_o \quad (22)$$

Integrating (19) with respect to *t*, we have

$$u_1(x,t) = v_o t + c_3$$

$$u_1(x,0) = 0 + c_{3+} 0 = 0$$

$$c_3 = 0$$

Thus

$$u_1(x,t) = v_o t \quad (23)$$

Integrating (20) with respect to *t*, we have

$$v_1(x,t) = -u_o t + c_4$$

$$v_1(x,0) = 0 + c_4 + 0 = 0$$

$c_4 = 0$

Thus

$v_1(x,t) = -u_o t$ (24)

Substituting equation (21), (22), (23) and (24) into equation (13) and (14), respectively yields,

$u(x,t) = u_o - fv_o t$ (25)

$v(x,t) = v_o - fu_o t$ (26)

Integrating equation (10) with respect to *y*, yields

$$\frac{\partial T}{\partial y} = -(f\frac{\overline{U}}{R} + \gamma)\phi \quad (27)$$

Thus the analytic solution to our model equations (8), (9) and (10) is giving as;

$u(x,t) = u_o - fv_o t$ (28)

$v(x,t) = v_o - fu_o t$ (29)

$T_{(\phi)} = T_{(O)} - (f\frac{\bar{u}}{R} + \gamma)\phi$ (30)

3.1 Data Consideration

The following data for the evaluation of our analytical solution where considered

u_o = 0.8, initial value for zonal wind speed

v_o = 5.4 initial value for meridional wind speed

t = 3.0 time

T_0 = 37^OC

γ = 0.0065

R = 8.3144598

Ubar "$\bar{u}$"=product of the mean value of zonal and meridional wind speed, and is giving

$$\bar{u} = \frac{\sum_i^n u_i}{n} \cdot \frac{\sum_i^n v_i}{n}, for\ i = 1,2...n \quad (31)$$

4.0 Results

This section shows the graphical solution obtained from the simulation of the equations (28), (29) and (30).

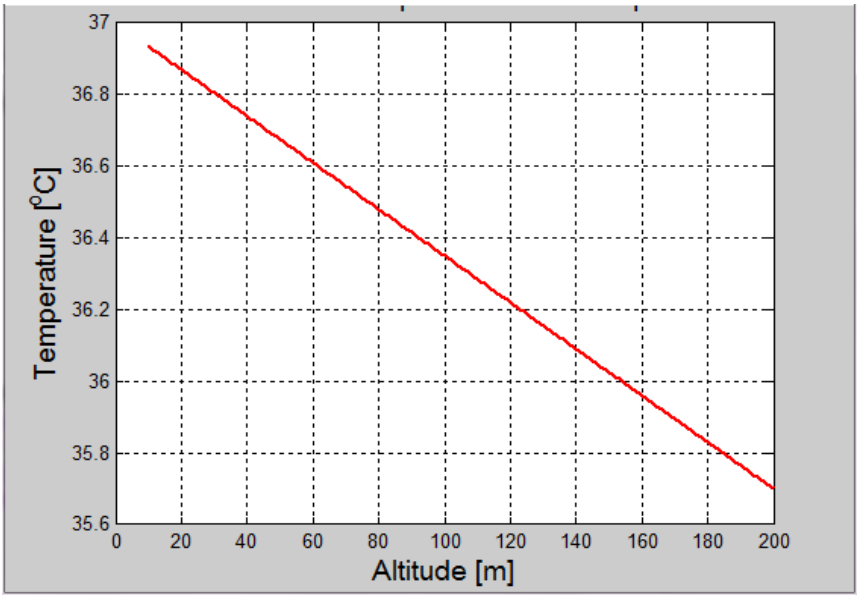

Figure 1: Graph of Temperature (^{0}C) against the atmospheric Altitude (m).

Figure 1 is the graphical solution to the simulation of the equations (28), (29) and (30) with the mean value of the zonal and meridional wind speed, using Matlab software.

Table 1: Predicted temperature extracted from figure 1

Altitude (m)	20	40	60	80	100	120	140	160	180
Temperature(^{0}C)	36.84	36.71	36.60	36.44	36.38	36.20	36.10	35.93	35.85

It can be observed from table 1, that the land surface temperature decreases as the atmospheric altitude increases, also the temperature increases as the altitude decreases. It can be see how the temperature gradually decreases from 36.84^{0}C to 35.85^{0}C for the altitude 0m to 200m.

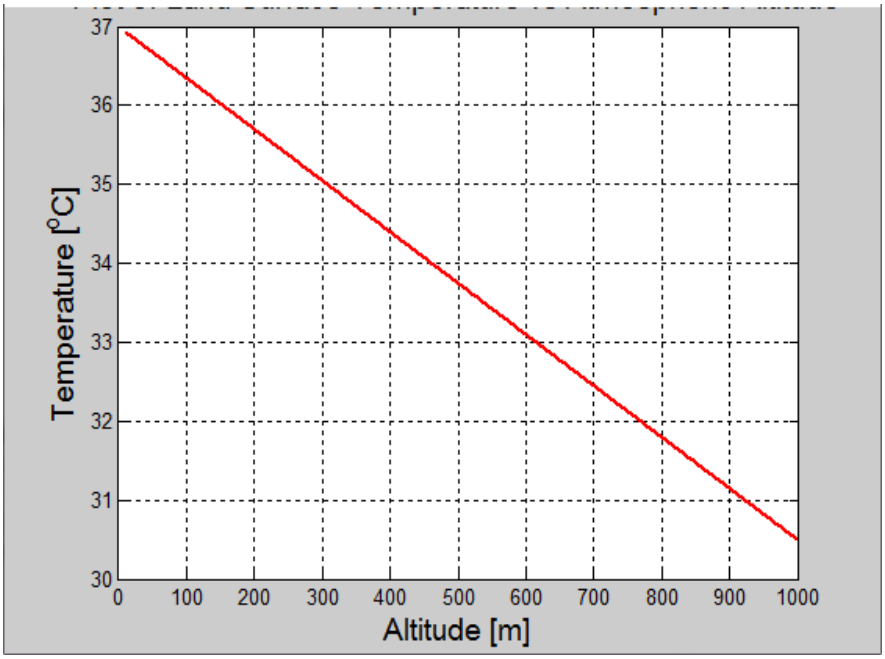

Figure 2: Graph of Temperature (^{0}C) against the atmospheric altitude (m).

Figure 2 is the graphical solution to the stimulation of the equations (28), (29) and (30) with the mean value of the zonal and meridional wind speed, using Matlab software.

Table 2: Predicted temperature extracted from figure 2

Altitude (m)	100	200	300	400	500	600	700	800	900
Temperature(^{0}C)	36.40	35.80	35.00	34.51	33.92	33.20	32.50	31.80	31.20

It can be observed from table 2, that the land surface temperature decreases as the atmospheric altitude increases, also the temperature increases as the altitude decreases. It can be see how the temperature gradually decreases from 36.40^{0}C to 31.2^{0}C for the altitude 0m to 1000m.

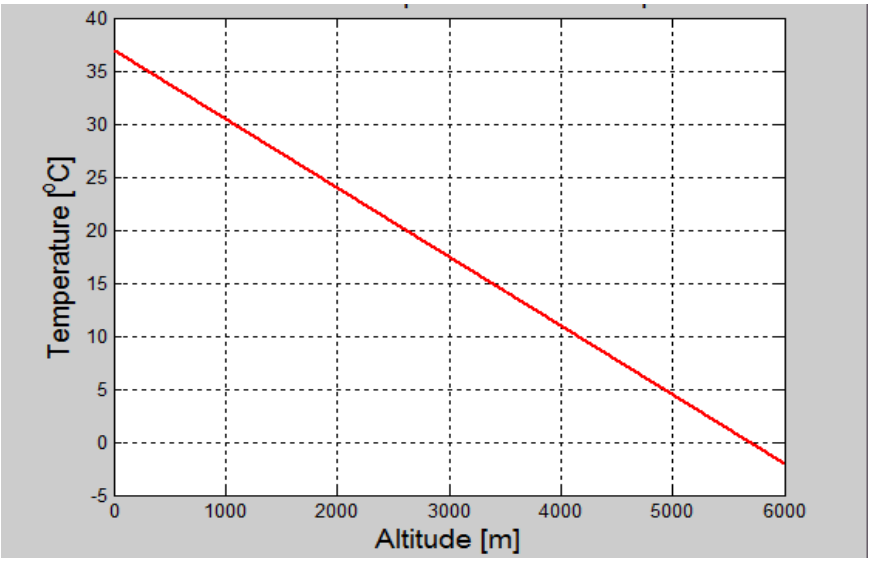

Figure 3: Graph of Temperature (^{0}C) against the atmospheric altitude (m)

Figure 3 is the graphical solution to the simulation of the equations (28), (29) and (30) with the mean value of the zonal and meridional wind speed , using Matlab software.

Table 3: Predicted temperature extracted from figure 3

Altitude (m)	1000	2000	3000	4000	5000	6000	7000	8000	5800
Temperature(^{0}C)	30.00	24.00	17.00	11.00	5.00	-2.00	-5.00	-7.00	-12.0

It can be observed from table 3, that the land surface temperature decreases as the atmospheric altitude increases, also the temperature increases as the altitude decreases. It can be seen how the temperature gradually decreases from 37^{0}C to -3^{0}C for the altitude 0m to 6000m.

5.0 Conclusion

This research work presents an analytical method for the prediction of Land Surface Temperature using the shallow water equation. The atmospheric behavior was carefully studied and most important parameters were identified and well represented accordingly as required in the prediction of Land Surface Temperature using the shallow water equation. The demographic profile of Nigeria meridional and zonal wind speed were used to study the behavior of this model. However, the behaviors exhibited

by both the atmosphere altitude and the land surface temperature in this analytic result shows that at any given time on the earth surface, "the higher the location of a particular area, the lower will be the temperature the people living in that environment will experience.

Information on weather dataset should be made available, accessible and usable for all researchers who take research in the area of Land Surface Temperature and other weather related areas. The Federal Government of Nigeria should establish commission for the training of weather and climate management and development for lecturers and students in Nigeria.

References

AchutaRao, K., Covey, C. & Doutriaux, C. (2004). An Appraisal of Coupled Climate Model Simulations, Lawrence Livermore National Laboratory report UCRL-TR-202550.

Ådlandsvik, B. (2008). Marine downscaling of a future climate scenario for the North Sea.Tellus, 60A, 451–458.

Albrecht, B. A., Betts, K. A. & Schubert, W. H. (2016). A model for the thermodynamic structure of the trade-wind boundary layer: I. Theoretical formulation and sensitivity tests. J. Atmos. Sci., 36, 73–89.

Alexander, L. V., & Arblaster, J. M (2009). Assessing trends in observed and modeled climate extremes over Australia in relation to future projections. Int. J. Climatol., 29,417–435.

Batteen, M. L. & Han, Y.-J. (1981). On the computational noise of finite-difference schemes used in ocean models, Tellus, 33, 387–396 .

Buhler, O. (1998). A shallow-water model that prevents nonlinear steepening of gravity waves. *J. Atmos. Sci*., 55, 2884–2891.

Hallberg, R. & Rhines, P. B. (2016). Buoyancy-driven circulation in an ocean basin with isopycnals intersecting the sloping boundary. J. Phys. Oceanogr., 26, 913–940.

Nelson G. & Markley A. (2014). Principles of Differential Equations. Pure and Applied Mathematics, Wiley-Interscience, Hoboken, NJ, USA, 99-105.

Nycander, J. & Doos, K (2003). Open boundary conditions for barotropic waves, Journal of Geophysical Research: Oceans, 108.

Mesinger, F. & Arakawa, A. (2017). Numerical methods used in atmospheric models, GARP technical report 17, WMO/ICSU. Geneva, Switzerland, 1, 17, 976.

Agreement between the Homotopy Perturbation Method and Variation Iterational Method on the Analysis of One-Dimensional Flow Incorporating First Order Decay

BY

***[1]Jimoh, O. R., [2]Aiyesimi, Y. M. and [3]Jiya, M.**
[1,2,3,4]Department of Mathematics,
Federal University of Technology, Minna, Nigeria.
*[1]razaq.jimoh@futminna.edu.ng
[2]yomiaiyesimi2007@yahoo.co.uk
[3]jiyason2010@gmail.com
*Corresponding author

Abstract

In this paper, a comparative study of reactive contaminant flow for constant initial concentration in one dimension is presented. The adsorption term is modeled by Freudlich Isotherm. An approximation of the one-dimensional contaminant flow model was obtained using homotopy-perturbation transformation and the resulting linear equations were solved semi-analytically by homotopy-perturbation method (HPM) and Variational Iteration Method (VIM). Graphs were plotted using the solution obtained from the methods and the results presented and discussed. The analysis of the results obtained show that the concentration of the contaminant decreases with time and distance as it moves away from the origin.

Keywords: Homotopy-perturbation, contaminant, advection, diffusion, adsorption, Variational Iteration Method

1.0 Introduction

Virtually every day, the Society generates a large number of pollutants which often find their ways into the environment. These happen intentionally during agricultural practices or unintentionally resulting from leakages of municipal wastes disposal sites.

Consequently, as many of these chemicals or pollutants enter the food chain, contamination of both surface and subsurface water supplies has become a critical issue. A high percentage of drinking water in Nigeria comes from groundwater. The effect of contamination of groundwater systems as a subject of discourse cannot be over-emphasized in assessing the hazards of public health. In order to predict the fate of such pollutants during their transport, an arduous task for hydro-geologists and scientists

emerges. The problem involves defining the flow path of groundwater in the aquifers, the travel time of the water along the flow lines and to predict the chemical reaction which alters the concentrations during transport.

2.0 Literature Review

Several researchers have been on the field in the study of hydrodynamic dispersion with various initial and boundary conditions. Aiyesimi (2004), Gideon and Aiyesimi (2005) and Gideon (2011) studied one dimensional contaminant flow problems by method of perturbation. Clint (1993) and Makinde and chinyoka (2010) employed numerical methods and Laplace Transform method (Singh *et al.*,2010) and Yadav and Kumar, 2011). Another well-known method, the Homotopy perturbation method was used to solve wide range of physical problems, eliminating the limitations of perturbation method (Rezania *et al.*,2009, Muhammad, 2010; Rajabi *et al.*, 2007; and Jiya, 2010). A semi-analytical solution of one-dimensional contaminant flow problem was handled by method of weighted residual method and the results approximate the behavior of the contaminant in the finite flow domain (Jimoh *et al*., 2017). Most of the researches done in the past either neglects the non-linear term or considers it as a constant, and they are mostly nonreactive. In this paper, we provide a comparative analysis of the non-linear reactive contaminant transport problem with initial continuous point source by Homotopy-Perturbation method and Variational Iteration method.

3 Methodology

3.1 Formulation of the Model

We consider an incompressible fluid flow through a homogeneous, saturated porous medium where the fluid is not solute-free, i.e. contaminated with solute of concentration C(x,t). The following assumptions are made (i) The flow is steady (ii) the solute transport is described by advection, molecular diffusion and mechanical dispersion (iii) the flow is one dimensional and in x-direction.

Under these assumptions, mass conservation of the contaminant may be combined with a mathematical expression of the relevant process to obtain a differential equation describing flow Jimoh *et al*., 2017. Following (Bear, 1997), (Yadav, *et al.* 2011), (Jimoh and Aiyesimi, 2012 and 2013), Ramakanta and Mehta (2010), Singh (2013) and Singh *et al*. (2015), the one dimensional partial differential equation describing hydrodynamic dispersion in adsorbing, homogeneous and isotropic porous medium can be written as

$$\frac{\partial C}{\partial t}+u\frac{\partial C}{\partial x}+\frac{pb}{\theta}\frac{\partial S}{\partial t}-D\frac{\partial^2 C}{\partial x^2}+\alpha C=0,\ 0<x<\infty,\ t>0 \tag{1}$$

where $S(x,t)$ is the mass of the contaminant absorbed on the solid matrix per unit mass of the solid, $p_b>0$ is the bulk density of the porous medium, $n>0$ is the porosity, $D>0$ accounts for both molecular diffusion and mechanical dispersion, u is the fluid velocity and α is the reaction parameter. We consider the non-linear flow equation with the associated boundary and initial conditions:

$$\begin{cases}\dfrac{\partial C}{\partial t}+u\dfrac{\partial C}{\partial x}+\dfrac{pb}{\theta}\dfrac{\partial S}{\partial t}-D\dfrac{\partial^2 C}{\partial x^2}+\alpha C=0,\\ C(0,t)=B,\ C(\infty,t)=0,\\ C(x,0)=Be^{-\lambda x}\\ \alpha>0,\ 0<x<\infty\end{cases} \tag{2}$$

Equation (2) can be rewritten as

$$\frac{\partial C}{\partial t}+\frac{\partial f(C)}{\partial t}+u\frac{\partial C}{\partial x}-D\frac{\partial^2 C}{\partial x^2}+\alpha C=0 \tag{3}$$

which can also be expressed in the form:

$$\frac{\partial C}{\partial t}+\frac{\partial f}{\partial C}.\frac{\partial C}{\partial t}+u\frac{\partial C}{\partial x}-D\frac{\partial^2 C}{\partial x^2}+\alpha C=0 \tag{4}$$

This can again be expressed as

$$\frac{\partial C}{\partial t}+\varepsilon\frac{\partial C}{\partial t}+u\frac{\partial C}{\partial x}-D\frac{\partial^2 C}{\partial x^2}+\alpha C=0 \tag{5}$$

where $\varepsilon=\dfrac{\partial f}{\partial C}$, the perturbation parameter.

That is,

$$(1-\varepsilon)\frac{\partial C}{\partial t}+u\frac{\partial C}{\partial x}-D\frac{\partial^2 C}{\partial x^2}+\alpha C=0 \tag{6}$$

3.2 Principle of Homotopy-Perturbation Method (HPM)

In order to explain the method of homotopy-perturbation, we consider the function:

$$A(u)-f(r)=0,\ r\in\Omega \tag{7}$$

with the boundary conditions:

$$B\left(u,\frac{\partial u}{\partial n}\right)=0,\ r\in\Gamma, \tag{8}$$

where $A, B, \mathrm{f(r)}$ and Γ are a general differential operator, a boundary operator, a known analytical function and a boundary of the domain respectively. The operator A can be divided into two parts L and N where L is linear and N is nonlinear. Equation (7) can therefore be rewritten as follows:

$$L(u)+N(u)-f(r)=0,\ r\in\Omega \tag{9}$$

By homotopy-perturbation method, we form a homotopy:

$$v(r,p):\Omega\times[0,1]\to R \tag{10}$$

which satisfies

$$H(v,p)=(1-p)(L(u)-L(u_0))+p(A(v)-f(r))=0,\quad p\in[0,1],\ r\in\Omega \tag{11}$$

where $p\in[0,1]$, is an embedding parameter, while u_0 is an initial approximation of (7), which satisfies the boundary conditions (He, 2000 and 2005). From equation (9), we have:

$$H(v,0)=L(v)-L(u_0)=0 \tag{12}$$

$$H(v,1)=A(v)-f(r)=0 \tag{13}$$

According to HPM, we can first use the embedding parameter p as a "small parameter", and assume that the solutions of equation (9) can be written as a power series in p:

$$v=v^{(0)}+pv^{(1)}+p^2v^{(2)}+p^3v^{(3)}+\ldots \tag{14}$$

and the best approximate solution is

$$u=\lim_{p\to1} v=v^{(0)}+pv^{(1)}+p^2v^{(2)}+p^3v^{(3)}+\ldots \tag{15}$$

The convergence of the above solution was discussed in Abdul-Sattar (2011).

3.3 Solution of the Contaminant flow problem by Homotopy perturbation method

By the Homotopy-perturbation transformation equation:

$$H(v,p)=(1-p)\left((1+\varepsilon)\frac{\partial C}{\partial t}\right)+p\left((1+\varepsilon)\frac{\partial C}{\partial t}+u\frac{\partial C}{\partial x}-D\frac{\partial^2 C}{\partial x^2}+\alpha C\right)=0 \quad (16)$$

Defining,

$$C(x,t)=v^{(0)}+pv^{(1)}+p^2v^{(2)}+p^3v^{(3)}+\ldots \quad (17)$$

Equation (18) is substituted in (17), we have

$$\begin{aligned}H(v,p)&=(1-p)\left((1+\varepsilon)\frac{\partial}{\partial t}\left(v^{(0)}+pv^{(1)}+p^2v^{(2)}+p^3v^{(3)}+\ldots\right)\right)\\&+p\begin{pmatrix}(1+\varepsilon)\frac{\partial}{\partial t}\left(v^{(0)}+pv^{(1)}+p^2v^{(2)}+p^3v^{(3)}+\ldots\right)+u\frac{\partial}{\partial x}\left(v^{(0)}+pv^{(1)}+p^2v^{(2)}+p^3v^{(3)}+\ldots\right)\\-D\frac{\partial^2}{\partial x^2}\left(v^{(0)}+pv^{(1)}+p^2v^{(2)}+p^3v^{(3)}+\ldots\right)+\alpha\left(v^{(0)}+pv^{(1)}+p^2v^{(2)}+p^3v^{(3)}+\ldots\right)\end{pmatrix}=0\end{aligned} \quad (18)$$

The following equations result from equating coefficients of corresponding terms on both sides of equation (18).

$$p^0:(1+\varepsilon)\frac{\partial}{\partial t}v^{(0)}(x,t)=0 \quad (19)$$

$$p^1:(1+\varepsilon)\frac{\partial}{\partial t}v^{(1)}(x,t)+u\frac{\partial}{\partial x}v^{(0)}(x,t)-D\frac{\partial^2}{\partial x^2}v^{(0)}(x,t)+\alpha v^{(0)}(x,t)=0 \quad (20)$$

$$p^2:(1+\varepsilon)\frac{\partial}{\partial t}v^{(2)}(x,t)+u\frac{\partial}{\partial x}v^{(1)}(x,t)-D\frac{\partial^2}{\partial x^2}v^{(1)}(x,t)+\alpha v^{(1)}(x,t)=0 \quad (21)$$

$$p^3:(1+\varepsilon)\frac{\partial}{\partial t}v^{(3)}(x,t)+u\frac{\partial}{\partial x}v^{(2)}(x,t)-D\frac{\partial^2}{\partial x^2}v^{(2)}(x,t)+\alpha v^{(2)}(x,t)=0 \quad (22)$$

$$p^4:(1+\varepsilon)\frac{\partial}{\partial t}v^{(4)}(x,t)+u\frac{\partial}{\partial x}v^{(3)}(x,t)-D\frac{\partial^2}{\partial x^2}v^{(3)}(x,t)+\alpha v^{(3)}(x,t)=0 \quad (23)$$

and so on.

The above equations (19)-(23) were solved successively and obtained the following results.

$$v^{(0)}(x,t) = Be^{-\lambda x} \tag{24}$$

$$v^{(1)}(x,t) = \frac{Be^{-\alpha x}\left(-\alpha + u\lambda + D\lambda^2\right)t}{1+\varepsilon} \tag{25}$$

$$v^{(2)}(x,t) = \frac{1}{2}\frac{Be^{-\lambda x}t^2\left(-\alpha + u\lambda + D\lambda^2\right)^2}{(1+\varepsilon)^2} \tag{26}$$

$$v^{(3)}(x,t) = \frac{1}{6}\frac{Be^{-\lambda x}t^3\left(-\alpha + u\lambda + D\lambda^2\right)^3}{(1+\varepsilon)^3} \tag{27}$$

$$C(x,t) = \lim_{p\to 1}\left(v^{(0)} + pv^{(1)} + p^2v^{(2)} + p^3v^{(3)} + ..\right) \tag{28}$$

Therefore,

$$C(x,t) = Be^{-\lambda x} + \frac{Be^{-\alpha x}\left(-\alpha + u\lambda + D\lambda^2\right)t}{1+\varepsilon} + \frac{1}{2}\frac{Be^{-\lambda x}t^2\left(-\alpha + u\lambda + D\lambda^2\right)^2}{(1+\varepsilon)^2} + \frac{1}{6}\frac{Be^{-\lambda x}t^3\left(-\alpha + u\lambda + D\lambda^2\right)^3}{(1+\varepsilon)^3} \tag{29}$$

3.4 Basic Idea of Variational iteration Method (VIM)

In order to throw light on the concept of Variational iteration Method (VIM), the following differential equation is considered:

$$Lu + Nu = g(t) \tag{30}$$

where L is a linear operator, N is a non-linear operator and $g(t)$ an inhomogeneous term. By VIM, the correctional functional can be constructed as follows:

$$U_{n+1}(t) = U_n(t) + \int_s^t \lambda\left(LU_n(s) + N\tilde{U}_n(s) - g(s)\right)ds \tag{31}$$

Where λ is the Lagrange multiplier (He, 2000), which can be obtained using the variational theory. The subscript n is the nth approximation and $\tilde{U}_n(s)$ is considered as the restricted variation (He, 2005).

3.5 Solution of the Contaminant Flow Problem by Variation of Parameter Method (VIM).

The transformed version of the equation (6) is solved by VIM as follows:

$$C_{n+1}(x,t) = C_n(x,t) + \int_0^t \lambda \begin{pmatrix} (1+\varepsilon)\frac{\partial}{\partial s}C_n(x,s) - D\frac{\partial^2}{\partial x^2}C_n(x,s) \\ + u\frac{\partial}{\partial x}C_n(x,s) + \alpha C_n(x,s) \end{pmatrix} ds \tag{32}$$

$$C_0(x,t) = Be^{-\lambda x} \tag{33}$$

The Lagrange multiplier is $\lambda = -1$ as obtained from the variational theory.

The iterations in equation (32) yield the following results:

$$C_1(x,t) = C_0(x,t) + \int_0^t (-1) \begin{pmatrix} (1+\varepsilon)\frac{\partial}{\partial s}C_0(x,s) - D\frac{\partial^2}{\partial x^2}C_0(x,s) \\ + u\frac{\partial}{\partial x}C_0(x,s) + \alpha C_0(x,s) \end{pmatrix} ds \tag{34}$$

i.e.,

$$C_1(x,t) = Be^{-\lambda x} + DB\lambda^2 e^{-\lambda x}t + uB\lambda e^{-\lambda x}t - \alpha B\lambda e^{-\lambda x}t \tag{35}$$

Further iterations give

$$C_2(x,t) = \frac{1}{2}Be^{-\lambda x}\begin{pmatrix} 2 + 2D\lambda^2 t + 2u\lambda t - 2\alpha t + t^2D^2\lambda^4 + 2t^2Du\lambda^3 - 2t^2D\alpha\lambda^2 \\ + t^2u^2\lambda^2 - 2t^2u\alpha\lambda + t^2\alpha^2 - 2t\varepsilon D\lambda^2 - 2t\varepsilon u\lambda + 2t\varepsilon\alpha \end{pmatrix} \tag{36}$$

$$C_3(x,t) = \frac{1}{6}Be^{-\lambda x}\begin{pmatrix} 6 + 3t^3u^2\lambda^4 D + 3t^3u\lambda^5 D^2 + 3t^3u\lambda\alpha^2 - 3t^3u^2\lambda^2\alpha \\ + 3t^3D\lambda^2\alpha^2 - 3t^3D^2\lambda^4\alpha - 6t^2D^2\lambda^4\varepsilon - 6t^2\varepsilon u^2\lambda^2 \\ + 6t\varepsilon^2 D\lambda^2 + 6t\varepsilon^2 u\lambda - t^3\alpha^3 - 12t^2D\lambda^3\varepsilon u + 12t^2\varepsilon u\alpha\lambda \\ + 12t^2D\lambda^2\varepsilon\alpha - 6t^3u\lambda^3 D\alpha + 6D\lambda^2 t + 6u\lambda t + 3t^2D^2\lambda^4 \\ + 3t^2u^2\lambda^2 + 6t\varepsilon\alpha - 6\alpha t + 3t^2\alpha^2 + 6t^2Du\lambda^3 - 6t^2D\alpha\lambda^2 \\ - 6t^2u\alpha\lambda - 6t\varepsilon D\lambda^2 - 6t\varepsilon u\lambda + t^3u^3\lambda^3 + t^3D^3\lambda^6 \\ + 6t^2\varepsilon\alpha^2 - 6t\varepsilon^2\alpha \end{pmatrix} \tag{37}$$

$$C_n(x,t)=\frac{1}{6}Be^{-\lambda x}\begin{pmatrix}6+3t^3u^2\lambda^4D+3t^3u\lambda^5D^2+3t^3u\lambda\alpha^2-3t^3u^2\lambda^2\alpha\\+3t^3D\lambda^2\alpha^2-3t^3D^2\lambda^4\alpha-6t^2D^2\lambda^4\varepsilon-6t^2\varepsilon u^2\lambda^2\\+6t\varepsilon^2D\lambda^2+6t\varepsilon^2u\lambda-t^3\alpha^3-12t^2D\lambda^3\varepsilon u+12t^2\varepsilon u\alpha\lambda\\+12t^2D\lambda^2\varepsilon\alpha-6t^3u\lambda^3D\alpha+6D\lambda^2t+6u\lambda t+3t^2D^2\lambda^4\\+3t^2u^2\lambda^2+6t\varepsilon\alpha-6\alpha t+3t^2\alpha^2+6t^2Du\lambda^3-6t^2D\alpha\lambda^2\\-6t^2u\alpha\lambda-6t\varepsilon D\lambda^2-6t\varepsilon u\lambda+t^3u^3\lambda^3+t^3D^3\lambda^6\\+6t^2\varepsilon\alpha^2-6t\varepsilon^2\alpha\end{pmatrix} \tag{38}$$

Therefore,

$$C(x,t)=\lim_{n\to\infty}C_n(x,t)$$

$$=\frac{1}{6}Be^{-\lambda x}\begin{pmatrix}6+3t^3u^2\lambda^4D+3t^3u\lambda^5D^2+3t^3u\lambda\alpha^2-3t^3u^2\lambda^2\alpha\\+3t^3D\lambda^2\alpha^2-3t^3D^2\lambda^4\alpha-6t^2D^2\lambda^4\varepsilon-6t^2\varepsilon u^2\lambda^2\\+6t\varepsilon^2D\lambda^2+6t\varepsilon^2u\lambda-t^3\alpha^3-12t^2D\lambda^3\varepsilon u+12t^2\varepsilon u\alpha\lambda\\+12t^2D\lambda^2\varepsilon\alpha-6t^3u\lambda^3D\alpha+6D\lambda^2t+6u\lambda t+3t^2D^2\lambda^4\\+3t^2u^2\lambda^2+6t\varepsilon\alpha-6\alpha t+3t^2\alpha^2+6t^2Du\lambda^3-6t^2D\alpha\lambda^2\\-6t^2u\alpha\lambda-6t\varepsilon D\lambda^2-6t\varepsilon u\lambda+t^3u^3\lambda^3+t^3D^3\lambda^6\\+6t^2\varepsilon\alpha^2-6t\varepsilon^2\alpha\end{pmatrix} \tag{39}$$

4. Results and discussion

The graphs in figures 1-6 were obtained using equations (29) and (39).

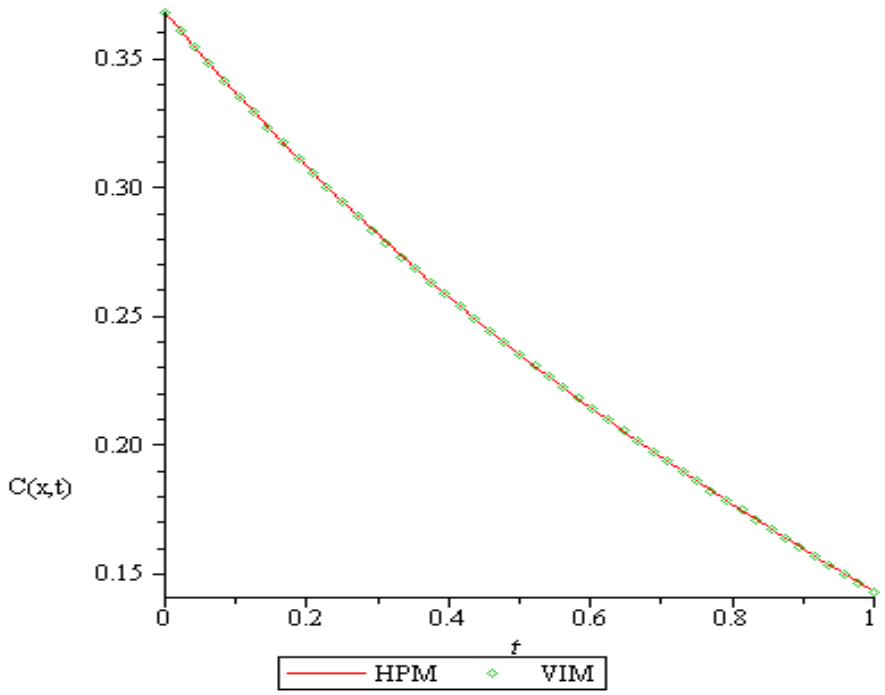

Figure 1: Graph of Concentration against time for the solution

obtained by VIM and HPM

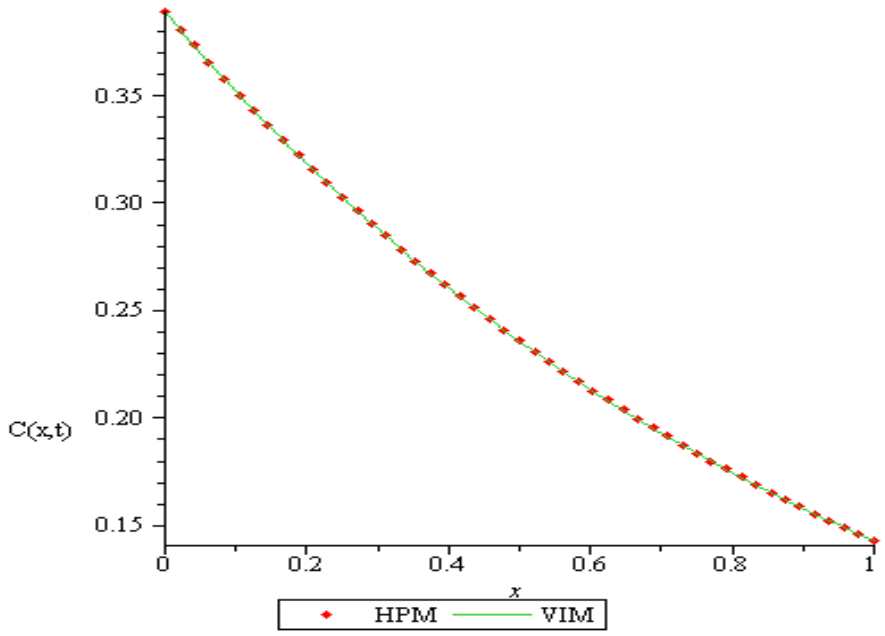

Figure 2: Graph of Concentration against distance for the solution obtained by VIM and HPM

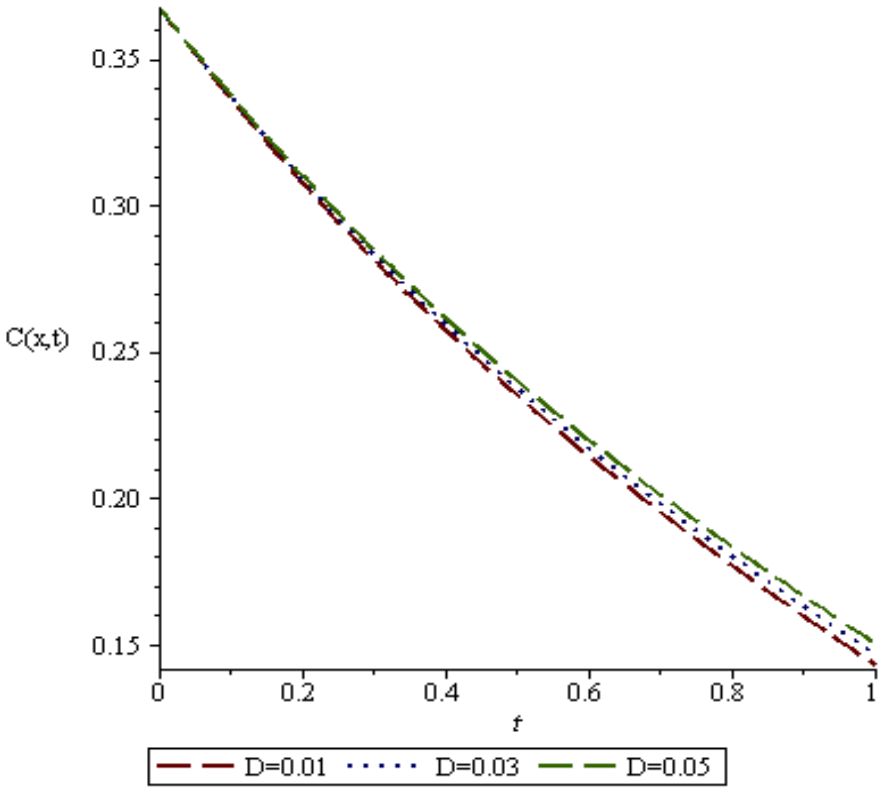

Figure 3: Concentration profile with time for varying dispersion coefficients

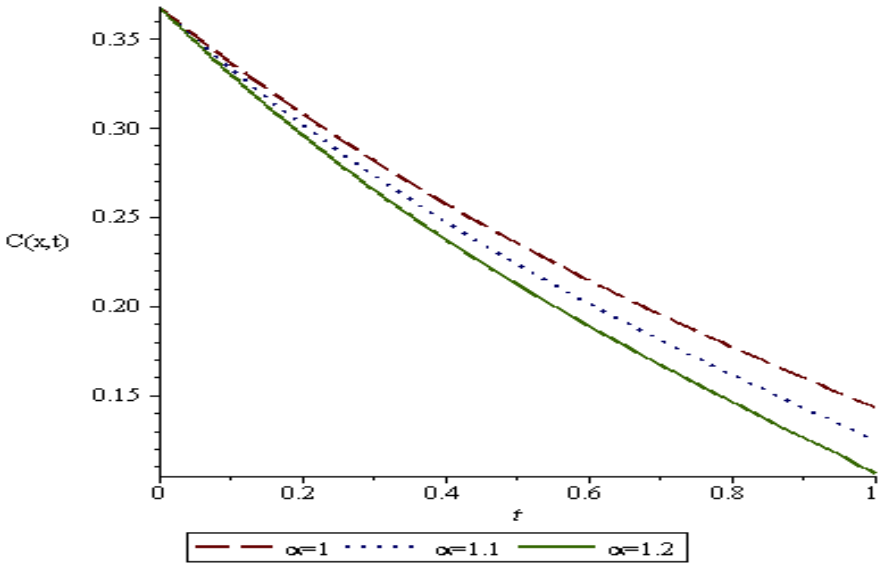

Figure 4: Concentration profile with time for varying decay parameter

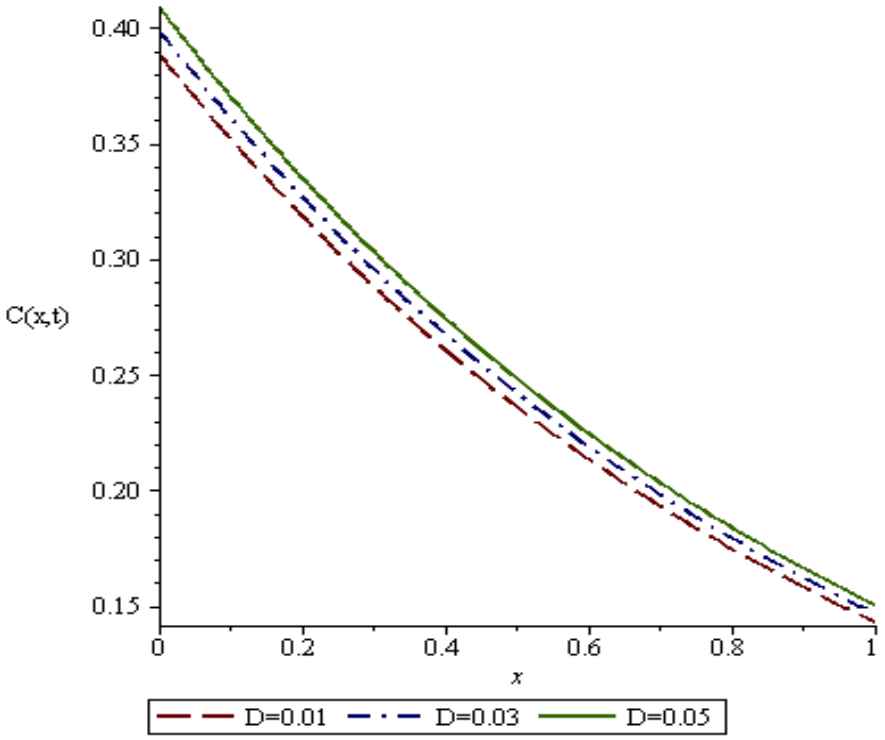

Figure 5: concentration profile with distance for varying dispersion coefficients

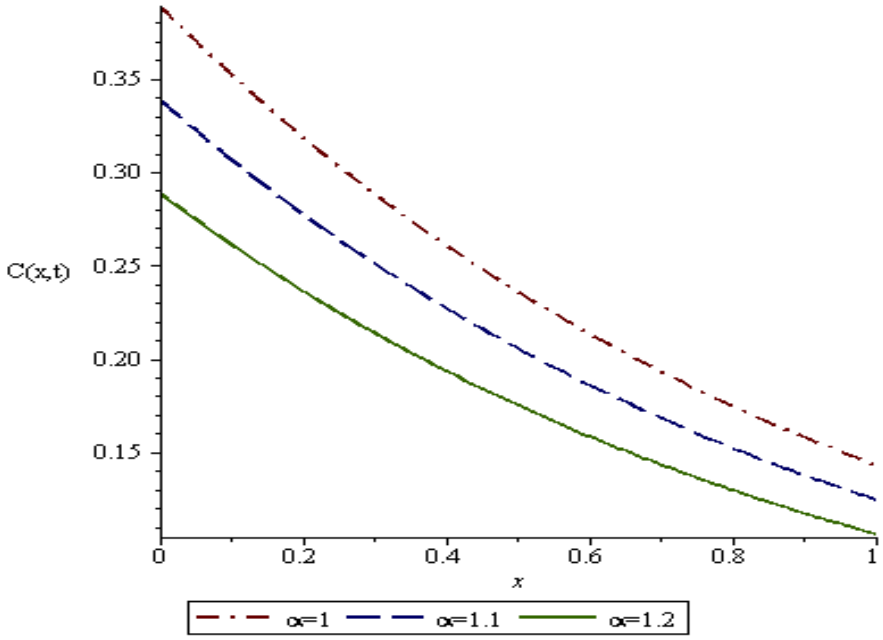

Figure 6: concentration profile with distance for varying dispersion coefficient

The graphs in figures 1 and 2 were plotted using the solutions obtained using HPM and VIM. The concentration profiles show how the two results overlapped. These show that the application of VIM performs equally as good as that of HPM. In both cases, the concentration of the contaminant decrease with increase in time and distance.

Figure 3 is the concentration profile with time for varying dispersion coefficient. The graph shows that as the dispersion coefficient decreases, the contaminant concentration decreases faster with time. Figure 4 is the graph of contaminant concentration against time for varying decay parameter. The graph shows that as the decay parameter increases, the contaminant concentration decreases faster with time.

Similarly, the concentration profile of the contaminant with distance for varying dispersion parameter is shown in figure 5. The graph shows that as the dispersion coefficient decreases, the contaminant concentration decreases with time. Lastly, figure 6 is the concentration profile of contaminant with distance for varying decay parameter. This shows the effect of varying the decay parameter. It shows that as the decay parameter decreases, the concentration of the contaminant decreases.

5. **Conclusion**

A one-dimensional contaminant flow model with non-zero initial concentration has been solved semi-analytically using the homotopy perturbation method and variational Iteration method. The study

shows that the result obtained from variational iteration method is as accurate as that of homotopy perturbation method. This can easily be seen from figures 1 and 2 as the graphs overlapped completely. The effects of change in the first order decay coefficients and the dispersion coefficient on the contaminant concentration along transient groundwater were shown in the figures 3 to 6. The study reveals that the contaminant concentration decreases with increase in time and distance from the origin.

References

Abdul-Sattar, J. Al-Saif, and Dhifaf, A. A (2011). The Homotopy Perturbation Method for Solving K(2,2) Equation. *Journal of Basrah Researches (Sciences).* 37(4):151-157..

Aiyesimi, Y. M. (2004): The mathematical analysis of environmental pollution of the Freudlich non-linear contaminant transport formulation. *Journal of Nigerian association of Mathematical physics,* 8: 83-86.

Aiyesimi, Y. M & Jimoh, O. R. (2012). "Computational Analysis of a One-dlmensional Non-linear Reactive Contaminant Flow with an Initial Continuous Point Source by Homotopy-perturbation Method". Journal of Nigerian Association of Mathematical Physics (JNAMP). 22: 543-546

Aiyesimi, Y. M & Jimoh, O. R. (2013). "A Homotopy-Perturbation Analysis of the Non-linear Contaminant Transport Problem in One Dimension with an Initial Continuous Point Source" Nigerian Journal of Technological Research (NJTR). 8(1): 43-46.

Bear, J (1997). *Hydraulics of groundwater.* McGraw-Hill, Newyork.

Clint N. D (1993): Analysis of an upwind-mixed finite element method for non-linear contaminant transport equations. *Society for industrial and applied Mathematics.*

He, J. H (2000). A coupling method of a Homotopy technique and a perturbation technique for nonlinear problems, International Journal of nonlinear Mechanics, 35: 37-43.

He, J. H (2005). Application of Homotopy perturbation to nonlinear wave equations, Chaos, Solitons Fractals, 26: 695-700.

Jimoh, O. R., Aiyesimi, Y. M., Jiya, M. and Bolarin, G. A. (2017): Semi-analytical Study of a One-dimensional Contaminant Flow in a Finite Medium. Journal of Science and Environmental Management. 21(3): 487-494.

Jiya, M. (2010). Application of Homotopy perturbation method for the solution of some Kumar, nonlinear differential equations. The pacific Journal of Science and Technology. 11(2): 268-272. http://www.akamaiuniversity.us/PJST.htm.

D. J and Kumar, A (2011): Analytical solution of advection-dispersion equation for varying pulse type input source in one dimension. *International Journal of Engineering, science and Technology*, 3: 22-29.

Makinde, O. D. and Chinyoka, T. (2010): Transient analysis of pollutants dispersion in a cylindrical pipe with a non-linear waste discharge concentration. *Computer and mathematics with applications*, 60:642-654.

Muhammad, A. N (2010). Iterative Methods for Nonlinear Equations Using Homotopy Perturbation Technique. Applied Mathematics & Information Sciences 4(2):27–235.

Okedayo, T. G. (2011): A regular perturbation of the nonlinear contaminant transport equation with an initial and instantaneous point source. *Australian Journal of Basic and applied sciences*, 5(8): 1273-1277.

Okedayo, G. T. and Aiyesimi, Y. M. (2005): The influence of retardation factors on the non-linear contaminant flow. *The Journal of education*, 4: 27-32.

Rajabi, A., Ganji, D. D and Taherian, H (2007). Application of homotopy-Perturbation method to nonlinear heat conduction and convection equations, International journal of nonlinear science and numerical simulation. 7(4): 413-420.

Ramakanta, M and Mehta, M. N. (2010): Effect of longitudinal dispersion of miscible fluid flow through porous media. Advanced theoretical and Applied Mechanics. 3(5):211-220.

Rezania, A., Ghorbali, A. R., Ganji, D. D and Bararnia, H (2009): Application on Homotopy perturbation and variational iteration methods for heat equation. *International journal of nonlinear science and numerical simulation.*(3): 1863-1874.

Singh, M. K. & Das, P. (2015). Scale dependent solute dispersion with linear isothern in heterogeneous medium. *Journal of Hydrology*, 520, 289-299.

Singh, M. K., Singh, P. S., Singh, V. P (2010): Analytical solutions of Solute transport along and against time dependent source concentration in homogeneous finite aquifer. *Advanced theoretical and applied Mechanics*. 3(3): 99-119.

Yadav, R. R., Kumar, D. J (2011): Two-dimensional analytical solutions for point source contaminants transport in semi-infinite homogeneous porous media. *Journal of Engineering*. 6(4): 459-468.

Boundary Value Technique for the Solution of Special Third Order Boundary Value Problems in Ordinary Differential Equations (ODEs)

Umaru Mohammed[1] Habibah Abdullah[2] Aliyu Alhaji Abdullahi[3] and Mikhail Semenov[4]
[1,2]Department of Mathematics, Federal University of Technology, Minna, Nigeria
[3]Department of Mechanical Engineering, Federal University of Technology, Minna, Nigeria
[4]School of Nuclear Science & Engineering, Tomsk Polytechnic University
[4]sme@tpu.ru
[3]aliuaabdullah@futminna.edu.ng
[2]bibalmaas@gmail.com
[1]umaru.mohd@futminna.edu.ng

Abstract

We develop a class of continuous modified multistep methods (CMMMs) which were use as boundary value methods for the numerical integration of special third order boundary value problems in ordinary differential equations. We investigate the basic properties of the methods and numerical experiments are given to show the performance of the approach.

Keywords: boundary value methods, continuous modified multistep methods

1. INTRODUCTION

Differential equations are important tools in solving real-world problems. These equations arise in several branches of sciences, engineering and technology, ranging from models that describe acoustic wave propagation in relaxing media, draining and coating flow problems to the deflection of a curved beam that has a constant or varying cross section. Boundary value problems also arise in these areas and as such numerical methods that are faster and accurate in solving them are of importance

Boundary value problems of third order have been discussed in many papers in recent years. Examples of such papers are (Abdullah *et al*2013; 2013) had developed a fifth order block method using constant step size with shooting technique to solve third order non-linear boundary value problems anddeveloped a fourth order two-point block method for solving non-linear third order boundary value problems.Khan and Aziz (2003) presented a forth order method that was based on quantic splines which was used to solve third order linear and non-linear boundary value problems. Collocation approximation was applied in deriving schemes that were applied as a block method to solve special third order initial value problems in Olabode (2009). Srivastava and Kumar (2011) andSahi*et al* (2013) had all worked in solving third order ordinary differential equations.Jator (2008) used a continuous linear multistep method to generate multiple finite difference methods that were assembled into a

single block matrix that was used to generate third order BVPs. A family of three step hybrid methods independent of first and second derivative components using Taylor approach were proposed to solve special third order ODEs in Jikantoro*et al* (2018), These were all done without reducing the ODEs to equivalent systems of first order ODEs.

Ahmed (2017) used the variational iteration method to get numerical solutions to third order ordinary boundary value problems after reducing them to a system of first order ODEs

In this paper, the considered special third order ordinary differential equation is of the form:

$$y''' = f(x,y), \qquad y(a) = y_0, y'(a) = \delta_0, y''(a) = \beta_0, y(b) = y_M \tag{1}$$

$$y''' = f(x,y), \qquad y(a) = y_0, y'(a) = \delta_0, y'(b) = y_M, y''(b) = y_N \tag{2}$$

2. METHODOLOGY

In this section, the construction of the continuous linear multistep methods via the interpolation and collocation approach is discussed, which will be used to produce several discreteschemes for solving (1) and (2)

Algorithm

Step 1: Construct the continuous LMM (CLMM) with continuous coefficients as:

$$U(x) = \alpha_v(x)y_{n+v} + \alpha_{v-1}(x)y_{n+v-1} + \alpha_0(x)y_n + h^3\sum_{j=0}^{k}\beta_j(x)f_{n+j} + h^3\beta_\mu(x)f_{n+\mu}, \tag{3}$$

Where $v = \begin{cases} \dfrac{k}{2} & for\ even\ k \\ \dfrac{k+1}{2} & for\ odd\ k \end{cases}$

Step 2: Obtain the main and additional methods by evaluating (3) in step 1 at x_{n+j} where

$$j = 1(1)2v,\ j \neq v-1, v$$

$$y_{n+j} + \alpha_v y_{n+v} + \alpha_{v-1}y_{n+v-1} + \alpha_0 y_n = h^3\sum_{i=o}^{k}\beta_i f_{n+i} + h^3\beta_w f_{n+w} \tag{4}$$

$$j = 1,\ldots,v-1, v+2,\ldots,2v$$

Step 3: Obtain the first and second derivative formulae which are used to obtain the additional methods by evaluating $U'(x)$ and $U''(x)$ at $x = x_{n+j}$, $j = 0(1)k$ as

$$U'(x) = \frac{1}{h}\left(\alpha_v'(x)y_{n+v} + \alpha_{v-1}'(x)y_{n+v-1} + \alpha_0'(x)y_n + h^3\sum_{i=0}^{k}\beta_i'(x)f_{n+i} + h^3\beta_\mu'(x)f_{n+\mu},\right)$$

$$U''(x) = \frac{1}{h^2}\left(\alpha_v''(x)y_{n+v} + \alpha_{v-1}''(x)y_{n+v-1} + \alpha_0''(x)y_n + h^3\sum_{i=0}^{k}\beta_i''(x)f_{n+i} + h^3\beta_\mu''(x)f_{n+\mu},\right)$$

by imposing that $U'(a) = y'_0, U'(b) = y'_N$ and $U''(a) = y''_0, U''(b) = y''_N$

Step 4: Combine the schemes obtained in steps 2 and 3 above to form a system of equations with form equivalent to $Ax = B$ where

$x = (M_0, M_1, M_2, \ldots, M_{N-1})^T$ and

$M_0 = (y_0, y_1, y_2, y_3)^T$, $M_1 = (y'_0, y'_1, y'_2, y'_3)^T$, $M_2 = (y''_0, y''_1, y''_2, y''_3)$

Step 5: Adopt matrix inversion algorithm to the system of equations in step 4 to obtain the values of the unknowns in the expected block method.

Theorem 2.1:*Let* $P_j(x) = 2xT_n(x) - T_{n-1}(x), n = 0(1)(k+3)$ *be the Chebyshev Polynomial used as basis function and W a vector given by* $W = (y_n, y_{n+v-1}, y_{n+v}, f_n, f_{n+1}, \ldots, f_k)^T$ *where T is the transpose. Consider the matrix V defined as*

$$V = \begin{pmatrix} P_0(x_n) & P_1(x_n) & \ldots & P_{k+3}(x_n) \\ P_0(x_{n+v-1}) & P_1(x_{n+v-1}) & \ldots & P_{k+3}(x_{n+v-1}) \\ P_0(x_{n+v}) & P_1(x_{n+v}) & \ldots & P_{k+3}(x_{n+v}) \\ P''_0(x_n) & P''_1(x_n) & \ldots & P'''_{k+3}(x_n) \\ P''_0(x_{n+1}) & P''_1(x_{n+1}) & \ldots & P'''_{k+3}(x_{n+1}) \\ \vdots & \vdots & \vdots & \vdots \\ P''_0(x_{n+\mu}) & P''_1(x_{n+\mu}) & \ldots & P'''_{k+3}(x_{n+\mu}) \\ P''_0(x_{n+k}) & P''_1(x_{n+k}) & \ldots & P'''_{k+3}(x_{n+k}) \end{pmatrix}$$

and V_j *obtained by replacing the jth column of V by the vector W and let (3) satisfy the following conditions*

$$U(x_{n+j}) = y_{n+j} \quad j = 0, v-1, v$$

$$U'''(x_{n+j}) = f_{n+j} \qquad j = 0(1)k \tag{4}$$

then the continuous representation (3) is equivalent to

$$U(x) = \sum_{j=0}^{k+4} \frac{\det(V_j)}{\det(V)} P_j(x) \tag{5}$$

Assuming the basis functions as

$$\begin{cases} \alpha_j(x) = \sum_{i=0}^{k+4} \alpha_{i+1,j} P_i(x), \\ h^3\beta_j(x) = \sum_{i=0}^{k+4} h^3 \beta_{i+1.j} P_i(x), \\ h^3\beta_\mu(x) == \sum_{i=0}^{k+4} h^3 \beta_{i+1.\mu} P_i(x), \end{cases} \tag{6}$$

where $\alpha_{i+1,j}$, $\beta_{i+1.j}$, $\beta_{i+1.\mu}$, are coefficients to be determined.

Substituting (6) into (3) yields

$$U(x) = \sum_{i=0}^{k+4} \alpha_{i+1,v} P_i(x) y_{n+v} + \sum_{i=0}^{k+4} \alpha_{i+1,v-1} P_i(x) y_{n+v-1} + \sum_{i=0}^{k+4} \alpha_{i+1,0} P_i(x) y_n +$$
$$h^3 \sum_{j=0}^{k} \sum_{i=0}^{k+4} \beta_{i+1,j} P_i(x) f_{n+j} + h^3 \sum_{i=1}^{k+4} \beta_{i+1,\mu} P_i(x) f_{n+\mu},$$

which is simplified as

$$U(x) = \sum_{i=0}^{k+4} \left\{ \alpha_{i+1,v} y_{n+v} + \alpha_{i+1,v-1} y_{n+v-1} + \alpha_{i+1,0} y_n + \sum_{j=0}^{k} h^3 \beta_{i+1,j} f_{n+j} + h^3 \beta_{i+1,w} f_{n+w} \right\} P_i(x)$$
$$\approx U(x) = \sum_{i=0}^{k+4} \Gamma_i P_i(x) \tag{7}$$

where $\Gamma_i = \alpha_{i+1}, 0, y_n, \ldots$

imposing conditions (4) on (7), we obtain a system of (k+5) equations which can be expressed as $VH = W$ where $H = (\Gamma_0, \Gamma_1, \Gamma_2, \ldots, \Gamma_{k+4})^T$ is a vector of (k+5) undetermined coefficients.

We proceed to find the elements of H using Cramer's rule, thus;

$$\Gamma_i = \frac{\det(V_j)}{\det(V)}, j = 0(1)(k+3)$$

replacing the jth column of V by W gives the value of V_j

$$\Rightarrow U(x) = \sum_{i=0}^{k+4} \frac{\det(V_j)}{\det(V)} P_i(x)$$

3. SPECIFICATION OF THE METHODS

Evaluating the CMMM (3) at $x_{n+i,} i = 1, \ldots, v-2, v+1, \ldots, k$ and using it to obtain the first derivative formulae given by

$$U'(x) = \frac{1}{h}\left(\alpha'_v(x) y_{n+v} + \alpha'_{v-1}(x) y_{n+v-1} + \alpha'_0(x) y_n + h^3 \sum_{j=0}^{k} \beta'_j(x) f_{n+j} + h^3 \beta'_w(x) f_{n+w}, \right) \tag{8}$$

effectively applied by imposing

$$U'(a) = y'_0, U'(b) = y'_N \tag{9}$$

to produce derivative formula of the form (8). The second derivative formula is also obtained from (3), this is given by

$$U''(x) = \frac{1}{h^2}\left(\alpha''_v(x) y_{n+v} + \alpha''_{v-1}(x) y_{n+v-1} + \alpha''_0(x) y_n + h^3 \sum_{j=0}^{k} \beta''_j(x) f_{n+j} + h^3 \beta''_w(x) f_{n+w}, \right) \tag{10}$$

effectively imposed by applying

$$U''(a) = y''_0, U''(b) = y''_N \tag{11}$$

to generate the formulae in (10)

4. CONVERGENCE OF THE METHOD

Here the convergence of the method is established. The equation (3) is evaluated at x_{n+1}, x_{n+2},…, x_{n+v-2}, x_{n+v+1},…, $x_{n+\omega}$, x_{n+2v} to give

$$y_{n+1} + \alpha_v^{(1)} y_{n+v} + \alpha_{v-1}^{(1)} y_{n+v-1} + \alpha_0^{(1)} y_0 = h^3 \sum_{i=0}^{k} \beta_i^{(1)} f_{n+i} + h^3 \beta_\omega^{(1)} f_{n+\omega}$$

$$y_{n+2} + \alpha_v^{(2)} y_{n+v} + \alpha_{v-1}^{(2)} y_{n+v-1} + \alpha_0^{(2)} y_0 = h^3 \sum_{i=0}^{k} \beta_i^{(2)} f_{n+i} + h^3 \beta_\omega^{(2)} f_{n+\omega}$$

$$\vdots$$

$$y_{n+v-2} + \alpha_v^{(v-2)} y_{n+v} + \alpha_{v-1}^{(v-2)} y_{n+v-1} + \alpha_0^{(v-2)} y_0 = h^3 \sum_{i=0}^{k} \beta_i^{(v-2)} f_{n+i} + h^3 \beta_\omega^{(v-2)} f_{n+\omega} \tag{12}$$

$$y_{n+v+1} + \alpha_v^{(v+1)} y_{n+v} + \alpha_{v-1}^{(v+1)} y_{n+v-1} + \alpha_0^{(v+1)} y_0 = h^3 \sum_{i=0}^{k} \beta_i^{(v+1)} f_{n+i} + h^3 \beta_\omega^{(v+1)} f_{n+\omega}$$

$$\vdots$$

$$y_{n+\omega} + \alpha_v^{(\omega)} y_{n+v} + \alpha_{v-1}^{(\omega)} y_{n+v-1} + \alpha_0^{(\omega)} y_0 = h^3 \sum_{i=0}^{k} \beta_i^{(\omega)} f_{n+i} + h^3 \beta_\omega^{(\omega)} f_{n+\omega}$$

$$y_{n+k} + \alpha_v^{(k)} y_{n+v} + \alpha_{v-1}^{(k)} y_{n+v-1} + \alpha_0^{(k)} y_0 = h^3 \sum_{i=0}^{k} \beta_i^{(k)} f_{n+i} + h^3 \beta_\omega^{(k)} f_{n+\omega}$$

$U'(x)$ is evaluated at x_{n+j} $j = 0(1)k$ and $x_{n+\omega}$ to give

$$hy'_n + \alpha_v'^{(0)} y_{n+v} + \alpha_{v-1}'^{(0)} y_{n+v-1} + \alpha_0'^{(0)} y_n = h^3 \sum_{i=0}^{k} \beta_i'^{(0)} f_{n+i} + h^3 \beta_\omega'^{(0)} f_{n+\omega}$$

$$hy'_n + \alpha_v'^{(1)} y_{n+v} + \alpha_{v-1}'^{(1)} y_{n+v-1} + \alpha_0'^{(1)} y_n = h^3 \sum_{i=0}^{k} \beta_i'^{(1)} f_{n+i} + h^3 \beta_\omega'^{(1)} f_{n+\omega}$$

$$\vdots \qquad (13)$$

$$hy'_n + \alpha_v'^{(\omega)} y_{n+v} + \alpha_{v-1}'^{(\omega)} y_{n+v-1} + \alpha_0'^{(\omega)} y_n = h^3 \sum_{i=0}^{k} \beta_i'^{(\omega)} f_{n+i} + h^3 \beta_\omega'^{(\omega)} f_{n+\omega}$$

$$hy'_n + \alpha_v'^{(k)} y_{n+v} + \alpha_{v-1}'^{(k)} y_{n+v-1} + \alpha_0'^{(k)} y_n = h^3 \sum_{i=0}^{k} \beta_i'^{(k)} f_{n+i} + h^3 \beta_\omega'^{(k)} f_{n+\omega}$$

And also evaluate $U''(x)$ to give

$$hy''_n + \alpha_v''^{(0)} y_{n+v} + \alpha_{v-1}''^{(0)} y_{n+v-1} + \alpha_0''^{(0)} y_n = h^3 \sum_{i=0}^{k} \beta_i''^{(0)} f_{n+i} + h^3 \beta_\omega''^{(0)} f_{n+\omega}$$

$$hy''_n + \alpha_v''^{(1)} y_{n+v} + \alpha_{v-1}''^{(1)} y_{n+v-1} + \alpha_0''^{(1)} y_n = h^3 \sum_{i=0}^{k} \beta_i''^{(1)} f_{n+i} + h^3 \beta_\omega''^{(1)} f_{n+\omega}$$

$$\vdots \qquad (14)$$

$$hy''_n + \alpha_v''^{(\omega)} y_{n+v} + \alpha_{v-1}''^{(\omega)} y_{n+v-1} + \alpha_0''^{(\omega)} y_n = h^3 \sum_{i=0}^{k} \beta_i''^{(\omega)} f_{n+i} + h^3 \beta_\omega''^{(\omega)} f_{n+\omega}$$

$$hy''_n + \alpha_v''^{(k)} y_{n+v} + \alpha_{v-1}''^{(k)} y_{n+v-1} + \alpha_0''^{(k)} y_n = h^3 \sum_{i=0}^{k} \beta_i''^{(k)} f_{n+i} + h^3 \beta_\omega''^{(k)} f_{n+\omega}$$

All the equations in (12) to (14) are of order $O(h^{k+})$ and can be compactly written in matrix form by introducing the following notations. Let P be a $3N \times 3N$ matrix defined by

$$P = \begin{pmatrix} P_{11} & P_{12} & P_{13} \\ P_{21} & P_{22} & P_{23} \\ P_{31} & P_{32} & P_{33} \end{pmatrix}$$ where P_{ij} are $N \times N$ matrices given as

$$P_{11}=\begin{pmatrix}
 & \alpha'^{(0)}_{v-1} & \alpha'^{(0)}_{v} & & \alpha'^{(0)}_{0} & & \\
 & \alpha''^{(0)}_{v-1} & \alpha''^{(0)}_{v} & & \alpha''^{(0)}_{0} & & \\
1 & \alpha^{(1)}_{v-1} & \alpha'^{(1)}_{v} & & \alpha^{(1)}_{0} & & \\
1 & \alpha^{(2)}_{v-1} & \alpha'^{(2)}_{v} & & \alpha^{(2)}_{0} & & \\
 & \vdots & \vdots & & \vdots & & \\
1 & \alpha^{(v-1)}_{v-1} & \alpha^{(v-1)}_{v} & & \alpha^{(v-1)}_{0} & & \\
1 & \alpha^{(v)}_{v-1} & \alpha^{(v)}_{v} & & \alpha^{(v)}_{0} & & \\
 & \vdots & \vdots & & \vdots & & \\
 1 & \alpha^{(k)}_{v-1} & \alpha^{(k)}_{v} & & \alpha^{(k)}_{0} & & \\
 & & & & \alpha'^{(0)}_{v-1} & \alpha'^{(0)}_{v} & \alpha'^{(0)}_{0} \\
 & & & 1 & \alpha^{(1)}_{v-1} & \alpha'^{(1)}_{v} & \alpha^{(1)}_{0} \\
 & & & & & \vdots & \vdots \\
 & & 1 & & \alpha^{(v-1)}_{v-1} & \alpha^{(v-1)}_{v} & \alpha^{(0)}_{0} \\
 & & 1 & & \alpha^{(v)}_{v-1} & \alpha^{(v)}_{v} & \alpha^{(v)}_{0} \\
 & & & & & \ddots & \ddots \\
 & & & 1 & \alpha^{(k)}_{v-1} & \alpha^{(k)}_{v} & \alpha^{(k)}_{0}
\end{pmatrix}$$

$$P_{21}=\begin{pmatrix}
\alpha'^{(1)}_{v-1} & \alpha'^{(1)}_{v} & \alpha'^{(1)}_{0} & & & \\
\alpha'^{(2)}_{v} & \alpha'^{(2)}_{v} & \alpha'^{(2)}_{0} & & & \\
\vdots & \vdots & \vdots & & & \\
\alpha'^{(k)}_{v-1} & \alpha'^{(k)}_{v} & \alpha'^{(k)}_{0} & & & \\
 & & & \alpha'^{(1)}_{v-1} & \alpha'^{(1)}_{v} & \alpha'^{(1)}_{0} \\
 & & & \ddots & \ddots & \ddots \\
 & & & \alpha'^{(k)}_{v-1} & \alpha'^{(k)}_{v} & \alpha'^{(2v)}_{0}
\end{pmatrix}$$

$$P_{31}=\begin{pmatrix}
\alpha''^{(1)}_{v-1} & \alpha''^{(1)}_{v} & \alpha''^{(1)}_{0} & & & \\
\alpha''^{(2)}_{v} & \alpha''^{(2)}_{v} & \alpha''^{(2)}_{0} & & & \\
\vdots & \vdots & \vdots & & & \\
\alpha''^{(k)}_{v-1} & \alpha''^{(k)}_{v} & \alpha''^{(k)}_{0} & & & \\
 & & & \alpha''^{(1)}_{v-1} & \alpha''^{(1)}_{v} & \alpha''^{(1)}_{0} \\
 & & & \ddots & \ddots & \ddots \\
 & & & \alpha''^{(k)}_{v-1} & \alpha''^{(k)}_{v} & \alpha''^{(2v)}_{0}
\end{pmatrix}$$

P_{12}, P_{13}, P_{23}, P_{32}, are $N\times N$ null matrices and P_{22}, P_{33} are $N\times N$ identity matrices. Similarly, another matrix Q which is a $3N\times 3N$ matrix defined as

$$Q=\begin{pmatrix}Q_{11} & Q_{12} & Q_{13}\\ Q_{21} & Q_{22} & Q_{23}\\ Q_{31} & Q_{32} & Q_{33}\end{pmatrix}$$

Where Q_{ij} are $N \times N$ matrices given as

$$Q_{11} = \begin{pmatrix} \beta_1'^{(0)} & \beta_2'^{(0)} & \cdots & \beta_k'^{()} & & & & & \\ \beta_1''^{()} & \beta_2''^{()} & \cdots & \beta_k''^{()} & & & & & \\ \beta_1^{(1)} & \beta_2^{(1)} & \cdots & \beta_k^{(1)} & & & & & \\ \vdots & \vdots & \cdots & \vdots & & & & & \\ \beta_1^{(v-2)} & \beta_2^{(v-2)} & \cdots & \beta_k^{(v-2)} & & & & & \\ \beta_1^{(v+1)} & \beta_2^{(v+1)} & \cdots & \beta_k^{(v+1)} & & & & & \\ \vdots & \vdots & \cdots & \vdots & & & & & \\ \beta_1^{(k)} & \beta_2^{(k)} & \cdots & \beta_k^{(k)} & & & & & \\ & & & & \beta_0'^{(0)} & \beta_1'^{(0)} & \cdots & \beta_k'^{(0)} & \\ & & & & \beta_0'^{(0)} & \beta_1'^{(1)} & \cdots & \beta_k'^{(1)} & \\ & & & & \vdots & \vdots & \cdots & \vdots & \\ & & & & \beta_0^{(v-2)} & \beta_1^{(v-2)} & \cdots & \beta_k^{(v-2)} & \\ & & & & \beta_0^{(v+1)} & \beta_1^{(v+1)} & \cdots & \beta_k^{(v+1)} & \\ & & & & \vdots & \vdots & \cdots & \vdots & \\ & & & & \beta_0^{(k)} & \beta_1^{(k)} & \cdots & \beta_k^{(k)} & \\ & & & & & \ddots & \ddots & \ddots & \\ & & & & & & \beta_0^{(k)} & \beta_1^{(k)} & \cdots & \beta_k^{(k)} \end{pmatrix}$$

$$Q_{21} = \begin{pmatrix} \beta_1'^{(1)} & \beta_2'^{(1)} & \cdots & \beta_k'^{(1)} & & & & \\ \vdots & \vdots & \cdots & \vdots & & & & \\ \beta_1'^{(k)} & \beta_2'^{(k)} & \cdots & \beta_k'^{(1)} & & & & \\ & & & & \beta_0'^{(1)} & \beta_1'^{(1)} & \cdots & \beta_k'^{(1)} \\ & & & & \vdots & \vdots & \cdots & \vdots \\ & & & & \beta_0'^{(k)} & \beta_1'^{(k)} & \cdots & \beta_k'^{(k)} \\ & & & & & \ddots & \ddots & \ddots \\ & & & & & & \beta_0'^{(k)} & \beta_1'^{(k)} & \cdots & \beta_k'^{(k)} \end{pmatrix}$$

$$Q_{31} = \begin{pmatrix} \beta_1''^{(1)} & \beta_2''^{(1)} & \cdots & \beta_k''^{(1)} & & & & \\ \vdots & \vdots & \cdots & \vdots & & & & \\ \beta_1''^{(k)} & \beta_2''^{(k)} & \cdots & \beta_k''^{(1)} & & & & \\ & & & & \beta_0''^{(1)} & \beta_1''^{(1)} & \cdots & \beta_k''^{(1)} \\ & & & & \vdots & \vdots & \cdots & \vdots \\ & & & & \beta_0''^{(k)} & \beta_1''^{(k)} & \cdots & \beta_k''^{(k)} \\ & & & & & \ddots & \ddots & \ddots \\ & & & & & & \beta_0''^{(k)} & \beta_1''^{(k)} & \cdots & \beta_k''^{(k)} \end{pmatrix}$$

$Q_{12},\ Q_{13},\ Q_{22}, Q_{23},\ Q_{32}, Q_{33}$ are $N \times N$ null matrices

And then the following vectors are defined

$$\bar{Y} = (y_{n+1},\ldots, y_{n+k}, hy'_{n+1},\ldots, hy'_{n+k}, h^2 y''_{n+1},\ldots, h^2 y''_{n+k})^T$$

$$Y = (y(x_{n+1}),\ldots, y(x_{n+k}), hy'(x_{n+1}),\ldots, hy'(x_{n+k}), h^2 y''(x_{n+1}),\ldots, h^2 y''(x_{n+k}))^T$$

$$F = (f_{n+1},\ldots, f_{n+2v}, hf'_{n+1},\ldots, hf'_{n+k}, h^2 f''_{n+1},\ldots, h^2 f''_{n+k})^T$$

$$L(h) = (l_1,\ldots, l_N, l'_1,\ldots, l'_N, l''_1,\ldots, l''_N)^T$$

$$C = (\beta_0'^{(0)} h^3 f_0 - hy'_0, \beta_0''^{(0)} h^3 f_0 - hy''_0, \beta_0^{(0)} h^3 f_0 - y_0, \beta_0^{(1)} h^3 f_0,\ldots, \beta_0^{(v-2)} h^3 f_0, \beta_0^{(v+1)} h^3 f_0,\ldots,$$
$$\beta_0^{(k)} h^3 f_0, 0,\ldots, 0, \beta_0'^{(1)} h^3 f_0 - \alpha_0'^{(1)} y_0, \beta_0'^{(k)} h^3 f_0 - \alpha_0'^{(k)} y_0, 0,\ldots 0, \beta_0''^{(1)} h^3 f_0 - \alpha_0''^{(1)} y_0,$$
$$\beta_0''^{(k)} h^3 f_0 - \alpha_0''^{(k)} y_0, 0,\ldots 0)^T$$

With $L(h)$ representing the local truncation error vector at the point x_n of the methods (12) to (14).

Theorem 4.1: Let (y_i, y'_i, y''_i) be an approximation to the solution vector $(y(x_i), y'(x_i), y''(x_i))$ for the systems (1) and (2). If $e_i = |y(x_i) - y_i|, e'_i = |y'(x_i) - y'_i|, e''_i = |y''(x_i) - y''_i|$, where the exact solution given by the vector $(y(x), y'(x), y''(x))$ is several times differentiable and if $\|E\| = \|Y - \bar{Y}\|$, then the BVMs are said to be convergent of order $k+1$ which implies that

$\|E\| = O(h^{k+1})$, where k is the step number.

Proof: Consider the exact form of the system formed from (12) to (14) and given by

$$PY - h^3 QF(Y) + C + L(h) = 0 \qquad (15)$$

where $L(h)$ is the truncation error vector obtained from the formulas (12) to (14). The approximate form of the system is given by

$$P\bar{Y} - h^3 QF(\bar{Y}) + C = 0 \qquad (16)$$

where $\bar{Y}$ is the approximate solution of vector Y.

Subtracting (15) from (16) and letting $E = |\bar{Y} - Y| = (e_1,\ldots e_N, e'_1,\ldots e'_N, e''_1,\ldots e''_N)^T$ and using the mean value theorem, we have the error system

$$(P - h^3 QB)E = L(h) \qquad (17)$$

where B is the Jacobian matrix and its entries $B_{rs}, r, s = 1,2,3,$ are defined as

$$B_{rs} = \begin{pmatrix} \frac{\partial f_1^{(r-1)}}{\partial y_1^{(s-1)}} & \cdots & \frac{\partial f_1^{(r-1)}}{\partial f_N^{(s-1)}} \\ \vdots & \vdots & \vdots \\ \frac{\partial f_N^{(r-1)}}{\partial f_1^{(s-1)}} & \cdots & \frac{\partial f_N^{(r-1)}}{\partial f_N^{(s-1)}} \end{pmatrix}$$

From (16) and $L(h)$

$$E = (P - h^3 QB)^{-1} L(h)$$

$$E = SL(h)$$

$$\|E\| = \|SL(h)\|$$

$$= O(h^{-3})O(h^{k+4})$$

$$= O(h^{k+1})$$

Which show that the methods are convergent and the global errors are of order $O(h^{k+1})$

Numerical Examples

Here, two numerical examples are considered.

Problem 1: Consider the third order boundary value problem (Jator*et al*, 2018)

$$y'''(x) - xy(x) = (x^3 - 2x^2 - 5x - 3)e^x, 0 \prec x \prec 1$$

$$y(0) = y(1) = 0, y'(0) = 1$$

Exact: $y(x) = (x - x^2)e^x$

The problem above was solved using the proposed method and the behaviour of the method was observed. The results gotten are compared with the results in Jator (2018) and the results gotten from the Extended Trapezoidal Methods (ETRs). Maximum of absolute error was obtained within the interval of integration. It is observed from Table 1 that the proposed methods did better than the methods of Jator (2018) and the ETRs in terms of accuracy.

Table 1: Comparison of the Proposed Methods, Jator (2018) and ETRs

N	Proposed Method	Jator (2018)	ETRs
6	8.33E-07	1.525E-05	1.089E-02
12	2.06E-08	9.257E-07	7.666E-05

24	7.0E-10	5.873E-08	5.108E-06
48	6.52E-11	3.683E-09	3.300E-07
96	4.31E-12	2.305E-10	2.098E-08
192	2.13E-13	1.428E-11	1.323E-09

Problem 2: $y''' = -2e^{-3y} + \frac{4}{(1+x)^3}, y(0) = 0, y(1) = \ln 2, y'(0) = 1, 0 \le x \le 1$

Exact: $y(x) = \ln(1+x)$

The proposed method was applied to the problem above and the results were compared to the results in Mohammed (2016). The maximum error was also obtained within the interval of integration. Table 2 suggests that the proposed methods generate results that are at least of approximate accuracy with Mohammed (2016).

Table 2: Comparison of the Proposed Methods and Mohammed (2016).

N	Proposed Method	Mohammed (2016)
6	1.24E-06	1.079E-06
9	-	1.290E-07
12	3.93E-08	2.770E-08
15	-	8.990E-09
24	2.45E-10	-
48	9.32E-12	-
96	4.69E-14	-
192	8.38E-16	-

Note tha:t Mohammed proposed a three step method with one off grid point for the solution of third order ODEs

5. CONCLUSION

In this paper, CMMMs have been proposed using the boundary value technique to integrate special third order boundary value problems in ordinary differential equations. This has been done without reducing the differential equations to systems of first order ODEs. The convergence of this class of methods was carried out and numerical examples were given. The efficiency of the methods was given in the tables 1 and 2. A future research will be carried out based on applying this approach to higher order ODEs while increasing the number of off grid points.

REFERENCES

Abdullah, A. S., Majid, Z. A. andSenu, N. (2013) Solving Third Order Boundary Value Problemwith Fifth Order Block Method. *Mathematical Methods in Engineering and Economics,* ISBN: 978-1-61804-230-9

Abdullah, A. S., Majid, Z. A. andSenu, N. (2013). Solving Third Order Boundary Value Problem Using Fourth Order Block Method. *Applied Mathematical Sciences,*Vol. 7(53), 2629-2645

Ahmed, J. (2017). Numerical Solutions of Third-Order Boundary Value Problems Associated with Draining and Coating Flows. *Kyungpook Mathematical Journal,* Vol. 57,651-665

Brugnano, L. andTrigiante, D. (1998).*Solving Differential Problems by Multistep Initial and Boundary Value Problems*. Gordon and Breach Science Publishers, London

Khan, A. and Aziz, T. (2003). The Numerical Solution of Third-Order Boundary Value Problems Using Quintic Splines. *Applied Mathematics and Computation,*Vol. 137, 253-260

Jator, S. N. (2008). On the Numerical Integration of Third Order Boundary Value Problems by a Linear Multistep Method. *International Journal of Pure and Applied Mathematics,* Vol. 46(3), 375-388

Jator, S., Okunlola, T., Biala, T., andAdeniyi, R. (2018). Direct Integrators for the General Third-Order Ordinary Differential Equations with an Application to the Korteweg–de Vries Equation. *Int. J. Appl. Comput. Math,* Vol. 4, 110

Jikantoro, Y. D., Ismail, F., Senu, N. & Ibrahim, Z. B. (2018). A New Integrator for Special Third Order Differential Equations with Application to Thin Film Flow Problem. *Indian J. Pure Appl. Math.,* Vol. 49(1), 151-167

Mohammed, U. (2016). *A Class of Block Hybrid Linear Multistep Methods for Solution of Second and Third Order Ordinary Differential Equations*. A PhD thesis submitted to the University of Ilorin, Ilorin, Nigeria

Olabode, B. T. (2009). An Accurate Scheme by Block Method for Third Order Ordinary Differential Equations.The Pacific Journal of Science and Technology, Vol. 10(1), 136-142

Sahi, R. K., Jator, S. N. and Khan, N. A. (2013). Continuous Fourth Derivative Method for Third Order Boundary Value Problems. International Journal of Pure and Applied Mathematics, *International Journal of Pure and Applied Mathematics,* Vol. 85(5), 907-923

Srivastava, P. K. and Kumar, M. (2011). Numerical Treatment of Nonlinear Third Order Boundary Value Problem. *Applied Mathematics,* Vol. 2, 959-964

A Note on the Existence of Unique Solution of In-Situ Combustion Oil Shale In Porous Medium

Oyubu, J.P.; Olayiwola, R. O.; Yahaya, Y.A.; Cole A. T

Department of Mathematics,
Federal University of Technology, Minna, Nigeria.
E-mail.: oyubuj@yahoo.com **Phone No:** +234-806-342-2423

Abstract

This paper establishes the criteria for the existence of unique solution of the equations governing the in-situ combustion of oil shale and examines the properties of solution. Our proof revealed that velocity, mass and temperature are increasing function of time.

Keywords and phrases: combustion, In-situ, oil recovery, oil shale, porous medium.

1. Introduction

Oil shale gains attention as a potential abundant source of oil whenever the price of crude oil rises. Though, oil shale mining and processing raise a number of environmental concerned such as land use, waste disposal, water use, waste-water management, greenhouse- gas emissions and air pollution. Oil shale is found all over the world, including China, Israel, and Russia. The United States, however, has the most shale resources. However, all the types of kerogen consist mainly of hydrocarbons; smaller amounts of sulphur, oxygen and nitrogen; and a variety of minerals.(Abdelrahman, 2015).

Deposits of oil shale have been found in 27 countries worldwide. Oil shale becomes an important alternative energy due to its huge reserves. It is quite possible to satisfy the future oil requirement. Upon being heated, kerogen in oil shale can be converted to oil and gas. The heating process is called pyrolysis or retorting (Zheng *et al*., 2017).

In situ processes introduce heat to the oil shale which is still embedded in its natural geological formation. One of the in situ methods is the in- situ combustion (ISC). In-situ combustion is simply combustion heating of in-place oil shale within a deposit at the fire front. The main idea in in-situ combustion is burning of a portion of oil shale to produce sufficient heat to retort the remainder. A great portion of the potentially recoverable shale oil resource is in low-grade deposits that may never be recovered by primary mining techniques. In-situ processing presents the opportunity of recovering shale oil from these low-grade deposits without the adverse environmental impacts normally related with mining and above ground processing which comprises three steps: conduction heating, hot gas injection, and in situ combustion. In the step of conduction heating, oil shale is heated, in the second step, hot gas is injected into the oil shale layer and the surrounding cool oil shale would be heated. In-situ combustion is the process whereby hot air is injected into the oil shale layer in order to react the organic component (kerogen). The combustion reaction produces enough heat to propagate with a combustion wave leading to cracking and vaporizations of lighter components. The pyrolysis of oil

shale is triggered by the combustion reactions in the absence of extra heat supply. Shale oil is obtained through the pyrolysis process (Zheng *et al*., 2017).

Several works have been done on the in-situ combustion of oil shale. Lapene *et al.* (*2007)* modeled coupled mass and heat transport in reactive porous medium using homogeneous description at a Darcy-scale. Local non-equilibrium transport of heat was treated with a two field temperature, one for the gas and one for the solid phase.

Olayiwola *et al*. (2011) extended Lapene *et al*.(2007) model to a situation where there is Arrhenius heat generation and chemical reaction. They made additional assumption that the reaction is in steady-state so that time derivatives are zero $\left(\frac{\partial}{\partial t}=0\right)$. They examined the properties of solution of the model and obtained the analytical solution using asymptotic expansion.

In another development, Olayiwola *et al*. (2012) studied coupled heat transport in Arrhenius reactive porous medium using a homogeneous description at the Darcy-scale. They assumed that there is a perfect contact between gas and solid phase. Eigenfunctions expansion technique was used and the outcome showed that the heat transfer increases as Frank-Kamenetskii number increases and scaled thermal conductivity decreases.

Zheng *et al.* (2017) focused on the numerical simulation of in situ combustion of oil shale. Numerical test was used for the stimulation of oil shale and their result showed that varying gas injection rate and oxygen was important in the field test in-situ combustion.

This paper aim at establish the criteria for the existence of unique solution and examine the properties of solution of the equations governing the in-situ combustion of oil shale as enhanced oil recovery technique in a porous medium.

3.0 Model Formulation

Here, we extend Olayiwola *et al*. (2012) model by incorporating combustion front velocity. Then, the equations that describe the in-situ combustion of oil shale are:

The continuity equation:

$$\frac{\partial \rho}{\partial t}+\frac{\partial\left(\rho u_c\right)}{\partial x}=0 \tag{1}$$

The momentum equation:

$$\rho\left(\frac{\partial u_c}{\partial t}+\frac{\partial u_c}{\partial x}\right)=-\frac{\partial p}{\partial x}+\frac{\partial}{\partial x}\left(\mu\frac{\partial u_c}{\partial x}\right) \tag{2}$$

Gas phase energy equation:

$$\left.\begin{aligned}\rho_g \varepsilon c_g\left(\frac{\partial \mathrm{T}_g}{\partial t}-u_c\frac{\partial \mathrm{T}_g}{\partial x}\right)+\rho_g \varepsilon c_g u_f\frac{\partial \mathrm{T}_g}{\partial x}=\frac{\partial}{\partial x}\left(\kappa_g\frac{\partial \mathrm{T}_g}{\partial x}\right)+\Gamma\left(\mathrm{T}_g-\mathrm{T}_s\right)+h\left(\mathrm{T}_e-\mathrm{T}_g\right)+\\ \varepsilon\Delta \mathrm{HAC}_f^{\alpha}C_{ox}^{\beta}e^{-\frac{\mathrm{E}}{R\mathrm{T}_s}}\end{aligned}\right\} \quad (3)$$

The solid phase energy equation:

$$\left.\rho_s(1-\varepsilon)c_s\left(\frac{\partial \mathrm{T}_s}{\partial t}-u_c\frac{\partial \mathrm{T}_s}{\partial x}\right)=\frac{\partial}{\partial x}\left(\kappa_s\frac{\partial \mathrm{T}_s}{\partial x}\right)-\Gamma\left(\mathrm{T}_g-\mathrm{T}_s\right)+h\left(\mathrm{T}_e-\mathrm{T}_s\right)+(1-\varepsilon)\Delta \mathrm{HAC}_f^{\alpha}C_{ox}^{\beta}e^{-\frac{\mathrm{E}}{R\mathrm{T}_s}}\right\} \quad (4)$$

The oxygen mass balance:

$$\varepsilon\rho_g\left(\frac{\partial C_{ox}}{\partial t}-u_c\frac{\partial C_{ox}}{\partial x}\right)+\varepsilon\rho_g u_f\frac{\partial C_{ox}}{\partial x}=\rho_g\varepsilon\frac{\partial}{\partial x}\left(D_{ox}\frac{\partial C_{ox}}{\partial x}\right)+\varepsilon \mathrm{AC}_f^{\alpha}C_{ox}^{\beta}e^{-\frac{\mathrm{E}}{R\mathrm{T}_s}} \quad (5)$$

The fuel mass balance:

$$(1-\varepsilon)\rho_g\left(\frac{\partial C_f}{\partial t}-u_c\frac{\partial C_f}{\partial x}\right)=(1-\varepsilon)\mathrm{AC}_f^{\alpha}C_{ox}^{\beta}e^{-\frac{\mathrm{E}}{R\mathrm{T}_s}} \quad (6)$$

Darcy's law

$$u_f=-\frac{\mathrm{K}}{\mu}\left(\frac{\partial \mathrm{P}}{\partial x}-\rho_g\nabla \mathrm{Z}\right) \quad (7)$$

Where

A is the frequency, E is the activation energy, α and β are orders of the gaseous reaction, ρ_g is gas density, R is the gas constant, u_c is combustion front velocity, κ_s is thermal conductivity of solid phase, κ_g is thermal conductivity of gas phase, μ is viscosity, t is time, x is position, ε is the porosity, c_s is heat capacity of solid phase, c_g is the heat capacity of gas phase, T_e is the external temperature, T_s is the temperature of solid phase, T_g is the temperature of gas phase, $\Delta \mathrm{H}$ is heat generation constant, h is heat transfer coefficient, C_{ox} is concentration of oxygen, C_f is fuel concentration, Γ is exchange term between the phases, K is the permeability , D_{ox} is the diffusion of oxygen, u_f is filtration velocity and P is the pressure.

3.1 Coordinate Transformation

Here, we shall neglect the gravitational effect due to the small size in the vertical direction and we let $\rho_g = \rho_s = \rho.$ it simple to eliminate the continuity equation (1) by means of streamline function

$$\eta(x,t) = \left(\rho^2\right)^{-\frac{1}{2}} \int_0^x \rho(s,t)ds \tag{8}$$

Then, the coordinate transformation becomes

$$\frac{\partial}{\partial x} \to \frac{\partial}{\partial \eta}\frac{\partial \eta}{\partial x} = \frac{\partial}{\partial \eta} \tag{9}$$

$$\frac{\partial}{\partial t} \to \frac{\partial}{\partial \eta}\frac{\partial \eta}{\partial t} + \frac{\partial}{\partial t} = -u_c \frac{\partial}{\partial \eta} + \frac{\partial}{\partial t} \tag{10}$$

Using the equations (9) and (10) can be simplified as:

$$\rho \frac{\partial u_c}{\partial t} = -\frac{\partial \mathrm{P}}{\partial \eta} + \frac{\partial}{\partial \eta}\left(\mu \frac{\partial u_c}{\partial \eta}\right) \tag{11}$$

$$\left.\begin{aligned} &\rho \varepsilon c_g \left(\frac{\partial \mathrm{T}_g}{\partial t} - 2u_c \frac{\partial \mathrm{T}_g}{\partial \eta}\right) + \rho \varepsilon c_g u_f \frac{\partial \mathrm{T}_g}{\partial \eta} = \frac{\partial}{\partial \eta}\left(\kappa_g \frac{\partial \mathrm{T}_g}{\partial \eta}\right) + \Gamma\left(\mathrm{T}_g - \mathrm{T}_s\right) + h\left(\mathrm{T}_e - \mathrm{T}_g\right) + \\ &\varepsilon \Delta \mathrm{H} A C_f^{\alpha} C_{ox}^{\beta} e^{-\frac{\mathrm{E}}{\mathrm{RT}_s}} \end{aligned}\right\} \tag{12}$$

$$\left.\begin{aligned} &\rho(1-\varepsilon)c_s \left(\frac{\partial \mathrm{T}_s}{\partial t} - 2u_c \frac{\partial \mathrm{T}_s}{\partial \eta}\right) = \frac{\partial}{\partial \eta}\left(\kappa_s \frac{\partial \mathrm{T}_s}{\partial \eta}\right) - \Gamma\left(\mathrm{T}_g - \mathrm{T}_s\right) + h\left(\mathrm{T}_e - \mathrm{T}_s\right) + \\ &(1-\varepsilon)\Delta \mathrm{H} A C_f^{\alpha} C_{ox}^{\beta} e^{-\frac{\mathrm{E}}{\mathrm{RT}_s}} \end{aligned}\right\} \tag{13}$$

$$\rho\varepsilon\left(\frac{\partial C_{ox}}{\partial t} - 2u_c \frac{\partial C_{ox}}{\partial \eta}\right) + \varepsilon\rho u_f \frac{\partial C_{ox}}{\partial \eta} = \rho\varepsilon \frac{\partial}{\partial \eta}\left(D_{ox} \frac{\partial C_{ox}}{\partial \eta}\right) + \varepsilon A C_f^{\alpha} C_{ox}^{\beta} e^{-\frac{\mathrm{E}}{\mathrm{RT}_s}} \tag{14}$$

$$(1-\varepsilon)\rho\left(\frac{\partial C_f}{\partial t} - 2u_c \frac{\partial C_f}{\partial \eta}\right) = (1-\varepsilon) A C_f^{\alpha} C_{ox}^{\beta} e^{-\frac{\mathrm{E}}{\mathrm{RT}_s}} \tag{15}$$

$$\frac{\partial \mathrm{P}}{\partial \eta} = -\frac{\mu}{\mathrm{K}} u_f \tag{16}$$

Here, we assume the porous space of the medium is filled initially with fuel and oxygen. The initial and boundary conditions were formulated as follows:

Initial conditions:

At $t=0$ and $\forall \eta$

$$u_c = u_{inj} \;\; \mathrm{T}_g = \mathrm{T}_0, \; C_{ox} = 0, \; C_f = C_{f0} \tag{17}$$

Boundary conditions:

$$\left.\begin{aligned} &\left.\frac{\partial \mathrm{T}_s}{\partial \eta}\right|_{\eta=0} = 0, \;\; \left.\frac{\partial \mathrm{T}_s}{\partial \eta}\right|_{\eta=L} = 0 \\ &\left.\mathrm{T}_g\right|_{\eta=0} = \mathrm{T}_{inj}, \;\; \left.\frac{\partial \mathrm{T}_g}{\partial \eta}\right|_{\eta=L} = 0 \\ &\left.C_{ox}\right|_{\eta=0} = C_{ox0}, \;\; \left.\frac{\partial C_{ox}}{\partial \eta}\right|_{\eta=L} = 0 \\ &\left.u_c\right|_{\eta=0} = u_{inj}, \;\; \left.u_c\right|_{\eta=L} = 0 \\ &\left.C_f\right|_{\eta=0} = C_{f0} \\ &\left.\mathrm{P}\right|_{\eta=L} = \mathrm{P}_{outlet} \end{aligned}\right\} \tag{18}$$

3.2 Existence and Uniqueness of solution

To Scientists and Engineers, the question of existence and uniqueness of solution remain to be a pivot in models and designs. When a problem is formulated we need to examine the solution(s) so as to predict the behavior of such solution(s). We are interested in the existence and uniqueness of solution of the system of equations (11) – (16) satisfying (17) and (18) in order to be able to predict the behavior of the solution. First, in the absence of convection and combustion front and assuming no thermal exchange and no heat transfer between phases. We let $\kappa_s, \kappa_g, D_{ox}$ be constants and we shall follow the approach used by Olayiwola (2015).

Theorem 3.1: let, $D_{ox} = \dfrac{\mathrm{K}_g}{\rho c_g} = D_1$ Then there exists a unique solution of problem (11) – (16) satisfy (17) and (18)

Proof: let, $D_{ox} = \dfrac{\mathrm{K}_g}{\rho c_g} = D_1, \;\; \psi = \left(\mathrm{T}_g - \dfrac{\Delta \mathrm{H}}{c_g} C_{ox}\right)$ and $\varphi = \left(\mathrm{T}_s - \dfrac{\Delta \mathrm{H}}{c_s} C_f\right)$

Then (19) – (22) become

$$\frac{\partial \psi}{\partial t} = D_1 \frac{\partial^2 \psi}{\partial \eta^2} \tag{19}$$

$$\psi(\eta,0)=\mathrm{T}_0, \quad \psi(0,t)=\left(\mathrm{T}_{inj} - \frac{\Delta \mathrm{H}}{c_g} C_{ox0}\right), \quad \psi_\eta(L,t)=0 \tag{20}$$

and

$$\frac{\partial \varphi}{\partial t} = \mathrm{K}_1 \frac{\partial^2 \mathrm{T}_s}{\partial \eta^2} \tag{21}$$

$$\varphi(\eta,0)=\left(\mathrm{T}_0 - \frac{\Delta \mathrm{H}}{c_s} C_{f0}\right), \quad \left.\frac{\partial \mathrm{T}_s}{\partial \eta}\right|_{\eta=0} = 0, \quad \left.\frac{\partial \mathrm{T}_s}{\partial \eta}\right|_{\eta=L} = 0 \tag{22}$$

Using Eigenfunction expansion technique, we obtain the solution of the problem (19) and (20) as

$$\psi(\eta,t)=\sum_{n=1}^{\infty} \frac{4\mathrm{T}_0}{(2n-1)\pi} e^{-D_1\left(\frac{(2n-1)\pi}{2L}\right)^2 t} \sin\left(\frac{(2n-1)\pi}{2L} x\right) \tag{23}$$

and by direct integration, we obtain the solution of problem (21) and (22) as

$$\varphi(\eta,t)=\left(\mathrm{T}_0 - \frac{\Delta \mathrm{H}}{c_s} C_{f0}\right) \tag{24}$$

Then, we obtain

$$\mathrm{T}_g(\eta,t)=\sum_{n=1}^{\infty} \frac{4\mathrm{T}_0}{(2n-1)\pi} e^{-D_1\left(\frac{(2n-1)\pi}{2L}\right)^2 t} \sin\left(\frac{(2n-1)\pi x}{2L}\right) + \frac{\Delta \mathrm{H}}{c_g} C_{ox}(\eta,t) \tag{25}$$

$$C_{ox}(\eta,t)=\frac{c_g}{\Delta \mathrm{H}}\left(\mathrm{T}_g(\eta,t) - \sum_{n=1}^{\infty} \frac{4\mathrm{T}_0}{(2n-1)\pi} e^{-D_1\left(\frac{(2n-1)\pi}{2L}\right)^2 t} \sin\left(\frac{(2n-1)\pi x}{2L}\right)\right) \tag{26}$$

$$\mathrm{T}_s(\eta,t)=\left(\mathrm{T}_0 - \frac{\Delta \mathrm{H}}{c_s} C_{f0}\right) + \frac{\Delta \mathrm{H}}{c_s} C_f(\eta,t), \tag{27}$$

$$C_f(\eta,t)=\frac{c_s}{\Delta \mathrm{H}}\left(\left(\mathrm{T}_s(\eta,t) - \left(\mathrm{T}_0 - \frac{\Delta \mathrm{H}}{c_s} C_{f0}\right)\right)\right) \tag{28}$$

Hence, there exists a unique solution of problem (11) – (16). This completes the proof.

We shall now consider an alternative method for the existence of unique solution of the problem.

Before delving into the method, we shall substitute the solutions (26) - (28) into the equations (11) - (16).

Therefore, the equation (11) – (16) in dimensionless form become:

$$\frac{\partial u}{\partial t}=-\frac{\partial \mathrm{P}}{\partial \eta}+\frac{1}{\mathrm{Re}}\frac{\partial}{\partial \eta}\left(\mu\frac{\partial u}{\partial \eta}\right) \tag{29}$$

$$\left.\begin{aligned}&\frac{\partial \phi}{\partial t}-2u\frac{\partial \phi}{\partial \eta}+v\frac{\partial \phi}{\partial \eta}=\frac{1}{\mathrm{Pe}}\frac{\partial}{\partial \eta}\left(\lambda_g\frac{\partial \phi}{\partial \eta}\right)+\sigma\left(\phi-\theta\right)+\gamma\left(a-\phi\right)+\delta\left(b\theta+C_{f0}\right)^{\alpha}\\&\left(c\phi+d\left(1-\sum_{n=1}^{\infty}\frac{4}{(2n-1)\pi}e^{-\frac{1}{\mathrm{Pem}}\left(\frac{(2n-1)\pi}{2}\right)^2 t}\sin\left(\frac{(2n-1)\pi\eta}{2}\right)\right)\right)^{\beta}e^{\frac{\theta}{1+\epsilon\theta}}\end{aligned}\right\} \tag{30}$$

$$\left.\begin{aligned}&\frac{\partial \theta}{\partial t}-2u\frac{\partial \theta}{\partial \eta}=\frac{1}{\mathrm{Pe}}\frac{\partial}{\partial \eta}\left(\lambda_s\frac{\partial \theta}{\partial \eta}\right)-\sigma_1\left(\phi-\theta\right)+\gamma_1\left(a_1-\phi\right)+\delta_1\left(b_1\theta+C_{f0}\right)^{\alpha}\\&\left(c_1\phi+d_1\left(1-\sum_{n=1}^{\infty}\frac{4}{(2n-1)\pi}e^{-\frac{1}{\mathrm{Pem}}\left(\frac{(2n-1)\pi}{2}\right)^2 t}\sin\left(\frac{(2n-1)\pi\eta}{2}\right)\right)\right)^{\beta}e^{\frac{\theta}{1+\epsilon\theta}}\end{aligned}\right\} \tag{31}$$

$$\left.\begin{aligned}&\frac{\partial \mathrm{X}}{\partial t}-2u\frac{\partial \mathrm{X}}{\partial \eta}+v\frac{\partial \mathrm{X}}{\partial \eta}=\frac{1}{\mathrm{Pem}}\frac{\partial}{\partial \eta}\left(D\frac{\partial \mathrm{X}}{\partial \eta}\right)+\delta_2\left(b_2\theta+C_{f0}\right)^{\alpha}\\&\left(c_2\phi+d_2\left(1-\sum_{n=1}^{\infty}\frac{4}{(2n-1)\pi}e^{-\frac{1}{\mathrm{Pem}}\left(\frac{(2n-1)\pi}{2}\right)^2 t}\sin\left(\frac{(2n-1)\pi\eta}{2}\right)\right)\right)^{\beta}e^{\frac{\theta}{1+\epsilon\theta}}\end{aligned}\right\} \tag{32}$$

$$\left.\begin{aligned}&\frac{\partial \mathrm{Y}}{\partial t}-2u\frac{\partial \mathrm{Y}}{\partial \eta}=\delta_3\left(b_3\theta+C_{f0}\right)^{\alpha}\\&\left(c_3\phi+d_3\left(1-\sum_{n=1}^{\infty}\frac{4}{(2n-1)\pi}e^{-\frac{1}{\mathrm{Pem}}\left(\frac{(2n-1)\pi}{2}\right)^2 t}\sin\left(\frac{(2n-1)\pi\eta}{2}\right)\right)\right)^{\beta}e^{\frac{\theta}{1+\epsilon\theta}}\end{aligned}\right\} \tag{33}$$

$$v=-Da\,\mathrm{Re}\eta\left(1-\eta\right) \tag{34}$$

With initial and boundary conditions

$$\left.\begin{aligned}
&\phi(\eta,0)=0, \quad \phi(0,t)=q, \quad \left.\frac{\partial\phi}{\partial\eta}\right|_{\eta=1}=0\\
&\theta(\eta,0)=0, \quad \left.\frac{\partial\theta}{\partial\eta}\right|_{\eta=0}=0 \quad \left.\frac{\partial\theta}{\partial\eta}\right|_{\eta=1}=0,\\
&\mathrm{X}(\eta,0)=0, \quad \mathrm{X}(0,t)=1, \quad \left.\frac{\partial \mathrm{X}}{\partial\eta}\right|_{\eta=1}=0\\
&\mathrm{Y}(\eta,0)=1, \quad \mathrm{Y}(0,t)=1\\
&\left.\mathrm{P}\right|_{\eta=1}=q_1\\
&u(\eta,0)=1,\ \left.u\right|_{\eta=0}=1,\ \left.u\right|_{\eta=1}=0
\end{aligned}\right\} \qquad (35)$$

Where

$\mathrm{Re}=\dfrac{\rho L u_{inj}}{\mu_0}=\dfrac{Lu_{inj}}{\upsilon}=$ Reynolds number, $pe=\dfrac{\rho\varepsilon c_g L u_{inj}}{\kappa_{g0}}$ = Peclet number, $pem=\dfrac{Lu_{inj}}{D_1}=$ Mass transfer peclet number, $\sigma=\dfrac{\Gamma L}{\rho\varepsilon c_g u_{inj}}$ = Heat exchange coefficient,

$\gamma=\dfrac{hL}{\rho\varepsilon c_g u_{inj}}$, $\delta=\dfrac{L\Delta \mathrm{HA}}{\rho c_g \in \mathrm{T}_0 u_{inj}} e^{-\frac{\mathrm{E}}{R\mathrm{T}_0}}$ = Frank-kameneskii parameter, $a=\dfrac{\mathrm{T}_e-\mathrm{T}_0}{\in \mathrm{T}_0}$, $b=\dfrac{c_s \in \mathrm{T}_0}{\Delta \mathrm{H}}$

$pem=\dfrac{Lu_{inj}}{D_1}=$ Mass transfer peclet number, $c=\dfrac{c_g \in \mathrm{T}_0}{\Delta \mathrm{H}}$, $d=\dfrac{c_g \mathrm{T}_0}{\Delta \mathrm{H}}$

We let $\dfrac{\partial \mathrm{P}}{\partial\eta}=\eta(1-\eta)$ and consider the following asymptotic expansion of temperatures θ and ϕ and concentrations X and Y and velocity u in $\in$

Let

$$\left.\begin{aligned}
u&=u_0+\in u_1+\ldots\\
\theta&=\theta_0+\in\theta_1+\ldots\\
\mathrm{X}&=\mathrm{X}_0+\in \mathrm{X}_1+\ldots\\
\mathrm{Y}&=\mathrm{Y}_0+\in \mathrm{Y}_1+\ldots
\end{aligned}\right\} \qquad (36)$$

and equate the powers of $\in$ in equation (29) – (35), we have

$\in^0$:

$$\frac{\partial u_0}{\partial t}=\frac{1}{\mathrm{Re}}\frac{\partial^2 u_0}{\partial \eta^2}-\eta(1-\eta) \tag{37}$$

$$\left.\begin{aligned}\frac{\partial \phi_0}{\partial t}&=\frac{1}{\mathrm{Pe}}\frac{\partial^2 \phi_0}{\partial \eta^2}+2u_0\frac{\partial \phi_0}{\partial \eta}+Da\,\mathrm{Re}\,\eta(1-\eta)\frac{\partial \phi_0}{\partial \eta}+\sigma(\phi_0-\theta_0)+\gamma(a-\phi_0)+\delta(b\theta_0+C_{f0})^{\alpha}\\ &\left(c\phi_0+d\left(1-\sum_{n=1}^{\infty}\frac{4}{(2n-1)\pi}e^{-\frac{1}{\mathrm{Pem}}\left(\frac{(2n-1)\pi}{2}\right)^2 t}\sin\left(\frac{(2n-1)\pi\eta}{2}\right)\right)\right)^{\beta}e^{\theta_0}\end{aligned}\right\} \tag{38}$$

$$\left.\begin{aligned}\frac{\partial \theta_0}{\partial t}&=\frac{1}{\mathrm{Pe}}\frac{\partial^2 \theta_0}{\partial \eta^2}+2u_0\frac{\partial \theta_0}{\partial \eta}+Da\,\mathrm{Re}\,\eta(1-\eta)\frac{\partial \theta_0}{\partial \eta}+\sigma_1(\phi_0-\theta_0)+\gamma_1(a-\phi_0)+\delta_1(b_1\theta_0+C_{f0})^{\alpha}\\ &\left(c_1\phi_0+d_1\left(1-\sum_{n=1}^{\infty}\frac{4}{(2n-1)\pi}e^{-\frac{1}{\mathrm{Pem}}\left(\frac{(2n-1)\pi}{2}\right)^2 t}\sin\left(\frac{(2n-1)\pi\eta}{2}\right)\right)\right)^{\beta}e^{\theta_0}\end{aligned}\right\} \tag{39}$$

$$\left.\begin{aligned}\frac{\partial \mathrm{X}_0}{\partial t}&=\frac{1}{\mathrm{Pem}}\frac{\partial^2 \mathrm{X}_0}{\partial \eta^2}+2u_0\frac{\partial \mathrm{X}_0}{\partial \eta}+Da\,\mathrm{Re}\,\eta(1-\eta)\frac{\partial \mathrm{X}_0}{\partial \eta}+\delta_2(b_2\theta_0+C_{f0})^{\alpha}\\ &\left(c_2\phi_0+d_2\left(1-\sum_{n=1}^{\infty}\frac{4}{(2n-1)\pi}e^{-\frac{1}{\mathrm{Pem}}\left(\frac{(2n-1)\pi}{2}\right)^2 t}\sin\left(\frac{(2n-1)\pi\eta}{2}\right)\right)\right)^{\beta}e^{\theta_0}\end{aligned}\right\} \tag{40}$$

$$\left.\begin{aligned}\frac{\partial \mathrm{Y}_0}{\partial t}&=2u_0\frac{\partial \mathrm{Y}_0}{\partial \eta}+\delta_3(b_3\theta_0+C_{f0})^{\alpha}\\ &\left(c_3\phi_0+d_3\left(1-\sum_{n=1}^{\infty}\frac{4}{(2n-1)\pi}e^{-\frac{1}{\mathrm{Pem}}\left(\frac{(2n-1)\pi}{2}\right)^2 t}\sin\left(\frac{(2n-1)\pi\eta}{2}\right)\right)\right)^{\beta}e^{\theta_0}\end{aligned}\right\} \tag{41}$$

$$\left.\begin{aligned}
&\phi_0(\eta,0)=0, \quad \phi_0(0,t)=q, \quad \left.\frac{\partial\phi_0}{\partial\eta}\right|_{\eta=1}=0\\
&\theta_0(\eta,0)=0, \quad \left.\frac{\partial\theta_0}{\partial\eta}\right|_{\eta=0}=0 \quad \left.\frac{\partial\theta_0}{\partial\eta}\right|_{\eta=1}=0,\\
&\mathrm{X}_0(\eta,0)=0, \quad \mathrm{X}_0(0,t)=1, \quad \left.\frac{\partial \mathrm{X}_0}{\partial\eta}\right|_{\eta=1}=0\\
&\mathrm{Y}_0(\eta,0)=1, \quad \mathrm{Y}_0(0,t)=1\\
&u_0(\eta,0)=1,\ u_0\Big|_{\eta=0}=1,\ u_0\Big|_{\eta=1}=0
\end{aligned}\right\} \tag{42}$$

$\in^1$:

$$\frac{\partial u_1}{\partial t}=\frac{1}{\mathrm{Re}}\left(\frac{\partial u_0}{\partial\eta}\right)^2+\frac{1}{\mathrm{Re}}\frac{\partial^2 u_0}{\partial\eta^2}+\frac{u_0}{\mathrm{Re}}\frac{\partial^2 u_0}{\partial\eta^2} \tag{43}$$

$$\left.\begin{aligned}
&\frac{\partial\phi_1}{\partial t}=\frac{1}{Pe}\left(\frac{\partial\phi_0}{\partial\eta}\right)^2+\frac{1}{Pe}\frac{\partial^2\phi_0}{\partial\eta^2}+\frac{\phi_0}{Pe}\frac{\partial^2\phi_0}{\partial\eta^2}+2u_1\frac{\partial\phi_1}{\partial\eta}+Da\,\mathrm{Re}\,\eta(1-\eta)\frac{\partial\phi_1}{\partial\eta}+\sigma(\phi_1-\theta_1)-\gamma\phi_1+\\
&c\delta\beta\phi_1(b\theta_0+C_{f0})^{\alpha}\left(c\phi_0+d\left(1-\sum_{n=1}^{\infty}\frac{4}{(2n-1)\pi}e^{-\frac{1}{\mathrm{Pem}}\left(\frac{(2n-1)\pi}{2}\right)^2 t}\sin\left(\frac{(2n-1)\pi\eta}{2}\right)\right)\right)^{\beta-1}e^{\theta_0}+\\
&b\delta\alpha\theta_1(b\theta_0+C_{f0})^{\alpha-1}\\
&\left(c\phi_0+d\left(1-\sum_{n=1}^{\infty}\frac{4}{(2n-1)\pi}e^{-\frac{1}{pem}\left(\frac{(2n-1)\pi}{2}\right)^2 t}\sin\left(\frac{(2n-1)\pi\eta}{2}\right)\right)\right)^{\beta}e^{\theta_0}+\theta_1e^{\theta_0}-\theta_0^2e^{\theta_0}
\end{aligned}\right\} \tag{44}$$

$$\left.\begin{aligned}
&\frac{\partial\theta_1}{\partial t}=\frac{1}{Pe}\left(\frac{\partial\theta_0}{\partial\eta}\right)^2+\frac{1}{Pe}\frac{\partial^2\theta_0}{\partial\eta^2}+\frac{\theta_0}{Pe}\frac{\partial^2\theta_0}{\partial\eta^2}+2u_1\frac{\partial\theta_1}{\partial\eta}+\sigma_1(\phi_1-\theta_1)-\gamma\theta_1+c_1\delta_1\beta\phi_1(b\theta_0+C_{f0})^{\alpha}\\
&\left(c_1\phi_0+d_1\left(1-\sum_{n=1}^{\infty}\frac{4}{(2n-1)\pi}e^{-\frac{1}{\mathrm{Pem}}\left(\frac{(2n-1)\pi}{2}\right)^2 t}\sin\left(\frac{(2n-1)\pi\eta}{2}\right)\right)\right)^{\beta-1}e^{\theta_0}+b_1\delta_1\alpha\theta_1(b_1\theta_0+C_{f0})^{\alpha-1}\\
&\left(c_1\phi_0+d_1\left(1-\sum_{n=1}^{\infty}\frac{4}{(2n-1)\pi}e^{-\frac{1}{pem}\left(\frac{(2n-1)\pi}{2}\right)^2 t}\sin\left(\frac{(2n-1)\pi\eta}{2}\right)\right)\right)^{\beta}e^{\theta_0}+\theta_1e^{\theta_0}-\theta_0^2e^{\theta_0}
\end{aligned}\right\} \tag{45}$$

$$\left.\begin{aligned}
&\frac{\partial \mathrm{X}_1}{\partial t}=\frac{1}{\mathrm{Pem}}\left(\frac{\partial \mathrm{X}_0}{\partial \eta}\right)^2+\frac{1}{\mathrm{Pem}}\frac{\partial^2 \mathrm{X}_0}{\partial \eta^2}+\frac{\mathrm{X}_0}{\mathrm{Pe}}\frac{\partial^2 \mathrm{X}_0}{\partial \eta^2}+2u_1\frac{\partial \mathrm{X}_1}{\partial \eta}+Da\,\mathrm{Re}\,\eta(1-\eta)\frac{\partial \mathrm{X}_1}{\partial \eta}+\\
&c_2\delta_2\beta\phi_1\left(b_2\theta_0+C_{f0}\right)^{\alpha}\\
&\left(c_2\phi_0+d_2\left(1-\sum_{n=1}^{\infty}\frac{4}{(2n-1)\pi}e^{-\frac{1}{\mathrm{Pem}}\left(\frac{(2n-1)\pi}{2}\right)^2 t}\sin\left(\frac{(2n-1)\pi\eta}{2}\right)\right)\right)^{\beta-1}e^{\theta_0}+b_2\delta_2\alpha\theta_1\left(b_2\theta_0+C_{f0}\right)^{\alpha-1}\\
&\left(c_2\phi_0+d_2\left(1-\sum_{n=1}^{\infty}\frac{4}{(2n-1)\pi}e^{-\frac{1}{pem}\left(\frac{(2n-1)\pi}{2}\right)^2 t}\sin\left(\frac{(2n-1)\pi\eta}{2}\right)\right)\right)^{\beta}e^{\theta_0}+\theta_1e^{\theta_0}-\theta_0^2e^{\theta_0}
\end{aligned}\right\}\quad(46)$$

$$\left.\begin{aligned}
&\frac{\partial \mathrm{Y}_1}{\partial t}=2u_1\frac{\partial \mathrm{Y}_1}{\partial \eta}+c_3\delta_3\beta\phi_1\left(b_3\theta_0+C_{f0}\right)^{\alpha}\\
&\left(c_3\phi_0+d_3\left(1-\sum_{n=1}^{\infty}\frac{4}{(2n-1)\pi}e^{-\frac{1}{\mathrm{Pem}}\left(\frac{(2n-1)\pi}{2}\right)^2 t}\sin\left(\frac{(2n-1)\pi\eta}{2}\right)\right)\right)^{\beta-1}e^{\theta_0}+b_3\delta_3\alpha\theta_1\left(b_3\theta_0+C_{f0}\right)^{\alpha-1}\\
&\left(c_3\phi_0+d_3\left(1-\sum_{n=1}^{\infty}\frac{4}{(2n-1)\pi}e^{-\frac{1}{pem}\left(\frac{(2n-1)\pi}{2}\right)^2 t}\sin\left(\frac{(2n-1)\pi\eta}{2}\right)\right)\right)^{\beta}e^{\theta_0}+\theta_1e^{\theta_0}-\theta_0^2e^{\theta_0}
\end{aligned}\right\}\quad(47)$$

$$\left.\begin{aligned}
&\phi_1(\eta,0)=0,\quad \phi_1(0,t)=0,\quad \left.\frac{\partial\phi_1}{\partial\eta}\right|_{\eta=1}=0\\
&\theta_1(\eta,0)=0,\quad \left.\frac{\partial\theta_1}{\partial\eta}\right|_{\eta=0}=0\quad \left.\frac{\partial\theta_1}{\partial\eta}\right|_{\eta=1}=0,\\
&\mathrm{X}_1(\eta,0)=0,\quad \mathrm{X}_1(0,t)=0,\quad \left.\frac{\partial \mathrm{X}_1}{\partial\eta}\right|_{\eta=1}=0\\
&\mathrm{Y}_1(\eta,0)=0,\quad \mathrm{Y}_1(0,t)=0\\
&u_1(\eta,0)=0,\ \left.u_1\right|_{\eta=0}=0,\ \left.u_1\right|_{\eta=1}=0
\end{aligned}\right\}\quad(48)$$

This question of existence and uniqueness of solutions to these equations has been addressed by Ayeni (1978) who consider a similar set of equations and showed among other results that existence and uniqueness are somewhat well known. In his work, he studied the following system of parabolic equations.

$$\left.\begin{aligned}
\frac{\partial \phi}{\partial t} &= \Delta\phi + f(x,t,\phi,u,v), \qquad x \in R^n, t > 0 \\
\frac{\partial u}{\partial t} &= \Delta u + g(x,t,\phi,u,v), \qquad x \in R^n, t > 0 \\
\frac{\partial v}{\partial t} &= \Delta v + h(x,t,\phi,u,v), \qquad x \in R^n, t > 0
\end{aligned}\right\} \tag{49}$$

$$\phi(x,0) = f_0(x)$$

$$u(x,0) = g_0(x)$$

$$v(x,0) = h_0(x)$$

$$x = (x_1, x_2, ..., x_n)$$

(S.1): $f_0(x)$, $g_0(x)$ and $h_0(x)$ are bounded for $x \in R^n$ .Each has at most a countable number of discontinuities.

(S.2): f, g, h satisfies the uniform Lipschitz condition

$$|\varphi(x,t,\phi_1,u_1,v_1) - \varphi(x,t,\phi_2,u_2 v_2)| \le \mathrm{M}(|\phi_1 - \phi_2| + |u_1 - u_2| + |v_1 - v_2|), \qquad (x,t) \in G$$

Where $G = \{(x,t) : x \in R^n, 0 < t < \tau\}$.

Our proof of existence of unique solution of the system of parabolic equations (37) – (42) will be analogous to his proof.

Theorem 3.2: There exists a unique solution $u_0(\eta,t), \phi_0(\eta,t), \theta_0(\eta,t), \mathrm{X}_0(\eta,t)$ and $\mathrm{Y}_0(\eta,t)$ of equations (37) – (41) which satisfy (42).

Lemma 3.1 (Ayeni(1978)) :

Let (f_0, g_0, h_0) and (f, g, h) satisfy (**S.1**) and (**S.2**) respectively. Then there exists a solution of problem (49),

Proof of lemma 3.1, see Ayeni (1978)

Proof of theorem (3.1):

We rewrite equations (37) – (42) as

$$\frac{\partial u_0}{\partial t} = \frac{1}{\mathrm{Re}}\frac{\partial^2 u_0}{\partial \eta^2} + f\left(\eta, t, u_0, \phi_0, \theta_0, \mathrm{X}_0, \mathrm{Y}_0\right), \quad \eta \in R^n, t > 0, \tag{50}$$

$$\frac{\partial \phi_0}{\partial t} = \frac{1}{\mathrm{Pe}}\frac{\partial^2 \phi_0}{\partial \eta^2} + g\left(\eta, t, u_0, \phi_0, \theta_0, \mathrm{X}_0, \mathrm{Y}_0\right) \quad \eta \in R^n,\ t > 0, \tag{51}$$

$$\frac{\partial \theta_0}{\partial t} = \frac{1}{\mathrm{Pe}}\frac{\partial^2 \theta_0}{\partial \eta^2} + h\left(\eta, t, u_0, \phi_0, \theta_0, \mathrm{X}_0, \mathrm{Y}_0\right) \quad \eta \in R^n,\ t > 0, \tag{52}$$

$$\frac{\partial \mathrm{X}_0}{\partial t} = \frac{1}{\mathrm{Pem}}\frac{\partial^2 \mathrm{X}_0}{\partial \eta^2} + \mathrm{Z}\left(\eta, t, u_0, \phi_0, \theta_0, \mathrm{X}_0, \mathrm{Y}_0\right) \quad \eta \in R^n,\ t > 0, \tag{53}$$

Where,

$$f\left(\eta, t, u_0, \phi_0, \theta_0, \mathrm{X}_0, \mathrm{Y}_0\right) = -\eta\left(1-\eta\right) \tag{54}$$

$$\left.\begin{aligned} g\left(\eta, t, u_0, \phi_0, \theta_0, \mathrm{X}_0, \mathrm{Y}_0\right) &= \sigma\left(\phi_0 - \theta_0\right) + \gamma\left(a - \phi_0\right) + 2u_0\frac{\partial \phi_0}{\partial \eta} + Da\,\mathrm{Re}\,\eta\left(1-\eta\right)\frac{\partial \phi_0}{\partial \eta} + \\ &\delta\left(b\phi_0 + C_{f0}\right)^{\alpha}\left(c\phi_0 + d\left(1 - \sum_{n=1}^{\infty}\frac{4}{(2n-1)\pi}e^{-\frac{1}{pem}\left(\frac{(2n-1)}{2}\pi\right)^2 t}\sin\left(\frac{(2n-1)\pi\eta}{2}\right)\right)\right)^{\beta} e^{\theta_0} \end{aligned}\right\} \tag{55}$$

$$\left.\begin{aligned} h\left(\eta, t, u_0, \phi_0, \theta_0, \mathrm{X}_0, \mathrm{Y}_0\right) &= \sigma_1\left(\phi_0 - \theta_0\right) + \gamma_1\left(a - \theta_0\right) + 2u_0\frac{\partial \theta_0}{\partial \eta} + \delta_1\left(b_1\theta_0 + C_{f0}\right)^{\alpha} \\ &\left(c_1\phi_0 + d_1\left(1 - \sum_{n=1}^{\infty}\frac{4}{(2n-1)\pi}e^{-\frac{1}{pem}\left(\frac{(2n-1)}{2}\pi\right)^2 t}\sin\left(\frac{(2n-1)\pi\eta}{2}\right)\right)\right)^{\beta} e^{\theta_0} \end{aligned}\right\} \tag{56}$$

$$\left.\begin{aligned} Z\left(\eta, t, u_0, \phi_0, \theta_0, \mathrm{X}_0, \mathrm{Y}_0\right) &= 2u_0\frac{\partial \mathrm{X}_0}{\partial \eta} + Da\,\mathrm{Re}\,\eta\left(1-\eta\right)\frac{\partial \mathrm{X}_0}{\partial \eta} + \delta_2\left(b_2\phi_0 + C_{f0}\right)^{\alpha} \\ &\left(c_2\phi_0 + d_2\left(1 - \sum_{n=1}^{\infty}\frac{4}{(2n-1)\pi}e^{-\frac{1}{pem}\left(\frac{(2n-1)}{2}\pi\right)^2 t}\sin\left(\frac{(2n-1)\pi\eta}{2}\right)\right)\right)^{\beta} e^{\theta_0} \end{aligned}\right\} \tag{57}$$

Ignoring the second term at the right hand side, the fundamental solutions of equations (50) – (53) are (see Toki and Tokis (2007)):

$$F\left(\eta, t\right) = \frac{\mathrm{Re}^{\frac{1}{2}}\eta}{2t\sqrt{\pi t}}\exp\left(-\frac{\mathrm{Re}\,\eta^2}{4t}\right) \tag{58}$$

$$G(\eta,t)=\frac{\mathrm{Pe}^{\frac{1}{2}}\eta}{2t\sqrt{\pi t}}\exp\left(-\frac{\mathrm{Pe}\eta^2}{4t}\right) \tag{59}$$

$$\mathrm{H}(\eta,t)=\frac{\mathrm{Pe}^{\frac{1}{2}}\eta}{2t\sqrt{\pi t}}\exp\left(-\frac{\mathrm{Pe}\eta^2}{4t}\right) \tag{60}$$

$$J(\eta,t)=\frac{\mathrm{Pem}^{\frac{1}{2}}\eta}{2t\sqrt{\pi t}}\exp\left(-\frac{\mathrm{Pem}\eta^2}{4t}\right) \tag{61}$$

Clearly

$$f(\eta,t,u_0,\phi_0,\theta_0,\mathrm{X}_0,\mathrm{Y}_0)=-\eta(1-\eta),$$

$$\left.\begin{aligned} g(\eta,t,u_0,\phi_0,\theta_0,\mathrm{X}_0,\mathrm{Y}_0)&=\sigma(\phi_0-\theta_0)+\gamma(a-\phi_0)+2u_0\frac{\partial\phi_0}{\partial\eta}+Da\,\mathrm{Re}\,\eta(1-\eta)\frac{\partial\phi_0}{\partial\eta}+\delta\left(b\phi_0+C_{f0}\right)^{\alpha}\\ &\left(c\phi_0+d\left(1-\sum_{n=1}^{\infty}\frac{4}{(2n-1)\pi}e^{-\frac{1}{pem}\left(\frac{(2n-1)}{2}\pi\right)^2 t}\sin\left(\frac{(2n-1)\pi\eta}{2}\right)\right)\right)^{\beta}e^{\theta_0}\end{aligned}\right\}$$

$$\left.\begin{aligned} h(\eta,t,u_0,\phi_0,\theta_0,\mathrm{X}_0,\mathrm{Y}_0)&=\sigma_1(\phi_0-\theta_0)+\gamma_1(a-\theta_0)2u_0\frac{\partial\theta_0}{\partial\eta}+\delta_1\left(b_1\theta_0+C_{f0}\right)^{\alpha}\\ &\left(c_1\phi_0+d_1\left(1-\sum_{n=1}^{\infty}\frac{4}{(2n-1)\pi}e^{-\frac{1}{pem}\left(\frac{(2n-1)}{2}\pi\right)^2 t}\sin\left(\frac{(2n-1)\pi\eta}{2}\right)\right)\right)^{\beta}e^{\theta_0}\end{aligned}\right\},$$

$$\left.\begin{aligned} Z(\eta,t,u_0,\phi_0,\theta_0,\mathrm{X}_0,\mathrm{Y}_0)&=2u_0\frac{\partial\mathrm{X}_0}{\partial\eta}+Da\,\mathrm{Re}\,\eta(1-\eta)\frac{\partial\mathrm{X}_0}{\partial\eta}+\delta_2\left(b_2\phi_0+C_{f0}\right)^{\alpha}\\ &\left(c_2\phi_0+d_2\left(1-\sum_{n=1}^{\infty}\frac{4}{(2n-1)\pi}e^{-\frac{1}{pem}\left(\frac{(2n-1)}{2}\pi\right)^2 t}\sin\left(\frac{(2n-1)\pi\eta}{2}\right)\right)\right)^{\beta}e^{\theta_0}\end{aligned}\right\}$$

are Lipschitz continuous .Hence by theorem 3.2, the results follow. This completes the proof.

3.3 Properties of Solution

Theorem 3.2: Let $\mathrm{Re}=\mathrm{Pe}=Da=\sigma=\sigma_1=\gamma=\gamma_1=\mathrm{Pem}=1$ and $\alpha=\beta=0$ in equation (37) – (41). Then $\frac{\partial u_0}{\partial t}\geq 0$, $\frac{\partial\phi_0}{\partial t}\geq 0$, $\frac{\partial\theta_0}{\partial t}\geq 0$, $\frac{\partial\mathrm{X}_0}{\partial t}\geq 0$, $\frac{\partial\mathrm{Y}_0}{\partial t}\geq 0$

In the proof, we shall make use of the following lemma of kolodner and Pederson (1966). **Lemma (Kolodner and Pederson (1966))**: Let $u(x,t)=0\left(e^{\alpha|x|^2}\right)$ be a solution on $R^n\times[0,t)$ of the differential inequality $\frac{\partial u}{\partial t}-\Delta u+k(x,t)u\geq 0$ where k is bounded from below if $u(x,t)\geq 0$, then $u(x,t)\geq 0$ for all $(x,t)\in R^n\times[0,t_0)$

Proof of Theorem 3.2: Given,

$$\frac{\partial u_0}{\partial t}-\frac{\partial^2 u_0}{\partial \eta^2}-\eta(1-\eta)=0 \tag{62}$$

$$\frac{\partial \phi_0}{\partial t}-\frac{\partial^2 \phi_0}{\partial \eta^2}-2u_0\frac{\partial \phi_0}{\partial \eta}-\eta(1-\eta)\frac{\partial \phi_0}{\partial \eta}+\theta-\delta e^{\theta_0}=0 \tag{63}$$

$$\frac{\partial \theta_0}{\partial t}-\frac{\partial^2 \theta_0}{\partial \eta^2}-2u_0\frac{\partial \theta_0}{\partial \eta}-\eta(1-\eta)\frac{\partial \theta_0}{\partial \eta}+\theta_0-\delta_1 e^{\theta_0}=0 \tag{64}$$

$$\frac{\partial \mathrm{X}_0}{\partial t}-\frac{\partial^2 \mathrm{X}_0}{\partial \eta^2}-2u_0\frac{\partial \mathrm{X}_0}{\partial \eta}-\eta(1-\eta)\frac{\partial \mathrm{X}_0}{\partial \eta}-\delta_2 e^{\theta_0}=0 \tag{65}$$

$$\frac{\partial \mathrm{Y}_0}{\partial t}-2u_0\frac{\partial \mathrm{X}_0}{\partial \eta}-\delta_3 e^{\theta_0}=0 \tag{66}$$

Differentiating with respect to t, we have

$$\frac{\partial}{\partial t}\left(\frac{\partial u_0}{\partial t}\right)-\frac{\partial^2}{\partial \eta^2}\left(\frac{\partial u_0}{\partial t}\right)=0 \tag{67}$$

$$\frac{\partial}{\partial t}\left(\frac{\partial \phi_0}{\partial t}\right)-\frac{\partial^2}{\partial \eta^2}\left(\frac{\partial \phi_0}{\partial t}\right)=\left(2u_0+\eta(1-\eta)\right)\frac{\partial}{\partial \eta}\left(\frac{\partial \phi_0}{\partial t}\right)+2\frac{\partial \phi_0}{\partial \eta}\frac{\partial u_0}{\partial t}+\left(\delta e^{\theta_0}-1\right)\frac{\partial \theta_0}{\partial t} \tag{68}$$

$$\frac{\partial}{\partial t}\left(\frac{\partial \theta_0}{\partial t}\right)-\frac{\partial^2}{\partial \eta^2}\left(\frac{\partial \theta_0}{\partial t}\right)+\left(1-\delta_1 e^{\theta_0}\right)\frac{\partial \theta_0}{\partial t}=\left(2u_0+\eta(1-\eta)\right)\frac{\partial \theta_0}{\partial \eta}\frac{\partial u_0}{\partial t}+2\frac{\partial \theta_0}{\partial \eta}\frac{\partial u_0}{\partial t} \tag{69}$$

$$\frac{\partial}{\partial t}\left(\frac{\partial \mathrm{X}_0}{\partial t}\right)-\frac{\partial^2}{\partial \eta^2}\left(\frac{\partial \mathrm{X}_0}{\partial t}\right)=\left(2u_0+\eta(1-\eta)\right)\frac{\partial}{\partial \eta}\left(\frac{\partial \mathrm{X}_0}{\partial t}\right)+2\frac{\partial \mathrm{X}_0}{\partial \eta}\frac{\partial u_0}{\partial t}+\delta_2 e^{\theta_0}\frac{\partial \theta_0}{\partial t} \tag{70}$$

$$\frac{\partial}{\partial t}\left(\frac{\partial \mathrm{Y}_0}{\partial t}\right)=2u_0\frac{\partial}{\partial \eta}\left(\frac{\partial \mathrm{Y}_0}{\partial t}\right)+2\frac{\partial \mathrm{Y}_0}{\partial \eta}+\delta_3 e^{\theta_0}\frac{\partial \theta_0}{\partial t}=0 \tag{71}$$

Let

$$m=\frac{\partial u_0}{\partial t},\ n=\frac{\partial \phi_0}{\partial t},\ r=\frac{\partial \theta_0}{\partial t},\ \ w=\frac{\partial \mathrm{X}_0}{\partial t},\ \ \mathrm{Z}=\frac{\partial \mathrm{Y}_0}{\partial t}$$

Then

$$\frac{\partial m}{\partial t}-\frac{\partial^2 m}{\partial \eta^2}=0$$

$$\frac{\partial n}{\partial t}-\frac{\partial^2 n}{\partial \eta^2}\geq 0 \text{ Since } \left(2u_0+\eta(1-\eta)\right)\frac{\partial n}{\partial \eta}+2\frac{\partial \phi_0}{\partial \eta}m+\left(\delta e^{\theta_0}-1\right)r\geq 0$$

$$\frac{\partial r}{\partial t}-\frac{\partial^2 r}{\partial \eta^2}+\left(1-\delta_1 e^{\theta_0}\right)r\geq 0 \quad \text{Since } \left(2u_0+\eta(1-\eta)\right)\frac{\partial r}{\partial \eta}+2\frac{\partial \theta_0}{\partial \eta}n\geq 0$$

$$\frac{\partial w}{\partial t}-\frac{\partial^2 w}{\partial \eta^2}\geq 0 \quad \text{Since } \left(2u_0+\eta(1-\eta)\right)\frac{\partial w}{\partial \eta}+2\frac{\partial \mathrm{X}_0}{\partial \eta}n+\delta_2 e^{\theta_0}r\geq 0$$

$$\frac{\partial \mathrm{Z}}{\partial t}\geq 0 \text{ Since } \quad 2u_0\frac{\partial \mathrm{Z}}{\partial \eta}+2\frac{\partial \mathrm{Y}_0}{\partial \eta}m+\delta_3 e^{\theta_0}r\geq 0$$

These can be written as

$$\frac{\partial m}{\partial t}-\frac{\partial^2 m}{\partial \eta^2}+k(\eta,t)m\geq 0$$

$$\frac{\partial n}{\partial t}-\frac{\partial^2 n}{\partial \eta^2}+k_1(\eta,t)n\geq 0$$

$$\frac{\partial r}{\partial t}-\frac{\partial^2 r}{\partial \eta^2}+k_2(\eta,t)r\geq 0$$

$$\frac{\partial w}{\partial t}-\frac{\partial^2 w}{\partial \eta^2}+k_3(\eta,t)w\geq 0$$

$$\frac{\partial \mathrm{Z}}{\partial t}-0\frac{\partial^2 \mathrm{Z}}{\partial \eta^2}+k_4(\eta,t)\mathrm{Z}\geq 0$$

Where

$$k(\eta,t)=0,\ k_1(\eta,t)=0,\quad k_2(\eta,t)=\left(1-\delta e^{\theta_0}\right),\quad k_3(\eta,t)=0,\quad k_4(\eta,t)=0$$

Clearly, k_2 is bounded from below and k, k_1, k_3 and k_4 are bounded everywhere. Hence, by Kolodner and Pederson's lemma, $r(\eta,t) \geq 0$, $m(\eta,t) \geq 0$, $n(\eta,t) \geq 0$, $w(\eta,t) \geq 0$ and $Z(\eta,t) \geq 0$, that is $\frac{\partial u_0}{\partial t} \geq 0, \frac{\partial \phi_0}{\partial t} \geq 0, \frac{\partial \theta_0}{\partial t} \geq 0$, $\frac{\partial \mathrm{X}_0}{\partial t} \geq 0$, and $\frac{\partial \mathrm{Y}_0}{\partial t} \geq 0$. This completes the proof.

4.0 Conclusion

To examine the properties of solution of the in-situ combustion of oil shale as enhanced oil recovery technique in porous medium, we used an approach by Ayeni (1978) and Kolodner and Pederson (1966).Our result revealed that velocity u ,mass X and Y , temperature θ and ϕ are increasing function of time.

References

Ayeni, R.O. (1978). Thermal Runaway. Unpublished PhD Thesis, Cornell University, USA.

Abdelrahman,.A.A.(2015). Geological overview of oil shale.. https:// www.researchgate.net//publication/282354048.

Burnham, A.K. (1993). Chemical Kinetic and Oil shale Process Design. A paper prepared for submittal to the NATO Advanced study institute Composition Geochemistry and conversion of oil shale, Akcay, Turkey.

Kolodner J. and Pederson R.H. (1966). Pointwise bounds for solutions of some semi-linear parabolic equations. Journal of Differential equations, 2, 353-364.

Lapene A, Martins M.F., Debenest G., Quintard M. and Salvador S. (2007).Numerical Simulation of oil shale combustion in a fixed bed: Modeling and chemical aspect. https//www.researchgate.net/publication/27333515. Alb, France.

Myint-U T. and Debnath L.(1987). Partial Differential Equation for Scientist and Engineers.PTR Prentice- Hall, Englewood Cliffs. New Jersey 07632.

Olayiwola R.O. (2011). A Mathematical Model of solid fuel Arrhenius combustion in a fixed –bed. International Journal of Numerical Mathematic Vol.6 NO.2 PP214-233

Olayiwola R.O. (July, 2012). Fixed – bed solid fuel Arrhenius combustion: Modeling and simulation.Journal of the Nigeria of Mathematical Physics vol.21, PP111-120.

Toki, C. J. and Tokis,J.N.(2007). Exact solutions for the unsteady free convection flows on a porous plate with time-dependent heating. Zamm-.Zeitchrift for Angewadte Mathematics Mechanics, 87, N0.1, 4- 13.

Zheng H. Shi W. Dig D. and Zhang C.(2017) .Numerical Simulation of in situ combustion of oil shale. Hindaw Geofluids Volume 2017, Article ID 3028974, 9 pages. Http//do.Org/10.115/2017/3028974.

Three Step Continuous Hybrid Block Method for the Solution of $y' = f(x, y)$

Cole A.T., Maryam O. J., Olayiwola R. O.

Department of Mathematics,
Federal University of Technology, Minna Niger State, Nigeria

Abstract

In this paper, we present a block method for the direct solution of first order initial value problems of ordinary differential equations. Collocation and interpolation approach was adopted to generate a continuous linear multistep method which was then solved for the independent solution to give a continuous block method. We evaluated the result at selected grid points to give a discrete block which eventually gave simultaneous solutions at both grid and off grid points. The three step block method is zero stable, consistent and convergent. Numerical experiments on some selected problems compared with the exact solution proved the efficiency and accuracy of the derived method.

Keywords: consistent, convergent, collocation, off grid points, interpolation, zero stable

1.0 Introduction

We consider the first order differential equation of the form:

$$y' = f(x, y), \quad y(x_0) = y_0 \tag{1}$$

With the advancement in Science and Technology, mathematical modeling of physical phenomenon into ordinary differential equation has been a subject of research.Ordinary differential equations (ODEs) are an indispensable tool for modeling such behaviors mathematically and first order ordinary differential equation is not an exemption. In order to understand the physical phenomenon, solution to the model is required and since most ODEs are not solvable analytically, numerical methods are implored to produce an approximate solution(Badmus, 2013).

Recent researches on numerical solutions of first order differential equation have been directed to increasing the efficiency and accuracy. Researchers developed direct methods for higher order ODEs among whom are Awoyemi *et al.* (2011), ObaruahandKayode (2013) and Adesanya *et al.* (2013) to address the challenges associated with method of reduction to system of first order.

In order to avoid these challenges, Jator (2010), Adesanya *et al.* (2012)andAnake *et al.* (2012) developed block methods in which approximations are simultaneously generated at different grid points in the interval of integration and is less expensive in terms of the number of function evaluations compared to linear multistep methods.

In this paper, we developed a three step linear multistep method with two off-grid points implemented in block method.

2.0 Development of Method

In this section, we want to derive the Hybrid Linear Multistep Method of the form:

$$\sum_{j=0}^{k}\alpha_j y_{n+j} = h\sum_{j=0}^{k}\beta_j f_{n+j} + h\beta_v f_{n+v} \qquad (2)$$

Where v_j is not an integer and α_j and β_j are continuous coefficient defined by;

$$\left.\begin{aligned}\alpha_j(x) &= \sum_{j=0}^{k}\alpha_j x^j \\ \beta_j(x) &= \sum_{j=0}^{k}\beta_j x^j\end{aligned}\right\} \qquad (3)$$

Now, the general form of the power series is given by:

$$y = a_0 + a_1 x + a_2 x^2 + a_3 x^3 + \ldots \qquad (4)$$

Discretizing equation (4) at one interpolation point, x_n and collocation points, $x_n, x_{n+\frac{1}{3}}, x_{n+\frac{2}{3}}, x_{n+1}, x_{n+2}, x_{n+3}$ where m, $1 \le m < k$ and $t, t > 0$ are the numbers of collocation and interpolation points respectively gives:

$$\sum_{j=0}^{m+t-1}\alpha_j x^j = y_{n+i},\ i = 0 \qquad (5)$$

$$\sum_{j=0}^{m+t-1}\beta_j x^j = f_{n+i},\ i = 0, \frac{1}{3}, \frac{2}{3}, 1, 2, 3 \qquad (6)$$

Equation (5) and (6) give a system of $(t+m)$ equations which is solved by Gaussian elimination method to obtain $\alpha_j(x)$, $\beta_j(x)$ and $\beta_v(x)$.

The general form of the proposed method with the addition of the two off grid points is expressed as:

$$\left.\begin{aligned} y(x) &= \alpha_0(x)y_n + \\ h&\left(\beta_n(x)f_n + \beta_{n+\frac{1}{3}}(x)f_{n+\frac{1}{3}} + \beta_{n+\frac{2}{3}}(x)f_{n+\frac{2}{3}} + \beta_{n+1}(x)f_{n+1} + \beta_{n+2}(x)f_{n+2} + \beta_{n+3}(x)f_{n+3}\right) \end{aligned}\right\} \quad (7)$$

In thisderivation, we use $t=1,\ m=6,\ k=3\ v=\frac{1}{3},\frac{2}{3}$ and also express $\alpha_j(x)$, $\beta_j(x)$ and $\beta_v(x)$ as a function of *t*, where $t=x-x_n$ to obtain the continuous form as follows:

$$\left.\begin{aligned} \alpha_0 &= 1 \\ \beta_0 &= -\frac{1}{240}\left(240t - \frac{760t}{h} + \frac{1100t^2}{h^2} - \frac{775t^3}{h^3} + \frac{252t^4}{h^4} - \frac{30t^5}{h^5}\right) \\ \beta_{\frac{1}{3}} &= \frac{27t}{320}\left(\frac{72t}{h} - \frac{160t^2}{h^2} + \frac{135t^3}{h^3} - \frac{48t^4}{h^4} - \frac{6t^5}{h^5}\right) \\ \beta_{\frac{2}{3}} &= \frac{27t}{1120}\left(\frac{180t}{h} - \frac{580t^2}{h^2} + \frac{585t^3}{h^3} - \frac{228t^4}{h^4} + \frac{30t^5}{h^5}\right) \\ \beta_1 &= \frac{t}{240}\left(\frac{360t}{h} - \frac{1280t^2}{h^2} + \frac{1515t^3}{h^3} - \frac{648t^4}{h^4} + \frac{90t^5}{h^5}\right) \\ \beta_2 &= -\frac{t}{480}\left(\frac{36t}{h} - \frac{140t^2}{h^2} + \frac{195t^3}{h^3} - \frac{108t^4}{h^4} + \frac{18t^5}{h^5}\right) \\ \beta_3 &= \frac{t}{6720}\left(\frac{40t}{h} - \frac{160t^2}{h^2} + \frac{235t^3}{h^3} - \frac{144t^4}{h^4} + \frac{30t^5}{h^5}\right) \end{aligned}\right\} \quad (8)$$

Substituting (8) into (7) and evaluating at $x_{n+\frac{1}{3}}, x_{n+\frac{2}{3}}, x_{n+1}, x_{n+2}, x_{n+3}$ respectively, we have:

$$y_{n+\frac{1}{3}} = y_n + h\left(\frac{6763}{58320}f_n + \frac{863}{2880}f_{n+\frac{1}{3}} - \frac{1177}{10080}f_{n+\frac{2}{3}} + \frac{709}{19440}f_{n+1} - \frac{13}{7776}f_{n+2} + \frac{211}{1632960}f_n\right) \quad (9)$$

$$y_{n+\frac{2}{3}} = y_n + h\left(\frac{389}{3645} f_n + \frac{83}{180} f_{n+\frac{1}{3}} + \frac{4}{45} f_{n+\frac{2}{3}} + \frac{13}{1215} f_{n+1} - \frac{1}{1218} f_{n+2} + \frac{83}{180} f_n\right) \quad (10)$$

$$y_{n+1} = y_n + h\left(\frac{9}{80} f_n + \frac{27}{64} f_{n+\frac{1}{3}} + \frac{351}{1120} f_{n+\frac{2}{3}} + \frac{37}{240} f_{n+1} - \frac{1}{480} f_{n+2} + \frac{1}{6720} f_n\right) (11)$$

$$y_{n+2} = y_n - h\left(\frac{1}{15} f_n - \frac{27}{20} f_{n+\frac{1}{3}} + \frac{54}{35} f_{n+\frac{2}{3}} - \frac{29}{15} f_{n+1} - \frac{1}{3} f_{n+2} + \frac{1}{140} f_{n+3}\right) (12)$$

$$y_{n+3} = y_n + h\left(\frac{57}{80} f_n - \frac{729}{320} f_{n+\frac{1}{3}} + \frac{729}{160} f_{n+\frac{2}{3}} - \frac{153}{80} f_{n+1} + \frac{261}{160} f_{n+2} + \frac{93}{320} f_n\right) (13)$$

3.0 Basic Properties of the Developed Method

3.1 Order of the Block

Let the linear operator $L\{y(x):h\}$ on (2) be:

$$L\{y(x):h\} = \sum_{j=0}^{k} \alpha_j y(x+jh) - h\sum_{j=0}^{k} \beta_j y'(x+jh) + h\beta_v y'(x+jh) \quad (14)$$

where the function $y(x)$ is assumed to have continuous derivatives of sufficiently high order (Lambert, 1973). Expanding (14) in Taylor series about the point *x* gives the expression:

$$L\{y(x):h\} = C_0 y(x) + C_1 y'(x) + \ldots + C_P y^p(x) + C_{p+1} y^{p+1}(x) + \ldots (15)$$

Definition: The linear operator L and associated block method are said to be of order p if $C_0 = C_1 = C_2 = \ldots = C_P = 0,\ C_{p+1} \neq 0$ *is called the error constant and implies that the truncation error is given by* $t_{n+k} = C_{p+1} h^{p+1} y^{p+1}(x) + O(h^{p+2})$.

Comparing the coefficient of h, the order ofthe method is six with error constant

$$C_6 = \left[-\frac{281}{14696640}, -\frac{31}{2755620}, -\frac{11}{544320}, \frac{17}{34020}, -\frac{13}{4032}\right]$$

3.2 Consistency

From (15),

$$\left.\begin{aligned} C_0 &= \sum_{j=0}^{k} \alpha_j = 0 \\ C_1 &= \sum_{j=0}^{k} \left(j\alpha_j - \beta_j \right) = 0 \end{aligned}\right\} \tag{16}$$

Since $C_0 = C_1 = 0$, then the method is consistent.

3.3 Zero Stability

The linear multistep method (2) is said to be zero stable if the zeros of the first characteristic polynomial are such that none is larger than one in magnitude and any zero equal to one in magnitude is simple (that is, not repeated).

For the developed method, we have for schemes (9)–(13), we have

$$\left.\begin{aligned} \rho(z) &= z^{\frac{1}{3}} - 1 \Rightarrow z = 1 \\ \rho(z) &= z^{\frac{2}{3}} - 1 \Rightarrow z = 1 \\ \rho(z) &= z - 1 \Rightarrow z = 1 \\ \rho(z) &= z^2 - 1 \Rightarrow z = 1, z - 1 \\ \rho(z) &= z^3 - 1 \Rightarrow z = 1 \end{aligned}\right\} \tag{17}$$

Equation (17) shows that the schemes (9)-(13) are zero stable.

3.4 Convergence

The schemes are convergent sine they are consistent and zero stable.

4.0 Numerical Examples

Problem 1:

$$y' = x + y, \quad y(0) = 1, \quad h = 0.01$$

Exact solution: $y(x) = 2e^x - (x+1)$

Problem 2:

$y' = -y + 20, \quad y(0) = 1, \quad h = 0.01$

Exact solution: $y(x) = 5 - 4e^{-4x}$

Table 4.1: Comparison of result of Problem 1with exact solution.

x	Exact Result	Computed Result	Error
0.01	1.010100334168340	1.010100334168330	1.0 E−14
0.02	1.020402680053510	1.020402680053510	0.0 E+00
0.03	1.030909067907030	1.030909067907030	0.0 E+00
0.04	1.041621548384780	1.041621548384770	1.0 E−14
0.05	1.052542192752050	1.052542192752040	1.0 E−14
0.06	1.063673093090720	1.063673093090710	1.0 E−14
0.07	1.075016362508430	1.075016362508430	0.0 E+00
0.08	1.086574135349920	1.086574135349910	1.0 E−14
0.09	1.098348567410420	1.098348567410420	0.0 E+00
0.1	1.110341836151300	1.110341836151290	1.0 E−14

Table 4.2: Comparison of result of Problem 2 with exact solution.

x	Exact Result	Computed Result	Error
0.01	1.00025002500166	1.00025002500166	0.0 E+00
0.02	1.00100040010668	1.00100040010668	0.0 E+00
0.03	1.00225202621554	1.00225202621556	2.0 E−14
0.04	1.00400640683213	1.00400640683214	1.0 E−14
0.05	1.00626565107425	1.00626565107425	0.0 E+00

0.06	1.00903247790016	1.00903247790023	7.0 E−14
0.07	1.01231022156300	1.01231022156307	7.0 E−14
0.08	1.01610283830835	1.01610283830840	5.0 E−14
0.09	1.02041491433388	1.02041491433402	1.4 E−14
0.1	1.02525167503344	1.02525167503359	1.5 E−14

5.0 Conclusion

In this paper, we have developed a three step hybrid linear multistep method for solving first order differential equation. The method was found to be zero stable, consistent and hence convergent. Numerical examples are used to show that our new method favorable performs well in comparison with the exact solution.

References

Adesanya, A. O., Udoh, M.O. & Alkali, A.M. (2012). A new block predictor-corrector algorithm for the solution of $y''' = f(x, y, y', y'')$, American Journal of Computational 2, 341-344.

Adesanya, A.O., Udoh, A. M. & Ajileye, A. M. (2013). A new hybrid block method for the solution of general third order initial value problems of ordinary differential equations, International Journal of Pure and Applied Mathematics 86(2), 37-48.

Anake,T. A., Awoyemi, D. O. & Adesanya, A.O. (2012). A one step method for the solution of general second order ordinary differential equations. International Journal of Science and Technology 2(4),159-163.

Awoyemi, D.O., Adebile, E.A., Adesanya, A. O. & Anake, T. A. (2011). Modified block method for the direct solution of second order ordinary differential equation. International Journal of Applied Mathematics and Computation 3(3), 181-188.

Badmus, A. M. (2013). Derivation of Multi-step Collocation Methods for the Direct Solution of Second and Third Order Initial Value Problems, PhD Thesis (Unpublished) Nigerian Defence Academy, Kaduna, Nigeria.

Jator, S. N. (2010). On a class of hybrid method for $y'' = f(x, y, y')$, Intern. J. of Pure and Appl. Math. 59(4), 381-395 .

Lambert, J. D., (1973), Computational Methods in Ordinary Differential Equations, John Wiley and Sons, New York.

Obarhua, F. O. & Kayode, S. J. (2013). Continuous y-function hybrid methods for direct solution of differential equations, International Journal of Differential equations and Applications 12(1), 365-375.

Application of Differential Equation to Economics

Yusuf, A., Bolarin, G., and David, M., O.

Department of Mathematics, Federal University of Technology, PMB 65, Minna, 00176-0000 Nigeria, Niger State, Nigeria
*Corresponding Author: yusuf.abdulhakeem@futminna.edu.ng

Abstract

In recent years, many Business analyst and Economist discovered the abnormality in price of products or commodities, rather than a fixed price or a little increase, the price increases drastically affecting the demand or supply of goods with respect to time, which in turn inflates the price of such commodities, and affects the various policy alternatives. These problems were modeled into differential equations and the solutions were obtained. With a closer view at the Evans Price Adjustment Model, which is a determinant factor of Price as regards quantity of Demand $D(t)$ and supply $S(t)$ with respect to time t. Variation of time clearly shows that as time increases, price increases, supply increases and demand decreases.

Keywords: Revenue function, Marginal revenue, profile function, Evans Price model.

1.0 INTRODUCTION

The relationship between the financial sector, business and economic growth is an important issue that has been examined in a wide range of research papers, both theoretical and empirical. Many of them have focused on the impact of the financial sector through derivative on economic growth. Pioneering studies that highlight the role of the financial sector in the dynamism of the economy include Wicksell (1934), Goldsmith (1969), which found that the financial system serves as an engine driving the economic activity.

On the other hand, Levine (1991) points out that stock markets facilitate long-term investments, helping to reduce risk and simultaneously offering liquidity to savers and funding to companies. The author concludes that stock markets do contribute to economic growth. Moreover, Levine and Zervos (1998) highlight that a significant number of empirical studies support the existence of a relationship between capital markets and economic growth in the long term.

Derivatives markets have experienced robust growth in recent decades. In December 2008, the volume of derivatives worldwide was approximately USD 592 trillion, much higher than the gross domestic product (GDP) of the United States (the world's largest economy), which was just over 13.8 trillion in 2007. In 2003, 92% of the 500 largest firms in the world used derivatives to manage risk in several ways, especially interest rate risk, according to information provided by the BIS (Bank for International Settlements). The derivatives market is not only an enormous market, but also one that is growing dramatically. Derivative contracts increased more than sevenfold in the period 1998-2014 . The role played by derivatives markets in boosting economic growth has been analyzed by authors such Sundaram (2013), Sipko (2011), Prabha*et al*. (2014), among many others. Most have found a positive relationship between the development of the derivatives market and economic growth; however, a

worldwide analysis of such a relationship has yet to be carried out. This research paper examines the impact of derivatives markets on economic growth in four major world economies. Specifically, we assess the impact of variables such as the volume of the derivatives market in US dollars and the volume of the derivatives market as a proportion of GDP on economic growth over the period 2002-2014 and it is a new development in the literature

2.0 MATHEMATICAL FORMULATIONS

Consider the differential equation of the form

$$\begin{aligned} D(t) &= \alpha_0 + \alpha_1 p(t) + \alpha_2 p'(t), \alpha_0 > 0, \alpha_1 > 0, \alpha_2 > 0. \\ S(t) &= \beta_0 + \beta_1 p(t) + \beta_2 p'(t), \beta_0 > 0, \beta_1 > 0, \beta_2 < 0. \end{aligned} \tag{2.1}$$

If $\alpha_2 = \beta_2 = 0$ we have the Evans price Adjustment Model in which $\alpha_1 < 0$ since when price increases, demand decreases and $\beta_1 > 0$ since when price increases, supply increases. In Allen's Model, co-efficients α_{2,β_2} accounts for effect of speculation.

The Evans price adjustment model, assumes that the rate of change of price p with respect to time t is proportional to the shortage $D - S$ so that

$$\frac{dp}{dt} = K(D - S) \tag{2.2}$$

$$D(t) = \alpha_0 + \alpha_1 p(t) \tag{2.3}$$

$$S(t) = \beta_0 + \beta_1 p(t) \tag{2.4}$$

From the above

$$\begin{aligned} D(t) &= \alpha_0 + \alpha_1 p(t) + \alpha_2 p'(t) \\ S(t) &= \beta_0 + \beta_1 p(t) + \beta_2 p'(t) \\ D(t) - S(t) &= (\alpha_0 - \beta_0) + (\alpha_1 - \beta_1) p(t) + (\alpha_2 - \beta_2) p'(t) \end{aligned} \tag{2.5}$$

At dynamic equilibrium $\alpha_2 = 0 = \beta_2$ (2.6)

D(t) – S(t) = 0

$$\Rightarrow D(t) = S(t)$$

$$\alpha_0 + \alpha_1 p(t) = \beta_0 + \beta_1 p(t) \tag{2.7}$$

Let

$$D(t) = S(t) = p$$
$$\frac{dp}{dt} = 0 \tag{2.8}$$

$$(\alpha_0 - \beta_0) + (\alpha_1 - \beta_1)p + (\alpha_2 - \beta_2)\frac{dp}{dt} = 0 \tag{2.9}$$

$$(\alpha_2 - \beta_2)\frac{dp}{dt} + (\alpha_1 - \beta_1)p = -(\alpha_0 - \beta_0)$$
$$(\alpha_2 - \beta_2)\frac{dp}{dt} + (\alpha_1 - \beta_1)p = \beta_0 - \alpha_0 \tag{2.10}$$

Divide through by $\alpha_2 - \beta_2$ we have

$$\frac{dp}{dt} + \frac{(\alpha_1 - \beta_1)}{\alpha_2 - \beta_2}p = \frac{\beta_0 - \alpha_0}{\alpha_2 - \beta_2} \tag{2.11}$$

Let

$$\frac{\alpha_1 - \beta_1}{\alpha_2 - \beta_2} = \gamma$$
and (2.12)
$$\frac{\beta_0 - \alpha_0}{\alpha_2 - \beta_2} = \xi$$

By substitution we have

$$\frac{dp}{dt} + \gamma p = \xi \tag{2.13}$$

By using application of linear differential equation of the form

$$\frac{dy}{dx} + p(x)y = Q(x) \tag{2.14}$$

Using integrating factor

$$\upsilon(t) = \ell^{\int \gamma dt} = \ell^{\gamma t} \tag{2.15}$$

The solution becomes

$$p(t) = \frac{\xi}{\gamma} + \left(p_0 - \frac{\xi}{\gamma}\right)\ell^{-\gamma t} \tag{2.16}$$

Let $\frac{\xi}{\gamma} = p_e$

$$p(t) = p_e + \left(p_0 - p_e\right)\ell^{-\gamma t} \tag{2.17}$$

$$p(t) = \frac{\alpha_0 - \beta_0}{\beta_1 - \alpha_1} \tag{2.18}$$

Where $D(t)$ represents demand and $S(t)$ represents supply, both with respect to time, and α, β are both co-efficients of demand and supply, while $P(t)$ is price with respect to time.

Case 1:

Assume a commodity is introduced with an initial price of 5 naira per unit and t months later, the price is $P(t)$ naira per unit. A case study indicates that at a time t ,the demand for the commodity will be $D(t) = 3 + 10e^{-0.01t}$ thousand units and that $S(t) = 2 + p$ thousand units will be supplied. Suppose that at each time t, the price is changing at the rate of 2% 0f the shortage $D(t) - S(t)$.

a) According to the given information, the unit price $P(t)$ satisfies

$$\frac{dp}{dt} = 0.02\left(D(t) - S(t)\right) = 0.02\left((3 + 10\ell^{-0.01t}) - (2 + p)\right) = 0.02 + 0.2e^{-0.01t} - 0.02p \tag{2.19}$$

Or equivalently,

$$\frac{dp}{dt} + 0.02p = 0.02 + 0.2e^{-0.01t} \tag{2.20}$$

Which we recognize as a first order linear differential equation with $P(t) = 0.02$ and $Q(t) = 0.02 + 0.2e^{-0.01t}$.

The integrating factor is

$$I(t) = e^{\int 0.02t} = e^{0.02t} \tag{2.21}$$

So the general solution is

$$P(t) = \frac{1}{e^{0.02t}}\left(\int \ell^{0.02t}(0.02 + 0.2\ell^{-0.01t}dt + c\right) = e^{-0.02t}\left(\frac{0.02\ell^{0.02t}}{0.02} + \frac{0.2\ell^{-0.01t}}{0.01} + c\right) \tag{2.22}$$

$$= 1 + 20e^{-0.01t} + ce^{-0.02t}$$

Since the initial price is $P(0) = 5$, we have

$$P(0)=5=1+20e^{-0.01t}+ce^{0}=1+20+c \tag{2.23}$$

So that $c=5-21=-16$

And

$$P(t)=1+20e^{-0.01t}-16e^{-0.02t} \tag{2.24}$$

b) After 6 months $(t=6)$ the price is

$$P(6)=1+20e^{-0.01(6)}-16e^{-0.02(6)} \quad 5.6446 \tag{2.25}$$
$$=$$

That is, approximately 5.64 naira per unit

c) To maximize the price, we first compute the derivatives

$$P'(t)=20\left(-0.01e^{-0.01(6)}\right)-16\left(-0.02e^{-0.02t}\right)=-0.2e^{-0.01t}+0.32e^{-0.02t} \tag{2.26}$$

And then note that $P'(t)=0$ when

$$P'(t)=-0.2e^{-0.01t}+0.32e^{-0.02t}=0 \tag{2.27}$$
$$0.32e^{-0.02t}=0.2e^{-0.01t}$$

Divide both sides by 0.2

$$\frac{0.32e^{-0.02t}}{0.2}=\frac{0.2e^{-0.01t}}{0.2} \tag{2.28}$$

Multiply both sides by $\frac{1}{e^{-0.02t}}$

$$\frac{e^{-0.01t}}{e^{-0.02t}}=\frac{0.32}{0.2}$$
$$e^{-0.01t(-0.02t)}=1.6$$
$$e^{-0.01+0.02t}=1.6 \tag{2.29}$$

Taking ln of both sides

$$0.01t=ln1.6$$

Taking logarithms of both sides

$$t=ln1.6$$

$$t = 47 \tag{2.30}$$

The critical number corresponds to a maximum, the largest price occur after 47 months

Since

$$P(47) = 1 + 20\ell^{-0.01(47)} - 16\ell^{-0.02(47)} = 7.25 \tag{2.31}$$

The largest unit price is approximately 7.25

Since

$$D(47) = 3 + 10\ell^{-0.01(47)} = 9.25$$
$$\textit{and} \tag{2.32}$$
$$S(47) = 2 + P(47) = 2 + 7.25 = 9.25$$

It follows that approximately 9.250 units will be both demanded and supplied at the maximum price of 7.25 naira per unit

d) Since

$$\lim_{t\to\infty} P(t) = \lim\left(1 + 20\ell^{-0.01t} - 16\ell^{-0.02t}\right) = 1 + 20(0) - 16(0) = 1 \tag{2.33}$$

The Price tends towards 1 naira per unit in the "Long run".

Case 2:- *Supply* $S(t)$ and *demand* $D(t)$ functions for a commodity are given in terms of the unit price $P(t)$ at time t. Assume that price changes at a rate proportional to the shortage $D(t) - S(t)$ with indicated constant of proportionality K and initial price P_0 in each problem:

a. Set up and solve a differential equation for $P(t)$
b. Find the unit price of the commodity when $t = 4$
c. Determine what happens to the price at $t \to \infty$.

$$S(t) = 2 + 3p; D(t) = 10 - p(t); k = 0.02; p_0 = 1$$

From equation (3.1)

$$\frac{dp}{dt} = K(D - S) \tag{2.34}$$

$$\frac{dp}{dt} = k\left(D(t) - S(t)\right) = k\left((10 - p) - (2 + 3p)\right) = k\left(D(t) - S(t)\right) = k\left(10 - 2 - (p + 3p)\right) \tag{2.35}$$
$$\frac{dp}{dt} = k(8 - 4p)$$

Or equivalently,

$$\frac{dp}{dt} = 0.02(8-4p) = 0.16 - 0.08p$$

$$\frac{dp}{dt} + 0.08p = 0.16 \qquad (2.36)$$

a) Implying it's a first order linear differential equation with $P(t) = 0.08 and Q(t) = 0.16$

b) The integrating factor is $I(t) = e^{\int 0.08dt} = e^{0.08t}$ (2.37)

So the general solution is

$$P(t) = \frac{1}{e^{0.08t}}\left(\int \ell^{0.08t}(0.16)dt + c\right) = e^{-0.08t}\left(\frac{0.16\ell^{0.08t}}{0.08} + c\right) = \ell^{-0.08t}\left(2\ell^{0.08t} + c\right) = 2 + c\ell^{-0.08t} \qquad (2.38)$$

Since the initial price is $P(0) = 1;\ \Rightarrow P(0) = 5 = 2 + ce^{-0.08t} = 2 + \ell^{-0.08(0)} = 2 + c$ (2.39)

So that $c = 1 - 2 = -1$

And

$$P(t) = 2 - e^{-0.08t} \qquad (2.40)$$

b) After 4 months $(t = 4)$ the price is

$$P(4) = 2 - e^{-0.08(4)} = 2 - e^{-0.032} \approx 1.2739 \qquad (2.41)$$

That is, approximately 1.27 naira per unit

c) Price $P(t)$ as $t \to \infty$ will become

$$\lim_{t\to\infty} P(t) = \lim\left(2 - \ell^{-0.08t}\right) = 2 - 0 = 2 \qquad (2.42)$$

The Price tends towards 2 naira per unit in the "Long run".

Case 3:

Assume

$S(t) = 1 + 4p(t); D(t) = 15 - 3p(t); k = 0.015; p_0 = 3$

$$\frac{dp}{dt} = K(D-S) \tag{2.43}$$

$$\frac{dp}{dt} = k\left(D(t)-S(t)\right) = k\left((15-3p)-(1+4p)\right) = k\left(15-3p-1-4p\right) = k\left(15-1-(3p+4p)\right)$$

$$\frac{dp}{dt} = k\left(14-7p\right)$$

Or equivalently,

$$\Rightarrow \frac{dp}{dt} = 0.015\left(14-7p\right) = 0.21-0.105p$$

$$\frac{dp}{dt} + 0.105p = 0.21 \tag{2.44}$$

Implying it's a first order linear differential equation with $P(t) = 0.105 and Q(t) = 0.21$ The integrating factor is $I(t) = e^{\int 0.105dt} = e^{0.105t}$

So the general solution is

$$P(t) = \frac{1}{e^{0.105t}}\left(\int \ell^{0.105t}(0.21)\,\mathrm{dt} + \mathrm{c}\right) = e^{-0.105t}\left(\frac{0.21\ell^{0.105t}}{0.105} + c\right) = \ell^{-0.105t}\left(2\ell^{0.105t} + c\right) \tag{2.45}$$

$$= 2 + c\ell^{-0.105t}$$

Since the initial price is $P(0) = 1$;

$$\Rightarrow P(0) = 3 = 2 + ce^{-0.105t} = 2 + \ell^{-0.105(0)} = 2 + c\ell^{0} = 2 + c \tag{2.46}$$

So that $c = 3-2 = 1$

And

$$P(t) = 2 + e^{-0.105t} \tag{2.47}$$

b) After 4 months $(t = 4)$ the price is

$$P(4) = 2 + e^{-0.105(4)} = 2 + e^{-0.042} \approx 2.6570$$

That is, approximately 2.6570 naira per unit

c) Price $P(t)$ as $t \to \infty$ will become

$$\lim_{t\to\infty} P(t) = \lim\left(2 + \ell^{-0.105t}\right) = 2 + 0 = 2$$

The Price tends towards 2 naira per unit in the "Long run".

Case 4:

Assume

$S(t)=2+p(t); D(t)=3+7\ell^{-t}; k=0.02; p_0=4$

From equation (3.1)

$$\frac{dp}{dt}=`K(D-S) \tag{2.48}$$

$$\frac{dp}{dt}=k(D(t)-S(t))=k\left((3+7\ell^{-t})-(2+p)\right)=k\left(3-2-7\ell^{-t}-p\right)=k\left(1+7\ell^{-t}-p\right)$$

$$\frac{dp}{dt}=k\left(1+7\ell^{-t}-p\right)$$

Or equivalently,

$$\Rightarrow \frac{dp}{dt}=0.02\left(1+7\ell^{-t}-p\right)=0.02+0.14\ell^{-t}-0.02p$$

$$\frac{dp}{dt}+0.02p=0.02+0.14\ell^{-t} \tag{2.49}$$

Implying it's a first order linear differential equation with $P(t)=0.02 and Q(t)=0.02+0.14\ell^{-t}$

The integrating factor is $I(t)=e^{\int 0.02\,dt}=e^{0.02t}$ (2.50)

So the general solution is

$$P(t)=\frac{1}{e^{0.02t}}\left(\int \ell^{0.02t}(0.02+0.14\ell^{-t})dt+c\right)=e^{-0.02t}\left(\frac{0.02\ell^{0.02t}}{0.02}+\frac{0.14\ell^{-t}}{-1}+c\right)$$

$$=\ell^{-0.02t}\left(\ell^{0.02t}-0.14\ell^{-t}+c\right)$$

$$P(t)=1-0.14\ell^{-1.02t}+c\ell^{-0.02t}$$

Since the initial price is $P(0)=4$;

$$\Rightarrow P(0)=4$$

$$=1-0.14\ell^{-1.02}+ce^{-0.02t}=1-0.14\ell^{-0.02(0)}+c\ell^{-0.02(0)}=1-0.14\ell^{0}+c\ell^{0}=1-0.14+c$$

So that $c=4-1+0.14=3.14$

And

$$P(t) = 1 - 0.14\ell^{-0.02t} + 3.14e^{-0.02t}$$

Or

$$P(t) = 1 - \frac{1}{7}\ell^{-0.02t} + \frac{22}{7}e^{-0.02t} \qquad (2.51)$$

b) After 4 months $(t = 4)$ the price is

$$P(4) = 1 - 0.14\ell^{-0.02(4)} + 3.14e^{-0.02(4)} = 1 - 0.14\ell^{-0.08} + 3.14e^{-0.08} = 3.7693 \qquad (2.52)$$

That is, approximately 3.7693 dollars per unit

c) Price $P(t)$ as $t \to \infty$ will become

$$\lim_{t\to\infty} P(t) = \lim\left(1 - 0.14\ell^{-0.02t} + 3.14\ell^{-0.02t}\right) = 1 - 0 + 0 = 1 \qquad (2.53)$$

The Price tends towards 1 naira per unit in the "Long run".

3.0 RESULTS AND DISCUSSION

With a closer view at the Evans Price Adjustment Model in chapter three, it's a determinant factor of Price as regards quantity of Demand $D(t)$ and supply $S(t)$ with respect to time t .variation of time clearly shows that as time increases, price increases, supply increases and demand decreases. This is the more reason we have to use MATLAB.

CASE 1

Table 3.1: Values of Price and Quantity functions (D(t) and S(t)) with respect to time t

t	0	6	12	18	24	30	36	42	48	54
p1	5.0000	5.6446	6.1524	6.5426	6.8320	7.0354	7.1655	7.2336	7.2494	7.2214
d1	13.0000	12.4176	11.8692	11.3527	10.8663	10.4082	9.9768	9.5705	9.1878	8.8275
s1	7.0000	7.6446	8.1524	8.5426	8.8320	9.0354	9.1655	9.2336	9.2494	9.2214

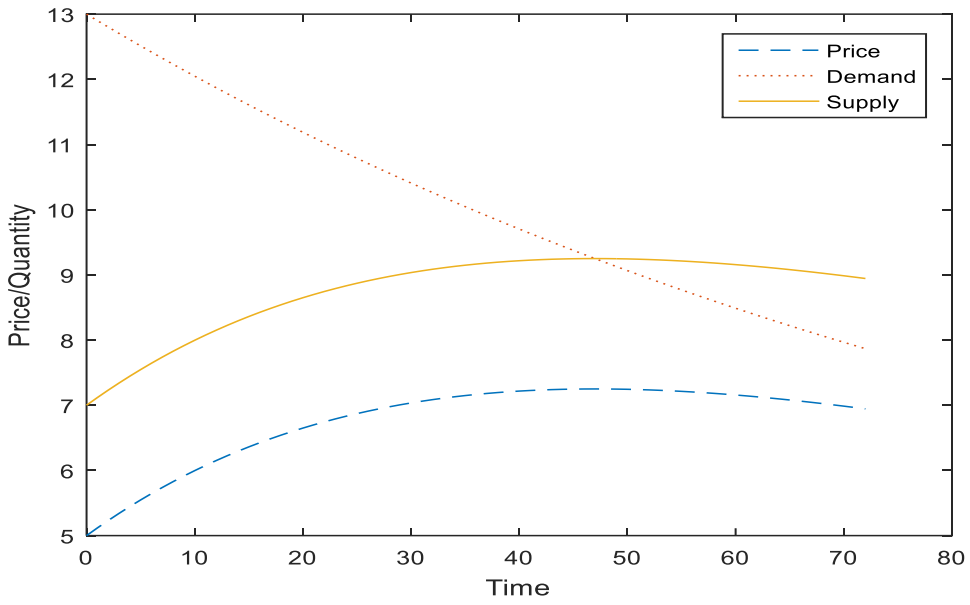

Figure 3.1: Graph of Price and Quantity functions (d(t) and s(t)) against time for case 1

$$p(t) = 1 + 20\ell^{-0.01t} - 16\ell^{-0.02t}, d(t) = 3 + 10\ell^{-0.01t}, s(t) = 2 + p$$

The above shows that within the period of 6 years as time increases there is an increase in price, and supply, while demand decreases drastically, at the point where demand equals supply, it said to be point of Equilibrium.

CASE 2

Table 3.2: Values of Price and Quantity functions (d(t) and s(t)) with respect to time t

t	0	6	12	18	24	30	36	42	48	54
p2	1.0000	1.3812	1.6171	1.7631	1.8534	1.9093	1.9439	1.9653	1.9785	1.9867
d2	9.0000	8.6188	8.3829	8.2369	8.1466	8.0907	8.0561	8.0347	8.0215	8.0133
s2	5.0000	6.1436	6.8513	7.2892	7.5602	7.7278	7.8316	7.8958	7.9355	7.9601

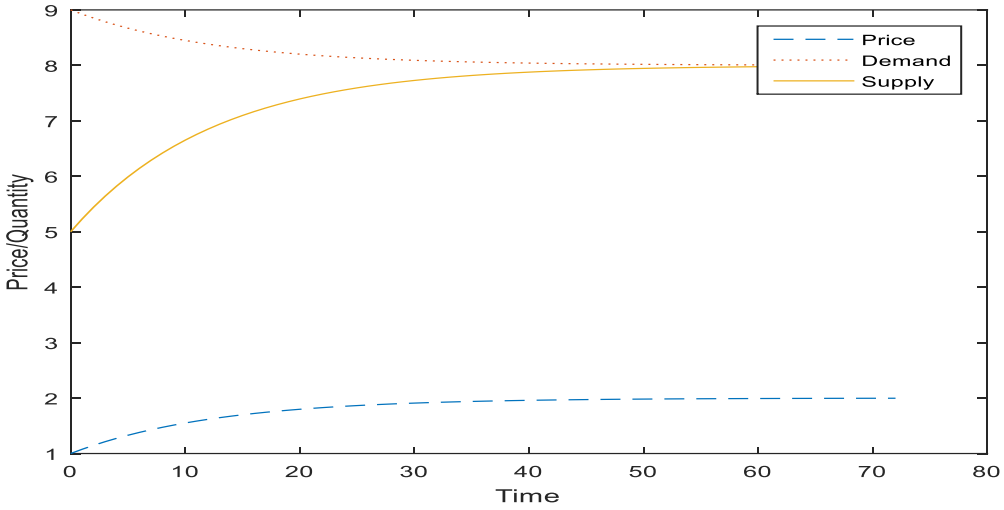

Figure 3.2: Graph of Price and Quantity functions (d(t) and s(t)) against time for case 2

$p(t) = 2 - \ell^{-0.08t}, \mathrm{d}(t) = 10 - 2p, \mathrm{s}(t) = 2 + 3p$

The above shows that within the period of 6 years as time increases there is an increase in price, and drastic increase in supply while demand decreases , at the point where demand equals supply, it said to be point of Equilibrium.

CASE 3

Table 3.3: Values of Price and Quantity functions (d(t) and s(t)) with respect to time t

t	0	6	12	18	24	30	36	42	48	54
p3	3.0000	2.5326	2.2837	2.1511	2.0805	2.0429	2.0228	2.0122	2.0065	2.0034
d3	6.0000	7.4022	8.1490	8.5468	8.7586	8.8714	8.9315	8.9635	8.9806	8.9897
s3	13.0000	11.1304	10.1346	9.6043	9.3218	9.1714	9.0913	9.0486	9.0259	9.0138

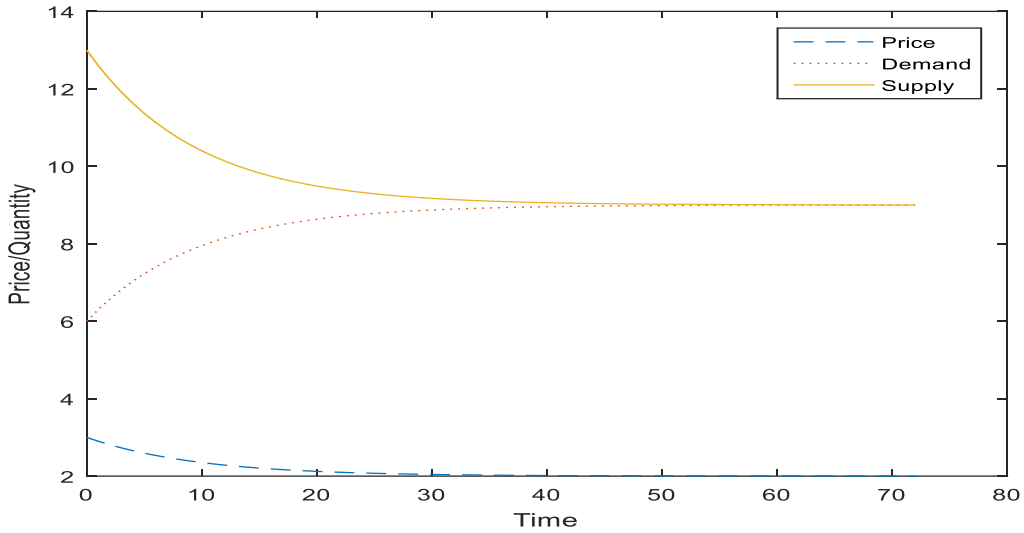

Figure 3.3: Graph of Price and Quantity functions (d(t) and s(t)) against time for case 3

$p(t)=2+\ell^{-0.105t}, d(t)=15-3p, s(t)=1+4p$

The above shows that within the period of 6 years as time increases there is a decrease in price, and supply decreases drastically while demand increases significantly, at the point where demand equals supply it said to be point of Equilibrium.

CASE 4

Table 3.4: Values of Price and Quantity functions (d(t) and s(t)) with respect to time t

t	0	6	12	18	24	30	36	42	48	54
p4	4.0000	3.6608	3.3599	3.0930	2.8564	2.6464	2.4603	2.2951	2.1487	2.0188
d4	10.0000	3.0174	3.0000	3.0000	3.0000	3.0000	3.0000	3.0000	3.0000	3.0000
s4	6.0000	5.6608	5.3599	5.0930	4.8564	4.6464	4.4603	4.2951	4.1487	4.0188

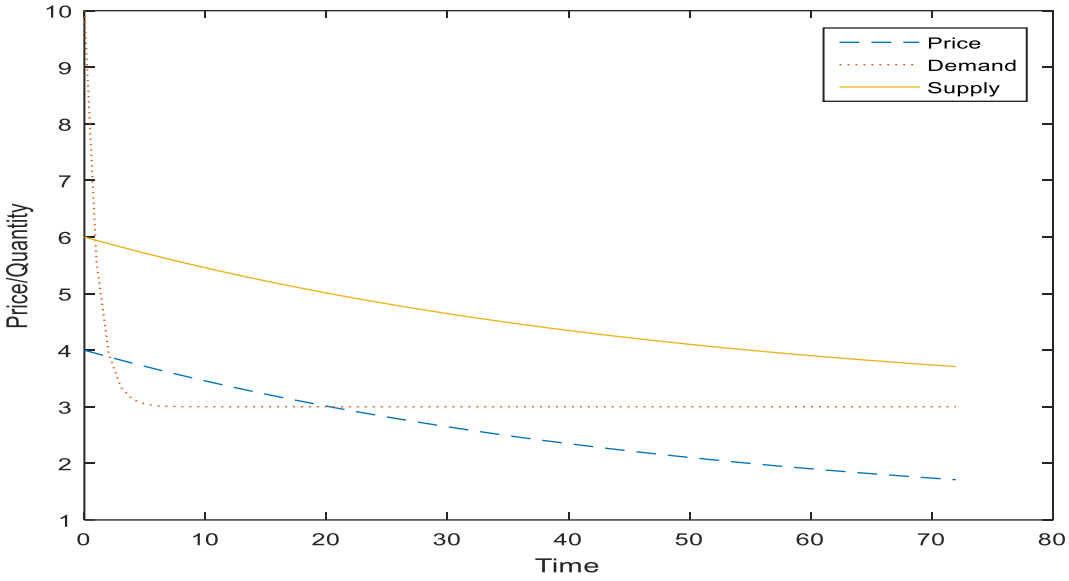

Figure 3.4: Graph of Price and Quantity functions (d(t) and s(t)) against time t case 4

$$p(t)=1-\frac{1}{7}\ell^{-0.02t}+\frac{22}{7}\ell^{-0.02t}, \mathrm{d}(t)=3+7\ell^{-t}, \mathrm{s}(t)=2+p$$

The above shows that within the period of 6 years as time increases there is an decrease in price, and supply, while demand decreases significantly, at the point where demand equals supply it said to be point of Equilibrium.

4.0 CONCLUSION

The problems formulated in this work were solved analytically using differential calculus through the application of Evans Price Adjustment Model, as the Price increases with respect to time, it gets to a point where it stops increasing and then begins to decrease until it gets to a fixed point which is the point of Equilibrium and also this in turn also affects the demand for the products and also supply which with respect to time, providing the Graphical summaries of the system responses.

REFERENCES

Goldsmith, R.W. (1969). *Financial Structure and Development*, Yale University Press, New Haven, USA.

Levine, R. (1991). Stock Market, Growth, and Tax Policy, *Journal of Finance*, 46(4), pp. 1445-1465.S

Levine, R. and Zervos, S. (1998). Stock Markets, Banks and Economic Growth, *The American Economic Review*, 88(3), pp. 537-558.

Prabha, A., Savard, K. and Wickramarachi, H. (2014). *Deriving the Economic Impact of Derivatives, Growth Trough Risk Management*, Working paper, Milken Institute, Los Angeles, USA.

Sipko, J. (2011). Derivatives and the Real Economy, *International Scientific Journal*, 1(1), pp. 33-43.

Sundaram, K.R. and Das, S.R. (2013). *Derivatives Principles and Practice*, McGraw Hill, New York.

Wicksell K.. (1934). *Lectures on Political Economy*, Routledge, London.

Panel Data Regression Method for Evaluating Financial Performance of Commercial Banks in Nigerian

By
YisaYakubu and Egopija, Sitamara Mercy

Department of Statistics, School of Physical Sciences
Federal University of Technology, Minna, Niger State, Nigeria

Abstract

Evaluation of financial performance of the banking sector is an effective measure and indicator to check the soundness of economic activities of a nation because thesector's performance is perceived as the nation's replica of economic activities.The key indicators of banks' financial performance are their return on assets (ROA), which indicates the proportion of profit a company makes in relation to its assets and return on equity (ROE), whichmeasures a corporation's profitability by revealing how much profit a company generates with the money shareholders have invested. Panel data are data on two or more entities for multiple time periods.Therefore, this study sought to model the overall performance of some sampled commercial banks (in terms of ROA and ROE) in Nigeria using panel data regression methods. This performance is modeled in relation to the factors that affect it, which include capital adequacy ratio(CAR), credit risk(CRISK), management, liquidity ratio(LIQ.RAT.) and bank size. The results revealed that capital adequacy ratio (CAR), credit risk (CRISK), and liquidity ratio (LIQ.RAT) have highly significant effects on the estimated ROA model at both 1% and 5% significance levels with the given p-values. This model accounted for over 82% of the total variability in the data. However, for the fitted ROE model, only credit risk (CRISK) and liquidity ratio (LIQ.RAT)

were observed to have highly significant effects at both 1% and 5% significance levels and the fitted model accounted for about 69% of the total variation in the ROE data.

1.0 INTRODUCTION:

Financial sectors play crucial role in a nation's economic growth and industrialization through channeling funds from surplus units- the depositors, to the deficit units, the borrowers, and in the process gaining from the spread of the different interests charged. Banks are important component of the financial sector of any economy because of their role as financial intermediaries that helps facilitate capital to promote productivity and thereby enhancing growth and development in the economy (Onyema*et al*, 2018).The financial performance of a bank is its ability to make use of available resources to boost shareholders' wealth and, at the same time, strengthen its capital base to ensure future survival and profitability.Evaluation of financial performance of the banking sector is an effective measure and indicator to check the soundness of economic activities of a nation. This is so because the banking sector's performance is perceived as the replica of economic activities of the nation. The stage of development of the banking industry is a good reflection of the development of the economy (Misra&Aspal, 2013). Therefore, to sustain the development of a nation's economy, the financial performance of the banking sectorneeds to be checked and evaluated periodically.This periodic evaluation will enable the shareholders to assess which banks they can deem suitable for financialinvestment. This will also enable the banks to determine the efficacy and long term viability of their management decisions or goals so thatthey can alter the course and make changes whenever it is appropriate.

The degree to which banks extend credits to the public for fruitful activities speeds up the0pace of0a0nation's economic0growth as well as the long-term0sustainability of the banking business (Kolapo, Ayeni&Oke, 2012). This explains why it is necessary to draft policies for the sector and why it is therefore0not0surprising that their0operations0are perhaps the0most0heavily0regulated of all businesses. In varying degrees, these policies are aimed at achieving macroeconomic objectives, stability, efficiency and soundness of the financial system (Adeusi and Familoni, 2004).

The productivity of a bank0largelydepends on the magnitude to which0it has performed0in the intermediation0procedure either0locally0or globally. Banks,through0their0intermediary role accrue0profits0and on the0other hand, might0incur0losses if not efficient0and0effective in0their operations.As rightly observed by (Flamini et al, 2009), bank earningsoffer asubstantial source of equity if reinvested into business. This could0lead to safe0banks, great profits and firmness in the

economy. Therefore, bank profitability is of great importance both to the individual and the society at large.

Financial performance measurement of any firm is vital in determining the tactics to be expressed to ensure that the firm is on the right track, (ECB, 2010). First of all, a bank must be able to produce incomes to remain in operation. Furthermore, it should be effective,that is, it should be able to create revenue from the given assets and make profits. Thirdly, it should be able to regulate its earnings to overcome the numerous risks associated, such as credit risk, and finally it should be able to improve its results through the approach it functions, (Kuria, 2013).

The stage of development of the banking industry in any nation is a good reflection of the development of the nation's economy (Misra&Aspal, 2013). To sustain the development of the economy, the performanceand health of the banking sector have to be checked and evaluated periodically. Differentapproaches are often used by different regulatory bodies and scholars to evaluate banks' financial performance. For example, there is CAMEL (Capital adequacy, Asset quality, Managementquality, Earnings and Liquidity) rating criterion, CLSA-Stress test, Bankometer S-score model, etc. The most frequently-used approach to assess and evaluate the performance andfinancial soundness of the activities of the bank is the CAMEL approach (see Rehana and Irum, (2012), Jaffar and Manarvi, (2011), Onyema*et al* (2018), etc., for details). However, this study use panel data regression approach to evaluate financial performance of some selected commercial banks in Nigeria by assessing a bank's return on assets (ROA) and its return on equity (ROE). The banks' financial performance were measured by their return on asset (ROA) and return on equity (ROE). The return on asset (ROA) is an economic ratio that indicates the proportion of profit a company makes in relation to its assets. It is the ratio of the net profit to total assets. ROA measures how successfully a bank's assets are managed to create profits (Golin, 2001).

$$ROA = Net\ income\ /\ Total\ assets$$

Return on equity (ROE) measures a corporation's profitability by revealing how much profit a company generates with the money shareholders have invested. It is given as

$$ROE = Net\ income\ /\ Total\ capital$$

This work seeks to model the relationship between the sampled banks' financial performance (measured in terms of these statistics) and some key factors that are believed to affect such performance. Such factors include

Capital Adequacy Ratio (CAR), which is a ratio of the capital of a bank to its risk. It is used to shield investors and stimulates the stability and effectiveness of economic systems. CAR is a vital measure to ascertain the condition of financial institutions and the wellness of banks (Kosmidou (2008). The capital adequacy ratio (CAR) can be calculated as the proportion of shareholders' equity to total assets, which is seen as the overall utilization of the financial leverage of the bank. That is,

$$CAR = \left(\frac{total\ equity}{total\ assets}\right)$$

Credit Risk: Credit risk is the risk that a financial loss will be suffered if a borrower does not fulfill his obligations according to the agreed terms. It is the ratio of the total loans to total assets.

$$Credit\ Risk\ = \left(\frac{total\ loans}{total\ assets}\right)$$

Management**:** Management is a substantive element that determines a bank's accomplishment. It is given as

$$\text{Management} = \left(\frac{\text{operating expenses}}{\text{total assets}}\right)$$

Liquidity**:** the liquidity of a bank is the ability to realize its short-term liability and sustain its affluence at the same time. Loan-to-deposit ratio is used to assess the liquidity of the bank by comparing its total loans to total deposits at the same time period and expressed as a percentage. If the ratio is too high, then the bank may not have sufficient liquidity to cover any unpredicted fund requirements and if it is too low, the bank may not be making as much as it is expected. It is given as

$$\text{Liquidity} = \left(\frac{\text{total loans}}{\text{total deposits}}\ x\ 100\right)$$

Bank size**:** The size of a bank is also a substantive element on its performance or profitability. The natural logarithm of total assets is used to indicate the size of a bank. That is, bank size = $ln(total\ assets)$.

Panel data are data on two or more entities for multiple time periods. Such data have a cross-section component and a time-series components as the values of the variables of interest are registered for several time periods or at several time points for each individual. Practice shows that panel data has an extensive use in biological and social sciences (Frees, 2004). There are considerable advantages of using panel data as opposed to using only time series or only cross-sectional data. They are

extensively addressed by Frees (2004). The panel data estimation methods require less assumptions and are often less problematic than simpler methods. One basic advantage of using panel data is the use of individual-specific components in the models.

2.0 RESEARCH METHODOLOGY

The population0of this0study comprises of all the commercial banks in Nigeria out of which five banks were sampled. The sampled banks include Zenith Bank, Guarantee Trust Bank (GTB), United Bank for Africa (UBA), Access Bank and First Bank. The data used for this work were secondary data gotten from the published and audited annual financial report of each of the banks for the period 2010 -2017.

Secondary data on each of the two dependent variables (ROA) and (ROE) and the five independent variables were generated from the published and audited annual financial report of each of the banks for the period 2010 -2017.Two estimation methods are used in this work, which include the pooled and the fixed effects models.

2.1 The pooled Model

The pooled model does not differ from the common regression equation. It regards each observation as unrelated to the others ignoring panels and time. No panel information is used. A pooled model can be expressed as:

$$y_{it} = \beta_0 + \beta_1 X_{1,it} + \beta_2 X_{2,it} + \cdots + \beta_k X_{k,it} + \epsilon_{it} \quad (1)$$

A pooled model is used under the assumption that the individuals behave in the same way, where there is homoscedasticity and no autocorrelation. Only then OLS can be used for obtaining efficient estimates. The assumptions for the pooled model are the same as for the simple regression model as described by Greene (2012).

2.2 The Fixed effects Model

One of the advantages of using panel data as mention in Section 1 above is that models like the fixed effects model can deal with the unobserved heterogeneity. The fixed effects model for factors can be expressed as

$$y_{it} = \alpha_i + \beta_1 X_{1,it} + \beta_2 X_{2,it} + \cdots + \beta_k X_{k,it} + \epsilon_{it} \quad (2)$$

Wherey_{it} denotes the observed outcome of entity i at time t,X_{it} is the (1xK) vector of covariates of this entity measured contemporaneously, and β is the corresponding (Kx1) vector of parameters to be

estimated. The α_i are stable, entity-specific characteristics. That is, α_i are unobserved effects capturing time-constant individual heterogeneity.$\epsilon_{it}$is an idiosyncratic error that varies across subjects and over time.

There is no constant term in the fixed effects model. Instead of the constant term $\beta_0$in the pooled model (1) above, now we have an individual-specific component α_i that determines a unique intercept for each individual. However, the slopes (the βparameters) are the same for all individuals.Two methods are available for computing the estimates of the fixed effects model (Josef and Volker, 2015), which include the within-groups method and least squares dummy variable method (LSDV).The two methods yield equivalent results. However, the technique of including a dummy variable for each variable (that is, the second method) is feasible when the number of individuals N is small. When the number of individuals is large, the within-groups method is the best because there will be too many dummy variables.

2.2.1The within-group method

Given the fixed effects model in (2) above, for the within-group method when the sample size is large, first, one has to compute the means of all observed variables within individuals across time as follows.

$$\bar{y}_{i.} = \frac{1}{T}\sum_{t=1}^{T} y_{it};\ \bar{x}_{l,i.} = \frac{1}{T}\sum_{t=1}^{T} x_{l,it},\quad l = 1, \dots, K$$

Equation (2) then takes the form

$$\bar{y}_{i.} = \alpha_i + \beta_1\bar{x}_{1,i.} + \beta_2\bar{x}_{2,i.} + \cdots + \beta_k\bar{x}_{k,i.} + \bar{\epsilon}_{i.} \qquad (3)$$

The term $\bar{\epsilon}_{i.}$is assumed to be 0. Also, since α_i is time-invariant, its mean across time would stay as the original value for each individual. Next, equation (3) is subtracted from equation (2) as

$$y_{it} - \bar{y}_{i.} = \beta_1\left(X_{1,it} - \bar{x}_{1,i.}\right) + \beta_2\left(X_{2,it} - \bar{x}_{2,i.}\right) + \cdots + \beta_k\left(X_{k,it} - \bar{x}_{k,i.}\right) + \left(\epsilon_{it} - \bar{\epsilon}_{i.}\right) \qquad (4)$$

By this subtraction, the individual specific component disappears. Also if a constant term had been used, it would have also disappeared.

Let $\tilde{y}_{it} = y_{it} - \bar{y}_{i.}, \tilde{X}_{l,it} = X_{l,it} - \bar{x}_{l,i.}$, for $l = 1, \dots, K$and $\tilde{\epsilon}_{it} = \epsilon_{it} - \bar{\epsilon}_{i.}$, then equation (4) can be written as

$$\tilde{y}_{it} = \beta_1\tilde{X}_{1,it} + \beta_2\tilde{X}_{2,it} + \cdots + \beta_k\tilde{X}_{k,it} + \tilde{\epsilon}_{it} \qquad (5)$$

The parameters and the individual-specific component can then be computed using the formulas:

$$\hat{\beta}_i = \frac{\sum\sum\tilde{X}_{l,it}\tilde{y}_{it}}{\sum\sum\tilde{X}_{l,it}^2};\ \hat{\alpha}_i = \bar{y}_{i.} - \hat{\beta}_1\bar{X}_{1,i.} - \hat{\beta}_2\bar{X}_{2,i.} - \cdots - \hat{\beta}_k\bar{X}_{k,i.}$$

These estimates are consistent.

2.2.2. The Fixed Effects Least-Squares Dummy Variable Model (LSDV)

Now, since this work considers five commercial banks (where N is not too large) for eight time periods, the LSDV is fitted to the collected data sets using ROA and ROE as the dependent variables.For our data with five banks, the fixed effects model with dummy variables, where intercepts α_i are different for different banks but each individual intercept does not vary over time is

$$y_{it} = \alpha_0 + \alpha_1 D_1 + \alpha_2 D_2 + \alpha_3 D_3 + \alpha_4 D_4 + \beta_1 X_{1,it} + \beta_2 X_{2,it} + \beta_3 X_{3,it} + \beta_4 X_{4,it} + \beta_5 X_{5,it} + \epsilon_{it} \quad (6)$$

WhereD_k denotes the k^{th} bank, $k = 1, \dots, 5$, (Zenith, First, UBA, GTB and ACCESS),Xdenotes cash adequacy ratio(CAR), credit risk, management, liquidity ratio, and size, respectively, i stands for the i^{th} bank,$i = 1, \dots, 5$ and t stands for the t^{th} time period ($t = 2010, \dots, 2017$).Thus the individual effect is picked up by the dummy variable $D_{mi}$where $m = n-1$ and the dummy variables are defined as

$$D_{1i} = \begin{cases} 1, & i = 1 \\ 0, & otherwise \end{cases}$$

$$D_{2i} = \begin{cases} 1, & i = 2 \\ 0, & otherwise \end{cases}$$

$$D_{3i} = \begin{cases} 1, & i = 3 \\ 0, & otherwise \end{cases}$$

$$D_{4i} = \begin{cases} 1, & i = 4 \\ 0, & otherwise \end{cases}$$

3.0 Results and Discussion

We first look at the correlation structure of the variables with themselves as given in the table below.

Table 3.1: Correlation0coefficients, using0the observations 1:1 - 5:8
5% critical0value (two-tailed) = 0.3120 for n = 40

	ROA	ROE	CAR	CRISK	MGT	LIQ__RAT	BANK_SIZE
ROA	1	0.9152	0.6293	0.3421	-0.0231	0.1442	-0.322
ROE		1	0.3508	0.1921	-0.1879	0.0971	-0.1229
CAR			1	0.6231	0.4356	0.1641	-0.7113
CRISK				1	0.5213	0.4528	-0.5318
MGT					1	-0.1389	-0.6121
LIQ__RAT						1	0.1744
BANK_SIZE							1

Correlation matrix above is used to assess the degree0of0relationship between each of the variables, most especially the independent variables, under study. The result shows that most of the variables are not highly correlated with each other. However, a few such as bank size and capital0adequacy ratio; credit risk and capital0adequacy ratio; and bank size and management have a correlation that is above average.

Test for multicollinearity using Variance Inflation Factors

Diagnostics: using n = 5 cross-sectional units

Table 3.2: Test for multicollinearity using Variance Inflation Factors

Variables	VIF
CAR	2.567
CRISK	3.11
MGT	1.961
LIQRAT	2.079
BANKSIZE	3.247
	2.5928

Table 3.2 above shows the testing of multicollinearity using VIF. There is serious case of multicollinearity whenever each VIF or the mean VIF is greater than 10. Hence, since the result of the test shows that no VIF was greater than 10 and the mean VIF is less than 10, we conclude that the model fitted does not suffer from the problem of multicollinearity.

3.1 Pooled Ordinary Least Square (OLS) Regression Model with ROA as dependent variable

Here we pool all observations together and run the regression model, neglecting the cross sections and time series nature of the data. By combining the commercial Banks and pooling the data, we deny the heterogeneity or individuality that may exist among the Banks. In other words, we assume that the five Banks are same.

Table3.3:Model 2: Pooled OLS, using 40 observations
Included 5 cross-sectional units
Time-series length = 8
Dependent variable: ROA

	Coefficient	*Std. Error*	*t-ratio*	*p-value*	
const	-2.92895	6.18757	-0.4734	0.63898	
CAR	26.7698	6.33202	4.2277	0.00017	***

CRISK	2.13311	2.23052	0.9563	0.34566	
MGT	-38.0696	14.951	-2.5463	0.01559	**
LIQ__RAT	-0.0156969	0.0169026	-0.9287	0.35961	
BANK_SIZE	0.221154	0.378657	0.584	0.56304	

R-squared=0.521 Adjusted R-squared = 0.451
F(5, 34) =7.397 P-value(F) = 0.0000

The predicted model for pooled cross-sectional model is given as

$$\boldsymbol{ROA_{it} = -2.928 + 26.769CAR + 2.133CRISK - 38.069MGT - 0.0156LIQ_{RAT} + 0.221BANK\_SIZE}$$

From table 3.3, the result obtained shows that *CAR* has a positive and significant effect on the ROA with p-value < 0.05 while the *CRISK*has a positive but insignificant effect on the ROA with a p-value greater than both 0.05 and 0.01. The MGT has negative but a significant effect on the ROA while the LIQ-RAT has a negative but insignificant effect on the ROA. The effect of the bank size was also observed from this Table to be positive but insignificant. The Table also revealed that about 52% of variation in the ROA of these banks was accounted for by this pooled OLS model. Hence, the model is adequate for predicting ROA. The F(5, 34) = 7.397 with p-value = 0.000 reveals that the model estimated was extremely significant.

Table3.4: Model 3: Pooled OLS, using 40 observations
Included 5 cross-sectional units
Time-series length = 8
Dependent variable: ROE

	Coefficient	*Std. Error*	*t-ratio*	*p-value*	
const	-3.38247	41.7323	-0.0811	0.93588	
CAR	94.2079	42.7066	2.2059	0.03425	**
CRISK	19.2032	15.0439	1.2765	0.21044	
MGT	-268.328	100.838	-2.661	0.01181	**
LIQ__RAT	-0.125465	0.114	-1.1006	0.27882	
BANK_SIZE	1.2023	2.55387	0.4708	0.64081	

R-squared=0.302 Adjusted R-squared = 0.200
F(5, 34) =2.952 P-value(F) = 0.0255

The predicted model for pooled cross-sectional model is given as

$$\boldsymbol{ROA_{it} = -3.382 + 94.207CAR + 19.203CRISK - 268.328MGT - 0.125LIQ_{RAT} + 1.202BANK\_SIZE}$$

From table 3.4, the result obtained shows that *CAR* has a positive and significant effect on the ROE with p-value < 0.05 while the *CRISK* has a positive but insignificant effect on the ROE with a p-value greater than both 0.05 and 0.01. The MGT has negative but a significant effect on the ROE while the LIQ-RAT has a negative but insignificant effect on the ROE. The effect of the bank size was also observed from this Table to be positive but insignificant. The Table also revealed that only about 30% of variation in the ROE of these banks was accounted for by this pooled OLS model. Hence, the model is inadequate for predicting ROE. The F(5, 34) = 2.952 with p-value = 0.0255 reveals that the model estimated was not too good.

3.2 The Fixed Effect LSDV Model Estimates

Using LSDV method, the fixed effects model estimates for ROA and ROE as dependent variablesare presented respectively below.

Table3.5: Fixed Effects LSDV Model Estimates with ***ROA*** as the dependent variable

Term	Coef	SE_Coef	T-Value	P-value
Const	-8.37	5.11	-1.64	0.112
ZENITH	0.317	0.427	0.74	0.464^{ns}
FIRST	-0.533	0.395	-1.35	0.187^{ns}
UBA	-0.319	0.469	-0.68	0.502^{ns}
GTB	2.08	0.33	6.31	0.000**
CAR	13.88	5.85	2.37	0.024*
CRISK	5.22	1.63	3.19	0.003**
MGT	-15.7	11.6	-1.35	0.187^{ns}
LIQ_RAT	-0.0423	0.0143	-2.95	0.006**
BANK_SIZE	0.642	0.326	1.97	0.058*

Model Summary: S = 0.606113, R-sq =83.12%, R-sq(adj) = 78.05%, R-sq(pred)=72.66%

The predicted fixed effects LSDV model is given as

$$ROA_{it} = -8.37 + 0.317ZENITH_{BANK} - 0.533FIRST_{BANK} - 0.319UBA + 2.08GTB + 13.88CAR + 5.22CRISK - 15.7MGT - 0.0423LIQ_{RAT} + 0.642BANK\_SIZE$$

From table 3.5 above, the effects of cash adequacy ratio (CAR), credit risk (CRISK), and liquidity ratio (LIQ.RAT) were observed to be highly significant at both 1% and 5% significance levels with the given p-values while BANK-SIZE was slightly significant at 5% level. The MGT effect was not significant. The fitted LSDV model accounted for over 83% of the total variation in the ROA, which indicates that the estimated model fits the data well.

The estimated ROA model for each of the banks are:

ACCESS BANK:

$$ROA_{it} = -8.37 + 13.88\,CAR + 5.22\,CRISK - 15.7\,MGT - 0.0423\,LIQ.RAT + 0.642\,BANK\,SIZE$$

GTB:

$$ROA_{it} = -6.29 + 13.88\,CAR + 5.22\,CRISK - 15.7\,MGT - 0.0423\,LIQ.RAT + 0.642\,BANK\,SIZE$$

UBA

$$ROA_{it} = -8.69 + 13.88\,CAR + 5.22\,CRISK - 15.7\,MGT - 0.0423\,LIQ.RAT + 0.642\,BANK\,SIZE$$

FIRST BANK

$$ROA_{it} = -8.90 + 13.88\,CAR + 5.22\,CRISK - 15.7\,MGT - 0.0423\,LIQ.RAT + 0.642\,BANK\,SIZE$$

ZENITH BANK

$$ROA_{it} = -8.05 + 13.88\,CAR + 5.22\,CRISK - 15.7\,MGT - 0.0423\,LIQ.RAT + 0.642\,BANK\,SIZE$$

Table3.6:Fixed Effects LSDV Model Estimates with ***ROE*** as the dependent variable

Term	Coef	SE_Coef	T-Value	P-value
Const	-29.2	38.6	-0.76	0.455
ZENITH	3.92	3.22	1.22	0.233
FIRST	-4.92	2.98	-1.65	0.109
UBA	-2.02	3.54	-0.57	0.573
GTB	12.47	2.49	5.01	0.000
CAR	-9.9	44.2	-0.22	0.824
CRISK	42.9	12.3	3.48	0.002

MGT	-124.9	87.8	-1.42	0.165
LIQ_RAT	-0.263	0.108	-2.43	0.021
BANK_SIZE	3.24	2.46	1.31	0.199

Model Summary: S =4.5755; R-sq = 69.21%; R-sq(adj)=59.97%; R-sq(pred)47.27%

The predicted fixed effects LSDV model is given as

$$ROE_{it} = -29.2 + 3.92ZENITH_{BANK} - 4.92FIRST_{BANK} - 2.02UBA + 12.47GTB - 9.9CAR + 42.9CRISK - 124.9MGT - 0.263LIQ_{RAT} + 3.24BANK\_SIZE$$

From table 3.6 above, it is only the effects of credit risk (CRISK) and liquidity ratio (LIQ.RAT) that were observed to be highly significant at both 1% and 5% significance levels with the given p-values, the other factor effects were not significant. The fitted LSDV model accounted for about 69% of the total variation in the ROE, which indicates that the estimated model fits the data well.However, when compared with that of the estimated ROA model above, the proportion of the total variability accounted for by this model is less than that of the ROA model.

For each of the banks, we have the estimated ROE models below.

ACCESS BANK:

$$ROE_{it} = -29.2 - 9.9\,CAR + 42.9\,CRISK - 124.9\,MGT - 0.263\,LIQ.\,RAT + 3.24\,BANK\,SIZE$$

GTB:

$$ROE_{it} = -16.7 - 9.9\,CAR + 42.9\,CRISK - 124.9\,MGT - 0.263\,LIQ.\,RAT + 3.24\,BANK\,SIZE$$

UBA

$$ROE_{it} = -31.2 - 9.9\,CAR + 42.9\,CRISK - 124.9\,MGT - 0.263\,LIQ.\,RAT + 3.24\,BANK\,SIZE$$

FIRST BANK

$$ROE_{it} = -34.1 - 9.9\,CAR + 42.9\,CRISK - 124.9\,MGT - 0.263\,LIQ.\,RAT + 3.24\,BANK\,SIZE$$

ZENITH BANK

$$ROE_{it} = -25.3 - 9.9\,CAR + 42.9\,CRISK - 124.9\,MGT - 0.263\,LIQ.\,RAT + 3.24\,BANK\,SIZE$$

3.3 Diagnostic plots

Figure 3.1 below gives the normal probability plot of the residuals, which indicates whether the residuals follow a normal distribution. From this plot, nearly all the points fall on the straight line. This indicates that, to some extent, the residuals were normally distributed. Thus there are no problems with our data.

Figure 3.1: Normal Probability plot of Residuals for the ROA LSDV Model

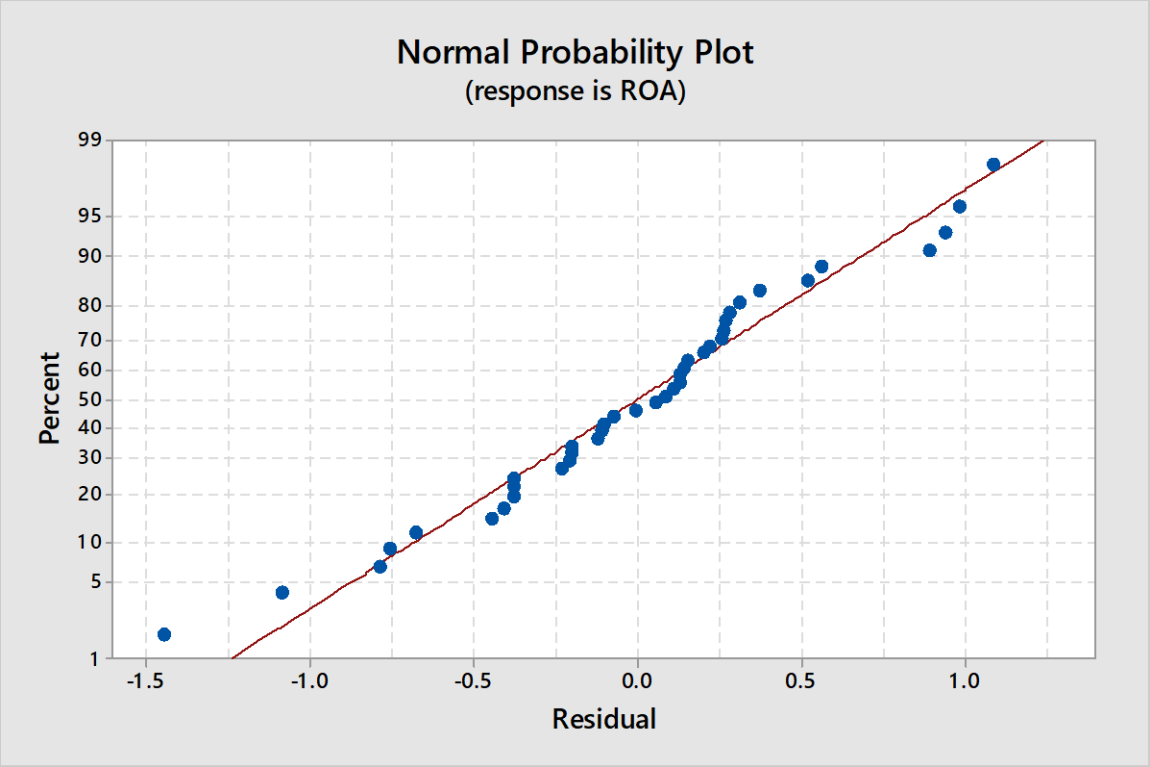

Figure 3.2 is a visual check for the assumption of constant variance. As can be directly seen, this plot is a random scatter with a consistent top to bottom range of residuals across the predictions on the X axis. Thus we can conclude here that our model satisfied the constant variance assumption.

Figure 3.2: Plot of Residuals versus the Fitted values for the ROA LSDV Model

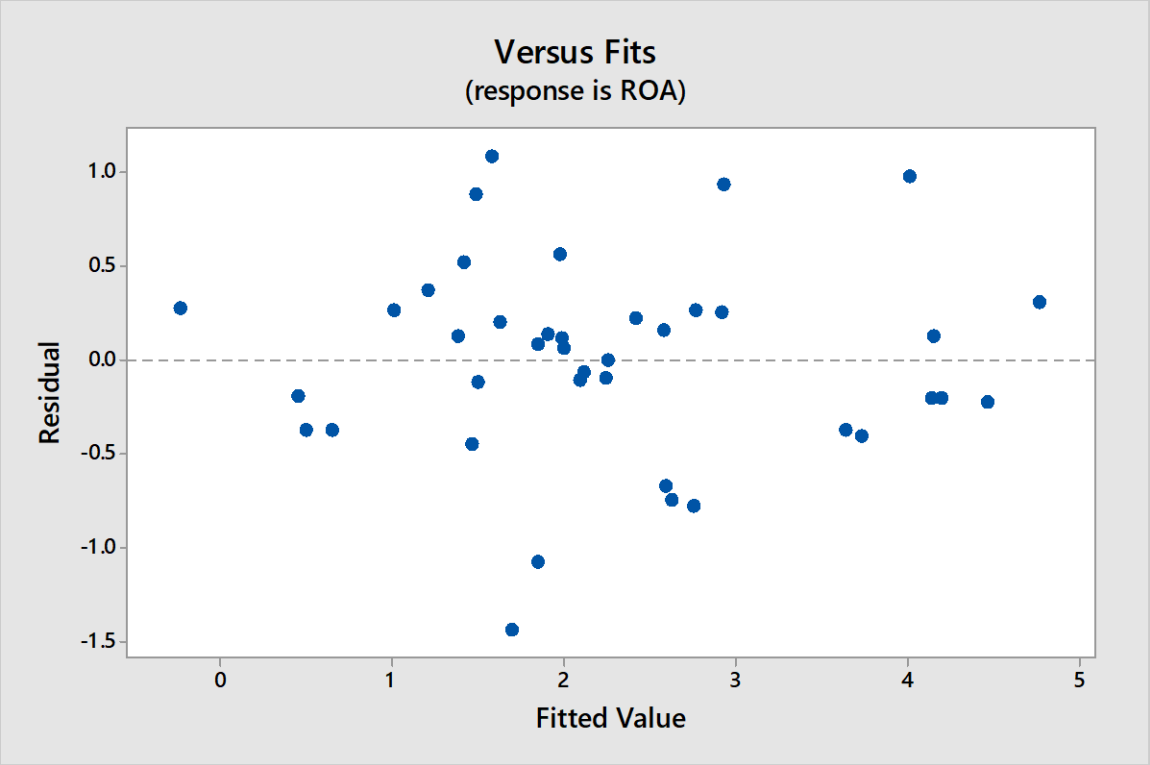

4.0 CONCLUSION AND RECOMMENDATIONS

Conclusion

Based on the findings from the preceding chapter, it can be0concluded that0capital structure has a relationship0with banks'0performance. It can also be concluded that there are other factors, aside the explanatory variables used in the analysis of this research work, that have a significant effect on the performance0of the banking0institution in0Nigeria. These may include the level of advertising, marketing strategies being implemented by the commercial banks, services being introduced into the market etc. These factors should be included into further studies relating to the performance of banks in0Nigeria.

Recommendations

Following the findings from the study, the following recommendations are made;

i. Capital structure should be0well0managed to ensure0that the firm0remains in operation0and is0able to finance its projects

ii. To improve0banks' performance, the banks need a good0regulatory environment that will0enable0expand their scope0of business. With a good regulation, the banks will be able to regulate unnecessary expenses.

REFERENCE

Abor, J. (2005). *The Effect of Capital Structure on Profitability: Empirical Analysis of Listed Firms in Ghana. Journal of Risk Finance, 6(5), 438 – 445.*

Ammar, A.G., (2013). *Impact of capital structure on banking performance: a case study of Pakistan. Interdisciplinary Journal of contemporary research in business, 4(10), 393 – 403.*

Anarfo, E.B. (2015). *Capital structure and bank performance: Evidence from Sub-Sahara Africa. European Journal of Accounting, Auditing and Finance Research, 3(3), 1 – 20.*

Burkhardt, J.H. & Wheeler, J.C. (2013). *Examining Financial Performance Indicators for Acute Care Hospitals. Journal of Health Care Finance, 39(3), 1 – 13.*

Chowdhury, A. & Chowdhury, P.S., (2010). *Impact of capital structure on firms' value: evidence from Bangladesh. Peer reviewed and open access Journal, 3(3) 111 – 115.*

Diamond, D. &Rajan, R. (2000). *A Theory of Bank Capital. Journal of Finance (55), 2431 – 2465.*

Ebaid, E.I (2009). *The Impact of Capital-structure Choice on Firm Performance: Empirical Evidence from Egypt. The Journal of Risk Finance, 10(5) 477 – 487.*

European Central Bank (2010). *Beyond ROE, how to Measure Bank Performance*

Fitch Rating, a subsidiary of Fitch Group, London and New York. (accessed from www.fitchratings.com)

Imala, O.I., (2005). *Challenges of banking sector reforms & bank consolidation in Nigeria. CBN bullion, 29(2).*

Kolapo, T.F., Ayeni, R.K., &Oke, M.O., (2012). *Credit risk and commercial banks' performance in Nigeria. European Journal of Economics, Finance and Administrative Sciences, 11.*

Modigliani, F & Miller, M (1958). *The cost of capital, corporation, finance and the theory of investment. The America Economic Review, 48(3), 261 – 297.*

Ogebe, P. & Joseph, O.O., (2013). *The impact of capital structure on firms' performance in Nigeria. MPRA paper No. 46173*

Oke, O.O., &Afolabi, B., (2008). *Capital structure and industrial performance in Nigeria: an empirical investigation. AAU Journal of management sciences, 1(1), 43 – 52.*

Saunders, A. & Cornett, M.M., (2007). *Financial institutions management: a risk management approach. The McGraw-Hill Edition, 2007, 6th Edition.*

www.accessbankplc.com

www.gtbank.com

www.irfbnholdings.com

www.ubagroup.com

www.zenithbank.com

Differential Transformation Method (DTM) for Solving Mathematical Modelling of Monkey Pox Virus Incorporating Quarantine

***[1]Somma S. A., [2]Akinwande N. I., [3]Abdurrahman N. O. and [4]Zhiri A. B.**

[1,2,3]Department of Mathematics, Federal University of Technology, Minna

*[1]sam.abu@futminna.edu.ng

[2]ninuola.wande@futminna.edu.ng

[3]abdurrahmannurat@gmail.com

[4]a.zhiri@futminna.edu.ng

Abstract

In this paper the Mathematical Modelling of Monkey Pox Virus Incorporating Quarantine was solved semi-analytically using Differential Transformation Method (DTM). The solutions of difference cases were presented graphically. The graphical solutions gave better understanding of the dynamics of Monkey pox virus, it was shown that effective Public Enlightenment Campaign and Progression Rate of Quarantine are important parameters that will prevent and control the spread of Monkey Pox in the population.

Keywords: differential transformation method; Monkey Pox Virus; semi-analytically; solution

Introduction

Differential Transformation Method (DTM) is a semi-analytical technique for solving linear and non-linear ordinary differential equations (ODEs). Differential Transformation Method (DTM) is one of the method uses to solve linear and nonlinear differential equations. It was first proposed Zhou (1986), for solving linear and nonlinear initial value problems in electrical circuit analysis. The DTM construct a semi-analytical numerical technique that uses Taylor series for the solution of differential equations in the form of a polynomial. DTM is a very effective and powerful tool for solving different kinds of differential equations. This technique has been used to solve different kind of problem by different people such as; Arikoglu. and Ozkol, (2007), Momani *et al.* (2008) used it to solved fractional differential equations, Ayaz (2004) solved differential algebraic equations, Moustafa,(2008) solved nonlinear oscillatory system and Biazar and Eslami (2010) solved quadratic Riccati differential equation. Akinboro *et al.* (2014) obtained the numerical solution of Susceptible Infected Recovered (SIR) model, Batiha (2015) obtained the solution of prey and predator problem, Soltanalizadeh (2012), solved fourth-order parabolic partial differential equations, Odibat (2008) solved Volterra integral equations and Arikoglu and Ozkol (2006) solved difference equations. The main advantage of this

method is that it can be applied directly to linear and nonlinear Ordinary Differential Equations (ODEs) without linearization, discretization or perturbation.

Monkey pox is caused by a rodent virus, which occurs mostly in West and Central Africa. The identification of monkey pox virus is based on biological characteristics and endonuclease patterns of viral DNA. In contrast to smallpox, monkeypox virus can infect rabbit skin and can be transmitted serially by intracerebral inoculation of mice. The four orthopoxviruses that may infect man produce macroscopically characteristic lesions on the inoculated chorioallantoic membrane of an embryonated chicken egg, (Jezek and Fenner, 1988).

The virus can spread from human to human by both respiratory (airborne) contact and contact with infected person's bodily fluids. Risk factors for transmission include sharing a bed, room, or using the same utensils with an infected patient. Increased transmission risk associated with factors involving introduction of virus to the oral mucosa, (Kantele, *et al.* 2016). Incubation period is 10–14 days. Prodromal symptoms include swelling of lymph nodes, muscle pain, headache, fever, prior to the emergence of the rash. The rash is usually only present on the trunk but has the capacity to spread to the palms and soles of the feet, occurring in a centrifugal distribution. The initial macular lesions exhibit a papular, then vesicular and pustular appearance, (Kantele, *et al.* 2016).

Literature Review

Che Hussin *et al.* (2010) proposed the generalization of differential transformation method to solve higher order of linear boundary value problem. They provided several numerical examples and compared the results with the exact solutions in order to show the accuracy of the proposed method.

Soltanalizadeh (2012) used the Differential Transformation method (DTM) to solved a fourth-order parabolic partial differential equations. In the end, some numerical tests are presented to demonstrate the effectiveness and efficiency of the proposed method.

Akinboro *et al.* (2014) investigated the application of differential transformation method and variational iteration method in finding the approximate solution of Epidemiology Susceptible Infected Recovered (SIR) model. Their result revealed that both methods are in complete agreement, accurate and efficient for solving systems of ODE.

Bhunu and Mushayabasa (2011) developed a mathematical modeling of pox- like infection, in their model they considered SIR model for both human and rodent/wild animals. They used Lyapunov approach to analyzed the global stability of the animal (nonhuman) endemic equilibrium.

Usman and Adamu (2017) developed a mathematical model for the dynamics of the transmission of monkeypox virus infection with control strategies of combined vaccine and treatment interventions. They used standard approaches to established two equilibria for the model namely: disease-free and endemic. They analyzed the disease-free equilibrium and endemic equilibrium. Basic reproduction

numbers for the humans and the non-human primates of the model were computed using next generation matrix

This paper reviews the paper of Bhunu and Mushayabasa (2011), by incorporating quarantine class and an enlightenment campaign parameter into the human population to control the spread of the disease in the population. The model equations are solve analytically and present the solutions graphically.

Table 2.1: The Fundamental Mathematical Operations by Differential Transformation Method (DTM)

Original Function	Transformed Function
$y(t)=f(t)\pm g(t)$	$Y(k)=F(k)\pm G(k)$
$y(t)=af(t)$	$Y(k)=aF(k)$
$y(t)=\frac{df(t)}{dt}$	$Y(k)=(k+1)F(k+1)$
$y(t)=\frac{d^2f(t)}{dt^2}$	$Y(k)=(k+1)(k+2)F(k+2)$
$y(t)=\frac{d^mf(t)}{dt^m}$	$Y(k)=(k+1)(k+2)\ldots(k+m)F(k+m)$
$y(t)=1$	$Y(k)=\delta(k)$
$y(t)=t$	$Y(k)=\delta(k-1)$
$y(t)=t^m$	$Y(k)=\delta(k-m)=\begin{cases}1, k=m\\0, k\neq m\end{cases}$
$y(t)=f(t)g(t)$	$Y(k)=\sum_{m=0}^{k}G(m)f(k-m)$
$y(t)=e^{(\lambda t)}$	$Y(k)=\frac{\lambda^k}{k!}$
$y(t)=(1+t)^m$	$Y(k)=\frac{m(m-1)\ldots(m-k+1)}{k!}$

Source: Hassan (2008).

Methodology

Model Equations

$$\frac{dS_h}{dt} = \Lambda_h + (1-\varepsilon)S_h - \left(\frac{\alpha_1 I_r}{N_h} + \frac{\alpha_2 I_h}{N_h}\right)S_h - \mu_h S_h \tag{3.1}$$

$$\frac{dI_h}{dt} = \left(\frac{\alpha_1 I_r}{N_h} + \frac{\alpha_2 I_h}{N_h}\right)S_h - (\mu_h + \delta_h + \tau)I_h \tag{3.2}$$

$$\frac{dQ_h}{dt} = \tau I_h - [\mu_h + \gamma_h + (1-\theta)\delta_h]Q_h \tag{3.3}$$

$$\frac{dR_h}{dt} = \gamma_h Q_h + \varepsilon S_h - \mu_h R_h \tag{3.4}$$

$$\frac{dS_r}{dt} = \Lambda_r - \frac{\alpha_3 I_r S_r}{N_r} - \mu_r S_r \tag{3.5}$$

$$\frac{dI_r}{dt} = \frac{\alpha_3 I_r S_r}{N_r} - (\mu_r + \delta_r)I_r \tag{3.6}$$

$$\left.\begin{aligned} 0 \le \varepsilon \le 1 \\ 0 \le \theta \le 1 \end{aligned}\right\} \tag{3.7}$$

$$N_h = S_h + I_h + Q_h + R_h \tag{3.8}$$

$$N_r = S_r + I_r \tag{3.9}$$

Table 3.1: Definition of Variables and Parameters

Variables/Parameters	Definition

S_h	susceptible Humans
I_h	Infected Humans
Q_h	Quarantine Infected Humans
R_h	Recovered Humans
S_r	Susceptible Rodents
I_r	Infected Rodents
Λ_h	Recruitment Rate of Humans
Λ_r	Recruitment Rate of Rodents
α_1	Contact Rate of Rodents to Humans
α_2	Contact Rate of Humans to Humans
α_3	Contact Rate of Rodents to Rodents
μ_h	Natural Death Rate of Humans
δ_h	Disease Induced Death Rate of Humans
γ_h	Recovery Rate of Humans
τ	Progression Rate from Infected to Quarantine
ε	Effectiveness Public Enlightenment Campaign
θ	Effectiveness of Quarantine and Treatment
μ_r	Natural Death Rate of Rodents
δ_r	Disease Induced Death Rate of Rodents
N_h	Total Population of Humans
N_r	Total Population of Rodents

Differential Transformation Method (DTM)

An arbitrary function $f(t)$ can be expanded in Taylor series about a point $t=0$ as

$$f(t)=\sum_{k=0}^{\infty}\frac{t^k}{k!}\left[\frac{d^k f}{dt^k}\right]_{t=0} \tag{3.10}$$

The differential transformation of $f(t)$ is defined as

$$F(t)=\frac{1}{k!}\left[\frac{d^k f}{dt^k}\right]_{t=0} \tag{3.11}$$

Then the inverse differential transform is

$$f(t)=\sum_{k=0}^{\infty}t^k F(t) \tag{3.12}$$

In Hassan (2008) if $y(t)$ and $g(t)$ are two uncorrelated functions with t where $Y(k)$ and $G(k)$ are the transformed functions corresponding to $y(t)$ and $g(t)$ then, the fundamental mathematical operations performed by differential transform can be proof easily and are listed as follows

Analytical Solution of the Model Equations using Differential Transformation Method (DTM)

In this section we are going to apply Differential Transformation Method to the Model equation and solve.

Let the model equation be a function $h(t)$, $h(t)$ can be expanded in Taylor series about a point $t=0$ as

$$h(t)=\sum_{k=0}^{\infty}\frac{t^k}{k!}\left[\frac{d^k h}{dt^k}\right]_{t=0} \tag{3.13}$$

Where,

$$h(t)=\{s_h(t), i_h(t),\ q_h(t),\ r_h(t), s_r(t),\ i_r(t)\} \tag{3.14}$$

The differential transformation of $h(t)$ is defined as

$$H(t)=\frac{1}{k!}\left[\frac{d^k h}{dt^k}\right]_{t=0} \tag{3.15}$$

Where,

$$H(t)=\{S_h(t), I_h(t), Q_h(t), R_h(t), S_r(t), I_r(t)\} \tag{3.16}$$

Then the inverse differential transform is

$$h(t)=\sum_{k=0}^{\infty} t^k H(t) \tag{3.17}$$

Using the fundamental operations of differential transformation method in table 2.1, we obtain the following recurrence relation of equation (3.1) to (3.6) as

$$S_h(k+1)=\frac{1}{k+1}\left[\Lambda_h-\frac{\alpha_1}{N_h}\sum_{m=0}^{k} S_h(m)I_r(k-m)-\frac{\alpha_2}{N_h}\sum_{m=0}^{k} S_h(m)I_h(k-m)-A_1 S_h(k)\right] \tag{3.18}$$

$$I_h(k+1)=\frac{1}{k+1}\left[\frac{\alpha_1}{N_h}\sum_{m=0}^{k} S_h(m)I_r(k-m)+\frac{\alpha_2}{N_h}\sum_{m=0}^{k} S_h(m)I_h(k-m)-A_2 I_h(k)\right] \tag{3.19}$$

$$Q_h(k+1)=\frac{1}{k+1}[\tau I_h(K)-A_3 Q_h(k)] \tag{3.20}$$

$$R_h(k+1)=\frac{1}{k+1}[\gamma_h Q_h(k)+\varepsilon S_h(k)-\mu_h R_h(k)] \tag{3.21}$$

$$S_r(k+1)=\frac{1}{k+1}\left[\Lambda_r-\frac{\alpha_3}{N_r}\sum_{m=0}^{k} S_r(m)I_r(k-m)-\mu_r S_r(k)\right] \tag{3.22}$$

$$I_r(k+1)=\frac{1}{k+1}\left[\frac{\alpha_3}{N_r}\sum_{m=0}^{k} S_r(m)I_r(k-m)-A_4 I_r(k)\right] \tag{3.23}$$

Where,

$$A_1 = [\mu_h - (1-\varepsilon)],\ A_2 = (\mu_h + \delta_h + \tau),\ A_3 = [\mu_h + \gamma_h + (1-\theta)\delta_h] \text{ and } A_4 = (\mu_r + \delta_r) \tag{3.24}$$

We consider $k = 0, 1, 2, 3$

We are considered six cases, the cases are variation of different values of effective enlightenment campaign ε and Quarantine Progression rate τ

Case 1: $\varepsilon = 0.25$

$$\left.\begin{aligned} S_h(t) &= 160000 + 125065.8824t + 49646.1959t^2 + 14545.7717t^3 + 4433.5931t^4 \\ I_h(t) &= 500 - 242.6324t + 65.4105t^2 - 10.6703t^3 + 1.4717t^4 \\ Q_h(t) &= 700 + 136.0750t - 71.7312t^2 + 14.7932t^3 - 1.9357t^4 \\ R_h(t) &= 400 + 40100.200t + 15402.8397t^2 + 4071.9851t^3 + 897.4495t^4 \\ S_r(t) &= 5000 - 100.4000t + 256.0816t^2 + 156.4111t^3 + 120.3063t^4 \\ I_r(t) &= 200 - 53.6000t + 7.1784t^2 - 0.6337t^3 + 0.0441t^4 \end{aligned}\right\} \tag{3.25}$$

Case 2: $\varepsilon = 0.50$

$$\left.\begin{aligned} S_h(t) &= 160000 + 85065.8823t + 24254.7254t^2 + 6278.5947t^3 + 2515.9404t^4 \\ I_h(t) &= 500 - 242.6324t + 63.6458t^2 - 10.7201t^3 + 1.4244t^4 \\ Q_h(t) &= 700 + 136.0750t - 71.7312t^2 + 14.4990t^3 - 1.9399t^4 \\ R_h(t) &= 400 + 80100.2000t + 20796.0750t^2 + 3955.6833t^3 + 773.5010t^4 \\ S_r(t) &= 5000 - 100.4000t + 256.0816t^2 + 156.4111t^3 + 120.3063t^4 \\ I_r(t) &= 200 - 53.6000t + 7.1784t^2 - 0.6337t^3 + 0.0441t^4 \end{aligned}\right\} \tag{3.26}$$

Case 3: $\varepsilon = 0.75$

$$\left.\begin{aligned} S_h(t) &= 160000 + 45065.8823t + 8863.2548t^2 + 3036.3687t^3 + 1930.6308t^4 \\ I_h(t) &= 500 - 242.6324t + 61.8812t^2 - 10.4758t^3 + 1.3780t^4 \\ Q_h(t) &= 700 + 136.0750t - 71.7312t^2 + 14.2049t^3 - 1.8874t^4 \\ R_h(t) &= 400 + 120100.2001t + 16189.3103t^2 + 2147.4699t^3 + 563.4094t^4 \\ S_r(t) &= 5000 - 100.4000t + 256.0816t^2 + 156.4111t^3 + 120.3063t^4 \\ I_r(t) &= 200 - 53.6000t + 7.1784t^2 - 0.6337t^3 + 0.0441t^4 \end{aligned}\right\} \quad (3.27)$$

Case 4: $\tau = 0.25$

$$\left.\begin{aligned} S_h(t) &= 160000 + 125065.8824t + 49645.6077t^2 + 14545.4655t^3 + 4433.5076t^4 \\ I_h(t) &= 500 - 117.6324t + 19.2009t^2 - 0.9992t^3 + 0.1967t^4 \\ Q_h(t) &= 700 + 11.0750t - 15.6053t^2 + 2.4467t^3 - 0.1620t^4 \\ R_h(t) &= 400 + 40100.200t + 15393.4647t^2 + 4074.7799t^3 + 896.9590t^4 \\ S_r(t) &= 5000 - 100.4000t + 256.0816t^2 + 156.4111t^3 + 120.3063t^4 \\ I_r(t) &= 200 - 53.6000t + 7.1784t^2 - 0.6337t^3 + 0.0441t^4 \end{aligned}\right\} \quad (3.28)$$

Case 5: $\tau = 0.50$

$$\left.\begin{aligned} S_h(t) &= 160000 + 125065.8824t + 49646.1959t^2 + 14545.7717t^3 + 4433.5931t^4 \\ I_h(t) &= 500 - 242.6324t + 65.4105t^2 - 10.6703t^3 + 1.4717t^4 \\ Q_h(t) &= 700 + 136.0750t - 71.7312t^2 + 14.7932t^3 - 1.9357t^4 \\ R_h(t) &= 400 + 40100.200t + 15402.8397t^2 + 4071.9851t^3 + 897.4495t^4 \\ S_r(t) &= 5000 - 100.4000t + 256.0816t^2 + 156.4111t^3 + 120.3063t^4 \\ I_r(t) &= 200 - 53.6000t + 7.1784t^2 - 0.6337t^3 + 0.0441t^4 \end{aligned}\right\} \quad (3.29)$$

Case 6: $\tau = 0.75$

$$\left.\begin{aligned} S_h(t) &= 160000 + 125065.8824t + 49646.1959t^2 + 14545.7717t^3 + 4433.5931t^4 \\ I_h(t) &= 500 - 367.6324t + 142.8701t^2 - 35..8982t^3 + 6.9457t^4 \\ Q_h(t) &= 700 + 261.0750t - 159.1071t^2 + 44.3491t^3 - 8.5354t^4 \\ R_h(t) &= 400 + 40100.200t + 15412.2157t^2 + 4067.6378t^3 + 898.5840t^4 \\ S_r(t) &= 5000 - 100.4000t + 256.0816t^2 + 156.4111t^3 + 120.3063t^4 \\ I_r(t) &= 200 - 53.6000t + 7.1784t^2 - 0.6337t^3 + 0.0441t^4 \end{aligned}\right\} \quad (3.30)$$

Results and Discussions

Difference variations of effective enlightenment campaign ε and progression rate from infected to quarantine τ are considered. Cases one to cases three are the variations of effective enlightenment campaign ε while cases four to cases six the variations of progression rate from infected to quarantine τ.

Figures 4.1 to 4.4 are graphical solutions of each compartment of human population and different proportions of effective enlightenment campaign ε. Figure 4.1 shows that as effective enlightenment campaign ε increases the susceptible population decreases. The more the people are being sensitize about the risk of monkeypox the less the transmission in the population. Figure 4.2 reveals that as the enlightenment campaign ε increases the infected human population decreases. It is assumed that those who have being enlightened effectively will not contact the disease and hence, moved to recovered class from susceptible class. Figure 4.3 is the graph of quarantine human population against the effective enlightenment campaign ε and it is observe that there is no effect of enlightenment campaign on quarantine population because people are already sensitized and so there no cause for outbreak in the population. Figure 4.4 shows that as enlightenment campaign ε increases the recovered human population increases.

Figures 4.5 to 4.8 are graphical solutions of each compartment of human population and different proportions of progression rate from infected to quarantine τ. Figure 4.5 shows no effect of the progression rate because it is the infected population that are quarantined. In Figure 4.6 it is observe that as the progression rate increases the infected population decreases. The more the people are quarantined the less the infected population. Figure 4.7 reveal that as progression rate increases the quarantine population increases. Figure 4.8 shows no effect of progression rate.

The solution of the model is for seven systems of ordinary differential equation while that Akinboro *et al.* (2014) is only three seven systems of ordinary differential equation. The graphical solutions makes this paper richer than theirs and also shows the usefulness of the method.

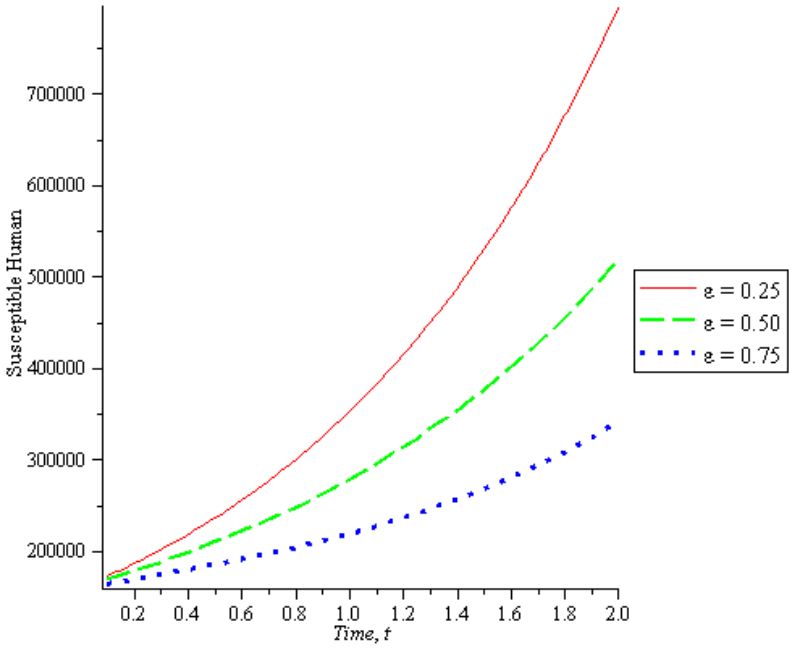

Figure 4.1: Susceptible Human against difference variation of Effective Enlightenment Campaign

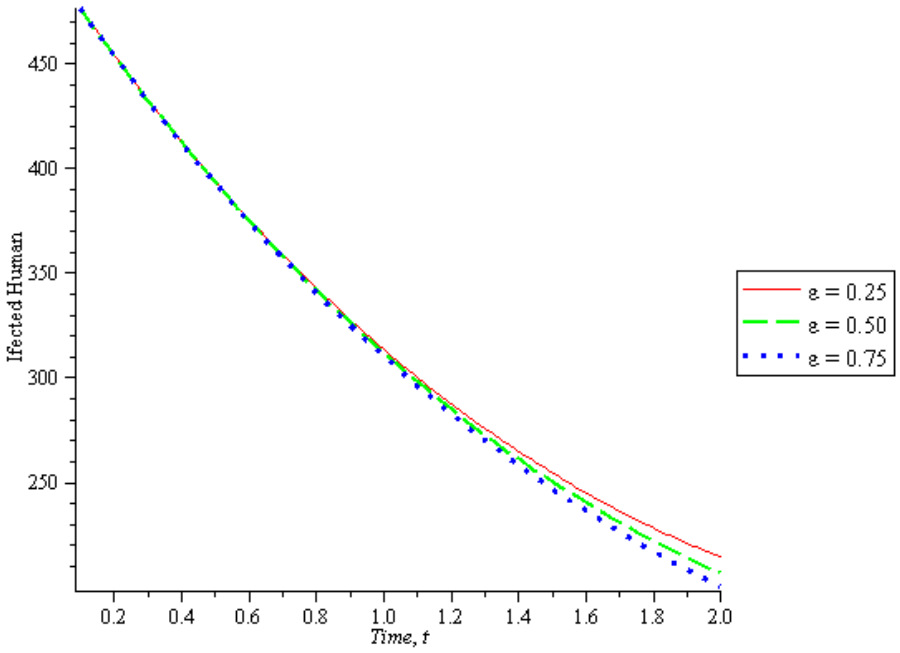

Figure 4.2: Infected Human against difference variation of Effective Enlightenment Campaign

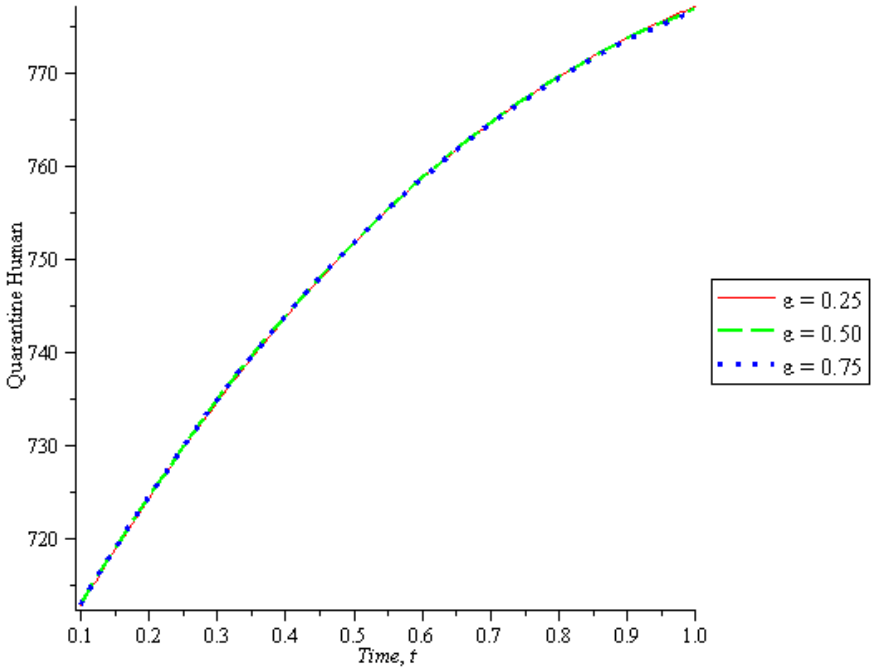

Figure 4.3: Quarantine Human against difference variation of Effective Enlightenment Campaign

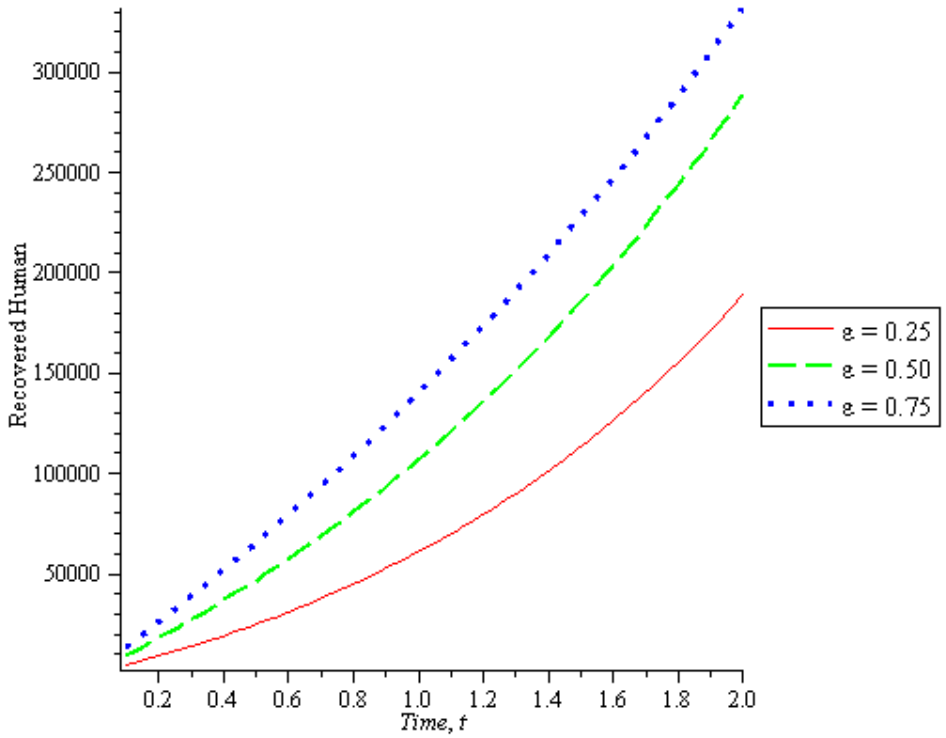

Figure 4.4: Recovered Human against difference variation of Effective Enlightenment Campaign

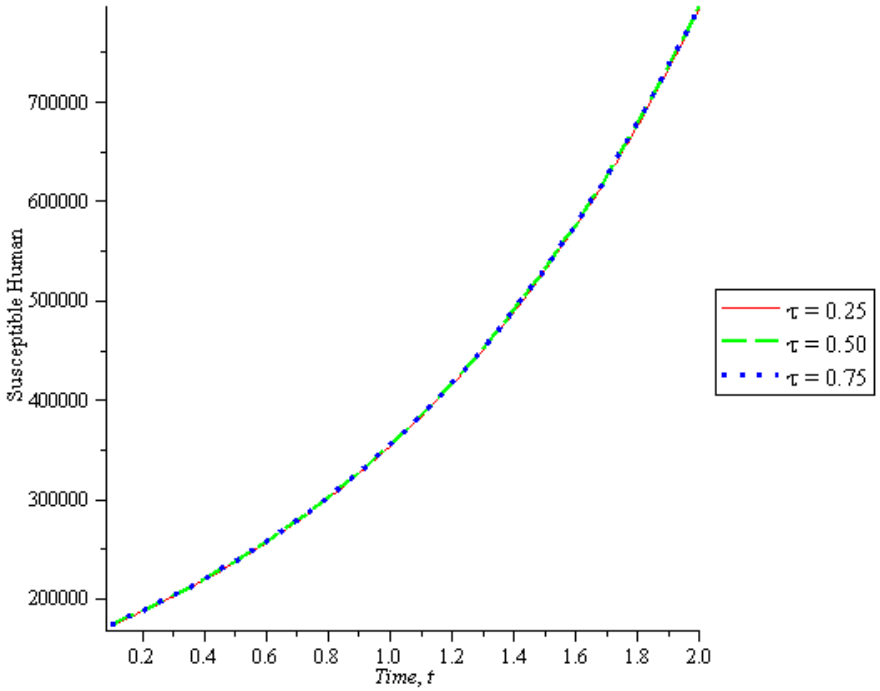

Figure 4.5: Susceptible Human against difference variation of Quarantine Progression Rate

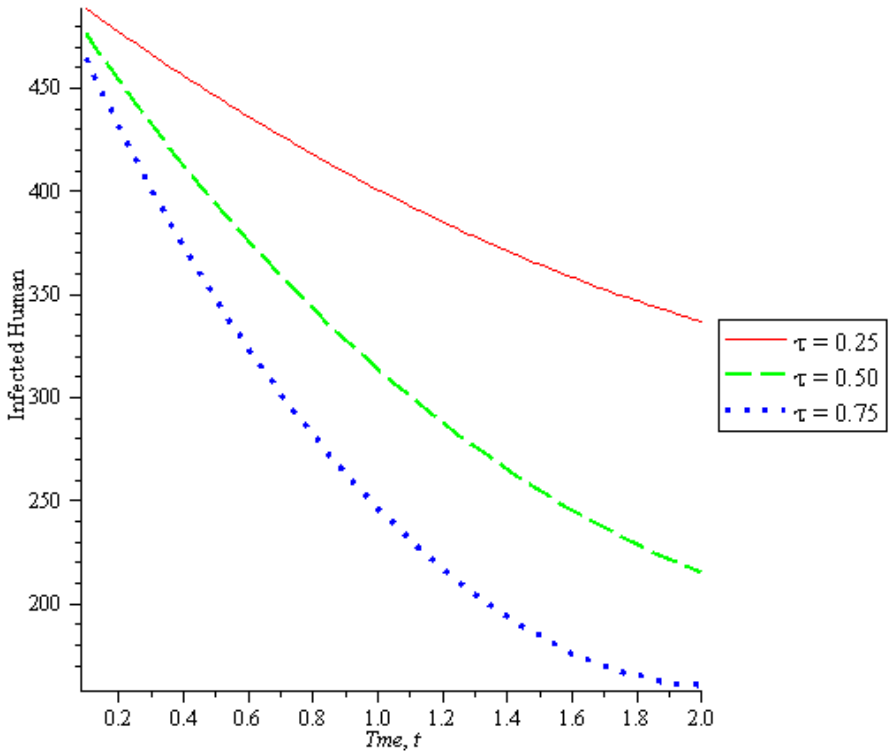

Figure 4.6: Infected Human against difference variation of Quarantine Progression Rate

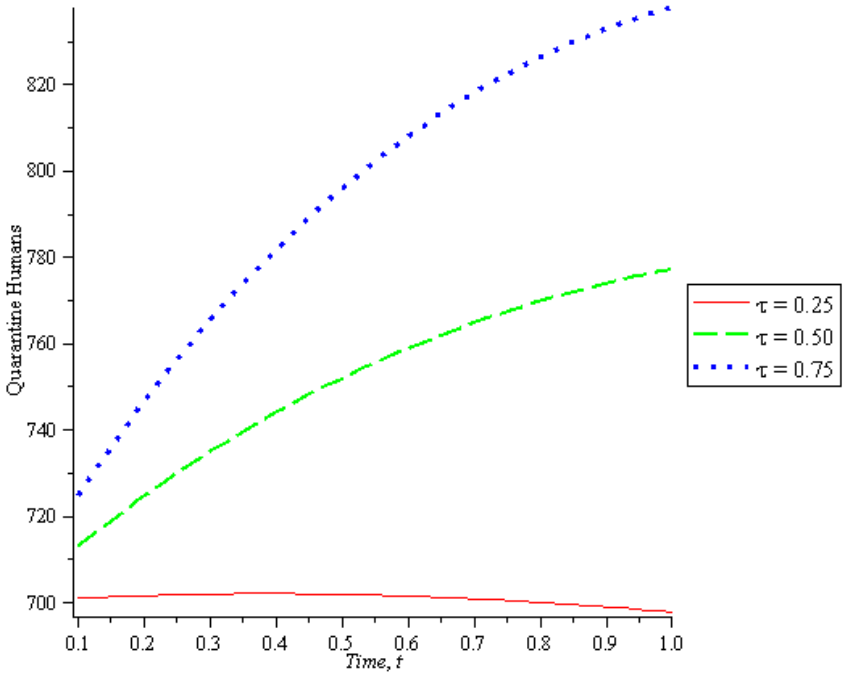

Figure 4.7: Quarantine Human against difference variation of Quarantine Progression Rate

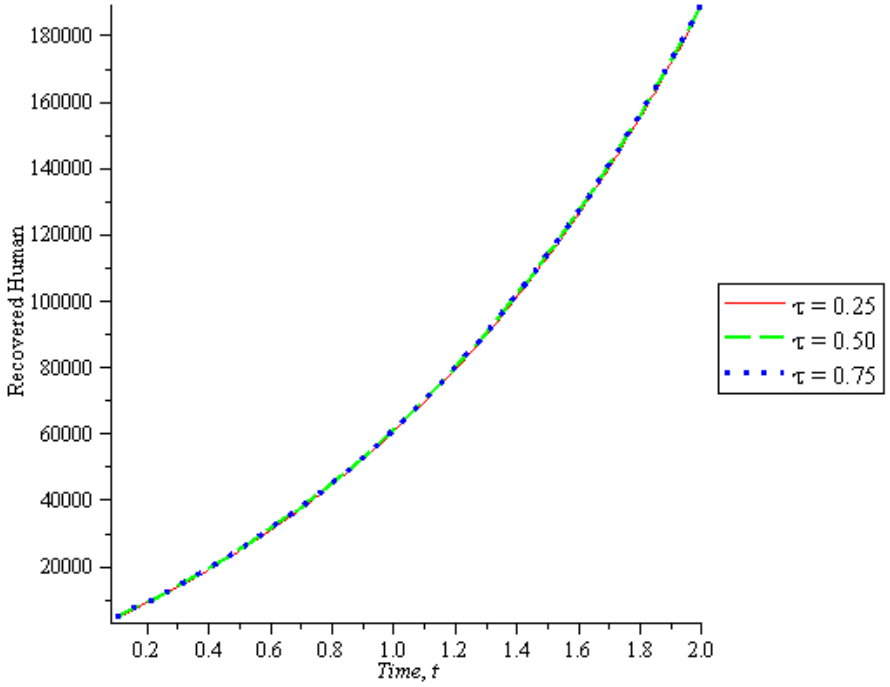

Figure 4.8: Recovered Human against difference variation of Quarantine Progression Rate

Conclusion

The Differential Transformation Method (DTM) is good method for solving non – linear differential equations. The solutions were presented graphically and it makes the understanding of the dynamics richer. The graphical solutions also show the parameters of the model that are important in eradicating monkey pox in the population. More effort should be made by relevant organizations to enlighten the public about the danger of the disease and how to go about the infected persons and also make effort to isolate the infected people from the others (Susceptible individuals).

References

Akinboro F. S., Alao S. and Akinpelu F. O. (2014), Numerical Solution of SIR Model using Differential Transformation Method andVariational Iteration Method. *Gen. Math. Notes;* 22(2):82-92. *Available free online at http://www.geman.in*

Arikoglu A. and Ozkol I., (2006). Solution of Difference Equations by Using DifferentialTransformation Method, *Applied Mathematics Computation*. 174, 1216-1228

Arikoglu A. and Ozkol I., (2007).Solution of Fractional Differential Equations by Using Differential Transform Method, *Chaos Solitons and Fractals*,34, 1473-1481.

Ayaz F., (2004). Application of Differential Transform Method to Differential Algebraic Equations, *Applied Mathematics and Computation*, 152,649-657.

Batiha B., (2015).The Solution of the Prey and Predator Problem by Differential Transformation Method. *International Journal of Basic and Applied Sciences*, 4(1): 36-43. www.sciencepubco.com/index.php/IJBAS c Science Publishing Corporation.doi: 10.14419/ijbas.v4i1.4034

Bhunu, C.P. and Mushayabasa, S. (2011) Modeling the Transmission Dynamics of Pox-Like Infections. International Journal of Applied Mathematics , 41, 2.

Biazar J. and Eslami M. (2010). Differential Transform Method for Quadratic Riccati Differential Equation, *International Journal of Nonlinear Science*,9(4) 444-447.

Che Haziqah C., Adem K. & Arif M. (2010). General Differential Transformation Method for Higher Order of Linear Boundary Value Problem, *Borneo Science* 27, 35-46.

Hassan I. H. A. (2008). Application to Differential Transformation Method for Solving Systems of Differential Equations, *Applied Mathematical Modelling,* 32 2552-2559.

Jezek, Z and Fenner, F. (1988). Human Monkeypox. Monographs in Virology, Vol. 17. 140

Kantele A., Chickering K., Vapalahti O. and Rimoin A. W. (2016). Emerging Diseases—the Monkeypox Epidemic in the Democratic Republic of the Congo. *Clinical Microbiology and Infection*. 22 (8): 658–659.

Momani S., Odibat Z. andHashim I.,(2008). Algorithms for Nonlinear Fractional Partial Differential Equations: *A selection of numerical methods, TopologyMethodNonlinear Analysis.*, 31, 211-226.

Moustafa E. S.,(2008).Application of Differential Transformation Method to Nonlinear Oscillatory Systems, *Communication Nonlinear Science Numerical Simulation*, 13,1714-1720.

Odibat Z. M., (2008). Differential Transformation Method for Solving VolterraIntegral Equations with Separable Kernels, *Mathematics ComputationModeling*., 48,1144-1149.

Soltanalizadeh B., (2012). Application of Differential Transformation Method for Solving a Fourth-Order Parabolic Partial Differential Equations. *International Journal of Pure and Applied Mathematics*, 78(3): 299-308. url: http://www.ijpam.eu*The World Factbook* (CIA).

Usman, S. and Adamu, I.I. (2017) Modeling the Transmission Dynamics of the Monkeypox Virus Infection with Treatment and Vaccination Interventions. *Journal of Applied Mathematics and Physics* , 5, 2335-2353.https://doi.org/10.4236/jamp.2017.512191

Zhou J. K. (1986). *Differential Transformation and its Applications for Electrical Circuits*, Huazhong University Press, Wuhan, China, (in Chinese).

Effective Human Resources Management as a Tool For Enhancing Quality Technical Teacher Education In Kaduna State, Nigeria

By

DANIEL, BobaiChristopher[1*], JOLLY, Charles Nairi[1]&UDUAFEMHE, Maxwell Emmanuel[2]

1 Department of Technical Education, NuhuBamalli Polytechnic, Zaria, Kaduna State, Nigeria.
2 Psychometrics Department, National Examinations Council, Minna, Niger State, Nigeria.
*__Corresponding Author__: bobbydekoknet@gmail.com

Abstract

This study examined ways of enhancing quality technical teacher education in Kaduna State, Nigeria through effective human resources management. The study was guided by four research questions. Descriptive survey research design was adopted for the study. The population of the study comprised of 19 administrators and 84 lecturers in the 3 technical teacher training institutions in Kaduna State. Data for the study were collected using a 23 item structured questionnaire whose reliability coefficient was calculated using Cronbach's Alpha and was found to be 0.88. Mean statistics and standard deviation were employed to answer the research questions. Findings of the study include among others that respondents strongly agree that recruitment should be carried out based on approved guidelines and that training and development should be carried out based on compliance with implementation of approved guidelinesin technical teacher training institutions towards enhancing quality technical teacher education. It was recommended among others that proper procedures for recruitment should be adopted by employers and administrators in order to recruit the qualified personnel to work in technical teacher training institutions. Seminars, workshops and conferences should be organised by employers and administrators for staff within and outside the institutions regularly to update their knowledge.

Keywords: Human Resources Management, Quality Technical Teacher Education, Technical Teacher Training Institutions

Introduction

In the quest for self-actualization, Nigeria as a nation has been making effort to develop her industrial sector. One of the steps taken is the training of people who will are expected to train people in technical colleges. The programme in which these teachers are trained is what is referred to as the Technical Teacher Education. Technical teacher education is the type of education that prepares individuals for teaching positions in technical colleges. The type of certification given to graduate of the institutions in question is the Nigeria Certificate in Education (Technical) or NCE(T).Three of such institutions exists in Kaduna State. They are Kaduna Polytechnic, Nuhu Bamali Polytechnic, Zaria and Kaduna

State College of Education, Gidan Waya. The Federal Republic of Nigeria (FRN, 2013) in the National Policy on Education (NPE) places considerable emphasis on technical teacher training programme by emphasizing that the Nigeria Certificate in Education (NCE) shall be expanded to cater for the requirements of diverse categories of education including technical education. The NCE (Technical) programme therefore is geared towards empowering individuals with requisite knowledge and skills for job creation and self-employment (Gopar, 2008). But this however is far from being achieved because there are incompetent human resources to effectively provide the necessary training towards producing these teachers. Hence, the need for effective HRM in the technical teacher training institutions cannot be overemphasized.

Human Resource Management (HRM) is a very vital approach used by authorities to enhance the performance of personnel of any organisation whether public or private. It is expected that when HRM practices are taken seriously, it enables organisations to function effectively. According to Mohammed, Bhatti, Jariko, and Zehri, (2013) and Khalid, Rehmanand Ilyas (2012)HRM enables authorities to employ individuals who are highly competitive and having valuable knowledge and skills and equally retaining the skilled, competent and motivated workforce towards meeting organisational goals and objectives. Hence, it has therefore become the responsibility of every organisation's administrators, to hire, train, pay, maintain and ultimately motivate employees such as teachers towards a better service delivery. This invariably means that for effectiveness of every organisation such as the educational system to be achieved, the HRM function must be properly constituted and maintained in order to achieve the goals and objectives of the school system. Human resources according to Adeyemi (2009) entail a collection of people or individuals within an organisation having aspirations, abilities and capacities that are geared towards meeting organisational goals and objectives.

In addition, it has been noted that the management of human resources in any organisation such as the school system is an effective way of achieving organisational performance and objectives(Karsten & Ghebregiorgis, 2007).On one hand, the school system in general and Teacher Training Institutions offering Technical courses in particular have been discovered according to Okoye and Arimonu (2016) to be lacking behind in the country in the area of achievement of the goals of Technical Education as stated in the National Policy on Education. This could be attributed to the inability of administrators to effectively manage their human resources thereby resulting to the decline in productivity of personnel as well as failure in the achievement of the goals and objectives of Technical Education in the country. Horgan and Muhlau (2006) and Fu (2013) stated that if effective HRM practices are implemented, it would enhance employees' knowledge, skills, abilities and motivation. It was equally argued by Mehmood, Awais Afzal Shahzadi and Khalid (2017) and Nkondola and Deuren (2017)that HRM has positive contribution to the quality of education and by implementing HRM practices, there will be increased acquisition of knowledge, skills and motivation of teachers. Therefore, for institutions offering technical teacher courses to perform better towards the achievement of goals and objectives of Technical Vocational Education and Training (TVET) as stated in the NPE, it requires that the HRM sections of Technical training institutions become proactive and ensure that the available human resources are effectively managed in the aspects of recruitment, training and development as well as welfare in order to achieve the goals of technical education in the country.

Staff recruitment in the technical teacher training institutions is the process in which individuals are screened, selected and employed to fill in the available positions. According toGusdorf (2008) and Inyiagu (2015), staff recruitment enables institutions to attract and recruit the right caliber of both academic and non-academic staff. It is expected that guidelines that governs the recruitment of personnel in the technical teacher training institutions should be strictly adhered to in order to maintain a quality human

resources workforce. To maintain a formidable human resource workforce in the technical teacher training programme, the place of training and human capital development cannot be overemphasized. According to Hervie and Winful (2018), training aims at increasing the skills, knowledge and expertise of an employee for doing a particular job. Training in the context of this study therefore is the process that provides employees the opportunity to gain knowledge that is required to operate within the systems and standards set by any institution or educational system.

The welfare of staff is equally a very fundamental component of human resources management in the technical teacher training programme because it is a gesture that enhances motivation of employees. According to Mazaki (2017) and Nnaeto and Ndoh (2017), effective HRM serves as motivation to employees and serves as one of the most effective means of organisational growth. It therefore becomes a necessity that critical areas of the welfare of employees is catered for in order to motivate the workers. Gachie (2016)further opined that employers are saddled with the responsibility of recruitment, training and development, promotion and motivation of employees through the provision of adequate welfare services. This shows that it is the duty of employers in the institutions where technical courses are offered, to provide good conditions of service to their employees in order for them to become more committed to their duties towards promoting quality technical teacher education in Kaduna State. It is therefore important for a study that would unravel the effective human resources management capable of enhancing quality technical teacher education in Kaduna State to be undertaken.

Statement of the Problem

A very careful look at the Nigerian educational system shows that teachers, school administrators, policy makers and even governments on daily basis are in a dilemma by frustrating employer-employee related challenges. The challenges include the inability of employers to hire the right workforce, provide appropriate training for the hired workforce and to equally provide the needed welfare to

employees. Nkondola and Deuren (2017) and Agi and Nnokam (2013) are of the opinion that these challenges in the Nigerian educational system in-turn put pressure on the human resource managers such as school administrators and equally result to lack of commitment on the path of teachers in the technical teacher training institutions thereby slowing down the achievement of the goals and objectives of technical education as stated in the National Policy on Education (NPE). According to Oyenenye (2006), the credibility of Nigerian educational system is at a deteriorating state both nationally and internationally whilst the products of tertiary level of education can no longer be compared with those at the same level of education in other parts of the world. This is an unpleasant situation especially when the human resource at the technical teacher training programmes are not properly recruited, trained and motivated thereby affecting the quality of services rendered by employees and on the long run affecting the quality of products that are graduated from the institutions every year. It is in order for the status quo to be changed that this study was embarked upon. Therefore, the problem of this study is effective human resources management as a tool for enhancing quality Technical Teacher Education in Kaduna State, Nigeria.

Purpose of the Study

The aim of the study was to provide insight on effective human resources management as a tool for enhancing quality technical teacher education in Kaduna State, Nigeria. Specifically, the study sought to identify:

1. How staff recruitment complies with approved guidelines towards enhancing quality technical teacher education in Kaduna State.
2. How staff training and development is implemented based on approved guidelines towards enhancing quality technical teacher education in Kaduna State.

3. How staff welfare is implemented based on established guidelines towards enhancing quality technical teacher education in Kaduna State.
4. The strategies adopted for effective human resources management towards enhancing quality technical teacher education in Kaduna State.

Research Questions

The following research questions were raised to guide the study:

1. How is staff recruitment in technical teacher training institutions complied with based on approved guidelines towards enhancing quality technical teacher education in Kaduna State?
2. Howis staff training and development in technical teacher training institutions implemented based approved guidelines towards enhancing quality technical teacher education in Kaduna State?
3. How is staff welfare in technical teacher training institutions implemented based on established guidelines towards enhancing quality technical teacher education in Kaduna State?
4. What are the strategies to be adopted for effective human resources management towards enhancing quality technical teacher education in Kaduna State?

Methodology

Descriptive survey design was adopted for the study. Descriptive survey research according to Salaria (2011)is to carry out a study which includes proper analysis and interpretation of data on a sampled population so that the result can be generalised on the entire population. The study was carried out in Kaduna State, Nigeria. The population of the study comprised of 19 administrators and 84 lecturers in the 3 technical teacher training institutionsin Kaduna State. Due to the manageable size of thepopulation, no sampling was involved. The instrument fordata collection was a four point structured

questionnaireof; Strongly Agree (SA=4), Agree (A=3), Disagree (DA=2), and Strongly Disagree (SD=1), which was validated by three experts.The instrument was then pilot tested on five administrators and 10 lecturers in Niger State. The reliability coefficient was calculated using Cronbach's Alpha and was found to be 0.88. The instrument was administered to respondents by the researcher with the help of three research assistants each from the institution the study was carried out. 100% return rate of questionnaire was achieved. Mean statistics and standard deviation were employed to analyse the data collected. Items with mean less than 2.50 were considered disagree, those with means 2.50 or higher were considered agreed. Additionally, the standard deviation of items was weighed against the normal deviate of 1.96.Where it was found equal to or less, it was interpreted to mean that that the responses of the respondents were clustered around the central means and so has reliability. However, where an item had a standard deviation that is higher than the normal deviate (1.96), it was interpreted to mean that the responses were too far dispersed from the central mean and so had low reliability.

Table 1
Mean Scores of respondents on compliance with approved guidelines for staff recruitment in technical teacher training institutions towards enhancing quality technical teacher education

S/N	Item Statement	$\bar{X}$	SD	Decision
1.	Recruitment intechnical teacher training Institutions should be based on areas of needs	3.61	0.51	SA
2.	Only candidates with requisites qualifications Should be employed to fill in vacant positions	3.65	0.57	SA
3.	Appropriate candidates should be selected and and employed through transparent process	3.64	0.56	SA
4.	Job related skills and competence should be considered during recruitment exercises	3.59	0.70	SA
5.	Due process should be adhered to during recruitment exercises	3.33	0.93	SA
6.	Only candidates that are certified to be physically and mentally fit should be recruited	3.58	0.76	SA

$\bar{X}$ = Average Mean, SD = Average Standard Deviation

Table 2
Mean scores of respondents on implementation of approved guidelines for staff training and development in technical teacher training institutions towards enhancing quality technical teacher education

S/N	Item Statement	$\bar{X}$	SD	Decision
1.	Staff should be given the opportunity to attend workshops/seminars and conferences within and outside their institutions	3.61	0.51	SA
2.	Orientation programmes should organised for new staff to enable them become familiar with the new job	3.63	0.56	SA
3.	Staff should be encouraged to embark self-development through study leave	3.59	0.70	SA
4.	Staff seminars should be organised to create room for staff to brainstorm for better workplace	3.50	0.59	SA
5.	Staff on training should be given allowances due for the training	3.23	1.03	A
6.	Staff should be selected based on area of specialization or professional development for training	3.37	0.81	A

$\bar{X}$ = Average Mean, SD = Average Standard Deviation

Table 3
Mean scores of respondents on implementation of established guidelines for staff welfare in technical teacher training institutions towards enhancing quality technical teacher education

S/N	Item Statement	$\bar{X}$	SD	Decision
1.	Payment of staff entitlements regularly and at when due	3.56	0.53	SA
2.	Provision of medical services to staff and their family members	3.48	0.59	A
3.	Provision of salary advance to staff in time of financial need	3.52	0.53	SA
4.	Provision of basic amenities such as shelter, water, electricity, roads and recreational environment	3.36	0.66	A
5.	Compensating staff whenever they work	3.50	0.56	SA

	overtime			
6.	Provision of conducive work environment and furnishings for staff	3.54	0.67	SA

$\bar{X}$ = Average Mean, SD = Average Standard Deviation

Table 4
Mean scores of respondents on strategies to be adopted for effective human resources management in technical teacher training institutions towards enhancing quality technical teacher education

S/N	Item Statement	$\bar{X}$	SD	Decision
1.	Due process and established guideline should be followed during recruitment of staff	3.50	0.49	SA
2.	Heads of Departments and Heads of Sections should be exposed to relevant training and development	3.71	0.46	SA
3.	Staff appraisals and promotions should follow established rules and guidelines	3.66	0.47	SA
4.	Welfare of staff should be accorded utmost priority in the institutions	3.57	0.52	SA
5.	Effective supervision and monitoring should be carried towards guaranteeing effectiveness in task performance	3.56	0.50	SA

$\bar{X}$ = Average Mean, SD = Average Standard Deviation

Findings and Discussion

The findings emerging from the opinions of the respondents with regards to compliance with approved guidelines forstaff recruitment in technical teacher training institutions towards enhancing quality technical teacher education (table 1) revealed that respondents strongly agreed with all the six items. This can therefore be deduced that all respondents strongly agreed that the recruitment of personnel in technical training institutions should be carried out based on approved guidelines.This is in conformity with the opinion of Gusdorf (2008) and Inyiagu (2015) who revealed that staff recruitment enables

institutions to attract and recruit the right calibre of both academic and non-academic staff in order to meet the goals of the institution.

The respondents accepted items 1, 2, 3 and 4 as Strongly Agree while equally Agreed with items 5 and 6 on the need to comply with implementation of approved guidelines for staff training and development in technical teacher training institutions towards enhancing quality technical teacher education (table 2). This is in agreement with Hervie and Winful (2018) who posited that training contributes immensely in increasing the skills, knowledge and expertise of an employee on the job and provides employees the opportunity to gain knowledge that is required to operate within the systems and standards set by the institution. It therefore signifies that there is need for steps to be taken towards professional development of staff in technical teacher training institutions.

With regards to staff welfare, the findings revealed that respondents strongly agreed with items 1, 3, 5 and 6 on the need for staff welfare services to be implemented in technical teacher training institutions towards enhancing quality technical teacher education (table 3). The findings are in consonance with Mazaki (2017) and Nnaeto and Ndoh (2017) who revealed that staff welfare should be the responsibilities of employers towards improving the working conditions of employees and serves as catalyst for motivation of employees. This therefore indicates that catering for the welfare of staff in any institution implies giving attention to critical areas of employees needs in the work place such as housing, remuneration, office accommodation and furnishing, transportation, good health care delivery and meeting any other basic needs of employees.

The findings of the study with respect to strategies to be adopted for effective human resources management towardsenhancing quality technical teacher education (table 4) revealed that respondents strongly agreed with all items. This agrees with the view of Gachie (2016) who stated that, it is the

duty of employers to recruit, train and develop her staff effectively, promote their staff and motivate employees towards attaining organisational goals and objectives.

Conclusion

It was concluded based on the findings that, it is the duty of employers and administrators in Technical Training Institutions to follow the approved guidelines for staff recruitmentand comply with established guidelines for staff training and development.Finally, it equally behoves on employers and administrators in Technical Teacher Training Institutions to adequately implementation staff welfare packages in order to motivate the workforce towardsenhancing quality technical teacher education in Kaduna State.

Recommendations

1. Proper procedures for recruitment should be adopted by employers and administrators in order to recruit the qualified personnel to work in technical teacher training institutions.
2. Seminars, workshops and conferences should be organised by employers and administrators for staff within and outside the institutions regularly to update their knowledge
3. Proper welfare of staff especially in the areas of health care services, accommodation should be made of paramount importance by employers in order to motivate employees.

References

Adeyemi, T. O. (2009). Human Resources Management in Education.In Babalola J. B. &Ayeni, O. A. (Eds).*Educational Management:Theories and Tales*. Macmillan-Nigeria Publishers Ltd. Lagos.

Agi, U. K. &Nnokam, N. C. (2013).Challenges of Human Resources Management for Effective Implementation of the Universal asic Education Programme in Rivers State.*Mediterranean Journal of Social Science*,*4*(5), 51-59.

Federal Republic of Nigeria (2013).*National Policy on Education.*NERDC Press, Lagos.

Fu, N. (2013). Exploring the Impact of High Performance Work System in Professional Service Firms: A Practices-Resources-Uses-Performance Approach.*Consulting Psychology Journal: Practice and Research*,*65*(3), 240-257.

Gachie, C. (2016). Relationship Between Human Resource Policies and Employees Job Satsifaction in a Local Non-Governmental Organisation in Kenya: A Case of Article 19 in Kenya. *Master's Degree Thesis.*Labour Management and Policy Departmment. University of Nairobi, Kenya.

Gopar, D. D. (2008). Teacher Training and Development for Effective Implementation of the 6-3-3-4 system of Education in Nigeria. A Paper Presented at the Conference Organised for Technical/Vocational Teachers in Plateau State, Nigeria.

Gusdorf, M. L. (2008). Recruitment and Selection: Hiring the Right Person. A Two-Part Learning Module for Undergraduate Students.Society for Human Resource Management.

Hervie, D. M. &Winful, E. C. (2018). Enhancing Teachers' Performance Through Training and Development in Ghana Education Service (A Case Study of Ebenezer Senior High School). *Journal of Human Resources Management, 6*(1), 1-8.

Horgan, J. &Muhlau, P. (2006). Human Resources Systems and Employee Performance in Ireland and the Netherlands: A Test of the Complementarity Hypothesis. *International Journal of Human Resource Management, 17*(3), 414-439.

Inyiagu, E. E. (2015). Technical and Vocational Teachers' Perception of the Influence of National Commission for Colleges of Education Accreditation Exercise on Some Quality Indicators in Nigeria Certificate in Education (Technical) Training Institutions.*International Journal of Vocational and Technical Education Research, 1*(4), 1-9.

Karsten, L. &Ghebregiorgis, F.(2007). Human Resources Management and Performance in a Developing Country: The Case of Eritrea. *International Journal of Human Resources Management, 18*(2), 321-332.

Khalid, M. M., Rehman, C. A.,&Ilyas, M. (2014). Human Resources Management Practices and Employee Performance in Public Sector Organisation in Pakistan: An Empirical Study. *International Journal of Management Sciences and Business Research, 3*(2), 69-73.

Mazaki, K. E. (2017). Staff Welfare and teachers' Performance in Public Primary Schools in Bugisu Sub-Region in Uganda. *Ph.D Thesis.*Institute of Management, Mbarara University of Science and Technology, Uganda.

Mehmood, M., Awais, M., Afzal, M. M., Shahzadi, I. & Khalid, U. (2017).Impact of Human Resources Management Practiceson Organisational Performance.*International Journal of Engineering and Information Systems,1*(9), 165-178.

Nkondola, A. A. &Deuren, R. V. (2017). Human Resources Management Challenges in Technical and Vocational Education in Developing Countries: The Case Study of Technical Institutions in Tanzania. International Journal of Business and Social Science, *8*(2), 156-162.

Nnaeto. J. O. &Ndoh, J. A. (2017). Impact of Motivation on Employee Performance: A study of Alvan-Ikoku Federal College of education. *Journal of Management and Strategy, 9*(1), 53-65.

Okoye, R. &Arimonu, M. O. (2016). Technical and Vocational Education in Nigeria: Issues, Challenges and a Way Forward. *Journal of Education and Practice, 7*(3), 113-118.

Oyenenye, O. Y. (2006). Current Issues in the Administration of University Education in Nigeria.A Status Report.Higher Education Policy.

Salaria, N. (2012). Meaning of the Term- Descriptive Survey Research Design.*International Journal of Transformation in Business Management, 1*(6), 1-7.

PHYSICAL/MATERIAL SCIENCS

Delineating Comparative Studies on Biogas Production from Camel, Donkey and Horse Dungs

B. SAMAILA[1*], M.N. YAHAYA[2], N. ABUBAKAR[3]

[1, 2, 3] Department of Physics with Electronics Federal University Birnin Kebbi, P.M.B 1157 Kebbi State, Nigeria.

kawara002@gmail.com

Abstract

The present work explores the production of biogas from animal wastes mixed with water in a digester. The high costs and health implications of using energy derived from hydrocarbon compound have necessitated the continuous search for alternative source of energy. The animal wastes (camel, donkey and horse) as a renewable source of energy supply has been proven to be very efficient. This study investigated and compared the production of biogas using camel, donkey and horse dungs collected from three different areas of kawara located in maiyama local Government, Kebbi State, Nigeria. A 150g of camel, horse and donkey dungs were used in this study. The digestion was carried out in a 1 L anaerobic digester for each dung at a certain range of temperature. The total volume of biogas (in cm^3) produced in five weeks and two days were found to be 4550 cm^3 for camel, 2210 cm^3 for donkey, 4000 cm^3 for horse. Thus biogas production from these dungs is a good and cheap alternative source of energy. The use of biogas will not only serve as a source of fuel but will also help in the management of waste in the area. It was observed that all the dung was stagnant for one week, and the more the retention time, the more gas is produced. This investigation reveals that biogas production was delayed till the seven day. This can be traced to the fact that most camels, donkeys, and horses feed on fibrous materials and microorganisms require a longer time to degrade fibrous materials. The gas produced is in order camel > horse > donkey.

Keywords: *Biogas, Digester, Camel, Donkey and Horse Dungs*

1. INTRODUCTION

It is much desirable that the renewable energy to be developed has no adverse effects on the environment. Surely, productions of renewable energy from materials that are readily and locally available are extremely advantageous and reduce the cost of its production. Environmentally friendly individuals may choose to compost their food waste to acquire a useful fertilizer or soil amendment; however, this process does not allow a means to capture the energy that is locked up in waste. Biogas-generating technology is a favorable dual-purpose technology at present: the biogas generated can be

used to meet energy requirements while the organic residue is a useful fertilizer. Biogas is a type of renewable energy that can be produced from the decomposition of animal and plant wastes and is composed of methane, carbon dioxide and trace impurities like hydrogen, hydrogen sulfide and some nitrogen (Deressaa L, et al *2015*). *Biogas is a mixture of colorless, flammable gases obtained by the anaerobic digestion of plant-based organic waste materials (Onwuliri FC* et al*, 2013) and animal waste. Biogas is typically made up of methane (50-70%) carbon dioxide (30-40%) and other trace gases. It is generally accepted that fuel consumption of a nation is an index of its development and standard of living. There have been increases in the use of and demand for fuel in terms of transportation and power generation in many nations including Nigeria. These have so far been met in Nigeria largely from the nation's stock of fossil fuel such as crude oil, which is finite in nature. Fossil fuels are not environmentally friendly and are also expensive. The use of alternative and more environmentally-friendly energy sources such as biogas has been advocated (Onwuliri FC* et al*, 2013). At present, the renewable energy sources (RES), that can be technologically used for electricity, heating and motor vehicle fuel production are biomass, biofuels, biogas, solar energy, water energy, wind energy and geothermal energy. Renewable energy sources are considered to be sources whose energy potential is permanently renewed by natural processes or human activity (Miroslav H* et al*, 2009). Renewable energy resources appear to be one of the efficient solutions to the problems resulting from the use of fossil fuels (O. C. Ozor* et al*, 2014).*

2. THEORITICAL BACKGROUND

As energy demand is increasing in the world, renewable energy sources are utilized. Biogas is a renewable energy source which helps us in conserving fossil fuel. There are favorable scenarios for using biogas energy in rural areas through an arrangement of community biogas plants. This technology is not only used in houses for lightening and cooking purposes but it also serves as a good fertilizer. It can also be used in various automotive applications. This study proposes the method to convert animal waste into biogas. Biogas is sustainable in long run. Underdeveloped countries should adopt this technology as a renewable energy source to meet their energy demands. It can be continued indefinitely in the future (Neeha F and Shafqat H, 2012).

Biogas, a clean and renewable form of energy could very well substitute (especially in the rural sector) for conventional sources of energy (fossil fuels, oil, etc.) which are causing ecological–environmental problems and at the same time depleting at a faster rate. Despite its numerous advantages, the potential

of biogas technology could not be fully harnessed or tapped as certain constraints are also associated with it. Most common among these are: the large hydraulic retention time of 30–50 days, low gas production in winter, etc. Therefore, efforts are needed to remove its various limitations so as to popularize this technology in the rural areas. Researchers have tried different techniques to enhance gas production (K.Vijay Kumar et al*, 2013).*

The rapid increase in energy consumption particularly in the past several decades has raised fears of exhausting the globe's reserves of petroleum and other resources in the near future. The huge consumption of fossil fuels has caused visible damage to the environment in various forms. Approximately 90% of our energy consumption comes from fossil fuels. Due to industrializations and population growth our economy and technologies today largely depend upon natural resources, which are not replaceable. The renewable sources are cost effective, user-friendly, so that they can easily beat the fossil fuels. By promoting renewable energy sources we can avoid, Air pollution, soil pollution and water pollution. Country's Economy will increase. Throughout the year these sources are available without affecting the Environment (Nada Kh. And M. A. Alrikabi, 2014).

A case study has been conducted for estimation of total large animal waste based biomass potential for meeting the growing power demand of the state and also making the state as power surplus state. During study it has been observed that district Bathinda has animal population (large animals) of 423375 and potential of animal dung is 1385247 GJ per year. The electrical energy that can be produced from surplus animal dung with conversion efficiency 35% is 384.8 GWH per year. The production of electrical energy by use of dung is reducing GHG emission, meeting rising power demand, appropriate use of surplus animal dung and renewable energy production (Gagandeep K et al*, 2014).*

The effectiveness of donkey dung for biogas production using a designed and constructed cylindrical field batch biogas digester was investigated. The donkey dung was collected from the University of Fort Hare's Honeydale Farm and was analyzed for total solids, volatile solids, total alkalinity, calorific value, pH, chemical oxygen demand and ammonium nitrogen. The biogas composition was analyzed using a gas analyzer. It was found that donkey dung produced biogas with an average methane yield of 55% without co-digesting it with other wastes. The results show that donkey dung is an effective substrate for biogas production (Mukumba P et al*, 2016).*

3. METHODOLOGY

3.1 Sample collection

Fresh dung of camel, horse and donkey were collected from three areas of kawara in maiyama L.G. Kebbi state, Nigeria. A clean container with cover was used for collection of the Waste. The dungs were dried under the sun for five days and then pulverized using a pestle and mortar. The pulverized dung was sieved and dried again for 28 hours.

3.2 Preparation of Slurry and digestion

150grams each of the fine powdered dungs were weighed and mixed with 900 cm^3 of distilled water measured by cylinder of 1000cm^3 and poured into one liter bio digesters respectively and were labeled as camel, donkey and horse on their respective digesters .The mixture was thoroughly stirred to achieve homogeneity. The digesters were connected to their respective gas collectors by the use of rubber tubes. Then observations and recording of gas produced from the slurries were taken after twenty four hours interval every day. Before readings were taken every day, the digesters were agitated gently in order to enhance the mixture of the slurry and ease release of the gas present in the digesters. The biogas produced under goes several stages. These stages include: Hydrolysis, Acidogenesis, Acetogenesis, and Methanogenesis. The hydrolysis stage is the first stage in which organic dungs transformed (breakdown) into a simple sugar. In acidogenesis stage, the simple sugar produced in hydrolysis stage transformed into propanoic acid and methanol acid e.t.c. In acetogenesis stage, the rest of the acidogenesis products that is, the propanoic acid and methanol are transformed by acetogenic bacteria into hydrogen, carbon dioxide and acetic acid. In methanogenesis stage, the hydrogen and acetic acid transformed to methane gas and carbon dioxide. The bacteria responsible for this conversion are called methanogens and are strict anaerobes. Waste stabilization is accomplished when methane gas and carbon dioxide are produced. Biogas comprised primarily of methane and carbon dioxide with other trace of gases, it burns more cleanly than coal, and emits less carbon dioxide per unit of energy (Calverton, 2008). The apparatus used in carried out the experiment are: three measuring cylinders (1000cm^3), Weighing balance, three retort stands and clamps, three Rubber tubes, three plastic basin (500cm^3), three one liter digesters. The stages in which biogas undergoes during the process can be presented in flow chart as shown below:

Figure 1.Flow chart presenting biogas production stages

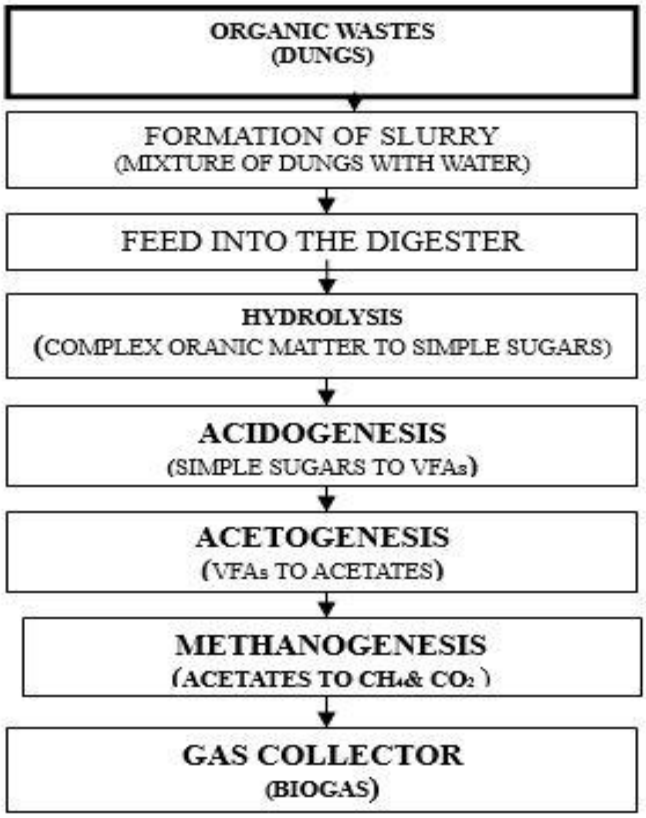

4. RESULT AND DISCUSSION

The biogas produced in this research work undergoes four stage processes as shown above. These include Hydrolysis, Acidogenesis, Acetogenesis, and Methanogenesis. The biogas production was delayed till the seven day. The readings were taken at every 24 hours, the total gas produced was calculated using the expression below:

$$\text{The total gas produced in 37 days} = X_1 + X_2 + X_3 + X_4 + X_5 + X_6 + X_7 \ldots\ldots\ldots X_N \quad (1)$$

Where $X_1 \ldots\ldots\ldots X_N$ *representing number of days. Each day the volume of gas produced was recorded and added up to the 37 days as shown in the equation 1 above. The total volumes of gas produced from each digester were tabulated below:*

Table 1.*total biogas produced in five weeks, two days (37 days)*

SLURRY (mixture of dungs and water)	*Total Volume of gas produced (cm^3)*
CAMEL	*4550*
DONKEY	*2210*
HORSE	*4000*
Total gas produced from camel, donkey and horse	*4550+2210+4000 = 10760 cm^3*

The highest total volume of biogas produced 4550 cm^3 was in the digesters that contained camel dungs follow by horse and then donkey. The result reported in this work, indicated that camel dungs produced more gas compare to donkey and horse. The total volume of biogas produced from three samples is equal to 10760 cm^3. The percentage of the volume of biogas produced from three samples were calculated using expression below

$$\text{Percentage of gas produced by camel dungs} = \frac{4550}{10760} \times 100 = 42.290\ \%$$

$$\text{Percentage of gas produced by donkey dungs} = \frac{2210}{10760} \times 100 = 20.540\%$$

$$\text{Percentage of gas produced by horse dungs} = \frac{4000}{10760} \times 100 = 37.175\ \%$$

The pie chart below shows the percentage of the total gas produced by each of the dungs collected from the study area.

Figure 2. Pie chart showing the percentage of total biogas produced in 37 days from three samples.

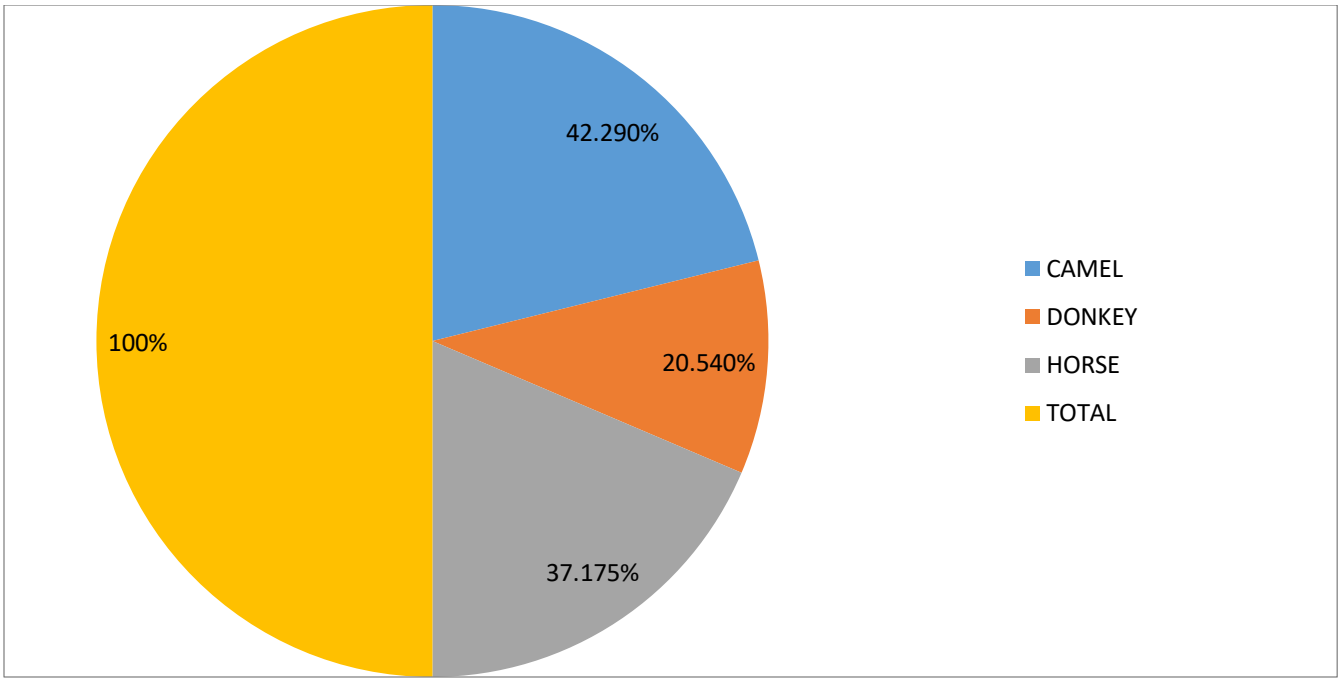

Conclusion

The findings shows that out of three samples collected, camel dung produced more gas as shown above in the table and could be used as a suitable substrate for biogas production. The result of this research on the production of biogas from camel, donkey and horse dungs has shown that flammable biogas can be produced from these wastes through anaerobic digestion for biogas production. These wastes are always available in our study area and can be used as a source of fuel if managed properly. The study revealed further that camel dung as animal waste has great potentials for production of biogas and its use should be encourage due to its early retention time and high volume of biogas yields. Biogas production, if carried out at commercial scale, would not only provide an alternative source of energy but would also be a means of waste disposal for Nigeria.

REFERENCE

*Claverton E.C, (2008). "*Biomethane fueled vehicles, the carbon neutral option*" claverton Energy conference, Bath, UK, October 24th 2008*

*Gagandeep Kaur, Yadwinder Singh Brar , D.P.Kothari "*Estimation of Large Animals Dung for Power Generation – A Case Study of District Bathinda, Punjab*", IOSR Journal of Electrical and*

Electronics engineering (IOSR-JEEE) e-ISSN: 2278-1676,p-ISSN: 2320-3331, Volume 9, Issue 5 Ver. III (Sep – Oct. 2014), PP 50-55, www.iosrjournals.org

*K.Vijay Kumar, V.Sridevi, K. Rani, M.Sakunthala and C. Santosh Kumar "*A review on production of biogas, fundamentals, applications & its recent enhancing techniques*", K.Vijay Kumar et al./ Elixir Chem. Engg. 57 (2013) 14073-14079, Available online at www.elixirpublishers.com (Elixir International Journal)*

*Leta Deressa, Solomon Libsu, R. B. Chavan, Daniel Manaye, Anbessa Dabassa, "*Production of Biogas from Fruit and Vegetable Wastes Mixed with Different Wastes*" Environment and Ecology Research 3(3): 65-71, 2015,* http://www.hrpub.org, *DOI: 10.13189/eer.2015.030303*

*Mukumba P, Makaka G, Mamphweli S. "*Anaerobic digestion of donkey dung for biogas production*". S Afr J Sci. 2016; 112(9/10), Art.2016-0013, 4pages.* http://dx.doi.org/10.17159/sajs.2016/20160013

*Nada Kh. M. A. Alrikabi "*Renewable Energy Type*s" Journal of Clean Energy Technologies, Vol. 2, No. 1, January 2014.*

*Neeha Farouqe and Shafqat Hameed "*Effective Use of Technology to Convert Waste into Renewable Energy Source*" life science journal, 2012 pp (654-661), (ISSN: 1097-8135).*

O. C. Ozor, M. V. Agah, K. I. Ogbu, A. U. Nnachi, O. E. Udu-ibiam, M. M. Agwu "Biogas Production Using Cow Dung From Abakaliki Abattoir In South-Eastern Nigeria*" International journal of scientific and technology research volume 3, issue 10, October 2014.*

*Onwuliri FC, Onyimba IA and Nwaukwu IA "*Generation of Biogas from Cow Dung*" Journal of Bioremediation & Biodegradation, 2013*

*Miroslav Hutňan, Igor Bodík, Andrea Blšťáková "*Production of biogas from renewable energy sources*" 36th International Conference of SSCHE, May 25–29, 2009, Tatranske Matliare, Slovakia. ISBN 978-80-227-3072-3.*

Threats of Climate Change on the Biodiversity of the Hadejia-Nguru Wetlands

[1]Abubakar, M. M., [2]Haruna, M., [2]Getso, B. U. and [2]Ahmad, M. M.

[1]Department of Biological Sciences, Federal University Dutse

[2] Department of Biology, Kano University of Science and Technology, Wudil

Abstract

This review highlights the manifestation of climate change in the Hadejia-Nguru wetlands. Warming of the earth surface is definitely taking place. And that most of the increase in global temperature is caused by greenhouse gases emitted as a result of human activities. The Hadejia-Nguru wetland ecosystem comprises permanent lakes and seasonally flooded pools connected by a network of channels. The wetland is an important site for biodiversity. The minimum essential characteristics of a wetland are recurrent, sustained inundation or saturation at or near the surface and the presence of physical, chemical and biological features reflective of the recurrent, sustained inundation or saturation. Functions of wetlands can be grouped broadly as habitat, hydrologic, or water quality. Many endangered plant and animal species are dependent on wetland habitats for their survival. The result of several studies shows that the most obvious manifestation of climate change in the Hadejia-Nguru wetlands is the steady increase in both water and atmospheric temperature. Climate change is global in its causes but its consequences are far more reaching in developing countries, particularly Nigeria.

Key Words: Biodiversity, Ecosystem, Habitat, Inundation, Temperature

INTRODUCTION

Freshwater is an indispensible resource and essential for life. Freshwater constitutes only 2.5 % of all freely available water on earth's surface, of which only 0.3 % is readily accessible in lakes, reservoirs and rivers (USEPA 2001). Some major problems that humanity is facing in the twenty-first century are related to water quantity and/or water quality issues (Medugu, 2009).

The sustainable development and management of the world's freshwater resources has been the focus of several international debates, conferences and workshops where a number of blueprints or guidelines on sustainable water resources development have been advanced. According to Inter-governmental Panel on Climate Change, which is the most authoritative team of experts on climate change, warming of the earth surface is definitely taking place. And that most of the increase in global temperature is caused by greenhouse gases emitted as a result of human activities. IPCC (2007)

concluded that wetlands are among the most vulnerable to climate change. And those inland freshwater wetlands will be most affected mainly through changes to precipitation, intense droughts, storms and floods.Many semi-arid areas, Hadejia-Nguru wetlands (HNW) inclusive are particularly exposed to impacts of climate change and are expected to suffer serious pressure on the resources of the wetland. This review highlights the manifestation of climate change in the Hadejia-Nguru wetlands.

DESCRIPTION OF THE HADEJIA-NGURU WETLANDS

The Hadejia-Nguru Wetlands is generally abbreviated as HNWs, hence in this review will be addressed as HNWs. The HNWs is an extensive floodplain created by the Hadejia and Jama'are rivers to form the Komodugu-Yobe River which drains into the Lake Chad. The HNWs lie on the southern edge of the Sahel savanna in northeastern Nigeria with central coordinates 10^{o} 33.00' East and 12^{o} 39.00' North, the wetlands covered an area of about 350, 000 ha and altitude 152-305 m (Birdlife international, 2015). The climate of the wetland is characterized by two distinct seasons; wet season (May- September) and dry season (October-April), The rainfall period is from June to October, and has annual mean of over 1,000 mm in the upstream Basement complex area and approximately 500mm in the Hadejia-Nguru Wetlands (Sanyu, 1994).

There is mean minimum temperature of 12°C during the month of December to January, to a maximum of 40°C during the month of April (Ogunkoya and Dami, 2007). The ecosystem comprises permanent lakes and seasonally flooded pools connected by a network of channels. The ecosystem is an important site for biodiversity, especially migratory water birds from Palearctic regions. For example, at one time, the floodplain supports over 423,000 birds of 68 species, including significant numbers of Ferruginous Duck (*Aythya nyroca*), Spur-winged Goose (*Plectropterus gambensis*), Black-tailed Godwit (*Limosa limosa*), and Ruff (*Philomachus pugnax*) (Birdlife international, 2010). Other wildlife species found include species of gazelle (*Gazella sp.*), duiker (*Cephalophus sp.*), jackal (*Canis sp*) and hyena (*Crocuta crocuta*) (Ogunkoya and Dami, 2007). In total, there are about 378 bird species listed for the wetland, 103 fish species, 250 species of flowering plants and more than 136 species of aquatic flora and fauna (Oduntan *et al*., 2010).

Three broad types of vegetation occur in HNWs. There is scrub savanna, which consist of upland farmland areas and *Acacia* woodlands. The second include the 'tudu' (raised areas) which are never

inundated with tree species of *Acacia* spp, *Ziziphus* spp., *Balanites aegyptiaca, Tamarindus indica* and *Adansonia digitata*, while common grasses include *Cenchrus biflorus*, *Andropogon* spp. and *Vetiveria nigritana*. In addition, pockets of riparian forests and woodlands, known as 'kurmi' comprise species of *Khaya senegalensis*, *Mitragyna inermis* and *Diospyros mespiliformis*. In some parts, the 'kurmi' has been replaced with orchards of mango *Mangifera indica* and guava *Psidium guajava* (Ezealor, 2001).

The third vegetation type consist the seasonally flooded marshes in which the tree *Acacia nilotica* is common while Dum palms (*Hyphaene thebaica*) grow on small raised islands (Ezealor, 2001). Aquatic grasses include *Echinochloa* and *Oryza* spp. while in drier parts *Dactyloctenium aegyptium*, *Setaria* spp. and *Cyperus* spp. occur and extensive vegetation of *Typha domingensis* along the shore of the wetlands.

Hausa, Kanuri and Fulani are the most dominant tribes in the wetlands with an estimated population of about 1.5 million, including farmers, herders and fishermen who entirely depend on the ecosystem for their livelihoods (Kaugama and Ahmed, 2014; Birdlife international, 2015). The wetlands provide essential income and nutrition benefits in the form of agriculture, grazing resources, non-timber forest products, fuel wood and fishing (Ramsar, 2007). The Hadejia-Nguru Wetlands is bordered by three states of Bauchi, Jigawa and Yobe (Blench, 2013).

Fishermen and farmers in the HNWs represent about 75% of the indigenous community population (Birdlife international, 2015), and the wetlands represents their entire source of livelihoods through farming and fishing activities. Farming in particular accounts for about 25%, major crops grown include rice, maize, sesame, sorghum, wheat, millet, and some vegetables such as tomato, pepper, onions, and carrot (Ogunkoya and Dami, 2007; Kaugama and Ahmed, 2014; Birdlife international, 2015). The financial benefits of major agricultural outputs in the wetlands has been estimated at US$ 75 million, while cattle trade annually contributes to about US$ 5 million (Eaton and Sarch, 1997).

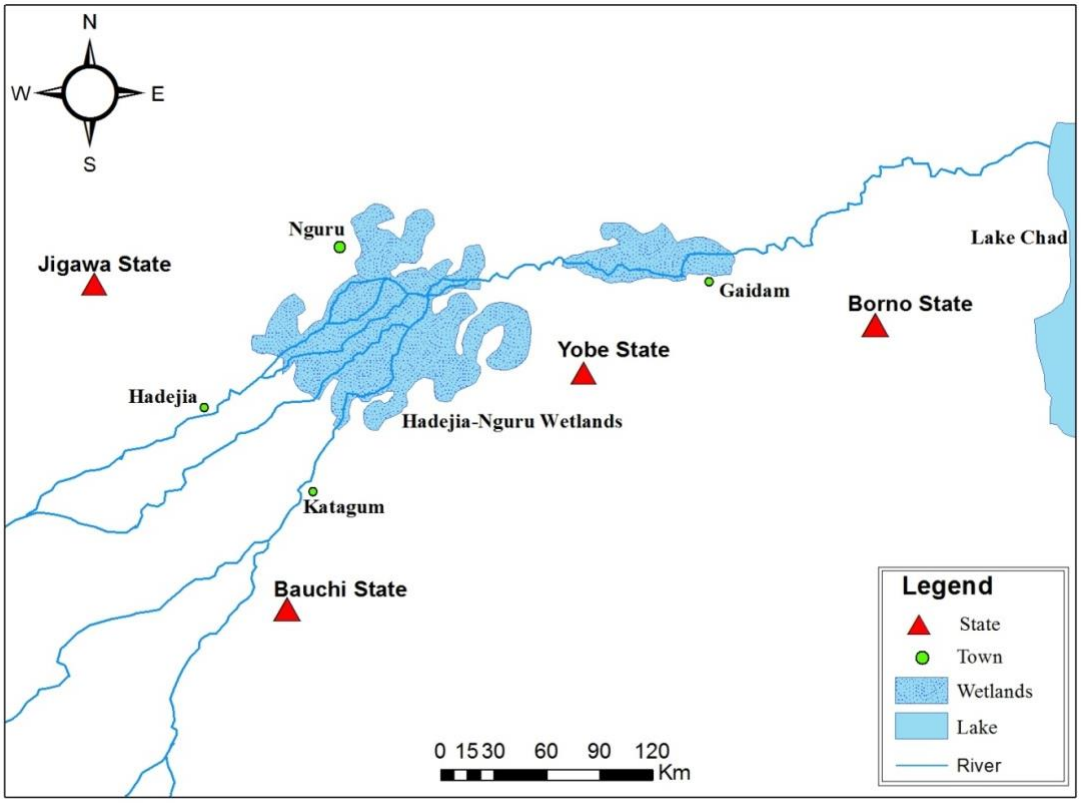

Figure. 1. Location of the HNWs

Source: (Eaton and Sarch, 1997)

DEFINITION OF WETLANDS

The term wetland has been defined by different people based on their profession and the needs for the ecosystem. There is no single definition accepted by all users of wetlands. Wetlands, as the term might suggest, are the collective terms for ecosystems whose formation, processes and characteristics have been dominated and controlled by water. The Ramsar convention defined wetlands as "areas of marsh, fen, peat land or water, natural or artificial, permanent or temporary with water that is static or flowing, fresh, brackish or salt, including areas of marine water, the depth of which at low tide does not exceed six meters" (Ramsar, 1994). Those concerned with the hydrology of a particular wetland may define it differently. Just like Hassan *et al.,* (2014) describe wetland as transition zones where the flow of water, the cycling of nutrients, and the energy of the sun meet to produce a unique ecosystem characterized by hydrology, soils and vegetation.

Some definitions are take into cognizance the processes of soil formation, in which case a wetland is defined as an ecosystem that arises when inundation by water produces soils dominated by anaerobic processes and forces the biota particularly rooted plants to exhibit adaptation to tolerate flooding Keddy(2010). Wetlands are also defined as sinks into which surface water or groundwater flows from a surrounding catchment (Mc Cartney *et al.,* 2010). NRC (2001) The minimum essential

characteristics of a wetland are recurrent, sustained inundation or saturation at or near the surface and the presence of physical, chemical and biological features reflective of the recurrent, sustained inundation or saturation. Dauda (2014) defined wetlands as natural lands perceived to be waste land that needs to be converted or put to use as agricultural land or development purpose. A wetland is a land area covered with water or where water is present at or near the soil surface all year or varying periods of the year (EPA, 2009). Nwankwoala (2012) referred to wetlands as those areas, which are capable of supporting water related vegetation. Asibor (2009) defined wetlands as any place that can support hydrophytes.

FUNCTIONS OF WETLANDS

Although the overall benefits of functions can be valued, determining the value of each wetland is difficult because they differ widely and do not all perform the same functions.

The value of a wetland is an estimate of the importance or worth of one or more of its functions to society. For example, a value can be determined by the revenue generated from the sale of fish that depend on the wetland, by the tourist money associated with the wetland, or by public support for protecting fish and wildlife. (EPA, 2001).Wetland functions are defined by Noviztki et al., (1997) as a process or series of processes that take place within a wetland. These include the storage of water, transformation of nutrients, growth of living matter, and diversity of wetland plants, and they have value for the wetland itself, for surrounding ecosystems, and for people. Functions can be grouped broadly as habitat, hydrologic, or water quality, although these distinctions are somewhat arbitrary and simplistic.

Habitat Functions

Perhaps wetlands are best known for their habitat functions, which are the functions that benefit wildlife. Habitat is defined as the part of the physical environment in which plants and animals live (Lapedes, 1976), and wetlands are among the most productive habitats in the world (Tiner, 1989). They provide food, water, and shelter for fish, shellfish, birds, and mammals, and they serve as a breeding ground and nursery for numerous species. Many endangered plant and animal species are dependent on wetland habitats for their survival. Coastal and estuarine wetlands provide food and habitat for estuarine and marine fish and shellfish, bird species, and some mammals (NOAA 1990a). Diverse species of plants, insects, amphibians, reptiles, birds, fish, and mammals depend on wetlands for food, habitat, or temporary shelter. Although wetlands make up only about 3.5 percent of U.S. land area, more than one-third of the United States' threatened and endangered species live only in wetlands

(Mitsch and Gosselink 1993). An additional 20% of the United States' threatened and endangered species use or inhabit wetlands at some time in their life.

Aquatic macrophytes play an integral role in the ecology of the wetlands. Aquatic macrophytes provide breeding and nursery sites, resting areas for migratory species, and refuge from predators (Crance 1988). Decomposed plant matter (detritus) released into the water is important food for many invertebrates and fish both in the wetland and in associated aquatic systems (Crance 1988). Physical and chemical characteristics such as climate, topography, geology, hydrology, and inputs of nutrients and sediments determine the rate of plant growth and reproduction (primary productivity) of wetlands (Mitsch and Gosselink 1993).A wetland with more vegetation will intercept more runoff and be more capable of reducing runoff velocity and removing pollutants from the water than a wetland with less vegetation (Richardson and McCarthy 1994). Wetland plants also reduce erosion as their roots hold the streambank, shoreline, or coastline. However, it is a well-known fact that the inundated or saturated conditions occurring in wetlands limit plant species composition to those that can tolerate such conditions.

The function of a wetland as a habitat is seriously impacted by fragmentation of the habitat. Wetland shape and size affect the wildlife community and the wetland's function as suitable habitat (Kent 1994b). The shape of the wetland varies the perimeter to area ratio. The amount of perimeter versus area has importance for the success of interior and edge species (Kent 1994b). Shape is also important for the possibility of movement of animals within the habitat and between habitats. Wetland size is particularly important for larger and wide ranging animals that utilize wetlands for food and refuge, such as lion or fox, since in many locations wetlands may be the only undeveloped and undisturbed areas remaining.

IMPACT OF CLIMATE CHANGE ON THE HNW

The most obvious manifestation of climate change in the Hadejia-Nguru wetlands is the steady increase in both water and atmospheric temperature, this is shown by the result of several studies (Abdullahi 1997, Indabawa 1998, Abubakar 2010, Abubakar and Yaji 2013 and Abubakar *et al*., 2015). Manifestation of climate change had been shown by changes in patterns of temperature and rainfall. According to Odjugo (2010) the temperature trend in Nigerian since 1901 showed increasing pattern. The increase was gradual until the late 1960s and this gave way to a sharp rise in air temperatures from

the early 1970s, which continued till date. The mean air temperature in Nigeria between 1901 and 2005 was 26.6^{o}C while the temperature increase for the past 105 years was 1.1^{o} C. This is obviously higher than the global mean temperature increase of 0.74^{0}C. Should this trend continue unabated, Nigeria may experience between the middle (2.5^{o}C) and high (4.5^{o}C) risk temperature increase by the year 2100.Medugu (2009) submitted that climate change refers to an increase in average global temperatures caused by natural events and human activities, which are believed to be contributing to an increase in average global temperatures. Increasing temperature will mean northward migration of mosquitoes and malaria fever which will extend from the tropical to warm temperate region while the sporogony of the protozoa causing the malaria accelerates from 25 days at 10^{0}C to 8 days at 32^{0}C (IPCC, 1998; Odjugo, 2000; DeWeerdt, 2007). About 200 million people could be affected by sea level rise, especially in Vietnam, Bangladesh, China, Indonesia, Thailand, Philippine, Indonesia, Nigeria and Egypt (*www.en.wikipedia.org*). The agricultural and food-distribution systems may be further stressed by shifting of temperature and precipitation belts, especially if changes are rapid and not planned for (see, for example, Adams *et al*. (1990). Malaria will also increase due to the preponderance of stagnant pools of water resulting from the sea-level rise related flooding. New evidence with respect to micro-climate change due to land-use changes such as swamp reclamation and deforestation suggest an increase spread of malaria to new areas (Munga et al. 2005; IPCC, 2007). Direct impacts of temperature increase include health problems induced by increasing incidences of heat waves. These could lead to more cases of cerebro-spinal meningitis (CSM), which today is found to correlate positively with the highest maximum temperature of the northern winter season, and inversely with absolute humidity to a lesser, although still significant, extent. The dryness has led to dry waterbeds and movement of people and their pasture to the southern regions thus causing tension and conflicts between the original inhabitants and the new comers. Another evidence of climate change in the HNW is a decline in rainfall. This is shown by frequent drought in the region. According to Odjugo (2010) the impact of climate change or global warming (as captured by average rainfall) revealed that all the Northern regions experienced decline (11.03%) during period under review (1971-2000), with North West region most affected (13.32%). The Southern region however, climate change (as captured by average rainfall) show a beneficial response with the exception of South east that recorded a decline (9.09%), while the South west show a high figure of 20.58% while South-south had an average of 2.45%. Findings indicate that the agricultural impacts of climate change in Nigeria need a holistic and quick interventions. The total average impact may be positive or negative depending on

the climate scenarios and zones. They are positive in the South particularly in the Southwest in most scenarios, but negative in the North in some scenarios. This is in agreement with the observations of NEST (2003) which shows that there is increasing rainfall in most coastal areas and decreasing rains in the continental interiors of Nigeria.Odjugo (2007) also observed that the number of rain days dropped by 53% in the north-eastern Nigeria and 14% in the Niger-Delta Coastal areas. Studies also showed that while the areas experiencing double rainfall maximal is shifting southward, the short dry season (August Break) is being experienced more in July as against its normal occurrence in the month of August prior to the 1970s. (IPCC 1996, Odjugo, 2005). These are major disruptions in climatic patterns of Nigeria showing evidences of a changing climate. The most devastating adverse impacts of climate change in Nigeria and other subtropical countries according to Ishaya and Abaje (2008) includes frequent drought, increased environmental damage, increased infestation of crop by pests and diseases, depletion of household assets, increased rural urban migration, increased biodiversity loss, depletion of wildlife and other natural resource base, changes in the vegetation type, decline in forest resources, decline in soil conditions (soil moisture and nutrients), increased health risks and the spread of infectious diseases, changing livelihood systems, (Reilly, 1999; Abaje and Giwa, 2007).According to NEST, (2003) apart from the two major effects of global warming, that is – Increasing temperatures and Rise in Sea level, other noticeable future and present impacts within our environment include disappearing African Rivers: Geologists recently projected a 10-20% drop in rainfall in North Western and Southern Africa by 2070. That would leave Botswana with just 23% of the surface-water flow it has now, Cape Town with just 42% of its river water. Apart from increased temperature and decreased rainfall the HNW is also experiencing other manifestations of climate change which include loss of biodiversity and the introduction of invasive species of plants, specifically *Typha* sp. that has grown to nonsense level, that it impedes almost all the uses of the water. According to Blench (2013) the bulrush, *Typha dominguensis*, has developed an invasive form in this region of Nigeria that is now a source of major economic losses. Studies by Abubakar (2012) showed significant differences in number and weight of fish caught between the infested and uninfested portions of Nguru Lake in the HNW. According to Blench (2013). The blackfaced dioch (*quelea quelea*) is a small finch that has developed intoa major pest since the 1970s. It forms large gregarious flocks and swarms over standing crops, stripping fields of grain. Its multiplication is probably associated with habitat change and biodiversity loss in the Sahelian region; as low-intensity cropping has spread so has the *quelea* bird. Studies by Abubakar *et al*., (2015) shows that the wildlife composition of the NHW shows a gradual species

reduction. Climate change negatively affects biodiversity conservation and management through exacerbated drought conditions, increased risk of wildfires leading to some extreme events like heat waves, river and coastal flooding, landslides, storms, hurricanes and tornadoes which culminate in environmental degradation (Agbogidi, 2011). So to fight these challenges, increase in the productivity level of pollution free product by application of advanced, environmental friendly technology, which can manage and allocate efficiently all resources for sustainable development of agriculture, is necessary (Basu, 2011; Bhadoria, 2011; Mahapatra, 2011; Mondal et al., 2011a). The National Adaptation Strategy and Plan of Action for Climate Change in Nigeria (NASPA-CCN 2011) revealed that climate change is already having significant impacts onNigeria. According to the report, recent estimates suggest that in the absence of adaptation, climate change could result in the loss of between 2% and 11% of Nigeria's GDP by 2020, rising to between 6%-30% by the year 2050. The impacts of climate change are expected to exacerbate the impacts of human pressure on biodiversity. This will further diminish the ability of natural ecosystems to continue to provide ecosystem services and may cause invasion of strange species that are favoured by climate change. Climate change is unarguably the biggest environmental issue of our time. Climate change is global in its causes but its consequences are far more reaching in developing countries, particularly Nigeria. Climate change is an environmental, social and economic challenge on a global scale (Scholze and Prentice, 2006; Mendelsohn and Williams, 2006). It can be exacerbated by human induced actions such as: the widespread use of land, the broad scale deforestation, the major technological and socioeconomic shifts with reduced reliance on organic fuel, and the accelerated uptake of fossil fuels (Millennium Ecosystem Assessment, 2005).

REFERENCES

Abaje I.B & Giwa P.N (2007). *Urban Flooding and Environmental Safety: A Case Study of Kafanchan Town in Kaduna State.* A Paper Presented at the Golden Jubilee (50th Anniversary) and 49th Annual Conference of the Association of Nigerian Geographers (ANG) Scheduled for 15th – 19th October, 2007 at the Department of Geography, University of Abuja, Gwagwalada-Abuja.

Abdullahi, B. A. (1997). Hydrobiology component. Biodiversity study of the aquatic fauna and flora of The Hadejia-Nguru wetlands. Hadejia- Nguru Wetlands Conservation Project. (HNWCP), Nguru, Nigeria. Pp79-86.

Abubakar, M. M., Kutama, A.S. and Sulaiman, M.I. (2015). Preliminary Survey of the wildlife biodiversity of the Hadejia- Nguru wetlands. *Dutse journal of Pure and Applied Sciences, 1(1)*. Pp 1-4.

Abubakar, M.M. (2010). *Some aspects of ecology and Fisheries of Nguru Lake*. (Unpublished) Ph.D. Thesis, Ahmadu Bello University, Zaria.

Abubakar, M.M. 2012**.** Impact of Emergent Macrophytes on Fish catch in Nguru Lake. *Bayero Journal of Pure and Applied Science (BAJOPAS).* Vol **5** No **2**. pp 47-50

Abubakar, M.M. and Yaji, A.J. (2013). Some aspects of the Limnology of Nguru Lake, northeastern, *Nigeria. International Journal of Basic and applied Sciences **2(2)***. 140-144

Asibor, G. (2009). Wetlands Values, Uses and Challenges. A paper presented to the Nigerian Environmental Society at the Petroleum Training Institute Effurun.

B., Jona, J. W., Boote, K. J. & Allen, L. H. 1990 Global climate change and US agriculture. *Nature, Lond*. 345, 219-224.

Basu, T.K. (2011). Effect of Cobalt, Rhizobium and Phosphobacterium Inoculations on Growth, Yield, Quality and Nutrient Uptake of Summer Groundnut (Arachis hypogaea). *American Journal of Experimental Agriculture,***1(1)**, 21-26.

Belewu, M.A. and Orire, I.O. (2011) PhysicNut: A Proactive Climate Change Risk Management Strategy. *British Journal of Environment & Climate Change 1(4):* 159-171

Bhadoria, P.B.S. (2011). Allelopathy: A Natural Way towards Weed Management. American *Journal of Experimental Agriculture,***1(1**), 7-20.

BirdLife International (2010). *In Nigeria, the BirdLife partner is assisting wetland restoration to safeguard ecosystem services.* Cambridge, United Kingdom.

BirdLife International (2015). *Important Bird Areas factsheet: Hadejia-Nguru wetlands*. Cambridge, United Kingdom.

Blench, R. (2013). An overview of the context of the Jewel project: Access rights and conflict over Common pool resources in the Hadejia-Nguru wetlands. *A report prepared for the JEWEL project in the Hadejia-Nguru wetlands, report of ITAD*, Cambridge CB1 2AL, United Kingdom.

Dauda, A.B. (2014). Salvaging Wetland Ecosystem in Nigeria. Towards Ensuring Sustainable Fish Production. *Nature and Science* 12(9). Pp 61-67

DeWeerdt S (2007). Climate change coming home: Global warming effect on populations. *World Watch*, 2(3): 6-13

Eaton, D., and Sarch, T. M. (1997). The economic importance of wild resources in the Hadejia-Nguru wetlands: Collaborative Research in the Economics of environment and Development (CREED).-London (International Institute for Environment and Development) (No.13). *WorkingPaper*. Pp 10-19

Ezealor, A. U. (2001). Important Bird areas in Africa and associated islands. *Report by Nigeria Conservation Foundation (NCF)*, Lagos, Nigeria. Pp 675-688.

Glenn, R. P., and T. L. Pugh. (2006). Epizootic shell disease in American lobster (Homarus H.L., Eds.Cambridge,; Cambridge University Press: UK.

Hassan, A.A., Jenyo-Oni, A. Dauda, A. B. (2014). Assessment of water quality, Ichthyofauna and Macroflora diversity of lower Ogun River Wetlands. *World Journal of Fish and Marine Sciences***6(1)**: 101-108

Indabawa, I. I. (1998). *Ecology of the phytoplankton of Hadejia-Nguru wetlands* (Unpublished) M.Sc. Thesis Bayero University Kano.

IPCC(1996): "*Technologies, policies, and measures for mitigating climate change*." Intergovernmental Panel on Climate Change Technical Report 1.

IPCC (1998). The Regional Impacts of Climate Change: An Assessment of Vulnerability. Special Report of IPCC Working Group II [Watson,R.T., Zinyowera, M.C., Moss, R.H. (eds.)] Intergovernmental Panel on Climate Change. Cambridge University Press, Cambridge, United Kingdom and New York, NY, USA, 517 pp.

IPCC (2007). Climate change: the physical science basis. In Contribution of Working Group I to the Fourth Assessment Report of the Intergovernmental Panel on Climate Change;

Ishaya, S.1 and Abaje, I. B (2008). Indigenous people‟s perception on climate change and adaptation strategies in Jema‟a local government area of Kaduna State, Nigeria. *Journal of Geography and Regional Planning* Vol. 1(8), pp. 138-143. Available online at http://www.academicjournals.org/J GRP ISSN 2070-1845

Kaugama, H. H., and Ahmed, B. A. (2014). Prospect and Challenges of Farming along the Hadejia-Nguru Wetland in Jigawa State, Nigeria. *International Journal of Academic Research in Economics and Management Sciences*, **3**:6, 43.

Keddy, P. A. (2010). *WetlandEcology: Principles and Conservation*(second Edition). Cambridge University Press: United Kingdom. Pp 497

Kennedy, V.S. (1990). "Anticipated Effects of Climate Change on Estuarine and Coastal Fisheries." *Fisheries* 15(6):16- 24.

Lapedes, D.N.,(1976)McGraw-Hill dictionary of scientific and technical terms: New York, McGraw-Hill Book Company, 1634 p.

Mahapatra, Sushanta Kumar (2011): *"Participatory Irrigation Management and Water Policy Reform: An Empirical Analysis of the Farmers Management of Irrigation Systems"*.A paper presented at the Southern Regional Research Paper Contest-2011 organised by the Navraj Academy for Managerial Excellence, held on12th November 2011 at the Conference hall hotel Sriram International Coimbatore.

Mc Cartney M., Rebelo L.M., Searatna Sellamuttu, S., de Silva, S.(2010). *Wetlands, Agriculture and Poverty reduction*. Colombo , Sri Lanka: International Water Management Institute (IWMI Research Report 137).

McCarthy, J., O. Canziani, N. Leary, D. Dokken, and K. White, eds. (2001). *Climate Change 2001: Impacts, Adaptation, Consequences of Climate Variability and Change.* U.S. Global Change Research Program, Washington, DC.

Medugu, N. I (2009) Nigeria: Climate Change A Threat to the Country's Development. http://www.allafrica.c om/nigeria/

Mendelsohn R, Dinar A, Williams L (2006). The distributional impact of climate Change on rich and poor countries. *Environment and Development Economics* 11: 159-178.

Millennium Ecosystem Assessment, (2005). *ECOSYSTEMS AND HUMAN WELLBEING:*

Mitsch, W., and J. Gosselink. (1993). *Wetlands.* 2nd Edition.New York Van Nostrand Reinhold,.

Mondal, P., Basu, M., Bhadoria, P.B.S. (2011a). Critical Review of Precision Agriculture Technologies and Its Scope of Adoption in India. *American Journal of Experimental Agriculture*,

1(3), 49-68.

Munga S., Minakawa N., Zhou G., Barrack O. O., Githeko A. K., Yan G. (2005). Oviposition site preference and egg hatchability of *Anopheles gambiae*: effects of land cover types. *J. Med. Entomol.*42, 993–997

National Research Council (2001). *Compensating for Wetland Losses under the clean Water Act.*WashintonDC,National Academy Press..

Nigerian Environmental Study Team (NEST), (2003),*Regional Climate Modelling and Climate Scenarios Development in Support of Vulnerability and Adaptation Studies: Outcome of Regional Climate Modeling Efforts over Nigeria,* NEST, Ibadan, Nigeria

Novitzki, R.P., Smith, R.D. and Fretwell, J.D. (1997). Restoration, Creation, and Recovery of intermolt duration *Journal of Crustacean Biology* 26(4):639-645..

Nwankwoala, H.O.(2012). Case studies on coastal Wetlands and Water Resources in Nigeria. *European Journal of Sustainable Development* 1(2): 113-126.

Odjugo PAO 2005. An analysis of rainfall pattern in Nigeria. *Global Journal of Environmental Science*, 4(2): 139-145.

Odjugo PAO 2007. The impact of climate change on water resources; global and regional analysis.. *TheIndonesian Journal of Geography*, 39: 23-41.

Odjugo, P.A. (2010).General Overview of Climate Change Impacts in Nigeria. *Journal of Human Ecology*, **29**(1). 47- 55

Odjugo, P.A.O. (2000). Global Warming and Human Health: Current and Projected Effects. *Environment Analer*., 4(2),49-60.

Oduntan, O. O., Akinyemi, A. F., Adetoro, A. O., and Osunsina, I. O. O. (2010). Seasonal availability of farmland and its contribution in wildbirds-landuse conflicts in Hadejia-Nguru wetlands, Nigeria. *African Journal of Agriculture*, **6**:3, 131-137.

Ogunkoya, O. O., and Dami, A. (2007). Information Sheet on Ramsar Wetlands (RIS) – 2006-2008 version: Dagona Sanctuary Lake, Hadejia- Nguru wetlands. *Annual report submitted to Ramsar*. Gland, Switzerland

Oguntuase, M.A. (1995).Environmental Impact of Groundwater Development Projects. *Proceedings of. Nig. Society of Agric. Engineers,*Akure, Nigeria PP 205

Ramsar (1994). *The Ramsar Convention on Wetlands*: Convention on Wetlands of international importance especially Waterfowl Habitat. Paris, 13 July 1994. Ramsar Convention Secretariat,

Gland, Switzerland.

Ramsar Convention Secretariat (2007). *Ramsar Handbook for the wise use of Wetlands* "Toolkit" (3rd Ed.). Ramsar Convention Secretariat, Gland Switzerland.

Reilly J (1999). What does climate change mean for agriculture in developing countries? A comment on Mendelsohn & Dinar. *World Bank Research Observer* 14: 295–305.

Rufous Hummingbirds. The Auk 115:240-245.

Sanyu (1994). *The study of the National Water Resources Master Plan*. Sanyu Consultants Inc. For Japan International Cooperation Agency.

Scholze M, Knorr W, Arnel NW, Prentice IC (2006). A climate-change risk analysis for world ecosystems. *Proceedings of the National Academy of Sciences* 103(35): 116-120.

Solomon, S., Qin, D., Manning, M., Chen, Z., Marquis, M., Averyt, K.B., Tignor, M., Miller, Tiner, R.W., (1989), Wetlands of Rhode Island: Newton Corner, Mass., U.S. Fish and Wildlife Service, National Wetlands Inventory, 71 p., appendix.

United States Environmental Protection Agency (2001). EPA 843-F-01-002c September 2001

WETLANDS AND WATER Synthesis. World Resources Institute, Washington, DC.

Wetlands. Wetland Functions, Values, and Assessment. National Water Summary on Wetland Resources**.** *United StatesGeological Survey Water Supply Paper 2425*

Environmental Audit of Camelite Paint Manufacturing Company Located at Agbor, Delta State, Nigeria. Case Study: Analysis of Effluent/Borehole water Discharge

By

Dr. C. O. Molua

College of Education, Agbor.

moluaogom@hotmail.com

Phone: +2348033596733

Abstract

An Environmental Audit (E.A) study of physiochemical and bacteriological effluent and borehole discharges of Camelite paint Manufacturing Company limited, Agbor was investigated. pH was determined using the pH meter pre-calibrated using buffer 4 and 9. TDS contents were estimated using Lovibond conductivity meter. Heavy meal concentrations were determined with Spectra AA varion 400 plus Atomic Absorption Spectrometer. Total aerobic bacterial counts were determined by the pour-plate technique technique. Total coliform counts were determined by the Most Probable Number (MPN) technique. The study revealed low pH, low TDS and small quantities of cations and heavy metal presence, and high total coliform bacteria counts of 42.2MPN/100ml which contributed to the bacteriological pollution of rivers and coastal waters resulting in limited possibilities of their use for recreation. It is suggested that to detect coliform organisms in water, either the multiple tube-fermentation-technique or the use of the Membrane Filter be employed because of the disadvantages associated with the so called Most-Probable-Number technique whose test is not sensitive to large fluctuations in coliform densities. Management of Camelite should consider pollution abatement and ensure compliance with environmental requirements.

Introduction

Environmental Audit, EA, is one of the available enforcement tools used as agent of sustainable growth comprising a systematic documented, periodic and objective evaluation of the process technology, equipment performance, raw materials in use, quality and quantity of waste generated and their effects on the air, soil, vegetation, underground and surface water, with the aim of facilitating management

control of environmental practices and assessing compliance with companies and meeting regulatory requirements.

In general, paint industries release significant amount of hazardous wastes to the environment, in particular, large quantities of untreated waste water are routinely discharged to the surface water ecosystem.

A close assessment of the chemical and bacteriological constituents of the studied parameters is often imperative for effective monitoring of their quality status.

Many scholars have conducted studies on these parameters within the sedimentary formations of Southern Nigeria (Etu-Efuotor, 1981; Amadi , 1989, Olobaniyi and Owoyemi, 2004).

The broad aims of this environmental Audit are to:

- Assess compliance with regulatory requirements (DPR, FEPA, WHO,etc) as well as company policies on environmental matters and sustainable development.
- Facilitate management control of environmental practices.
- Help local management to control the quality of existing operations and develop strategies for improvement in anticipation of future needs by:

i Identifying and proffering measures to minimize actual or potential company exposure to environmental liabilities.

ii Documenting the company's environmental status.

iii Transferring know-how on cost effective environmental techniques, as measures and procedures, as well as giving timely warning of situations that may need improvement.

iv Providing assurance that operations do not have unacceptable environmental effects.

Environmental Audit acts as internal control process to ensure that environmental protection and management procedures are being enforced vigorously. It will also ensure that enforcement of company policy, procedures and standards are in line with management's responsibility and in compliance with environmental legislation

Apart from the three major attributes of physical, chemical and biological considerations examined, it also includes the need to:

- Evaluate time management systems, plant operations, monitoring practices and data procedures and plans.
- Identify current and potential environmental problems through groundwater and effluent discharge study.
- Recommend improvement to the management of the operations, and especially pollution abatement.
- Evaluate company policy
- Assess the current environmental status of the company and evaluate compliance with existing regulatory requirements.

2.0 Materials and Methods

2.1 Area of study

The study was carried out at Camelite Paint Manufacturing Company Ltd, Agbor, Delta state, Nigeria. The study area lies between latitude $6^{o}16'0''$ North and longitude $6^{o}9'0''$ East (fig. 1). The main source of water in the factory is bore hole.

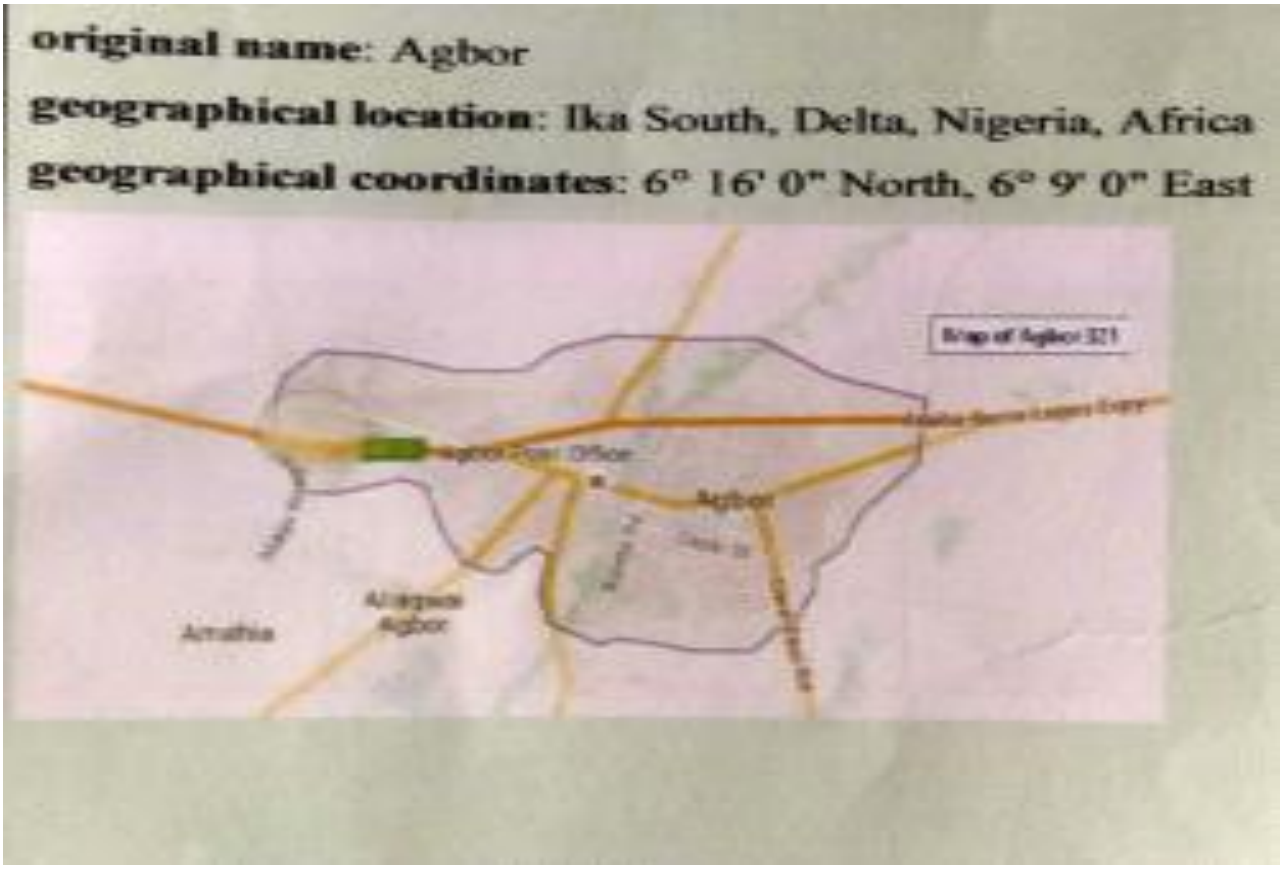

Fig.1: Map of Agbor showing the general coordinates

2.2 Climatic Conditions

The study of the physical features of the entire area shows two topographic highs separated by a valley. Within the valley is river Asimiri,, which flows in a southwest northeast direction (fig. 2). The area lies within the subequatorial climate with wet season of about 96 weeks and annual rain fall of over 2000mm. The area is also humid with average temperature of between 24^{o}C - 27^{o}C, (Iloeje, 1981), which adequately supports rainforest kind of vegetation.

2.3 Effluent sampling and Preservation

Water samples were collected into clean 1 litre plastic cans from each sampling point. For metal concentration determination, one of the points was stabilized with acid. Samples were also collected into sterilized 1 litre plastic cans for biological investigation. The procedures for obtaining these

different parameters were conducted in the chemistry and integrated science laboratories, College of Education, Agbor, Delta state.

Effluent water samplings were done at six points using a Ruttner Sampler. Separate samples were collected for the following determinations; Exchangeable cations, Heavy metals, and general phyisco-chemical analysis (using 2 litre plastic bottles)

Samples were preserved in ice chest cooler.

Samples were collected from the only Separator pit in the factory and also from other points within and also from other points within and outside the factory. The borehole sample was first collected for physco-chemical parameters and later for coliform test after steaming the pump head and allowing the pump to run for about 10 minutes. This was to ensure that a true and representative water sample was collected.

Table 1: The Effluent/Borehole sampling points

S/No	Effluent Sample	Sample point Description	Activities
1	Effluent, $\propto$	Beside Pre assembly and Premix	Resin, Pigment and solvent are mixed to produce an even mill base
2	Effluent, β	Beside Pigment grinding/milling	Mill base produced at the pre-mixing process is sent to the dispenser to finely disperse the pigment particles
3	Effluent, γ	Product finishing/blending	Resin, addictive agents are added to the mill base, the dispersion is now completed. Also, the colour phase is adjusted
4	Effluent, φ	Product filtering, filling and packaging	Blended and toned paint is filtered and packed into a container
5	BHW	Borehole water near the canteen	

6	SEP	Separator Pit	Gravity device that uses centrifugal force to separate particles from suspension

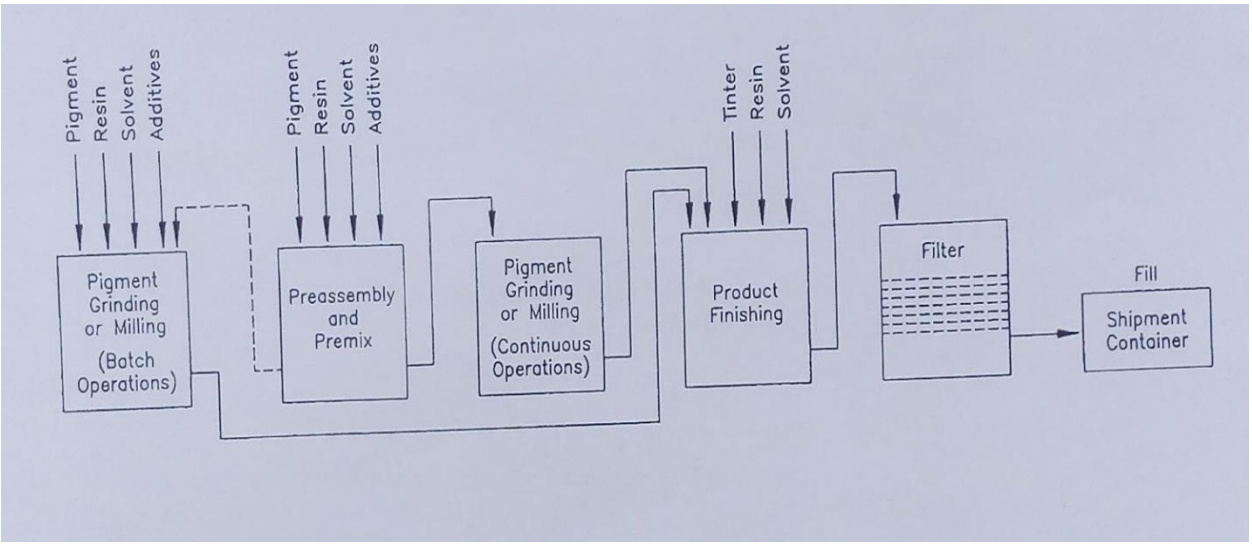

Fig. 3.Flow diagram of paint manufacturing process.

2.5 Physico-chemical study

The analytical procedures for physical, chemical and bacteriological parameters were determined generally in accordance with the overall specifications of American Public Health Association (APHA, 1985). T

The pH of the effluents was determined using glass electrode pH meter which was pre-calibrated using buffer 4 and 9 (APHA, 1992). Temperatures were measured in situ on the field.

The TDS contents of the samples were estimated using Lovibond conductivity meter.

The concentration of Na^+ and K^+ were determined using a flame photometer. Ca^{2+} and mg^{2+} were measured by EDTA titrimetriy, while Cl^-, HCO_3^{2-} and CO_3^{2-} were measured using titrimetric methods. NO_3^- content of the samples was determined by the Braine-Sulphate method (APHA, 1995).

SO_4^{2-} was determined by the turbidimetry method. Colloidal Barium sulphate was formed by the reaction of sulphate with barium ion in a barium chloride – hydrochloric acid solution in the presence of glycerol and ethyl alcohol.

Po_4^{2-} was determined by the stannous chloride (APHA, 1995).

The concentrations of heavy metals (Fe, Pb, Zn, Mn) were determined with spectra AA Varian 400 plus Atomic Adsorption Spectrometer. This analysis was carried out twice and the average values were obtained. Total aerobic bacterial counts were determined by the pour-plate technique while Total Coliform counts were performed by the Most Probable Number (MPN) technique.

3.0 Results and Discussion

The results of the physic-chemical study are as presented in tables2, 3 and 4.

Table 2 Physical Parameters Results of Effluent and Borehole samples.

Points	pH	Temp.^oC	TDS	EC	THC
A	7.0	28.0	24.0	44.5	21.0
B	6.5	27.0	40.1	80.2	28.5
Γ	5.4	26.7	15.2	27.8	13.4
Φ	5.7	28.5	14.7	23.6	28.8
BHW	5.5	26.0	12.3	22.0	8.0
SEP	4.9	26.5	41.2	88.2	29.7

TDS in mg/L

EC in µs/cm

THC in mg/L

Table 3

Chemical Parameters Results of Effluent and Borehole samples

Points	Na^+	K^+	Ca^{2+}	Mg^{2+}	Fe^{2+}	Zn^{2+}	Mn^{2+}	Pb^{2+}	HCO_3^-	CO_3^{2-}	Cl^-	SO_4^{2-}	NO_3^-	PO_4^{2-}
A	4.5	1.7	4.1	0.5	0.41	0.62	0.03	0.02	12.0	0.10	4.5	0.20	0.10	0.10
B	10.3	2.8	7.3	1.4	0.35	0.60	0.02	0.01	12.0	0.70	4.2	4.0	2.4	2.4
Γ	4.1	1.2	1.6	0.8	0.21	0.73	0.02	0.00	4.0	0.80	5.1	0.80	0.7	0.7

Φ	2.5	0.8	2.5	2.0	0.11	0.20	0.02	0.00	4.0	0.80	8.4	0.30	0.2	0.2
BHW	2.5	0.8	2.5	0.4	0.11	0.18	0.02	0.00	4.0	0.60	9.3	0.10	0.2	0.2
SEP	10.4	3.8	8.0	0.9	0.28	0.51	0,02	0.00	3.0	0.40	16.2	2.0	1.7	1.7

All measurements in mg/l

Table 4

Bacteriological Analysis results of Effluent and Borehole Samples

Points	Total Aerobic Counts (cfu/ml	Total Coliform (MPN/100ml)S
A	12	29
B	36	58
Γ	149	43
Φ	372	28
BHW	24	42
SEP	12	53

Table 5

Effluent Samples and bacteriological composition compared to DPR/FEPA/WHO standard for drinking water

N=6 Parameters	Minimum Value	Maximun Value	Mean	DPR/FEPA/WHO permissible limit
pH	4.9	7.0	5.83	6.5-8.5
Temp.^{o}C	26.0	28.5	27.1	-
TDS	12.3	41.2	24.6	1500
EC	22.0	88.2	47.7	1500
THC	8.0	29.7	21.6	500

Na^+	2.5	10.4	5.73	500
K^+	0.8	3.8	1.85	50
Ca^{2+}	1.6	8.0	4.33	200
Mg^{2+}	0.4	1.4	1.00	150
Fe^{2+}	0.11	0.41	0.25	0.03-1.00
Zn^{2+}	0.18	0.73	0.47	5.00
Mn^{2+}	0.02	0.03	0.02	0.1-0.20
Pb^{2+}	0.00	0.02	0.005	0.01
HCO_3^-	3.00	12.0	6.50	500
CO_3^{2-}	0.10	0.80	0.57	-
Cl^-	4.2	16.2	7.95	500
SO_4^{2-}	0.10	4.00	1.23	400
NO_3^-	0.10	2.40	0.88	40-70
PO_4^{2-}	0.10	1.20	0.37	-
Total Aerobic counts (cfu/ml)	12	372	199.8	-
Total Coliform (MPN/100ml)	28	58	42.2	0/100ml

Discussion

pH

The pH of the samples has a minimum value of 4.9 at point SEP and a maximum value of 7.0 at point α with a mean value of 5.83 (Table 2 and 5). The pH values at all the points are within the permissible limits for industrial effluents and borehole water set by DPR/FEMA/WHO.

Temperature

The temperature values ranged from 26.0ºC to 28.5ºC. The minimum value was at point BHW and the maximum value was at point γ with a mean value of 27.1ºC (Tables 2 and 5).

Total Dissolved Solids (TDS)

The TDS value has a minimum of 12.3 at point BHW and a maximum value of 40.1 at point β with an average value of 24.6. The DPR/FEPA/WHO permissible limit for TDS is 1500mg/l (Table 2 and 5). The borehole water has a low dissolved solid value of 12.3mg/l and falls within acceptable limit for portable water.

Electrical Conductivity, EC

The electrical conductivity of the effluent water samples varied widely. The least value of 22.0µs/cm was obtained at point BHW while the maximum value of 88.2 µs/cm was obtained at point SEP.

Total Hydrocarbon Content (THC)

The effluent samples have the least THC of 8.0 at point BHW and a maximum value of 29.7 at point SEP. The mean value was 21.6 which is below th permissible standard by DPR/FEPA/WHO.

Exchangeable cations (Na^+, K^+, Ca^{2+}, Mg^{2+})

All the cations analysed for namely, Na^+, K^+, Ca^{2+}, Mg^{2+}, were detected in varying degrees in all the sampled points (Table 3)

Heavy Metal (Fe, Zn, Mn, Pb)

Heavy metals were detected in small quantities in all the sampled points.

Apart from the points α and β which had 0.02 and 0.01 respectively for Pb^{2+}, all other points did not detect Pb^{2+}, (Table 3).

Nitrate (NO_3^-)

The nitrate content of effluent samples showed some variations. It has minimum of 0.10 at α and maximum of 1.7 at point SEP (Table 3). It has a mean value of 0.88 which is very low compared to the permissible limit of 40-70 by DPR/FEPA/WHO.

Chloride (Cl)

The chlorine values from the sampled points ranged from 4.2 at point β to 16.2 at point SEP, with a mean value of 7.95. This is in conformity with the required standards by WHO, (Tables 3 and 5).

Sulphate (SO_4^{2-})

Sulphate was detected in all the sampled points. The minimum value was at point BHW (0.10) and maximum value of 4.00 at point β, (Table 3)

Phosphate (PO_4^{3-})

Phosphate was detected in the samples in small quantities. The mean value was 0.37.

Bacteriological quantity

The result of the bacteriological analysis from the study is as presented in table 4 above. Total aerobic bacteria counts range between 12cfu/ml and 372cfu/ml while the coliform counts have values from 28 to 58 MPN/100ml with a mean value of 42.2MPN/100ml. This value far exceeded the WHO standard requirement of 0/100ml., (Tables 4 and 5). This means the samples were all contaminated with pathogenic micro organisms.

Conclusion

The study revealed low pH and low TDS. These are characteristics of tropical regions of high rainfall, (Rose, Hawkes and Webb, 2000).

Also, the low EC within the study area is indicative of low salinity sodium hazards. The study also revealed contaminated effluent waste water with pathogenic micro organisms due to total coliform count whose mean value was 42.2 MPN/100ml compared to 0/100ml permissible by DPR/FEPA/WHO.

This high value contributes to the bacteriological pollution of rivers, coastal waters, resulting in limited possibilities of their use for recreation. It is therefore necessary to disinfect it, control its bacteriological quantity, especially when discharged into surface waters used for recreational purposes.

References

Akpoborie, I. A., Ekakittie, O. A. and Adaikpoh, E. O. (2000): The qualityofgroundwater from dug wells in part of the Niger Delta. Knowledge Review, 2/5, pp72-79.

Amadi, P. A., Ofoegbu, C. O. and Morrison, T. (1989): Hydrological Assessment of groundwater in parts of Niger Delta, Nigeria. Environmental Geology. 14/3. Pp195-202.

APHA (1995); Standard Methods for the Examination of water and wastewater

APHA, (1992): Standard Methods of Water and Waste Examination, 18th Edition. American Public Health Association, NY. Washinton DC. Pp 2-172.

Ayodele, J. T., Momoh, R. U. and Aminu, M., (1991): Determination of heavy metals in Sharada Industrial effluents. In : Book of Abstrack: Second National Environmental Seminar. Pp. 14: FEPA. F.M.H. National Water resources Institute; WHO, Kaduna State Water Board.

DPR: Department of Petroleum Resources, 2002. Environmental Guidelines and Standards for Petroleum Industries in Nigeria.

Etu-Efeotor, J. O. (1981): Preliminary hydro-chemical investigation of sub-surface waters in parts of the Niger Delta. *Journal of Mining and Geology. 18/6, Pp103-107.*

Federal Environmental Protection Agency, (FEPA), 1998. Guidelins and standards for environmental Pollution Control in Nigeria. Decree 58 of 1998. Pp. 238.

FEPA (1991); Federal Environmental Protection Agency. Guideline and standards for environmental pollution in Nigeria, FEPA, Nigeria.

HACH, 1997. Water Analysis Handbook, 3rd edition, HACH Company, Loveland, Colorado, USA.

Iloeje, N. P.(1981): A new geography of Nigeria. Longman, Nigeria. 201p

Mallman, W. and Frank, R. P., (1961): Multiple-Tube dilution and Membrane Filter methods. Water and sewage works. 108 (10), 384

Offodile, M. E, (1992): An approach to groundwater study and development in Nigeria. Mecon Services Ltd, Jos.243p.

Olobamiyi, S. B. and Owoyemi, F. B. (2004): Quality of ground water in the Deltaic plains and aquifer of Warri and environs, Delta state of Nigeria, Water Resources. Journal of the Nigerian Association of Hydrogeologists. 15, Pp38-45.

Olobanji, S. B., Ogban, F. E., Ejechi, B. V. and Ugbe, F. C. (2004): Assessment of groundwater across Delta state: effects of man, geology and hydrocarbon exploration. Final report., Delta State University, 100p.

Onuegbu, T. U., Okoye, I. O.,Dioha, J. J., Okoye , P. A. and Nwako, P. A., (2008): Treated effluents and sludges. J. Chem. Oc. Nigeria. Vol. 33 No 1. Pp 6-9.

Rose, J. B., Dickson, L. J., Farrah, S. R., and Carnahan, R. P., (1996): Removal of Pathogenic and indicator micro-organisms by full scale water reclamation facility. Wat. Res. 30, (11), 2786.

Rose, O. N., Hawkes, H. E. and Webb, J. S. (2000): Geochemistry in Mineral exploration. Academic press, London 55p.

Singare, P.U., Lokhand, R.S.andJangtap, A. G., (2010): Study of Physiochemical quality of Indusrial area of Maharashtra, India: Dispersion of heavy metal and toxic effects. *International journal of of global Environmental issue.*

Technical Proposal for waste water treatment plant for based paints, CAIROMATIC Company, Egypt, 1999.

WHO, Guidelines for safety Recreational Water Environments; Draft for consultation. World Health Organization, Geneva, 1998.

World Healt Organisation, 1993: International Standard for drinking water and guidelines for water quality. WHO. Geneva.

World Healt Organisation, 1996: International Standard for drinking water and guidelines for water quality, 2nd edition, Health criteria and other supporting information. WHO., Geneva.

Protective Shielding Parameters for Diagnostic X-Ray Rooms In Some Selected Hospitals In Agbor - Delta State

BY

Molua, O.C, Eseka, K and Ukpene, A.O

College of Education, Agbor,

E-mail : **moluaogom@hotmail.com**

+2348034050646

ABSTRACT

A research work for the determination of protective shielding parameters of diagnostic x- ray rooms at some selected hospitals in Agbor, Delta State have been carried out with the aid of Geiger Muller Counter 320 plus.The hospitals includes central hospital Agbor, central hospital Abavo and Nkonye hospital Agbor.The workload ,use factors of each x-ray machine together with their operational potential were evaluated and used to ascertain the level of effectiveness of the secondary and primary structural shielding barrier at the x-ray units of these hospitals. The wall thickness around the x-ray units at central hospital Agbor, central hospital Abavo and Nkonye hospital Agbor are found to be 310 ± 3.0 x 10^{1} mm, 300 ± 3.0 x10^{1} mm and 280 ± 6.0 x10^{1} mm, and these values are found to be adequate as effective protective structural barriers when compared with international standard value of 74 ± 7.4 x10^{-1} mm for diagnostic x- ray units.

INTRODUCTION

Since the discovery of X-rays by Wilhelm Comrade Roentgen in 1895, x-rays have become very useful in the field of science especially in medical science all over the world. The production and scattering of x-rays provide additional examples of the quatum nature of electromagnetic radiation. X-

rays are produced when rapidly moving elections that have been accelerated through a potential difference of the order of 10^3 to 10^6 V strike a metal target (University Physics 9th edition).

In an x-ray machine, sufficient intensity of electrons flow when high voltage power supply of 50 kVp to 125 kVp is applied, producing diagnostic x-rays for clinical diagnosis and treatment (Agba., et al 2011). Abdominal and chest examinations are normally performed at about 70 – 80 kVp and 100 kVp (Benjamin, 1982). X-rays have may practical applications in medicine and industry. They can penetrate several centimeters of solid matter and can be used to visualize the interiors of materials that are opaque to ordinary light such as bones or defects in structural steel. It is generally known that over exposure to x-rays is capable of producing serious damaging health effects and can even lead to death at a higher level of exposure (Agba., et al 2011). Due to the ionizing nature of x-rays, it has become very necessary that exposure to x-rays from x-ray rooms be minimized. External radiation in radiology can be minimize or reduced by limiting the duration (time) of exposure, increasing distance between source and patients and placing a shielding material between the radiation source and the patients (Camber & Johnson 2009). Since x-ray radiation exposure from x-ray machines is considered as an external radiation, it effect can easily be minimized using source and structural shield in and around diagnostic and therapeutic x-ray rooms.The objective of this work therefore, is to determine the shielding parameters of diagnostic x-ray rooms in some selected hospitals in Agbor,Delta State with a view to determining the effectiveness of the primary and secondary protective shielding of the x-ray rooms.

BASIC THEORETICAL CONCEPT.

The physical parameters that determines the primary and secondary structural shielding of x-ray radiology rooms include, tube workload, use factor, operating potential and occupancy factor. These parameter are related by the equaation

$$K = \frac{Pd^2}{WUT}$$ ……(Zuk, 2002).

K is exposure per unit workload at unit exposure.

P is the maximum permissible exposure in R/week for controlled area.

D is distance (m) from the target to primary area.

W is the workload (MA – mm/week)

T is the occupancy factor and U is the use factor.

Akodele and Okunade, (2001) gave the following definition:

i Workload: this is the amount of x-rays emitted per week (MA –mm/week)

ii Occupancy factor (T) is the fraction of time that a maximally present individual is present in the area while the beam is on and the barrier protecting the area is being irradiated.

iii Use factor (U) is the fraction of primary beam workload that is directed to a

MATERIALS AND METHODS

A nuclear radiation detector Geiger Muller Counter 320 plus was used for the measurement of radiation in all the selected hospitals to ascertain the exposure of x-ray machines at exactly 1m from the primary source.

The work was carried out for a period of 4 weeks in each of the selected centers The patients examination records containing types of examination each day,peak tube voltage, tube current and exposure time including the actual number of films used were obtained. Atotal of 145 patients were examined in central hospital Agbor, 110 in central hospital Abavo and 125 in Nkonye hospital Agbor for a period of 4 weeks.

The following distances were measured:

Primary distance

Leakage distance

Scattered distance

Wall thickness (with the aid of measuring tape).

The primary distance measured for the x-ray tube focal spot was at 0.4 m beyond the wall to serve as the primary barrier while the distance from the source to the scattered distance was measured from the surface of the patients (scattering material) to 0.4 m beyond the primary barrier.

The exposure per week contributed by the primary exposure, scattered exposure and the leakage exposure were evaluated .The method used here has also been used by other researchers.

Results and Discussion

The results obtained after some series of computations arising from the measurement of radiographic parameters and shielding distances at the selected hospitals are as shown in the tables below.

Table1. Measured Radiographic parameters at the various hospitals.

	Hospitals		
Measured parameters	Central hospita l Agbor	Central hospital Abavo	Nkonye hospital Agbor
Tube voltage (kvp)	100	100	100
Exposure rate (mr/hr)	$25.2 \pm 1.3 \times 10^1$	$9.4 \pm 0.3 \times 10^1$	$5.6 \pm 1.8 \times 10^1$
Exposure time (s)	1	1	1
Field size (cm^2)	1275	1275	1250

Table 2. Measured shielding distances at various hospitals

Measured parameters	Hospitals		
	Central hospita l Agbor	Central hospital Abavo	Nkonye hospital Agbor
Primary distance (m)	2.52	2.41	2.12
Secondary distance (m)	0.91	0.82	0.99
Leakage distance (m)	2.31	1.91	2.11
Scattered distance (m)	1.36	1.01	1.20
Source image distance (m)	1.35	1.50	1.23
Film to coat distance (m)	0.35	0.39	0.41
Wall thickness (m)	$0.31 \pm 3 \times 10^{-2}$	$0.30 \pm 3 \times 10^{-2}$	$0.28 \pm 2.6 \times 10^{-2}$

Table 3. Measured shielding distances at various hospitals

Measured parameters	Hospitals		
	Central hospita l Agbor	Central hospital Abavo	Nkonye hospital Agbor
Tube workload (mA-min/wk)	48.40	30.30	98.35
Use factor	0.42	0.41	0.39
Occupancy factor	1	1	1
X-ray tube output (mR/mA-min) at 1m from source	4.2×10^{-3}	3.98×10^{-3}	3.0×10^{-3}
Exposure toward (mR/wk)	0.68	0.49	0.35

primary beam

Exposure per unit workload (mR/wk) `			
toward primary beam at unit dist.	0.64	0.50	0.41
Exposure per unit workload			
toward secondary barrier	0.014	0.04	0.005

From table 3, it was observed that the tube workload of 48.40, 30. 30 and 98.35 mA – min per week recorded for central hospital Agbor, central hospital Abavo and Nkonye hospital Agbor were found to be lower than the NCRP 49 (1970) recommendation which is 250 mA – min per week for a solo practice and 1000 mA – min per week for busy radiographic units.

We can attribute the high level of tube workload recorded at Nkonye hospital which is higher than that obtained from the other hospitals may be due to the fact that the x – ray machine is the busiest of the other entire x – ray machines employed in these hospitals.

The findings from this work shows that the workload lies between the range of 73 to 530 mA min/wk recommended for arthopeadie facilities and 500 mA min /wk for shielding design purposes and this is in agreement with the recommendation by Bushing and Glaze (1983). Braestrup (1970) reported that so many results have shown that the weekly workload does not exceed 100 mA – min even for very busy radiographic x-ray room and this is also in agreement with the results obtained in this work from the three hospitals investigated.

From table 3 also, the exposures per week without shielding at posititon of 0.3 m above the primary/secondary protective barriers in the three hospitals are found to be lower that the recommended standard value for exposure limit/week of 2 mR/wk.

These values are 0.68 and 0.64 for central hospital Agbor, 0.49 and 0.50 for central hospital Abavo and 0.35 and 0.4 mr/wk

From the results obtained in this investigation, it was observed that the primary and secondary shielding barrier of the concrete thickness of the walls of the x – ray rooms at these hospitals are 310 + 3.0 x 10^1 mm for central hospital Agbor, 300 + 30 x 10^1mm for central hospital Abavo and 280 + 2.6 x 10^1 mm for Nkonye Hospital Agbor.These results are in agreement with the findings of Agba., et al (2011) and it shows that the walls of the x-ray units of these hospitals have adequate primary shielding effectiveness and this in effect takes care of the secondary protective shielding at these hospitals.

Conclusion

Findings have shown that the results obtained from the three hospitals investigated in this work are found to be inconformity with the recommendations of National Commission on radiological and protection NCRP 70 and (116) protocols. This is because the protective shielding parameters results obtained in this work are lower than the standard recommended maximum values.

This work,therefore have finally shown that the walls of the x-ray rooms of these hospitals investigated have adequate shielding and therefore do not necessarily required any additional primary structural shielding barriers.

REFERENCES

Agba, E.H., Gemanam,S., and Sombo T.(2011): Protectective shielding parameters for diagnostic x-ray rooms in some selected hospitals in Makurdi and Gboko towns of Benue State, Nigeria. Nigerian Journal of Physics Vol.22 (1) 2011

Bushong, S.C. and Glaze,A. (1983): Radiographic workload and use factors for Orthopaedic facilities. Health Physics, Pp 44 53-59

ICRP (1991): Recommendations of the International commission on Radiological Protection. Annals of ICRP 194 (46).

NCRP 116 (1993): Limitations of Exposure to Ionizing Radiations, Bethesda,MD NCRP; NCRP Report No 116.

NCRP Publication 49 (1970): Structural shielding design and evaluation for Medical use of x-rays and gamma rays of energies up to 10 MeV. NCRP Report No 49.

Zuk, W.M (2002): X-ray Equipments in medical diagnosis part A. www.google.com, Ontario 2005.

Nuclear Energy in Nigerian Energy Matrix: Problems and Prospects

***[1]Oche O. C., [2]Olarinoye O. I**

*[1 &2] Department of Physics, Federal University of Technology, Minna, Niger State, Nigeria.

Ochegabasphysics@gmail.com

Leke.olarinoye@futminna.edu.ng

correspondence Author

Abstract

The need for energy globally is continuously on the increase and hence the need for more efficient ways to produce energy to meet this demand cannot be overemphasized. Nigeria currently produces approximately 4 Gigawatt of Electrical power for a population of over 0.181 Billion people leading to an abysmally low level of industrial productivity as evident from the country's per capita income owing to erratic supply of electricity. Sources of generating electricity used the world over includes Solar, wind, hydro, Geothermal, Biomass, Gas, Coal and Nuclear Power. Most countries rely heavily on a robust mix of the afore-listed sources of energy while Nigeria yet battles with more of gas and less of hydro. The world over is battling with the menace of global warming and air pollution/environmental that created the need for greener and eco-friendly sources of electrical power. This applauds the use of nuclear energy for electricity generation. Its challenge has been that of reactor accidents, material proliferation and waste managements. Nuclear reactors have in the last six decades become a lot safer. The Uranium Extraction (UREX+) and Plutonium, Uranium extraction (PUREX) methods have been reviewed as viable methods to be used to curb against proliferation of nuclear materials- a major cause of disapproval of the nuclear energy. This paper also outlines the various technologies used which has made nuclear reactor waste management and recycling safer and practicable

Keywords: Energy, Gen IV Reactors, Nuclear, PUREX, UREX+

1.0 INTRODUCTION

Energy is the physical driving force, the life blood of modern civilization. Every activity of man is hinged on its availability. Energy services are essential for human welfare and contribute to enhanced social stability through improved standards of living. It is a critical input to economic development and prosperity (OECD, 2000). Between 1970 and 2006, the world's total energy requirement increased by a factor of 2.5 even with measures set up to enhance energy production and its utilization (Ferenc, 2008). Holistically speaking, as countries gear towards sustainable developments, their energy needs increase so as to achieve such sustenance. Developed nations have over the years been able to utilize their energy production vis-à-vis its sustainability as they achieve more vibrant economies. A lot more countries in the developing and the less developed cadre suffer one form of energy crisis or another. Nigeria isn't an exception. With over 0.181 Billion people, Nigeria currently suffers from acute power shortage which has seriously affected the country's economy without any viable solution thus far (Salawu and Oche, 2017). Electricity is the key source of power for socio-economic development of any country (Mollah et al., 2015). In Nigeria, energy serves as a pillar of wealth creation evident by being the nucleus of operations and engine of growth for all sectors of the economy (Adegbemi et al., 2013). The current mix for the country includes Hydro, coal and gas stations and the current surge for other renewable sources like solar, biomass amongst others. Despite Nigeria's steady access to fossil based and renewable energy resources, its per capita electricity has been one of the lowest in Africa. Indeed the tenth largest exporter of oil in the world and Africa's one time largest economy has only a grid capacity of 6000 MW while the consumable power fluctuates between 2 – 3 GW (Lowbeer, 2010). Nigeria is endowed with enormous energy resources such as gas, petroleum, coal, tar, silica, uranium, solar energy, winder and geothermal potentials. However, Nigeria is yet to exploit these huge available energy potentials with less environmental and climatic impacts (Lowbeer, 2010). The output of the energy sector (electricity and petroleum products) usually consolidates the activities of the other sectors which provides essential services to direct production activities in agriculture, manufacturing, mining, commerce etc. (Adegbemi et al., 2013) . As a developing country, the need for energy is high and this need has not been met by the current output because of inadequate/epileptic supply and the fact that developing these sources to full capacity may not suffice without the utilization of a good electrical source matrix whose combination will produce more than enough for the nations usage in both industrial and household usage (Yehuwdah et al., 2013). Suffering from age long mismanagement, lack of investment and general neglect, the domestic energy industry in Nigeria has consistently failed to meet the demands of consumers. Research has highlighted major reasons for this inadequacy to include (Chidi et al., 2008);

- General low-level capacity of power stations
- Problems associated with ageing hydropower plants
- Seasonal variations in water levels in hydropower dams.

- Capriciousness of gas supplies to the gas thermal stations, sometimes resulting from gas pipeline vandalization and corrosion attacks.
- A thriving business of importation of power generating sets – a major contributor of greenhouse gases (GHGs).

The reasons why the solutions to the problems listed above may be difficult can be given as follows;

- The plants currently in use are old models which in other developed countries have phased out due to innovations and upgrades due to more power requirements. The problem here is that of purchasing and installations which may seem very costly owing to non-local manpower hence the need to manage existing plants.
- Seasonal variations in water levels are perennial problems which we may not have direct control over. Because the amount of rainfall a year possesses is a deciding factor for the rise and fall of the water collectable in dams. Similarly, Climate change is another factor. It also may cause a stretch in the dry seasons in a place and hence a dip in the water collection index.
- Pipeline vandalization and youth restiveness has evaded possible solutions thus far due to massive corruptions that are involved when monies meant for the developments of the lands (Niger delta – Southern Nigeria) are being usurped by politicians and supposedly representatives of these lands.
- Unless the use of power generating sets in Nigeria is totally eradicated by the presence of power from the national grid, the problem of importations of power sets would never stop thriving. We can note also that people are enjoying the problem caused by inadequate supply of power because it means good business.

As power demand studies have projected a medium to long term electricity demand of 30,000 MW and 192,000 MW respectively, there will be a need of substantial improvement in the energy production and supply sector if this demand is to be met (Famous, 2014) . Hence the need for Nigeria to consider taking the right steps towards adding viable power sources into its energy matrix. In developed countries, a sustainable energy mix has driven renewable energy considerations. However, in developing countries, the push for sustainable energy is mostly bolstered by the need to combat energy shortage in order to encourage development in the rural areas (Ayoola et al., 2017). This paper presents the current status and the challenges

of the Nigerian energy sources matrix, suggests nuclear option as a viable choice for a good mix as it regards its prospects. Also the review discusses the art of nuclear technology and the current fail-safe technology. Reviews of various scholars on the prospects and problems associated with the technology, the way forward for Nigeria, and the Generation IV nuclear reactors as anti-proliferation agent in the midst of a global threat of weaponization of nuclear wastes.

2.0 Electrical Power in Nigeria

2.1 Current State

Most research shows that Nigeria has been battling with the seemingly 4GW barrier. In that all combined efforts have not been able to yield better efforts at surpassing that mark. The National energy supply is at present almost entirely dependent on fossil fuels (conventional energy sources) which are depleting fast. In 2004, use of liquid and solid fossil fuels accounted for approximately 58% of the gross national consumption with natural gas and hydroelectricity contributing 34% and 8% respectively. Fidelis *et al*. (2011) puts the figures at 25% hydro, 12% Thermal (oil) and 63% thermal (gas). Coal, nuclear and 'some' renewable are not yet part of the primary energy mix used to produce electricity (Sambo et al., 2012). Although coal was used some decades ago in powering locomotives and currently by some companies (such as Dangote) for private energy production (Sunnewsonline, 2018).

There is a total number of 23 on grid connected generating plants currently under the Nigeria Electricity Supply Industry (NESI) totaling an installed capacity of 10,396.0 MW out of which only about 58% is available. Owing to the fact that most of our power comes from thermal plants, out of the existing 8457.6 MW installed capacity, only about 4996 MW (83%) of installed capacity is produced. Three major hydro power plants contributes a total installed capacity of 1,938.4 MW of which 1,060 MW is available (Okoye, 2014).

The current situation in Nigeria is paradoxical because, despite Nigeria's rich oil and gas sector, many communities do not have access to electricity which is a secondary form of energy fueled by the petroleum with which Nigeria is richly endowed (Sambo et al., 2012).

The Nigeria situation is such that the current electricity provision is short of the electricity demand in the country. At 126 kWh per capita, Nigeria lags far behind other developing nations in terms of grid-based electricity consumption. Based on the country's GDP and global trends, electricity consumption ought to be four to five times higher than its current value. For example, Ghana's per capita consumption (361 kWh) is 2.9 times higher than that of Nigeria, and South Africa's (3,926 kWh) is 31 times higher. (Power Africa, 2015)

Ironically, while Nigerian energy resources, particularly oil, are exported to other countries; its people and economy suffer from severe shortages of the same product. This is manifested by the epileptic supply of electricity and perennial shortage of most petroleum products (Adegbemi et al., 2013).

Furthermore, unreliable power supply forces both households and industry to rely on privately owned generators for much of their power. Nigerians get a significant portion of their electricity from private generators at a higher cost (NGN 62 - 94/kWh) than grid-based (NGN 26 - 38/kWh) power (Power Africa, 2015). The consequence of these is seen in the current state of the economy. There is a huge deficit of power needed to fast track and sustain national development.

A study by Adegbami and Babatunde (2013) showed that the demand for power (peak load)is projected to rise from 5,746 MW in 2005 to 297,900 MW in the year 2030 which translates to construction of 11,686 MW every year to meet this demand. The current matrix is inadequate for such a projection. It was also reported that industrial capacity utilization has plummeted from 78.7% in 1977 to 30.1% in 1987 before resurgence to 53.3% in 2007 and 53% in 2010. Currently, industries are paying too high to produce their own power while most have relocated to other countries thereby reducing the export potentials. Investors are forced to go elsewhere. The coexistence of vast wealth in natural resources and extreme personal poverty referred to as the "resource curse" or 'Dutch disease' afflicts Nigeria (Adegbemi et al., 2013) These problems can be apportioned to be responsible to this problems which includes;

- Insufficient Funding of Existing power stations
- Inadequate and/or delayed maintenance of facilities and plants
- Inadequate generation availability.

- Lack of continuous implementation of a futuristic power development blueprint

2.2 Available Energy Resource in Nigeria

Research has shown that the potential of Nigeria in generating about 15 GW of power via hydro, 83 million untapped tones/annum of biomass crop residue, 61 million tones/annum of biomass animal waste, biomass fuel wood of forest land circa 13 million hectares of land; solar radiation of a mean of circa 5.25 KWh/sqm/day and annual wind of an average of 10.5 Km/h at a height of 10.0m (Ismaila and Olusola, 2015); Fidelis *et al., 2014;* Famous, 2014). Even though costly, the solar technology will prove to be a veritable mix element in any power-serious driven nation. (Fidelis et al., 2014) Gives the coal reserve in the country to about 2.7 billion tons. In his paper, Anyaegbunam (2015) gave another renewable source for the country as 'Over 50 Million vehicles plying the road with a growth rate of 15% (2012 figure).' This technology is based on power generation from speed breakers generators. Chidi *et al*. (2008) reports Uranium and thorium occur (unquantified) in Gombe, Plateau and sokoto states of Nigeria. Meaning apart from its export potentials, Nigeria can actually tap from this energy source for its own energy and diverse other reasons. Geothermal energy (GTE) is another source of energy which needs serious attention in the country. It is energy produced from decay of radioactive minerals found in the earth's core as combined with solar heating of the water at its surface. Ikogosi warm-spring in southern Nigeria is an example. GTE produces about 12 GW of electricity world over. This represents about 0.3% supply of the global energy demand (Eyinla et al., 2016). Its advantages ranges from cost effectiveness, base load generation ability, sustainability and environmentally friendliness. These sources of energy would prove a great resource to be added into the Nigerian energy matrix. But out of all these resources, one stands out as a resource amongst resources. It's one of the fastest growing sector in the world and its importance cannot be overemphasized.

3.1 A Nuclear Option for Nigeria

The initiation of Nigeria's Nuclear Program was initiated by the establishment of the Nigerian Mining Company (NUMCO) in the late 1970s. It would be noted that the original interest was military focused [Lowbeer (2010) Ayoola *et al., (*2017)]. A research by Lowbeer (2010) indicated that the motion was primarily a response to South Africa's acquisition of nuclear weapons and India's test of a nuclear device. In 1978 The Nigerian Uranium Mining cooperation was founded

for self-sufficiency, having the French mining company as partners with the federal government of Nigeria. The Nigerian atomic energy commission (NAEC) was then created with three other training and research centers viz;

I. The center for energy Research and development (CERD) Located at Obafemi Awolowo University, Ife

II. Center for Energy Research and Training (CERT) in Ahmadu Bello Zaria. And;

III. Nuclear Technological center at the Sheda science and technology complex (SHETSCO), Abuja. (Ayoola et al., 2017) In 1995, the Nigerian Nuclear Regulatory Agency (NNRA) was established by the nuclear Safety and Radiation Protection Act. NNRA began operation in 2001 and subsequently implementing safety regulations (Lowbeer, 2010).

Nigeria Currently has no Nuclear power reactor. Its first research reactor was commissioned at ABU in 2004. It is a 31.1KW, Chinese Tank in pool miniature Neutron source Reactor - MNSR (90% enriched) light water cooled and moderated with metallic Beryllium as reflectors (Lowbeer, 2010). However a 2.5 MW multipurpose research Nuclear reactor (NIRR-7) to be stationed in Sheda, Abuja is also in its design phase. (Ayoola et al., 2017)

3.2 Rationale for adopting Nuclear energy in the Nigerian national grid.

3.2.1 Economic Value/Potentials

In 2010, IMF placed Nigeria on the 31st position on the world economies scale with regards purchasing power parity. Thus the frantic effort being done by the government its position among the 1st 20 economies in the world by developing the vision 20:2020 blueprint (Fidelis et al., 2014). This is a call for the country to grow her Real GDP annual growth from the present rate of 2.1% see (Fig 3.1) to about 14% per annum which would translate into a per capita income of circa 8500 USD (current exchange rate). One vital key to such realization is energy. In Africa, SouthAfrica is the only country that has utilized the energy gotten from nuclear deposits with capacity of about 12.7 terawatts in 2011(about 0.5% of the world's total consumption share) (Fidelis et al., 2014) Projections have placed Nigeria's Real GDP growth rate to lie between 1.9%(2019) and

2.2%(2023) (IMF,2018) . When compared with Bangladesh (see Fig 3.3), a country with about 0.167 Billion people (92.3% of Nigeria's population),

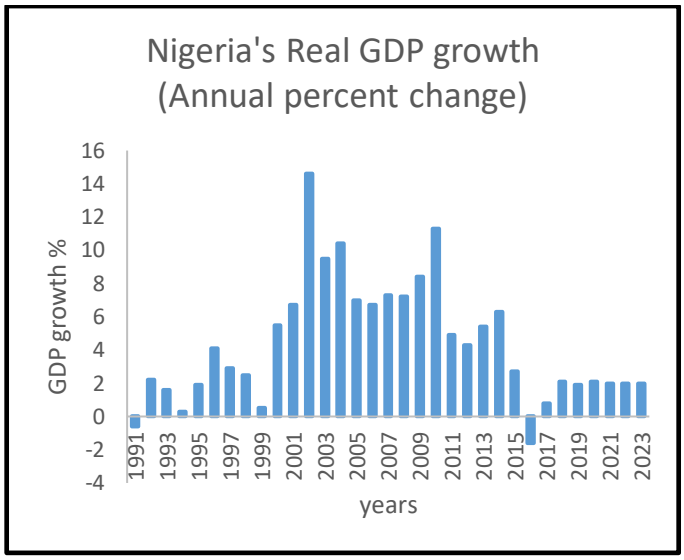

Fig 3.1 GDP growth rate for Nigeria from 1991-2021 as projected (data gotten from (IMF,2018))

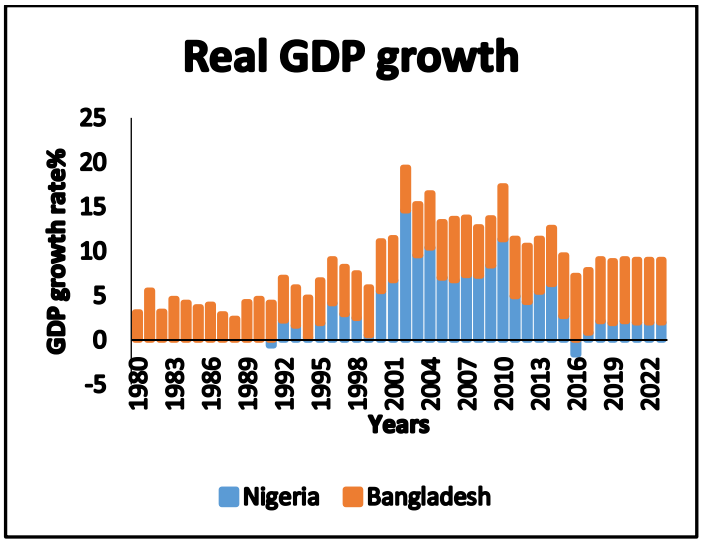

Fig 3.2 GDP growth rate compared for Nigeria and Bangladesh from 1991-2021 as projected (data used gotten from (IMF,2018))

The trend (Fig 3.2) shows a rise and fall with time for Nigeria while that of the compared nation has been increasing even though slowly. The elevation of a country's population is usually greeted

with an increase in demand for more energy. An attachment of importance to this fact is the beginning of self-sufficiency in energy production, utilization and maybe, exportation. An online publication by "why electricity matters" shows Bangladesh is now able to boast of 90% connection of its citizens to the national grid (Why electricity Matters, 2018). Nigeria can borrow a leaf from such a nation whose governmental policies have been translated into favorable growth rate it's their GDP. They have been able to acquire a good mix of various sources into their national grid.

Nuclear power would provide base-load generation at relatively stable prices, avoiding the current price fluctuations of oil products. This would then mean a reduction in local demand for petroleum thereby leading to increase foreign exchange earnings from the oil industry. Nuclear reactor technology is very efficient. Uranium is one of the chief fuel source of nuclear energy and it is possible to extract 10,000 times more energy per unit mass from uranium than from other sources thus making it an immensely large reservoir of energy consisting of a small amount of fuel extracted, processed, stored and transported for each KWh of electricity produced (OECD, 2000). This would then be the needed push for Nigeria to become a world leader in the export of energy and thus more source of income to pilot its affairs. In addition, research on extracting uranium from seawater shows promise of a virtually inexhaustible future supply. These known resources clearly provide for many future generations without competing for limited fossil fuel materials or for the air and land required for waste disposal and deployment of extensive decentralized generating systems American Nuclear Society.

A nuclear powered and effectively managed grid will increase the influx of local/international manufacturers who will need to take advantage of the available power (low cost of production) to produce goods thereby increasing local production, employment and reducing restiveness in the country especially in the less industrialized/developed part of the country.

3.2.2 Environmental Issues and climate change.

Nigeria's energy sector currently dangles at the mercy of the pipeline vandals and pirates/oil bunkering due to the production of electricity from the natural gas produced from the region. Bringing nuclear reactor technology amongst other options would help remove our total dependence on thermal plants. Global warming is an ever pressing danger that calls for concern all over the world. The ways in which energies are supplied largely determine the health and

environmental impacts of the sector. Nuclear reactors under normal operations do not produce environmental pollutants. Nuclear energy creates a new and abundant energy source that would not exist otherwise, extending the world's energy resource base and hence assuring maximum energy security and diversity through its unique attributes (OECD, 2000). Its application can revolutionize our agricultural, health, science and technological sectors reducing the need for personal exoduses on medical tourism, increasing direct investments as well as persons with different health/research needs into the country.

The nuclear electricity generation chain does not release gases or particles that acidify rains or contribute to urban smog or deplete the ozone layer. CO_2 emissions are very negligible. A single large nuclear power plant of 1GWe capacity offsets the emission of about 1.75 Million tonnes of carbon each year if it displaces coal, about 1.2 million tonnes if its displaces oil and 0.7 million tones if it displaces natural gas (OECD, 2000). A nuclear power plant basically contributes significantly to guaranteeing high air quality. Imagine what this would do to the current air pollution problems in cities like Port-Harcourt and Lagos that are densely populated (industrially which affects the air quality). Comparatively speaking, Nuclear energy is more advantageous when compared to the amount of waste each source produces. This is a comparison between the amount of heat produced and the consequent waste for every source of energy. For instance, a single 1000 MW coal-fired plant produces over 300,000 tonnes of ash, 44,000 tons of sulphur dioxides, 22,000 tonnes of Nitrous Oxide and 6 million tonnes of carbon. In contrast, a 1000MW of nuclear power plant produces a mere 3 cubic meters of wastes after reprocessing the spent fuel, 300 tonnes of radioactive wastes and 0.20 tonnes of plutonium. (Mollah *et al*., 2015). There are several concerns associated with the use of nuclear power, one of which is operation safety. Critiques of Nuclear technology never fail to scare people away from it while it seems very few information is given to the public about new safety parameters included in recent safety reactor designs since Three Mile island (TMI), Chernobyl and Fukushima which includes passive safety features and also the globalization of operation experience in the nuclear industry and most recently the generation IV reactor (Ferenc, 2008).

3.2.3 Wastes Recycling potential

Most anti-nuclear scholars are always quick to judge the waste produced by nuclear reactors. The capacity for recycling nuclear fuel is a unique feature that sets it apart from fossil fuels which once

burned are largely dispersed into the environment in gaseous or particulate forms (OECD, 2000). Nuclear spent fuel contains fertile materials which may be converted to fissile plutonium as can be made possible by inherent designs of special reactors. By the conversion of bulk uranium resource to fissile materials in breeder reactors it is possible to multiply the energy produced from a given amount of uranium 60times and more as compared with present reactors using the once-through fuel cycle. Such facts could mean a conversion of our fuel storage facility into a veritable mine of nuclear fuel (OECD, 2000) and the Yucca Mountain repository would basically be enough to contain the minor actinides (which may be transmuted) and the fission products. Long-lasting Reserves Known fuel resources for nuclear power plants can provide about 250 years of consumption using current "once through" commercial reactor technology. The technology exists (though it is not yet significantly deployed), with multipass fuel usage and fast reactors, to utilize even more energy from each fuel sample. Recycling of uranium and plutonium could extend the fuel supply for up to 10,000 years of consumption American Nuclear Society. Recycling is a commercial business as is being carried out by nations like France (world leader in the business), United States (U.S), China, and Japan. For the current time in our phase of nuclear technology development, this may prove to be costlier than the once-through nuclear fuel. However, the next generation reactors (Gen IV) may come with viable ways to curb production of these hazardous wastes.

3.2.4 Nuclear power acceptability and the Human Reliability Program (HRP)

Countries model solutions to its problems by giving due consideration to the peculiar nature of their environment and the way of living of their people. The HRP has been used successfully to solve problems in the United States. A Human Reliability Program (HRP) ensures that personnel who –either via their professional position, privileges or other appointments – have access to materials, devices, data, instrument, or facilities meet the highest standards of reliability including mental wellness in carrying out assigned duties (Dahunsi *et al* 2017). Results of study carried out by Dahunsi *et al* (2017) showed that aberrant behaviors can be detected by a vibrant HRP program. Systems such as this exists and is functional in the United States of America which is also a multi-ethnic society. This would douse the cries from several quarters about the problem of nepotism, favoritism and sectionalism which may have characterized Nigeria's public service systems over the years.

3.3 Risks perceptions and public Fears

A survey carried out by Salawu and Oche (2017) on the acceptability of nuclear electricity generation showed a high support (68% of their sample population) for the introduction of nuclear energy to provide a lasting solution to the country's energy crises. Similar survey was conducted in the U.S in 2008 indicating about 74% acceptance. Also in Bangladesh, similar research records that about 70% of the sampled population favour the nuclear energy (Mollah, 2010). Reactor accidents are not events that occur frequently. There are so far three nuclear accidents that have occurred of a large magnitude. They include the Three Mile Island (TMI), the Chernobyl and the Fukushima accidents. Nuclear reactors are very safe. The building of reactors includes safety measures which ensures that the failsafe protocols are enhanced as soon as there are bad eventualities. The analysis of causes of the three major accidents have led to significant improvements to reactor safety.

It's true that people tend to be more concerned about low probability/high consequence events than about more probable/low consequence events (OECD, 2000). Such as aircraft accidents and road accidents. The growth of the aviation industry in Nigeria has led to a concomitant rise in aviation disasters. A survey by Salawu and Oche (2017) reported a total of 38 air crashes occurred in Nigeria between the year 1960 – 2011 and this gives an average of circa one air crash per year. During this period, a total of 1514 persons were killed in the air crashes giving an average of about 39 deaths per year. Therefore, air transportation is by far safer, as compare to road transport in Nigeria with an average of over 6500 deaths per year but yet by death figure riskier than nuclear Reactors. To meet the ever increasing demand of electrical energy in Bangladesh Saiful and Ziaur (2016) wrote that it had become essential to think about Nuclear power plants (NPP) which has led to an Inter-Governmental Agreement (IGA) signed by Bangladesh and Russia in 2011 to install two units of 1200 MW. These units will be manufactured and installed complying with all the post Fukushima safety features. All nuclear accidents teach manufacturers a vital lesson about safety and hence subsequent models of reactors have safety features installed to address previous errors and providing a safer product.

3.4 Waste storage

There are issues bordering on the waste produced from nuclear reactors which may be hazardous for a very long time. Some wastes such as long lived isotopes and heavy metals are such examples. Technologies like Plutonium, Uranium extraction (PUREX) and Uranium extraction (UREX+) can easily be deployed into conversion of Spent Nuclear Fuel (SNF). PUREX technology has been used in the United States and is currently used in other nations such as France and the U.K. The UREX+ process have the following products;

- Uranium ^{238}U, Which can be reused or disposed as Low level wastes (LLW)
- A mixture of Plutonium/actinide, which can fuel fast/conventional(candu) reactors or could be transmuted
- The Fission products goes for storage in repository consuming little space.
- Other minor actinides which can undergo transmutation to more stable products.

This obviously depicts that innovations in nuclear waste managements would prove to be very useful in the nearest future owing to the fact that nuclear wastes need not be stored but reused especially with cheaper technologies as the time goes by.

3.5 Proliferation and global terrorism

This danger doesn't only stream from the peaceful uses of nuclear energy; renouncing it would not eliminate the already existing risk of nuclear proliferation (OECD, 2000). From the early days of nuclear power development there has been prevalent concern that increased use of nuclear power would lead to the deviation of nuclear materials to surreptitious weapons production. The system of international safeguards implemented by the IAEA, however, has been effective in preventing diversions of nuclear materials from commercial power reactors or reprocessing plants. The effectiveness of the safeguard program is aided by the extreme technical difficulties inherent in converting nuclear material produced in power reactors to weapons-grade material (American Nuclear Society). Nigeria was among the first countries to sign and ratify the 1968 Nuclear Non-Proliferation treaty (NPT) and is therefore committed to using nuclear energy exclusively for peaceful purposes. These and many more treaties are guiding factors to the peaceful use of the technology in the country.

4.0 Generation IV reactors (The Future)

4.1 Generation IV nuclear reactors and anti-proliferation potentials

The degree of safety at a nuclear facility improves more or less continuously with the introduction of new technologies and stricter safety regulations (Matilda, 2013). Research is a continuum. In order to eliminate failures and drawbacks by and of earlier models of reactors, researchers have continuously sought after answers to key problems like nuclear proliferation and weaponisation of plutonium which is one of the products of nuclear reactions. With the aim to resolve some of the difficulties facing today's nuclear power, striving for sustainability, waste minimization and proliferation resistance, a new generation of nuclear energy systems is being pursued: Generation IV Reactors (Matilda, 2013). An integral part of many Gen IV systems is metal-cooled reactors operating with a fast neutron spectrum, or in short, "fast reactors" (FRs), in which no moderator is present to slow down the neutrons. These reactor concepts address central issues for nuclear power, such as safety, sustainability, economy and non-proliferation [Matilda (2013); Grapen *et al.,* 2014]. Advanced fuel recycling are additives developed with these reactors. Deployment of advanced fuel cycles, where the fuel is repeatedly recycled in fast reactors, could significantly extend the long-term availability of nuclear power from hundreds to thousands of years (Matilda, 2013). Matilda (2013) gave some achievable goals of the Generation IV reactors which agrees with that given by (Grapen et al 2014) to include that the generation IV nuclear energy systems will ensure the following;

4.2 Sustainability

1. Provide sustainable energy generation that vis-à-vis clean air objectives, promote durability of systems, and effective fuel utilization for global energy production.
2. Reduce to the barest minimum/manage their nuclear waste and notably reduce the long-term stewardship burden, thereby improving protection for the public health and the environment.

4.3 Economics

1. Have a distinct life-cycle cost advantage comparatively with other energy sources.
2. Have a level of financial risk comparable (positively) to other energy projects.

4.4 Safety and Reliability

1. Excel reliably in safety (Matilda, 2013).
2. Have a very low likelihood and degree of reactor core damage.
3. Demand no need for offsite emergency response.

4.5 Proliferation Resistance and Physical Protection

1. Increase the guarantee that wastes are useless to proliferators and provide increased physical protection against acts of terrorism.

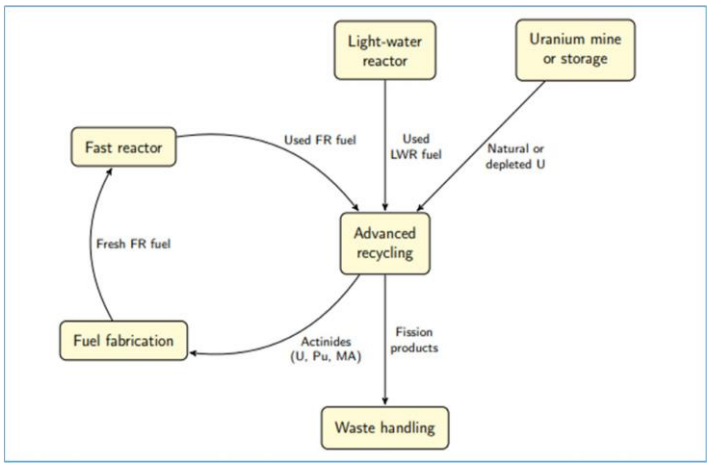

Figure 4.1: Some advanced recycling techniques (source: Matilda, 2013)

The implication of the "once-through" fuel cycle is that uranium is mined, enrichment is done to about 3-5%, and fuel assemblies are made from the enriched material which as the loaded fuel. In the most dominant type of reactors of today; LWRs, the fuel is irradiated in the reactor for about five years. After that, the fissile content has decreased due to fission of U and Pu, and the fuel is treated as waste and sent to storage before being sent to a perpetual disposal in e.g. a geological storehouse (Matilda, 2013). However, as mentioned above, there is still a significant amount of extractable energy in terms of heavy nuclei in the discarded fuel assembly. Some countries have chosen to recycle the used fuel in order to recover U and Pu for repeated use in light-water reactors (LWRs). In the separation process, Pu and U are separated from the fission products using a solvent extraction technique called Purex. The new fuel, which encompasses the recycled material, is called Mixed Oxide fuel (MOX). With FRs technologies, a new fuel cycle option emerges; the advanced closed fuel cycle (see fig 4.1). One advantage of fast reactors is their ability to burn all

long-lived actinides, such as Pu (a target for proliferators) from used nuclear fuel. The long-lived minor actinides can also be incinerated in fast reactors, which is an advantage from a waste management perspective. Thus, by launching fast reactors, one may adopt a closed fuel cycle, where actinides are separated and reused several times (see figure 4.1 above). This option requires less uranium mining and gives rise to smaller amounts of long-lived waste than the classical closed fuel cycle. In addition, the required repository space can be minimized. The resulting waste will also be less radiotoxic after the removal of actinides and it cannot be used for nuclear weapons production. Several advanced recycling techniques are available (UREX+) and under development, one of which is called Ganex (Group actinide extraction). See (Matilda, 2013). Ganex has the potential to enhance proliferation resistance (Matilda, 2013). Lastly as a seldom discussed advantage, breeder reactors (BRs) producing their own plutonium during operation may eliminate the need for enriched-uranium based fuels and hence the need for uranium enrichment facilities (Grapen et al 2014).

5.0 Conclusion

The need for energy to foster national/economic development cannot be overemphasized. The present production and distribution of electricity in Nigeria has less significance to the manufacturing and production sectors due to its erratic supply and in most cases total scarcity which raises the cost of production, and discourages investments. Two giant energy sources provide enough baseload to power any country; coal and nuclear. Coal has a large disadvantage perKWh because of the danger is portends environmentally. This leaves us to the nuclear option. There is an urgent need for the inclusion of nuclear electricity production into our grid which has been proven to be safe, environmentally friendly, continuous and base-load efficient. Gen IV reactors have given mankind the hope of having safer reactors which eliminates the global threat to weaponization of weapon-grade Uranium. Every nation has a peculiar problem when it comes to technological acceptance and adoption, thus, Nigeria is not an exception. The Establishment of a well-developed HRP can mitigate any unwanted risk involving the implementation, general peaceful application and eventual operation of the Nigerian nuclear program hence solving the precarious situation of nepotistic tendencies of the country's public sphere. This is not to shove aside the potential brought about by other renewables such as solar, GTEs, wind, Biomass and others. A good and healthy mix of these together with a base load efficient source is what every

developing nation like Nigeria needs. The Nigerian government can start by first investing immensely in science and technology especially in the aspects of training and development of our institutions of research. Developing a huge man power resource which are indigenous is an immense potential for any industrial-revolution-ready nation. This would include bringing specialists in various technologies to train and/or sending our nationals to learn these technologies such that the nation not need spend so much in the management and building of similar power technologies in the future. Departments of Nuclear science/ Renewable energies and Engineering can be created in special universities across the country aside other departments and institutes of research where serious funding would go into ensuring developing skilled manpower for Nigeria. Similarly, the old existing power stations need to be revitalized. The issue of infrastructural and managerial negligence is crippling the power sector. This can be cushioned by conscious and wholesome efforts at provision of funds/resources while maintaining a strict supervision for total compliance to the power blueprint. GTE also can be looked into as a viable source which has been seen in various research as a huge energy resource aside solar which also lays untapped(circa-few investment), wind and other renewable sources.

6.0 References

Abdulhameed Salawu and Oche O. C. (2017); Risks Comparison between Nuclear Generated Electricity and Other Electricity Generation Sources in Nigeria; FUOYE Journal of Engineering and Technology, Volume 3, Issue 1, March 2018 pp 122-126.

Adegbemi B. O., Adegbemi O. O. Olalekan A. J. S. Babatunde O. O. (2013); Nigeria Energy consumption and Nigerian economic growth: An empirical analysis; European Scientific Journal February 2013 edition vol.9, No.4 ISSN: 1857 – 7881 (Print) e - ISSN 1857- 7431 pp (25-40)

American Nuclear Society; Nuclear Power: A Sustainable Source of Energy; www.ans.org

Anyaegbunam F.N.C. (2015); Power Generation from a Renewable Energy Source - Speed Breaker Generators; International Journal of Electrical & Computer Sciences IJECS-IJENS Vol:15 No:05;

Arinze Okoye(2014); The Nigerian electric power sector; https://www.researchgate.net/publication/264084026

Avisory Team/Power Africa (2015); Nigeria Power Baseline Report; www.nesistats.org,

Ayoola T. B. Ahmed S. Samuel S. Isa K. (2017); Sustainable energy development in Nigeria: Wind, hydropower, geothermal and nuclear (Vol. 1); Renewable and Sustainable Energy Reviews 74 (2017)474–490;

Chidi E. Akujor a,b , Oluwasogo A. Ogungbenro , Gregory A. Alozie and Okey K. Nwofor (2008); A Nuclear Energy Option for Nigeria

Eyinla D. S., Oladunjoye M. A., Ogunribido T.H.T. and Odundun O. A. (2016) ;An Overview of Geothermal Energy Resources in Nigeria; Environtropica, March 2016, Vols. 12 & 13, pp61-71

Famous O. Igbinovia (2014); An overview of renewable energy potentials in Nigeria: Prospects, challenges and the way forward; https://www.researchgate.net/publication/319450558

Ferenc L. Toth (2008); Prospects for nuclear power in the 21st century: a world tour; Int. J. Global Energy Issues, Vol. 30, Nos. 1/2/3/4, 2008

Fidelis I. Abam Bethrand N. Nwankwojike Olayinka S. Ohunakin Sunday A. Ojomu (2014); Energy resource structure and on-going sustainable development policy in Nigeria: a review; Intl Journal of Energy, Environment Engineering (2014) 5:102

IMF,(2018)www.imf.org/external/datamapper/NGDPRPCH@WEO/OEMDC/ADVEC/WEOWORLD#list 01/08/2018 0400GMT+1

Ismaila Y. P. Olusola O. B. (2015); Renewable Energy: Comparison of Nuclear Energy and Solar Energy Utilization Feasibility in Northern Nigeria; Asian Transactions on Engineering (ATE ISSN: 2221-4267) Volume 05 Issue 02; pp 19-23

Matilda Åberg Lindell (2013); Proliferation resistances of Generation IV recycling facilities for nuclear fuel; A Licentiate thesis, Uppsala University, Department of Physics and Astronomy.

Mollah A. S., Sabiha Sattar, M. A. Hossain, A.Z.M. Salahuddin, H. AR-Rashid (2015); Prospects of Nuclear Energy for Sustainable Energy Development in Bangladesh International Journal of Nuclear Energy Science and Engineering (IJNESE) Volume 5, 2015; pp 28-39

Mollah A.S., (2010); An Overview for Achieving Public Understanding and Acceptance of Nuclear Energy: Bangladesh Perspective, Proc. of ICONE18, 2010.

Nathaniel Lowbeer-Lewis (2010); Nigeria and Nuclear Energy: Plans and Prospects; Nuclear Energy Futures Pap e r No. 11. The Centre for International Governance Innovation (CIGI)

OECD (Organisation for Economic Co-operation and Development), (2000); Nuclear Energy in a Sustainable Development Perspective; OECD PUBLICATIONS (2), rue André-Pascal, 75775 PARIS CEDEX 16

Saiful I., Md. Ziaur R. K. (2016); A review of energy sector of Bangladesh; Energy Procedia 110 (2017) 611 – 618; pp 611-618

Sambo A. S., Bala E. J., ZARMA I. H., Dawuda A. A. (2012); Implementation of energy plans: A solution to Nigeria's Energy Crisis; A paper presented at NAEE/IAEE International Conference https://www.researchgate.net/publication/321342659

Sophie Grapen, Staffan Jacobsson Svärd, Carl Hellesen, Peter Jansson, Matilda Åberg Lindell (2014); New perspectives on nuclear power—Generation IV nuclear energy systems to strengthen nuclear nonproliferation and support nuclear disarmament; Energy Policy 73 (2014) 815–819

Stephen Dahunsi, John D. Auxier, Joseph R. Stainback, IV, Howard L. Hall (2017); Aligning Technology, Policy, and Culture to Enhance Nuclear Security: A Comparative Analysis of Nigeria and the U.S. ; International Journal of Nuclear Security, Vol. 3, No. 1, 2017 pp 1-15

Sunnewsonline (2018) http://sunnewsonline.com/gas-shortages-dangote-cement-resorts-to-use-of-coal-to-power-factory Retrieved 22/10/2018 0216hours GMT+1

Why Electricity matters. (2018) https://whyelectricitymatters.com/2018/08/08/bangladesh-leading-example-electricity-access-can-powerdevelopment. Accessed 8/9/2018, 0557GMT+1

Yehuwdah E., Chad-Umoren, Bamidele F. Ebiwonjumi (2013). Nigeria's Nuclear Power Generation Project. Current State and Future Prospects. Journal of Energy Technologies and Policy. ISSN 22243232, Vol.3, No.7

Gamma-rays shielding parameters of two new Ti-based bulk metallic glasses

***Olarinoye, I.O[1]., Oche, C.O[1].**

[1]Department of Physics, Federal University of Technology, Minna, Nigeria

Leke.olarinoye@futminna.edu.ng

Ochegabasphysics@gmail.com

****correspondence Author***

Abstract

Two new low density Ti-based bulk metallic glasses (BMG) ($Ti_{32.8}Zr_{30.2}Ni_{5.3}Cu_9Be_{22.7}$ and $Ti_{31.9}Zr_{33.4}Fe_4Cu_{8.7}Be_{22}$) were investigated for their photon shielding capacities. The mass attenuation coefficients, half value layers, effective atomic numbers and exposure buildup factors of the two BMG were calculated for photon energies between 15 keV and 15MeV. The XCOM and auto-Z_{eff} software were used for the computation of the mass attenuation coefficients and effective atomic numbers respectively while the geometric progression procedure was used for calculating the exposure buildup factors of the BMG. The calculated photon shielding parameters for the BMG were compared with those of lead (Pb) and heavy concrete and also analyzed according to their elemental compositions. The results showed that though Pb has better photon shielding capacity, Ti-BMG attenuate photons better than heavy concrete. It is concluded that Ti based BMG with high strength and low density have potential applications in high radiation environments particularly in nuclear engineering for source and structural shielding.

Keywords: Bulk metallic glasses; photons; structural shielding; exposure buildup factors

Introduction

The quest for reducing energy consumption and operational cost has encouraged material scientist and engineers to investigate low density structural materials. Consequently, low density materials with superior mechanical and physical properties [1-5] have always been a subject of active research in the material science community for some time now. Among such novel materials which have attracted much interest are Bulk Metallic Glasses (BMG). These are metallic alloys having amorphous atomic arrangement obtained by rapid cooling from a high temperature [5]. The amorphous nature of the BMG gives them high yield strength in excess of 2 Giga Pascal (GPa) [6-9]. Furthermore, BMG exhibit other interesting properties such as low stiffness, high hardness, low surface roughness, low shrinkage during casting and high corrosion resistance [1-4, 10]. These properties have attracted BMG based on different metals to potential applications in biomedical, automobile, defense and aerospace industries [11-14]. Unfortunately, the deployment of many BMG for these applications have been hindered by their low Glass Forming Ability (GFA). Consequently, the improvement of GFA of metallic alloys has led to the design of BMG alloy compositions based on empirical rules [5, 15-19].

For structural engineering purpose, Ti-based BMG are currently the most suitable low density BMG [5, 10]. This is due to their low densities (4-7 gcm-3); high strength and toughness; fabrication ease due to low temperature requirement; high mechanical properties similar to crystalline Ti and low cost

of production. To this end, research in recent times has improved the GFA of Ti-based BMG [5]. Recently, two Ti-based BMG - $Ti_{32.8}Zr_{30.2}Ni_{5.3}Cu_9Be_{22.7}$ (T1) and $Ti_{31.9}Zr_{33.4}Fe_4Cu_{8.7}Be_{22}$ (T2) [16,19] with high compressive fracture strength of about 1800 MPa and GFA greater than 50 was reported. These materials were adjudged to be good materials in structural engineering applications. The potential use of these materials for structural engineering applications also suggest that they may be good material for structural radiation shield.

Traditionally, structural radiation shielding materials include high density concrete and lead (Pb). The poisonous nature of Pb has limited its application for this purpose, concrete on the other hand, surfers from cracking and unstable properties due to temperature changes which leads to changes in its hydrogen content [20]. Consequently, a tough material with lower density compared to Pb such as Ti-based BMG would be a potentially good alternative for radiation shielding purpose. Furthermore, the applications of Ti-based BMG may extend to environments where it could be exposed to radiation such as space, accordingly, the study of radiation interaction processes of the material is essential. In addition, the study of radiation shielding capacity of Ti-based BMG is very scarce in the literature to the best of our knowledge. The aim of this research is thus to evaluate the photon shielding parameters of $Ti_{32.8}Zr_{30.2}Ni_{5.3}Cu_9Be_{22.7}$ (T1) and $Ti_{31.9}Zr_{33.4}Fe_4Cu_{8.7}Be_{22}$ (T2) with the view to determine their suitability for structural shielding purpose. The mass attenuation coefficient, half value layer, effective atomic number (Z_{eff}), exposure buildup factor for photon energies in the range of 15 keV to 10 MeV were calculated and also compared to those of Pb and heavy concrete.

Calculation of Shielding Parameters

Mass Attenuation Coefficient

When a beam of monochromatic photons is incident on a thin absorbing medium of mass thickness *t*, the intensity is reduced on emerging from the medium according to the equation:

$$I = I_o e^{-\mu_m t} \qquad (1)$$

where I, I_o and μ_m are respectively the transmitted (attenuated), incident photon densities and the mass attenuation coefficient of the material medium. The μ_m measures the mean number of photo-interactions between the incident photons and the absorbing medium at a given mass thickness. The μ_m can be used to compare the photon shielding capacity of different material at specific photon energy.

It is experimentally determined using equation 1 or theoretically through the use of computer codes such as MCNP5 and XCOM [21, 22]. For composite material, the $\mu_m$is estimated using the mixture rule from the equation [23]:

$$\mu_m^c = \sum_i^n w_i \mu_m^i \quad (2)$$

where μ_m^c, μ_m^i and w_i are the mass attenuation coefficients of the composite material, and the i^{th} component in the material and the weight fraction of the i^{th} component of the composite material respectively.

Half Value Layer (HVL)

The HVL is the thickness of an absorbing material required to reduce the density of incident photon of a specific energy by 50%. The HVL is calculated from the mass attenuation coefficient according to the equation:

$$HVL = {}^{0.693}/_{\rho\mu_m} \quad (3)$$

The HVL can also be used as a quantity to describe the relative shielding capacity of different shielding materials.

Effective Atomic Number (Z_{eff})

Many of the photon interaction mode depends on the atomic number (Z) of the interacting medium. Though, many of the materials used in many photon applications are composite material containing more than one pure elements, the effective atomic number is a convenient parameter used similarly to represents its atomic number as if it were a pure element. Unlike Z, Z_{eff} is not a constant over all photon energies but varies depending on the comparative importance of photon interaction processes. The Z_{eff} is an important parameter for radiation dose measurement and shielding calculations [24]. Effective atomic number cam be estimated using the equation [25]:

$$Z_{eff} = \frac{\sum_i f_i A_i (\mu_m)_i}{\sum_j f_j \frac{A_j}{Z_j} (\mu_m)_j} \quad (4)$$

Where f_i, A_i and Z_i are the fractional abundance, atomic weight and atomic number of element i.

Exposure Buildup Factor

For many practical applications, radiation shields are not thin and photons may not be monochromatic and collimated, consequently, equation 1 is always modified to account for multiple photon scattering and buildup in the thick absorber. The buildup factor (*B*) accounts for the ratio of broad beam to that of collimated beam and directly influences radiation absorption for absorbed dose or shielding calculations. Data for photon buildup factors for 23 elements (Be, B, C, N, O, Na, Mg, Al, Si, P, S, Ar, K, Ca, Fe, Cu, Mo, Sn, La, Gd, W, Pb and U), one compound (water) and two mixtures (air and ordinary concrete) for standard photon energies in the range 15 keV -15 MeV and for penetration depth up to 40 mean free path (mfp) by the American Nuclear Society [26]. This data is usually used as a standard for estimating buildup factors for undefined substances via Geometric Progression (GP) fitting method [27-30]. Generally, the evaluation of buildup factors using the G.P method requires three distinct procedures:

Calculation of equivalent atomic number, Z_{eq}

To do this for any material, the Compton partial interaction coefficient (μ_c) and mass attenuation coefficients (μ_m) is calculated for the photon energy range 0.015 MeV– 15 MeV using the XCOM software. The ratio $R = {}^{\mu_C}/_{\mu_m}$ of each material is then calculated and matched at the standard energies to the corresponding ratios of elements up to the heaviest element. If the value of the radio matches any of the elements', then the atomic number of that element becomes the equivalent atomic number of the material. However, if the value of *R* obtained for the considered material does not match that of any element but rather falls between the ratios for two successive elements then, the Z_{eq} of such material is interpolated using the expression [27-30]:

$$Z_{eq} = \frac{Z_1(\log R_2 - \log R) + Z_2(\log R - \log R_1)}{\log R_2 - \log R_1} \qquad (5)$$

Here, R_1 and R_2 are the ratios (${}^{\mu_C}/_{\mu_m}$) of the two successive elements of atomic numbers Z_1 and Z_2 respectively within which *R* falls at each energy.

Evaluation of GP fitting parameters

Five (5) fitting parameters are required for the evaluation of photon buildup factors by the GP fitting method [27, 28]. These parameters (*b*, *c*, *a*, X_k, and *d*) depend on Z_{eq} and photon energy. The GP fitting coefficients of the material is also interpolated using the logarithmic interpolation formula:

$$P = \frac{P_1(\log Z_2 - \log Z_{eq}) + P_2(\log Z_{eq} - \log Z_1)}{\log Z_2 - \log Z_1} \quad (6)$$

Where P_1 and P_2 are the G-P fitting parameters obtained from ANS data base corresponding to the atomic numbers Z_1 and Z_2 respectively.

Estimation of Exposure buildup factor

The exposure buildup factors ($EBF(E,x)$) for a given material is then estimated from the fitting parameters for a given incident energy (E) in the spectrum (0.015 MeV -15 MeV) for different penetration depth (x) up to 40 mfp by the equations [27, 28]:

$$EBF(E,x) = 1 + \frac{(b-1)(K^x - 1)}{K-1}, \quad \text{for } K \neq 1 \quad (7)$$

$$EBF(E,x) = 1 + (b-1)x, \quad \text{for } K = 1 \quad (8)$$

$$K(E,x) = cx^a + d\frac{\tanh\left(x/X_\kappa - 2\right) - \tanh(-2)}{1 - \tanh(-2)} \quad \text{for } x \leq 40\ mfp \quad (9)$$

Results and Discussion

The mass attenuation coefficient (μ_m) of T1, T2, lead (Pb) and that of heavy concrete (StMg) obtained theoretically from the XCOM code are presented in figure 1. The chemical composition (by weight %) and density of the heavy concrete were as follows: H= 0.51; O= 15.70; Mg= 0.58; Al= 0.66; Si= 2.68; P= 0.08; S= 0.06; Ca= 3.95; Mn= 0.07; Fe= 75.73 and 5.11 g/cm^3 respectively [31] . From figure 1, the $\mu_m$of the four materials were high for low photon energies and gradually decreased as the energy increased. This trend is due to the fact that high energetic photons are more penetrating and consequently, μ_m are lower in this region for all materials. The density of a composite material plays a vital role in its ability to absorb photons at low energy. This is so because the interaction processes dominant for low energy are dependent on atomic number and density of such material [31-33]. Consequently, the relative μ_m of the four materials for energies below 0.1 MeV compares directly with the values of their density. There was no much difference between the μ_m of the two Ti-based BMG within this energy range due to the almost equal density of 5.56 g/cm^3 and 5.57 g/cm^3 respectively. Beyond 0.10 MeV, it appears the density had little or no effect on the mass attenuation coefficients of the four materials. This could be attributed to predominance of pair production effect in this energy region beyond 0.1 MeV which is independent of material density. Although the μ_m of the two BMG

were less than that of Pb for the energy spectrum considered, still the Ti-based BMG are better shielding material Compared to heavy concrete.

Similarly, the HVL of Pb is lowest compare to T1, T2 and StMg concrete, however the thickness of of Ti-based BMG required for the reduction of photons of energy lower than 15 MeV is smaller than that required for heavy concrete (figure 2). Equation 3 explains the trend observed in figure 2 as HVL is inversely related to both μ_m and density.

The Z_{eff} of the Ti- BMG were evaluated using Auto-Z_{eff} software [34] and the results are depicted in table 1. From the results, it is clear that the Z_{eff} was not constant across the energy spectrum but vary similarly with energy for the two BMG. The Z_{eff}values was also noticed to lie between the minimum and maximum atomic numbers of the constituents elements (i.e. 4-40). The maximum Z_{eff} was observed at 40 keV with values of 23.17 and 23.50 respectively for T1 and T2 respectively. While the minimum values of 12.10 and 12.35 was observed at photon energy of 1.5 MeV for T2 and T2 respectively. The Z_{eff} values generally increased from 15 keV to 50 keV , thereafter it decreased steadily up to 1.5 MeV before it start increasing again. The changes of the effective atomic number with energy could be explained based on the partial photon interaction coefficients. For the energy spectrum considered, only the photoelectric effect, Compton scattering and the pair production processes are the major partial interaction modes of importance. The photoelectric effect interaction coefficient is dependent on the fifth power of the effective atomic number, while the Compton and the pair production interaction coefficients are directly proportional to Z_{eff} and the square of Z_{eff} respectively [23, 29, 35]. Consequently, the maximum values recorded at low energy region, could be attributed to the dominance of the photoelectric effect in this region. Conversely, the minimum values of Z_{eff} at 1.5 MeV could be as a result of the dominance of the Compton interaction process which has the least dependence on the effective atomic number of the material. At all energies, the Z_{eff} values of T2 were slightly greater than those of T1. This is attributed to the higher concentration of high atomic number Zr atoms in T2 (33.4) compare to T1 (32.8). This also explains why the mass attenuation of T2 was slightly greater than of T1.

The equivalent atomic number and G.P fitting parameters of T1 and T2 calculated using equations 5 and 6 are given in table 1. The variation of the exposure buildup factors of T1 and T2 with photon energy and depth up to 40 mfp are shown in figures 3 and 4. The variations are similar with respect to energy and depth. It is observed from the figures that the *EBF* values for T1 and T2 are low at lower and higher photon energies but maximum for intermediate energies. This is as a result the partial photoelectric and pair production processes which dominates at the lower and higher regions of the energy spectrum considered respectively. Both processes remove photon completely from photon thus resulting low photon density (buildup) after interaction. On the other hand, in the intermediate energy region, the Compton (incoherent) scattering dominates the photon interaction mode. Consequently, multiple photon scattering takes place and photon of lower energies are produced and hence high buildup of photons are recorded in this region [23, 35]. The EBF of T1 and T2 are almost equal at all energies and depth. This could be attributed to their similar elemental composition and mass

attenuation coefficients. A comparison of the EBF of T1, T2, StMg concrete and Pb at selected energies of 150 keV and 1.5 MeV as a function of depth is presented in figures 5 and 6. The figures showed an inverse relationship between mass attenuation coefficient and buildup factor. Consequently, the EBF of Pb is the least implying better photon shielding capacity while the EBF of heavy concrete was higher than the values of the BMG. Furthermore, at lower energy (0.15MeV), and for depth greater than 30 mfp, the Ti based BMG had the least EBF and thus are better photon shield compare to Pb and heavy concrete at this thickness.

Conclusion

The mass attenuation coefficients, half value layer, effective atomic number and exposure buildup factors of two new Ti-based bulk metallic glasses ($Ti_{32.8}Zr_{30.2}Ni_{5.3}Cu_9Be_{22.7}$ and $Ti_{31.9}Zr_{33.4}Fe_4Cu_{8.7}Be_{22}$) were calculated for photon energy in the range of 15 keV to 15 MeV and compared to those of lead and heavy concrete- two traditional shielding materials. The results showed that the photon shielding capacities of the two Ti- based BMG was better than that of heavy concrete but inferior to that of Pb. The differences in the photon shielding capacity of the materials is attributed to the differences in their elemental composition and physical density. The results showed that $Ti_{32.8}Zr_{30.2}Ni_{5.3}Cu_9Be_{22.7}$ and $Ti_{31.9}Zr_{33.4}Fe_4Cu_{8.7}Be_{22}$ are superior photon absorbers compared to heavy concrete. Consequently, it can be concluded that both Ti-based BMG with high fracture strength and low density can be used for structural shielding purpose, protection of sealed nuclear sources and other applications in high radiation environment such as space and nuclear facilities.

References

1. S. Chen, J. Tu, Q. Hu, X. Xiong, J. Wu, J. Zou, X. Zeng, Corrosion resistance and in vitro bioactivity of Si-containing coating prepared on a biodegradable Mg-Zn-Ca-bulk metallic glass by micro-arc oxidation, J. Non-Cryst. Solids 456 (2017) 125–131.
2. A. Inoue, A. Takeuchi, Recent development and application products of bulk glassy alloys, Acta Mater. 59 (2011) 2243–2267.
3. H. Li, S. Pang, Y. Liu, L. Sun, P.K. Liaw, T. Zhang, Biodegradable Mg–Zn–Ca–Sr bulk metallic glasses with enhanced corrosion performance for biomedical applications, Mater. Des. 67 (2015) 9–19., 986.
4. D. Wang, Y. Li, B.B. Sun, M.L. Sui, K. Lu, E. Ma, Bulk metallic glass formation in the binary Cu–Zr system, Appl. Phys. Lett. 84 (2004) 4029–4031.
5. Jian-Zhong Jiang, Douglas Hofmann, David John Jarvis and Hans-J. Fecht. (2014). Low-density high-strength bulk metallic glasses and their composites: a review. *Advanced Engineering Materials*, DOI:10.1002/adem.201400252.
6. C. A. Schuh, T. C. Hufnagel, U. Ramamurty, Acta Mater. 2007, 55, 4067.
7. M. F. Ashby, A. L. Greer, Scr. Mater. 2006, 54, 321.

8. L. Y. Chen, Z. D. Fu, G. Q. Zhang, X. P. Hao, Q. K. Jiang, X. D. Wang, Q. P. Cao, H. Franz, Y. G. Liu, H. S. Xie, S. L. Zhang, B. Y. Wang, Y. W. Zeng, J. Z. Jiang, Phys. Rev. Lett. 2008, 100, 075501.

9. L. Y. Chen, H. T. Hu, G. Q. Zhang, J. Z. Jiang, J. Alloys Compd. 2007, 443, 109.

10. S. Lin, D. Liu, Z. Zhu, D. Li, H. Fu, Y. Zhuang, H. Zhang, H. Li, A. Wang, H. Zhang, New Ti-based bulk metallic glasses with exceptional glass forming ability. *Journal of Non-Crystalline Solids, https://doi.org/10.1016/j.jnoncrysol.2018.06.038*

11. W.H., Wang, C. Dang, C.H. Shek, Mater. Sci. Eng. R.44, 45 (2004).
12. C. Suryyanarayana, A. Inoeu, Bulk Metallic Glasses RC, Press, (2010).
13. L. Huang, C. Pu, R.K. Fisher, D.J. Mountain, Y. Gao, P.K., Liaw, W., Zhang, W. He. A Zr-based bulk metallic glass for future stent applications: Materials properties, finite element modelling and in vitro human vascular cell response. Acta Biomater. 2015, 25, 356-368.
14. H., Li, Y. Zheng. Recent advances in bulk metallic glasses for biomedical applications. Acta Biomater, 36, (2016) 1-20.
15. P. Gong, K.F. Yao, X. Wang, Y. Shao, A new centimeter-sized Ti-based quaternary bulk metallic glass with good mechanical properties, *Adv. Eng. Mater*. 15 (2013) 691–696.
16. K.F. Xie, K.F. Yao, T.Y. Huang, A Ti-based bulk glassy alloy with high strength and good glass forming ability, *Intermetallics* 18 (2010) 1837–1841.
17. L. Zhang, Z.W. Zhu, A.M. Wang, H. Li, H.M. Fu, H.W. Zhang, H.F. Zhang, Z.Q. Hu, A $Ti_{36.2}Zr_{30.3}Cu_{8.3}Fe_4Be_{21.2}$ bulk metallic glass with exceptional glass forming ability and remarkable compressive plasticity, J. Alloys Compd. 562 (2013) 205–210.
18. L. Zhang, M.Q. Tang, Z.W. Zhu, H.M. Fu, H.W. Zhang, A.M. Wang, H. Li, H.F. Zhang, Z.Q. Hu, Compressive plastic metallic glasses with exceptional glass forming ability in the Ti–Zr–Cu–Fe–Be alloy system, J. Alloys Compd. 638 (2015) 349–355.
19. M.Q. Tang, H.F. Zhang, Z.W. Zhu, H.M. Fu, A.M. Wang, H. Li, Z.Q. Hu, TiZr-base bulk metallic glass with over 50 mm in diameter, J. Mater. Sci. Technol 26 (2010) 481–486.
20. V. P. Singh, Huseyin O. Tekin, N.M. Badiger1, T. Manici, E.E. Altunsoy. Effect of Heat Treatment on Radiation Shielding Properties of Concretes, *Journal of Radiation Protection and Research* (2018) 43(1):20-28 https://doi.org/10.14407/jrpr.2018.43.1.20
21. RSICC Computer Code Collection (2008). MCNP- A General Monte Carlo N-particle Transport Code, Version 5;
22. M.J. Berger, J.H. Hubbel, XCOM: Photon Cross section Database, Web Version 1.2 available at http://physics.nist.gov/xcom. National Institute of Standards and Technology, Gaithersburg, M.D 208899, USA, 1987, p. 99, Originally published as NBSIR 87-3597 "XCOM:Photon Cross Sections on Personal Computer.
23. James E.M., Physics for Radiation Protection: A Handbook.Copyright WILEY- VCH Verlag GmbH and Co. KGaA, Weinheim, 822, (2006)
24. Jackson, D.F., Hawks. D. J. (1981). X-rays attenuation coefficients of elements and mixtures, Phys. Rep. 70, 169-233).
25. El-Mallawny, R., Sayyed, M.I., Dong, M.D. (2017). Comparative Shielding Properties of Some Tellurite Glasses. Journal of Non-Crystalline Solids (2017), http://dx.doi.org/10.1016/j.jnoncrysol.2017.08.011.

26. ANSI/ANS-6.4.3. (1991). Gamma-ray attenuation coefficient and buildup factors for engineering materials. American Nuclear Society, La Grange Park. IL.
27. Harima,Y., Sakamoto, Y., Tanaka, S., Kawai, M. (1986). Validity of the geometric progression formula in approximating gamma ray buildup factors. *Nucl. Sci. Eng*. 94, 24-35.
28. Harima, Y. (1983). A historical review and current status of buildup factor calculations and applications. *Radiation Physics and Chemistry*, 41, 631-672.
29. Olarinoye, I.O. (2017). Photon buildup factors for tissues and phantom Materials for penetration depth up to 100 mfp. *Journal of Nuclear Research and Development*, 13, pp. 57-67.
30. Manohara, S.R., Hanagodimath, S.M., Gerward, L., 2010. Energy absorption buildup factors for thermoluminescent dosimetric materials and their tissue equivalent. *Radiation Physics and Chemistry*, 79, 575-582.
31. V. P. Singh and N. M. Badiger. Investigation on Radiation Shielding Parameters of Nuclear Technology & Radiation Protection (2014), 29 (2), 149-156.
32. M.I. Sayyed, Investigation of gamma ray and fast neutron shielding properties of tellurite glasses with different oxide oxide compositions, Can. J. Phys. 94 (2016) 1133-1137.
33. M.I. Sayyed, Investigation of shielding parameters of smart polymers, *Chin. J. Phys*. 54, (2017) 408-415Taylor, M.L., Smith, R.I., Dossing, F., Franich, R.D. Robust Calculation of effective atomic numbers: the auto-Z_{eff} software. Medical Physics, 39, 1769-1778.
34. Cevik U., Damla N. andCelik A. Effective atomic numbers and electron densities for Cdse and Cdte semiconductors, *Radiat. Meas.*, (2008) 43 1437-1442. Figure1. Mass attenuation coefficients of T1, T2, Pb and StMg

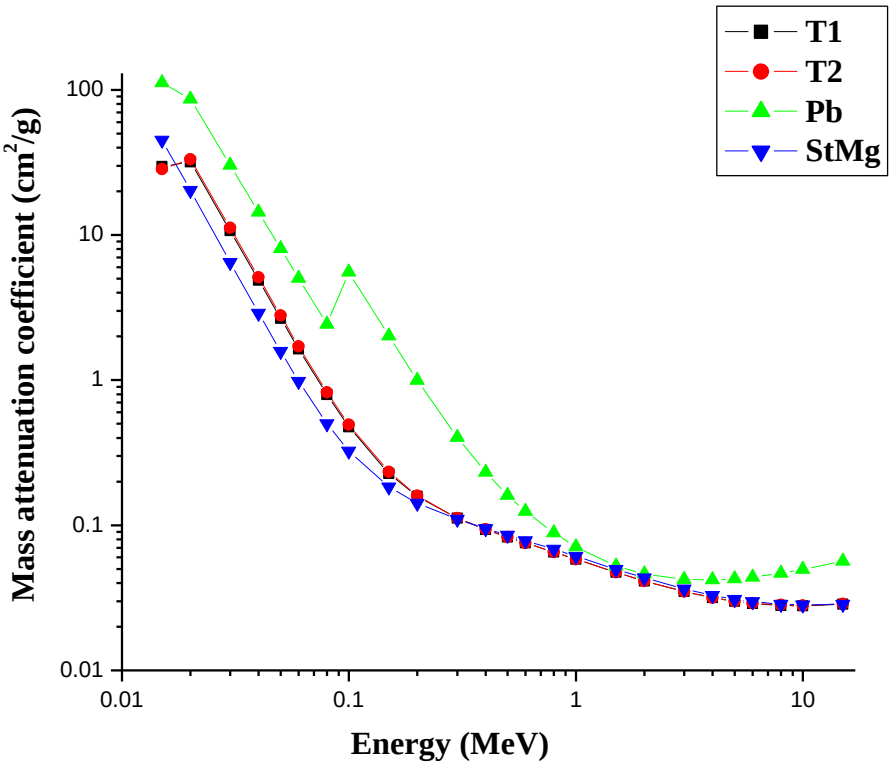
T1
T2
Pb
StMg
Mass attenuation coefficient (cm²/g)
Energy (MeV)
100
10
1
0.1
0.01
0.01
0.1
1
10

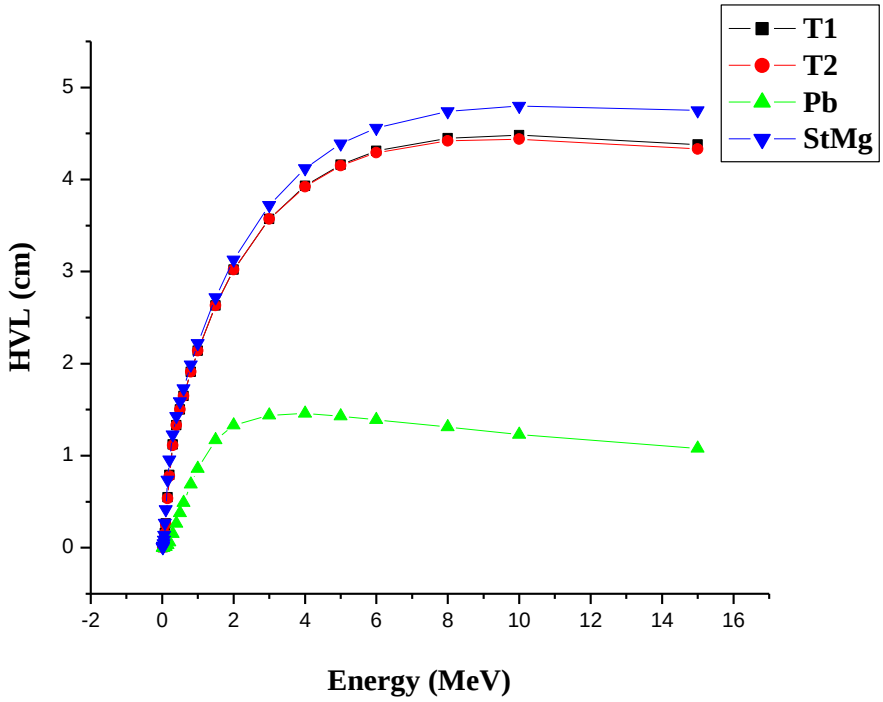

Figure 2. Half Value Layer (HVL) of T1, T2, Pb and StMg as function of photon energy

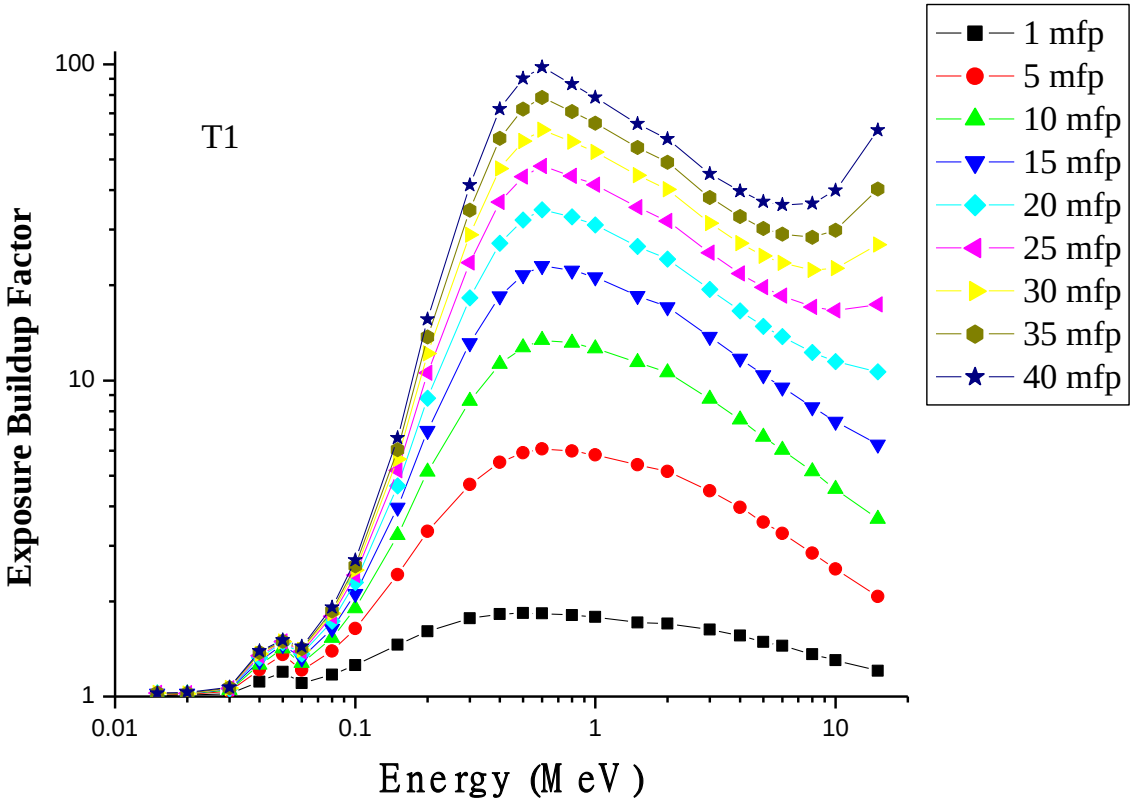

Figure3. Exposure buildup factor of T1 as a function of energy at different depths (mfp)

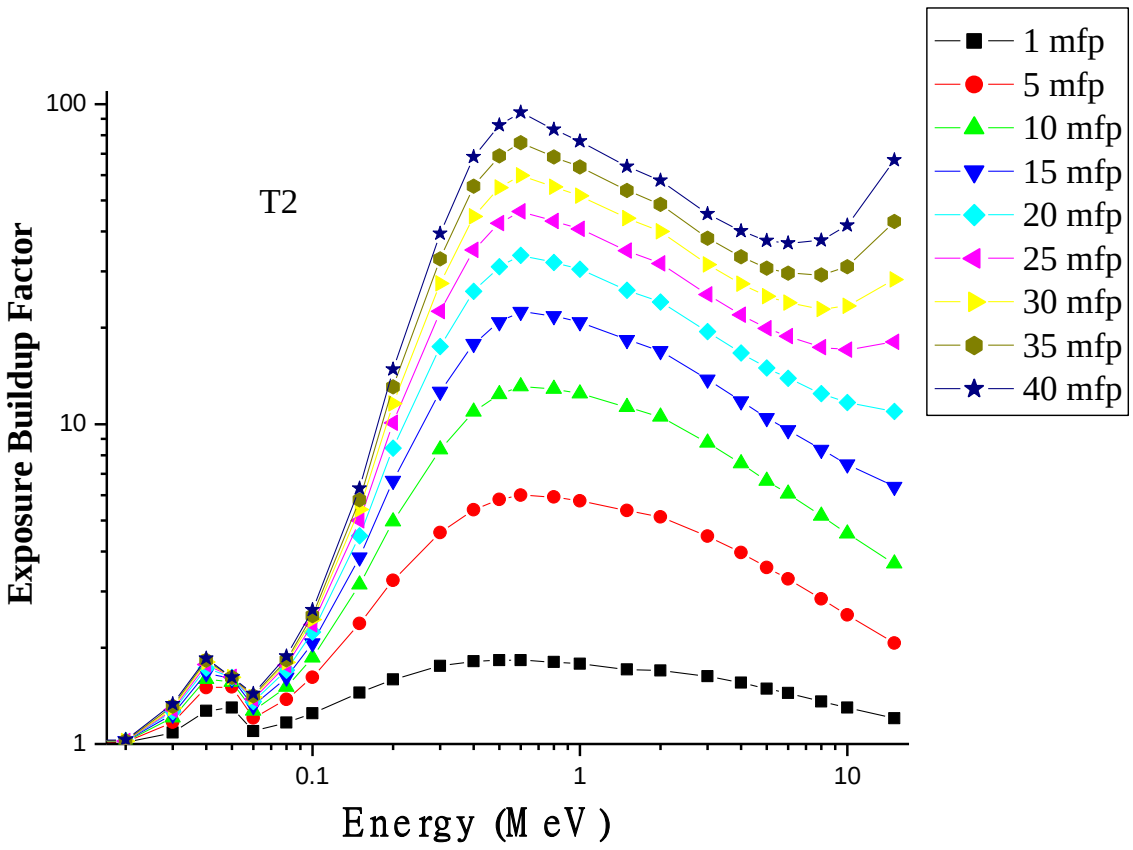

Figure 4. Exposure buildup factor of T2 as a function of energy at different depths (mfp)

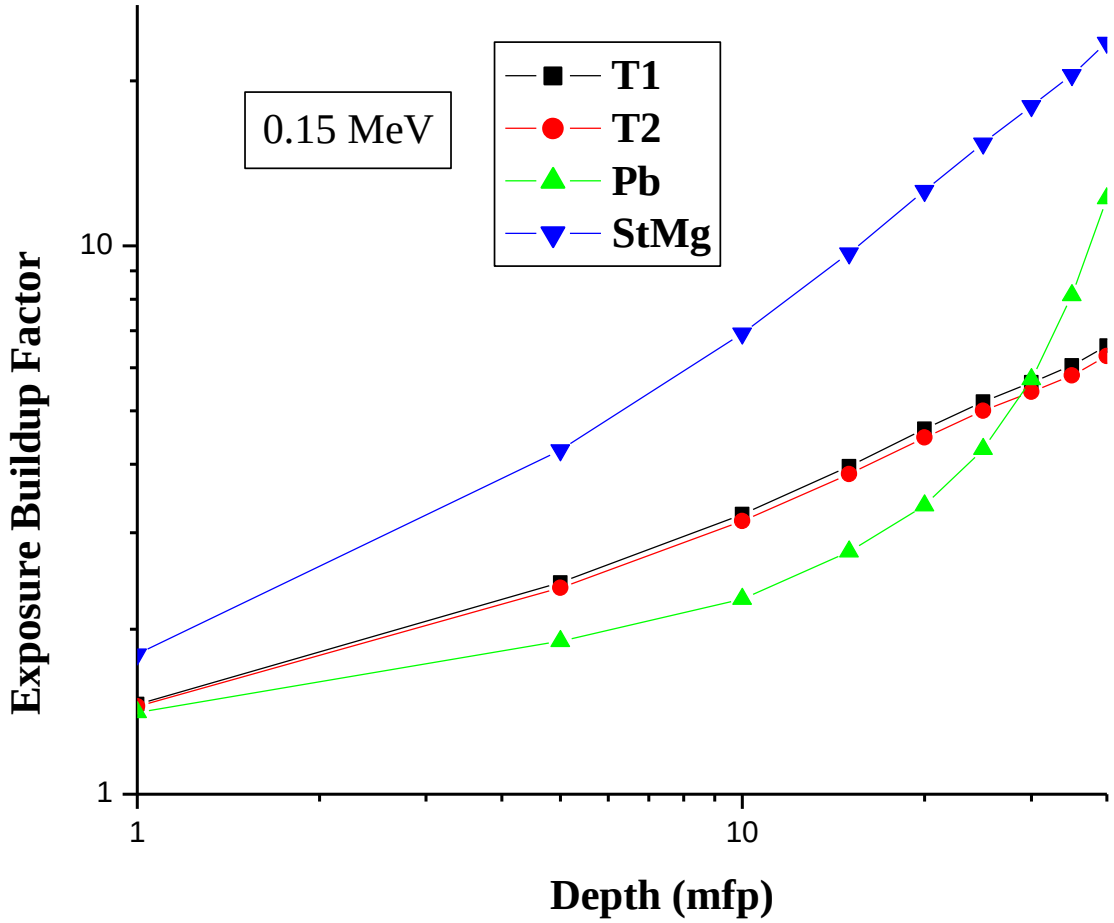

Figure 5. Exposure buildup factor of T1, T2, Pb, and StMg as a function depths (mfp) at 150 keV

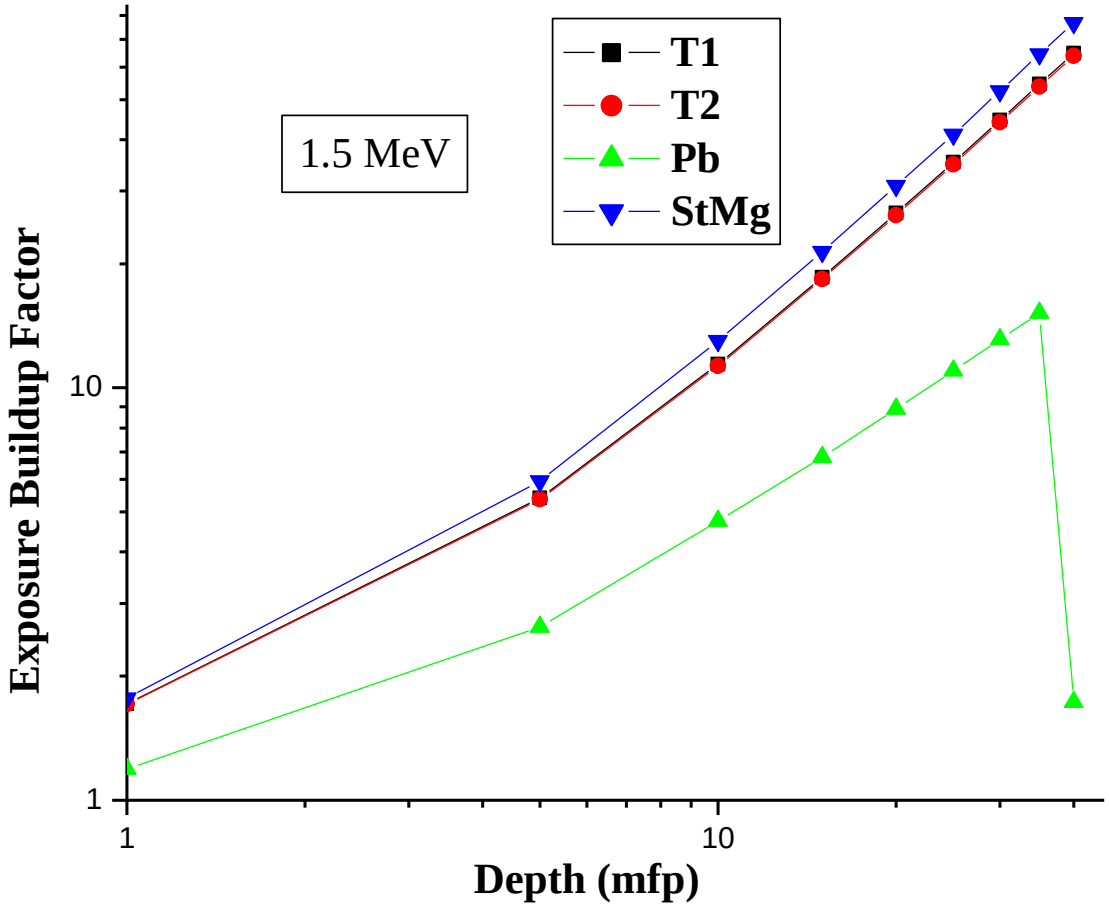

Figure 6. Exposure buildup factor of T1, T2, Pb, and StMg as a function depths at 1.5 MeV

Table1. Effective and equivalent atomic numbers, G.P fitting parameters, effective and equivalent atomic numbers of T1 and T2

E (MeV)	T1							T2						
	Z_{eff}	Z_{eq}	b	c	a	X_k	D	Z_{eff}	Z_{eq}	b	c	a	X_k	d
0.015	17.97	20.72	1.00646	0.76976	-0.0825	6.77252	0.16922	17.88	20.71	1.0066	0.72449	-0.0556	6.83959	0.15875
0.02	22.61	28.44	1.00997	0.11177	0.71725	10.978	-0.9168	23.01	28.44	1.00953	0.10781	0.73835	10.8887	-0.982
0.03	23.01	29.25	1.02066	0.36024	0.20376	13.4312	-0.073	23.41	29.27	1.08498	0.37726	0.20263	12.606	-0.0574
0.04	23.17	29.89	1.11469	0.33038	0.23418	14.8541	-0.0961	23.57	29.88	1.26869	0.33122	0.22368	15.7346	-0.0959
0.05	23.17	30.32	1.19551	0.33247	0.21243	13.1273	-0.1284	23.59	30.31	1.29807	0.31149	0.18724	13.3227	-0.1182
0.06	23.07	30.63	1.10103	0.38221	0.22619	13.6083	-0.1269	23.50	30.62	1.09666	0.39221	0.22025	13.6458	-0.1225
0.08	22.57	31.08	1.17186	0.43149	0.20347	13.8594	-0.1196	23.04	31.08	1.16576	0.42632	0.20755	13.8201	-0.1232
0.1	21.73	31.39	1.2568	0.48439	0.17934	13.7399	-0.1044	22.23	31.41	1.24848	0.47816	0.18329	13.6985	-0.1078
0.15	18.68	31.88	1.4584	0.62917	0.11979	13.7727	-0.0678	19.25	31.89	1.44689	0.62032	0.12362	13.7307	-0.0701
0.2	16.04	32.21	1.60653	0.773	0.07258	13.8675	-0.0455	16.54	32.22	1.5925	0.76316	0.07585	13.9068	-0.0469
0.3	13.67	32.84	1.76661	0.93706	0.02841	13.0849	-0.0301	14.04	32.81	1.75429	0.92629	0.03134	13.1569	-0.0314
0.4	12.88	33.35	1.82156	1.04006	0.00412	12.3686	-0.0216	13.19	33.35	1.81215	1.02971	0.00653	12.4676	-0.0225
0.5	12.55	33.8	1.83682	1.09587	-0.0088	11.5581	-0.0169	12.84	33.77	1.82961	1.08657	-0.0068	11.7217	-0.0176
0.6	12.37	34.1	1.83244	1.12877	-0.0163	10.7646	-0.0149	12.65	34.08	1.82709	1.12052	-0.0145	10.9759	-0.0155
0.8	12.21	34.4	1.80866	1.14336	-0.0212	9.93533	-0.0129	12.47	34.44	1.80523	1.13596	-0.0198	10.1953	-0.013
1	12.13	34.47	1.78428	1.14186	-0.0218	10.1687	-0.0121	12.39	34.55	1.78148	1.13638	-0.0208	10.4064	-0.0121
1.5	12.10	32.15	1.71228	1.16823	-0.0335	16.9024	0.00786	12.35	32.25	1.70892	1.16551	-0.033	16.6659	0.00742

2	12.22	28.69	1.7008	1.12168	-0.021	8.58249	-0.0047	12.48	28.55	1.69744	1.12129	-0.021	8.76666	-0.0044
3	12.62	25.91	1.62839	1.06018	-0.0056	12.1239	-0.0125	12.89	25.82	1.62734	1.05928	-0.0052	12.0223	-0.013
4	13.04	25.17	1.55714	1.02265	0.00539	12.7565	-0.0186	13.33	25.20	1.55549	1.02398	0.00524	12.8255	-0.0188
5	13.43	24.92	1.48887	1.00289	0.0127	13.1411	-0.0252	13.73	24.95	1.48694	1.0049	0.01247	13.1342	-0.0254
6	13.77	24.81	1.44639	0.97535	0.023	13.3235	-0.0342	14.07	24.78	1.4451	0.97672	0.023	13.3372	-0.0346
8	14.31	24.68	1.36017	0.96531	0.02956	13.6136	-0.0407	14.62	24.64	1.35851	0.96764	0.02941	13.6233	-0.0411
10	14.70	24.59	1.3016	0.94469	0.04056	13.8636	-0.0522	15.03	24.59	1.30041	0.9458	0.04093	13.8911	-0.0532
15	15.32	24.59	1.20479	0.94512	0.04929	14.2367	-0.0582	15.65	24.57	1.20331	0.94815	0.04922	14.2708	-0.0585

Thermal Characterization of Bida Basin Kerogen

Iliyasu Kudu Mohammed[1*]Abubakar Garba Isah[2]*Alhassan Mohammed[3]*Mohaammed Umar Garba[4]* and Nda Idris Abdullahi[5]

Department of Chemical Engineering, Federal University of Technology Minna, Nigeria

[1]Iliyasu43@gmail.com

[2]abubakar.Isah@futminnaedu.ng

[3]Moh.alhaa@futminna.edu.ng

[4]Dr.m.u Garba.tamuya@yahoo.com

Abstract

In this study Kerogen from Bida Basin was used as a source of hydrocarbon for the production of oil.Different thermal characterization such as Thermogravimetric analysis (TGA) and Rock Eval (R.E) Pyrolysis was studied on kerogen sample from Bida Basin Area of Niger State, Nigeria.Thermal breakdown of the kerogen content of the oil shale using TGA and R.E takes place mainly at the temperature range of 400 to 600^0C.The analysed kerogen sample from R.E have Total Organic Carbon (TOC) content of 2.50wt% and constitute of oil prone kerogen type I and II.Thermal characteristics of analysed sample obtain by TGA is in conformity with R.E parameters.The results from R.E Pyrolysis reveal that oil shale constitute adequate good quality kerogen to generate oil and gas during pyrolysis process.

Keywords: Kerogen, Thermogravimetric analysis, Rock Eval Pyrolysis, Total Organic Carbon

1.0 Introduction

Energy is very important resources of any nation. It can be seen that increase of industrial growth of nation is a function of the quantity of energy available in that nation and the extent it is utilized (Osueke and Ezugwu,2011).Among the energy sources crude oil remained the world leading fuel that is accounting for 32.9% of the world energy consumption. However as a result of the increase in economics activities lead to the high demand for energy most especially crude oil all over the world. The record levels is at increase in OPEC which states that there is increase in consumption

rate from 1.6million barrel per day to 38.2 million barrel per day, exceeding the previous records reached in 2012.The production rate in Brazil (+180,000 b/d), Russia (+140,000 b/d), UK and Canada (+110,000 b/d) (BP.,2016).Nigeria is a developing nation in Africa where application of renewable energy technology is situated. However, it is largely remain untapped as a result of insufficient knowledge skills about energy resources. Therefore, there is need to look at the energy deficiency and find an everlasting solution to it (Saifuddin et al., 2016).Energy to be specific oil and gas has continued to contribute more than 70% of Nigeria's National Income.25% of Gross Domestic Product (GDP) has been on crude oil for many years ago. Nigria is the world's tenth biggest reserve of crude oil estimated to be about 36 billion barrels Onshore drilling refers to drilling deep holes under the earth surface whereas offshore drilling refers to drilling underneath the seabed These drilling methods are used in order to extract natural resources usually oil and gas.(Oyedepo,2012). The most exploited natural resource in Nigeria is petroleum. However recent findings suggest that petroleum potentials of Nigeria have not been fully realized, particularly with emphasis to its inland basins. Nigeria's inland basin have been highly under explored basically as a result of abundance of oil in the Niger Delta. Examples of inland basin in Nigeria are Anambra Basin, Benue Trough, Benin Basin, Bida Basin, Borno Basin, Niger Delta Basin and Sokoto Basin (Geologin, 2012).The technology of exploring in inland Basin is Seismic. Seismic technology has been used by oil and gas companies to findout the roak where there is potential for hydrocarbons. Seismic technology operates with sound waves to predict what lies in the ground. Other technologies are magnetic geophysical method, gravitational, passive, magnetic electric, sonic and radioactive processing, aerial and satellite remote sensing (LAND SAT), 2- dimensional, 3-dimensional and 4-dimensional are used to carried out detailed evaluation of the nature and distribution of rock units as well as frequency, orientation and geological history of folds that will

serve as trap for the migrating hydrocarbons. After the exploration process has been carried out within the acceptable standard, the next process is to drill for oil and gas. The major types of drilling are horizontal, directional, slant rotary, electro and turbo drilling (Akinwale,2016).Kerogen (Petroleum Source Rock) can simply be defined as a fined grained sediment with sufficient amount of organic matter which can generate and release enough hydrocarbon to form a commercial accumulation of oil or gas (Al Areeq,2018).Kerogen is usually stable on heating and its consist of Carbon (C),Hydrogen (H), Nitrogen (N),Sulphur (S) and Oxygen (O) (Adegoke et al.,2015).The major methods of pyrolysis are combustion (presence of oxygen), thermal/cracking (350 -900^{0}C),catalysis/cracking (catalyst),hydrocracking (hydrogenation),gray –king pyrolysis (fixed bed pyrolysis) and micro wave pyrolysis (Olufemi,2016).

2 Literature Review

Sonibare et al (2005) studied thermal decomposition of Lokpanta Kerogen sample from Nigeria using Thermogravimetric (TG) and Differential Thermal Analysis (DTA) within a temperature range of 25 – 600^{0}C .Rock Eval (R.E) pyrolysis was used to studied the geochemical characteristics of kerogen within a temperature range of 300 – 570^{0}C.The activation energy is evaluated within a range of 73.2 – 75.0 KJ/Mol.Tiwari and Deo (2012) studied the behavioir of kerogen from Green Rivel Oil U.S.A using Thermogravimetric Analysis (TGA) combined with online Mass Spectrometry (TGA-MS).The activation energy was determined between the range of 90 – 230 KJ/Mol in relation to conversion.Han et al (2015) used TGA to studied kerogen and kinetics at 10,20,30 and 40^{0}C/min heating rate on two kerogen samples from Huandian and Fushun in northeast China.Characterizes the hydrocarbon released during pyrolysis weight loss at 400 – 550^{0}C using TGA and hydrocarbon generation using R.E at 400 – 575^{0}C.The activation energy

obtained is 10KJ/Mol (Huandian) and 1KJ/Mol (Fushun).Liu et al (2017) studied the pyrolysis kinetics characteristics of kerogen from mudanjiang using Rock Eval pyrolysis.The heating (10,15,20,25 and 30^0C/min) and temperature range of 200 – 600^0C.kinetics model was used to evaluate the activation energy and frequency factor respectively.The aim of these research is to study the thermal behaviour of Bida Basin Kerogen using TGA and R.E.

3 Methodologies

3.1 Sample

The dark black carbonaceous kerogen sample was drilled at kudu Bida Basin area of Niger State Nigeria.The sample was crushed to a particle size <65µm and prepared according to ASTM standards (ASTM D 2013-72).

3.2 Equipment and Procedure

The Thermogravimetry Analysis (TGA) and Differential Thermogravimetry (DTG) was performed using perkin elmer analyzer.The sample is 10mg placed in a platinum holder and heated from 25 to 550^0C in the presence of nitrogen gas .Experiment was carriedout at heating rate of 10^0C/min.

The Rock Eval (R.E).pyrolysis was used in analyzing the organic matter contained in the oil shale with respect to quantity, quality or type and thermal maturity. Rock Eval pyrolysis was carried out using Rock Eval equipment. The sample was heated in the absence of oxygen to a temperature of 418^00C using a special temperature program. The analysis of the peaks are as follows.The first peak (S1) stand for hydrocarbons already present in the sample at about temperature of 300^0C.The

second peak (S2) stand for hydrocarbon gotten from thermal cracking of kerogen of the kerogen at about temperature of 300 – 550^0C and the third peak (S3) stand for the CO_2 which is generated from kerogen during thermal cracking. The equipment also provide information about the maximum S2 peak (Tmax) and the Total organic content (TOC) of the oil shale. The amount of organic matter in the shale was deduced from the Total Organic Carbon Content (TOC).The sum of S1 and S2 gives the Genetic Potential (GP), the Hydrogen Index HI (S2/TOC) and the Oxygen Index OI (S3/TOC) were used to analyse the kerogen type. A plot of these indices in place of normal Van Krevelen Diagram reveals the type of organic matter constituted in the oil shale. The maturity of the kerogen,S1/(S1+S2) and Tmax S1(S1+S2) is normally known as the transformation ratio (TR) or Production Index (PI).

4 Results and Discussion

4.1 Thermogravimetric Analysis (TGA) and Differential Thermogravimetry (DTG)

TGA was used to measure changes in physio-chemical characteristics of the temperature was elevated with constant heating rate. It is used to study the thermal attributes of samples due to degradation. It was done using a TGA analyzer Perkin Elmer with a sample measurement of 10mg at a degree of heating of 10^0C/min. Derivative Thermogravimetry (DTG) is also determined from TGA data, to elevate the degree of weight loss when temperature is elevated. The TGA and DTG data is often applied in the study of chemical kinetics of the degradation process and also the decomposition of behavior of samples.

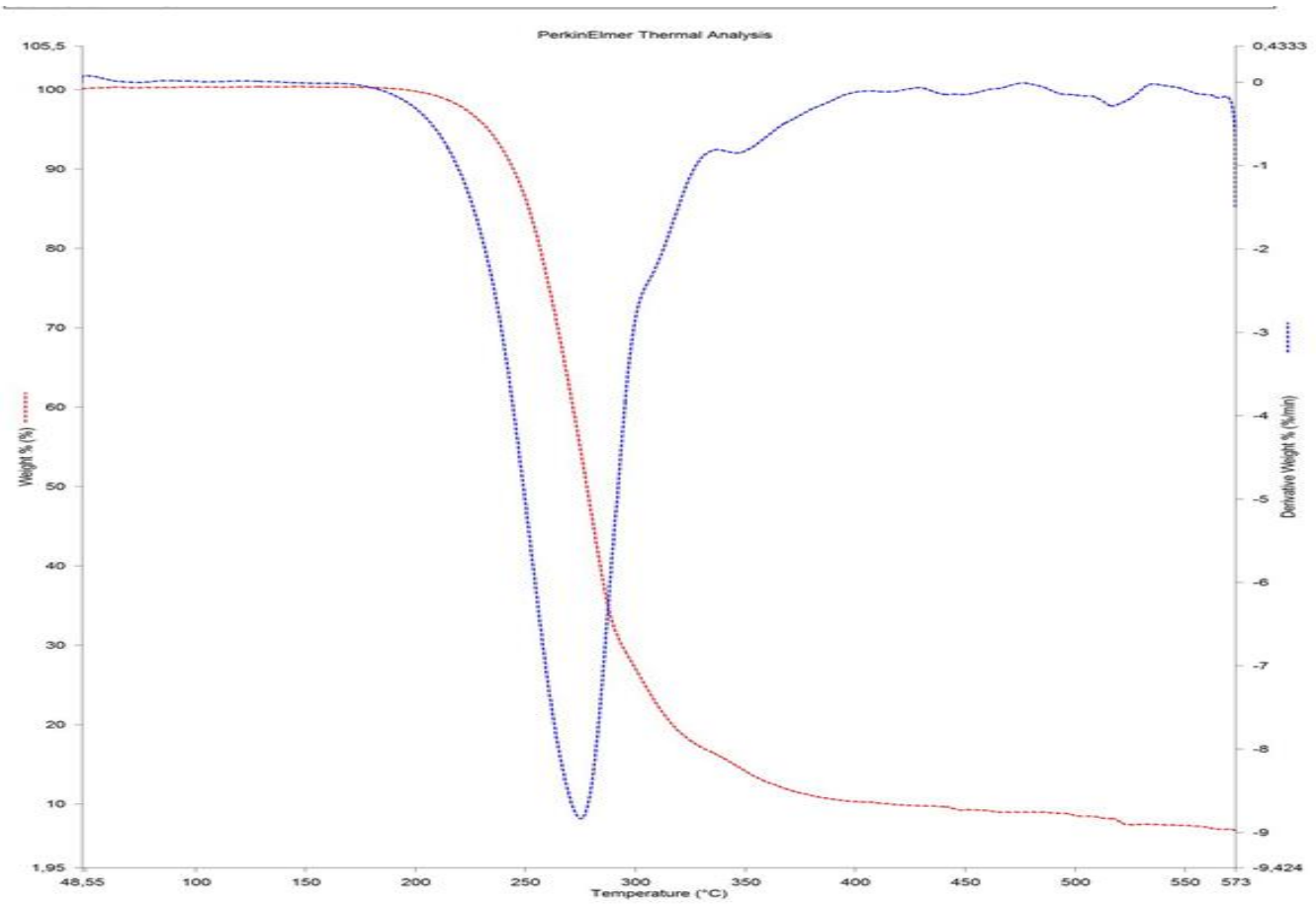

Figure 4.1: TG and DTG Curves of Kerogen

Thermogravimetric analysis (TGA) is a technique that is used to study the thermal decompositional behavior of oil shale sample. It gives a measure of the weight loss of a sample material as a function of temperature or time. The decomposition characteristics of oil shale sample is given in figure 4.1 from the TGA curve .It can be seen that weight loss increased with the increase in pyrolysis temperature. It has been reported from literature that the degradation of of oil shale involves three main stages, which are moisture content elimination, decomposition of sample and continues slight valorization (White et al., 2011).The TGA curve of oil shale shows that the decomposition is divided into 3 stages which is due to the varying composition of oil shale. In the initial stage of the decomposition which began at room temperature up to 200^0C, there was a gradual weight loss

about 10.0wt% which can be attributed to the release of moisture and partial hydrolysis of some extractives. In the second stage it is observed that an accelerated decomposition of oil shale sample which constituted organic matter is observed within a temperature range of 200^0C to 500^0C with an approximate weight loss of about 82%.The last stage which is observed above 550^0C shows a constant residue ratio which can be attributed to complete loss of the decomposable fractions. The maximum yield usually occurs between the temperature ranges of 280^0C to 500^0C (Almeida et al., 2008, white et al., 2011 and Dewangan, 2014)

4.2 ANALYSIS OF ROCK-EVAL PYROLYSIS

Rock –Eval Pyrolysis was used as standard techniques for knowing hydrocarbon generative potential of oil shale organic matter. The results of parameter obtain by Rock – Eval Pyrolysis is presented in Table 4.1.

TABLE 1: ROCK EVAL PYROLYSIS RESULTS

TOC	S1	S2	S3	Tmax	HI	OI	S2/S3	S1/TOC×100	PI
2.50	0.05	1.04	0.57	418	41.60	22.80	1.80	2 .00	0.05

4.2.1QUANTITY OF ORGANIC MATTER: The total organic carbon (TOC) serve as measure of determine the amount of organic matter including the quantity of kerogen organic matter in

sedimentary rock is 2.50wt% as shown in Table 4.1 the TOC value indicate that the source rock has excellent generative capacity compare with standard.

S1 represent the quantity of free hydrocarbon present in the source rock sample which signifies that the quantity of hydrocarbon present in the source rock is 0.05. S2 represents the quantity of hydrocarbons obtained through thermal cracking of nonvolatile organic matter which is 1.04.S3 represents the quantity of CO_2 generated during pyrolysis of source rock sample which is 0.57.The S1 value is as result of low maturity of source rock sample not to poor generative capacity. Tmax is equivalent to the temperature of the maximum production of hydrocarbon during pyrolysis (S2 peak maximum). Tmax result of 418^0C signifies immature to early mature stage. The Rock Eval Pyrolysis was carried out at Getamme Laboratory in Portharcourt

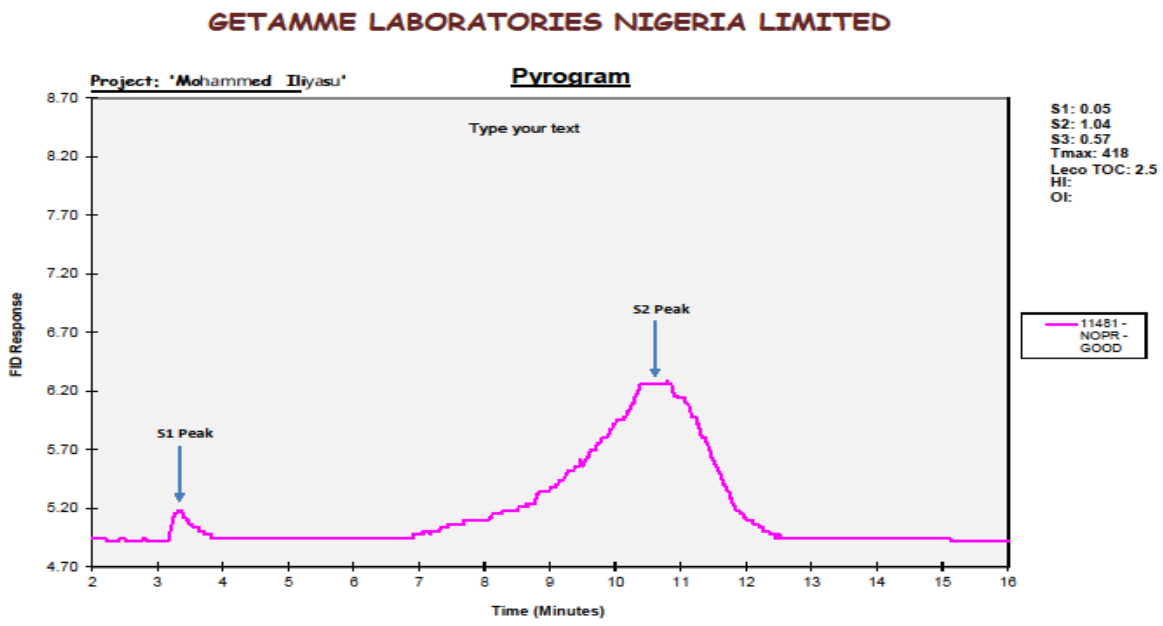

FIGURE 4.2: Relationship between flame ionization detection (FID) Response and Time

Figure 4.2 shows the relationship between flame ionization detection (FID) responses with Time. It can be seen that FID and Time increases progressively until its reaches its optimal conditions. The S1 and S2 signals successively determined with FID equivalent to first quantity of hydrocarbons and second peak representing the hydrocarbons produced from thermal cracking of source rock sample

4.2.2 QUALITY OF ORGANIC MATTER: The result of hydrogen index (HI) is 46.1, oxygen index (OI) is 22.8, S2/S3 is 1.80, S1/TOC×100 is 2 and PI is 0.05 respectively. The hydrogen index (HI) of 41.6% indicates that 35% oil and 6.6% gas. The analysis signifies that the source rock contain type I and II kerogen.

4.2.3 MATURITY OF ORGANIC MATTER: Production index (PI) is 0.05, which implies that the hydrocarbons quantity has been produced naturally in relation to the total quantity of hydrocarbons which the source rock sample can produce. The PI value of 0.05 signifies that it is a mature organic matter in corformity with low S1 value of 0.05 resulted from low thermal maturity.

4.2.4 HYDROCARBON GENERATIVE POTENTIAL: The results from Table 1.0 significantly shows that organic matter of sample is immature to early mature. Hydrocarbon production capacity depends on organic matter type and quantity.TOC, HI, OI, S2/S3 reveal that sample has potential for organic matter represented by oil prone kerogen I and II .In Rock –Eval terminology, the TOC consists of pyrolysable (PC) and residual (RC) carbon. PC equivalents to the carbon content in the HCs (S1+S2).100PC/TOC>30% are typical for an oil prone source rock while 100PC/TOC<30% shows a gas prone source rock. Most of the samples have 100PC/TOC is range from 55 to 65% (Carthy et al.,2011,Obaje et al.,2013 and Gajica G.D et al.,2017)

4.3 Abbreviations

TGA: Thermogravimetric Analysis

DTG: Differential Thermogravimetry

TGA-MS: Thermogravimetric Analysis Microscopy

R.E: Rock Eval

TOC: Total Organic Carbon

S1: Hydrocarbon already present in the sample

S2: Hydrocarbon obtain from thermal cracking process

S3: CO_2 which is generated from kerogen during thermal cracking process

Tmax: Maximum Temperature at S2 peak

HI: Hydrogen Index

OI: Oxygen Index

GP: Genetic Potential

PI: Production Index

TR: Transformation Ratio

5.0 Conclusion

In this study, the thermal characteristics of Bida Basin oil shale under pyrolysis process was studied.The oil shale was also analyzed by Rock Eval 6 instrument in order to know the hydrocarbon potentials of the oil shale.The oil shale constituted adequate quantity and types of kerogen to generate oil and gas upon pyrolysis process respectively.

References

Adegoke A.D., Abdullah W.H.,Yandoka, B.M.S and Abubakar, M.B.(2015).Kerogen Characterisation and Petroleum Potential of late cretaceous sediments,chad (Borno) Basin,northeastern Nigeria.Bulletin of the Geology society of Malaysia Vol 61,30 – 33.

Akinwale Y.O.(2016).Harnessing Science Technology and Innovation for Enhancing Marginal Oil and Gas field development in Nigeria.A comparative analysis.International Journal of ebusiness and eGovernment studies North West University (vaal campus),South Africa ,Vol 8 issue 2,49 - 50.

Al- Areeq, N.M.(2018).Petroleum Source Rocks Characterization and Hydrocarbon Generation.Recent insight in petroleum science and engineering.13-16/

Almeida, D and Marquez, M.D.F.(2016).Thermal and Catalytic pyrolysis of plastic waste polymers Vol 26,44-55.

BP Stats (2016) Statistical Review of World Energy June, 25 -26.

Carthy K.M.,Niemann, M.,Palmowski, D.,Peters, K., Stankiewicz,A.(2011).Basic Petroleum Geochemistry for Source Rock Evaluation 38.

Dewangan,A.K.(2014).Co-pyrolysis of lignocellulose biomass and synthetic polymer.Unpublished project report, Department of Chemical Engineering,National Institute of Technology Rourkela India.45-46.

Gajica, G.D., Sajnovic, A.M and Stojanovic K.A.(2017). The Influence of Pyrolysis type on shale oil generation and its Composition (Upper Layer of Aleksinac Oil Shale, Serbia), Journal of Serbian Chemical Society Vol 82 issue12 ,1468 – 1471.

Geologin,D. (2012).Geology and Petroleum Potentials of Nigeria Sedimentary Basins,8-9.

Han,H.,Zhon,N.N.,Huang,C.X., and Zhang,W.(2015).Pyrolysis Kinetics of oil shale from northeast china:Implications from Thermogravimetric and Rock Eval Experiment Vol 159,778-779.

Lin,H and Wang,J.(2017).Pyrolysis mechanism and Kinetics model of Mudanjiang oil shale in the Songhow Basin China.Energy Exploration and Exploitation Vol 35 issue 4.504-505.

Obaje N.G.,Balogu, D.O., Nda, A.I.,Goro I.A.,Ibrahim, S.I., Musa, M.K.,Dantata, S.H.,Yusuf, I.,Dadi, N.M and Kolo I.A.(2013).Preliminary Integrated Hydrocarbon Prospectivity Evaluation of the Bida Basin in North Central Nigeria.Petroleum Technology Journal (ISSN 1595-9104).An International Journal Vol 3 issue 3, 37- 42.

Olufemi, O, A.(2016).Conventional and Microwave Pyrolysis remediation of crude oil contaminated soil.PhD thesis.University of Nottingham.8-12.

Osueke and Ezugwu.(2011).Study of energy Resources and its consumption.International Journal of Scientific and Engineering research Vol 2 issue 12.34-37.

Oyedepo,S.O (2012).Renewable and Sustainable Energy Review Journal Homepage:www.elsevier.com/locate.2585.

Saifuddin.N.,Bello.S.,Fatihah.S and Vigna K.R.(2016).Improving Electricity Supply in Nigeria – Potential for Renewable Energy from Biomass.International Journal of Applied Engineering Research.ISSN 0973 – 4562 Vol 11, issue 14, 8322 – 8323.

Sonibare,O.O.,Ehinola,O.A., Egashira,R.(2005).Thermal and geochemical characterization of Lokpanta oil shales,Nigeria.Energy Conversion and Management 46.2338-2343.

Tiwari,P and Deo.M.(2012).Compositional and Kinetics analysis of oil shale pyrolysis using TGA-Ms.333-334.

White J.E, Catallo W.J and Legendre B.L (2011).Biomass pyrolysis kinetics a comparative critical review with relevant agricultural residue case studies J Anal Appl pyrol, Vol 9,11-13.

Possible Teleconnection between the Indian Ocean Dipole and the rainfall distribution over Nigeria.

Ezedigboh Ugochukwu*[1,2], Usman Mohammed[1], Suleiman Mohammed[1], Bello Emmanuel[2], Orisakwe Ikenna[2,3], Aganbi Blessing[2]

[1]Federal University of Technology, Minna, Nigeria. [2]Nigerian Meteorological Agency, Abuja, Nigeria. [3]African Center of Meteorological Applications

for Development, Niamey Niger.

Corresponding author's email: ugochukwuezedigboh@gmail.com. Tel: +234 (0) 8037817755

ABSTRACT

The El Nino Southern Oscillation (ENSO) has some level of control over the weather of Nigeria and Africa seasonally but there has been enough debate as to the extent of the control. ENSO magnitudes do not necessarily translate into impacts in the same direction hence, attempt to investigate possible teleconnections with the Indian Ocean Dipole Mode Index (IODMI) phases over equatorial Indian Ocean that could explain the subsisting gaps in the knowledge of large scale controls on Nigerian Monsoon Seasonal Rainfall (NMSR) pattern is the basis of this paper. Daily rainfall data was obtained from Nigerian Meteorological Agency (NiMet) and Sea Surface Temperatures (SSTs) over the Indian Ocean and the Pacific Ocean were obtained from NOAA site. Pearson correlation coefficient method was used to assess the spatial and temporal relationship between the IODMI/NMSR and ENSO/NMSR while the test-of-significance of the correlation results were carried out using two methods- Critical r value and p-value. The results revealed that there is a significant correlation at 10% level between the IODMI and NMSR over the selected stations with contrasting tendencies to increase rainfall at a certain period of the year or decrease it at another period. However, the comparison of the influence of IODMI and ENSO indices negates their effects on NMSR which is dependent on the strength of correlation, thus with both having a decreasing north to south spatial pattern. Hence, the incorporation of IODMI for the climate prediction of the monsoon rainfall over Nigeria would improve the resilience of different specific sectors of the economy especially agriculture.

Keywords: ENSO, IODMI, Teleconnection, Rainfall, Climate change

INTRODUCTION

Rainfall variability and change impacts are already being felt in many parts of the world especially Africa, and are likely to worsen in the future, with clear evidences of changes in climate and weather patterns in many parts of the world based on assessment reports produced by the working groups of the Inter-Governmental Panel on Climate Change (IPCC, 1995; 2001; 2007; 2012; 2013). However, these climate extremes is being felt in Nigeria having resultant effects on increased frequency and intensity of floods/ droughts, delayed onset, early cessation and irregular distribution of rainfall (Ukhurebor and Abiodun, 2018).

The rainfall over the western region of Africa are directly affected over the Atlantic and indirectly by the Indian Ocean. (Preethi, 2015). Among the tropical indo-pacific climate drivers, the canonical El Nino Southern Oscillation (ENSO), (Ramussen and Carpenter, 1983; Guanghan et al. 2016), plays a dominant role in rainfall distribution over various parts of Africa during all the seasons (Janowiak, J. E. 1988; Janicot et al., 1998).

The El Niño Southern Oscillation (ENSO) has been recognized as an important manifestation of the tropical ocean-atmosphere-land coupled system. However, the more recently discovered Indian Ocean Dipole (IOD; Saji et al., 1999; Behera et al., 1999; Webster et al, 1999) is another important manifestation of the tropical air-sea interaction.

The IOD is defined by the **difference in Sea Surface Temperature (SST) between two areas** (or poles, hence a dipole) – a western pole in the **Arabian Sea** (western Indian Ocean) and an eastern pole in the **eastern Indian Ocean** south of Indonesia. IOD develops in the equatorial region of Indian Ocean from April to May peaking in October. The climate variability in the Indian Ocean is dominated by the Indian Ocean Dipole (IOD) during September–November, which is related to the inherent ocean and atmosphere coupling processes (Saji et al., 1999; Yamagata et al., 2004; Behera et al., 2006).

IOD also known as the Indian Nino, is an irregular oscillation of Sea Surface Temperature (SST) in which the western Indian Ocean becomes alternately warmer and cooler than the eastern part of the ocean. This leads to a coupled ocean-atmospheric phenomena in which convection, winds, SST and thermocline take part actively (Vinayachandran, et al 2007).

It involves an aperiodic oscillation of SST between “positive”, “neutral” and “negative” phases. A positive phase peaks is in September-October (Murtugadde et al., 1999) and has been shown to be

associated with greater than average SST and greater precipitation in the western Indian Ocean region with a corresponding cooling of waters in the eastern Indian Ocean, which tends to cause droughts in adjacent land areas of Indonesia and Australia (Saji et al., 1999; Ashok et al., 2001; Behera et al., 2006). On the other hand, the negative phase of the IOD brings about the opposite conditions with warmer water and greater precipitation in the eastern Indian Ocean and cooler and drier conditions in the west. Hence, the negative phase of IOD can be considered as an intensification of the normal state where as positive phase of the IOD represents conditions nearly opposite to the normal (Ashok et al., 2001; Vinayachandran, et al 2007).

The positive phase SST anomaly can be accompanied by above average rainfall in eastern Africa and the tropical western Indian Ocean and diminished rainfall over Indonesia and the tropical southeastern Indian Ocean (Saji et al., 1999, Webster et al., 1999, Black et al., 2002). During the positive phase of IOD, unusually strong winds from the east push warm surface water towards Africa, allowing cold water to upwell along Sumatran coast. Strong zonal wind anomalies trapped to the equatorial Indian Ocean are a characteristic of atmospheric feature during such Sea Surface Temperature Anomalous (SSTA) events (Murtugudde et al., 2000).

Rainfall pattern in Nigeria can be affected by a lot of factors – large scale monsoon circulation, the migration/oscillation of ITD and by regional orography but the effect of Indian Ocean Dipole (IOD) on rainfall pattern over Western Africa with Nigeria as a case study is the aspect this research was focused on since it has already been established to have direct influence on East African rainfall pattern (Black et al, 2002, Behera et al., 2005) though a weak influence on South Sudan rainfall pattern (Omay, 2015).

Having established the facts that ENSO plays a huge role in the determination of the rainfall regime in Africa (Preethi et al., 2015), this study focused on investigating the unexplored influence of IOD SST anomalies on rainfall distribution over Nigeria against the backdrop of the propagation of active mesoscale convective systems (line squall) from the tropical western Indian ocean affecting both the Zonal (east-west) circulation and the meridional (north-south) circulation in the troposphere, as shown in the RGB satellite imagery in Figure 1, that could explain the subsisting gaps in the knowledge of large scale controls on Nigerian Monsoon Seasonal Rainfall (NMSR) pattern which would improve the resilience of different specific sectors of the economy especially agriculture.

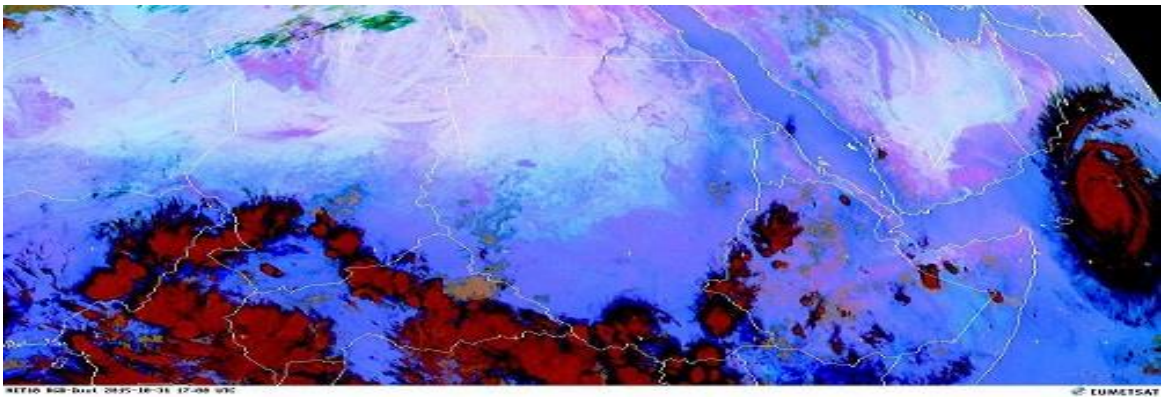

Fig. 1.: Showing mesoscale convective clouds in RGB-Dust Meteosat imagery (saved on 2015-10-31 at 17:00 UTC). NIMET, 2015.

LITERATURE REVIEW

The perception that the Indian Ocean is passive and merely responds to the atmospheric forcing has been shown to be untrue. The discovery of the IOD and the studies that followed have demonstrated that the Indian Ocean can sustain its own intrinsic coupled ocean-atmosphere processes and is not merely a slave to the events happening over the Pacific Ocean in connection with ENSO. (Schott et al., 2009; Cherchi & Navara 2013).

El Niño and IOD events account for 30% and 12% of the tropical Indian Ocean SST variability respectively (Saji et al., 1999; Gaughan et al., 2016). It means that both of the aforementioned phenomena explain most of the tropical Indian Ocean variability. The IOD events have a strong influence on the climate of the immediate neighboring regions such as East Africa, Indonesia and southern Africa (Saji et al., 1999; Black et al., 2003; Gaughan et al., 2016), and also on the Indian summer monsoon region (Ashok et al., 2001;Gouda et al., 2017), East Asia (Saji and Yamagata, 2002b, Guan et al., 2002), the Mediterranean, Australia, and Brazil (Saji and Yamagata, 2002b)

Significant increase in rainfall is seen in eastern Africa in association with canonical El Nino and positive IOD events. This significant positive correlation observed between the East African rainfall and IOD events during October-December season are in general agreement with the earlier studies (Black et al., 2003; Ummenhofer et al., 2009) which show that the East African short rains are predominantly driven by the warm SST anomalies in the western equatorial Indian Ocean.

However, the IOD event has been observed to affect east African rainfall independent of ENSO especially during September and November period (Behera et al., 2005). Hence, in a research work carried out on the relationship between IOD and ENSO using observed sea surface temperature data from 1871-1998 and observed wind data from 1958-1998, by Ashok et al., (2001) discovered Indian Ocean Dipole (IOD) is a physical entity.

However, there has also been observed changes in the spatio-temporal distribution of rainfall over Nigeria resulting in changes in onset, cessation, frequency, intensity and duration of rainfall that is influenced by alot of factors which include; large scale monsoon circulation, the migration/oscillation of ITD, orography and other forcing functions. Several studies have been carried out on the influence of the forcing functions on rainfall over Nigeria, (Nicholson, 2012; Sylla et al., 2013) but little or no study has considered the influence of the IOD on rainfall in Nigeria.

There is ample evidence in literature, some reviewed here, of a statistical relationship between both the Indian Ocean Dipole Mode Index (IODMI) and ENSO as well as the spatial and temporal characteristics of rainfall variability over Africa, especially East Africa, South Sudan, (Saji et al., 1999; Black et al., 2003; Omay, 2015) respectively and the world, but gaps still persist with respect to Nigeria.

Therefore this study was designed to fill the gaps and to provide climate information needed in advance early warning systems. It evaluated temporal and spatial characteristics of rainfall and the impacts of IOD events on variability of rainfall over Nigeria.

DATA AND METHODOLOGY

The rainfall database consisting of sixteen (16) synoptic Nigeria stations as shown in Figure 2, having 33years of daily rainfall records covering the period from 1983-2015 were obtained from the Nigerian Meteorological Agency. Moisture Quality Index (MQI), (Usman, 2000) was the rainfall derivative that was used for the analysis.

$$MQI = \frac{r_{mm} \times Nbi}{{R_i}^2} \ldots\ldots\ldots\ldots\ldots\ldots\ldots\ldots\ldots\ldots\ldots\ldots\ldots\ldots\ldots\ldots\ldots\ldots \ldots\ldots \; equation 1$$

where;

I= Year identifier rmm=

Highest weekly rainfall total for the month R=

Monthly rainfall total Nb=

Number of 'breaks' in rainfall per month. A break is taken as any pentad period with less than 5mm of rain.

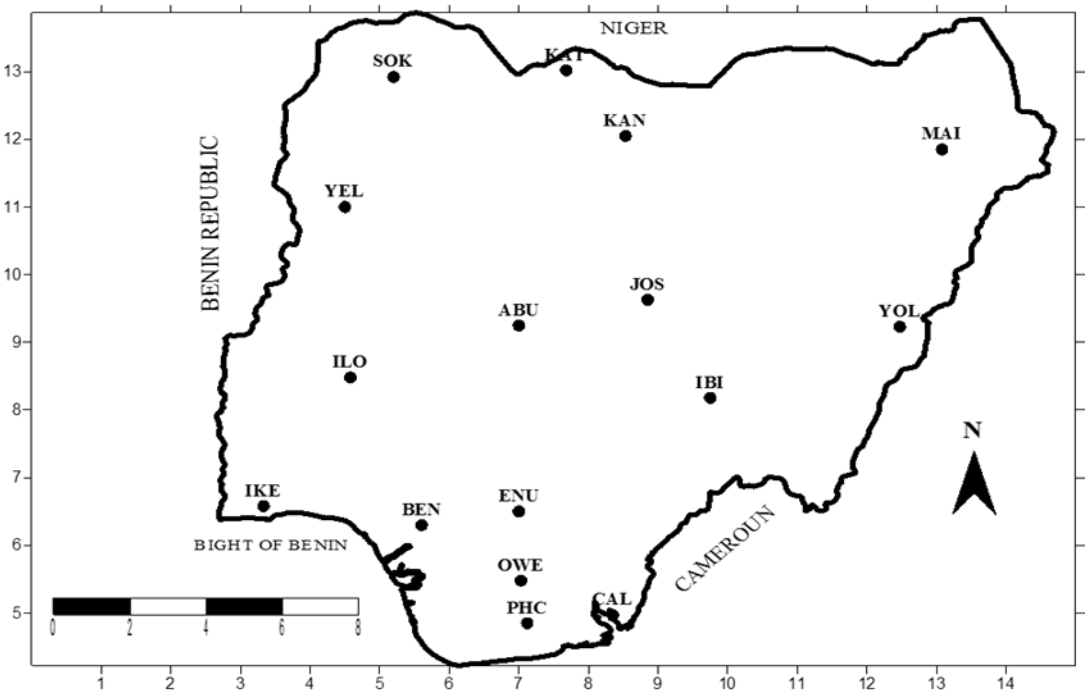

Figure. 2. Map showing the selected stations of Nigeria. Source: (NIMET, 2018).

Furthermore, Monthly SSTs over Indian Ocean (IODMI) and over Pacific Ocean (ENSO) were obtained from NOAA website: http://www.esrl.noaa.gov/psd/gcos_wgsp/Timeseries/DMI and

http://www.esrl.noaa.gov/psd/gcos_wgsp/Timeseries/Nino34/ respectively for the same study period.

The three months moving average of monthly MQI, IODMI and ENSO data was done specifically during the Monsoon Period - **MAM** (March, April, May), **AMJ** (April, May, June), **MJJ** (May, June, July), **JJA** (June, July, August), **JAS** (July, August, September), **ASO** (August, September, October) and **SON** (September, October, November). So for any of the given period j, the moving average was calculated using these formula respectively;

$$MQI_j = \frac{1}{3}\sum_{i=1}^{3} MQI_i \ldots\ldots\ldots\ldots\ldots\ldots\ldots\ldots\ldots\ldots\ldots\ldots\ldots\ldots\ldots\ldots\ldots\ldots\ldots\ldots\ldots\ldots\ldots\ldots\ldots\ldots \; equation\ 2$$

$$DMI_j = \frac{1}{3}\sum_{i=1}^{3} DMI_i \ldots\ldots\ldots\ldots\ldots\ldots\ldots\ldots\ldots\ldots\ldots\ldots\ldots\ldots\ldots\ldots\ldots\ldots\ldots\ldots\ldots\ldots\ldots\ldots\ldots\ldots\ldots \; equation\ 3$$

$$ENSO_j = \frac{1}{3}\sum_{i=1}^{3} ENSO_i \ldots\ldots\ldots\ldots\ldots\ldots\ldots\ldots\ldots\ldots\ldots\ldots\ldots\ldots\ldots\ldots\ldots\ldots\ldots\ldots\ldots\ldots\ldots\ldots\ldots \; equation\ 4$$

Thereafter, Pearson Coefficient correlation was used to quantify the teleconnection between the Nigerian Monsoon Seasonal Rainfall (NMSR) with the IODMI and ENSO respectively using

$$r_{xy} = \frac{1/n \sum_{i=1}^{n}(x_i - \bar{x})(y_i - \bar{y})}{\sqrt{1/n \sum_{i=1}^{n}\{(x_i - \bar{x})^2 \,.\, 1/n \sum_{i=1}^{n}\{(y_i - \bar{y})^2\}}}$$

$$\ldots\ldots\ldots\ldots\ldots\ldots\ldots\ldots\ldots\ldots\ldots\ldots . \; equation\ 5$$

where x is MQI, DMI and ENSO.

However, P-value and Critical Value r methods were used to test the significance of the Pearson correlation between NMSR/IODMI and NMSR/ENSO at 10% level based on these hypotheses

H_0= “the correlation coefficients is not significant at the 10% significant level.”

H_1= “the correlation coefficients is significant at the 10% significant level.”

Finally, spatial pattern analysis using Quantum GIS (QGIS) software, Bar Charts and Tables were used to show the nature of the teleconnection between the NMSR/IODMI and NMSR/ENSO.

RESULTS AND DISCUSSION

Firstly, the analysis was carried out to assess the relationship between IODMI and rainfall during monsoon seasons starting with MAM, AMJ, MJJ, JJA, JAS, ASO and SON over each station. The values of the Pearson correlation coefficient analysis was computed using equation 5 and presented in three periods (1983-1993), (1994-2004), (2005-2015) as shown in Table 1-3. However, the red and blue colored results show the correlation coefficient ≥ +0.5 or -0.5 respectively that have some significant relationship.

Tables 1-3 agrees with the fact that the Pearson coefficient correlation analysis shows very strong significant values using the 3-months moving average during the monsoon period (Black et al 2003, Omay, 2015). In other words, it indicates that there is an existence of a relationship between the Nigerian Monsoon Seasonal Rainfall (NMSR) and Indian Ocean Dipole Mode Index (IODMI).

It also shows that Years with dominant positive correlation were 1984, 1985, 1986, 1990, 1992, 1996, 1997, 2004, 2006, 2010, 2013 and 2014 while years with dominant negative correlation were 1983, 1987, 1988, 1991, 1993, 1995, 1998, 1999, 2000,2001,2002, 2003, 2007, 2008, 2011, 2012 and 2015.

Table 1: 3 months moving average correlation analysis results between MQI and DMI during monsoon season for 1983-1993

Stns	1983	1984	1985	1986	1987	1988	1989	1990	1991	1992	1993
ABU	-0.6	0.7	0.6	0.7	-0.8	-0.7	-0.4	0.6	-0.5	0.0	-0.8
BEN	-0.9	-0.4	-0.2	-0.3	0.1	0.1	0.4	0.0	-0.7	0.9	-0.4
CAL	-0.8	0.7	-0.2	0.0	-0.1	-0.6	0.3	-0.2	-0.6	0.9	-0.8
ENU	-0.9	-0.1	0.8	0.7	-0.7	-0.7	0.2	0.6	-0.5	0.9	-0.7
IKE	0.1	-0.4	-0.3	-0.1	-0.4	0.1	0.5	0.5	-0.7	-0.2	-0.1
ILO	-0.2	-0.4	0.9	0.7	-0.9	0.1	-0.5	0.7	-0.5	0.5	-0.8
JOS	-0.8	-0.6	-0.1	0.6	-0.9	-0.5	-0.2	0.7	-0.7	-0.1	-0.7
KAN	-0.4	0.7	-0.3	0.4	0.6	-0.8	-0.8	-0.8	-0.7	0.8	0.6
KAT	-0.7	-0.6	-0.3	-0.6	-0.2	-0.9	-0.8	0.7	-0.8	0.6	-0.4
MAI	-0.6	0.3	-0.3	-0.4	0.6	-0.9	-0.6	0.6	-0.7	-0.3	-0.7
OWE	-0.4	-0.4	0.8	0.5	-0.8	0.0	0.3	-0.1	-0.5	0.7	-0.1
PHC	-0.3	-0.1	0.7	0.4	-0.7	0.1	0.5	-0.1	-0.6	0.5	0.5
SOK	-0.4	-0.7	-0.6	-0.6	-0.9	-0.8	0.6	-0.9	-0.8	-0.5	-0.7
YEL	-0.8	0.5	0.4	0.4	-0.9	0.0	0.5	0.7	-0.4	-0.5	0.6
YOL	-0.1	0.4	0.6	0.8	-0.7	0.1	0.6	0.6	-0.6	0.7	-0.6
IBI	-0.8	-0.4	0.5	0.7	-0.8	-0.6	-0.6	0.6	-0.6	0.7	0.6

Source- Author's Analysis, (2018)

Table 2: 3 months moving average correlation analysis results between MQI and DMI during monsoon season for 1994-2004

Stns	1994	1995	1996	1997	1998	1999	2000	2001	2002	2003	2004
ABU	-0.4	-0.3	0.6	0.5	-0.4	0.0	-0.9	-0.3	0.7	-0.8	0.5
BEN	0.0	-0.6	-0.3	0.0	-0.3	-0.4	-0.9	-0.5	0.4	-0.5	0.4
CAL	-0.1	-0.1	-0.6	-0.5	0.6	-0.9	-0.2	0.0	0.1	-0.4	0.3
ENU	-0.1	-0.2	0.8	0.5	-0.5	0.0	0.1	-0.6	0.2	-0.7	0.0
IKE	0.8	-0.2	-0.7	-0.4	-0.1	0.1	-0.9	0.0	-0.2	0.8	0.4
ILO	0.1	-0.6	0.6	0.6	-0.7	-0.1	-0.5	0.2	0.6	-0.2	0.5
JOS	0.1	0.0	0.1	0.6	0.6	-0.2	0.0	-0.6	-0.3	-0.2	0.7
KAN	-0.9	-0.6	-0.5	0.2	0.3	0.1	-0.7	0.7	-0.7	-0.8	0.4
KAT	-0.8	-0.7	-0.8	0.3	-0.3	-0.9	0.0	0.7	-0.7	-0.8	0.8
MAI	-0.8	-0.7	0.7	0.5	0.0	-0.4	-0.5	0.9	-0.5	-0.9	0.8
OWE	-0.5	-0.2	-0.6	0.1	-0.5	-0.4	-0.1	-0.5	-0.6	0.2	0.0
PHC	-0.3	-0.4	-0.3	-0.2	-0.3	-0.1	-0.7	-0.4	0.0	-0.3	0.0
SOK	0.5	-0.7	-0.8	-0.5	0.2	-0.2	-0.1	0.9	-0.2	-0.7	0.8
YEL	-0.4	-0.6	0.7	-0.4	-0.5	-0.8	0.0	-0.7	-0.5	-0.5	0.6
YOL	0.1	-0.6	-0.9	0.6	-0.5	-0.3	-0.7	-0.8	-0.6	-0.8	0.6
IBI	0.1	-0.5	0.6	0.3	0.8	-0.7	-0.6	-0.7	0.0	-0.3	0.8

Source- Author's Analysis, (2018)

Table 3: 3 months moving average correlation analysis results between MQI and DMI during monsoon season for 2005-2015

Stns	2005	2006	2007	2008	2009	2010	2011	2012	2013	2014	2015
ABU	-0.3	0.5	0.1	-0.9	-0.1	-0.1	0.4	-0.2	0.6	0.8	0.7
BEN	-0.3	0.5	-0.5	-0.5	0.4	0.7	0.2	-0.6	0.6	0.5	0.3
CAL	-0.8	-0.9	-0.5	-0.7	0.3	0.7	-0.3	-0.6	0.4	0.5	-0.9
ENU	-0.2	0.6	0.1	-0.8	0.4	0.0	0.4	-0.6	0.6	0.7	-0.8
IKE	-0.8	-0.2	-0.6	-0.2	-0.8	0.0	-0.3	0.6	-0.1	0.3	0.2
ILO	-0.3	-0.5	0.1	-0.9	0.1	-0.5	0.0	-0.5	0.7	0.8	-0.6
JOS	0.5	-0.5	0.5	-0.7	0.1	0.7	0.1	0.3	0.7	-0.1	-0.8
KAN	0.8	0.8	0.5	-0.4	0.1	0.5	-0.7	0.4	0.7	0.7	0.6
KAT	-0.1	0.7	-0.6	-0.8	-0.2	0.6	0.7	0.4	0.7	0.9	0.7
MAI	0.7	-0.8	-0.8	-0.2	0.4	0.6	0.2	0.3	0.8	-0.3	-0.5
OWE	-0.3	0.6	-0.1	-0.2	0.5	-0.3	0.1	-0.5	0.6	0.8	-0.5
PHC	-0.3	0.6	-0.5	-0.3	0.2	-0.1	0.2	-0.4	0.2	0.7	0.3
SOK	-0.5	0.7	-0.7	-0.8	0.1	0.7	0.8	0.5	0.6	0.8	-0.7
YEL	0.5	-0.7	0.6	-1.0	0.5	-0.3	-0.8	0.0	-0.6	0.8	-0.8
YOL	-0.1	-0.3	0.0	-0.8	0.0	0.8	-0.7	0.1	-0.6	-0.1	-0.9
IBI	0.1	-0.6	0.1	-0.5	0.4	-0.7	-0.8	0.1	0.6	0.7	0.0

Source- Author's Analysis, (2018)

However, various researchers like Saji et al 1999, Yamagata et al, 2004 and from Bureau of Meteorology (BOM) website-www.bom.gov.au/climate/iod/, agreed to some positive and negative IOD years to cover the study period as follows; Positive IOD years (1983, 1991, 1994, 1997, 2003, 2006, 2007, 2008, 2012, 2015) while Negative IOD years (1985,1989, 1990, 1992, 1996, 1998, 2005, 2010).

Therefore, the comparison of the NMSR and IODMI Pearson correlations during the positive and negative IOD years as shown in Table 4, reveals that there is a negative correlation between NMSR and IODMI during some Positive IOD years- (1983, 1991, 2003, 2007, 2008, 2012 and 2015), while there is a positive correlation between NMSR and IODMI during some Negative IOD years- (1985, 1986, 1990, 1992, 1996 and 2010), hence, the contrasting tendencies to increase rainfall at a certain period of the year or decrease it at another period.

Table 4- Showing the comparison of the (pIOD) years/Negative correlation years and (nIOD) years/Positive correlation years

Positive (IOD) Years	Negative Correlation Yrs.	Negative (IOD) Years	Positive Correlation Yrs.
1983	**1983**	**1985**	**1985**
	1987		1986
	1988	**1990**	**1990**
1991	**1991**	**1992**	**1992**
	1995	**1996**	**1996**
	2000		1997
2003	**2003**		2004
2007	**2007**		2006
2008	**2008**	**2010**	**2010**
2012	**2012**		2013
2015	**2015**		

Source- Author's Analysis, (2018)

Table 4 also shows that the tendency of IODMI to reduce rainfall were expected during Positive IOD years while its tendency to increase rainfall were expected during Negative IOD years, however, this was also observed for all season (MAM, JJA and SON) in South Sudan (Omay, 2015).

Thus, the spatial pattern correlation analysis revealed a better nature of the contrasting tendencies of IODMI to either increase or decrease rainfall over the study area at certain periods of the Positive years (2003 and 2012) and Negative years (1990 and 2010) respectively, as shown in Figures 3 & 4.

Note: The red color depicts rainfall scenario while the blue color depicts drought scenario.

Moreover, Figure 3a shows the negative correlation between the NMSR and IODMI during the positive IOD in 2003, with observed widespread rainfall decrease which was also in agreement with the first quarter of Standardized Precipitation Index (SPI) hydrological bulletin that showed drought incidences in most synoptic stations in 2003, (E. Bello, Unpublished data). Hence, the contrasting effects during Positive IOD in 2012 may not be unconnected to the high incidence of rainfall that translated into a widespread flooding in 2012 amidst decreased rainfall in the southern Nigeria as shown in Figure 3b. However, it was termed the worst in 40yrs by National Emergency Management Agency, (NEMA) which affected 30 Nigeria's 36 states that killed 363people and displaced 2.1 million. (Reuter: November 5, 2012, retrieved November 26, 2012.).

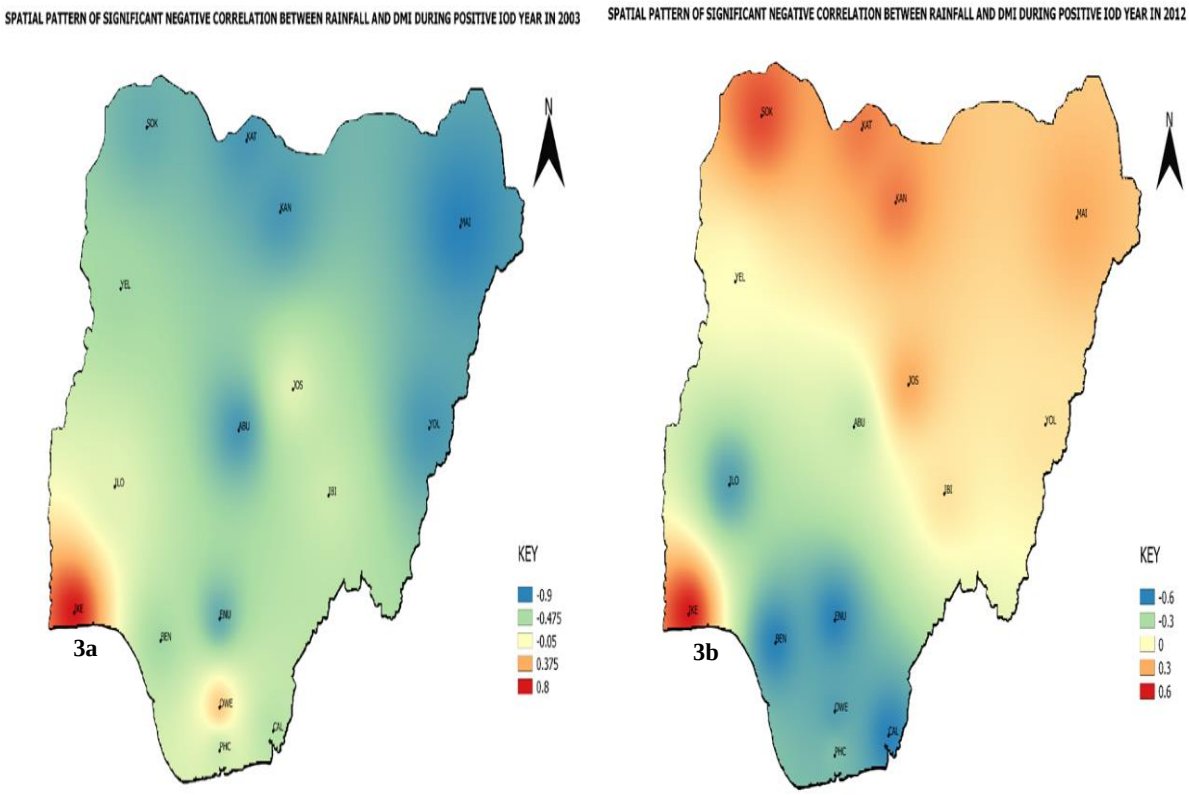

Figure- 3: Spatial Pattern of contrasting decreased and increased rainfall during Positive IOD in 2003 and 2012 respectively.

Thus, the positive correlation between the NMSR and IODMI during the 1990 negative IOD in Figure 4a, showed widespread rainfall increase that was in agreement with the reports of the observed 1990 flooding that took place in April 1990 which destroyed almost all the structures, worth over 2million naira and claimed more than 30 lives, damaged 100 houses, and over 15,000 rendered homeless near the major rivers in the city of Ibadan in the southwest region (Olawumi et al., 2015).

However, the contrasting effect of Negative IOD in 2010 shown in figure 4b, cannot be unrelated to the flood incidence that occurred in 2010 Usmanu Danfodiyo University Sokoto and other parts of the state, Magami et al. (2014) and also in Katsina which claimed 44 people with 20 missing and destroyed more than 500 houses. (Xinhua News Agency, retrieved on 17th July, 2017)

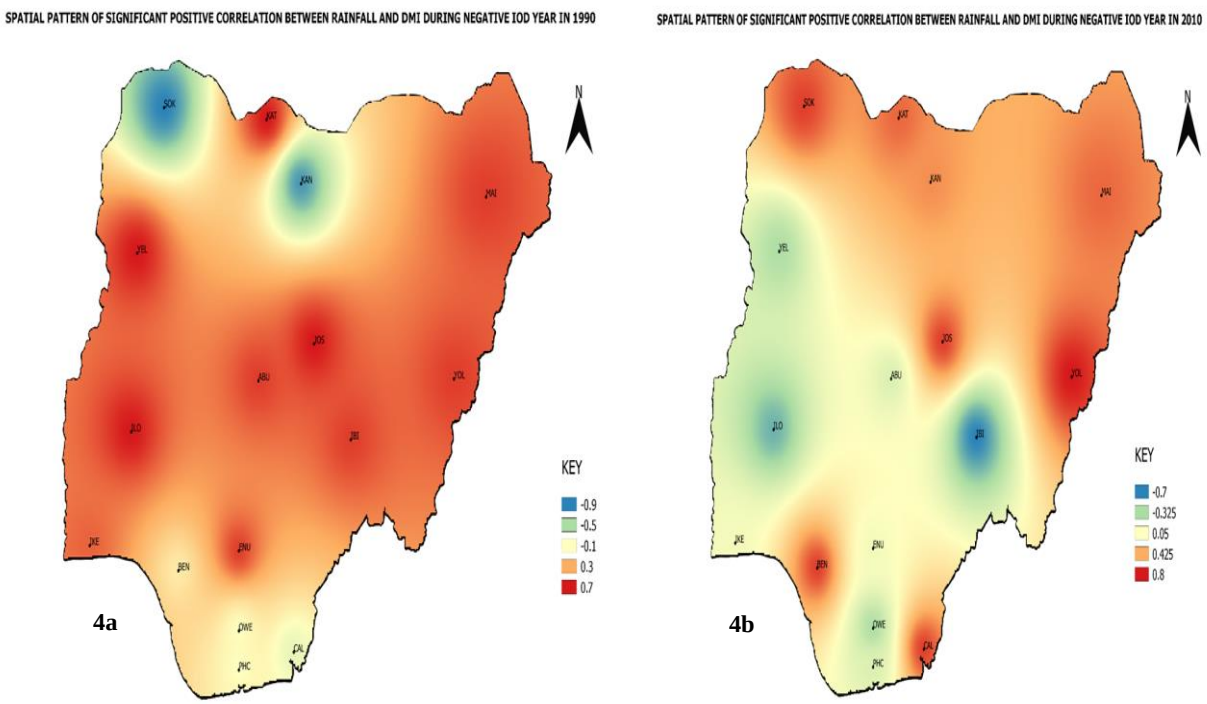

Figure- 4: Spatial Pattern of contrasting increased and decreased rainfall during Negative IOD in 1990 and 2010 respectively.

Furthermore, the test of the significance of the Pearson correlation coefficient (r) between the NMSR and IODMI was done using two methods namely;

i) P-value
ii) Critical r value

However, both methods showed that the correlation is significant at 10% level in some years within the study period with most of the stations in the northern part of the country for instance, Sokoto, Kano, Katsina, Maiduguri, Yelwa, Yola, Jos, Abuja and Ibi while the stations like Enugu, Calabar, Ilorin, Ikeja, Benin, Owerri, Portharcourt, over the southern part of the country had fewer significant correlations as shown in Table 5.

Table 5- Years with significant Pearson correlation between MQI and DMI during monsoon period at 10% level of significance

NORTHERN STATIONS	**POSITIVE CORRELATION YEARS**	**NEGATIVE CORRELATION YEARS**	**No. of Yrs. with non-Sig. r from 1983-2015**	**No. of Yrs. with Sig. r from 1983-2015**	**No. of Yrs. with Sig. r coefficient (%) from 1983-2015**
SOKOTO	2001,2004,2006,2010,2011, 2014	1984,1987,1988,1990,1991,1993,1995, 1996, 2003,2007, 2008,2015	15	18	54
KANO	1984,1992,2001,2005,2006, 2013, 2014	1988,1989,1990,1991,1994,2000,2002, 2003, 2011	17	16	48
KATSINA	1990,2001,2004,2006,2011, 2013, 2014	1988,1989,1991,1994,1996,1999,2002, 2003, 2008	17	16	48
MAIDUGURI	1996,2001,2004,2005,2013	1988,1991,1993,1994,2003,2006,2007	21	12	36
YELWA	1990,1996,2014	1983,1987,1999,2001,2006,2008,2011, 2015			33
JOS	1990,2004,2010,2013	1983,1987,1991,1993,2008,2015	23	10	30
YOLA	1986,1992,2010	1996,2001,2003,2008,2001,2015			27
IBI	1992,1998,2004,2014	1983,1987,1999,2011	25	8	24
SOUTHERN STATIONS	**POSITIVE CORRELATION YEARS**	**NEGATIVE CORRELATION YEARS**	**No. of Yrs. with non-Sig. r from 1983-2015**	**No. of Yrs. with Sig. r from 1983-2015**	**No. of Yrs. with Sig. r coefficient (%) from 1983-2015**

ENUGU	1985,1986,1992,1996,2014	1983,1986,1987,1988,2003.2008,2015	22	11	33
CALABAR	1984,1992,2010	1983,1993,1999,2005,2006,2008,2015	23	10	30
ILORIN	1985,1986,1990,2014	1987,1993,1998,2008	25	8	24
IKEJA	1994,2003	1991,1996,2000,2005,2009	26	7	21
BENIN	1992,2010	1983,1991,2000	28	5	15
OWERRI	1985,1992,2014	1987	29	4	13
PORTHARCOURT	1985,2014	1987,2000	29	4	12

Source- Author's Analysis, (2018). Correlation is significant at the 10% level (2-tailed).

Furthermore, the comparison of the nature of the teleconnection between NMSR with IODMI and ENSO indices, showed that Positive IOD index negated the effects of ENSO which resulted in increased Nigerian Monsoon Seasonal Rains in 1983, 1994, 1997 and 2003 as shown in Table -6.

Table 6- shows how the Positive IOD and ENSO negates their effects in 1983, 1994, 1997 and 2003. Negative IOD negates ENSO effects in 1990.

Stns	Positive IOD -1983	ENSO - 1983	Negative IOD -1990	ENSO-1990	Positive IOD-1994	ENSO-1994	Positive IOD-1997	ENSO-1997	Positive IOD-2003	ENSO-2003
ABU	-0.6	-0.3	0.6	-0.4	-0.4	0.2	0.5	0.4	-0.8	0.3
BEN	-0.9	0.4	0.0	0.7	0.0	0.6	0.0	-0.2	-0.5	0.6
CAL	-0.8	0.6	-0.2	0.8	-0.1	0.6	-0.5	-0.7	-0.4	0.6
ENU	-0.9	0.7	0.6	-0.4	-0.1	0.6	0.5	0.3	-0.7	0.0
IKE	0.1	-0.9	0.5	-0.6	0.8	0.4	-0.4	-0.3	0.8	0.3
ILO	-0.2	-0.6	0.7	-0.5	0.1	0.7	0.6	0.5	-0.2	0.8
JOS	-0.8	0.8	0.7	-0.3	0.1	0.8	0.6	0.5	-0.2	0.7
KAN	-0.4	0.8	-0.8	-0.1	-0.9	-0.8	0.2	0.0	-0.8	0.2
KAT	-0.7	0.9	0.7	-0.2	-0.8	-0.5	0.3	0.2	-0.8	-0.5
MAI	-0.6	0.9	0.6	-0.3	-0.8	-0.6	0.5	0.3	-0.9	-0.3
OWE	-0.4	-0.6	-0.1	0.8	-0.5	0.2	0.1	-0.2	0.2	0.9
PHC	-0.3	-0.6	-0.1	0.8	-0.3	0.4	-0.2	-0.4	-0.3	0.6
SOK	-0.4	0.9	-0.9	0.3	0.5	0.9	-0.5	-0.7	-0.7	0.3
YEL	-0.8	0.8	0.7	-0.4	-0.4	0.3	-0.4	-0.6	-0.5	0.6
YOL	-0.1	-0.8	0.6	-0.4	0.1	0.7	0.6	0.5	-0.8	-0.5
IBI	-0.8	0.8	0.6	-0.4	0.1	0.7	0.3	0.2	-0.3	0.6

(Source- Author's Analysis, 2018).

However, it agrees with what has been demonstrated in the works done by (Behera et al. 1999, Webster et al., 1999) where a Positive IOD index often negated the effect of ENSO that resulted to increased monsoon rains in some ENSO years like the 1983 and 1994.

Meanwhile, 2003 Positive IOD year coincided with the Negative correlations between the NMSR/IODMI while in the same year the Pearson correlation coefficient between the NMSR/ENSO were positive. Hence, Positive IOD = Negative Correlation while ENSO of the same year = Positive Correlation as shown in table 6. However, this is supported with Figures 5a&b that shows the spatial pattern of the contrasting relationship of IODMI and ENSO indices with NMSR in 2003.

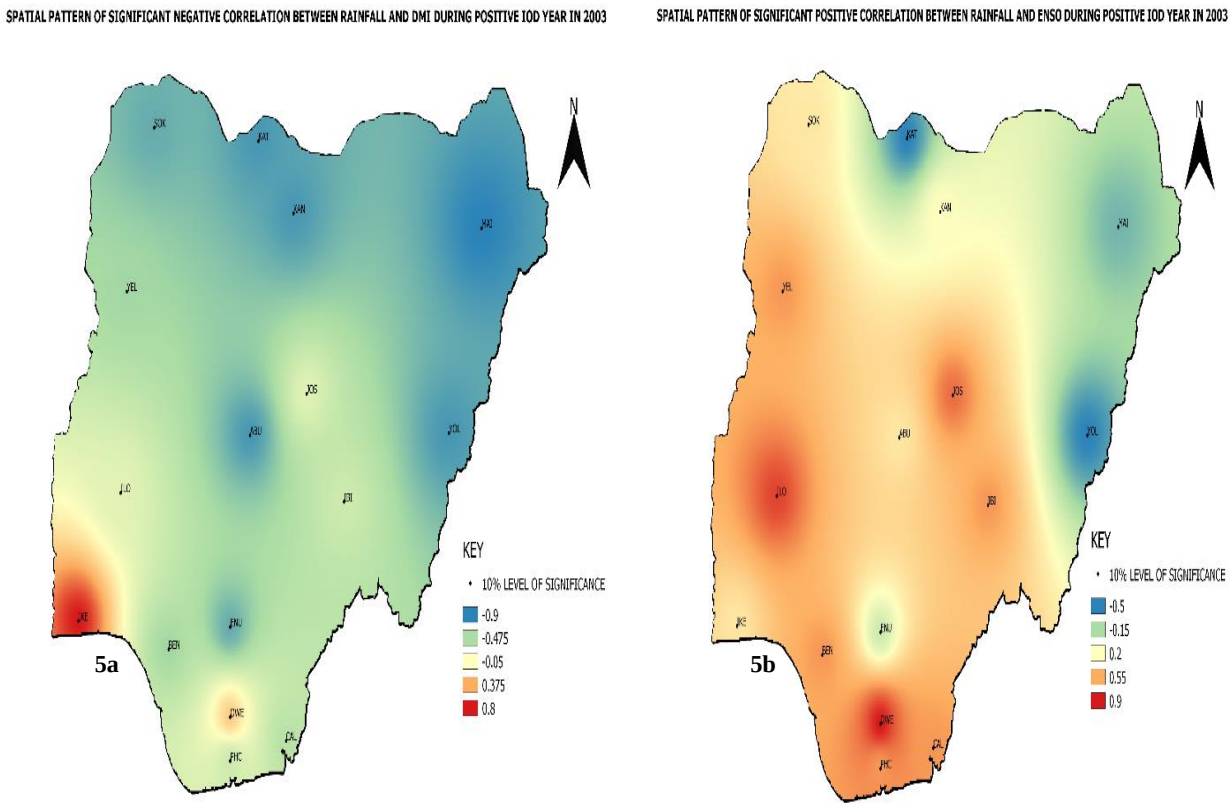

Figure 5: Spatial Pattern of the reverse effects of relationship between Positive IOD and ENSO on NMSR in 2003

In contrast to the aforementioned, during the 1990 Negative IOD year it coincided with the Positive Correlations between the NMSR/IODMI while in the same year, the Pearson correlation coefficient between the NMSR/ENSO were weaker Positive correlations as shown in Table 6. Hence, Negative IOD = Positive Correlation while ENSO of the same year = Negative Correlation however, this is supported with Figures 6a&b that shows the spatial pattern of the contrasting relationship of IODMI and ENSO indices with NMSR in 1990.

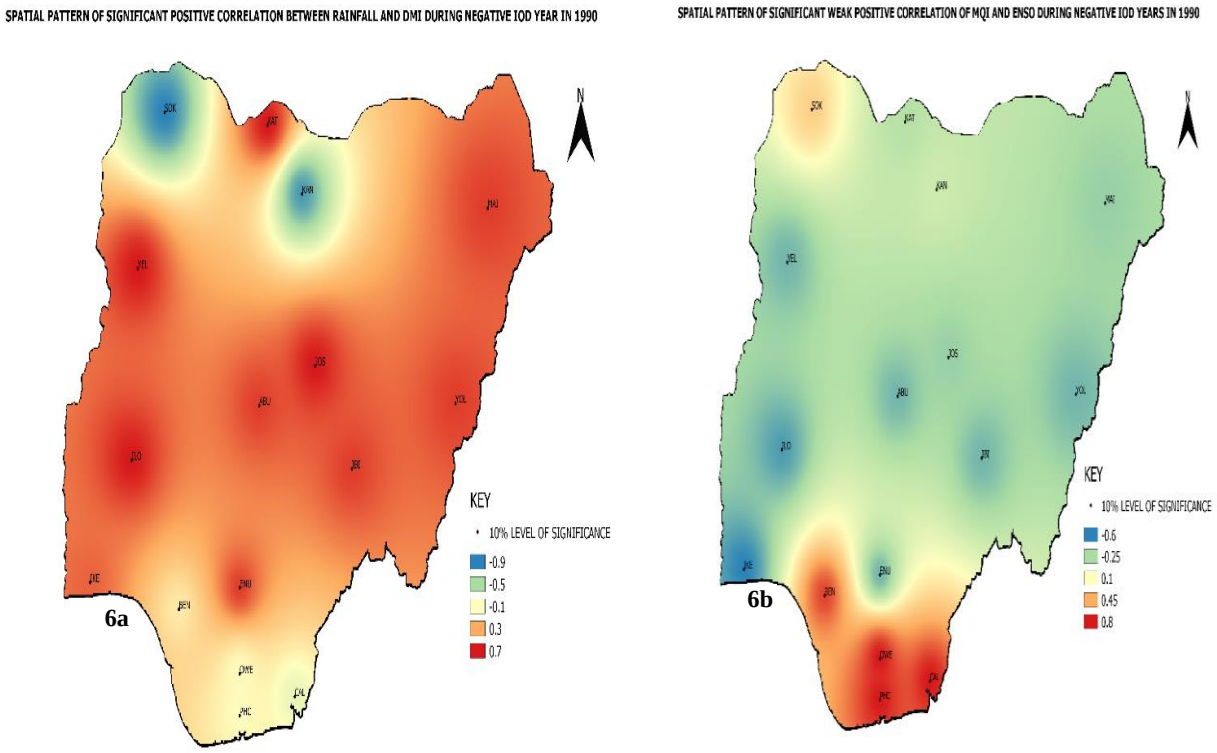

Figure 6: Spatial Pattern of the reverse effects of relationship between Negative IOD and ENSO on NMSR in 1990

Interestingly, this suggests that in 2003, the positive correlation between NMSR and ENSO resulted to negative correlation with the IODMI. Therefore, this means that the higher correlation between NMSR/ENSO was responsible for the reduced rainfall over the most parts of the selected synoptic stations during the 2003 Positive IOD year as shown in Figure 3a. However, in 1990 the weaker positive correlation between the NMSR and ENSO resulted to positive correlation with the IODMI, hence the weaker positive correlations between ENSO/NMSR was responsible for the high rainfall on most parts of the selected synoptic stations as shown in Figure 4a.

This is in agreement with the work by Ashok et al (2001), that whenever the ENSO- Indian Summer Monsoon rainfall (ISMR) correlation is low (high) the IOD-ISMR correlation is high (low.) where for instance, in 1990 a weak correlation between the Indian Monsoon and ENSO resulted to an intense and frequent Dipole Mode events.

Furthermore, the research shows that Pearson correlation coefficient between IODMI and NMSR were significant at 10% level with more percentage of significance over the stations in the northern part compared to stations in the southern part of the country as shown in bar chart and spatial pattern map in Figure- 7a &8a.

Conversely, the Pearson correlation coefficient between ENSO and NMSR were significant at 10% level with a strong and broad percentage of significance across all the stations except for Lagos that had the lowest significant correlation as shown in Figure-7b & 8b. The low significant correlation over Lagos is in agreement with the work done by Nnawuike, (2016) that revealed that ENSO has no significant relationship with the rainfall over the southwestern Nigeria.

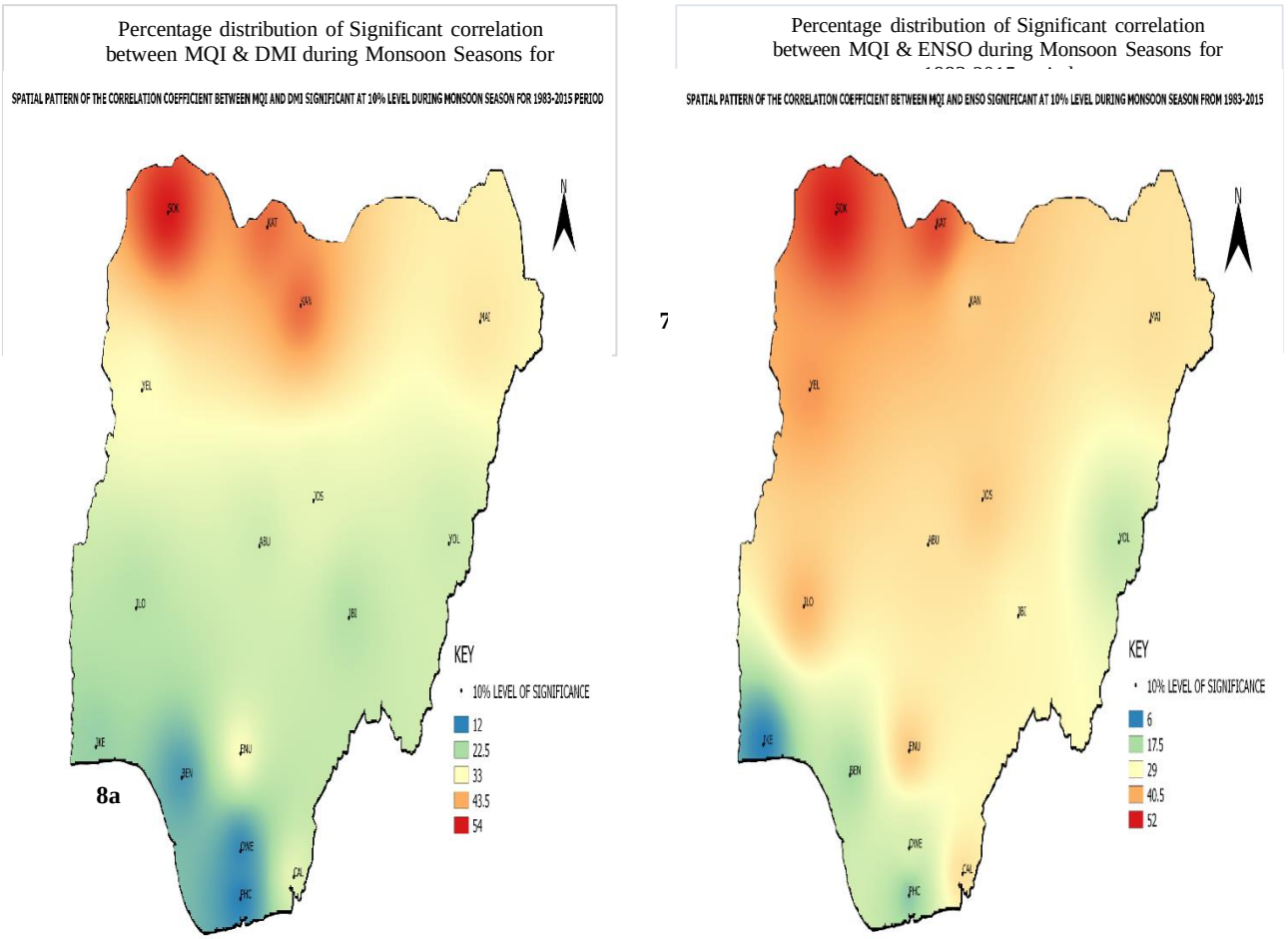

Figure 7- shows the percentage distribution of significant correlation between MQI&DMI (left) and MQI&ENSO (right) during the Monsoon Seasons for 1983-2015 period.

Figure 8: Spatial Correlation Coefficient between the NMSR/IODMI and NMSR/ENSO significant at 10% level from 1983-2015.

CONCLUSION AND RECOMMENDATION

This research work has to a great extent found the existence of a teleconnection between the Nigerian Monsoon Seasonal Rainfall, (NMSR) and the Indian Ocean Dipole based the Pearson correlation coefficient results that were tested by two different tests of significance (Critical r and p-Value) and were found to be significant at 10% over the selected synoptic stations in Nigeria over the 33yrs period, (1983-2015).

This research has also further proven that the El Nino Southern Oscillation (ENSO) which is one of the major indices used by Nigerian Meteorological Agency (NiMet) for weather and climate predictions may not be the only indices that have teleconnection with the weather outcomes over Nigeria.

However, the analysis showed that the impact of IODMI is felt more over the Sahel region of Nigeria, perhaps with ENSO impact in dominance over the selected stations in Nigeria especially over the Sahel region. Hence, the results showed similar pattern of influence of IODMI and ENSO on NMSR to decrease from north to south over selected stations in Nigeria.

Recommendations:

This study examined only the teleconnection between sea surface temperature (SSTs) over Indian Ocean and equatorial Pacific Ocean with the Nigerian Monsoon Seasonal Rainfall. Hence, further research should include other indices affecting monsoon rainfall over Nigeria for instance Outgoing Long-wave Radiation (OLR), winds and pressure systems etc.

Government and relevant agencies like NiMet, Nigerian Hydrological Services Agency (NIHSA), National Emergency Management Agency (NEMA) etc. should work harmoniously to enhance the resilience of Nigerian communities through mainstreaming and incorporating Indian Ocean SSTs as part of the weather components in weather monitoring and forecasting especially for the seasonal rainfall prediction (SRP) to various weather-dependent sectors like agricultural production and food

security sector and in prevention/ mitigation of weather related hazards like flooding, drought etc. especially in this era of climate change.

References:

Adeniyi, M. O. (2014). Variability of daily precipitation over Nigeria. *Meteorology and Atmospheric Physics, 126(3-4):161-176.* DOI: 10.1007/s00703-014-0340-6.

Ashok, K., Guan, Z., &Yamagata,T. (2001). Impact of the Indian Ocean Dipole on the relationship between the Indian monsoon rainfall and ENSO, Geophys.Res.Lett., 28, 4499–4502, doi:10.1029/2001GL013294.

Behera S. K., R. Krishnan & T. Yamagata, (2005)*.Paramount impact of the Indian Ocean Dipole on the East African short rains: A CGCM Study. J. Climate 18, 4514–4530.

Behera, S. K., R. Krishnan & T. Yamagata, (1999)*. Unusual Ocean-Atmosphere conditions in the tropical Indian Ocean during 1994. Geophys. Res. Lett. 26, 3001-3004.

Black, E.,Slingo, J.& Sperber, K. R. (2003). An observational study of the relationship between excessively strong short-rains in coastal East Africa and Indian Ocean SST,*Mon. Weather Rev.*, **131**,74–94.

Cherchi, A., and Navara, A. (2013). Influence of ENSO and of the Indian Ocean Dipole on the Indian summer monsoon variability. Clim. Dyn. 41:81-103

Guanghan, A., Stanb, C., Hoell, A., Weaver, A., &Waylen, P. (2016). Inter- and Intra-annual precipitation variability and relationships to ENSO and the IOD in the southern Africa. *Int. J. of Climatol.* 36:1643-1656, doi:10.1002/joc.4448

Gouda, K., Sahoo, S., Samantray, P., & Shivappa, H. (2017). Comparative Study of Monsoon Rainfall Variability over India and the Odisha State. Climate, Vol.5,79 doi:10.3390/cli5040079

Janicot, S., Harzallah, A., Fontaine, B. & Moron, V. (1998). West African Monsoon dynamics and eastern equatorial Atlantic and PacificSST anomalies (1970-1988). *J. Climate* **11,** 1874–1882.

Janowiak, J. E. (1988). An investigation of interannual rainfall variability in Africa. *J. Climate* **1,** 240–255.

Magami, I., Yahaya, S., and Mohammed, K., (2014). Causes and Consequences of flooding in Nigeria: A Review. Biological and Environmental Sciences Journal for the Tropics 11(2), June, 2014, ISSN 0794-9057, pp 154-162.

Murtugudde, R. G., McCreary, J. P., & Busalacchi, A. J., (2000). Oceanic processes associated with anomalous events in the Indian Ocean with relevance to 1997–1998. *J. Geophys. Res.*, **105,** 3295–3306.

Nicholson, S.E. (2012). The West African Sahel: A Review of Recent Studies on Rainfall Regime and its interannual variability. ISRN Meteorology, Vol. 2013, Article ID 4535221, pp.1-32,http://dx.doi.org/10.1155/2013/453521.

Nigerian Meteorological Agency (NIMET), (2015). Monthly historical rainfall data, NiMet Archive. Retrieved July, 15, 2015.

Nnawuike, N (2016). Assessment of the impact of El Nino- Southern Oscillation (ENSO) events on rainfall amount in South-Western Nigeria. J. Physical Science and Environmental Studies, Vol.2 (2) PP.23-29. ISSN 2467-8775.

NOAA, (2014). Aglobal merged land, air and sea surface temperature reconstruction based on historical observations (1880-1997), J. Clim., 18, 2021-2036.

Olawumi, O.P.,Popoola, A.S., Blukale, A.T., Eluyele, K.P., Adegoke, J.O., (2015). An Assessment of the Factors Responsible for Flooding in Ibadan Metropolis, Nigeria. J.Environ.and Earth Sci., vol.5, 1-7, ISSN224-3216(Paper).

Preethi, B., Sabin, T. P., Adedoyin, J. A., Ashok, K. (2015). Impacts of the ENSO Modoki and other Tropical Indo-Pacific Climate-Drivers on African Rainfall. Sci. Rep. 5, 16653, doi:10.1038/srep16653

Rasmussen, E. M. & Carpenter, T. H. (1983). The relationship between eastern equatorial Pacific sea surface temperatures and rainfall over India and Sri Lanka. *Mon. Wea. Rev*. **111,** 517–528

Saji N. H., Goswami B. N., Vinayachandran P. N. & Yamagata T. (1999). A dipole mode in the tropical Indian Ocean. Nature 401, 360–363. [PubMed].

Saji, N. H.,&Yamagata, T. (2003). Structure of SST and surface wind variability during Indian Ocean Dipole mode events: COADS observations, *J. Clim.*, **16**, 2735–2751.

ScienceDirect, (1977). *Hydrology and Water Resources in Tropical Africa*, vol.8,pp. 2-6, 11-208. edited by Jaroslav Balek.

Schott, F.,&McCreary, J. P. (2001).The monsoon circulation of the Indian Ocean, *Prog.Oceanogr.*, **51**, 1–123.

Sylla, M.B., Diallo, I. & Pal, J.S. (2013). West African Monsoon in State-of-the-Science Regional Climate Models. INTECH open science/open minds. pp. 1-36. http://dx.doi.org/10.5772/55140.

Ummenhofer C. C., Sen G. A., England M. H. & Reason C. J. C. (2009). Contributions of Indian Ocean Sea surface temperatures to enhanced East African rainfall. J. Climate 22, 993–1013.

Ukhurebor, K.E & Abiodun, I.C (2018). Variation in Annual Rainfall Data of Forty Years (1978-2017) for South-South, Nigeria, J. Appl. Sci. Environ. Manage. Vol. 22(4), 511-518.

Usman M.T. (2000). An instability index for monsoon onset characterization over Nigerian Sahel. Environ.Rev,3(1):367-379.

Vinayachandran, P. N.,Kurian, J. & Neema, C. P. (2007), Indian Ocean response to anomalous conditions in 2006, *Geophys. Res. Lett.*, **34**, L15602, doi:10.1029/2007GL030194

Construction and Synthesis of Carbon Nanostructures via Domestic Microwave Oven

Kure Nicodemus, Ahmad Danladi Adamu, Daniel Isaac Hyuk & Ismail Lakin

Abstract

In this work, a quick and effective method to synthesize carbon nanotubes (CNTs) is presented. Here a 600 W commercial microwave oven operating at 2.45 GHz was utilized to synthesize CNTs from plasma catalytic decomposition of polyethylene. It is shown that the use of carbon source, catalyst, and commercial microwave oven to induce plasma is necessary to carry on this synthesis. The CNTs were synthesized at 750 °C under atmospheric pressure of 0.81 mbar. Field Emission Scanning Electron Microscope (FESEM), Thermogravimetric Analysis (TGA), and Raman spectroscopy were utilized to confirm the presence and quality of produced carbon nanomaterials. Finally a comparison between the use of Polyethylene and Rick Husk as the carbon precursor was also presented.

1. Introduction

The synthesis of novel structure of carbon nanotubes (CNTs) using commercial microwave oven has received much attention in recent years. This increased focus was due to synthesis techniques becoming more expensive and time consuming. The microwave assisted synthesis technique has attracted much attention over the conventional techniques such as chemical vapour deposition (CVD), laser ablation, Hipco, and arc discharge due to its advantages, which include volumetric heating, rapid reaction time, economic and environmental friendliness [1]. Carbon structures have proven strong potentials in revolutionizing wide range of applications globally. CNTs are made of hexagonal network of sp^2 hybridization of carbon atoms that is similar to graphene [1]. CNTs are the strongest materials due to carbon-carbon σbonds and can be mainly categorized into single wall carbon nanotubes (SWCNTs) and multiwall carbon nanotubes (MWCNTs) [2]. They consist of honeycombed lattice carbon sheets with interlayer spacing of 0.32–0.35 nm and 2 to 50 sheets tubules range of wall thickness [3].

Novel structure of CNTs has led to their remarkable properties including high chemical stability, excellent electrical conductivity, and high mechanical properties [4]. Compared to CNTs, graphene possesses special features, for instance, high reactivity of graphene edge [5] and high light transmittance [6]. Exceptional electrical, mechanical, thermal, and electrochemical properties are exhibited by CNTs; it is widely used in semiconductor, sensor, superconductive electrode, drug delivery, and other forms of electronics [7].

Innovative approach was employed in this study, with an attempt to develop a technique that can synthesize CNTs economically within the shortest possible time by using a commercial microwave oven in a batch synthesis process. To date, solid carbon materials are good microwave absorbers due to their dielectric properties which makes them conducting polymers and gives them crucial roles in

CNTs growth. The plasma created as a result of electromagnetic interactions provides the required temperature for catalytic decomposition of the starting materials.

2. Experiment

This section presents detailed experimental procedure carried out.

2.1. Synthesis of Carbon Nanomaterials

The commercial microwave oven was modified with quartz tube of volume 1860 mL. Polyethylene ((C_2H_4)) [8] and Rice husks (RH) [9] were used as carbon source. The carbon source has a very high dielectric tangent loss at 2.45 GHz [10] which enables fast decomposition into carbon species over the catalyst nanoparticles. The catalyst (Iron oxides) was impregnated on the silicon substrate using drop casting process and was calcinated in a furnace at 200 °C for 30 minutes to evaporate the ethanol residue [11]. The sample was then placed at the centre of the quartz tube inside the microwave oven (Samsung M539 MAN200405W), 600 W power and 2.45 GHz frequency (household microwave frequency). Prior to microwave plasma irradiation, the quartz tube was evacuated into base pressure of 0.81mbar. Deposition time was employed for 4 - 38 minutes. It has also been reported that under plasma radiation amorphous carbon forms if the process exceeds 40 minutes. The tube pressure was controlled by a rotary pump and a leak valve. No additional heater was installed in the system for substrate heating; however the substrate temperature could increase with increasing growth time. A K-type thermocouple was used to measure the synthesis temperature at 750 °C. The final products were allowed to reach room temperature and then collected for characterizations. The time this method took from turning on the microwave till collecting the sample was about 1 hour.

2.2. Material Characterization

The microstructure morphological analysis was performed using a field emission scanning electron microscope (FESEM) operated at 10 kV. High resolution of the sample was viewed using High Resolution Transmission Electron Microscope (HRTEM) and Dispersed X-rays (EDX) analysis were obtained using a FEI Tecnai G2 F20 XTWIN. The crystalline structure was investigated via Raman spectroscopy using Witec Alpha 300R with laser excitation wavelength of 532 nm. To determine the amount of catalyst impurities thermal gravimetric analysis (TGA) under air was utilized.

3. Results and Discussion

Figures 1 show the schematic diagram of Household Microwave Oven technique for derivation of carbon nanomaterials from the carbon precursors. The Raman analysis of polyethylene carbon precursor showed in Figure 2(a) indicates two prominent peaks at 1604 cm^{-1} and 1336 cm^{-1}, corresponding to ordered carbon atom, G-band and disordered carbon atom, and D-band, respectively, as a result of first-order Raman scattering [8] as compared with RH [9]. These peaks were associated with both CNTs and graphite [2]; the CNTs quality can be estimated from intensity ratio of D-band (*I*D) and G-band (*I*G) [3, 11]. Intensity ratio of these peaks, *I*G/*I*D, is calculated to be 0.98, which indicates that the graphitized material has defects [12] compared with RH which has 1.013 [9]. The high intensity of D-band arises from the distorted carbon atoms on the surface and edges as well as sp^3 bonding which serve as impurity [1]. The small peaks at 135.81 cm^{-1} and 240.29 cm^{-1} are described as radial breathing mode (RBM), associated with SWCNTS while the peak at 519.88 cm^{-1} represents signal from Si substrate as depicted in Figure 2(b), also present in RH carbon precursor. The diameter, *d*, of the SWCNTs is estimated from the RBM peak position, ωas $d = 248\ (cm^{-1})\ (nm)/\omega\ (cm^{-1})$ [13], which yield diameters of about 1.83 nm and 1.03 nm, respectively.

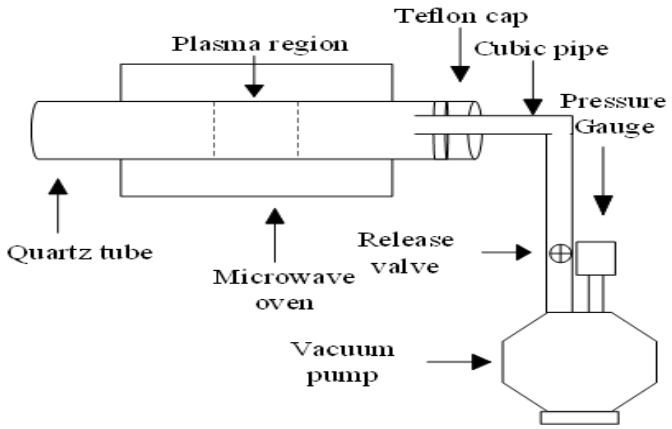

Figure 3. Schematic of experiments setup

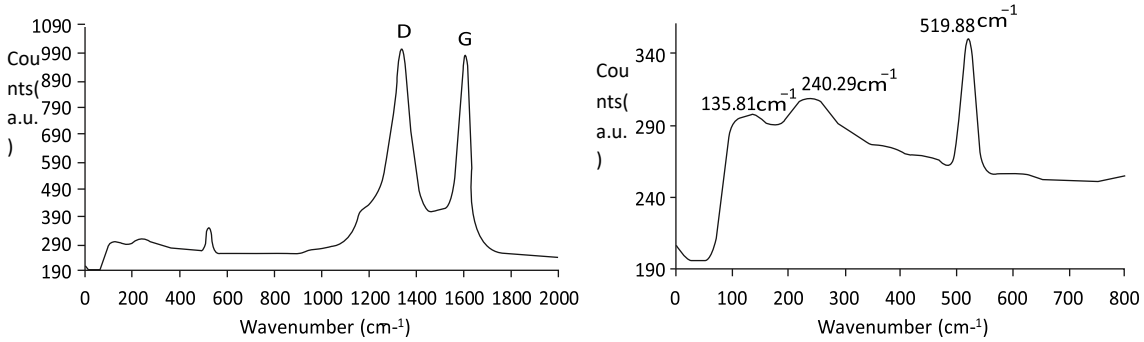

Figure 2. (a) Raman spectra showing the RBM, the D and G peaks of the CNTs (b)Raman spectra showing RBM mode of CNTs at different scale.

Figures 3(a) and 3(b) show FESEM morphological images of CNTs grown on silicon substrate, obtained from plasma catalytic decomposition of polyethylene as carbon precursor. The CNTs consist of SWCNTs and MWCNTs which we could confirm due to the presence of RBM [2]. CNTs diameters are in the range of 1.03–25.00 nm and are formed in entangled bundles due to catalyst nanoparticles movement under microwave irradiation when carbon species diffuses across substrate. The CNTs are elongated and measured about 0.85 μm. At high magnification, sample shows the CNTs are made up of entangled individual CNTs. The irregularities in CNTs shape and diameter are attributed to high D-band level. The arrows indicate the presence of catalyst embedded within the tube walls which is one of the characteristics of most CNTs synthesized in microwave oven[1,8, 14].The encapsulated catalyst within the tubes was due to capillarity action possibly as a result of interaction between the catalyst and substrate [1]. Figures 3(c) and 3(d) show HRTEM images which indicate CNTs are graphitized in conformity with Raman spectra and FESEM results. From these images the interlayer spacing between CNTs lattice was measured to be in the range of 3.2˚A to 4.2˚ A. Based on the EDX result, the percentage of elementary composition in the sample was revealed as shown in Table 1. Carbon is the dominant element while oxygen percentage was quite negligible.

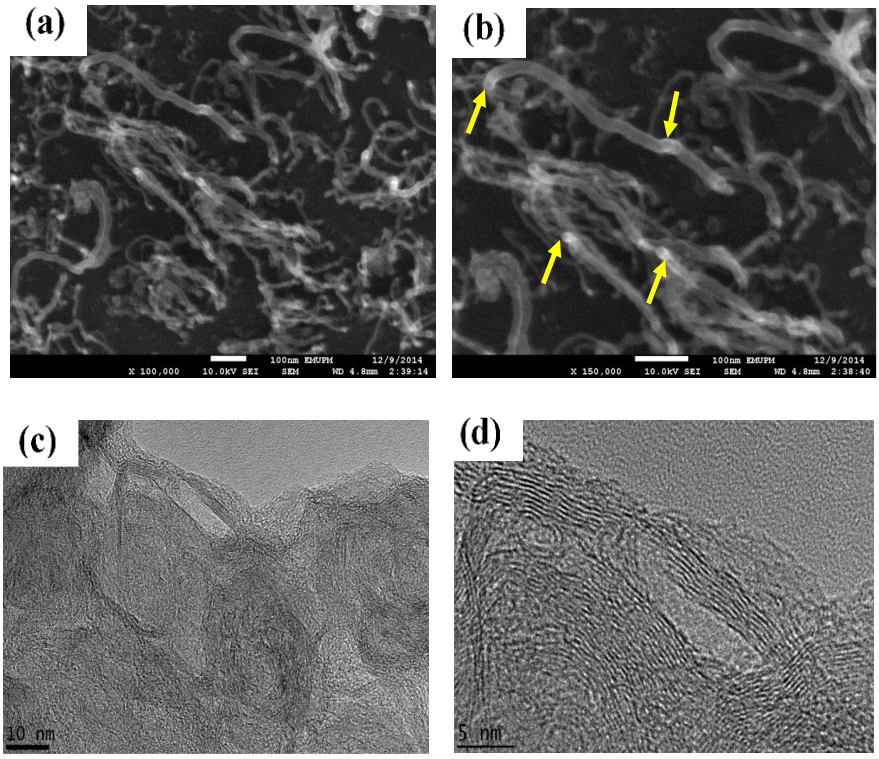

Figure 3. (a) - (b) FESEM image of CNTs at different magnification (c) - (d) HRTEM image of CNTs at different magnification.

Table 1. EDX of the CNTs.

Element	Weight (%)	Atomic (%)
C(K)	99.86	99.90
N(K)	0.00	0.00
O(K)	0.10	0.08
Si(K)	0.02	0.00
Fe(K)	0.00	0.00

The TGA result shown in Figure 5 indicates a rapid oxidation of CNTs from 540°C to 640°C with 90% sample weight loss; the sharp peak observed from DTGA result corresponds to this region. At

640 °C the sample contains 2% residue which continues to drop gradually to 1.3% at 1000 °C. From these results we could conclude that the growth mechanism of CNTs via microwave irradiation is similar to the CVD method in which the carbon atoms dissolve in catalyst particles until the dissolved materials reach saturation which results in CNTs growth. Decomposition of polyethylene and RH molecules to individual carbon atoms as a result of volumetric heating via plasma induced by microwave irradiation [15] would be the main difference in this technique with CVD.

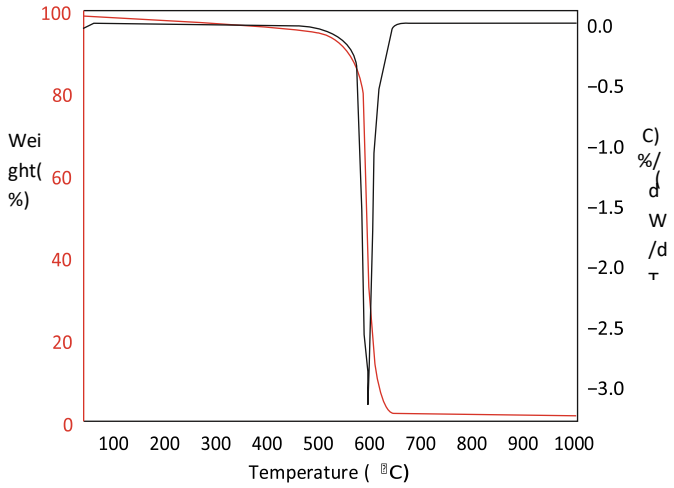

Figure 4. TGA and DTGA result of as-synthesized CNTs.

4. Conclusion

This study have demonstrated a short period of time process using the commercial microwave oven as the heating system of Carbon Precursors (Polyethylene and RH). It offers an alternative technique of synthesizing CNTs at low cost using efficient procedures which can be scaled up for mass production. It is necessary to use carbon source, catalyst, and commercial microwave oven to induce plasma. The plasma enhances and speeds up the catalytic decomposition of the carbon precursors in presence of catalyst. CNTs was obtained, similar to most chemical vapor deposition techniques. Raman spectroscopy and FESEM analysis reveal CNTs produced are in diameter range of 1.03–25.00 nm with length of about 0.85 μm. HRTEM confirms that CNTs are graphitic in structure. EDX analysis shows that CNTs are produced with about 98% carbon purity.

5. Reference

[1] Bajpai R and Wagner H D 2015 *Fast growth of carbon nanotubes using a microwave oven. Carbon.***82** 327–336

[2] Dresselhaus M S,Dresselhaus G, Jorio A, Souza Filho A G and Saito R 2002*Raman spectroscopy on isolated single wall carbon nanotubes. Carbon.***40**(12) 2043–2061
[3] Liu W W, Chai S P, Mohamed A R and Hashim U 2014 *Synthesis and characterization of graphene and carbon nanotubes: a review on the past and recent developments. Journal of Industrial and Engineering Chemistry*. **20**(4)1171– 1185
[4] Hong E H, Lee K H, Oh S H and Park C G 2003 *Synthesis of carbon nanotubes using microwave radiation. Advanced Functional Materials*.**13**(12) 961–966
[5] Whitener K E and Sheehan P E 2015*Graphene synthesis. Diamond and Related Materials.***46**25–34
[6] Nair R R, Blake P, Grigorenko A N 2008 *Fine structure constant defines visual transparency of graphene. Science*.**320**(5881) 1308
[7] De Volder M F L, Tawfick S H, Baughman R H, and Hart A J 2013 *Carbon nanotubes: present and future commercial applications, Science*.**339**(6119) 535–539
[8] Kure N, Hamidon M N and Azhari S 2017 *Simple microwave-assisted synthesis of carbon nanotubes using polyethylene as carbon precursor. Journal of Nanomaterials*. **2017**1-4.
[9] Asnawi M,Azhari S, Hamidon M N, Ismail I, Helina I 2018 *Synthesis of Carbon Nanomaterials from Rice Husk via Microwave Oven. Journal of Nanomaterials*. **2018** 1-5
[10] Hotta M, Hayashi M, Lanagan M T, Agrawal D K and Nagata K 2011 *Complex permittivity of graphite, carbon black and coal powders in the ranges of X-band frequencies (8.2 to 12.4 GHz) and between 1 and 10 GHz. ISIJ International*. **51** (11)1766–1772
[11] Z. Yunusa Z, Abdul Rashid S, Hamidon M N, Hafiz S, Ismail I and Rahmanian S 2015 *Synthesis of Y-tip graphitic nanoribbons from alcohol catalytic chemical vapor deposition on piezoelectric substrate. Journal of Nanomaterials*. **2015**1-7
[12] Hojati-Talemi P and Simon G P 2010 *Preparation of graphene nanowalls by a simple microwave-based method. Carbon.*48(14) 3993–4000

Flood Warning And Mitigation: the Critical Issues of Water Level Forecasting

Ocheme, J. E.; Octache, M. Y.; Musa, J. J.; and Ezekiel, L. P

Department of Agricultural and Bioresources Engineering, Federal University of Technology,Minna.

ochemejohn1211@gmail.com

Abstract

Prediction of the pattern of water level is one of the benchmark in flood forecasting and analysis; this has become one of the most important issues in hydrological research. Water level is an essential component in the process of flood warning and mitigation strategies. This review revealed that water level study is an essential component in any purported flood warning and mitigation designs. Worthy of mentioning in this context is the need for effective water levelforecasting. However, the development of any forecasting system is highly fraught with encumbrances like hysteresis in the stage hydrograph due to random behaviour of river flow regime and uncertainty. Thus, within the general context of the discourse, the critical issues are the determination of appropriate forecast model, forecast lead time, and suitable water level for standby alarms and areal alert.

Keywords: Floods, flood warning, water level prediction, emerging issues

1. Introduction

Flooding is considered as one of the major threats to human civilization and is directly attributed to heavy rainfall leading to loss of human life, properties, infrastructure damage, as well as huge economic losses (Kundzewicz, 2002, Singh *et al.*, 2018). Climate change, intense natural resource exploitation and inappropriate land use have altered the hydrological response of catchments (Egbenta*et al.*, 2015). These factors increase the frequency and magnitude of flood events. It was estimated that Nigeria suffered combined losses of over $16.9b in damaged properties, oil production, agricultural and other losses due to flood events in 2012 alone (AmangabraandObenade, 2012, Egbenta*et al.*, 2015). Similarly, a combination of an exposed, vulnerable and ill-prepared population may enhance such situations which generate additional risks. The insufficient capacity of public

authorities and rescue services to act diligently in these situations also increases risks (ISDR, 2017). High population density in urban area present a higher disaster risk (Flood Warning Guide: FWG, 2010). They are expected to experience the effects of climate change with the increment of intensity and frequency of harmful events such as flash floods (Flood Early Warning System Reference Guide: FEWSRG, 2010). The flooding that affects the vast majority of the world's regions is fluvial flooding or river flooding. This type of flood occurs when the rivers overflow or burst their banks due to excessive rainfall over an extended period of time and spill onto the floodplain (Alfieri *et al*., 2018; Maggioni and Massari, 2018). Other flood that can also be experienced is pluvial flooding or surface water flooding which is a problem in many cities and occurs when there are high intensity of rainfall; here, the sewage and drainage system become overwhelmed and excess water cannot be absorbed into the soil. This also can be due to sewage and drainage blockage by human waste. This problem is enhanced in cities with insufficient or non-existent sewer systems. It suffices to note however that fluvial floods are more disastrous than pluvial flooding as they do have high return period. Pluvial floods come with less damage but, the frequency is higher and the cumulative damage over the years can be just as high as with fluvial flooding events (Jiang. *et a*l., 2018; Ten Veldhuis, 2011). Floods are among the most devastating natural disasters in the world, claiming more lives and causing more property damage than any other natural phenomena. In Nigeria, though not leading in terms of lives claimed, flood affects and displaces more people than any other disaster; it also causes more damage to properties. For instance, fluvial flood experienced in Nigeria in 2012 is the worst in living memory (Social Action, 2012). At least 20 per cent of the population is at risk from one form of flooding to another (Social Action, 2012). These losses are expected to escalate in the future due to climate change, land use change, deforestation, rising sea levels, and population growth in flood-proneareas, causing the number of people vulnerable to flood disasters globally to increase to two billion by 2050 (Bogardi, 2004, Vogogel*et al*., 2011; ICHARM, 2009).

Therefore, to avoid further disaster by flood, flood warning program must be introduced to increase lead time for watches and warnings at locations subject to flood risk. The information can be used to predict whether a flood is about to occur, when it will arrive, and how severe it will be. The warning system allows Organizations and individuals to develop their preparedness and response regimes accordingly; with this, the concomitant impacts can be mitigated.

2. Flood warning and mitigation in perspective

A flood warning is an information in the form of a prediction about a flood that is likely to happen. This information is usually targeted at and communicated to people who are in the path of the flood in advance of the flood occurring, with the intention of enabling them to avoid harm. Such information may also be communicated to infrastructure providers (e.g., electrical power companies) to enable them to take actions to avoid the disruptive effects of power outages and also to those operating flood barriers. Many population centers are protected from flooding by flood forecasting and warning systems that operate in conjunction with large-scale flood barriers that are closed when forecast thresholds are reached. Warnings are also provided for professional emergency responders so that they are alerted, for example, to evacuate people from an area likely to be flooded (Parker, 2017).

A successful flood warning system consists of several interacting components such as: continuous monitoring and forecasting of weather patterns, particularly precipitation, and water levels; detection of potentially hazardous situations; definition and implementation of rules on when, how and whom to warn in case of rising flood water levels and what to communicate in order to activate organizations in charge of civil protection as well as potentially affected people; and an adequate and effective response to the unfolding flood situation (e.g. Parker *et al*., 1994; Parker and Priest, 2012). Hence, a flood warning system is more adequately addressed as a flood-forecasting, warning and response system (FFWRS; Parker and Priest, 2012). In a FFWRS, several organizations have to collaborate and information has to be communicated, disseminated and interpreted correctly along a chain of different stakeholders, including the general public, which opens the door for many pitfalls that reduce the system's overall efficiency. Consequently, redundancies are seen as an important principle at all levels (Parker and Priest, 2012). Flood warning components in this context is as depicted by Figure 1.

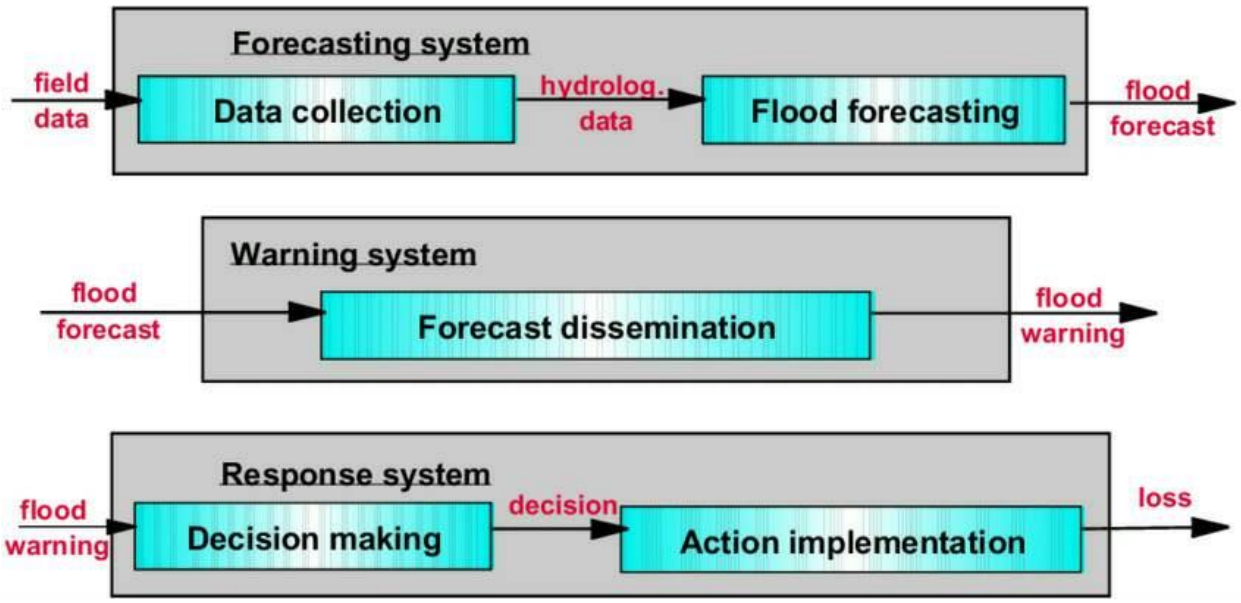

Figure 1.The flood forecasting, warning, and response system (FFWRS)

Source: (Krysztofowiczand Davis, 1983)

The components of an early warning system consists of a chain of subsystems. The first link is the forecasting system which consists of data gathering component, a component for transmission of the data to the forecasting center, and a component of forecast preparation. In the forecasting center, the data are converted into a forecast, which then is transmitted to the decision maker. The decision maker then uses the forecasts to prepare and release a warning, depending on his evaluation. Then the response system is activated. The warning is transferred to the local authorities, who have to take appropriate preventive action and pass the warning on to people in a form so that they can react (Krysztofowiczand Davis, 1983).

Therefore, for a real-time solution, an effective flood warning should be based on the regular collection of water level data, this can be done through routine monitoring in which the operating personnel make visit to stream gauging stations or hydrometric stations to collect information on temporal water levels.The objective of this is to have an idea of the transient change in the level of the river so that at critical peak flow period, warning can be issued.

3 Water level forecasting for flood and general river system management

Water level is the depth of flow above the river bed which is used to estimate the discharge; thus, because of this, water level is considered as a critical component in river flow forecasting especially water issues like hysteresis effects and uncertainty in stage-discharge relationship are taken into reckoning. River stage forecasting is crucial in water resources management and real-time prediction of extreme floods.Over any given region, the water level as well as the quantity of water flowing in streams may vary widely in both time and space. The fluctuation in discharge and water level results from variation in duration, frequency, intensity, areal cover of precipitation and variation in the catchment characteristics. Knowledge of river flow and its variability is an essential requirement for assessment, management and control of surface water resources. The basic data required for flood frequency studies, flood inundation modelling, design of flood protection and warning systems, river sediment management, water supply engineering, drought studies and geomorphologic studies are records of discharge measurement in river (WMO, 2011a).

Development of optimal flood forecasting and viable flood risk management systems have been advocated as measures of flood preparedness (Arduino*et al*., 2005, WMO, 2011a) for a variety of reasons. Due to the uncertainties surrounding the magnitude, timing and place of occurrence, geographical extent, and geophysical interactions of floods, it is often not possible to completely control them. As a result, complete protection from floods is not always considered as a viable alternative (Moore *et al*., 2005). Therefore, accurate water level forecasting that results from hydro-meteorological variations and anthropogenic disturbances are very vital for environmental protection and flood management strategy (Hofmann *et al*., 2008). During flood events, reliable water level prediction enable the use of both early warning systems to alert the population and for real time control of hydraulic structures, like diversion, gates etc., to mitigate flood effect. Water level fluctuations are dependent on diverse factors such as the spatial and temporal distribution of precipitation, topography, soil type, vegetation, land-use, catchment hydrology and the built environment, making flood forecasting a difficult exercise (White, 2001).

Therefore, Information on the flood evolution must be provided with a reasonable lead time to be effective, but this is not an easy task, particularly in Nigeria where the historical data needed for forecasting are not readily available; this situation makes real-time prediction of hydrological phenomenadifficult.Therefore, managing river systems that flow across borders is complex and

multifaceted. The issue encompasses theoretical and practical debates that, in some form, have been present since the beginning of mankind, as they reflect human attitudes and values. As such, effective prediction approaches play an important role; for instance in the studies of lakes. They can be used to simulate the water level variations based upon the available measured data and predict the possible responses under different scenarios, supporting management decisions of valuable water resources.

3.1 Methods / approaches adopted for water level forecasting

The knowledge of the surface water system has a wide range of applications in life. Regular monitoring and studying of river water level behavior is important from several perspectives most especially for timely forecasting of floods and dry spells and this is exemplified by numerous references (Chinh*et al*., 2009; Koutrouli*set al*., 2010; Valle Venencio and García, 2011). In this sense, the analysis of the change in water level as well as water level forecast have been subjects of numerous research activities, though, it has been possible thus far to reliably predict water level of river a few days in advance. Hydrologists are now developing, with the aid of river level data from the last six decades, a calculation model that enable longer-term water level predictions. Therefore, In terms of forecasting techniques, it is reported that many analyses of water level forecasting approaches had been done in hydrological problems. The choice of the forecasting model is an important factor in order to improve the forecasting accuracy (Areekul*et al*., 2010).

In the last decade a new type of data-driven models, based on artificial intelligence and soft computing technique have been applied in water level forecasting. In particular, Artificial Neural Network (ANN) is one of the most widely used technique in the forecasting field (Hsu *et al*., 1995). Most applications based on these models consider the discharge as forecasting variable (Imrie*et al*., 2000; Dawson *et al*., 2002; Moradkhany*et al*., 2004), probably because of a historical contiguity with the classes of conceptual and physically based rainfall-runoff models. Such an approach requires the knowledge of the rating curve in the cross section of interest (i.e. the basin outlet) to parameterize the model. However, the knowledge of the water level is required within the framework of a flood warning system and thus the rating curve has to be used also to transform the forecasted flows into water levels.

Altunkaynak (2007)applied an artificial neural network model to accurately predict dynamic changes of surface water level in the lake. Van. Yarar*et al*. (2009) estimated level changes of Lake Beysehir in Turkey using the adaptive neuro-fuzzy inference system (ANFIS), ANN, and seasonal autoregressive integratedmoving average (SARIMA) approaches. Kisi *et al*. (2012) also forecasted daily lake levels by artificial intelligence approaches. However, detailed comparison of the time series forecasting and ANN models with the physically based models has not yet been studied in lakes.

Models based on ANN, FL, etc., and, more in general, all data-driven models, can be designed to forecast water levels directly, given their very nature. For instance, Campolo*et al*. (1999), See and Openshaw (1999), See and Openshaw (2000), Thirumalaiah and Deo (2000), Campolo*et al*. (2003), Young (2001, 2002), developed models based mainly on applications of the ANN techniques, while Krzysztofowicz (1999, 2001), Krzysztofowicz and Kelly (2000), Krzysztofowicz and Herr (2001) developed a Bayesian forecasting system which produces a short-term probabilistic river level forecast based on a probabilistic quantitative precipitation forecast.

On the other hand, physically based numerical models are constructed using a set of governing equations that address conservation laws of mass/momentum and transport processes. In contrast to a simple zero-dimensional mass balance computation for elevation and storage, these models can provide more detailed spatial-temporal patterns of water level, circulation, vertical stratification/mixing, and other aspects of lake physics (Kimura*et al*., 2012; AnyahandSemazzi, 2009). Young *et al*. (2015) used physically based hydrodynamic model to accurately predict water level fluctuations. To address these issue of water level forecasting, time series modelling has been also explored over time.

In this regard, well-known technique such as ARIMA and SARIMA are most commonly used for time series forecasting, however, they have limitations in applications due to linearity issue.Time series forecasting methods that define the trend or stochastic processes of variables have also been applied to predict water level fluctuation in lakes. One of the most commonly used approaches is the autoregressive integrated moving average (ARIMA) model, where the autoregressive and moving average filters account for systematic effects and internal shock effects in the endogenous variable, respectively. But, ARIMA models require a stationary time series without data missing (Ediger and Akar, 2007). Based on the observations time series, an identified underlying process can be

constructed under the assumptions of linearity, normality, and homoscedasticity. Thus, for better prediction accuracy and variability in endogenous variables, an autoregressive moving average with exogenous (ARMAX) model includes the explanatory variables in the cause-effect technique.

One of the most common methods, based on times series analysis, are models based on the combination of autoregressive model and moving average model to increase efficiency and accuracy of water level forecasting.Therefore, the implementation of water level forecasting requires both human and computing resources. Sufficient resources must be in place to support not only the development of the system but to operate and maintain it through time. Thus, in general,water level forecasting is constrained by many issues such as the availability and types of data and their representativeness and quality. Specifically, the issues of immediate concern here are as discussed in the next section.

4.0 Emerging issues in water level forecasting

Water levels are designed to make local authority aware of the level of danger posed by the rising water level so that a necessary emergency arrangement could be initiated for the welfare of the local community affected by the river. As the water level forecasting could reduce the damage from the impact of flooding in agriculture, public uses, avoid both life and economic loss, it is therefore important to predict its fluctuation. Prediction of the pattern of water level is one of the benchmark points in the flood forecasting analysis and has been one of the most important issues in hydrological research. Water level is an essential component in the process of forecasting flood resources evaluation and is considered as a central problem in hydrology (Ekhwah*et al*., 2009).

The most critical issues involved in water level forecasting are:

a) Choice of time horizon for the practicalities of flood protection:

In general, water level changes seasonally (e.g., high in the rainy season and low in the dry season) with sharp rising/falling limbs during flood events, but not in a simple periodic mode;this give rise to hysteresis in the hydrograph with associated problem in the development of an effective rating curve for a particular river section. Therefore, it is a serious challenge to thehydrologists to decide the time suitable for flood protection especially due to the lack of the following vita information, namely:

1. Amount of rainfall occurring on a real time basis
2. The rate of change in river stage on a real time, which can help indicate the severity and immediacy of the threat.
3. Knowledge about the type of storm producing the moisture, such as duration, intensity and areal extent, which can be valuable for determining possible severity of the flooding.
4. Knowledge about the characteristics of river's drainage basin, such as soil moisture conditions, ground temperature, topography, vegetation cover, and impermeable land area, which can help to predict how extensive and damaging a flood might become.

Against this backdrop therefore, the appropriate time horizon to be chosen for flood forecasting for the practicalities of flood protection such as alerting the appropriate authorities, issuing of warnings to industries and households in the vicinity and protection of property become an issue of great concern because the catchment is not continually monitored by the agency or government institutions and bodies responsible for flood defence (Environmental Protection Agency: EPA, 2002).

b) Choice of appropriate or critical water level for the assurance of standby alarms to duty officer and area alert;

Flood response levels for Agency/ Jurisdiction will be based on river stage for a given river at a given hydrometric station so that when the water levels at the station reached the required height (m) based on historical data, the standby alarm to duty officers monitoring the catchment will be triggered. According to EPA (2002), an area alert is activated when the level reaches 3.5m and flood warning is issued as the level continues to rise but in Nigeria today, the choice of appropriate water level has been a great issue due to the fact that the agencies in charge of monitoring lack the requisite capacity to do. So, this is compounded by inadequate data on water level rises as well as absence of telemetering gauges for real-time transmission of information and corresponding analysis.

According to Sample Flood Safety Plan (2011), flood stage monitoring comprises of observing the readings from specific real-time, telemetered stream gauge that report the conditions on water courses that affect potential flooding in the area. For each gauge location on a stream or water course, stages or flows have been categorized into three levels: monitoring stage, danger stage, or flood stage but responding to these stages have been a challenging issues due to its complex nature especially

due to inability of agencies shouldered with responsibility to put the necessary structures to access the real time gauge through the internet hence they cannot directly monitor the outflow at the various areas that are been affected. Thus, deciding the choice of water level remains a challenging issue especially in an area where there is no levee patrols when the elevation reaches the assumed height at the location for a named river as well as monitoring and surveillance information to decide if it is necessary to begin flood operation or direct flood fight resources to specific area where flooding is occurring or may occur soon. Concisely, lack of or improper use of technical information have been the issue; these technical information include:

1. **Radio Reporting Rain Gauges:**According to Flood Warning Systems Manual, (2012), gauges have two primary functions—sensing and communicating. Sensing involves detection of an "event", which is the smallest unit of measurement desired, such as 1 millimeter of rain, 1/100 inch of stage height, etc. Communicating involves reporting the event to a user location. For maximum flexibility, nearly all gauges are designed to allow multiple sensors at a particular site to report through a single communications platform. The gauge assigns a unique identifier to each individual sensor type (rain, stream, temperature, wind speed, etc.), and communicates both. This radio reporting rain gauge is usually needed in remote areas where commercial power is unavailable; but appropriate disseminating this information has become an issue.
2. **Stream Gauge:** In small watersheds, stream flow observations are not noted so it is difficult to calibrate watershed models and verify forecasts from models, or trigger alarms when flooding is impending or occurring. The placement of stream gauges is not usually guided by public warning requirements and forecast model requirements. Gauges used for stage alarms are at times not even located at key points of potential damage and at points that are far enough upstream to yield enough warning time for downstream locations.
3. **Communications Media:**Alert gauges and other forms of radio transmissions are susceptible to interference from man-made electrical noise, atmospheric conditions, and other transmitters on the same or adjacent frequencies. Because multiple alert transmitters share common radio frequencies, there are instances when simultaneous transmissions occur. Most VHF/UHF radio-based communications platforms do not use the alert radio transmission protocol, which transmits in real time when each sensor event occurs. Alert systems may be fast, have good resolution, and low operating costs, but they have a limited transmission range. Therefore, remote areas are at risk during flood events.

4. **Software:**The primary function of automated flood warning system (AFWS) software is to collect and interpret raw data sent from remote gauge locations. Most software also includes one or more applications that enable the user to view the data as graphical or text information, both locally and on the internet. Obviously most of the agencies in Nigeria do not have this software and even if they do, it is not properly managed. Agencies of Government like Nigerian Emergency Management Agency:NEMA and Nigerian Hydrological Services Agency: NHSA may not have been operationally organisedto technically address the issues mentioned here.

c) Data collected in terms of type, size and quality:

There are important challenges facing Federal Agencies that collect and manage hydrologic data. One of these challenges is related intrinsically to the type of problems for which hydrologic data are being used. The analysis of problems related to floods and droughts requires specific information about extreme events, which can be developed only after conducting decades or substantial period of precipitation and streamflow monitoring across a variety of different climatic and hydrologic setting. In general, the broad spectrum of present and future scientific water problems nationwide requires monitoring systems that function reliably over both large and small temporal and spatial scales. Unfortunately, the observational networks to measure various water characteristics have been in decline during the last 30 years due to political and fiscal instabilities (NRC, 1991; Entekhabi*et al*., 1999); this is basically not in term of the number of available institutions but rather the capacity and the associated service delivery.

In general, most often than not, the situation leads to imperfect characteristics of the produced data such as missing data and inconsistent value of data are therefore issues of great concern. Datapre-processing such as consistency and extension and infilling through either interpolation or extrapolation can also influence the performance of the prediction model (Zhang, 2002) because a large element of uncertainty exists in extrapolation process. It is difficult to categorically comment on the existing stations of Government Agencies to adequately handle these issues considering mal-functional nature of government agencies and interrelated problem of function duplication..

d) Choice of Model/ Model Performance:

The transformation of precipitation into channel flow by determining its depth(level) is a highly complex physical process. A common practice is to use a hydrological model to represent watershed

process. Many different hydrological models have been produced by government agencies, universities, and private companies. They offer a wide range of process simulation options, differing levels of complexity and data requirements, and various degrees of technical support and training. Their application also depends on the forecasting objective, geographical and environmental factors, as well as institutional capabilities. Therefore, the selection of a "best choice" flood forecasting model needs to be based on a systematic approach (Lettenmaier and wood, 1993).

It is therefore imperative to note that Comparing Hydrological Flood Forecasting Models (HFFMs) is not a new idea, but assembling the required data for model forecasting is challenging and complex.A traditional approach is to select a gallery of models for comparison, and a watershed where models can be run. But the common data set to be assembled include meteorological data, observations of flow and stage, soil characteristics, and all other data that might be used to parameterize the models which are not readily available. Each model is configured for the watershed using the assembled data. Performance metrics are defined, and calculated for each model in the inter-comparison. The models are then ranked based on the performance metrics. This process may be repeated for a variety of different watersheds in various climates or regions of the world representing different hydro-meteorological conditions. The general idea is to select a single, most appropriate model for a particular set of hydro-meteorological and institutional conditions. Therefore, the spatial and temporal resolution of models depend on a wide range of factors. The temporal resolution depends on the frequency of input data and data assimilation as well as the forecast purpose. The spatial resolution depends on the density of the observing network, interpolation possibilities, variability of the flow conditions and the spatial characteristics of the area for which the forecast is issued (Lettenmaier and wood, 1993). But alarming in this regard is the haphazard nature of how things are being handled; institutions that are supposed to handle this critical component are not taken into proper contextual / operational reckoning.

5. Conclusion

Floods are among the most devastating natural disasters in the world, claiming more lives and causing more property damage than any other natural phenomena. Therefore to avoid further disaster by flood, flood warning program must be introduced to increase lead time for monitoring and warning

at location subject to flood risk. This information can be used to predict whether a flood is about to occur, when it will arrive and how severe it will be; for real-time solution, an effective flood warning should be based on the regular but temporal collection of water level data that would allow for the fastest possible response to flood event. In this regard, effective prediction approaches play an important role in the study of river which can be used to simulate water level fluctuations. This water level forecasting is constrained by many issues such as choice of time horizon, appropriate water level for standby alert, type of model to be applied, and data availability in terms of quality and type. In general, addressing water resources concerns in the future will require increasingly substantial data base: in this regards, both Streamflow and water level data are needed to support important public policy decisions concerning towns located in the floodplains of rivers.

Refrences

Alfieri, L.; Cohen, S.; Galantowicz, J.; Schumann, G.J.-P.; Trigg, M.A.; Zsoter, E.; Prudhomme, C.; Kruczkiewicz, A.; de Perez, E.C.; Flamig, Z.(2018). A global network for operational flood risk reduction. Environ. Sci. Policy, 84, 149–158.

Arduino, G., Reggiani, P., and Todini, E., (2005). Recent advances in flood forecasting and flood risk assessment. Hydrology and Earth Sciences, 9 (4), 280–284. doi:10.5194/hess-9-280.

Amangabra, G.T. andObenade, M., (2015). Flood vulnerability assessment of Niger Delta states relative to 2012 flood disaster in Nigeria. *American Journal of Environmental Protection*, **3**(3), pp. 76–83.

Anyah, R. O., and Semazzi, F. (2009). "Idealized simulation of hydrodynamic characteristics of Lake Victoria that potentially modulate regional climate," *International Journal of Climatology*, vol. 29, no. 7, pp. 971–981.

Altunkaynak, A. (2007). "Forecasting surface water level fluctuations of lake van by artificial neural networks," *Water ResourcesManagement*, vol. 21, no. 2, pp. 399–408.

Areekul,P., Senjyu, T., Toyama, H and Yona, A. (2010).*A Hybrid ARIMA and Neural Network Model for Short-Term Price Forecasting in Deregulated Market. Japan*, Department of Electric and Electron, Engineer University of the Ryukyus, Nishihara.

Bogardi J. (2004). Update.unu.edu. The newsletter of the United Nations University and its international network of research and training centres/programmes. Issue 32. (Available online athttp://update.unu.edu/archive/issue32.htm

Basheer, I. A., and Hajmeer, M. (200). "Artificial neural networks— fundamentals, computing, design, and application," *Journal ofMicrobiological Methods*, vol. 43, no. 1, pp. 3–31.

Campolo, M., Andreussi, P., and Soldati, A. (1999). River flood forecasting with neural network model, WaterResour. Res., 35(4), 1191– 1197.

Campolo, M., Andreussi, P., and Soldati, A. (2003). Artificial neural network approach to flood forecasting in the river Arno, Hydrol. Sci. J., 48(3), 381-398.

Chinh, L., Hiramatsu, K. and Mori, M. H. M. (2009). Estimation of water levels in a main drainage canal in a flat low-lying agricultural area using artificial neural network models, *Agricultural Water Management* 96: 1332–1338.

Dawson, C. W., Harpham, C., Wilby, R. L., and Chen, Y. (2002). Evaluation of artificial neural network technique in the River Yangtze, China, Hydrol. Earth Syst. Sci., 6, 619–626, **SRef-ID: 1607-7938/hess/2002-6-619**.

Egbenta, I.R., Udo, G.O. andOtegbulu, A.C., (2015). Using hedonic price model to estimate effects of flood on real property value in Lokoja Nigeria. *Ethiopian Journal of Environmental Studies and Management*, **8**(5), pp. 507–516. http://dx.doi.org/10.4314/ejesm.v8i5.4

Entekhabi, D., G. R. Asrar, A. K. betts, K. J. Beven, R. L. Bras, C. J. Duffy, T. Dunne, R. D. Koster, D. P. Lettenmaier, D. B. Mclaughlin, W. J. Shuttleworth, M. T. VanGenuchten, M. Y. Wei, and Wood, E. F.,(1999). An agenda for land surface hydrology research and a call for the second international hydrological decade. Bull. Amer. Meteor. Soc. 80:2043-2058.

Environmental Protection Agency: EPA, (2002). National Water Quality Inventory – 2000 report: EPA-841-R-02-001. Washington DC: EPA.

Ediger V. S., and Akar, S. (2007). "ARIMA forecasting of primary energy demand by fuel in Turkey," *Energy Policy*, vol. 35,no. 3, pp. 1701– 1708.

Ekhwah, M. T.,Juahir, H.,Mokhtar, M., Gazim, M. B., Abdullah, S. M. S., and Jaafar, O. (2009). "Predicting for Discharge characteristics in Langat River, Malaysia using Neural Network Application Model," Research *Journal of Earth Sciences*, vol. 191, pp. 15-21.

Hofmann, H.,Lorke, A., andPeeters, F. (2008): "Temporal scales of water-level fluctuations in lakes and their ecological implications," *Hydrobiologia*, vol. 613, no. 1, pp. 85–96.

Hsu, K. L., Gupta, H. V., and Sorooshian, S. (1995). Artificial neural network modeling of the rainfall-runoff process,WaterResour. Res., 31(10), 2517–2530.

ICHARM Report, (2009). Global trends in water related disasters: an insight for policymakers. International Centre for Water Hazard and Risk Management (UNESCO), Tsukuba, Japan, http://www.icharm.pwri.go.jp.

International Strategy for Disaster Reduction (ISDR). UNISDR Terminology on Disaster Risk Reduction. Available online: https://www.unisdr.org/we/inform/publications/657 (accessed on 24 July 2017).

Imrie, C. E., Durucan, S., and Korre, A. (2000). River flow prediction using artificial neural networks: generalizations beyond the calibration range, J. Hydrol., 233, 138–153.

Jiang, Y.;Zevenbergen, C.; Ma, Y. (2018). Urban pluvial flooding and stormwater management: A contemporary review of China's challenges and 'sponge cities' strategy. Environ. Sci. Policy, 80, 132–143.

Kundzewicz, Z.W. (2002). Non-structural flood protection and sustainability. Water Int. 27, 3–13.

Kisi,O., Shiri, J., and Nikoofar, B. (2012). "Forecasting daily lake levels using artificial intelligence approaches," *Computers andGeosciences*, vol. 41, pp. 169–180.

Kimura, N., Liu, W. C., Chiu, C. Y., Kratz, T. K., and Chen, W. B. (2012)."Real-time observation and prediction of physical processes in a typhoon-affected lake," *Paddy and Water Environment*, vol. 10, no. 1, pp. 17–30.

KRZYSZTOFOWICZ R and DAVIS DR (1983). A methodology for evaluation of flood forecast-response systems (1. Analysis and Concepts). *Water Resour. Res.* **19** (6) 1423-1429.

Krzysztofowicz, R. (1999) Bayesian theory of probabilistic forecasting via deterministic hydrologic model, Water Resour. Res., 35(9), 2739–2750.

Krzysztofowicz, R. and Kelly, K. S. (2000). Hydrologic uncertainty processor for probabilistic river stage Forecasting, Water Resour. Res., 36(11), 3265–3277.

Krzysztofowicz, R. and Herr, H. D. (2001). Hydrologic uncertainty processor for probabilistic river stage forecasting: precipitationdependent model, J. Hydrol., 249, 46–68, 2001.

Krzysztofowicz, R. (2001). Integrator of uncertainties for probabilistic river stage forecasting: precipitation-dependent model, J. Hydrol. 249, 69–85.

Koutroulis, A. G., Tsanis, I. K. and Daliakopoulos, I. N. (2010). Seasonality of floods and their hydrometeorologic characteristics in the island of Crete, *Journal of Hydrology* 394: 90–100.

Lettenmaier, D. P., and Wood, E. F., (1993). Hydrological Forecasting, Chapter 26 in Handbook of Hydrology. (D. Maidment, ed.), McGraw-Hill. D.P.

Maggioni, V.; Massari, C. (2018). On the performance of satellite precipitation products in riverine flood modeling: A review. J. Hydrol. 558, 214–224.

Makridakis S, Wheelwright SC, Hyndman RJ (1998). Forecasting Methods and Applications, JHON WILEY and SONS.

Moore, R.J., Bell, V.A., and Jones, D.A.(2005). Forecasting for flood warning. ComptesRendus Geosciences, 337 (1), 203–217. doi:10.1016/j.crte.2004.10.017.

Moradkhany, H., Hsu, K. L., Gupta, H. V., and Sorooshian, S. (2004). Improved streamflow forecasting using self-organizing radial-basis function artificial neural networks, J. Hydrol., 295, 246–262.

National Weather Services, (2012): Flood Warning Systems Manual. US department of commerce. Version 1.0.

National Research Council (NRC). (1991): Opportunities in the Hydrologic Science. Washington, DC: National Academy Press

Parker, D.J. (2017). Flood Warning Systems and Their Performance. In Oxford Research Encyclopedia of Natural Hazard Science; 2017; Available online:

http://naturalhazardscience.oxfordre.com/view/10.1093/acrefore/9780199389407.001.0001/acrefore-9780199389407-e-84.

Parker, D. J. and Priest, S. J. (2012). The Fallibility of Flood Warning Chains: Can Europe's Flood Warning be Effective? Water Resour. Manag. 26, 2917–2950.

Parker, D. J., Fordham, M., &Torterotot, J-P. (1994). Real-time hazard management: Flood forecasting, warning and reponse. In E. C. Penning-Rowsell& M. Fordham (Eds.), *Floodsacross Europe: Flood hazard assessment, modelling and management* (pp. 135–166). London: Middlesex University Press.

Social action (2012). The 2012 Floods. Social Action Briefing, No. 5 December, 2012 pp. 2-14

Singh, P.; Sinha, V.S.P.; Vijhani, A.; Pahuja, N. (2018). Vulnerability assessment of urban road network from urban flood. Int. J. Disaster Risk Reduct. 28, 237–250.

See, L. and Openshaw, S. (1999). Applying soft computing approaches to river level forecasting, Hydrol. Sci. J., 44(5), 763–778.

See, L. and Openshaw, S. (2000). A hybrid multi-model approach to river level forecasting, Hydrol. Sci. J., 45(4), 523–536.

Sample flood safety (2011). California department of water resources.

Ten Veldhuis, J.A.E. (2011). How the choice of flood damage metrics influences urban flood risk assessment. J. Flood Risk Manag. 4, 281–287.

Thimuralaiah, K. and Deo, M. C. (2000). Hydrological forecasting Using Neural Networks, J. Hydrol. Eng., 5(2), 180–189.

Valle Venencio, M. and García, N. O. (2011). Interannual variability and predictability of water table levels at Santa Fe Province (Argentina) within the climatic change context, *Journal of Hydrology* 409: 62–70.

Vogel, R.M., Yaindl, C., and Walter, M.(2011). Non stationarity: flood magnification and recurrence reduction factors in the United States. Journal of the American Water Resources Association, 47 (3), 464–474. doi:10.1111/j.1752-1688.2011.00541.x.

World Meteorological Organization. Guidelines on Early Warning Systems and Application of Now casting and Warning Operations; Pws-21, No. 1559; World Meteorological Organization: Geneva, Switzerland, 2010; p. 25

WMO.(2011a). Workshop on Intercomparison of Flood Forecasting Models, 14–16, Koblenz, Germany.

White, W.R.(2001). Water in rivers: flooding. Proceedings of the Institution of Civil Engineers – Water and Maritime Engineering 2 (2), 107–118.

Yarar A., Onucyildiz, M., and Copty, N. K., (2009). "Modelling level change in lakes using neuro-fuzzy and artificial neural networks," *Journal of Hydrology*, vol. 365, no. 3-4, pp. 329–334.

Young, P C. (2001). Data-based mechanistic modelling and validation of rainfall-flow processes, in: Model Validation: Perspectives in Hydrological Science, edited by: Anderson, M. G. and Bates, P. D., Wiley, Chichester, pp. 117–161.

Young, P. C. (2002). Advances in real-time flood forecasting, Philosophical Transactions of the Royal Society: Mathematical, Physical and Engineering Sciences.

Young, C.C.; Liu, W.C. (2015). Prediction and modelling of rainfall–runoff during typhoon events using a physically-based and artificial neural network hybrid model. Hydrol. Sci. J.60, 2102–2116.

Zhang, G. P. (2002).Time Series Forecasting Using Hybrid ARIMA and ANN Model," Neurocomputing, vol. 50, pp. 159-175.

Effect of Agrochemicals on Water Quality in Parts of Rivers Niger and Kaduna Catchments, North Central, Nigeria.

BY

IDRIS, Aliyu Ja'agi[1*]Yahaya, T. I.[1]Abubakar, A. S.[1]andJigam, A. A.[2]

[1]Department of Geography, Federal University of Technology Minna, Niger State, Nigeria

[2]Department of Biochemistry, Federal University of Technology Minna, Niger State, Nigeria

*Corresponding Author: aliyuidrisjaagi@yahoo.com, +2348034576625

Abstract

Effect of agrochemicals on water quality in parts of Rivers Niger and Kaduna Catchments, north central, Nigeria was investigated. Data from the study of agrochemical residue levels in the area remains scanty and therefore needed. Extensive field survey was conducted using various participatory appraisals techniques involving key stakeholders in the area, following which total of sixteen samplesof water andsediments for minerals and physico-chemical determinations were collectedand transported to the laboratory for analysis. Survey result showed that lower zone ranked the highest with use of agrochemicals (39.4%); upper zone ranked second with 33.5% and middle zone ranked the least with 24.5%. Out of 100% of the respondents, 2.7% disaffirmed the use of pesticides and fertilizers in their farms due to inadequate financial support to farming and inadequate legit borrowing facilities in the study area. Plant minerals NO_3^-, NO_2^-, and PO_4^-concentrations ranging from 0.02 to 5.771ppm weredetected in sediments and surface water samples.Most of the findings were above permissible level.Physico-chemical parameters analysed include COD, BOD, Total hardness, Sulphate, Manganese, PH and Chloride. The findings shows considerable number of the parameterswere above permissible level. In view, of the aforementioned, we suggest that farmers should be educated and urged to adopt sustainable agrochemical usage. These will guarantee cleaner and healthier environment for all.

Keywords: Agrochemicals,Physico-chemicals, Plant minerals, Sediments, Water quality

1. Introduction

Agrochemicals (fertilisers and pesticides) are intended to facilitate plant growth and protections. Although initially used to improve crop production,however, in achieving this essential mission to care for crops, they have been reported to have negative effects on water quality (Jokha, 2015). Apart from the obvious effects on crops and the food chain, agrochemicals have a wide area of application. Due to these many uses, they move into the surrounding water bodies, therefore having a widespread effect on the physical, chemical and biological processes within aquatic ecosystems (Lakhani, 2015; Bassi *et al.*, 2016; Joko *et al.*, 2017).

Environmental protection has become global focus and important aspect of sustainable development. Proactive measures are being taken by regulatory agencies and relevant stakeholders to address all environmental issues with special attention on chemical pollutants (National Environmental Standards and Regulations Enforcement Agency, 2009).

The amount of agrochemicals usage continue to grow in the study area and most of the users lack awareness of the socioeconomic effects and environmental management plan to prevent or reduce possible environmental issues from their applications. This has become an issue of serious concern in the study area. Managing environmental burden resulting from agrochemical usage continue to frighten the relevant authorities who seem not to be concerned or lack effective capacity to deal with the negative health and environmental situation in this regard.

Environmental management in agriculture sector involving agrochemicals usage is very important to ensure products consumers, nearby communities and the natural environments are protected from the resulting negative effects of their applications. However, if agrochemicals are not used sustainably, it could lead to serious socioeconomic problems thereby endangering existence of life. Nowadays, the environmental issues arising from agrochemicals uses are too numerous which are the direct consequences of improper regulations and enforcement policies particularly in developing countries (NESREA, 2014).

A good number of agriculture chemicals such as endosulfan and dichlorodiphenyltrichloroethane (DDT) have been restricted from use by authorities due to socioeconomic reasons but are still being used in developing countries including Nigeria (Keri and Directorate, 2009; Ojo, 2016).The use of synthetic fertilizers and pesticides in many parts of the world is on the increase (Ramteke and Shirgave, 2012). Rivers Niger and Kaduna sub-catchments are arable land where people practice

farming involving intense use of agrochemicals (Ogwueleka, 2014). This practice can eventually cause degradation of water quality and disproportionate effect on the socio-economic wellbeing of the communities in the area.

Further, a research finding by Ogwueleka (2014) suggest that Kaduna Basin and its sub-catchments in part of the study area are highly affected by intense agricultural activities and requires continue monitoring of its resources. Considering the threats from unsustainable agrochemicals usage and weaknesses in conservation of aquatic resources measures, resulting in more adverse effects on socioeconomic wellbeing of communities than expected.Jokha, (2015)andKnauer, (2016)observed that, rapid population growth in addition to change in climate has resulted to a driving force for farmers to use more agrochemicals in agricultural activities near Rivers.

Communities' dependant on the resources from Rivers in the area for livelihood and lack of enough research information about the area that represent risk of agrochemical pollution informed the need for immediate assessment of qualities of its resources to guaranty socioeconomic sustainability. There is presently little research attention on agrochemicals effects on aquatic resources in the area and has resulted to scanty research information about the proposed study area that represent risk of agrochemical pollution. The levels of agriculture chemicals residues in the area under consideration remain under studied to date. Data from the study of agrochemical residue levels in the area is therefore needed. Hence, informed the need for immediate investigation in the area.Finding of this study will provideopportunity for relevant government authorities and all stakeholders in this sector to improve on overall environmental performance.

2. Literature Review

Agrochemicals exposure and poisoning is a highly neglected public health issue in Nigeria and most other developing countries (Ojo, 2016). Citizens and policy makers are not generally aware of this problem due to a lack of valid information on the subject. In view of extensive exposures, adverse health effects and over-stretched health care resources in many developing countries including Nigeria, prevention of pesticide poisoning emerges as the most viable option to reduce the harmful

impact on the population (Lewis *et al.*, 2016). This study provides a local scientific basis for the development of strategies to reduce and control poisoning in farming communities by preventing agrochemicals exposures in the environment.

A number of studies on pollution of aquatic environment caused by various chemicals have been carried out on Rivers Niger and Kaduna Basin Catchments in north central Nigeria and reported by various researchers. These include: Assessment of water quality and identification of pollution sources of Kaduna River in Niger State, Nigeria (Ogwueleka, 2014). Ojutiku*et al.*, (2016) worked on Distribution of Phytoplankton and Physico-Chemical Characteristics of Agaie-Lapai Dam, Minna, Niger State, Nigeria. Sidi, *et al.*, (2016) worked on Assessment of Chemical Quality of Water from Shallow Alluvial Aquifers in and around Badeggi, Central Bida Basin, Nigeria. These research were notspatial enough had no specific consideration for agriculture pesticides. Even though little literatures (specifically) on risk of agrochemicals use researches have been found in the study area, a lot of studies related to this topic have been carried out in other parts of Nigeria and these include; Distribution of ecological risk assessment of pesticide residues in surface water, sediment and fish from Ogbesse River, Edo state, Nigeria by Lawrence *et al.*, (2015); Pesticides distribution in surface waters and sediments of lotic and lentic ecosystems in Agbede wetlands by Dirisu *et al.*, (2016;. Assessment of Dichlorvos and Endosulfan pesticide residue levels in selected fruits and vegetables sold in some major markets in Ibadan, Oyo state, Nigeria by Bamigboye *et al.*,(2017); Assessment of pesticide residue levels in vegetables sold in some markets in Lagos state, Nigeria by Njoku *et al.*, (2017;. However these research were also not spatial enoughand had no consideration for plant nutrients. Thus, this study attempted to fill this gap.

3. Methodology

Study area

The study area for the investigation is communities in parts of Rivers Niger and Kaduna Sub-catchments, Niger State which lies between Longitude 3˚30'N and 7˚20'E and Latitude 8˚22'N and 11˚30'N; located at the Guinea Savanah vegetation zone in the north central part of Nigeria (Figure 1). Rivers Niger and Kaduna sub-catchments are arable land where people practice agricultural activities close to the Rivers (Ja'agi& Baba, 2015; Ogwueleka, 2014). The study area was divided

into zones according to altitude. Along River Niger, the Upper zone is from Rabba village in Mokwa Local Government Area (LGA), Middle zone is at Muregi and the Lower zone is after Muregi in Mokwa LGA down to Baro village in Agaie LGA. Study area along River Kaduna was divided into two zones. Upper zone is from Wuya village in Lavun LGA and the Lower zone from half way down to Muregi. The major economic activities of the communities living around the area are agriculture and fishing. These are the leading sector in terms of employment, income earning and overall contribution to the socio-economic wellbeing of the people.

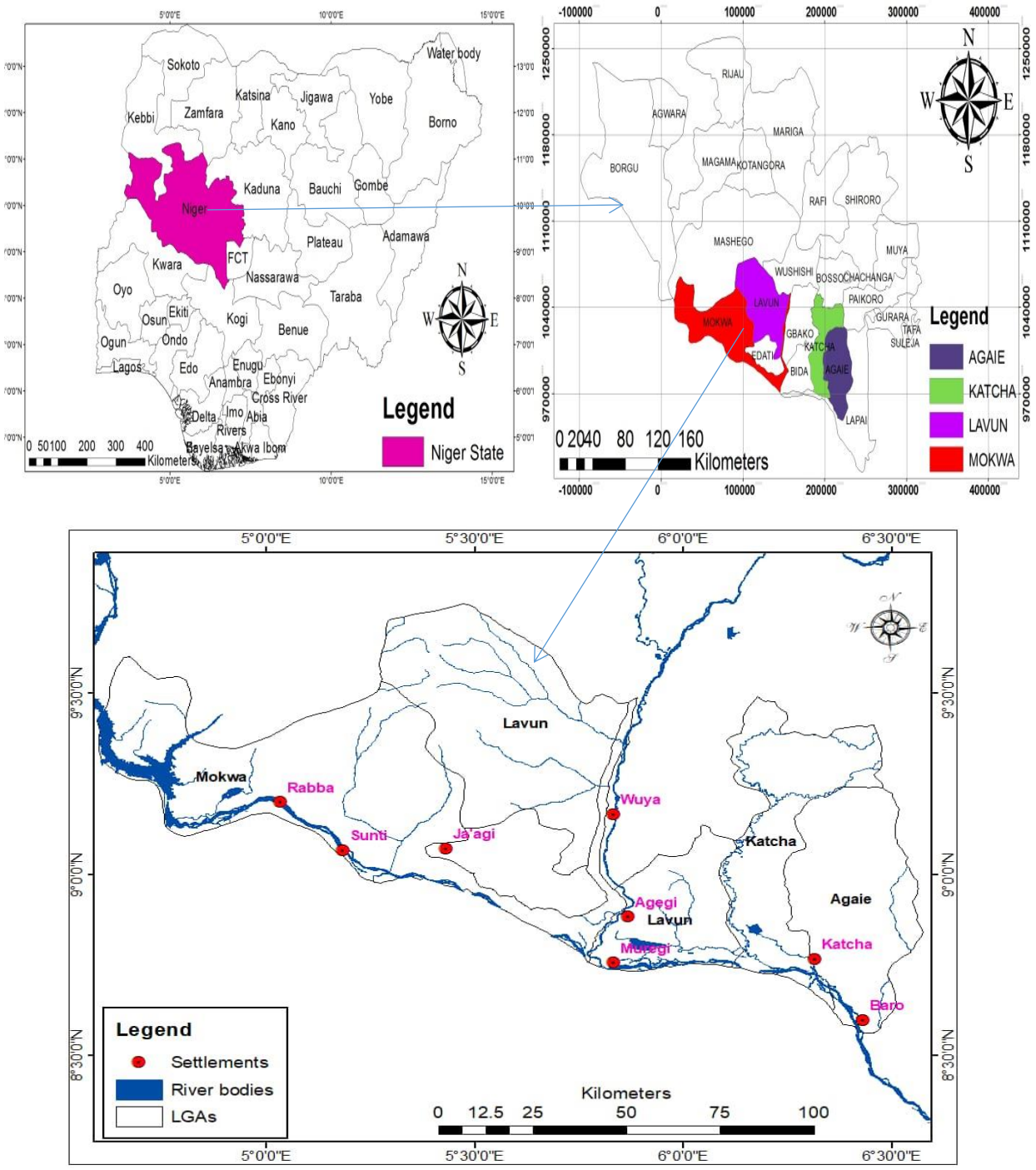

Figure 1: The study Area (Parts of Rivers Niger and Kaduna Basin, Niger State)

Sampling point's identification: Water and Sediment samples were collected from eight selected sampling points in the study area (Table. 1). The eight sampling points was based on altitude and

information from key stakeholders in the area. In order to ascertain the proper points for water and sediment samples collection, qualitative information from initial field survey were used. Samples were collected using standard procedures for water and sediment samples collection and preservation. Each sampling point was georeferenced using Global Position System (GPS) device.

Table.1 Description of the surface water and sediment sampling sites

s/n	Site Reference/Zones	Coordinates	Site Characteristics
1	Upper Zone (RN) S1 & W1 S2 & W2 S3 & W3	 9°14’53” N 5°83’37”E 9°11'09" N 5°26'19” E 9°11'43” N 5°18'38” E	Domestic activities, farming, fishing and settlements
2	Middle Zone (RN) S4 & W4	 8°45'25” N 5°50’38” E	Domestic activities, farming, fishing and settlements
3	Lower Zone (RN) S5 & W5 S6 & W6	 8°35'11” N 6°25'59” E 8°46'12” N 6°18'42” E	Domestic activities, farming, fishing and settlements
4	Upper Zone (RK) S7 & W7	 9°09'24” N 5°49'39” E	Domestic activities, farming, fishing and settlements
5	Lower Zone (RK) S8 & W8	 8°50'35” N 5°50'39” E	Domestic activities, farming, fishing and settlements

RN = River Niger, RK = River Kaduna, W = Water sampling site, S = Sediment sampling sites

Water Sampling and Preservation

A total of sixteen samples of water and sediments for minerals and physico-chemical determinations were collected, water samples were analysed insitu for a number of physicochemical parameters, preserved, kept in cool boxes and later transported to the laboratory for analysis. In the Laboratory, water and sediments samples for Minerals and physico-chemical determinations were analysed immediately upon arrival.

*Laboratory Analysis:*Plant Minerals was analysed spectrophotometrically following the methods outlined by APHA/AWWA/WEF. (2005). Physico-chemical analysis was conducted using HENNA Multiparameter Analyser for insitu analysis and other parameters were determined following method outlined by Federation & American Public Health Association APHA. (2005).

Statistical Analysis

Data obtained from administered questionnaire and interview schedules of farmers and key stakeholders in the area was analysed for agrochemicals use pattern using descriptive statistical methods (frequency, percentage and mean).

4. Results and Discussion

4.1 Agrochemicals Use Attributable to Water Quality Degradation in Farming Activities in the Study Area

Use of Fertilizer and Pesticide in Farming

As indicated in Table 1, there were high use of pesticide and fertilizer in farming activities by the respondents in the study area. Lower zone ranked the highest with use of pesticides and fertilizer (39.4%); upper zone ranked second with 33.5% and middle zone ranked the least with 24.5%. Out of 100% of the respondents, 2.7% disaffirmed the use of pesticides and fertilizers in their farms due to inadequate financial support to farming and inadequate legit borrowing facilities in the study area. The types of fertilizers used in the study area by the respondents includeNitrogen Phosphate

Potassium NPK,Nitrogen Phosphate, Prilled Urea, Calcium Ammonium Nitrate and Ammonium Sulphate Nitrate. The pesticides used by the respondents in the study area include Cypermethrin, 2.4 D - Dichlorophenoxy-acetic acid,Gramaxonesuper and Prime force (Dichlovos). This implied that majority of respondents used fertilizer and pesticide for farming activities in the study area.

Table 1:Use of Fertilizer and Pesticide in Farming

Options	Upper zone		Middle zone		Lower zone	
Yes	117	33.5%	85	24.3%	138	39.6%
No	06	1.8%	01	0.3%	02	0.6%
Total	123	35.2%	86	24.6%	141	40.2%

Source: Field Survey (2019)

Fertilizer Application per Hectare

As indicated in Table 2, fertilizer application per hectare ranges from 50kg to 170kg in the study area. 121 – 170kg fertilizer application ranked the highest in lower zone and 101 – 120kg ranked the least in middle zone. This implies that the respondents in the study area applied high rate of fertilizer during farming activities and it improved crop yield but in turn lead to water quality degradation.

Table 2:Fertilizer Application per Hectare

Options	Upper zone		Middle zone		Lower zone	
50 – 100kg	47	13.4%	21	6.0%	41	11.7%
101 – 120kg	45	12.9%	20	5.7%	31	8.8%
121 – 170kg	31	8.9%	45	12.9%	69	19.7%
Total	123	35.2%	86	24.6%	141	40.2%

Source: Field Survey (2019)

Pesticide Application per Hectare

As indicated in Table 3, pesticide application per hectare ranges from 5 to 10litres in the study area. 10 litres and above of pesticide application ranked the highest in lower zone with 69 respondents and 5 – 7 litres ranked the least in middle zone with 19 respondents. This implies that the respondents in the study area applied high rate of pesticide during farming activities and it improved crop yield but in turn lead to water quality degradation.

Table 3: Pesticide Application per Hectare

Options	Upper zone		Middle zone		Lower zone	
5 – 7litres	41	11.7%	19	5.4%	41	11.7%
8 – 9litres	45	12.9%	20	5.7%	31	8.8%
10 litres and above	37	10.6%	47	13.4%	69	19.7%
Total	123	35.2%	86	24.6%	141	40.2%

Source: Field Survey (2019)

4.2 Extent of Occurrence of Agrochemicals in Surface Water and Sediment Samples, and Water Quality Status in the Study Area

As revealed in Table 4, Manganese values within the study area ranges from 0.08 in W1 to 0.74 in W7. The maximum permitted level is 0.2 and the ones within this range include 0.08 and 0.16 in W1 and W3. The remaining six sample points contains manganese as toxic element which can cause neurological disorder in human. For Nitrite, the maximum permitted level is 0.2 and the sample points within this range were W1, W2, W3 and W4 with values of 0.05, 0.02, 0.16 and 0.18. The sample points above the maximum permitted level include W5 to W8 with values of 0.25, 0.28, 0.34, and 0.56. This can leads to blue baby syndrome in infants under 3 months. The high nitrite level could be attributed to fertilizer application on agricultural activities in the study area.

Table 4: Physicochemical Analysis on Water Samples

Parameter (ppm)	W1	W2	W3	W4	W5	W6	W7	W8
Nitrates	0.256	N.D	0.893	1.764	1.080	1.142	1.274	2.626
Nitrite	0.05	0.02	0.16	0.18	0.25	0.28	0.34	0.56
Ammonium	-	-	-	-	-	-	-	-
Phosphate	N.D	N.D	N.D	0.715	0.229	3.969	4.564	1.294
Sulphate	2.07	0.69	1.02	1.57	1.68	1.88	2.15	
Manganese	0.08	0.25	0.16	0.57	0.62	1.06	0.74	0.65
Chloride	35.5	53.3	71.0	71.0	60.40	63.90	35.6	106.5
COD	30.05	25.65	35.70	32.06	28.30	40.07	24.80	45.06
BOD	12.25	9.82	15.60	13.20	12.00	16.02	10.85	18.15
TSS	45.6	30.0	52.00	49.62	35.02	40.52	38.65	53.05
Total Hardness	7.50	8.60	7.01	6.85	10.52	7.60	8.00	4.60
Potassium	0.56	0.35	1.27	1.54	0.13	2.07	1.68	1.75

Note: W =Water samples, N.D =not detected

Nitrate ranged between 0.256ppm and 2.626ppm at the study area as indicated in Table 4. The acceptable limit for Nitrate is 1-2ppm and water sample W8 (2.626ppm) have exceeded that level which could have serious negative health implications on the inhabitants of the study area. Nitrates are an essential source of nitrogen (N) for plants. When nitrogen fertilizers are used to enrich soils, nitrates may be carried by rain, irrigation and other surface waters through the soil into groundwater which may be the cause of high nitrate level in W8 of the water sample. Human and animal wastes within the study area can also contribute to nitrate contamination of the Rivers. Nitrates can be

harmful to humans if they exceed acceptable limits because our intestines cannot break them down into nitrites which affect the ability of red blood cells to carry nitrogen. Nitrates can also cause serious illness in fish and death there decreases fish population. This agreed with the finding of Eziashi (2015) and Waite (2011).

The relatively high levels of BOD (9.82-18.15 ppm) can be attributed to the presence of decaying organic matter from possible use of herbicides. BOD has been a fair measure of cleanliness of any water on the basis that values less than 1-2 ppm are considered clean, 3 ppm fairly clean, 5 ppm doubtful and 10 ppm definitely deity.

Table 5: Physicochemical Analysis on Sediment Samples

Parameter (ppm)	S1	S2	S3	S4	S5	S6	S7	S8
Nitrates	2.004	2.098	2.095	2.144	2.137	1.896	2.556	3.147
Nitrite	0.07	0.63	0.71	0.69	0.75	0.54	1.02	1.16
Ammonium	-	-	-	-	-	-	-	-
Phosphate	1.546	2.552	1.965	1.269	2.099	4.564	5.771	3.776
Sulphate	15.06	5.28	6.57	10.06	12.58	22.68	8.65	7.96
Manganese	0.20	0.65	0.42	1.49	1.60	2.79	1.95	2.45
Chloride	23.08	37.31	48.28	41.89	35.64	40.90	22.78	72.42
COD	NA	NA	NA	NA	NA	NA	NA	NA
BOD	NA	NA	NA	NA	NA	NA	NA	NA
TSS	NA	NA	NA	NA	NA	NA	NA	NA
Total Hardness	NA	NA	NA	NA	NA	NA	NA	NA
Potassium (mg/kg)	35.02	12.56	40.65	55.65	10.56	62.75	45.09	58.25

Note: NA = Not Available, S = Sediment samples

Nitrate ranged between 1.896ppm and 3.147ppm at the study area as indicated in Table 5. The acceptable limit for Nitrate is 1-2ppm and sediment samples S1, S2, S3, S4, S5, S7 and S8 have exceeded that level which in turn will affect the health of the inhabitants of the study area. Maximum permitted level for Potassium ranges between 3.6 – 5.2ppm and all the sediment samples has higher values which in turn can cause kidney and heart diseases in human health. Phosphates and nitrates are important nutrients to plant bloom and the eutrophication of lakes rate of plant growth observed in the river.

5. Conclusion

In conclusion, people in the study area are looking at surface water in the rivers as an infinite resource thereby, ignoring its real value. Rather, more attention is given to the farming sectors which in turn degraded the water quality. The surface water quality of study area is not fit in this present form to serve the domestic purpose of drinking, washing, cooking for the local inhabitants without further treatment. Taking into account the travelling delay of surface water in the rivers, these results indicate that the poor water quality in the surface water of the catchment probably is not only due to recent (excessive) fertilisation as well as pesticides use in surrounding parcels, but can also be attributed to historical pollution in parcels located at a greater distance. In view, of the aforementioned, we suggest that farmers should be educated to change farming practices and adopt sustainable agrochemical usage. In the future, the proliferation of environmental policies, research and the collation of knowledge will hopefully improve the ways in which sustainable farming interacts with surface water resources precisely the rivers in the study area to promote and reach overall environmental quality standards.

References

Federation, W. E., & American Public Health Association. (2005). Standard methods for the examination of water and wastewater.American Public Health Association (APHA): Washington, DC, USA.

APHA/AWWA/WPCF. (2005). Standard Methods for the Examination of Waters and Wastewaters, 21st ed. *Washington*, DC, USA.

Bamigboye, A. Y., Adepoju, O. T. & Olalude, C. B. (2017). “Assessment of Dichlorvos and Endosulfan Pesticide Residue Levels in Selected Fruits and Vegetables Sold in Some Major

Markets in Ibadan, Oyo State, Nigeria" *Journal of Applied Science and Technology*, 22(5), 1-6.

Bassi, A. P., Ramyil, M. C., Ogundeko, T.O., Abisoye-Ogunniyan, A, Builders, M..... & Nwankwo B. (2016). "Farmer: Agrochemical Use and Associated Risk Factors in Fadan Daji District of Kaura LGA, Kaduna State, Nigeria." *American Journal of Medical and Biological Research*, 3, 33-41. doi:10.12691/ajmbr-4-3-1.

Dirisu, A. R., Ekaye, S. A., & Olomukoro, J. O. (2016). Pesticides distribution in surface waters and sediments of lotic and lentic ecosystems in Agbede wetlands. *Ethiopian Journal of Environmental Studies and Management*, 9 (2), 997-1008.

Eziashi, Y. (2015). A probabilistic approach for the groundwater vulnerability to contamination by pesticides: the VULPEST model. *Ecological Model*, 51, 47–58.

Ja'agi, A. I., & Baba, J. M. (2015). The Effects of Environmental Consciousness in Public Healthcare Institutions and Community Awareness in Mokwa Local Government Area, Niger State, Nigeria. *Journal of Environments*,2 (1), 1-4.

Joko, T., Anggoro, S., Sunoko, H. R., & Rachmawati, S. (2017). Pesticides Usage in the Soil Quality Degradation Potential in Wanasari Subdistrict, Brebes, Indonesia. Applied and Environmental Soil Science.

Jokha, M. (2015). Effects of Agricultural Pesticides and Nutrients Residue in Weruweru Sub-Catchment, Tanzania (Doctoral dissertation, Kenyatta University).

Keri, H. J., & DIRECTORATE, E. I. (2009). Nigeria's status on pesticide registration and maximum residue levels. *In The workshop on pesticide Maximum Residue Levels (MRLs) held in Alexandria*, Egypt.

Knauer, K. (2016). Pesticides in surface waters: a comparison with regulatory acceptable concentrations (RACs) determined in the authorization process and consideration for regulation. *Environmental Sciences Europe*, 28(1), 13-18.

Lakhani, L. (2015). "How to Reduce Impact of Pesticides in Aquatic Environment" *International Journal of Research Granthalaayah, a knowledge respiratory, Social Issues and Environmental Problems*, 3 (Iss.9: SE), 2394-3629.

Lewis, K. A., Tzilivakis, J., Warner, D. J., & Green, A. (2016). An international database for pesticide risk assessments and management. Human and Ecological Risk Assessment: *An International Journal*, 22 (4), 1050-1064.

Lawrence, E., Ozekeke, O. & Isioma, T. (2015). Distribution and ecological risk assessment of pesticide residue in surface water, sediment and fish from Ogbesse, River State, Nigeria. *Journal of Environmental Chemistry and Ecotoxicology*, 7(2), 20-30.

National Environmental Standards and Regulations Enforcement Agency, (2009). National Guidelines for Environmental Audit in Nigeria. pp. 1-3.

National Environmental Standards and Regulations Enforcement Agency, NESREA, (2014). "*Training Manual" Environmental Compliance Monitoring*.pp. 23-36.

Njoku, K. L., Ezeh, C. V., Obidi, F. O. & Akinola, M. O. (2017). "Assessment of Pesticide Residue Levels in Vegetables sold in some Markets in Lagos State, Nigeria". *Journal of Biotechnology*. 32 53-60, DOI: 10.4314/njb.v32i1.8.

Ogwueleka, T. C. (2014). Assessment of the water quality and identification of pollution sources of Kaduna River in Niger State (Nigeria) using exploratory data analysis. *Water and environment journal*, 28(1), 31-37.

Ojo, J. (2016). "Pesticides use and health in Nigeria". *Ife Journal of Science*, 18(4), 981-991.

Ojutiku, R. O., Kolo, R. J., & Yakubu, M. A. (2016). Spatial Distribution of Phytoplankton and Physico-Chemical Characteristics of Agaie-Lapai Dam, Minna, Niger State, Nigeria. *Journal of Biology and Life Science,* 7 (2), 1-12.

Ramteke, A.A and Shirgave, P.D. (2012). Study the Effect of Common fertilizers on Plant Growth Parameters of Some Vegetable Plants. *Journal of National Production and Plant Resources*, 2(2), 328-333.

Sidi A, Waziri N.M, Maji A.T, Okunlola I.A, Umar A, & Waziri S.H. (2016). Assessment of Chemical Quality of Water from Shallow Alluvial Aquifers in and around Badeggi, Central Bida Basin, *Nigeria Journal of Earth Sciences and Geotechnical Engineering,* 6, (3), 133-145.

Waite, R. (2011). Regional estimation of groundwater vulnerability to non-point sources of agricultural chemicals. *Water Science Technol.*, 33, 241–247.

Characterization of Hospital Wastewater and Management Treatment Practices in Minna, Niger State, Nigeria

A. Abubakar [1], M. A. Emigilati[1], T. I. Yahya [1]. and M. N. Muhammed [2]

[1]Department of Geography, Federal University of Technology, P. M. B. 46, Minna, Niger State, Nigeria

[2]Department of Chemistry, Federal University of Technology, P. M. B. 46, Minna, Niger State, Nigeria.

[1]tangwagee@gmail.com[1]M.emigilati@fut minna.edu.ng

[2]muhdndamitso@futminna.edu.ng

Abstract

Hospitals generate large quantities of both solid and liquid wastes. High public health and environmental risks are involved in managing these wastes. Objectives of this study were: To determine the characteristics of hospital wastewater and examine the current wastewater management practices system. Hospital wastewater contains various potentially amount of hazardous pathogenic organisms, organic and heavy metals, as well as hazardous chemicals, and one of the most important source of pollution factors. In this study, two general government hospitals in Niger State were selected for this studied, i.e., General Hospital Minna, and New General Hospital Minna. Wastewater characteristics were determined by taking samples from each hospital. Results were compared with World Health Organization (WHO). Measurements and monitoring of ten environmental parameters determined. Physical properties: pH, Total Suspended Solids (TSS). Chemical properties: Biological Oxygen Demand (BOD), Chemical Oxygen Demand (COD), trace elements, Dissolved Oxygen (DO), Chloride, Sulphate. Microbiological properties: Total Coliforms (TC), Faecal Strep (FS) and Faecal Wastewater analysis revealed that BOD, COD and Chloride concentrations were more than the permissible limits prescribed in WHO. Coliforms others indicators such as physiochemical and biological indicated that the quality of wastewater in the investigated hospitals was similar to domestic wastewater. Physiochemical parameters studied revealed that the hospital wastewaters showed most of parameters values are within WHO and Federal Ministry of Environment Nigeria acceptable limits. The study of wastewater treatment and disposal methods clarified that the discharge to municipal wastewater collection system will be able to discharge their wastewater into sewerage network. This process is the best solution for wastewater management in General Hospitals Minna. The researchers recommended that the hospitals have to select onsite separate wastewater treatment

alternative. Indeed, efforts must be undertaken by hospitals to integrate environmental control and safe programme to avoid a higher risk safety factor of hospital facility operational facilities Key words: Hospital, Wastewater, Water quality, Wastewater treatment.

INTRODUCTION

Hospital wastewater are known sources of several chemicals including remnants of disinfectants, medicine, pharmaceuticals, radionuclides and antineoplastic drugs are widely used in hospitals for medical purposes and research are regarded as risky wastewater for humans and the environment and if left untreated, these could lead to outbreak of communicable diseases, water contamination, and radioactive pollution (Gautam *et al.*, 2007). Medical waste (MW) is an environmental as well as public health issue that attracts attention in both advanced and developing countries this is because both, liquid and solid waste generated from medical activities has become a serious concern because of its implications on the environment and public health Nazik, (2010). Hospitals generate on average 750 liters of wastewater by bed per a day which loaded with pathogenic microorganisms, pharmaceutical partially metabolized, radioactive elements and other toxic chemical substances (Babanyara *et al.,* 2013). The huge volume of hazardous wastewater needs special attention, left untreated; these could lead to outbreak of communicable diseases, water contamination and radioactive pollution Evens *et al.* (2014) and Babanyara *et al.* (2014).

Discharge and penetration of these substances into the human environment especially groundwater and surface water would cause major hazards and health implications. Therefore, we need to monitor hospital effluent precisely and provide necessary measures in order to prevent from entry of non-treated hospital wastewater into human environment. Also, we have to protect surface water and groundwater from wastewater disposal, otherwise serious contamination and diseases will spread among healthy peoples Ashouri and Sadhezari (2016)

The UN Basel Convention considers health care waste as the second most dangerous wastes after nuclear wastes. WHO, WPRO; (2011). Health care waste includes all the waste generated by all health care establishments, health research facilities, and health-related laboratories. It also includes waste generated by home health care activities, such as dialysis, insulin injections WHO (Retrieved 23-5-2018). There are many potential hazards associated with handling health care wastewater through transmission of diseases posing risks not only to the patients and health care workers and their families, but also to, their relatives, environment and neighborhood communities especially

children due to their fragility, developing immune systems and for the fact that they often play at such sites increases their contact with medical waste, thus exposing them to injuries and infections. WHO, (2011).Despite the great potential for environmental hazards and public health risks of hospital wastewater, its proper handling and management is substantially undermined in many developing countries. The hazardous waste has a small portion of healthcare waste, but the absence of appropriate waste segregation practices leads mixing hazardous waste with general (non-hazardous) waste results the entire bulk of waste becoming potentially hazardous. Esubalew **(**2015). The management of health care waste is an integral part of a national healthcare system. However, many countries do not have minimum standards or practices, essentially in developing countries. Research conducted by (Chimchirian *et al*., 2007), revealed that the use of ground water for supplying drinking water has profoundly increased and in case of failure in effective management wastewater treatment plant as well as controllingcontamination, hospital wastewater spreads into surface and ground water (Seifrtová *et al*., 2008), Pena *et al*, (2010). Consequently, this,leads to prevalence of different kind of diseases. Therefore, huge costs would be imposed on the public and the government. For that reason, investigating hospital wastewater treatment is germane.

Medical waste management has not received sufficient attention and the priority it deserves in developing countries such as Nigeria, where health concerns are competing with limited resources Abahand and Ohimain, (2011);Ibijoke *et al.*,2013).In this case hazardous medical wastes are still handled and disposed-off together with non- hazardous wastes thus posing a great health risk to the healthcare workers, the public and the environment (Silva *et al.*,2005; Ogbonna e*t al.*,2012;Ibijoke *et al.*,2013).

In Niger State, MWs in different hospitals are managed improperly in which they are dumped in open landfills, surface dumping sites or by the use of sub-standard incinerators. In addition, unavailability of adequate data with regards to waste generation rate, composition and management practices have posed profound challenges in planning appropriate MW management methods in the state. Furthermore, both non-hazardous and infectious MWs in the state are burnt together in incinerators leading to the more accumulation of more heavy metals as well as organic compounds and other cancer causing organics in the bottom ash of the incinerators which if not properly disposed of can pollute the environment and pose public health problems such as acute respiratory syndromes,

gastrointestinal abnormalities and various cancers. These has been proved in the studies conducted by (Zhao *et al.*, 2010; Auta and Morenikeji, 2013; Mohajer *et al.*, 2013).

Hospital waste management in Nigeria and Niger State in particular has not also received sufficient attention and the priority it deserves both at local and national levels. Some studies have been carried out on solid waste management of hospitals but little or no previous data is available on wastewater in the state Shaibu (2014). However, practices from daily observation indicate that, most health facilities had not put in place an organized management system to address Health Care Waste Management. In countries' where the management of healthcare wastes is often poor; they could pose a potential risk to public health through the circulation of agents in the environment, animals and people Babanyara *et al.* (2014)

2. MATERIALS AND METHODS

2.1 *Description of the Study Area*

The study area is located in Minna town, Chanchaga Local Government Area of Niger State, Nigeria. Minna is the Capital of Niger State and also the largest commercial centre in the state and its proximity to Federal Capital attract more population. The study area lies between latitude 9º33 to 9º4 N and longitude 6º29 to 6º35 E. The mean annual rainfall is between 1334mm and 3000mm, the mean monthly temperature is highest in March at 39.5 ºC and lowest in August at 22.3ºC. (Ministry of Land and Housing Minna, 2015). Minna has a total population of approximately 201,429 people out of the total population of Niger State, which has 3,950,249 with an annual growth rate of 2.3%. (National Population Commission, 2006). Also, Minna has become a cosmopolitan city with most of residents engaging in white collar jobs. As a state capital, majority of the inhabitants are civil servants, the proximity to Abuja capital of Nigeria influence the increasing influxes of population and boosted commercial activities a result, the volume of wastewater generated has increased due to increase number of inpatients and outpatients that visited the hospital Shaibu (2014). Figure 1.1 shows the location of the study area

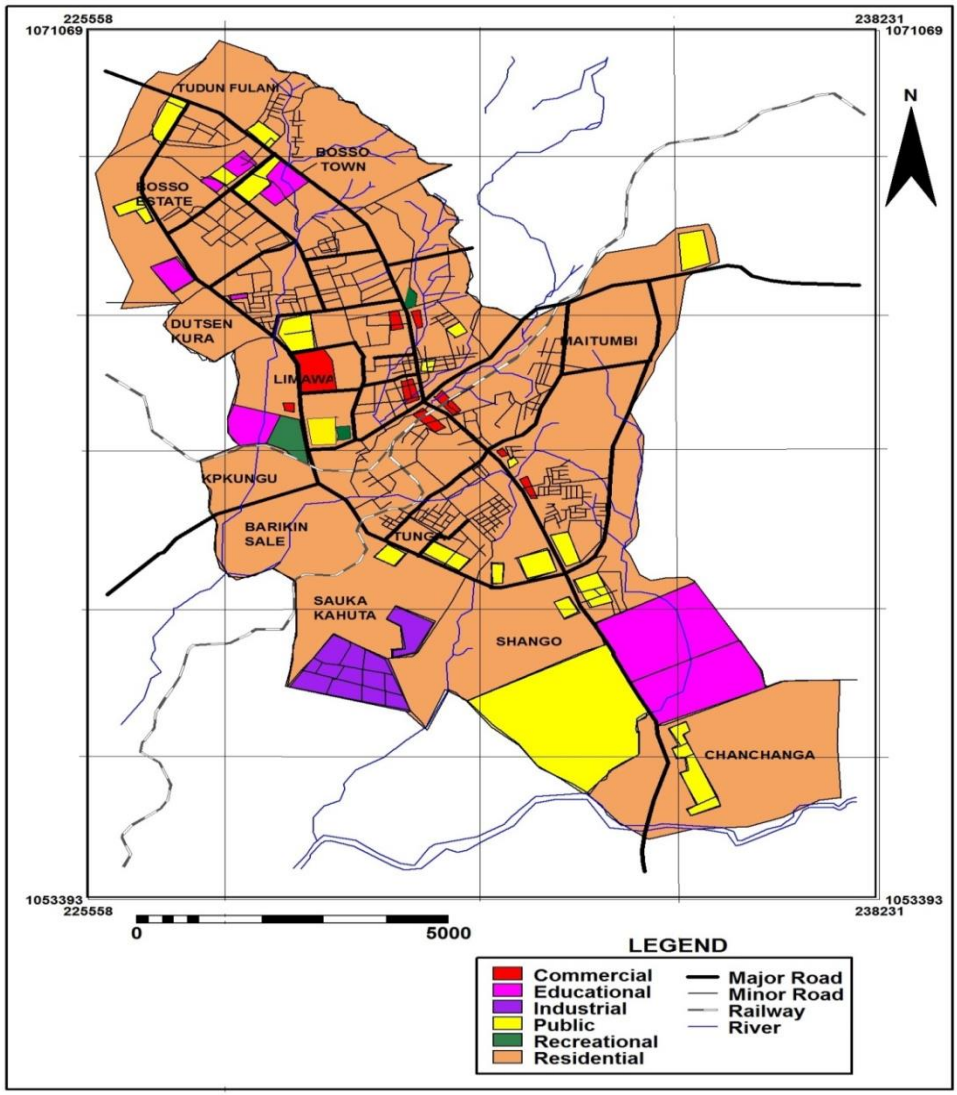

Figure 1.1: Location of the Study Area

Source: Ministry of Land and Housing, 2015

The General Hospital has six wards: Surgical, Pediatrics, Gynecology and obstetrics, Ophthalmology, Pharmaceutical, Medical, and Labor wards, with 296 maximum bed capacities More so, Minna General Hospital has a new extension located at opposite site with 150 bed capacities. These are the largest hospital which generate considerable amount of wastewater and the outpatient flow on

average is 150-200 per day. The hospitals consumes considerable amount of water. It is one of the largest hospital which releases considerable amount of wastewater to the soaker- way

In this study, management and quality of wastewater in the government hospital in Minna Niger State, Nigeria have been investigated. The raw wastewater discharge of the hospital was collected to determine various physico-chemicals, trace organic pollutants, trace elements, biochemical indicators (BOD and D.O) and microbiological measurements. The wastewater quality was compared with WHO limits (1996) and Nigeria Federal Ministry of Environment (1991). In addition, the current wastewater management practices was equally examine. All of the examinations were performed according to the instructions of "Standard Methods for the Examination of Water and Wastewater" (APAH, 2005). Similarly, Focus Group Discussion and Field Observations were utilizedfor the investigations of wastewater management treatment practices

2.2 *Sampling Collection and Analysis of Wastewater*

There were several wards in the selected hospitals. Each ward generated wastewater having different characteristics. All these wastewaters discharge into soaker-ways untreated. Collection tank of disposal station not available in both hospital selected in this study. To take a representative sample, it was decided to collect wastewater from each of the soaker way to form a composed sample. The testing procedures for the parameters tested are mentioned in Table 1. The heavy metals in the wastewater were analysed.

Table 1. Parameters tested and the testing procedures.

Parameters	**Testing Method**
PH @ 25.0 0C	APHA
Suspended Solid (mg/L)	COLOMETRIC
COD (mg/L)	APHA 5220 (D)
BOD (mg/L)	APHA 5210B

D.O (mg/L)	APHA 4500-OC
Chlorides (mg/L)	APHA 4500 Cl-(B)
Sulphate (mg/L)	APHA 4500 SO4 E
Tata Coliform (Cfu/100ml)	APHA 9222 B
Faecal Strep (Cfu/100ml)	APHA 9222 B
Faecal Coliforms (Cfu/100ml)	APHA 9222 B

- C.O.D = Chemical Oxygen Demand
- D.O = Dissolved Oxygen
- B.O.D = Biological Oxygen Demand

All the testing methods are based on Standard Methods for the Examination of Water and Wastewater, 20th edition (1998), www.standardmethods.org.

3.0 RESULT AND DISCUSSION

3.1 *Characteristics of Hospital Wastewater*

Hospital wastewater quality and management has become a critical issue as it poses potential damage to the environment and health risks as well, which has taken a central place in the national health policies of many countries Hanan and Amira, (2011). Hospitals investigated had no wastewater treatment plant. The results of physico- chemical parameters are presented and compared with WHO in Table 2 that indicated the quality characteristics of raw wastewater in the investigated hospital for pH, TSS, D.O, BOD, COD,T.C, F.C. F.S, Sulpate and Chloride.

3.1.1. *pH- Value*

One of the most germane parameters in biological waste water treatment processes is pH and its variances. Overall, suitable pH for bacteria growth and activity ranges between 6.5 to 8.5. The activity

of most of bacteria effective on wastewater treatment is disrupted or stopped at pH> 9.5 (Emmanuel *et al*., 2001). While, acceptable effluent pH for discharge into surface water and rivers ranges between 6.5 to 8.5, and for agricultural purposes and green spaces irrigation ranges between 6 to 8.5 (Giger *et al* 2003). In the current study, hospitals raw wastewater and effluent was measured to be 7.31 and 7.49, respectively. These values were within the permissible limits of WHO (5-9) and Nigeria Federal Ministry of Environment (6-9),these amount are acceptable. Similar results were obtained in other studies. Beyene and Redaie, determined pH value in hospital wastewater to be 7.4. Study on hospital wastewater in India showed pH value of 7.36 (Gautam *et al*., 2007). Other environmental studies (Onesios, *et al*., 2009 and Metcalf and Eddy, 2003) that within WHO limits (pH: 5-9) (WHO, 1996). All these results agree with the current study results and therefore, safe for discharge into surface water and rivers

Table 2. Physicochemical characterizations of hospital wastewater

Parameter	General Hospital	General Hospital Extension	WHO (Permissible Limit)
P^H	7.31	7.21	5-9
TSS (mg/L)	212	49	100
COD (mg/L)	215	23	60
BOD (mg/L)	86	10	50
DO (mg/L)	1.60	1.80	6.0
Chloride (mg/L)	62,70	59.9	1000
Sulphate (mg/L)	63.0	11.0	250
Total Coliform (CFU/100 mL)	1100	72000	1000
Faecal Strep (CFU/100 mL)	402	34000	1000
Faecal Coliform (CFU/100 mL)	400	60000	1000

3.1.2 *Total Suspended Solids (TSS)*

This is one of the common parameters used in defining a wastewater. The result indicates that TSS concentration of hospital raw wastewater from the General hospital was 212mg/L. This concentration is more than the 100 mg/L permissiblelimit by the WHO and Nigeria Federal Ministry of Environment of 30 mg/L. Similar studies which investigated wastewater samples of some government hospitals obtained TSS concentrations in the range of 120-400mg/L (Metcalf and Eddy, 2003).The value of this parameter in the current study of the New General Hospital Extension was 49mg/L which is lower than theWHO 100 mg/L permissiblelimit but, closed to Nigeria Federal Ministry of Environment limit of 30mg/L. Other studies measured TSS value to be 50 mg/L and 49.27 mg/L Ashouri and Sadhezari (2016) and all these values are lower than theWHO standard limit but similar to the one obtained for the New General Hospital Extension.

3.1.3 *Dissolved Oxygen (DO)*

Dissolved oxygen is one of the most important bio- monitoring parameters of water quality in the aquatic environment.The DO values in the current study hospitals obtained to be 1.60 and 1.80 mg/L respectively, these values were lower than theWHO 6.0 mg/L permissiblelimit. Therefore, safe for discharge into surface water and rivers

3.1.4 *BOD and COD*

The parameters of BOD and COD are widely used to characterize the organic matter contents of wastewater (Puangrat and Nattapol, 2010). BOD is an index of the oxygen-demanding properties of the biodegradable materials in water that are useful in assessing water pollution loads and for comparison purposes. Also, COD is a measure of pollutant loading in terms of complete chemical oxidation using strong oxidizing agents. It provides a good index of chemical-oxygen demanding properties of natural waters. BOD and COD values in the studied hospitals varied from 10 mg/L to 86 mg/L and 23 mg/L to 215 mg/L respectively.These concentrations are higher than the permissiblelimits of WHO (COD: 60, BOD: 50 mg/L). Highest concentrations of BODand COD were obtained for the General Hospital. Generally, values of hospital wastewater BOD vary due to differences in their medical services (Purdara, *et al.*, 2004). In some studies, the BOD values of 272.98 mg/L and 240 mg/L have been reported; Ashouri and Sadhezari (2016) and Rafaat *et al*, (2010) respectively. The findings in thecurrent study not in accord with all of these results. Another

study conducted in Imam Khomeini Hospital, with theBOD contents of 60.5 which is closed to 86 of BOD contend in the current study. Similarly, the results of CODin hospital raw wastewater were 792, 628 and 629 mg/L respectively were reported (Sabzevari *et al*., 2005). All these results are higher than the findings of current study. According to the WHO standard, the maximum allow able concentration of BOD and COD in effluent discharge into surface water are 50 mg/L and 60 mg/L respectively, while for agricultural purposes and green spaces irrigation, the maximum allowable concentration is 100 mg/L (Giger, *et al*., 2003). Therefore, the contends of BOD and COD in the current study of General Hospital are not safe for discharge in to surface water and this calls for special attention.

3.1.5 *Chlorides and Sulphates*

The result of Table 2 reveals that the parameters; chlorides and sulphatesobtained were 62.7, 59.9 and 63.0 and 11.0 mg/L respectively for the General Hospital and the General Hospital Extension. These values are less than the WHO limits and Nigeria Federal Ministry of Environment of 250 mg/L for discharge into surface water. Therefore, the results of this findings in the current study of General Hospital are safe for discharge in to surface water and this calls for regular monitoring and evaluation for it sustainability.

3.1.6*Microbiological Pollutants*

Treatment of patients with enteric diseases is a critical problem during outbreaks of diarrhoeal diseases, therefore, the knowledge of the microbial quality of hospital wastewater is very critical (Pauwels, *et al*., 2006). To achieve this, some bacteriological indicators are used to reflect the presence of pollution pathogens in wastewater. These include the determination of TC. FC and FS that are the most world-wide knownparameters used for the establishment of contamination (Hanan and Amira, 2011). The microbiological quality of water varies from hospital to another due to variations in the consumption of water by the hospitals during the study. The acceptable limit of TC, FC and FSin hospital effluent discharge into surface water, for agricultural purposes and green spaces irrigation are 1000, and 400 MPN/100 ml, respectively Majlesi(2001)

Table 2 indicates that the average TC, FC and FS in the wastewater samples of the current study were 1100, 400 and 402 CFU/mLrespectively in the case of General Hospital while for the New General Hospital extension, the values obtained were 72000, 60000 and 34000 CFU/mL respectively. This

means that, the number of TC, FC and FS are higher than the 1000 MPN/100 mLgiven by WHO,indicating higher bacterial contamination.Accordingly, these hospital effluents are not ripe for discharge into surface water. These high values could be as a result of the fact that proper wastewater treatment process is not on priority list of most of the managements of the selected hospitals in this study since none of them hasa wastewater treatment plant. Another studies, the TC, FC and FS values of 99.57, 97.45, 90.63 and 29.87, 31.2 30.54 MPN/100ml, respectivelyrespectively have been reported;(Majlesi and Yazdanbakhsh,2008)and (Ashouri and Sadhezari, 2016). All these results are lower than the results of current study.This means that lack of bacterial

contamination and good treatment plant efficiency in those hospitals.

3.1.7*Study on wastewater treatment and disposal*

The result of Focus Group Discussion and Field Observationsreveals that, the two General Hospitals in this study have no wastewater treatment plant and finally dispose their wastewaters directly into their septic tanks (soaker-way). This may permit the discharge of infectious agents into groundwater and other environments which may be a hazard for both hospital personnel and the nearby community. Therefore, this present situation calls for urgent interventions by the concerned authorities in addressing these critical environmental and health risk factors.

4.0 CONCLUSIONS AND RECOMMENDATIONS

Since wastewater treatment is not a priority of some managements of the selected hospitals because none of them haseven a wastewater treatment plant, the BOD, COD,TC, FC and FS of the wastewater samples of most of the hospitals are above the limits prescribed by WHO thus making it unsafe for direct discharge of these wastewaters into surface water. This is because this may harm the aquatic life and even human health. Therefore, this calls for special urgent attention by these establishments by way of establishing wastewater treatment plantsand improving the operation and maintenance practices by employing experienced operators in order to meet effluent discharge standards.

Furthermore since wastewater treatment and disposal methods clarified that the discharge to municipal wastewater collection system will be able to discharge their wastewater into sewerage network, this process may be the best for wastewater management in the general hospitals studied in

this work. It is also the recommendation of this study that the hospitals select onsite separate wastewater treatment alternatives that will integrate environmental control and safe programmes aimed at avoiding high risks in safety factors of hospital facility operations.

References

Abahand, S. O., Ohimain, E.I. (2011). Healthcare waste management in Nigeria: A case study *Journal of Public Health and Epidemiology, Vol.* 3(3) 99-110,

APAH, AWWA, WEF (1998). *Standard Methods for the Examination of Water and Wastewater.* 20th ed. United BookPress. Baltimore.

Ashouri, A and Sadhezari, B. (2016). Qualitative and Quantitative Assessment of The Effects of Hospital Wastewater Pollutants on Treatment Plants Performance Of Medical Sciences University Of Shiraz Hospitals. *Journal of Proceedings of 14th Research World International Conference, Auckland, New Zealand*, ISBN: 978-93-85973-63-5.

Auta, T. and Morenikeji, O.A. (2013). Heavy mental concentrations around a hospital incineration and a municipal dumpsite in Ibadan City, South-West Nigeria, *Journal of Applied Sciences and Environmental Management, vol.* 18, no 3. 419-422.

Babanyara, Y. Y., Israhim, D. B., Garba, T., Bogoro, A. G., and Abubakar, M. Y. (2013). Poor Medical Waste Management practices and its risks to human health and the Environment; a literature review. *International journal of Oral Health CommunityDentistry,* 7(1). 43-52.

Chimchirian, R., Suri, R., andFu H. (2007). Free synthetic and natural estrogen hormones in influent and effluent of three municipal wastewater treatment plants. *Water Environ Res.*79(9):969-74.

Beyene, H. and Redaie, G. (2011). Assessment of waste stabilization ponds for the treatment of hospital wastewater: the case of Hawassa university referral hospital. *World Applied Sciences Journal* 15(1): 142-150.

Emmanuel, E., Perrodin, Y., Blanchard, J.,andVermande, P. (2001). Chemical, Biological and Ecotoxicological of Hospital Wastewater. *Journal of Science and Technology;* 2: 31-38.

Esubalew, T. (2015). Waste generation, composition and management in the Amhara National Region State, Ethiopia. A PhD Dissertation submitted to the School of Graduate Studies of Addis Ababa University.

Evens, E., Yves, P., Gerard, K., Jean-Marie, B., Paul, V. (2014). Effects of Hospital Wastewater on Aquatic Ecosystem. *Journal of Ecotoxicological and sanitary risk assessment related to Hospital Wastewater*. Retrieved 5th August, 2018 from www.researchgate. Net/232724983.

Nigeria, Federal Ministry of Environment (1991). Guidline and Standards for Environmental Pollution Control in Nigeria

Gautam, A.K., Kumar, S., and Sabumon, P.C. (2007). Preliminary study of physicochemical treatment options for hospital wastewater. *Journal of Environmental Management* 83: 298-306.

Giger, W., Alder, A.C., and Golet, E.M. (2003). Occurrence and fate of antibiotics as trace contaminants in wastewater, Sewage Sludge and Surface Water. Chimin; 57(9):485-491.

Hanan, A. E., and Amira M. A (2011). Assessment of Aquatic Environmental for Wastewater Management Quality in the Hospitals. *Australian Journal of Basic and Applied Sciences*, 5(7): 474-782, 2011 ISSN 1991-8178.

Ibijoke, A., Babajide, A., Williams, A., and Rafid, K. (2013). Profile of medical waste management in two healthcare facilities in Lagos, Nigeria.*Waste management and research, Vol*.31.pp494-501.

Mahvi, A., Rajabizadeh, A., Fatehizadeh, N., Yousefi, H., and Ahmadian, M. (2009). Survey Wastewater Treatment Condition and Effluent Quality of Kerman Province Hospitals, *World Applied Sciences Journal*, 7(12): 1521-1525.

Majlesi, N. M., and Yazdanbakhsh, A. R. (2008). Study on wastewater treatment systems in hospitals of Iran. *Iran Journal of Environment, Health Science Engineer*; 5(3):211-215.

Majlesi, N. M. (2001). Study of wastewater disposal and effluent quality in ShahidBeheshti university of medical sciences hospitals. *Pajouhandeh Journal*; 6(24): 371-372, 2001.

Metcalf and EddyInc (2003). *Wastewater Engineering: Treatment and Reuse*. 4th Edition.

McGraw-Hill. New York.

Mohajer, R., Salehi, M. H., Mohammadi, J., Emami, M. H., and Azarm, T. (2013). The status of lead and cadmium in soils of high prevalenct gastrointestinal cancer region of Isfahan. *Journal of Research in Medical Sciences, vol.* 18, no. 3. 210-214.

Nazik, A. E. (2010). Assessment of Medical Waste Management in Khartoum State Hospitals a PhD Thesis Submitted to the University of Khartoum

Ogbonna, D. N., Chindah, A., Ubani, N. (2012) "Waste management options for health care wastes in Nigeria: A case study of Port Harcourt hospitals" *Journal of Public Health and Epidemiology. Vol.* 4(6), 156-169.

Pauwels, B., Ngwa, F., Deconinck, F.,and Verstraete, W. (2006). Effluent quality of a conventional activated sludge and a membrane bioreactor system treating hospital wastewater. *Journal of Environmental Technology*, 27: 395- 402.

Pena, A., Paulo, M., Silva, L., Seifrtová, M., Lino, C., andSolich, P. (2010). Tetracycline antibiotics in hospital and municipal wastewaters: a pilot study in Portugal. *Analytical Bioanal Chemistry*.396(8):2929-36.

Purdara,H., Zini M., and Fallah,J. (2004). Estefadeyemojadadazpasabtasfieyesho debimarestanibarayeabyarifazayesabz. Ab vafazelab *Journal*, 49: 43- 49.

Raf'at, S., Nemati, F., and Allahabadi, A. (2010). Characteristics of sewage of Mobini Hospital, Sabzevar, Iran.*The Journal of Research Committee of Students at Sabzevar University of Medical Sciences ,Iran*; 15(3,4)

Sabzevari, A., Binavapour, M., Omidi, S., and Mohammad, T.(2005). Study of wastewater treatment plant operation of Atiesazan hospital of hamedan. *Proceeding of 8th Congress on Environmental Health*, Tehran University of Medical Sciences; 1245-1253, 2005.

Seifrtová, M., Pena, A., Lino, C., andSolich, P. (2008). Determination of fluoroquinolone antibiotics in hospital and municipal wastewaters in Coimbra by liquid chromatography with a monolithic column and fluorescence detection. Anal Bioanal; 391(3):799-805.

Shaibu, I. (2014). An Assessment of Hospital Wastes Management in Minna Towards a Waste Management Approach in a Growing Urban Area. *Greener Journal of Medical Sciences* 5.98 Vol. 4 (1), 001-015.Retrieved 27 May, 2018 from www.gjournals.orgs

Silva, C.E., Hoppe, A.E., Ravanello, M. M., andMello, N. (2005). Medical waste management in the south of Brazil. *Journal of Waste Management, Vol*. 25(6) 600–605.

World Health Organization. Waste from Health Care Activities. (Online); 2011. Retrieved 21 May, 2018 from:http://www.wpro.

WHO, World Health Organization (2018). Health care waste management, Western Pacific Region. Retrieved 23 May, from: http://www.who.int/ mediacentre/factsheets/fs253/en/.

WHO, World Health Organization(1996). Fact sheets on environmental sanitation. Epidemic diarrhoeal diseases control.4 (1):43-50. Geneva, World Health Organization. WHO/EOS/96.4.

Zhao, L., Zhang, F.S., Chen, M., Liu, Z., and Wu, D.B. (2010).Typical pollutants in bottom ashe from a typical medical waste incineration.*Journal of Hazardous Materials*, vol. 173, no. 1-3. 181-185.

Assessing the Effect of Rainfall Variability in Parts of Benue State, Nigeria

Iornongo Terseer[1] T.I Yahaya[2] Ojoye Samsedeen[3]
Department of Geography, Federal University of Technology, Minna, Nigeria
[1]terseeriornongo84@gmail.com

Abstract

The aim of this study was to investigate the effect of rainfall variability in parts of Benue State. CMAP and TRMM (Tropical Rainfall Measuring Mission) rainfall data were collected using orbiting satellite for the period of 30 years from 1988 to 2017 over Benue State. Data collected were subjected to various statistical analysis which include Coefficient of Variation which was used to determine the rainfall variability and Precipitation Variability Index (PVI) which was used to show the tendency of drought. The result shows that the mean rainfall distribution is normal since the mean annual precipitation is greater than 1000mm. The precipitation Variability Index in all the selected LGAs within the three zones indicates that the tendency of drought is much higher in the Northern zone of the State followed by the West and the South. Vandeikya LGA in the Western zone have Precipitation Variability Index of 19.50% in August which is an indication of least variability of moisture with high rainfall intensity, it is concluded that, in all the zones in Benue State agricultural activities should be carried out during the month of May, hence the Precipitation Variability Index values in April exceeds 30% which is an indication of higher rainfall variability.

Keywords*: Drought, Moisture, Precipitation, Rainfall, Variability*

Introduction

Rainfall variability has become a topical issue in recent times largely because of its impacts on natural and human systems. Labiru (2016) noted that most frequently cited activities that are likely to be affected by rainfall variability include agriculture, forestry, hydrology and fisheries. Agriculture which is the mainstay of local socio- economic and National Gross Domestic Product (GDP) in some African countries is the most vulnerable to rainfall variability. This is because in spite of recent technological advances, weather and climate are still the most important determinants in agricultural production. The long term crisis between farmers and herdsmen mostly in the north central part of Nigeria is primarily attributed to climate change and rainfall variability. This is because northern parts of Nigeria are getting drier and herdsmen have to move down South in search for greener

pasture. Farmers on the other hand need to expand on their farm size in order to maximize higher yield as a result of the danger posed by climate change.

Rainfall is the leading climatic factor that influences crop growth and productivity. Rainfall variability is increasingly becoming a source of concern, particularly in the rain fed agricultural regions of the world; this is due to its variability, pattern, distribution and seasonality. In a typical rain fed agricultural region, scarcity of water and uncertainties in both the amount received and spread, remains a major threat to agricultural development which is usually associated with significantly poor yield and high variability in crop production on yearly basis (Agidi, 2014). Therefore a change or unpredictable pattern of rainfall onset, cessation and length of growing season in a location can have a negative effect on the farmers in the area who depend on rainfall for their farming activities (Agidi, 2017). In Benue, rainfall variability is known to affect the rain-fed agriculture in which many of the population depend on. In this region crop lose their viability and the farmers lose their source of income as well (Obasakin, 2011).

Literature Review

Nigeria's population and economy are linked to climate sensitive activities including rain-fed agriculture. An understanding of current and historical rainfall trends and variation is inevitable to her future development especially in agriculture and hydrological sectors. Adamgbe and Ujoh, (2012) observed that despite great advances made in the understanding and dealing with the problem of rainfall variability impact on crop yield at the international level, awareness and concern for the problem at the national and local levels remain poor or in some cases non- existent. Without knowledge and awareness of climate variability and its possible effects on agriculture there will be little or no adaptation strategies to cope with the challenge. Akpenpuun (2013) in their study of the impact of crop yield in Kwara State showed that variation in the tuber crop yields in the State can be attributed to climate variation. Emmanuel and Fanan (2013) also found out that rainfall is highly variable in Makurdi as well as yield of maize. They reviewed further that changes in onset and cessation are the main reason for maize yield decline in Makurdi. Despite the great potential of Nigeria in crop production, the frequent occurrence of drought occasioned by erratic rainfall distribution and/or cessation of rain during the growing season is the greatest hindrance to increase production and this is more serious in the northern part of the country where most of the tubers are produced particularly in Benue State.

The Study Area

Benue State lies within the lower river **Benue** trough in the middle belt region of Nigeria. Its geographic **coordinates** are Latitude 6° 25' to 8° 8' North and longitude 7° 47' to 10° 0' East. The State shares boundaries with five other states namely: Nasarawa **State** to the north, Taraba **State** to the east, Cross-River **State** to the south, Enugu **State** to the south-west and Kogi **State.** The state has a total land area of 30,800 sq. km (National Bureau of Statistics, 2012). The total population is estimated to be 4,253,641 (National Bureau of Statistics, 2012). The State generally has about 5-7 months of rainfall. Temperatures are constantly high throughout the year, with average temperatures ranging from 23°C-32°C. This work focus areas will comprise of twelve out of the twenty three Local Government Areas in the State four Local Government Areas from each zones where agricultural activities is at maximum. The zones include Northern zone (Ushongo, Vandeikya, Ukum and Kwande), Eastern zone (Gboko, Gwer- West, Makurdi and Tarka) and Southern zone (Gwer- East, Ado Ohimini and Otukpo)

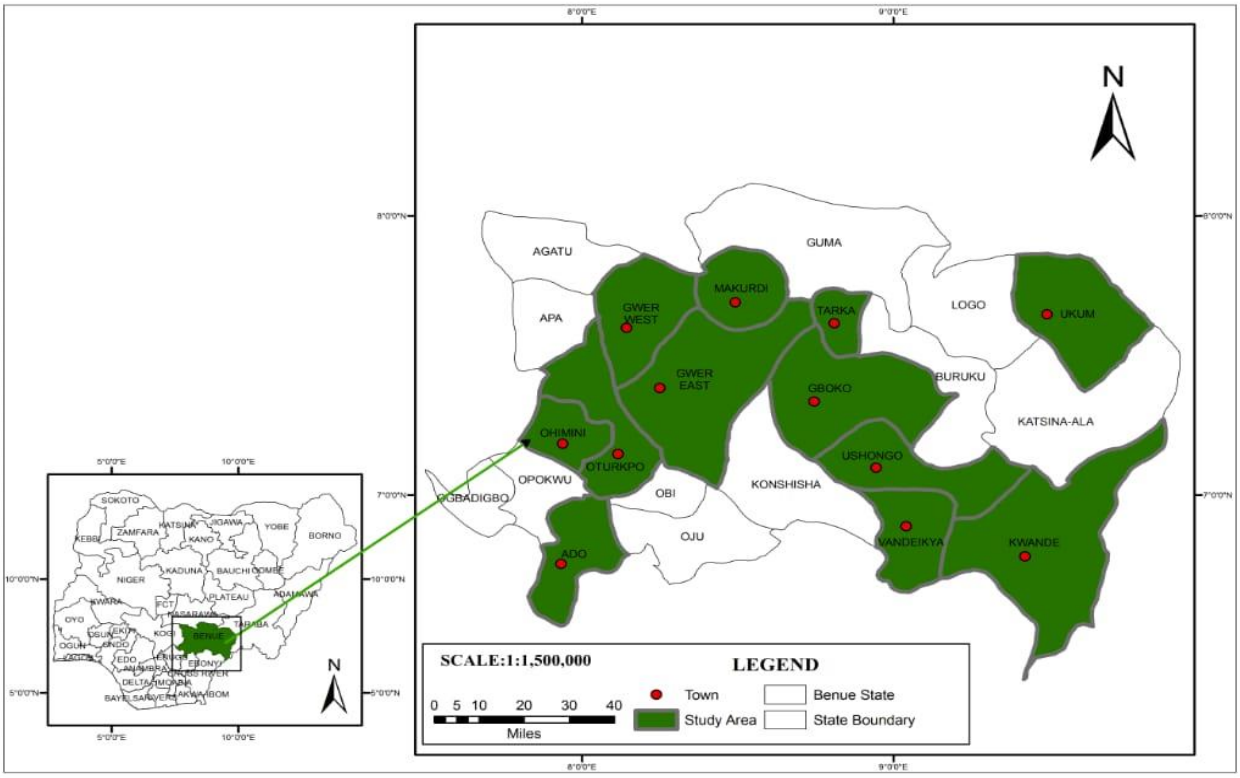

Fig1.1 **The study Areas**

Source: Geography Department, Federal University of Technology, Minna, 2019.

Material and Methods

The daily rainfall records was obtained from Tropical Rainfall Measuring Mission (TRMM) data version and CMAP data for a period of 1988 to 2017 across the twelve LGAs under study which were extracted and computed to get the daily, mean monthly, seasonal and annual rainfall records from which other relevant precipitation indices were derived.

Coefficient of Variation (CV) is a measure of relative variability which comprises of mean and standard deviation will be used to determine the variability. This can be expressed as:

$$\mathrm{CV} = \left[\frac{SD}{\overline{RF}}\right] \times 100\%$$

Standard deviation (sd) is defined by

$$\mathrm{SD} = \frac{(RF - \overline{RF})}{N}$$

where RF = the annual rainfall for a given period

$\overline{RF}$ = the average annual

N= number of variable

Precipitation Variability index (PVI)

This model (Precipitation Variability index) is a modification of precipitation periodicity index (PPI) developed by Hassan (2012) and later modified by (Hassan and Usman, 2015). It can be expressed as:

$$\mathrm{PVI} = \left(\frac{A}{Y} - \frac{B}{Y}\right) 100\% = \frac{Hd}{M} - \frac{Ld}{My}$$

Where PVI is Precipitation Variation Index

Hd= highest daily rainfall in a month

Ld= lowest daily rainfall in a month

M= monthly rainfall total

My= Monthly total* annual total

Y= Total annual rainfall

PVI is an improve version of Precipitation Periodicity Index (PPI) developed by Hassan (2012). This model can explain the tendency of drought in a given rainy season. It has three threshold levels that explain the regions variability in the dryness and vulnerability to drought. That is

Table 1.1 Precipitation Periodicity Index (PPI)

S/No	Precipitation periodicity Index	Implication
1	=≤ 20%	Least variability
2	=≥20% but ≤30%	Moderate variability
3	=≥30%	High variability

Source: Adapted from Hassan (2012)

1. is a normal distribution rainfall with adequate moisture for cropping period
2. is a moderately rainfall distribution with enough moisture but may require some measure of moisture supplement during the cropping season
3. Is prone to dry spells during the cropping season which certainly require some form of irrigation to complement the rain waters.

Results and Discussion

To understand the rainfall data in this study, it is very important to know how these Local Government Areas are been categorized into their zones in Benue State as shown in table 1.2

Table 1.2 Distribution of selected LGAs and their respective zones

S/N	Local Government Areas	Zones
1	Makurdi	Northern
2	Gwer-West	Northern
3	Tarka	Northern
4	Gboko	Northern

5	Otukpo	Southern
6	Ado	Southern
7	Ohimini	Southern
8	Gwer-East	Southern
9	Kwande,	Western
10	Vandeikya,	Western
11	Ukum	Western
12	Ushongo	Western

Source: (Author, 2019)

Table 1.2 shows the distribution of the selected LGAs and their respective zones in Benue State. The Northern zone comprises of Makurdi, Gwer-West, Tarka and Gboko, the Southern zone comprises of Otukpo, Ado, Ohimini and Gwer-East and Western zone comprises of Kwande, Vandeikya, Ukum and Ushongo. This constituted a total of 12 selected LGAs in Benue State to be considered.

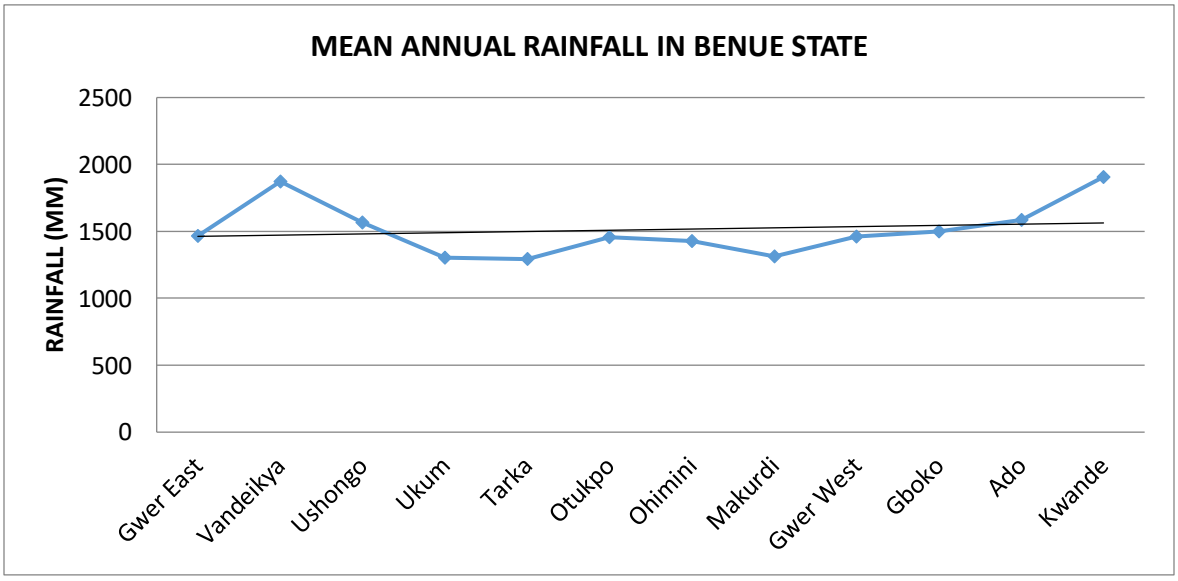

Fig. 1.2 Mean annual Rainfall in Benue State

The distribution of rainfall in Benue State indicates that all the selected LGAs have a mean annual rainfall of above 1200mm. Kwande LGA in the Western zone has the highest mean annual rainfall of 1906.8mm. The LGA which has the lowest mean annual rainfall is recorded in Tarka with total of 1292.8mm. The trend line indicates a normal mean annual rainfall in Benue State since all the LGAs have above 1200mm annually, which agrees with Adejuwon (2006) and Odekunle (2004) that the total rainfall distribution in Nigeria is generally normal if the mean is greater than 750mm. Therefore, the trend line shows a normal distribution of mean annual rainfall in Benue State.

Precipitation Variability Index (PVI)

Precipitation variability index for each Local Government in Benue State for the three zones was calculated and the results presented in fig 1.3. For clearer understanding and ease of interpretation, PVI distributions are presented in months for each Local Government Area. This will give an idea of the months with high or low tendency of moisture stress or drought. The PVI is presented in percentage of drought tendency in those areas. It gives more insight of moisture requirements for agriculture. This allow us understand tiny details that could otherwise be lump up in sum and means of precipitation. It is a known fact that the average annual or seasonal rainfall at a place does not give sufficient information regarding its capacity to support crop production. Daily, monthly and Seasonal rainfall pattern does.

		April	May	June	July	August	September	October
	Makurdi	37.23	26.76	26.40	22.48	23.19	23.55	24.98
Northern zone	Gwer West	36.32	26.46	25.40	22.47	21.53	22.94	36.34
	Tarka	39.24	32.34	27.64	23.60	23.62	26.02	26.41
	Gboko	35.23	26.92	26.51	22.85	21.86	35.45	23.71

	Otukpo	36.85	27.44	25.25	22.87	21.70	23.01	22.69
Southern zone	Ado	35.35	26.23	25.77	25.39	34.00	22.81	24.00
	Ohimini	36.09	25.68	25.55	22.86	21.07	22.65	23.54
	Gwer east	36.28	26.4276	24.70	22.86	20.30	22.18	37.34
	Kwande	31.99	27.92	21.01	20.04	21.41	21.37	25.09
Western zone	Vandeikya	31.68	25.92	25.42	22.43	19.50	23.07	23.73
	Ukum	24.55	38.25	26.09	22.21	22.99	22.59	24.55
	Ushongo	32.12	25.82	26.23	23.04	22.16	23.98	42.46

Table 1.3 shows the summary of PVI in (%) in the three zones of Benue State

Source: (Author, 2019)

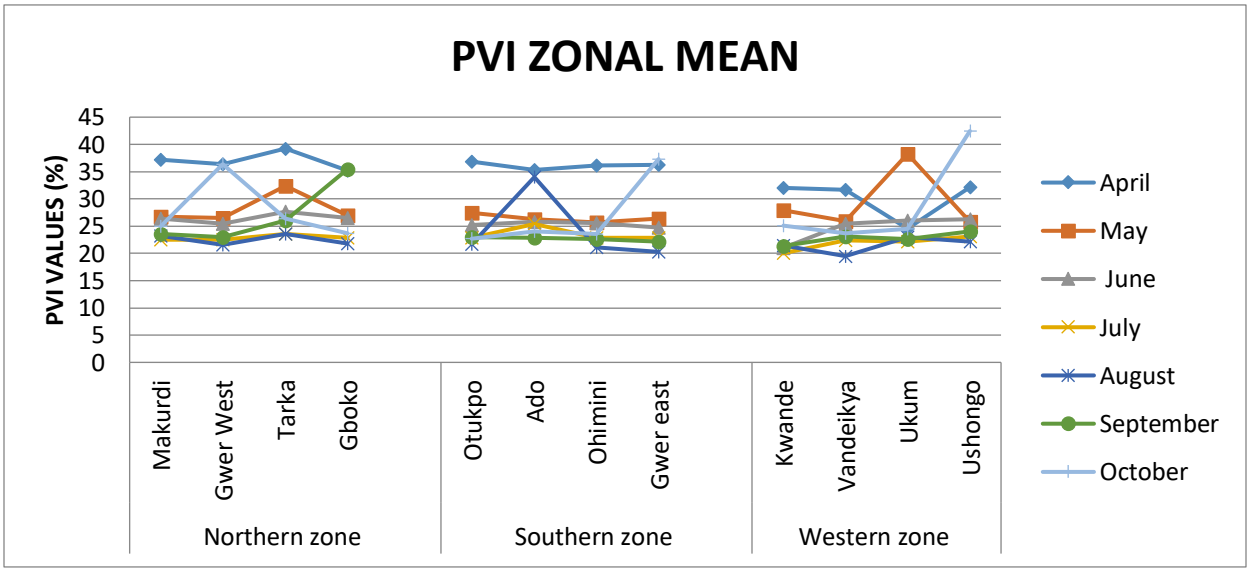

Fig 1.3 PVI Mean for Western, Northern and Southern zones of Benue State

Fig 1.3 is the summary of PVI in the Northern, Western and Southern zone of Benue State.

The Northern zone is categorized into four selected LGA which includes, Makurdi, Gwer- West, Tarka and Gboko. The mean precipitation index in this zone indicate that apart from April in all the LGA, May, September and October in Tarka, Gboko and Gwer- West, all the remaining months shows moderate variability of moisture. Gwer-West LGA has 4 months with moderate variability from May – September which is good for farming activities and perhaps encourages high crop yield. This indicates that rain fed agricultural activities in Gwer- West LGA may not suffer water availability. While Makurdi, Tarka and Gboko has four months which most of the months have PVI of greater than 25% which implies that, the rain fed agricultural activities will be subjected to drought except an alternative means of moisture to support rainfall will be put in place to have maximum yield. Farmers in this zone need to delay planting around April – May to avoid water stress that may affect plant growth which will lead to low yield.

The southern zone on the other hand, has the following LGA which include, Otukpo, Ado, Ohimini and Gwer- East. The mean PVI shows that only Otukpo from May- October have moderate variability of moisture, that is PVI is greater than 20% but less than 30%. Month of April for all the LGA have PVI of high moisture variability. Otukpo and Ohimini has 6 months (May- October) with moderate variability, while Ado and Gwer –East has 5 months of moderate variability in May, June July, September, October and May- September respectively. This shows that for adequate farming activities to succeed, other alternative source is needed in this zone hence most of the month have high moisture index which will be subjected to drought and may affect the growing season.

The Western zone has the following LGA which includes, Kwande, Vandeikya, Ukum and Ushongo. The month of April is considered as the dry month within the zone except in Ukum Local Government with a PVI of 24.55% which is an indication of moderate variability of moisture. Kwande, Vandeikya and Ukum has 6 months of moderate variability Exception of Ushongo with only 5 months. The highest PVI recorded in this zone is in Ushongo in October with 42.46%. This implies that there is high variability of moisture in Ushongo and there should be an alternative source of moisture other than rainfall, this will enhance in rain fed farming activities in Ushongo. In this zone, planting should not be done during the month of April especially in Kwande, Vandeikya and Ushongo to avoid poor growth.

Conclusion

The study focus on rainfall variability in Parts of Benue State, considering the perception of rainfall variability, TRMM and CMAP data were used from 1988 to 2017. Moisture variability distribution is high in the Northern zone and least in the Western and Southern zone of the State. It is concluded that, agricultural activities should be carried out in the month of May in all the three zones, hence the onset of rain normally take place in late April and early May..

References

Adamgbe, E. M. and Ujoh, F. (2012). Variation in Climate Parameters and Food Crops yields: Implications on Food Security in Benue State Nigeria. *Confluence Journal of Enotol. Stad 7:59-67.*

Adejuwon, J. O. (2006). Climate Change and Adaptation: Ibadan: University Press Limited.

Agidi, V.A. (2014). Inter Annual Rainfall variability and crop yields in Nasarawa State. Unpublished Master's Thesis, University of Abuja.

Agidi, V.A. (2017). Inter- Annual Rainfall Variability and Crop Yields In Nasarawa State. Unpublished Ph.D. Thesis, University of Abuja.

Akpenpuun, T.A. (2013). Impact of climate on tuber crops yield in Kwara State.Nigeria, *American international journal of contemporary research. 3(10), 52-57.*

Emmanuel, M.A. and Fanan, U. (2013). Effect of rainfall variability on maize yield in Gboko, Nigeria. *Journal of earth and Environmental Science 2(1) 26.*

Hassan, S.M. (2012). Climate Variability and crop zones classification for the Federal Capital Territory. *Conference Journal of Environmental Science 2(3) 45-53*

Igwebuike, M.N., Odoh, F.C., Ezeugwu, N.F. & Oparku, O.U. (2014). Climate Change, Agriculture and food security. International Institute of Tropical Agriculture (IITA). Hybrids Maize farming In Nigeria Time To Start Your Planting For This Season.

Ityo, S. A. (2013). "Analysis of Rainfall Distribution Pattern at Genyi-yandev, Benue State," Unpublished Research Project Submitted to the Department of Geography, Benue State University, Makurdi.

Labiru (2016). The economic impacts of climatic change: Evidence from agricultural profits and random fluctuations in weather. *Journal of Economic Research. 97(2) 354-385.*

Nigerian Bureau of statistics (2012). Nigeria poverty profile report. Abuja.

Obasakin, C.B. (2011). “The Changing Rainfall Pattern” The press Institute.

Odekunle, T.O. (2004). Rainfall and the length of the growing season in Nigeria *International Journal of Climatology*. *24 (4) 467-479.*

Thermo-Economic Analysis of Solid Oxide Fuel Cell Fuelled with Biomass from Human Waste

Sunday Kelechi,[1*] Afolabi E. A,[2] Abdulkareem, A. S[3]

Department of Chemical Engineering, Federal University of Technology, Minna,

Nigeria

[3]kasaka2003@futminna.edu.ng,[2]elizamos2001@yahoo.com

[1]kelechi.sunday@ymail.com

Abstract

Thermo-economic analysis of solid oxide fuel cell fuelled with biomass from human waste is a research work aimed at generating more hydrogen gas via simulation as fuel from producer gas contained in the biomass of human waste to fuel solid oxide fuel cell for 200kW power generation. Thermolib 5.4 one-month trial version, a MATLAB/Simulink's was used for simulating the configuration drawn for the two adapted processes. From the simulated result, the energy analysis revealed that producer gas gasification had a thermal efficiency of 82.2% while that of producer gas slow pyrolysis was 34.69% owing to the lower heating value of both gases calculated to be 113.1414kJ/mole (gasification) and 466.3725kJ/mole (slow pyrolysis). The exergy efficiency indicates that for both processes, auto-thermal reformer had an efficiency of 99.7092% (gasification) and 99.645% (slow pyrolysis) while that for solid oxide fuel cell indicates that the producer gas gasification had an efficiency of 57.5937% and producer gas slow pyrolysis 72.4978%. The cost analysis indicates that the total annual cost of $204,947 for producer gas slow pyrolysis configuration is more expensive as compared to that of producer gas gasification configuration where the total annual cost is $133,560. Thus, for the set targeted 200kW power generation; the exergy performance of the solid oxide fuel cells supports the claims that carbon monoxide is also a fuel for the equipment alongside hydrogen gas that was the main fuel to be generated. Producer gas gasification was more efficient due to its low lower heating value and a lighter hydrocarbon content (methane) while that of slow pyrolysis for the set power was not because of the higher energy content of the gas (lower heating value) which implied that the gas had a high capacity of generating more power higher than 200kW.

Keywords: energy analysis, exergy analysis, hydrogen, producer gas, solid oxide fuel cell

1. Introduction

Hydrogen is becoming a fast growing fuel replacement for the traditional fossil fuel whose use would make the energy systems to become more reliable, cleaner, and effective; therefore ensuring the sustenance of energy security and environmental sustainability. It is however proposed that for the future sustainable energy supply, hydrogen and electricity would be the leading energy carriers; thus the search for pathways of generating hydrogen from readily available sources (Kristin, 2006). The utilization of biomass derived fuel in fuel cells aids in the reduction of cost of operation (Gaurav and Valerie, 2012). Human faeces have been proven to be a feasible source of energy (Dawid *et al.,* 2016).

2. Literature Review

Solid oxide fuel cell is a device which carries out the conversion of chemical energy of a matter into electricity (Abdussalam, 2010). For an efficient thermo-economic analysis the following reviews were made: Dincer and Ratlamwala (2013), worked on the importance of exergy for analysis, improvement, design, and assessment as well as how performance assessment efficiencies are defined and Querol *et al.,* (2013), Amir *et al.,* (2011), Yoshihiko *et al.,* (2013), Truls (2009), and Young (2015), all worked on the concept of exergy (physical and chemical exergy) and formulated their equations for calculations. Furthermore, Tesfayohanes *et al.,* (2018) carried out a research work on the pyrolysis of human faeces: gas yield analysis and kinetic modelling via laboratory experiment. From the result obtained, based on the valued energy output and operation of a slow pyrolysis system the gas evolved at 450°C was optimum; while Onabanjo *et al.,* (2016) in the research work "energy recovery from human faeces via gasification: a thermodynamic equilibrium modelling approach" used Aspen plus to develop a thermodynamic equilibrium model of the gasification scheme, in which the suitability of human faeces as feedstock for gasification was investigated involving a non-stoichiometric chemical equilibrium established approach. It was deduced that the adiabatic gasification of human faeces at 979K yielded the best energy and exergy product gas quality attributed to the carbon and hydrogen as the ultimate composition of the fuel. Bijan (2004) did a comparison of auto-thermal reforming of hydrocarbons in which the factors that affect the performance of an ATR was considered while Takashi *et al.,* (2002), worked on "R&D on hydrogen production by auto-thermal reforming. The aim of the research included evaluation of auto-thermal reforming reactions and development of a high-efficiency hydrogen production technology through reforming of naphtha fraction to kerosene fraction and hence, it was confirmed that the lower the class of hydrocarbon, the higher the reforming reactivity. Hence, this research would be exploring

the feasibility of generating 200kW of electricity by fuelling SOFC with producer gas from human waste (Faeces).

3. Methodology

3.1 Selection of Configuration

Configurations for the simulation of the reforming process for producer gas generated via slow pyrolysis and gasification process to fuel SOFC with hydrogen and carbon monoxide. The adapted producer gases (syngas) were from Onabanjo *et al.,* (2016) obtained via simulation at 979K and Tesfayohanes *et al.,* (2018) obtained experimentally at 723K as reviewed under literature review with modification using the configuration from Takashi *et al.,* (2002); which was augmented and simulated with the SOFC Demo and Reforming process in the Thermolib 5.4 one-month trial version, a MATLAB/Simulink's toolbox.

Table 1: Adapted Producer Gas Compositions for Simulation

Composition	Gasification at 979K	Slow Pyrolysis at 723K
Hydrogen	0.194	0.138
Carbon monoxide	0.221	0.221
Carbon dioxide	0.049	0.281
Water	0.027	-
Methane	0.004	0.232
Nitrogen	0.505	-
Ethane	-	0.128

3.2 Description of process

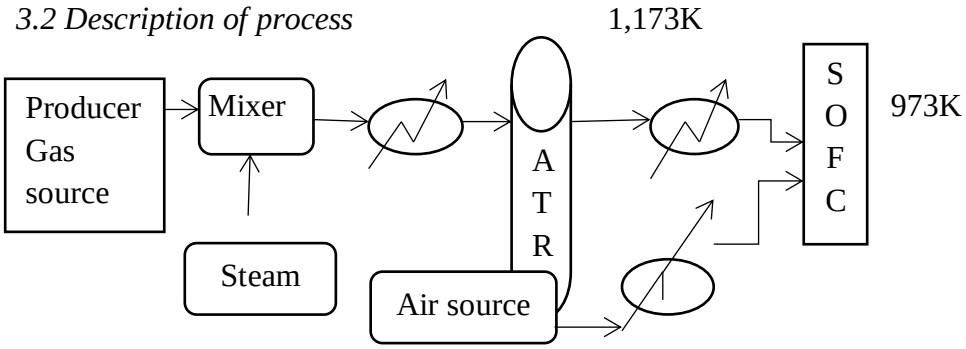

Flow diagram 1: Simulation flow diagram

The producer gas (fuel) was compressed and mixed with steam from a water source and channelled to heat exchanger 1 to raise the temperature and preheat the fuel mixture before been pumped to a reformer operated at 1,173K. At the reformer conversion of the hydrocarbons take place yielding a high fraction of hydrogen as fuel and lower carbon monoxide alongside non- combustible element within the reformate gas and increased in CO_2 as a diluent. The reformate gas was channelled to anode inlet port of SOFC operated at 973K where the hydrogen gas, carbon monoxide and methane trace under goes oxidation; while the oxygen from air reduction process to yield electricity and water as by product. However, before the electrochemical process takes place preheated air flow rate from heat exchanger 2 comprising of 79% nitrogen and 21% oxygen was fed to the cathode inlet port and both reactions takes place in the electrolyte of the Stack. Heat was recycled back to the system from the SOFC Stack exhaust gas stream via a 3 way valve that splits the after burner exhaust gas stream into two equal parts and then channelled to the two heat exchangers where heat is extracted to preheat the air stream supplied to the cathode side of the SOFC and also provide additional heat for the mixed feed stream. Various lower heating values of the gases were also calculated based on the combustible gases as adapted from the authors.

3.2 Energy and Exergy Analysis

Energy analysis is a thermodynamic technique that allows energy or heat losses to be assessed, nevertheless this analysis does not give any information about the ideal conversion of energy (Stephen *et al.*, 2017) while exergy analysis, a thermodynamic analysis technique is based principally on the second law of thermodynamics (Dincer and Ratlamwala, 2013). Exergy when compared to

energy is generally not conserved but destroyed by the irreversibility's within the system which may be internal or external (Colpan, 2009).

3.3 Figures and Tables

The configurations for producer gas are presented in Figures 1 and 2 below

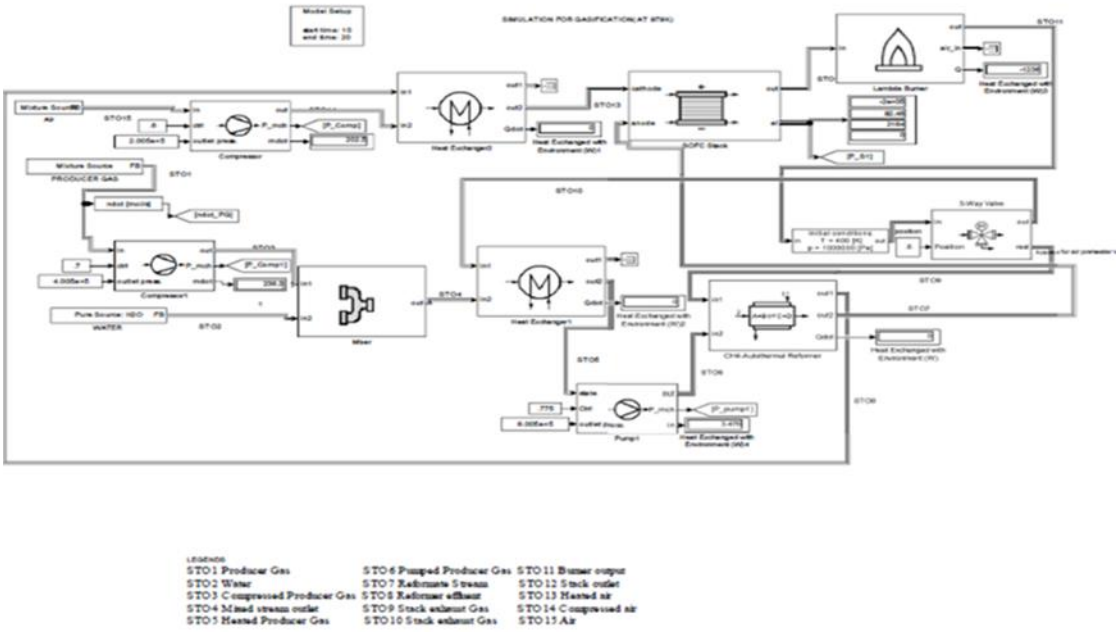

Figure 1: Configuration for simulated producer gas (Gasification)

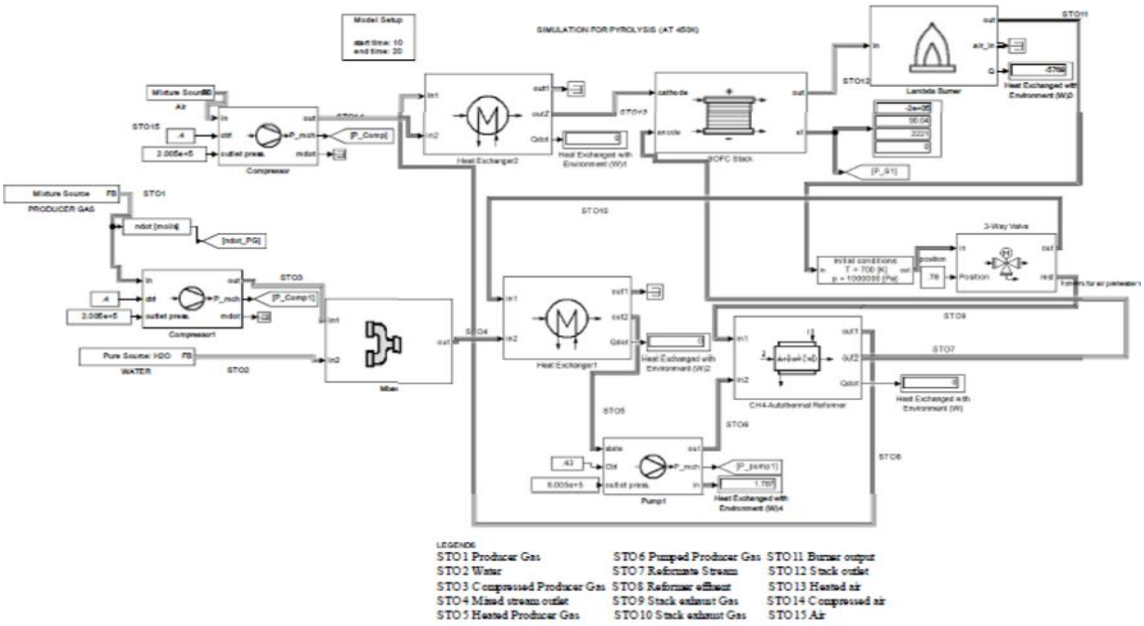

Figure 2: Configuration for slow pyrolysis at 723K

3.4 Equations

Exergy balance is given as

$\bar{E}x = \bar{E}xPH + \bar{E}xCH$..... (1)

(Khalid and Seong, 2016)

Physical exergy

$\bar{E}xPH = Cp.(T - To) - To\,[Cp.ln\,(T/To) - R\,ln\,(P/Po)]$ ..... (2) (Truls, 2009)

Chemical exergy

$\bar{E}xCH == \sum xi * e$ì°..... (3)

(Querol *et al.*, 2013)

Lost work or exergy destroyed

$\bar{E}xD = \bar{E}xf - \bar{E}xp$..... (4)

Exergy efficiency

$\eta ex = Useful\ exergy\ output\ /Total\ exergy\ input$ ..... (5)

(Dincer and Ratlamwala, 2013)

Overall exergetic efficiency

$= power\ generated\ /heat\ exergy\ generated\ by\ the\ fuel$ …….. (6)

(Anozie and Ayoola, 2012)

Energy balance

$\frac{du}{dt} = \sum \dot{H}in\grave{\imath} - \sum \dot{H}out^{\,j}$…….... (7)

Where,

U = internal energy of the component (Eutech, 2016).

$\dot{H}_{in\grave{\imath}}$, $\dot{H}_{out\,j}$ = Enthalpy in and out

4. Results and Discussion

The simulated results are presented in the following tables below

4.1 Energy Analysis

From Tables 2 – 3, the negative values indicate that the equipment in which the reactions were taking place actually lost energy to the environment implying that the reactants energy were higher than that of the product which is an exothermic reaction except for the SOFC and compressor 1where the output energy was higher and for the positive values endothermic reaction was taking place with energy gained into the system (Jessie, 2019). The result revealed that the most energy requiring equipment's are the pumps, and the heat exchangers. ATR energy flow indicates that the reformers needed negligible amount of energy as shown in the tables as 0.123kW and 0.1053kW which is attested for by the slight increase in molar output flow rate of the streams; in comparison to what was reported by Kristin (2015) that ATR do not require additional heat (energy). The compressor energy represents the power required to compress the feed and air up to the desired level before entering the next equipment (Kristin, 2015).

Table 2: Producer gas (gasification at 973K)

Equipment	Energy in (kW)	Energy out (kW)	Energy required (kW)	Energy produced (kW)
Compressor1	-92.0102	-463.742	-	371.7318
Mixer	-923.66	-923.66	-	-
Heat Exchanger1	-1073.707	-734.16	339.543	-

Pump	-734.164	-197.309	536.855	-
ATR	-297.341	-297.128	0.123	-
SOFC	-48.139	-248.15	-	200.011
Lambda Burner	-248.15	-249.386	-	1.236
3Way valve	-250.079	-250.079	-	-
Heat Exchanger2	-89.412	148.957	238.369	-
Compressor	12.0341	10.62	-	1.411

Table 3: Producer gas (Slow pyrolysis at 723K)

Equipment	Energy in (kW)	Energy out (kW)	Energy required (kW)	Energy produced (kW)
Compressor1	-131.875	-674.105	-	542.23
Mixer	-1070.663	-1070.66	0.003	-
Heat Exchanger1	-1295.339	-998.096	297.243	-
Pump	-998.096	-212.704	785.392	-
ATR	-276.0751	-275.9698	0.1053	-
SOFC	-82.124	-282.143	-	200.019
Lambda Burner	-282.143	-287.912	-	5.769
3Way valve	-288.05	-288.0501	-	0.0001
Heat Exchanger2	-11.5837	11.4031	22.9868	-

Compressor	72.9031	68.2311	-	4.672

The Table 4 below shows the overall energy efficiency for both configurations as obtained as part of the data from the software shows that of producer gas (gasification) had a better energy efficiency of 82.2% due to the product lower heating value (LHV) content of 113,141.4J/mole for a 200kW power output generation having only methane as its only hydrocarbon content (a hydrocarbon with a single carbon that efficiently combusted as fuel (Lambok, 2015) and for that of slow pyrolysis, the energy efficiency was low due to the fact that its lower heating value of 466,372.52J/mole which was four times higher than that of the LHV of producer gas from gasification had more capacity and fuel quality of generating more power output higher than 200kW which was the targeted power to be generated during the simulation.

Table 4: Energy efficiency

Configuration	Efficiency (%)
Producer gas (gasification)	82.2
Producer gas (pyrolysis)	34.69

4.2 Exergy Analysis

From Tables 5 – 6, the high exergies showed that the irreversibility of the equipment came along with corresponding high entropy due to the mixing of reactants, temperature difference, chemical reaction and fluid friction in the equipment (Dincer and Rosen, 2007). Therefore, the higher the temperature of a stream and high exergy value of the hydrocarbon content, the higher its corresponding total exergy value that would be obtained (Wall, 2009). For the SOFC of both configurations, it would be observed that the PG gasification had an exergy in of 502.0524kW and an output of 289.1507kW with 212.9017kW lost and that for slow pyrolysis had an input exergy of 807.2384kW and an output of 585.2297kW with a higher exergy destroyed of 222.0087kW an indication of lost exergy due to the irreversibility of the electrochemical reaction taking place at the electrolyte and heat loss in the solid oxide fuel cell stack (Young 2015). Thus, the high standard exergy for methane and ethane

accounts for the high chemical exergy according to the mole fractions of these hydrocarbon contents of the streams.

Table 5: Producer gas (gasification)

Equipment	Physical Exergy in (kW)	Chemical Exergy in (kW)	Total Exergy in (kW)	Physical Exergy out (kW)	Chemical Exergy out (kW)	Total Exergy out (kW)
Compressor1	8.5722	229.432	238.0042	43.2629	1156.5096	1199.7725
Mixer	63.2634	1175.5096	1238.773	57.1794	1175.1421	1232.3215
Heat Exchanger1	190.4974	1214.9233	1405.4207	173.1193	1175.1421	1348.5314
Pump	173.1192	1175.1421	1348.2613	64.0069	338.074	402.0809
ATR	152.8858	364.5934	517.4792	170.841	348.1472	518.5314
SOFC	170.5782	331.4724	502.0524	222.3702	66.7805	289.1507
Lambda Burner	222.3923	67.7267	289.0119	221.3502	66.7805	288.1307
3Way valve	222.1967	66.2974	288.4941	222.2019	66.2981	288.5
Heat Exchanger2	101.538	36.3639	137.9019	88.5538	9.8446	98.3984
Compressor	14.4393	11.22	25.6593	12.7214	9.8446	22.566

Table 6: Producer gas (slow pyrolysis)

Equipment	Physical Exergy in (kW)	Chemical Exergy in (kW)	Total Exergy in (kW)	Physical Exergy out (kW)	Chemical Exergy out (kW)	Total Exergy out (kW)
Compressor 1	18.9589	471.8464	490.8053	97.0657	2414.4091	2509.4748
Mixer	159.7382	2431.4091	2591.1473	156.9713	2412.6229	2569.5942
Heat Exchanger1	308.0756	2743.5065	3051.5821	218.8181	2412.6229	2631.441
Pump	218.8181	2431.6237	2650.4418	94.5679	606.217	700.7849
ATR	137.3096	698.9633	836.2729	95.1074	744.145	839.2524
SOFC	144.5803	662.6581	807.2384	184.6277	400.602	585.2297
Lambda Burner	203.3122	400.602	603.9142	193.6567	400.5767	594.2334
3Way valve	194.2791	399.8548	594.1339	194.2955	400.2603	594.5558
Heat Exchanger2	73.7478	94.529	168.2768	78.2665	6.5631	84.829
Compressor	48.0323	7.0125	55.0448	44.9542	6.5631	51.5173

Table 7 - 8 shows the exergetic performance and equipment lost work. The lost work analysis showed that the highest irreversibility occurred in compressor1 due to the increased molar flow rate of the output stream resulting in lower efficiencies in both configuration and the least also when compared to the efficiency of other equipment. The efficiency of the SOFC simulated during the process indicates that the efficiencies obtained were higher than that stated in literature (45-55%) and with the power output of 200kW; the simulated SOFC indicates that the equipment is independent of size as there both operated at different areas but same temperature (Wei 2006). The ATR, mixer, lambda burner and the 3 way valve had negligible losses and thus had high efficiencies.

Table 7: Exergetic Performance of the Equipment and their Lost Work obtained (Gasification)

Equipment	Lost Work	Efficiency %
Compressor1	961.7683	19.8374
Mixer	6.4515	99.4792
Heat Exchanger1	56.8893	95.9522
Pump	946.1804	29.8222
ATR	1.5090	99.7092
SOFC	221.9017	57.5937
Lambda Burner	1.9883	99.3147
3Way valve	0.0059	99.9980
Heat Exchanger2	39.5035	71.3539
Compressor	3.0933	87.9447

Table 8: Exergetic Performance of the Equipment and their Lost Work obtained (slow pyrolysis)

Equipment	Lost Work	Efficiency%

Compressor1	2018.6695	19.5581
Mixer	21.5531	99.1682
Heat Exchanger1	420.1411	86.2320
Pump	1949.6569	26.4403
ATR	2.9795	99.6450
SOFC	222.0087	72.4978
Lambda Burner	9.6808	98.3970
3Way valve	0.4219	99.9290
Heat Exchanger2	83.4472	50.4108
Compressor	3.5275	93.5916

Table 9: Overall Exergetic Efficiency

Configuration	Lost Work (kW)	Efficiency %
Producer gas (gasification)	2230.2912	53.8
Producer gas (slow pyrolysis)	4732.0862	36.9

4.3 Cost Analysis

From Table 10, it is observed that the PG slow pyrolysis had the highest equipment, operating and corresponding total annual cost. Hence, making the reforming process of slow pyrolysis most expensive.

Table 10**:** Total Annual Cost

Variable Description	Producer gas	Producer gas (Slow

	(Gasification)	Pyrolysis)
Depreciation cost ($)	21935	23533
Interest ($)	2031	2179
Maintenance cost ($)	1316	1412
Insurance cost ($)	439	471
Taxation cost ($)	119	127
Capital cost ($)	25840	27722
Operating cost ($)	107,720	177225
Total cost ($)	133560	204947

Conclusion

This research work actually achieved its set objectives as hydrogen mainly alongside carbon monoxide were generated through the reformation of the hydrocarbon content of the adapted producers gas from the two separate production routes namely: gasification and slow pyrolysis in addition to the fractions that came in with feed and was fed as fuel with other reformate gas composition to the anode port of the SOFC and 200kW the set power output was produced. Deducing from all the analysis carried out, the configuration for producer gas (gasification) had a better energy and exergetic performance and also is cost effective.

References

Abdussalam Goma. (2010), Investigation of Sustainable Hydrogen Production from Steam Biomass Gasification. 1, 3, 27, 42, 64, 75

Amir Vosough, Aminreza Noghrehabadi, Mohammed Ghalambaz and Sadagh Yosough. (2011), *International Journal of Multidisciplinary Sciences and Engineering.* Vol. 2, (4) 49-51

Anozie, A.N., and Ayoola P. O. (2012), The Influence of Throughput on Thermodynamic Efficiencies of a thermal Power-Plant. *Internal Journal of Energy Engineering* doi:10.5923/j/ijee.20120205.11.2

Bijan F. Hagh (2004). Comparison of Auto-thermal Reforming for Hydrocarbon Fuels. 144

Colpan Can Ozgur (2009). Thermal Modelling of Solid Oxide Fuel Cell based on Biomass Gasification Systems. 17-21, 49,102,104,107,111,114

Dawid P. Hanak, Anthanasios J. Kolios, Tosin Onabanjo, Stuart T. Wagland, Kunar Parchigolla, Beatriz Fidalgo, Vasilije Manovic, Ewan McAdam, Alison Packer, Leon Williams, Sean Tyrrel and Elise Cartmell (2016). Conceptual Energy and Water Recovery System for Self-Sustained Nano Membrane Toilet. 353

Dincer, I. and T. A. H Ratlamwala (2013). Importance of Exergy for Analysis, Improvement, Design and Assessment. 2, 335-338.doi:10.1002/wene 63

Dincer, I. and Rosen M. A. (2007). Exergy: Energy, Environment and Sustainable Development. 14

Eutech Scientific Engineering GmbH (2016). Thermolib User's Manual. Thermodynamic Systems Library, Release 5.4. 18, 26

Gaurav Nahar and Valerie Dupont, (2012). Resent advances in hydrogen production via Auto-thermal reforming process (ATR). *A Review of Patents and Research Articles.* 1

Jessie A (2019). Introductory Chemistry-1st Canadian Edition Chapter 7. Energy and Chemistry. Retrieved from http://open textbc.ca/introductory Chemistry/chapter/stoichiometry-Calculations-using-enthalpy-2 2/219

Khalid Zouhri and Seong Young Lee (2016). Exergy Study on the Effect of Material Parameters and Operating Conditions on the Anode Diffusion Polarization of the SOFC. *Int J. Energy Environ Eng*. 7, 215.doi:10.1007/s40095-015-0201-1

Kristin Hew McGlocklin (2006). Economic Analysis of various Reforming Techniques and Fuel Sources for Hydrogen Production. 6, 24

Kristin Skerbergene (2015). New Technologies for the Purification and Carbon Capture in Hydrogen Production from Natural Gas. 10, 11, 12

Lambok Parulian Simbolon (2015). Potential Human Sewage into Renewable Energy and Organic fertilizer plants in society. *International Journal of Science and Technology* (1).1.171

Onabanjo T, Patchigolla K, Wagland S. T, Fidalgo B, Kolios A, McAdam, Parker A, Williams L, Tyrrel S and Cartmell E (2016). Energy Recovery from Human Faeces via Gasification: A Thermodynamic Equilibrium Modelling Approach: 366, 368, 370 - 371.

Querol E, Gonzalez – Regueral B, Perez – Benedilo, J. L (2013). Practical Approach to Exergy and Thermo-Economic Analyses of Industrial Processes. Retrieved from http:// www.springer.com/978-1-4471-4621-6. 11/10/18

Stephen R. Allent, Geoffery P. Hammond, Russell C. Mckenna (2017). The Thermodynamic Implications of Electricity End use for Heat and Power. Proceedings of the Institution of Mechanical Engineers, Part A: *Journal of Power and Energy*. http://doi.org/10.1177/0957650917693483. 7, 10, 17

Takashi Suzuki, Katsume Miyamoto Shuichi Kobayashi, Noriyuki Aratani, Tomoyuki Yogo (2002). R and D on Hydrogen Production by Auto-thermal Reforming. 2

Tesfayohanes, W., Yacob, Richard (chip) Fisher, Karl G. Linden and Alan W. Weimer (2018) Pyrolysis of Human Faeces: Gas yield Analysis and Kinetic Modelling. Waste Management, volume 79. 96

Truls Gundersen (2009). Introduction to Concept of Exergy and Energy Quality. 3

Wall G. (2009). Exergetics. Retrieved from http:// www.exergy.se/ffp/exergetics.pdf 5/2/19

Wei Zhang (2006). Simulation of Solid Oxide Fuel Cell-Based Power Generation Processes with CO_2 Capture. 12, 49

Yoshihiko Soeno, Hiromitsu Ino, Kiiti Siratori and Kohmei Halada (2013) Exergy Analysis to Evaluate Intergrated Environmental Impacts. Vol.44(7) 1244-1250

Young Duk Lee (2015). Thermodynamic, Economic and Environmental Evaluation of Solid Oxide Fuel Cell Hybrid Power –Generation Systems. 26, 81

Appraisal of global rainfall forecasting models on heavy rainfall days over the Guinea Savanna Zone, Nigeria

Audu, E.B.[1]; Abubakar, A.S.[2]; Ojoye, S.[2]; Muhammed, M.[2]. and Nsofor, G.N.[2]

[1]Government Secondary School, Abuja@30, Pegi, Federal Capital Territory, Nigeria

[2]Department of Geography, Federal University of Technology, Minna, Niger State, Nigeria

Correspondence author: audu_ebamaiyi@yahoo.com (+234-803-585-6619).

Abstract

Numerical models are vital tools in forecasting rainfall globally. In most cases, these models underperform. This has formed the basis for this research which was aimed at the appraisal of global rainfall forecasting numerical models on heavy rainfall days over the Guinea Savanna Zone, Nigeria (GSZN) which served as the study area. Nine (9) meteorological stations were chosen from the study area for the purpose of data collection due to their long history of data. These stations included Makurdi, Lokoja, Ibi, Ilorin, Lafia, Abuja, Minna, Jos and Kaduna. Secondary data were used for the study. These included the observed daily rainfall data obtained from the Nigerian Meteorological Agency (Nimet), Oshodi, Lagos and rainfall forecasts obtained from the European Centre for Medium-Range Weather Forecasts (ECMWF) as well as the United Kingdom Met Office (UKMet). Data were presented in figures as well as tables and analysed using the probability of detection (POD), root mean square error (RMSE), mean absolute error (MAE) and rainfall intensities. The results indicated that both global numerical models appraised performed well in categorical rain forecasting over the study area, but under-estimated the total rainfall on the nine (9) events appraised. It was therefore suggested among others that both models be dynamically downscaled to

take into consideration local peculiarities over Nigerian domain and local numerical model such as the artificial neural network (ANN) be developed to forecast various degrees of rainfall intensities.

Key words: Rainfall, heavy rainfall, numerical models, COSMO, observed rainfall

Introduction

Rainfall remains the most important weather variable in Nigeria because the most important occupation in Nigeria which is agriculture is majorly rain-fed. Other sectors of the socio-economic activities in Nigeria such as hydrology/water resources, inland water transport, hydro electric power generation as well as domestic water supply are heavily dependent on rainfall both directly and indirectly. Similarly, rainfall is highly variable than other weather parametres. Hulme *et al* (2005) cited in Lawal *et al* (2012) observed that rainfall exhibits notable spatial and temporal variability over Nigeria. It is therefore inevitable to embark on rainfall forecast. Heavy rainfall is one of the derived rainfall parameters in Nigeria. According to Audu *et al* (2018), heavy rainfall is that total amount of rainfall which is $\geq$ 50 mm within 24 hours (1 day). This amount of rainfall can occur in any month of the year within the study area. However, it is mostly concentrated within the peak of the wet season that is, August over the study area (Audu *et al*, 2019).

Commenting on the need for the use of numerical models in weather forecast, Anthes (1984) cited in Ajayi *et al* (2010) argued that; if human can modify climate and weather inadvertently, they should be able to intentionally modify weather most especially rainfall in a constructive way. Ajayi *et al* (2010) used the ICTP Regional Climate Model ($RegCM^3$) to analyse the impact of land-cover changes on rainfall in West Africa. The study of Agboluaje and Dangana (2014) utilized the SARIMA and ARIMA models for the seasonal modeling and forecasting of rainfall in Badeggi-Bida Area of Niger State, Nigeria. The study carried out by Akinsanola *et al* (2014) on the diagnostic evaluation of precipitation over West Africa using three of the Coordinated Regional Climate Downloading Experiment (CORDEX) Africa simulations, used three (3) of the Regional Climate Model (RCM). The Nigerian Meteorological Agency (NiMet), adopted the use of Consortium for Small Scale Modelling (COSMO) which is a non-hydrostatic, high resolution, limited area atmospheric prediction model in 2012 in collaboration with the German Meteorological Office (DWD) (NiMet, 2018a) in

weather forecast. It is a regional numerical weather prediction system with additional components such as data assimilation and interpolation of boundary conditions from driving model. As good as these models are in the area of performance, they are limited because they are not global in nature.

There are several global numerical models used for rainfall forecast. Some of these models include European Centre for Medium-Range Weather Forecasts (ECMWF), United Kingdom Met Office (UKMet), Action de Recherche Petite Echelle Grande (ARPEGE) (Asaniyan, 2006), Meteo-France (Ibrahim, 2006) and Global Forecasting System (GFS). This study aimed at the appraisal of the most commonly used global rainfall forecasting numerical models on heavy rainfall days over the Guinea Savanna Zone, Nigeria which are the ECMWF and UKMet models.

Study area

The study area is the Guinea Savanna Zone, Nigeria (GSZN) which lies between longitudes 4^{o}–10^{o}E and latitudes 6^{o}–$11^{o}30^{1}$N (Figure 1). The Sudano–Sahelian Zone, Nigeria (SSZN) bordered it to the north, while the forest vegetation zone, Nigeria (FVZN) bordered it to the south.

There are two (2) seasons in the area namely, wet and dry. Wet season is experienced between April and October, while dry season is experienced between October and April (Mohammed, 2010). The total annual rainfall ranges between 697.10 mm–2456.9 mm (Audu *et al*, 2018). Mean annual temperature is between 28.03^{o}C-31^{o}C (MS, 2013) cited in (Musa *et al*, 2013). August has the highest mean monthly rainfall (NiMet, 2018). The Tropical Maritime Air mass (mT) also called the South–West (SW) trade wind which is described as moisture laden and brings rainfall across the area and the Tropical Continental (cT) air mass also called the North–East (NE) trade (harmattan) wind which blows in the dry season between November and February are the two (2) major air masses that affect the area (Iwena, 2000; Malik, 2004 cited in Musa *et al*., 2012). The wind speed is about 10km/hr (MMS, 2013) cited in (Musa *et al*, 2013).

The study area consists of gently undulating plain with some hills, ridges and plateaux whose heights are between 300m-900m (Ola, 2001) cited in (Obateru, 2017). It also consists of part of the western upland as well as the Niger–Benue Trough (Falola *et al*, 2015). The highest elevation is about 1500m. There are numerous rivers in the area such as Rivers Niger, Benue, Katsina Ala, Kaduna, Gurara, Awum, Donga and Usuma. The confluence of Rivers Niger and Benue is found at Lokoja (Audu,

2001). There are two (2) main artificial or man–made lakes such as the Kainji Lake on River Niger and Shiroro Lake on River Kaduna in the region and few dams such as Kainji Dam and Jebba Dam located on River Niger, Shiroro Dam located on River Kaduna (all in Niger State) as well as the Jabi and Lower Usuma Dams in Abuja–FCT (Iwena, 2000).

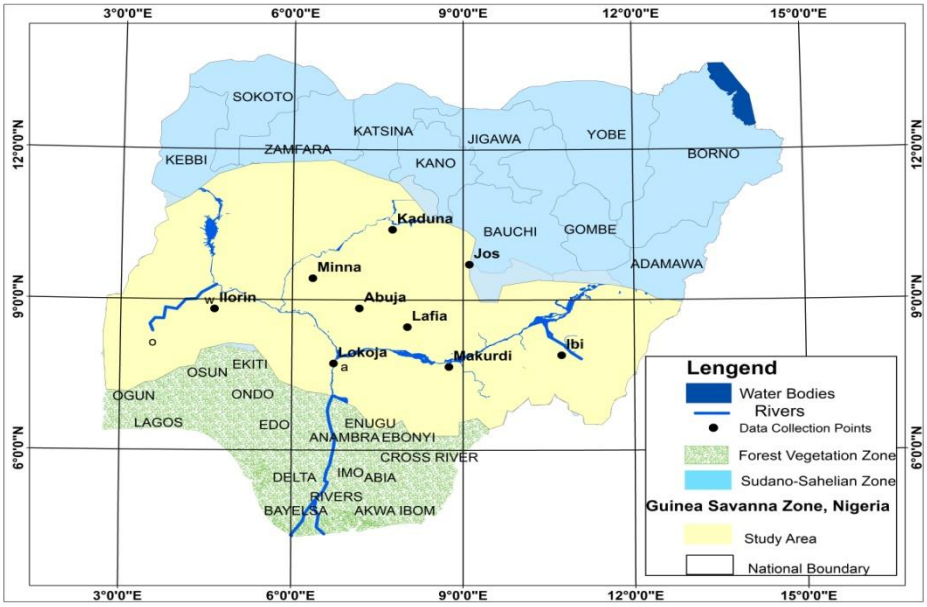

Figure 1: The Study Area

Source: National Space Research and Development Agency (NSRDA), Abuja (2019)

The zone is the largest vegetation belt in Nigeria, the Guinea Savanna with the presence of gallery forests mainly along Rivers Niger and Benue (Bello, 2007). The geology of the study area is predominantly Precambrian basement as well as various sedimentary rocks (Ayuba *et al*, 2013; MMS, 2013 cited in Musa *et al*, 2013; Dan–Hassan *et al*, 2015). The major land uses in the study area include settlement, construction, farming, trading, small scale manufacturing and tourism (Odekunle *et al*, 2007; Shehu, 2014; Gonap *et al*, 2018).

Materials and methods

Secondary data on daily rainfall (in mm) were obtained from Nigerian Meteorological Agency (NiMet), Oshodi, Lagos, and rainfall forecasts from two (2) most popular global numerical models obtained from European Centre for Medium-Range Weather Forecasts (ECMWF) and United Kingdom Met Office (UKMet) were used for this study. The data were from 2007 to 2015 and covered nine (9) data collection points namely, Makurdi, Lokoja, Ibi, Ilorin, Lafia, Abuja, Minna, Jos and Kaduna. Heavy rainfall data were extracted from daily rainfall using micro soft excel in which all cells containing the considered data were selected. Conditional formatting was chosen in a manner that cells rules were highlighted and greater than was clicked. The available text box with desired threshold value of ≥ 50 mm was then clicked and all dates with rainfall value ≥ 50 mm appeared. Tigge data were retrieved online from ECMWF and UKMet using python script and Grid Analysis and Display System (GRADS).

Probability of detection (POD) (Gaili *et al*, 2016) was used to determine the fraction of observed "yes" events which were correctly forecasted. It was determined using the equation:

$$POD = \frac{Hits}{Hits+misses} \qquad 1$$

Where: Hits is the number of rainfall forecast that matches with observed rainfall, while misses is the number of rainfall forecasts that did not match with the observed rainfall. Hits range between 0 1. 1 means perfect score for the events.

The magnitude of forecast errors was determined using root mean square error (RMSE). It measures average error, weighted according to the square of the error. It ranges from 0 to ∞. 0 means perfect score. It puts greater influence on large errors than smaller errors. It was calculated after Gaili *et al* (2016) as thus:

$$RMSE = \sqrt{\frac{1}{N}\sum_{i=1}^{N}(F_i - O_i)^2} \qquad 2$$

The magnitude absolute error (MAE) was used to determine the average of the forecast error. It was calculated after Gaili *et al* (2016) as follows:

$$MAE = \sqrt{\frac{1}{N}\sum_{i=1}^{N}/F_i - O_i/} \qquad 3$$

From equations 2 and 3, F_i means the forecast values, O_i means the observed values, N means the number of events and perfect score=0

Rainfall varies in intensity over time and space. Rainfall intensity (RI) is described as the ratio of total amount of rain (rain depth) falling during a particular period to the duration of the period. It is shown in depth units/unit time usually as mm per hour (mm/hr). It is measured as the height of the water layer covering the ground in a period of time. Rainfall forecasts from the two (2) global numerical models and the observed rainfall were also compared with rainfall intensities. Table 1 shows the rainfall intensities.

Table 1: Rainfall intensities

Descriptive Term Used	**Rainfall Amount (mm/day)**
No rain	0.0
Very light	0.1–2.4
Light rain	2.5–7.5
Moderate rain	7.6–35.5
Rather heavy	35.6–64.4
Exceptionally heavy rain at or this term will be used only	When the amount is a value near about the heaviest recorded rainfall near the station for the month or season. However, when the actual rainfall amount exceeds 12 cm (120 mm)
Heavy rain	64.5–124.4
Very heavy rain	124.5–244.4
Extremely heavy rain	> 244.5

Source: Meera and Priyanca (2015)

Results and Discussion

The relationship between model forecasts and observed rainfall is the model performance which could be accurate, near accurate or inaccurate. Figures 2 to 19 show the results on the model forecasts

by ECMWF and UKMET for nine (9) events under appraisal. Both models were able to capture the rain forecast over the study area.

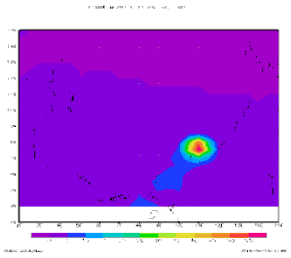

Fig. 2: ECMWF forecast, 16th Aug, 2007

Source: Authors' computation, 2018

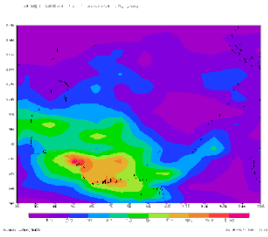

Fig. 3: UKMet forecast, 16th August, 2007

Source: Authors' computation, 2018

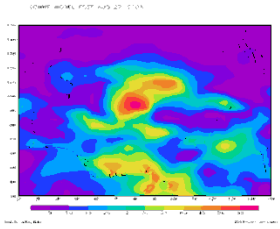

Fig. 4: ECMWF forecast, 27th August, 2008

Source: Authors' computation, 2018

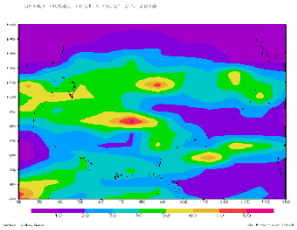

Fig. 5: UKMet forecast, 27th Aug. 2008

Source: Authors' computation, 2018

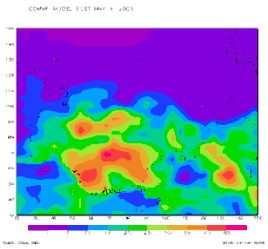

Fig. 6: ECMWF forecast, 4th May, 2009

Source: Authors' computation, 2018

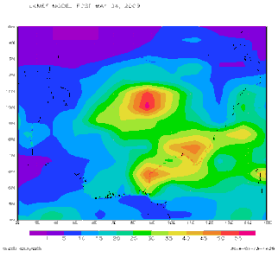

Fig. 7: UKMet forecast, 4th May, 2009

Source: Authors' computation, 2018

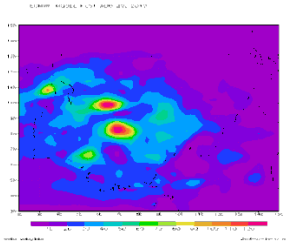

Fig. 8: ECMWF forecast, 20th Aug, 2010

Source: Authors' computation, 2018

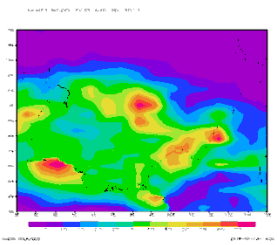

Fig. 9: UKMet forecast, 20th Aug, 2010

Source: Authors' computation, 2018

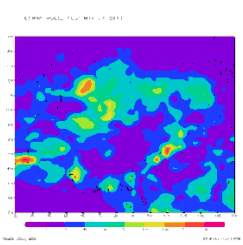

Fig. 10: ECMWF forecast, 27th May, 2011

Source: Authors' computation, 2018

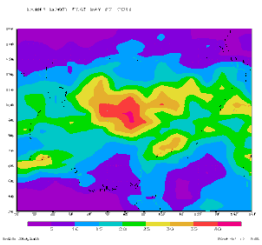

Fig. 11: UKMet forecast, 27th May, 2011

Source: Authors' computation, 2018

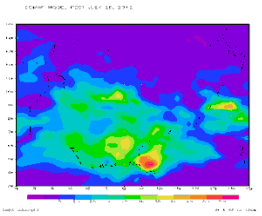

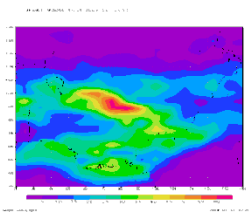

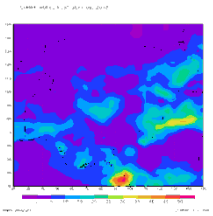

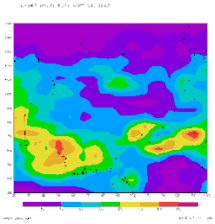

Fig. 12: *ECMWF forecast on 26th July, 2012* ***Fig. 13:*** *UKMet forecast on 26th July, 2012* ***Fig. 14:*** *ECMWF forecast on 9th Sep, 2013* ***Fig. 15:*** *UKMet forecast on 9th Sep, 2013*

Source: Authors' computation, 2018 **Source:** Authors' computation, 2018 **Source:** Authors' computation, 2018 **Source:** Authors' computation, 2018

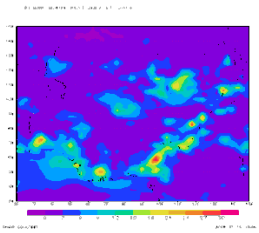

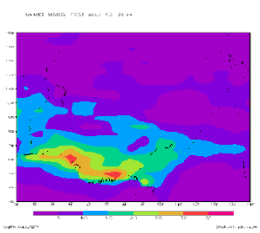

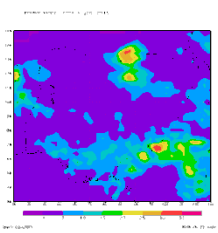

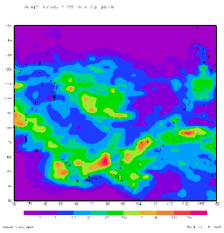

Fig. 16: *ECMWF forecast on 13th Jul, 2014* ***Fig. 17:*** *UKMet forecast on 13th Jul, 2014* ***Fig. 18:*** *ECMWF forecast on 20th Aug, 2015* ***Fig. 19:*** *ECMWF forecast on 20th Aug 2015*

Source: *Authors' computation, 2018* ***Source:*** *Authors' computation, 2018* ***Source:*** *Authors' computation, 2018* ***Source:*** *Authors' computation, 2018*

Both the ECMWF and UKMet numerical models performed very well in the area of categorical rainfall forecast since the observed "yes" events were equal to forecast "yes" events (figs. 19 and 20). The UKMet model values are higher than the ECMWF model values. However, the two (2) models underestimated all the nine (9) events under investigation (fig. 20). Heavy rainfall was not forecast by the two (2) global models.

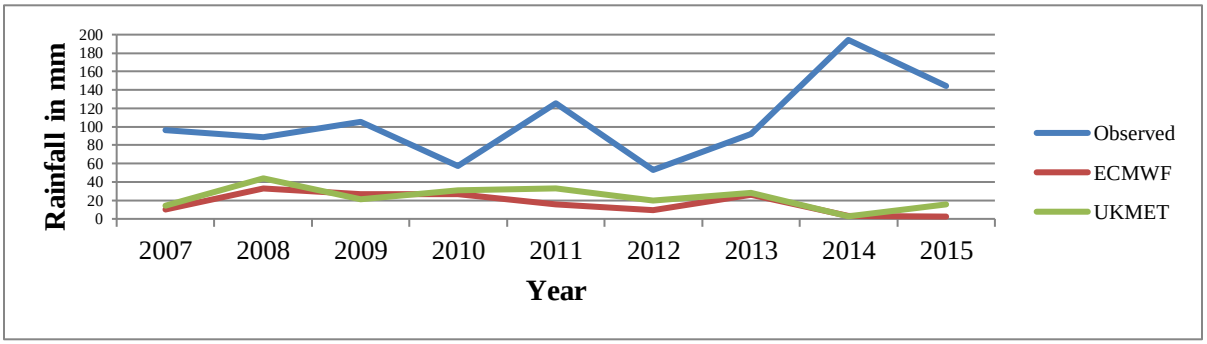

Figure 20: ECMWF and UKMet forecasts and observed rainfall on heavy rainfall days, 2007-2015 over the study area

Sources: Nigerian Meteorological Agency, Oshodi, Lagos (2018b) and ECMWF (2018)

Figure 20 shows the differences between ECMWF and UKMet forecasts and observed rainfall on heavy rainfall days, 2007-2015 over the study area. The observed rainfalls were higher than the forecasts by both numerical models appraised which means that the models were unable to forecast heavy rainfall over the area. Reasons for the inability of the two (2) numerical models to forecast heavy rainfall over the study area could be that they are not producing high vertical motion at the top of the boundary layer, some parametization schemes such as cloud microphysics and convection used in the models may not work well over the Nigerian domain; and that they did not consider the local peculiarities over the Nigeria's domain owing to the parametization schemes used.

Results on probability of detection (POD) for both ECMWF and UKMet are one (1) each which implies perfect score. The Root Mean Square Error (RMSE) of the ECMWF rainfall forecast is 101.43, while that of the UKMet is 96.33. This implies that the error magnitude of the ECMWF rainfall forecast was greater than the UKMet. The result on mean absolute error (MAE) for ECMWF forecast is 89.22, while that of UKMet is 83.03. This implies that, there exist large variations between the numerical models rain forecasts and the observed rainfall. However, the MAE of UKMet is lower than that of the ECMWF because the rainfall model forecasted values by UKMet are higher than the ECMWF which implies that, although these two (2) models forecasted rainfall over the study area; UKMet model performed better in Quantitative Rainfall Forecast (QRF).

Results on rainfall forecasts by ECMWF and UKMet numerical models as well as the observed rainfall were further compared with rainfall intensities as shown in tables 2-10. The observed rainfall is the actual rainfall recorded over a particular location. This is the rainfall value that is used for planning in the areas of agriculture, water resources, construction, drainage, erosion, landslide and flood management.

Table 2: Comparism between ECMWF and UKMet models rainfall forecasts, observed rainfall and rainfall intensities on 16th August, 2007 over the study area.

S/N	Descriptive terms Used*	Rainfall amount (mm/day)	ECMWF forecast**	UKMet forecast**	Observed heavy rainfall (mm)**
1.	No rain	0.0	-	-	-

2. Very light rain	0.1-2.4	-	-	-
3. Light rain	2.5-7.5	-	-	-
4. Moderate rain	7.6-35.5	10	14	-
5. Rather heavy rain	35.6-64.4	-	-	-
6. Exceptionally heavy rain	120 +	-	-	-
7. Heavy rain	64.5-124.4	-	-	96
8. Very heavy rain	124.5-244.4	-	-	-
9. Extreme heavy rain	>244.5	-	-	-

Sources: *Adapted from Meera and Priyanca (2015) **ECMWF (2018) *** NiMet (2018b)

According to table 2, the ECMWF and UKMet numerical models were able to forecast rainfall over the study area on 16th August, 2007. Both models forecasted moderate rainfall intensity, while the observed rainfall intensity was heavy rainfall. Both models therefore underestimated the rainfall intensity for the day over the study area.

Table 3: *Comparism between ECMWF and UKMet models rainfall forecasts, observed rainfall and rainfall intensities on 27th August, 2008 over the study area.*

S/N	Descriptive terms Used*	Rainfall amount (mm/day)	ECMWF forecast**	UKMet forecast**	Observed heavy rainfall (mm)**
1.	No rain	0.0	-	-	-
2.	Very light rain	0.1-2.4	-	-	-

3.	Light rain	2.5-7.5	-	-	-
4.	Moderate rain	7.6-35.5	33	-	-
5.	Rather heavy rain	35.6-64.4	-	44	-
6.	Exceptionally heavy rain	120 +	-	-	-
7.	Heavy rain	64.5-124.4	-	-	88.7
8.	Very heavy rain	124.5-244.4	-	-	-
9.	Extreme heavy rain	>244.5	-	-	-

Sources: *Adapted from Meera and Priyanca (2015) **ECMWF (2018) *** NiMet (2018b)

ECMWF rainfall forecast, UKMet model rainfall forecast and observed rainfall over the study area on 27th August, 2008 and rainfall intensities are presented in table 3. The ECMWF model forecasted moderate rain while UKMet model forecast indicated rather heavy rain. Meanwhile, while the observed rainfall was heavy rainfall intensity. The two (2) models performed fairly well, but underestimated rainfall intensity for the day.

Table 4: Comparism between ECMWF and UKMet models rainfall forecasts, observed rainfall and rainfall intensities on 4th May, 2009 over the study area.

S/N	Descriptive terms Used*	Rainfall amount (mm/day)	ECMWF forecast**	UKMet forecast**	Observed heavy rainfall (mm)**
1	No rain	0.0	-	-	-
2	Very light rain	0.1-2.4	-	-	-
3	Light rain	2.5-7.5	-	-	-
4.	Moderate rain	7.6-35.5	30	25	-

5.	Rather heavy rain	35.6-64.4	-	-	-
6.	Exceptionally heavy rain	120 +	-	-	-
7.	Heavy rain	64.5-124.4	-	-	105.4
8.	Very heavy rain	124.5-244.4	-	-	-
9.	Extreme heavy rain	>244.5	-	-	-

Sources: *Adapted from Meera and Priyanca (2015) **ECMWF (2018) *** NiMet (2018b)

Table 4 shows the results on ECMWF and UKMet model forecasts as well as the observed rainfall on 9th September, 2009 in relation to intensities of rainfall. Both models forecasted moderate rainfall intensities, while the observed rain was heavy rainfall intensity. The two (2) models performed poorly due in the area of heavy rainfall forecast over the study area.

Table 5: Comparism between ECMWF and UKMet models rainfall forecasts, observed rainfall and rainfall intensities on 20th August, 2010 over the study area

S/N	Descriptive terms Used*	Rainfall amount (mm/day)	ECMWF forecast**	UKMet forecast**	Observed heavy rainfall (mm)**
1.	No rain	0.0	-	-	-
2.	Very light rain	0.1-2.4	-	-	-
3.	Light rain	2.5-7.5	-	-	-
4.	Moderate rain	7.6-35.5	27	31	-

5. Rather heavy rain	35.6-64.4	-	-	57
6. Exceptionally heavy rain	120 +	-	-	-
7. Heavy rain	64.5-124.4	-	-	-
8. Very heavy rain	124.5-244.4	-	-	-
9. Extreme heavy rain	>244.5	-	-	-

Sources: *Adapted from Meera and Priyanca (2015) **ECMWF (2018) *** NiMet (2018b)

The results on ECMWF and UKMet models forecasts as well as the observed rainfall on 20th August, 2010 are shown in table 5. Both models forecasted moderate rainfall intensity, while the observed rainfall intensity was rather heavy. The two (2) models forecasts were near-accurate.

Table 6: Comparism between ECMWF and UKMet models rainfall forecasts, observed rainfall and rainfall intensities on 27th May, 2011 over the study area.

S/N	Descriptive terms Used*	Rainfall amount (mm/day)	ECMWF forecast**	UKMet forecast**	Observed heavy rainfall (mm)**
1	No rain	0.0	-	-	-
2	Very light rain	0.1-2.4	-	-	-
3	Light rain	2.5-7.5	-	-	-
4.	Moderate rain	7.6-35.5	16	33	-
5.	Rather heavy rain	35.6-64.4	-	-	-
6.	Exceptionally heavy rain	120 +	-	-	125.6
7.	Heavy rain	64.5-124.4	-	-	-
8.	Very heavy rain	124.5-244.4	-	-	-

9.	Extreme heavy rain	>244.5	-	-	-

Sources: *Adapted from Meera and Priyanca (2015) **ECMWF (2018) ***** NiMet (2018b)**

Table 6 presents the comparism between ECMWF model rain forecast, UKMet model rain forecast and observed rainfall in relation to rainfall intensities on 27th May, 2011. Both numerical models forecasted moderate rain intensity, while the observed rainfall intensity was exceptionally heavy. The performance of the two (2) models is therefore poor even though they were able to forecast rainfall intensities.

Table 7: Comparism between ECMWF and UKMet models rainfall forecasts, observed rainfall and rainfall intensities on 26th July, 2012 over the study area.

S/N	Descriptive terms Used*	Rainfall amount (mm/day)	ECMWF forecast**	UKMet forecast**	Observed heavy rainfall (mm)**
1.	No rain	0.0	-	-	-
2.	Very light rain	0.1-2.4	-	-	-
3.	Light rain	2.5-7.5	-	-	-
4.	Moderate rain	7.6-35.5	9.5	20	-
5.	Rather heavy rain	35.6-64.4	-	-	53.1
6.	Exceptionally heavy rain	120 +	-	-	-
7.	Heavy rain	64.5-124.4	-	-	-

8. Very heavy rain	124.5-244.4	-	-	-
9. Extreme heavy rain	>244.5	-	-	-

Sources: *Adapted from Meera and Priyanca (2015) **ECMWF (2018) *** NiMet (2018b)

Table 7 presents the results on model forecasts, ECMWF and UKMet as well as the observed rainfall in relation to rainfall intensities on 26th July, 2012. Both models forecasted moderate rain intensity, while the observed rainfall intensity is rather heavy rain. The two (2) models under-estimated rainfall intensity.

Table 8: *Comparism between ECMWF and UKMet models rainfall forecasts, observed rainfall and rainfall intensities on 9th September, 2013 over the Guinea Savanna Zone, Nigeria (GSZN).*

S/N	Descriptive terms Used*	Rainfall amount (mm/day)	ECMWF forecast**	UKMet forecast**	Observed heavy rainfall (mm)**
1.	No rain	0.0	-	-	-
2.	Very light rain	0.1-2.4	-	-	-
3.	Light rain	2.5-7.5	-	-	-
4	Moderate rain	7.6-35.5	26	28	-
5.	Rather heavy rain	35.6-64.4	-	-	-
6.	Exceptionally heavy rain	120 +	-	-	-
7.	Heavy rain	64.5-124.4	-	-	92.1
8.	Very heavy rain	124.5-244.4	-	-	-

9.	Extreme heavy rain	>244.5	-	-	-

Sources: *Adapted from Meera and Priyanca (2015) **ECMWF (2018) *** NiMet (2018b)

Table 8 presents the results on model rain forecasts for ECMWF and UKMet, observed rainfall and rainfall intensities on 9th September, 2013. Both models forecasted moderate rain intensity while heavy rainfall intensity was observed.

Table 9: Comparism between ECMWF and UKMet models rainfall forecasts, observed rainfall and rainfall intensities on 13th July, 2014 over the Guinea Savanna Zone, Nigeria (GSZN).

S/N	Descriptive terms Used*	Rainfall amount (mm/day)	ECMWF forecast**	UKMet forecast**	Observed heavy rainfall (mm)***
1.	No rain	0.0	-	-	-
2.	Very light rain	0.1-2.4	-	-	-
3.	Light rain	2.5-7.5	3.1	2.8	-
4.	Moderate rain	7.6-35.5	-	-	-
5.	Rather heavy rain	35.6-64.4	-	-	-
6.	Exceptionally heavy rain	120 +	-	-	194.3
7.	Heavy rain	64.5-124.4	-	-	-
8.	Very heavy rain	124.5-244.4	-	-	-
9.	Extreme heavy rain	>244.5	-	-	-

Sources: *Adapted from Meera and Priyanca (2015) **ECMWF (2018) *** NiMet (2018b)

Table 9 presents the results on model forecasts for both ECMWF and UKMet, observed rainfall and rainfall intensities on 13th July, 2014. Both models forecasted light rain intensity, while the observed rainfall indicated exceptionally heavy rain. Therefore, both models underestimated rainfall intensity for that day over the study area.

Table 10: Comparism between ECMWF and UKMet models rainfall forecasts, observed rainfall and rainfall intensities on 20th August, 2015 over the study area.

S/N	Descriptive terms Used*	Rainfall amount (mm/day)	ECMWF forecast**	UKMet forecast**	Observed heavy rainfall (mm)***
1.	No rain	0.0	-	-	-
2.	Very light rain	0.1-2.4	-	-	-
3.	Light rain	2.5-7.5	2.5	-	-
4.	Moderate rain	7.6-35.5	-	16	-
5.	Rather heavy rain	35.6-64.4	-	-	-
6.	Exceptionally heavy rain	120 +	-	-	144.6
7.	Heavy rain	64.5-124.4	-	-	-
8.	Very heavy rain	124.5-244.4	-	-	-
9.	Extreme heavy rain	>244.5	-	-	-

Sources: *Adapted from Meera and Priyanca (2015) **ECMWF (2018) *** NiMet (2018b)

Table 10 shows the results on model forecasts- ECMWF and UKMMet; actual rainfall as well as rainfall intensities on 20th August, 2015. ECMWF model forecasted light rain intensity; UKMet model forecasted moderate rain intensity; while the observed rain was exceptionally heavy rain intensity. Generally, rainfall intensities forecasted by both models over the study area were under-estimated.

Conclusion and recommendations

The two (2) numerical models appraised performed well in the area of categorical rainfall forecast on the nine (9) events investigated. Out of the nine (9) events appraised, the models performed well by forecasting moderate rain on 16th August, 2007; 4th May, 2009; 20th August, 2010; 27th May, 2011; 26th July, 2012 and 9th September, 2013. The models also performed well by forecasting light rain intensity on 13th July, 2014. On the contrary, the models did not forecast same rain intensities on 27th August, 2008 and 20th August, 2015. On a whole, both numerical models under performed in the area of heavy rainfall forecast. Due to this inadequacies, the Nigerian Meteorological Agency (NiMet) which is the most authoritative agency saddled with the responsibility of weather forecast in Nigeria has adopted the use of a regional model called Consortium for small scale modeling (COSMO) alongside other global numerical models. It is hereby recommended that NiMet should work on both numerical models by dynamically downscaling them in such a way that local peculiarities over the Nigerian domain are considered in the physics and dynamics of the models. This will also create room for possible tuning of the model to get the best configuration and set up during heavy rainfall effects. Further, the use of artificial neural network (ANN) is advocated to forecast all the degrees of rainfall intensities especially heavy rain over Nigeria in view of the fact that heavy rainfall has been causing colossal loss to both lives and property annually in Nigeria.

References

Agboluaje, A.A. and Dangana, K. (2014). Seasonal modeling and forecasting of rainfall in Badeggi-Bid Area of Niger State, Nigeria. Development Journal of Science and Technology Research (DJOSTER). 3(1):165-179.

Ajayi, V.O., Abiodun, B.J. and Omotosho, J.A. (2010). Impact of land-cover changes on rainfall in West Africa. Preliminary result. In C.O. Akoshile, A.A. Adeloye, T.R. Fayeye and T.B. Ajibola (eds). Nigerian Meteorological Society proceedings of the annual conference on climate change impact and adaptation: Is Nigeria Ready? Pp. 236-237.

Akinsanola, A.A. Ajayi, V.O., Adefisan, E.A. and Ogunjobi, K.O. (2014). Diagnostic evaluation of precipitation over West Africa using three of the CORDEX-Africa simulation. In Tyubee, B.T.' Ocheri, M.I. and Mage, J.O. (eds). Nigerian Meteorological Society international conference Book of proceedings on climate change and sustainable economic development. Pg. 120.

Asaniyan, T. (2006). Monitoring Convective System over the Sahelian West Africa using Global Models: Case Study of 6th August, 2005. *Journal of the Nigerian Meteorological Society*. 6(1): 50–59.

Audu, E.B. (2001). The Hydrological Consequences of Urbanization in Nigeria: Case Study of Lokoja, Kogi State, Nigeria. Unpublished M. Tech Thesis. Post Graduate School, Federal University of Technology, Minna, Niger State, Nigeria. Pp. 1, 2, 5 &6.

Audu, E.B. (2012). A Descriptive Analysis of Rainfall for Agricultural Planning in Lokoja Local Government Area of Kogi State, Nigeria. *International Journal of Science and Technology*.2(12),850–855.

Audu, E.B., Abubakar, A.S.,Ojoye, S., Mohammed, M. and Mohammed, S.Y. (2018). Characteristics of annual rainfall over Guinea Savanna Zone, Nigeria. *Journal of Information, Education, Science and Technology (JIEST).* School of Technology Education Federal University of Technology, Minna, Niger State, Nigeria. In press.

Audu, E.B; Abenu, A; Usman, M.T; Yahaya, T.I. and Mohammed, S.Y. (2019). Analysis of heavy rainfall in Guinea Savanna Zone, Nigeria. Submitted.

Ayuba, R; Omonona, O.V. and Onwuka, O.S. (2013). Assessment of Ground Water Quality of Lokoja Basement Area, North–Central Nigeria. *Journal Geological Society of India*. 82: 413–420.

Bello, A.O. (2007). Regional Geography of Nigeria. In Eno, J.E (ed). Perspective of Geography. Tamaza Publication Company Limited. Pg131.

Dan–Hassan, M. A.; Amadi, A. N; Yaya, O.O. and Okunlola, I.A. (2015). Managing Nigeria's Groundwater Resources for Safe Drinking Water. Nigeria Association of Hydrological Sciences (NAHS). International Conference on Sustainable Water Management in a Changing Environment, Ahmadu Bello University, Zaria, Kaduna State, Nigeria. Pp. 85– 86.

European Centre for Medium-Range Weather Forecasts (2018). Models rainfall forecasts.

Falola, T.O; Udo, R.K; Ajayi, J.F.A; Kirk–Greene, A.H.M. (2015). Nigeria. Pg. 4.

Gaili, W., Dan, W., Ji, Y. and Liping, L. (2016). Evaluation and Correction of Quantitative Precipitation Forecast by Storm-Scale NWP Model in Jiangsu, China. Research Article. Np.

Gonap, E.G., Gontul, T.K., Iirmdu, T.O., Timchang, N.M. and Abenu, A. (2018). Words of Mouths, WOMs as main Information Source to Tourists in Plateau State. *Journal of Science, Technology, Mathematics and Education (JOSTMED).* Department of Science Education, Federal University of Technology, Minna, Nigeria, Africa. 14(2):9-18.

Ibrahim, I. (2006). Severe Thunderstorms in study over January in Southern Nigeria–A case study over Akure. *Journal of the Nigerian Meteorological Society*. 6(1): 60–69.

Iwena, O.A. (2000). Essential Geography for Senior Secondary Schools. Tonad Publishers Limited. Pp. 187.

Lawal, M.K., Bello, U.S. and Abubakar, A. (2012). Preparing for climate change related dissters: Role of relevant stakeholders in Sokoto State. In M.A. Iliya, M.A. Abdulrahim, I.M. Dankani and A. Opponkumi (eds). Climate change and sustainable development. Geography

Department, Usumanu Danfodiyo University, Sokoto and Association of Nigerian Geographers. Pg. 48.

Meera, N. and Priyanca, F. (2015). Daily Weather Forecasting using Artificial Neural Network. *International Journal of Computer Applications*. 121(22):9–13.

Mohammed, H. (2010). Mean monthly rainfall pattern of the Shiroro (HEP) during the Pre and Post Dam periods. Department of Geography, Federal University of Technology, Minna, Niger State, Nigeria. Pg.8

Musa, J., Bako, M.M., Yunusa, M.B., Garba, I.K. and Adamu, M. (2012). An Assessment of the Impact of Urban Growth on Land Surface Temperature in FCT, Abuja Using Geospatial Technique. *Sokoto Journal of the Social Sciences*. 2(2):144-160.

Musa, J.J; Abdulrazak, N; Olaniyan, O.A; Ojo, A.C. and Adeyeye, J. (2013). Trend Analysis of wind variation in Minna, Nigeria. *Journal of Science, Technology, Mathematics and Education (JOSTMED).* 10(1):72-81.

National Space Research and Development Agency, Abuja (2019). The Study Area.

Nigerian Meteorological Agency (NiMet) (2018a). Climate Review Bulletin. Pp. 11 and 55.

Nigerian Meteorological Agency (NiMet) (2018b). Rainfall data.

Obateru, O.C. (2017). Impact of Climate Variability on some Tuber Crop Yields in the Federal Capital Territory. School of Post Graduate Studies, University of Abuja. Pg. 50.

Odekunle, T.O; Orinmoogunje, I.O.O. and Ayandele, A. (2007). Application of Geographic Information System (GIS) to assess Rainfall Variability Impacts on Crop Yield in Guinean Savanna Part of Nigeria. *African Journal of Biotechnology*. 6(18):2100–2113.

Shehu, A.A. (2014). An Assessment of Impact of Traffic Congestion on Road Users in Minna Metropolis using Remote Sensing Techniques. Department of Geography, Federal University of Technology, Minna, Niger State, Nigeria. Pg. 6.

Using Artificial Neural Networks to Forecast Rainfall Over Guinea Ecological Zone, Nigeria

Audu, E.B.,[1] Musa, S.D.,[2] Yahaya, T.I.,[3] Emigilati, M.A.[3] and Yisa, C.L.[4]

[1]Government Secondary School, Abuja@30, Pegi, Federal Capital Territory, Nigeria

[2]Departmnt of Geography and Environmental Planning, Kogi State University, Anyigba, Nigeria

[3]Department of Geography, Federal University of Technology, Minna, Niger State, Nigeria

[4]Department of Geography, Niger State College of Education, Minna, Nigeria

Correspondence author: audu_ebamaiyi@yahoo.com (+234-803-585-6619).

Abstract

Rainfall forecast is very crucial in view of the fact that Nigeria is not left out in the global rainfall variation and climate change occurrence. This research used the artificial neural networks to forecast rainfall for 2019 over the Guinea Ecological Zone, Nigeria (GEZN) and comparing its results with the Nigerian Meteorological Agency (NiMet) Seasonal rainfall Prediction (SRP) for the same region in the corresponding year. Daily rainfall data which spanned through 1981 to 2015 and obtained from NiMet, Oshodi, Lagos; were used. The NiMet rainfall forecast with its margin of error were obtained from 2019 SRP by NiMet. The data were trained using artificial neural networks (ANNs). The test dataset was used to evaluate the performance of the networks by computing the Root Mean Square Errors (RMSEs). Fuzzy logics were also used for the neural networks training. The neural networks outputs were probability of density of rainfall, regression and margin of error. Margin of errors were also calculated for the data collection points. Results were shown in figures. According to the results from ANNs were able to forecast rainfall over the study area. Onset and cessation of rains are April and October, while August has the highest mean rainfall. Both NiMet and ANN forecasts showed near accurate annual rainfall over Abuja, Ibi, Kaduna, Lokoja and Makurdi while discrepancies were observed over Ilorin, Minna, Lafia and Jos. It was then recommended that rainfall review should be carried out at the end of 2019 to evaluate the performance of the ANNs so as to ascertain its suitability for future use.

Keywords: Rainfall, rainfall forecast, rainfall variability, models, artificial neural networks.

Introduction

Rainfall is very important in Nigeria not only because it is a weather variable, but also because of its role in agriculture, ecology and hydrology including the hydrological cycle. It is also a major determinant of crop germination, growth, maturation and yield. According to the Nigerian Meteorological Agency (NiMet) (2017), the 2017 rainfall season favoured the agricultural sector particularly in crop production as it was characterized by normal rainfall pattern in most parts of the country and above normal over places like Jos, Lafia, Nguru, Ilorin, Kaduna, Yelwa, Enugu, Calabar and Lagos. In hydrology, heavy/frequent/prolonged rainfall leads to floods, especially flash floods; landslides and erosion. According to NiMet (2018), in Nigeria; there were levee failures in 2012 and 2018 because water levels in major dams were observed to be above normal due to heavy rainfall occurrence recorded in August and September in some northern states leading to flash floods which greatly impacted catchment areas and aquifers.

The derived rainfall parameters which require forecast include onset, cessation, duration, wet spells, dry spells, drought, frequency, intensity and total amount. According to NiMet (2019), annual rainfall amount is the total amount of rainfall observed and recorded in the year under reference. Rainfall forecast could be for a very short term, short term, medium term and long term. This forecast is for a long term because it covers a year.

Rainfall forecast is done using different methods. However, in recent times; the use of Numerical Weather Prediction (NWP) and other numerical models are very common because they have high accuracy and reliability. Nigeria adopted the use of Consortium for Small Scale Modelling (COSMO) since 2012 in collaboration with German Meteorological Office (DWD) and has proven its ability to forecast deep convection successfully; that performed quite well for many heavy convection events

including the explicit simulation of deep convention during 2017 rainy season (NiMet, 2017). According to NiMet (2017), NWP consists of numerical models that stimulate dynamical, radiation and thermo-dynamical atmospherical physics and further processes on the earth boundary layer as well as on a large variety of different observation data which are focused into a coherent state of the atmosphere by data assimilation techniques.

Agogbuo *et al* (2017) evaluated selected NWP models for a case of widespread rainfall over Central and Southern Nigeria on 21st March, 2015 using data from ECMWF, UKmet, NCEP Global Forecast System (GFS) and Weather Research and Forecast (WRF) model. The rainfall forecasts were compared with observed rainfall at station and gridded observation points using the Method of Objective-based Diagnostic Evaluation (MODE), Grid statistics and point statistics. Results showed that ECMWF, UKMet and GFS underestimated the rainfall amount when compared to the WRF regional models.

Capacci *et al* (2004) conducted a research on the probability of precipitation estimation using SEVIRI-LIKE data and artificial neural networks. The ANNs techniques were adopted to establish an indirect procedure to estimate Probability of Precipitation (PoP). Result shows that a new SEVIRI-based scheme could provide better estimation of precipitation.

As good as these models are in terms of categorical rainfall forecast, the ANNs were not used to forecast rainfall in year 2019 over the GEZN hence this research which aimed at forecasting annual rainfall over the GEZN and comparing its result with the NiMet forecast for 2019.

Study area

The Guinea Ecological Zone, Nigeria (GEZN) is the study area. It is located between longitudes 4°–10°E and latitudes 6°–11°30[1]N. It shares boundaries with the Sudano–Sahelian Zone, Nigeria (SSZN) to the north and the forest vegetation zone, Nigeria (FVZN) to the south (Figure 1).

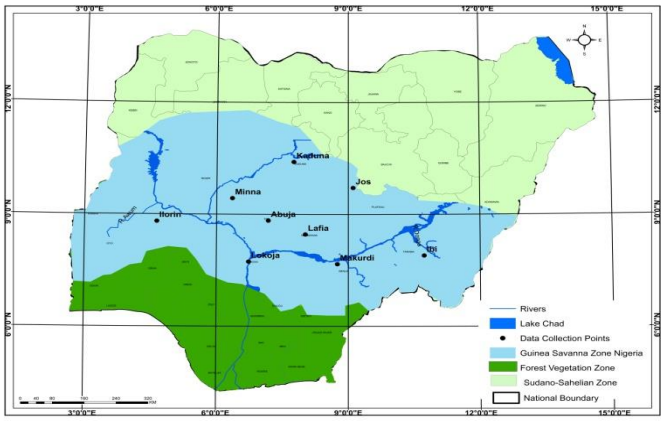

Figure 1. *The Study Area*

Source: *National Space Research and Development Agency (NASRDA) (2019).*

The GSZN has two (2) distinct seasons which are rainy and dry. The onset of rain is April while its cessation is October. Dry season period is November to March, while the harmattan is experienced between November and February (Malik, 2004 cited in Musa *et al*., 2012). There is inter-annual variation in rainfall over the area (Ibrahim *et al*, 2018). Total annual rainfall is over 1220 mm in most years (Abdulkadir, 2007; Yusuf, 2012, FUT Minna, 2014). The highest mean monthly rainfall occurs in August (Obateru, 2017; NiMet, 2018). Mean annual temperature is about 31°C except for Jos Plateau where it is lower (MS, 2013 cited in Musa *et al*, 2013). In dry season, relative humidity is about 30%, while during the rainy season, it is about 70% (Audu, 2001; Audu, 2012). The two (2) predominant air masses that influence the weather and climate of the area are the Tropical Maritime Air mass (mT) also called the South–West (SW) trade wind which is moisture laden and the Tropical Continental (cT) air mass. (Iwena, 2000).

The study area consists of gently undulating plain, hills, ridges and plateaux whose heights are between 300m-1500m (Ola, 2001 cited in Obateru, 2017; Gonap *et al*, 2018). There are numerous rivers in the area such as Rivers Niger, Benue, Katsina Ala, Kaduna, Gurara, Awum, Donga and Usuma (Audu, 2019). These rivers and the associated features such as flood plains and islets are of great economic importance such as fishing, irrigation farming especially in the dry season, hydroelectric power generation, industrial uses and tourism. However, these potentials are grossly under harnessed. Two (2) prominent man–made lakes found in the area are Kainji Lake on River Niger and Shiroro Lake on River Kaduna. Few dams within the study area include the Kainji and Jebba Dams located on River Niger, Shiroro Dam located on River Kaduna as well as the Jabi and Lower Usuma Dams in Abuja–FCT (Iwena, 2000). The vegetation is guinea in nature with pockets of gallery forest around water courses (Bello, 2007).

The geology of the study area is mainly Precambrian basement and sedimentary rocks (Ayuba *et al*, 2013). The major occupations are farming, hunting, little lumbering and little mining.

Materials and methods

Secondary data were used for this research. These data included the daily rainfall and annual rainfall forecast (mm) by Nimet (2019) for Makurdi, Lokoja, Ibi, Ilorin, Lafia, Abuja, Minna, Jos and Kaduna. The period covered in the data is from 1st January, 1981 to 31st December, 2015 (35 years). The data points are evenly distributed across the study area. The secondary data were sourced from the Nigerian Meteorological Agency, Oshodi, Lagos.

Artificial neural networks (ANNs) were used to train the daily rainfall data on time series (using year and day of year as inputs). The data were arranged in four columns such as day of year sum of rainfall,

day of year index of rainfall, day of year daily rainfall and actual annual rainfall, . Fifty networks were simulated varying the number of hidden neurons from 1–50. Before the training, the daily rainfall data were split into three in this manner: Training=70%; Validation=15% and Testing=15%. The test dataset was used to evaluate the performance of the networks by computing Root Mean Square Errors (RMSEs). Fuzzy logics were also used for the neural networks training. The neural networks outputs were densities of rainfall. Rainfall amount for a day was obtained using the following equation:

$$\frac{probability\ density\ for\ the\ day\ (PDD)}{sum\ of\ probability\ densities\ for\ the\ year\ (SPDDY)} x \frac{Rainfall\ cummulative\ for\ the\ year\ (mm)}{1} \qquad 1$$

Where: *PDD* = an index for indicating rainfall amount for the day,

RCY= rainfall cumulative (total annual rainfall) in mm for the year; and

SPDDY= sum of probability densities for all the days in the year

The RMSE was determined using the following equation:

$$RMSE=\sqrt{\sum \frac{(x-f)^2}{n}} \qquad 2$$

Where:$x\ = observed\ rainfall\ in\ mm$, f= rainfall forecast from the network, n=15% of data point (in days) used for testing.

$$H_{vm}=\tanh(iwm * ivm + B_1) \qquad 3$$

tanh is the hyperbolic tangent of trigonometric function. Input weight matrix (iwm) is a parameter of the network which is obtained after the network training. Input variable matrix (ivm) contains the inputs for the neural networks.

$$O_{vm}=B_2 + L_{wm} * H_{vm} \quad 4$$

Both $B_1$and B_2 (called bias vectors) are parameters of the network that are obtained after the training. They are constant vectors. Layer weight matrix (L_{wm}) is also a parameter of the network which is obtained after the training. It is a constant matrix.

Eqns 3 and 4 are respectively functions of the neural networks representing the transfer functions from the in input to the hidden layer and from the hidden layer to the output layer.

$$FL = A - R = B \quad 5$$

Where: $A\ and\ B$ are fuzzy sets, R is a fuzzy relation and $A - R$ stands for the composition of A with R.

To determine the expression for the linear regression, the following equation was used:

$$y = mx + c \quad 6$$

Where: y =which is the output (predicted annual rainfall in mm),$m\ is\ slope\ of\ the\ line$

$x = O_{vm}$ (observed annual rainfall in mm), c is the *intercep*t of the line ($m\ and\ c$ are constants in the equation).

The neural network diagram is shown in Figure 2.

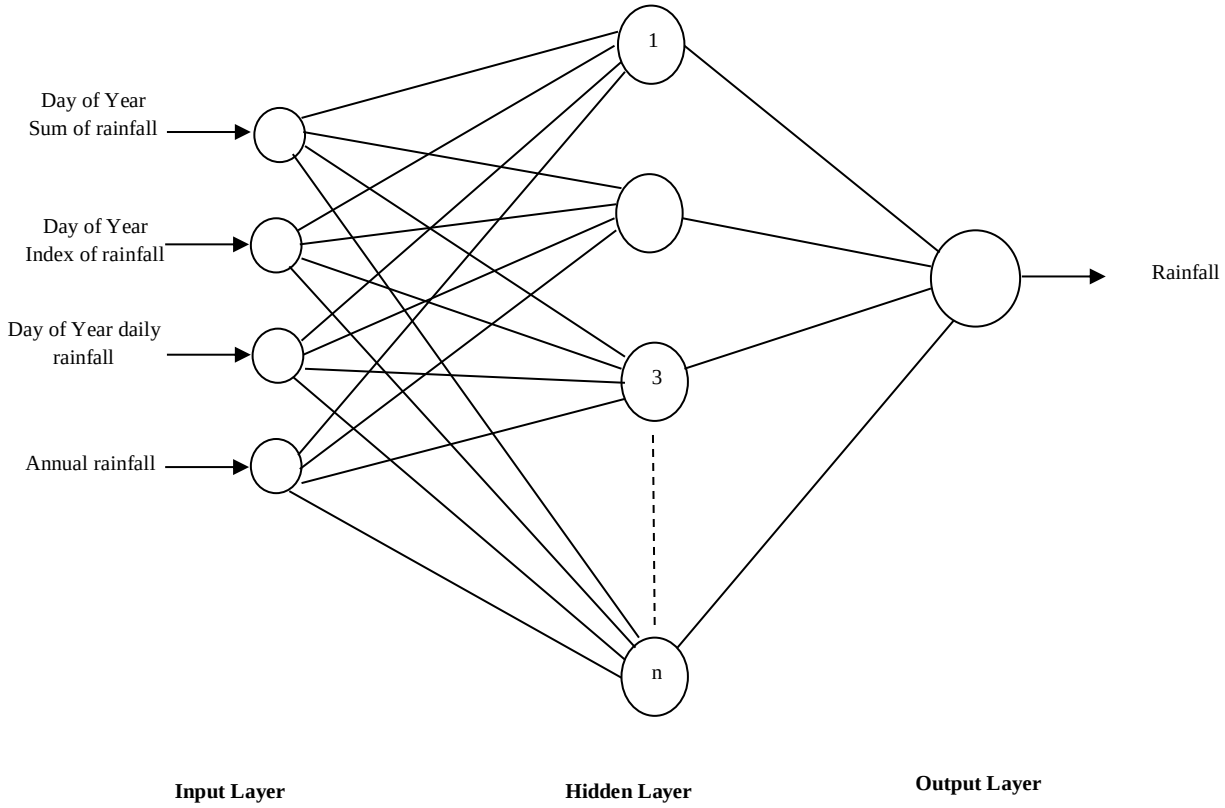

Figure 1: *Neural Networks diagram*

Source: Authors' computation, 2019

To take care of the errors in the total annual rainfall forecast by ANNs, margin of errors (MEs) were calculated for all the data collection points. A margin of error is the range of values below and above the sample statistic in a confidence interval. MEs were calculated using the following equation:

$$ME = z_{\frac{\alpha}{2}} x\ \sigma \qquad 7$$

Where: ME = margin of error,

$Z\frac{\alpha}{2}$ = critical value which is 1.96 based on the 95 % level of confidence for this study,

σ = standard deviation

Results and discussion

Figures 3-12 show the total monthly rainfall forecast by ANNs over the study area. Ilorin and Makurdi are expected to experience rainfall in January and February. In March, all the stations are expected to experience rainfall except Kaduna and Lafia. All the stations are expected to have rains in April-October except Jos where rain is not expected in October. Abuja, Ilorin and Makurdi are expected to have rains in November, while rains are expected over Ibi and Ilorin in December. In the study area, April-October marks the rainy season (Audu, 2012; Obateru, 2017).

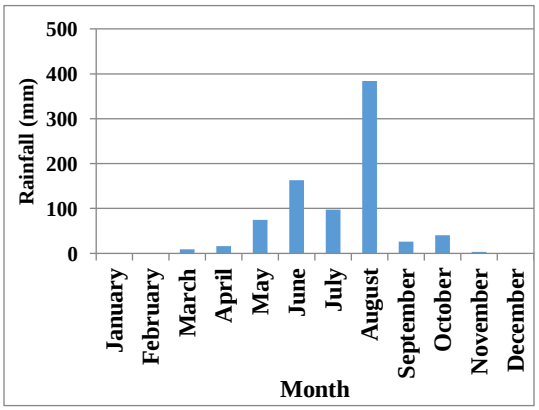

Fig.3: Monthly rainfall forecast by ANNs over Abuja in 2019

Source: Authors' computation, 2019

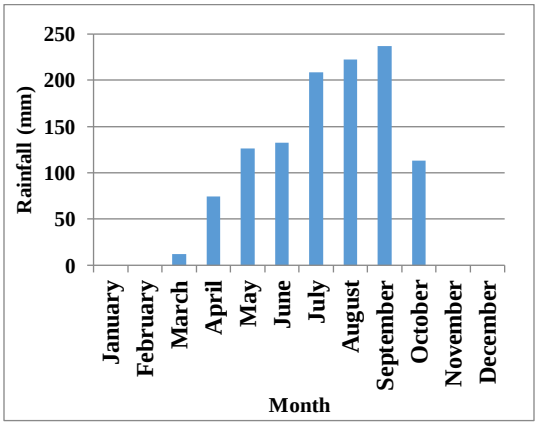

Fig.4: Total monthly rainfall forecast by ANNs over Ibi in 2019

Source: Authors' computation, 2019

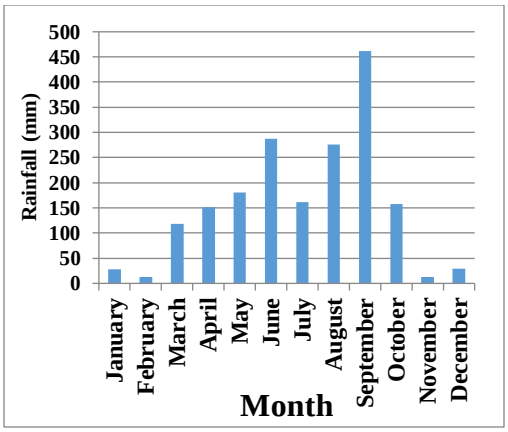

Fig.5: Total monthly rainfall forecast by ANNs over Ilorin in 2019

Source: Authors' computation, 2019

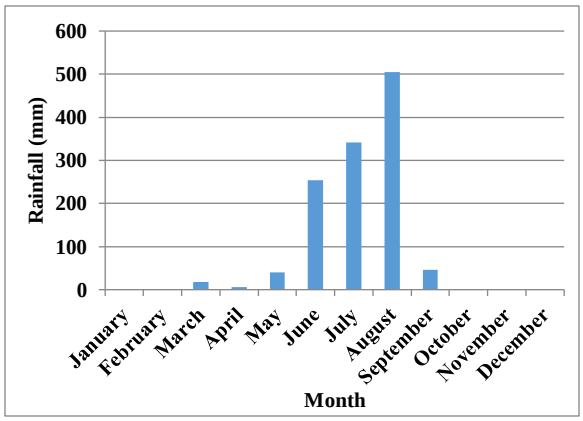

Fig.6: Total monthly rainfall forecast by ANNs over Jos in 2019

Source: Authors' computation, 2019

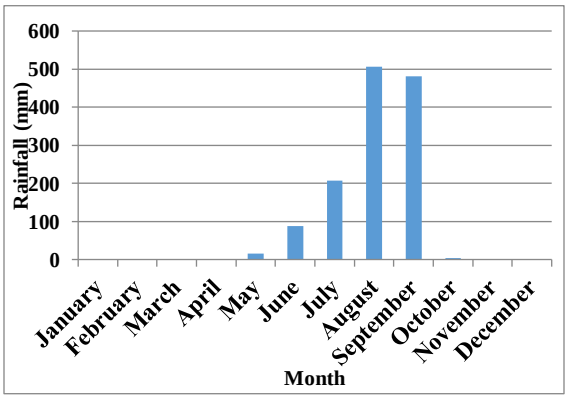

Fig.7: Total monthly rainfall forecast by ANNs over Kaduna in 2019

Source: Authors' computation, 2019

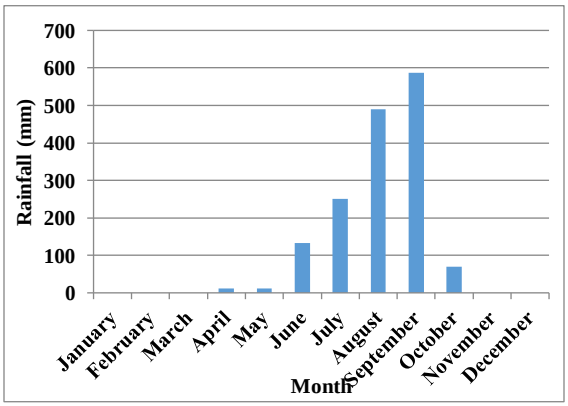

Fig.8: Total monthly rainfall forecast by ANNs over Lafia in 2019

Source: Authors' computation, 2019

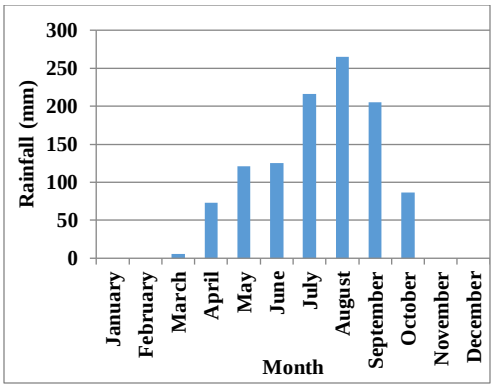

Fig.9: Total monthly rainfall forecast by ANNs over Lokoja in 2019

Source: Authors' computation, 2019

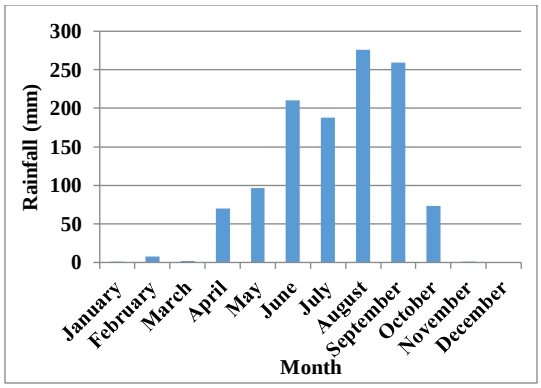

Fig.10: Total monthly rainfall forecast by ANNs over Makurdi in 2019

Source: Authors' computation, 2019

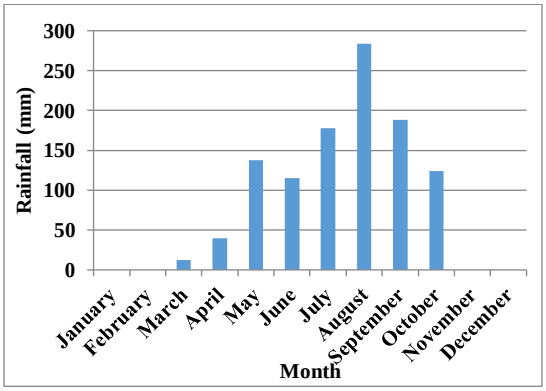

Fig.11: Total monthly rainfall forecast by ANNs over Minna in 2019

Source: Authors' computation, 2019

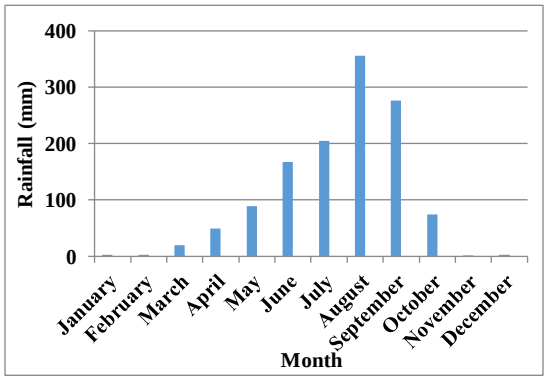

Fig.12: Mean monthly rainfall forecast by ANNs over GEZN IN 2019

Source: Authors' computation, 2019

In Abuja, highest rainfall is expected in August (fig. 3). Obateru (2017) opined that highest mean monthly rainfall over Abuja occurs in August. There is also a sign of double maxima rainfall in June and August. In fig.4, Ibi is expected to have high values of monthly rainfall which is over 50 mm between April-October with the highest in September. According to fig.5, Ilorin is expected to have

rainfall throughout the year with March-October having monthly rainfall of over 100 mm. there is double maxima rainfall over the station with September having the highest rainfall. A delayed onset of rain was observed over Jos and Kaduna (figures 6 & 7). May is the onset, while September is the cessation with August having the highest rainfall. Figure 8 depicts that Lafia will experience onset of rain in June and cessation will be in October, while the highest rainfall is in September. Over Lokoja and Makurdi (figures 9 & 10), April is the onset of rain, October is the cessation while August has the highest. Makurdi shows a sign of double maxima rainfall with a reduction of rain in July. In Minna (figure 11), onset of rainfall is in May, cessation is in October, while highest rainfall is in August. According to figure 12, April is the onset of rain over the GEZN, October is the cessation while the highest rainfall is in August with single maximum.

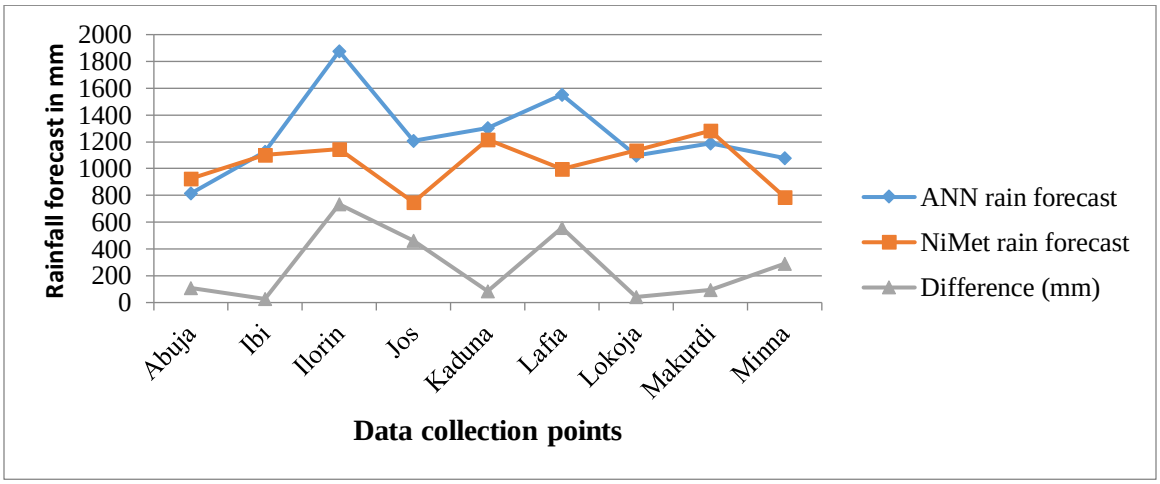

Fig. 13: Rain forecasts by ANNs and NiMet for 2019

Sources: 1. NiMet (2019) 2. Authors' computation, 2019

According to figure 13, NiMet annual total rainfall for the data collection points shows below normal rainfall over all the points for the year 2019 except for Kaduna and Makurdi where normal rainfall is expected. The artificial neural network (ANNs) forecasts show below normal rainfall over Jos, Kaduna and Makurdi, while above normal rainfall forecast was made over Ilorin and Lafia. Results from NiMet forecast also shows a decline in total annual rainfall over the stations except Kaduna and Makurdi, while ANN forecasts show downward trend in annual rainfall over Abuja. In a research conducted by Audu *et al* (2019), it was discovered that Abuja and Ibi are experiencing downward trend in total annual rainfall in recent time.

According to Audu (2019), no forecast is 100% accurate; hence the need for margin of error (ME) to be calculated for every forecast. The margin of error for this study is shown in fig. 14.

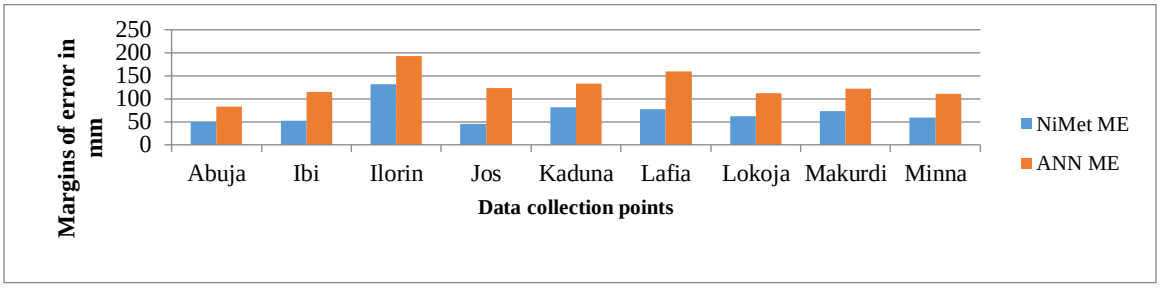

Fig. 14: Margin of error over the data collection points in GEZN.

Source: Authors' computation, 2019

According to figure 14, all the data collection points have NiMet ME that is above 50 mm except for Abuja and Jos, while the ANNs ME is higher than 50 mm in all data collection points. In ANNs ME, Abuja has the least, while Ilorin has the highest. The mean NiMet ME is 70.2 mm, while ANN ME is 128 mm. Generally; the ANNs MEs are higher than NiMet ME.

Conclusion and recommendation

The artificial neural network (ANNs) was able to forecast rainfall over the GEZN for the year 2019. According to the forecast, there were significant rains in March, but the onset of rain is April, while its cessation is October. The ANNs mean annual rainfall over the study area is August. The ANNs forecast performed well when compared with the NiMet's forecast except for Ilorin, Minna, Jos and Lafia. It is therefore recommended that a rainfall review should be carried out at the end of 2019 to evaluate the performance of the ANN so as to ascertain its suitability for forecast in the future.

References

Abubakar, A.S. (2015). Hydrometeorology: Enhancing the Capacity for Hydroelectricity Generation in our Homes and Industries. Inaugural Lecture Series 36. Published by University Seminar and Coloquium Committee, Federal University of Technology, Minna, Niger State, Nigeria. Pg. 8.

Agogbuo, C.N., Nwagbara, M.O., Bekele, E. and Olusegun A. (2017). Evaluation of selected Numerical Weather Prediction Models for a case of widespread rainfall over Central and Southern Nigeria. J Environ Anal Toxicol 7 491 doi:1-9

Audu, E.B. (2001). The Hydrological Consequences of Urbanization in Nigeria: Case Study of Lokoja, Kogi State, Nigeria. Unpublished M. Tech Thesis. Post Graduate School, Federal University of Technology, Minna, Niger State, Nigeria. Pp. 1, 2, 5 &6.

Audu, E.B. (2012). A Descriptive Analysis of Rainfall for Agricultural Planning in Lokoja Local Government Area of Kogi State, Nigeria. *International Journal of Science and Technology*.2(12):850–855.

Audu, E.B. (2019). Development of heavy rainfall forecasting model using meteorological parameters in Guinea Savanna Zone, Nigeria. Department of Geography, Federal University of Technology, Minna, Niger State, Nigeria. Pg. 15.

Audu, E.B., Abubakar, A.S., Ojoye, S., Muhammed, M. and Mohammed, S.Y. (2019). Characteristics of annual rainfall over Guinea Savanna Zone, Nigeria. In press.

Ayuba, R; Omonona, O.V. and Onwuka, O.S. (2013). Assessment of Ground Water Quality of Lokoja Basement Area, North–Central Nigeria. *Journal Geological Society of India*. 82: 413–420.

Bello, A.O. (2007). Regional Geography of Nigeria. In Eno, J.E (ed). Perspective of Geography. Tamaza Publication Company Limited. Pg131.

Capacci, D., Bryan, C. and Porcu, F. (2004). Probability of precipitation estimation using SEVIRI-LIKE data and artificial neural networks. Researchgate. 1:8.

Federal University of Technology (FUT), Minna, Nigeria (2014). Postgraduate School Prospectus. Pg. 1.

Gonap, E.G., Gontul, T.K., Iirmdu, T.O., Timchang, N.M. and Abenu, A. (2018). Words of Mouths, WOMs as main Information Source to Tourists in Plateau State. *Journal of Science, Technology, Mathematics and Education (JOSTMED).* Department of Science Education, Federal University of Technology, Minna, Nigeria, Africa. 14(2):9-18.

Ibrahim, I., Emigilati, M.A., Suleiman, Y.M., Ojoye, S. and Yahaya, T.I. (2018). Effectiveness of Early Warning Methodology and Standardized Precipitation Index for Drought Monitoring over Guinea Savanna Zone, Nigeria. *Journal of Science, Technology, Mathematics and Education (JOSTMED).* Department of Science Education, Federal University of Technology, Minna, Nigeria, Africa. 14(2):1-8.

Iwena, O.A. (2000). Essential Geography for Senior Secondary Schools. Tonad Publishers Limited. Pp. 187.

Musa, J., Bako, M.M., Yunusa, M.B., Garba, I.K. and Adamu, M. (2012). An Assessment of the Impact of Urban Growth on Land Surface Temperature in FCT, Abuja Using Geospatial Technique. *Sokoto Journal of the Social Sciences*. 2(2):144-160.

Nigerian Meteorological Agency (NiMet) (2018). Climate Review Bulletin. Pp. 11-12 & 52.

Nigerian Meteorological Agency (NiMet) (2019). Seasonal Rainfall Prediction (SRP). Pp. 35-35 & 56-57.

Nsofor, G.N. (2019). Climate change, paradoxes and mapping the tragedy of the commons. Inaugural Lecture Series 71. Federal University of Technology, Minna. Pg. 28.

Obateru, O.C. (2017). Impact of Climate Variability on some Tuber Crop Yields in the Federal Capital Territory. School of Post Graduate Studies, University of Abuja. Pg. 50.

The Nigerian Meteorological Agency (NiMet) (2017). Climate Review Bulletin. Pg. 59.

Wannah, B.B. and Mbaya, L.A. (2012). Adaptation to climate change: vulnerability assessment for Gombe State. In M.A. Iliya, M.A. Abdulrahim, I.M. Dankani and A. Opponkumi (eds). Climate change and sustainable development. Geography Department, Usumanu Danfodiyo University, Sokoto and Association of Nigerian Geographers. Proceedings of the 52nd Annual Conference. Pp. 169-170.

Yusuf, Y.O. (2012). An Assessment of Spatial Distribution of Rainfall Amount in Zaria, Kaduna State. In M.A. Iliya, M.A. Abdulrahim, I.M. Dankani and A. Oppokumi (eds). Climate Change and Sustainable Development. Geography Department, Usumanu Dan Fodio University, Sokoto and Association of Nigerian Geographers (ANG). Proceedings of 52nd Annual Conference of ANG. Pg. 69.

Yusuf, Y.O. and Mohammed, N.A. (2012). An assessment of spatial distribution of rainfall amount in Zaria, Kaduna State. In M.A. Iliya, M.A. Abdulrahim, I.M. Dankani and A. Opponkumi (eds). Climate change and sustainable development. Geography Department, Usumanu Danfodiyo University, Sokoto and Association of Nigerian Geographers. Proceedings of the 52nd Annual Conference. Pg. 70.

Effect of Grain Size/Grain Boundaries on the Electrical Conductivity of SnS Thin Film of $0.2 < t \leq 0.4$ Mm Thicknes For Transistor Application

Thomas Ojonugwa Daniel[1*], Uno Essang Uno[2], Kasim Uthman Isah[3] and Umaru Ahmadu[4]

[1]Department of Physics/Geology/Geophysics, Alex Ekwueme-Federal University Ndufu-Alike, Ikwo, Abakaliki, Ebonyi state, Nigeria.

[1,2,3&4]Department of Physics, Federal University of Technology, Minna, Nigeria.

[4]umaruahmadu@futminna.edu.ng

[3]kasim309@futminna.edu.ng

[2]uno.uno@futminna.edu.ng

[1]danielojonugwathomas@gmail.com;

*Corresponding author

Abstract

SnS semiconductor thin films of 0.20, 0.25, 0.30, 0.35, 0.40 μm were deposited using aerosol assisted chemical vapour deposition on glass substrates and were investigated for use in a field effect transistor. Profilometry, Scanning electron microscope, Energy dispersive X-ray spectroscopy and hall measurement were used to characterise the microstructural and electrical properties of the SnS thin film. The SnS thin films were found to consist of Sn and S elements whose composition varied with increase in thickness. The film conductivity was found to vary with grain size and grain boundary which is a function of the film thickness. The SnS film of 0.4 μm thickness shows a more uniform grain distribution and growth with a grain size of 130.31 nm signifying an optimum for the as deposited SnS films as the larger grains reduces the number of grain boundaries and charge trap density which allows charge carriers to move freely in the lattice thereby causing a reduction in resistivity and increase in conductivity of the films which are essentially parameters for a transistor semiconductor material.

Key words: conductivity; grain boundary; grain size; SnS; thin film.

1.0.Introduction

Field effect transistors are unipolar devices employing only the free majority carriers in the conduction region. The operation of a field effect transistor with a low operating voltage and high carrier concentration is essentially dependent on the choice of semiconductor channel layer material and the gate dielectric among other parameters since the threshold voltage (V_{th}), which is the voltage required in switching a transistor is dependent on the semiconductor material(Du *et al.*, 2015). More so the minimum gate to source voltage differential that is needed to create a conducting path between the source and drain is dependent on the semiconductor channel layer.

However, the reported modulation of electronic states in a field effect transistor have been so far realised only on oxides, nitrides, carbon nanotubes and organic semiconductor. Therefore, the application of the electric double layer field effect transistor technique to other classes of semiconductor solids has become one of the emerging interests for novel electronic phenomena. This trend is increasingly important for the achievement and development of novel device concepts, applications and tuning of physical properties of materials (Yuan *et al*., 2011).

Metal chalcogenides (MX-where M denote metal (usually transistion metal) and X denote chalcogen) such as Tin(II) sulphide (SnS) and metal dichalcogenides (MX_2, where M and X denote metal and chalcogen respectively) such as Tin(IV) sulphide (SnS_2) are of interest as potential candidates for the transport channel of field effect transistor and have also found vital applications in solar cells, photoconductive materials, thermoelectric materials, rewritable memory, studying of dopant induced superconductivity and charge density formation. Chalcogenides are materials containing a transition element and one or more chalcogen elements (Silicon, Selenium,Polonium and Tellunum). SnS is abundance in the earth's crust, SnS is one of the Tin chalcogenides layered semiconductors in group IV-VI, it possess the layered orthorhombic structure with eight atoms per unit cell forming biplane layers normal to the largest c axis and the constituent elements are abundant in nature (Thiruramanathan *et al*., 2015). SnS does not contain any toxic or expensive elements; it is a p type semiconducting material with carrier concentration on the order of $10^{16}cm^{-3}$, hole mobility of 1.4 $cm^2V^{-1}s^{-1}$ and low resistivity (Hegde *et al*., 2011). SnS thin film is relatively unexplored for application in a field effect transistor, as literatures pertaining to the application of SnS as semiconductor or transport channel of a field effect transistor is relatively scanty.

Hence SnS thin film is a promising candidate to test the feasibility of the chalcogen family for transport channel of a field effect transistor and to determine the optimum deposition parameters that will give suitable properties for its usage. The SnS thin film has been rarely reported for use as a semiconductor in a field effect transistor. A parameter of interest is the film thickness which is a function of the film structure and microstructure. The investigation and control of film thickness is important in semiconductor processing as the film thickness influences the grain size/grain boundary which is essential in defining the electrical and properties of a semiconductor material (Soonmin *et al*., 2013). The deposition method of interest in the study is the aerosol assisted chemical vapour deposition (AACVD). AACVD offers the competitive advantage of usage of less-volatile precursors, thus widening the types of molecules that can be used to deposit thin films.

A thickness range of 0.20-0.40 μm was selected from the average values and method of thickness variation obtained in literatures for a field effect transistor. Preliminary deposition and profilometry was carried out to determine the starting precursor concentrations to achieve the thickness range and also the substrate temperature to use.

2.0. Experimental procedure

Soda lime glass substrates were cleaned using the cleaning methods described as follows: **a.** the substrates were washed in sodium lauryl sulphate (SLS) solution to remove oil and protein. **b.** To remove the organic contaminants, the substrates were immersed in piranha solution (H_2SO_4: H_2O_2 (3:1)) for 30 minutes. **c.** The substrates were then ultrasonically cleaned in distilled water using a sonicator and kept in methanol until it is ready to be used. **d.** Finally, to use the substrate for deposition process, the substrate were taken from the methanol and dried in air at 150℃. SnS semiconductor thin films was deposited using 0.1 M Tin chloride dehydrates and 0.2 M of Thiourea which was weighed in stoichiometric proportion and dissolve in ethanol solvent. The two solutions were then mixed and stirred for 1 hour using a magnetic stirrer at room temperature, after which the resulting solution was filtered through a 0.22 μm syringe filter and then deposited on the substrate by aerosol assisted chemical vapour deposition (AACVD) at a constant substrate temperature of 258 ℃, nozzle distance of 6.8 mm, substrate to nozzle distance of 3 cm, spray volume of 0.2 mL and spray rate of 0.04 ml/min. Five samples of SnS thin films were deposited at thickness of 0.4 μm, 0.35 μm, 0.30 μm, 0.25 μm and 0.20 μm (Labelled as Sample 2, Sample 3, Sample 4, Sample 5 and Sample 6) which was achieved by keeping the initial concentration of the SnS precursors constant using 1 ml of

the precursor while varying the concentration of the ethanol solvent through 0 ml, 0.5 ml, 1.0 ml, 1.5 ml, and 2.0 ml. The as deposited films samples were allowed to cool to room temperature after which they were placed in petri dishes before undergoing film characterisation as follows:

2.1. Characterisation of SnS thin film semiconductor

2.1.1. Scanning Electron Microscopy (SEM)/Energy dispersive spectroscopy (EDS)

The morphology and the microstructure of the SnS thin films was characterized using High Resolution Scanning Electron Microscopy (HR-SEM, Zeiss) while the elemental composition of the films were determined by an Energy dispersive X-ray spectroscopy (EDS; Oxford instrument). The instrument was operated at a voltage of 20 kV while the images were captured at 5 kV. Average grain size and grain size distribution histogram was obtained using imagej software.

2.1.2. Surface profilometry

Surface Profilometry (VEECO DEKTAK 150) was used to carry out measurement of the thickness of the deposited films.

2.1.3. Electrical Characterisation

The carrier density, carrier mobility and carrier type were determined by an ECOPIA Hall Effect measurement system (HMS 3000 Hall measurement system) based on Van der pauw configuration. The current was varied from $\pm$ 1 mA to 1 mA at room temperature. A magnetic field of 8000 gauss was employed for the Hall Effect measurement. The polarity of the current was reversed during each measurement and average values were taken in order to eliminate thermo electric and thermo magnetic effects. The hall measurements were carried out by passing the current through AC and measuring the P.D across BD by applying a homogeneous magnetic field perpendicular to the plane of the films.

3.0. RESULTS AND DISCUSSION

3.1. Surface profilometry and Physical properties

The thickness of the as deposited SnS thin films as obtained from surface profilometry are 0.20 μm, 0.25 μm, 0.30 μm, 0.35 μm and 0.40 μm. The deposited films were smooth and strongly adherent to

the surface of the substrate. A colour change was observed with increase in film thickness from 0.20 µm to 0.40 µm. The colour changed from pale yellow to gray via brown with the increase of film thickness. The SnS films grown at lower thickness of 0.20 µm, 0.25 µm, and 0.30 µm were more transparent than the films grown with thickness of 0.35 µm and 0.40 µm. Plate I, shows the as deposited SnS thin films of 0.20 µm, 0.25 µm, 0.30 µm, 0.35 µm and 0.40 µm thickness.

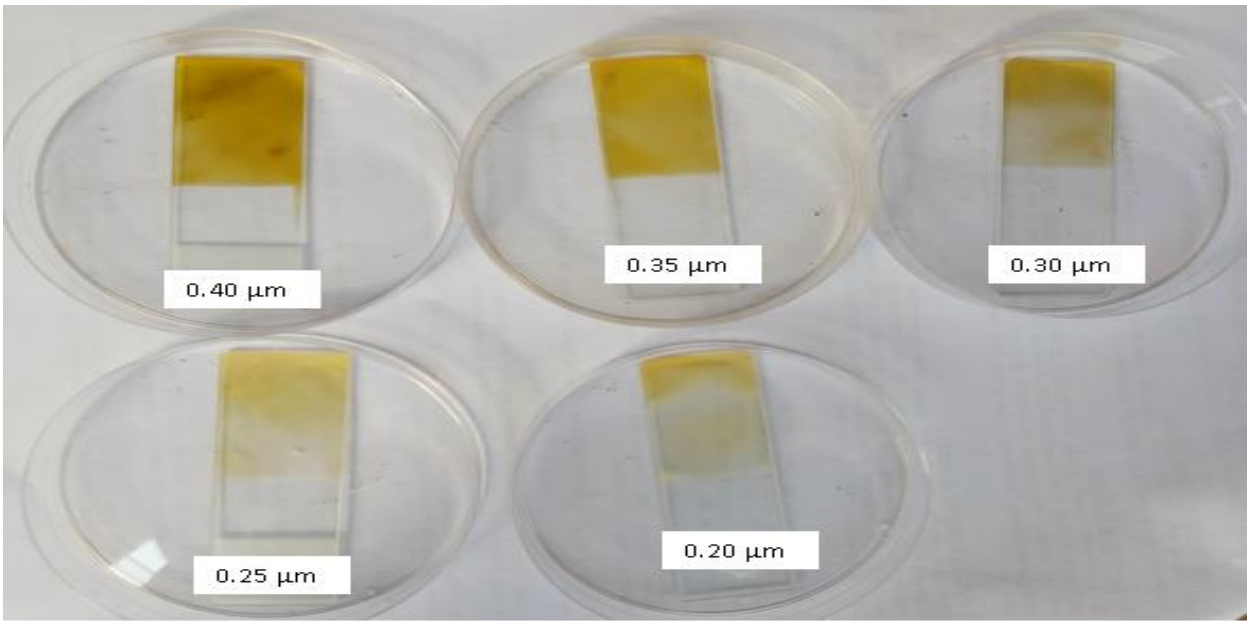

Plate I: As-deposited SnS thin films of 0.20 µm, 0.25 µm, 0.30 µm, 0.35 µm and 0.40 µm thickness.

3.2. Compositional analysis of as deposited SnS thin films (0.2 to 0.4 µm thickness)

Figure 1(a-e) shows the EDX spectrum of the as deposited SnS thin film at thickness of 0.2, 0.25, 0.30, 0.35 and 0.40 µm. It is evident from the figure that the film is made up of Sn and S elements. Other elements were also observed due to their presence in the soda lime glass substrate. These elements include Sodium (Na), Calcium (Ca), Silicon (Si) and Chlorine (CI) which correlates with the reports of Guneri *et al*. (2010). The elemental composition of the SnS films in terms of its atomic percent (%) is shown in Table 1 while the variation of Sn/S ratio with film thickness is shown in figure 2.

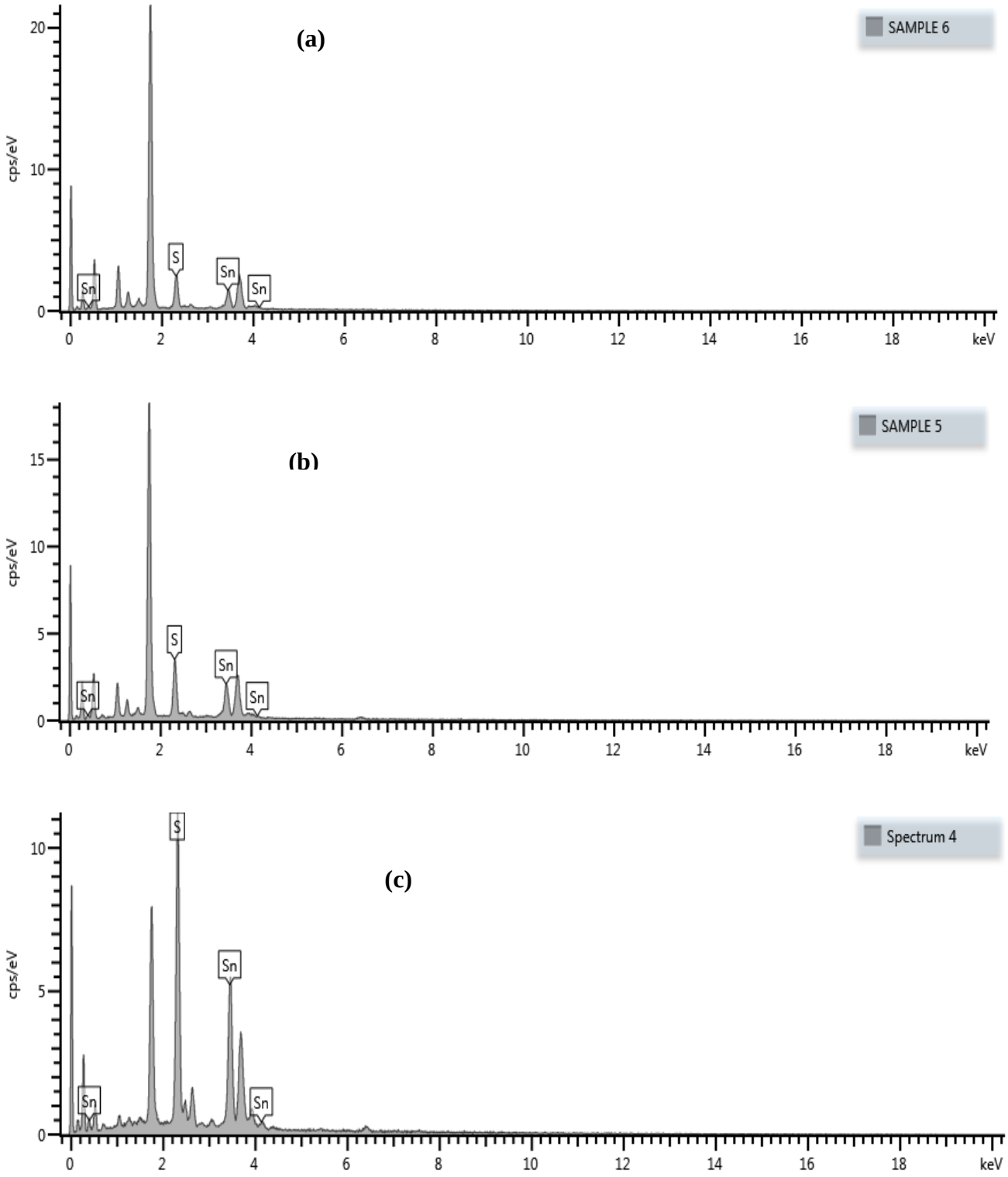
(a)
SAMPLE 6
cps/eV
keV
Sn
S
Sn
Sn
(b)
SAMPLE 5
cps/eV
keV
S
Sn
Sn
Sn
(c)
Spectrum 4
cps/eV
keV
S
Sn
Sn
Sn

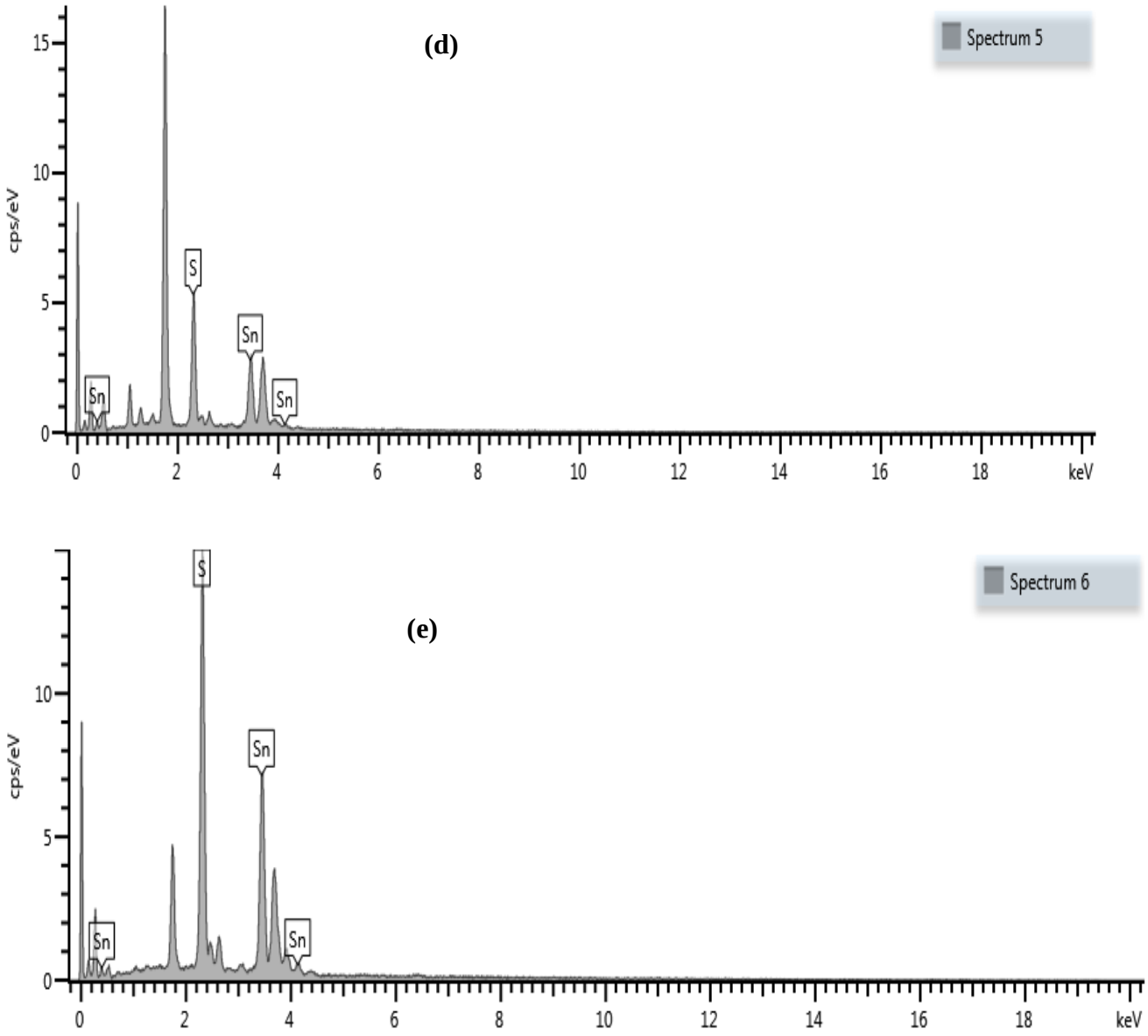

Figure 1(a-e): EDS spectrum of the SnS thin films of 0.20 µm, 0.25 µm, 0.30 µm, 0.35 µm and 0.40 µm thickness.

Table 1: As deposited SnS thin film composition in terms of atomic percent

Thickness (nm)	Sn (at.%)	S (at.%)	Sn/S at ratio	SnS (Total)
0.20	55.57	44.43	0.80	100
0.25	56.44	43.56	0.77	100

0.30	59.52	40.48	0.68	100
0.35	62.50	37.50	0.60	100
0.40	63.60	36.40	0.57	100

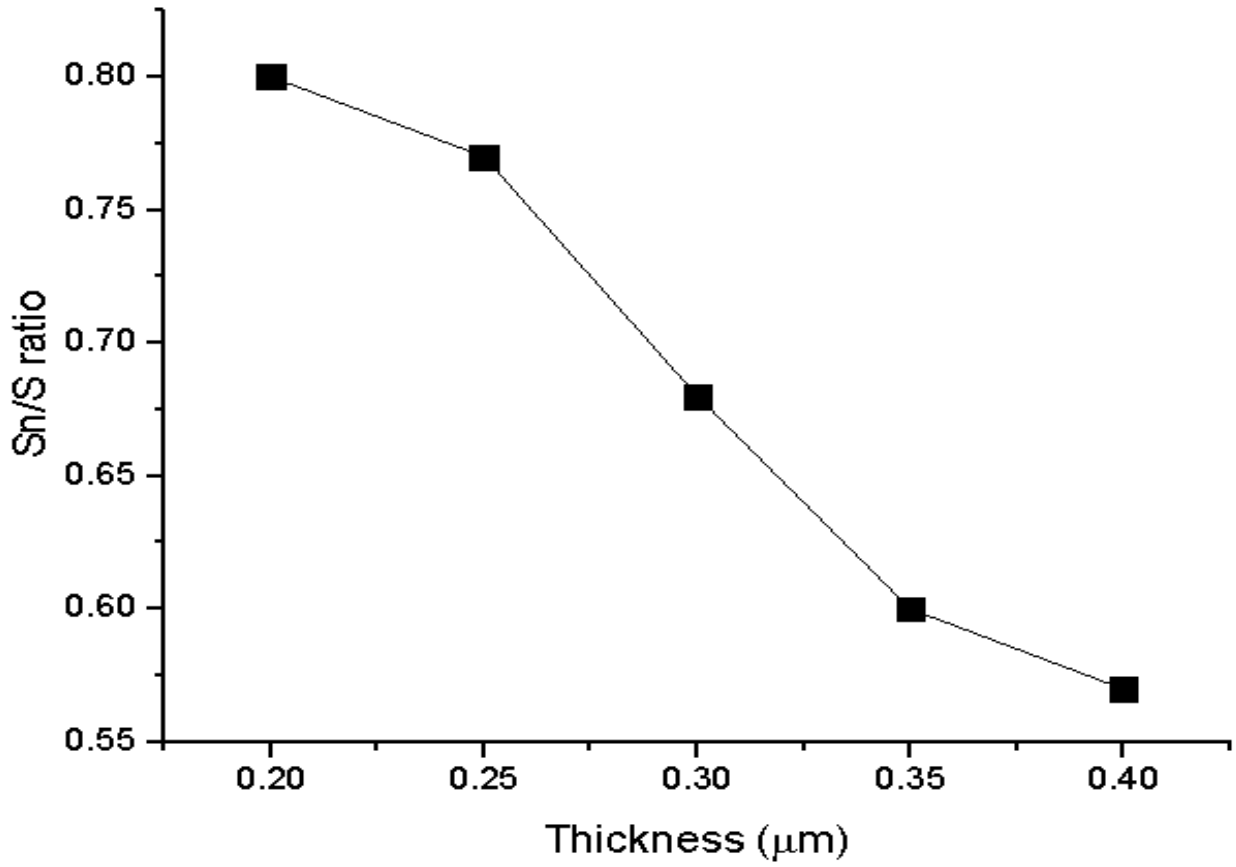

Figure 2: Sn/S atomic percent (at.%) ratio as a function of film thickness.

From table 1, the sulphur content was observed to increase with increase in film thickness. For a film of varying thickness deposited by chemical vapour deposition on a substrate, the substrate temperature is of interest in the formation and determination of the composition of the film as it enhances the kinetics of the film formation. A constant substrate temperature of 258 ℃ was used for the deposition of all the SnS thin film. Sn/S ratio was observed to slightly decrease with increase in SnS film thickness which correlates with the report of Reddy and Kumar (2016); Devika *et al*. (2007). The AACVD deposition method employed involves chemical reactions with precursors, mostly

reacting components undergoing reaction at the substrate surface or in the vicinity of the substrate. As a result the evaporated sulphur and tin atoms could reach the substrate surface with different velocities and energies due to their different vapour pressures. Since Sulphur tends to have a greater vapour pressure compared to tin, more of the sulphur atoms will arrive on the substrate than tin as observed in table 1. Some of the S atoms have the tendency of been scattered back on arrival at the substrate surface which could be attributed to adatom mobility, lower sticking coefficient or heat radiant effect between the substrate surface and the deposited SnS thin film hence resulting in lower sulphur content or a large deficiency at lower thickness as compared to higher thickness. The effect however tends to reduce at higher thickness as a result of reduction in scattering loss due to a decrease in heat gradient with the formation of clusters of SnS crystallites at higher SnS thin film thickness and agrees with the findings of Prathap *et al*. (2008).

3.3. Scanning electron microscopy (SEM)

The surface morphology of the as deposited SnS thin films of 0.2, 0.25, 0.30, 0.35 and 0.40 μm thickness as examined with SEM is shown in figure 3 (a-e). The average grain size of the SnS thin films were calculated using imageJ software (Rasband, 2014). Otsu's thresholding method and particle analysis (Julio *et al,* 2008) was used after which statistical analysis of the data was made with histogram generated to study the grain distribution and average grain size determine from the average particle size assuming round/spherical particles as confirmed by the analysis. The particle analyser was configured in a size range of 0 nm^2 to infinity in other to allow for coverage of smaller particles. No restriction was also made for particle circularity.

The SnS films of 0.2 to 0.40μm thickness exhibited two distinguishable microstructural features consisting of a portion of agglomerates and some defined spherical grains. The agglomerates increases for films of 0.2 to 0.30 μm thickness after which it decreases for films of 0.35 to 0.40 μm thickness leading to a more defined grain structure and growth for the films of 0.40 μm thickness. The SnS films of 0.2 to 0.30 μm thickness exhibited a non-uniformly distributed grain sizes. No observable crack or hole in the deposited SnS thin films as they were randomly positioned on the surface of the SnS films. As the thickness increases, the deposited SnS thin film tends to have a porous and uneven grain growth leading to an uneven film surface and poor surface morphology of the deposited films. With increase in SnS film thickness to 0.35 and 0.40 μm, the films contain more

uniform and tightly bonded grains with the most improved grain and crystal structure been at the thickness of 0.40 μm.

Furthermore with increase in film thickness, the deeper layers of film atoms are subjected to stronger interatomic forces leading to the formation of a compact structure, while for a thinner film the atoms near the surface are subjected to weaker interatomic force to form a loosely packed grain structure. This consistent with the reports of Jain *et al*. (2007) and Jain *et al*. (2013).

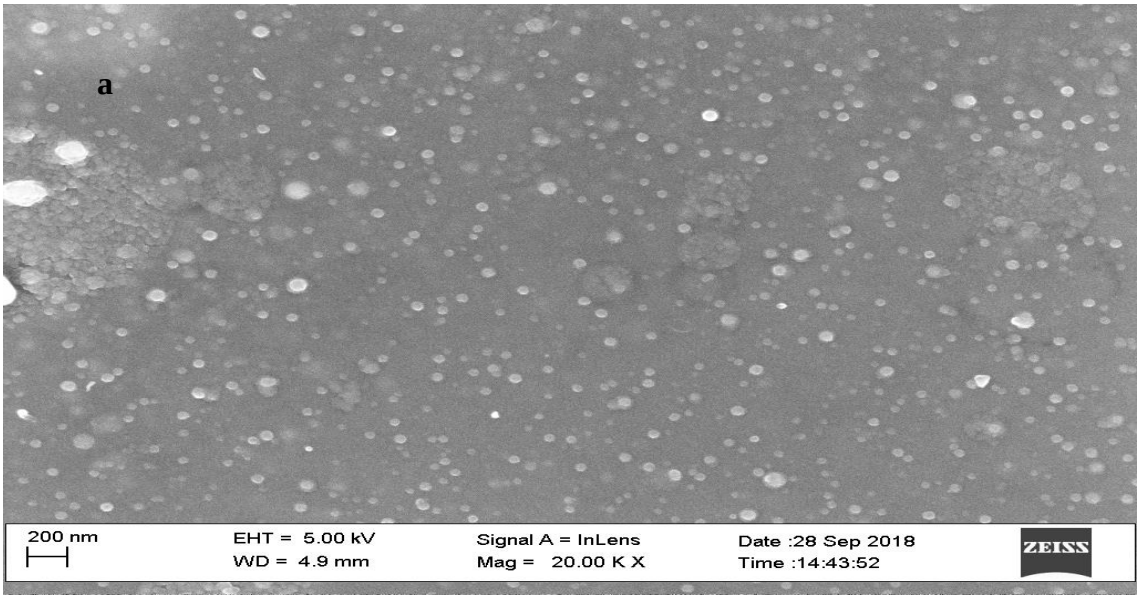

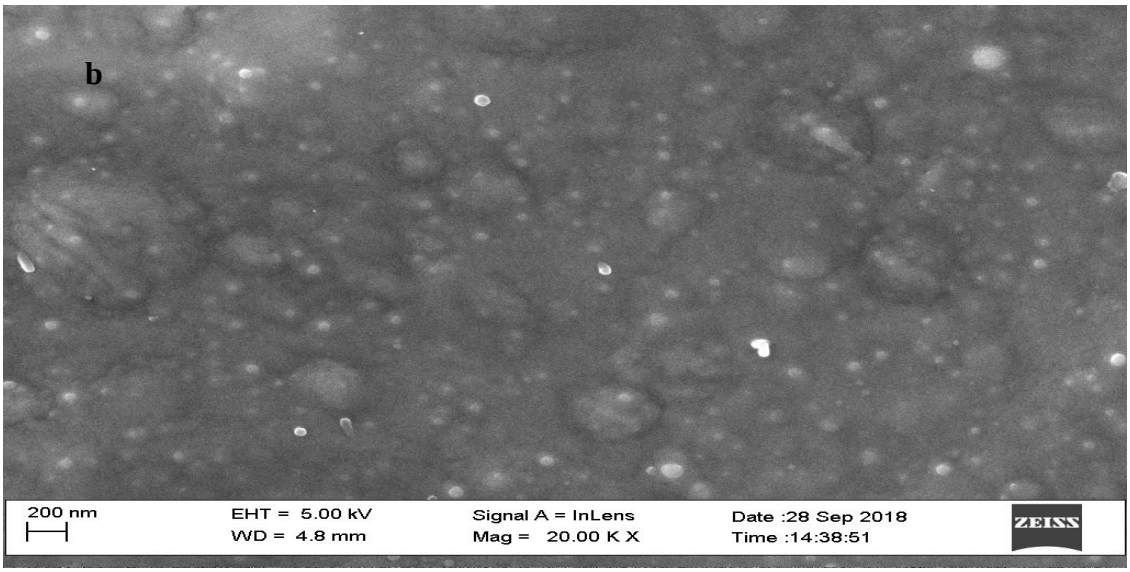

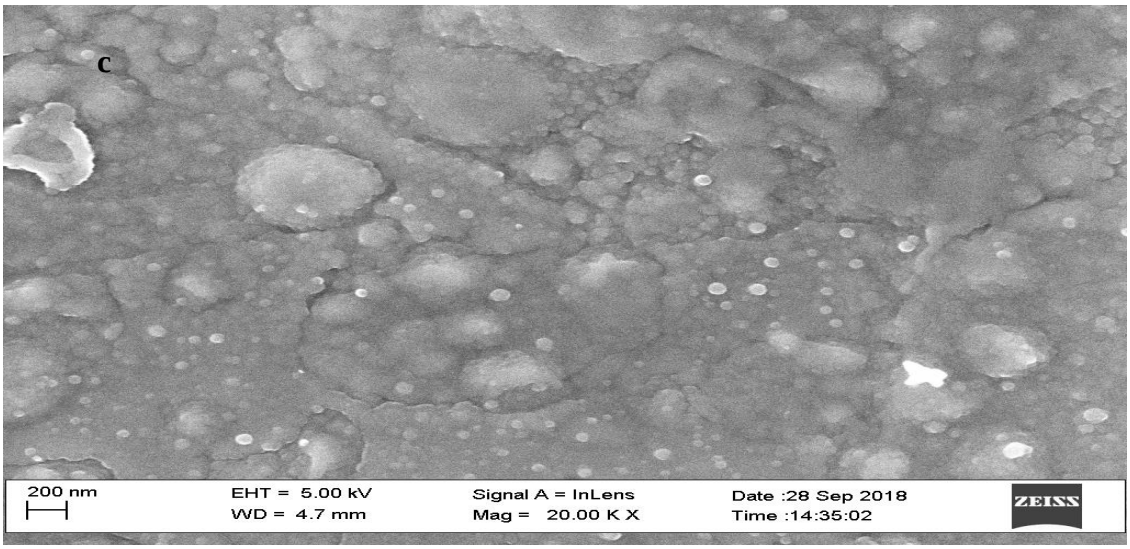
c
200 nm
EHT = 5.00 kV
WD = 4.7 mm
Signal A = InLens
Mag = 20.00 K X
Date :28 Sep 2018
Time :14:35:02
ZEISS

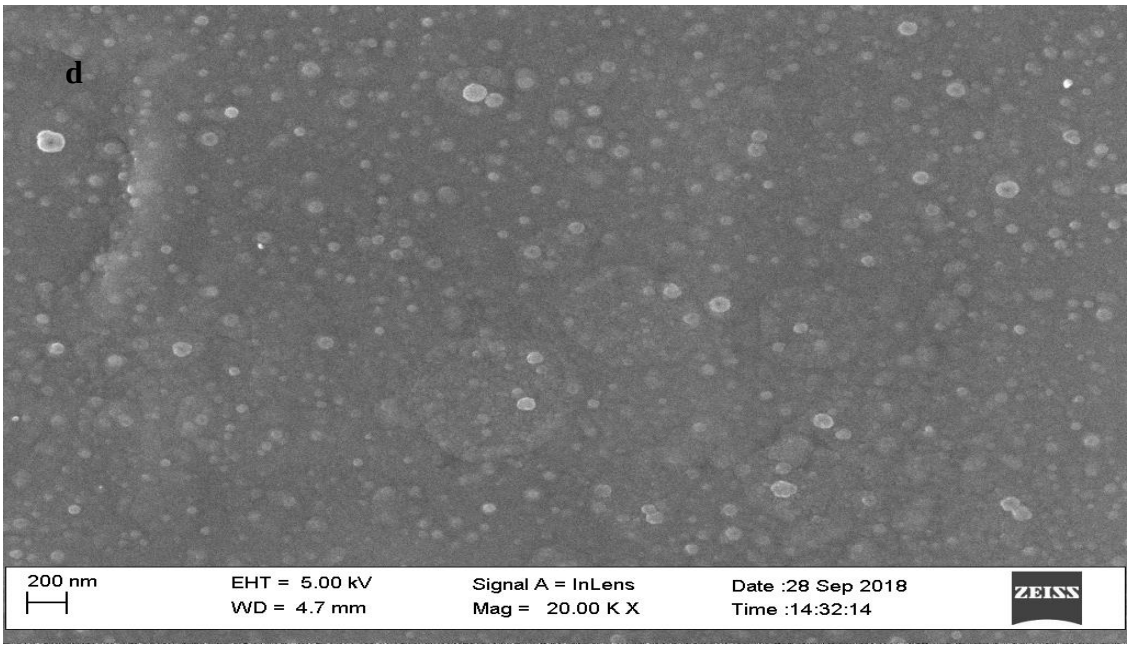
d
200 nm
EHT = 5.00 kV
WD = 4.7 mm
Signal A = InLens
Mag = 20.00 K X
Date :28 Sep 2018
Time :14:32:14
ZEISS

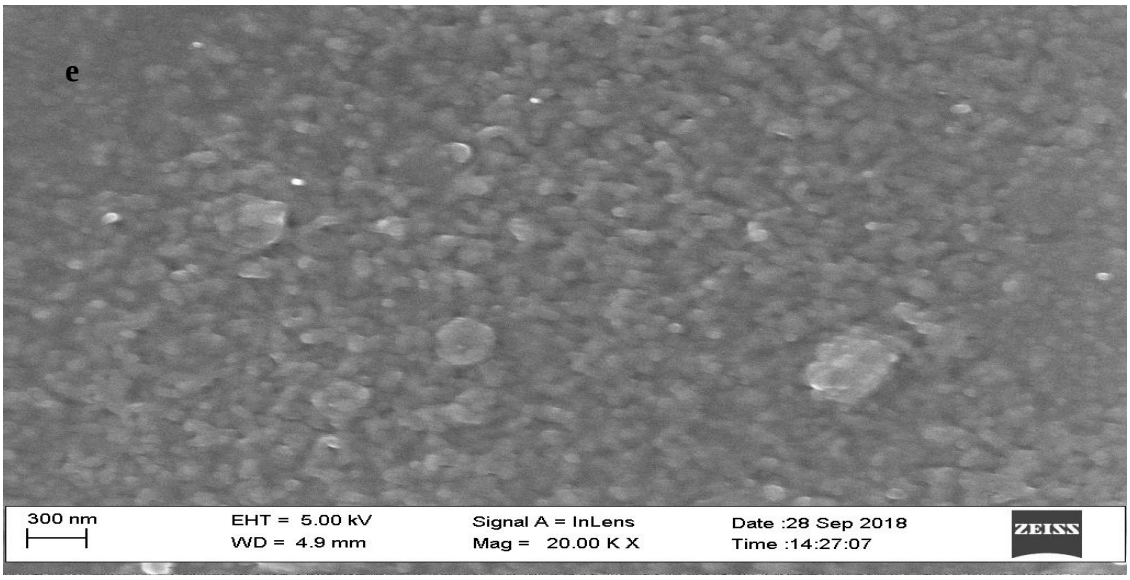

Figure 3 (a-e): The surface morphology of the as deposited SnS thin films of 0.2, 0.25, 0.30, 0.35 and 0.40 μm thickness.

The grain size distribution histogram plot for SnS samples of 0.2, 0.25, 0.30, 0.35 and 0.40 μm thickness is shown in figure 4, while the composite average grain size plot for 0.2, 0.25, 0.30, 0.35 and 0.40 μm thickness is shown in figure 5.

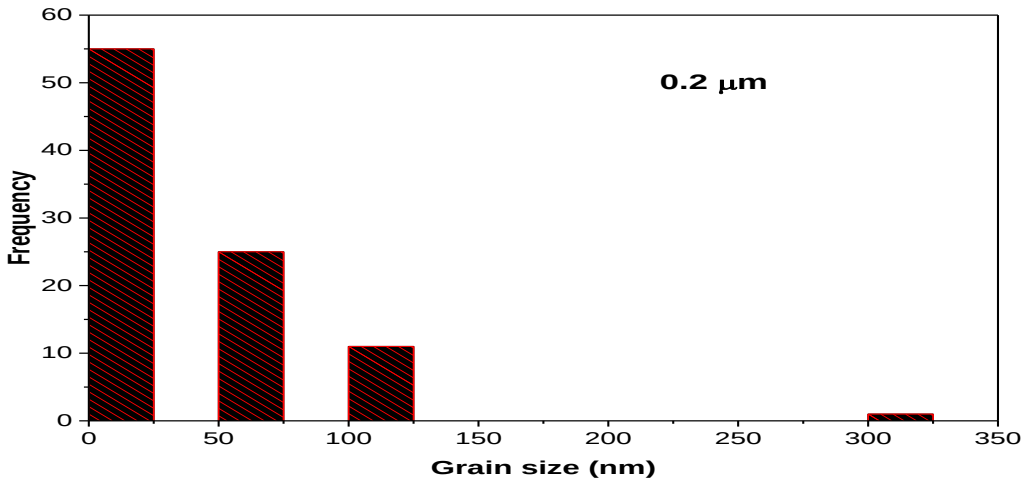

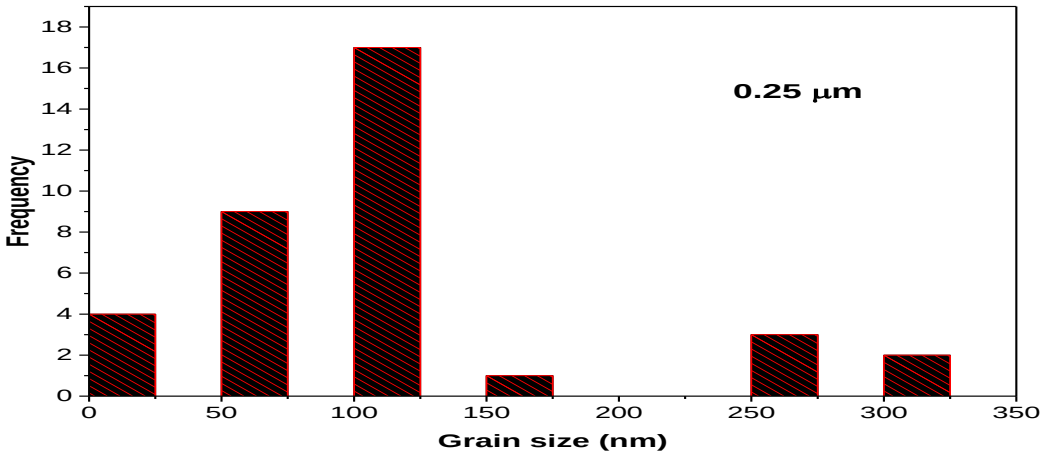
0.25 μm
Frequency
Grain size (nm)
0
2
4
6
8
10
12
14
16
18
0
50
100
150
200
250
300
350

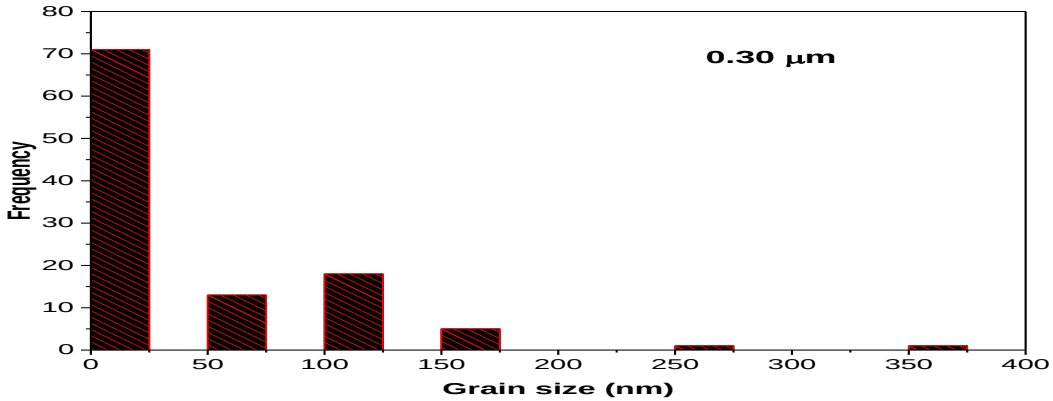
0.30 μm
Frequency
Grain size (nm)
0
10
20
30
40
50
60
70
80
0
50
100
150
200
250
300
350
400

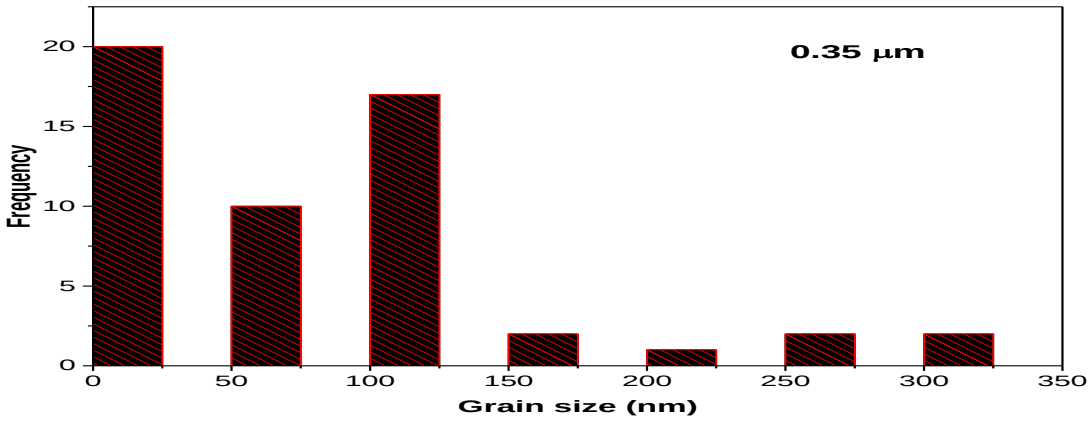
0.35 μm
Frequency
Grain size (nm)
0
5
10
15
20
0
50
100
150
200
250
300
350

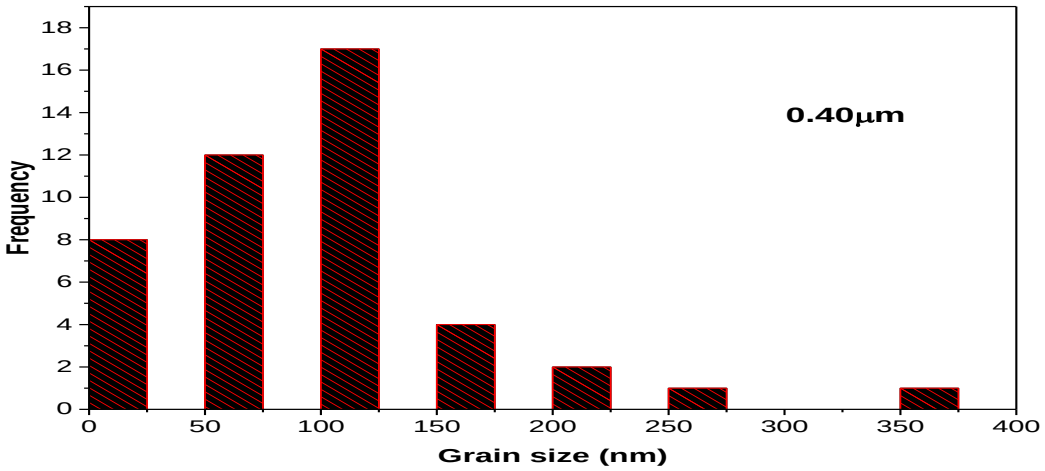

Figure 4: Grain size histogram plot for SnS samples of 0.20, 0.25, 0.30, 0.35 and 0.40µm.

From figure 4, the histogram shows a non-uniform grain concentration and distribution at grain size range of 0.0 to 100 nm for all the as-deposited SnS thin films. The grain size distribution at 0.0 to 100 nm is larger than that of 100 to 400 nm range. There tend to be a preferred grain distribution and growth defining factor or pattern at 100 nm for all the films which could be related to the preferred crystal growth orientation earlier defined by the XRD results. The preferred grain distribution increases with increase in film thickness, with the most prominent distribution at the film of 0.4 µm thickness. The increase in grain distribution from 0 to 100 nm range is followed by a decrease from 100 to 400 nm for the 0.4 µm thickness which could be attributed to initialisation of grain stability and uniformity at the range of 250 to 400 nm. The absence of grain at 300 nm within the range of 250 to 400 nm of the 0.4 µm thickness could be attributed to grain boundary effect of crystal system defects. The as-deposited 0.4 µm thickness shows a more uniform grain distribution and growth which could signify an optimum for the as deposited films.

Figure 5 reveals that the average grain size which is as labelled on each column increases with increase in film thickness. The increase in thickness necessitated the growth of smaller grains into larger grains which could be attributed to the coalescence of small grains into bigger grains with an evident improvement in the film grain size which are more densely packed.

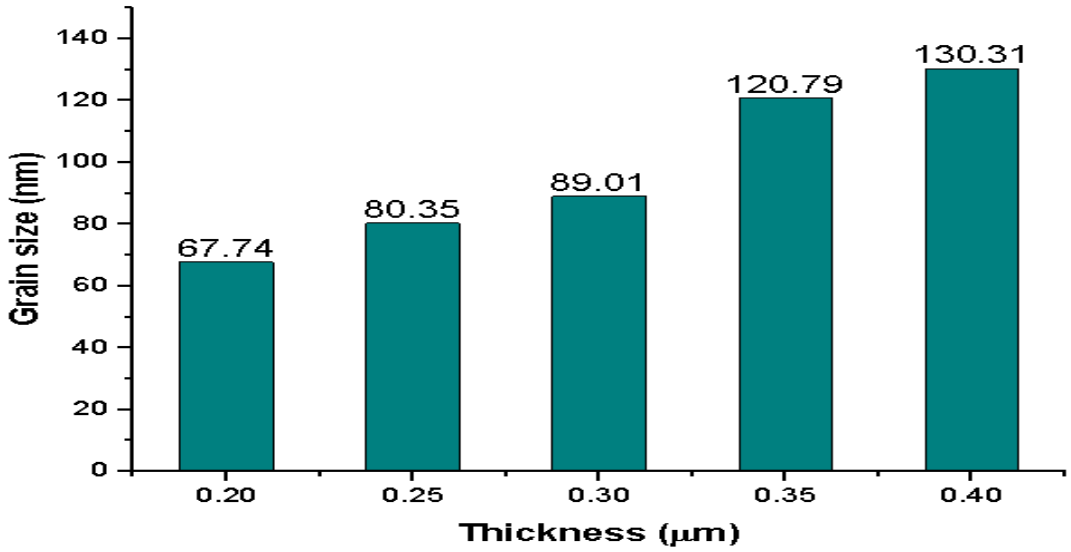

Figure 5: Composite average grain size plot for 0.20, 0.25, 0.30, 0.35 and 0.40µm SnS thin film thickness.

3.4. Hall effect measurement of 0.20, 0.25, 0.30, 0.35 and 0.40 µm SnS film thickness

The electrical properties of the as deposited SnS thin film as a function of film thickness is shown in Table 2. The electrical properties were determined by the Vander Pauw method and are summarised in the table 2.

Table 2: Electrical parameters of SnS thin films of 0.20, 0.25, 0.30, 0.35 and 0.40 µm SnS film thickness

Thickness (μm)	**Bulk concentration N_b (cm^{-3})**	**Average Hall coefficient R_H (cm^3/c)**	**Carrier mobility µ (cm^2/Vs)**	**Resistivity ρ (Ωcm)**	**Conductivity σ $(\Omega cm)^{-1}$**
0.20	2.572×10^9	2.224×10^9	5.257×10^2	4.230×10^6	2.364×10^{-7}
0.25	2.807×10^9	2.427×10^9	9.132×10^2	2.658×10^6	3.762×10^{-7}
0.30	2.990×10^9	2.642×10^9	1.714×10^3	6.081×10^5	1.645×10^{-6}
0.35	1.438×10^{10}	4.342×10^9	2.063×10^3	4.085×10^5	2.448×10^{-6}

0.40	2.238×10^{10}	6.928×10^{9}	4.337×10^{3}	3.612×10^{5}	2.768×10^{-6}

From the table, the average hall coefficient of all the as deposited samples were positive which indicates that all the films exhibits p-type carrier conductivity. Similar SnS thin film conductivity type has been reported for SnS thin films by Reddy and Kumar (2016); Gao and Shen (2012) among others. The variation of electrical resistivity of deposited SnS thin films has been reported by several researchers to depend on lattice defects (e.g interstitials, vacancies and presence of binary phases of films), residual stress and grain size. From the EDS studies no binary phases of SnS film was noticed but the grain size of the deposited films increases with increase of thickness. Hence the variation in the electrical conductivity with thickness could be attributed largely to the grain size of the films. The high resistivity for thin films of 0.20 and 0.25 μm thickness could be attributed to the presence of higher number of lattice defects, poor crystallinity and presence of inter crystalline regions which affects the growth of grains to a sufficiently large size. A further increase in film thickness from 0.30μm to 0.40μm causes the film crystallinity to improve gradually leading to a more uniform structure with grains which are comparably larger. The larger grains reduces the number of grain boundaries and charge trap density hence allowing the carriers to move freely in the lattice leading to a reduction in resistivity and increase in conductivity of the films. For thinner films, presence of defects acts as scattering centres which could enhance the formation of trap states capable of trapping carriers and number of free carriers available for conduction. The carrier traps could become electrically charged after trapping mobile carriers by creating a potential energy barrier which impedes the motion of charge carriers from one crystallite to another hence reducing carrier mobility and number of free carriers available for electrical conduction (Jain *et* al., 2007; Moreh *et al., 2014*).

Hall measurement further revealed that the SnS films have hole concentrations in the range of 2.807×10^{12} to $1.438 \times 10^{13} cm^{-3}$ and hole mobility in the range of 1.663×10^{3} to $9.132 \times 10^{3} cm^{2} v^{-1} s^{-1}$. The low carrier concentrations could be attributed to slight deviations from stoichiometry leading to native point defects such as Sn^{+2} vacancies which is a basic define factor for the p-type conductivity of the SnS thin films.

4.0. Conclusion

The SnS thin film semiconductor of varying thickness were deposited using Aerosol assisted chemical vapour deposition (AACV). The SnS thin film was found to be polycrystalline consisting of Sn and S elements in varying composition. No noticeable change was noticed in the crystal structure of the film. The presence of large grain size reduces the number of grain boundaries and charge trap density hence allowing the carriers to move freely in the lattice leading to a reduction in resistivity and increase in conductivity of the film. The high carrier concentration of $1.438 \times 10^{13} cm^{-3}$ and low resistivity of $3.612 \times 10^{5}\ \Omega$cm indicates the possibility of usage or application of SnS thin film as a semiconductor channel in an electric double layer field effect transistor.

Acknowledgements

This research did not receive any specific grant from funding agencies in the public, commercial, or not-for-profit sectors. However, the authors acknowledged the Staff and management of Alex Ekwueme Federal University Ndufu Alike Ikwo, Ebonyi state, Federal University of Technology Minna, Sheda Science and Technology (SHESTCO), Namiroch research laboratory Abuja, iThemba Laboratory South Afica and the electron microscopy unit of the University of Western Cape, South Africa where the laboratory preparation of the film/ device and characterisations were carried out.

REFERENCES

Devika, M., Koteeswara, N.R., Ramesh, K., Gunasekhar, K.R., Gopal, E.S.R., & Ramakrishna, R.K.T. (2006). Influence of annealing on the physical properties of evaporated SnS films. Semiconductor science and technology, 21, 1125-1131.

Du, H., Lin, Xi., Xu, Z., & Chu, D. (2015). Electric double layer field effect transistors: a review of recent progress. Review springer.doi:10.1007/s10853-015-9121-y

Gao, C., & Shen, H. (2012). Influence of the deposition parameters on the properties of orthorhombic SnS films by chemical bath deposition. *Thin solid films*, 2012, 520, 3523-3527.

Guneri, E., Gode, F., Ulutas, C., Kirmizigul, F., Altindemir, G., & Gumus, C. (2010). Properties of P-type SnS thin films prepared by chemical bath deposition. *Chalcogenides letters*, 7(12), 685-694.

Hedge, S.S., Kunjomana, A.G., Chandrasekharam, K.A., Ramesh, K., & Prashantha, M. (2011). Optical and electrical properties of SnS semiconductor crystals grown by physical vapour deposition technique. Physica B 406 (2011) 1143-1148. doi.10.1016/j.physb.2010.12.068

Jain, A., Sagar, P., & Mehra, R.M. (2007). Changes of structural, optical and electrical properties of sol-gel derived ZnO films with their thickness. *Materials science-poland,* 25 (1) 2007, 233-241.

Jain, P., & Arun., P. (2013). Parameters influencing the optical properties of SnS thin films. *Journal of semiconductors,* 34 (9), 1-6.

Julio, G., Merindano, M.D., Canals, M., & Rallo, M. (2008). Image processing techniques to quantify micro projections on outer corneal epithelial cells. Journal of anatomy, 212, 879-886. doi:10.1111/j.1469-7580.2008.00898.X

Moreh, A.U., Momoh, M., Yahaya, H.N., Hamza, B., Saidu, I.G., & Abdullahi, S. (2014). Effect of thickness on structural and electrical properties of $CuAlS_2$ thin films grown by two stage vacuum thermal evaporation technique. *International journal of mathematical, computational, physical and computer engineering,* 8(7), 1084-1088.

Prathap, P., Revathi, N., Subbaiah, S., & Reddy, K.T.R. (2008). Thickess effect on the microstructure, morphology and optoelectronic properties of ZnS films, Journal of Physics: condense matter, 20, 035205-035215.

Rasband, W.S. (2014). ImageJ, National institute of health, Bethesda, Maryland, USA, http://imagej.nih.gov/ij/1997-2014

Reddy, T.S., & Kumar, M.C. (2016). Co-evaporated SnS thin films for visible light photo detector applications. *Royal society of chemistry*, 2016, 6, 95680-95692. doi: 10.1039/c6ra20129f.

Soonmin, H., Kassim, A., & Weetee, T. (2013). Thickness dependent characteristics of chemically deposited Tin sulphide films. *Universal journal of chemistry,* 1(4), 170-174.

Thiruramanathan, P., Hikku, G.S., Krishna-Sharman, R., & Siva Shakthi, M. (2015). Preparation and characterisation of indium doped SnS thin films for solar cell applications. *International journal of technochem research*, 1(1), 59-65.

Yuan, H., Liu, H., & Shimotani, H. (2011). Liquid gated ambipolar transport in ultrathin films of a topological insulator Bi_2Te_3. *Nano letters,* 11, 2601-2605.

The Role of Solar Thermal Energy in Resolving the Energy Crisis towards National Development

By
I.K. Magaji, B. Usman & I.G Usman

Zamfara State College of Education, Maru.
magajiibrahim2014@gmail.com

Abstract

Renewable energy is regarded as an alternative energy source of that can replace the fossil fuels and provide a clean energy to the environment thereby resolving the national energy crisis. Solar thermal technology is one of the promising technologies that can be used for harnessing solar energy to generate thermal energy or electrical energy. This technology could produce a wide range of thermal energy from low, medium to high temperature depending on its solar thermal collector design. For production of low and medium temperature, flat plate collectors are usually used. However, for much higher temperature, mirrors or lenses are usually adopted where they are able to concentrate sunlight. This is known as concentrated solar thermal (CST) technology. This paper focuses on the role of different aspects of solar thermal energy in producing energy and point out how they can be used in resolving energy crisis in Nigeria.

1.1 INTRODUCTION

Due to the increase in electricity demand, issue in global warming and greenhouse effect as well as depletion in source of fossil fuels has forced the scientist around the world to look for alternative clean sources of energy (Thomas et al., 1993). Solar energy is one of the potential renewable sources of energy especially to the country that receive high solar radiation such as in Nigeria. The implementation of solar thermal technology can be used to replace fossil fuel electricity generation in Nigeria. However, the implementation of this type technologies were not given much attention in Nigeria (Ijeoma Vincent-Akpu, 2012). According to World Energy Council, in 2015 the world energy consumption shows an increased growth in renewable energy consumption. Similarly, most of the energy consumption is still coming from fossil fuels (oil, coal, and gas) as shown in Figure 1. Although the usage of renewable sources is still low, but depletion of non-renewable sources encourages the world to shift the energy policy towards renewable energy sources.

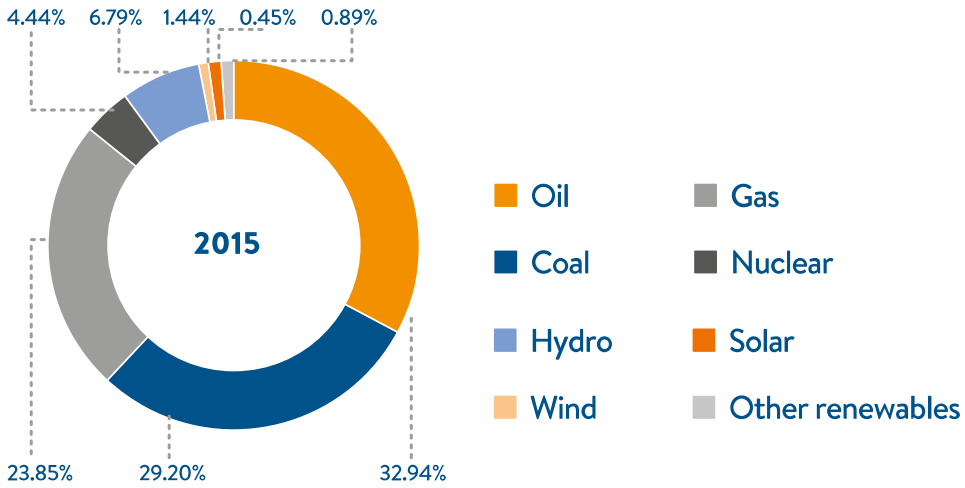

Figure 4: Energy Consumption in 2015 (World Energy Council, 2016)

1.2 SOLAR ENERGY CONVERSION

The conversion of solar energy radiation can be roughly divided into two categories: the heat/electric systems and radiation into electricity generation; the photovoltaic.

1.2.1 The Heat/Electric or Concentrated Solar Energy Conversion.

Concentrated solar thermal energy involves the collection and conversion of solar energy from the sun at a certain wavelength in the solar spectral region into heat. The application of concentrated solar thermal collectors are generally classified into two different groups: The first subgroup is a CSP electricity generation system at a high temperatures (500 - 1000 ^{0}C), which is regarded as the most attractive fields in solar thermal technology for the generation of electricity while the second subgroup is the medium temperatures (100 ^{0}C – 250 ^{0}C), which considered to be industrial process heat applications such as water heating, space heating, cooking, refrigeration, cooling and drying etc.

1.3 THE CONCENTRATED SOLAR POWER (CSP) SYSTEM

The CSP technology based on heat to electricity conversion is a highly desirable renewable alternative. The CSP systems used for this purpose are; , parabolic dish, power tower, linear Fresnel reflector and parabolic trough solar concentrators (Lertsatitthanakorn et al., 2014). One of the most prevalent applications of the concentrated solar thermal energy is the hot water production, which requires temperature below 100 ^{0}C for these applications (Ibrahim et al, 2011).

Many countries currently implemented the water solar heating systems and some promoting this type of technology. Among this country, Israel with more than 90 % of the solar thermal systems retrofitted into existing buildings. Nevertheless, Spain current legislation included in the building code requires that all new domestic hot water installations and covered swimming-pool heating should have a solar system to supply a certain amount of the energy demanded. Similarly, Portugal, introduces the requirement of solar thermal installations into their new Portuguese building code (Fernandez-Garcı´a, 2011). In Nigeria, lack of public awareness and understanding of the potential benefits of solar water heating system, high cost of the original WHS, inappropriate roofing structures are some of the factors affecting the installation of WHS in Nigeria.

There are two types of solar thermal collectors: Concentrating and non-concentrating/stationary collectors (Kalagirou, 2014). Concentrating solar collectors are the solar tracking collectors and are the type of solar thermal collectors that has the surface area larger than the receiver's or absorbing area, the parabolic reflecting surfaces of this type of concentrators intercept and focus the sun's beam radiation in a smaller receiving area, while non-concentrating collectors refers to the solar thermal collectors that has intercepting area the same as that of the absorbing solar radiation.

Table 1: Concentrated Solar Thermal Collectors

Tracking system	Type of Collector	Type of Receiver
Stationary Collectors	Evacuated tube collector (ETC)	Flat
	Flat plate collector (FPC)	Flat
	Compound parabola collector (CPC)	Tabular

Single-axis tracking	Parabolic trough collector (PTC)	Tabular
	Linear Fresnel reflector (LFR)	Tabular
	Cylindrical trough collector (CTC)	Tabular
Two-axes tracking parabolic	Heliostat field collector (HFC)	Point
	Dish reflector (PDR)	Point

1.3.1 Advantages and Dis advantages of Concentrated Solar Collectors

The concentrated solar thermal technology has many advantages and some disadvantages compared to other types of solar energy system. The following are some of the advantages of the concentrated solar power (CSP) systems:

- It works noiselessly with less thermal losses
- It works with higher temperature at a higher thermal efficiency with small surface collector for a given power requirement.
- It has no risk of reaching dangerous stagnation temperatures.
- It has high performance and is considered to be a reliable system;
- It is a clean technology, which does not produce any toxic waste or radioactive material;
- It is a low maintenance system.

Some of the disadvantages are:

- It needs innovative absorber design due to its non-uniform cooling;
- Its maintenance and installation cost increases due its solar-tracking system.
- It is expensive and has high installation cost.
- It is not compatible with the present roofing system.
- It needs a larger space for separate systems (water heating and electricity generation).

Conclusively, this type of system utilizes only direct beam solar radiation, therefore it is geographically limited at very high humidity and wind speed operation.

1.4 CLASSIFICATION OF CONCENTRATED SOLAR POWER (CSP).

The classification of the concentrated solar power are as follows:

1.4.1 The Parabolic Trough Solar Collectors (PTSC)

PTC's represents the most matured, inexpensive as well as the most efficient source of electricity and steam generation. It consists of parabolic reflecting surface with a support structure and receiving tube (Thomas and Guven, 1993). In most applications, the PTC reflector is a single axis linear parabola, designed to concentrate reflected solar radiation onto the receiver tube located along its focal plane.

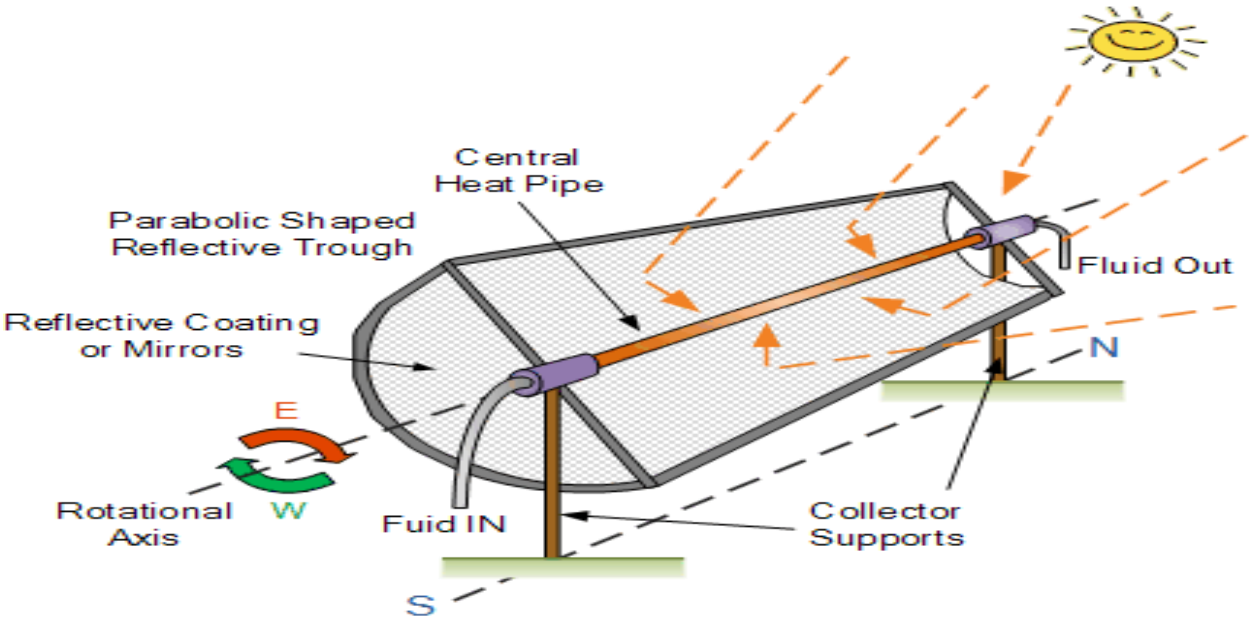

Figure 2. Schematic representation of parabolic trough solar concentrator.

1.4.2. The Parabolic Dish Concentrator

A parabolic dish reflector is usually regarded as a point-focus concentrator that tracks the solar radiation in two axes, concentrating solar energy onto a receiver located at the focal point of the dish. The dish structure must track fully the sun to reflect the beam into the thermal receiver. The receiver absorbs the radiant solar energy, converting it into thermal energy in a circulating fluid. The thermal energy can then either be converted into electricity or it can be transported to the pipes to central

power conversion system. The dish focus collectors are successfully used for low temperature applications in manycountries throughout world (Mohammed et al., 2012). Parabolic dish can be able reach a temperature of up to 1500ºC (Mohit Bhargva, 2012).

Figure 3. Parabolic Dish Concentrator (Mohit Bhargva, 2012)

1.4.3 The power Tower System.

A power tower is a large tower surrounded by tracking mirrors called heliostats. These mirrors align themselves and focus sunlight on the receiver at the top of tower, collected heat is transferred to a power station. The average solar flux impinging on the receiver has values between 200 and 1000 kW/m2. This high flux allows working at relatively high temperatures of more than 1500ºC (Mohit Bhargva, 2012).

1.4.4 The Linear Fresnel System

Linear Fresnel is regarded as a collector with an array of linear mirror strips which concentrate light on to a fixed receiver mounted on a linear tower. The field of the linear Fresnel can be made-up like broken-up parabolic trough reflector, but not have in a parabolic shape, large absorbers can be constructed and the absorber does not have to move.

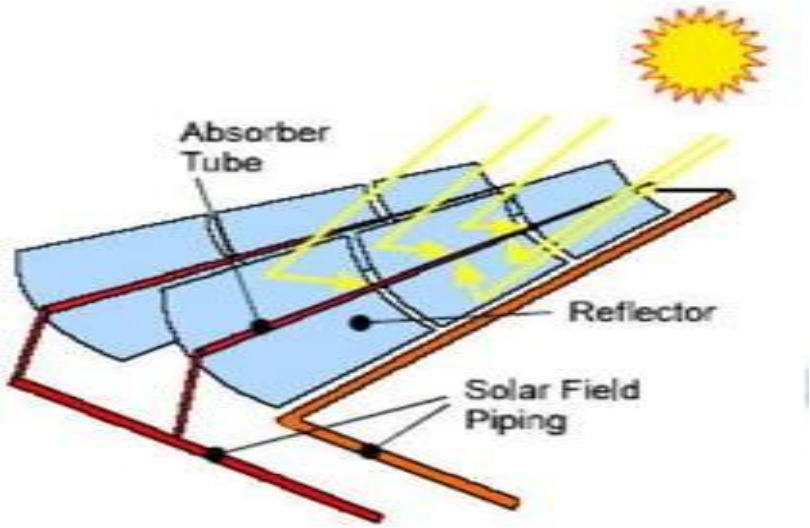

Figure 5. Linear Fresnel Reflector (Falah Abd Alhasan Mutlak, 2012).

1.5 THE PHOTOVOLTAIC ENERGY CONVERSION

Solar energy can also be used to meet our electricity requirements. Through Solar Photovoltaic (SPV) cells, solar radiation gets converted into DC electricity directly. This electricity can either be used as it is or can be stored in the battery. This stored electrical energy then can be used at night. SPV can be used for a number of applications such as: domestic lighting , electricity generation, street lightening, hot water generation etc.

1.6 THE ROLE OF SOLAR THERMAL ENERGY TOWARDS RESOLVING ENERGY CRISIS AND NATIONAL DEVELOPMENT.

Solar thermal energy can play a significant role in resolving energy crisis and national development in Nigeria if properly implemented. The following are some of the roles of solar thermal energy:

1. Nigeria is located at the equatorial region with a higher solar energy potential that would enable the country to build large scale solar thermal power. Solar energy can be regarded as the best choice for future energy power generation, this is due it's low maintenance cost, independent of fuels source, environmental friendly, and its contributions to lower carbon emissions. Solar thermal power method of generating electricity is considered as the matured in term of electricity. Therefore, if the establishment/installation of solar thermal power technology is given priority by the Nigerian government. It can play a major role in resolving the energy conflict and at the same time supplementing/replacing the dependence on the thermal gas method of generating electricity in Nigeria that courses high emission of CO2 to the environment. However,
2. A significant amount of megawatts (MW) of energy can be generated through solar thermal and photovoltaic energy conversion for domestic and industrial applications such as, cooking, refrigeration, cooling, drying, hot-water generation, and above all electricity generation in Nigeria.
3. Most of the developed solar concentrators for research purpose in Nigeria were carried out by individuals or groups with or without support from their various institutions and research centers. Government intervention of full support in funding relevant researches in this area is yet to be fully felt (Abdulrahim Abdulbaqi Toyin., 2014). If the Nigerian Government can give proper attention on solar thermal energy. It can definitely bust a competitive research, development, commercialization and installation of solar thermal energy in Nigeria.

1.7 Conclusion

From the forgoing, it was found that different aspects of solar thermal technology have been reportedly designed, developed, evaluated/experimentally analyzed for research purpose, domestic and industrial applications or generation of electricity. Some aspects of the solar thermal systems are now even in operation. However, the performance of those reported concentrators were mostly implemented under normal environmental weather where there is uninterrupted degree of solar irradiation like some parts of Nigera. Therefore, the establishment/implementation of this type of technology in Nigeria has no doubt will definitely play a significant role in resolving the energy crisis and contribute positively to the national development.

1.8 References.

Abdulrahim Abdulbaqi Toyin, 2014. "Solar Concentrators's Developments in Nigeria: Prospect and Challenges". Journal of Emerging Trends in Engineering and Applied Sciences (JETEAS) Vol. 5. No. 7. PP. 73-77.

Fernandez, A.G., Zarza, E., Valenzuela, L., & M., Perez. 2010. "Parabolic trough solar Collectors and their applications". Renewable and sustainable energy. Vol. 14. March. PP. 1695-1721.

Ijeoma Vincent-Akpu, 2012. Renewable energy potentials in Nigeria. Energy Future: The Role of Impact Assessment, 32nd Annual Meeting of the International Association for Impact Assessment. 27 May- 1 June 2012, Centro de Congresso da Alfândega, Porto – Portugal.

Kalogirou, S. A., 2014. "Solar thermal collectors and their applications". Progress in Energy a and Combustion science. Vol. 30. February. PP. 231-295.

Lertsatitthanakorn, C., Jamradloedluk, J., & M., Rungsiyopas. 2014. "Electricity generated from a parabolic solar concentrator coupled to a thermo-electric module". Energy procedia Vol. 52. PP. 150-158.

Mohit Bhargva, 2012. "Modeling, Analysis, Evaluation, Selection and Experimental Investigation of Parabolic trough Solar Collector System": (Master Thesis). Thapar University, Patiala – 147004.

Thomas, A., 1996. "Solar steam generation systems using parabolic trough concentrators". Energy Convers. Vol.37. No.2. March. pp. 215-245.

Thomas, A., & H.M., Guven. 1993. "Parabolic trough concentrators Design, construction and evaluation". Energy covers. Mgmt. Vol. 34. No. 5. August. pp. 401-416.

Analysis of Rain Attenuation for Earth-Space Communication Links at Ku and Ka-Bands

K. C. Igwe* and J. A. Joshua

Department of Physics, Federal University of Technology, Minna, Nigeria

*Corresponding author

Abstract

Rain rate and rain attenuation predictions are very vital considerations when designing microwave satellite communication systems. In this research work, rainfall data bank of 33 years (1983-2015) was obtained from the Nigerian Meteorological Agency (NIMET) for Gombe and Akwa-Ibom States which was used for the prediction of rain rate and rain attenuation. Chebil rain rate model was used to predict the point rainfall rate, while ITU-R P. 618-9 model was used for the prediction of the rain attenuation for the two locations. The rain attenuation values computed were at horizontal polarization and for links to Nigerian Communication Satellite-1 Replacement (NIGCOMSAT-1R). The results obtained from this work will be good as preliminary design tools for earth-space communication links and will also provide a broad idea of rain attenuation for microwave engineers.

Keywords: Earth-space link, Ka-band, Ku-band, Rain attenuation, Rainfall rate.

1. Introduction

Signal energy degradation that occurs as a result of absorption, scattering and refraction of microwave energy by rain drops is a major challenge to satellite transmission operating at a frequency of 10 GHz and above. Attenuation caused by rain may be measured directly from beacon experimental setups and it can as well be predicted from rain-rate or raindrop size distributions. To predict rain attenuation of satellite signals from rain rate along the satellite link path, the statistics of point rainfall rate characteristics peculiar to the location of interest must be available (Mandeep *et al.*, 2008).

Empirical and physical methods are the two types of prediction methods for rain attenuation on earth space paths. Empirical method is the method for measurement of data bases from stations in different climatic zones within a given territory. Physical method is used to recreate the physical behaviour involved in the attenuation process. Not all the input parameters needed for analysis when using the

physical method is available, therefore empirical method is mostly used for methodologies (Crane, 1980).

The rainfall rate of 1-minute integration time necessary for the study of rain induced impairment to telecommunication signal especially in the tropical region is scarce or totally unavailable. This is because global national weather institutions were established to satisfy more traditional requirements such as those for agriculture, hydrology and forest management. A method for converting the specific rain rate data to the equivalent 1-minute rain rate cumulative distribution is therefore needed (Ajayi and Ofoche, 1983).

Satellite communication systems are already migrating to higher frequency bands due to increase in demand for wide bandwidth as a result of developments in the complex multimedia applications. However, these higher frequency bands are affected adversely by rain-induced degradation. This has thus demanded for the pragmatic necessity for careful and detailed analysis of the effects of rain-induced degradation on system performance in these frequency bands (Panagopoulos *et al*, 2009, Igwe *et al.*, 2019).

2. Relevant Theory

2.1 Rain Rate Model

2.1.1 Chebil Rain Rate Model

Chebil-Rahman (Chebil and Rahman, 1999) came up with an experimental technique for estimating rainfall rate conversion element by using the conversion process from 60-minute and 1-minute integration time of rainfall intensity data in Malaysia. The 1-minute rainfall data were obtained from 3 different tipping bucket stations over 3 years period and the 60-minute rainfall data were acquired from Malaysia Meteorological Department (MMD) formerly known as Malaysia Meteorological Service (MMS) for 35 stations and for a period of 12 years. The proposed conversion formula is expressed as follows:

$$\rho 60(\mathrm{P}) = R_1(P)/R_{60}(P) \quad (1)$$

where $R_{60}(\mathrm{P})$ is the precipitation rate in 60 minute integration time and $\rho 60(\mathrm{P})$ is the rainfall rate at 1-minute integration time. $\rho 60(\mathrm{P})$is expressed as a mixed power-exponential law:

$$\rho 60(\mathrm{P}) = aP^b + ce^{(dp)} \quad (2)$$

where a, b, c and d are the regression variables analysed from statistical analysis of rainfall data. The accuracy of this method has been further tested for other lower integration time intervals to estimate $R_{0.01}$.

The use of Chebil's model is suitable since it allows the usage of long-time mean annual accumulation, M at the location of interest.

The power law relationship of the model is given by:

$$R_{0.01} = aM^{\beta} \quad (3)$$

where α and β are the regression coefficients. Chebil has made a comparison between some models based on measured values of $R_{0.01}$, and M in Malaysia, Indonesia, Brazil, Singapore and Vietnam. The regression coefficients α and β are defined as:

$\alpha = 12.2903$ and $\beta = 0.2973$

2.2 Rain Attenuation Model

2.2.1 The ITU-R P. 618 model

The ITU-R P. 618-9 model (ITU-R, 2007) provides the estimation of the long-term statistics of the slant path rain attenuation at a given location for frequencies up to 55 GHz. The model was developed based on the data obtained from ITU-R data storage using a satellite beacon with elevation angles from 6° to 82.5°. The model uses mainly rainfall information at one probability level ($R_{0.01}$) to calculate the attenuation. The ITU-R model provides global rain statistics by dividing the earth into rain regions and assigning a rain rate to each region along with the probability of that rain being exceeded (Seybold, 2005). This model uses the rain rate at 0.01% probability level for the estimation of attenuation and an adjustment factor is applied to the predicted rain fade depth for other probabilities. It can be used for the frequencies from 4 - 55 GHz and 0.001 – 5% percentage probability range. It is based on log-normal distribution and both rain intensity and path attenuation distribution conform to the same log-normal distribution.

The method consists of the following procedure, which is proposed to calculate the long-term statistics of the slant path rain attenuation at a frequency up to 30GHz. The method consists of several steps shown below.

The following parameters are required:

$R_{0.01}$: point rainfall rate for the location for 0.01% of an average year (mm/h)

h_s: height above mean sea level of the earth station (km)

θ: elevation angle (degrees)

φ□: latitude of the earth station (degrees)

f : frequency (GHz)

R_e : effective radius of the Earth (8500 km).

If local data for the earth station height above mean sea level is not available, an estimate can be obtained from the maps of topographical altitude given in Recommendation ITU-R P.1511.

The geometry is illustrated in Fig. 1

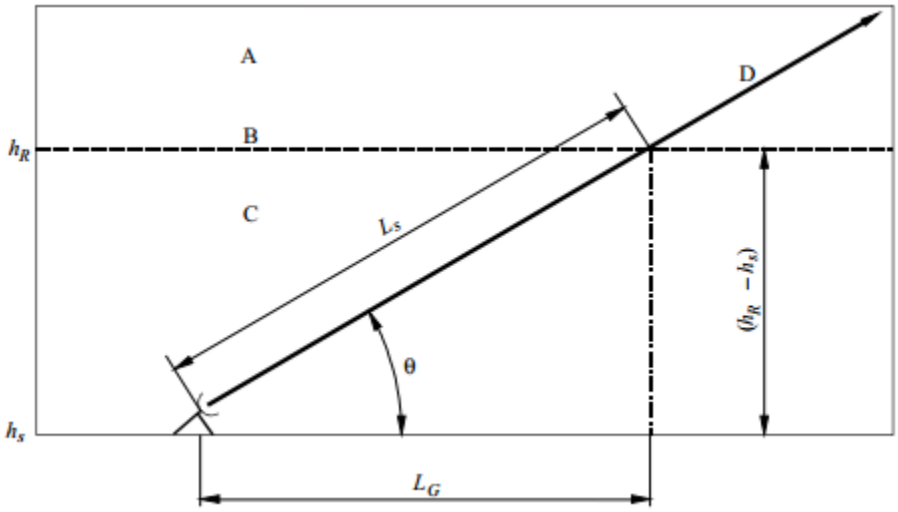

Fig. 1: Schematic presentation of an Earth-space path.

A: frozen precipitation

B: rain height

C: liquid precipitation

D: Earth-space path

Step 1: Determine the rain height, h_R, as given in Recommendation ITU-R P.839.

Step 2: For $\theta \geq 5°$ compute the slant-path length, L_S, below the rain height from:

$$L_S = \frac{(h_R - h_s)}{\sin\theta} \text{ km} \quad (4)$$

For $\theta < 5°$, the following formula is used:

$$L_S = \frac{2(h_R - h_s)}{\left(\sin^2\theta + \frac{2(h_R - h_s)}{R_e}\right)^{1/2} + \sin\theta} \text{ km} \quad (5)$$

If h_R-h_s is less than or equal to zero, the predicted rain attenuation for any time percentage is zero and the following steps are not required.

Step 3: Calculate the horizontal projection, L_G, of the slant-path length from:

$$L_G = L_S \cos\theta \text{ km} \quad (6)$$

Step 4: Obtain the rainfall rate, $R_{0.01}$, exceeded for 0.01% of an average year (with an integration time of 1 min). If this long-term statistics cannot be obtained from local data sources, an estimate can be obtained from the maps of rainfall rate given in Recommendation ITU-R P.837.

If $R_{0.01}$ is equal to zero, the predicted rain attenuation is zero for any time percentage and the following steps are not required.

Step 5: Obtain the specific attenuation, γ_R using the frequency-dependent coefficients given in Recommendation ITU-R P.838 and the rainfall rate, $R_{0.01}$ determined from Step 4 by using:

$$\gamma_R = k\,(R_{0.01})^{\alpha} \text{ dB/km} \quad (7)$$

Step 6: Calculate the horizontal reduction factor, $r_{0.01}$, for 0.01% of the time:

$$r_{0.01} = \frac{1}{1 + 0.78\sqrt{\frac{L_G \gamma_R}{f}} - 0.38\,(1 - e^{-2L_G})} \quad (8)$$

Step 7: Calculate the vertical adjustment factor, $v_{0.01}$, for 0.01% of the time:

$$\zeta = \tan^{-1}\left(\frac{(h_R - h_s)}{L_G r0.01}\right) \quad \text{degrees} \tag{9}$$

For $\zeta > \theta$ $$L_R = \frac{L_G r0.01}{\cos\theta} \quad \text{km} \tag{10}$$

Else, $$L_R = \frac{(h_R - h_s)}{\sin\theta} \quad \text{km} \tag{11}$$

If $|\varphi| < 36°$, $$\chi = 36 - |\varphi| \quad \text{degrees} \tag{12}$$

Else, $$\chi = 0 \quad \text{degrees} \tag{13}$$

$$v_{0.01} = \frac{1}{1 + \sqrt{\sin\theta}\left(31\,(1 - e^{-(\frac{\theta}{1+\chi})})\right)\frac{\sqrt{LR\gamma R}}{f2} - 0.45} \tag{14}$$

Step 8: The effective path length is:

$$L_E = L_R v_{0.01} \quad \text{km} \tag{15}$$

Step 9: The predicted attenuation exceeded for 0.01% of an average year is obtained from:

$$A_{0.01} = \gamma_R L_E \quad \text{dB} \tag{16}$$

Step 10: The estimated attenuation to be exceeded for other percentages of an average year in the range 0.001% to 5% is determined from the attenuation to be exceeded for 0.01% for an average year:

If $p \geq 1\%$ or $|\varphi| \geq 36$: $\beta = 0$ (17)

If $p < 1\%$ and $|\varphi| < 36$ and $\theta \geq 25$: $\beta = -0.005(|\varphi| - 36)$ (18)

Otherwise: $$\beta = -0.005(|\varphi| - 36) + 1.8 - 4.25\sin\theta \tag{19}$$

$$A_p = A_{0.01}\left(\frac{P}{0.01}\right)^{-(0.655 + 0.033\ln(p) - 0.045\ln(A_{0.01}) - \beta(1-p)\sin\theta)} \tag{20}$$

This method provides an estimate of the long-term statistics of attenuation due to rain. When

Comparing measured statistics with the prediction, allowance should be given for the rather large year-to-year variability in rainfall rate statistics.

3. Methodology

The rainfall data of 33 years (January, 1983 to December, 2015) collected from the Nigerian Meteorological station (NIMET) in Akwa-Ibom and Gombe was analysed using the Chebil rain rate model and the ITU-R P. 618-9 rain attenuation model stated in section 2.

4. Results and Discussion

4.1 Point Rainfall Rate for the Study Area

The point rainfall rate obtained using Chebil rain rate model is given in Table 1. Attenuation varies from location to location due to different rainfall rate experienced in the various locations. Akwa-Ibom State has a higher rainfall rate when compared to Gombe State, hence there will be more signal attenuation occurrence.

Table 1: Point rainfall for the study area.

Study Area	Gombe	Akwa-Ibom
Point Rainfall	94.75 mm/h	136.72 mm/h

The parameters used in the analysis of rain attenuation are shown in Table 2

Table 2: Rain attenuation parameters for the study area.

LOCATION	GOMBE	AKWA-IBOM
Longitude	11.02º	7.57º
Latitude	10.19º	5.00º
Elevation	42.5º	42.5º
Height above sea level	0.422 Km	0.163 Km
Polarisation	Horizontal	Horizontal
Operating frequencies	11 GHz for downlink and 14 GHz for Uplink Ku-band.	11 GHz for downlink and 14 GHz for Uplink in Ku-band.
	20 GHz for downlink and 40 GHz for Uplink Ka-band.	20 GHz for downlink transmission and 40 GHz for Uplink Ka-band.

4.2 Rain Attenuation for the Study Area

The predicted rain attenuation for the study area at 11 GHz and 14 GHz downlink and uplink frequencies respectively and 20 GHz and 40 GHz downlink and uplink frequencies respectively at 0.01% exceedance are given in Table 3.

Table 3: The predicted attenuation at 0.01%

Frequency(GHz)	Gombe	Akwa-Ibom
11	13.6229	18.0471
14	27.7331	29.8146
20	44.3253	57.5429
40	117.2618	147.9524

Rain does not occur all the time in a year and its rate does not remain the same all the time when it occurs, therefore the amount of rain fade margin needed to compensate for the rain effect varies with time. Figures 2-5 show the graphical comparison of the rain attenuation for a horizontally polarised signal at different percentages of time for Ku-band downlink (11 GHz) and uplink (14 GHz) and Ka-band downlink (20 GHz) and uplink (40 GHz) frequencies.

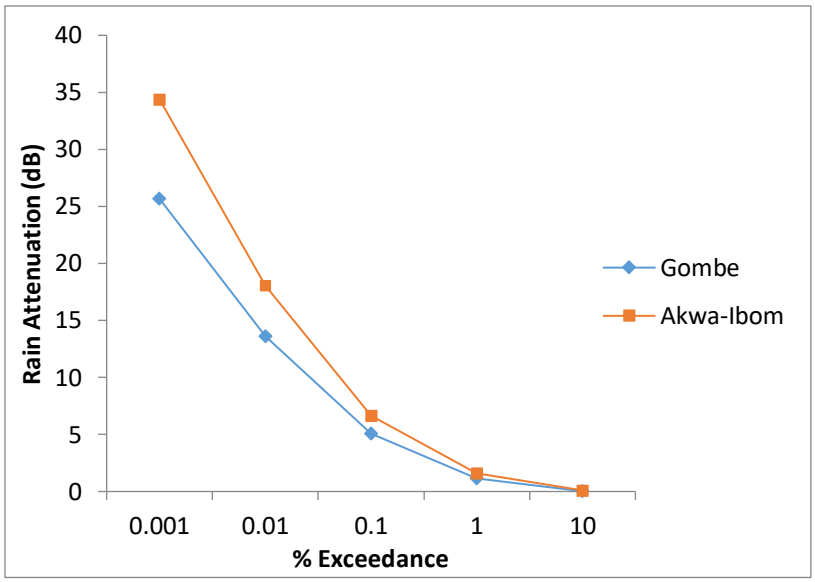

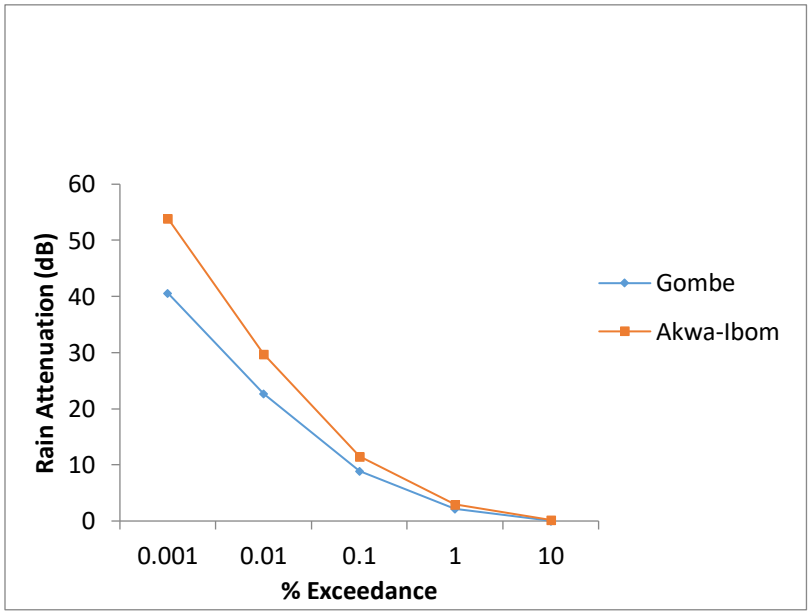

Figure 2: Rain attenuation at 11 GHz

Figure 3: Rain attenuation at 14 GHz

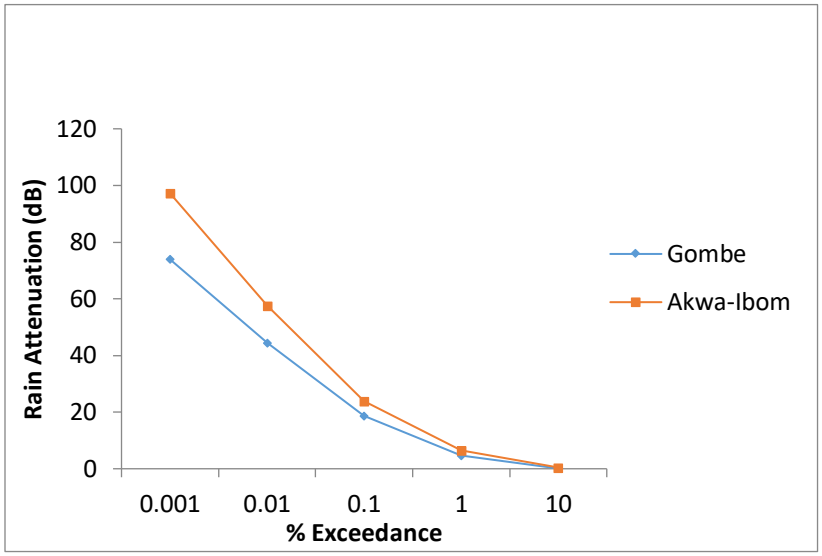

Figure 4: Rain attenuation at 20 GHz

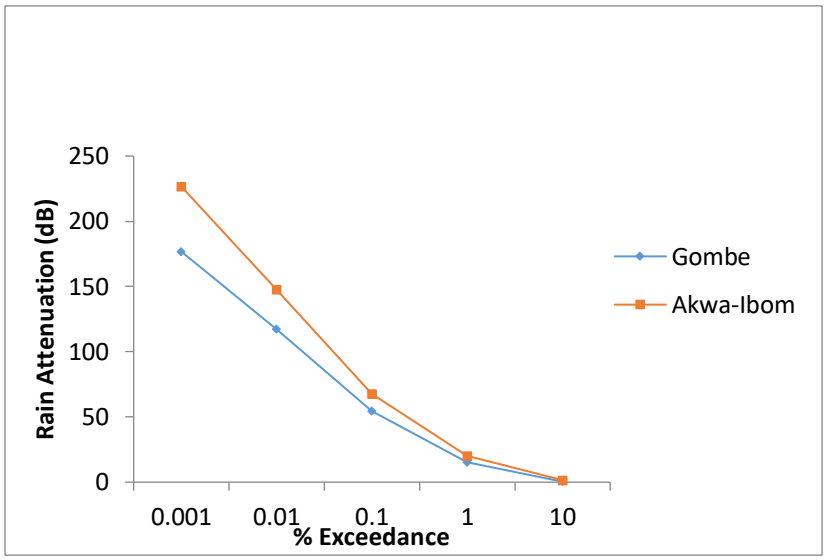

Fig. 5: Rain attenuation at 40 GHz

For 0.01% of the year (99.99% availability), the rain attenuation in Gombe at Ku-band downlink and uplink frequencies are 13.62 dB and 22.73 dB respectively. At Ka-band downlink and uplink frequencies, the attenuation is 44.33 dB and 117.26 dB respectively.

Similarly in Akwa-Ibom, the rain attenuation for Ku-band downlink and uplink frequencies are 18.05 dB and 29.81 dB respectively. At Ka-band downlink and uplink frequencies, the attenuation is 57.54 dB and 147.95 dB respectively. This shows that attenuation experienced in Gombe is lesser in

comparison to that experienced in Akwa-Ibom. Attenuation is also a function of frequency which is also true from the results obtained, as increase in frequency leads to a corresponding increase in signal attenuation.

5. Conclusion

The effect of rainfall on earth-space communication link at Ku and Ka-bands have been investigated for links to Nigerian communication satellite-1 Replacement (NIGCOMSAT-1R) based on local input data. Rain attenuation for Gombe and Akwa-Ibom States were predicted for 0.001-10% time exceedance using the ITU-R P. 618-9 attenuation model. For the downlink and uplink frequencies of Ku-band, 13.62 dB and 22.73 dB respectively were predicted, while 44.33 dB and 117.26 dB were predicted for the downlink and uplink frequencies respectively of Ka-band at 0.01% for Gombe State. For Akwa Ibom State, 18.05 dB and 29.81 dB were predicted for the Ku-band downlink and uplink frequencies respectively, while 57.54 dB and 147.95 dB were predicted for the Ka-band downlink and uplink frequencies respectively. The results obtained clearly show that satellite links in Akwa Ibom State will surfer more rain attenuation than those in Gombe State. These results are the consequent effects of the point rainfall rate values deduced for the two States.

References

Ajayi, G. O. & Ofoche, E. B. C. (1983). Some tropical rainfall rate characteristics at Ile-Ife for microwave and millimetre wave application, *Journal of Climate and Applied Meteorology*, 23, 562 – 567.

Chebil, J. & Rahman, T. A. (1999). Rain rate statistical conversion for the prediction of rain attenuation in Malaysia. *Electronics Letters,* 35, 1019-1021.

Crane, R. K. (1980). Prediction of attenuation by rain. *IEEE Transactions on Communications,* 28, 9, 1717 – 1733.

Igwe, K. C., Oyedum, O. D., Ajewole, M. O. & Aibinu, A. M. (2019): Evaluation of some rain attenuation prediction models for satellite communication at Ku and Ka bands. *Journal of Atmospheric and Solar-Terrestrial Physics, 188, 52-61.*

ITU-R. (2001). Rain height model for prediction methods. *Recommendation P.839-3, ITU-R P Series, International Telecommunication Union,* Geneva, 1-2.

ITU-R. (2001). Topography for Earth-to-space propagation modelling. *Recommendation P.1511, ITU-R P Series, International Telecommunication Union,* Geneva, 1-2.

ITU-R. (2005). Specific attenuation model for rain for use in prediction methods. *Recommendation P.838-3, ITU-R P Series, International Telecommunication Union,* Geneva, 1-8.

ITU-R. (2007). Propagation data and prediction methods required for the design of earth-space telecommunication systems. *Recommendation P.618-9, ITU-R P Series, International Telecommunication Union,* Geneva, 1-7.

Mandeep, J. S., Hassan, S. I., Ain, M. F. & Tanaka, K. (2008). Rainfall propagation impairments for medium elevation angle satellite-to-earth 12 GHz in the tropics. *International Journal of Satellite Communications and Networking, 26 (4), 317-327.*

Panagopoulos D. J., Chavdoula, E. D. & Margaritis, L. H. (2009). Bio-effects of mobile telephony radiation in relation to its intensity or distance from the antenna. *International Journal of Radiation Biology, 86(5), 345-357.*

Seybold, J. S. (2005). Introduction to RF propagation. Wiley-Interscience, John Wiley and Sons Inc. ISBN-13978-0-471-65596-1.

Synthesis and Thermal Characterization of NZP Compounds $Na_{1-x}li_xzr_2(Po_4)_3$(X= 0.00-0.75)

Ahmadu U. and Yusuf A.S.

Department of Physics, Federal University of Technology, Minna, Nigeria

****corresponding author: u.ahmadu@yahoo.com***

Abstract

NZP composition $Na_{1-x}Li_x(PO_4)_3$, x=0.00-0.75 has been synthesized by the method of solid state reaction from $Na_2CO_3.H_2O$, Li_2CO_3, ZrO_2 and $NH_4H_2PO_4$, sintering at 1050-1250^oC for 8hours only in other to determine the effect on thermal and other properties, such as the phase formation of the compound. The materials have been characterized by TGA and DTA thermal analysis methods from room temperature to 1000^oC. It was observed that the increase in lithium content of the samples increases thermal stability of the samples and the DTA peaks shifted towards higher temperatures with increase in lithium content. The thermal stability regions for all the sample is observed to be above 640^oC.The sample with the highest lithium content, x= 0.75 exhibited the greatest thermal stability over the temperature range.

Keywords: thermal analysis; sodium zirconium phosphate; NASICON

1. Introduction

One of the most important materials that is being presently studied in materials science is sodium Zirconium Phosphate, $NaZr_2(PO_4)_3$, otherwise popularly known as NASICON or NZP. The material has been found to have very unique properties such as being the only substance that can accommodate atoms of different sizes in its various lattice sites[1]. The Na, Zr and Phosphorus can all be substituted, except oxygen, resulting in compositions with varying physical and chemical properties suitable for diverse applications. Several studies have been undertaken reflecting the various potential applications such as its use as substrate material for oxide-coating [1-2], for demobilisation of nuclear wastes [3], applications in zero or negative thermal expansion materials [4-6] and as electrode for rechargeable lithium battery applications [7] and gas sensors[8], among others.

We are carrying out series of characterizations on the NZP, beginning with thermal analysis of lithium substituted composition $Na_{1-x}Li_x(PO_4)_3$ (x=0.00-0.75), with the ultimate objective of

determining their suitability for applications as electrolytes for energy applications. Many studies have been carried out on NZP materials that were synthesized through various routes in other to obtain materials of good thermal and electrical characteristics, in particular by appropriate configuration of the sintering times and temperatures. This has ultimately lead to the synthesis of pure phase and good crystalline materials with enhanced properties. Studies have shown that the minimum sintering temperature required for the formation of NASICON is about 1100^{o}C [9] at different sintering times which may be as low as possible, but generally varying from 16hours [10] to as much as 20hours [11], aside from other intermediate and higher values. The authors in ref.[12] in their study of two different NASICON compositions have examined the balance between these two factors on the formation of the phases of the NASICON compound and found that there is indeed a particular balance that exists between them for the formation of NASICON to ensue. The present study is therefore expected to elucidate this further by using a sintering time of only 8 hours for both the sintering and other preliminary steps in the solid state synthesis of the materials, making the aggregate time to be much less than had hitherto been reported in literature. By maintaining a high temperature at the expense of the sintering time and improving on sample preparation through thorough grinding and regrinding of sample for many hours, we wish to determine whether NZP of good crystallinity and phase purity could be formed within this period at a sintering temperature of 1050-1250^{o}C.Thus we studied four compositions that to our knowledge have not been systematically analysed and thermally examined their stability with respect to increasing lithium content between room temperature and 1000^{o}C using DTA and TGA thermal analysis methods. We are interested particularly in structural transformations that may take place and how this will affect the other parameters to be determined ultimately. Moreover, we also observe the systematic degradation of the compound with temperature and the reasons behind them. Here we report the results of the thermal characterizations while the ongoing research on XRD, among others, is taking place to determine the phases and other relevant parameters relating to the materials.

2. Experimental

2.1 Synthesis

The preparation of these samples was carried out at the Centre for Energy Research and Development (CERD), O.A.U. Ile-Ife. Basic starting materials of analytical grade (>99%) were used, that is, $Na_2CO_3.H_2O$, ZrO_2, Li_2CO_3 and $NH_4H_2PO_4$. Stoichiometric amounts of these materials were

mixed and thoroughly ground in an agate mortar four about five hours in each case. The solid solution was then dried in air for about four (4) hours. Acetone was added in appropriate quantity to homogenize the mixture. Pellets of discs of 13mm diameter and 6mm thickness were prepared for sintering purposes under pressure of 7.42 x $10^6 N/m^2$. The sintering was carried out at the National Metallurgical Development Centre (NMDC), Jos. All the samples were placed inside a gas-heated furnace for eight (8) hours at successive temperatures 200, 500, 1050,1100,1150,1200 and 1250^oC, respectively. Between each temperature, the samples were allowed to furnace-cool to room temperature and the samples were thoroughly ground, re-mixed, pelletized and placed back into the furnace for the next round of heating. The maximum sintering temperature was 1250^oC.

2.2. Thermal characterization

Specimens of the virgin powder samples were used for the measurement on DTA machine NETZCHDTA404PC in air, at the Centre for Energy Research and Development (CERD), O.A.U. Ile Ife. The readings were conducted between room temperature and 1000^oC at heating rate of 20.0K/min. The results are shown in fig.2 (a-d). The TGA was performed on virgin powder specimens from room temperature to about 1000^oC on an TGA Shimadzu DT-30 thermal analyser in air at a heating rate of 20.0K/min at the University of Witwatersrand, South Africa. The plot of Weight (Wt %) versus Temperature (T^oC) of the samples are shown in fig.3 (a-d) together with the composite plot, fig.4.

3. Results and Discussions

For the sample x=0.00, there is only one exothermic peak at 188.9^oC which began from 140-220^oC in the DTA plot. This can be attributed to the loss of water and water of hydration. The absorbed heat continued to increase until it reached a plateau between 680-760^oC, showing the establishment of equilibrium. This shows that the sample is stable in this region, fig.1 and is confirmed by the TGA plot in fig.5 where the sample showed stability from 600^oC to 1000^oC.

Similar work by the authors [13] on the sample, for example, has about eight peaks in the DTA plots, three are endothermic and the rest are exothermic. They attributed the endothermic (largest) peak which they found at 120^oC to the elimination of water from the mixture. Their work and others showed that using different precursors of the starting materials leads to different results, particularly, the peaks and their positions. The area of the peak in this sample is the smallest,

comparatively, showing that the reaction involving the evolution of water released the least amount of heat. In the system $Li_{1+x}Ti_{2-x}Al_x$ $(PO_4)_3$(0.5<x<0.9) the DTA did not show any structural changes on heating, though melting was observed above 800oC [14]. Similarly, [15] observed the DTA peaks in a temperature region different from the TGA in $Li_{1+x}GaTi_{2-x}$ $(PO_4)_3$ with x=0.1-0.9.

Ref. [16] studied NZP x =0.00 by sol-gel preparation and had one exothermic peak in the DTA at 270°C from 220--280°C and overall weight loss is 29%, RT--1000°C and it similarly, had approximately four temperature regions and shows stability around 600°C upwards.

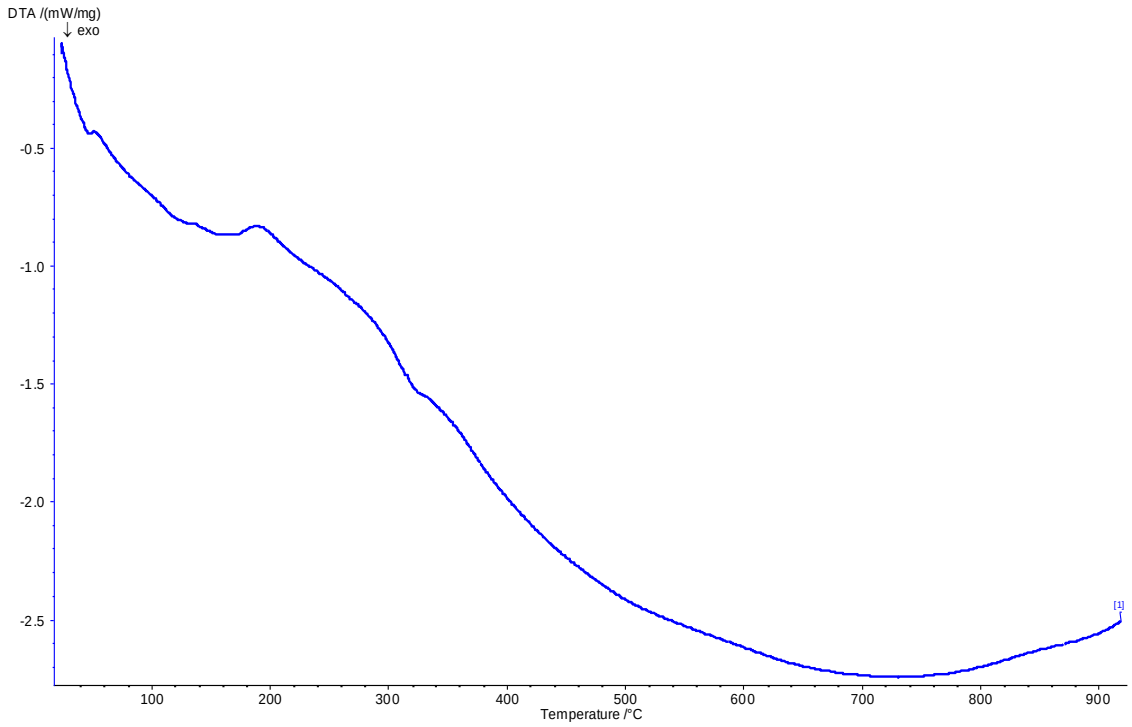

Fig.1. DTA plot of sample x=0.00 showing the exothermic peak at 188.9°C.

The sample x=0.25 showed one sharp exothermic peak at 200°C, starting from 180-250°C which is also ascribed to the loss of water and water of hydration. A plateau exists from 670-760°C showing that the stability region for this sample began at an earlier temperature, fig.2. This means that the increment of lithium content in the sample has increased the thermal stability of the compound compared to the x=0.00 sample.

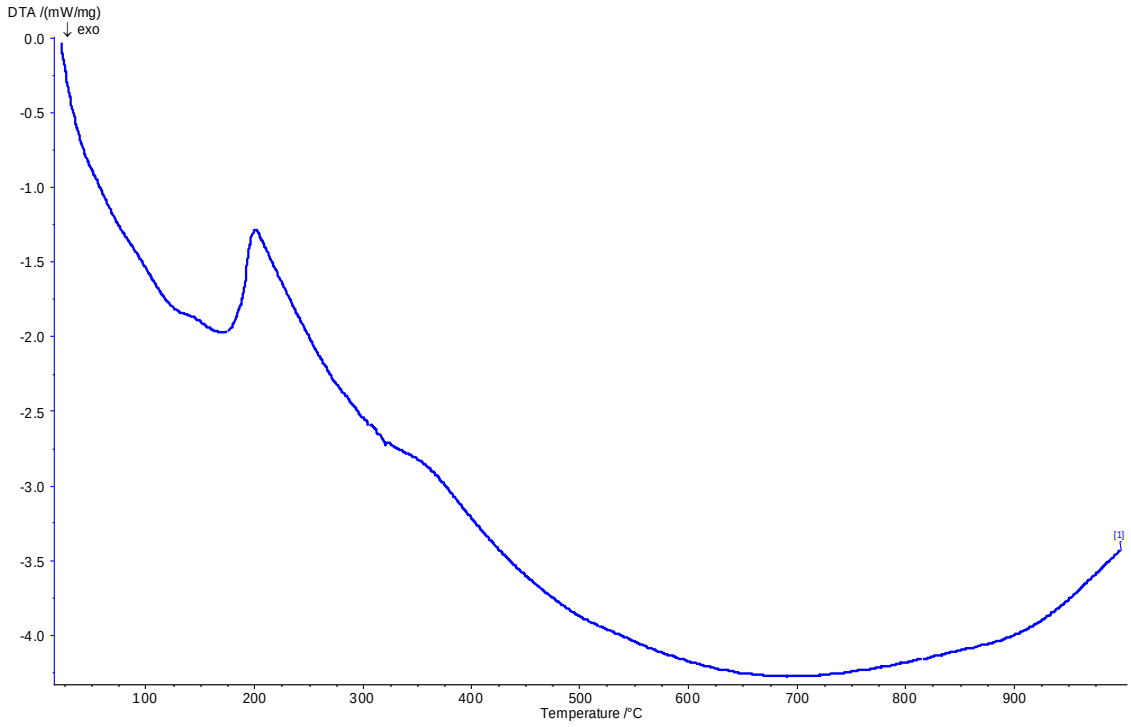

Fig.2. DTA plot of sample x=0.25 showing the exothermic peak at 200.0^{o}C.

In the case of x=0.50 sample, there is a sharp exothermic peak at 196.4^{o}C from 163-250^{o}C is also attributed to the loss of water of hydration and moisture. A plateau is observed between 580-700^{o}C, fig.3 which is wider than the previous samples. There is a broad exothermic peak at about 800^{o}C which may point to the beginning of crystallization process.

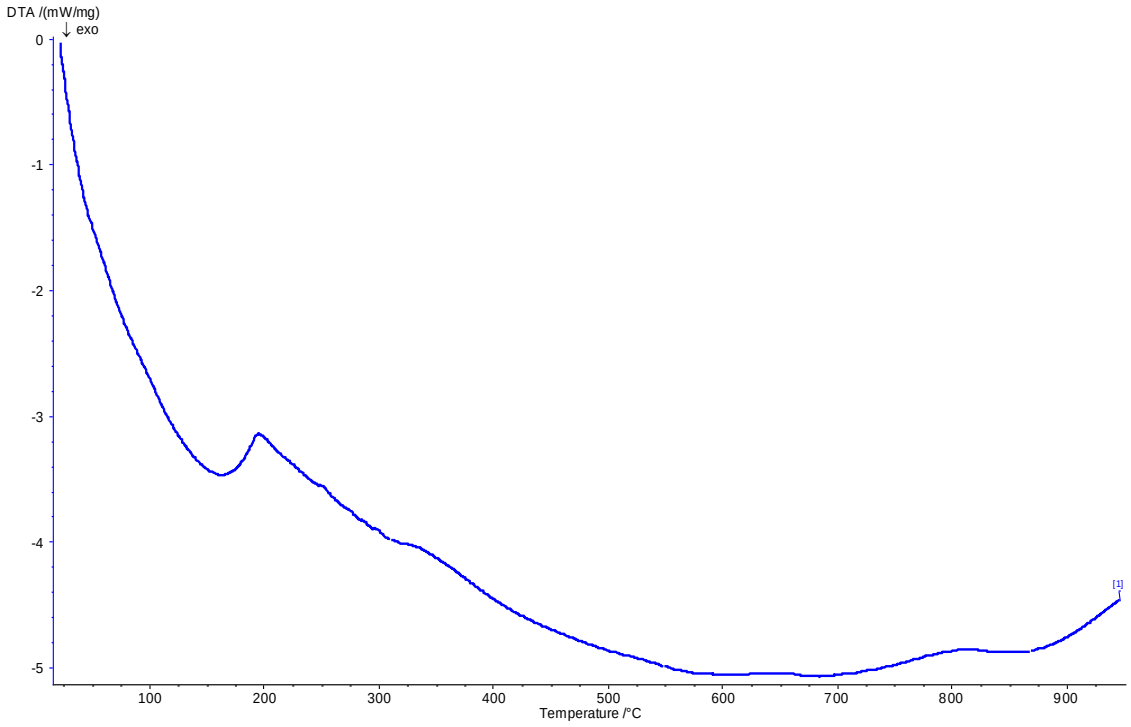

Fig.3. DTA plot of sample x=0.50 showing the exothermic peak at 196.4^{o}C.

The last sample, x=0.75 showed the largest and broadest exothermic peak at 202.6. ^{o}C between 140-250^{o}C showing the loss of water and water of hydration. Similarly, a plateau at 650-720^{o}C is observed which is the widest region of stability compared to the others, fig.4.This is a confirmation of the fact that increasing lithium content brings about thermal stability of the sample, by decreasing the rate of loss of weight of the sample, as confirmed by the TGA results below. Also the positions of the exothermic peaks are shifted towards higher temperatures with increasing lithium contents.

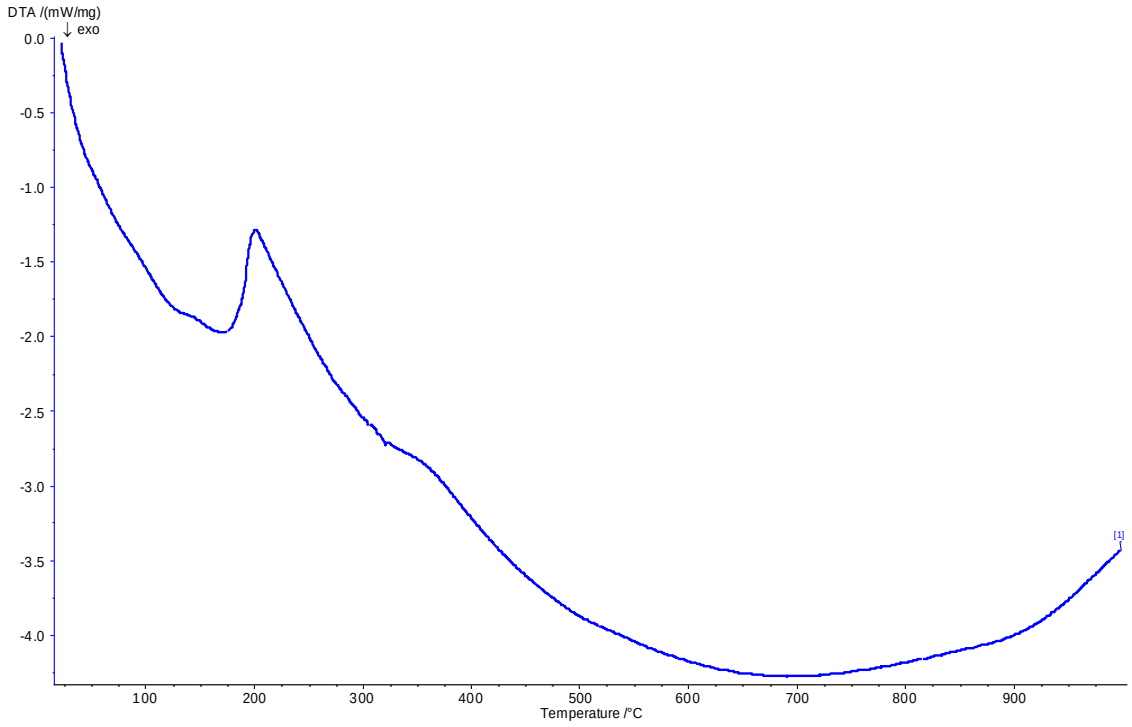

Fig.4. DTA plot of sample x=0.75 showing the exothermic peak at 201.7°C.

The position of the peaks is shifting with increased lithium content, implying that the lithium increases the thermal stability of the samples, delaying the temperature at which these losses occur. This is confirmed by the TGA plot. The TGA for all the samples show the same character and can be approximately broken into four temperature ranges: 1) RT- 60°C, 2) 60-180°C, 3) 180-360°C and 4) 360-1000°C, with the first range being the smallest almost invisible in the x=0.50 and 0.75 samples. In all the samples 600-1000°C is the thermal stability region, as the weight loss is about 1% only. The rate of mass loss decreases with increasing temperature through the regions, until it becomes virtually constant from above 600°C upwards in all the samples. The TGA plot is not shown beyond 800°C because of the limitation of the EXCEL PROGRAM which was used to plot the data, as it is limited to 32,000 data points only (OFFICE 2007 PROGRAM) and becomes unstable beyond this range. Nevertheless, the weight loss is virtually constant beyond this temperature range. The composite TGA plot is shown to 600°C.

Thus for sample x= 0.00, the weight loss is 7% in the first region, approximately 5% in the second region, 15% weight in the third and 2% in the fourth region. The weight loss is greatest in the third and is within the region of the exotherm, as observed in the DTA. Overall there was a weight

loss of about 29% from room temperature to about 1000°C, fig.5.The TGA shows that the sample is stable from around 600°C and this is in agreement with that of [13] and the general characteristics of the plots are the same in terms of mass losses in the various regions. This implies the formation reaction of the product is complete at this temperature. This is also in agreement with the DTA results discussed above for the sample. In their study of $Li_{1+x}Ti_{2-x}Al_x$ $(PO_4)_3(0.5<x<0.9)$ ref. [14] did not observe any mass losses in the TGA from room temperature up to 800°C.

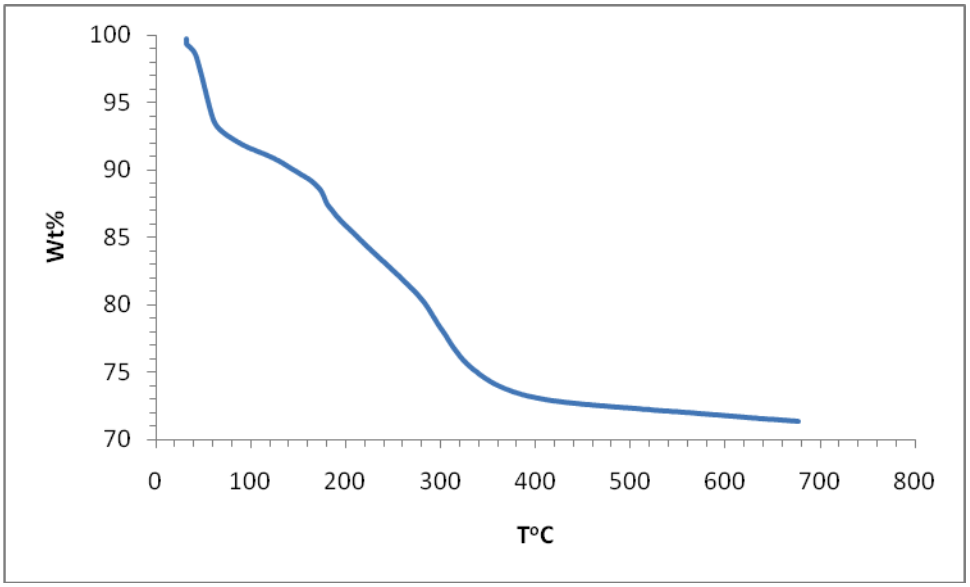

Fig. 5. TGA Plot of sample x=0.00 showing the four temperature regions of weight losses

In the same region for sample x= 0.25, the weight loss are 6%, 4%, 16% and 2.5% respectively. Similarly, the weight loss is the greatest in the third region, almost the same amount with the x=0.00 sample. Overall weight loss is approximately 29%, fig.6, as in the sample x=0.00 and correlates with the sample x=0.00 in terms of the greatest amount of mass loss in the third region. Similarly, the rate of weight loss with changing temperature has now decreased, showing that the material has become more stable with increase in lithium content.

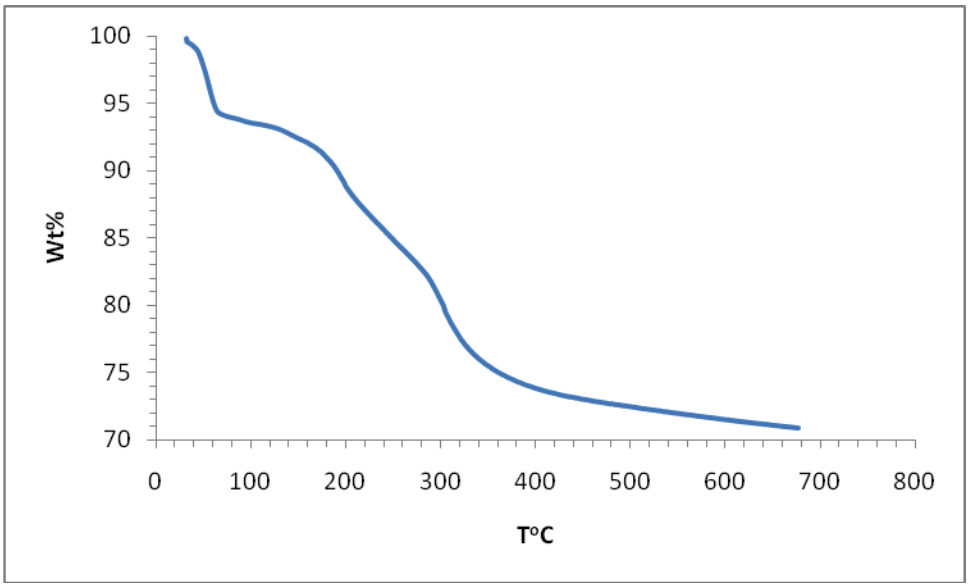

Fig. 6. TGA Plot of sample x=0.25 showing the four temperature regions of weight losses

Similarly, for x= 0.50 respective weight losses in the regions are 5%, 3%, 13% and 2% confirming further the activity in the exothermic region, i.e. , third region. Again there is a slight decrease in the rate of weight loss with changing temperature compared to the earlier samples. Overall weight loss is 23%., fig.7, and further evidence of the comparative stability of this sample.

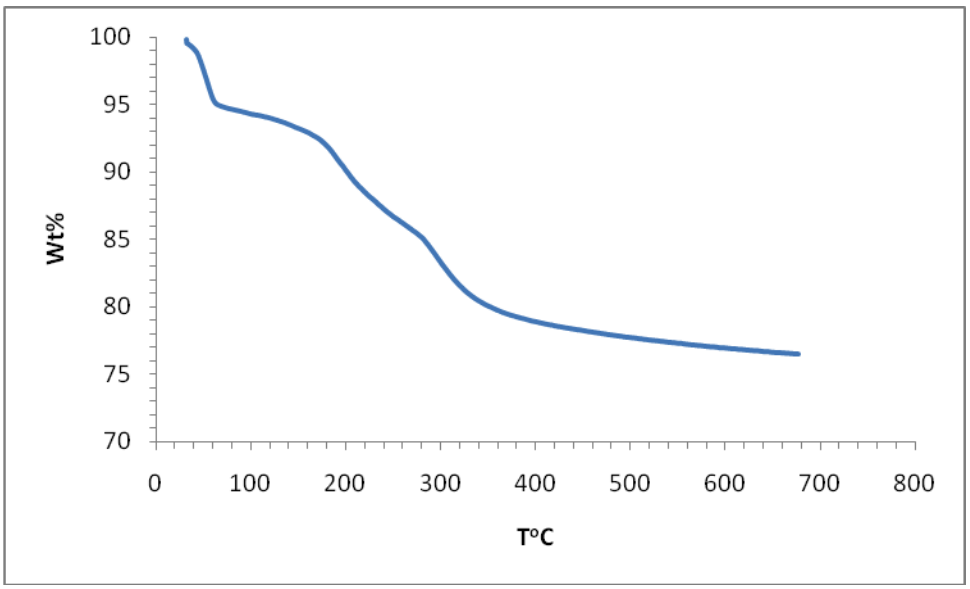

Fig.7. TGA Plot of sample x= 0.50 showing the four temperature regions of weight losses

The last sample, x= 0.75 has respectively, 2%, 2.5% and 5% in the regions with overall weight loss of 25%, fig.8.The weight loss has drastically reduced in the third region to only 5% and beyond, showing that the lithium content at this level has dramatically increased the stability of the sample with the rate of weight loss with increased temperature being the lowest. The results show an increasing stability of the samples with increased lithium content.

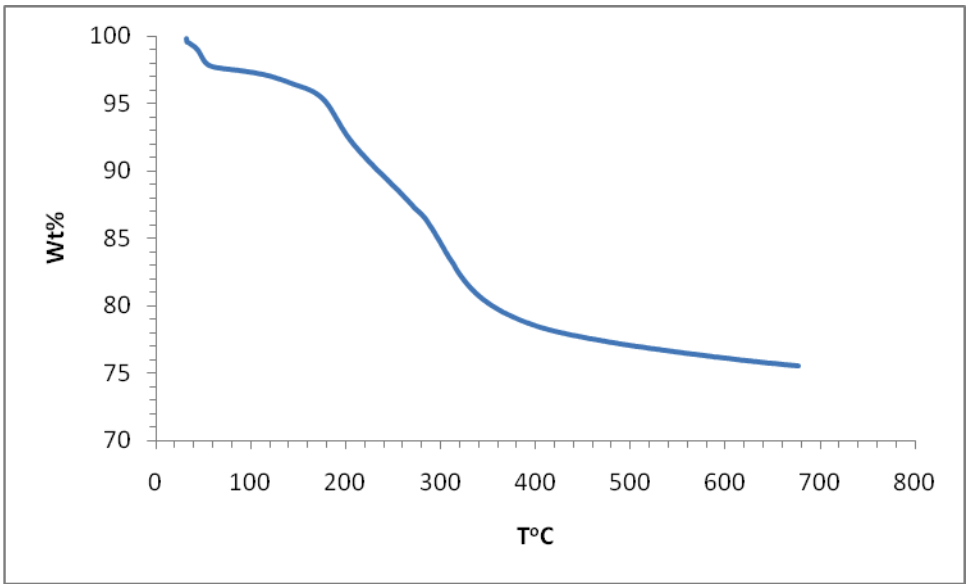

Fig. 8. TGA Plot of sample x=0.75 showing the four temperature regions of weight losses

The composite TGA plot is shown in fig.9 for comparison and it is clear that the samples exhibited the same characteristics, with the four temperature domains clearly visible and weight losses occurring at about the same temperature range. Within the temperature range RT-60^{o}C, x=0.00 showed the highest weight loss of about 30%, with x= 0.75 being the least. Similarly, between RT-360^{o}C, the plots maintained a particular order in terms of weight loss with x=0.75<0.50<0.25<0.00. The weight loss decreases with increasing lithium content. Beyond this temperature the weight loss for the x=0.00 > x = 0.25 up to about 500^{o}C, thereafter they maintain virtually the same weight loss. Whereas the x= 0.50 sample became more stable, with less loss in weight than x= 0.75 and beyond 360^{o}C. The x= 0.50 and 0.25 have the same weight loss from RT-170^{o}C, about 5%.The fourth region has the least loss in weight in all the samples and almost the same magnitude. The composite plot is shown in fig.9.

The small weight loss from RT-60^{o}C, visible in all samples except x=0.75, may be attributed to loss of the homogenizer acetone. Moreover, loss of Ammonia and water can also be attributed to

the weight loss at up to 150°C whereas weight loss of CO_2 takes place at 260-428°C [17].The fact that no weight increase was observed throughout, except very small bulges at 81.17, 82.61, 85.70 and 87.61°C in increasing order of sample concentration, which may point to slight increments in weight in the compositions, indicates that the material is stable in air to oxidation [18]. It seems reasonable to say that the decomposition of Na_2CO_3 at 831°C and Li_2CO_3 at 723°C to produce the Na and Li respectively, imply that the latter, although decomposes earlier, is thermally more stable owing to the higher melting (181°C) and boiling points (1342°C) of the elemental substituent (Li) and hence when the substitutions take place in the x≠0.00 samples, the composition becomes increasingly more thermally stable. The dehydration of the $Na_2CO_3.H_2O$ is expected between 100-150°C[19].This is also certainly helped by the high reactivity of lithium and thus its bonding within the framework becomes stronger. This therefore explains why the sample x=0.00(no lithium) is the least stable from the composite TGA plots.

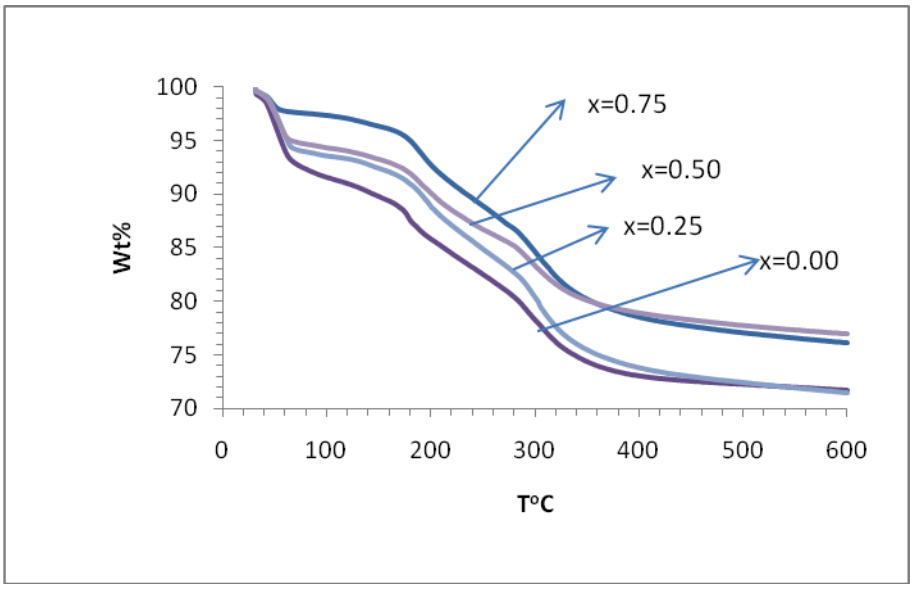

Fig. 9. Composite TGA Plot of $Na_{1-x}Li_xZr_2(PO_4)_3$ showing the compositions.

4. Conclusion

The systematic Increase in the lithium content of the samples increases the thermal stability of the compounds in particular from 50°C to 350°C owing to the greater thermal stability of lithium. However, x= 0.50 and 0.75 are more stable throughout the temperature range, as they are clearly separated from the x= 0.00 and x= 0.25 and are on the upper side indicating lower weight loss. The samples x=0.00 and 0.25 remained clearly distinguished in their thermal behaviour from 69°C until

425^{o}C when they became indistinguishable.Whearas x=0.50 and 0.75 had a shorter period of distinguishable thermal behaviour from 69 to 317^{o}C before they became closer. It may be concluded that the threshold for increased thermal stability for the compositions is when the composition is x= 0.50, as the compositions appear clearly separated in into twos. The exothermic peaks were observed to shift towards higher temperatures with increased lithium content just as the process itself shifted towards higher temperatures from its lower limits in agreement with the TGA results. Consequently, the thermal stability regions become wider with increased lithium content. There were no peaks observed that could be attributed to any form of structural transformation in the compositions since the NZP is not expected to begin to form until far above 1050^{o}C, beyond the temperature limit of the TGA/DTA. This is very important for electrical conductivity measurements and for structural analyses purposes. It was also possible to establish the sintering temperature for the compositions, which are similar, for the solid state synthesis of these materials. Work is ongoing to characterize the phase and other properties of the compositions before conclusive deductions can be made, though the materials seem to exhibit the typical NZP character from the thermal point of view.

Acknowledgements

The authors would like to thank Eng. Shehu Ahmed Isah, of NMDC, Jos, for help with the Furnace work, Mr. A.S. Afolabi of the University of Witwatersrand, South Africa and Mr. A. Jegede of CERD, OAU, Ife, for thermal characterization. Also we thank Prof. Sunday Thomas, D-G. Shestco, Abuja and Dr. T. Salkus of Vilnius University, Lithuania for their various roles in the synthesis of the materials.

References

[1] A. K. Dinesh, H. Girish, B. Else, R. Rustum, J. Mater. Res., 11 (1996) 3160.

[2] W. Y. Lee, K. M. Cooley, C. C. Berndt, D. L.Joslin, D. P. Stintin, J. Am. Ceram. Soc., 799 (1996) 2759-62.

[3] S. Nakayama, K. Itoh, J. Nucl. Sci. Tech., 40 (2003) 631-633.

[4] R. M. Hazen, L. W. Finger, D. K. Agrawal, H. A. McKinstry, A. J. Perrotta, J. Mater.

Res., 2 (1987) (329-337)

[5] P.S. Tantri, K. Greetha, A. M. Umarji,S. K. Ramasesha, Bull. Mater. Sci., 23 (2000) 491-499.

[6] B. Angadi, V. M. Jali, M. T. Lagure, N. S., Kini, A. M. Umarji, Bull. Mater. Sci., 25 (2002) 191-196.

[7] J. M. Taracson, M. Armand, Nature, 414 (2001) 362.

[8] E.D. Tsagarakis, PhD dissertation, Der Christian Albrechts Universitat, Kiel University (2004).

[9] R. O. Fuentes, D. G. Lamas, M.E. Fernandez,D. E. Rapp, F. M. Figuiredo, J.R. Frade,F. M. B. Marques, J. J. Franco, Boll. De la Soc. Ceram, 14 (2004) 777.

[10] P. P. Kumar, Y. Yashonath, J. Chem. Soc., 118 (2006) 147.

[11] N. Anantharamulu, G. Prasad, M. Vithal, Bull. Mater. Sci., 31 (2008) 134.

[12] H. B.Kang, N. H. Cho, J. Mater. Sci., 34 (1999) 5006.

[13] A.H. Naik, N.V. Thakkar, S.R. Darwatkar, K.D.S. Mudher, V.V.Venagopal, J. Therm. Anal. Cal., 76 (2004)707-713.

[14] F. E. Mouahid, M. Zahir, P. M. Maldonado-Manso, S. Bruque, E. R. Losilla, M. A. G. Aranda, A. Rivera, C. Leona, J. Santamaria, J. Mater. Chem., 11 (2001) 3258-3263.

[15] K. Oda, S. Takase, Y. Shimizu, Mater. Sci. Forum, 544-545 (2007)1033-1036.

[16] J. V. Bothe, P. W. Brown, (2003). Low Temperature Formation of NZP Ceramics.www.netl.doe.gov/publications/proceedings/03/ucr-hcbu/Brown/pdf.

[17] J. Judes, V. Kawaraj, Mater. Sci. Pol., 27(2009)3.

[18] M. N. Kutukcu, M.Sc thesis, Georgia Institute of Technology (2004).

[9] O.A. Smirnova , V.V. Kharton, F.M.B. Marques, Bol. Soc. Esp. Ceram.,3(2004) 679- 685.

Evaluation of Physico-Chemical Properties of starches from *DisocoreaRotundata*species

Umaru Ahmadu[a], Yusuf A.S.[a] and Oluwatoyin Odeku[b]

[a]Department of Physics, Federal University of Technology, Minna, Nigeria

[b]Department of Pharmaceutics and Pharmacy , University of Ibadan, Nigeria

Corresponding author:u.ahmadu@yahoo.com

Abstract

Three species of starches from *dioscorearotundata:Giwa, Lagos, Sule and Kwasi* were investigated and characterized by X-ray diffraction, EDX/XRF/PIXE/SEM with Proximate composition determined.Yams tarches were found in all the *D.R.* species.XRD peaks of highest intensity are at~17.02,17.12 and 17.26°2θ with relative crystallinities (%) ~ 18.25$\pm$1.25, 22.25$\pm$5.75, and 18.75$\pm$0.75%, respectively.A distinctive characteristic is that all the species contain elements Ru(18.37 to 27.71) and K (11.48 to 21 w/w%)in major concentrations. Their microstructure has grain sizes of 3.59, 3.54 and 3.19 µm, respectively, for*Giwa, Lagos*and*Sule.* The grains are generally uniform/oval in shape and mixtures of B and C-crystal types.The crystallite sizes are ~2.5, 3.0 and 2.4 nm, for *Giwa*, *Lagos*and*Sule*, respectively.Whole profile fitting of the patterns with subsequent refinement using GSAS II suite of programs, together with instrumental resolution curve fitting and peak profile analysis show agreement factors (*Rwp)* of 1.49, 2.66 and 1.75%, and were all indexed as orthorhombic cells.It is concluded that the starches can be stored safely due to their low moisture content, the possibility of some mineral deposits in the soil and that they have physico-chemical properties that may be suitable for application in the starch industry, particularly when modified.

A. Introduction

Yam tuber is one of the most staple foods eaten in sub-Saharan Africa and constitutesabout 15% of total calories and 81% of protein of the average Nigerian diet(Odebami*et al.*,2007), compared to the UK , for example,where it is about 30% of diet by weight(Wang *et al.*, 1998). White yam (guinea

yam or African yam) belongs to the *DioscoreaRotundata* (*D.R.*) family with over 600 species in which only seven are edible (Polycarp *et al.*, 2012; Amani *et al.*, 2005) or cultivated for food and medicine. According to the International Institute of Tropical Agriculture(IITA), in 2005 yams were produced in 47 countries (Polycarp *et al.*, 2012) in tropical and subtropical regions of the world and out of the 47.8 million tons produced, 97% were from sub-Saharan Africa, Nigeria being the leading producer with 34 million tons.

Dioscorea species contain carbohydrates which essentially are starches of different origins with varying degrees of crystallinity of between 15 -45%(Napaporn*et al.*, 2001) and can be extracted from various starch bearing tubers, roots or cereals. Inspite of the predominance and relevance of this species there is dearth of literature in the area of work carried out on yam starch and particularly, on exploiting their favourable physical properties for industrial applications with major data bases reporting less than 1%(Amani *et al.*,2005; Satin, 2006) compared to other sources such as potato, corn,maize and rice.Further, there is little attempt at correlating the various properties of the *dioscorearotundata*species found within and outside Africa with different local names with the view to classifying them based on their similar properties

Native starches are composed of amylose and amylopectin which form the amorphous and crystalline components, respectively(Napaporn*et al.*,2001; Karin *et al.*, 2003) and their crystallinity have been classified as A, B or C based on Wide Angle X-ray Diffraction(WAXD)(Riley *et al.*, 2006;Frost *et al.*, 2009). Detailed structure of starch and other relevant features have been described by Karin *et al.*(2003) and Whaig*et al.*,1997). Starch has been studied by various techniques to elucidate some of its physical properties, such as *in situ* SAXD(Small Angle X-ray Diffraction), WAXD(Jenkins and Donald, 1997), SEM, NMR, AFM and TEM(Cornnejols and Perèz,2010) and impedance spectroscopy, among others (WawroKazimierczak, 2008; German*et al.*, 2012).

The above underscores the relevance**,** challenges and necessity to understand the physical, chemical and material properties of starch biopolymers from *D.R.* sources in sub-saharan Africa. It also underlines the importance of correlation studies within and outside Africa of the properties of *D.R.* species. In this work the results from proximate composition, material properties, mineral composition, microstructure and X-ray diffraction studies of starch have been analysed fort hree local varieties of*D.R.*, namely, *Giwa (G), Lagos (L) and Sule (S)*). The results have been correlated with similar *D.R.* species' properties and evaluated for suitability in relevant starch industries.

B. Experimental

1. Sample.

Three species of*D. R.*, i.e., G, L and S were harvested from Pmazi village in Bosso,Minna, Niger state, Nigeria. They were harvested fresh from the farm and a month later extraction of starch was carried out.

2. Specimen preparation

Each tuber of the yam cultivars was weighed in a top loading balance before being peeled and reweighed. This was followed by cutting in pieces and blending with 100ml of distilled water using electrical blender. It was followed by sieving with five litres of distilled water which was allowed to settle for about ten minutes and decanted. Decantation was repeated three times. The starch collected was then spread on a clean plastic tray and allowed to dry at room temperature for about 24h. The dry starch was reweighed and the percentage starch contained in each tuber was determined.

3. Data Collection

Three specimens of each sample were subjected to X-ray diffraction to ensure consistency and repeatability of results. The measurements were carried out with a Philips X'pert pro working at 30

mA, 40 kVin a continuous scanning mode in reflection-transmission mode at 0.0670° 2Θ step size in the 2Θ range 5.07 to 8.96° with Cu $k_{\alpha 1} = 1.5405\ A^o$ at 25°C and Cu $k_{\alpha 2} = 1.54443\ A^o$.

Specimen starch powders were gold-sputtered and analysed in a scanning electron microscope, ESEM 30, Philips, Kassel, Germany at an accelerating voltage of 2 kV.Particle size distributions were determined by laser light diffractometry using a dry feeder (Malvern 2600C, Malvern Instruments, Worcestershire, U.K.). The feeder was set at a pressure of 400 kPaand the injector to a pressure of 6 kPa.The focal distance was 300 mm and the measuring time was 25-35 s. The mean particle size was determined in quadruplicate.

The apparent particle densities of specimens of all equilibrated starches were determined by helium pcnometry(Acupye 1330,micrometrics, Norcross, GA, USA) in triplicates (Picker and Mielck(1996).

Bulk and tap densities were determined in a 250 ml cylinder suing a volumeter(stampfvolumeterStav 2003, J.Engelsmann AG, Ludwigshafen, Germany). Determinations were also made in triplicate according to the European pharmacopoeia (EP, 2007).

Proximate composition analysis for ash and lipids contents was carried out according to*Association of Official Analysis Chemists* AOAC(2000)methods. Protein content was estimated from the nitrogen content determined by elemental analyses based on a conversion factor of 1.25(Gebre-Mariam and Schmidt, 1998). The phosphorus content was determined from the starch ash by mixing the starch with 1%(w/w) sodium carbonate and ignited in a furnace at 550°C for 6h.The phosphorus content in the starch was determined colorimetically based on the method described by Murphy and Riley(1962).The amylose content was determined colorimetically using the method described by William *et al*.(1970).All determinations were done in triplicate and the results were presented as mean and standard deviations.

Powder flowability:The flowability of the starches wasassessed using the Hausner ratio and the Carr index (Carr, 1965).The Carr index was calculated as followings:

$$\text{Carr index} = \text{Compressibility} = \frac{\text{tap density - bulk density}}{\text{tap density}} \times 100$$

The flow rate of the starch powders were determinedusing a steel funnel on a Pharmatest flow rate apparatus (Sartorius Pharmatest, Apparatebau GmbH, Hainburg, Germany) with an orifice of 15 mm. All determinationswere performed in triplicate.

Swelling power and water binding capacity: Swelling power and solubility: The swelling power at room temperature (27˚C ± 2 ˚C) was determined using the method described by Leach *et al*. (1959), whilethe water binding capacity was determined using the method of Ring (1985). All determinations were done in triplicates.

Similarly, elemental analysis and microstructure were carried out on the samples using Rigaku Supermini WD-XRF, 50 kV /200 W using three techniques for complementarity and validation purposes to cover trace concentrations, i.e., SEM-EDX (Carl Zweiss EVO 40 EP, 30 kV)/XRF/PIXE.

C. Results and Discussion

1. Proximate composition of *D.R.* starches

Table 1presents the determinedparameters of the starches with sample S having the highest moisture content in the order S>L>G. Their protein/crude fat/total ash/fibreand carbohydrate contents are similar. The values of their amylose contents are also similar with G being slightly higher.

Table 1: The proximate composition of *Dioscorea* starches

Starch	Moisture content (%)	Crude protein (%)	Crude fat (%)	Total ash (%)	Crude fibre (%)	Crude carbohydrate (%)	Amylose content (%)
Lagos	9.67	1.23	0.385	1.06	1.08	86.596	23.06
Giwa	9.58	1.27	0.426	1.03	1.10	86.609	23.16
Sule	9.98	1.36	0.439	1.09	1.13	86.022	22.86

The work of Odeku and Picker-Fryer(2007) on *D.R.* species showed higher amount of moisture (11.96±0.06%) and amylose (28.830±0.65%) contents, compared to the average value obtained for the same parameters in this work. However, the amounts of crude proteins, lipids and ash reported in their work (0.28±0.08%, 0.02±0.01% and 0.015±0.01%), respectively, are much smaller than our results. In the case of phosphorus determined from proximate analysis in their work (0.022±0.001%),it is lower than the value obtained in this work (0.028±0.002%).Work on four *D.R.*species carried out in Ghana(Ransford, 2012) determined moisture, ash, crude protein, crude fat, crude fibre and carbohydrate contents as(w/w%) 7.22 to 7.82, 0.24 to 0.86,~1.31,~ 0.04, 0.1 to 0.15 and 40.13 to 91.06, respectively; amylose and amylopectin were reported as(%) 27.48±0.47 to 31.55±0.47 and 68.45±0.47 to 72.52±0.47, respectively.The low moisture content determined for the species is far below the threshold of 13%(w/w)(Odeku and Picker-Fryer, 2007) which makes them safe for storage.

2. Material Properties

The results of material properties determined for the *D.R.* species are presented in Table 2.

Table 2: Material properties of *Dioscorea* starches

Starch	Particle size (µm)	Particle shape	Apparent particle density (g/cm^3)	Bulk density (g/cm^3)	Tapped density (g/cm^3)	Carr's Index (%)	Angle of repose (^{o})	Swelling Capacity (ml)	Water binding capacity
Lagos	3.54	Oval- angular	1.59	0.509	0.635	19.84	65.60	1.20	0.57
Giwa	3.59	Oval	1.57	0.599	0.790	24.17	57.00	1.29	0.67
Sule	3.19	Oval- Oblong	1.49	0.506	0.715	28.81	65.90	1.19	1.20

All the species have small particle sizes. Sample G has higher particle size, followed by L, S being the smallest. The particle shapes are generally uniform and oval, while the apparent/bulk/tap densities are all similar. The values of particle sizes reported by Odeku(2012) and Odeku and Picker-Fryer(2007) are much higher($29.85\pm0.17\mu$m, $18.68 \pm 0.85\ \mu$m) when compared to those reported in this work. Figure 1(A to C) shows the microstructure of the surfaces of the *D.R.* species at magnification of x 200.On the other hand, the average particle densities reported by Odeku and Picker-Fryer(2007) (1.53 g/cm^3) are almost the same as that of this work. However, the values of bulk and tap densities reported in their work are higher. The Carr's index for *Lagos* species is the lowest and indicates fair flowerbility whereas *Sule*and *Giwa*have poor flowerbility (but higher compressibility) due to their higher values (Anisko and Piroska*et al,* 2014;Odeku and Picker-Fryer, 2007).The poor flowerbility is due to strong force of cohesion between starch particles which is reinforced by the very small particle sizes providing high surface areas that promote interparticle attraction. These parameters are relevant for application as pharmaceutical excipients.

The work of Otebayo*et al.*(2005) on six species of *D.R.*reported average grain sizes in the range 18.4 ± 5.0 to $40.9\pm3.0\ \mu$m. Riley *et al*(2006) on the other hand, reported polygonal and rodlike shapes for the grains with mean diameters of 27.33 μm.The results indicate grain sizes that are much higher

and wider in range, with the shapes generally in conformity with literature on *D.R.* species as reported in the work of Ransford (2012). Ransford (2012), working on four *D.R.* species in Ghana reported mean grain sizes in the range7.10 to 66.99 µm, swelling power and water binding capacities (%) as 1.05±0.04 to 12.48±0.02 and 1.73±0.26 to 1.02±0.25. Our results therefore show grain sizesthat are much smaller and narrower which has implications for industrial applications such as the paper industry. This is also true of the swelling power and water binding capacities which are both larger and wider in range, and larger and narrower in range, respectively.

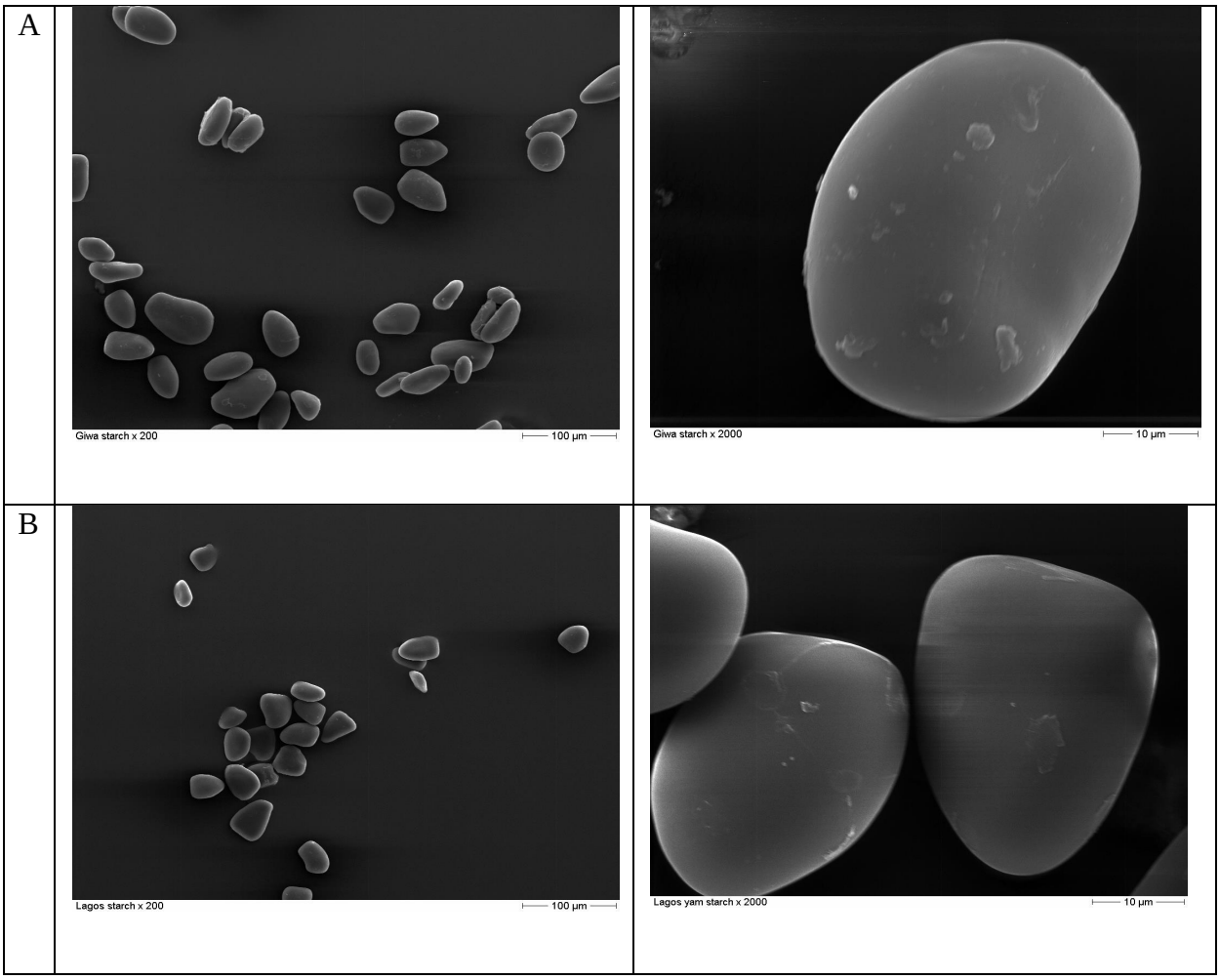

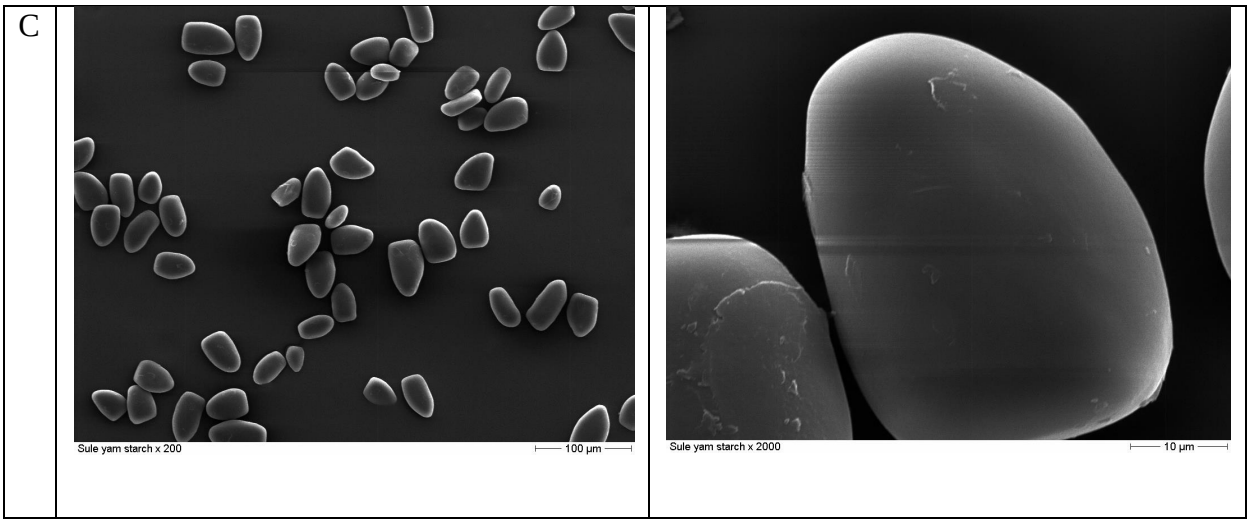

Figure 1. SEM of the different cultivars of yam starches: A,Giwa; B,*Lagos*; C. *Sule*

3. Elemental analysis

Qualitative EDX results ran on samples G, L and S showed the presence of the elements C, K, Al and O, while Cu was observed in sample L in addition. Qualitative XRF resultsalso revealed the presence in sample G of the elements K, Ca, Mn, Zn, Fe, Ru, Cu, Mo, Ni, Br, Sr, As, Cr Se and Co. Samples L and S have similar elemental compositions, except that Ca is absent in both. PIXE results show presence of the elements Mg, Al, Si, P, S, K, Fe, Zn in sample G; Mg and Zn are missing in samples L and S. The most significant results are the quantitative values(w/w%) obtained from XRF with elemental concentrations of K(17.29$\pm$2.34) and Ru(26.78$\pm$3.75)constituting major concentrations in G;Sample L has K(17.28$\pm$2.54), Ru(18.37$\pm$3.55) and Mo(10.26$\pm$1.39); whereas sample S has K (11.48$\pm$2.10) and Ru(27.71$\pm$4.30). The presence of Ru has not been reported,but the fact that it is present in major concentrations in all the *D.R* .species make the results not only unique but important owing to the relevance of Ru (as the mineral Rutile(TiO_2)) in the manufacture of optical components.Those present in minor concentrations in sample G are Mo(8.85$\pm$1.09); Cu(8.82$\pm$0.48) in sample L and Cu(8.08$\pm$0.44) in sample S. The concentrations of Cu are almostthe same in all the *D.R.* species. Further, the amount of P determined from PIXE (w/w%) (0.022$\pm$0.002-G,

0.035±0.002-L and 0.024±.002-S) and that reported using the method of Murphy and Riley (1962) for *D.R.* species found in south west Nigeria are in good agreement(0.022±0.001) (Odeku and Picker-Fryer(2007). Though the values reported in our present work areslightly higher. Qualitative work reported on mineral compositions of *D.R.* species found in south west Nigeria by Odebumi*et al.*(2007) found the elements Mn, Fe, Zn, Ca and Mg, all of which were detected in our samples. Work of Polycarp *et al.*(2012)on *D.R.* species show the presence of elements (w/w%)K (0.475±0.003), Na (0.070±0.004),Ca (0.100±0.005), Mg (0.035±0.005) and P(0.158±0.017), all less than the values for the present work, particularly, the K. However, the P concentrationreported is much higher than our results and those reported in literature (as mentioned elsewhere).Na was not found in our work.Tubers are associated with high P content(Aprianita, 2010)and haveenormous implications for many physical properties of starch such as viscosity, gelatinization temperature, transparency, among others. These variations have been attributed to geographical and botanical origins, amongst others.

4. X-ray Diffraction

Composite XRD patterns using XPowder program (Martin, 2008) for the three D.R.species are shown in Figure 2 on a normalized relative intensity scale for the species.It is observed that the positions of the central/largest peaks are all coincident and the reflection intensities show good counting statistics compared to those reported in literature. Sample S has the most intense peak amongst them.Table 3 is a summary of the peak($2\Theta^{o}$) positions, crystallinity (%) and the proposed crystal typesof the *D.R.* species.

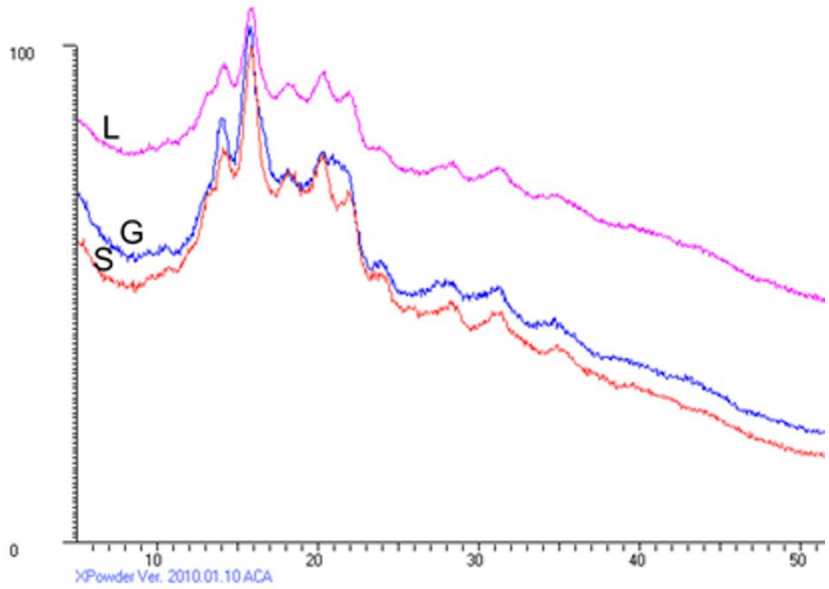

Figure 2.Composite XRD patterns of *Lagos(L), Giwa(G)* and *Sule(S)* on a normalized intensity scale.

Table 3.Summary of peak (2Θ) positions (most intense), crystallinity and crystal type forthree *D.R.* species.

Starch species	**2Θ(º)**	**Crystallinity (%)**	**Crystal type**
Sule	5.43,14.03,15.34,17.26,19.82,22.16,24.05	18.75±0.75	B
Giwa	5.27,15.14,17.02,21.96,23.93,34.37	18.25±1.25	B,C
Lagos	5.37,14.01,15.11,17.12,19.91,22.14,23.85	22.25 ±5.75	B,C

There are a number of discernible peaks in the diffractograms of some of the *D.R.* species compared to those reported literature (Riley, 2006; Ao*et al.*, 2007;Yuan *et al.*, 2007;Maria *et al.*, 2010). The strongest peaks occur at 17.02 º,17.12 ºand 17.25 º for samples G, L and S, respectively. Comparison

of the data with those reported at the same wavelength in literature show that they are consistent with reported diffractograms obtained from different starch sources, including*D.R.* species.

Phase composition analysis shows that all the *D.R.* species belong to yam starches. However, based on the reference patterns (ICDD): 00-052-2246(lentil starch), 00-052-2248(yam starch), 00-052-1802(maize starch) and 00-052-2247(potato starch) some of the 2Θ values could be related to these patterns. One of the peaks (17.23^o) of sample G for example, corresponds thatreported in maize starch (Maria *et al.*,2010) while the peak at 17.2^o corresponds to that reported for potato(Yuan *et al.*, 2007) in samples L and S. This is validated by the reference patterns. *D.R.* has been found to exhibit the open hydrated patterns of B-type typical of tuber starches with strong diffraction peaks at ~5.8^o, a single sharp peak at 17.5^o and two identifiable peaks at 22.5^o and 24^o(Riley, 2000). These figures indicate that the species belong to the *D.R.* family and the crystalline types may be hypothesized to be a mixture of B and C polymorphs (Odeku and Picker-Fryer,2007,2009) because the FT-Raman spectra of *D.R.* are similar to that of maize starch which couldfurther lead to a similarity of molecular structures.XRD patterns of *D.R.* have been shown to vary from B to C-type(Odeku, 2012). Samples L and G may therefore be mixtures of B- and C-crystal types while S may be B-type. The computed relative crystallinities are as presented in the table 3determined from XPowder program(Martin,2008) and show that sample G has the lowest crystallinity of the species.Thesevalues are within the range reported for starches of various origins, 15-45% (Napaporn*et al.*, 2001) and indicate that some of the starches have moderate crystallinity.

The crystallite sizes (D) were analysed by the XPowder program using Debye-Scherer equation ($D = \frac{k\lambda}{10.\beta Cos\theta_\beta}$, (nanometers),with k=1; whereβ, λ and θ_β are the fullwidth at half maxima(FWHM), wavelength and Bragg peak, respectively).Values (for 2Θ=16.34^o,16.47^o) for sample G are 2.4 and

2.3 nm, respectively; whereas for sample L, we have (2Θ=17.039°,17.172°) crystallite sizes of 2.5 and 2.4 nm, respectively,after$k_{\alpha 1}$, broadening correction and neglecting strain. The results indicate that Samples S and G have similar crystallite sizes. The crystallites are very small hence the broadenings observed in the XRD patterns which are attributed to sample size effects only (after instrumental correction).The small size of the crystallites explains the modest crystallinities of the species.Table 4 is a summary of the profile parameters for calculating the crystallite size. Theasymmetry, shape factor and instrumental Cagliotti coefficients for selected 2Θvalues based on simple Gaussian analysis are shown.

Table 4.Profile parameters and Instrumental Cagliotti coefficients

Species	**2Θ°**	***FWHM(2Θ°)**	**Crystallite size(nm)**	**Assymetry**	**Shape factor**	**Instrumental Cagliotti Coefficients**		
						U	**V**	**W**
Giwa	16.34	3.79	2.5	-0.31	0.63	0.014680	0.005190	0.005800
Sule	17.04	3.56	2.4	-0.33	0.61	0.014680	0.005190	0.005800
Lagos	15.87	3.02	3.0	1.50	0.51	0.014680	0.005190	0.005800

*All FWHM are after $k_{\alpha 2}$and Instrumental broadening corrections.

5. Full Profile Fitting, Refinement and Indexing

Whole(and single peak) profile fittingsfor samples S, G and L and subsequent refinement were carried out with GSASIIprogram (Von Dreel and Torby, 2010) for peak positions, intensity and background, while the peak widths were fitted using Gaussian and Lorentzian parameters as shown in Figure 4(A–F). Figure 4(A, B) for sample Grepresentssingle peak fit and Gaussian and Lorentzian fits for instrumental functions. The plot shows the resolution curves corresponding to values of the Gaussian (U, V, W), and Lorentzian X, Y coefficients. The '+' marks show the individual values based on sigma and gamma values for the peaks (i.e., deviations).The discontinuities seen in the data points are bad reflections which were omitted during refinement. The green continuous line is the fit while the blue lines are the data points. The overall fitting parameter based on weighted agreement factoris $R_{wp} = 1.49\%$. The fitting is best in sample G but not so perfect in L. The agreement factors aregenerally low due to the high background. Similar analysis has been made for the other samples. All the instrumental and sample widths plots generally follow the same pattern as reported in literature, the FWHM falls with increasing 2Θ. The Gaussian+Lorentziangenerally have the same features and shows that it is significant for sample L.

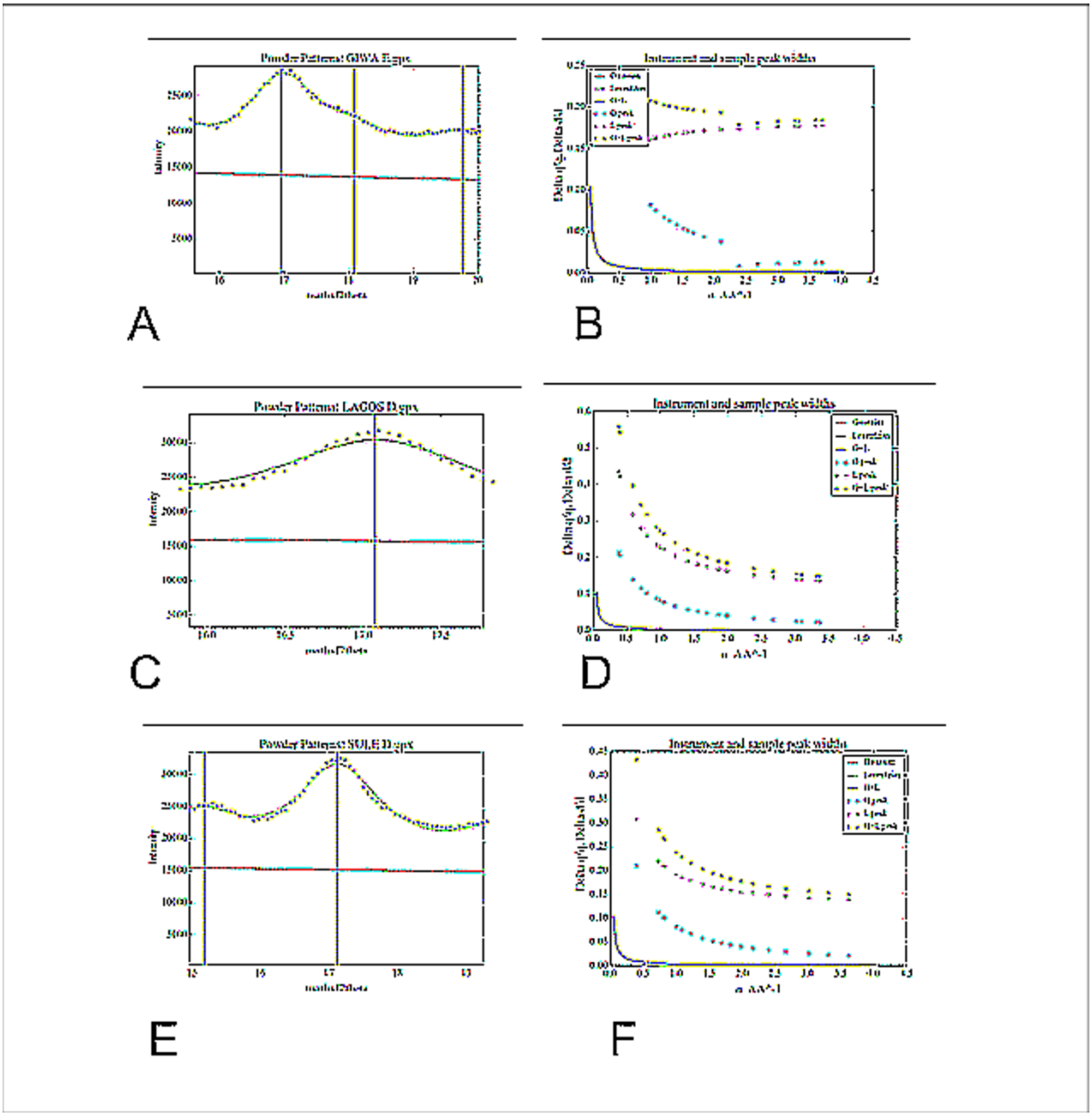

Figure 4. Profile fitting for peak of strongest intensities and Gaussian and Lorentzian fitsof instrumental profilesfor samples G, L and S. The fitting for L is shown in Figure 4(C,D) with $R_{wp} = 2.66\%$ together with the corresponding Gaussian and lorentzian broadenings. Figure 4(E, F) profile fitting for one peak and Gaussian and Lorentzian fits of instrumental profiles for sample L.The agreement factor is $R_{wp} = 1.75\%$.

Indexing was carried out on the XRD data by including peaks of small intensitiesin some cases to obtain at least M20 required for successful indexing. Table 5 shows the indexing results usingCMPR program (Brian, 2010) and the refined lattice parameters of the unit cells. All the cells were indexed on orthorhombic lattice with fairly high M(20) and F values for six strong reflections.

Table5. Indexing results based on orthorhombic symmetry and lattice parameters for three species of *D.R.*

Species	**h k l**	**F(6)**	**M(6)**	**a**Å	**b** Å	**c** Å	$\alpha°$	$\beta°$	$\gamma°$
Lagos	120	80	20	8.0635	16.893	7.449	90	90	90
	111								
	031								
	200								
	002								
	132								
Giwa	200	200	50	11.742	15.689	6.245	90	90	90
	111								
	121								
	031								
	230								
	221								
Sule	110	224	56	7.624	11.158	5.803	90	90	90
	001								
	011								

120	
021	
030	

6. Conclusion

Three starch samples were studied from the *dioscorearotundata* species:*Giwa*, *Sule and Lagos.* Proximate analysis shows that the moisture and amylose contents are relatively lower than reported. Similarly, carbohydrate found in this work is relatively high. The low moisture content implythe species have stability/longer storage time.

The particle sizes of the *D.R.*species are generally similar and oval in shape. Grains of relatively smaller and narrower distribution of sizes were obtained. The shapes and small sizesof the grains may have implications for applications in the paper, textile and cosmetic industry.

Elemental compositions of the *D.R.* species are generally the same with the most important finding being the presence of the element Ru, which is found in major concentrations (up to ~27%) and K (up to ~21%). The element Ru is appliedin the electronic industry as an optical component. The work suggests the presence of some important mineral deposits in the soil.

The starches exhibited the characteristic features of tuber starches and are all of the B-type, except *Giwa* and *Lagos* which are mixtures of B- and C-types. The crystallinity varied between 18-29% and while thecrystallite sizesare 2.5, 3.0 and 2.4nm, respectively, for *Giwa*, *Lagos* and *Sule*) and reflect the broadenings observed in the XRD patterns which are attributed to sample size. All the species of *D.R.* were indexedon orthorhombic lattice.With appropriate modifications of the native starch, *Lagos*

may find applications as pharmaceutical excipients and al, the species exhibit relatively competitive grain sizes that may compete with maize potato starches.

References

Amani, N. G., Rolland-Sabaté, A. K. A. Colonna, P.(**2005**). ''Stability of yam starch gels during processing'', African Journal of Biotechnology, **4**, 94-101.

Cornuéjols, D. and Pérez, S. (**2010**). ''Starch: a structural mystery'', science in school, issue 14, 2010.

Frost , K., Kaminski, D., Kirwan, G., Lascaris, E., Shanks, R. (**2009**). ''Crystallinity and structure of starch using wide angle X-ray scattering'', Carbohydrate Polymers, **78,** 543–548.

Germán Ayala, G., Ana Agudelo, A.,Rubén Vargas, R.(**2012**). ''Effect of glycerol on the electrical properties and phase behavior of cassava starch biopolymers'',*Dyna*, **79**, 138-147.

Jenkins, P. J. and Donald, A. M. (**1997**). ''Breakdown of crystal structure in potato starch during gelatinization'' J. Appl. Polym. Sci., **66**, 225–232.

Karin, K. (**2003**). ''Aqueous-based amylose-rich maize starch solution and dispersion: a study on free films and coatings, Ph.D dissertation, university of Helsinki.

Martin, J. D. (**2008**). A Software Package For Powder X-Ray Diffraction Analysis, Qualitative, quantitative and microtexture, Version 2004.04.82.

Napaporn, A., Sujin, S., Pavinee, C., Saiyavit, V. (**2001**). ''Study of Some Physicochemical Properties of High-Crystalline Tapioca Starch'',Starch/Stärke, **53**, 577–581.

Odebunmi, E.O., Oluwaniyi, O. O, Sanda, A. M. and Kolade, B. O.(**2007**). ''Nutritional Compositions of selected tubers and root crops used in Nigerian food preparations.'' International Jour. Chem., **17**, 37-43.

Polycarp, D., Afoakwa, E. O., Budu, A. S. and Otoo, E. (**2012**). ''Characterization of chemical composition and anti-nutritional factors in seven species within the Ghanaian yam *(Dioscorea)*germplasm'', International Food Research Journal, **19**, 985-992.

Riley, C. K. , Wheatley, A. O., and Asemota, H. N.(**2006**). ''Isolation and Characterization of Starches from eight *Dioscorea alata* cultivars grown in Jamaica'', African Journal of Biotechnology, **5**, 1528-1536.

Satin, M. (**2006**). ''Functional properties of starches FAO Agricultural and Food Engineering Technologies Service,www.**fao.org**/ag/magazine/pdf/**starches**.pdf. Accessed 20th October, 20012.

Von Dreel, R. B. and Torby, B. H. (**2010**). General Structure Analysis System(GSAS)–II. Argonne national Laboraroty, 2010.

Waigh, T. A., Hopkinson, I., Donald, A. M., Butler, M. F., Heidelbach, F. and Riekel, C. (**1997**). ''Analysis of the native structure of starch granules with X-ray microfocus diffraction'', Macromolecules, ***30***, 3813-3820.

Wang, T. L., Bogracheva, T. Y. and Hedley, C. L. (**1998**). ''Starch: as simple as A, B, C?'', Journal of Experimental Botany, **49**, 481–502.

Wawro, D., Kazimierczak, J.(**2008**).'' Forming conditions and mechanical properties of potato starch films'', fibres & textiles in Eastern Europe, **16**, 106-112.

Aprianita, A. (**2010**). Assessment of underutilized starchy roots and their tubers for their application in the food industry. M.Sc.Thesis, Victoria University, Australia.

Ransford, N.A.A.(**2012**).Comparative Study on the properties of yam(*Disocorea Rotundata*) varieties in Ghana: A Case Study in Asante Mampong, Unpublihed M.Sc., thesis, Kwame Nkrumah University of Science and Technology.

EP (**2007**).Directorate for the Quality of Medicines of the Council of Europe: European Pharmacopoeia, 5th ed., Strasbourg.

A.O.A.C.(**2000**). Official Methods of Analysis, 17th ed. Association of Official Analysis Chemists (A.O.A.C.), Washington, DC, USA.

Gebre-Mariam, T. and Schmidt, P.C.(**1998**).''Some physicochemical properties of Dioscorea starch from Ethiopia''.Starch/Stärke,**50**, 241–246.

Murphy, J. and Riley, J.P.(**1962**).''A modified single solution method for determination of phosphate in natural water''.Anal. Chem. Acta,***27***, 31–36.

Williams, P.C.,Kuzina, F.D. and Hlynka, I.(**1970**).''A rapid calorimetric procedure for estimating the amylose content of starches and flours''.Cereal Chem.

Picker, K.M. and Mielck, J.B.(**1996**).''True density of swellable substances at different relative humidities: a new approach to its determination''.Eur. J. Pharm. Biopharm., ***42***, 82–84.

Carr, R.L.(**1965**).''Evaluating flow properties of solids''.Chem Eng., ***72***, 163–168

Leach, H.W., McCowen, L.D. and Schoch, T.J. (**1959**). ''Structure of the starch granule. I. Swelling and solubility patterns of various starches''. Cereal Chemistry**36**: 534

Ring, S. G. (**1985**). Some studies on gelation. Starch, **37**, 80–87.

Anikó, S., Piroska, S-R., János, B., Péter,K.Jr., Miklós, N., Roland, P., Attila J. K., Klára, P-H.(**2014**). Characterization and Utilization of StarchesExtracted from Florencia and Waxy Maize Hybrids for Tablet Formulation: CompactionBehaviour and Tablet Properties.American Journal of Plant Sciences**, 5,** 787-798.

Assessment of Wind Energy Potential In Minna, Niger State, Nigeria

GIMBA, Michael[1], OYEDUM, Onyedi David [2] EICHIE, Julia Ofure[3]

Department of Physics, Federal University of Technology, P.M.B. 65, Minna, Niger State, Nigeria
**Corresponding author E-mail: michaelgimba@futminna.edu.ng*

Abstract

This study assesses the wind energy resources in Minna, Niger State, Nigeria by reviewing the existing literature on the subject matter and also evaluating the wind potential in Minna. Five years (2012–2016) wind speed data obtained from the Federal University of Technology Minna, Physics department weather monitoring station at Bosso campus, were used in the study. Weibull two-parameter statistical model was employed in the analysis. Assessment of the wind-energy resources in the study location reveals that wind speed in Minna is from 0.49ms^{-1} to 1.61ms^{-1} at 4m above ground level, while wind energy potential in Minna has wind power density which varies from 0.10Wm^{-2} to 5.27Wm^{-2} at 4m above ground level. Thus, Minna is not suitable of large-scale and small-scale wind power generation for electricity because of the poor wind potential at surface level. However at higher heights of 30m above ground level, having wind power density of 160 Wm^{-2} will be suitable for pumping water using wind power.

Keywords: *Weibull Distribution Function; Wind Speed; Wind Power Density.*

Introduction

The energy demand for electricity and agricultural purposes is grossly inadequate and this poses a serious challenge to the nation. The conventional fossil energy is fast diminishing from the oil reserves and the environmental pollution by emission of carbon monoxide and the general health hazard of fossil fuel is of concern to the world (Ohunakin, 2011).
The available power as at 2007 was 4914MW, while presently approximately 6000MW is being supplied, which is still grossly inadequate for the teaming population of Nigeria (Maiyama *et al.*,2013; Nigeria Electricity Hub, 2017).

About 60 million Nigerians spend 1.6 trillion naira on generators annually. Companies and Businesses have relocated from Nigeria to neighbouring countries due to the inability of the national electricity power supply to meet their demand, while homes across the nation are forced to adapt to the epileptic power supply, or in some cases, total blackout (Olaoye *et al.*, 2016).

The commonly used source of power generation in Nigeria are hydro and thermal power generation which are burdened with a lot of issues (such as broken down turbines, bunkering of gas pipeline and general infrastructural problem) which have to insufficient and poor power generation.
Nigeria is an energy-rich nation with both non-renewable and renewable energy (Akinbami, 2001). The country is endowed with wind energy resources which have not been exploited to generate

power. Nigeria has a wind farm project at Lambar Rimi in Katsina State, which is at an advance stage of completion and has generation capacity of 10MW.
Wind energy can be harnessed for electricity generation, pumping of water, grinding and irrigation farming. The wind energy application suitable for a specific location, solely depend on the wind energy potential of that location (Olomiyesan, 2018).
This study is aimed at assessing the wind energy potential in Minna, Niger State at 4 m above ground level

MATERIALS AND METHOD

Data collection

Wind speed measured at 4 metres above the groud level was used in this study. The data set span for a period of five years (2012 – 2016) and was collected from the Federal University of Technology Minna, Physics Department weather monitoring station at the Bosso campus.

Statistical analysis of wind data

The analysis of wind distribution in the selected sites was carryout using Weibull distribution function. Weibull probability density function, fw(v), and the corresponding cumulative probability function, Fw(v), can be expressed as

$$fw(v)=\left(\frac{k}{c}\right)\left(\frac{v}{c}\right)^{k-1} exp\left[-\left(\frac{v}{c}\right)^{k}\right] \quad (1)$$

$$Fw(v)=1- exp\left[-\left(\frac{v}{c}\right)^{k}\right] \quad (2)$$

where;
fw(v) =Weibull Probability density function

$F_w(v)$ = Cummulative probability function

k = Shape factor (dimensionless)

c =Scale factor (m/s)

v = wind speed (m/s)
Justus *et al.*,(1978) describes how to determine Weibull parameters k and c as,

$$k = \left(\frac{\sigma}{v_m}\right)^{-1.086} \quad (3)$$

$$c = \frac{v_m}{\Gamma\left(1+\frac{1}{k}\right)} \quad (4)$$

Also, c can be determined from the expression given by (Justus *et al.*, 1978):

$$c = v_m \left(\frac{k^{2.6674}}{0.184+(0.816k^{2.73859})}\right) \quad (5)$$

$$\sigma = \left[\frac{1}{N-1}\sum_{i=1}^{N}(v_i - v_m)^2\right]^{1/2} \quad (6)$$

where;

σ = standard deviation

v_m = mean wind speed (ms^{-1})

v_i = observed wind speed (ms^{-1})

N = number of months considered and

$\Gamma(x)$ = gamma function expressed as $\Gamma(x) = \int_0^{\infty}(t^{x-1}\, e^{-t}\, dt)$ (7)

Similarly, the wind power density, P(v), can be expressed either in term of the wind speed or in terms of the Weibull shape and scale parameters, k and c, using the correlation given function (Ohunakin *et al.,* 2011) :

$$P(v) = {}^{1}/_{2}\rho\, v^3 \quad (8)$$

$$P(v) = {}^{1}/_{2}\rho c^3\, \Gamma(1+3k) \quad (9)$$

where:

P(v) = Wind Power Density (Wm^{-2})

v=Wind speed (ms^{-1})

c =Weilbull scale parameter (ms^{-1})

k =Weibull shape parameter (dimensionless)

ρ =Air density at the site, which can be expressed in the form:

$$\rho = \rho o - 1.194\times10^{-4}\times H_m \quad (10)$$

where ρo is the air density value at sea level usually taken as 1.225 kgm^{-3} and H_m is the site elevation in meters.

Results and discussion

The graphic representation of the monthly mean wind speed recorded for the entire study period of five years presented in Figure 1.

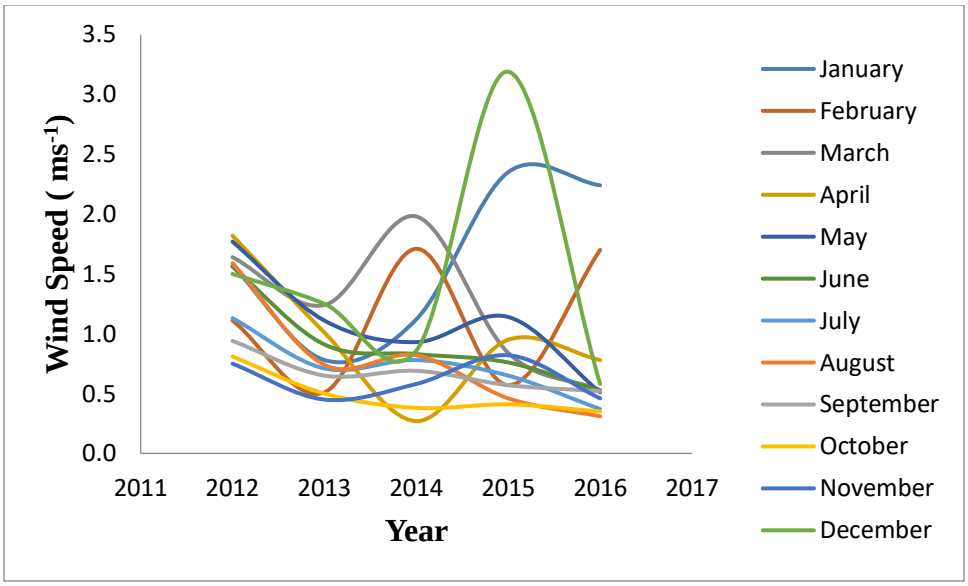

Figure 1: Monthly wind speed for Minna (2012 - 2016).

Figure 1 reveals that wind speeds fluctuate from year to year. During the period under study, the highest monthly mean wind speed recorded was 3.19 ms^{-1} in December, 2015 while the lowest monthly mean wind speed was 0.27 ms^{-1} in April, 2014. The annual mean wind speed recorded for the period of the study was: 0.98 ms^{-1}

Wind speed frequency distribution

The monthly probability density and cumulative distribution derived from the time series data for the whole period are shown in Figures 2 and 3 respectively. The PDF and CDF plots show that all the curves of the monthly wind profiles follow a similar distribution pattern. The variation in shapes of PDF and CDF plots are due to the varying values of the Weilbull parameters c and k. The parameter, c, determines the spread of the distribution, while the shape parameter, k, indicates the peak of the wind distribution.

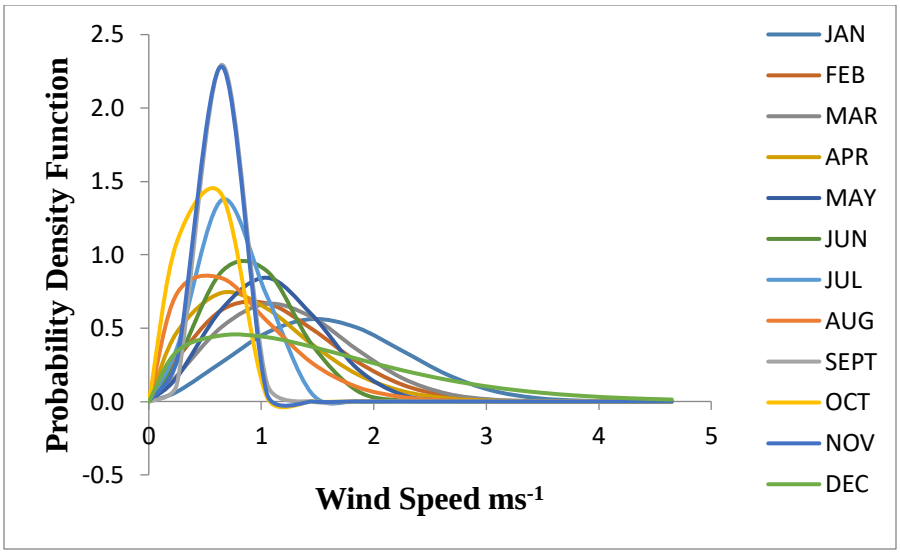

Figure 2: Monthly Wind Distribution for Minna PDF

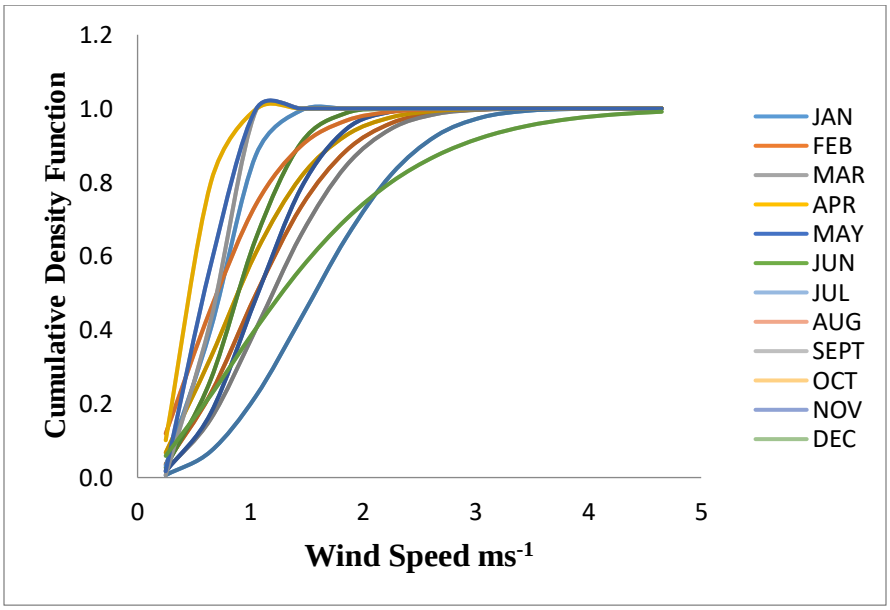

Figure 3: Monthly Wind Distribution for Minna CDF

The plot of the probability density function (PDF) illustrates the fraction of time for which a given wind speed possibly prevails at a location. The peak of the PDF curve indicates the most frequent velocity, whereas the plot of the cumulative distribution function is used for estimating the time for which wind speed is within a certain speed interval. The plots of the monthly PDF shown in Figures 2 and 4 demonstrate that the wind profiles for the study location and months follow the same distribution pattern. It can further be noted that the PDF plot for Minna shows a minimal data.

Similarly, the CDF plots in Figure 3 show that at Minna, most of the data are not in the wind speed range of 0.8 and 2.4 ms^{-1} and others falls below.

The annual probability and cumulative density functions obtained using the Weibull distribution function for Minna are shown in Figures 4 and 5.

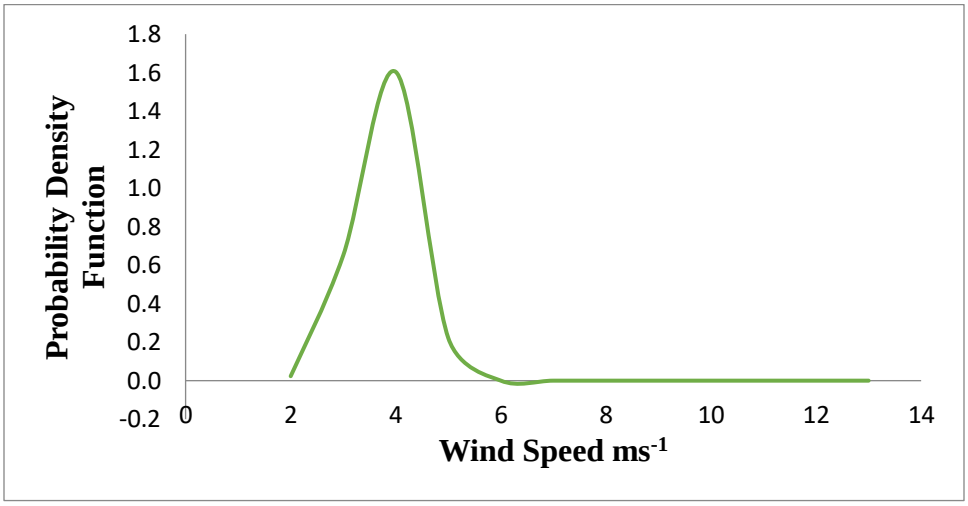

Figure 4: Annual PDF for Minna

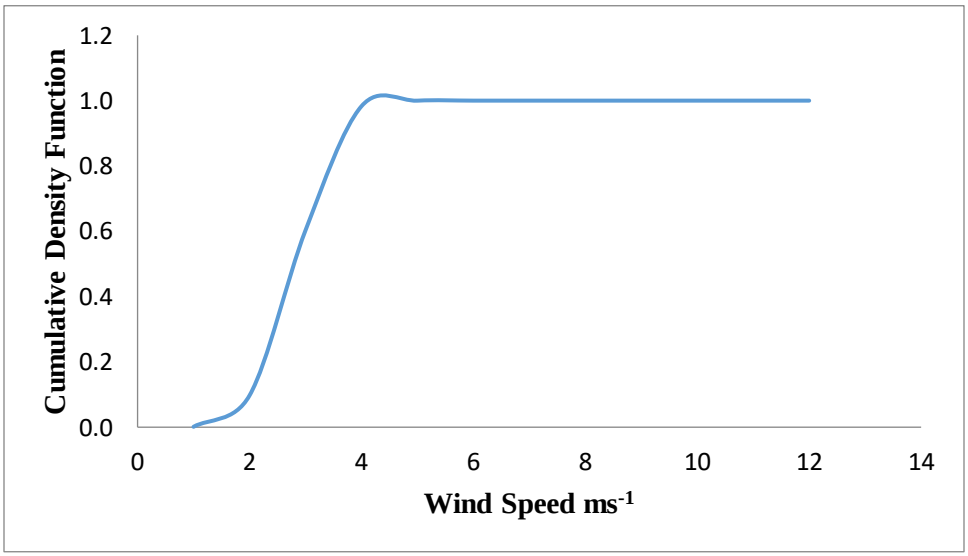

Figure 5: Annual CDF for Minna

From Figure 4, it can be noted that the annual mean and most frequent wind speeds for Minna is about 2.3 ms^{-1}. The cut-in wind speed which contributes to the generation of electricity from wind in most new wind turbine designs is about 2.5 ms^{-1} and above. However, if wind turbines with cut-in

wind speed of 3.5 ms^{-1} is selected for use in the site, it can be observed from the CDF curve in Figure 5 shows that, the CDF value is 2.8 ms^{-1} wind speed. Thus, Minna is not viable for wind power generation. This is in agreement with the findings of previous works (Adaramola and Oyewola, 2011).

Wind power density

The result of analysis of monthly and annual variations of the annual mean wind power densities calculated from the measured wind data and those obtained by using Weibull parameters for Minna is shown in Figure 6.

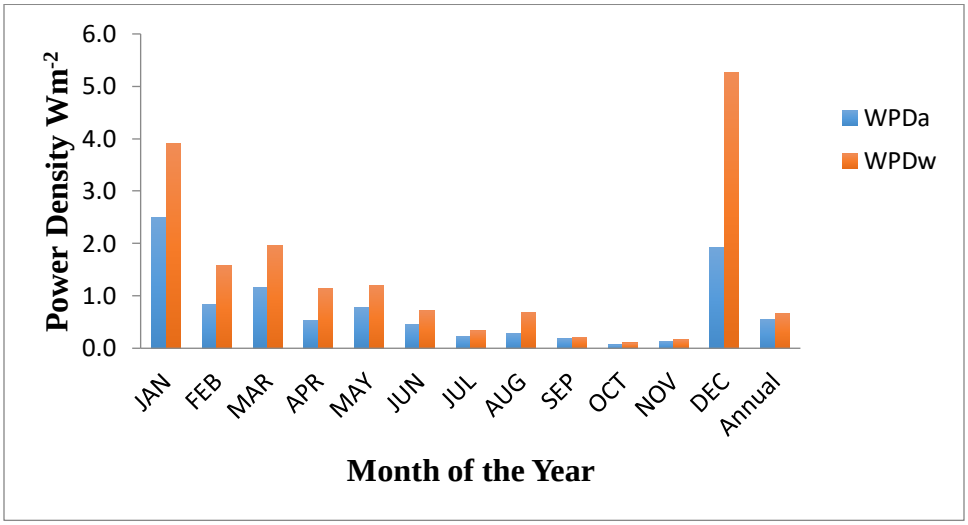

Figure. 6**:** Plot Showing monthly Variations of the Power Density Distributions for Measured and Weibull Values for Minna.
NOTE: WPDa is the actual Wind Power Density; WPDw is the Weilbull Wind Power Density

The monthly variations of the actual and Weibull power densitiy for the Minna in Figure 6 indicates that the estimated Weilbull wind power density are slightly higher than the actual power density for every month of the year and on annual basis. This supports the assertion that, 'Weilbull probability distribution is suitable for analysing and interpreting data of measured wind speed (Olayinka, 2011) and is not discriminative between location with high and low mean wind speeds. For Mjnna the monthly Weibull WPD is in the range of 0.1 – 5.3 Wm^{-2}, which falls into the Wind Classes of 1 of the PNL wind classification (Olomiyesan *et al*., 2017). The estimated annual wind power density for Minna is 0.66 Wm^{-2}. Thus, Minna does not have a good prospect for wind power generation.

Conclusion

In this study, the predictive ability of Weibull distribution function in analyzing wind speed data was assessed in Minna with mean wind speed. The results of the analysis show that the Weibull function is suitable for analyzing measured wind speed data and for predicting the wind-power density in a location. Other relevant findings of this study can be summarised as follows:
i. The annual mean wind speed recorded during the period of the study is: 0.98 ms^{-1}

ii. The annual values of the most probable wind speeds and the maximum energy carrying wind speeds are respectively 0.56 and 0.66 ms^{-1}.
iii. Based on the estimated annual values of the Weibull wind power density, the wind energy resource in Minna can be classified as class 1 in the PNL wind classification. Therefore, does not have a good prospect for wind energy for electricity generation.

References

Adaramola, M. S., & Oyewola, O. M. (2011). Wind Speed Distribution And Characteristics In Nigeria. 6(2), 82–86.

Akinbami, J. K. (2001). Renewable Energy Resources And Technologies In Nigeria : Present Situation , Future Prospects And Policy. (Wced 1987), 155–181.

Justus, C,G., Hargraves, W.R., Milhail, A., & Grabber, D.(1978). Method for estimating wind speed frequency distribution. Journal of Applied meterology, 17(3), 350-353'

Maiyama, B. A., Argungu, G. M., & Momoh, M. (2013). Assessment Of Wind Energy Potential For Electricity Generation In Sokoto,Nigeria. 2(6), 601–614.

Nigeria Electricity Hub, https://www.nigeriaelectricityhub.com/2017/03/10/electricity. Retrieved 29 Nov. 2018.

Ohunakin, O S, Adaramola, M. S., & Oyewola, O. M. (2011). Wind energy evaluation for electricity generation using WECS in seven selected locations in Nigeria. Applied Energy, 88(9), 3197–3206. https://doi.org/10.1016/j.apenergy.2011.03.022

Ohunakin, Olayinka S. (2011). Assessment of wind energy resources for electricity generation using WECS in. Renewable and Sustainable Energy Reviews, 15(4), 1968–1976. https://doi.org/10.1016/j.rser.2011.01.001

Olaoye, T., Ajilore, T., Akinluwade, K., Omole, F., & Adetunji, A. (2016). Energy Crisis in Nigeria : Need for Renewable Energy. 4(1), 1–8. https://doi.org/10.12691/ajeee-4-1-1

Olomiyesan, B M, Oyedum, O. D., Ugwuoke, P. E., & Abolarin, M. S. (2017). *Assessment of wind energy resources in Nigeria – a case study of north-western region of Nigeria*. *5*(2), 83–90. https://doi.org/10.14419/ijpr.v5i2.8327

Olomiyesan, Boluwaji Moses. (2018). *Performance evaluation of Weibull function for wind data analysis in two selected locations in*. *6*(1), 18–24. https://doi.org/10.14419/ijpr.v6i1.9053

Determination of yearly Degradation Rate of Electrical Parameters of Polycrystalline Silicon (p Si) Photovoltaic module in Minna. Nigeria

AHMADU. Aliyu, 'EZENWORA. Joel Aghaegbunmam , IGWE, Kingsley

Department of Physics, Federal University of Technology Minna, Niger State.

Abstract

There is need for accurate knowledge of degradation rate and lifespan of photovoltaic (PV) module in every location for an effective solar PV power system. Outdoor degradation analysis was carried out on polycrystalline silicon PV module rated 10w using CR1000 software base Data acquisition system (DAS). The PV module under test and meteorological sensors were installed on a metal support structure at the same test plane in the laboratory guarding of Federal University of Technology, Minna . The data monitoring was from 09:00am to 06:00pm hours each day continuously for a period of four years, from December 2014 to November 2018. Annual yearly averages of the performance variables were carried out to ascertain the degradation rate and lifespan of the module. It was observed that open circuit voltage (Voc), short circuit current (Isc), Power(W) ,Maximum current(Imax) A ,and Maximum power(W) has average yearly degradation of 0.286V, 0.004A, 0.024W, 0.276Vmax, 0.0042I,max, 0.0343WmaxDetermination of yearly Degradation Rate of Electrical Parameters of Polycrystalline Silicon (p Si) Photovoltaic module in Minna. Nigeria

Introduction

Photovoltaic solar energy is a form of renewable energy; it can generate electricity by converting the solar radiation and by using the photovoltaic effect. The installation of photovoltaic systems is mainly dictated for optical performance by its geographical context as the location and conception of the sun expose by several factors such as solar irradiation, ambient temperature, humidity, wind, shading and dust accumulation; these factors can accelerate the degradation rate. There is need for accurate knowledge of degradation rate and lifespan of photovoltaic (PV) module in every location for an effective solar PV cells and module due to their exposure to atmospheric parameters such as solar irradiance temperature wind speed relative humidity which depreciate the electrical parameter of the limited lifetime is as a result of several factor that are in play simultaneously, The performance of PV module has been observed to gradually decrease with operation time (Dunlop and Halton, 2006) long time performance of pv module is vital if they have to pay back to the consumer. It is important to investigate the performance parameters of modules

With rapid economic growth and important in living standard, there has been a marked increase in energy consumption in many third world countries. Most countries use fossil fuel. Hydroelectric

power and nuclear power as a source of energy, Nuclear and fossil fue have adverse effect on the environment such as large amount of greenhouse gases emission and pollution from the burning of fossil fuel (Rene, 2005, Azhar and Abdul, 2012)

Since fossil fuel and nuclear power of energy are not renewable, it is necessary to explore other sources of energy that are cost effective especially in the developing countries that rely heavily on imported fossil fuel, Renewable energy such as sunlight. Wind tides and wave can be particularly suitable for developing countries especially in rural and remote areas where transmission and distribution of energy generated from fossil fuel can be difficult and expensive Producing renewable energy locally can offer a viable alternative.

Technology advances are opening up a huge new market for solar power, Even though they are typically poor, use inefficient energy system like kerosene lamp and stoves. Power cost half as such as lighting with kerosene, (Dnke et al, 2010)

The energy conversion efficiency of a PV module or array as a group of electrically connected PV module in the same plane is defined as the ratio between electrical power conducted away from the module and the incidence power of the sun (Rakovect et al 2011)

This conversion efficiency of photovoltaic (PV) module by manufactures is done under standard Test condition (STC) The standard Test conditions are module temperature of 25c Irradiance of 1000W/m2 and Air mass of 1.5.Different PV module technologies now exist in the market these Includes crystalline module such as mono crystalline, polycrystalline and amorphous modules. The module available are rated by manufacture depending on their power output such as 5watt, 10watt, 15watts The choice of the module to use depend on the power output needed by the consumer and its efficiency photovoltaic {PV} modules are often considered as the most reliable elements in PV system . However, photovoltaic module reliability data are not shows on commercial data sheets in the same way as it is with other product such as electronics devices and electronics power supplies Conversely, the high reliability associated with PV module are indirectly reflected in the output power warranties usually provided in the industry, which range from 25- 30 years As a matter of fact, PV module have a low return time .the exception being the catastrophic failures. The performance of PV modules decreases when deployed outdoors over time. After several years of operation, this decrease will affect PV module reliability (manuel and ignacio, 2008) degradation rate of electrical

parameters of polycrystalline silicon PV module and the finding can be used to fairly design an effective PV modules.

2, Materials and Method

2.1 Method of Data acquisition

The degradation rate of the polycrystalline silicon PV module to ambient weather parameters; temperature, wind speed and relative humidity, irradiance was monitored in Minna environment, with the help of CR1000 software-based data logging system with computer interface. The PV modules under test, and meteorological sensors, were installed on support structure at the same test plane at about three meters of height, so as to able or ensure adequate exposure to insolation and enough wind speed, since wind speed is proportion to height. Also the PV was elevated above the ground to ensure that it is free from any shading from shruds and also protect from damage or interference by intruders and the entire system is secured. The modules are titled at approximately 10^0 (since Minna is on latitude $09^0$37N) to horizontal and south-facing to ensure maximum insolation (Strong and Scheller, 1991; Ugwuoke et al., 2005. Ezenwora, 2016). The data monitoring was from 9:00am to 6:00pm local time, each day continuously for a period of four years spanning from December 2014 to November, 2019.

Data acquired in the past 5 years was used to validate the data to support analysis. The experiment was carried out near Physics Department, Federal University of Technology, Minna (Latitude $09^0$37'N), longitude $06^0$32E and 249 meters above sea level. Te sensor are connected directly to CR1000 Campbell Scientific data, while the modules are connected to the logger via electronic loads. The logger was programmed to scan the load current from 0 to 1 A at intervals of 50mA every 5 minute and average value of short circuit current I_{ce}, open-circuit voltage V_{oc} current at maximum power, I_{max}, voltage at maximum power, V_{max}, power and maximum power obtained from the modules together with the ambient parameters are recorded and logged. Data download at the data acquisition site was performed every 7 days to ensure effective and close monitoring of the data acquisition system (DAS). At the end of each month and where necessary, hourly. Daily and monthly averages of each of the parameters-solar irradiance, solar insolation, wind speed, ambient and module temperature, and the output response variables (open-circuit voltage, V_{oc}, short-circuit current, I_{sc}, voltage at maximum power, V_{max}, current at maximum power, I_{max}, efficiency, Eff, and fill factor,

FF) of the photovoltaic modules were obtained. The global solar radiation was monitored using Li-200SA M200 Pyranometer, manufactured by LI-COR Inc. USA, with calibration of 94.62 microamperes per 1000W/m^2. The ambient temperature and relative humidity was monitored using HC2S3-L Rotronic HygraClip2 temperature/relative humidity probe, manufactured in Switzerland. Wind speed was monitored using 03002-L RM Young Wind Sentry Set. And module temperature was monitored using 110PV-L Surface-Mount Temperature probe: All sensors are installed in the CR1000 Campbell Scientific data logger with measurement and control module.

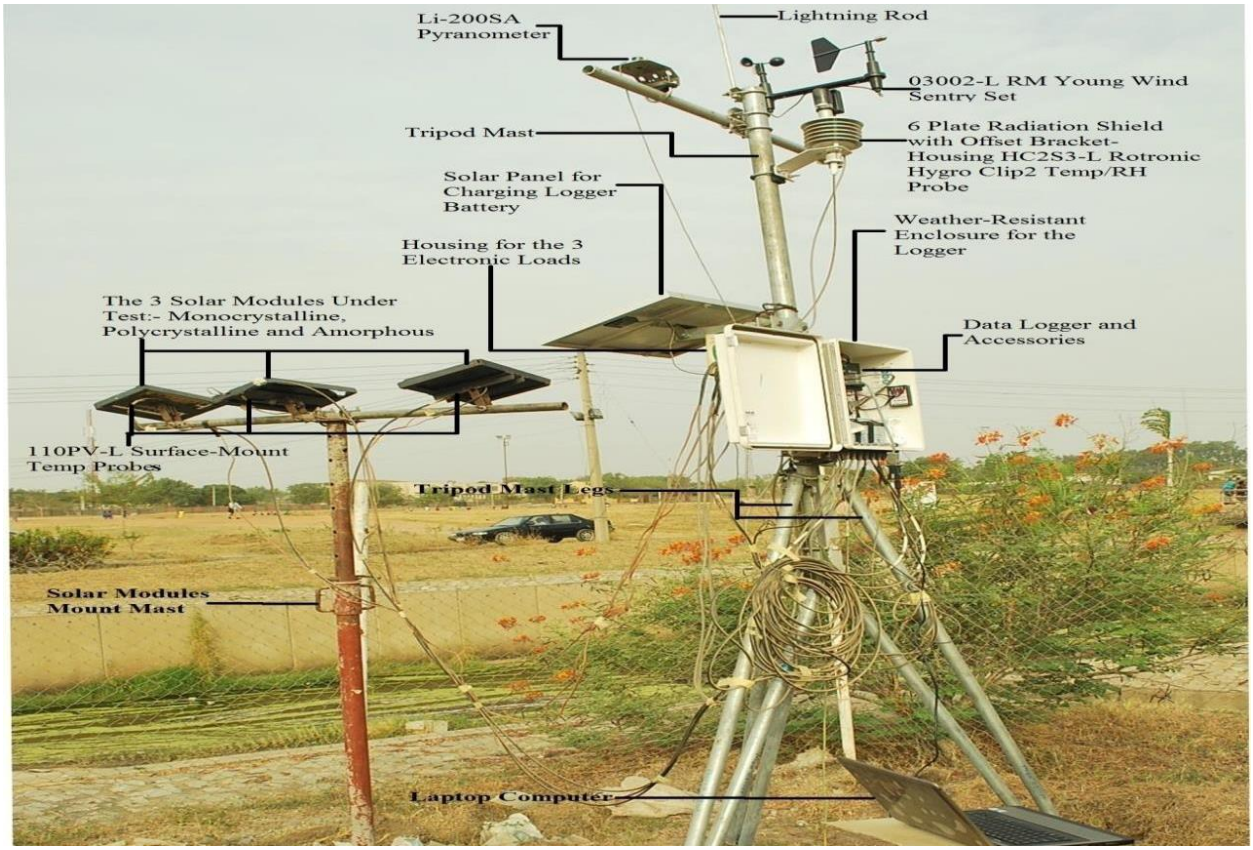

Plate 1: The experimental set up (Near physics Department, FUT Minna).

2.2 Method of Data Analysis

The situation responses of the polycrystalline module to ambient weather considering some parameters was analyzed in terms of Isc short-circuit current, Voc, open-circuit voltage, voltage at maximum power, V max, Imax , efficiency, Eff and fill factor, Ff, current at maximum power,.

FF, Efficiency, Eff, Fill Factor, and Module Performance Ratio (MPR) were evaluated using the following expressions (Ugwuoke, 2005. Ezenwora, 2016).

ill Factor, FF $=I_{max}\ V_{max}/I_{sc}V_{oc}$ 1

Efficiency, Eff $=I_{max}\ V_{max}/P_{in}= I_{sc}V_{oc}FF/P_{in} = I_{sc}V_{oc}FF/AE_e$ 2

The I-V curve were achieved by plotting current against voltage produced by the logger in scanning the electronic load current from 0 to 1 A at intervals of 50 mA. The maximum power point, P_{max}, that is the operating point of the module, was also note down by the logger. This maximum power point also corresponds to the largest area of the rectangle that fits into the curve. The current and voltage at this point are I_{max} and V_{max}.

Table 1: Annual Average of ambient parameters and Performance Variables for the Polycrystalline Silicon Module

T (Years)	WS (m/s)	T_a (^{0}C)	RH (%)	T_{mod} (^{0}C)	H_g (W/m^2)	Voc (v)	I_{sc} (A)	P (W)	V_{max} (V)	I_{max} (A)	P_{max} (W)	FF	Eff (%)
YEAR 1 (2015)	1.65	25.5	48.3	36.4	507	5.66	0.045	0.693	5.66	0.145	0.977	3.213	0.06
YEAR 2 (2016)	1.57	31.4	49.7	36.7	520	5.46	0.040	0.658	5.47	0.136	0.911	3.388	0.05
YEAR 3 (2017)	1.34	32.3	47.1	37.5	502	5.88	0.046	0.636	5.88	0.135	0.891	2.926	0.05
YEAR 4 (2018)	1.03	32.7	53.1	37.5	485	5.64	0.044	0.621	5.65	0.132	0.874	2.986	0.05
AVG	1.40	30.5	49.6	37.0	504	5.66	0.044	0.652	5.66	0.137	0.913	3.128	0.05

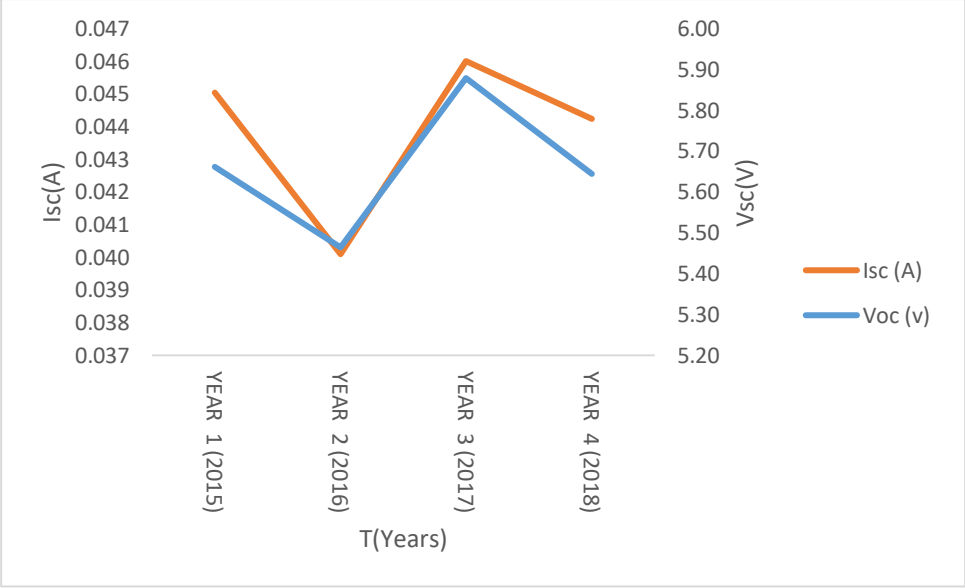

Figure 1: Variation of short circuit current and open circuit voltage as a function of years

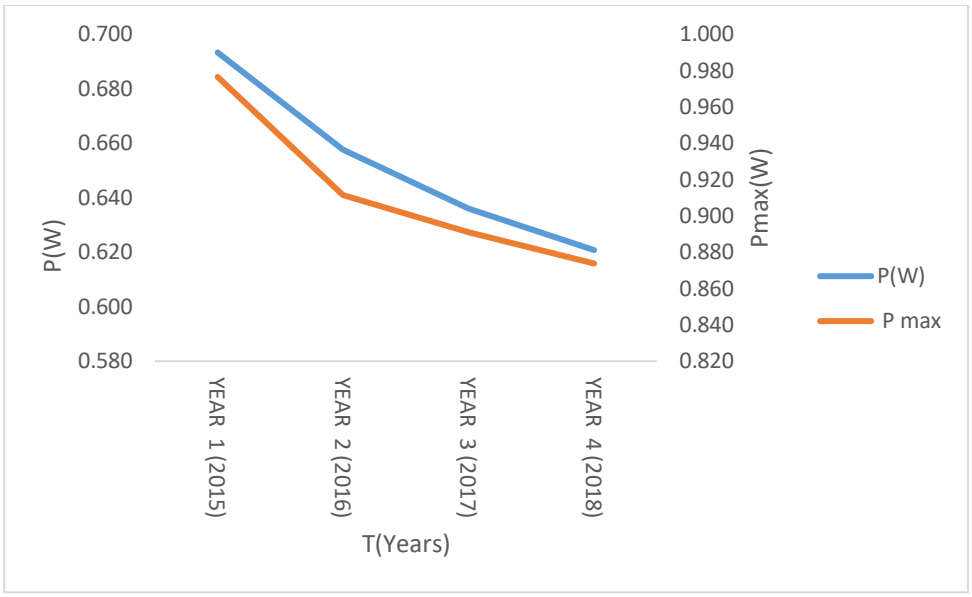

Figure 2: variation 0f power and maximum power as a function of years

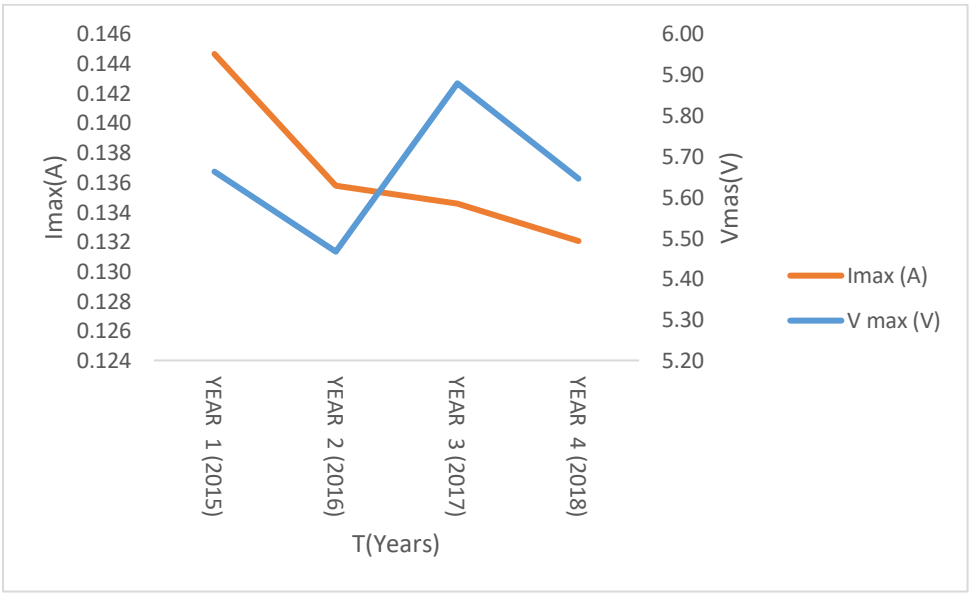

Figure 3: variation of maximum current and maximum voltage as a function of years

Result and Discussion

In fig 1: it was discover that I_{sc} degradation steadily throughout fours the years but for V_{oc} that increased between 2016 and 2017 and this increase was due to the decrease observed in the solar irradiance for 2016 and 2017 which is in consouad with Ezenwaro, *el at.*,2018.

From fig 2:it was discover that both the power and power maximum degrades steadily throughout four the years From fig 3:it was observed that I_{max} degraded steadily though out the four years but for V_{max} that increased between 2016 and 2017 and this was due to the decrease in solar irradiance seen from the for the year 2016 and 2017

From table 1 it was observed that V_{oc} and I_{sc} has a yearly decrease of 0.286Vand 0.004A after difference of four years with averaging and divided by 3 from 2017 and 2018 are slight increase throughout fours the years and increase was due to the decrease observed in solar irradiance, for P(w) and $P(w_{max})$ has observed that is degrades steadily throughout four the years by 0.024W and $0.0343W_{max}$ However from 2015 to 2016 v_{max} is decreased and from 2017 to 2018 is slight increase by $0.276V_{Max}$ and I_{max} degrades throughout four the years by $0.0042I_{max}$ Annual average of ambient parameter and performance variables for the polycrystalline silicon module.

Conclusion

It is conclude that the yearly determination of degradation rate of polycrystalline photovoltaic modules in Minna local environment reveals that all the performance variables of the modules degraded significantly from year to year for the four years of study. It was observed that the Electrical parameters of the module has an average degradation rate of V_{oc} 0.286v for I_{sc} 0.004A for P 0.024W for P_{max} $0.0343W_{max}$ for I_{max} $0.0042A_{max}$ for V_{mxa} $0.276V_{max}$ From

It was observed that electrical parameters of the module has an average degradation rate of V_{oc}= $5.66v_{1,}$ for I_{sc} = $0.044I_{sc}$, for P (W) 0.652W, For V_{max}. $5.66V_{max}$, For 1_{max} $0.137A_{max.}$ for $P(W_{max})$ $0.913W_{max.}$ for the four years of study. It was also observed from the table that V_{oc} and $I_{sc.}$ Has a yearly decrease rate of 0.286V and 0.004A from year 2017 to 2018 and a slight increase of 0.24V show that there is increase in solar irradiance and I_{sc} steadily decrease throughout the four years. By 0.004A, it was observed that P (w) and P (W_{max}) are degrade throughout the four years. By 0.0241W and $0.0343W_{max.}$ from the 2015 to 2016 V_{max} decrease steadily by $0.2V_{max,}$ but from 2017 to 2018 it shows that there is a increment in solar irradiance and there is slight increment by $0.23V_{max}$ showing that there is increase in solar irradianee I_{max} was observed that is degrades throughout the four years. By

$0.042I_{max}$ it has observed that P_{max} was degrades throughout the four years by $0.0343P_{max.}$ (Ezenwora *et*:*al*, 2018).

It is recommended that outdoor, yearly degradation studies should be carried out on all commercially available PV modules in every location of developing countries where this is lacking. Results will furnish policy makers, designers PV power system installers the vital information on the degradation rate or lifespan of all commercially available PV modules for effective and reliable PV power system.

Acknowledgement

It is my appreciation to acknowledge and thank Joel A. Ezenwora's Photovoltaic Lab for the data used for this research work.

References

Azhar G. and Abdul M. (2012). The performance of Three Different Solar Panel for Solar Electricity Applying Solar Tracking Devices Under The Malaysiaon Climate Condition. *Energy and Environment Reseach,* 2: 235-243.

Akachuku B. (2012). Prediction of optimum Angle of Inclination for flat plane solar collector in Zaria, Nigeria. *Agricultural Engineering International Journal, Commision International du Genie Rural,* 13: 1-11.

Duke R., Graham S., Mark H., Arne J., Daniel M., Osawa B., Simone P. and Erika W.. (1999). Field Performance Evaluation of Amorphous Silicon (a-Si) Photovaltaic Systems in Kenya: Methods and measurements in Support of a Sustainable Commerical Solar Energy Industry. *A Project of Energy Alternatives Africa (EAA) and Renewable Appropriate Energy Laboratory (RAEL) and Energy and Resources* Group (ERG), University of Clifornia Berkele

Dunlop E. and Halton D. (2006). The Performance of Crystalline Silicon Photovaltaic Solar Modules after 22 years of Exposure. Progress in Protovoltaic. *Research applications.* 7:16-23.

Ezenwora J. A. (2016) development of a prototype photovoltaic power system based on characterization and performance Evaluation of photovoltaic in Minna Nigeria *Ph'D Thesis Department of Physics Federal University of Technology Minna pp 45-140.*

Ezenwora J. A., Oyedum D. O., Ugwuke P. E. (2018) Comparative Study on Different types of Photovoltaic Modules under outdoor Operating Condition in Minna, Nigeria. *International Journal of Physical Research* 6 (1) pp 35-48.

Manuel V. and Ignacio R. (2018). Photovoltaic Modules Reliability Model Based on Field Degradation Studies. *Progress Report on Photovoltaic: Research and Applications,* 10: 825-1 Muyiwa S. A., Gabriel T. and Isa'ac A. E. (2007) Reliability and Degradation of solar PV Module, - case study of 19 years old Polycrystalline Module in Ghana.

Rakovect J. and Klement Z. (2011). Orientation and Tilt Dependence of a Fixed PV Array Energy Yield Base on Measurement of Solar Energy and Ground Albedo – A case Study of Slovenia. *Progress Report on Photovoltaic: Research and Application,* 13: 42-51.

Rene J. (2005). *Introduction to polymer solar cells*. Eindhoven University of Technology, Netherlands. 3Y280.

S. J. Strong & W . G./ Scheller, (1991). The Photovoltaic Room. 2nd ed. Sustainability Press, Massachusetts.

Polverini Davide and'Dunlop Ewan 2013. Polycrystallline suiron PV Modules Performance and Degradation over 20 years

Determination of Yearly Degradation Rate of Electrical Parameters of Amorphous Silicon (a-Si) Photovoltaic Module in Minna, Nigeria

MATTHEW, Samuel Oluwatobi*, EZENWORA, Joel Aghaegbunam and EICHIE, Julia Ofure

Department of Physics, Federal University of Technology, P.M.B. 65, Minna, Nigeria

**Corresponding author E-mail:sammyline4all@yahoo.com*

Abstract

There is need for accurate knowledge of degradation rate and lifespan of photovoltaic (PV) module in every location for an effective solar PV power system. Outdoor degradation analysis was carried out on amorphous silicon PV module rated 10 W using CR1000 software-based Data Acquisition System (DAS). The PV module under test and meteorological Sensors were installed on a metal support structure at the same test plane. The data monitoring was from 09:00 to 18:00 hours each day continuously for a period of four years, from December 2014 to November 2018. Annual yearly averages of the performance variables were carried out to ascertain the degradation rate and lifespan of the module. It was observed that Open-Circuit voltage (V_{oc}), Short-Circuit Current (I_{sc}), Power-Output (P), Maximum Voltage (V_{max}), Maximum Current (I_{max}) Maximum Power (P_{max}), fill-factor (FF) and Efficiency has average yearly degradation of 2.34V, 0.021A, 0.185W, 2.35V, 0.70A, 0.236W, 2.551 and 0.011%.

Keywords*: Amorphous; Module; Photovoltaic.*

1. Introduction

There is need for accurate knowledge of degradation rate and lifespan of photovoltaic (PV) module in every location for an effective solar PV power system. PV cells/modules due to their exposure to atmospheric parameters such as solar irradiance, temperature, wind speed, Relative humidity which depreciates the electrical parameters of these modules. The limited lifetime is as a result of several factors that are in play simultaneously. The performance of PV modules has been observed to gradually decrease with operation time (Dunlop and Halton, 2006). Long term performance of PV modules is vital if they have to pay back to the consumer. It is important to investigate the performance parameters of the modules.

With rapid economic growth and improvement in living standards, there has been a marked increase in energy consumption in many third world countries. Most countries use fossil fuel, hydroelectric power and nuclear power as a source of energy. Nuclear and fossil fuels have adverse

effects on the environment such as large amounts of greenhouse gases emissions and pollution from the burning of fossil fuel (René, 2005, Azhar and Abdul, 2012).

Since fossil fuel and nuclear sources of energy are not renewable, it is necessary to explore other sources of energy that are cost effective especially in the developing countries that rely heavily on imported fossil fuel. Renewable energy such as sunlight, wind tides and wave can be particularly suitable for developing countries especially in rural and remote areas where transmission and distribution of energy generated from fossil fuels can be difficult and expensive. Producing renewable energy locally can offer a viable alternative.

Technology advances are opening up a huge new market for solar power. Even though they are typically poor, these people have to pay far more for lighting than people in rich countries because they use inefficient energy systems like kerosene lamps and stoves. Solar power costs half as much as lighting with kerosene. According to (Duke *et al*., 2010). An estimated three million households get power from small solar panels.

The energy conversion efficiency of a PV module or array as a group of electrically connected PV modules in the same plane is defined as the ratio between electrical power conducted away from the module and the incidence power of the sun (Rakovect *et al.*, 2011).

This conversion efficiency of photovoltaic (PV) modules by manufacturers is done under Standard Test Conditions (STC). The Standard Test Conditions are module temperature of 25^{o} C, Irradiance of 1000W/m^2 and Air mass of 1.5).

Different PV module technologies now exist in the market. These include crystalline modules such as mono/single crystalline, poly/multi crystalline and amorphous modules. The modules available are rated by manufacturer depending on their power output such as 5Watts, 10Watts, 15 Watts. The choice of the module to use depends on the power output needed by the consumer and its efficiency. Photovoltaic (PV) modules are often considered as the most reliable elements in PV systems. However, PV module reliability data are not shown on commercial data sheets in the same way as it is with other products such as electronic devices and electric power supplies. Conversely, the high reliabilities associated with PV modules are indirectly reflected in the output power warranties usually provided in the industry, which range from 25-30 years. As a matter of fact, PV modules have a low return time, the exceptions being the catastrophic failures. The performance of PV modules decreases when deployed outdoors over time. After several years of operation, this decrease will affect PV module reliability (Manuel and Ignacio, 2008). Therefore, this study was carried out with

the-state-of-the-art DAS to determine the yearly degradation rate of electrical parameters of amorphous silicon PV module and the findings can be used to plan/design an effective and reliable PV Power system in any location.

2. Materials and Method

2.1. Method of Data acquisition

The degradation rate of the amorphous silicon PV module was monitored in Minna environment, using CR1000 software-based data logging system with computer interface. The PV modules under test, and meteorological sensors, were installed on support structure at the same test plane, at about three meters of height, so as to ensure adequate exposure to insolation and enough wind speed, since wind speed is proportional to height. The elevation equally ensures that the system is free from any shading from shrubs and also protected from damage or interference by intruders. Also, the whole experimental set up is secured in an area of about four meters in diameter. The modules are tilted at approximately 10^o (since Minna is on latitude 09^o 37'N) to horizontal and south-facing to ensure maximum insolation (Strong and Scheller, 1991; Ugwuoke et al., 2005; Ezenwora, 2016). The data monitoring was from 9.00am to 6.00pm local time, each day continuously for a period of four years, spanning from December 2014 to November 2018. The experiment was carried out near physics department, Federal University of Technology, Minna (latitude $09^o37'$N, longitude $06^o32'$E and 249 meters above sea level). The sensors are connected directly to the CR1000 Campbell Scientific data logger, while the module is connected to the logger via electronic loads. The logger was programmed to scan the load current from 0 to 1 A at intervals of 50mA every 5 minutes, and average values of short-circuit current, I_{sc}, open-circuit voltage, V_{oc}, current at maximum power, I_{max}, voltage at maximum power, V_{max}, power and maximum power obtained from the modules together with the ambient parameters are recorded and logged. Data download at the data acquisition site was performed every 7 days to ensure effective and close monitoring of the data acquisition system (DAS). At the end of each month and where necessary, hourly, daily and monthly averages of each of the parameters-solar irradiance, solar insolation, wind speed, ambient and module temperatures, and the output response variables (open-circuit voltage, V_{oc}, short-circuit current, I_{sc}, voltage at maximum power, V_{max}, current at maximum power, I_{max}, efficiency, Eff, and fill factor, FF) of the photovoltaic modules were obtained. The global solar radiation was monitored using Li-200SA M200 Pyranometer, manufactured by LI-COR Inc.USA, with calibration of 94.62 microamperes per 1000W/m^2. The ambient temperature and relative humidity was monitored using HC2S3-L Rotronic

HygraClip2 temperature/relative humidity probe, manufactured in Switzerland. Wind speed was monitored using 03002-L RM Young Wind Sentry Set. And module temperature was monitored using 110PV-L Surface-Mount Temperature probe. All sensors are installed in the CR1000 Campbell Scientific data logger with measurement and control module.

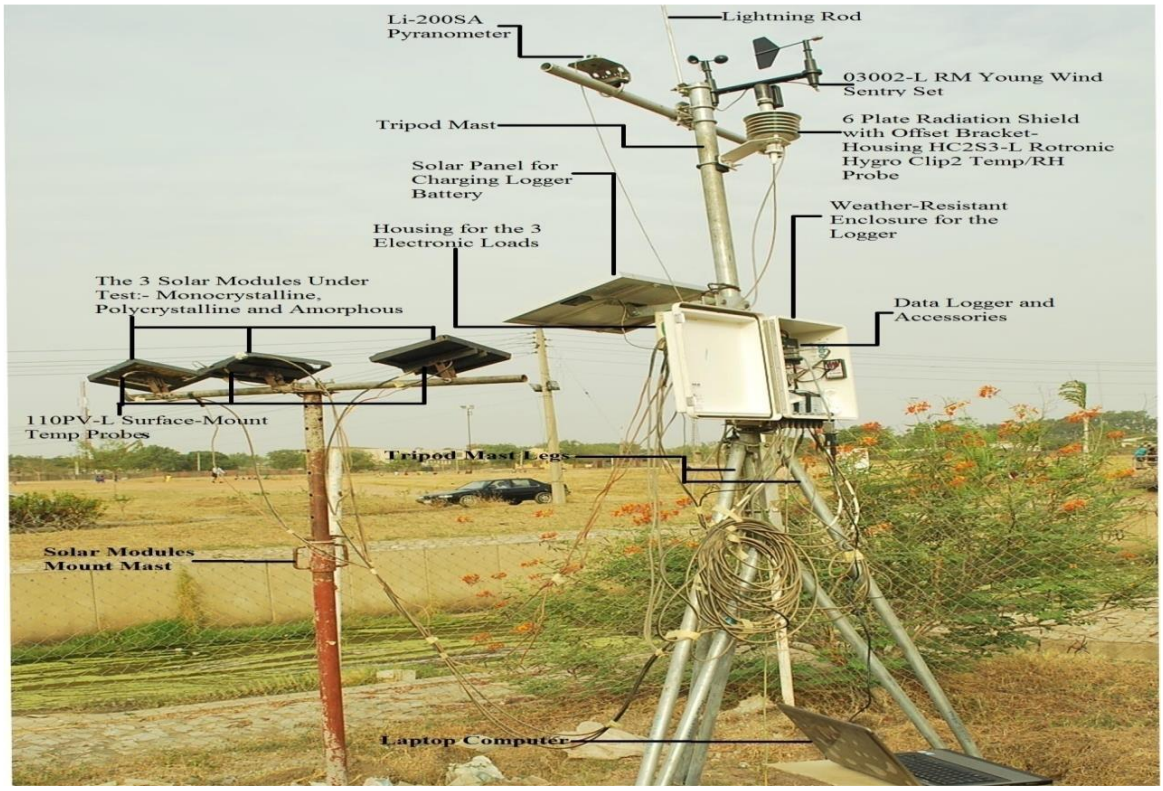

Plate 1: The Experimental Set Up (Near Physics Department, FUT Minna).

2.2. Method of Data Analysis

Degradation rate of the amorphous module was investigated in terms of open-circuit voltage, V_{oc}, short-circuit current, I_{sc}, voltage at maximum power, V_{max}, current at maximum power, I_{max}, efficiency, Eff, and fill factor, FF. Fill factor, FF, and Efficiency, Eff, were evaluated using the following expressions (Ugwuoke,2005; Ezenwora, 2016):

Fill factor, $FF = I_{max} V_{max}/I_{sc} V_{oc}$ **(1)**

Efficiency, $Eff = I_{max} V_{max} /P_{in} = I_{sc} V_{oc} FF/P_{in} = I_{sc} V_{oc} FF/AEe$ **(2)**

The maximum power point, P_{max}, which is the operating point of the module, was recorded by the logger. This maximum power point also corresponds to the largest area of the rectangle that fits the curve. The current and voltage at this point are I_{max} and V_{max} respectively.

3. Results and discussions

Figure 1 to 3 shows the degradation rate for the performance variables been investigated. It was discovered that Isc decreased steadily from year 2015 to 2018 but for I_{max} that started degrading after the third year. However, it was observed that the degradation trend was distorted in 2018 where V_{oc} and V_{max} were high. This is due to the fact that according to earlier work of (Ezenwora, 2016). V_{oc} and V_{max} are known to be affected negatively by high module temperature which accounted for the sudden increase of V_{oc} and V_{max} in year 2018 when a decrease in temperature was noticed as shown in table 1. The other parameters worthy of note are power (P) and maximum power (P_{max}). From the plots of figure 3, it was observed that there was an increase from 2015 to 2016 before it starts decreasing. The reason for the increase in the first year is not farfetched, according to (Ezenwora *et al*., 2018), Increase in solar irradiance (Hg) and module temperature (T_{mod}) increases P_{max}, I_{max} and P. Therefore, increase in Hg and T_{mod} as seen in table 1 has accounted for the increase noticed for the three performance variables in the first year.

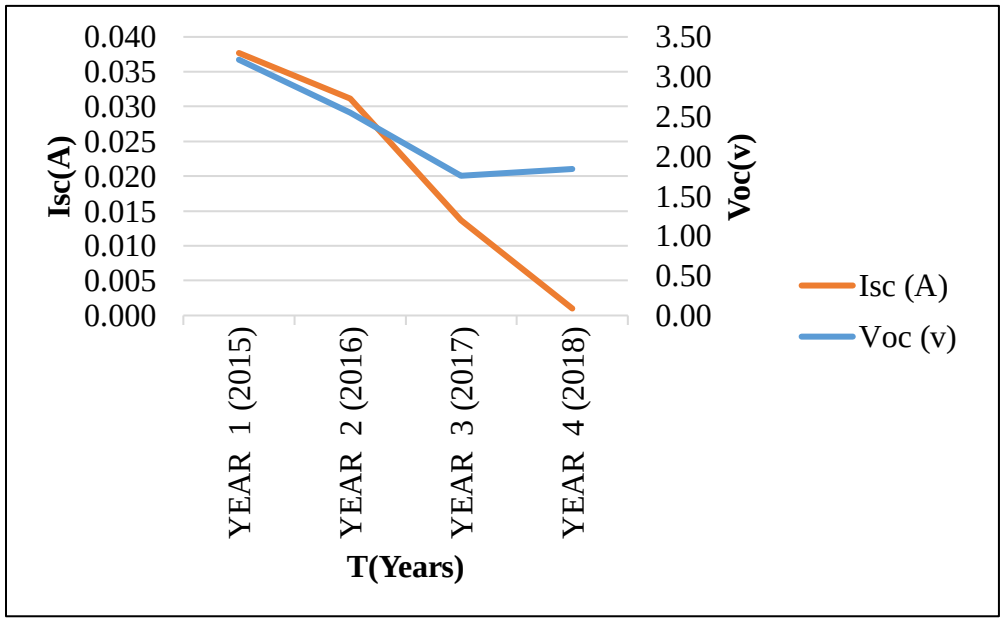

Figure 1: Variation of short circuit current and open circuit voltage as a function of years

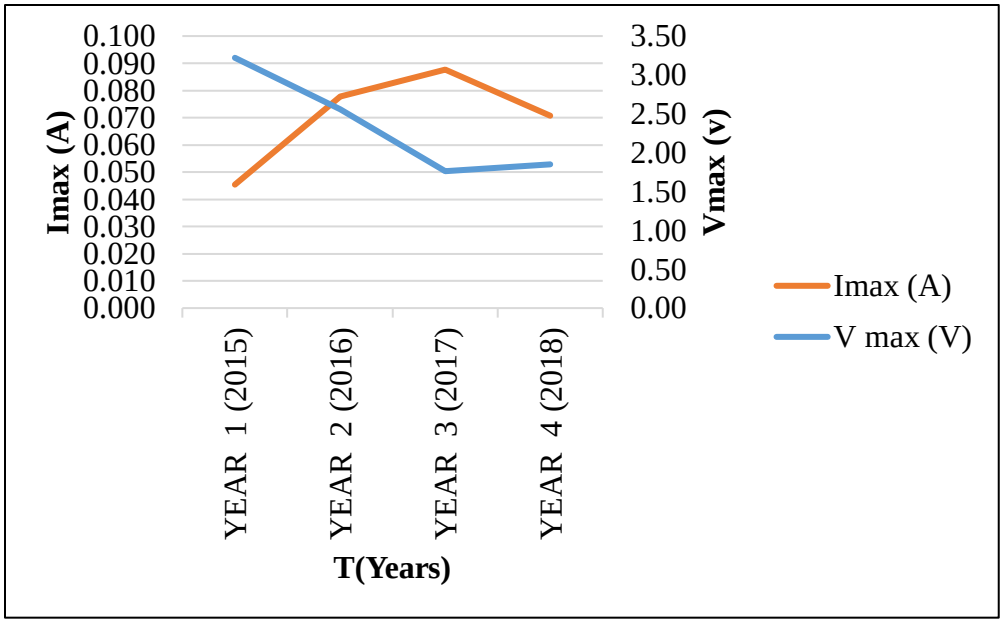

Figure 2: variation of maximum current and maximum voltage as a function of years

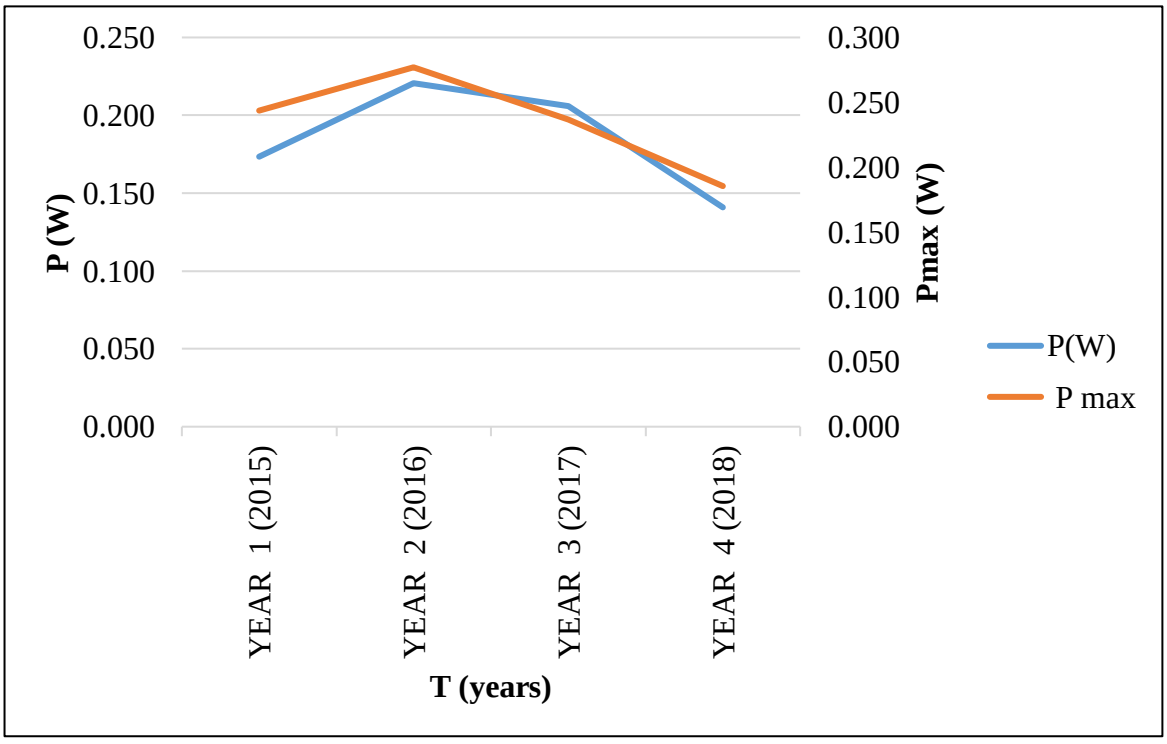

Figure 3: variation of power and maximum power as a function of years

From table 1, It was observed that V_{oc} and I_{sc} has a yearly decrease of 0.7V and 0.01A from year 2015 to 2016, 0.8V and 0.02A from 2016 to 2017, 0.01A for I_{sc} from 2017 to 2018 and a slight increase of 0.08V from 2017 to 2018 for V_{oc}. V_{max} was observed to decrease by 0.7V from 2015 to 2016, 0.8V from 2016 to 2017 and a slight increase of 0.1V from 2017 to 2018. I_{max} was observed to decrease from 2017 to 2018 by 0.02A despite observing increments in the preceding years suggesting that I_{max} could begin to degrade after the third year. Furthermore, P and P_{max} decreased by 0.02W and 0.04W from 2016 to 2017, 0.07W and 0.05W from 2017 to 2018 suggesting that P and P_{max} degrades steadily after a slight increment of 0.05W and 0.03W observed in the first year. Annual average values of the module performance variables and ambient parameters for the four years duration of this study is shown in Tables 1for the amorphous silicon module.

Table 1: Annual Averages of Ambient Parameters and Performance Variables for the Amorphous Silicon Module

T (Hours)	WS (m/s)	T_a (^{0}C)	RH (%)	T_{mod} (^{0}C)	H_g (W/m^2)	V_{oc} (v)	I_{sc} (A)	P (W)	V_{max} (V)	I_{max} (A)	P_{max} (W)	FF	Eff (%)
2015	1.65	25.4	48.3	35.4	507	3.21	0.038	0.173	3.22	0.045	0.244	1.207	0.0100
2016	1.57	31.4	49.7	35.5	520	2.55	0.031	0.221	2.55	0.078	0.277	2.508	0.0132
2017	1.34	32.3	47.1	36.4	502	1.76	0.014	0.206	1.76	0.088	0.237	6.418	0.0106
2018	1.03	32.7	53.1	36.1	485	1.84	0.001	0.141	1.85	0.071	0.185	0.071	0.0093
AVG	1.40	30.5	49.6	35.9	504	2.34	0.021	0.185	2.35	0.070	0.236	2.551	0.0108

4. Conclusion

The yearly determination of degradation rate of amorphous photovoltaic modules in Minna local environment reveals that all the performance variables of the modules degraded significantly from year to year for the four years of study. It was observed that the Electrical parameters of the module has an average degradation rate of 2.34V for V_{oc} , 0.021A for Isc, 0.185W for P, 2.35V for V_{max}, 0.70A for I_{max}, and 0.236W for P_{max} for the four years of study. Similarly, it was also observed from table that V_{oc} and I_{sc} has a yearly decrease of 0.7V and 0.01A from year 2015 to 2016, 0.8V and

0.02A from 2016 to 2017, 0.01A for I_{sc} from 2017 to 2018 and a slight increase of 0.08V from 2017 to 2018 for V_{oc}. V_{max} was observed to decrease by 0.7V from 2015 to 2016, 0.8V from 2016 to 2017 and a slight increase of 0.1V from 2017 to 2018. I_{max} was observed to decrease from 2017 to 2018 by 0.02A despite observing increments in the preceding years suggesting that I_{max} could begin to degrade after the third year. Furthermore, P and P_{max} decreased by 0.02W and 0.04W from 2016 to 2017, 0.07W and 0.05W from 2017 to 2018 suggesting that P and P_{max} degrades steadily after a slight increment of 0.05W and 0.03W observed in the first year. Module temperature was therefore observed to have significant influence on the general degradation of the modules especially V_{oc} and V_{max} hence the increase when temperature decreased in 2018. In addition to the temperature effects on the degradation of the module is solar irradiance which is seen to affect P, P_{max} and I_{max}, hence the increase when temperature and solar increased in the first year of study which is in consonant with the (Ezenwora *et al*., 2018).

It is recommended that outdoor, yearly degradation studies should be carried out on all commercially available PV modules in every location of developing countries where this is lacking. Results will furnish policy makers, designers, PV power system installers the vital information on the degradation rate or lifespan of all commercially available PV modules for effective and reliable PV power system.

Acknowledgment

It is my desire to acknowledge and thank Dr. Joel A. Ezenwora's Photovoltaic laboratory for the data used for this research work.

References.

Azhar G. and Abdul M. (2012). The performance of three Different Solar Panels for Solar Electricity Applying Solar Tracking Device under the Malaysian Climate Condition. *Energy and Environment Research,* **2** : 235-243.

Duke R., Graham S., Mark H., Arne J., Daniel M., Osawa B., Simone P. and Erika W. (1999). Field Performance Evaluation of Amorphous Silicon (a-Si) Photovoltaic Systems in Kenya: Methods and measurements in Support of a Sustainable Commercial Solar Energy Industry. *A*

Project of Energy Alternatives Africa (EAA) and Renewable Appropriate Energy Laboratory (RAEL) and Energy and Resources Group (ERG), University of California, Berkeley.

Dunlop E. and Halton D. (2006). The Performance of Crystalline Silicon Photovoltaic Solar Modules after 22 years of Exposure**.** *Progress in Photovoltaic. Research applications*, **7**:16-23.

Ezewonra, J.A; (2016). Development of a Prototype Photovoltaic Power System based on Characterization and Performance Evaluation of Photovoltaic Modules in Minna, Nigeria. *PhD Thesis, Department Of Physics, Federal University of Technology, Minna.* pp 45-140.

Ezewonra, J.A; Oyedum, D.A; Ugwoke, P.E. (2018). Comparative Study on Different types of Photovoltaic Modules under outdoor Operating Conditions in Minna, Nigeria. *International Journal of Physical Research.* 6(1), pp 35-48.

Manuel V. and Ignacio R. (2008). Photovoltaic Module Reliability Model Based on Field Degradation Studies. *Progress Report on Photovoltaics: Research and Applications,* **10**: 825-1002.

Rakovect J. and Klemen Z. (2011). Orientation and Tilt Dependence of a Fixed PV Array Energy Yield Based on Measurements of Solar Energy and Ground Albedo- A Case Study of Slovenia. *Progress Report on Photovoltaics: Research and Applications,* **13**: 42-51.

René J. (2005). *Introduction to polymer solar cells*. Eindhoven University of Technology, Netherlands. 3Y280.

S.J. Strong & W.G. Scheller, (1991). The Photovoltaic Room. 2nd ed. Sustainability Press, Massachusetts

Hydrothermal Synthesis of ZnO

HARUNA Isah, MUHAMMAD MustaphaKpanje, ABUBAKAR Sadiq, MOHAMMED Isah Kimpa and KASIM Uthman Isah

Department of Physics, Federal University of Technology Minna,

P. M. B 64, Minna, Niger State. Nigeria.

Corresponding email: kasim309@futminna.edu.ng

Abstract

This paper outlines explicit highlights of hydrothermal synthesis of zinc oxide nanoparticles. Hydrothermal synthesis permits control of the ZnO nanostuctural morphology and nanoparticle size since the synthesis factors can be fluctuated to influence these features. In this survey, the hydrothermal synthesis factors and their effects on the particulate properties are unraveled.

Keywords : Hydrothermal, synthesis, ZnO, Sintering temperature.

1. Introduction

The investigation of materials on nano-scale has turned out to be central in science and innovation as decrease in a material's size brings forth novel electrical, mechanical, chemical, optical properties coming about because of surface and quantum confinement [1, 2].

ZnO is a compound semiconductor (transparent to visible light) with a wide band-gap of 3.37eV and high exciton restricting vitality of 60 meV [2, 3]. Synthesis of ZnO thin films had begun during the 1960s when ZnO materials were connected in sensors, transducers and as photocatalysts [1]. ZnO nanaostructures have various innovative applications in optoelectronics, surface acoustic wave channels or filters, photonic crystals, photodetectors, light radiating diodes, photodiodes, gas sensors, optical modulator waveguides, solar cells [4, 5] and varistors [1, 3, 6].

Nanomaterials are typically classified into three groups: 0-dimensional, 1-dimensional, and 2-dimensional. 0-dimensional nanostructures, referred to as quantum dots or nanoparticles with an aspect ratio near unity, have been extensively used in biological applications [7, 8]. 2- dimensional nanomaterials, such as thin films, have also been widely used as optical coatings, corrosion

protection, and semiconductor thin film devices. Zinc oxide crystals can be prepared in the form of nanopowders, films, ceramics, and single crystals [9]. One-dimensional (1D) semiconductor nanostructures such as nanowires, nanorods (short nanowires), nanofibres, nanobelts, and nanotubes have been of intense interest in both academic research and industrial applications because of their potential as building blocks for other structures [10]. 1-D nanostructures are useful materials for investigating the dependence of electrical and thermal transport or mechanical properties on dimensionality and size reduction (or quantum confinement) [11]. They also play an important role as both interconnects and functional units in the fabrication of electronic, optoelectronic, electrochemical, and electromechanical nanodevices [12]. Among the one-dimensional (1D) nanostructures, zinc oxide (ZnO) nanowire is one of the most important nanomaterials for nanotechnology in today's research [13].

2. Basic synthetic approaches and growth mechanisms

The synthetic techniques used for the synthesis of ZnO are broadly divided into three types: chemical, biological, and physical methods [14].

In the physical (also called gaseous phase [6]) method, physical forces are involved in the attraction of nanoscale particles and formation of large, stable, well-defined nanostructures[15]. This method of synthesis uses gaseous environment in closed chambers with high temperatures from 500°C to 1500°C to carry out the synthesis. Its examples includecolloidal dispersion method, vapor condensation, amorphous crystallization, physical fragmentation, vapour phase transport (which includes vapour solid (VS) and vapour liquid solid (VLS) growths), physical vapour deposition (PVD), chemical vapour deposition (CVD), metal organic chemical vapour deposition (MOCVD), thermal oxidation of pure zinc and condensation, microwave assisted thermal decomposition and many others are expensive and complicated [1].

Biosynthesis of nanoparticles (NPs) is an approach of synthesiswhich uses microorganisms and plants for the formation of ZnO NPs having biomedical applications. This approach is an environment-friendly, cost- effective, biocompatible, safe, green approach [16]. Green synthesis can be carried out through plants, bacteria, fungi, algae etc. They allow large scale production of ZnO NPs free of additional impurities [17].

The chemical (also called solution phase)method is done in water with growth temperatures less than the boiling point of waterwhich makes it simple and has tolerable growth conditions[1]. Chemical reactions in aqueous systems are usually considered to be in a reversible equilibrium, and the driving force is the minimization of the free energy of the entire reaction system, which is the intrinsic nature of wet chemical methods [2, 6]. ZnO solution phase synthesis methods include: Sol-gel method (a chemical solution processused to make ceramic and glass materials in the form of thin film, fibers or powder), Co-precipitation method, Hydrothermal method (method of synthesis of single crystal that depends on the solubility of minerals in hot water under high pressure [2, 18, 19]), Pulsed laser deposition method (a physical vapour deposition technique where a high-power pulsed laser beam is focused inside a vacuum chamber to strike a target of the material that is to be deposited)[1, 2, 20].

Hydrothermal method unlike other methods is attributed with the following favorable circumstances which makes it more appropriate and suitable than different other methods for ZnO synthesis: utilization of simple equipment, minimal effort and low cost, catalyst-free growth, enormous area uniform circulation of as-grown particles [21], less perilous and natural agreeableness, does not require the utilization of natural solvents or extra handling of the item (crushing and calcinations) which makes it basic, the likelihood of completing the synthesis at low temperatures nonattendance of complex vacuum setup [22],assorted shapes and dimensions of the subsequent crystals relying upon the piece of the beginning mixture and the procedure temperature and pressure, high level of crystallinity of the as-orchestrated product, high purity of the material acquired, it very well may be utilized on large areaand/or flexible substrates, can be utilized for creation of unsupported nanostructures, accomplishment of exact control of the nanostructure size and direction [21]. Therefore, it has been a subject of exceptional research lately.

2.1 Zinc oxide crystal structure

The ZnO crystal is hexagonal wurtzite and exhibits partial polar characteristics [48, 49] with lattice parameters a = 0.3296 and c = 0.52065nm [4, 49]. The structure of ZnO can be described as a number of alternating planes composed of tetrahedrally coordinated O^{2-} and Zn^{2+} stacked alternately along the c-axis. The piezoelectric and pyroelectric properties are ascribed to the absence of inversion symmetry in ZnO which gives rise to tetrahedral coordination [49].

Another important characteristic of ZnO is polar surfaces. The most common polar surface is the basal plane (0001) [48]. One end of the basal polar plane terminates with partially positive Zn lattice sites and the other end terminates in partially negative oxygen lattice sites. The oppositely charged ions produce positively charged Zn-(0001) and negatively charged O-(0001) surfaces, resulting in a normal dipole moment and spontaneous polarization along the c-axis as well as a variance in surface energy. To maintain a stable structure, the polar surfaces generally have facets or exhibit massive surface reconstructions, but ZnO± (0001) surfaces are exceptions: they are atomically flat, stable and exhibit no reconstruction [41, 42]. Efforts to understand the superior stability of the ZnO± (0001) polar surfaces are at the forefront of research in today's surface physics [43–46, 49].

3. ZnO nanostructures through hydrothermal growth

Generally speaking, ZnO is expected to crystallize by the hydrolysis of Zn salts in a basic solution that can be formed using strong or weak alkalis [6]. An assortment of materials with different morphological structures and sizes of metal oxides such as NiO, α-Fe_2O_3 , ZnO, Ga_2O_3 , and CuO, SnO_2, F:SnO_2, SnO, Fe_2O_3, indium tin oxide (ITO), Ti_{1-x} Sn_x O_2, Y_2O_3, Na_2SiO_3, and $Li_2Si_2O_5$, carbon-coated SnO_2, TiO_2/$SrTiO_3$, titanate and TiO_2, In_2O_3, CeO_2, MgO, CeO_2/TiO_2e.t.c. is achievable by hydrothermal batch and flow reaction systems [18, 23]. Reports of hydrothermal synthesis in aqueous medium are available in the literature.

3.1 Growth in general alkaline solutions

An alkaline solution is essential for the formation of ZnO nanostructures because normally divalent metal ions do not hydrolyze in acidic environments. Generally speaking, the solubility of ZnO in an alkali solution increases with the alkali concentration and temperature. The commonly used alkali compounds are KOH and NaOH [6]. KOH is thought to be preferable to NaOH, because K^+ has a larger ion radius and thus a lower probability of incorporation into the ZnO lattice [6, 9]. The electrical conductivity of ZnO depends on the amount of Zn^{2+} ions with respect to O^{2-} (sample stoichiometry) and the real structure of the crystal (intrinsic defects associated with the presence of Zn at the interstitial, Zn_i^{2+}, or the defects associated with the oxygen vacancies V_O, playing the role of donors). The point defects (Zn_i, *V*O) determine high conductivity of ZnO crystals; usually, the resistivity of crystals grown hydrothermally does not exceed 104 Wcm [6]. Furthermore, it has been

suggested that Na^+ is attracted by the OH^- around the nanocrystal and forms a virtual capping layer, thus, inhibiting the nanocrystal growth.

$$Zn^{2+} + 2OH^- \longleftrightarrow Zn(OH)_2 (1)$$

$$Zn(OH)_2 + 2OH^- \longleftrightarrow [Zn(OH)_4]^{2-} (2)$$

$$[Zn(OH)_4]^{2-} \longleftrightarrow ZnO_2^{2-} + 2H_2O \quad (3)$$

$$ZnO_2^{2-} + H_2O \longleftrightarrow ZnO + 2OH^- (4)$$

$$ZnO + OH^- \longleftrightarrow ZnOOH^- \quad (5)$$

The main reactions involved in the growth are illustrated in the above equations [6, 9].

3.2 Growth mediated by hexamethylenetetramine (HMTA) aqueous solution

The most commonly used chemical agents in the existing literature for the hydrothermal synthesis of ZnO nanoparticles are $Zn(NO_3)_2$ and HMTA. In this case, $Zn(NO_3)_2$ provides Zn^{2+} ions required for building up ZnO nanowires. When HTMA (a nonionic cyclic tertiary amine [9]) and $Zn(NO_3)_2$ are chosen as precursor, the chemical reactions can be summarized in the following equations [24].

$$(CH_2)6N_4 + 6H_2O^- \rightarrow 6HCHO + 4NH_3 (1)$$

$$NH_3 + H_2O \longleftrightarrow NH_4+ + OH^- (2)$$

$$2OH^- + Zn^{2+} \rightarrow Zn(OH)_2 (3)$$

$$Zn(OH)^{2-} \rightarrow ZnO + H_2O (4)$$

H_2O molecules in the solution, not at all like for the instance of alkali-mediated growth, provides and gives O^{2-} ions. It has been recommended that HMTA amid the ZnO nanowire growth goes about as a bidentate Lewis base that directs and extends two Zn^{2+} ions and furthermore goes about as a frail base and pH buffer. Contingent upon the given pH and temperature, Zn^{2+}can exist in a progression of intermediates, and ZnO can be framed by the lack of hydration of these intermediates [6]. On the off chance that a ton of $OH^-$is created in a brief period, the Zn^{2+} ions in the arrangement will

precipitate out rapidly because of the high pH condition, and, along these lines, Zn^{2+} would contribute little to the ZnO nanowire development and in the long run outcome in the quick utilization of the supplement and forbid further development of the ZnO nanowires [25]. In this manner, the convergence of OH^- ought to be controlled in the solution to keep up low supersaturation levels amid the entire nanowire development process [24].

Table 1.0: **Summary of hydrothermal method of obtaining Zinc Oxide with different morphologies and sizes**

S /N	Precursors	Synthesis conditions	Properties and applications	Reference
1	Nitrate,ethylene glycol, NaOH	reaction temperature**:**180 ^oC	flower 5µm and rods	[26]
2	Acetate dihydrate, ethylene glycol	reaction temperature:160 ^oC	sphere 5µm and nanorods	[27]
3	Acetate dihydrate, ethylene glycol	reaction temperature: 180 ^oC	sphere 5µm and nanocrystallites 10 nm	[28]
4	Acetate dihydrate, ethylene glycol	reaction temperature: 160 ^oC	sphere0. 12 µm and ovoids 10 nm	[29]
5	$ZnCl_2$, NaOH	reaction: 5–10 h, 100–220 °C in teflon-lined autoclave	particle morphology: bullet-like (100–200 nm), rod-like (100–200 nm), sheet (50–200 nm), polyhedron (200–400 nm), crushed stone-like (50–200 nm)	[30]

6	tetramethylammonium hydroxide (TMAH), Ethanolic solution of zinc acetate dihydrate	heating temperature: : room temperature	particle morphology: snowflakes sized from 10 to 20nm	[31]
7	$Zn(CH_3COO)_2$, NaOH, HMTA (hexamethylenetetramine)	reaction: 5–10 h, 100–200 °C; HMTA concentration: 0–200 ppm	particlesize and morphology: diameter 55–110 nm, spherical shape	[32]
8	$Zn(CH_3COO)_2$, $Zn(NO_3)_2$, LiOH, KOH, NH_4OH	reaction: 10–48 h, 120–250 °C	particlesize and morphology:hexagonal (wurtize) structure, microcrystallites: 100 nm–20 μm	[33]
9	$Zn(CH_3COO)_2$, NH_3, zinc 2-ethylhexanoate, TMAH, ethanol, 2-propanol	reaction time and pH of solution: 15 min, 2–72 h, final pH: 7–10	particles with irregular ends and holes; aggregates consist particles of 20–60 nm, *BET*: 0.49–6.02 m^2/g	[34]
10	Trimethylamine N-oxide, 4-picoline N-oxide, HCl, toluene, ethylenediamine	reaction time and temperature: 24–100 h, 180 °C	particlesize and morphology:hexagonal structure, nanorods (40–185 nm), nanoparticles (24–60 nm)	[35]

	(EDA), tetramethylethylene diamine (TMEDA)			
11	$Zn(NO_3)_2{\cdot}2H_2O$, NaOH, CTAB	reaction time and temperature: 120°C for 24 h	particlesize and morphology:nanorods with diameters ~0.5–1 μm and lengths ~5–6 μm [without additive], nanoflowers with diameter ~4–5 μm [with additive].	[36]
12	$Zn(CH_3COO)_2$, $Zn(NO_3)_2$, ethanol, imidazoliumtetrafluoroborate ionic liquid	reaction temperature: 150–180 °C; drying temperature: 80 °C in vacuum oven; calcination temperature: 500 °C	particlesize and morphology:hexagonal (wurtize) structure, hollow microspheres (2–5 μm) consisted nano-sized particles and contained channels (10 nm); hollow microspheres consisted of nanorods (~20 nm); flower-like microspheres (2.5 μm)	[37]
13	zinc acetylacetonate, methoxy-ethoxy- and n-butoxyethanol, zinc oximate	precursor concentration: 2.5–10 wt%; heatingtime and temperature: in 800 W microwave, 4 min; drying temperature: 75 °C in air	particlesize and morphology: zincite structure; average crystallite size: 9–31 nm; diameter: 40–200 nm; *BET*: 10–70 m^2/g	[38]

14	$Zn(NO_3)_2$, deionized water, HMT (hexamethylenetetramine)	heating time and temperature:90 °C in microwave for 2 min. dryingtime and temperature: 2 h at 60 °C	particlesize and morphology: hexagonal wurtize structure, nanorod and nanowire shape (*L*: ~0.7 μm, *D*: ~280 nm); application: electronic and optoelectronic devices	[39]
15	Zinc nitrate hexahydrate, ammonium hydroxide	heating temperature: 120 ^oC in an autoclave with pH adjusted to 7.5	particlesize and morphology:powdered form nanoparticles	[40]
16	$Zn(NO_3)_2$, ammonia	heating time and temperatures: 100 ^oC, 150 ^oC and 200 ^oC for 2 hrs	particlesize and morphology:rod-like to polyhedral	[1]
17	Ethanolic solution of zinc acetate dihydrate	heating temperature: room temperature	particlesize and morphology:snowflakes (10-20 nm)	[1]
18	Zinc acetate in supercritical water	reaction: continuous tubular reactor	particlesize and morphology:sphere (39-320 nm)	[1]

3.3 Different structures

ZnO can be controlled into an assortment of structures, morphologies and sizes including nanowires, nanobelts, tubes/rings, twinning structures, progressive structures, and heterostructures with zinc oxide material, appearing incredible adaptability of wet chemical strategies [6] relying upon at least one of the factors that influence the auxiliary morphology and size of as-synthesized ZnO nanoparticles. These factors include concentration of precursors, pH of solution, reaction time and

reaction temperature, mechanical stirring duration, heatingrate, additives or template and substrate type.

The concentration of precursors affects ZnO nanoparticle by advancing its formation. In this manner, formation of the nanoparticles (nucleation rate) increases with increase in alkaline concentration of the precursors [51]. Varying the time of reaction influences the diameter of the as-synthesized ZnO particle such that the diameter increases with increase in reaction time and vice-versa. The rate at which heating is ramped up directly influence the kinetics of nucleation and precipitation severely. The reaction temperature guarantees that a ZnO phase is formed changing from 1D to 2D and then to 3D as reaction temperature is increased from 90-100 ^{o}C, and from 120-160 ^{o}C, and then from 180-200 ^{o}C [50]. A high temperature and heating cause increase in the average diameter of the as-synthesized ZnO nanoparticle [50, 51].

Table 2.0: **Modification Methods of Zinc Oxide**

Classification of modifiers	**Type of modifying agents**	**Modification effect**
Inorganic compound	Si2O, Al2O,$LiCo_2O$,metal ions	Change of surface area and particle size, reduced photocatalytic action of the oxide; improvement of dispersion degree of ZnO particles.
Organic compound	Carboxylic acids, silanes	Introduced characteristic groups on the surface ZnO and altered its physicochemical properties, increased the compatibility of ZnO with an organic matrix, reduced aggregation of particles and enhanced the long-term stability in an organic matrix, improved ZnO dispersion in rubber mixtures.

Polymer matrices	Poly(ethylene glycol), polystyrene, poly(methyl methacrylate), poly(methacrylic acid), chitin	Improved electrical, thermal and optical properties of ZnO/polymer composite

4. Characterization of ZnO

Under general conditions, ZnO is single crystalline and exhibits a hexagonal wurtzite structure. The optical properties could be obtainable from UV-Visible absorption spectroscopic analysis. The structure of ZnO nanowires could be revealed by Light Microscopy, X-ray diffraction (XRD) and scanning electron microscopy (SEM). Further structural characterizations can be carried out by transmission electron microscopy (TEM), Raman spectroscopy, Scanning Force Microscopy (SFM), high resolution transmission electron microscopy (HRTEM) and Rietvelt Refinement [1, 2, 6, 16, and 40].

The composition analysis could be carried out through X-ray absorption spectroscopy (XAS), energy dispersive spectroscopy (EDS), energy dispersive X-ray (TEDX), X-ray fluorescence spectroscopy (XRF), Auger electron spectroscopy (AES), proton induced X-ray emission spectroscopy (PIXE), atomic absorption spectroscopy (AAS), neutron absorption spectroscopy (NAS), Fourier transform infrared spectroscopy (FTIR), X-ray photoelectron spectroscopy (XPS), wave length dispersive spectroscopy (WDS).

5. Conclusion

This survey paper portrays ZnO hydrothermal synthesis for ZnO nanoparticle development and formation utilizing diverse zinc salts and alkali solutions, its focal points over different other methods and its characterization techniques. The hydrothermal synthesis technique is cordial, costless, straightforward and effective and it has gotten expanded consideration because of the extreme utilization of ZnO in research and industry holding to its remarkable highlights. A blend of zinc nitrate and hexamine is the most well known decision of antecedent for hydrothermal synthesis. In

light of this paper, the morphology and dimension of nanostructures incorporated by hydrothermal method are enormously impacted by precursor concentration, pH of solution, reaction time, reaction temperature, mechanical mixing or stirring duration, heating rate, additive or template and substrate type. Thus the need to comprehend the ZnO hydrothermal synthesis to empower designing and refined the as-combined ZnO nanoparticles to wanted prerequisite.

References

[1] Sunandan Baruah and Joydeep Dutta. Hydrothermal Growth of ZnO Nanostructures. Sci. Technol. Adv. Mater. 10 (2009) 013001 (18pp) doi:10.1088/1468-6996/10/1/013001.

[2] Yangyang Zhang,Manoj K. Ram, Elias K. Stefanakos, and D. Yogi Goswami. Synthesis, Characterization, and Applications of ZnO Nanowires. Hindawi Publishing Corporation Journal of Nanomaterials. Volume 2012, Article ID 624520, 22 pages doi:10.1155/2012/624520.

[3] Agnieszka Kołodziejczak-Radzimska and Teofil Jesionowski.Zinc Oxide—From Synthesis to Application: A Review *Materials* 2014, *7*, 2833-2881; doi:10.3390/ma7042833.

[4] Gratzel M 2005 MRS Bull. 30 39374.

[5] Baxter J B, Walker A M, van Ommering K and Aydil E S 2006 Nanotechnology 17 S304.

[6] Sheng Xu and Zhong Lin Wang. One-Dimensional ZnO Nanostructures: Solution Growth and Functional Properties.Nano Res.ISSN 1998-0124. DOI 10.1007/s12274-011-0160-7.

[7] W. Liu, A. B. Greytak, J. Lee et al., "Compact biocompatible quantum dots via RAFT mediated synthesis of imidazolebased random copolymer ligand," *Journal of the AmericanChemical Society*, vol. 132, no. 2, pp. 472–483, 2010.

[8] A. Hoshino, K. Fujioka, T. Oku et al., "Quantum dots targeted to the assigned organelle in living cells," *Microbiologyand Immunology*, vol. 48, no. 12, pp. 985–994, 2004.

[9] L. N. Demianets, D. V. Kostomarov, I. P. Kuz'mina, and S. V. Pushko (2002). Mechanism of Growth of ZnO Single Crystals from Hydrothermal Alkali Solutions. *Crystallography Reports, Vol. 47, Suppl. 1, 2002, pp. S86–S98.*

[11] Y. Xia, P. Yang, Y. Sun et al., "One-dimensional nanostructures: synthesis, characterization, and applications," *Advanced Materials*, vol. 15, no. 5, pp. 353–389, 2003.

[12] G. C. Yi, C.Wang, andW. I. Park, "ZnO nanorods: synthesis, characterization and applications," *Semiconductor Scienceand Technology*, vol. 20, pp. S22–S34, 2005.

[13] Z. L. Wang, "Ten years' venturing in ZnO nanostructures: from discovery to scientific understanding and to technology applications," *Chinese Science Bulletin*, vol. 54, no. 22, pp. 4021–4034, 2009.

[14] Ayesha Naveed Ul Haq, Akhtar Nadhman, Ikram Ullah, Ghulam Mustafa, Masoom Yasinzai, and Imran Khan. Synthesis Approaches of Zinc Oxide Nanoparticles: The Dilemma of Ecotoxicity. Hindawi Journal of Nanomaterials Volume 2017, Article ID 8510342, 14 pages https://doi.org/10.1155/2017/8510342.

[15] Happy Agarwal, S. Venkat Kumar, S. Rajeshkumar," A review on green synthesis of zinc oxide nanoparticles –An eco-friendly approach,'' Resource-Efficient Technologies 3 (2017) 406–413.

[16] H. Abdul, R. Sivaraj, R. Venckatesh, Green synthesis and characterization of zinc oxide nanoparticles from Ocimum basilicum L. Var. Purpurascens Benth.- lamiaceae leaf extract. Mater. Lett 131 (2014) 16–18, doi: 10.1016/j.matlet.2014. 05.033 .

[17] R. Yuvakkumar, J. Suresh, A.J. Nathanael, M. Sundrarajan, S.I. Hong, Novel green synthetic strategy to prepare ZnO nanocrystals using rambutan (Nephelium lappaceum L.) peel extract and its antibacterial applications, Mater. Sci. Eng. C. 41 (2014) 17–27, doi: 10.1016/j.msec .2014.04.025.

[18] Hiromichi Hayashi and Yukiya Hakuta (2010). Hydrothermal Synthesis of Metal Oxide Nanoparticles in Supercritical Water. *Materials* **2010**, *3*, 3794-3817; doi:10.3390/ma3073794.

[20] Lawrence Choi, Jacqueline Feng, Alexei Owen, Sohum Pawar. Synthesis of Zinc Oxide Nanomaterials Via Solution Synthesis Method. Published on Aug. 20, 2013.

[21] Aleksandra B. Djurisic, Yan Y. Xi, Yan F. Hsu and Wai K. Chan. Hydrothermal Synthesis of Nanostructures.Recent Patent on Nanotechnology 2007, 1, 121-128.

[22] M.D. Tyona, R.U. Osuji and F.I. Ezema. A review of zinc oxide photoanode films for dye-sensitized solar cells based on zinc oxide nanostructures. *Advances in Nano Research, Vol. 1, No. 1 (2013) 43-58.*

[23] A.B. Djurisic, X.Y. Chen and Y.H. Leung. Recent Progress in Hydrothermal Synthesis of Zinc Oxide Nanomaterials. *Recent Patents on Nanotechnology,* 2012, *6,* 124-134

[24] M. Ladanov, M. K. Ram, G. Matthews, and A. Kumar, "Structure and opto-electrochemical properties of ZnO nanowires grown on n-Si substrate," *Langmuir*, vol. 27, no. 14, pp. 9012–9017, 2011.

[25] S. Xu, C. Lao, B. Weintraub, and Z. L. Wang, "Densitycontrolled growth of aligned ZnO nanowire arrays by seedless chemical approach on smooth surfaces," *Journal of MaterialsResearch*, vol. 23, no. 8, pp. 2072–2077, 2008.

[26] X. Qi. 'Synthesis and characterization of 3D superstructures via a template-free hydrothermal method', Power Technol., 18(2007)455604.

[27] S. Ashoka, G. Nagaraju, C. N. Tharamani, G. t. Chandrapp. 'ZnO architectures', Mater. Lett., 63(2009) 873-876.

[28] D. Jezequel, J. Guuenota, N. Jouinia, F.Fievet. 'Submicronic zinc oxide particles. Elaboration in poly medium and morphological characteristics', J. Mater. Res., (1995) 77-83.

[29] Y. Y. Tay, S. Li, F. Boey, Y. H. Cheng, M. H. Liang. 'Growth mechanism of spherical ZnO nanostructures synthesized via colloid chemistry', Physical B, 394(2007)372-376.

[30] Xu, S.; Adiga, N.; Ba, S.; Dasgupta, T.; Wu, C. F. J.; Wang, Z. L. Optimizing and Improving the Growth Quality of ZnO Nanowire Arrays Guided by Statistical Design of Experiments. *ACS Nano* **2009**, *3*, 1803–1812.

[31] Musi´ c S, Popovi´ c S, Maljkovi´ c M and Dragˇ cevi´ c D 2002 J. Alloys Compd. 347 324

[32] Pearton, S. J.; Norton, D. P.; Ip, K.; Heo, Y. W.; Steiner, T. Recent Progress in Processing and properties of ZnO. *Prog.Mater. Sci.* **2005**, *50*, 293–340.

[33] Klingshirn, C. ZnO: From basics towards applications. *Phys. Status Solidi B* **2007**, *244*, 3027–3073.

[34] Schmidt-Mende, L.; MacManus-Driscoll, J. L. ZnO— nanostructures, defects, and devices. *Mater. Today* **2007**, *10*, 40–48.

[35] Zang, J. F.; Li, C. M.; Cui, X. Q.; Wang, J. X.; Sun, X. W.; Dong, H.; Sun, C. Q. Tailoring zinc oxide nanowires forhigh performance amperometric glucose sensor. *Electroanal.***2007**, *19*, 1008–1014.

[36] L. Wang, Y. Fan, H. Bala, G. Sun. 'Controllable synthesis of hierarchical ZnO microstructures via a hydrothermal route', Micro Nano Lett., 6(2011)741-744.

[37] Baruah, S.; Dutta, J. pH-dependent growth of zinc oxide nanorods. *J. Cryst. Growth* **2009**, *311*, 2549–2554.

[38] Xu, S.; Shen, Y.; Ding, Y.; Wang, Z. L. Growth and transfer of monolithic horizontal ZnO nanowire superstructures onto flexible substrates. *Adv. Funct. Mater.* **2010**, *20*, 1493–1495

[39] Li, W. J.; Shi, E. W.; Zhong, W. Z.; Yin, Z. W. Growth mechanism and growth habit of oxide crystals. *J. Cryst.Growth* **1999**, *203*, 186–196.

[40] C. Richard Brundle, Charles A. Evans, Jr., Shaun Wilson (1992). *Encyclopedia of Materials Characterization*. Materials Characterization Series, Surfaces, Interfaaces, Thin Film.

[41] Emanetoglu. N. W., Gorla C, Liu Y, Liang S. and Lu Y. 1999 Mater. Sci. Semicond. Process 2 247

[42] Chen Y, Bagnall D and Yao T 2000 Mater. Sci. Eng. B 75 190

[43] Liang S, Sheng H, Liu Y, Hio Z, Lu Y and Chen H 2001 J. Cryst. Growth 225 110

[44] Saito N, Haneda H, Sekiguchi T, Ohashi N, Sakaguchi I and Koumoto K 2002 Adv. Mater. 14 418

[45] Lee J Y, Choi Y S, Kim J H, Park M O and Im S 2002 Thin Solid Films 403 533

[46] Mitra A, Chatterjee A P and Maiti H S 1998 Mater. Lett. 35 3

[47] Akhiruddin, Sugianto, andIrmansyah.The Influence of Hydrothermal Duration on Structures and Optical Properties of ZnO Nanoparticles. *Journal of Materials Physics and Chemistry, 2014, Vol. 2, No. 2, 34-37* Available online at http://pubs.sciepub.com/jmpc/2/2/4 © Science and Education Publishing DOI:10.12691/jmpc-2-2-4.

[48] Wang Z L 2004 J. Phys.: Condens. Matter 16 R829

[49]Sunandan Baruah and Joydeep Dutta. Topical Review Hydrothermal Growth Of Zno Nanostructures. *Sci. Technol. Adv.* Mater. 10 (2009) 013001 (18pp) doi:10.1088/1468 6996/10/1/013001.

[50]Dairong Chen, Xiuling Jiao, Gang Cheng.Hydrothermal synthesis of zinc oxide powders with differentmorphologies. Solid State Communications 113 (2000) 363–366.

[51]Ken Elen, Heidi Van den Rul, An Hardy,Marlies K Van Bael1, Jan D'Haen, Roos Peeters, Dirk Francoand Jules Mullens. Hydrothermal synthesis of ZnO Nanorods: A Statistical Determination of the Significant Parameters in View of Reducing the Diameter. *Nanotechnology*20 (2009) 055608 (8pp) doi:10.1088/09574484/20/5/055608

Three Dimensional GrapheneElectrode for Lithium Ion Batteries: Opportunities and Chalenges

Ramalan, A. M.,Buba, A. D. A, Umaisha R.T , Yusuf A.S and Musa H

Department of Physics, University of Abuja

Abstract

Graphene has been considered to be extremely attractive and ideally suited for implementation in energy storage applications andto bring a huge improvement in the performance of lithium ion batteries (LIBs)due to its large electrical conductivity, vast surface area, unique heterogeneous electron transfer and charge carrier rates, widely applicable electro-catalytic activity, and low production costs.Despite the unique properties of 2D graphene, restackingof the graphene sheets has been one of the greatest setbacks in their applications in LIBs. To overcome this, 2D graphene is fabricated into 3D hierarchical frameworks, thebalanced space organization radically relieves the self-restacking of graphenelayers. The 3D materials also inherit intrinsic physical properties of 2D graphene.This study starts with a brief introduction, concept and working principle of LIBs, graphene and highlighting thefunction of 3D graphene as electrode materials. The preceding sections laid the foundation for the discussion on the review of various electrodes used in LIBs, the issues and efforts to offer solutions to these problems.

Keywords: lithium ion battery (LIB), 3D graphene, electrode, energy storage.

1.0 Introduction

The ever increasing global energy demands havecalled for more efficient, sustainable and renewable energy resources and most of the available renewable energy sources are intermittent. To make energy affordable, availablein amounts, and at times and places that are different from those when and where one is in need of it, thenthere is a need for development of electrical energy storage systems. Thus, methods to store and transport energy fromplace to place can be of great importance. Lithium ion batteries (LIBs), electrochemical capacitors (ECs) (also known as supercapacitors or ultracapacitors) and metal air batteries are the most prominentand fast-growing energy storage devices (Li and Zhi, 2018).

Comparatively, LIBs generally possess higher energy density due to their different energy storage principles (Liu *et al.*, 2018; Li *et al.*, 2017).However,the current lithium-ion battery technology is approaching itslimit especially in terms of specific energy (per weight) andenergy density (per volume), incapable of satisfying the everincreasingdemand for diverse applications in expanded fieldssuch as mobile electronic devices,vehicle electrification and renewable energy integration (Chen*et al.*, 2018).To relieve this situation, a good number of electrode (anode andcathode) materials with theoretically high specific capacitieshave thus far been widely scanned and/or revisited in recentyears in order to enhance the energy density and power density of the LIBs (Fan*et al.*, 2015).

There has been a concerted effort to synthesis advanced electrode materials with tailored structure, composition and morphology. Significantly, engineering the nanostructured active materials into highly conductive matrix offers desirable functionality and great potential to achieve excellent energy storage, high rate capabilities and long lifespan for electrode materials (Cabana*et al.*, 2010; Lee*et al.*, 2011; Zhou*et al.*, 2011; Peng*et al.*, 2012). Among the materials pursued to offer solutions to the limitations and challenges related to theseelectrode materials for LIBs, recent research hasshown that graphene, a typeof two-dimensional carbon material, is a promisingcandidate to overcome these issues owing to its unique physical and chemical properties(Li and Zhi, 2018).Graphene is extremely attractive and ideally suited for implementation in energy storage applications due to its reported large electrical conductivity, vast surface area, unique heterogeneous electron transfer and charge carrier rates, widely applicable electro-catalytic activity, and low production costs (Brownson*et al.*, 2011).

Despite the attracting properties of 2D graphene, restackingof the graphene sheets still occurred in many cases, where a partially-turbostratic structure that reduces the specific capacity forms (Kim*et al.*, 2018). On the other hand, if 2D graphene is fabricated into three-dimensional (3D) hierarchical frameworks, thebalanced space organization radically relieves the self-restacking of graphenelayers. The 3D materials also inherit intrinsic physical properties of graphene.Through the formation of porous channels, the 3D spongy form of graphene hasshown much higher surface area than aggregates of 2D sheets. Especially in energy-related applications, the porosity becomes a determinative advantage for 3Dporous graphene networks over its 2D counterparts.To acquire materials for high-performance energy storage, a 3Dgraphene with an interconnected cellular network is a promising candidate among various porous scaffolds (Xu*et al.*, 2017).The 2D grapheme

sheet can be assembled or processedinto 3D structures that exhibit desired physical andchemical properties(Ferrer, Mace, Thomas, & Jeon, 2017).

Three dimensional (3D)graphene structures can be synthesised using either templateor template-free methods; the template method employs some predetermined structures as the template(Choi, Yang, Hong, Choi, & Huh, 2012; Huang, Sun, Su, Zhao, & Wang, 2014; Shi, Peng, Zhu, Zhu, & Zhang, 2015) whileon the other hand, the template-free approach is targeted at modifying the 2Dgraphene using chemical etching or some other means(Ferrer, Mace, Thomas, & Jeon, 2017; Lee, et al., 2010; Chen & Yan, 2011; Zhang, Chen, Hedhili, Zhang, & Wang, 2012).Template-assisted synthesis methods are attracting more attention basically because morphology and architecture of resulting 3D graphene and its composites are determined by the templates used duringthe synthesis(Choi, Yang, Hong, Choi, & Huh, 2012; Wen, Zhang, Yan, Zhang, & Shi, 2013).A range of templates has been reported in the literature which are soft and hard templatesincluding polymers, carbon spheres, inorganicparticles, micelles, ionic liquids, and nanostructuredsubstrates(Ferrer, Mace, Thomas, & Jeon, 2017; Meng, Wang, Zhang, & Wei, 2013; Choi, Yang, Hong, Choi, & Huh, 2012; Huang, et al., 2014; Huang, et al., 2012).(Fan, et al., 2013).(Zhang & Li, 2018; Losurdo, Giangregorio, Capezzuto, & Bruno, 2011; Cen, Sisson, Qin, & Liang, 2018).Therefore, this study briefly underscores the concept and working principle of LIBs and application of 3D graphene-based electrode materials in LIBs.The discussion on the various electrodes used in LIBs, the issues and efforts to offer solutions to these problems are undertaken.

2.0 Graphene: Fundamental and its Energy Storage Applications

Fascination with graphene has been growing very rapidly in recent years and the science of graphene is now becoming one of the most interesting and fast-moving topics in material science (Aoki and Dresselhaus, 2014). The horizon of graphene is ever becoming wider, where physical concepts go hand in hand with advances in experimental techniques. On the other hand, graphene attributed properties such as high surface area, excellent transparency, light absorption, and charge transport properties have significantly aroused interest from different research fields concerned with energy conversion and environmental pollution remediation (Tahir, et al., 2016).

Graphene is the first truly 2D crystal ever observed in nature and this is remarkable because the existence of 2D crystals has often been doubted in the past mainly due to Mermin-Wagner theorem

stating that a 2D crystal loses its long-range order, and thus melts, at any small but non-zero temperature as a result of thermal fluctuations (Fuchs and Goerbig, 2008). According to Zhen and Zhu (2018), graphene is an allotrope of carbon in the form of a 2D, atomic-scale, hexagonal lattice in which one atom forms each vertex with sp^2 hybridization as shown in Figure 2.

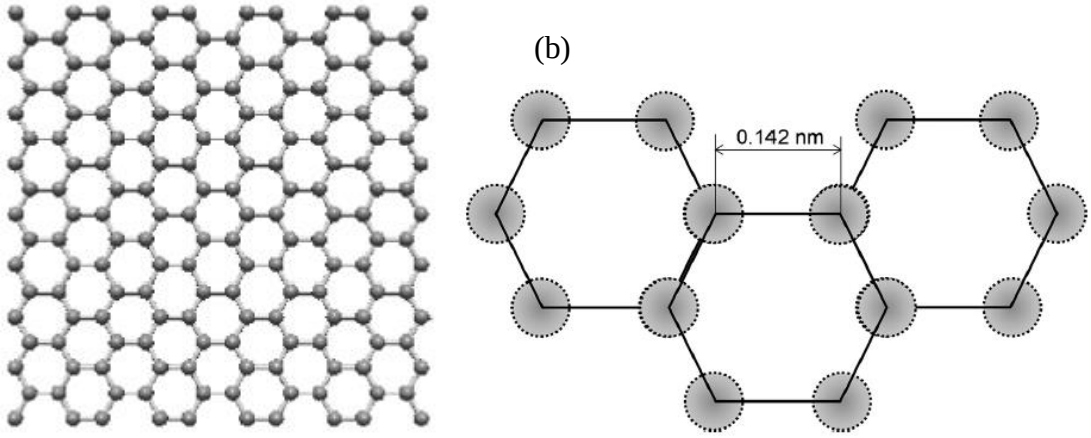

Figure 5 (a) Two-dimensional (2D) graphene (Wong & Akinwande, 2011) (b) Hexagonal lattice of graphene (Zhen & Zhu, 2018)

The unit structure of graphene is a hexagonal carbon ring with an area of 0.052 nm^2, carbon-carbon bond length is about 0.142 nm and a stable hexagonal structure is formed through strong connections by three σ bonds in each lattice (Zhen & Zhu, 2018; Harris, 2018). In graphene, each carbon atom uses 3 of its 4 outer orbital electrons to form 3 sigma bonds 120^0 apart with 3 adjacent carbon atoms in the same plane, leaving the 4th electron free to move, therefore, electrons in graphene behave just like massless relativistic particles without crystal lattices restrictions (Wei, et al., 2018; Stankovich S. , et al., 2006; Li & Kaner, 2008). As such, graphene possesses excellent electrical conductivities in two dimensions at room temperature (more than 200,000 $cm^2\ V^{-1}\ s^{-1}$) (Si & Samulski, 2008).

As a 2D material, graphene has zero band gap with a single molecular layered structure (Wei, et al., 2018); the electrical conductivity of graphene is mostly attributed to the π bond located vertically to the lattice plane (Zhen & Zhu, 2018). Graphene's stability is ascribed to its tightly packed carbon atoms and a sp^2 orbital hybridization—a combination of orbitals s, p_x, and p_y that constitute the σ-bond. The final p_z electron makes up the π-bond. The π-bonds hybridize together to form the π-band and π^*-bands. These bands are responsible for most of graphene's notable electronic properties, via the half-filled band that permits free-moving electrons (Zhen & Zhu, 2018). Moreover, graphene is

known for its tranparancy in the visible region which is attributed to its extreme thinness, this is found useful in DSSC's conductive substrate (Chae, et al., 2017; Nair, et al., 2008; Britnell, et al., 2013).

3D

3.0 Lithium Ion Battery (LIB): Concept and Working Principle

Lithium-ion battery (LIB) typically consists of anode (negative electrode), cathode (positive electrode), electrolyte and separator. The basic components and principle of a LIB is illustrated in Figure 1.

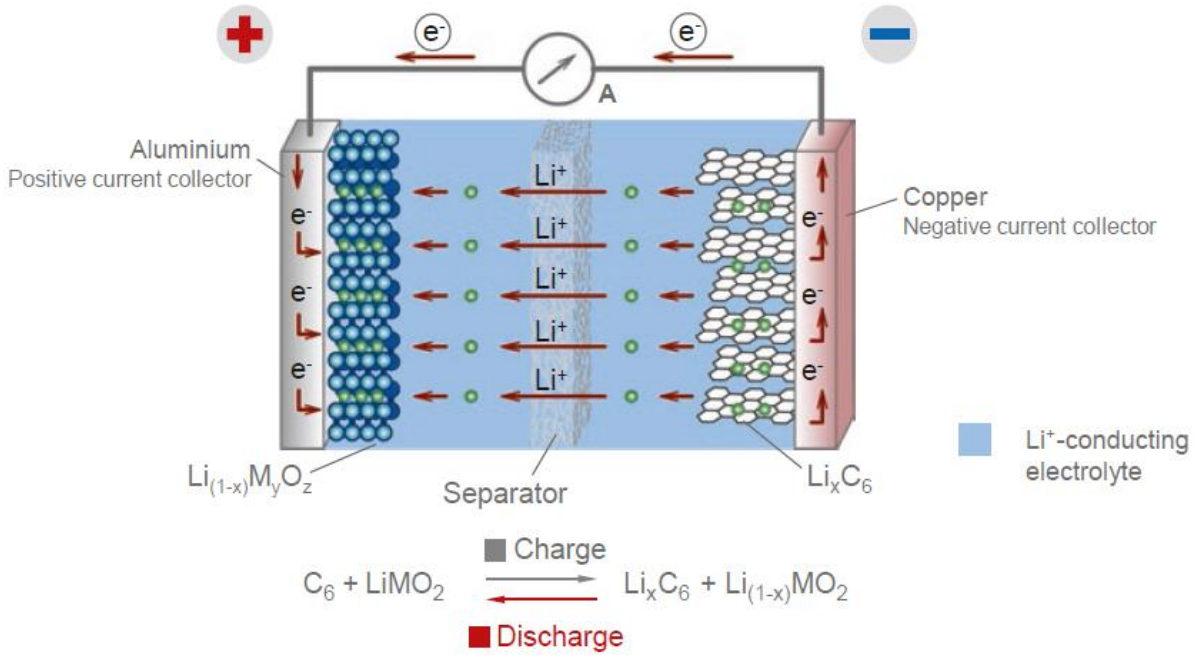

Figure 6: Scheme of lithium-ion battery: discharging process (Leuthner, 2018)

The most widelyused anode materials are graphite and other carbon materials, this is due to their high abundance, lowcost, and stable performance in Li storage while Li metal oxides ($LiCoO_2$, $LiMn_2O_4$), and Li metalphosphates ($LiFePO_4$) are common cathode materials. The electrolyte is usually a solution containing lithium hexafluorophosphate ($LiPF_6$) dissolved in carbonate-based solvents such as a mixture of ethylene carbonateand dimethyl carbonate(Feng, et al., 2018; Vuorilehto, 2018).Separator is a porous membrane (a layer of Li ion permeablemembrane) that prevents the direct contact between anodeand cathode i.e. it electricallyisolates the two electrodes from each other, LIB separators are mostly based on polyolefins(Weber & Roth, 2018). The ion-

conducting electrolyte (containing a dissociated lithium conducting salt)is situated between the two electrodes (anode and cathode) with the separator isolating the two electrodes from each other. The anode is relatively at lower potential with respect to Li^+/Li while cathode is at higher potential. Lithium is intercalated into anode materials (graphite and amorphous carbon compounds). The electrode materials are powders that are applied as coatingson current collectors, resulting in composite electrodes. The positive currentcollector is aluminum foil, typically 15 to 20 μm thick. Aluminum has a high conductivityand it is rather stable even at the high potential of the positive electrode.The negative current collector is copper foil, typically 8 to 18 μm thick. Aluminumwould be lighter and cheaper but it cannot be used at the low potential of the negativeelectrode due to parasitic formation of a lithium/aluminum alloy (Vuorilehto, 2018).

During charging and discharging process, there is a back and forth migration of Li^+between the electrodes as well as intercalation and de-intercalation of the Li^+into the electrode materials. Figure 1 illustrate discharging process of Li-ion battery, during discharging Li is de-intercalated from the anode and electrons are released to copper which functions as current collector and at the same time, the Li^+ (lithium ions) migrate from the anode through the electrolyte and theseparator to the cathode. The released electrons (current electricity) migrate from the anode via an outer electricalconnection (cable) to the cathode through aluminum which also functions as current collector.During charging, this process is reversed: Li ions migrate from the cathode through the electrolyte and the separator to the anode (Leuthner, 2018).

The performance of LIB is largely defined by its nominal capacity, electric energy and power. Capacity describes the amount of electric charge a power source can deliver underspecific discharge conditions. This depends on the discharging current, the cut-off voltage,the temperature, and the type and amount of active electrode materials, and the unit is Ah(Leuthner, 2018).The energy of LIB is calculated as the product ofcapacity and average discharge voltage,the unit is Wh. Specific energy refers to themass of the LIB and its unit is Wh/kg. Energy density refers to thevolume of the LIB and its unit is Wh/l(Leuthner, 2018). The power of LIB is Power is the product of current and voltage calculated duringdischarging and its unit is W. The efficiency of the battery is gottenby the energy released divided by the energy stored during charging (Leuthner, 2018).

4.0 3D Graphene Electrode for Lithium-Ion Batteries

Lithium-ion batteries being hi-tech devices are made of complex materials. The basic components of the device feature different materials for their composition.This review highlights the use of 3D graphene network in the LIB application.

4.1 Graphene Cathode for LIB

Nitta*et al.*(2015) described a cathode or an intercalation cathode as a solid host network, which can store guest ions; the solid host network creates a platform for the insertion and removal of the guest ions from the host network reversibly. In LIBs, the host network compounds could be metal chalcogenides,transition metal oxides, and polyanion compounds while the guest ion is Li^+(lithium ion). Some metal chalcogenides which have been studied as possible cathode materials include TiS_3, $NbSe_3$ and $LiTiS_2$; out of various chalcogenides, $LiTiS_2$ is more attractiveowing to its high gravimetric energy density combined with longcycle life (1000+ cycles)(Nitta, Wu, Lee, & Yushin, 2015; Whittingham, 2004). Recently, transition metal oxide and polyanioncompounds have been the focus of current LIB cathode research due to their higher operating voltage and the resultinghigher energy storage capability(Nayak, et al., 2018; Whittingham, 2004; Nitta, Wu, Lee, & Yushin, 2015).Based on different crystal structures, cathode materials are grouped into four classes in this work namely layered, spinel, olivine, and tavorite.

4.1.1 Layered Cathodes

Layered Cathodes can be layered chalcogenide such as TiS_3, $NbSe_3$ and $LiTiS_2$ as well as layered transition metaloxides.Nayak *et al.*(2018) and Graf (2018) noted that layered lithiated transition metaloxides is the most frequently examined system of cathode materials. These materials consist of layeredoxides with the chemical formula $LiMO_2$ (M = Co and/or Ni and/or Mn and/or Al) and they are probably most widely usedcathode materials. Examples of that layered transition metaloxides include lithium cobalt oxide ($LiCoO_2$, LCO)(Cho, Kim, Kim, Lee, & Park, 2003), $LiNiO_2$ (LNO), $LiMnO_2$ (LMO), $LiNi_{0.33}Mn_{0.33}Co_{0.33}O_2$, $LiNi_{0.8}Co_{0.15}Al_{0.05}O_2$, and Li_2MnO_3.Layered transition metal oxide compounds are very attractive and probably the most widely used cathode materialsbecause of their relatively high theoretical specific capacity, high theoretical volumetric capacity, low self-discharge, high discharge voltage, and good cycling performance(Nitta, Wu, Lee, & Yushin, 2015). However, LCO suffers drawbacks such as high cost (because of the high cost of Co), low thermal stability, and fast capacity fade at high current rates or during deep cycling; pure

LNO cathodes are not favourable because the Ni^{2+} ions have a tendency to substitute Li^{+} sites during synthesis and delithiation, blocking the Li diffusion pathways(Rougier, 1996), it also suffers from thermal instability(Arai, 1998); and the cycling performance of LMO is still not satisfactory because its layered structure has a tendency to change into spinel structure during Li ion extraction(Gu, 2012) and alsoMn leaches out of LMO during cycling(Nitta, Wu, Lee, & Yushin, 2015).

Continuous research efforts on improving the cathode materials has led to the doping ofthelayered transition metal oxide resulting to the development of layered transition metal oxide analog materials (composite layered cathode)(Nayak, et al., 2018). Nevertheless, these materials is yet to meet the required electronic conductivities for high battery performance. Of the materials sought to fulfil this purpose, graphene is considered very attractive,due to its relative high conductivity,to play a critical role in composite cathodematerials which is believed to fundamentally enhance the electrochemical performance of the LIB, though graphene is not to be a direct replacement of the existing cathode materials(Akbar, Rehan, Haiyang, Rafique, & Akbar, 2018; Guan, Li, Li, & Ren, 2017).The utilisation of graphene in LIB have been found beneficial in terms of cycling and rate capability(Nayak, et al., 2018; Goosey, 2012). Li et al (2017) used graphene with $LiNi_{1/3}Mn_{1/3}Co_{1/3}O_2$as a composite cathode in LIB, the result showed an improved specific capacity over ordinary $LiNi_{1/3}Mn_{1/3}Co_{1/3}O_2$ cathode. Venkateswara et al. (2011) similarly observed that the composites exhibited higher rate capability, longer cycle performance, and improved specific capacity.

4.1.2 Spinel(LiM_2O_4; M=Mn, Co, Ni) Cathodes

In exploring alternatives for commonly used toxic and expensive $LiCoO_2$, $LiMn_2O_4$ compounds (lithium manganese oxide, LMO spinel) were developed and these materials crystallize inthe spinel type structure which pose less safety hazard and characterised with ease of synthesis. However, due to the presence of John–Teller effect inlattice during the charge/discharge, its structure is prone todistort, resulting in the rapid decay of the capacity, especiallyat higher temperatures (Wu, Liu, & Guo, 2014; Lee, Cho, Song, Lee, & Cho, 2012). $LiMn_2O_4$ and its doping variants are attractivebecause of their easy availability and abundance but their low electrical conductivity brings about a low rate capacity (Zhang, et al., 2012; Akbar, Rehan, Haiyang, Rafique, & Akbar, 2018). However, many research advances have pointed towards grapheneas viable operators for enhancing the rate capacityand conductivity of spinel cathode materials. The use of $LiMn_2O_4$ graphene

composite as LIB cathode materials has reportedly showed enhanced electrochemical characteristics of the cathode(Akbar, Rehan, Haiyang, Rafique, & Akbar, 2018; Nitta, Wu, Lee, & Yushin, 2015).

4.1.3 Olivine ($LiMPO_4$; M = Fe, Mn, Co, Ni)Cathodes

Olivine cathodematerialsare sometimes referred toas phosphate cathode in the literature (Graf, 2018). Olivine cathode material was introduced in1997 and crystallizes like the natural mineral lithiophilite in the olivine structure (Graf, 2018; Padhi, Nanjundaswamy, & Goddenough, 1997).It is a polyanionic material, the polyanions ($(PO_4)^{3-}$) occupy lattice positions and increasecathode redox potential while also stabilizing its structure(Nanjundaswamy & al., 1996). Lithium ferrous phosphate ($LiFePO_4$; LFP) is probably most researched cathode material with olivine structure,owing to its high theoretical capacity(170 mAh g^{-1}), acceptable operating voltage (3.4 V vs.Li^+/Li), good cycling stability, low toxicity, good thermalstability, and low cost (Doughty & Rother, 2012; Graf, 2018; Nitta, Wu, Lee, & Yushin, 2015; Wu, Liu, & Guo, 2014).Other olivine materialssuch as $LiMnPO_4$ (lithium manganese phosphate; LMP) has been developed, this material offers about 0.4 V higher average voltage compared to olivine LFP, resulting to higher specific energy, but at the expense of lowerconductivity. $LiCoPO_4$, $LiNi_{1/2}Co_{1/2}PO_4$, and $LiMn_{1/3}Fe_{1/3}Co_{1/3}PO_4$, (LCP, NCP, MFCP) also exhibit relatively high operating voltage and goodcapacity, butfurther improvements are required in terms power, stability and energy density (Nitta, Wu, Lee, & Yushin, 2015; Li, Mu, vanAken, & Maier, 2013).

The biggest benefit of LFP is non-toxic compared to other olivine cathode $LiMPO_4$ (M = Co, Mn, and Ni) but unfortunately, LFP intrinsically exhibits poor electrical as well as ionic conductivityand low average potential which limits its electrochemical performance, especiallythe rate capability, as cathode in LIBs(Kang, Ma, & Li, 2011; Fisher, Prieto, & Islam, 2008; Andersson, Kalska, Haggstrom, & Thomas, 2000; Wu, Liu, & Guo, 2014).Various approaches have been attempted to improve the both the electrical and ionic conductivities by doping the LFP with other metals ions, reducing the particle size, coating with conductive carbon layer and aliovalent doping(Wu, Liu, & Guo, 2014; Chung, Bloking, & Chiang, 2002; Chung, Jang, Ryu, & Shim, 2004; Xu, Chang, & Gao, 2012). The results show that these approaches have been beneficial somewhat in achieving the aimed intended for but critical improvements are still required. Graphene in the recent times has been pursued as a material of choice to significantly, in combination with LFP, improve the electrochemical performance of LIBs.

It has been noted that 3D graphene-metaloxidestructures such as porous graphene films,graphene foams, and graphene ball hybrids are moresignificant than their 2D in energy storage fields. 3D graphene structures are said to maintain the superior intrinsic properties ofgraphene sheets which include large surface area and excellent electrochemicalproperties; the addition of metal oxides can furtherimprove the functions of these structures(Choi, Lee, & Kang, Three-dimensional porous graphene-metal oxide composite microspheres: Preparation and application in Li-ion batteries, 2015; He, et al., 2013; Cao, Yin, & Zhang, 2014; Huang, et al., 2014; Cao X. H., et al., 2014). More importantly, a 3D graphene structure with porousmorphology allow easyelectrolyte penetration and fast Li^+ diffusion for Li-ionbatteries (LIBs). Thus, 3Dgraphene-metal oxide composites are said to exhibit excellent electrochemical properties for awide range of energy storage applications(Cao, Yin, & Zhang, 2014).Yang*et al.*, (2013) used LFP/3D graphene composite in LIB cathode,the result showed that the conducting 3D graphene nano-network, enablesboth Li^+ and electrons to migrate andreach each of LFP particles, hence realizingthe full potential of the active materials which in return led to an enhanced electrochemical performance of the device.Similarly, 3D graphene LFP composite was developed by Zhou et al. (2011) as a Li-ion battery cathode material withexcellent high-rate capability and cycling stability. The composite was prepared with LiFePO4nanoparticles and graphene oxide nanosheets by spray-drying and annealing processes. It was reported that the presence of abundant voids betweenthe $LiFePO_4$ nanoparticles and graphene sheets was beneficial for Li^+ diffusion. The composite cathodematerial was able to deliver a capacity of 70 mAh g^{-1} at 60C discharge rate and showed a capacity decay rateof <15% when cycled under 10C charging and 20C discharging for 1000 times(Zhou, Wang, Zhu, & Liu, 2011).

4.1.4 TavoriteCathodes

Another type of cathode materials is tavorite-sructured cathodes such as $Li_3V_2(PO_4)_3$(LVP) and $LiFeSO_4F$ (LFSF).Tavorite-sructured cathode materials are another attractive cathode materials owing to their high cell voltage and reasonable specific capacity. Electrochemically active lithium iron sulfate fluoride ($LiFeSO_4F$) with tavorite structure was firstreported in 2010 by These materials are said to hold promise for the future of LIB cathode materials(Nitta, Wu, Lee, & Yushin, 2015; Masquelier & Croguennec, 2013).

4.2 Graphene LIB Anode

Materials for LIB anode are required to exhibit certain characteristics such as high lithium storage capability androbust structure for repeated charge/discharge cycles(Mao, Lu, & Chen, 2015).Carbon-based materials especially graphite are most widely used as anode in Li-ion (Sobkowiak, 2015). Graphite anodes possess ahigh electronic conductivity and high practical capacity of approximately350 mAh/g i.e. maximum one Li atom can bestored per six C atoms (LiC_6) based on the intercalationof Li, which give a theoretical maximum capacity of 372mAh/g (Campbell, et al., 2016; Ferrer, Mace, Thomas, & Jeon, 2017). In addition, the crystalline carbon allotrope graphite is almost exclusively utilized due to a much flatter cycling curve profile, and low operation voltage averaging about 0.125 V vs. Li/Li^+.Interestingly, using graphene as anode, two Li atomscan be stored per six C (Li_2C_6) because both sides of grapheneare able to store lithium ions, giving a theoreticalcapacity of 744 mAh/g; and moreLi atoms can be intercalated in defective sites and edgesof graphene, which could lead to even higher capacitythan 744 mAh/g(Ferrer, Mace, Thomas, & Jeon, 2017; Bonaccorso, et al., 2015; Zhu, Yin, Yan, & Zhang, 2014; Sun, Wu, & Shi, 2011).

On the other hand, many alternative non-carbon based materials have been demonstrated as potential anodematerials for LIBs due to their high specific capacities. The alternative non-carbon based anode materials that have attractedconsiderable attention recently are Li-alloys with different p-block elements,Li_xM, (M = Si, Sn, Sb, Al, etc.)(Croguennec & Palacin, 2015; Li & Dahn, 2007; Obrovac & Chevrier, 2014; Mao, Lu, & Chen, 2015)as well as conducting polymers such as polypyrrole (ppy)(Xia, Chao, Zhang, Shen, & Fan, 2015). These materials possess theoreticalcapacities of up to ten times higher than that of the carbon materials, for instance, Sn exhibits 981 mAh/g,SnO_2 exhibits 1491 mAh/g, and Si exhibits 4200 mAh/g compared with those of carbon-based materials (372 mAh/g for graphite)(Mao, Lu, & Chen, 2015). However, non-carbon based anodessuffer from significant capacity degradation,volume change (expansions and contractions)during Li^+ insertion/extraction cycles, which causes thepulverization of the anodes and electrical detachment of theactive materials from the current collector(Sobkowiak, 2015; Mao, Lu, & Chen, 2015).The issues of volume changes during lithiation anddelithiation, and extensive internal stresses have limited theirutilizationas anode materials despite the high theoretical capacity.

Various attempts have been made in using the graphene/non-carbon based electrode nanocomposite with the view to facilitate the transport of electronsand ions, and reduce the stress of thecollective electrode during lithiation anddelithiation process. Yet, most of the reported composites either with

reduced graphene oxide (rGO) or 2D graphene framework are far from practically serving as anodesdue to low Coulombic efficiency in the first cycle and unsatisfactorycycling performance(Mao, Lu, & Chen, 2015). Restacking of rGO or 2D graphene due to the van der Waals forces can significantly reduce the surface area and limit electron andion transport.3D graphene eliminates restacking issues and provide a large specific surface area, porous structure,and fast electron transport(Chen, et al., 2011; Han, Wu, Li, Zhang, & Feng, 2014).

Several composites combining 3D graphene with various non-carbon based high-capacity anode materials have been demonstrated to be promising in LIB. The non-carbon based anode materials include Sn(Qin, et al., 2014), SnO_2(Huang, et al., 2013), Si(Luo, et al., 2012; Zhu, Zhang, Xu, Yan, & Xue, 2014), Fe_3O_4(Chang, et al., 2013), Fe_2O_3(Cao X. H., et al., 2014; Cao X. , et al., 2014),MnO(Lee, Choi, Lee, & Kang, 2014),MnO_2(Li, Zhang, Zhu, Wei, & Shen, 2014; Zhu, Zhang, Xu, Yan, & Xue, 2014), TiO_2(Jiang, et al., 2014; Shen, Zhang, Li, Yuan, & Cao, 2011),NiO(Choi, Ko, Lee, & Kang, 2014), MoO2(Choi & Kang, 2014), V_2O_5(Choi & Kang, 2014), Co_3O_4(Choi, et al., 2012), CoO(Ma, et al., 2014), MoS_2(Xu, Lin, Huang, Liu, & Duan, 2013; Wang, et al., 2014), Ni_3S_2,(Zhao, et al., 2014)186 Ge(Ma, et al., 2014), S(Wang, et al., 2014), and also conducting polymers(Xia, Chao, Zhang, Shen, & Fan, 2015).

For instance, Qin et al. (2014) employed 3D graphene/Sn composite as a LIB anode through CVD technique, the composite anode exhibited good capacities of 1022 mAh/g at 0.2 C, 865 mAh/g at 0.5 C, 780 mAh/g at 1 C,652 mAh/g at 2 C, mAh/g at 5 C, and 270 mAh/g at10 C, where 1 C is 1 A/g.Long cycling stability was alsoand maintaining approximately 96.3% after 1000 cycles. The result demonstrated that the anode pecific capacity and good capacity retention surpass many other carbon/Sn composites(Mao, Lu, & Chen, 2015; Li, Dhanabalan, Gu, & Wang, 2012; Xu, et al., 2013). The observed enhanced electrical conductivity was ascribed to the porosity, highelectrical conductivity, large surface area, and high mechanicalflexibility of the graphene/Sn composite structure.

Another study carried out by Huanget al. (2013)obtaining 3Dgraphene/SnO_2 compositesthrough a two-step assembly method indicateda large surface area, several macropores, and a low mass density.The the result showed that the composite provided multidimensionalchannels for electron transport and electrolyte access, and enabled the rapid diffusion of lithium ions from the electrolyte to theelectrode. A high capacity of 830 mAh/gfor up to 70 charge/discharge cycles at 100 mA/gwith

good cyclingstabilitywas achieved. The composite have been reportedly doped by other workers in order to either tune the electronic properties of the composite or improve the lithium storage properties(Mao, Lu, & Chen, 2015; Wang, Xu, Sun, Gao, & Yao, 2014).

5.0 Conclusion and Perspective

The revolution in the landscape of the battery technology through the invention of LIBs and the continued development of the materials via intensive research has been a monumental feat.The success of LIBs have affected our everyday life positively ranging from portable electronics to the large-scale energy-storage devices, such as electric vehicles.The present LIB technology could boast of high energy density,high cycle life, and good efficiency, yet there is a need to push the boundaries ofcost, energy density, power density, cycle life, and safety in order to meetthe ever increasing demand for the enhanced energy storage devices.To achieve this, this will require inexpensivehigh capacity electrode materials with good electrical/ionic conductivity as well as cyclic stability, environmental benignity and excellent lithium storage properties. 3D graphene networks has been demonstrated to be a promising candidate due to its unique properties such as excellentmechanical strength, large specific surface area, desirable flexibility, and good electronicconductivity.

Presently, the 3D graphene composite as electrode material is considered as suitable strategy to practically improve LIB performance; theelectrochemical performance can be improved due to availability of more active sites, the porosity of the 3D graphene networks can facilitate the ion diffusion,issues of safety and of cyclic stability can be addressed with 3D graphene composite electrode. However, there are still notable concerns related to the high cost and synthesis of 3D graphene composite electrode which have to be addressed to make the LIBs using 3D graphene composite electrode commercially viable. Future work should be directed towards reducing the current high cost of production with focus on mass producing high-quality 3D graphenecomposite electrode. In addition, effective synthesis design is essential to maximise LIB performance, structure and morphology of the composite which has to be environmentally benign, simple, affordable and scalable.

References

Akbar, S., Rehan, M., Haiyang, L., Rafique, I., & Akbar, H. (2018). A brief review on graphene applications in rechargeable lithium ion battery electrode materials. *Carbon Letters, 28,* 1-8.

Andersson, A. S., Kalska, B., Haggstrom, L., & Thomas, J. O. (2000). Lithiumextraction/insertion in LiFePO4: an X-ray diffraction and Moss bauer spectroscopy study. *Solid State Ionics, 130*(1-2), 41–52. doi:10.1016/S0167-2738(00)00311-8

Arai, H. (1998). *Solid State Ionics, 109* (3), 295.

Bonaccorso, F., Colombo, L., Yu, G., Stoller, M., Tozzini, V., Ferrari, A. C., . . . Pellegrini, V. (2015). Graphene, related two-dimensional crystals, andhybrid systems for energy conversion and storage. *Science, 347,* 6217.

Britnell, L., Ribeiro, R. M., Eckmann, A., Jalil, R., Belle, B. D., Mishchenko, A., . . . Novoselov, K. S. (2013). Strong Light-Matter Interactions in Heterostructures of Atomically Thin Films. *Science, 340*(6138), 1311-1314. doi:10.1126/science.1235547

Cai, M., Thorpe, D., Adamson, D. H., & Schniepp, H. C. (2012). Methods of graphite exfoliation. *J. Mater. Chem., 22*, 24992–25002.

Campbell, B., Ionescu, R., Tolchin, M., Ahmed, K., Favors, Z., Bozhilov, K. N., . . . Ozkan, M. (2016). Carbon-coated, diatomite-derived nanosilicon asa high rate capable Li-ion battery anode. *Scientific Report, 6,* 33050.

Cao, X. H., Yin, Z. Y., & Zhang, H. (2014). Three-dimensionalgraphene materials: Preparation, structures and applicationin supercapacitors. *Energy Environ. Sci., 7*, 1850–1865.

Cao, X. H., Zheng, B., Rui, X. H., Shi, W. H., Yan, Q. Y., & Zhang, H. (2014). Metal oxide-coated three-dimensional grapheneprepared by the use of metal–organic frameworks as precursors. *Angew. Chem. Int. Ed, 53*, 1404–1409.

Cao, X., Zheng, B., Rui, X., Shi, W., Yan, Q., & Zhang, H. (2014). *Angew. Chem., Int. Ed.,, 124*, 1428–1433.

Cen, Y., Sisson, R. D., Qin, Q., & Liang, J. (2018). Current Progress of Si/Graphene Nanocomposites forLithium-Ion Batteries. *Journal of Carbon Research, 4*, 1-14. doi:10.3390/c4010018

Chae, S., Jang, S., Choi, W. J., Kim, Y. S., Chang, H., Lee, T. I., & Lee, J. -O. (2017). Lattice Transparency of Graphene. *Nano Letters, 17*(3), 1711-1718. doi:10.1021/acs.nanolett.6b04989

Chang, Y., Li, J., Wang, B., Luo, H., He, H., Song, Q., & Zhi, L. (2013). *Journal of Materials Chemistry A, 1*, 14658—14665.

Chen, W., & Yan, L. (2011). In situ self-assembly of mild chemical reduction graphenefor three-dimensional architectures. *Nanoscale, 3*(8), 3132–3137.

Chen, Z., Ren, W., Gao, L., Liu, B., Pei, S., & Cheng, H. -M. (2011). *Nat. Mater., 10*, 424–428.

Cho, J., Kim, Y. -W., Kim, B., Lee, J. -G., & Park, B. (2003). A Breakthrough in the Safety of Lithium Secondary Batteries by Coating the Cathode Material with AlPO4 Nanoparticles . *Angewandte Chemie International Edition, 42*(14), 1618 - 1621. doi:10.1002/anie.200250452

Choi, B. G., Chang, S. J., Lee, Y. B., Bae, J. S., Kim, H. J., & Huh, Y. S. (2012). *Nanoscale, 4*, 5924–5930.

Choi, B. G., Yang, M., Hong, W. H., Choi, J. W., & Huh, Y. S. (2012). 3D macroporousgraphene frameworks for supercapacitors with high energy and powerdensities. *ACS Nano, 6*(5), 4020–4028.

Choi, S. H., & Kang, Y. C. (2014). *ChemSusChem, 7*, 523–528.

Choi, S. H., & Kang, Y. C. (2014). *Chem. – Eur. J., 20*, 6294–6299.

Choi, S. H., Ko, Y. N., Lee, J. K., & Kang, Y. C. (2014). *Scientific Report, 4*, 5786.

Choi, S. H., Lee, J. -K., & Kang, Y. C. (2015). Three-dimensional porous graphene-metal oxide composite microspheres: Preparation and application in Li-ion batteries. *Nano Research, 8*(5), 1584–1594.

Chung, H. -T., Jang, S. -K., Ryu, H. W., & Shim, K. -B. (2004). Effects of nanocarbonwebs on the electrochemical properties in LiFePO4/Ccomposite. *Solid State Communications, 131*(8), 549–554.

Chung, S. Y., Bloking, J. T., & Chiang, Y. M. (2002). Electronically conductivephospho-olivines as lithium storage electrodes. *Nature Materials, 1*(2), 123–128.

Croguennec, L., & Palacin, M. R. (2015). Recent Achievements on Inorganic Electrode Materials for Lithium-Ion Batteries. *Journal of the American Chemical Society, 137* (9), 3140–3156.

Doughty, D., & Rother, E. P. (2012). *Electrochem. Soc. Interface, 21*(2), 35.

Fan, Z., Yan, J., Ning, G., Wei, T., Zhi, L., & Wei, F. (2013). Porous graphene networks ashigh performance anode materials for lithium ion batteries. *Carbon, 60*, 558–561.

Feng, K., Li, M., Liu, W., Kashkooli, A. G., Xiao, X., Cai, M., & Chen, Z. (2018). Silicon-Based Anodes for Lithium-Ion Batteries: FromFundamentals to Practical Applications. *Small, 1702737*, 1-33. doi:10.1002/smll.201702737

Ferrer, P. R., Mace, A., Thomas, S. N., & Jeon, J. -W. (2017). Nanostructured porous graphene and its composites for energy storage applications. *Nano Convergence, 4*(29), 1-19. doi:10.1186/s40580-017-0123-0

Fisher, C. A., Prieto, V. M., & Islam, M. S. (2008). Lithium batterymaterials LiMPO4 (M = Mn, Fe Co, and Ni): insights into defectassociation, transport mechanisms, and doping behavior. *Chemistry of Materials, 20*(18), 5907–5915. doi:10.1021/cm801262x

Goosey, M. (2012). short introduction to graphene and its potential interconnect applications. *Circuit World, 38*, 83-86.

Graf, C. (2018). Cathode materials for lithium-ion batteries. Ninu R. Korthauer, *Lithium-Ion Batteries: Basics and Applications* (oju ewe 29 - 43). Ber;lin, Germany: Springer-Verlag.

Gu, M. (2012). *ACS Nano, 7*(1), 760.

Guan, X., Li, G., Li, C., & Ren, R. (2017). Synthesis of porous nano/micro structuredLiFePO4/C cathode materials for lithium-ion batteries byspray-drying method. *Transactions of Nonferrous Metals Society of China, 27*(1), 141 - 147. doi:10.1016/s1003-6326(17)60016-5

Han, S., Wu, D., Li, S., Zhang, F., & Feng, X. (2014). *Advanced Materials, 26*, 849–864.

Harris, P. J. (2018). Transmission Electron Microscopy of Carbon: A Brief History. *Journal of Carbon Research, 4*(4), 1-17. doi:10.3390/c4010004

He, Y. M., Chen, W. J., Li, X. D., Zhang, Z. X., Fu, J. C., Zhao, C. H., & Xie, E. Q. (2013). Freestanding three-dimensionalgraphene/MnO2 composite networks as ultralight and flexiblesupercapacitor electrodes. *ACS Nano, 7*, 174–182.

Huang, X., Qian, K., Yang, J., Zhang, J., Li, L., Yu, C., & Zhao, D. (2012). Functionalnanoporous graphene foams with controlled pore sizes. *Advanced Materials, 24*(32), 4419–4423.

Huang, X., Sun, B., Su, D., Zhao, D., & Wang, G. (2014). Soft-template synthesis of3D porous graphene foams with tunable architectures for lithium-O2 batteries and oil adsorption applications. *Journal of Materials Chemistry A, 2*(21), 7973–7979.

Huang, X., Yu, H., Chen, J., Lu, Z. Y., Yazami, R., & Hng, H. H. (2014). Ultrahigh rate capabilities of lithium-ion batteries from 3D ordered hierarchically porous electrodes with entrappedactive nanoparticles configuration. *Adv. Mater., 26*, 1296–1303.

Huang, Y. S., Wu, D. Q., Han, S., Li, S., Xiao, L., Zhang, F., & Feng, X. L. (2013). *ChemSusChem, 6*, 1510—1515.

Natural Radioactivity Concentration in Soil Samples from Rayfield Mining Site Jos-Plateau, Nigeria

[1*]Atipo, M.K., [2]Olarinoye, I.O., [2]Awojoyogbe, O. B.

[1]Nigerian Nuclear Regulatory Authority (NNRA), Makurdi, Nigeria.

[2]Department of Physics, Federal University of Technology, Minna, Nigeria.

*[1]kolaxatip@yahoo.com

[2]Leke.Olanrinoye@futminna.edu.ng

[2]awojoyobge@yahoo.com

*Corresponding Author

Abstract:

The natural radioactivity in contaminated soil of a mining site in Rayfield area of Jos-Plateau, Nigeria was carried out in order to ascertain the level of primordial radioisotopes present. The activity level was determined using gamma-ray spectrometric procedure via a hyper-pure germanium (HPGe) detector. The obtained result showed that the mean activities of ^{238}U, ^{232}Th and ^{40}K in the soil samples ranged from145.65 ± 8.13 Bq/kg to 525.42 ± 28.23 Bq/kg; from 263.97 ± 16.99 to 1915.41 ± 110.82

Bq/kg and 78.62 ± 6.39 to 2091.4 ± 114.01 Bq/kg respectively with mean values of 299.03 Bq/kg, 682.51 Bq/kg and 664.99 Bq/kg for ^{238}U, ^{232}Th and ^{40}K respectively. The caculated absorbed dose rate, (D) and radium equivalent mean values were 578.12nGy/h and 1326.23Bq/Kg respectively. Also estimated annual external effective dose rate and external hazard index ranged from 0.30 to 1.73 mSv/yr and 1.52 to 8.81 respectively. The mean values of measured activity concentrations and estimated radiological safety parameters were all higher than their corespondence average values in soil and recommended safety limits. The result showed that the level of radiological contamination of the soil in the study area is alarming and may pose health and ecological challenge to the people and the environment.

Keywords: Effective-Dose, NORMs, Radioisotopes, Nuclear Safety.

Introduction.

The mineral survey carried out in northern Nigeria between 1904 – 1909 revealed the abundance of tin ore over a wide area of modern day Jos, Plateau State of Nigeria. Ever since then, more cassiterite and columbite have been discovered and mined in the area (Masok *et al.*, 2015a Masok *et al.*, 2015b). Consequently, tin mining activities have been going on in Jos and environs for more than a century (Masok *et al.*, 2015a). The tin production in Jos peaked around 1.5 metric tons and gradually rose to 17740 metric tons by 1943 (Onwuka *et al.*, 2013). Unfortunately, the mining processes come with accompanying inevitable environmental damage and hazards (UNSCEAR, 2000; Jibiri *et al.*, 2007). The disturbance in the natural distribution of Natural Occuring Radioactive Materials (NORM) such as ^{238}U, ^{232}Th and ^{40}K and the consequent increase in ionizing radiation in the environment is one of the environmental hazards associated with mining. Furthermore, monazite, thorite and other materials which are by products of tin mining process contain radioactive heavy metals whose concentrations in the biosphere may also increase within the mining vicinity. In 1996, De-Wet establishes that many food items grown near mining area contained radium – a radioactive nuclide. Also, research conducted and concluded in 2015 by Marvic *et al.* around tin mining dumpsites in Rayfield area of Jos suggested high values in the concentrations of ^{226}Ra, ^{232}Th and ^{40}K and associated radiological parameter in the soils of the dumpsites. Similar elevated levels have been reported by many previous

research conducted on Jos and its environs (Abba *et al.*; 2018, Usikalu *et al.*; 2011; Ibeanu, 2003; Arogunjo, 2009; Masok *et al.*; 2015b).

In view of the health hazard associated with uncontrolled increase in radiation exposure, it has become greatly important for continuous environment impact assessment of mining activities whenever they are carried out. This will reveal the extent of damage done to the environment and the health risk associated with the mining and milling processes. Such impact assessment includes the measurement of NORM and associated radiological parameters within the mining field's vicinity. Generally, the three NORM species are measured for this purpose. Also ^{226}Ra, another radionuclide of concern is a decay product of ^{238}U which is also widely distributed in many geological formations such as soils, water and rocks. It decays to ^{222}Rn (gas) with a half-life of about 4 days). This gas has been reported to be a major cause of lung cancer among non-smokers (IARC, 2012). The fact that many active and abandoned mining sites in Jos are located around residential area is a cause for concern. It has thus become important that the radiological risk parameters of the population in the said area be evaluated. This research reports the concentrations of ^{238}U, ^{232}Th and ^{40}K in the soils around a mining site at Rayfield, Jos North part of Plateau state. The radiological risk parameters associated with the NORM distribution is also presented. Data from this research is important to government, mining company, and individual who work or live around the area under study as it will give the level of environmental hazard caused by the mining operations, provide basic radiological data for evaluating environmental impact and for judgment of future impacts and also provide data on the future health risk such as cancer associated with working and living in the area.

Study area

The area known as Jos is the capital of the north central state of Plateau in Nigeria. The area is bounded by latitudes 9˚30' and 10˚10' N and longitudes 8˚15' and 9˚15' E and about 4062 feet above sea level. Climatically, it is dominated by tropical dry and wet conditions with annual rainfall and temperature ranging between 1500 – 2000 mm and 20˚C – 25 ˚C respectively (Wapwera *et al.*; 2015). The topography is characterized by series of highlands of variable heights and flat topography. Also, the vegetation consists of stunted trees, tall grasses and shrubs.

The geology of Jos is in the north central basement complex of Nigeria containing plutonic and volcanic rock types. These rocks are classified into: younger granites, Precambrian rocks and intrusive older granites (migmatites, gneisses, crystalline basement rocks) (Badejo, 1975; Wright, 1976; Turner, 1976). According to Badejo (1975), these rocks are host to cassiterite and columbite ores. This explains why these ores have been mined, milled and processes for tin for a very long time in Jos and its environs. Other minerals such as tantalite, xenotime, thorite, monazite and zirconium are also known to be associated with the geology of Jos (Arogunjo, 2009).

Materials and methods

Sample collection, preparation and activity determination

Twelve soil samples were collected from different locations evenly distribute across the active mining site in Rayfield, Jos through the use of digger and hand trowel in polythene bags. Also one soil sample was collected at Living Faith School fence about 100m away from the site. The soils were collected within a depth of 20cm from the top of the soil. The collected soils were transported to the laboratory where they were sundried to remove soil moisture content until a content soil weight was attained. The dried soil samples were then crushed and sieved using a 500 µm mesh sieve to remove debris, organic materials and uncrushed stones. The homogenized soil samples were weighted each at 500 g and packed in marinelli beaker and sealed. The sealed beakers were left for 31 days to allow for secular radioactive equilibrium between ^{238}U and its short lived daughters (^{222}Rn, ^{214}Pb, ^{226}Rn). The radioactivity concentrations of ^{238}U, ^{232}Th and ^{40}K were determined using a 53.4 mm x 59 mm hyper-pure germanium (HPGe) crystal detector (Canberra Co-axial (n-type) with an energy resolution of 0.0024MeV) (FWHM) at gamma energy of 1.33 MeV of ^{60}Co and a relative efficiency of 50%. A proper shielding for the detector was provided in orders to suppress external background radiation coming from other sources. The detector was calibrated using standard IAEA referenced source soil (GG U- 238), RG Th-332, R9G K-40 with same geometry and density as that of the prepared soil samples were placed on the detector and using the spectrometer and Multichannel analyzer, gamma energy spectra were accumulated for each of the soil samples using a counting time of 20000s. The ^{238}U activity concentration was calculated using the 609.3 KeV peak from the ^{214}Bi decay, while the 2.614 MeV peak of ^{208}Tl was used to determine the concentration of ^{232}Th and the single 1.46 MeV gamma line of ^{40}K was used to determine the concentration of ^{40}K in the soil samples.

The activity of the radionuclides was determined using the equation (Usinkalu *et al*., 2011):

$$A_i = \frac{C_n}{E_\gamma M_s I_\gamma} \quad (1)$$

where A_i is the activity concentration of radionuclides (^{235}U, ^{232} Th and ^{40}K) in the assigned soil sample, C_n is the net count per second of the sample under the corresponding photo peak, E_γ is the efficiency of the detector at the specific gamma ray energy of interest, M_s is the mass of assigned soil sample and I_γ is the intensity of the gamma rays at the interested energy being counted.

3.2 Evaluation of Radiological dose and risk Parameters

Absorbed Dose Rate (*D*)

The absorbed dose rate (D) in air associated with the activity concentrates of ^{238}U ^{232} Th and ^{40}K Present in each of collected soil sample was evaluated using equation (2) (UNCEAR, 2000, Abba *et al*., 2018).

$$\mathrm{D(nGy}h^{-1}) = \sum_{i=1}^{3} A_i\, C_i \quad (2)$$

Where A_i is the measured activity concentrations (Bg/kg) of ^{238}U, ^{232}Th and ^{40}K and C_i are their conversion factor to dose rate given as 0.462, 0.604 and 0.0417 respectively.

Radium equivalent (R_{eq}).

The radium equivalent (R_{eq}) is a radiological safety parameter which is calculated using equation (3) (Berekta and Mathew, 1985; UNSCEAR, 2000, Odoh *et al.*, 2018).

$$Ra_{eq} = A_U + 1.43A_{Th} + 0.077A_K \quad (3)$$

A_U, A_{Th} and A_K are the activity concentration as defined in equations 1 and 2. Equation 3 is based on the fact that 1 Bg/kg of ^{238}U, 1.43 Bq/Kg of ^{232}Th and 0.077 Bq/kg of ^{40}K yield equal adsorbed gamma radiation dose rates. Thus the R_{eq}, acts as a single and simple index which can be used to compare the specific activity concentrations in materials containing different amount of ^{238}U, ^{232}Th and ^{40}K.

Annual outdoor Effective dose rate (E_{out} (mSv/y)).

In order to assess the long term hazard due to exposure to radiation, the outdoor annual effective dose rate at 1m above the ground level in air was estimated via equation 4 (UNSEAR, 2000 ICRP, 2008).

$$E_{out}(\frac{mSv}{y}) = D\left(\frac{nGy}{h}\right) \times 8760(\frac{h}{y}) \times 0.2 \times 0.7 \times 10^{-6}(\frac{mSv}{nGy}) \quad (4)$$

The external hazard index was estimated using equation (5)

$$H_{ex} = \frac{A_u}{370} + \frac{A_{Th}}{259} + \frac{A_k}{4810} \leq 1 \quad (5)$$

The H_{ex} should be ≤ 1 in order for the external dose rate not to exceed 1.5mGy. It also ensure that the maximum permissible level of Ra_{eq} does not go exceed 370 Bq/kg i.e $H_{ex} = \frac{R_{acq}}{370(B}(Bq/kg)$

Results

The measuerd mean activities of the three primordial radionuclide in the contaminated soil samples in the mine are depicted in figure 1.

The activity concentration of ^{238}U, ^{232}Th and ^{40}K radioisotopes varies in the range from 145.65 ± 8.13Bq/Kg to 525.42 ± 28.23Bq/Kg, 263.97Bq/Kg, to 1915.41±11, and 78.62 ± 6.39, 2091.4 ± 114.01 respectively in the collected soil samples. The corresponding mean values of measureed activity concentrations are299.03 Bq/Kg, 682.51Bq/Kg and 664.99Bq/Kg for ^{238}U, ^{232}Th and ^{40}K respectively. Also shown in the figure is the world average concentration of 32, 45, and 420 Bq/Kg for U, Th, and K respectively according to UNSCEAR(2000). The result showed that the mean measured activity concentration of ^{238}U in all the samples was at least nine times the world average value while the mean concentration of ^{232}Th and K were fifteen and two times the world average values respectively, The elevated values of the primodial radionuclide concentrations could be attributed to the mining and milling processes taking place at the location. The soil samples at the

mining site could have been contaminated with mine tailing which are dumped indiscriminately at the mine. The high concentration of radionuclides in samples S3, S5 and S12 which were collected close to the mining pit further buttress this point. The variation in the radionuclide concentrations can be attributed thus to the level of the contamination in the locations. The activity of radionuclides in samples S5,S6 and S12 follows the order of world average distribution of the three radionuclides i.e $^{40}K > ^{232}Th > ^{238}U$. However only in S1 was the concentration of ^{238}U more than both ^{232}Th and ^{40}K. In the other samples the order was $^{232}Th > ^{40}K > ^{238}U$. The mean distribution of the radionuclide in the entire studied samples is depicted in Figure 1. The natural abudance of ^{40}K suggest that it content in undisturbed soil should be higher compare to the other two radionuclides, however the presence of mineral ore high in ^{232}Th such as thorite explains the higher average concentrations of ^{232}Th in the samples. Furthermore ^{232}Th tends to be insoluble while ^{40}K and ^{238}U dissolve in water depending on the alkalinity of the solution (Arogunjo, 2009). Similar distribution of ^{238}U, ^{232}Th and ^{40}K in mining tailings and contaminated soils have been compared and presented and compared in table 1.

Obviously, the radioactivity levels in Jos and its environs are higher than normal. The calculated values of Ra_{eq} of the collected soils and their coresponding absorbed dose rates are presented in figure 3. The values of Ra_{eq} varied between 563.49 to 3263.83 Bq/Kg with an average value of 1326.23Bq/Kg.

The estimated Ra_{eq} of all soil samples collected were higher than the world refrence limit of 370 Bq/Kg (UNSCEAR 2000) The mean value of the radium equivalent was though lower than the mean value of 31.2×10^3 Bq/Kg reported by Ademola in 2008 while working on mine tailing from a mining site in Jos area. The values of the absorbed dose rate (D) in air calculated using equation 2 are presented in figure 3 as well. It ranged from 244 to 1408 nGy/h with a mean of 578 nGy/h. All the soil samples analised presented Raeq that were greater than the international refrence of 80 $nGyh^{-1}$ set by the UNSCEAR (2000). The elevated primodial radionuclide content of soil due to the mining activities and geology of the soil are chiefly/majorly responsible for this high value of *D*.

The annual effective dose rate (E_{out}) and external hazard index (H_{ex}) values estimated via equations 4 and 5 are given in figure 4. The average E_{out} was 0.71 $mSvy^{-1}$ while that of H_{ex} was 3.58. The highest values of D and H_{ex} were obtained from soil sample S3 which was collected from a one of the mine points.

Conclusion.

Assesment of the radioactivity concentrations of ^{238}U, ^{232}Th and ^{40}K have been carried out in contaminated soils from a tin mine site in Jos- Plateau using gamma spectrometric procedure. Obtained radioactive concentration levels of the three primordial radionuclide were generally higher than their respective world average and safely values consequently the ambient radiation dose in the viscinity of the mine has been enhanced due to the mining activities going on in the said area. The elevated background radiation in the area can pose a potential health and ecological risk to the inhabitant of Rayfield area of Jos. Furthermore dwellers in the viscinity of the mine and the mine workers are potential candidates of radon induced lung cancers as a results of the elevated ^{238}U and ^{232}Th burdens in the soil of the area. Consequently, assessment of internal radiation contamination of mine workers and inhabitants of the mine area is very importants. It is also important that local authorities prevent the use of mine contaminated soils and tailings as building materials or farm soil so as to prevent the elevated level of primodial radionuclides from getting into food chain and also contaminate indoor air.

References.

Abba, H.T., Hassan, W.M; and Saleh, M.A. (20180. Evaluation of environmental natural radioactivity levels in soils and ground water of Baarkin Ladi, Plateau state Nigeria. Malaysian Journal of Fundamental and Applied Science, 14(3), 338-342.

Ademola J.A. Exposure to high background radiation level in the tin mining area of Jos Plateau, Nigeria. J Radiol Prot. 2008;28: 93–99.

Ajayi I.R. An evaluation of the equivalent dose due to natural radioactivity in the soil around the consolidated tin mine in Baukuru-Jos, plateau state of Nigeria. Iran J Radiat Res. 2008; 5:203–206.

Arogunjo, A.M., Hollriegl, V., Giussani, A., Leopeld, K., Gerstmann, U., Veronese, I., Oeh, U.(2009) Uranium and thorium in soils, minerals sands water and food samples in a tin mining area in Nigeria with elevated activity. Journal of Environmental Radioactivity 100;(232-240).

Badejo T A 1975 Evidence of magmatic differentiation in the origin of the younger granites of Nigeria *J. Mining Geol.* **10,** 67

Beretka J and Mathew P. J 1985 Natural radioactivity of Australian building materials, industrial wastes and by-products. *Health Phys.* **48** 87–95

De-Wet, P. D. (1996).The occurrence and bio-accumulating of Seleted metals and radionuclides in aquatic and terrestrial ecosystem on the wil water sand, Unpublished PhD. Thesis, and Africans University, Johannesburg.

Ibeanu I.G.E(2003). Tin mining and processing in Nigeria: cause for concern? J. Environ Radioact. 64, 59-66

Jacobson, R.R.E, Webb, J.S.(1946). The pegmatite of central Nigeria. Geological Survey of Nigeria, Bulletin 17.

Jibiri N.N, Alausa SK, Farai IP. Assessment of external and internal doses due to farming in high background radiation areas in old tin mining localities in Jos-plateau, Nigeria. Radioprotection. 2009;44:139–151.

Jibiri NN, Farai IP, Alausa SK. Estimation of annual effective dose due to natural radioactive elements in ingestion of foodstuffs in tin mining area of Jos-Plateau, Nigeria. J Environ Radioact. 2007;94: 31–40.

Masok, F.B., Masiteng, P.L., & Jwanbot, I. D (2015). Natural radioactivity concentration and effective dose rate from tin mining dumpsites in Rayfield, Nigeria. Journal of environment and earth science 5(12), 51-55.

Masok,F.B, Ike-Ogbonna, M. I, Dawam, R. B, Jwanbet, D. I. And Yenle, N. M. (2015). Cancer risk due to radionuclide Concentration in tinOre and sediments at Barkin-Ladi, Plateau State, North Central, Nigeria. International Journal of Environmental Monitoring and Analysis 3(5), 260-64.

Olise F.S., Oladejo O.F., Almeida, S.M., Owoade, O.K., Olaniyi, H.B., Freitas M.C.(2014). Instrument neutron activation analyses of uranium and thorium in samples from tin mining and processing sites. J. Geochem. Explur. 142, 36-42.

Olise, F.S., Owoade, O.K, Olaniyi, H.B., Obiajunwa, E.I.(2010). Acomplimentry tool in the determination of activity concentrations of naturally occuring radionuclides. J.Environ Radioactivity, 101, 910-914.

Onwuka, S., Duluora, J., Okoye., C. and Onaiwu O. 2013. Social economic impacts of tin mining in Jos, Plateau state, Nigeria. International Journal of Engineering Science Invention2: 30 – 34.

Onyeanuna, GC(2016). Interpretation of Ring structures in Jos Plateau using NigeriaSat 1 Imagery. International Journal of mathematics and physical sciences Research , 4(2), 95-104

Patterson, G.(1986). Lake Pidong. A preliminary survey of a Volcanic Crater Lake Durham! Department of Geography. University of Durham.

Turner, D.C.(1976) ‘‘Structure and Petrology of the Younger Granite Ring Complexes of Nigeria.’’ In Geology of Nigeria edited by Kogbe, C.A. Lagos Nigeria: Elizabethan Publ. Co.

UNSCEAR. Sources and effects of ionizing radiation. New York, NY: United Nations Scientific Committee on the Effects of Atomic Radiation; 2000.

Usikalu, M. R, Anoka, O. C. And Balogun, F. A. (2011).Radioactivity measurement of the Jos tin mine tailings in Norther Nigeria, Achives of Physic research 2(2), 80-86

Wapwera S.D. Ayanbimpe, G.M., and Odita, C. E. (2015). Abandoned Mine Potential home for the people: a case study of Jos Plateau tin –mining region. Journal of Civil Engineering and Architecture 9, 429 – 445.

Wright J.B.(1976).A Critical Reviiew of the Geollogy of Nigeria. Edited by Kogbe, C.A Elizabethan, Publisher Company, Lagos Nigeria, PP309 – 317.

Table 1. Comparison of activity concentrations with other mining areas in Nigeria

Activity Concentrations of Radionuclides (Bq/Kg)			**Tin Mine Location**	**Reference**
^{238}U	^{232}Th	^{40}K		
145.65 – 525.42	263.97 – 1915.41	78.62 – 2091.4	Rayfield, Jos	This Study
3779.1	8175.2	-------	Jos	Ibeanu, 2003
722	1680	____	Jos	Ademola, 2008
776	2.72	35.4	Bukuru-Jos	Ajayi, 2008
8.7-51	16.8 – 98	-------	Bitsichi – Jos	Arogunjo, 2009
_____	147 – 451	466 – 1062	Bitsichi & Bukuru Jos	Jibiri *et al.*, 2009
1.0 – 40	6 – 170	-------	Bitsichi, Bukuru & Kuru	Olise *et al.*, 2014
0 – 27420	50 – 35800	30 – 670	Bitsichi, Bukuru & Kuru	Olise *et al.*, 2010

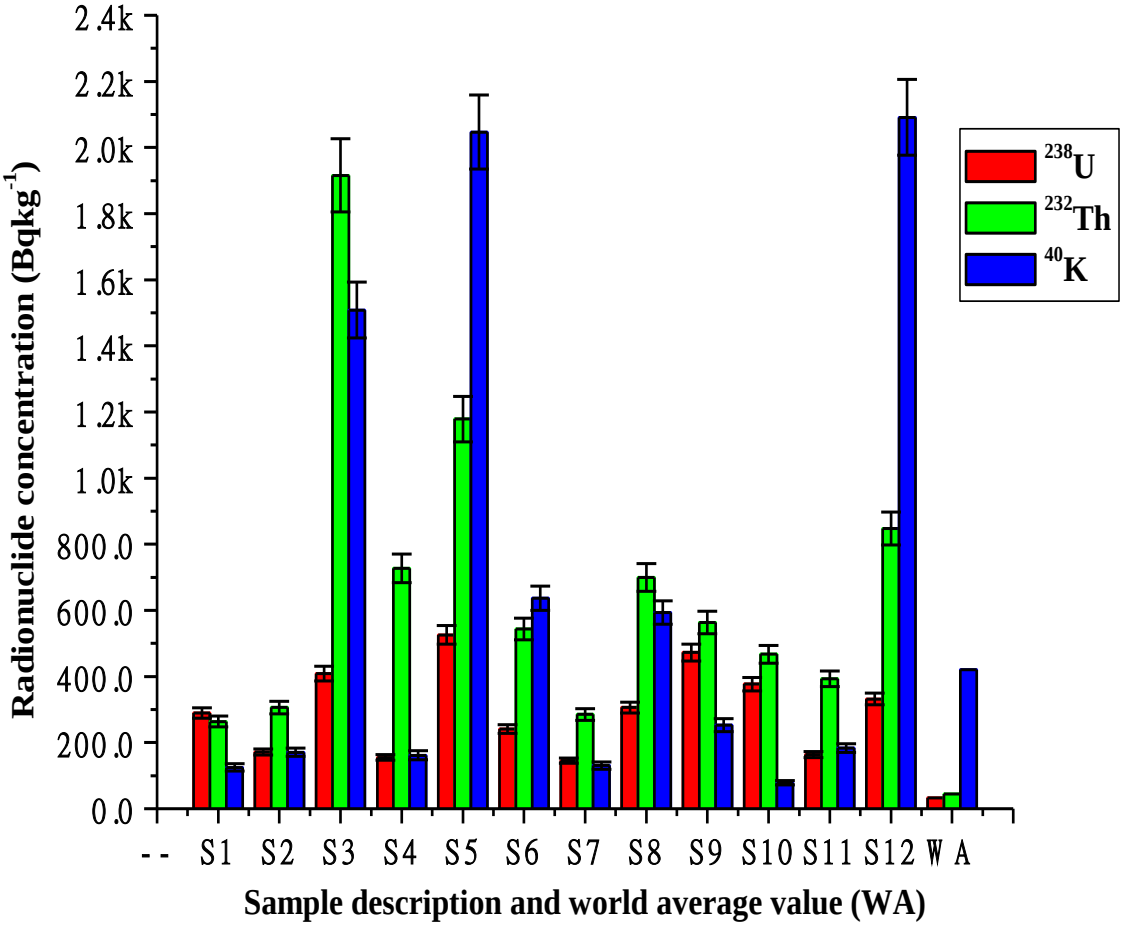

Figure 1. NORM distribution in the mine soil samples.

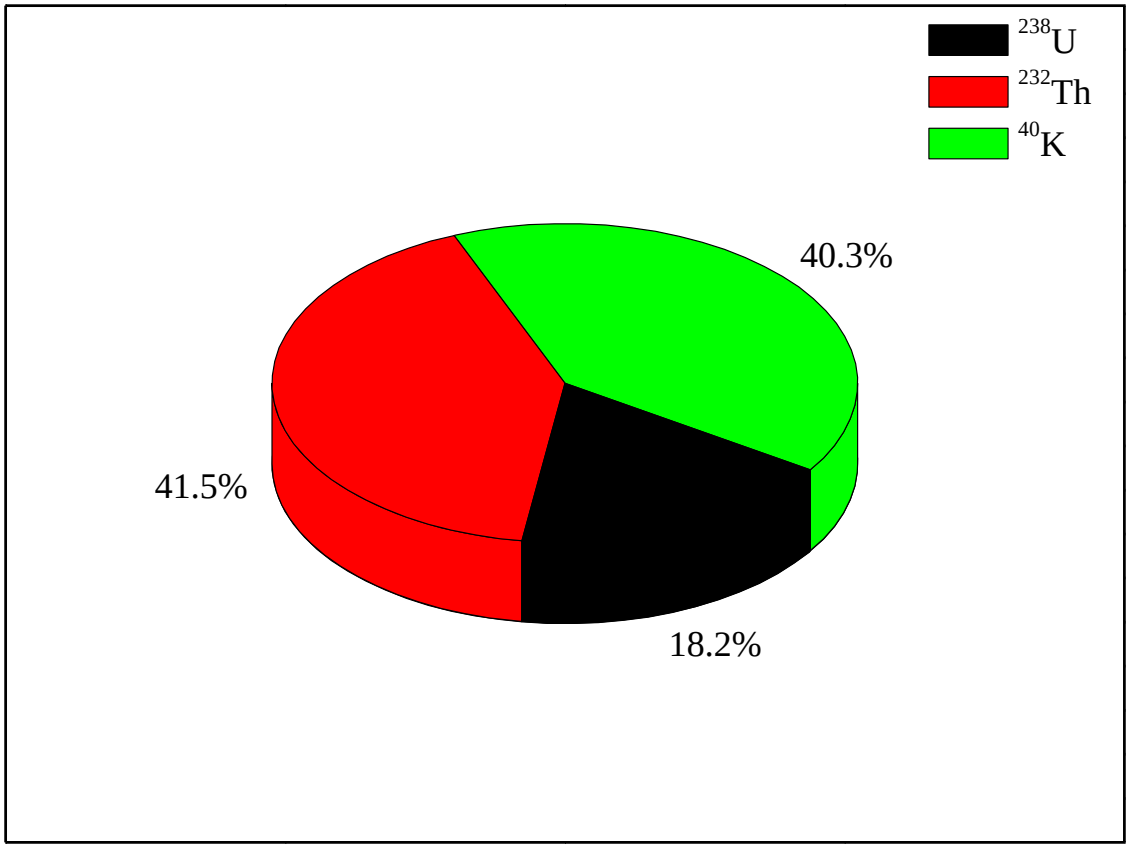

Figure 2. Relative ^{238}U, ^{232}Th and ^{40}K Activity concentrations in studied soil samples

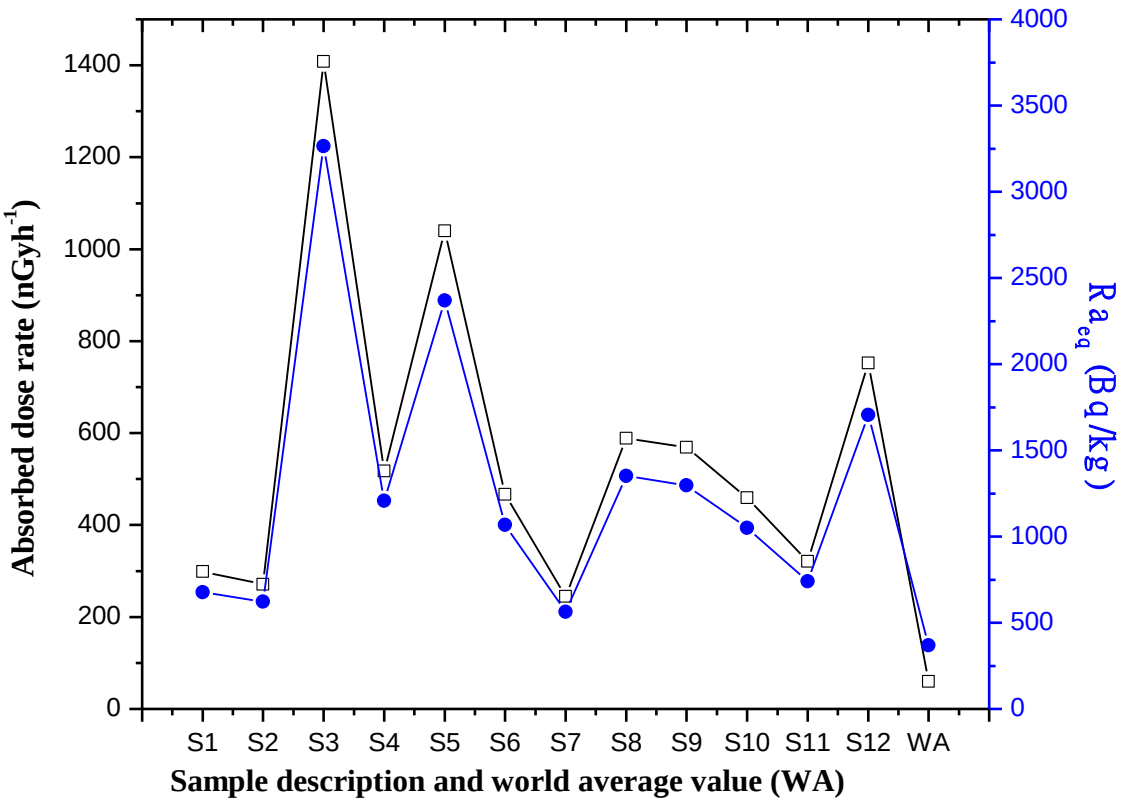

Figure 3. Distribution of absorbed dose rate in the study area

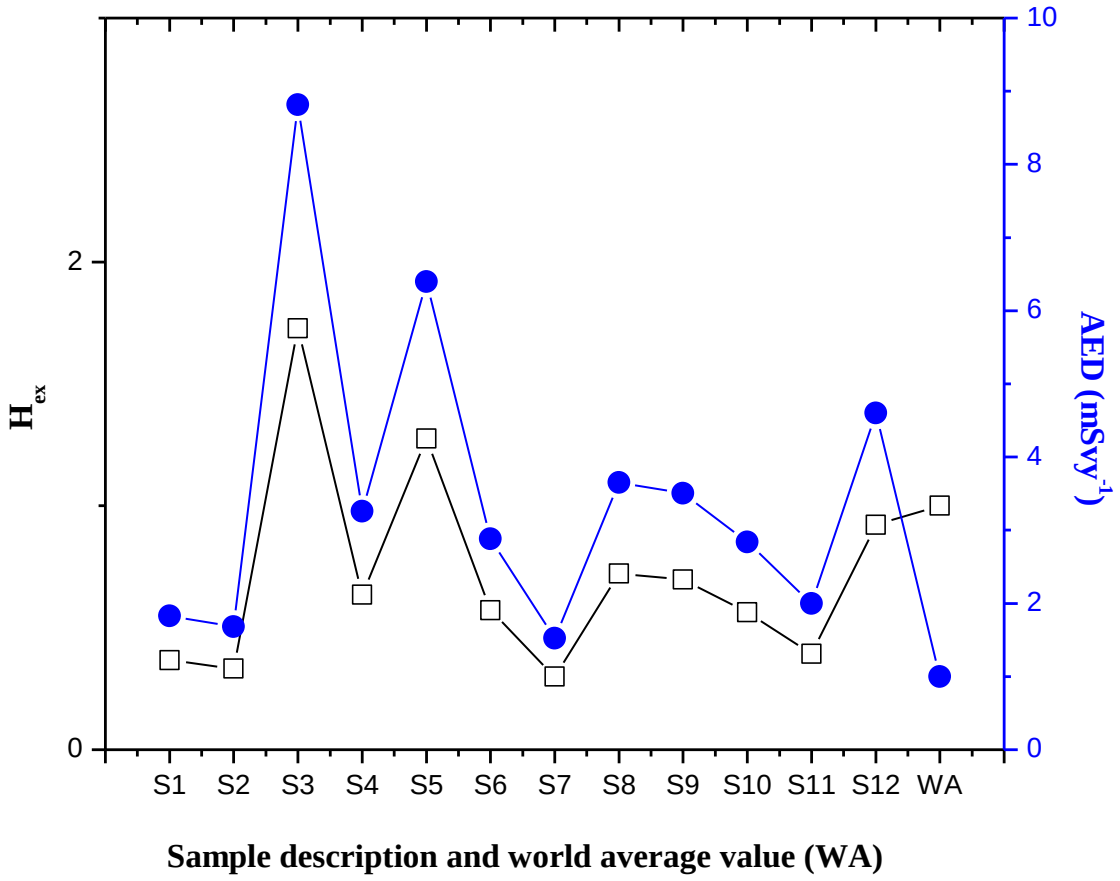

Figure 4. Distribution of annual effective dose rate (E_{out}) and external hazard index (H_{ex}) in soil samples

Determination of the Coverage Areas of VHF Television Signal in Ilorin, Kwara State, Nigeria.

[1]*Adewuni O.T, [1] Moses A.S

Department of Physics, Federal University of Technology, Minna, Niger State, Nigeria

E-mail: [1*] adewuniosenitaiwo959@gmail.com

*Corresponding Author

Abstract:

This study investigates the coverage areas of Nigerian Television Authority (NTA), Ilorin in Kwara State by means of quantitative measurement of the television signal level. The signal levels of NTA Ilorin, Channel 9, were measured radially along several routes with the transmitting station at focus. Their corresponding distances from the transmitting station and locations were also measured. These measurements were taken using Digital Signal Level Meter, GE-5499 and GPS 72 – Navigator. Measurements were taken radially along several routes in Ilorin Local Government Area and environs until the signal faded away completely. From the data obtained, surfer 8 application software was used to draw the contour maps of the signal levels around the transmitting station to show the coverage areas around the state. The results obtained showed that the present configurations of the transmitter for the television station did not give an optimum coverage area. The television signal, covers only 7.66% of the entire land mass of Kwara State.

Keywords: Coverage area, radio propagation, signal level, transmitter, VHF

Introduction

Radio propagation is the behavior of radio waves when they are transmitted, or propagated from one point on the earth to another, or into various parts of the atmosphere (Westman, 1968). As a form of electromagnetic radiation, like light waves, radio waves are affected by the phenomena of reflection, refraction, diffraction, absorption, polarization and scattering (Demetrius *et al*., 1969).

Radio propagation is also affected by the daily changes of water vapor in the troposphere and ionization in the upper atmosphere, due to the Sun. Understanding the effects of varying conditions on radio propagation has many practical applications, from choosing frequencies for international shortwave broadcasters, to designing reliable mobile telephone systems, to radio navigation and operation of radar systems.

Radio waves at different frequencies propagate in different ways. At extra low frequencies (ELF) and very low frequencies the wavelength is very much larger than the separation between the earth's surface and the D layer of the ionosphere, so electromagnetic waves may propagate in this region as a waveguide. Indeed, for frequencies below 20 kHz, the wave propagates as a single waveguide mode with a horizontal magnetic field and vertical electric field (Hall and Barclay, 1989).

The coverage areas of broadcast stations are usually classified into primary, secondary and fringe areas. The size of each of these areas depends on the transmitter power, the directivity of the aerial, the ground conductivity and the frequency of propagation. The coverage area decreases with increase in frequency and reduction in the ground conductivity (Ajayi and Owolabi, 1975).

The primary coverage area is defined as a region about a transmitting station in which the signal strength is adequate to override ordinary interference in the locality at all times. The primary coverage area corresponds to the area in which the electric field strength is greater than 60dBµV. The appropriate value of the electric field strength for this quality of service is dependent on the atmosphere and man-made noise in the locality. The relevant electric field strength also depends on whether the locality is rural, industrial or urban.

The secondary coverage area is a region where the electric field strength is often sufficient to be useful but is insufficient to overcome ordinary interference completely at all times. The service provided in this area may be adequate in rural areas where the noise level is low. The secondary coverage area corresponds to the area in which the electric field strength is at least 30 dBµV but less than 60 dBµV. The quality of service enjoyed in this area can be regarded as Grade B1.

The fringe service area can be regarded as that in which the electric field strength can be useful for some periods, but its service can neither be guaranteed nor be protected against interference. This is an area in which the electric field strength is greater than 0 dBµV but less than 30 dBµV. Such an area may be said to enjoy Grade B2 service (Moses *et al*., 2013).

Study Area

Ilorin is located in Kwara State, North-central Nigeria and its geographical coordinates are latitude: 8.5° N and longitude: 4.55° E. Ilorin is a confluence of cultures but populated majorly by people of Yoruba extraction. Its combine population is between 500 thousand and 1 million. It is the state capital of Kwara state which is one of the 36 states in the federal republic of Nigeria. Kwara state has a geographical area of 36,825km^2. Kwara state shares common boundary with Niger and Sokoto state to the north, Oyo, Ondo and Edo state to the south, and Benue, Plateau and Federal capital territory to the east. It maintains an international boundary with the republic of Benin to the west. The mineral resources available in Kwara state are limestone, marble, feldspar, clay, kaolin, quartz and granite rocks. Recently Kwara state has witnessed an increase in telecommunication companies (stations) (http://en.wikipedia.org/wiki//Kwara,state, 2013).

Figure 1: Location of Ilorin in Kwara state, Nigeria (8.5° N, 4.55° E)

Data collection and analysis

This work was carried out using the VHF television signal transmitted by the Nigeria Television Authority (NTA), channel 9, Ilorin. NTA, Ilorin, channel 9 has one working transmitter operating at the transmitting station at Ganmo, Ilorin, during the period of this research work, the power of the transmitter being 5 kW and the transmitting power fluctuate between 2.2 – 3.2 kW. NTA Ilorin transmits at 203.25.4 MHz for video signal and the transmitting antenna is mounted on an antenna tower height of 150 m, located at a site of 418 m above sea level.

The signal levels of Nigeria Television Authority (NTA) Ilorin, channel 9 were taken radially along several routes with the transmitting station at focus. Their corresponding distance and locations were also measured. These measurements were taken using GPS 72- Personal Navigator type and Digital Signal Level Meter GE- 5499 ranges from 30 dBµV -12030 dBµV. The Measurement were taken in Ilorin Local Government Areas and environs in Kwara State until the signals faded away completely.

From the data obtained, Surfer 8 software application was used to draw the contour maps of the signal levels around the transmitting station to determine the coverage areas of the station.

Table 1: Data obtaining along one of the radial routes considered in Ilorin, Kwara State

Signal Levels(dBμV)	Latitude(°N)	Longitude(°E)	Elevation(m)	Distance(km)
94.5	8.43190	4.60826	418	0
90.6	8.42960	4.60565	406	0.385
76.7	8.42529	4.60007	381	1.16
39.5	8.49328	4.56963	280	8.05
38.8	8.50107	4.55351	304	9.78
56.4	8.52013	4.55492	287	11.44
56.0	8.53909	4.55331	309	13.88
46.9	8.57301	4.55784	292	16.66
36.7	8.58987	4.5968	298	18.38
43.9	8.60294	4.54869	282	20.14
54.4	8.61985	4.53522	319	22.41
43.1	8.63868	4.52385	273	24.82
30.6	8.65761	4.52304	328	26.82
43.5	8.67582	4.51970	336	28.85
41.2	8.69158	4.50711	368	30.97
35.2	8.69803	4.49124	335	32.30
40.6	8.70545	4.47398	343	33.85
37.4	8.71076	4.45760	340	35.19
Low	8.71321	4.44541	356	36.08

RESULTS

Figure 1 and 2 shows the contour map of the signal levels around the transmitting stations and coverage area in the state, while Figure 2 shows the elevation of the ground around the coverage area of the station under study. Tables 2 to 6 show the television signal coverage areas relative to the percentage of the total land mass and the local government areas. The results obtained show that:

(a) The contour maps need for repeater stations at appropriate intervals to provide reception of television signals for the entire state.

(b) The present configurations of the transmitter of the television stations do not give an optimum coverage of the state. Only 7.66% of the entire land mass of Kwara State has television signal coverage.

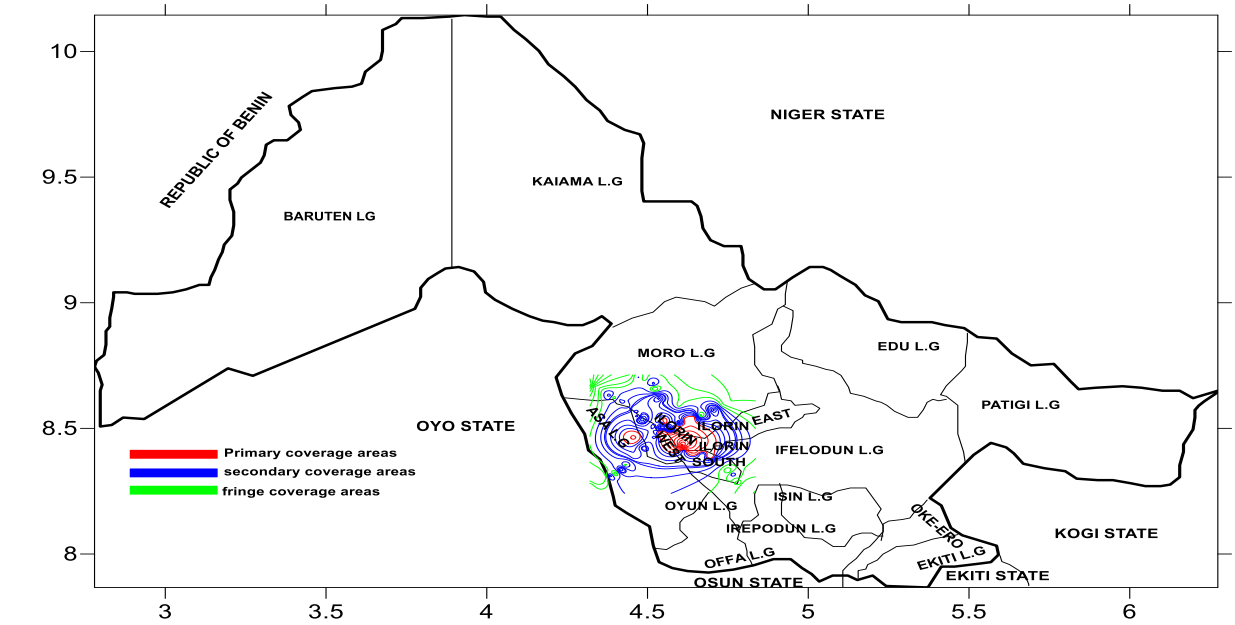

Figure 1. Coverage area of NTA, Ilorin channel 9 transmitting station in Kwara State

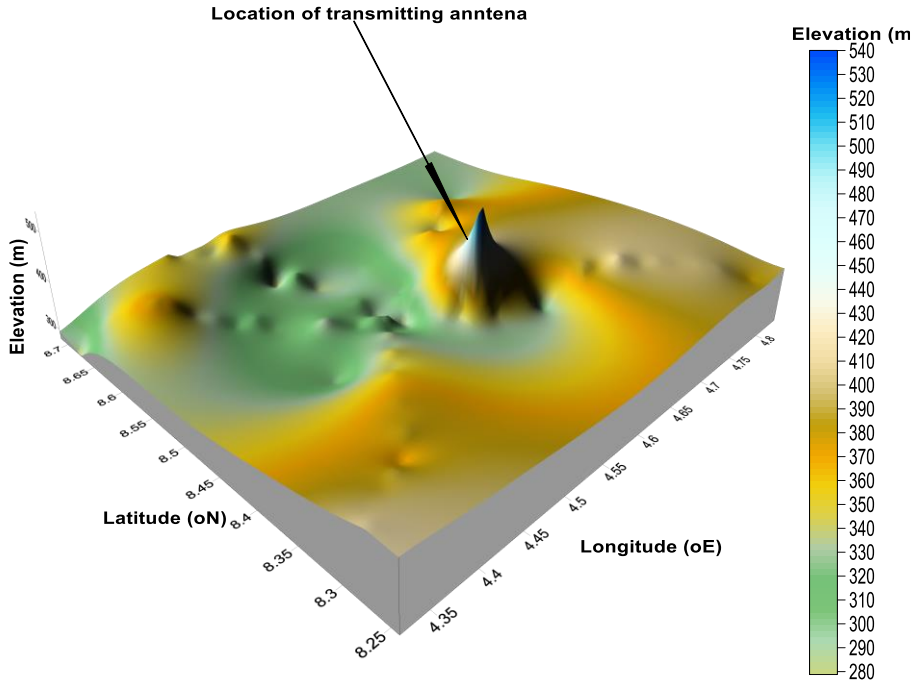

Figure 2. Surface Map showing the elevation of the ground above the Sea level around the Coverage Area of the Television transmitting station in Kwara State

Coverage Areas of NTA Ilorin, Channel 9

Table 2: Some of the towns and villages in NTA, llorin, primary Coverage Area

L .G. A	Lat(^{0}N)	Long(^{0}E)	Elevation (m)	Average Distance (km)	Towns/Villages
Moro	8.61	4.53	319	11.44	Kwasu, Shobi
Asa	8.45	4.51	331	10.86	Eyenkorin
Ilorin South	8.43	4.60	418	1.55	Ganma, Offa Road
Ilorin East	8.53	4.61	325	10.94	Oke-Oyi, Kwara Poly,
Ilorin West	8.50	4.52	306	12.65	Adabata, Oloje

Table 3: Some of the towns and villages in NTA llorin secondary coverage Area

L .G.A	Lat(^{0}N)	Long(^{0}E)	Elevation(m)	Average Distance (km)	Towns/Villages
Moro	8.60	4.54	282	17.60	Shao, Oke-Oyi
Asa	8.51	4.50	318	19.41	Ote, Madala, Ogidi,
Ilorin South	8.50	4.55	287	11.44	Molete

Ilorin East	8.46	4.52	335	19.13	Moraba, Sango, Ose
Ilorin West	8.50	4.53	323	11.09	Alimi

Table 4: Some of the towns and villages in NTA, Ilorin, Fringe Coverage Area.

L. G.A	Lat(^{0}N)	Long(^{0}N)	Elevation (m)	Average Distance (km)	Towns/Villages
Moro	8.60	4.75	324	25.72	Old-Jebba,
Asa	8.30	4.36	385	21.15	Iresa-adu, Gbede
Ilorin South	8.24	4.81	385	30.45	Ajase
Ilorin East	8.55	4.68	370	14.55	Oke-oyi
Ilorin West	8.32	4.40	366	25.94	Aduegba
Ifelodun	8.25	4.80	380	28.88	Ajasepo, Igbomina

Table 5: The percentage of the Local Government Areas covered by the NTA Ilorin, Channel 9, Transmitting Station in Kwara State.

L.G.A	Average Distance(km)	% of L.G.A. with Primary Coverage.	% of L.G.A. with Secondary Coverage.	% of L.G.A. with Fringe Coverage.	Total % of L.G.A. Coverage Area.
Ilorin West	19.25	20%	80%	0%	100%
Ilorin South	10.97	16.6%	66.7%	16.67%	100%
Ilorin East	13.44	33.3%	16.6%	8.3%	58.2%
Asa	25.88	6.06%	33.3%	12.1%	51.4%
Moro	31.45	4.16%	15.2%	16.6%	35.9%
Ifelodun	31.65	1.13%	3.40%	4.54%	9.07%

Table 6: The Percentage of the Coverage Area of the Television Transmitting Station relative to the total land mass of Kwara State.

Station	% of Primary Coverage	% of Secondary Coverage	% of Fringe Coverage	Total % of Coverage Area
N.T.A. Ilorin Channel 9	1.14%	4.0%	2.52%	7.66%

Summary and Conclusion

This study presents the contour map of signal level around the transmitting station to show the coverage area of VHF television signal of Nigeria Television Authority (NTA), Ilorin, Kwara state, by means of quantitative measurement of the television signal level. The percentage of the coverage area of the television transmitting station relative to the total land mass is 7.66%. The percentages of the Local Government Areas covered by the NTA Ilorin television station are: 35.96% for Moro Local Government Area, 51.46% for Asa Local Government Area, 100% for Ilorin West Local

Government Area, 58.2% for Ilorin East Local Government Area, 100% for Ilorin South Local Government Area and 9.07% for Ifelodun Local Government Area. The signal from the television station is not a potential interference to any of the local television station in the neighboring states. In summary, only 7.66% of the entire land mass of Kwara State has television signals coverage. More than 92.34% of Kwara State does not received television signals in the state. Thus, the present configurations of the transmitter of the station do not give optimal coverage of the total land mass of Kwara State.

References

Ajayi, G.O. and Owolabi, I.E. (1975). Medium Wave Propagation Curves (for use in medium wave transmission planning and design). Technical Report of the Radio wave propagation Research Group, Department of Electronics and Electrical Engineering, University of Ife, Nigeria, pp. 3-4)

Demetrius, T.P., and Kenneth, F. (1969). Hurd, Basic Electromagnetic Theory. McGraw Hill, New York. ISBN 0-07-048470-8, pp.8

Hall, M.P. and Barclay, L. (1989). Radiowave Propagation, edited and Published by Peter Peregrinus Limited, ISBN 0-86341-156-8

Kwara State, taken from http://en.wikipedia.org/wiki//Kwara,State.

Ajewole, M.O, Oyedum, O.D, Adedeji, A.T, Moses, A.S, and Eichie, J.O (2013): Spartial Variability of VHF/UHF Electric Field Strength in Niger State, Nigeria, International of Digital Information and Wireless Communications Vol. 3(3), Pp26-34.

Westman, H.P. (1968). Reference Data for Radio Engineers, (5th edition). Howard Sams and Company. Library of Congress Card, 43-14665, 26-1.

Design Presentation of a Solar Powered Microcontroller-Based Weather Station for the Acquisition of Atmospheric Parameters

Ughanze I. J, Ibrahim A. G and Eichie J. O.

Department of physics, Federal University Of Technology Minna, Niger State – Nigeria

E-mail: ughanzeifeanyi@yahoo.com

Abstract

Accessing real time weather information is still a challenge to atmospheric researchers. This work developed a solar powered Arduino microcontroller weather station that will measure atmospheric temperature, relative humidity, pressure and wind speed and wind direction using appropriate meteorological sensors such as DHT22 sensors for atmospheric temperature and humidity measurement, BMP180 sensors for pressure measurement, a three cup anemometer with reed switch sensor for wind speed measurement and a wind vane with a variable resistor for wind direction measurement. An Arduino Atmega 2560 microcontroller processes the output of the sensors, transfer them to the LCD for display and also transmit it to the Wi-Fi module which uploads the data to an online server to enable out-of-site end users to access the measured weather information.

Keywords: Weather station, Microcontroller, Monitoring Sensors, Wi-Fi module, solar panel.

1.0 INTRODUCTION

Weather tracking is of great importance in agriculture, communications, air transportation, industries and to atmospheric physicist (Anthony *et al*.,2017). For example in agriculture, weather determines how much success that can be recorded, because crop yield depend on weather in providing energy and water for it sustenance (Abubakar and Sulaiman,2018). Research has proved that climate change will have great effect on agricultural yield and human activities in the next century (Walthall *et al*.,2018). Hence there is need to have an effective means of monitoring atmospheric parameter at all times. Such a weather station should have an independent power source such as solar energy, for all time weather monitoring. A microcontroller weather station reads and records atmospheric parameters using sensors without any external intervention (Tajedinn and Abdelrasoul, 2015). The recorded atmospheric parameters can be processed as wired information, which means that it will be

downloaded in a computer or through a server as in wireless communication. The aim of this work is to design a low cost solar powered weather station which will transmit real time weather information to an online server for multiple retrievals.

2.0 METHODOLOGY

The block diagram of the design considered for the solar powered weather station is shown in figure 1:

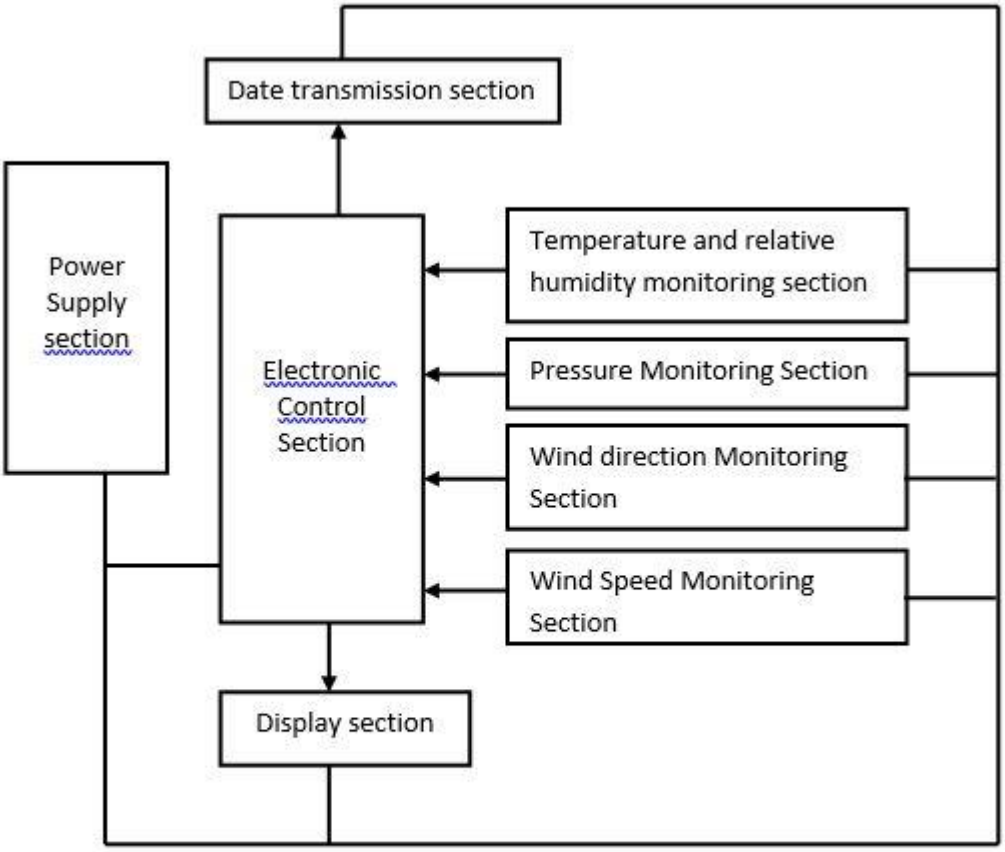

Figure 1: Block Diagram of the Device

The section by section design of the block diagram is explained below:

2.1 Power supply section

The power supply section provides the electrical energy required by the device. For round the clock monitoring device, a renewable energy is appropriate. As such, the device shall be powered using the enormous energy of the tropical African sun, solar energy. The block diagram of the power supply section is shown in Figure 2.

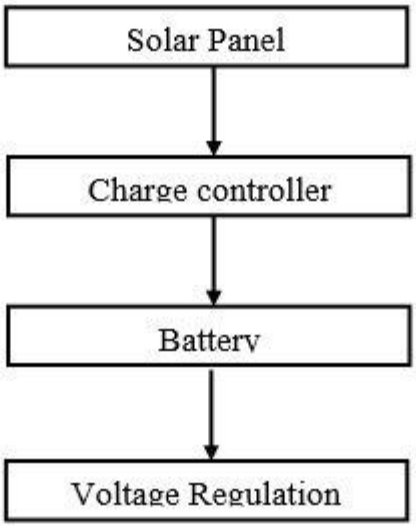

Figure 2: Block Diagram of the Power Supply Section

Sub sections of the proposed power supply design are explained below:

2.1.1 Solar Panel

A monocrystalline solar panel provides DC voltage source to the system to enhance continuous atmospheric data acquisition. The electrical rating of the solar panel considered is given in Table

Table 1: **Electrical Rating of Solar Panel**

ELECTRICAL RATING	VALUES
Maximum power (P_{max})	50W
Open circuit (V_{oc})	21.5V
Short circuit current (I_{sc})	3.05A
Maximum power current (I_m)	2.77A
Output tolerance (%)	+3
Operating temperature (^oC)	-40^{o}C - +80^{o}C

Length (mm)	670
Width (mm)	540
Height (mm)	30
Weight (kg)	4.35

All data at standard test condition (STC) E = 1000Wm^{-2}, AM = 1.5, T_c = 25^{o}C.

The 50W, 18V rating of the solar panel significantly provide the needed guide to choosing the panel.

2.1.2 Charge Controller

The charge controller acts as a switching device between the solar panel and the battery, it regulate the output voltage from the solar panel to the required charging voltage of the battery, the charge controller switches off the charging of the battery when it is fully charge to prevent over charging. It also prevent the battery from draining back it charge to the solar panel when it is not charging it. A 10A, 12V charge controller is appropriate so as to match the battery it is interfacing.

2.1.3 Battery

A 12V rechargeable deep cycle battery provides the DC voltage source to the device. The battery discharges very small current for a lengthy period.

2.1.4 Voltage Regulation

Voltage regulation is necessary to peg the 12V output from the battery to a level tolerated by constituent components. A maximum of voltage of +5V is sufficient and as such, a 7905 voltage regulator was chosen.

2.2. Electronic control sections

The electronic control unit is made up of Arduino Atmega2560 microcontroller. It is responsible for the reception of analogue and digital signal from the atmospheric sensors .The microcontroller process the output of the sensors using c++ programming language into useful weather information for the purpose of analysis. Arduino Atmega2560 microcontroller has 54 digital input/output pins and 16 analogue input pins.4 UARTS (hard ware serial pins),a 16MHz crystal oscillator. The table below shows the features of Arduino Atmega2560

Table 2: Features of the Arduino Atmega2560

Specification	**Values**
Operating Voltage	5V
Input Voltage	7-12V
Input Voltage (limits)	6-20V
Didital I/O pins	54(of which 14 provide PWM output)
Analog input pins	16
DC Current per 1/O pins	40 Ma
DC Current for 3.3 V pin	50 mA
Flash Memory	256 KB used by bootloader
SRAM	8 KB
EEPROM	4 KB
Clock speed	16 MHz

All the atmospheric sensors will be connected to the microcontrollers input via appropriate pins, it manipulates such inputs in line with programmed instructions and produce output through the output pins to the output devices.

2.3 Temperature and Relative Humidity Monitoring Section

This section has the DHT22 sensor. It has capacitive humidity sensing element and a high precision temperature measuring device. DHT22 sensor is small in size, low power consumption and long distance transmission. DHT22 sensor has the following features as shown in Table 3.

Table 3: Features of DHT22

Specification	**Values**
Model	DHT22
Power supply	3.36V DC
Output signal	Digital signal via single-bus
Sensing element	Polymer capacitor
Operating range	Humidity 0-100%RH;temperature -40-80Celsius
Accuracy	Humidity +-2%RH(Max+-5%RH);temperature <+-0.5 Ceius
Resolution or sensitivity	Humidity 0.1%RHtempeture o. 1Celsius
Repeatability	Humidity +-1%RHtemperatture 0+.2Celsius
Humidity hysteresis	+-0.3%RH
Long-term stability	+-.5%RH/year
Sensing period	Average;2s

DHT22 has a single-bus data communication with the microcontroller. When microcontroller sends start signal, DHT22 change from low power consumption mode to running mode when microcontroller finishes sending the start signal, DHT22 will send response signal that reflect the relative humidity and temperature information.

2.4 PRESSURE MONITORING SECTION

This section has BMP180 sensor which measures atmospheric pressure and give analogue output to the microcontroller. The microcontroller converts the analogue signal from the BMP180 to digital signal and display on the LCD. BMP180 makes use of I^2C communication protocol. The specifications of the BMP180 atmospheric pressure sensor ire enumerated below:

- Operating voltage of BMP180: 1:3V – 3.6
- Input voltage of BMP180MODULE: 3:3V to 5:5V
- Peak current : 100uA
- Consumes 0.1uA standby
- Maximum voltage at SDA, SCL : VCC + 0.3V
- Operating temperature: - 40^0C to 80^0C

2.5 WIND SPEED MONITORING SECTION

A three cup anemometer device is used to measure the wind speed. The three cup anemometer is mounted on a shaft at the base of the shaft there is a magnet attached to the shaft and a reed switch is positioned so that it is perpendicularly facing the magnet. When the three cup anemometer rotate due to the effect of wind, and the magnet passes, the reed switch for every rotation, this triggers the reed switch to send a logic zero to the microcontroller. The process continues and the microcontroller counts the triggers. For every rotation made after the selected interval of time the microcontroller calculate the wind speed using Davis equation;

$$V = P(2.25/T) \quad (1)$$

where V is the speed in miles per hour (m/h), P is the number of pulse during sampling period and T is the period per second.

2.6 WIND DIRECTION MONITORING SECTION

A wind vane is assembled such that the shaft is coupled directly to a continuous moving variable resistor that gives an output of 0V to 5V which is mapped to 0^o to 360^o, north direction serves as the reference degree which is 0^o while east, south and west are 90^o, 180° and 270^o respectively.

2.7 DISPLAY SECTION

The display section has 84 by 48 pixel LCD display with 8 input pins which are connected to the microcontroller through which measured atmospheric data are displayed as output. The LCD uses serial peripheral interface (SPI) communication protocol.

2.8 DATA TRANSMISSION SECTION

A Wi-Fi module serves as the data transmission link using universal asyndrionous receiver and transmitter (UART). The Wi-Fi module sends signal to the microcontroller during it initialization process, thereafter the microcontroller sends signals of processed atmospheric data to the Wi-Fi module to upload to an online server. Through the online server, real time weather information can be accessed.

3.0 RESULT AND DISCUSSION

The result of the design description presented so far constitutes the overall design and when in visuals; it's the overall circuit diagram. The diagram shows all the sections intra connections, inter connections and signal flow. The overall circuit diagram of the proposed Arduino microcontroller weather station is shown in Figure 3.

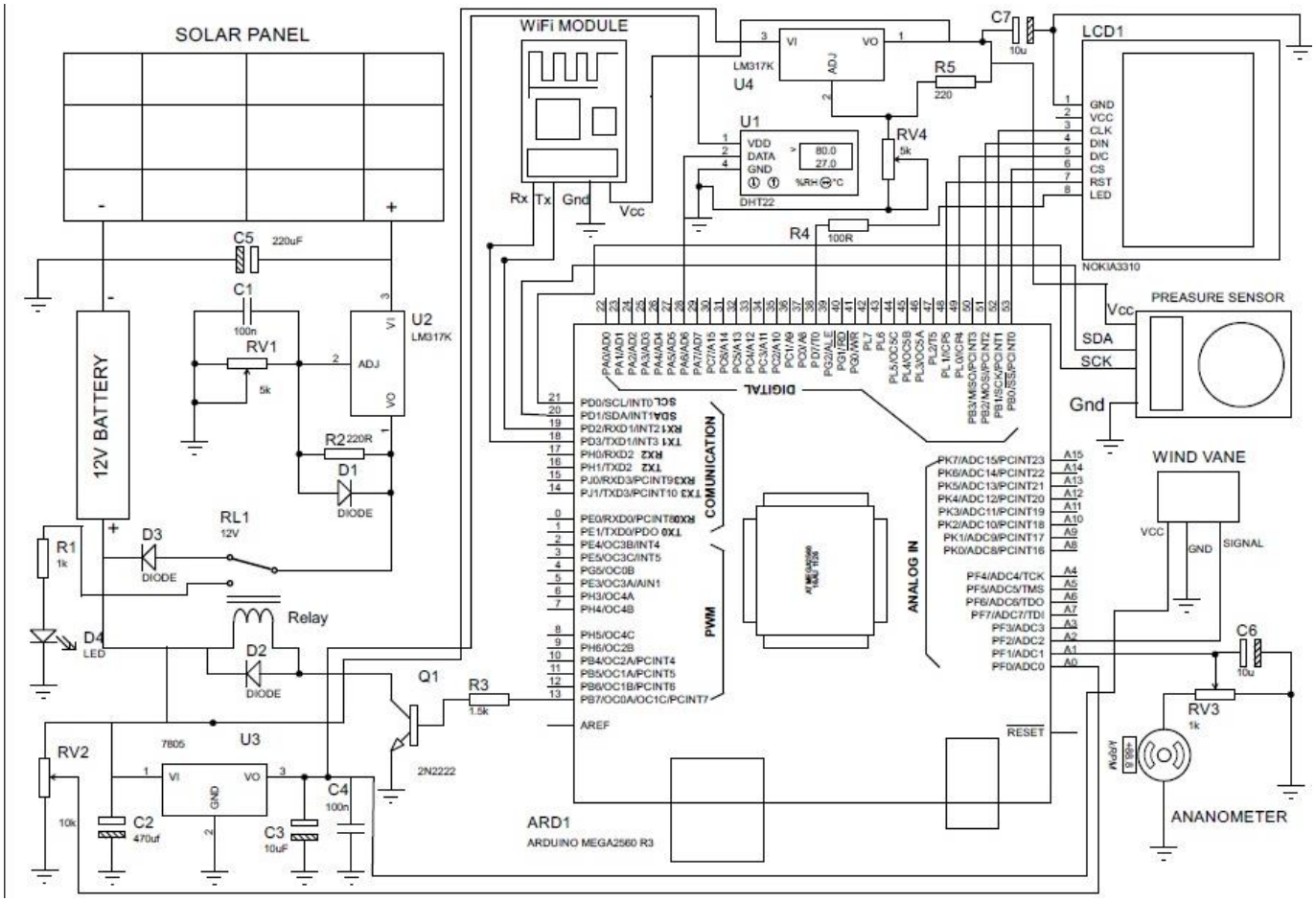

From the above circuit diagram, it is clear that the central part of the design is the microcontroller. All sensors which interact with atmospheric elements were directly connected to it and all channels in which the manipulations of the sensed inputs are expressed were all connected from it. Its role is similar to that of the human heart connected to veins and arteries. Hence, the heart of the device is the microcontroller and from where the device derived its name, "microcontroller-based" weather station. All sections of the design, hardware and software are therefore expected to function in perfect synergy for overall electrical and signal harmony of the system. The choice of solar power considering the study area, Minna, North-central Nigeria is a guarantee for all day and all year long uninterrupted power for the acquisition of atmospheric data.

4.0 CONCLUSION

The aim of this work which is to design a low-cost, mobile, microcontroller-based weather station that can provide real time weather information has been achieved. The focus of future research borders on:

1. Transforming the design concept of this work into physical reality for the benefit of mankind.
2. Performance evaluation of the constructed device by comparing acquired data using the device with those acquired using other weather measuring devices for same location and period. This is to help place performance comment on the device with respect to accuracy and error margin.

The designed microcontroller based weather station combined the benefit of low-cost, portability, real-time acquisition and efficiency all in one, thus making weather information acquisition, storage, transmission and reception possible from the comfort zone of the end user.

References

Abubakar Ibrahim Musa, Sulaiman Muhammad Bashir, (2018) Micro-controller Based Mobile Weather Monitor Station. American Journal of Embedded Systems and Applications. Vol. 6, No. 1, pp. 23-29.

Anthony U. Adoghe, Segun I. Popoola, Onyedika M. Chukwuedo, Abel E. Airoboman, Aderemi A. Atayero, (2017). Smart Weather Station for Rural Agriculture using Meteorological Sensors and Solar Energy Proceedings of the World Congress on Engineering Vol I WCE.

Karishma, P., Mansi, M., Rashmi, G., Shraddha, R., & Gaurav, G. (2016). Weather Monitoring System using Microcontroller, International Journal on Recent and Innovation Trends in Computing and Communication, Volume 4, Issue 1, pp. 78-80

Murugan, T., Periasamy A., & Muruganand, S. (2012). Embedded based Industrial Temperature Monitoring System using GSM, International Journal of Computer Applications, vol. 58, p. 0975 – 8887, 2012.

Tajedinn Abdelgawi Baker 1, Abdelrasoul Jabar Kizar Alzubaidi (2015) Design and implementation of a real-time remote measurement and monitoring of weather parameters system. IOSR Journal of Engineering Vol. 05, (P) 2278-8719.

Walthall, C. L., Hatfield, J., Backlund, P., Lengnick, L., Marshall, E., Walsh, M., Ziska, L. H. (2012) Climate change and Agriculture in the United States: Effects and adaptation (USDA Technical Bulletin 1995) Washington, DC: USDA].

Estimation of Incident Solar Ultraviolet (UV) Radiation in Minna, Niger State, Nigeria.

*** ILEDARE, Taiwo Abigail, OYEDUM, Onyedi David, EZENWORA, Joel Aghaegbunam.**

Department of Physics, Federal University of Technology, P.M.B. 65, Minna, Niger State, Nigeria
**Corresponding author E-mail: kingsolx@futminna.edu.ng*

Abstract

This study evaluates the level of UV radiation in Minna, Niger State, Nigeria. It has become a thing of concern as a lot of health hazard is associated with exposure to UV radiation. This research evaluates the level of UV index in Minna using one year (2015) data obtained from F.U.T. Minna weather station Bosso campus. The data was analyzed using MS excel. The result shows a high values of UV radiation in the months of march, April and May, a low UV radiation in the months of October, November and December Also there is strong correlation between the high and low in all the sampled yearly data, it therefore implies that safety measures should be taken by the public to avoid direct exposure on their body.

Keywords: *Sola Radiation, electromagnetic energy, Ultraviolet rays, UV index*

INTRODUCTION

The sun emits energy over a broad spectrum of wavelengths: Visible light that can be perceived, Infrared radiation that can be perceived as heat, and Ultraviolet (UV) radiation that cannot be seen or perceived. Solar radiation is a radiant energy emitted by the sun from nuclear fusion reaction that is a form of electromagnetic energy. Solar radiation comes in many forms such has visible light, radio wave, infrared, X-rays and ultraviolet rays. Measurements of solar radiation give higher values on clear sunny days and lower values on cloudy days. When the sun is down, at night, or when there are heavy clouds blocking the sun, solar radiation is at its barest minimum (EPA, 2010).

Ultraviolet radiation has a shorter wavelength and higher energy than visible light. It affects human health both positively and negatively. Scientists classify UV radiation into three types or bands: UVA, UVB, and UVC. The ozone layer absorbs some, but not all, of these types of UV radiations.

UVA: Wavelength in the range 320-400 nm. Not absorbed by the ozone layer.

UVB: Wavelength in the range 290-320 nm. Mostly absorbed by the ozone layer, but some do reach the Earth's surface.

UVC: Wavelength in the range 100-290 nm. They are completely absorbed by the ozone layer and atmosphere (EPA,2010). Short exposure to UVB radiation generates vitamin D, but can also lead to

sunburn, depending on an individual's skin type. Fortunately for life on Earth, the atmosphere's stratospheric ozone layer shields people from most UV radiation. However, Some UV radiation that escapes through the ozone layer however can cause the following problems, particularly for people who spend unprotected time outdoors (Elli *et al*., 2002):

Skin cancer, Cataracts Suppression of the immune system and Premature aging of the skin

UV radiation, from the sun and from tanning beds, is classified as a human carcinogen, according to the U.S. Department of Health and Human Services and the World Health Organization (WHO) (Rene *et al.*,2002). Since the benefits of sunlight cannot be separated from its damaging effects, it is important to understand the risks of overexposure, so as to take necessary precautions to protect one-self.

Location and The Climate of Study Area

The study was carried out in Minna, the capital of Niger State which is in the North-Central part of Nigeria, located on latitude 9° 36' 50" North and longitude 6° 33' 25" East at altitude of 249 meters above sea level. The state lies partially within the semi–arid Sahelian belt of West Africa.

Fig.1.1: Niger State showing position of Minna
Source: Ajayi *et al.*, (2014)

The climate of this zone is characterized by two distinct and well defined season, namely the wet (rainy) and dry seasons. These seasons correspond to Northern hemisphere summer and winter respectively. Average wet and dry season ambient temperatures in Minna are 28.0°C and 30.7°C respectively, while relative humidity is 70.8 and 39.9 respectively, and wind speed is 1.68ms^{-1} for wet season and 1.82ms^{-1} for dry season.

The annual onset and cessation of the dry and wet seasons follow the quasi-periodic north-south to and fro movement of the inter-tropical convergence zone (ITCZ). The ITCZ demarcates the dry dust laden north-east trade wind from the moisture-laden south–west trade wind. The dry season in the Sahel zone of Nigeria sets in about October each year and persists till about May of the next year. This is the period when the ITCZ is displaced to the south and the prevailing north-east trade wind transports large quantity of dust and smoke from the Sahara Desert and biomass burning into the atmosphere over the entire region (Anuforo *et al*.,2007).

Dust and smoke aerosol affect the climate system at local level, as well as regional and global scales in a number of ways. Due to its direct radioactive impact, dust aerosol affects atmospheric temperature, thereby modifying the vertical temperature distribution in the troposphere, because of the changes in heating and cooling rate at different altitude (Quijano, 2000). However, Minna is endowed with annual average sunshine hours of about 9.00 hours.

Similarly, it has an annual average daily solar irradiation of about 7.00 kWh/m^2/day of energy from the sun (Bala *et al*., 2000). Therefore, Minna is expected to have a tendency of high incidence of UV radiation.

MATERAILS AND METHOD

Data collection

Davis vantage pro 2 weather equipment was used to collect the ultraviolet (UV) radiation data ultraviolet index (UVI) for Minna Metropolis for the period of one year (2015).

Data Analysis

The ultraviolet radiation data obtained was separated as monthly and daily data, the data was filtered for the periods when noticeable amount of (UV) was measured, which is from 10:00 am to 4:00 pm result obtain were presented in graphs using Microsoft Excel.

RESULT AND DISCUSSION

It is observed that the highest and lowest UV index occurred in March and December, respectively in the dry season. This is expected, since the month of March is characterized by heavy sunshine and clear atmosphere, while the month of December is characterized by both reduced insolation winter

and harmattan haze which further greatly reduces the intensity of solar radiation (Babatunde, 2001; Ekpe and Nnabuchi, 2012).

Figures 2.1and 2.2 are the graphs of the daily UV index for the months of March and April, which are month in the dry season. in this month it is expected to have high UV index but in this case it was noted that there was more UV.

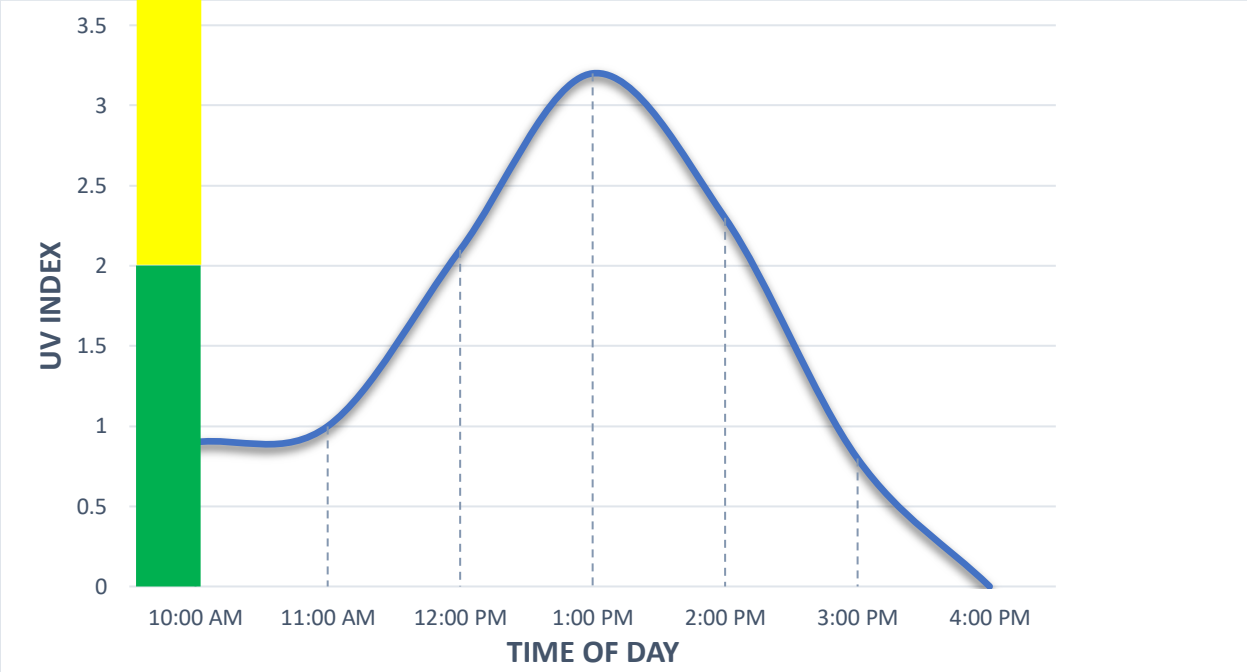

Figure 2.1 Hourly variation of UV Index in March

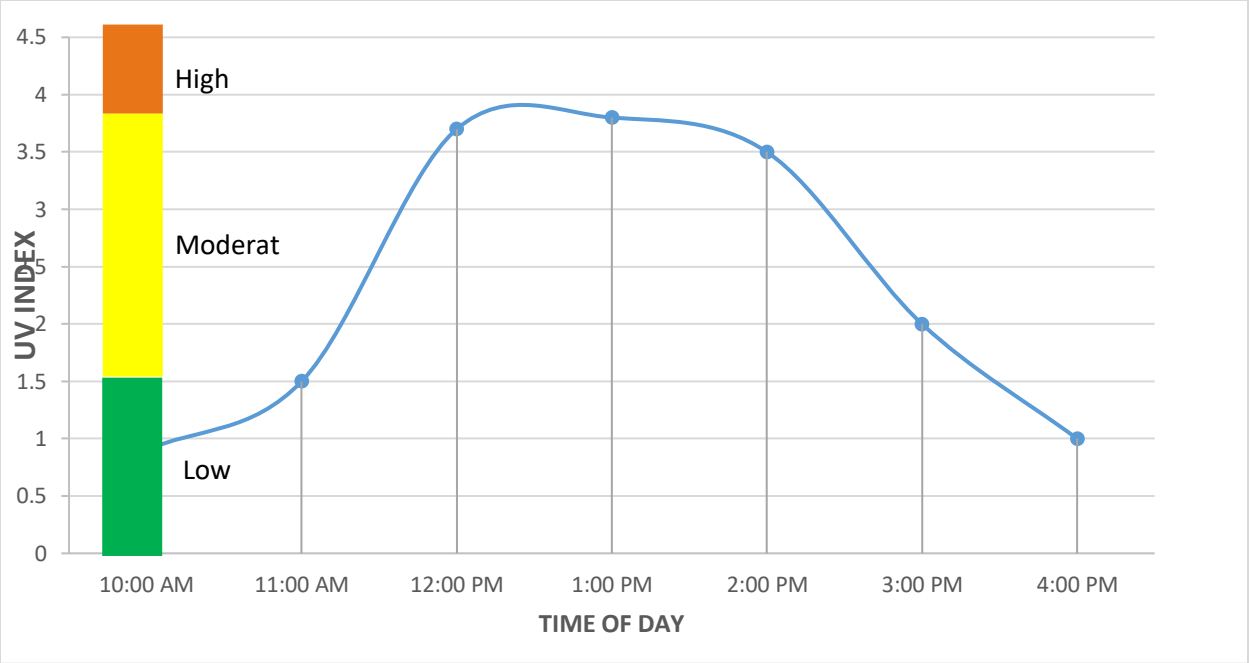

Figure 2.2 Hourly variation of UV index in April

The graphs in Figure 2.3 and 2.4 show that it is possible for us to have harmful UV index even in the wet season some days in the wet season which is generally assumed to be season without harmful effect UV index. may be harmful if care is not taken.

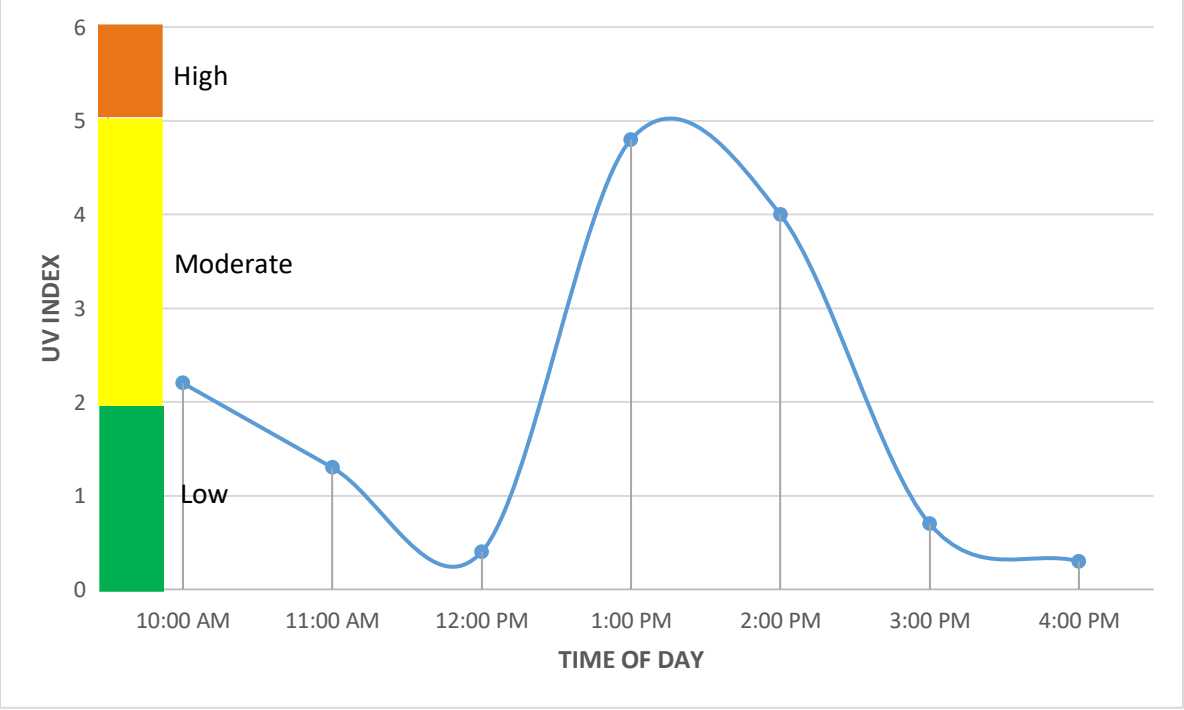

Figure 2.3: Hourly variation of UV index in July

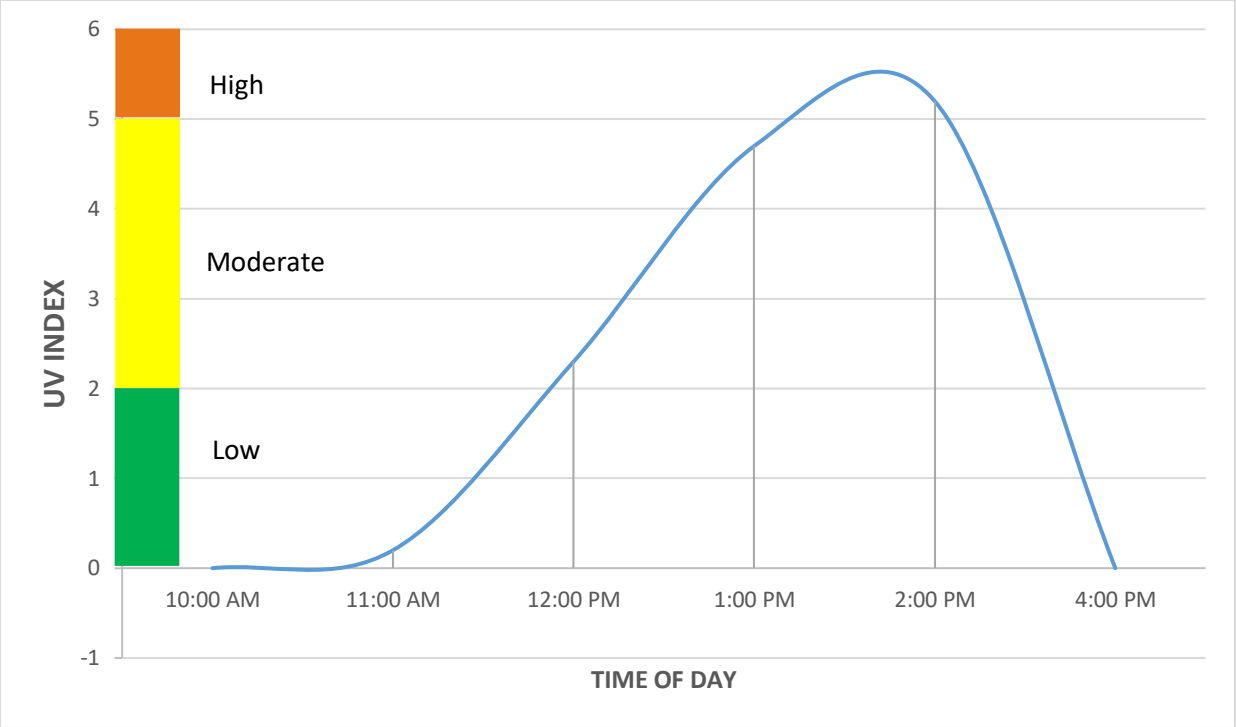

Figure 2.4: hourly variation of UV Index in August

Figures 2,5 and 2,6 are the monthly sum and the monthly average of the UV index for the year. This graph shows what happens in the course of the year, and it is noted that there were high values of UV index in the months of March, April and May, but low UV index is discovered in the months October, November and December due to the harmattan season in those month.

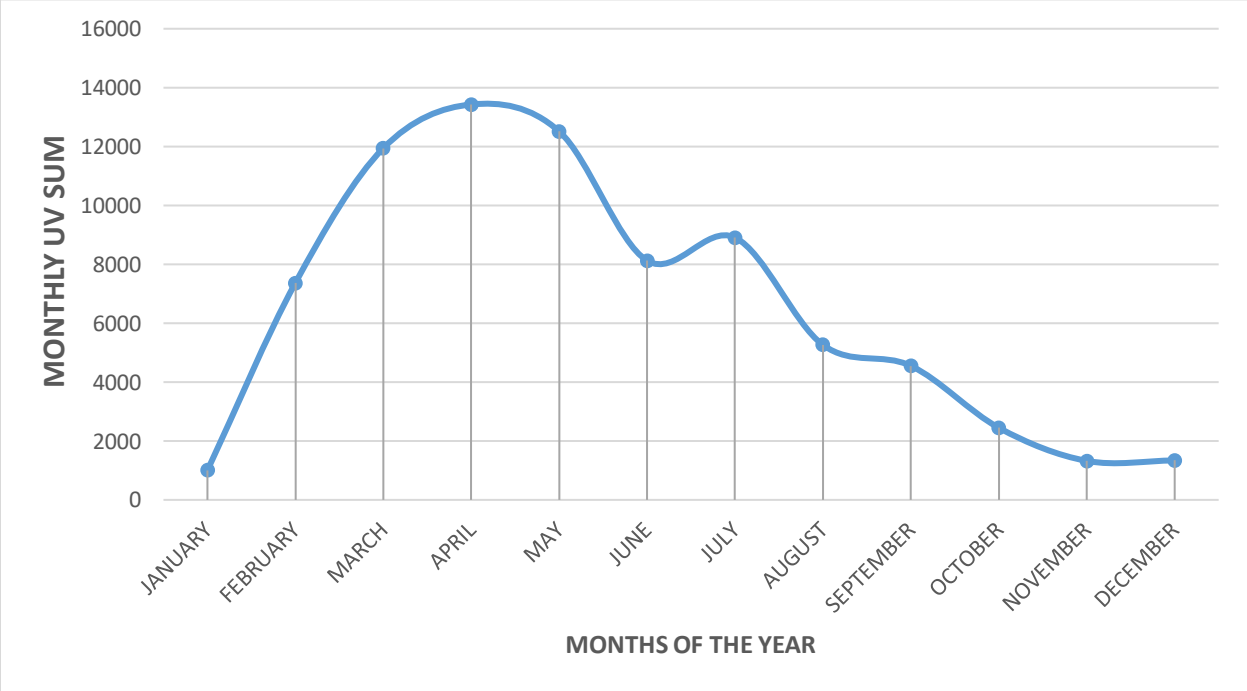

Figure: 2.5 The Monthly sum of the (UV) index for the year

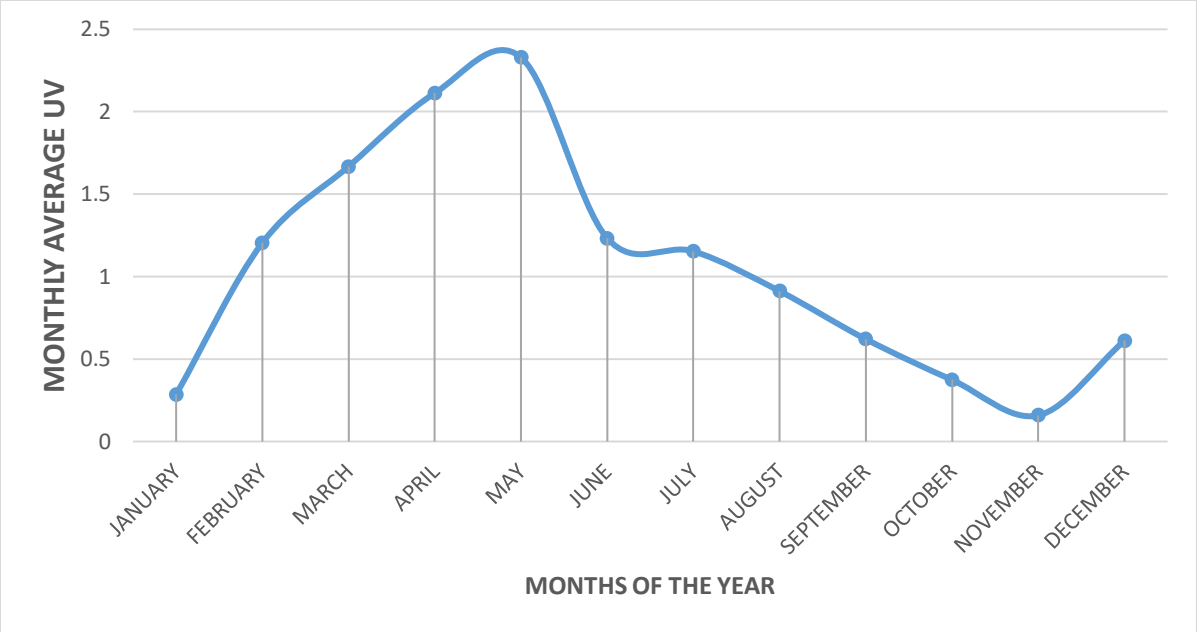

Figure: 2.6 Monthly average UV index for the year

CONCLUSION

Measurement of ultraviolet radiation index made for one year in Minna Niger State, Nigerian. has been analyzed, this measurement was used to characterize the incidence UV index in Minna. It was observed that Minna has moderate UV index except on rare occasions when high UV index occurred and even in the wet seasons we have UV index that are harmful to the heath, the incident ultraviolent index for each month was shown and it shows that solar UV began to rise in the morning corresponding to the sunrise around 10:00 am and drop at sunset around 4:00 pm.

Based on this research work an insight on the incidence UV in Minna was gained on the time and the season for high, moderate and low. that even in wet season someone may be at risk of the damaging effect of UV in Minna.

REFERENCES

Anuforom,A.C,. Akeh, L.E., Okeke, P.N. &Opara, F.E., (2007).Inter-Annual Variability

and Long Term Trend of UV-Absorbing Aerosols During Harmattan Season in Sub Saharan West Africa. Atmosphiric Environment 41,1550-1559.

Bala,E.J.,Ojosu, J.O& Umar,I H.(2000). Government Policies And Programmes On The Development Of Solar PV Sub-Sector In Nigerian.Nigerain Jounrnalof

Renewable Energy 8(1&2)Pp1-6

Diffey, B. L. (2002). *Sources and measurement of ultraviolet radiation* (Vol. 28).

EPA 430-F-10-025 June 2010 www.epa.gov/ozone/strathome.html retrieved on 20 Nov, 2018

Elli, K., René, S., & Joseph, H. G. (n.d). Effect of Solar Radiation on the Skin. Retrieved 08 29, 2015.

Gallagher, R. P., Lee, T. K., Bajdik, C. D., & Borugian, M. (2014). *Ultraviolet radiation.*

Guide On Exposure To Solar Ultraviolet Radiation (Uvr). (2013).

Quijano,A.L.(2000).Radiative Heating and Direct Radiative Forcing by Mineral

Dust in Cloud Atmospheric Condition.Journal of Geophysical Research

105(D10),12,207-12,219.

Safe Work Australia, August, 2013 Website: www.swa.gov.au retrieved on

Shittu, A. (2018). Measurement of Ultraviolet (UV) Solar radiation at Ilorin Kwara State , Nigerian.

You, D. (2010). *UV Radiation.*

Zeus Technical Whitepaper http://www.zeusinc.com retrieved on

Renewable Energy: Benefits, Environmental Impact and Strategies for Optimum Exploitation for Sustainable Development

Sani Garba Danjumma[1]* Sahabi Suleiman[2]
Department of Sciences, Kebbi State Polytechnic, Dakingari, Nigeria.
[1]garbadsani@gmail.com
[2]suleimansahabiyauri@gmail.com
***Corresponding author**

Abstract
The inevitable increase in population and the economic development that must necessarily occur in many countries have serious implications for the environment, because energy generation processes (e.g., generation of electricity, heating, cooling, or motive force for transportation vehicles and other uses) are harmful and pollutes the ecosystem. Energy is considered to be a key player in the generation of wealth and also a significant component in economic development. It is central to sustainable development and poverty reduction efforts. It affects all aspects of development; social, economic, and environmental including livelihoods, access to water, agricultural productivity, health, population levels, education, and gender related issues. This makes energy resources extremely significant for every country in the world. The aim of this paper is to highlight, renewable energy sources, their economic benefits for sustainable development, environmental impact including global warming, advantages and disadvantages and strategies for optimum exploitation for sustainable development.

Keywords: economic benefits, environmental impact, optimum exploitation, renewable energy sources, sustainable development

1. Introduction
Energy commonly defined as the ability to do work, is the capacity of matter to perform work as a result of its motion or its position in relation to forces acting on it. The sun is the source of light and heat to our planet and provides plants with energy to produce the chemicals they need for growth. Energy associated with motion is known as kinetic energy while that related to position is called potential energy. Thus, a swinging pendulum for example has maximum potential energy at the terminal points, but it possesses both kinetic and potential energy at varying proportion at the intermediate positions (Umar and Abubakar, 2014). The World Energy Committee states that there exists no risk free energy resource and for this reason, while choosing the energy resources, cost factors must be considered with environmental effects. Today, prevention of environment pollution and conservation of environment have a dimension exceeding national borders (Grigoriu, 2008). The risks that result from using of fossil fuels increasingly (petroleum, coal and gas) must be decreased. To decrease such risks and maximise energy productivity, energy resources that emit less harmful gas in the atmosphere (like Carbon-dioxide (CO_2) must be preferred in addition to renewable energy. Otherwise, destruction of ecological balance and disasters in future will be inevitable (Keith, 2009). The negative effects of renewable energy resources on environment are lesser than the conventional energy resources. Costs of renewable energy resources are lesser than the fossil origin fuels (Bozkurt, 2010). There are so many sources of renewable energy, however the following are highlighted.

2. Solar Energy
Solar radiation reaches the Earth's surface at a maximum flux density of about 1.0 kWm^{-2} in a wavelength band between 0.3 and 2.5μm (Oji *et al.*, 2012). This is called short wave radiation which includes the visible spectrum. For inhabited areas, this flux varies from about 3 to 30 MJm^{-2} day^{-1}, depending on place, time and weather (Gencoğlu, 2008). This is an energy flux of very high thermodynamic quality, from an accessible source of temperature very much greater than from conventional engineering sources. The flux can be used both thermally (e.g. for heat engines) or, more importantly, for photochemical and photo-physical processes (e.g. photovoltaic power and photosynthesis) (John and Tony, 2006). Solar energy is an energy resource that comes from the sun and

varies between the values of 0-1100 W/m^2 on earth. Solar energy is clean, costless and limitless. Firstly, solar energy was used as heat energy but in recent years, it is also being used as an electric energy source together with developed technology (Unal, 2008). The electric energy is being obtained by means of solar panels and photovoltaic (PV) cells with decreasing as the day goes by (Guney and Onat, 2008).

2.1 Economic Benefits for Sustainable Development

In developing nations, the PV generation system plays an important role in total electrical energy demand, and solar photovoltaic energy has gained a lot of attention because it is renewable, friendly to the environment, and flexible for installation (Guney and Onat, 2008). Solar energy is inconsumable energy resource that does not cause environment pollution. Because of the increase in fuel prices experienced in recent years, solar energy that was not considered economical few years ago, has become very economical in most areas. Solar energy, alternative to energy resources like petroleum and coal, is highly promising (Liqun and Zhixin, 2009).

Buildings could be heated by either orienting them toward the sun (passive solar heating) or pumping a liquid such as water through roof top collectors (active solar heating). Several solar thermal systems can collect and transform radiant energy from the sun into high-temperature thermal energy (heat), which can then be used directly for domestic activities or converted to electricity. These approaches are used mostly in desert areas with ample sunlight. Solar cells that convert sunlight to electricity can be incorporated into roofing materials or windows, and the expectation is that the high cost installation of will fall in due course (Umar and Abubakar, 2014). The renewable energy sector employed 9.8 million people in 2016, an increase of 1.1% over 2015. By technology, solar PV and biofuels provided the largest number of jobs. Employment shifted further towards Asia, which accounted for 62% of all renewable energy jobs (not including large-scale hydropower), led by China. During 2016, at least 75 GWdci of solar PV capacity was added worldwide, equivalent to the installation of more than 31,000 solar panels every hour. More solar PV capacity was installed in 2016 (up 48% over 2015) than the cumulative world capacity five years earlier. By year's end, global solar PV capacity totalled at least 303 GW as shown in Figure 1. (Paris REN21, 2017).

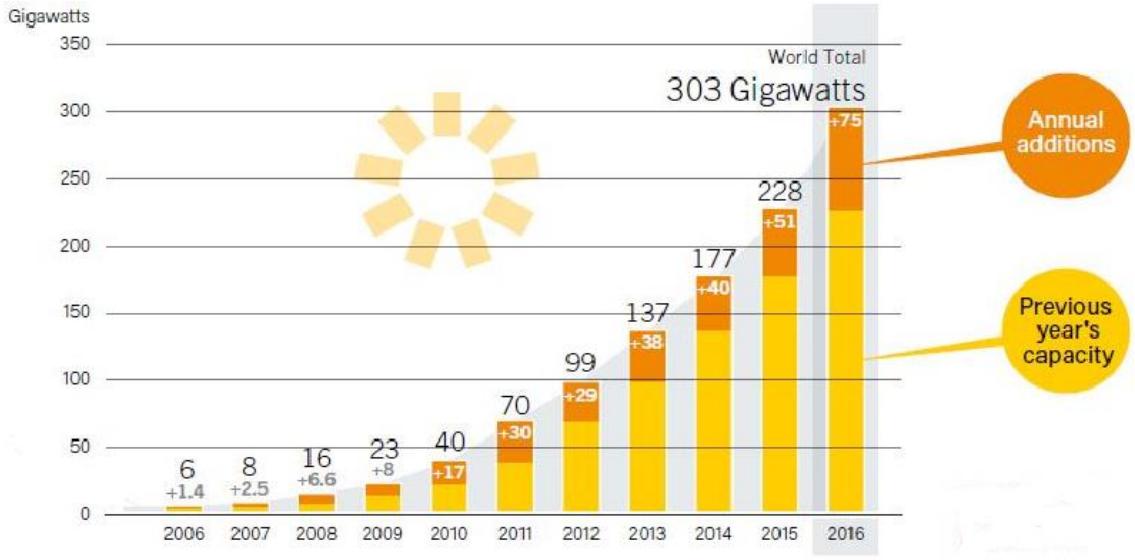

Figure 1. Solar PV Global Capacity and Annual Additions, 2006-2016
(Paris REN21, 2017)

2.2 Environmental Effects of Solar Energy

Photovoltaic is now a proven technology which is inherently safe, as opposed to some dangerous electricity generating technologies. Over its estimated life a photovoltaic module will produce much more electricity than was used in its production. A 100 W module will prevent the emission of over two tonnes of CO_2. Photovoltaic systems make no noise and cause no pollution while in operation. PV cell technologies that have relatively lower environmental risks compared to other types of electric sources. However, chemicals used in PV cells could be

released to air, surface water, and groundwater in the manufacturing facility, the installation site, and the disposal or recycling facility (Klugmann-Radziemska, 2011).
The production of photovoltaic devices involves the use of variety of chemicals and materials (eg.1,1,1-trichloroethane, acetone, ammonia, isopropyl alcohol, and methanol) (California Energy Commission, 2003). Depending on their location, larger utility-scale solar facilities can raise concerns about land degradation and habitat loss and impacts from utility-scale solar systems can be minimized by sitting them at lower-quality locations such as abandoned mining land, or existing transportation and transmission corridors (Hand, 2012).

2.3 Strategies for Optimum Exploitation of Solar Energy

i. Setting up and maintaining a comprehensive information system on available solar energy resources and technologies.
ii. Providing adequate resources to Energy Commissions, to domesticate solar and other renewable energy technologies.
iii. Providing adequate incentive to local manufacturers for solar energy system.

2.4 Advantages of Solar Energy

i. The energy from the Sun is free.
ii. The sun does not produce greenhouse gases and therefore is environmentally friendly.
iii. The sun will always be there during our lifetime. It does not run out.
iv. It prevents unnecessary and excessive commercial energy consumptions of buildings by using the natural heating and cooling systems.
v. It meets the energy need in areas lack of electric network.

2.5 The Disadvantages of Solar Energy

i. It is relatively expensive to build solar power stations.
ii. PV cells operate in low output.
iii. Effect of planar collector systems on environment is in negligible level. However, in some conditions, there may be dangerous situations in respect to health because of high temperatures and poisonous heat transformation fluids.
iv. When it is cloudy or at night there is no enough light, so no electricity can be produced.
v. During the production of solar cells, workers expose to poisonous matters.

3. Wind Energy

The greater heating of the earth at the equator than at the poles and the earth's rotation set of flows of air called wind. This indirect form of solar energy can be captured by wind turbines and converted into electricity. Since 1990, wind power has been the world's fastest growing source of energy with its use increasing almost sevenfold between 1995 and 2004 (Oyedepo, 2012). Europe is leading the way into the age of wind energy. Still much of the world potentials for wind power remain untapped (Umar and Abubakar, 2014). The development of modern wind energy is an impressive example of successful policies to promote renewable energy. Global wind energy capacity has grown from a few hundred megawatts (MW) in 1990 to 48 000 MW in 2004 (Adil and Cutler, 2003). The annual growth rate between 2000 and 2004 was 28 % (Enete and Alabi, 2011).

3.1 Economic Benefits for Sustainable Development

Wind energy has become an affordable and reliable source of alternative, renewable energy. Continued research and development has led to consistently larger turbines, though the average size is only 2 MW. Despite the advances in wind energy and turbine technology, wind energy remains a minor contributor to global energy (Adil and Cutler, 2003). Though, the high installation and maintenance cost of wind turbines coupled with limited output curtails wind energy's potential as a major source of renewable energy but yet, wind energy plays a vital role in electricity generation. Wind power alone already provides a significant share of electricity in some areas: for example, 14% in the U.S. State of Iowa, 40% in the northern German State of Schleswig-Holstein, and 49% in Denmark (Enete and Alabi, 2011). The wind energy is a clean energy resource that can contribute to the usual energy production as

an energy resource under suitable conditions (Umar and Abubakar, 2014). As shown in Figure 2, it has been estimated that, until year 2017, the windmills installed capacity covers up about 10% of the planet's electrical energy needs. Almost 55 GW of wind power capacity was added during 2016, increasing the global total about 12% to nearly 487 GW. Gross additions were 14% below the record high in 2015, but they represented the second largest annual market to date. By the end of 2016, over 90 countries had seen commercial wind power activity, and 29 countries representing every region – had more than 1 GW in operation (Paris REN21, 2017).

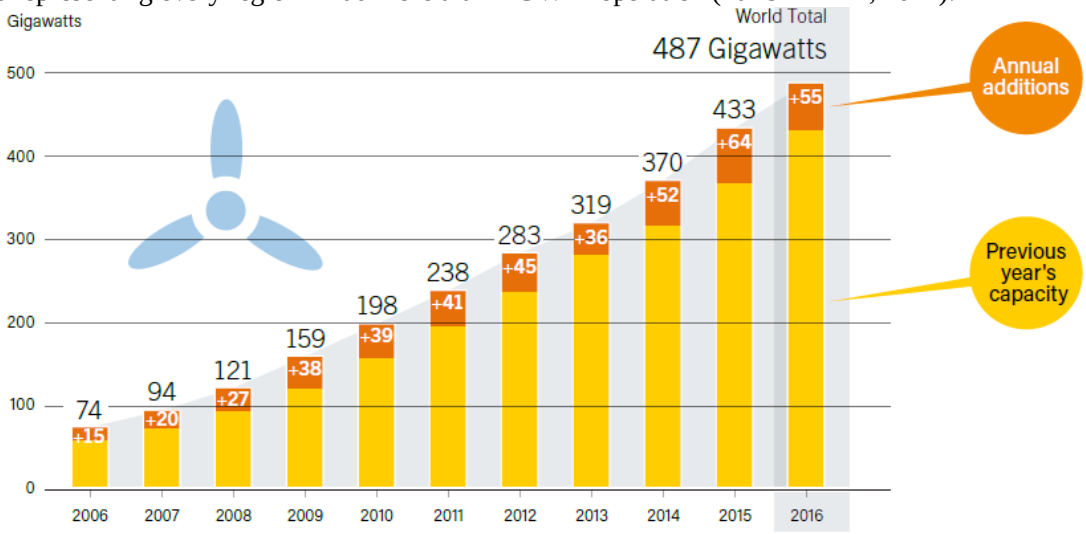

Figure 2. Wind Power Global Capacity and Annual Additions, 2006-2016 (Paris REN21, 2017).

3.2 Environmental Effects of Wind Energy

A wind farm, when installed on agricultural land, has one of the lowest environmental impacts of all energy sources. It occupies less land area per kilowatt-hour (kWh) of electricity generated than any other energy conversion system, apart from rooftop solar energy, and is compatible with grazing and crops; it generates the energy used in its construction in just 3 months of operation, yet its operational lifetime is 20–25 years. Greenhouse gas emissions and air pollution produced by its construction are very tiny and declining (Ewa, 2014). However, wind energy is noisy and cause bird deaths and make parasites on radio and TV receivers. For this reason, in many European countries, mainly in England, the wind turbines are banned to be installed within boundaries of national parks or nearby to them because of their environmental effects. The wind energy is one of the clean energy resources and has positive effects on environment. A 500kW wind turbine realizes the CO_2 cleaning process equal to 57000 trees (Ozyurt and Donmez, 2005).

3.3 Strategies for Optimum Exploitation of Wind Energy

i. Developing skilled manpower for provision of basic engineering infrastructure for local production of components and spare parts of wind power system.
ii. Developing extension programmers to facilitate the general use of wind energy technology.
iii. Providing appropriate incentive to producers, developers and consumers of wind power system.
iv. Training skilled local craftsmen to ensure the operation and maintenance of wind energy system.

3.4 Advantages of Wind Energy

i. Wind is free and will not run out
ii. Continuous sources of energy
iii. Clean source of energy. Wind power generation does not create greenhouse gases
iv. Wind Energy can be used directly as mechanical energy.
v. In remote areas, wind turbines can be used as great resource to generate energy (eg. electricity).
vi. Land around wind turbines can be used for other uses, e.g. Farming.

3.5 Disadvantages of Wind Energy

i. Windmills can be used only in areas where there is a lot of wind.
ii. A lot of turbines are needed to make a lot of electricity.
iii. Wind energy requires expensive storage during peak production time.
iv. Noise pollution problem is usually associated with wind mills.
v. Requires large open areas for setting up wind plants.
vi. It can be a threat to wildlife. Birds do get killed or injured when they fly into turbines.
vii. Maintenance cost of wind turbines is high as they have mechanical parts which undergo wear and tear over the time.

4. Biomass Energy

Plant materials and animal wastes can be burned to provide heat or electricity or converted into gaseous or liquid bio-fuels. Biomass consists of plant materials (such as wood and agricultural waste) and animal wastes that can be burned directly as a solid fuel or converted into gaseous or liquid biofuels (Umar and Abubakar, 2014). Biomass is the first-ever fuel used by humankind and is also the fuel which was the mainstay of the global fuel economy till the middle of the 18th century when fossil fuels took over because they were not only more abundant and denser in their energy content, but also generated less pollution when burnt compared to biomass (Abbasi and Abbasi, 2010). In recent years, there is a resurgence of interest in biomass energy because biomass is perceived as a carbon-neutral source of energy unlike net carbon-emitting fossil fuels of which copious use has led to global warming and ocean acidification. Biomass is an indirect product of solar energy because it consists of combustible organic compounds produced by photosynthesis (Keith, 2009).

4.1 Economic Benefits for Sustainable Development

Burning wood and animal manure for heating and cooking, it supplies 11% of the world's energy and 30% of the energy used in developing countries. Almost 70% of the people living in developing countries heat their homes and cook their food by burning wood or charcoal. However, 2.7 billion people in these countries cannot find, or are too poor to buy, enough fuel wood to meet their needs (Abbasi and Abbasi, 2010). Bacteria and various chemical processes can convert some forms of biomass into gaseous and liquid bio fuels. Example is biogas (a mixture of 60% methane and 40% CO_2), liquid ethanol, and liquid methanol (Umar and Abubakar, 2014). Figure 3 shows that, Global bio-power capacity increased an estimated 6% in 2016, to 112 GW. Generation rose 6% to 504 terawatt-hours (TWh). The leading country for electricity generation from biomass in 2016 was the United States (68 TWh), followed by China (54 TWh), Germany (52 TWh), Brazil (51 TWh), Japan (38 TWh), India and the United Kingdom (both 30 TWh) (Paris REN21, 2017).

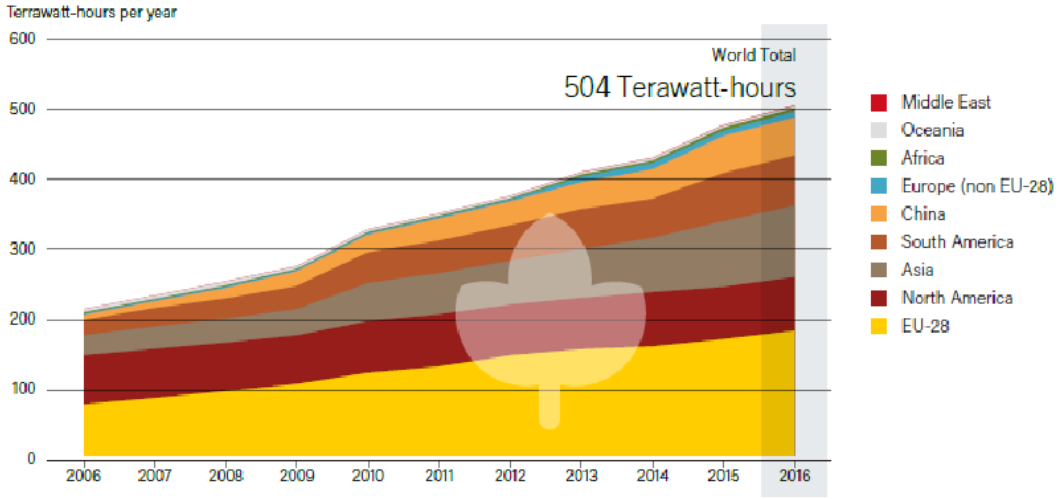

Figure 3. Global Bio-Power Generation, by Region, 2006-2016 (Paris REN21, 2017)

4.2 Environmental Effects of Biomass

If we use biomass as a fuel, the pollutants in the form of carbon and nitrogen are increased in air which may cause air pollution and pollutants at levels high than from traditional fuel sources such as coal or natural gas in some cases. Utilization of wood biomass, as a fuel can also produce fewer particulate and other pollutants than open burning as seen in wildfires or direct heat applications. According to a survey conducted, biomass is recorded as a second largest contributor to global warming (Sukhleen *et al*., 2016). The size of biomass power plant is decided by the availability of the biomass in the nearby surrounding as the transportation plays a vital role in the economy of the plants. So it is found that railway and shipment via waterways can reduce the cost of transport which has led to a global biomass market, to build plants of 1 MW generation economically. In the process of combustion, carbon from biomass is released as carbon dioxide in atmosphere. In the dry wood, the amounts of carbon contents are approximately 50% (Umar and Abubakar, 2014).

4.3 Strategies for Optimum Exploitation of Biomass Energy

i. Afforestation should be encouraged.
ii. Development of domestic capacity in Biomass production and usage so as to reduce the health implication associated with it.

4.4 Advantages of Biomass Energy

i. It's a renewable source of energy.
ii. It's a comparatively lesser pollution generating energy.
iii. It provides manure for the agriculture and gardens.
iv. There is tremendous potential to generate biogas energy.
v. Biomass energy is relatively cheaper and reliable.
vi. Growing biomass crops use up carbon dioxide and produces oxygen.

4.5 Disadvantages of Biomass Energy

i. Continuous supply of biomass is required to generate biomass energy.
ii. Transportation of biogas through pipe over long distances is difficult.
iii. Many easily grown grains like corn, wheat are being used to make ethanol. This can have bad consequences if too much of food crop is diverted for use as fuel.
iv. Crops which are used to produce biogas energy are seasonal and are not available over whole year.
v. Cost of construction of biogas plant is high, so only rich people can use it.

5. Hydropower

Hydropower is electricity generated using the energy of moving water. Rain or melted snow, usually originating in hills and mountains, create streams and rivers that eventually run to the ocean. This energy has been exploited for centuries. Water flowing in rivers and streams can be trapped in reservoirs behind dams and released as needed to spin turbines and produce electricity. Solar energy evaporates water and deposits it as water and snow in other areas through the water circle. Water flowing from higher to lower elevations in rivers and streams can be controlled by dams and reservoirs and used to produce electricity (Senpınar and Gencoğlu, 2006). It is also a flexible source of electricity since the amount produced by the station can be changed up or down very quickly to adapt to changing energy demands.

5.1 Economic Benefits for Sustainable Development

Hydroelectricity is the term referring to electricity generated by hydropower; the production of electrical power through the use of the gravitational force of falling or flowing water. It is the most widely used form of renewable energy, accounting for 16 percent of global electricity generation (3,427 terawatt-hours of electricity production in 2010) and is expected to increase about 3.1% each year for the next 25 years. Hydropower is produced in 150 countries, with the Asia-Pacific region generating 32 percent of global hydropower in 2010. China is the largest hydroelectricity producer, with 721 terawatt-hours of production in 2010, representing around 17 percent of domestic electricity use. There are now four hydroelectricity stations larger than 10 GW, the Three Gorges Dam and Xiluodu Dam in China, Itaipu Dam across the Brazil/Paraguay border, and Guri Dam in Venezuela. The cost of hydroelectricity is relatively low, making it a competitive source of renewable electricity (Askari *et al*., 2015).

Shown in figure 4 shows a Global utilisation of hydropower. More than one-third of new hydropower capacity was commissioned in China. After China, the countries adding the most capacity in 2016 were Brazil, Ecuador, Ethiopia, Vietnam, Peru, Turkey, Lao PDR, Malaysia and India. China also was the leading installer of pumped storage capability during the year, followed by South Africa, Switzerland, Portugal and the Russian Federation (Paris REN21, 2017).

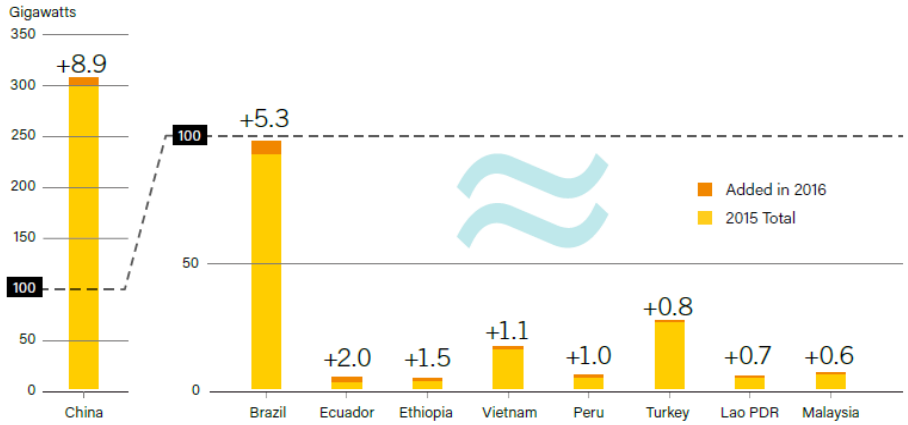

Figure 4. Hydropower Capacity and Additions, Top 9 Countries for Capacity Added, 2016 (Paris REN21, 2017)

5.2 Environmental Effects of Hydropower

The hydroelectric power plants have climatic, hydroelectric, ecological, socio-economic and cultural effects. The water collecting part of a hydroelectric power plant (reservoir) creates environmental effect when it is in operation. As the surface area of a reservoir is wider than a river and as the vaporizing increases, climatic effects occur. In this manner, humid rate in air increases, air movements change and temperature, raining and wind events differ (Unal, 2008). The hydrological effects result from flowing regime of stream and changing of physicochemical parameters. To convert rivers to reservoirs cause vaporizing of water and increasing of quantity of salt and other minerals in water. In transition from stream to lake, natural cleaning capacity decreases depending on decrease in water speed diffusion and oxygen taking capacity and the lake enters into mortification process. Blocking of migration ways both on land and in water, living areas remaining under water and annihilation of some important species cause occurring of ecological effects (Bozkurt, 2010). As a result of the expropriation made depending on size and quality of the land under water, internal and external migration events are experienced and value of land changes. However, because of the manpower movement during construction phase, the regional economy enlivens and infrastructure services and social services cause positive effects especially in integrated projects. The barrage lake is a resource for recreation and production of water products. However, unless the natural resources and historical assets in the region are protected, cultural values may disappear (Unal, 2008).

5.3 Strategies for Optimum Exploitation of Hydropower Energy

i. Ensuring increased indigenous participation in the planning, design and construction of hydropower stations.
ii. Providing basic engineering infrastructure for the production of hydropower plants, equipment and accessories.
iii. Encouraging the private sector, both indigenous and foreign, in the establishment and operation of hydropower plants.

5.4 Advantages of Hydropower

i. Once a dam is constructed, electricity can be produced at a constant rate.
ii. If electricity is not needed, the sluice gates can be shut, stopping electricity generation.
iii. The lake that forms behind the dam can be used for water sports and leisure/pleasure activities. Often large dams become tourist attractions in their own right.

iv. When in use, electricity produced by dam systems do not produce greenhouse gases.
v. Renewable: Hydroelectric energy is renewable. This means that we cannot use up.
vi. Flexible: As previously mentioned, adjusting water flow and output of electricity is easy. At times where power consumption is low, water flow is reduced and the magazine levels are being conserved for times when the power consumption is high.
vii. Hydroelectricity is much safer. There is no fuel involved.

5.5 *Disadvantages of Hydropower*

i. Dams are extremely expensive to build and must be built to a very high standard.
ii. The flooding of large areas of land means that the natural environment is destroyed.
iii. The building of dams for hydroelectric power can also cause a lot of water access problems.
iv. By building a dam, the nearby area has to be flooded and this could affect nearby wildlife and plants.

6.0 Geothermal Energy

It is defined as hot water, vapour and gases arising from the heat accumulated in various depths of the earth crust and of which temperatures are above the atmospheric temperature. The geothermal energy is the heat potential accumulated extraordinarily in accessible depths of the earth crust that can be benefited economically (Akinbami, 2001). This energy is a clean renewable energy. By aid of the energy transformation technologies, electric production is realized from hot water and vapour or they are directly used for purpose of heat energy. The waste fluid of which energy is benefited is re-injected to underground because of its negative environmental effects (Senpınar and Gencoğlu, 2006).

Geothermal energy manifests in the form of heat and has its source in the earth's core, where some nuclear reactions are assumed to occur. The earth's core temperature is estimated to be ~5,000 K, and due to rock conductivity the temperature at about 4 km below the earth's surface can reach ~90 ^{0}C (Oyedepo, 2012). However, at places where geysers, hot springs, hot rocks, or volcanoes exist, there is a much larger local potential for geothermal energy. The total estimated amount of geothermal energy is on the order of 10^{16} PJ (where 1 PJ is 10^{15} J). The geothermal heat flows from the earth's core to the surface at a rate of about 44 TW (where 1 TW is 10^{12} W), which is more than double the world's energy consumption rate of ~15 TW. However, since this heat is too diffuse (~0.1 W/m^2), it cannot be recovered unless a geographic location (i.e., geothermal site) shows a higher intensity geothermal resource. A simple calculation yields that at the consumption rate of 44 TW the geothermal heat will be exhausted after ~10^{12} years (Enete and Alabi, 2011).

6.1 Economic Benefits for Sustainable development

This energy is a clean renewable energy and is used for electricity generation. 27% of total electric production in Philippines and 7% in California State are being covered from geothermal plants and 56MW capacity geothermal electric energy production is made in Papua New Guinea. 75% of energy need of gold mining is covered from geothermal. 86% of total heat energy (city heating) in Iceland is covered from geothermal (Senpınar and Gencoğlu, 2006). Figure 5 shows the countries with the largest amounts of geothermal power generating capacity at the end of 2016 were the United States (3.6 GW), the Philippines (1.9 GW), Indonesia (1.6 GW), New Zealand (1.0 GW), Mexico (0.9 GW), Italy (0.8 GW), Turkey (0.8 GW), Iceland (0.7 GW), Kenya (0.6 GW) and Japan (0.5 GW). Indonesia added about 200 MW of new capacity in 2016, ending the year with 1.64 GW. By early 2017, the country also had started commercial operations at the 110 MW Sarulla plant, one of the largest geothermal plants in the world. The plant is notable for being a combined-cycle operation, analogous to a Turkish plant coming online in 2017, where conventional flash turbines are supplemented with a binary system to extract additional energy from the post-flash turbine steam, maximising energy extraction and efficiency (Paris REN21, 2017).

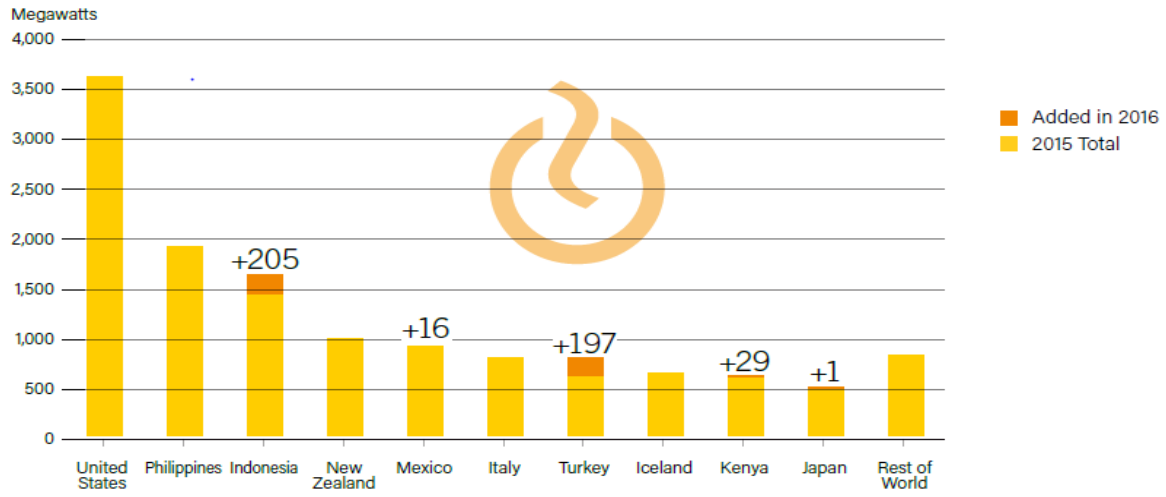

Figure 5. Geothermal Power Capacity and Additions, Top 10 Countries, 2016
(Paris REN21, 2017)

6.2 Environmental Effects of Geothermal Energy

As many countries that use geothermal energy apply reinjection, geothermal energy is considered the most positive energy resource in respect to environment. When geothermal energy is used in electric production, it comes before fossil fuels with its almost zero waste even though it is only evaluated with sulphide emissions. In geothermal power plants, azoth oxide emissions have much lower values than the power plants that use fossil fuels. For this reason, geothermal power plants are considered as a clean energy resource as they are classified risk free in respect to its effect on ozone layer and health (Senpınar and Gencoğlu, 2006).

6.3 Advantages of Geothermal Energy

Among the advantages of geothermal energy are;

i. It is environmentally friendly; it produces no greenhouse gasses.
ii. It does not need fossil energy to heat and vaporize water and it uses natural resources.
iii. The energy source is free and does not run out.

6.4 Disadvantages of Geothermal Energy

i. Geothermal energy requires re-injection because of emission of gases like hydrogen sulphide and carbon dioxide.
ii. Harmful gases and minerals may occasionally come up from the ground below. These can be difficult to control (Ozyurt and Donmez, 2005).

7. Challenges and Recommendations

Below are the challenges in the renewable Energy sector in Nigerian and recommendations for solution

7.1 Renewable Energy Challenges in Nigeria

According to Oji *et al*. (2012), some of the factors militating against the growth of the renewable energy in Nigeria include:

i. *Financial constraints*: A basic barrier to the development of renewable energy technology in Nigeria as a developing country lies in high initial costs and long payback times.
ii. *Technological incapability:* Though the technologies for harnessing renewable energy are being developed in Nigeria, most components have to be imported which further pushes the investment costs higher.
iii. *Absence of a Comprehensive National Energy Policy:* There was virtually no comprehensive energy policy in Nigeria until very recently. Only sub-sectorial policies relating to energy exist.

iv. *Low level of Public Awareness:* The level of awareness about the immense socio-economic and environmental benefits derivable from renewable energy is very low in Nigeria. The current flow of information about the development, various applications, dissemination and diffusion of solar energy resource and technologies is inadequate.

7.2 Recommendations

For effective and efficient utilization of renewable energy in Nigeria, the following recommendations will be useful.

i. More research into the techno-economics involving the initial and subsequent costs of renewable energy plants and their power efficiencies is encouraged.
ii. Government should subsidize the cost of importation of Renewable Energy Technologies (RET) to bring down the high cost in Nigeria.
iii. Private individuals and organisations should be encouraged by appropriate authorities to invest in energy-based technologies in the country.
iv. Consequently, the wide chasm between research bodies (universities, polytechnics and research institutes) and manufacturing industries must be bridged.
v. Government should create more awareness on the advantages derivable from Renewable Energy Technologies (RET).
vi. Government can also consider placing restrictions on the importation of diesel and petrol engine generators because of its adverse effects on the environment even as the global community gear towards clean (green) energies.
vii. Funding of energy technology researches and development initiatives in Nigerian Universities, Polytechnics and Research Institutes so as to develop renewable energy plants with increased efficiency that will be adaptable to our environment is advocated as is obtainable in developed countries.

8. Conclusion

The nature has resources and opportunities sufficient enough enabling people to live in balance without giving damage to the environment and even, to obtain comfortable life level by being industrialized. Most renewable energy sources are harmless to living things with the ability of producing a lot of energy. Although, some renewable energy plants are expensive but harnessing them can be a very big step in protecting the resources in the world and reducing greenhouse gases that affect the environment greatly. Renewable energy sources such as hydropower, biomass, geothermal, solar and wind energy should be considered and seriously supported by governments and private sectors. Sustainable energy systems are necessary to save the natural resources avoiding environmental impacts which would compromise the development of future generations.

Reference

Abbasi, T. and Abbasi, S. A. (2010), Biomass Energy and the Environmental Impacts Associated with its Production and Utilization, *Renewable and Sustainable Energy Reviews*, Vol. 14(3), 919-937.

Adil, N. and Cutler, J. C. (2003), Energy and Sustainable Development at Global Environmental Summits: An Evolving Agenda, *Environment, Development and Sustainability*. Vol. 5, 117–138.

Akinbami, J. F. K. (2001), Renewable Energy Resources and Technologies in Nigeria - Present Situation, Future Prospects and Policy Framework, Mitigation Adaptation Strategies, *Global Change*, Vol. 6, 155-181.

Askari, M. B., Mirzaei, V., Mirhabibi, M. and Dehghani, P. (2015), Hydroelectric Energy Advantages and Disadvantages, *American Journal of Energy Science*, Vol. 2(2), 17-20.

Bozkurt, I. (2010), Energy Resources and Their Effects on Environment, *WSEAS Transactions on Environment and Development*, Vol. 5(6), 327-324.

Enete, C. I. and Alabi, M. O. (2011), Potential Impacts of Global Climate Change on Power and Energy Generation, *Journal of Knowledge Management, Economics and Information, Technology*, Vol. 6, 1–14.

Ewa, K. (2014), Environmental Impacts of Renewable Energy Technologies, *2014 5th International Conference on Environmental Science and Technology*, Vol. 69(21), 104-109.

Gencoğlu, M. T. (2008), Water Pumping System Feeding Solar Energy, *Journal of 3E Electrotech*, Vol. 168, 94-97.

Grigoriu, M. (2008), Basis of Energy Efficiency Economical and Ecological Approach Method for Pumping Equipments and Systems, *WSEAS Transactions on Environment and Development*, Vol. 5(1), 1-12.

Guney, I. and Onat, N. (2008), Technological Status and Market Trends of Photovoltaic Cell Industry, *WSEAS Transactions on Electronics*, Vol. 5(7), 303-312.

Hand, M. M., Baldwin, S., DeMeo, E., Reilly, J.M., Mai, T., Arent, D., Porro, G., Meshek, M. and Sandor, D. (2012), Renewable Electricity Futures Study, *National Renewable Energy Laboratory (NREL)*.

John, T. and Tony, W. (2006), *Renewable Energy Resources*, 2nd Ed., Taylor and Francis E-Library, New York. Pp85.

Keith, S., (2009), *Environmental Hazard: Assessing Risk and Reducing Disasters*, 5th ed., Routledge, 11 New Fetter Lane, London EC4P 4EE.

Klugmann-Radziemska, E. (2011), Environmental Impact of Photovoltaic Technologies; *Low Carbon Earth Summit*, 19-26.

Liqun, L. and Zhixin, W. (2009), A Variable Voltage MPPT Control Method for Photovoltaic Generation System, *WSEAS Transactions on Circuits and Systems*, Vol. 8(4), 335-349.

Oji, J. O., Idusuyi, N., Aliu, T. O., Petinrin, M. O., Odejobi, O. A. and Adetunji, A. R. (2012), Utilization of Solar Energy for Power Generation in Nigeria, *International Journal of Energy Engineering*, Vol. 2(2): 54-59.

Oyedepo, S. O. (2012), Efficient Energy Utilization as a Tool for Sustainable Development in Nigeria. *International Journal of Energy and Environmental Engineering*, Vol. 3(11), 1-12.

Ozyurt, M. and Donmez, G. (2005), Assessment of Environmental Effects of Alternative Energy Sources, *Proceedings of the 3rd National Renewable Energy Sources Conference*, 39-42.

Paris REN21, (2017). *Renewables 2017 Global Status Report*, Paris REN21 Secretariat, Paris France. Senpınar, A. and Gencoğlu, T. M., (2006). Comparison of Renewable Energy Sources in Terms of Environmental Effects, *Fırat University East Anatolian Researches,* 49-54.

Sukhleen, K., Vandana, M., Kamal, K. S. and Inderpreet, K. (2016), Major Global Energy (Biomass). *Computational Intelligence in Data Mining Proceedings of the International Conference on CIDM*, 847.

Umar, D. A. and Abubakar, M. M. (2014), Effects of Energy Utilization on the Environment. *Discovery*, Vol. 25(90), 93-99.

Unal, O., Karagoz, S., Ulger, G., Yuce, E. and Erkul, S. (2008), How Expensive the Global Warming, *2nd International Economics Conference*, Eskisehir, Turkey.

Analysis of Degradation of Mono-Crystalline Photo Voltaic Modules after Four (4) Years of Outdoor Exposure in Minna, North-Central Nigerial

ALILU, Saliu Olakanmi*, EZENWORA Joe Aghabgunam, Moses Abiodun Stephen
Department of Physics, Federal University of Technology Minna,Niger State. Nigeria

Abstract

The understanding of degradation modes and mechanism is very important in order to ensure the lifetime of a Photovoltaic (PV) modules and to predict the total lifespan. In the present study, degradation analysis of mono-crystalline silicon PV modules under test and meteorological sensors installed on a metal support Mask at the Experimental Garden near Physics Department of Federal University OF Technology, Minna, has been carried out after 4 years of outdoor operation in a composite climate of Central Nigeria. A comprehensive analysis has been carried out on Mono-crystalline PV Module rated 10W using CR1000 software-based Data Acquisition System (DAS) through visual inspection, Open-Circuit Voltage (Voc), Short-Circuit Current (Isc),I-V characteristic. The data monitoring was from 09:00am to 18:00 pm hours each day continuously for four years, from December 2014 to November 2018. Annual yearly average of the performance variables were calculated to have the full knowledge of the degradation rate and the lifespan of the module. It was observed that Open-Circuit Voltage (V oc), Short-circuit Current (I sc), Power (W), Maximum Voltage (Vmax), Maximum Current (I Max) and Power Maximum (P Max) has average yearly degradation of 1.07V; 0.007A, P(W), 0.08W, 1.7V, 0.017A and 0.14W for the four years

1. Introduction

It is importance to know that the sun is the nearest star and therefore the source of all renewable energy on earth which provide sustenance for both plants and animals. Photovoltaic module in the local environment will establish performance comparison between the locally available modules types. The result of this investigations will assist the designers, scientists and Energy Research centers to get first-hand information on the modules performance in the local environment before they proceeds on design and installation for power supply. Indeed, solar energy is used for industry, Communities as well as individual needs. Over the past decade, the photovoltaic (PV) market has experienced unprecedented growth and beside these, photovoltaic market has reached a cumulative installed capacity of roughly 40 GW world-wide, with an annual added capacity of 16.6 GW (EPIA, 2011).

However, there is little information on PV modules degradation modules in terms of frequency, speed of evolution and degree of impact on module lifetime and reliability. Research on photovoltaic modules is rather focused on the race to develop new technologies without sufficient experience feedback on already operational technologies (Laronde, 2009; Tiwari and Dubey, 2010). For economy development in a society, the rate at which the demands for electricity will be increases, let us consider the present situation, primary energy account for 40% of the global energy used for power generation, and solar or renewable energy only account for 3.6% (Nasiro,S:Rev.2018,95 194-202).It is importance to know that the sun is the nearest star and therefore the source of all renewable energy

on earth which provide sustenance for both plants and animals.(Joel. E 2016).The investigating of the performance of mono-crystalline photovoltaic module in the local environment will establish performance comparison between the locally available modules types. The result of this investigations will assist the designers, scientists and Energy Research centers to get first-hand information on the modules performance in the local environment before they proceeds on design and installation for power supply.

2. Material and Method

2.1 Method of Data acquisition.

The research was carried out at the premises of Bosso Campus of Federal University of Technology, Minna, Niger State. The studied of the specific effect of ambient weather parameters which includes: Temperature, Solar irradiance, wind speed and relative humidity on performance of mono-crystalline photovoltaic module ,analyzing the observed data and convert to compare with the producer specification as the result will indicate any variance resulted from the meteorological effects indicate the degradation.

The research process involved two process which include Date acquisition by continuous monitoring and Date analysis.

3.1 Monitoring State

The performance response of the mono-crystalline PV modules to ambient weather parameters; solar irradiance, temperature, wind speed and relative humidity, was monitored in Minna environment, using CR1000 software-based data logging system with computer interface. The PV modules under test, and meteorological sensors, were installed on support structure at the same test plane, at about three metres of height, so as to ensure adequate exposure to insolation and enough wind speed, since wind speed is proportional to height. The elevation equally ensures that the system is free from any shading from shrubs and also protected from damage or interference by intruders. Also, the whole experimental set up was secured in an area of about four metres in diameter. The modules were tilted at approximately 10o (since Minna is on latitude 09o37' N) to horizontal and south facing to ensure maximum insolation (Ezenwora .J, 2016; Scheller *at el.*, 1991; and Ugwuoke *at al.*, 2006). The data monitoring was from 8.00 am to 6.00 pm local time, each day continuously for a period of four year, starting from December 2014 to November 2018, so as to cover the two distinct and well defined climate seasons of the area. The experiment was carried out at Experimental Guarding at Bosso

Campus of Federal University of Techology, Minna (latitude 09o37' N, longitude 06o32' E and 249 meter above sea level). The sensors were connected directly to the CR1000 Campbell Scientific data logger, while the modules are connected to the logger via electronic loads. The logger was programmed to scan the load current from 0 to 1 A at intervals of 50 mA every 5 minutes, and average values of short-circuit current, Isc, open-circuit voltage, Voc, current at maximum power, Imax, voltage at maximum power, Vmax, power and maximum power obtained from the modules together with the ambient parameters are recorded and logged. Data download at the data acquisition site was performed every 7 days to ensure effective and close monitoring of the DAS. At the end of each month and where necessary, hourly, daily and monthly averages of each of the parameters - solar irradiance, solar insolation, wind speed, ambient and module temperatures, and the output response variables (open-circuit voltage, V_{oc}, short-circuit current, I_{sc}, voltage at maximum power, Vmax, current at maximum power, Imax, efficiency, Eff and fill factor, FF) of the photovoltaic modules were obtained. The global solar radiation was monitored using Li-200SA M200 Pyra-nometer, manufactured by LI-COR Inc. USA, with calibration of 94.62 microamperes per 1000 W/m2. The ambient temperature and relative humidity were monitored using HC2S3-L Rotronic Hy-groClip2 Temperature/Relative

Humidity probe, manufactured in Switzerland. Wind speed was monitored using 03002-L RM Young Wind Sentry Set. And module temperature was monitored using 110PV-L Surface-Mount Temperature probe. All sensors were installed in the CR1000 Campbell Scientific data logger with measurement and control module as show below.

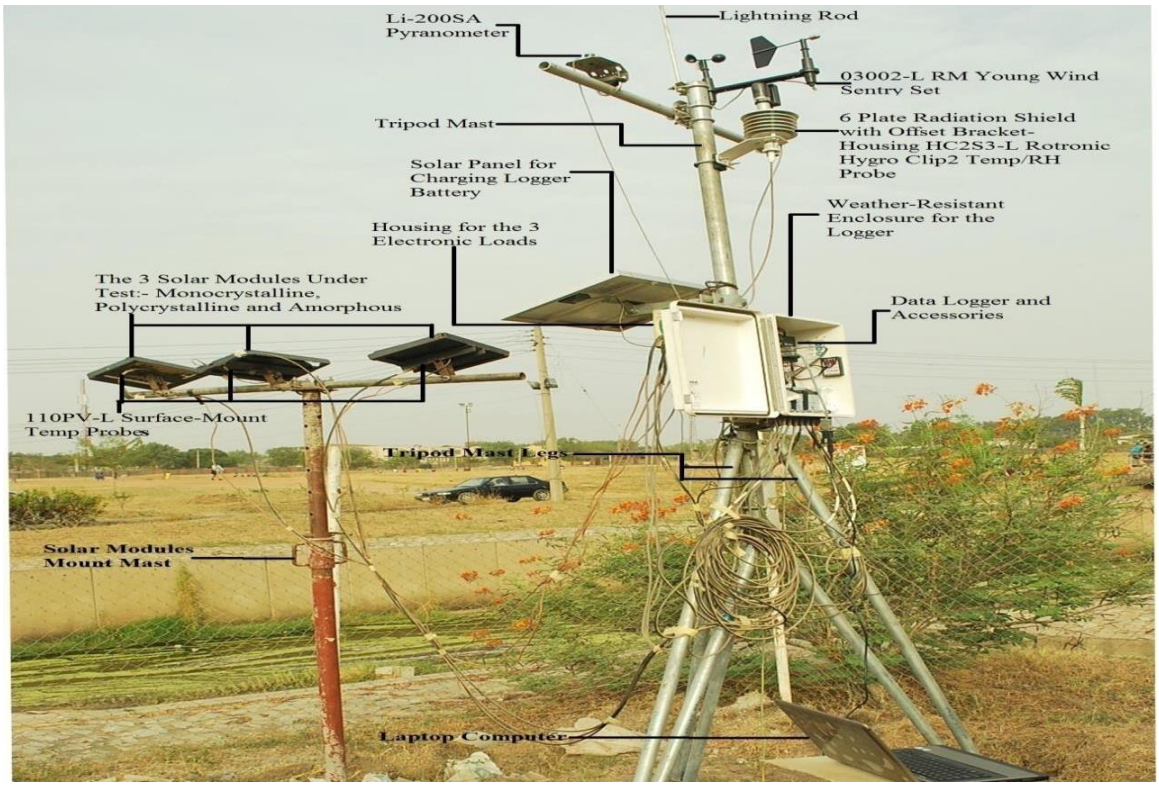

Plate 1:The Experimental set Up (Near Physics Department, FUT Minna)

2.2. Method Data Analysis

Analysis of the yearly degradation rate of the mono-crystalline module by solar irradiance was investigated in terms of open circuit voltage (Voc),Short-circuit current (Isc) Voltage at Maximum power (Pmax),current at maximum power(Imax),Efficiency(Eff) and Fill factor(FF).All the parameters and module performance Ratio (MPR) were evaluated using the following expressions(Ugwuoke,2005;Ezenwora, 2016)

Fill factor (FF) = $I_{max}V_{Max}/I_{SC}\ Voc$ (1)

Efficiency (Eff) = $I_{Max}V_{max}/P_{in}$ = $I_{sc}VocFF/P_{in}$= $I_{sc}V_{OC}/AE_e$ (2)

Module Performance Ration (MPR) = Effective Efficiency/Efficiency at STC (3)

The maximum power (P max) which is the operating point of the module, was recorded by the logger it was corresponds to the large area under the I-v curve .The current and voltage at this point are Imax and Vmax respectively.

3. Results and Discussions

T (Years)	WS (m/s)	T_a (^{0}C)	RH (%)	T_{mod} (^{0}C)	H_g (W/m^2)	V_{sc} (v)	I_{sc} (A)	P (W)	V_{max} (V)	I_{max} (A)	P_{max}	FF	Eff (%)
YEAR 1 (2015)	1.65	25.4	48.3	38.9	477	4.62	0.038	0.342	4.62	0.095	0.543	2.477	0.03
YEAR 2 (2016)	1.57	31.4	49.7	39.3	520	3.91	0.039	0.282	3.91	0.087	0.439	2.235	0.02
YEAR 3 (2017)	1.34	32.3	47.1	40.8	502	4.02	0.045	0.274	4.03	0.094	0.455	2.112	0.03
YEAR 4 (2018)	1.03	32.7	53.1	41.0	485	1.64	0.034	0.094	1.64	0.057	0.154	1.701	0.01
AVERAGE	1.40	30.5	49.6	40.0	496	3.55	0.039	0.248	3.55	0.083	0.398	2.131	0.02

Table 1: Annual Average f Ambient Parameters and Performance Variables For the Mono-Crystalline Module.

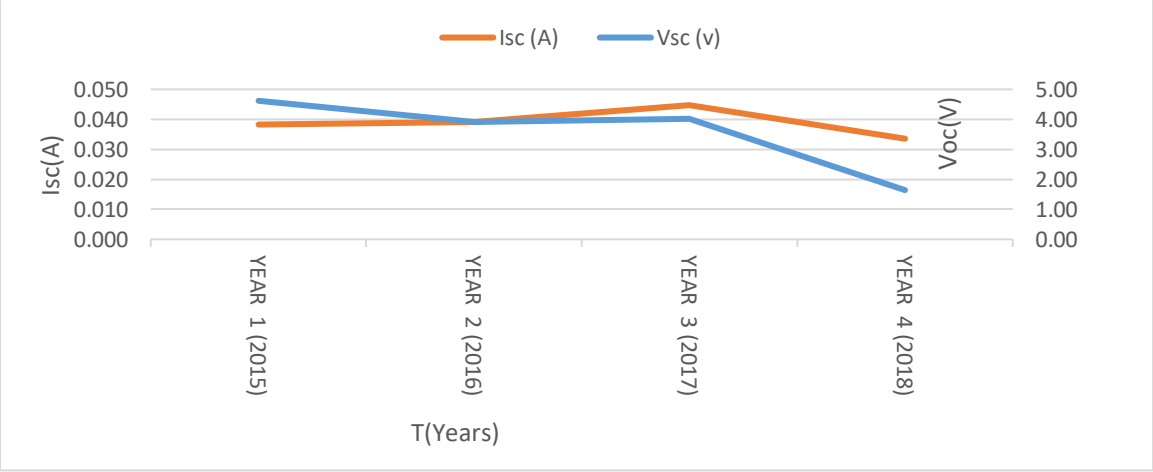

Figure 1: Yearly Variation of Short Circuit Current and Open-Circuit Voltage.

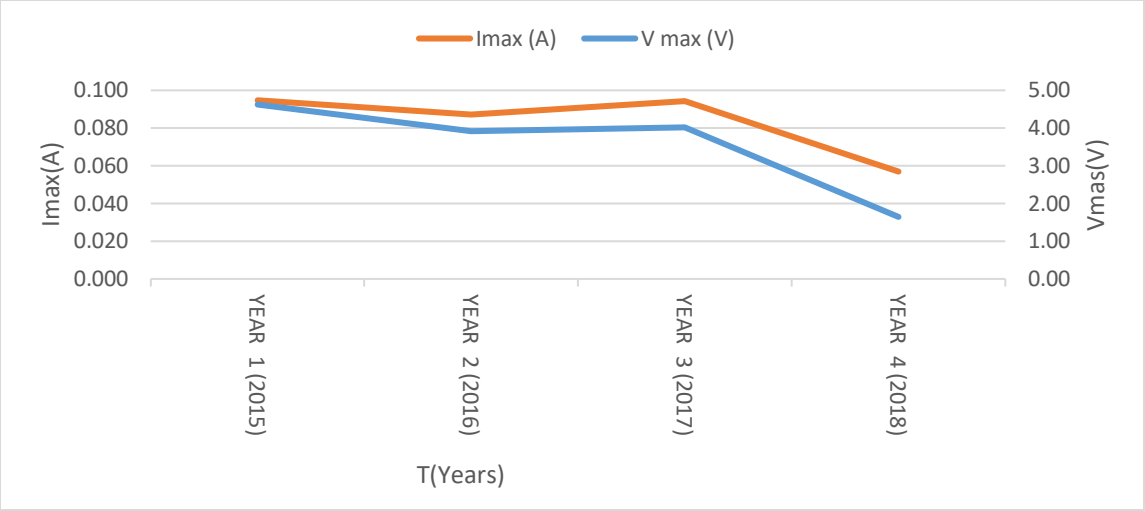

Figure 2: The yearly variation of maximum current and maximum voltage.

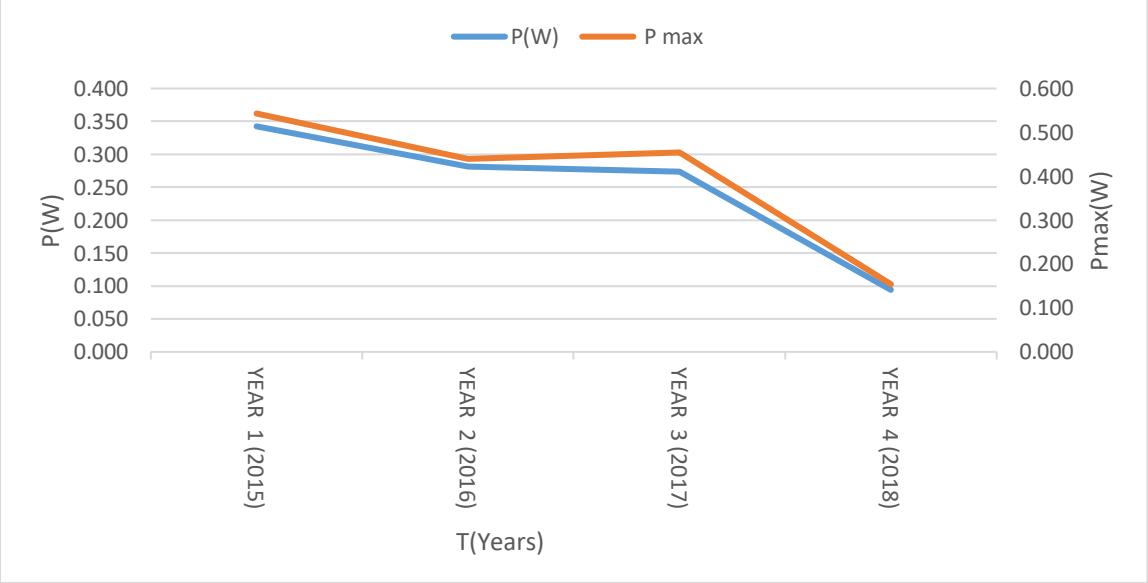

Figure 3: Yearly variation of Power (W) and Maximum Power (W)

In figure (1) shows the yearly variation of I-V characteristics of Short circuit currents and open circuit voltage, gradual degradation was observed by the open circuit voltage in 2015 from 4.62V to 3.91V In 2016 and further rise to 4.02V in 2017 then degraded to 1.64V in 2018.While the short circuit currents slightly increases from 2015 to 2017 by 0.001A and further increased by 0.006A in 2017,the rise in Isc from 2015 to 2017 was due to high in module temperature which accounted for the

increases. Therefore, increases in Hg Tmod as seen in table has accounted for the increases for the three performance variable (Ezenwora,2016),then drastically degraded by 0.01A in 2018.

In Figure (2), Current at maximum (Imax) decreases slightly from 0.095A to 0.087A in 2016 and increases drastically to 0.94 A in 2017 and degraded in 2018 by 0.037A while Voltage at maximum decreases down from 4.62V in 2015 to 3.91V in 2016 and from here, an increases was observed by 0.12V in 2018 follows by a drastic degraded to 1.63V.

In figure (3), the Maximum power decreases by 0.1W from 2015 to 2016and a slight increases in 2016 from 0.439W to 0.455W and further degraded by 0.30W in 2018.The maximum current decreases by 0.008W between 2015 to 2016 and slightly increases to 0.094W in 2017 but finally degraded by 0.037W in 2018.

4.0 Conclusion

The yearly Analysis of degradation of mono-crystalline photovoltaic module was carried out in Minna local environment and the result shows that all the performance variables of the modules degraded significantly from year to year for the four years of studied. It was observed that the electrical parameters variables of the modules has an average degradation rate of 3.55V for Voc,0.039A for Isc,0.248W for P(W),3.55V for Vmax,0.083A for Imax and 0.398W for Pmax for the four years of study. Similarly, it was noticed from table 1 that, Voc and Isc has a yearly decreases of 0.7V and 0.001A from 2015 to 2016, 0.1V and 0.11A from 2016 to 2017,0.02.40V and 0.11A from 2017 t0 2018. Imax was observed to have decreases by 0.037A from 2017 to 2018 after the increments in the preceding years suggesting that Imax could begin to degrade after the third year. Furthermore, P and Pmax decreased by yearly average of 0.08W and 0.0.14W from 2015 to 2018.Module temperature was therefore observed to have significant influence on the general degradation of the module especially Voc and Vmax hence they increase when temperature decreased in 2015.In addition to the temperature effects on the degradation of the module is the solar irradiance which is seen to affect P, Pmax and Imax, hence, the increases when temperature and solar irradiance increased in the first year of study which is in line with early observation.(Ezenwora et al.,2018).By compering this result with that from (Pramod Rajput et al.,2016), with an average power degradation rate of 90 PV period of 22 years of outdoor exposure in the composite climate of India which was found to be about 1.9%/year with maximum rate of power degradation 4.1%/year and minimum is 0.3%/year. This is to concludes that they are correlate and it is therefore recommended that outdoor, yearly degradation studies should be carried out on all commercially available PV modules in every location of developing countries where this is not realizable .Result should furnish the policy makers, designers, PV power system installers the vital information on the degradations rate and lifespan of all commercially available PV modules for effective and reliable PV power system.

Acknowledgement:

It wish to express my profound gratitude and appreciation to Joel A. Ezenwora's photovoltaic laboratory for the provision of data used for this research work.

References.

Dubey, R., Chattopadhyay, S., Kuthanazhi, V., John, J.J., Arora, B.M., Kottantharayil, A., Narasimhan, K.L., Solanki, C.S., Kuber, V., Vasi, J., 2010. All-India Survey of Photovoltaic Module Degradation, pp. 1–237.

EPIA: European Photovoltaic Industry Association, 2011. Global Market

Outlook for Photovoltaic until 2015.

Ezenwora,J.A;(2016).Development of a prototype photovoltaic power system based on characterization and performance Evaluation of photovoltaic Modules in Minna,Nigeria.phD Thesis, Department of Physics Federal University of Technology,Minna.pp 45-140.

Ezenwora,J.A;Oyedun,D.A;Ugwoke,P.E.(2018).Comparative study on Different types of photovoltaic Modules under outdoor Operating Conditions in Minna,Nigeria.International Journal of physical Research.6(1),pp35-48

Laronde, R., Charki, A., Bigaud, D., 2012. Lifetime Estimation of a Photovoltaic Module Subjected to Corrosion Due to Damp Heat Testing. Journal of Solar Energy Engineering 135 (2). http://dx.doi.org/10.1115/1.4023101.

Laronde, R., Charki, A., Bigaud, D., 2010. Reliability of photovoltaic modules based on climatic measurement data. International Journal of Metrology and Quality Engineering 1 (01), 45–49. http://dx.doi.org/ 10.1051/ijmqe/2010012.

Morita, K., Inoue T., Kato T., Tsuda I., Hishikawa Y., 2003. Degradation factor analysis of crystalline-Si PV modules through long-term field exposure test. In: 3rd World Conference on Photovoltaic Energy Conversion, Osaka, Japan, pp. 1948–1951.

Osterwald, C.R., Anderberg, A., Rummel, S., Ottoson, L., 2002. Degradation

Analysis of Weathered Crystalline-Silicon PV Modules. In: 29th

IEEE Photovoltaic Specialists Conference, New Orleans, Louisiana.

Pramod Rajput et al.,(2015).Degradation of Mono-Crystalline photovoltaic Modules after 22 years of outdoor exposure in the composite climate of India. International Journal.

Tiwari, G.N., Ghosal, M.K., 2010. Renewable Energy Resources: Basic Principles and Applications. Narosa Publishing House, New Delhi.

Strong,S.J. & Scheller,W.G (1991).The solar electric house. massachusetts: sustainability press.